AD-A213 561

DNA-TR-87-239-V2A-10A

THE NORSE MANUAL

Volume 2A-10A—Local Thermal Equilibrium Molecular Band Shape Parameters

T. Gorman
R. Parker
J. Generosa
Physical Research Inc.
2201 Buena Vista S.E.
Suite 301
Albuquerque, NM 87106

1 November 1988

Technical Report

CONTRACT No. DNA 001-88-C-0030

Approved for public release;
distribution is unlimited.

THIS WORK WAS SPONSORED BY THE DEFENSE NUCLEAR AGENCY
UNDER RDT&E RMC CODE B3200A76 0D SA SA 00183 25904D.

DTIC
ELECTE
OCT 11 1989
S B D

Prepared for
Director
Defense Nuclear Agency
Washington, DC 20305-1000

89 10 11 054

DISTRIBUTION LIST UPDATE

This mailer is provided to enable DNA to maintain current distribution lists for reports. We would appreciate your providing the requested information.

- ☐ Add the individual listed to your distribution list.
- ☐ Delete the cited organization/individual.
- ☐ Change of address.

NAME: _____

ORGANIZATION: _____

OLD ADDRESS	CURRENT ADDRESS
_____	_____
_____	_____
_____	_____

TELEPHONE NUMBER: (___) _____

SUBJECT AREA(s) OF INTEREST:

_____ _____

_____ _____

_____ _____

DNA OR OTHER GOVERNMENT CONTRACT NUMBER: _____

CERTIFICATION OF NEED-TO-KNOW BY GOVERNMENT SPONSOR (if other than DNA).

SPONSORING ORGANIZATION: _____

CONTRACTING OFFICER OR REPRESENTATIVE: _____

SIGNATURE: _____

CUT HERE AND RETURN

Director
Defense Nuclear Agency
ATTN: TITL
Washington, DC 20305-1000

Director
Defense Nuclear Agency
ATTN: TITL
Washington, DC 20305-1000

UNCLASSIFIED
SECURITY CLASSIFICATION OF THIS PAGE

REPORT DOCUMENTATION PAGE

1a REPORT SECURITY CLASSIFICATION UNCLASSIFIED	1b RESTRICTIVE MARKINGS
2a SECURITY CLASSIFICATION AUTHORITY N/A since Unclassified	3 DISTRIBUTION/AVAILABILITY OF REPORT Approved for public release; distribution is unlimited.
2b DECLASSIFICATION/DOWNGRADING SCHEDULE N/A since Unclassified	
4 PERFORMING ORGANIZATION REPORT NUMBER(S) PRi-NM-88-R002	5 MONITORING ORGANIZATION REPORT NUMBER(S) DNA-TR-87-239-V2A-10A
6a NAME OF PERFORMING ORGANIZATION Physical Research, Inc. 6b OFFICE SYMBOL (If applicable)	7a NAME OF MONITORING ORGANIZATION Director Defense Nuclear Agency
6c ADDRESS (City, State, and ZIP Code) 2201 Buena Vista SE Suite 301 Albuquerque, NM 87106	7b ADDRESS (City, State and ZIP Code) Washington, DC 20305-1000
8a NAME OF FUNDING SPONSORING ORGANIZATION 8b OFFICE SYMBOL (If applicable) RAAE/Schwartz	9 PROCUREMENT INSTRUMENT IDENTIFICATION NUMBER DNA 001-88-C-0030
8c ADDRESS (City State and ZIP Code)	10 SOURCE OF FUNDING NUMBERS PROGRAM ELEMENT NO: 63220C; PROJECT NO: SA; TASK NO: SA; WORK UNIT ACCESSION NO: DH200780

11 TITLE (Include Security Classification)
THE NORSE MANUAL
Volume 2A-10A—Local Thermal Equilibrium Molecular Band Shape Parameters

12 PERSONAL AUTHOR(S)
Gorman, Thomas; Parker, Ronald; Generosa, John

13a TYPE OF REPORT	13b TIME COVERED	14 DATE OF REPORT (Year Month Day)	15 PAGE COUNT
Technical	FROM 870201 TO 870901	881101	614

16 SUPPLEMENTARY NOTATION
This work was sponsored by the Defense Nuclear Agency under RDT&E RMC Code B3200A7600D SA SA 00183 25904D.

17 COSATI CODES			18 SUBJECT TERMS (Continue on reverse if necessary and identify by block number)
FIELD	GROUP	SUB-GROUP	NORSE, Nuclear Effects, MOLECULAR SPECTRA, Optics, Band Models, Molecular Effects, RADAR SYSTEMS, (TES)
12	8		
20	6		

19 ABSTRACT (Continue on reverse if necessary and identify by block number)

The NORSE (Nuclear Optical and Radar System Effects) Code is being developed by DNA as a systems analysis tool. This report describes the local Thermal Equilibrium Emissions data base used by the NORSE code. Graphs of the Weakline and Strongline parameters in the spectral region of 10 cm^{-1} to 10,000 cm^{-1} are presented. A brief description of the band models used by NORSE is given.

20 DISTRIBUTION/AVAILABILITY OF ABSTRACT	21 ABSTRACT SECURITY CLASSIFICATION
☐ UNCLASSIFIED/UNLIMITED ☒ SAME AS RPT ☐ DTIC USERS	UNCLASSIFIED
22a NAME OF RESPONSIBLE INDIVIDUAL Bennie F. Maddox	22b TELEPHONE (Include Area Code) (202) 325-7042 22c OFFICE SYMBOL DNA/CSTI

DD FORM 1473, 84 MAR 83 APR edition may be used until exhausted
All other editions are obsolete

SECURITY CLASSIFICATION OF THIS PAGE
UNCLASSIFIED

PREFACE

This Manual is a graphical compendium of the NORSE LTE infrared data base. The complete NORSE data base is shown. Whenever possible the assumptions used to generate this information have been given. The theoretical background of the NORSE transmission model is briefly discussed.

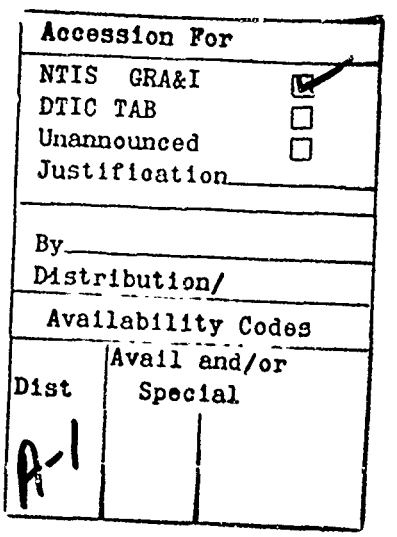

Conversion factors for U.S. Customary to metric (SI)
Units of Measure

MULTIPLY ----------► TO GET ◄----------	BY ----------► BY ◄----------	TO GET DIVIDE
angstrom (A)	1.000 000 X E -10	meters (m)
atmosphere (normal)	1.013 25 X E +2	kilo pascal (kPa)
bar	1.000 000 X E +2	kilo pascal (kPa)
barn	1.000 000 X E -28	meter^2 (m^2)
British thermal unit (thermochemical)	1.054 350 X E +3	joule (J)
calorie (thermochemical)	4.184 000	joule (J)
cal (thermochemical)/cm^2	4.184 000 X E -2	mega joule/m^2 (MJ/m^2)
degree (angle)	1.745 329 X E -2	radian (rad)
degree Fahrenheit	$t_K=(t_F+459.67)/1.8$	degree kelvin (K)
electron volt	1.692 19 X E -19	joule (J)
erg	1.000 000 X E -7	joule (J)
erg/second	1.000 000 X E -7	watt (W)
foot	3.048 000 X E -1	meter (m)
foot-pound-force	1.355 818	joule (J)
gallon (U.S. liquid)	3.785 412 X E -3	meter^3 (m^3)
inch	2.540 000 X E -2	meter (m)
joule/kilogram (J/kg) (radiation dose absorbed)	1.000 000	Gray (Gy)
kilotons	4.183	terajoules
kip (1000 lbf)	4.448 222 X E +3	newton (N)
kip/inch^2 (ksi)	6.894 757 X E +3	kilo pascal (kPa)
ktap	1.000 000 X E +2	newton-second/m^2 ($N-s/m^2$)
micron	1.000 000 X E -6	meter (m)
mil	2.540 000 X E -5	meter (m)
mile (international)	1.609 344 X E +3	meter (m)
ounce	2.834 952 X E -2	kilogram (kg)
pound-force (lbs avoirdupois)	4.448 222	newton (N)
pound-force inch	1.129 848 X E -1	newton-meter (N.m)
pound-force/inch	1.751 268 X E +2	newton/meter (N/m)
pound-force/foot^2	4.788 026 X E -2	kilo pascal (kPa)
pound-force/inch^2 (psi)	6.894 757	kilo pascal (kPa)
pound-mass (lbm avoirdupois)	4.535 924 X E -1	kilogram (kg)
pound-mass-foot^2 (moment of inertia)	4.214 011 X E -2	kilogram-meter^2 ($kg.m^2$)
pound-mass/foot^3	1.601 846 X E +1	kilogram/meter^3 (kg/m^3)
rad (radiation dose absorbed)	1.000 000 X E -2	**Gray (Gy)
roentgen	2.579 760 X E -4	coulomb/kilogram (C/kg)
shake	1.000 000 X E -8	second (s)
torr (mm Hg, 0°C)	1.333 22 X E -1	kilo pascal (kPa)

*The becquerel (Bq) is the SI unit of radioactivity; 1 Bq = 1 event/s.
**The Gray (Gy) is the SI unit of absorbed radiation.

TABLE OF CONTENTS

Section		Page
	PREFACE	iii
	CONVERSION TABLE	iv
	LIST OF ILLUSTRATIONS	vii
	LIST OF TABLES	xxviii
1	INTRODUCTION	1
	1.1 DESCRIPTION OF THE DATA	1
	1.2 DATA SOURCES	1
	1.3 LTE DATA BASE	2
	1.4 FUTURE EFFORTS	2
2	BACKGROUND	3
	2.1 TRANSMISSION BAND MODELS	3
	2.2 BAND MODEL PARAMETERS	7
3	SAMPLE CALCULATIONS	10
4	DIATOMIC MOLECULES	15
	4.1 CARBON MONOXIDE	16
	4.2 HYDROXYL	45
	4.3 NITROGEN	70
	4.4 NITROGEN OXIDE	87
	4.5 OXYGEN	146
5	POLYATOMIC MOLECULES	160
	5.1 AMMONIA	160
	5.2 CARBON DIOXIDE	168
	5.3 DINITROGEN OXIDE	197
	5.4 METHANE	220
	5.5 NITRIC ACID	233
	5.6 NITROGEN PEROXIDE	237
	5.7 OZONE	260
	5.8 SULFUR DIOXIDE	283
	5.9 WATER	291

TABLE OF CONTENTS (Continued)

Section		Page
6	METAL OXIDES	314
	6.1 ALUMINUM OXIDE	314
	6.2 COPPER OXIDE	343
	6.3 IRON OXIDE	372
	6.4 LITHIUM OXIDE	401
	6.5 MAGNESIUM OXIDE	430
	6.6 SILICON OXIDE	459
	6.7 TITANIUM OXIDE	488
	6.8 URANIUM OXIDE	517
7	LIST OF REFERENCES	575
APPENDICES		
A	BIBLIOGRAPHY	577
B	GLOSSARY	579
C	LIST OF SYMBOLS	581

LIST OF ILLUSTRATIONS

Figure		Page
1	Weak-line parameter for 626 CO_2	12
2	Inverse line spacing for 626 CO_2	13
3	Transmittance for 626 CO_2	14
4	Weak-line parameter for CO	17
5	Inverse line spacing for CO	18
6	Weak-line parameter for CO at 200°K	19
7	Weak-line parameter for CO at 300°K	20
8	Weak-line parameter for CO at 500°K	21
9	Weak-line parameter for CO at 750°K	22
10	Weak-line parameter for CO at 1000°K	23
11	Weak-line parameter for CO at 1500°K	24
12	Weak-line parameter for CO at 2000°K	25
13	Weak-line parameter for CO at 3000°K	26
14	Weak-line parameter for CO at 5000°K	27
15	Weak-line parameter for CO at 7000°K	28
16	Weak-line parameter for CO at 10000°K	29
17	Weak-line parameter for CO at 12000°K	30
18	Weak-line parameter for CO at 18000°K	31
19	Strong-line parameter for CO at 200°K	32
20	Strong-line parameter for CO at 300°K	33
21	Strong-line parameter for CO at 500°K	34
22	Strong-line parameter for CO at 750°K	35
23	Strong-line parameter for CO at 1000°K	36
24	Strong-line parameter for CO at 1500°K	37
25	Strong-line parameter for CO at 2000°K	38
26	Strong-line parameter for CO at 3000°K	39

LIST OF ILLUSTRATIONS (Continued)

Figure		Page
27	Strong-line parameter for CO at 5000°K	40
28	Strong-line parameter for CO at 7000°K	41
29	Strong-line parameter for CO at 10000°K	42
30	Strong-line parameter for CO at 12000°K	43
31	Strong-line parameter for CO at 18000°K	44
32	Weak-line parameter for OH	46
33	Inverse line spacing for OH	47
34	Weak-line parameter for OH at 200°K	48
35	Weak-line parameter for OH at 300°K	49
36	Weak-line parameter for OH at 500°K	50
37	Weak-line parameter for OH at 750°K	51
38	Weak-line parameter for OH at 1000°K	52
39	Weak-line parameter for OH at 1500°K	53
40	Weak-line parameter for OH at 2000°K	54
41	Weak-line parameter for OH at 3000°K	55
42	Weak-line parameter for OH at 5000°K	56
43	Weak-line parameter for OH at 7000°K	57
44	Weak-line parameter for OH at 10000°K	58
45	Strong-line parameter for OH at 200°K	59
46	Strong-line parameter for OH at 300°K	60
47	Strong-line parameter for OH at 500°K	61
48	Strong-line parameter for OH at 750°K	62
49	Strong-line parameter for OH at 1000°K	63
50	Strong-line parameter for OH at 1500°K	64
51	Strong-line parameter for OH at 2000°K	65
52	Strong-line parameter for OH at 3000°K	66

LIST OF ILLUSTRATIONS (Continued)

Figure		Page
53	Strong-line parameter for OH at 5000°K	67
54	Strong-line parameter for OH at 7000°K	68
55	Strong-line parameter for OH at 10000°K	69
56	Weak-line parameter for N_2 at 500°K	71
57	Weak-line parameter for N_2 at 750°K	72
58	Weak-line parameter for N_2 at 1000°K	73
59	Weak-line parameter for N_2 at 1500°K	74
60	Weak-line parameter for N_2 at 2000°K	75
61	Weak-line parameter for N_2 at 3000°K	76
62	Weak-line parameter for N_2 at 5000°K	77
63	Weak-line parameter for N_2 at 7000°K	78
64	Weak-line parameter for N_2 at 10000°K	79
65	Weak-line parameter for N_2 at 12000°K	80
66	Weak-line parameter for N_2 at 18000°K	81
67	Weak-line parameter for N_2^+ at 5000°K	82
68	Weak-line parameter for N_2^+ at 7000°K	83
69	Weak-line parameter for N_2^+ at 10000°K	84
70	Weak-line parameter for N_2^+ at 12000°K	85
71	Weak-line parameter for N_2^+ at 18000°K	86
72	Weak-line parameter for NO	89
73	Inverse line spacing for NO	90
74	Weak-line parameter for NO at 200°K	91
75	Weak-line parameter for NO at 300°K	92
76	Weak-line parameter for NO at 500°K	93
77	Weak-line parameter for NO at 750°K	94
78	Weak-line parameter for NO at 1000°K	95
79	Weak-line parameter for NO at 1500°K	96

LIST OF ILLUSTRATIONS (Continued)

Figure		Page
80	Weak-line parameter for NO at 2000°K	97
81	Weak-line parameter for NO at 3000°K	98
82	Weak-line parameter for NO at 5000°K	99
83	Weak-line parameter for NO at 7000°K	100
84	Weak-line parameter for NO at 10000°K	101
85	Weak-line parameter for NO at 12000°K	102
86	Weak-line parameter for NO at 18000°K	103
87	Strong-line parameter for NO at 200°K	104
88	Strong-line parameter for NO at 300°K	105
89	Strong-line parameter for NO at 500°K	106
90	Strong-line parameter for NO at 750°K	107
91	Strong-line parameter for NO at 1000°K	108
92	Strong-line parameter for NO at 1500°K	109
93	Strong-line parameter for NO at 2000°K	110
94	Strong-line parameter for NO at 3000°K	111
95	Strong-line parameter for NO at 5000°K	112
96	Strong-line parameter for NO at 7000°K	113
97	Strong-line parameter for NO at 10000°K	114
98	Strong-line parameter for NO at 12000°K	115
99	Strong-line parameter for NO at 18000°K	116
100	Weak-line parameter for NO^+	118
101	Inverse line spacing for NO^+	119
102	Weak-line parameter for NO^+ at 200°K	120
103	Weak-line parameter for NO^+ at 300°K	121
104	Weak-line parameter for NO^+ at 500°K	122
105	Weak-line parameter for NO^+ at 750°K	123

LIST OF ILLUSTRATIONS (Continued)

Figure		Page
106	Weak-line parameter for NO^+ at 1000°K	124
107	Weak-line parameter for NO^+ at 1500°K	125
108	Weak-line parameter for NO^+ at 2000°K	126
109	Weak-line parameter for NO^+ at 3000°K	127
110	Weak-line parameter for NO^+ at 5000°K	128
111	Weak-line parameter for NO^+ at 7000°K	129
112	Weak-line parameter for NO^+ at 10000°K	130
113	Weak-line parameter for NO^+ at 12000°K	131
114	Weak-line parameter for NO^+ at 18000°K	132
115	Strong-line parameter for NO^+ at 200°K	133
116	Strong-line parameter for NO^+ at 300°K	134
117	Strong-line parameter for NO^+ at 500°K	135
118	Strong-line parameter for NO^+ at 750°K	136
119	Strong-line parameter for NO^+ at 1000°K	137
120	Strong-line parameter for NO^+ at 1500°K	138
121	Strong-line parameter for NO^+ at 2000°K	139
122	Strong-line parameter for NO^+ at 3000°K	140
123	Strong-line parameter for NO^+ at 5000°K	141
124	Strong-line parameter for NO^+ at 7000°K	142
125	Strong-line parameter for NO^+ at 10000°K	143
126	Strong-line parameter for NO^+ at 12000°K	144
127	Strong-line parameter for NO^+ at 18000°K	145
128	Weak-line parameter for O_2 at 200°K	147
129	Weak-line parameter for O_2 at 300°K	148
130	Weak-line parameter for O_2 at 500°K	149
131	Weak-line parameter for O_2 at 750°K	150

LIST OF ILLUSTRATIONS (Continued)

Figure		Page
132	Weak-line parameter for O_2 at 1000°K	151
133	Weak-line parameter for O_2 at 1500°K	152
134	Weak-line parameter for O_2 at 2000°K	153
135	Weak-line parameter for O_2 at 3000°K	154
136	Weak-line parameter for O_2 at 5000°K	155
137	Weak-line parameter for O_2 at 7000°K	156
138	Weak-line parameter for O_2 at 10000°K	157
139	Weak-line parameter for O_2 at 12000°K	158
140	Weak-line parameter for O_2 at 18000°K	159
141	Weak-line parameter for NH_3	161
142	Inverse line spacing for NH_3	162
143	Weak-line parameter for NH_3 at 200°K	163
144	Weak-line parameter for NH_3 at 300°K	164
145	Weak-line parameter for NH_3 at 500°K	165
146	Weak-line parameter for NH_3 at 750°K	166
147	Weak-line parameter for NH_3 at 1000°K	167
148	Weak-line parameter for CO_2	169
149	Inverse line spacing for CO_2	170
150	Weak-line parameter for CO_2 at 200°K	171
151	Weak-line parameter for CO_2 at 300°K	172
152	Weak-line parameter for CO_2 at 500°K	173
153	Weak-line parameter for CO_2 at 750°K	174
154	Weak-line parameter for CO_2 at 1000°K	175
155	Weak-line parameter for CO_2 at 1500°K	176
156	Weak-line parameter for CO_2 at 2000°K	177
157	Weak-line parameter for CO_2 at 3000°K	178

LIST OF ILLUSTRATIONS (Continued)

Figure		Page
158	Weak-line parameter for CO_2 at 5000°K	179
159	Weak-line parameter for CO_2 at 7000°K	180
160	Weak-line parameter for CO_2 at 10000°K	181
161	Weak-line parameter for CO_2 at 12000°K	182
162	Weak-line parameter for CO_2 at 18000°K	183
163	Strong-line parameter for CO_2 at 200°K	184
164	Strong-line parameter for CO_2 at 300°K	185
165	Strong-line parameter for CO_2 at 500°K	186
166	Strong-line parameter for CO_2 at 750°K	187
167	Strong-line parameter for CO_2 at 1000°K	188
168	Strong-line parameter for CO_2 at 1500°K	189
169	Strong-line parameter for CO_2 at 2000°K	190
170	Strong-line parameter for CO_2 at 3000°K	191
171	Strong-line parameter for CO_2 at 5000°K	192
172	Strong-line parameter for CO_2 at 7000°K	193
173	Strong-line parameter for CO_2 at 10000°K	194
174	Strong-line parameter for CO_2 at 12000°K	195
175	Strong-line parameter for CO_2 at 18000°K	196
176	Weak-line parameter for N_2O	198
177	Inverse line spacing for N_2O	199
178	Weak-line parameter for N_2O at 200°K	200
179	Weak-line parameter for N_2O at 300°K	201
180	Weak-line parameter for N_2O at 500°K	202
181	Weak-line parameter for N_2O at 750°K	203
182	Weak-line parameter for N_2O at 1000°K	204
183	Weak-line parameter for N_2O at 1500°K	205

LIST OF ILLUSTRATIONS (Continued)

Figure		Page
184	Weak-line parameter for N_2O at 2000°K	206
185	Weak-line parameter for N_2O at 3000°K	207
186	Weak-line parameter for N_2O at 5000°K	208
187	Weak-line parameter for N_2O at 7000°K	209
188	Strong-line parameter for N_2O at 200°K	210
189	Strong-line parameter for N_2O at 300°K	211
190	Strong-line parameter for N_2O at 500°K	212
191	Strong-line parameter for N_2O at 750°K	213
192	Strong-line parameter for N_2O at 1000°K	214
193	Strong-line parameter for N_2O at 1500°K	215
194	Strong-line parameter for N_2O at 2000°K	216
195	Strong-line parameter for N_2O at 3000°K	217
196	Strong-line parameter for N_2O at 5000°K	218
197	Strong-line parameter for N_2O at 7000°K	219
198	Weak-line parameter for CH_4	221
199	Inverse line spacing for CH_4	222
200	Weak-line parameter for CH_4 at 200°K	223
201	Weak-line parameter for CH_4 at 300°K	224
202	Weak-line parameter for CH_4 at 500°K	225
203	Weak-line parameter for CH_4 at 750°K	226
204	Weak-line parameter for CH_4 at 1000°K	227
205	Strong-line parameter for CH_4 at 200°K	228
206	Strong-line parameter for CH_4 at 300°K	229
207	Strong-line parameter for CH_4 at 500°K	230
208	Strong-line parameter for CH_4 at 750°K	231
209	Strong-line parameter for CH_4 at 1000°K	232

LIST OF ILLUSTRATIONS (Continued)

Figure		Page
210	Weak-line parameter for HNO_3	234
211	Inverse line spacing for HNO_3	235
212	Weak-line parameter for HNO_3 at 300°K	236
213	Weak-line parameter for NO_2	238
214	Inverse line spacing for NO_2	239
215	Weak-line parameter for NO_2 at 200°K	240
216	Weak-line parameter for NO_2 at 300°K	241
217	Weak-line parameter for NO_2 at 500°K	242
218	Weak-line parameter for NO_2 at 750°K	243
219	Weak-line parameter for NO_2 at 1000°K	244
220	Weak-line parameter for NO_2 at 1500°K	245
221	Weak-line parameter for NO_2 at 2000°K	246
222	Weak-line parameter for NO_2 at 3000°K	247
223	Weak-line parameter for NO_2 at 5000°K	248
224	Weak-line parameter for NO_2 at 7000°K	249
225	Strong-line parameter for NO_2 at 200°K	250
226	Strong-line parameter for NO_2 at 300°K	251
227	Strong-line parameter for NO_2 at 500°K	252
228	Strong-line parameter for NO_2 at 750°K	253
229	Strong-line parameter for NO_2 at 1000°K	254
230	Strong-line parameter for NO_2 at 1500°K	255
231	Strong-line parameter for NO_2 at 2000°K	256
232	Strong-line parameter for NO_2 at 3000°K	257
233	Strong-line parameter for NO_2 at 5000°K	258
234	Strong-line parameter for NO_2 at 7000°K	259
235	Weak-line parameter for O_3	261

LIST OF ILLUSTRATIONS (Continued)

Figure		Page
236	Inverse line spacing for O_3	262
237	Weak-line parameter for O_3 at 200°K	263
238	Weak-line parameter for O_3 at 300°K	264
239	Weak-line parameter for O_3 at 500°K	265
240	Weak-line parameter for O_3 at 750°K	266
241	Weak-line parameter for O_3 at 1000°K	267
242	Weak-line parameter for O_3 at 1500°K	268
243	Weak-line parameter for O_3 at 2000°K	269
244	Weak-line parameter for O_3 at 3000°K	270
245	Weak-line parameter for O_3 at 5000°K	271
246	Weak-line parameter for O_3 at 7000°K	272
247	Strong-line parameter for O_3 at 200°K	273
248	Strong-line parameter for O_3 at 300°K	274
249	Strong-line parameter for O_3 at 500°K	275
250	Strong-line parameter for O_3 at 750°K	276
251	Strong-line parameter for O_3 at 1000°K	277
252	Strong-line parameter for O_3 at 1500°K	278
253	Strong-line parameter for O_3 at 2000°K	279
254	Strong line parameter for O_3 at 3000°K	280
255	Strong-line parameter for O_3 at 5000°K	281
256	Strong-line parameter for O_3 at 7000°K	282
257	Weak-line parameter for SO_2	284
258	Inverse line spacing for SO_2	285
259	Weak-line parameter for SO_2 at 200°K	286
260	Weak-line parameter for SO_2 at 300°K	287
261	Weak-line parameter for SO_2 at 500°K	288

LIST OF ILLUSTRATIONS (Continued)

Figure		Page
262	Weak-line parameter for SO_2 at 750°K	289
263	Weak-line parameter for SO_2 at 1000°K	290
264	Weak-line parameter for H_2O	292
265	Inverse line spacing for H_2O	293
266	Weak-line parameter for H_2O at 200°K	294
267	Weak-line parameter for H_2O at 300°K	295
268	Weak-line parameter for H_2O at 500°K	296
269	Weak-line parameter for H_2O at 750°K	297
270	Weak-line parameter for H_2O at 1000°K	298
271	Weak-line parameter for H_2O at 1500°K	299
272	Weak-line parameter for H_2O at 2000°K	300
273	Weak-line parameter for H_2O at 3000°K	301
274	Weak-line parameter for H_2O at 5000°K	302
275	Weak-line parameter for H_2O at 7000°K	303
276	Strong-line parameter for H_2O at 200°K	304
277	Strong-line parameter for H_2O at 300°K	305
278	Strong-line parameter for H_2O at 500°K	306
279	Strong-line parameter for H_2O at 750°K	307
280	Strong-line parameter for H_2O at 1000°K	308
281	Strong-line parameter for H_2O at 1500°K	309
282	Strong-line parameter for H_2O at 2000°K	310
283	Strong-line parameter for H_2O at 3000°K	311
284	Strong-line parameter for H_2O at 5000°K	312
285	Strong-line parameter for H_2O at 7000°K	313
286	Weak-line parameter for $A\ell O$	315
287	Inverse line spacing for $A\ell O$	316

LIST OF ILLUSTRATIONS (Continued)

Figure		Page
288	Weak-line parameter for AℓO at 200°K	317
289	Weak-line parameter for AℓO at 300°K	318
290	Weak-line parameter for AℓO at 500°K	319
291	Weak-line parameter for AℓO at 750°K	320
292	Weak-line parameter for AℓO at 1000°K	321
293	Weak-line parameter for AℓO at 1500°K	322
294	Weak-line parameter for AℓO at 2000°K	323
295	Weak-line parameter for AℓO at 3000°K	324
296	Weak-line parameter for AℓO at 5000°K	325
297	Weak-line parameter for AℓO at 7000°K	326
298	Weak-line parameter for AℓO at 10000°K	327
299	Weak-line parameter for AℓO at 12000°K	328
300	Weak-line parameter for AℓO at 18000°K	329
301	Strong-line parameter for AℓO at 200°K	330
302	Strong-line parameter for AℓO at 300°K	331
303	Strong-line parameter for AℓO at 500°K	332
304	Strong-line parameter for AℓO at 750°K	333
305	Strong-line parameter for AℓO at 1000°K	334
306	Strong-line parameter for AℓO at 1500°K	335
307	Strong-line parameter for AℓO at 2000°K	336
308	Strong-line parameter for AℓO at 3000°K	337
309	Strong-line parameter for AℓO at 5000°K	338
310	Strong-line parameter for AℓO at 7000°K	339
311	Strong-line parameter for AℓO at 10000°K	340
312	Strong-line parameter for AℓO at 12000°K	341
313	Strong-line parameter for AℓO at 18000°K	342

LIST OF ILLUSTRATIONS (Continued)

Figure		Page
314	Weak-line parameter for CuO	344
315	Inverse line spacing for CuO	345
316	Weak-line parameter for CuO at 200°K	346
317	Weak-line parameter for CuO at 300°K	347
318	Weak-line parameter for CuO at 500°K	348
319	Weak-line parameter for CuO at 750°K	349
320	Weak-line parameter for CuO at 1000°K	350
321	Weak-line parameter for CuO at 1500°K	351
322	Weak-line parameter for CuO at 2000°K	352
323	Weak-line parameter for CuO at 3000°K	353
324	Weak-line parameter for CuO at 5000°K	354
325	Weak-line parameter for CuO at 7000°K	355
326	Weak-line parameter for CuO at 10000°K	356
327	Weak-line parameter for CuO at 12000°K	357
328	Weak-line parameter for CuO at 18000°K	358
329	Strong-line parameter for CuO at 200°K	359
330	Strong-line parameter for CuO at 300°K	360
331	Strong-line parameter for CuO at 500°K	361
332	Strong-line parameter for CuO at 750°K	362
333	Strong-line parameter for CuO at 1000°K	363
334	Strong-line parameter for CuO at 1500°K	364
335	Strong-line parameter for CuO at 2000°K	365
336	Strong-line parameter for CuO at 3000°K	366
337	Strong-line parameter for CuO at 5000°K	367
338	Strong-line parameter for CuO at 7000°K	368
339	Strong-line parameter for CuO at 10000°K	369

LIST OF ILLUSTRATIONS (Continued)

Figure		Page
340	Strong-line parameter for CuO at 12000°K	370
341	Strong-line parameter for CuO at 18000°K	371
342	Weak-line parameter for FeO	373
343	Inverse line spacing for FeO	374
344	Weak-line parameter for FeO at 200°K	375
345	Weak-line parameter for FeO at 300°K	376
346	Weak-line parameter for FeO at 500°K	377
347	Weak-line parameter for FeO at 750°K	378
348	Weak-line parameter for FeO at 1000°K	379
349	Weak-line parameter for FeO at 1500°K	380
350	Weak-line parameter for FeO at 2000°K	381
351	Weak-line parameter for FeO at 3000°K	382
352	Weak-line parameter for FeO at 5000°K	383
353	Weak-line parameter for FeO at 7000°K	384
354	Weak-line parameter for FeO at 10000°K	385
355	Weak-line parameter for FeO at 12000°K	386
356	Weak-line parameter for FeO at 18000°K	387
357	Strong-line parameter for FeO at 200°K	388
358	Strong-line parameter for FeO at 300°K	389
359	Strong-line parameter for FeO at 500°K	390
360	Strong-line parameter for FeO at 750°K	391
361	Strong-line parameter for FeO at 1000°K	392
362	Strong-line parameter for FeO at 1500°K	393
363	Strong-line parameter for FeO at 2000°K	394
364	Strong-line parameter for FeO at 3000°K	395
365	Strong-line parameter for FeO at 5000°K	396

LIST OF ILLUSTRATIONS (Continued)

Figure		Page
366	Strong-line parameter for FeO at 7000°K	397
367	Strong-line parameter for FeO at 10000°K	398
368	Strong-line parameter for FeO at 12000°K	399
369	Strong-line parameter for FeO at 18000°K	400
370	Weak-line parameter for LiO	402
371	Inverse line spacing for LiO	403
372	Weak-line parameter for LiO at 200°K	404
373	Weak-line parameter for LiO at 300°K	405
374	Weak-line parameter for LiO at 500°K	406
375	Weak-line parameter for LiO at 750°K	407
376	Weak-line parameter for LiO at 1000°K	408
377	Weak-line parameter for LiO at 1500°K	409
378	Weak-line parameter for LiO at 2000°K	410
379	Weak-line parameter for LiO at 3000°K	411
380	Weak-line parameter for LiO at 5000°K	412
381	Weak-line parameter for LiO at 7000°K	413
382	Weak-line parameter for LiO at 10000°K	414
383	Weak-line parameter for LiO at 12000°K	415
384	Weak-line parameter for LiO at 18000°K	416
385	Strong-line parameter for LiO at 200°K	417
386	Strong-line parameter for LiO at 300°K	418
387	Strong-line parameter for LiO at 500°K	419
388	Strong-line parameter for LiO at 750°K	420
389	Strong-line parameter for LiO at 1000°K	421
390	Strong-line parameter for LiO at 1500°K	422
391	Strong-line parameter for LiO at 2000°K	423

LIST OF ILLUSTRATIONS (Continued)

Figure		Page
392	Strong-line parameter for LiO at 3000°K	424
393	Strong-line parameter for LiO at 5000°K	425
394	Strong-line parameter for LiO at 7000°K	426
395	Strong-line parameter for LiO at 10000°K	427
396	Strong-line parameter for LiO at 12000°K	428
397	Strong-line parameter for LiO at 18000°K	429
398	Weak-line parameter for MgO	431
399	Inverse line spacing for MgO	432
400	Weak-line parameter for MgO at 200°K	433
401	Weak-line parameter for MgO at 300°K	434
402	Weak-line parameter for MgO at 500°K	435
403	Weak-line parameter for MgO at 750°K	436
404	Weak-line parameter for MgO at 1000°K	437
405	Weak-line parameter for MgO at 1500°K	438
406	Weak-line parameter for MgO at 2000°K	439
407	Weak-line parameter for MgO at 3000°K	440
408	Weak-line parameter for MgO at 5000°K	441
409	Weak-line parameter for MgO at 7000°K	442
410	Weak-line parameter for MgO at 10000°K	443
411	Weak-line parameter for MgO at 12000°K	444
412	Weak-line parameter for MgO at 18000°K	445
413	Strong-line parameter for MgO at 200°K	446
414	Strong-line parameter for MgO at 300°K	447
415	Strong-line parameter for MgO at 500°K	448
416	Strong-line parameter for MgO at 750°K	449
417	Strong-line parameter for MgO at 1000°K	450

LIST OF ILLUSTRATIONS (Continued)

Figure		Page
418	Strong-line parameter for MgO at 1500°K	451
419	Strong-line parameter for MgO at 2000°K	452
420	Strong-line parameter for MgO at 3000°K	453
421	Strong-line parameter for MgO at 5000°K	454
422	Strong-line parameter for MgO at 7000°K	455
423	Strong-line parameter for MgO at 10000°K	456
424	Strong-line parameter for MgO at 12000°K	457
425	Strong-line parameter for MgO at 18000°K	458
426	Weak-line parameter for SiO	460
427	Inverse line spacing for SiO	461
428	Weak-line parameter for SiO at 200°K	462
429	Weak-line parameter for SiO at 300°K	463
430	Weak-line parameter for SiO at 500°K	464
431	Weak-line parameter for SiO at 750°K	465
432	Weak-line parameter for SiO at 1000°K	466
433	Weak-line parameter for SiO at 1500°K	467
434	Weak-line parameter for SiO at 2000°K	468
435	Weak-line parameter for SiO at 3000°K	469
436	Weak-line parameter for SiO at 5000°K	470
437	Weak-line parameter for SiO at 7000°K	471
438	Weak-line parameter for SiO at 10000°K	472
439	Weak-line parameter for SiO at 12000°K	473
440	Weak-line parameter for SiO at 18000°K	474
441	Strong-line parameter for SiO at 200°K	475
442	Strong-line parameter for SiO at 300°K	476
443	Strong-line parameter for SiO at 500°K	477

LIST OF ILLUSTRATIONS (Continued)

Figure		Page
444	Strong-line parameter for SiO at 750°K	478
445	Strong-line parameter for SiO at 1000°K	479
446	Strong-line parameter for SiO at 1500°K	480
447	Strong-line parameter for SiO at 2000°K	481
448	Strong-line parameter for SiO at 3000°K	482
449	Strong-line parameter for SiO at 5000°K	483
450	Strong-line parameter for SiO at 7000°K	484
451	Strong-line parameter for SiO at 10000°K	485
452	Strong-line parameter for SiO at 12000°K	486
453	Strong-line parameter for SiO at 18000°K	487
454	Weak-line parameter for TiO	489
455	Inverse line spacing for TiO	490
456	Weak-line parameter for TiO at 200°K	491
457	Weak-line parameter for TiO at 300°K	492
458	Weak-line parameter for TiO at 500°K	493
459	Weak-line parameter for TiO at 750°K	494
460	Weak-line parameter for TiO at 1000°K	495
461	Weak-line parameter for TiO at 1500°K	496
462	Weak-line parameter for TiO at 2000°K	497
463	Weak-line parameter for TiO at 3000°K	498
464	Weak-line parameter for TiO at 5000°K	499
465	Weak-line parameter for TiO at 7000°K	500
466	Weak-line parameter for TiO at 10000°K	501
467	Weak-line parameter for TiO at 12000°K	502
468	Weak-line parameter for TiO at 18000°K	503
469	Strong-line parameter for TiO at 200°K	504

LIST OF ILLUSTRATIONS (Continued)

Figure		Page
470	Strong-line parameter for TiO at 300°K	505
471	Strong-line parameter for TiO at 500°K	506
472	Strong-line parameter for TiO at 750°K	507
473	Strong-line parameter for TiO at 1000°K	508
474	Strong-line parameter for TiO at 1500°K	509
475	Strong-line parameter for TiO at 2000°K	510
476	Strong-line parameter for TiO at 3000°K	511
477	Strong-line parameter for TiO at 5000°K	512
478	Strong-line parameter for TiO at 7000°K	513
479	Strong-line parameter for TiO at 10000°K	514
480	Strong-line parameter for TiO at 12000°K	515
481	Strong-line parameter for TiO at 18000°K	516
482	Weak-line parameter for UO	518
483	Inverse line spacing for UO	519
484	Weak-line parameter for UO at 200°K	520
485	Weak-line parameter for UO at 300°K	521
486	Weak-line parameter for UO at 500°K	522
487	Weak-line parameter for UO at 750°K	523
488	Weak-line parameter for UO at 1000°K	524
489	Weak-line parameter for UO at 1500°K	525
490	Weak-line parameter for UO at 2000°K	526
491	Weak-line parameter for UO at 3000°K	527
492	Weak-line parameter for UO at 5000°K	528
493	Weak-line parameter for UO at 7000°K	529
494	Weak-line parameter for UO at 10000°K	530
495	Weak-line parameter for UO at 12000°K	531

LIST OF ILLUSTRATIONS (Continued)

Figure		Page
496	Weak-line parameter for UO at 18000°K	532
497	Strong-line parameter for UO at 200°K	533
498	Strong-line parameter for UO at 300°K	534
499	Strong-line parameter for UO at 500°K	535
500	Strong-line parameter for UO at 750°K	536
501	Strong-line parameter for UO at 1000°K	537
502	Strong-line parameter for UO at 1500°K	538
503	Strong-line parameter for UO at 2000°K	539
504	Strong-line parameter for UO at 3000°K	540
505	Strong-line parameter for UO at 5000°K	541
506	Strong-line parameter for UO at 7000°K	542
507	Strong-line parameter for UO at 10000°K	543
508	Strong-line parameter for UO at 12000°K	544
509	Strong-line parameter for UO at 18000°K	545
510	Weak-line parameter for UO^+	547
511	Inverse line spacing for UO^+	548
512	Weak-line parameter for UO^+ at 200°K	549
513	Weak-line parameter for UO^+ at 300°K	550
514	Weak-line parameter for UO^+ at 500°K	551
515	Weak-line parameter for UO^+ at 750°K	552
516	Weak-line parameter for UO^+ at 1000°K	553
517	Weak-line parameter for UO^+ at 1500°K	554
518	Weak-line parameter for UO^+ at 2000°K	555
519	Weak-line parameter for UO^+ at 3000°K	556
520	Weak-line parameter for UO^+ at 5000°K	557
521	Weak-line parameter for UO^+ at 7000°K	558

LIST OF ILLUSTRATIONS (Continued)

Figure		Page
522	Weak-line parameter for UO^+ at 10000°K	559
523	Weak-line parameter for UO^+ at 12000°K	560
524	Weak-line parameter for UO^+ at 18000°K	561
525	Strong-line parameter for UO^+ at 200°K	562
526	Strong-line parameter for UO^+ at 300°K	563
527	Strong-line parameter for UO^+ at 500°K	564
528	Strong-line parameter for UO^+ at 750°K	565
529	Strong-line parameter for UO^+ at 1000°K	566
530	Strong-line parameter for UO^+ at 1500°K	567
531	Strong-line parameter for UO^+ at 2000°K	568
532	Strong-line parameter for UO^+ at 3000°K	569
533	Strong-line parameter for UO^+ at 5000°K	570
534	Strong-line parameter for UO^+ at 7000°K	571
535	Strong-line parameter for UO^+ at 10000°K	572
536	Strong-line parameter for UO^+ at 12000°K	573
537	Strong-line parameter for UO^+ at 18000°K	574

LIST OF TABLES

Table		Page
1	Spectroscopic Data For CO.	16
2	Spectroscopic Data For OH.	45
3	Spectroscopic Data For NO.	87
4	Spectroscopic Data For NO^+.	117
5	Spectroscopic Data For NO_2	237
6	Spectroscopic Data For O_3	260
7	Spectroscopic Data For AℓO.	314
8	Spectroscopic Data For CuO.	343
9	Spectroscopic Data For FeO.	372
10	Spectroscopic Data For LiO.	401
11	Spectroscopic Data For MgO.	430
12	Spectroscopic Data For SiO.	459
13	Spectroscopic Data For TiO.	488
14	Spectroscopic Data For UO.	517
15	Spectroscopic Data For UO^+.	546

SECTION 1
INTRODUCTION

1.1 DESCRIPTION OF THE DATA.

This manual describes the NORSE LTE (Local Thermodynamic Equilibrium) database including, when possible, the input assumptions used to generate the data. The NORSE LTE data base consists of values for the weak-line parameter (S/d - SOD) and the inverse line spacing (1/d- DEI) arranged by wavenumber, temperature and molecule. This information is used by NORSE for thermal emission calculations.

The NORSE database contains emission information for twenty-six molecules and thirteen temperatures. The spectral range of this data is from 10 cm^{-1} (far infrared) to 100,000 cm^{-1} (visible).

The spectral data presented later in this report represents the NORSE LTE data base 87244.

1.2 DATA SOURCES.

The data sources for this database include: Band model programs, Air Force Geophysical Laboratory Line Atlas, Air Force Weapons Laboratory opacity database and other sources. Some of the information within this database originated over twenty years ago. During that time period the source of the data and the assumptions used to generate the information have been lost. When possible the source of the LTE data and the input assumptions will be presented in sections describing individual molecules.

1.3 LTE DATA BASE.

The LTE data base is stored as an ASCII file at the Los Alamos National Laboratory Central Computing Facility. The data base consists of over 260,000 eighty character lines of information. Further . ıformation about the structure and contents of the data base is contained in the NC RSE Manual 4-10 Model Data Files[1].

1.4 FUTURE EFFORTS.

Enhancement and verification of the LTE data base is a continuing effort. The Local Thermal Equilibrium (LTE) data base is upcated and reviewed on a regular basis. Work is underway to bring this data in line with current spectroscopic data.

SECTION 2

BACKGROUND[2]

2.1 TRANSMISSION BAND MODELS.

The presentation in this section has been adapted from a discussion given in reference 2. Given a spectral line atlas it is possible to calculate photon transport along an optical path with varying temperature and pressure. In practice, a line-by-line calculation is impractical because of the large number of lines which need to be considered. To simplify the numerics, various band models have been developed.

Band models differ in their method of treating rotation lines; in fact, a rotational line-by-line reconstruction (or prediction) is often called the "line-by-line model" recognizing that even in the most painstaking predictions, there are assumptions, improper methods of including coupling, etc., which prevent the accurate representation of the actual situation.

A brief review of the different types of band models follows. As an introduction, it can be shown from radiative transfer considerations that the energy, E_a, absorbed through a path length s, in a solid angle Ω and reaching an area A is given by

$$\frac{d^2E_a}{dAd\Omega} = \int_0^\infty I_\nu^o \left[1 - \exp\left(-a_\nu s\right)\right] d\nu \qquad (1)$$

whereas the energy emitted, E_e, to A by a gas is given by

$$\frac{d^2E_e}{dAd\Omega} = \int_0^\infty I_\nu^b \left[1 - \exp(-a_\nu s)\right] d\nu \qquad (2)$$

where I_ν^o is the incident intensity at wavenumber ν, I_ν^b is the Blackbody emission intensity, and a_ν, is the line absorption coefficient. It will be assumed that a_ν is zero, except in the small wavenumber interval near to a_ν. For small path lengths, the integrals in Eqns. (1) and (2) will be large only within this narrow interval, so that the integration need only be performed over this interval. Within this interval, I_ν^o and I_ν^b are assumed to be constant, at their value of ν. Then the two equations become

$$\frac{d^2E_a}{dAd\Omega} = I_{\nu_{ij}}^o \int_0^\infty [1-\exp(-a_{\nu_{ij}}s)]\, d\nu \tag{3}$$

and

$$\frac{d^2E_e}{dAd\Omega} = I_{\nu_{ij}}^b \int_0^\infty [1 - \exp(-a_{\nu_{ij}}s)]\, d\nu \tag{4}$$

where *ij* indicates the two levels involved in the line transition. The absorbed energy as well as the emitted energy for the line in question are seen to be dependent on the same integral; this integral is called "effective line width" $\bar{A}_{ij}$, i.e.,

$$\bar{A}_{ij} = \int_0^\infty [1 - \exp(a_{\nu_{ij}}s)]\, d\nu \tag{5}$$

and has the units of ν (cm^{-1}). $\bar{A}_{ij}$ can be interpreted as follows. If $a_{\nu_{ij}}$ is considered infinitely large, and there is no absorption outside this line, $\bar{A}_{ij}$ can be considered as the width of a black line centered at ν_{ij} that produces the identical emission as the actual line.

$\bar{A}_{ij}$ can be evaluated for two limiting cases. If the product ($a_{\nu_{ij}}$ s) is small (i.e., « 1) an expansion of the exponent in Eqn. (5) gives:

$$1 - \exp(-a_{\nu_{ij}} s) = a_{\nu_{ij}} s - \frac{(a_{\nu_{ij}} s)^2}{2!} + \ldots \tag{6}$$

Keeping only the first term, Eqn. (5) becomes

$$\bar{A}_{ij} = s \int_0^\infty a_{\nu_{ij}} \, d\nu \tag{7}$$

where the integral represents the "integrated absorption coefficient." The effective line width is therefore linear with path length, s, regardless of the line profile; a line with this linear behavior is called a "weak-line." [*"Line profiles" arise because the upper and lower energy levels, which determine the energy of a spectral "line", are in reality a distribution of levels; transitions from one distribution (say,the upper) to another distribution (lower) gives rise to a spectral line "profile". Depending on the statistical nature of these distributions, profiles are called Lorentzian, Gaussian, or Voigt (a convolution of Lorentzian and Gaussian). For our purposes, the major cause of Gaussian profiles is Doppler broadening, the term we will use in this work. The importance of line profiles cannot be overemphasized*].

The other limit concerns a large optical path (optically thick). In this limit, $a_{\nu_{ij}} s \gg 1$, the absorption coefficient is written

$$a_{\nu_{ij}} = b_{ij} \int_0^\infty a_{\nu_{ij}} \, d\nu \tag{8}$$

where b_{ij} is the line profile. Using the Lorentz profile for b_{ij}, substituting Eqn. (8) into Eqn. (7) and performing integration and rearrangements, it is found that

$$\bar{A}_{ij} = (2s\gamma_L \int a_{\nu_{ij}} \, d\nu)^{1/2}, \tag{9}$$

where γ_L is the Lorentzian width at half-maximum. Thus, the "strong-line" approximation leads to an absorption varying with the square root of the path length (s) in contrast to the "weak-line" approximation where it varies linearly with s.

In a similar manner, an "effective band width", $\bar{A}_\ell$ can be defined as

$$\bar{A}_\ell = \int_{band} [1 - \exp(-a_{\nu_{ij}} s)]\, d\nu \qquad (10)$$

The boundaries of the band can be defined as the wavenumber interval outside of which there is only a predetermined fractional contribution to $\bar{A}_\ell$. As the path length increases, the width of the wavenumber interval increases slowly due to absorption taking place in the wings of the line profiles (the profiles are bell shaped). Note that $\bar{A}_\ell$ for the band is the sum of the $\bar{A}_{ij}$ for all the lines that constitute the band, only if all the $\bar{A}_{ij}$ do not overlap. Since the lines overlap, each line absorbs less energy than if there were no overlap.

In the derivation of appropriate band models, simplified forms of the absorption coefficient a_ν must be devised. The two more common types of band models are the Regular and Random Band Models.

The most familiar of the Regular techniques is due to Elsasser. In this model, the individual lines all have the same profile, the same height and the same spacing. Elsasser's approach uses the Lorentz line profile (the Doppler and Voigt profiles may also be used). The absorption coefficient at a specified wavenumber is calculated by adding all the contributions from neighboring lines. If the specified position is ν_o, the distance of the centers of the other lines from the specified wavenumber ν_o is $|\nu_o - 0|$, $|\nu_o - d|$, $|\nu_o - 2d|$, ... Summing the contributions results in:

$$a(\nu_o) = \frac{\int a_L d\nu}{2\pi} \sum_{-\infty}^{\infty} \frac{\gamma_L}{\frac{\gamma_L^2}{4} + (\nu_o - nd)^2} \qquad (11)$$

where $a(\nu_o)$ is the absorption coefficient at the specified wavenumber (ν_o), $\int a_L\, d\nu$ is the integrated absorption coefficient for each line, n is the number of lines contributing, d is the spacing between adjacent peaks and γ_L is the Lorentzian width.

This function is substituted in Eqn. (7). By using the "weak-line" and "strong-line" limits, analytic solutions are practical, otherwise numerical methods are necessary.

The Random (or Statistical) band model uses a statistical array of individual lines. In this case, there can be a random spacing of identical or dissimilar lines. In order to apply this model, probability distributions of line strengths and positions must be assumed. Once the nature of a line, and its position, are chosen, the effective band width $\bar{A}_\ell$ is calculated from Eqn. (10). Note that $\bar{A}_\ell$ depends on the line spacing, the width of the line profile, and the integrated absorption. Since these parameters rely on temperature and density, it is necessary to know how they change with temperature and pressure.

2.2 BAND MODEL PARAMETERS.

An important source of radiation from low-altitude fireballs is thermal emission due to equilibrium processes in the hot gas. The magnitude of the radiation is determined by the temperature and the optical absorption properties of the fireball. For infrared wavelengths, the vibrational-rotational bands of

molecular species are major contributors to thermal emission. Particularly important emitters in a fireball are CO_2, CO, NO and NO^+. Other potential infrared emitters include O_3, NO_2, N_2O, H_2O, OH and metal oxides (MeO).

A procedure has been developed for the NORSE[3] code that uses band absorption models to calculate fireball thermal emission. These models require the fireball sight-path length, the average pressure over the path, an isothermal temperature of the emitting gas, and the population of species in the fireball. The spectral radiance of the path length is then calculated as a function of wavenumber. The models described in Section 2.1 include:

- o Elsasser model. This model is appropriate for a band of lines with uniform intensity, width and spacing.
- o Random Elsasser model. This model assumes n randomly superimposed Elsasser bands. The limit n corresponds to the statistical model, while n = 1 corresponds to the Elsasser model.
- o Statistical model. This model assumes lines with arbitrary strength and width distributions, and random spectral frequency.

For molecules of the asymmetrical top (three moments of inertia, all unequal) form, such as H_2O, the rotational structure is quite irregular, and the statistical model is clearly preferred. Symmetric top (rotor) molecules, such as diatomic or linear polyatomic species, have more regular rotational structures. Such a structure is best described by the Elsasser or random Elsasser models for lower temperatures. At elevated temperatures, many such regular bands will overlap. If the number of bands is $n > 10$, there is little difference between the predictions of the random Elsasser and statistical models. Since the statistical model offers the advantage of rapid calculation, and requires a minimum number of parameters to be determined from often scanty data, it is used in the fireball thermal emission model.

In many situations, lines show both Doppler and Lorentz profiles characterized by broadening widths denoted by γ_D and γ_L, respectively. If $\gamma_L \gg \gamma_D$, the absorption predicted by a pure Lorentz line shape is an excellent approximation. The corresponding approximation does not hold for $\gamma_D \gg \gamma_L$, however. In this case, the center of the line will reflect the Doppler profile, while the wings will reflect the Lorentz shape. For small path length, the absorption is well approximated by a pure Doppler line shape. For larger path lengths absorption by the line wings will dominate, so the Lorentz profile is needed.

Stephens[4] discusses the details of the transmission model. Of interest herein is the fact that in either limit of Doppler or Lorentz shapes, the value of transmission over an optical path of varying temperature, composition, and pressure (affecting the Lorentz profile) can be reduced to functions of γ_L, γ_D, pressure, and so-called weak-line parameters, average line strength, SOD, and effective inverse line spacing, DEI, for individual species. For temperature T and wavenumber ν

$$\mathrm{SOD}(T,\nu) = \sum_i S_i/\Delta\nu \tag{12}$$

$$\mathrm{DEI}(T,\nu) = \left[\sum_i (S_i)^{1/2}/\Delta\nu\right]^2 / \mathrm{SOD}(T,\nu) \tag{13}$$

where $\Delta\nu$ refers to a small wavenumber interval within which there are a limited number of individual quantum mechanical lines of strength S_i.

Thus, calculations of radiation transport are reduced to calculations involving the weak-line parameters SOD and DEI which approximate molecular absorption processes as a function of energy and temperature.

SECTION 3
SAMPLE CALCULATIONS

A sample transmissivity calculation for CO_2 gas in LTE is presented. The data used for this calculation are a subset of the CO_2 data presented in section 5.2 of this report. For simplicity, only data for the 626 (the 626 label denotes the ^{16}O-^{12}C-^{16}O molecule) isotopic species of carbon dioxide will be used. The temperature, path length, and mole fraction for the absorbing CO_2 gas are chosen to match the experimental conditions as reported.[5] This exercise will show how the data contained in this volume may be used to predict transmissivity and emissivities using the statistical band model approach.

The transmissivity predicted by various forms of the statistical band model is given by:

$$\tau = \exp[\, -F(x)(2\pi\gamma_L/d_\nu)\,] \tag{14}$$

where the curve of growth for the particular model is defined as, $-\ln(\tau)$. The variable x is defined here as:

$$x = (S/d)_\nu\, u(2\pi\gamma_L/d_\nu)^{-1} \tag{15}$$

where

γ_L is the full width at half maximum for a single line with Lorentzian shape

$$\gamma_L = \gamma_L^o(T_o/T)^\eta \tag{16}$$

d_ν is the mean line spacing

$(S/d)_\nu$ is the weak-line parameter

u is related to the number of absorber/emitters

$$u = LX\ P(T_o/T) \tag{17}$$

where X is the mole fraction of the absorbing/emitting species, P is the pressure, T is the temperature, L is the path length and η is an empirical parameter which is usually about 0.5.

Here it is assumed that all lines have the Lorentz shape and equal widths. The function F(x) is determined by the distribution of line strengths. For example, the probability distribution

$$P(S) \propto (1/S)\ \exp\ (-S/S_o) \tag{18}$$

results in

$$F(x) = (1/\pi)[(1+2\pi x)^{1/2} - 1\ ] \tag{19}$$

As $x \to 0$ the function F(x) becomes proportional to x and the curve of growth is said to be in the linear (weak-line) region . The square root (strong-line) region of the curve of growth obtains when $x \to \infty$. The curve of growth or F(x) is then proportional to $(x)^{1/2}$. Different choices of the distribution function P(S), will result in the same form for the curve of growth (or F(x)) for the asymptotic regions. However, for intermediate values of u (where $x \approx 1$) the various curve of growth functions will be different, with the exponential S^{-1} probability distribution having the largest change between the two asymptotic forms[6].

The statistical curve of growth which results from the distribution function given in Eqn. 18 is assumed and predictions are made of the transmissivity for a

given optical depth and temperature. In Figure 1 the weak-line parameter as a function of wavenumber is plotted for the 626 isotopic species of the CO_2 molecule for a temperature of T = 292 °K. The weak-line parameter is the absorption coefficient for the linear region of the curve of growth. Note the strong P and R branch lobes from the ν_3 fundamental transition located about the band center near 2350 cm^{-1}.

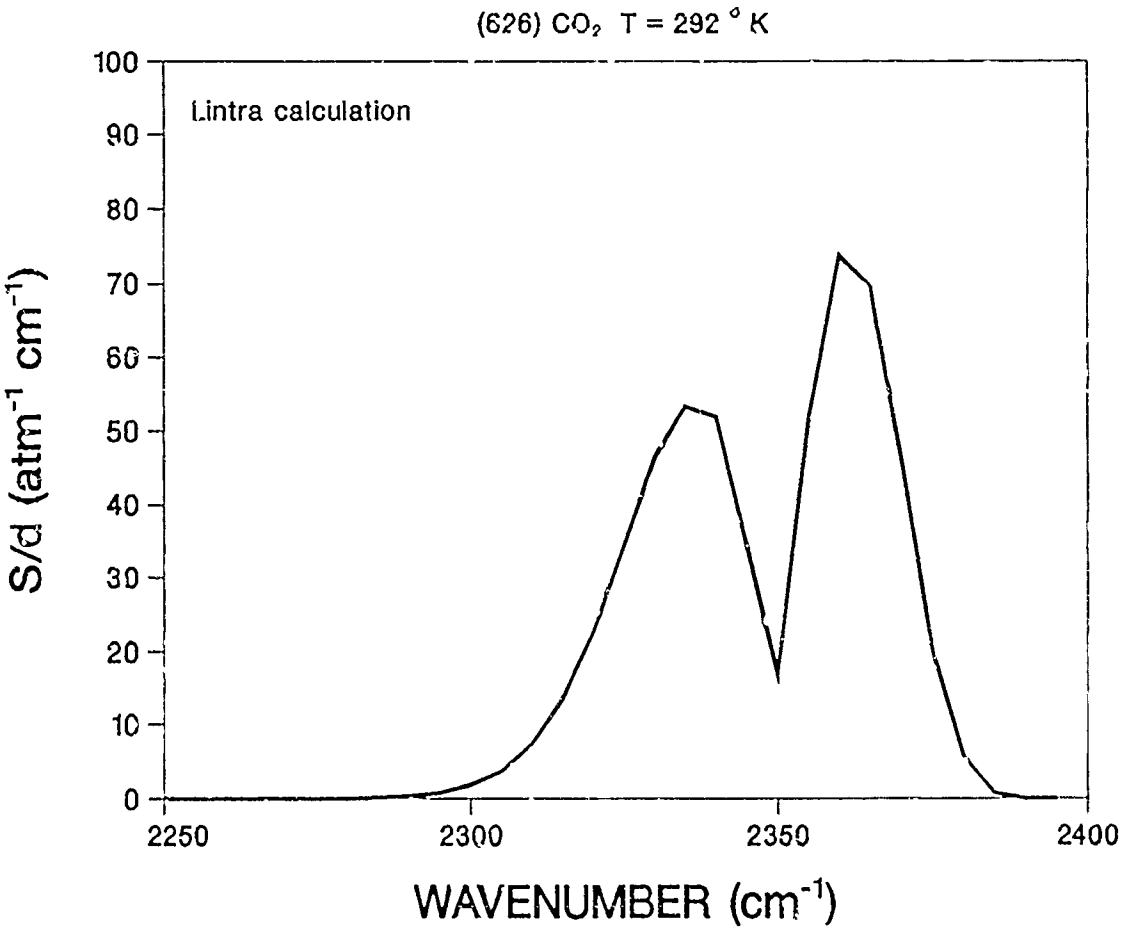

Figure 1. Weak-line parameter for 626 CO_2.

In Figure 2 the inverse line spacing parameter is displayed as a function of wavenumber for a temperature T = 292 °K. The two band model parameters listed in this report are the weak-line parameter $(S/d)_\nu$ and the strong-line parameter used by Malkmus[7]. The strong line parameter is related to the inverse line spacing parameter by

$$A = (S/d)_\nu(2\pi\gamma_L/d_\nu)^{-1} = x/u \tag{20}$$

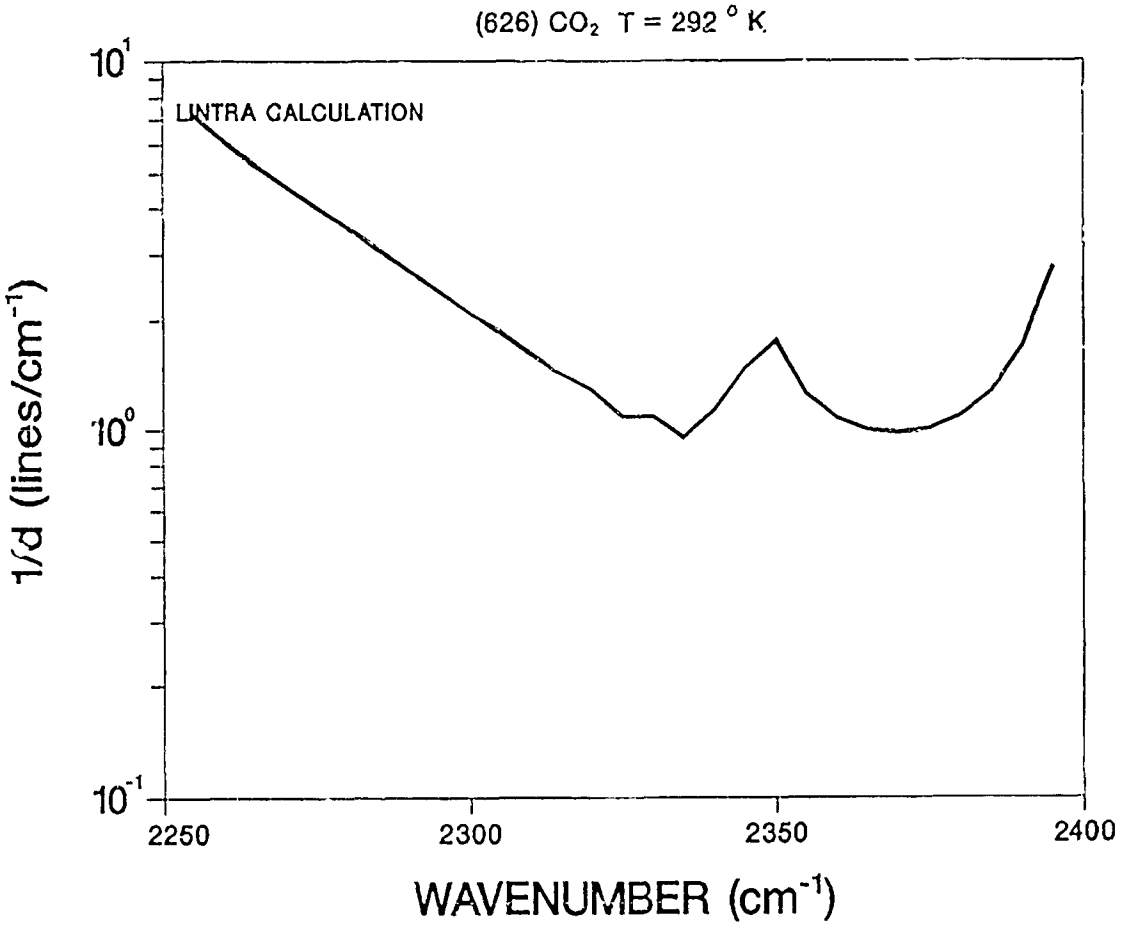

Figure 2. Inverse line spacing for 626 CO_2.

The weak-line and inverse line spacing parameters are input to the statistical model (Eqn. 14) with the optical conditions of a homogenous sample of gas at a temperature of T = 292 °K. The path length is 9.84 cm and the total pressure of the gas is 0.6128 atm, with the mole fraction for CO_2, χ = 0.0230. The statistical band model gives the transmissivity shown in Figure 3. This predicted transmissivity curve agrees with recent experimental data taken under the same conditions[5].

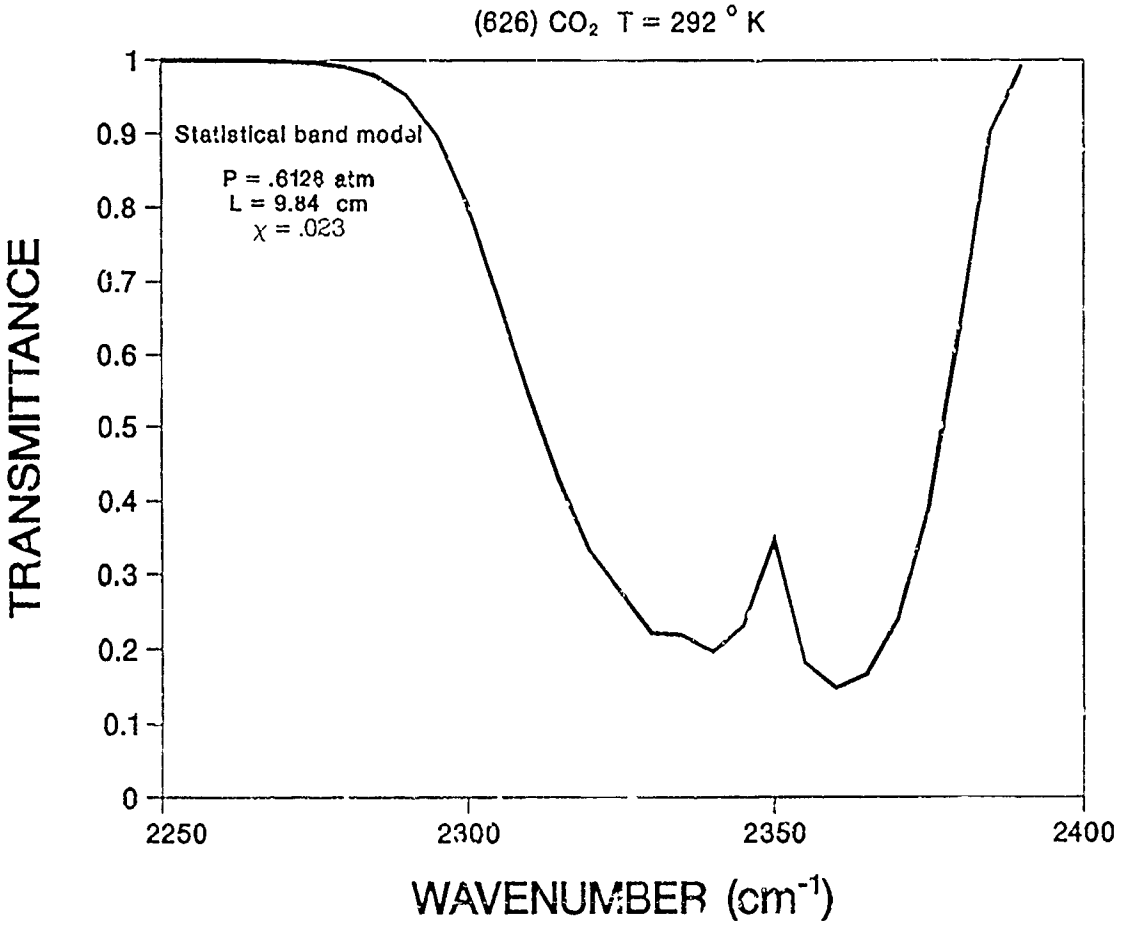

Figure 3. Transmittance for 626 CO_2.

SECTION 4
DIATOMIC MOLECULES

Local thermal equilibrium emission spectra for all diatomic molecules within the spectral range 10 - 10,000 cm^{-1} have been computed using the DiAtomic Thermal Emissions (DATE) code[8]. In the case of certain molecules, NO, N_2, N_2^+ and O_2, data available in the spectral range 5,000 - 100,000 cm^{-1} was obtained from the VisiDyne Corporation using a database developed by the Air Force Weapons Laboratory (AFWL) in the late sixties and used by the RADiation FLOw (RADFLO) code.

The band strengths given in this section are listed in cm^{-2} atm^{-1} at STP.

4.1 CARBON MONOXIDE (CO).

Data for the CO molecule in the spectral range 10 - 12,000 cm^{-1} has been computed using the DATE code.

Table 1. Spectroscopic data for CO.

$X\ ^1\Sigma^+$

$\omega_e = 2169.8233^*$	$\omega_e x_e = 13.2939^*$	$\omega_e y_e = 0.01158^*$
$\omega_e z_e = -1.119 \times 10^{-5\ b}$	$\omega_e a_e = 2.85 \times 10^{-6*}$	$\omega_e b_e = -4.94 \times 10^{-8*}$
$\alpha_e = 0.017513^*$	$B_e = 1.931271^*$	$\gamma_e = 2.96 \times 10^{-6*}$

$S_{10} = 260.0^\dagger$ $S_{20} = 2.06^\dagger$ $S_{30} = 0.0132^\dagger$

$\gamma_\ell(300°K) = 0.06^\ddagger$

Data Source:

*J.T. Yardley, J. Mol. Spectrosc. 35, 314 (1970).

†R.A. Toth, R.H. Hunt, and E.K. Plyler, J. Mol. Spectrosc. 32, 85 (1969).

‡Fit to the data of D.A. Draegert, and D. Williams, J. Opt. Soc. Am. 58 1399 (1968).

Figure 4. Weak-line parameter for CO.

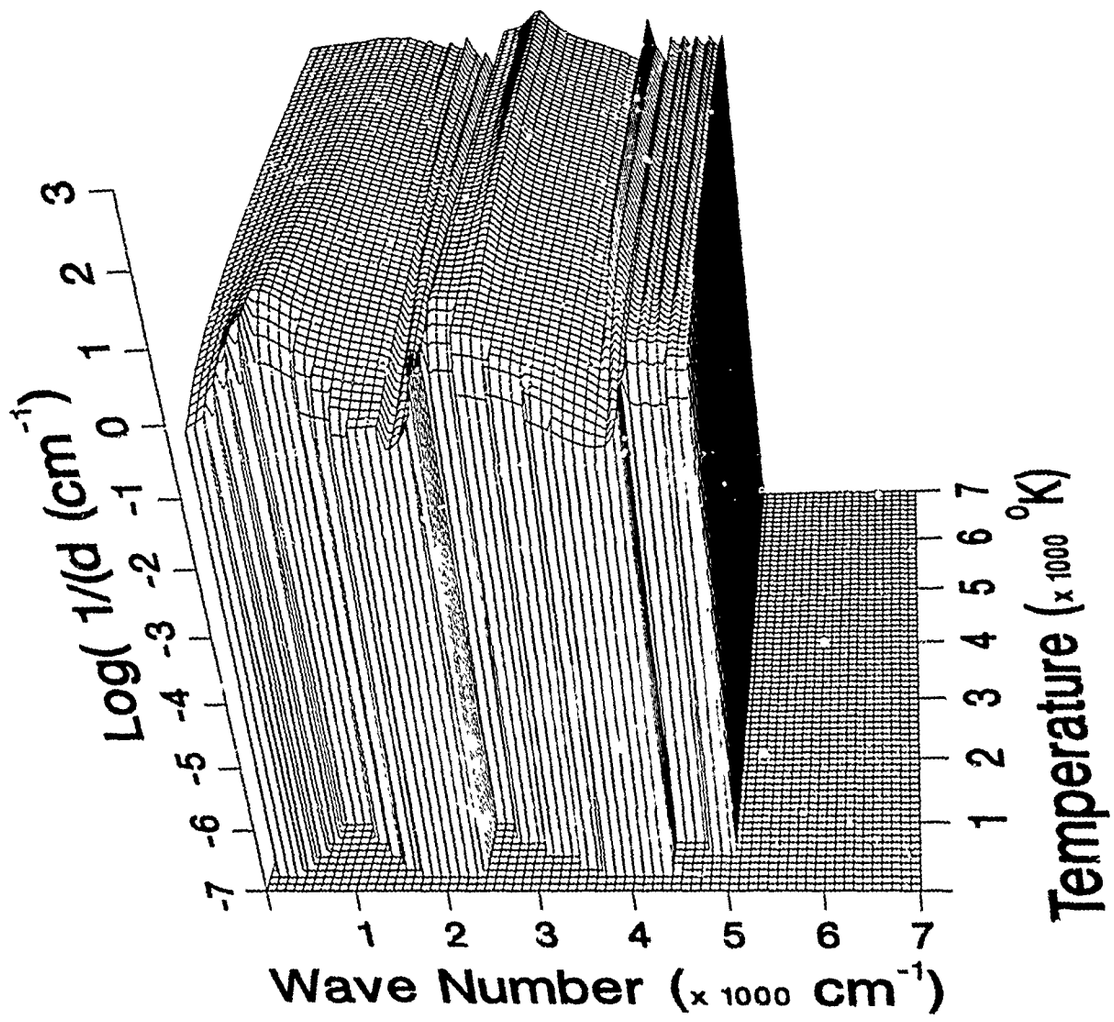

Figure 5. Inverse line spacing for CO.

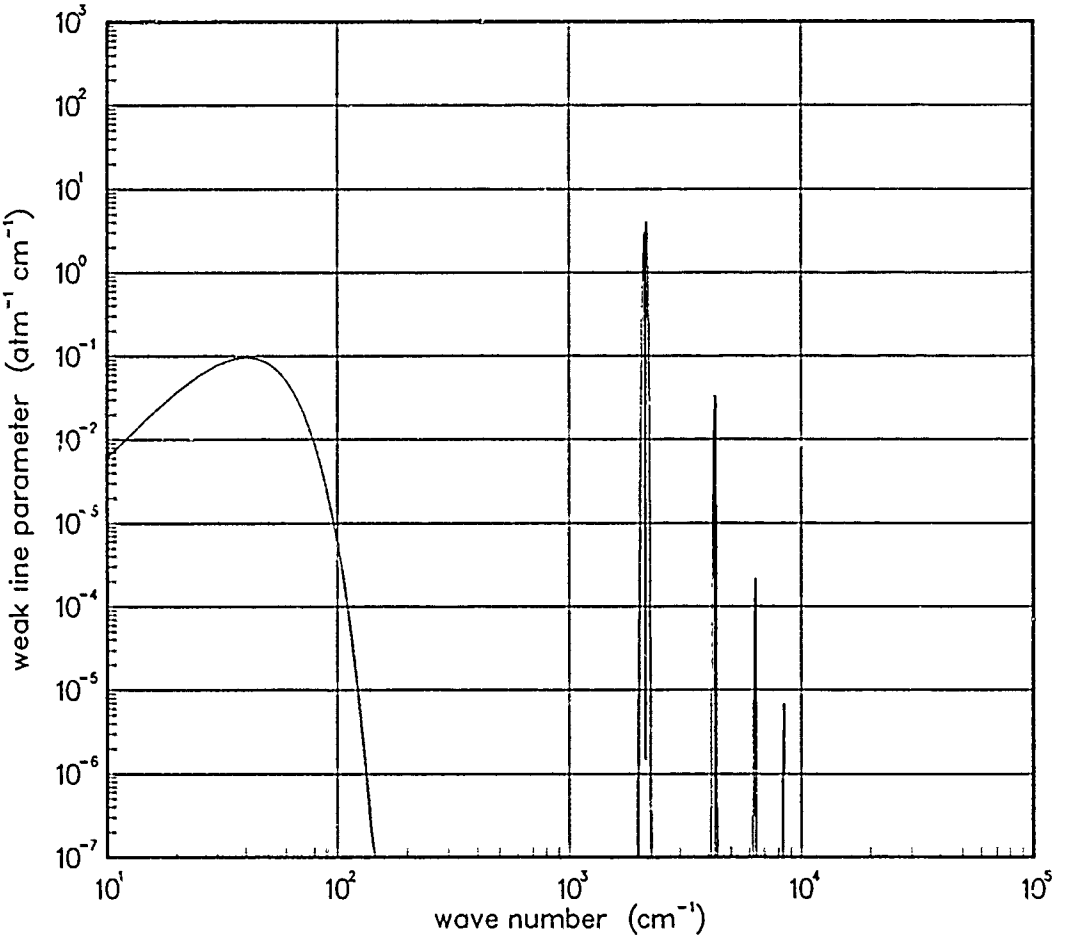

Figure 6. Weak-line parameter for CO at 200°K.

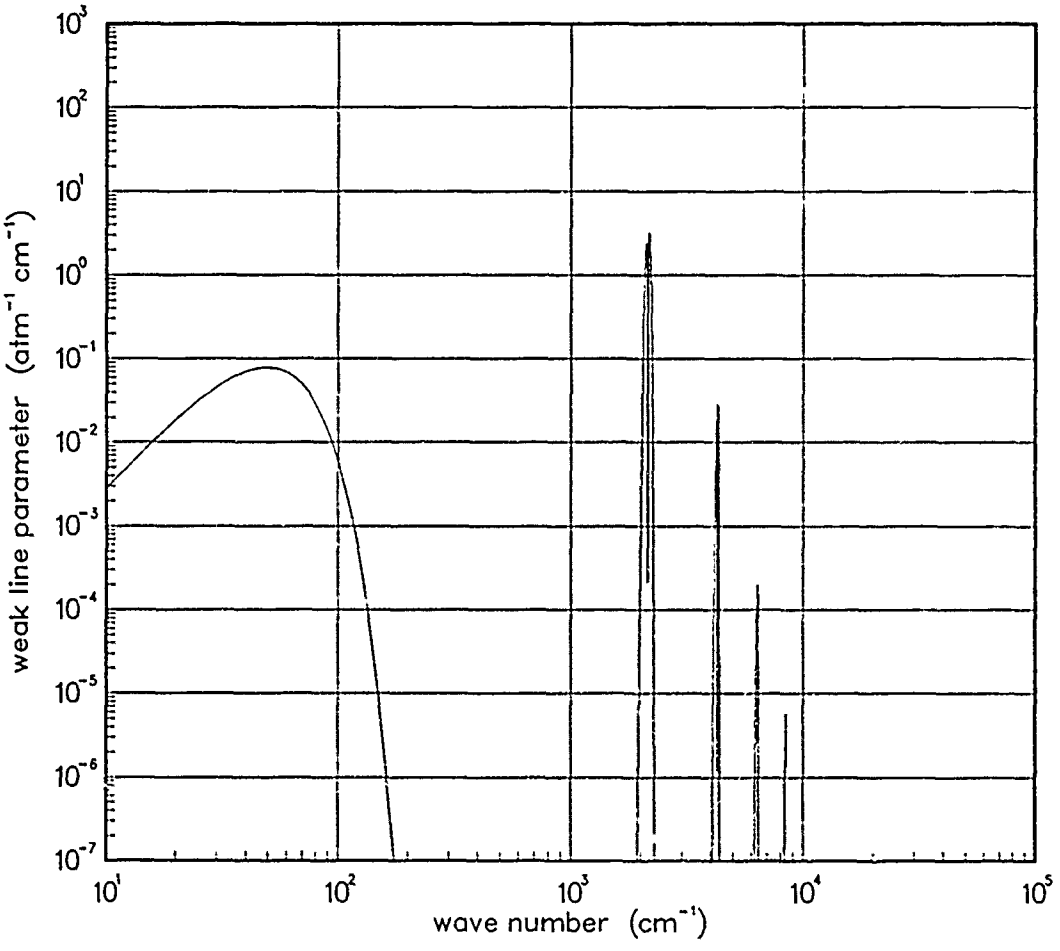

Figure 7. Weak-line parameter for CO at 300°K.

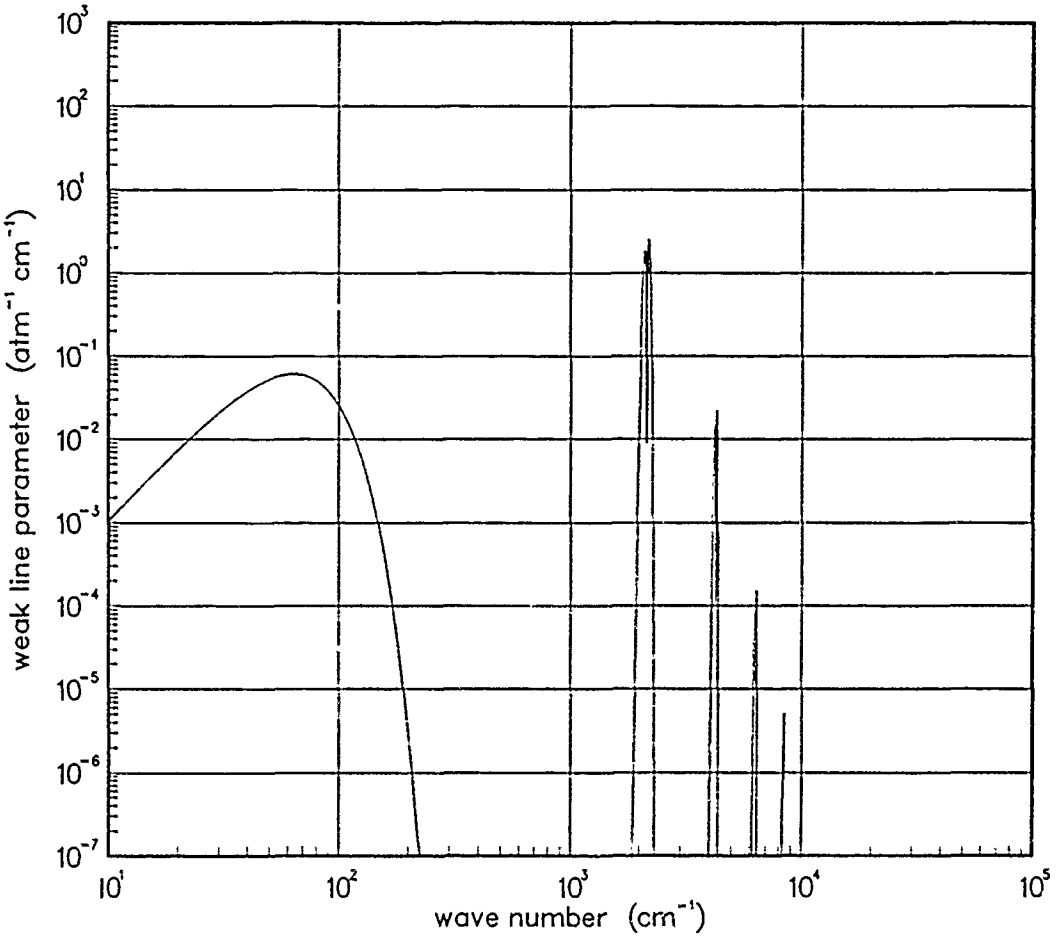

Figure 8. Weak-line parameter for CO at 500°K.

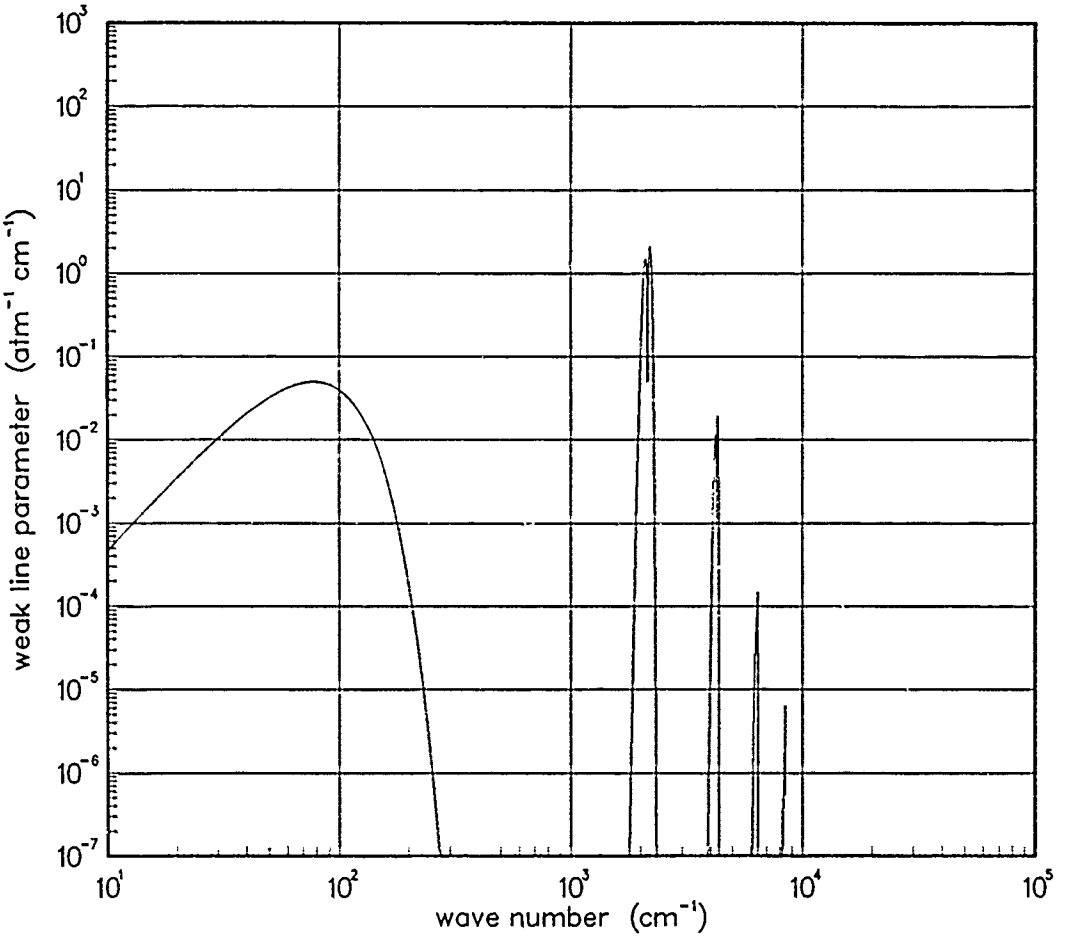

Figure 9. Weak-line parameter for CO at 750°K.

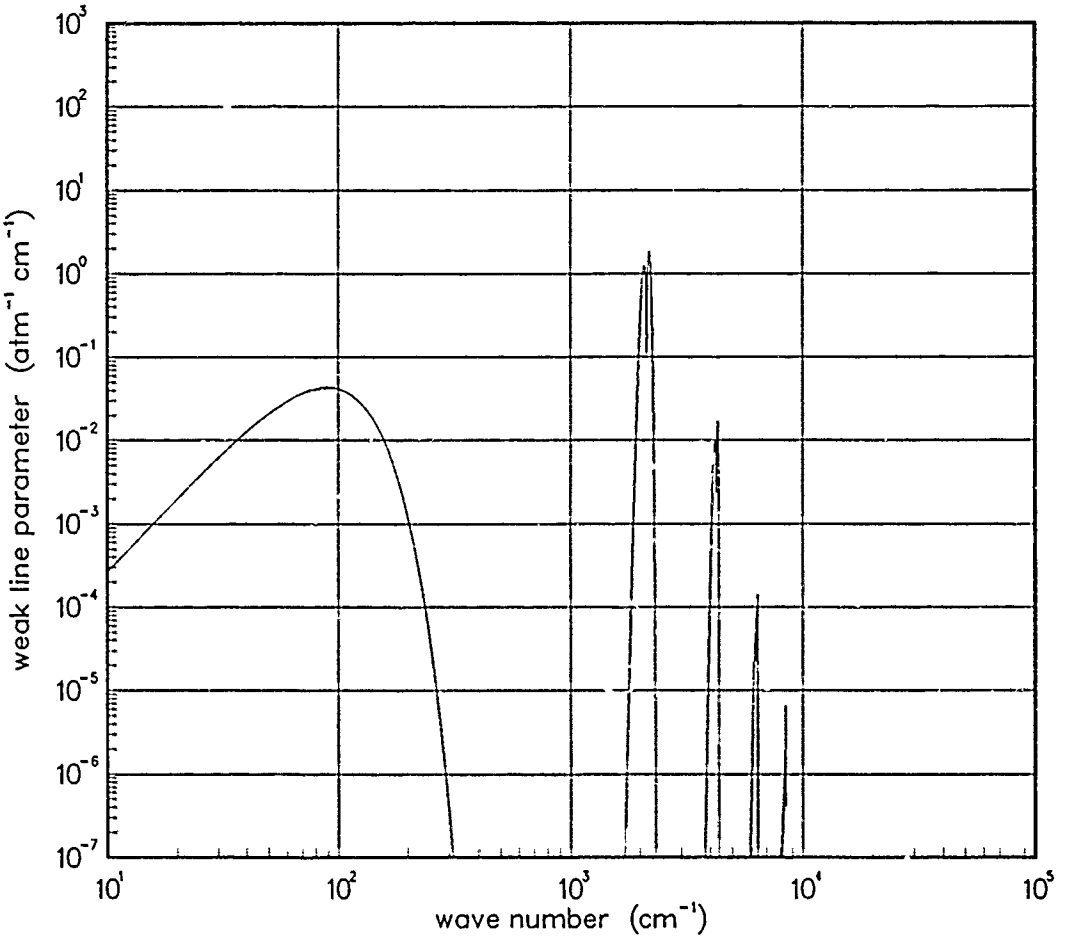

Figure 10. Weak-line parameter for CO at 1000°K.

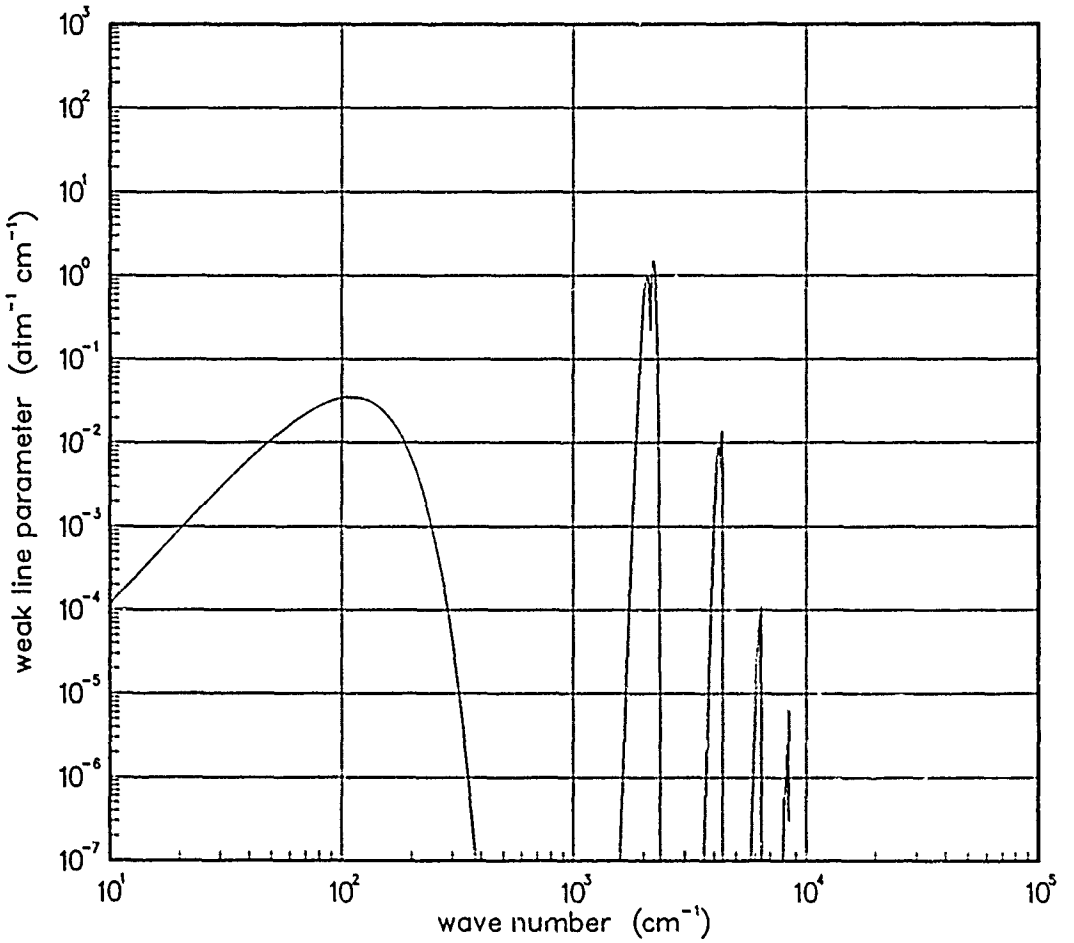

Figure 11. Weak-line parameter for CO at 1500°K.

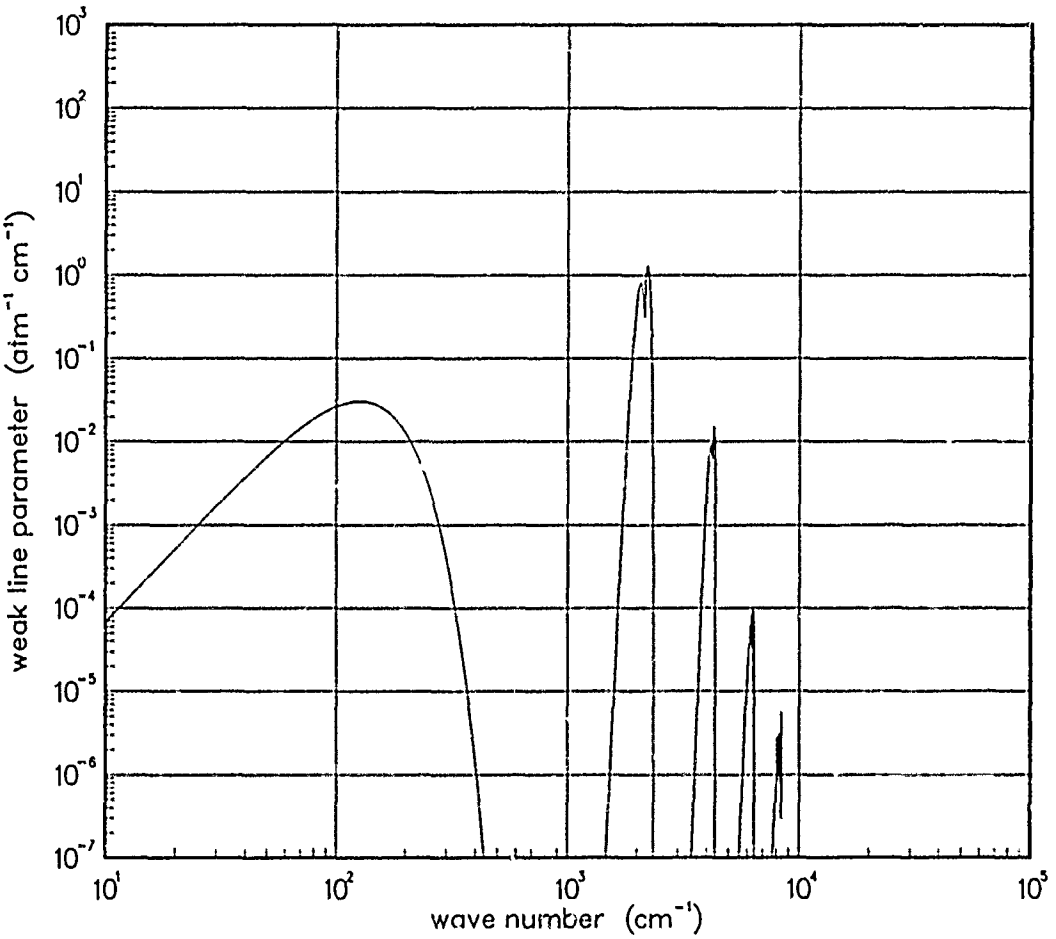

Figure 12. Weak-line parameter for CO at 2000°K.

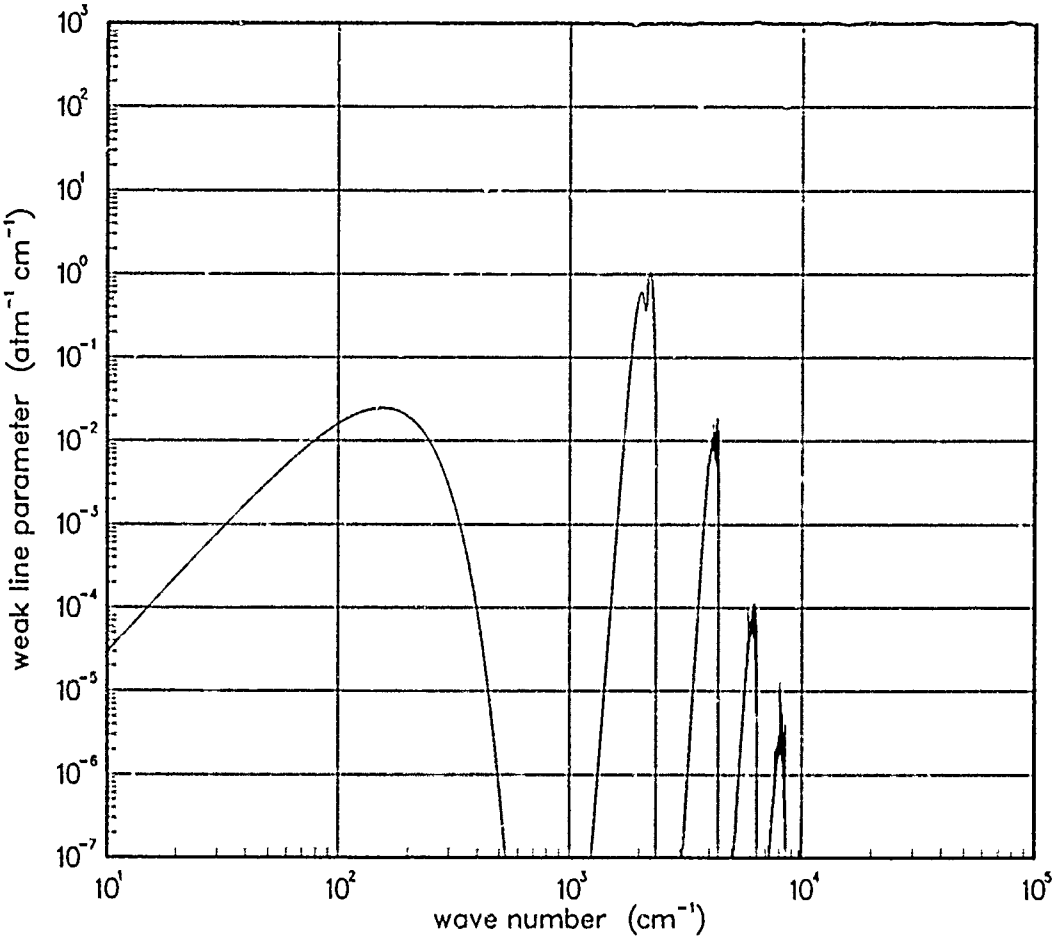

Figure 13. Weak-line parameter for CO at 3000°K.

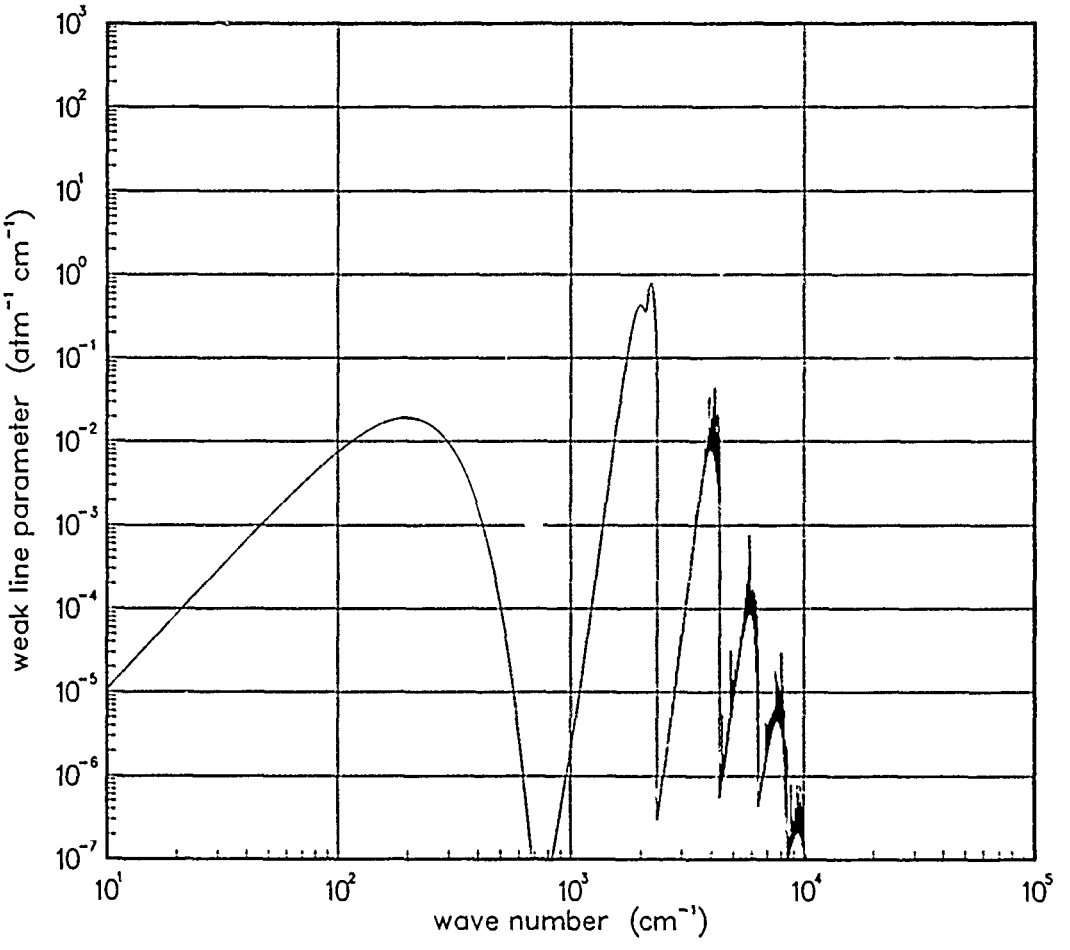

Figure 14. Weak-line parameter for CO at 5000°K.

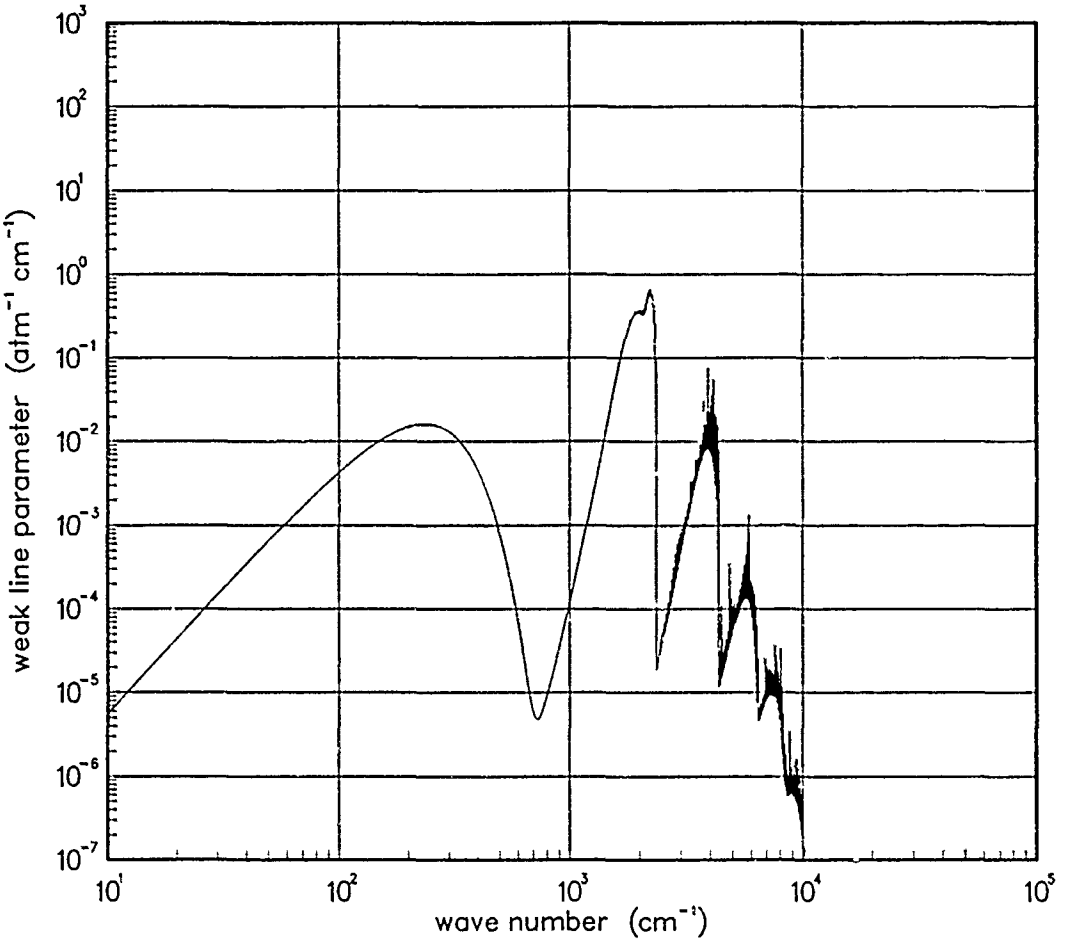

Figure 15. Weak-line parameter for CO at 7000°K.

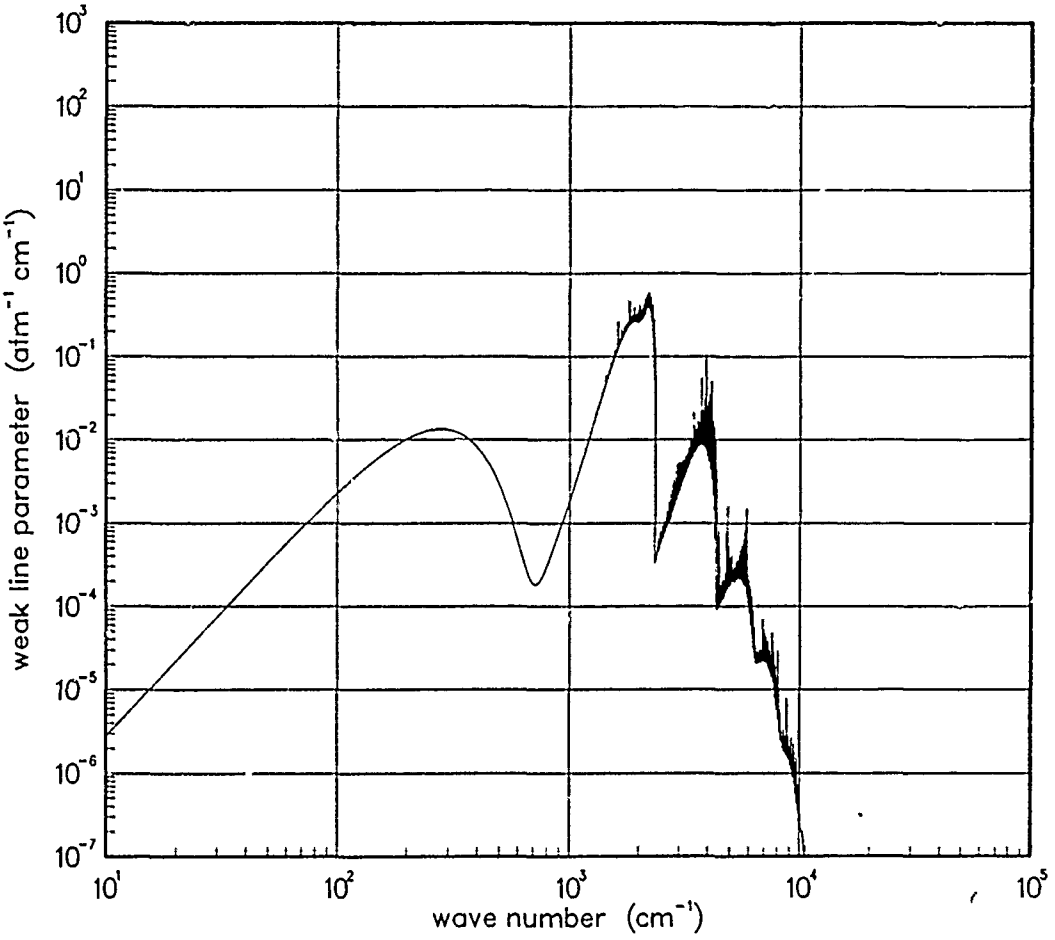

Figure 16. Weak-line parameter for CO at 10000°K.

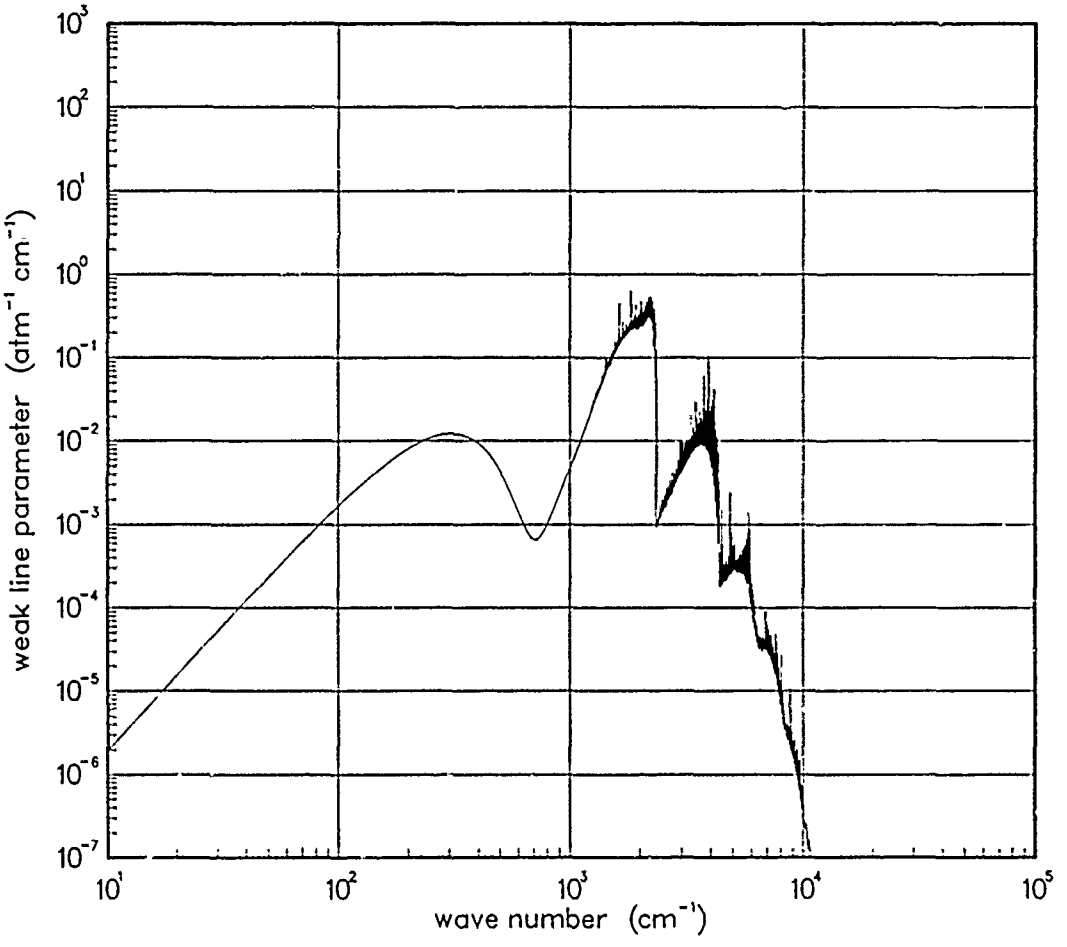

Figure 17. Weak-line parameter for CO at 12000°K.

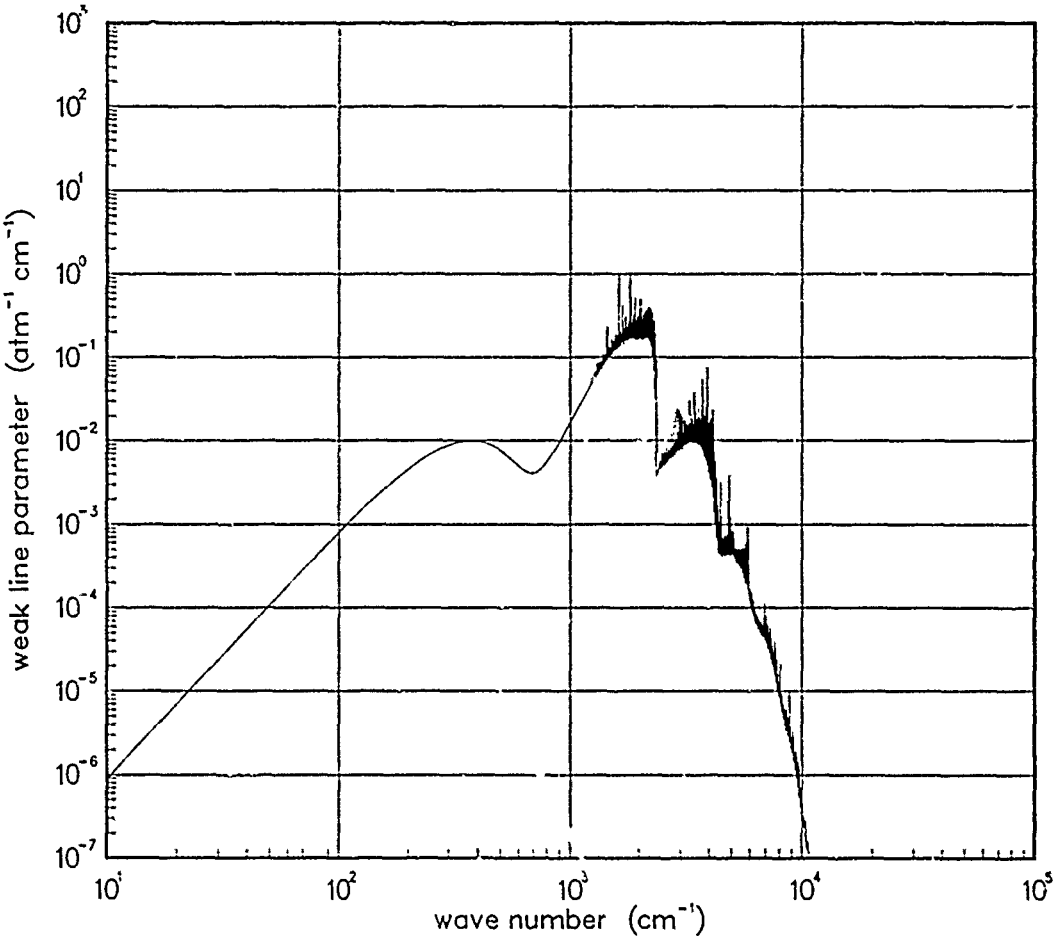

Figure 18. Weak-line parameter for CO at 18000°K.

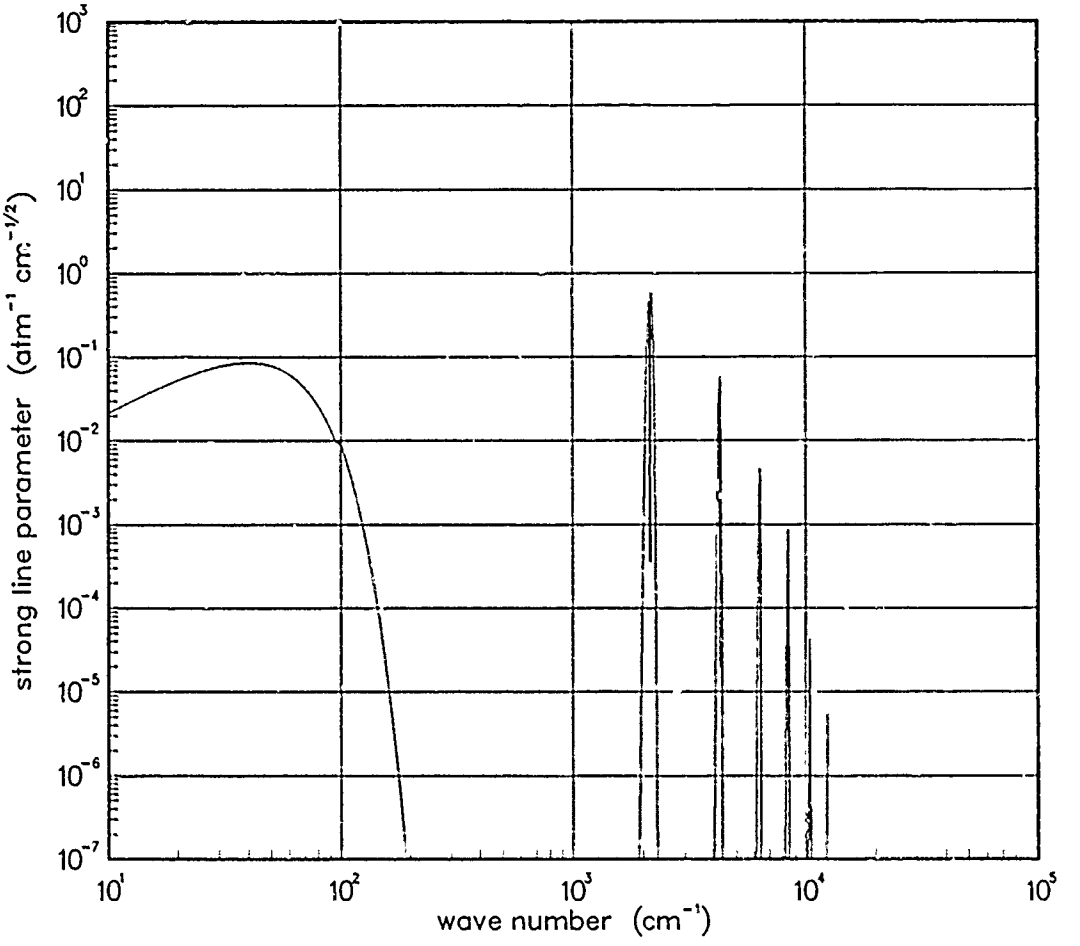

Figure 19. Strong-line parameter for CO at 200°K.

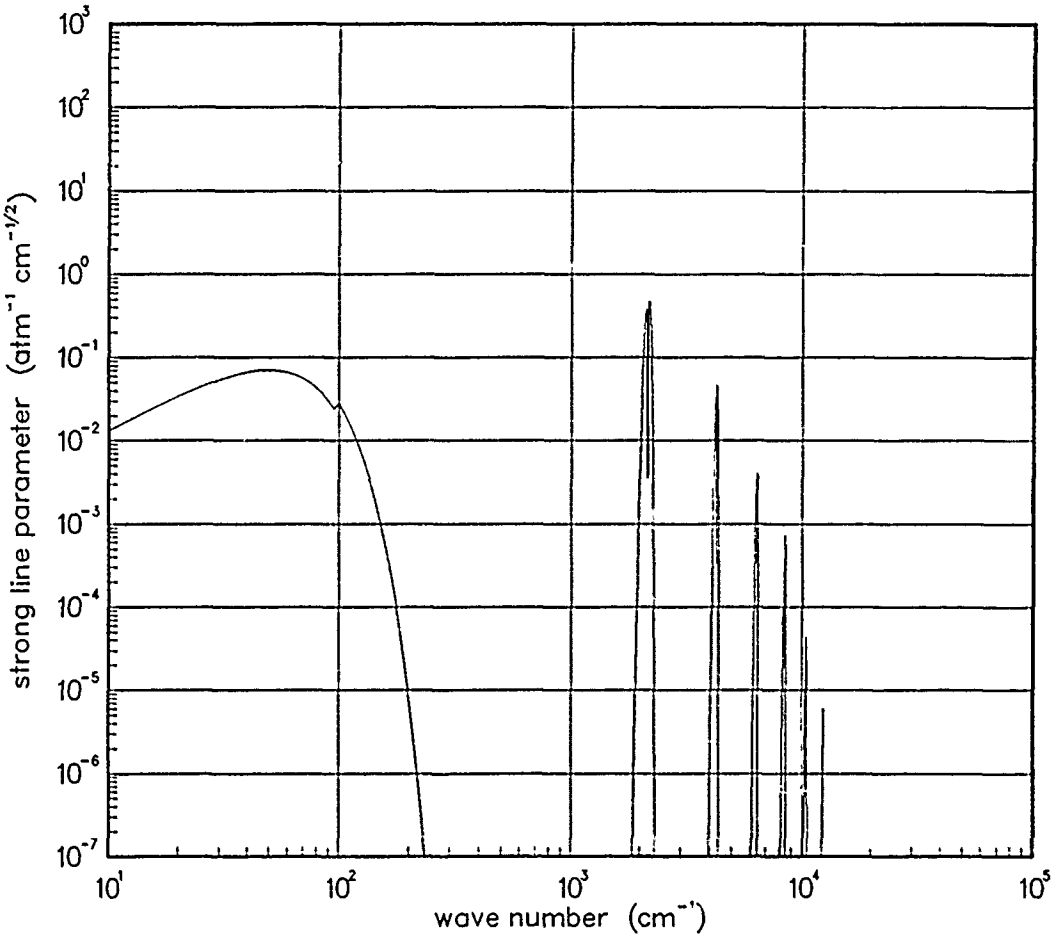

Figure 20. Strong-line parameter for CO at 300°K.

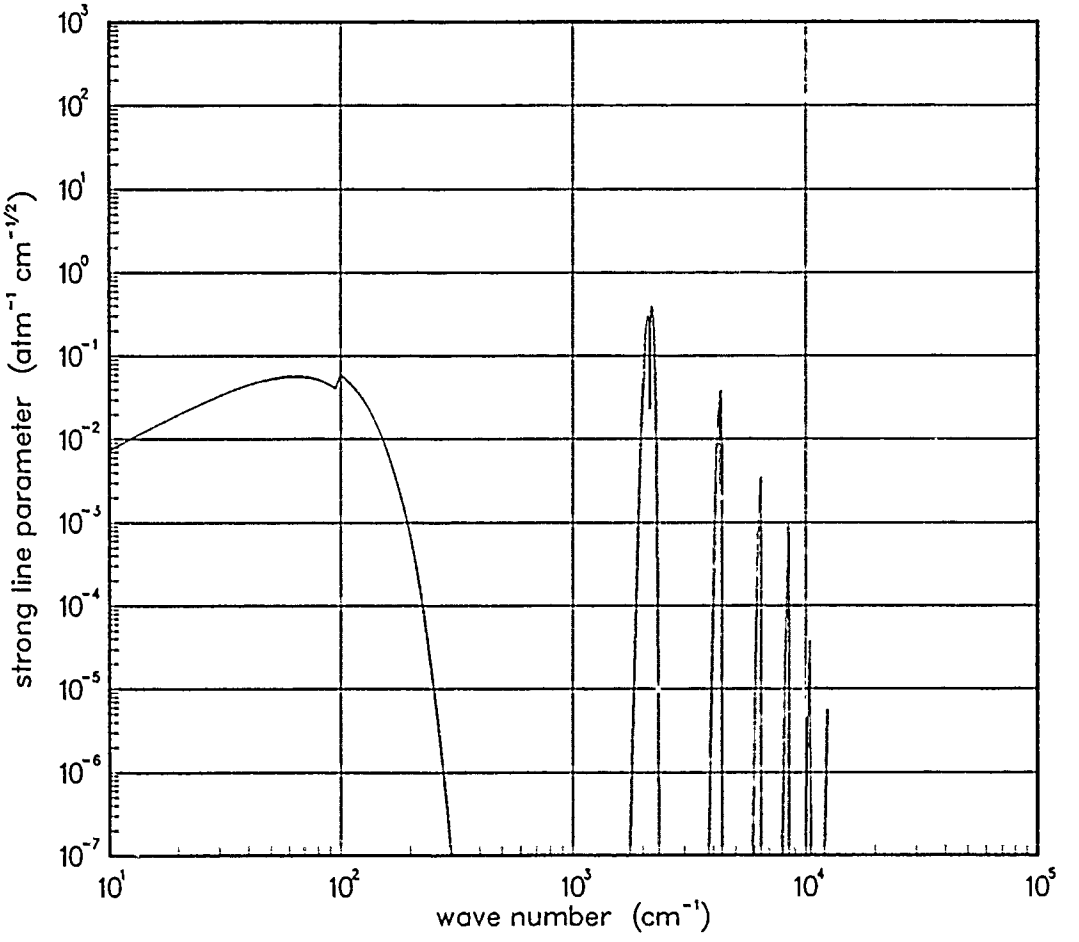

Figure 21. Strong-line parameter for CO at 500°K.

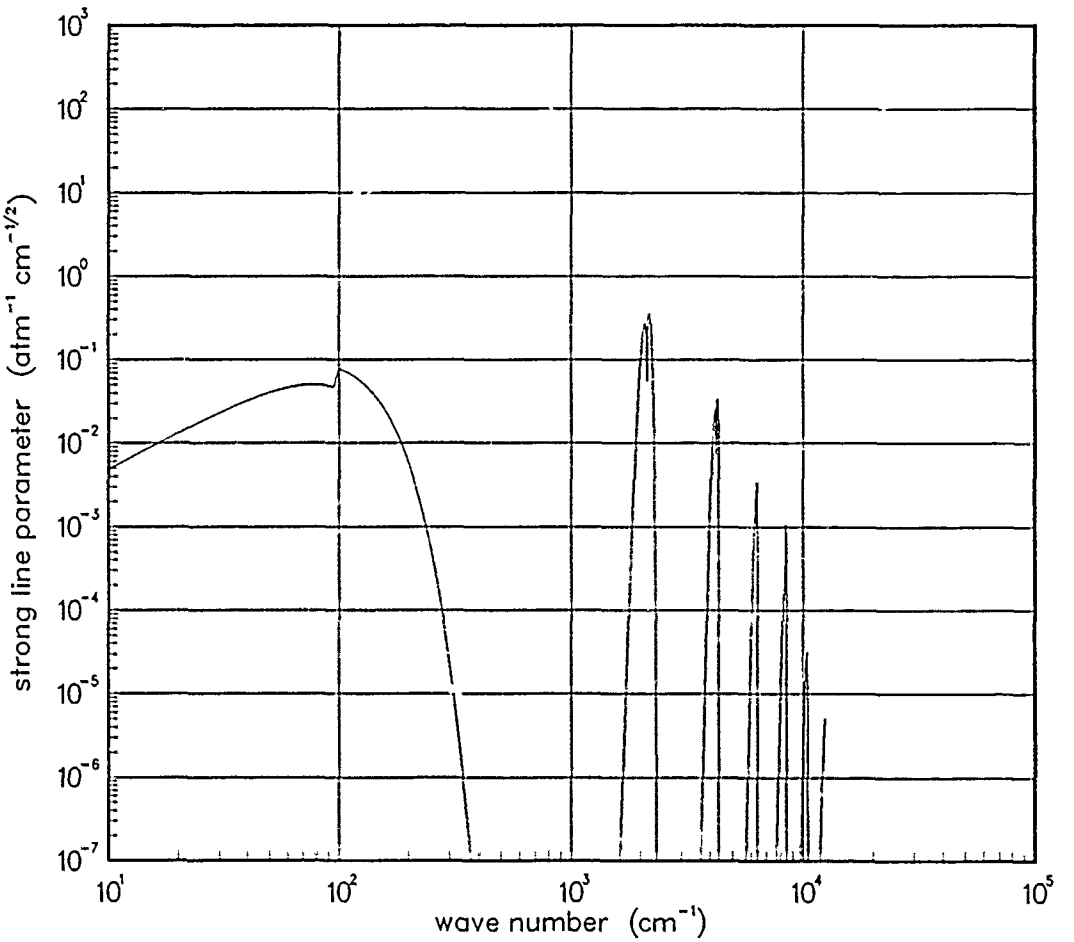

Figure 22. Strong-line parameter for CO at 750°K.

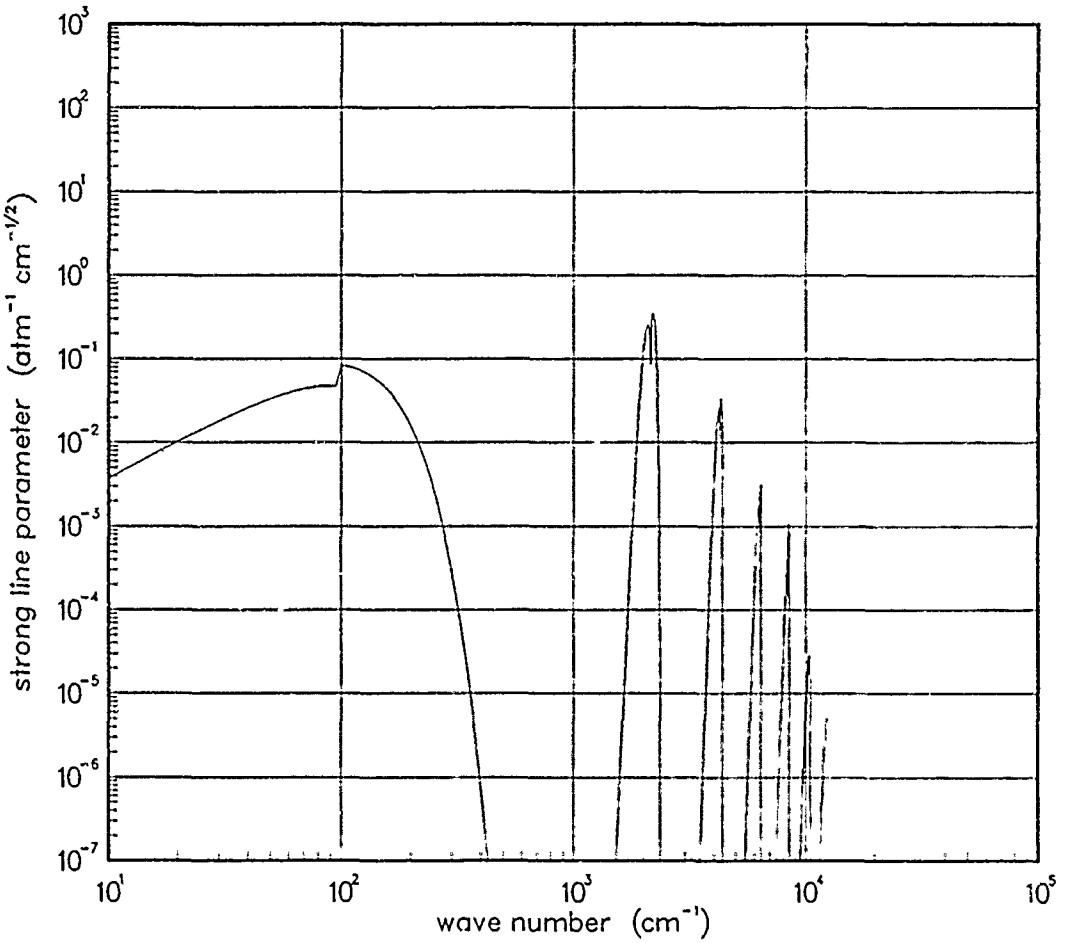

Figure 23. Strong-line parameter for CO at 1000°K.

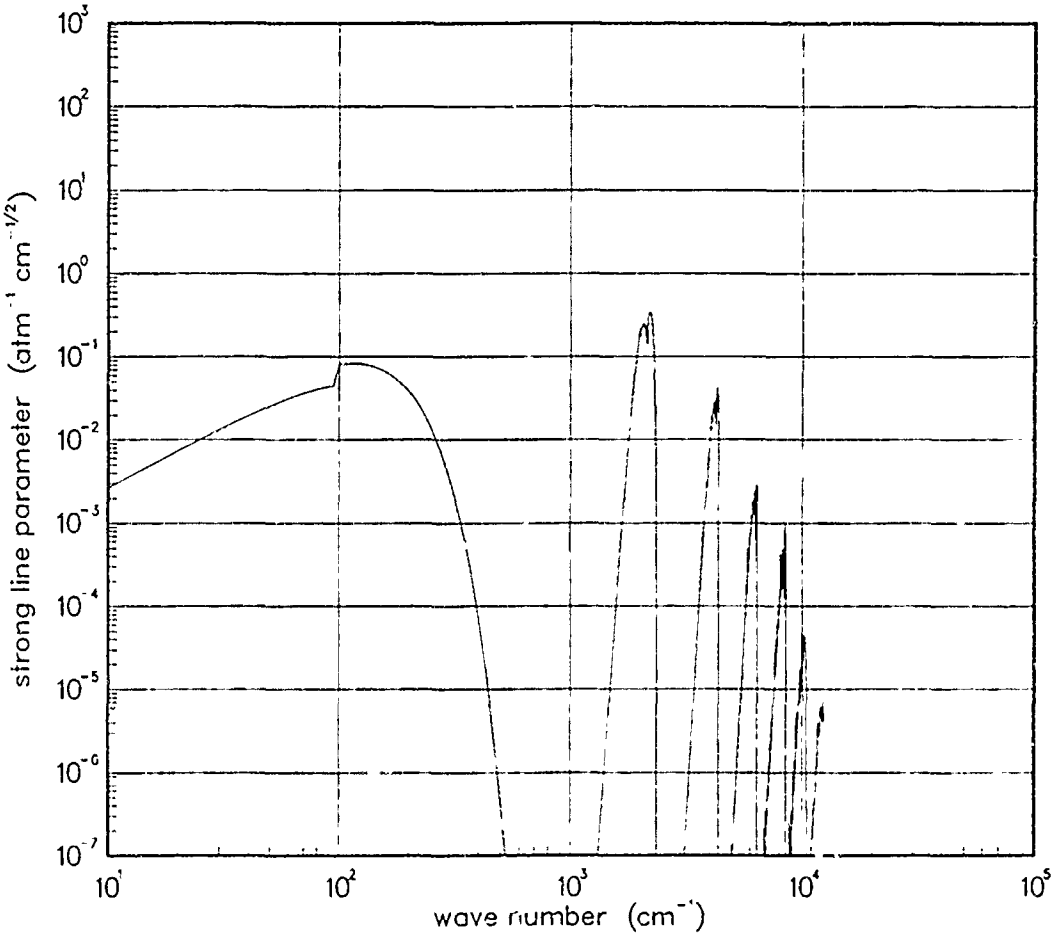

Figure 24. Strong-line parameter for CO at 1500°K.

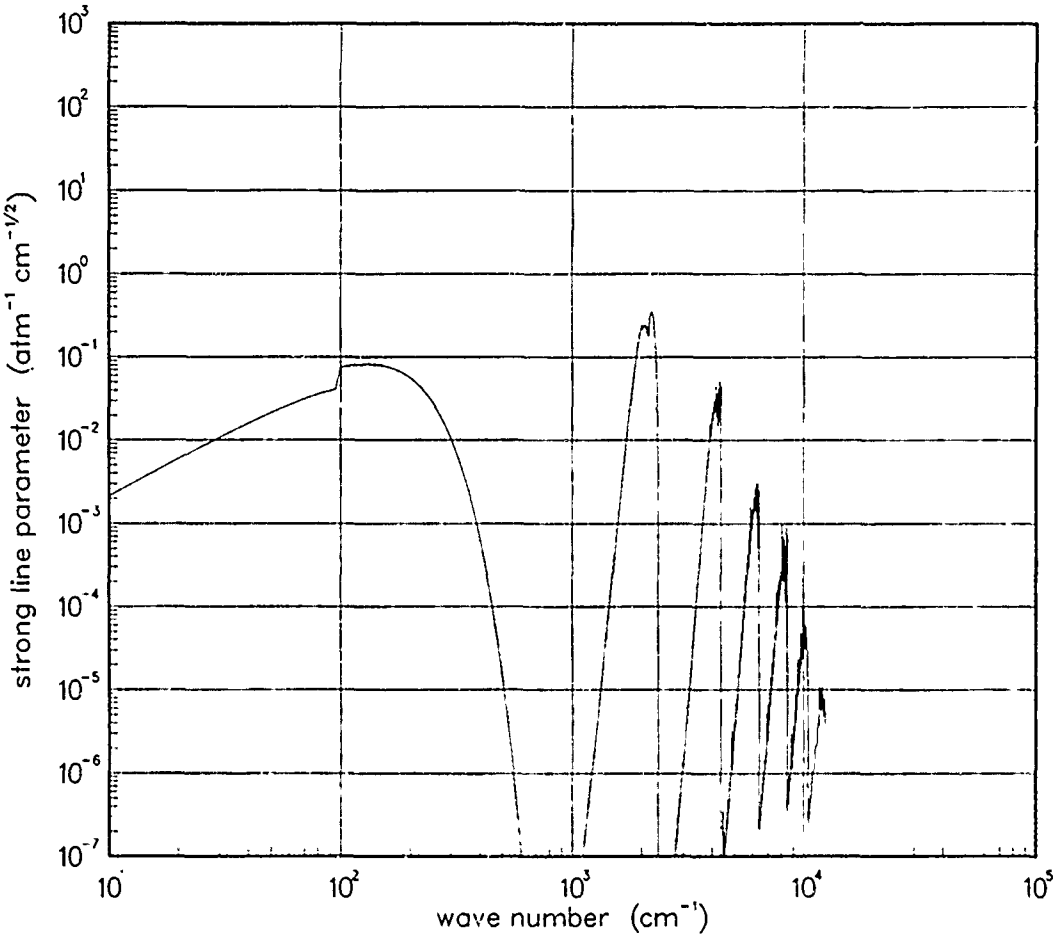

Figure 25. Strong-line parameter for CO at 2000°K.

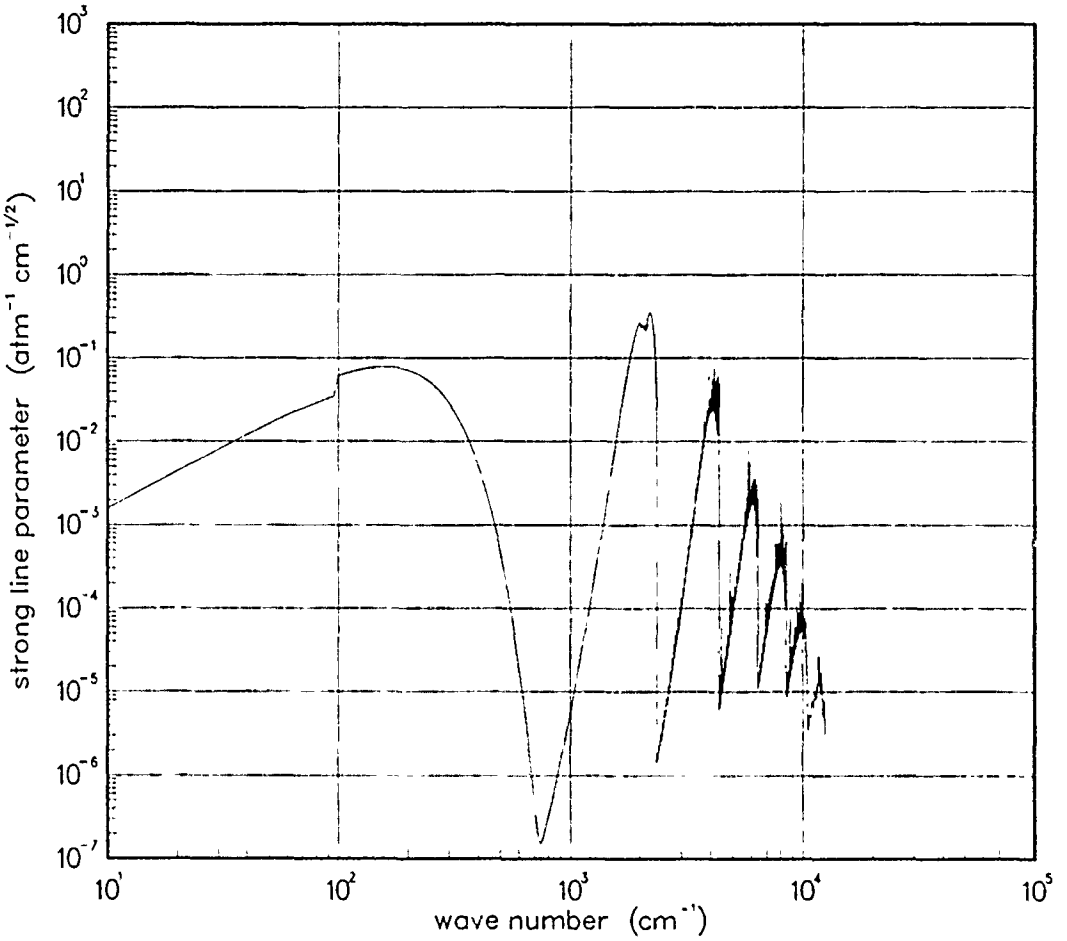

Figure 26. Strong-line parameter for CO at 3000°K.

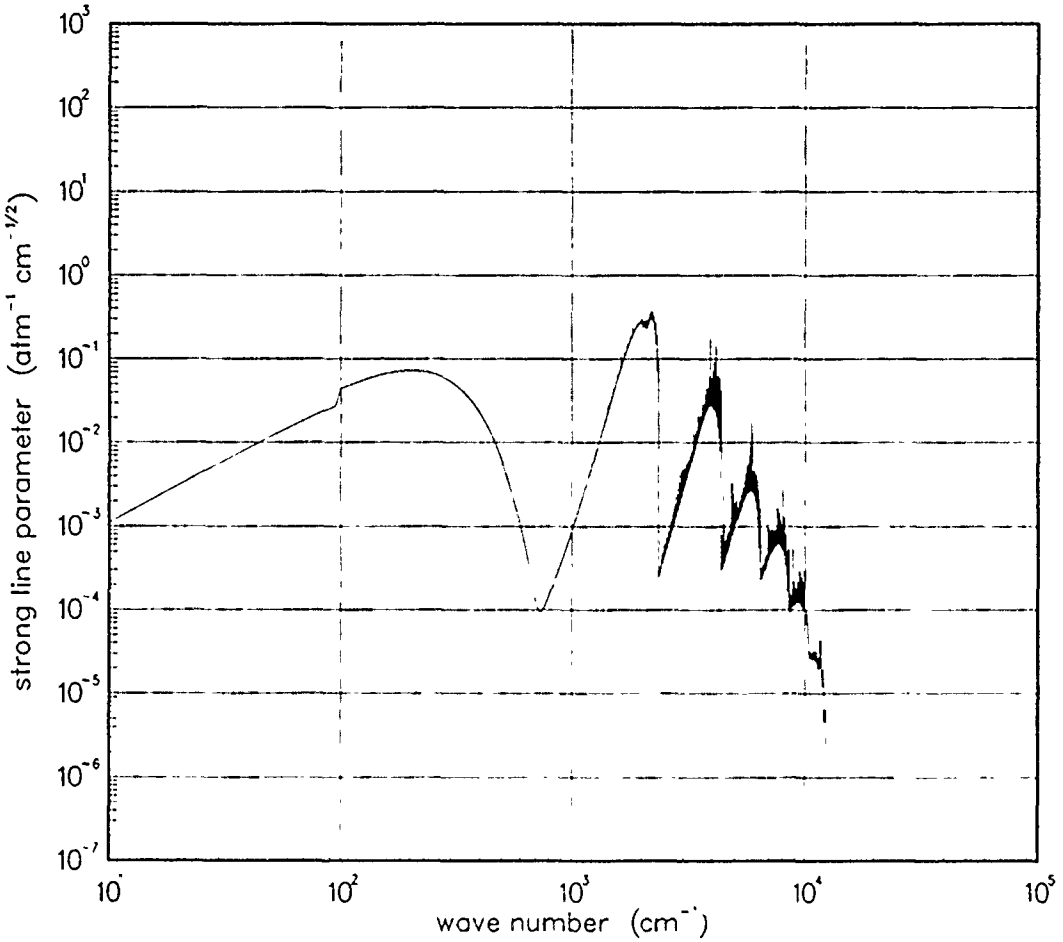

Figure 27. Strong-line parameter for CO at 5000°K.

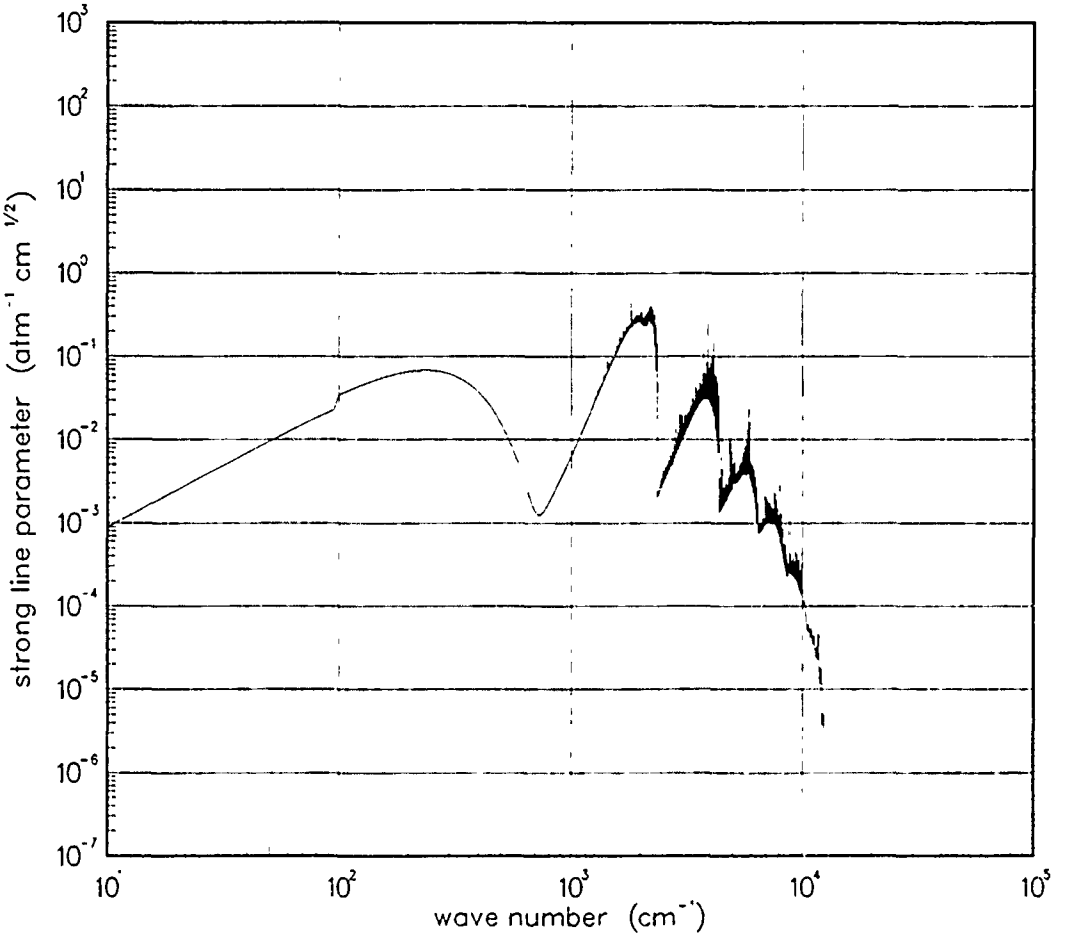

Figure 28. Strong-line parameter for CO at 7000°K.

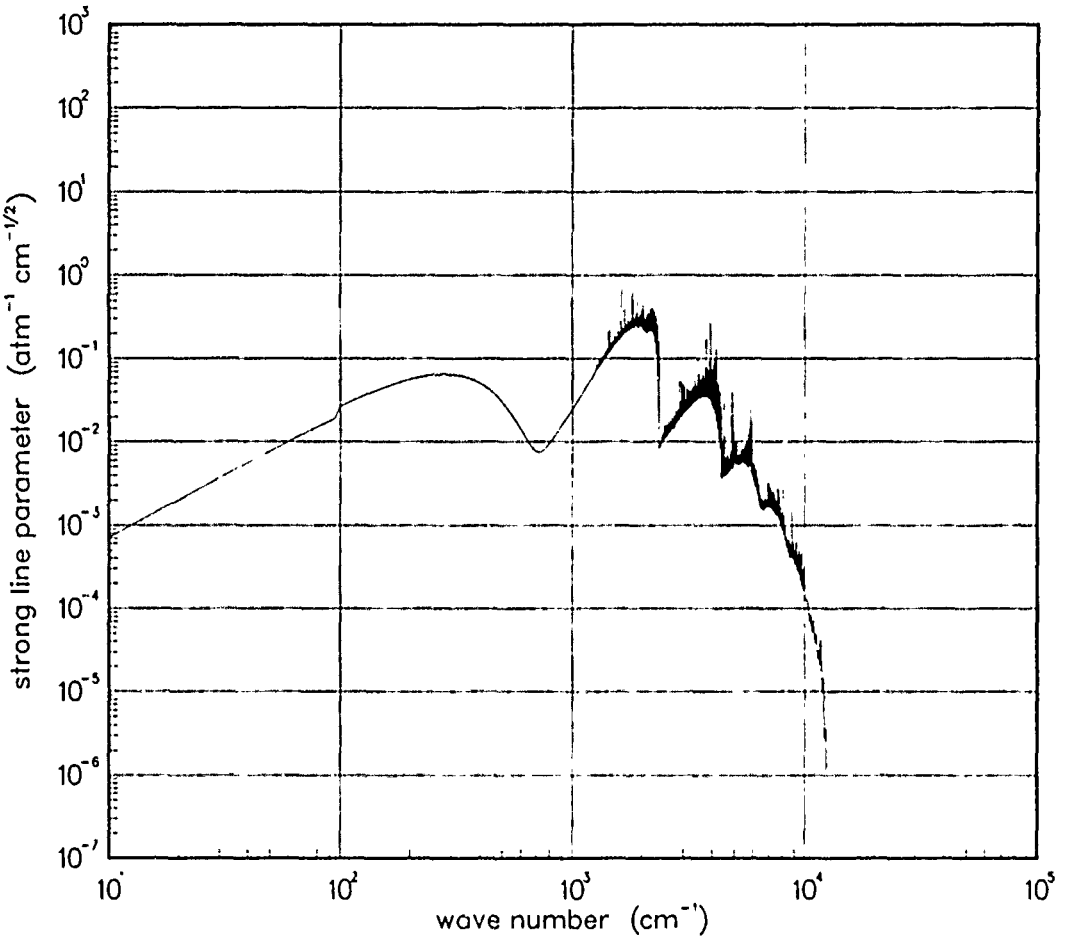

Figure 29. Strong-line parameter for CO at 10000°K.

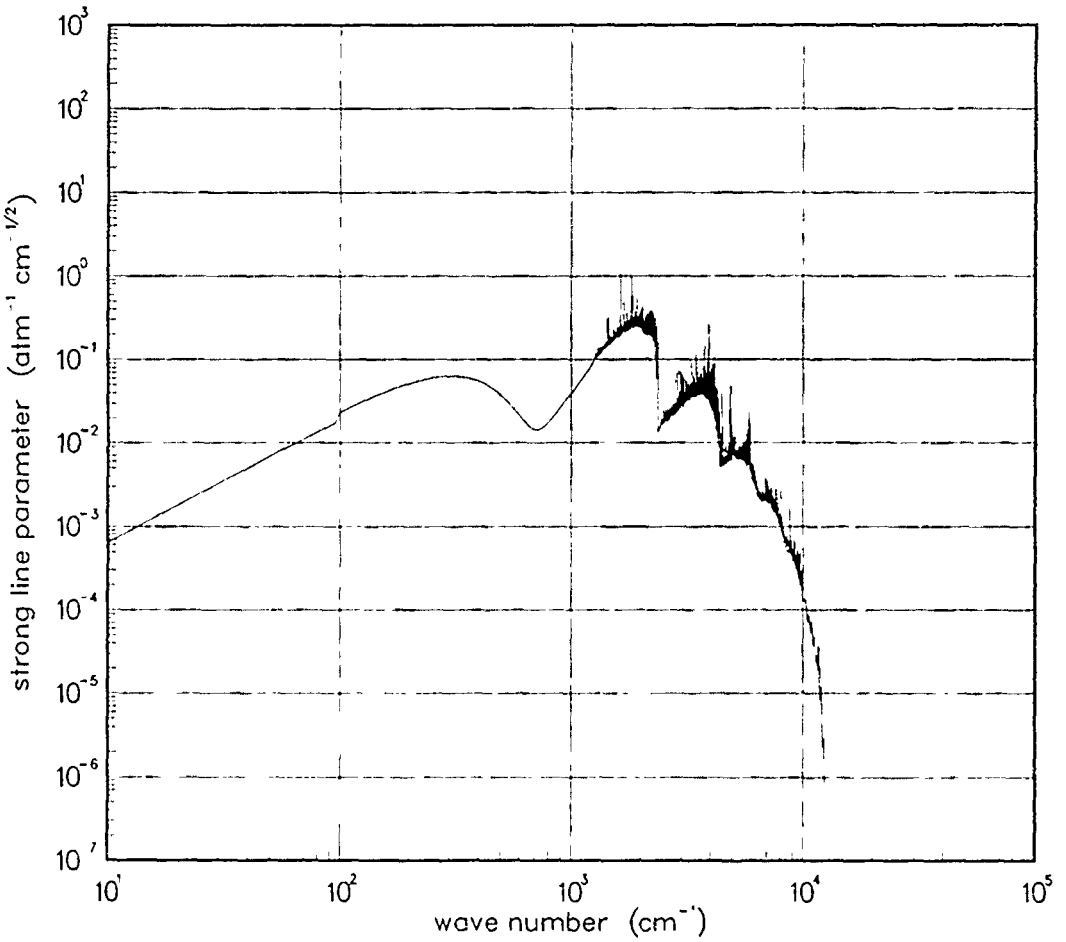

Figure 30. Strong-line parameter for CO at 12000°K.

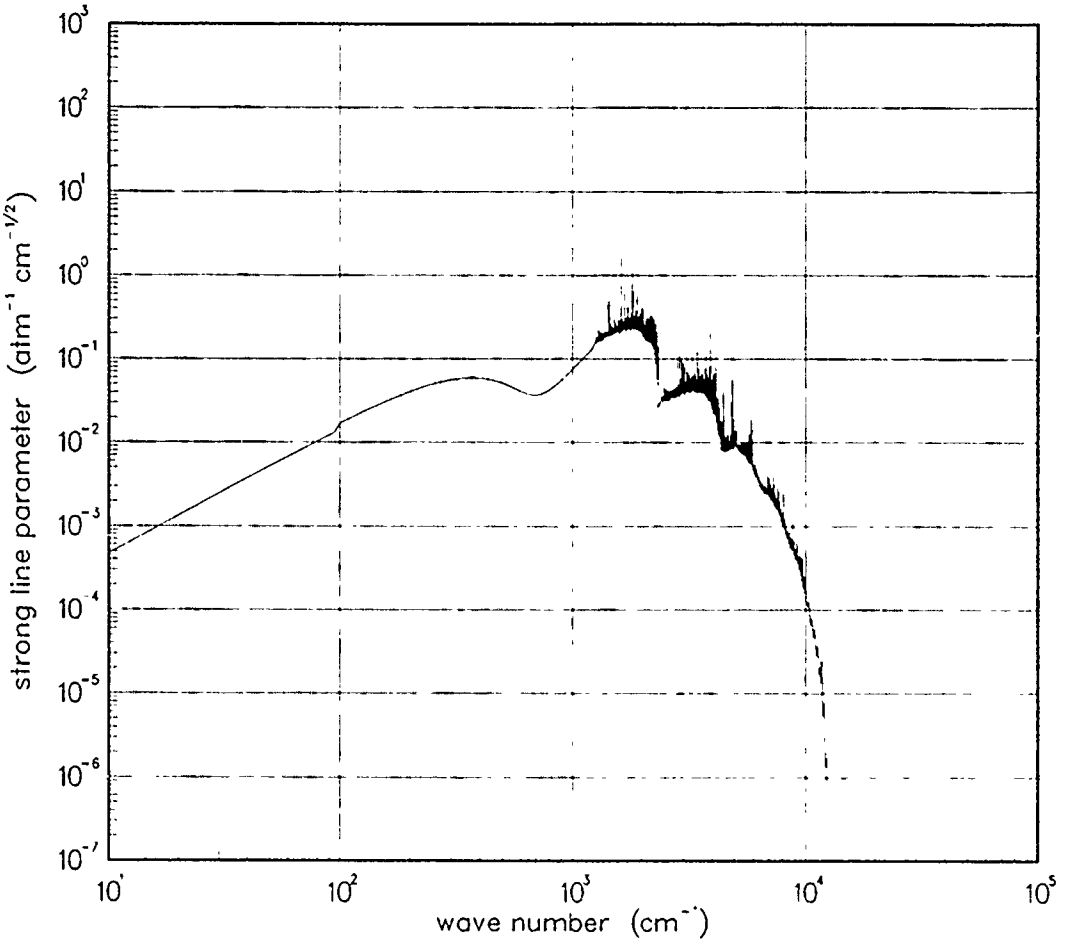

Figure 31. Strong-line parameter for CO at 18000°K.

4.2 HYDROXYL (OH).

Table 2. Spectroscopic data for OH.

Ground Electronic State

ω_e = 3735.21 cm^{-1}* $\omega_e x_e$ = 82.82 cm^{-1}*
α_e = 0.714 cm^{-1}* B_e = 18.871 cm^{-1}*

S_{10} = 120 atm^{-1} cm^{-2}*

γ_ℓ(300 °K) = 0.06†

Data Source:

*W.S. Benedict, and E.K. Plyler, High-Resolution Spectra of Hydrocarbon Flames in the Infrared, Energy Transfer in Hot Gases, National Bureau of Standards Circular 523, p. 57 (1954).

†D. Bastard, et al, Spectroscopic Hertzienne -- Etude experimental dela saturation de l'absorption hertzienne du radical OH, C.R. Acad. Sc. Paris, vol 284, Series B, p. 445 (1977).

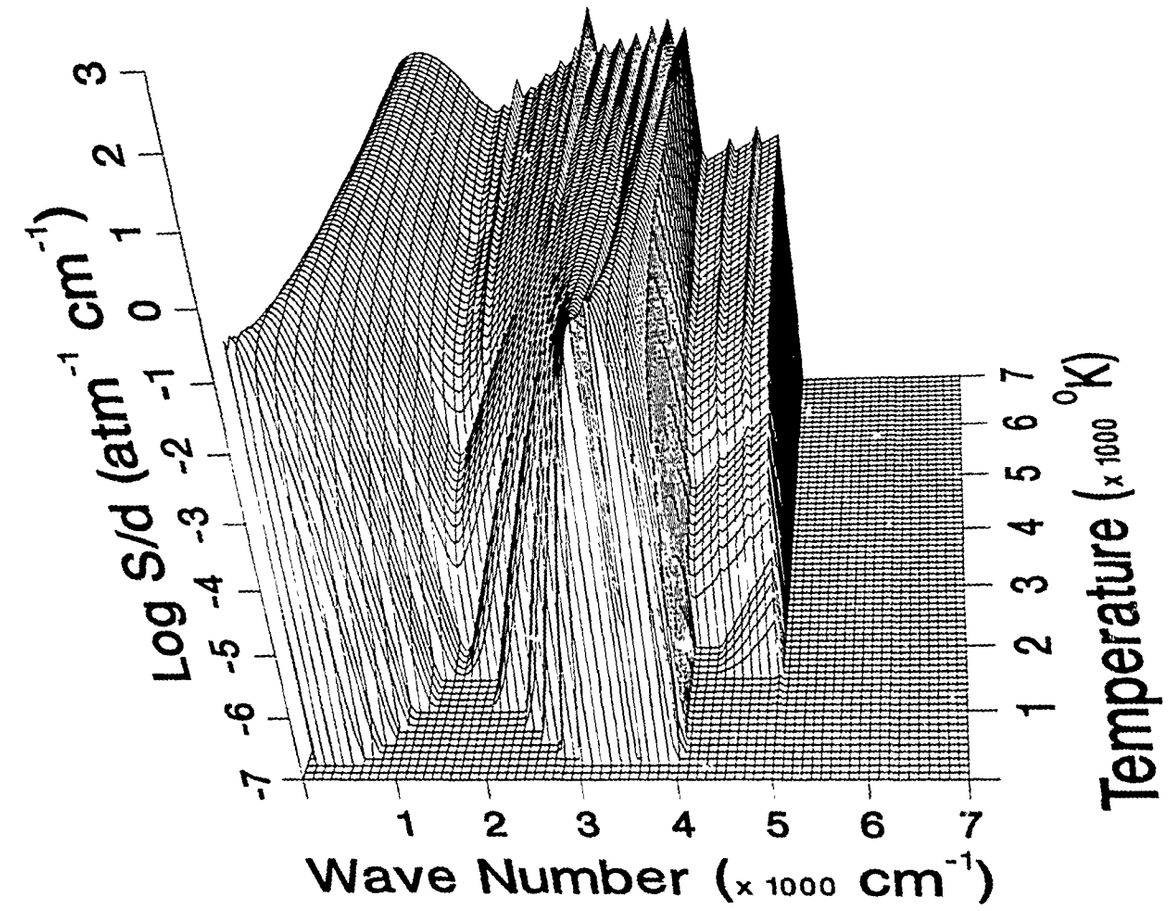

Figure 32. Weak-line parameter for OH.

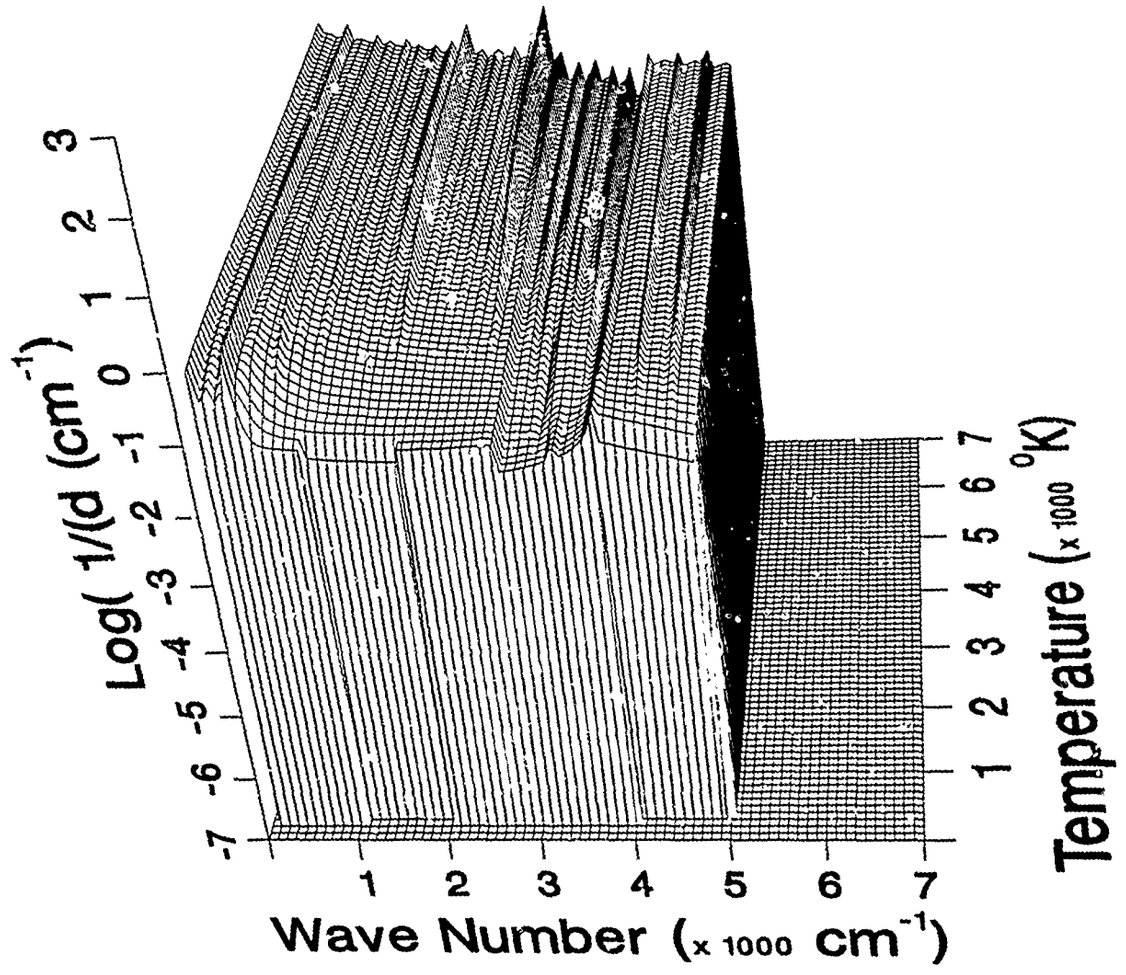

Figure 33. Inverse line spacing for OH.

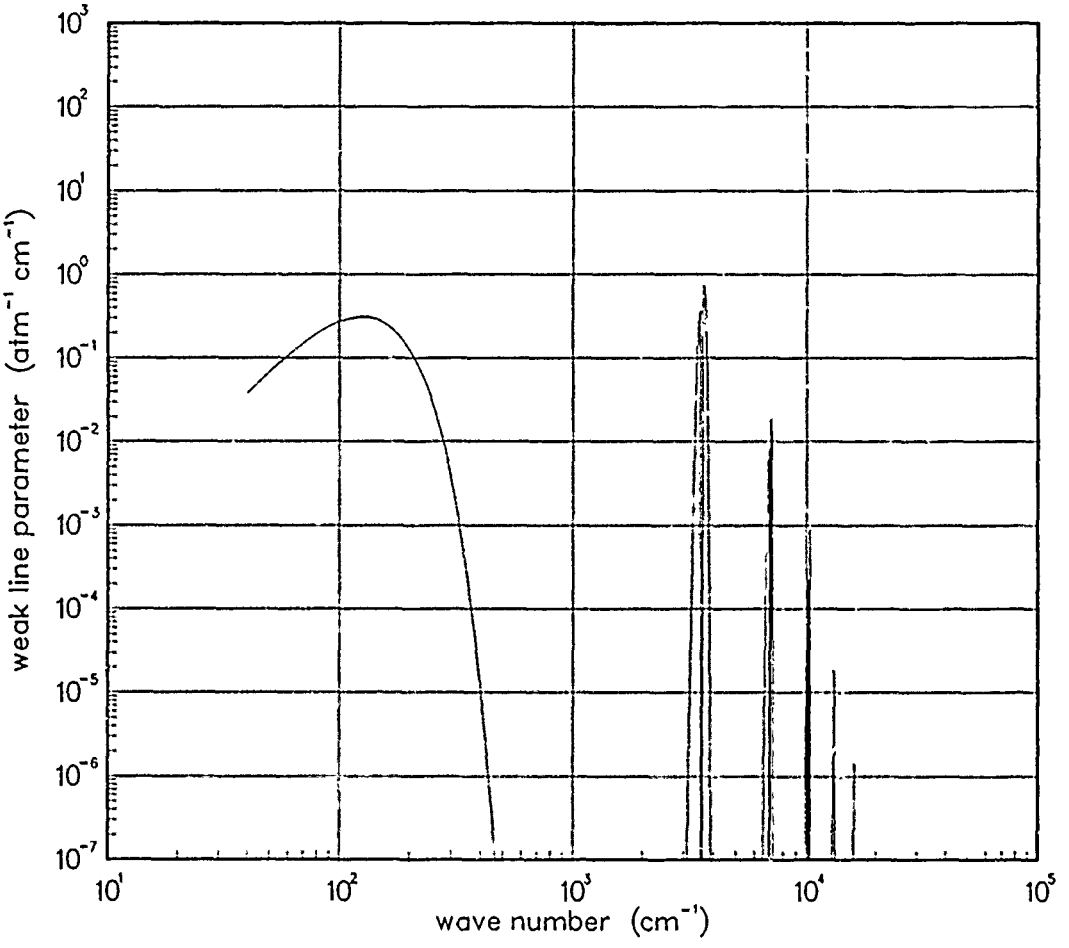

Figure 34. Weak-line parameter for OH at 200°K.

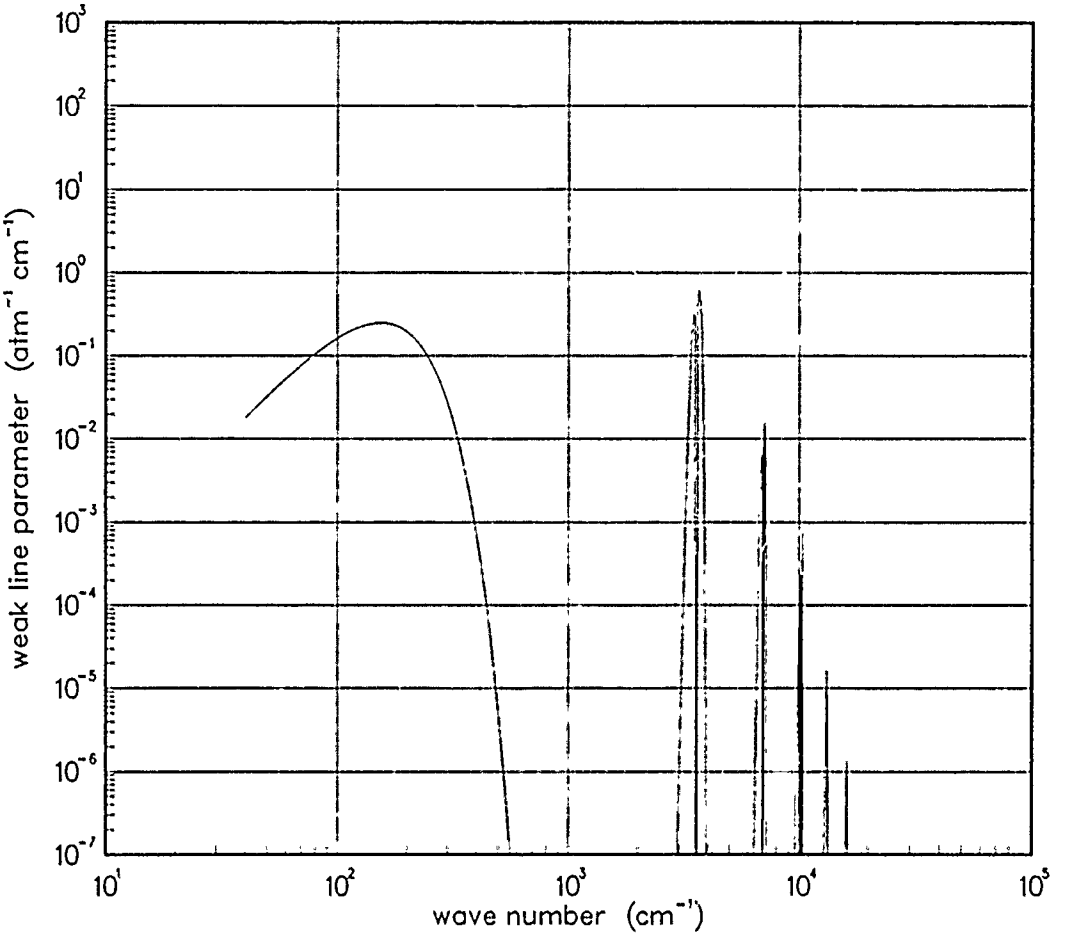

Figure 35. Weak-line parameter for OH at 300°K.

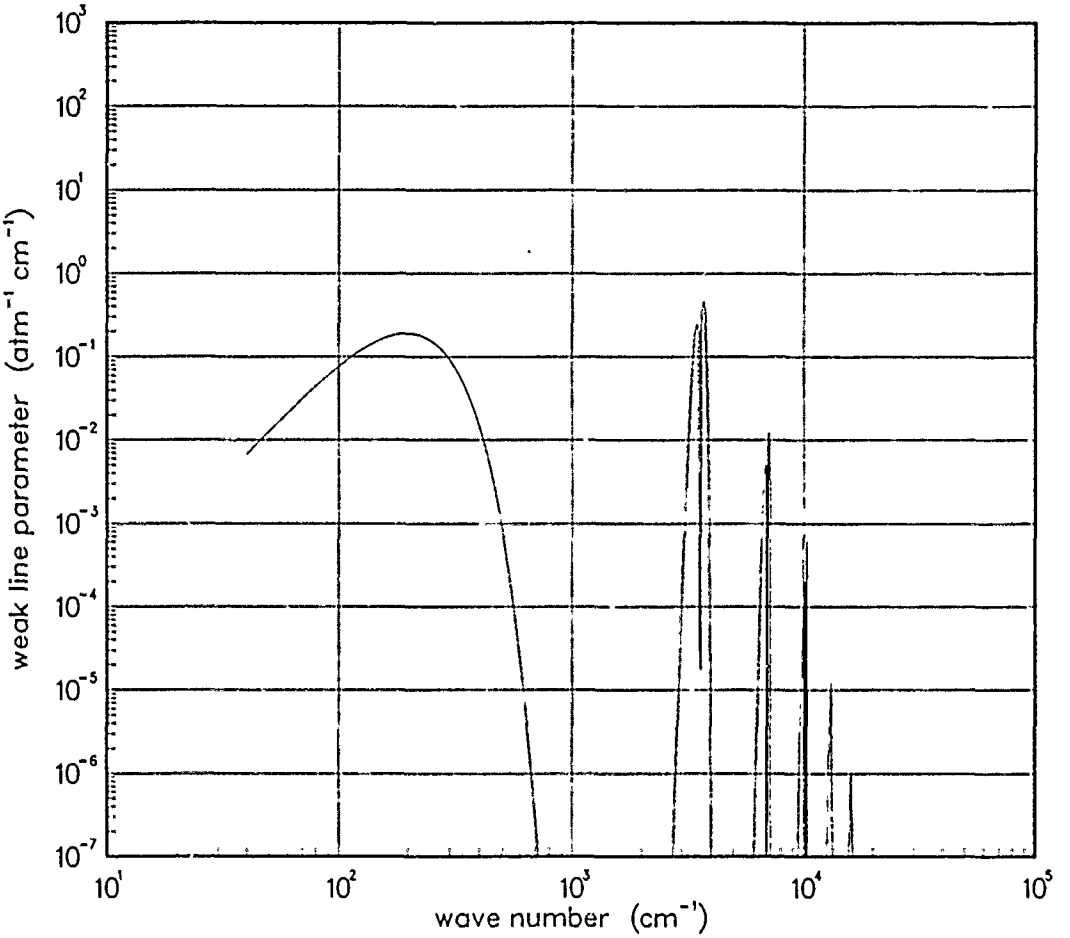

Figure 36. Weak-line parameter for OH at 500°K.

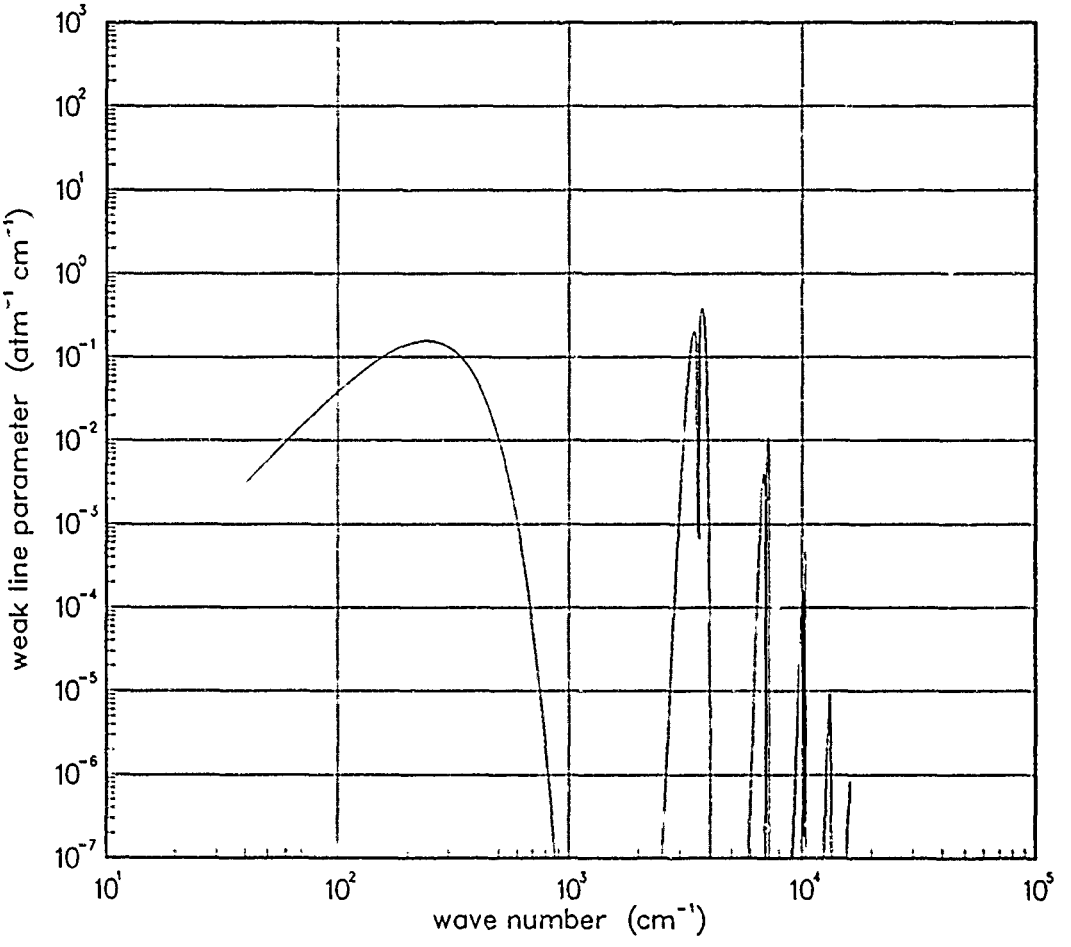

Figure 37. Weak-line parameter for OH at 750°K.

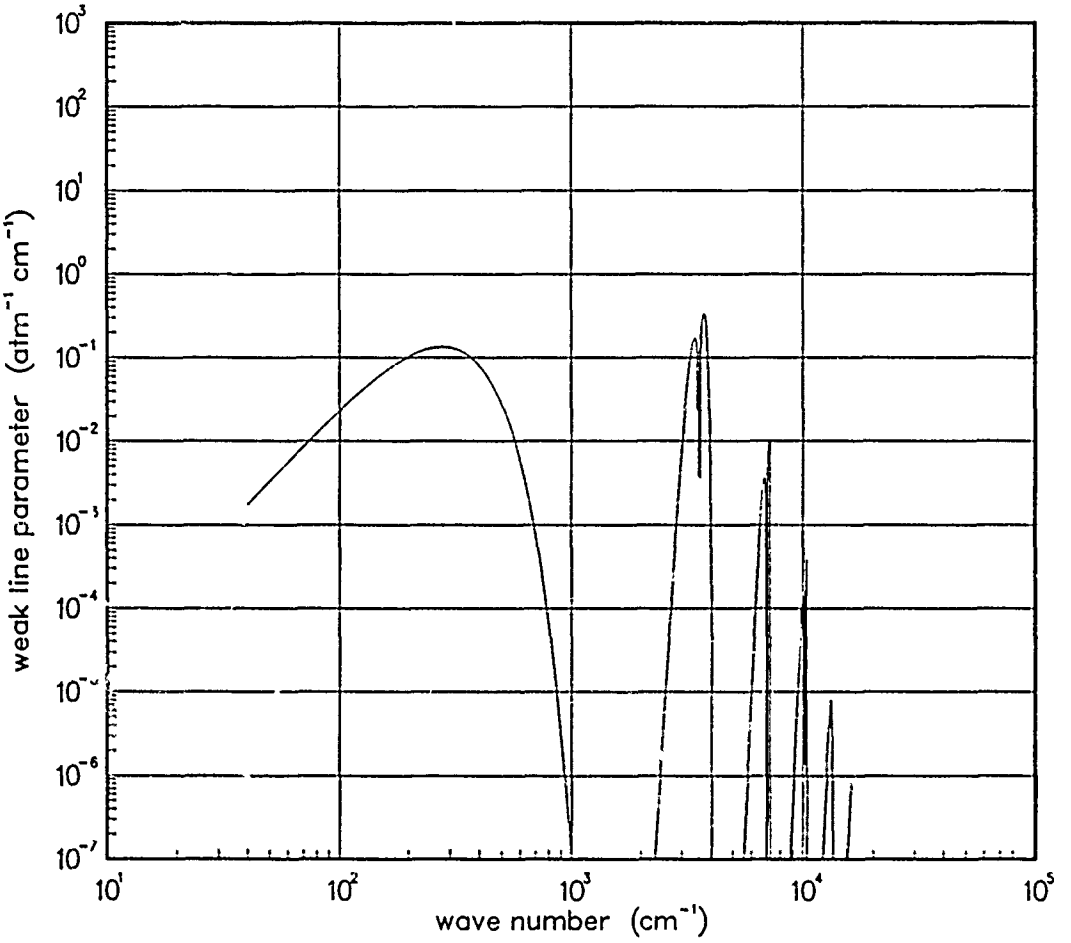

Figure 38. Weak-line parameter for OH at 1000°K.

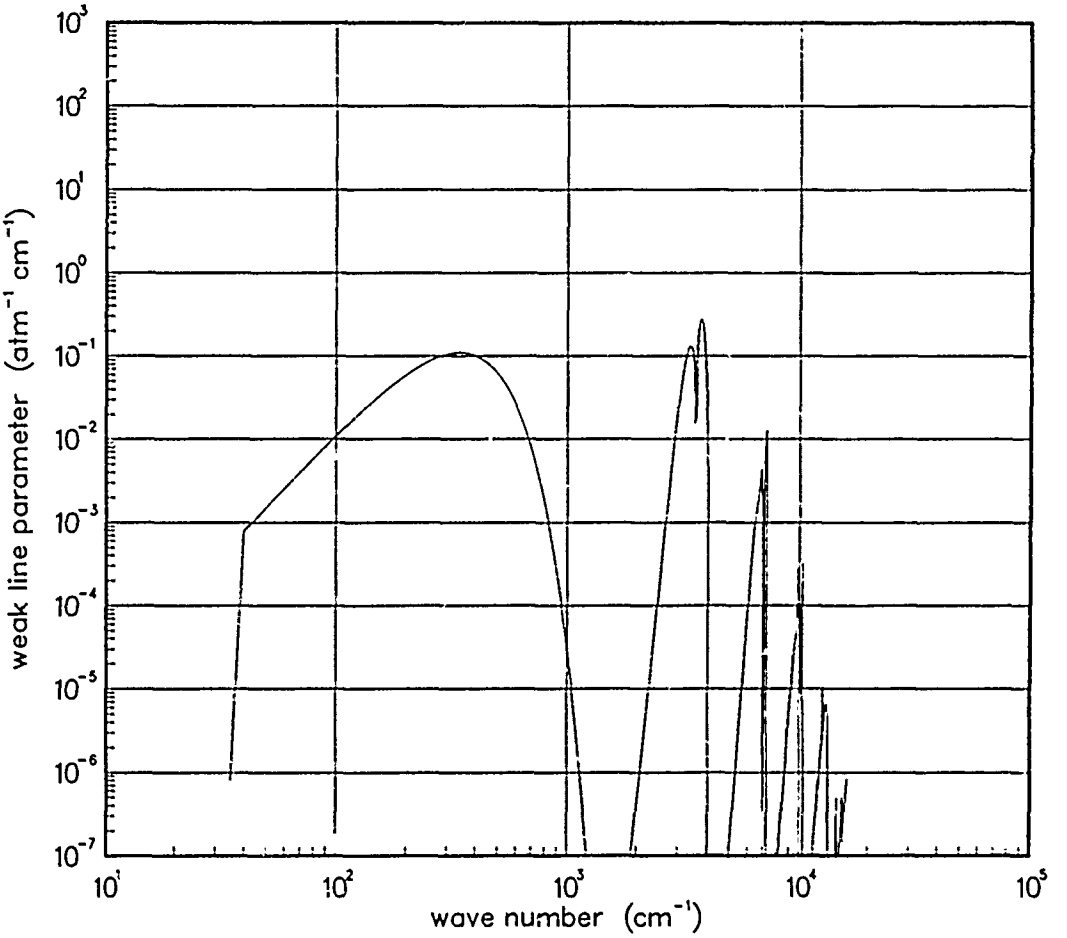

Figure 39. Weak-line parameter for OH at 1500°K.

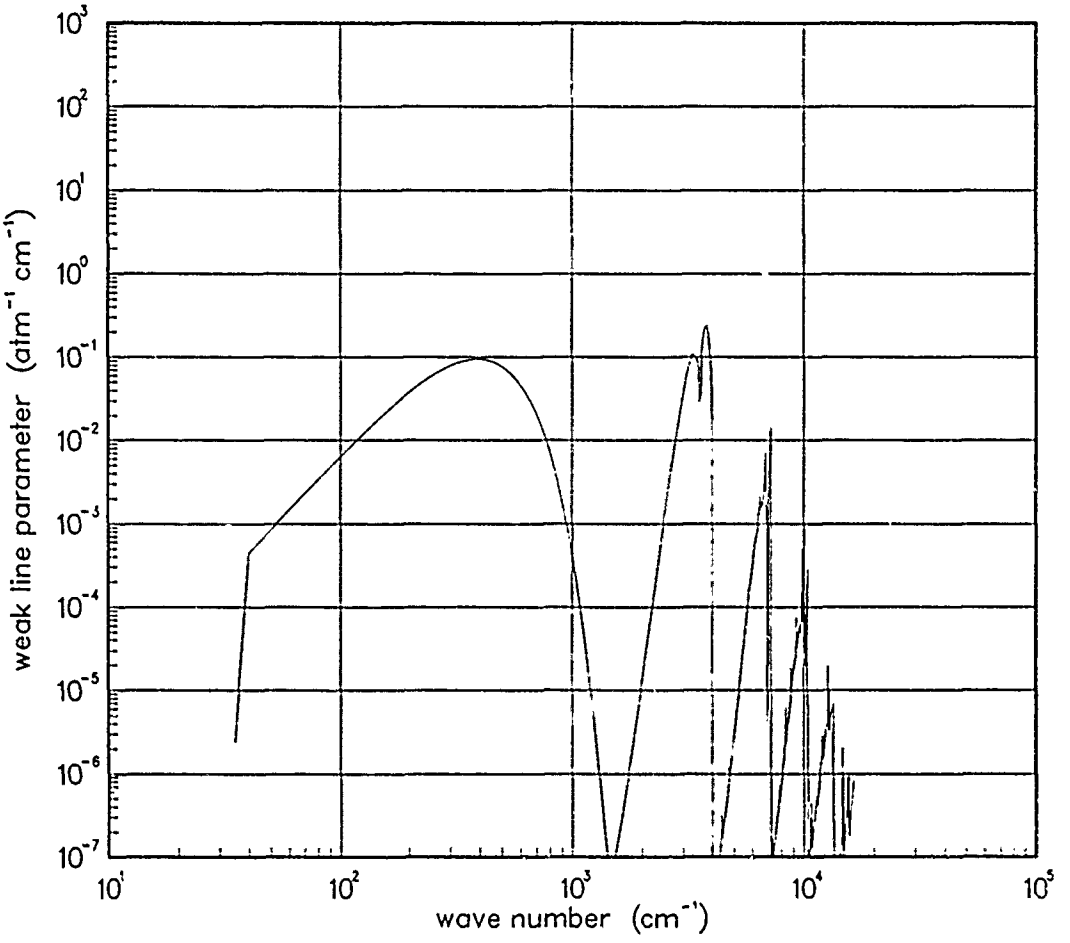

Figure 40. Weak-line parameter for OH at 2000°K.

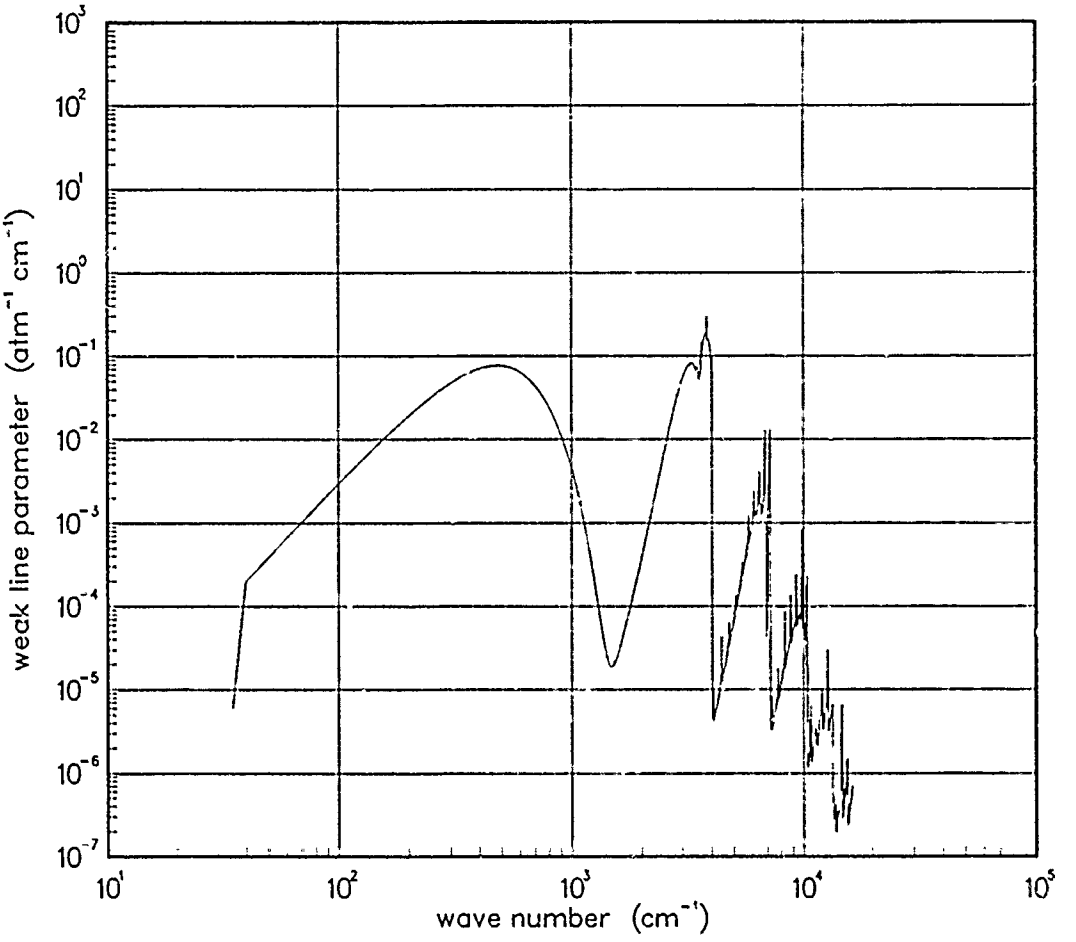

Figure 41. Weak-line parameter for OH at 3000°K.

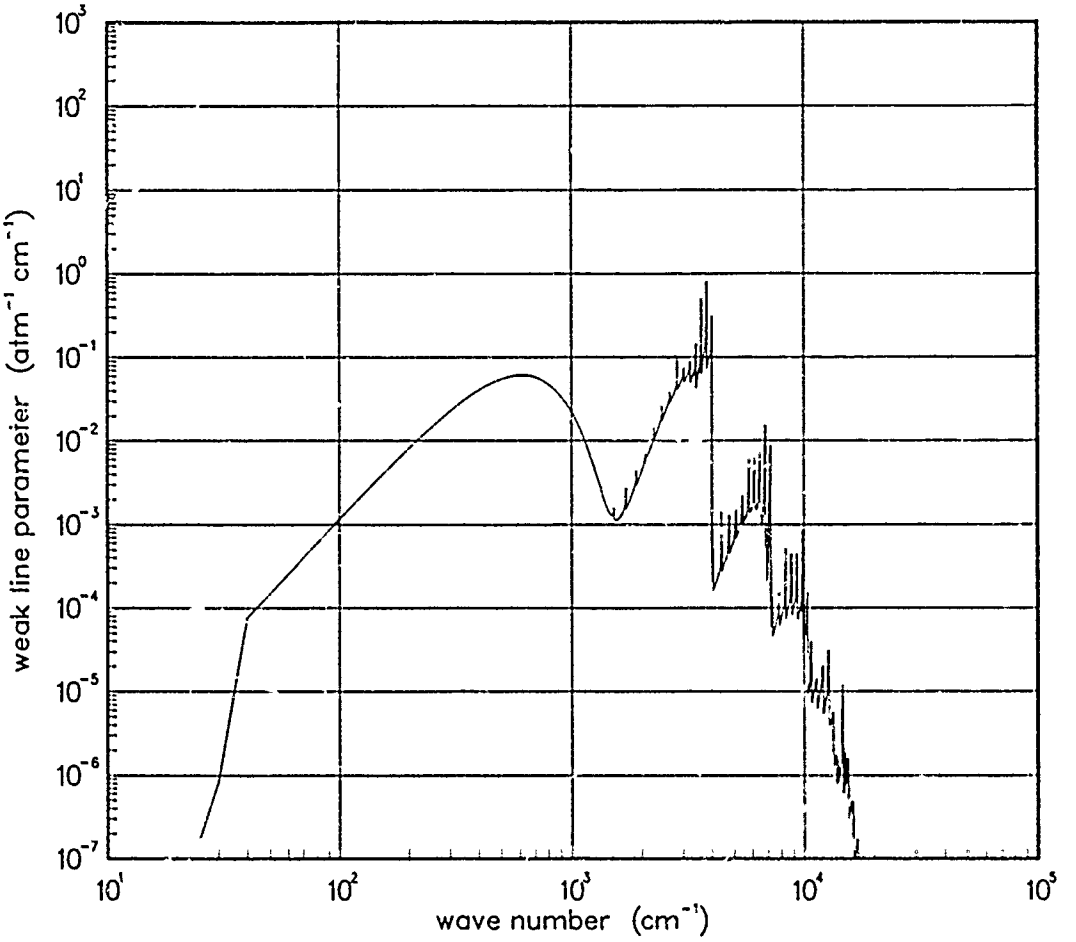

Figure 42. Weak-line parameter for OH at 5000°K.

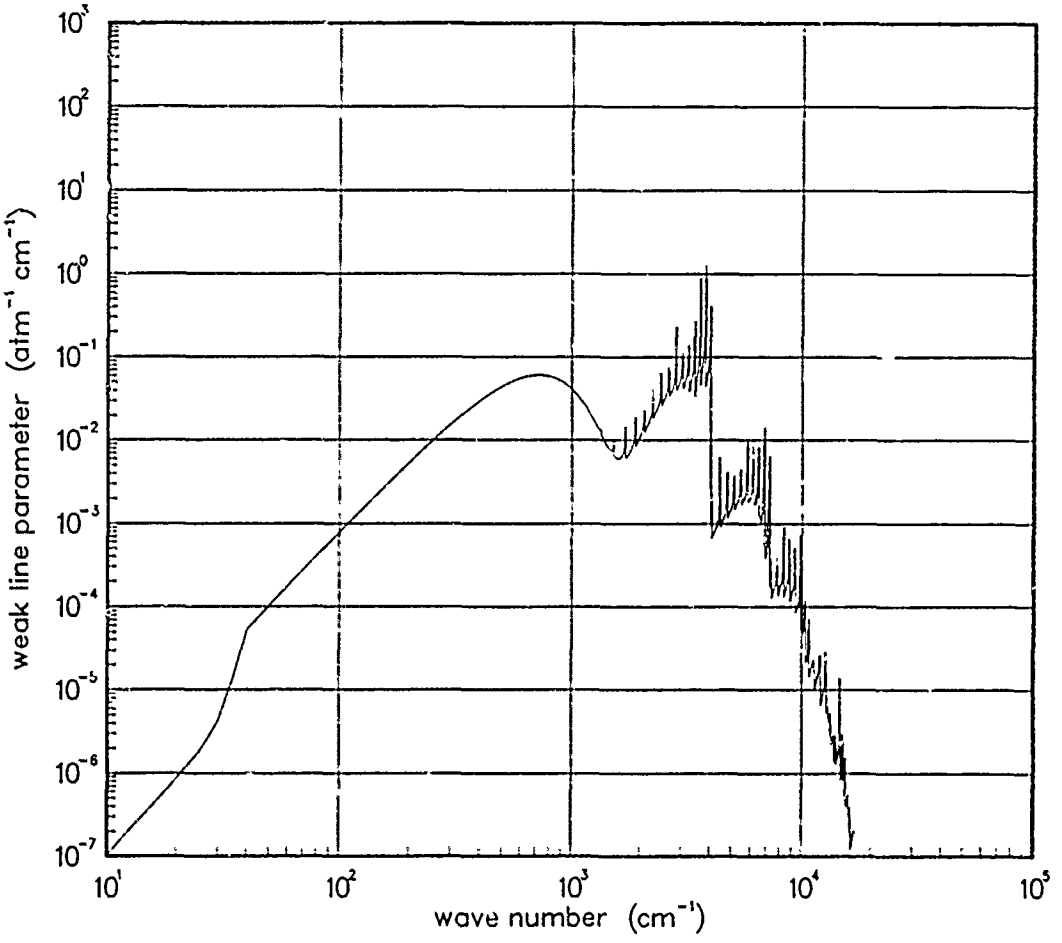

Figure 43. Weak-line parameter for OH at 7000°K.

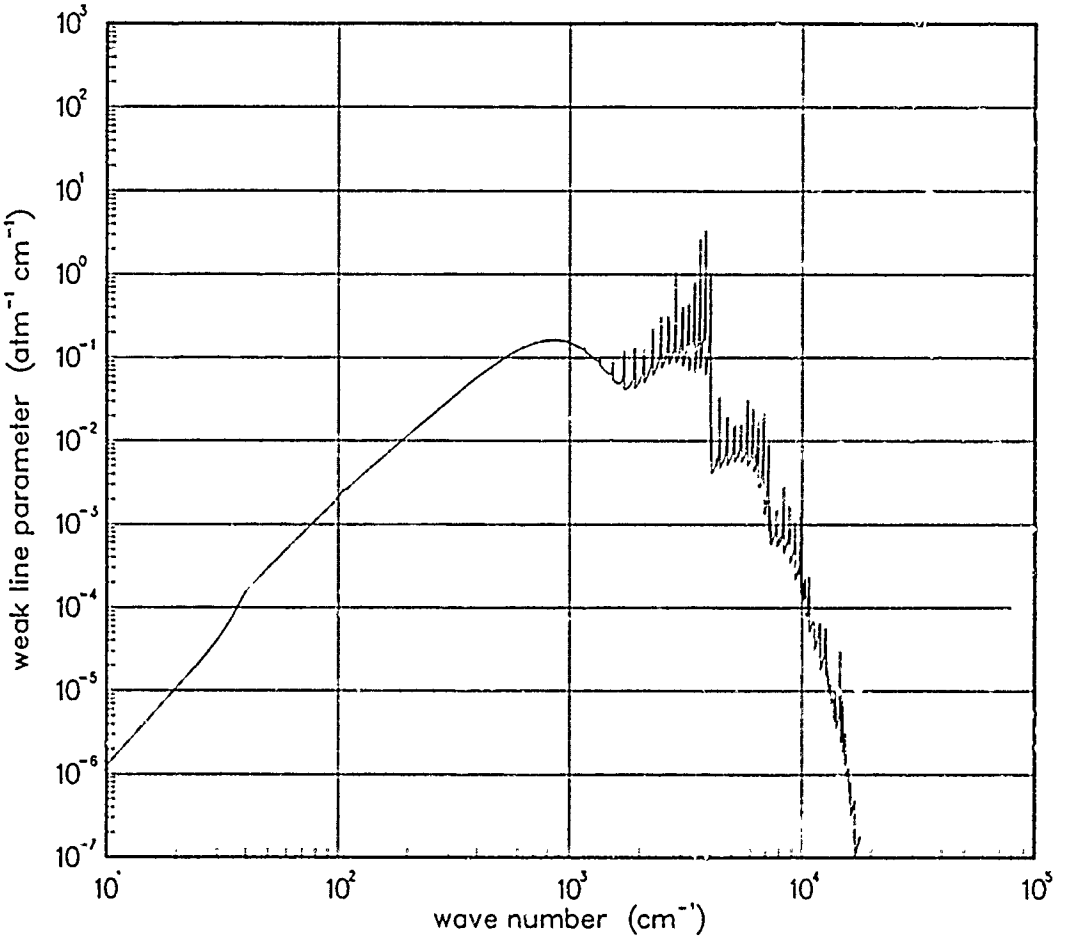

Figure 44. Weak-line parameter for OH at 10000°K.

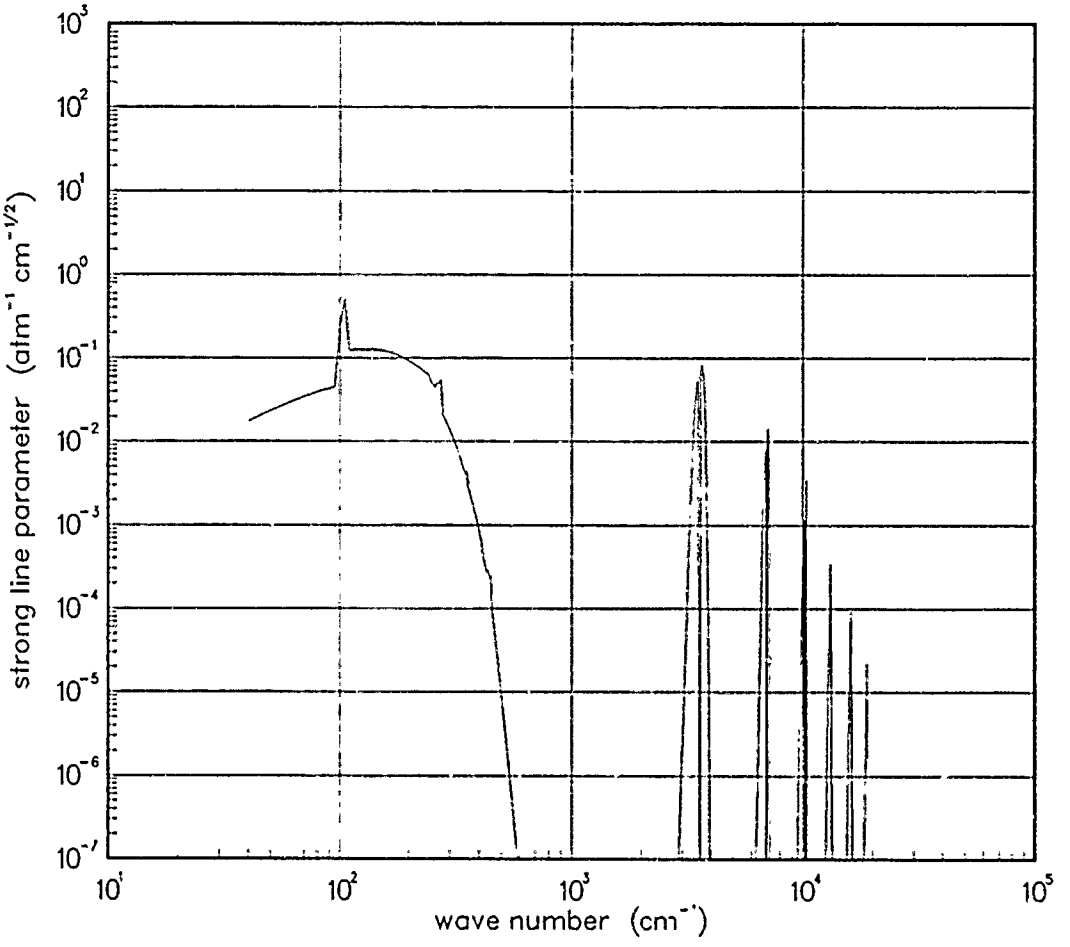

Figure 45. Strong-line parameter for OH at 200°K.

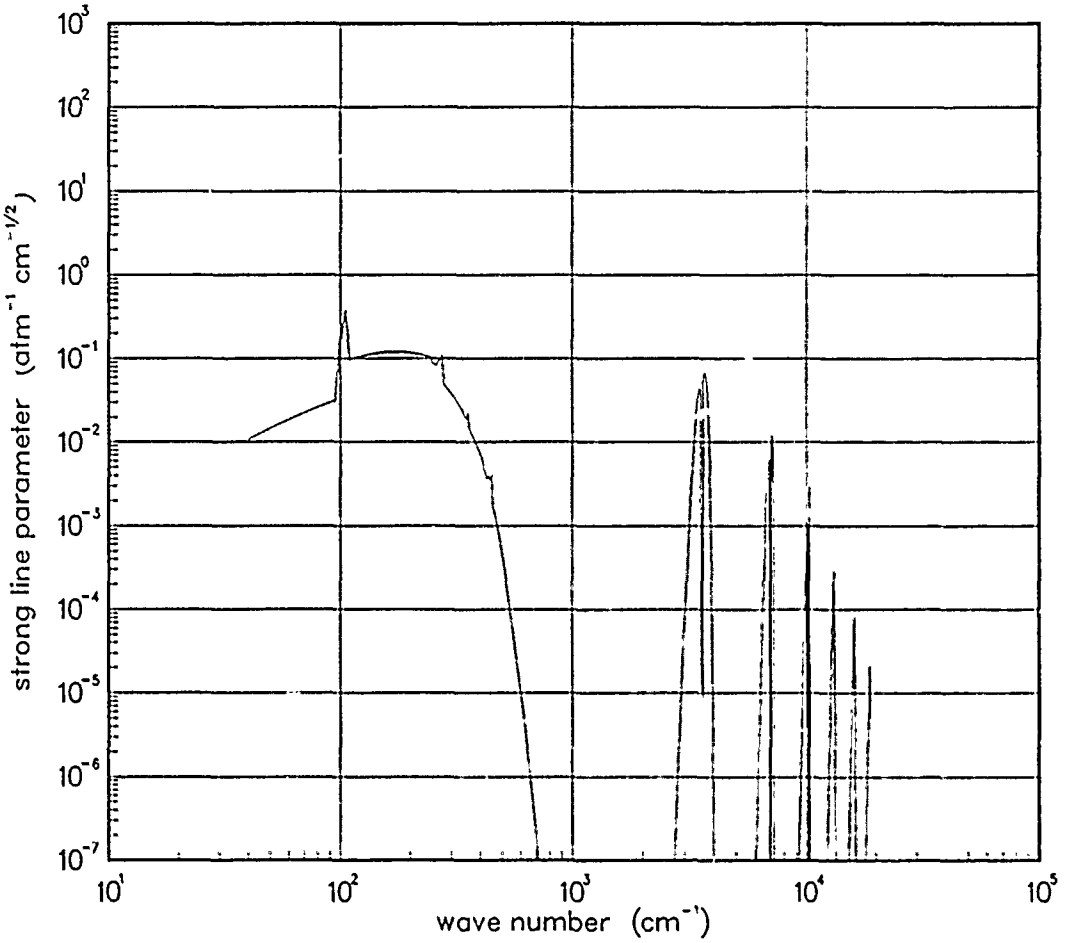

Figure 46. Strong-line parameter for OH at 300°K.

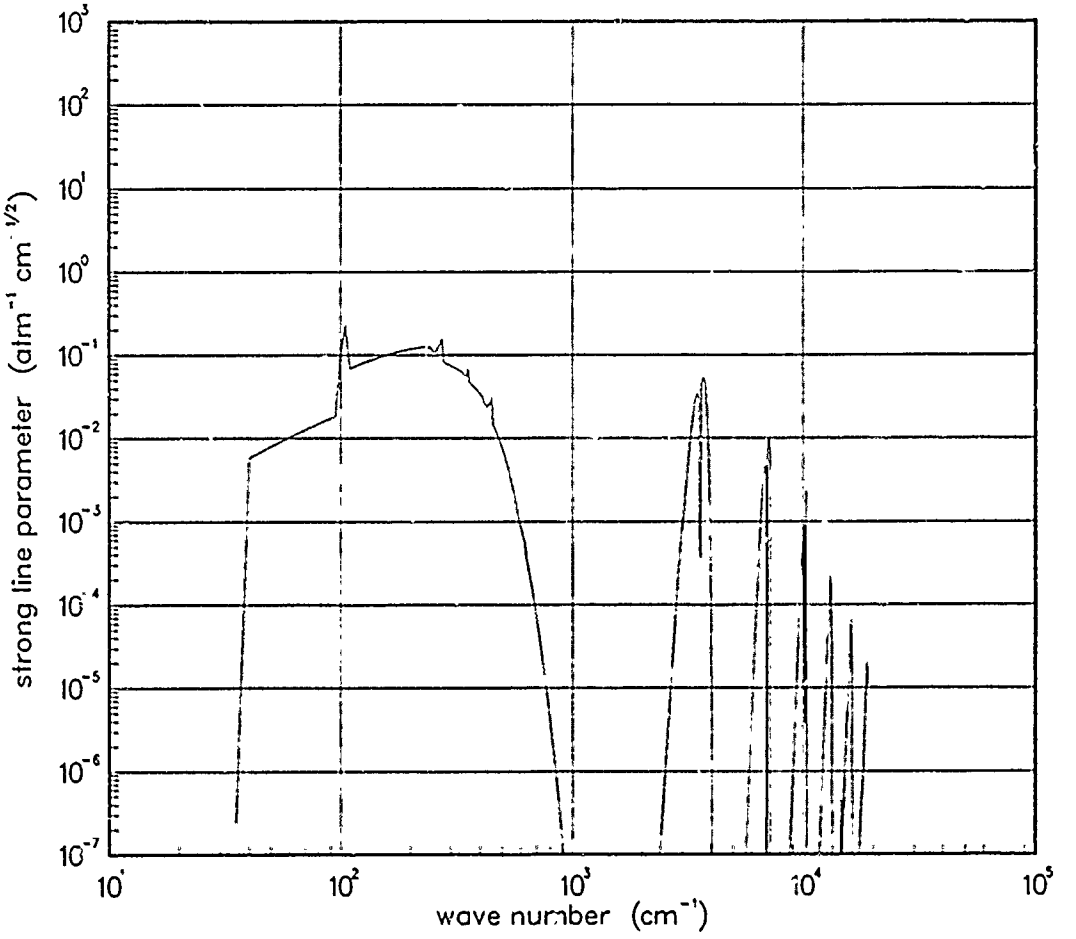

Figure 47. Strong-line parameter for OH at 500°K.

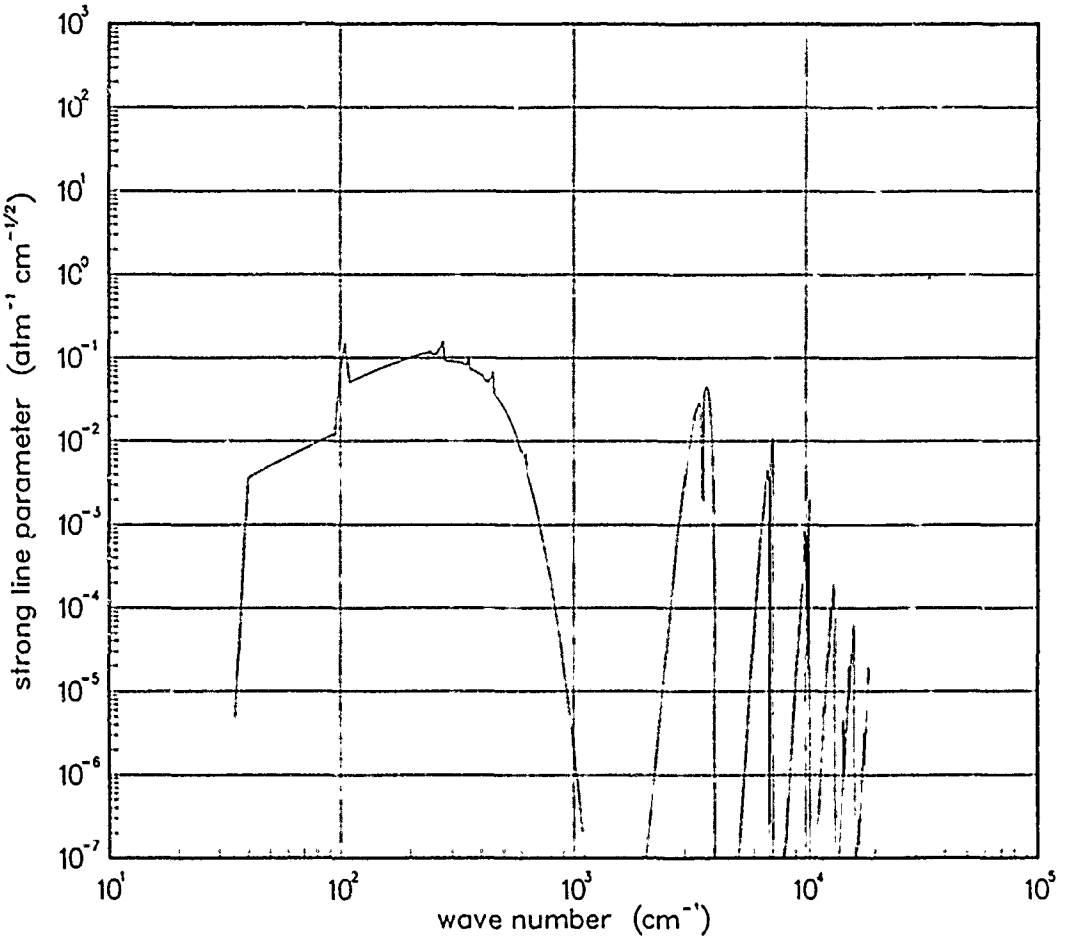

Figure 48. Strong-line parameter for OH at 750°K.

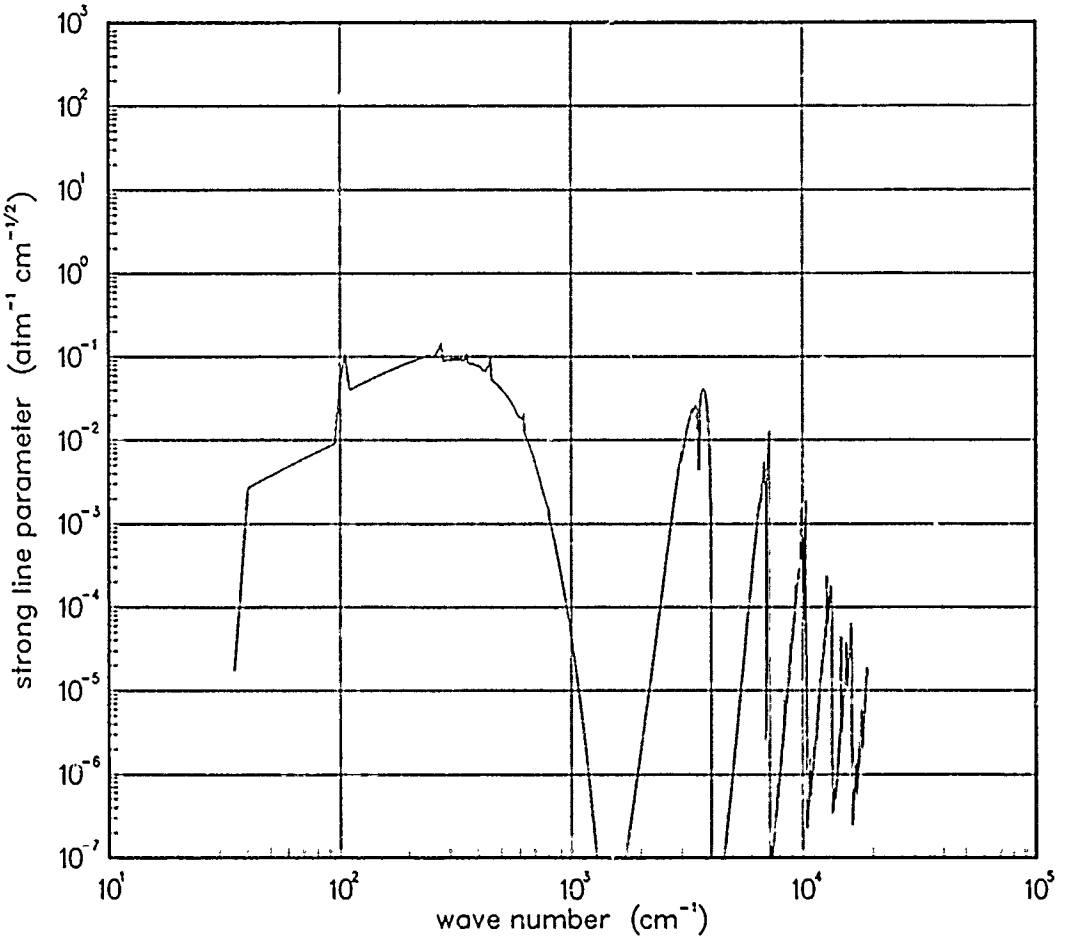

Figure 49. Strong-line parameter for OH at 1000°K.

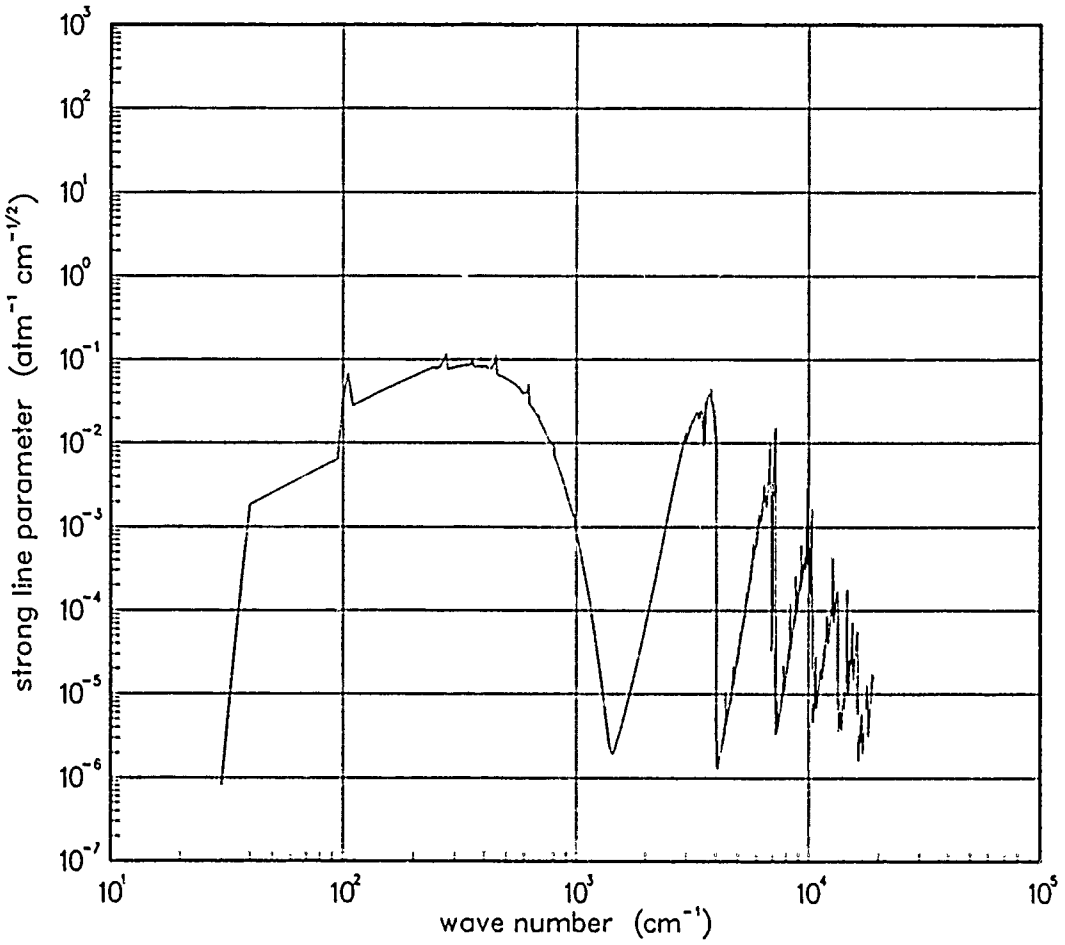

Figure 50. Strong-line parameter for OH at 1500°K.

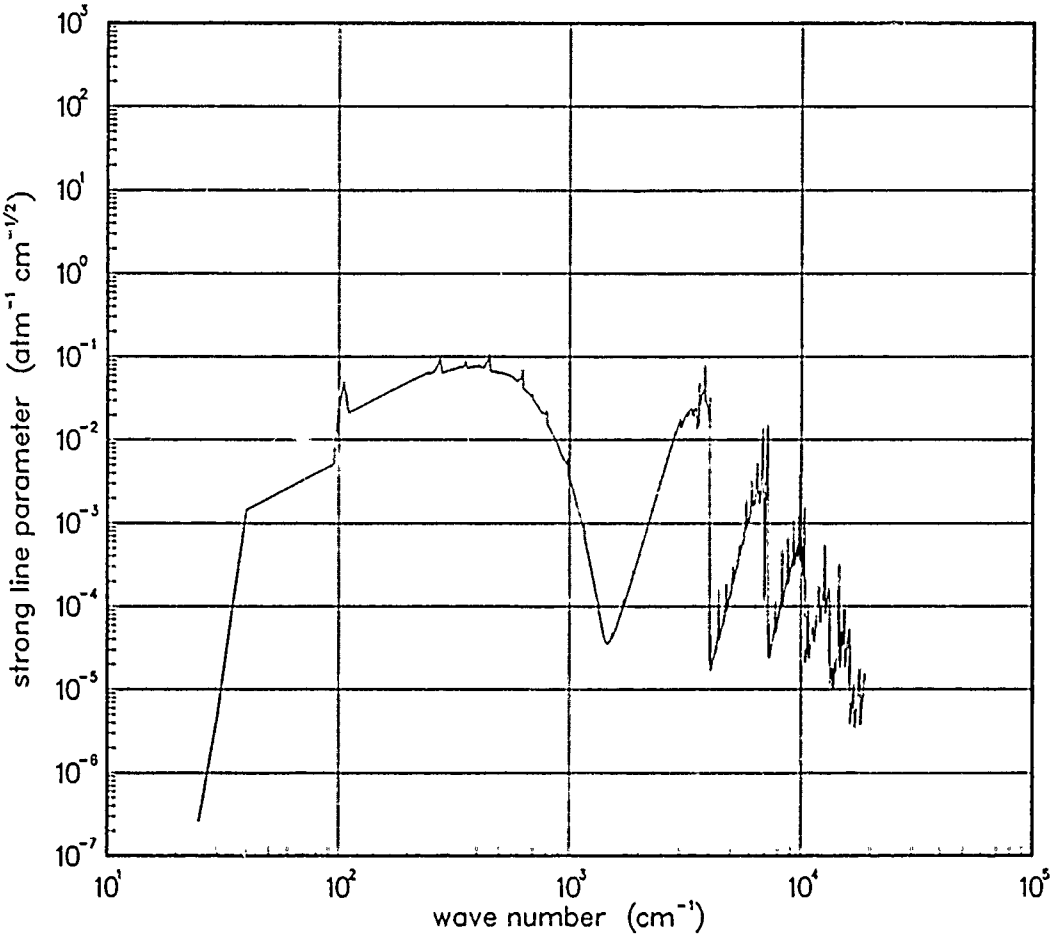

Figure 51. Strong-line parameter for OH at 2000°K.

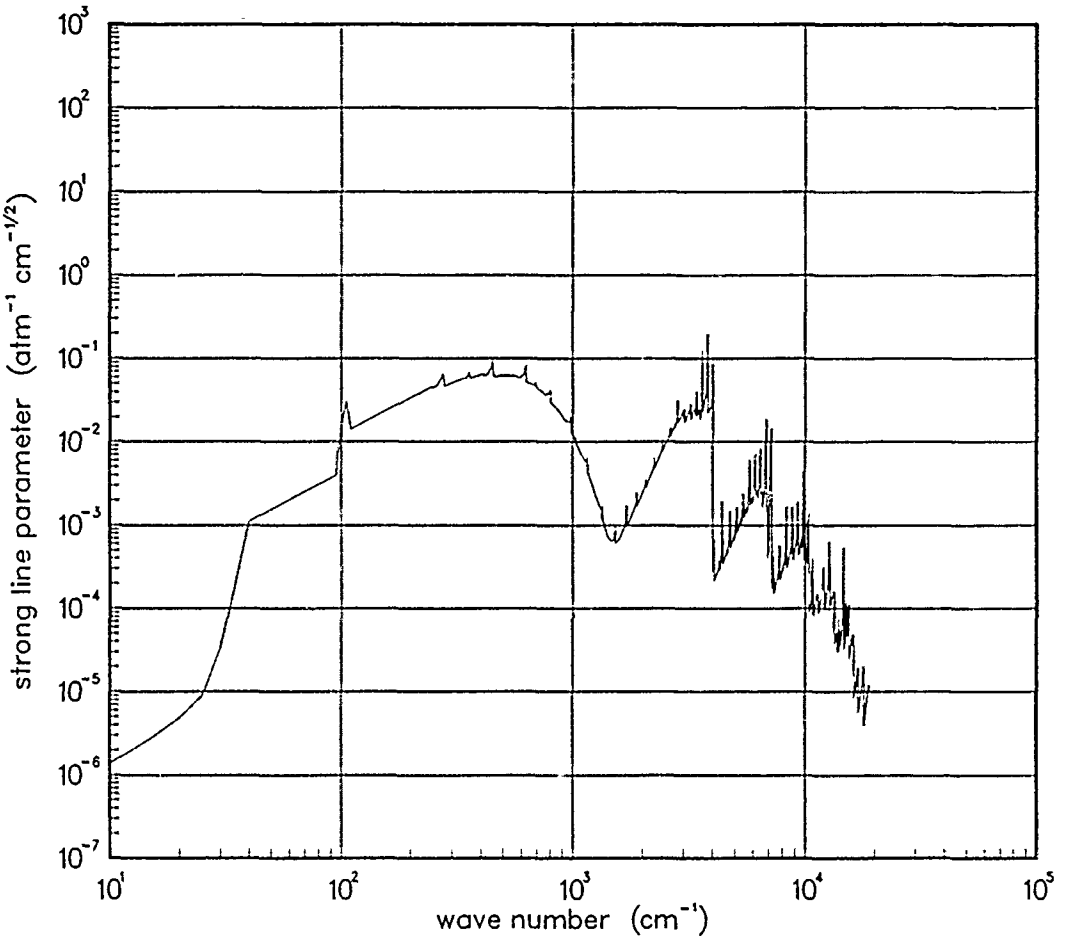

Figure 52. Strong-line parameter for OH at 3000°K.

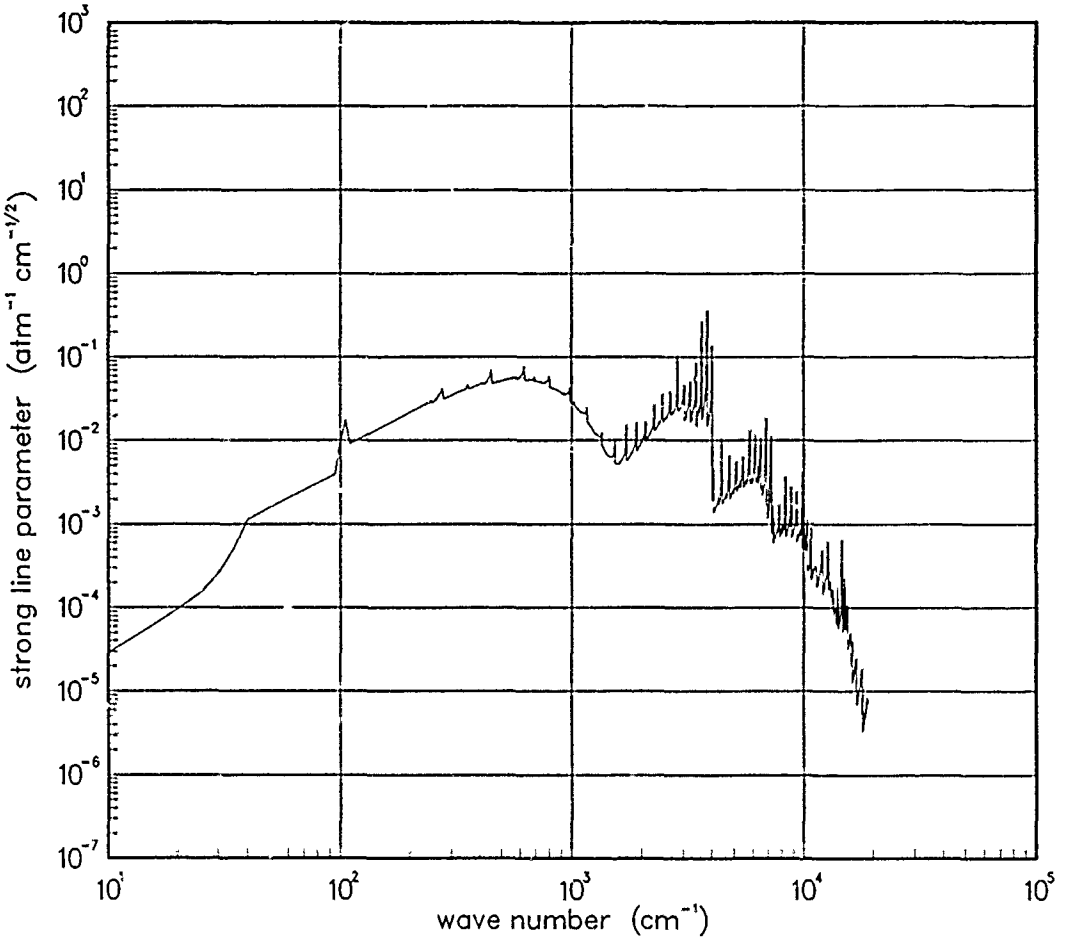

Figure 53. Strong-line parameter for OH at 5000°K.

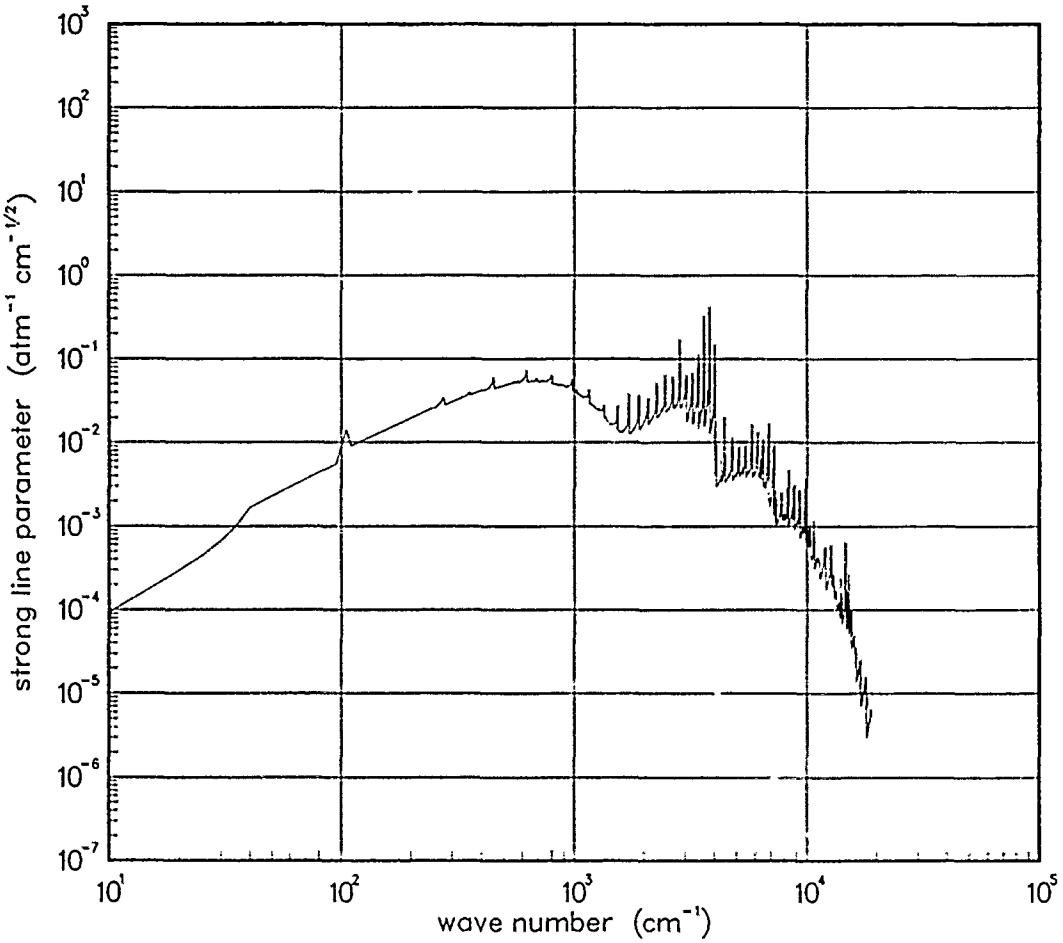

Figure 54. Strong-line parameter for OH at 7000°K.

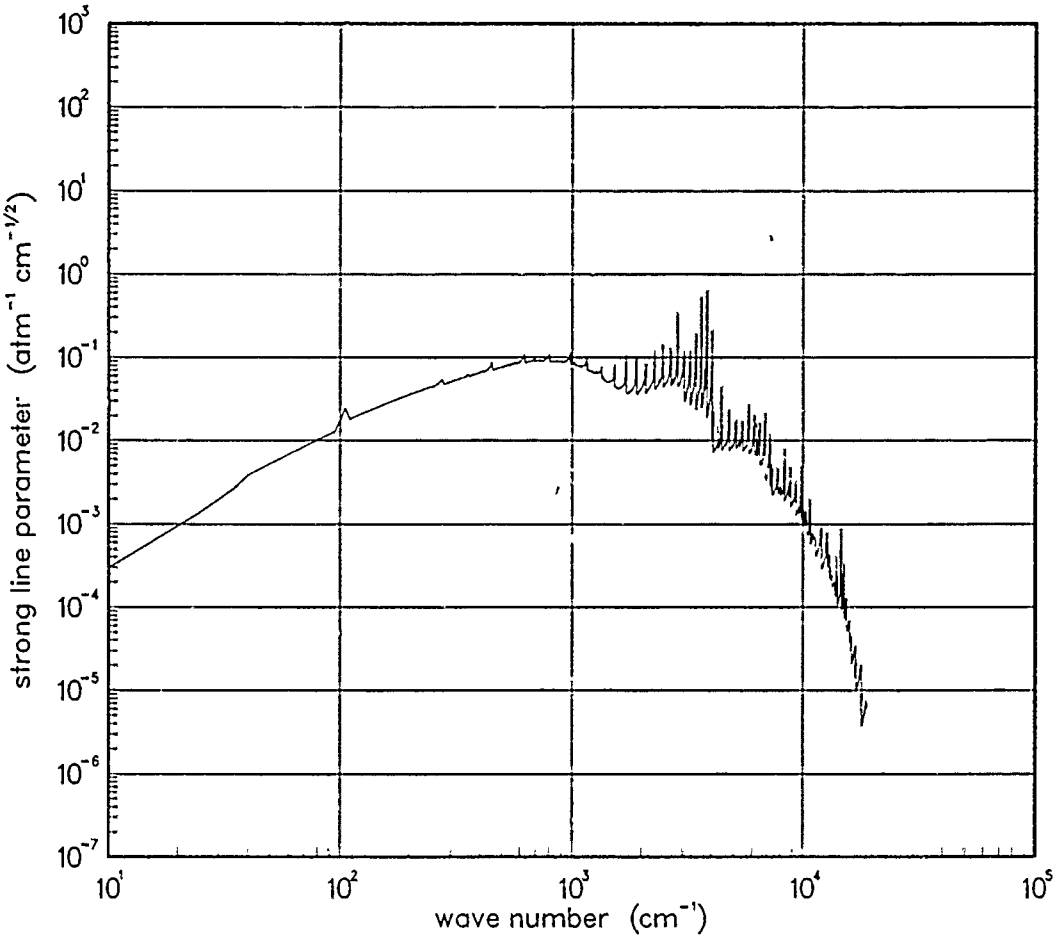

Figure 55. Strong-line parameter for OH at 10000°K.

4.3 NITROGEN (N_2).

The Nitrogen species were calculated by the VisiDyne* Corporation from the RADFLO opacity data base developed by the Air Force Weapons Laboratory in the late sixties. Data for the weak-line parameter for N_2 and N_2^+ in the visible region (5,000 cm^{-1} - 100,000 cm^{-1}) is available. There is no inverse line spacing information available in this region.

Data Source:

*H. Smith, T. Keneshea, VisiDyne Corporation, private communication (1986).

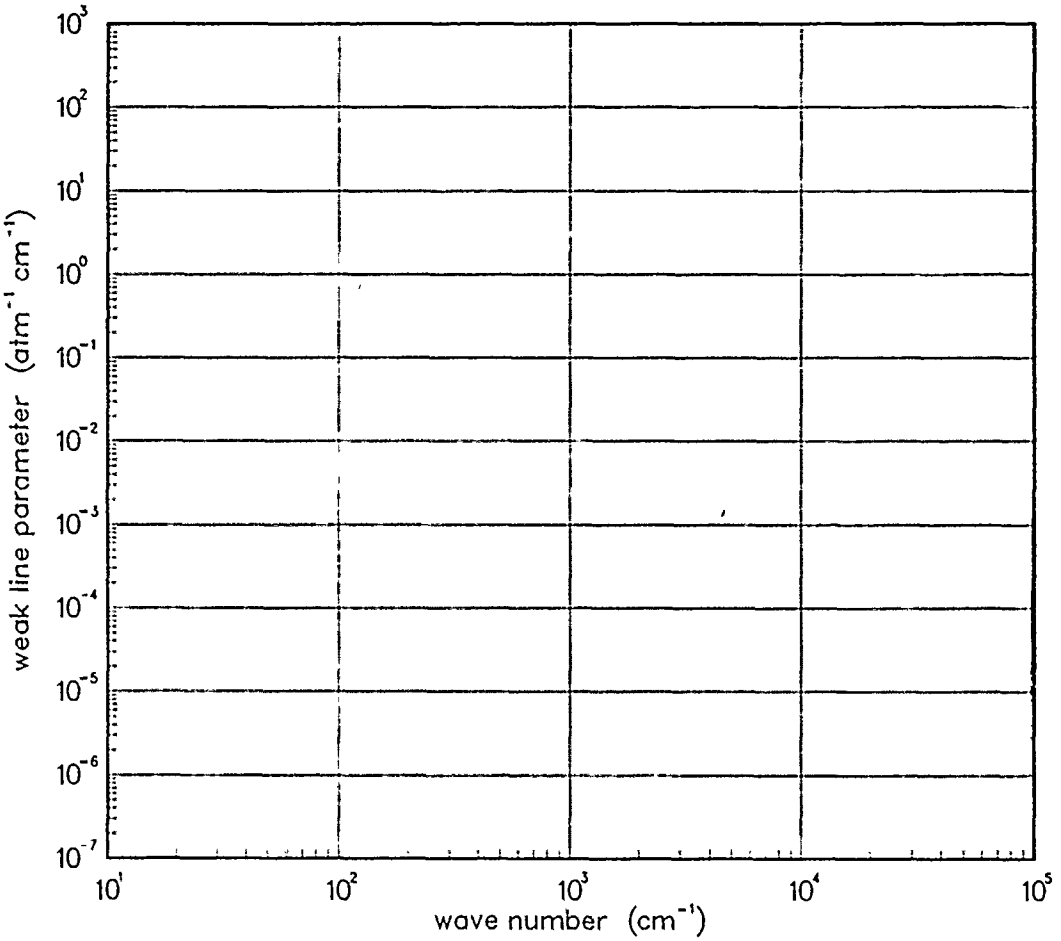

Figure 56. Weak-line parameter for N_2 at 500°K.

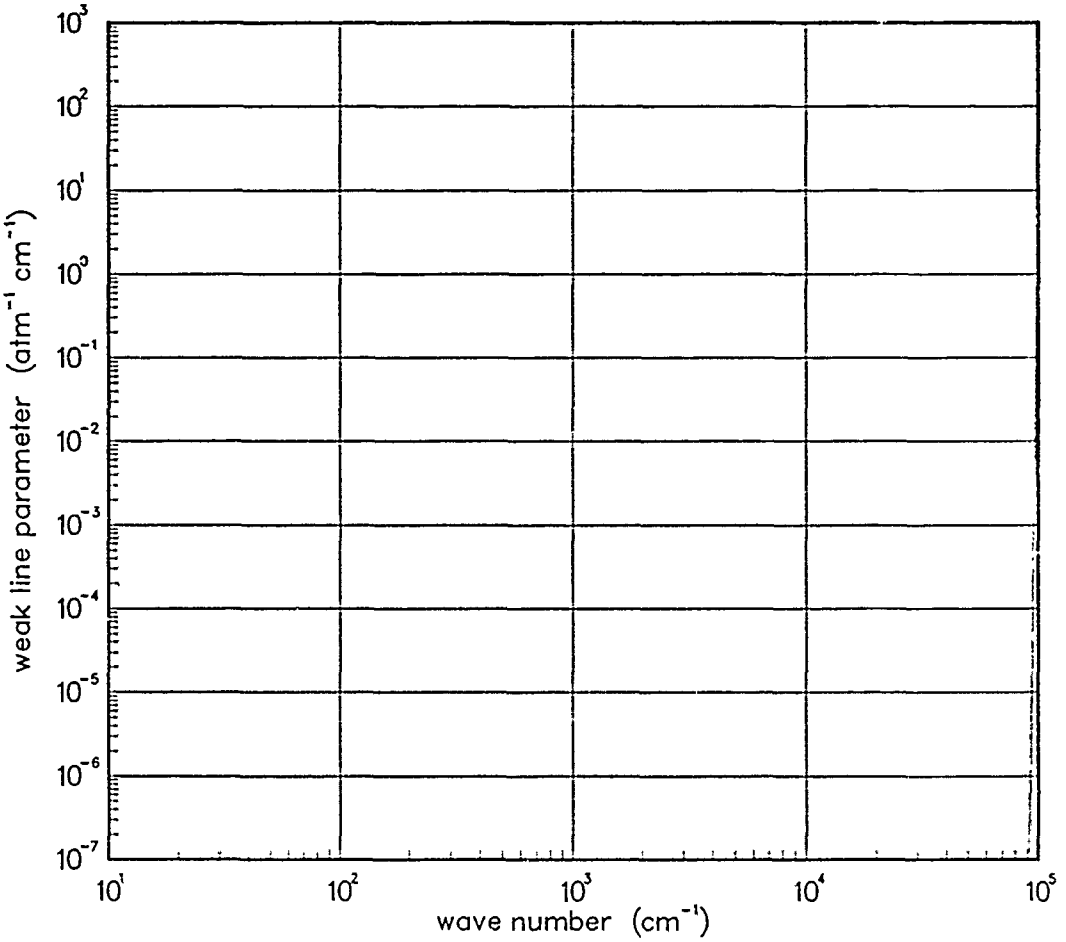

Figure 57. Weak-line parameter for N_2 at 750°K.

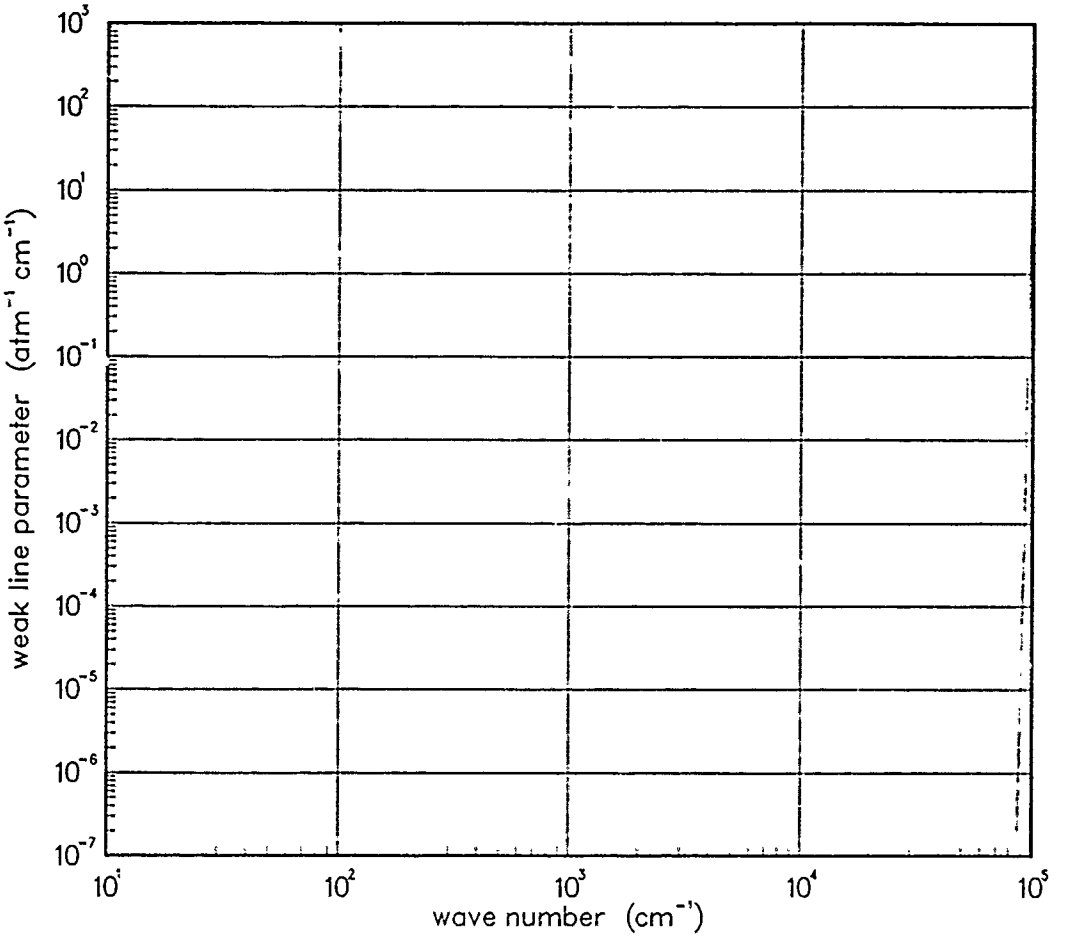

Figure 58. Weak-line parameter for N_2 at 1000°K.

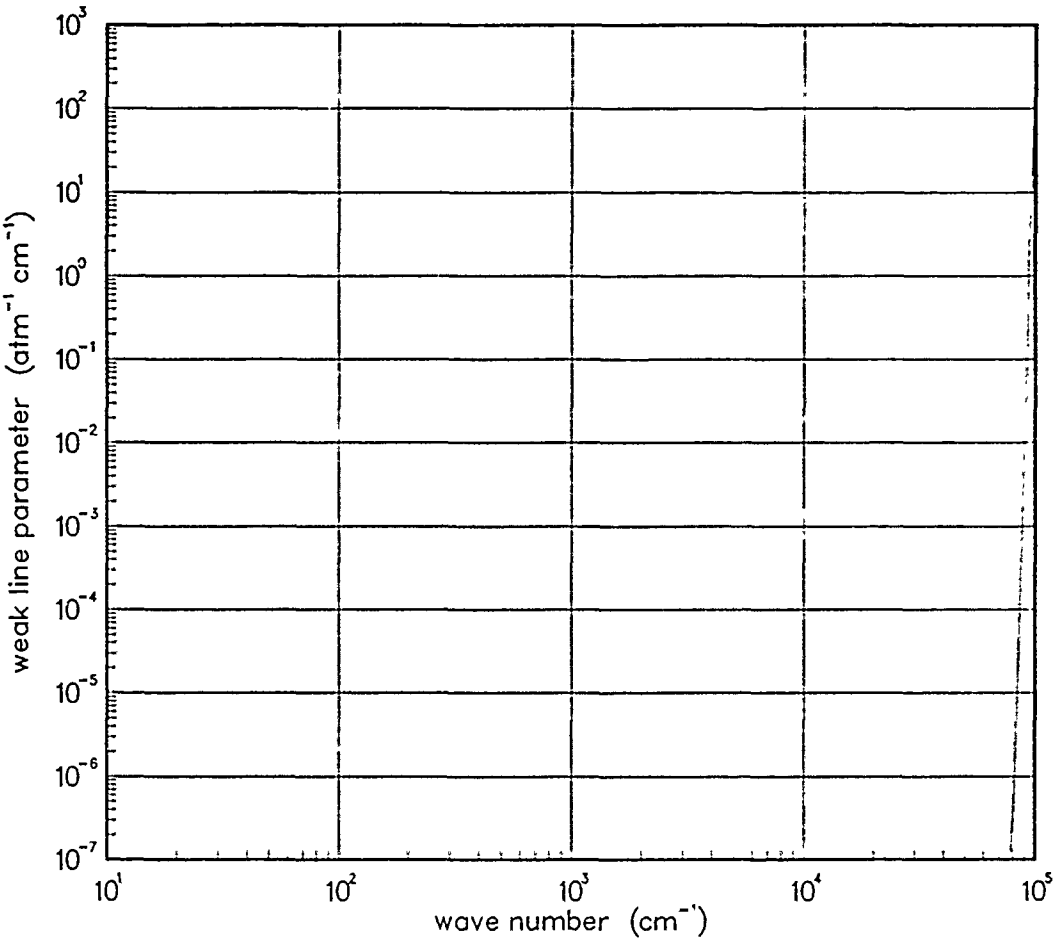

Figure 59. Weak-line parameter for N_2 at 1500°K.

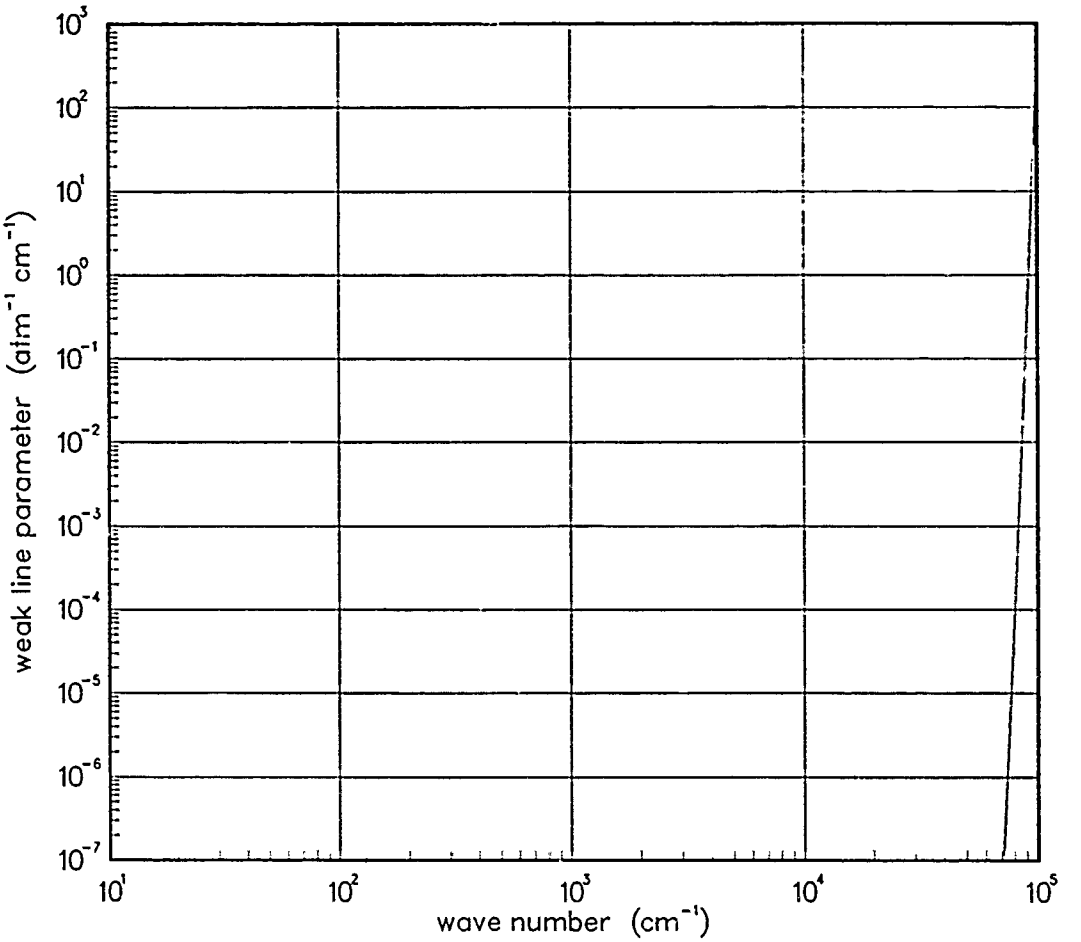

Figure 60. Weak-line parameter for N_2 at 2000°K.

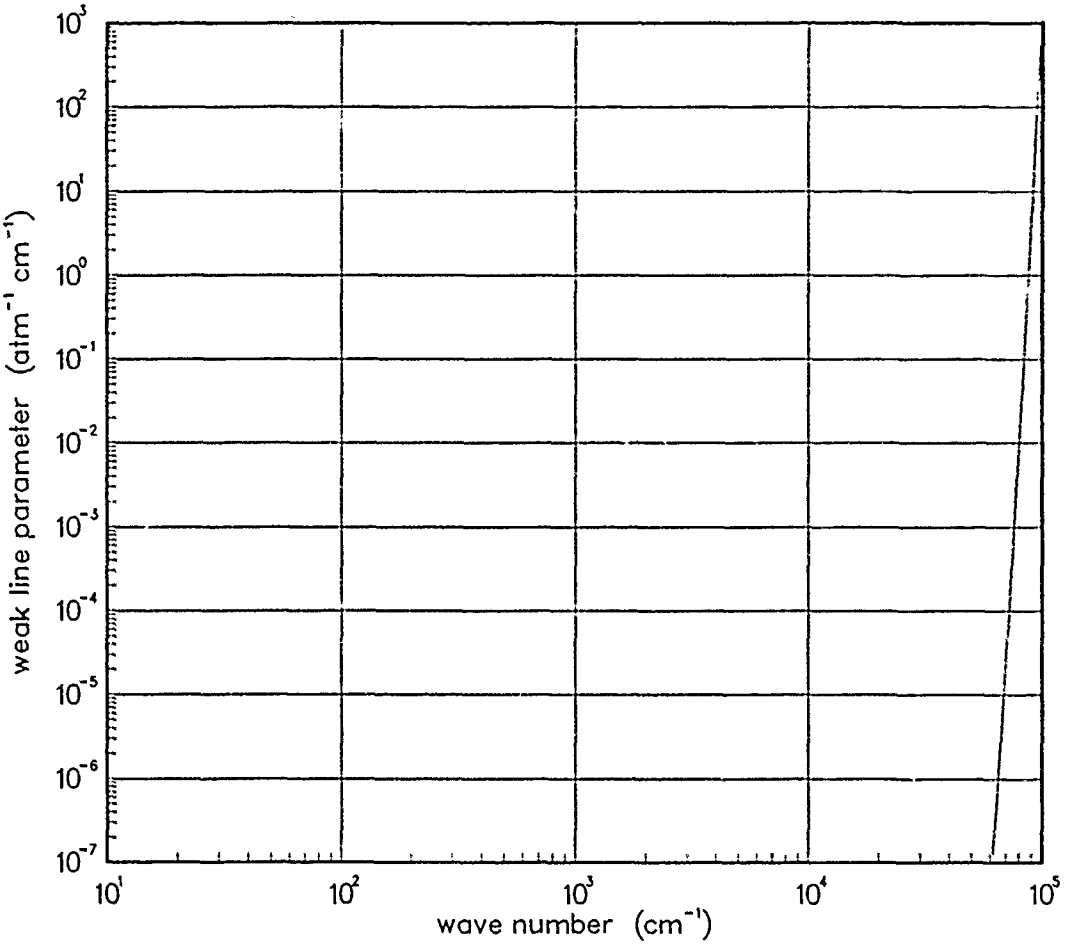

Figure 61. Weak-line parameter for N_2 at 3000°K.

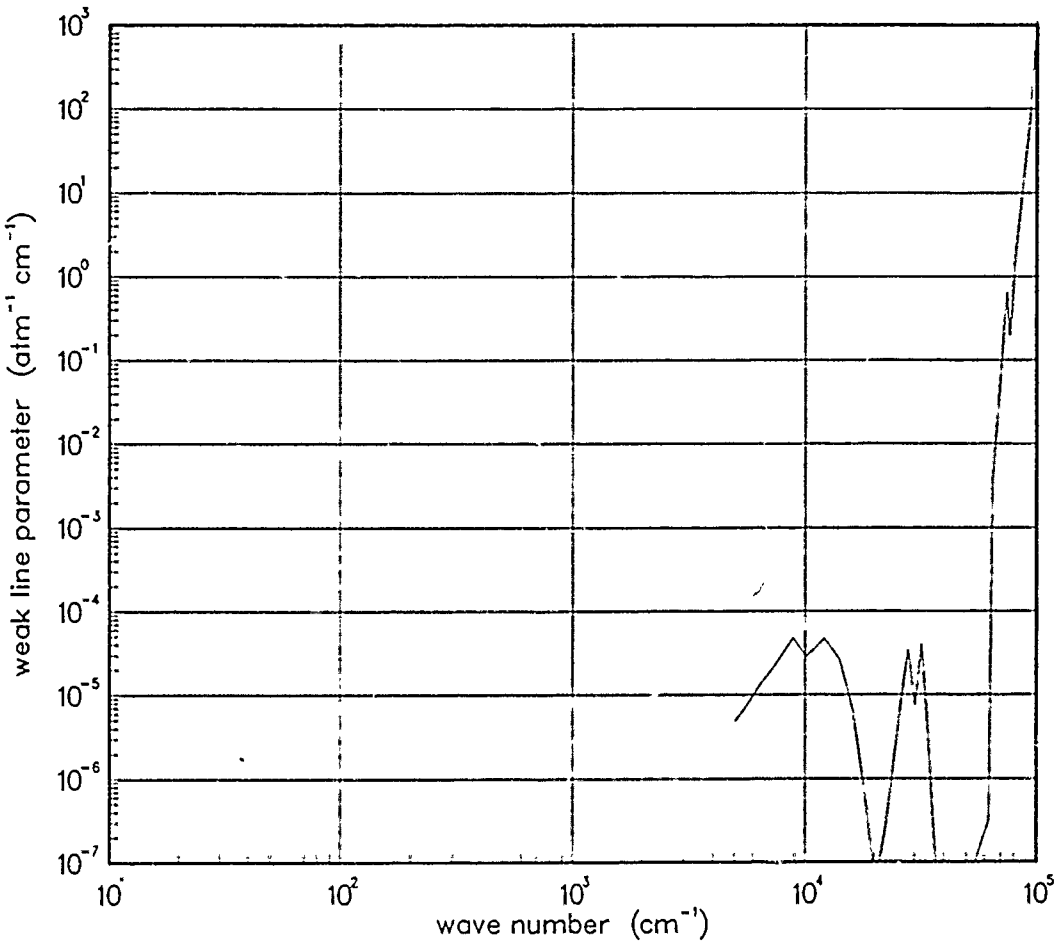

Figure 62. Weak-line parameter for N_2 at 5000°K.

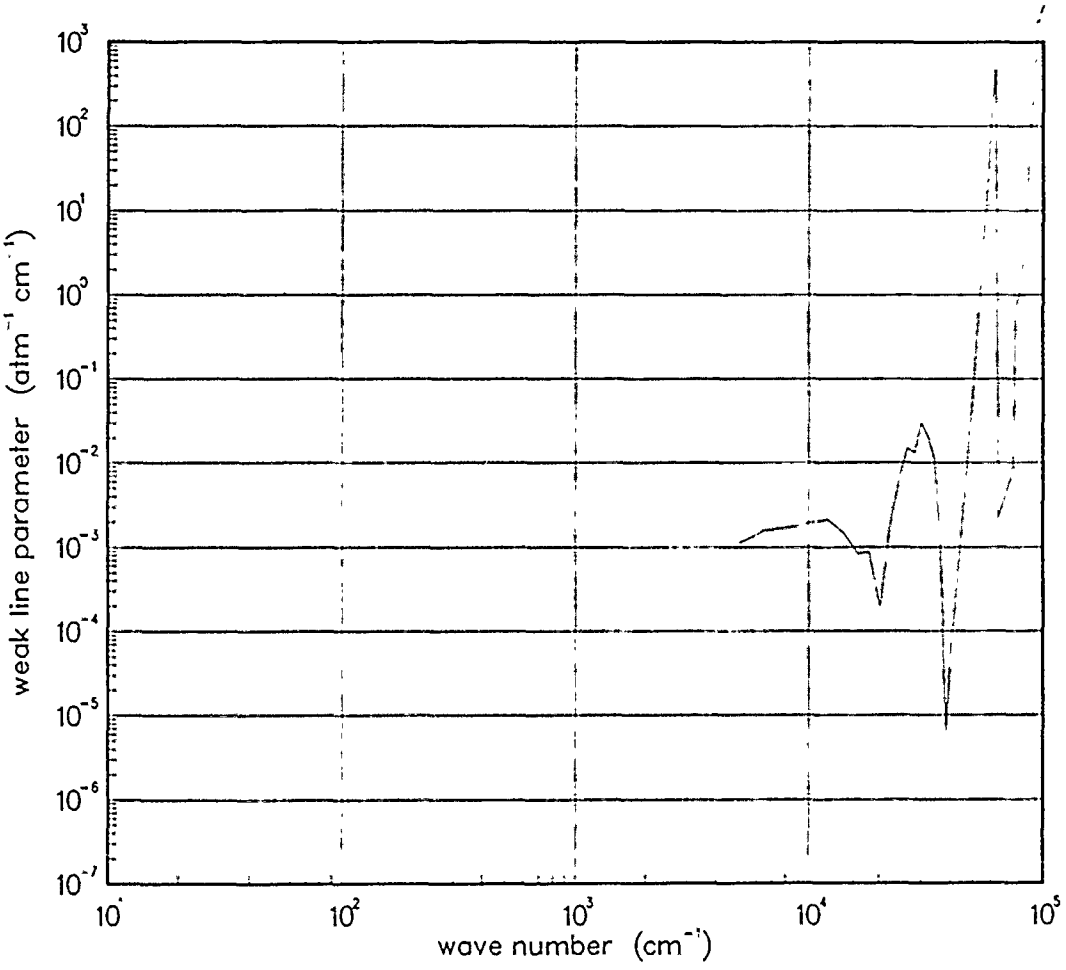

Figure 63. Weak-line parameter for N_2 at 7000°K.

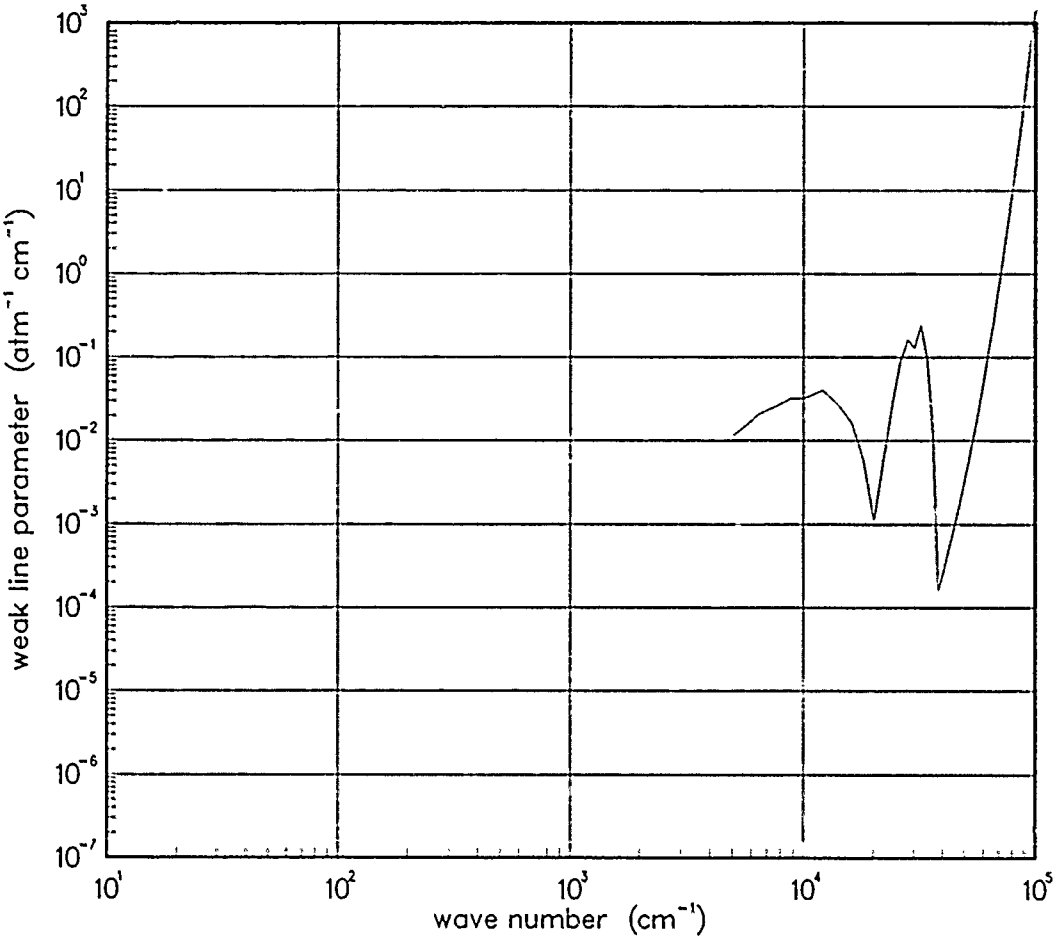

Figure 64. Weak-line parameter for N_2 at 10000°K.

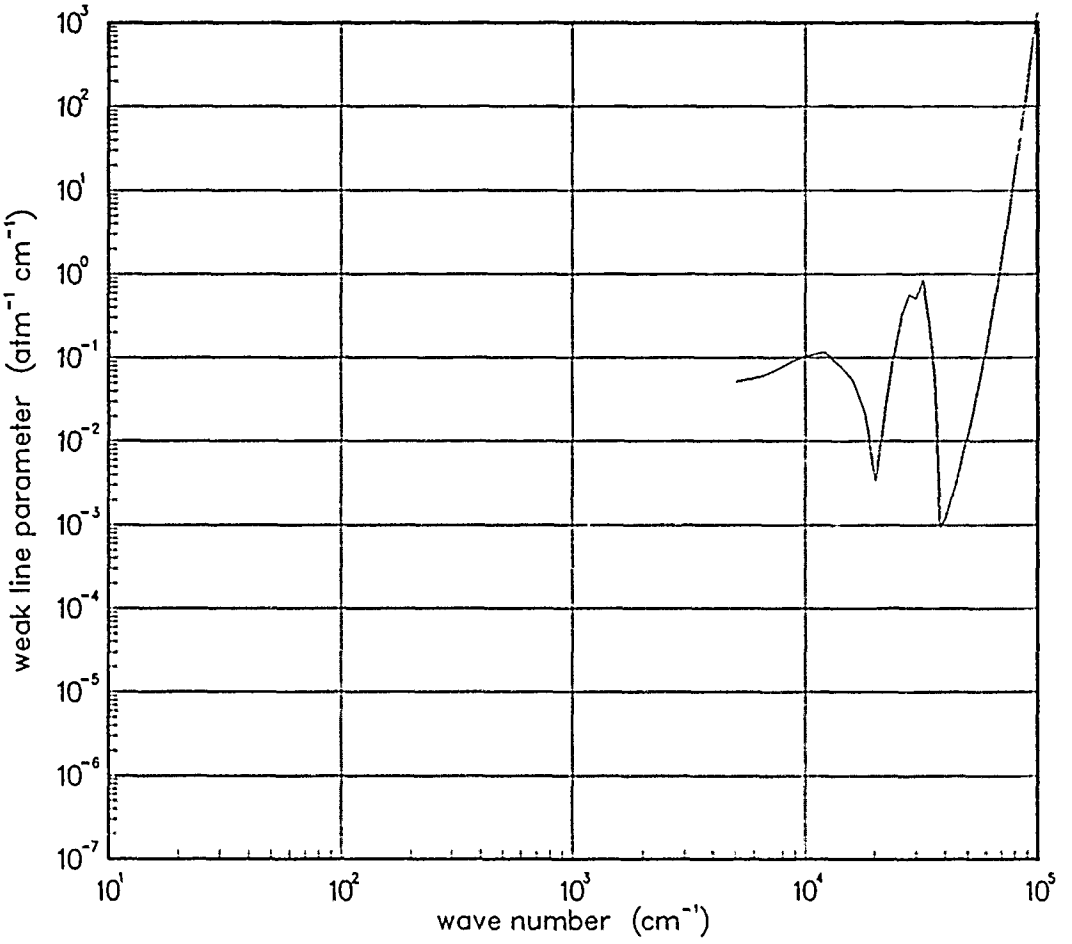

Figure 65. Weak-line parameter for N_2 at 12000°K.

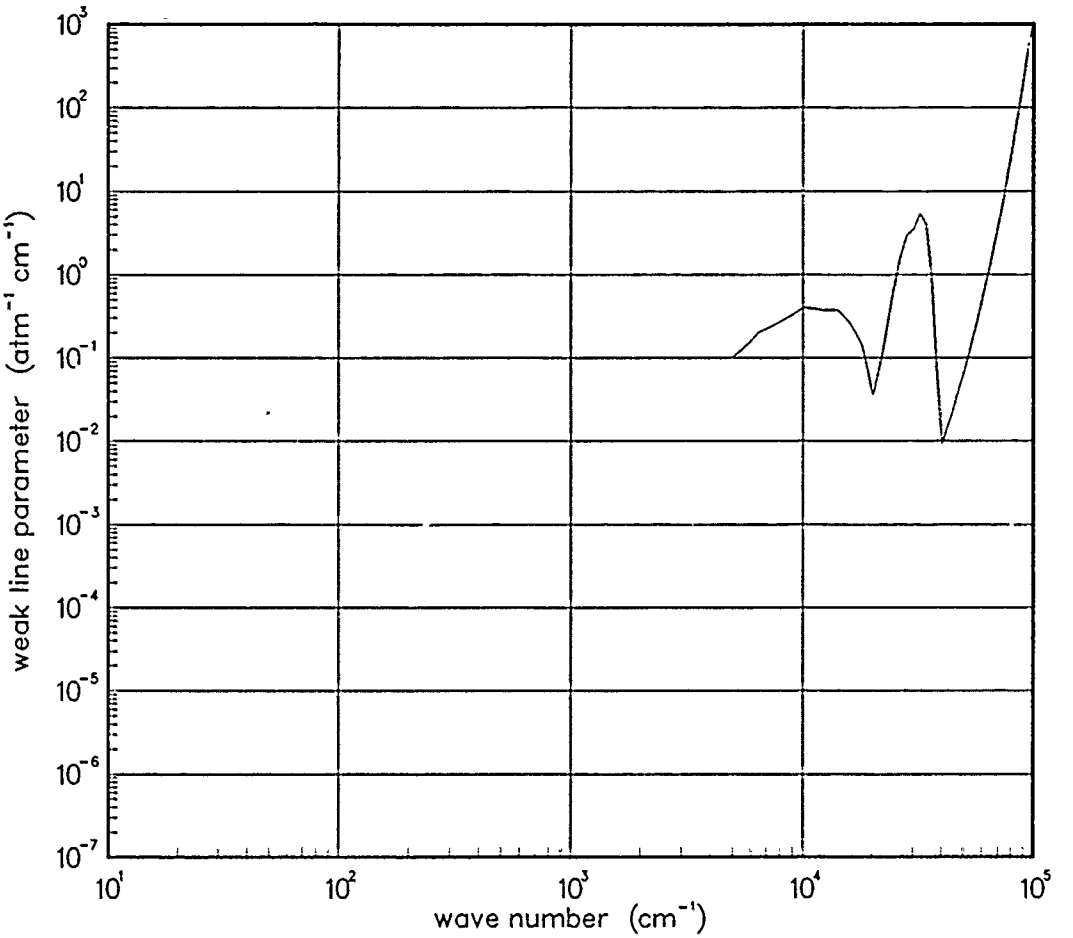

Figure 66. Weak-line parameter for N_2 at 18000°K.

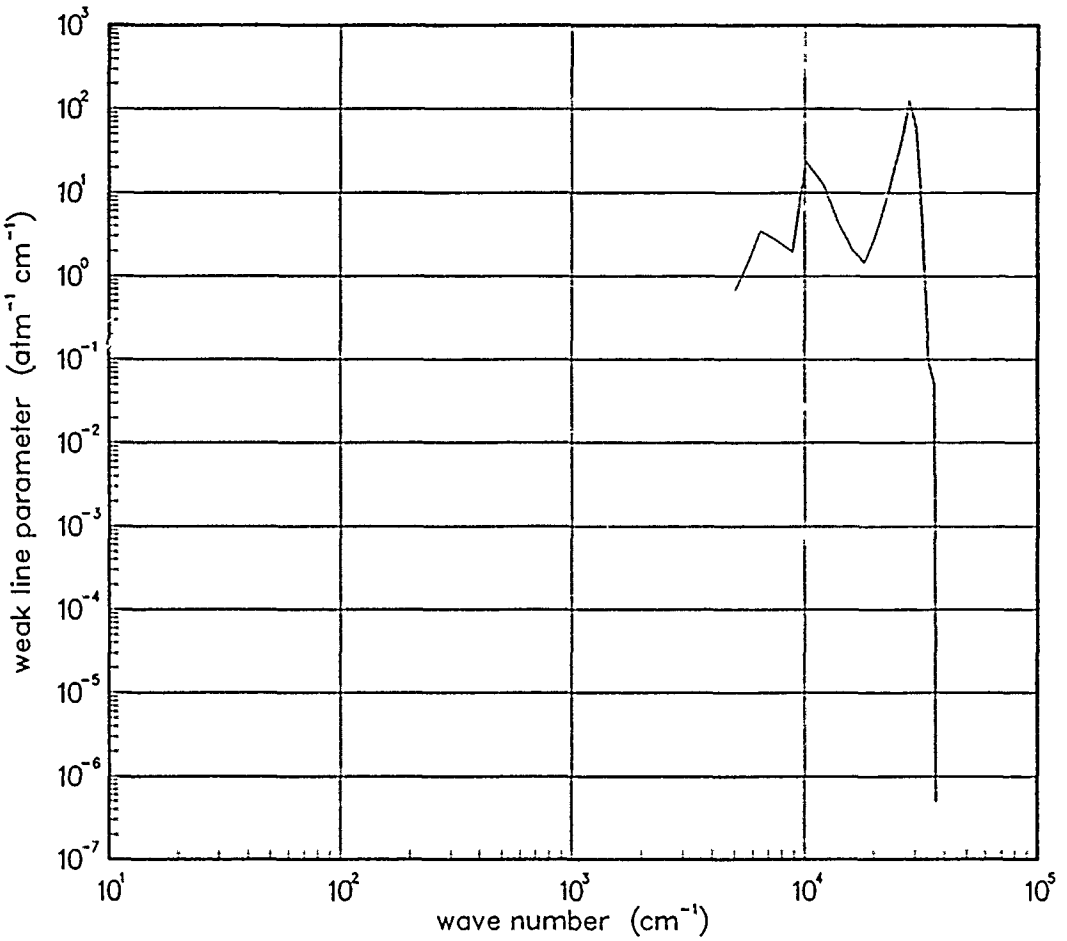

Figure 67. Weak-line parameter for N_2^+ at 5000°K.

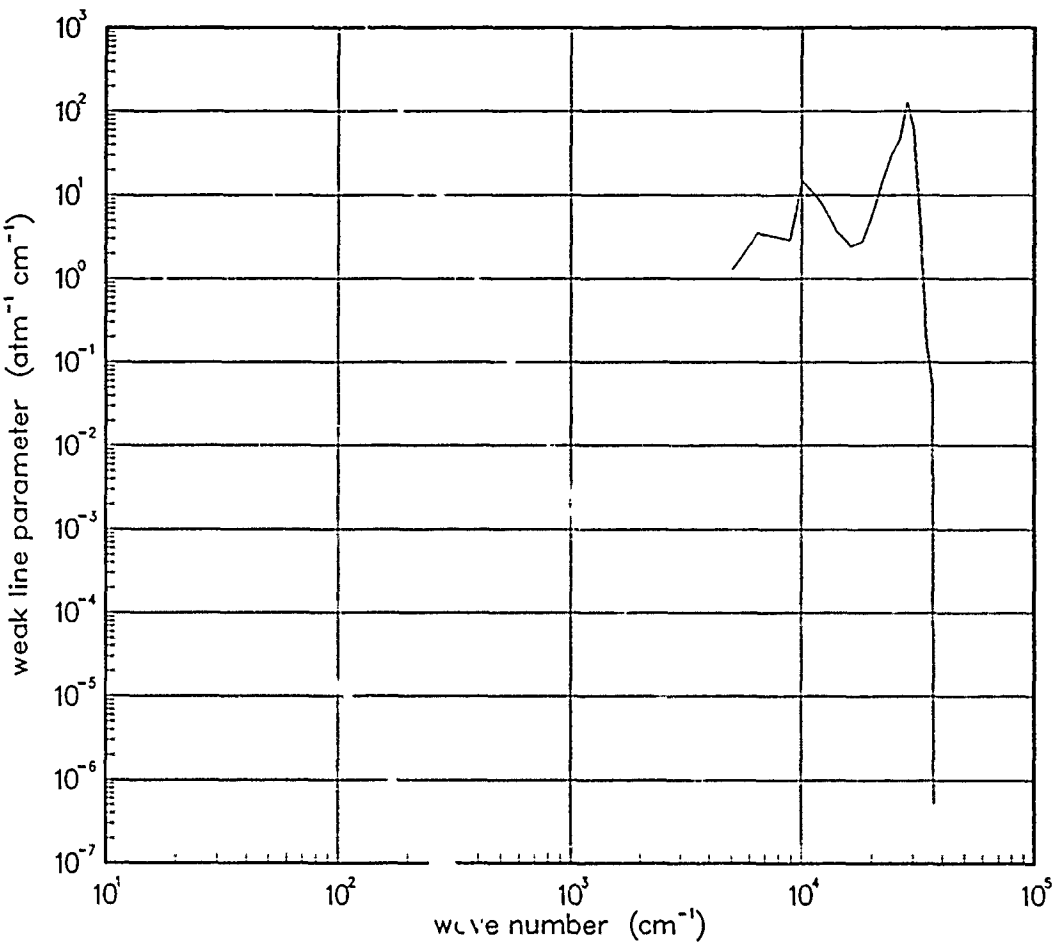

Figure 68. Weak-line parameter for N_2^+ at 7000°K.

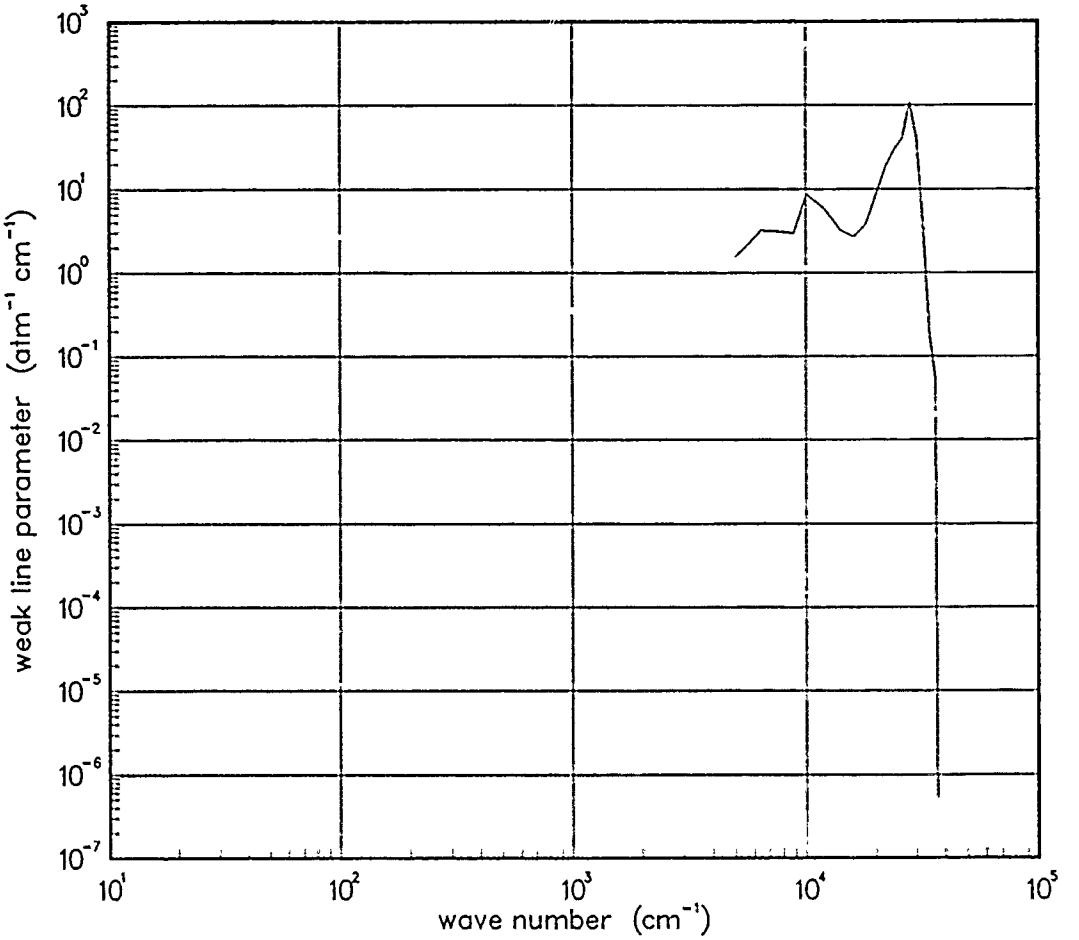

Figure 69. Weak-line parameter for N_2^+ at 10000°K.

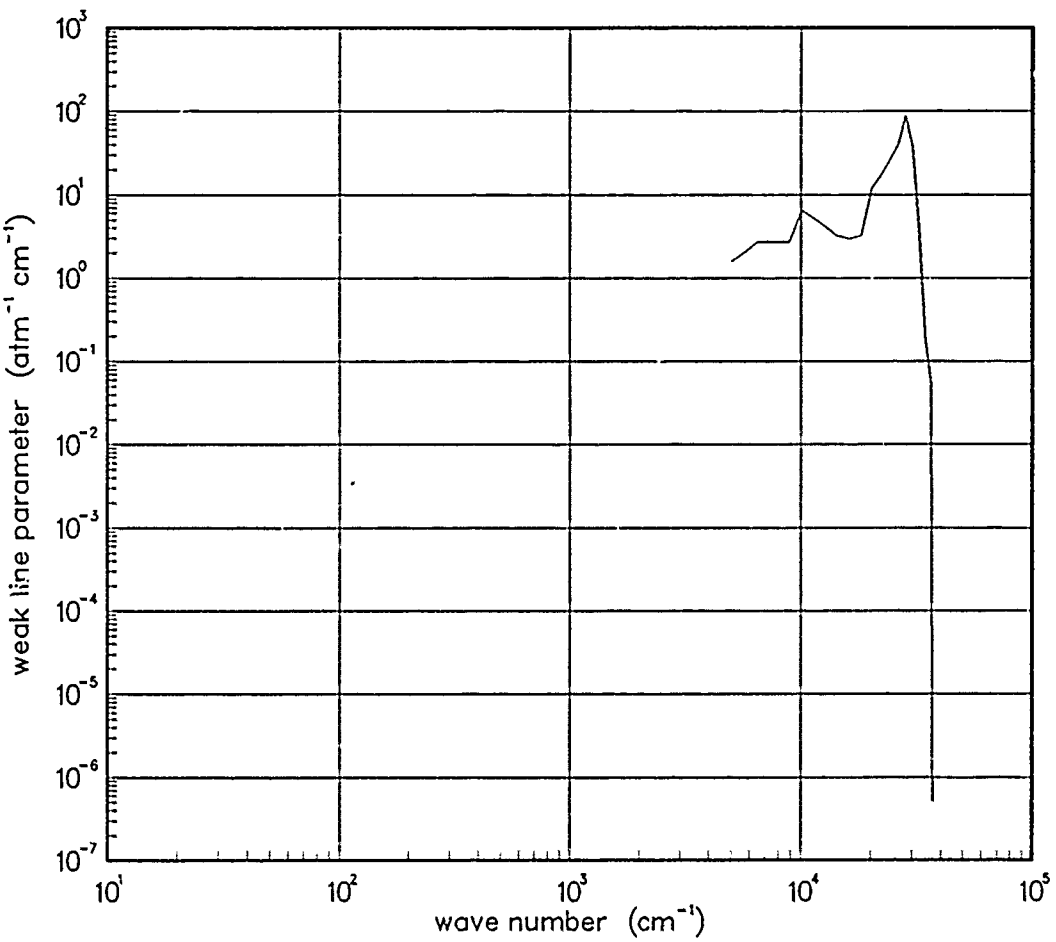

Figure 70. Weak-line parameter for N_2^+ at 12000°K.

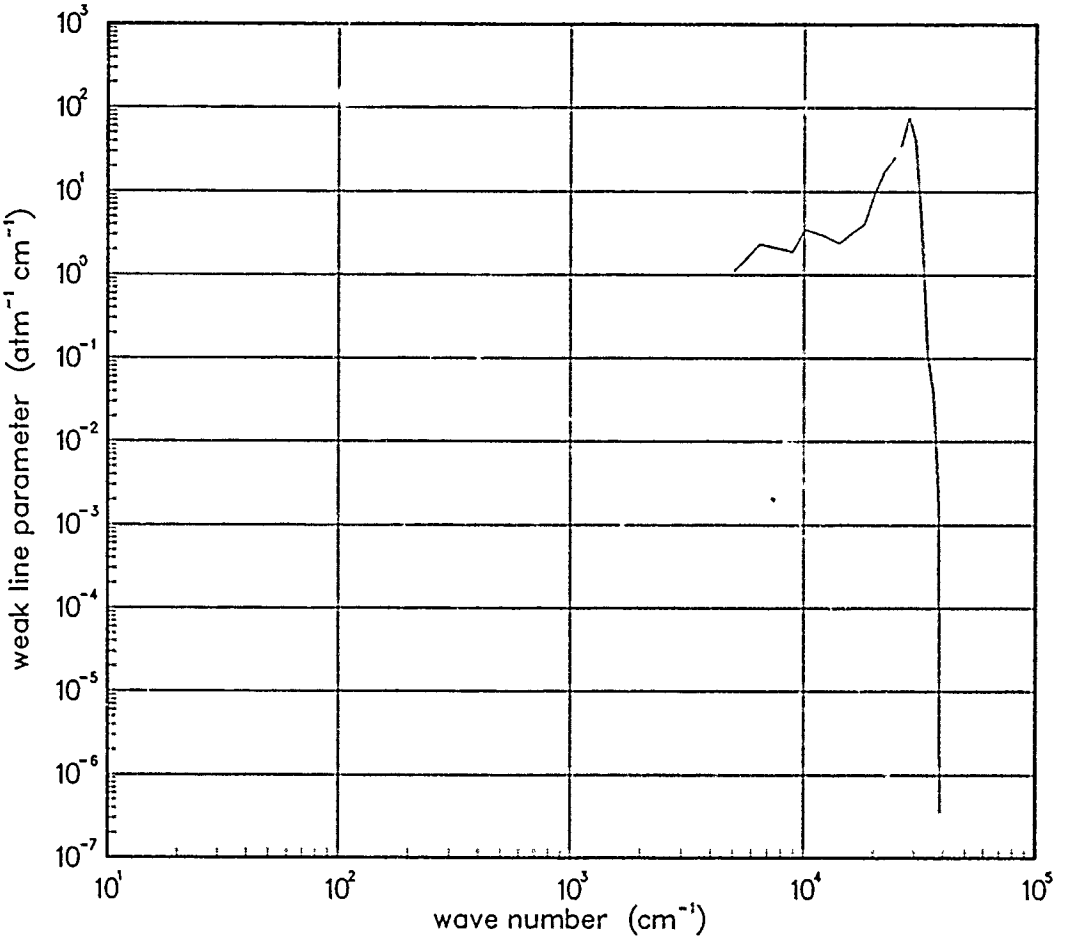

Figure 71. Weak-line parameter for N_2^+ at 18000°K.

4.4 NITROGEN OXIDE (NO).

Data for the NO and NO^+ molecule in the spectral range 10 - 12,000 cm^{-1} has been computed using the DATE code.

The Nitrogen oxide was also calculated by the VisiDyne Corporation[‖] from the RADFLO opacity data base developed by the Air Force Weapons Laboratory in the late sixties. Data is available for the weak-line parameter in the visible region (5,000 cm^{-1} - 100,000 cm^{-1}). The inverse line spacing is not available in this region.

Table 3. Spectroscopic data for NO.

$X\ ^2\Pi$

$\omega_e = 1904.087^*$ $\quad \omega_e x_e = 14.044^*$
$\alpha_e = 0.017612^‡$ $\quad B_e = 1.70509^†$ $\quad A_e = 123.61^*$

$S_{10} = 125.0^*$ $\quad S_{20} = 2.11^‡$ $\quad S_{30} = 0.0458^‡$

$\gamma_\ell(300°K) = 0.040^§$

Data Source:

*M.D. Olman, M.D. McNelis, and C.D. Hause, J. Mol. Spectrosc., 14, 62 (1964)

†U.P. Oppenheim, Y. Aviv, and A. Goldman, Appl. Opt. 6, 1305 (1967).

‡B. Schurin, and R.E. Ellis, J.Chem. Phys., 45, 2528 (1966).

§Fit to the data of: L.L. Abels, and J.H. Shaw, J. Mol. Spectrosc., 20, 11, (1966).

‖H. Smith, T. Keneshea, VisiDyne Corporation, private communication (1986).

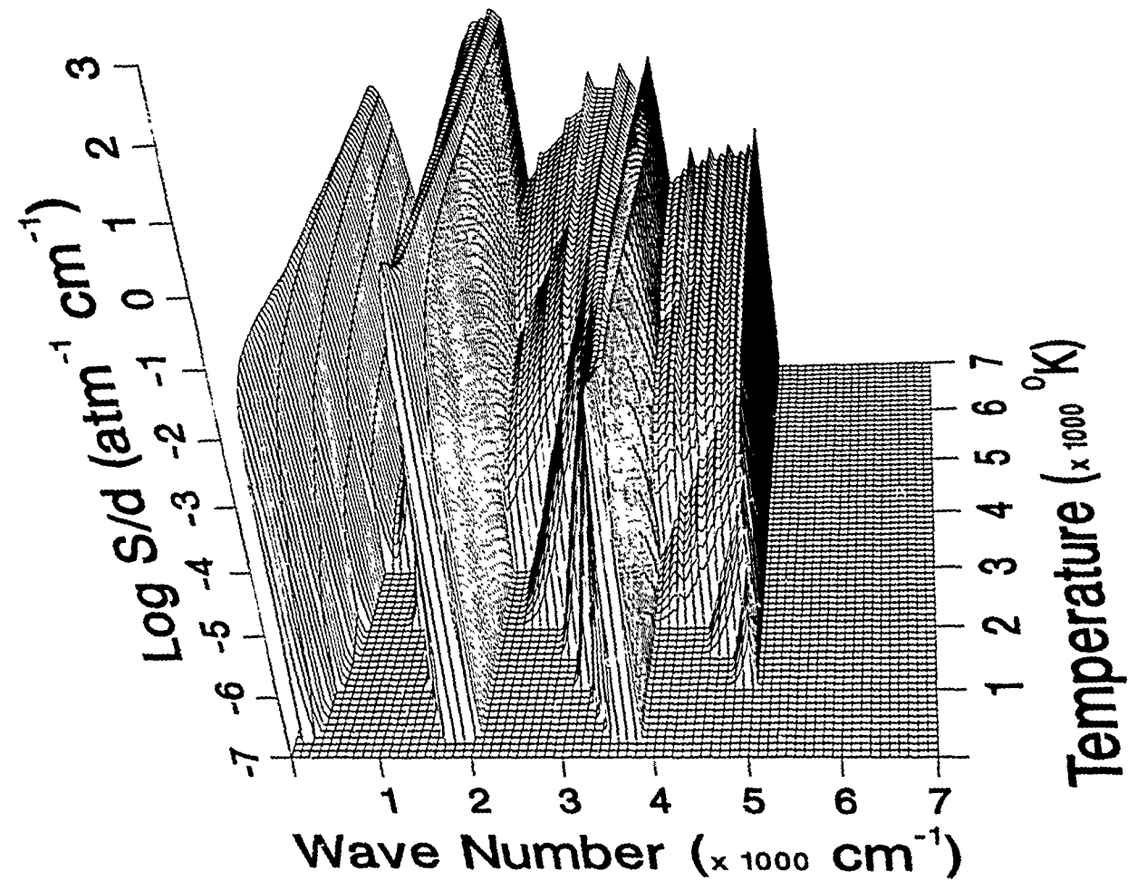

Figure 72. Weak-line parameter for NO.

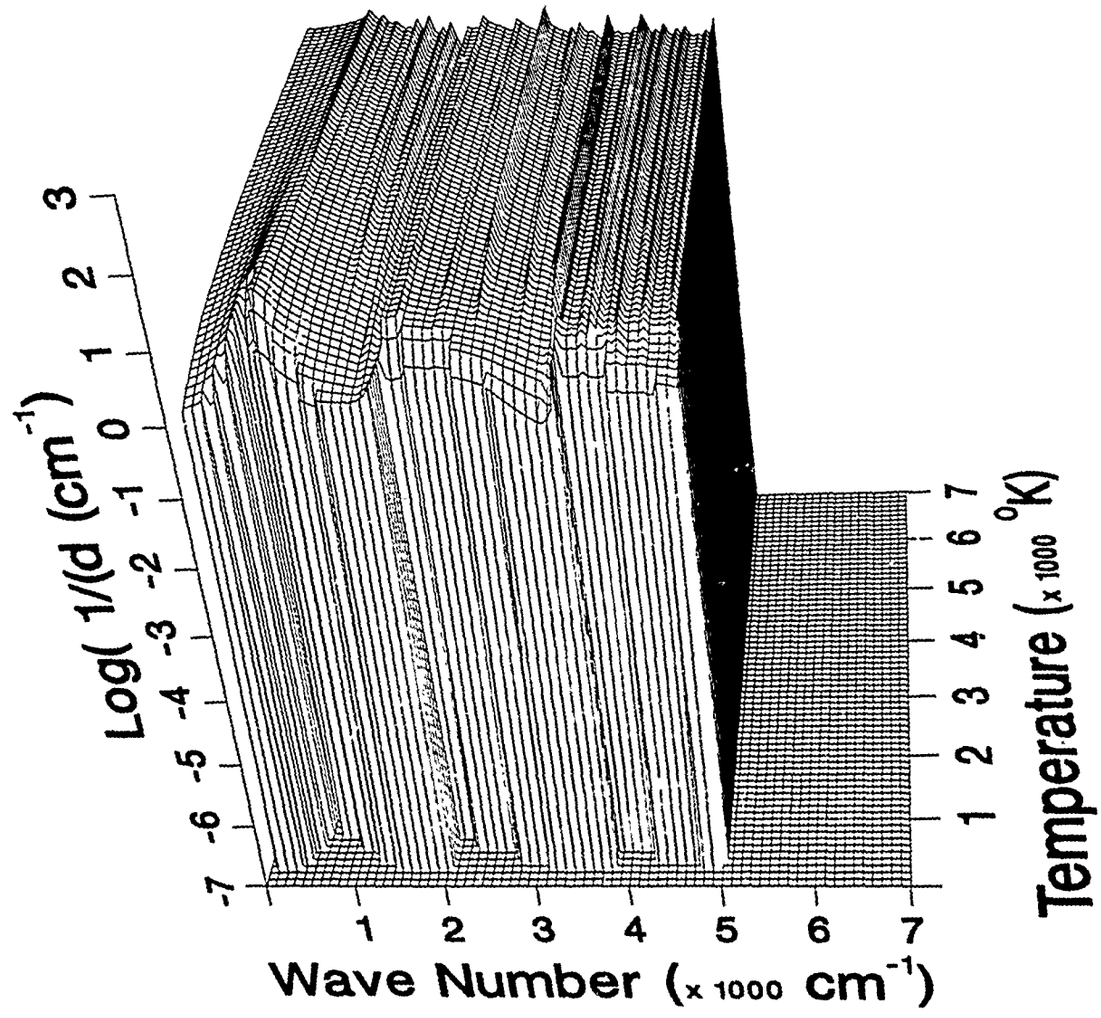

Figure 73. Inverse line spacing for NO.

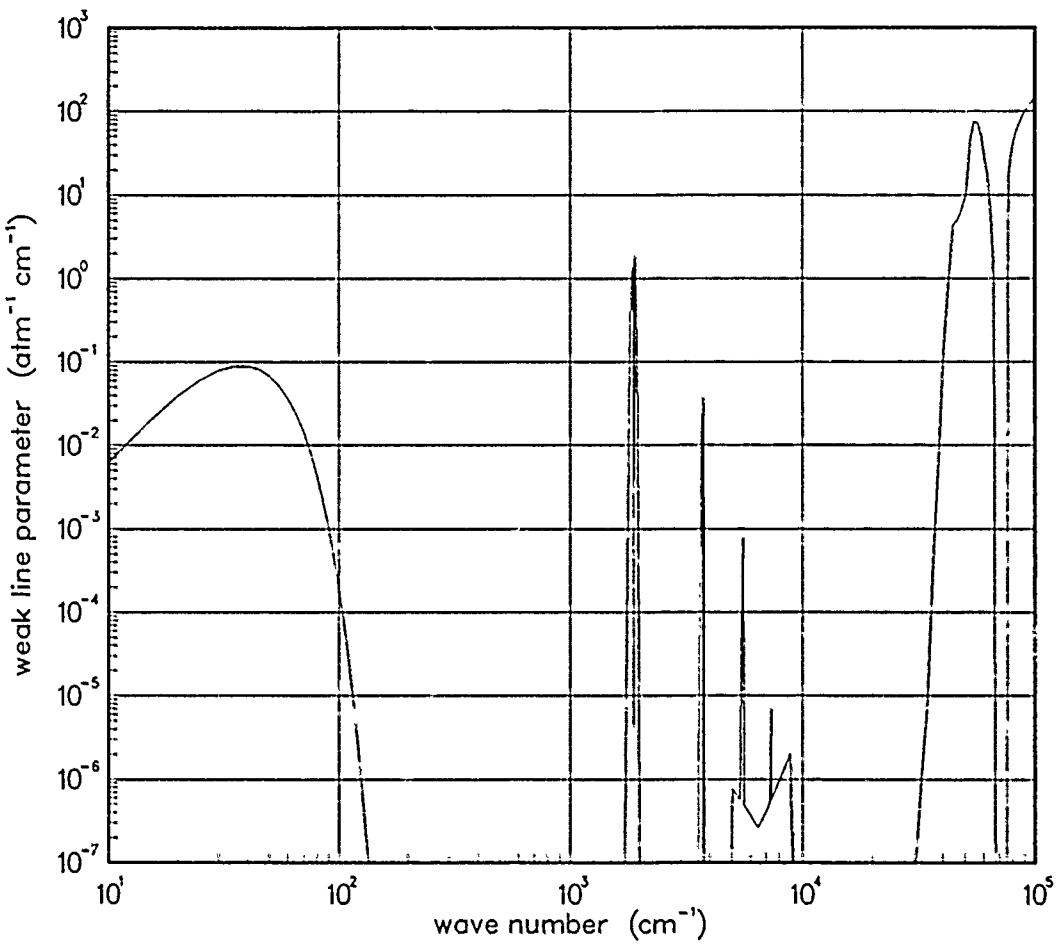

Figure 74. Weak-line parameter for NO at 200°K.

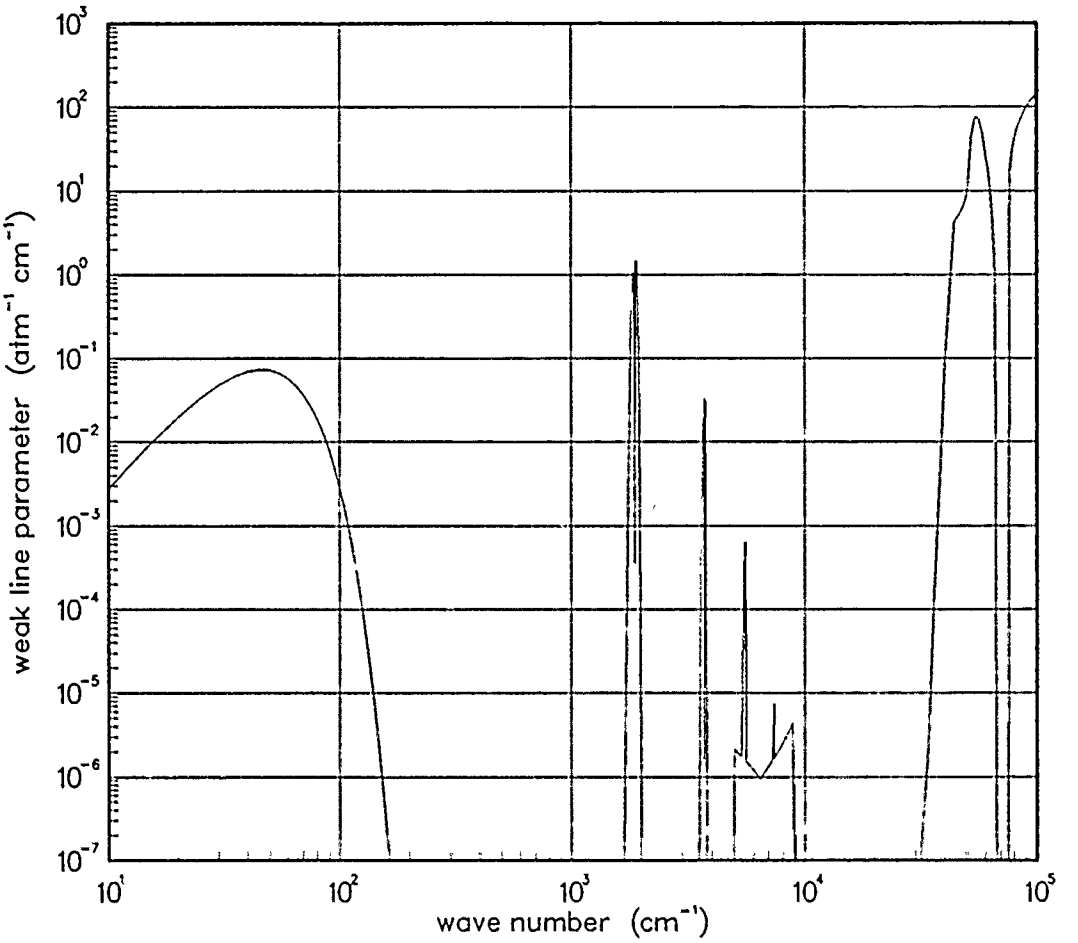

Figure 75. Weak-line parameter for NO at 300°K.

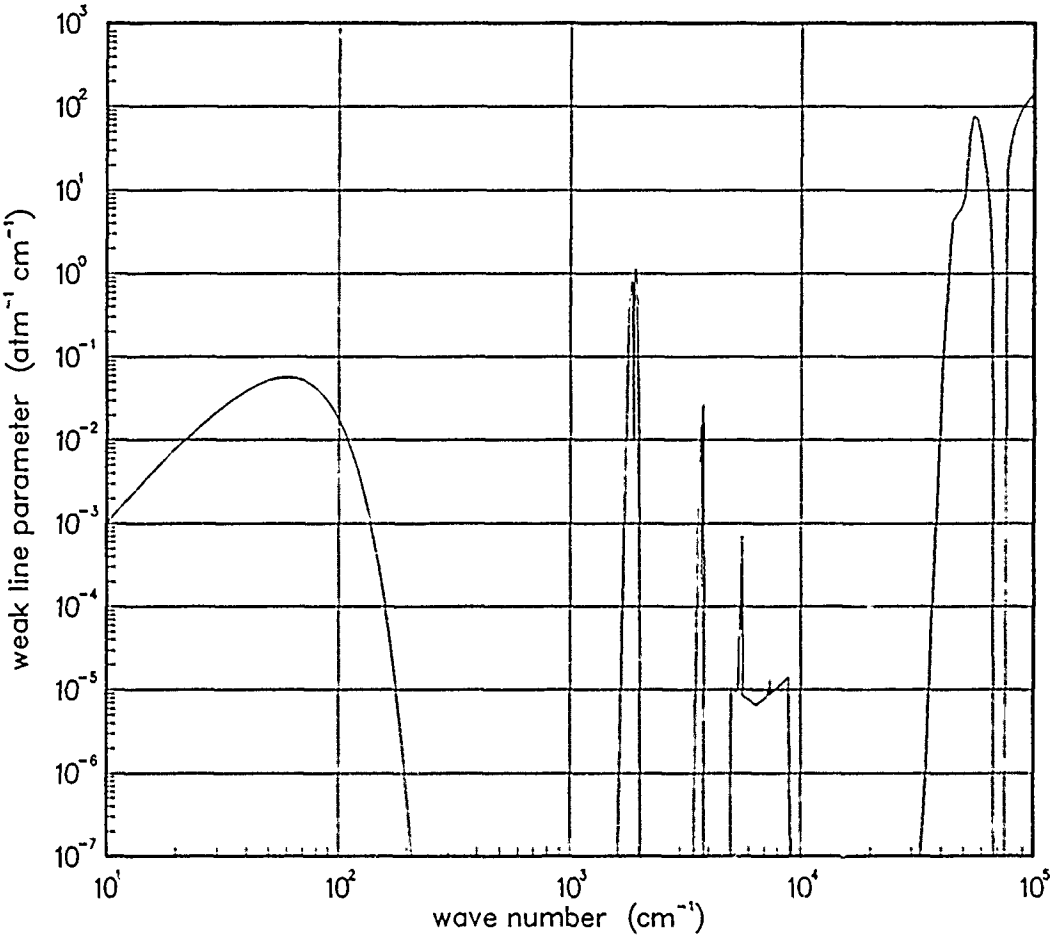

Figure 76. Weak-line parameter for NO at 500°K.

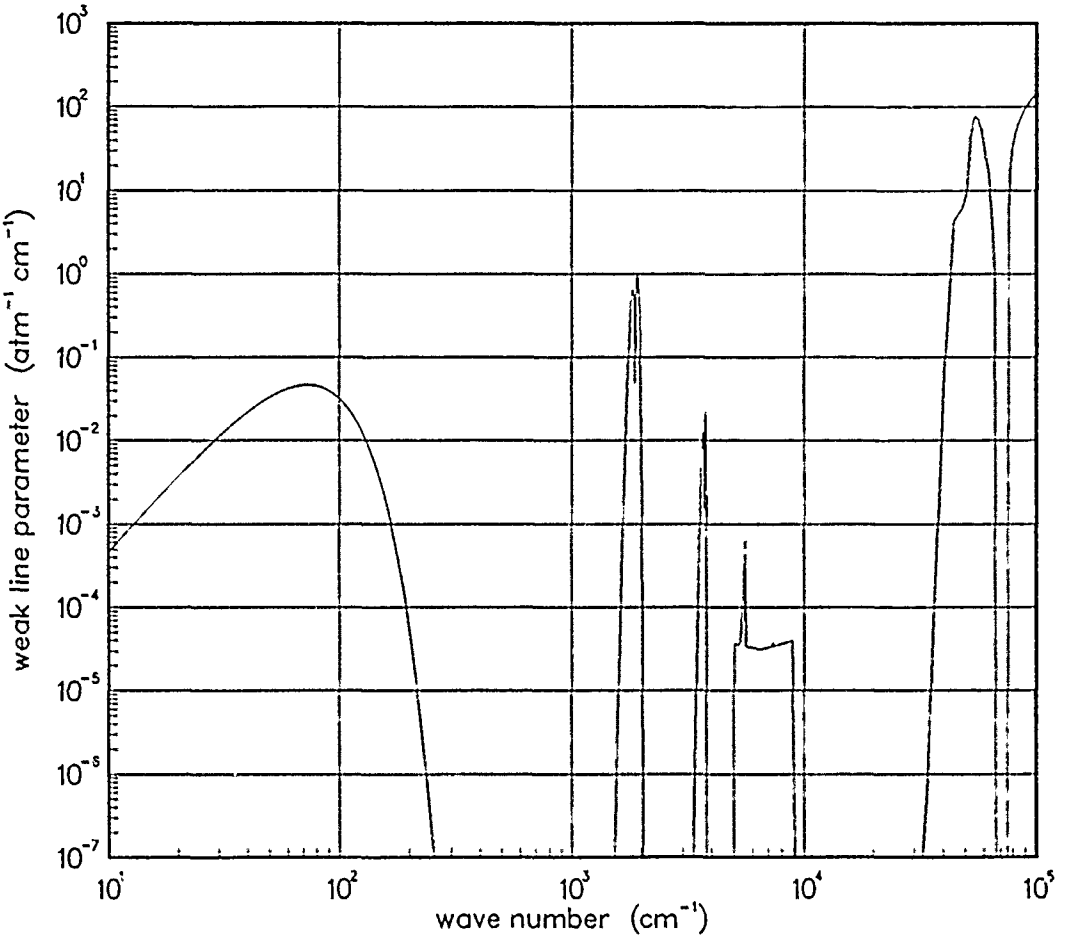

Figure 77. Weak-line parameter for NO at 750°K.

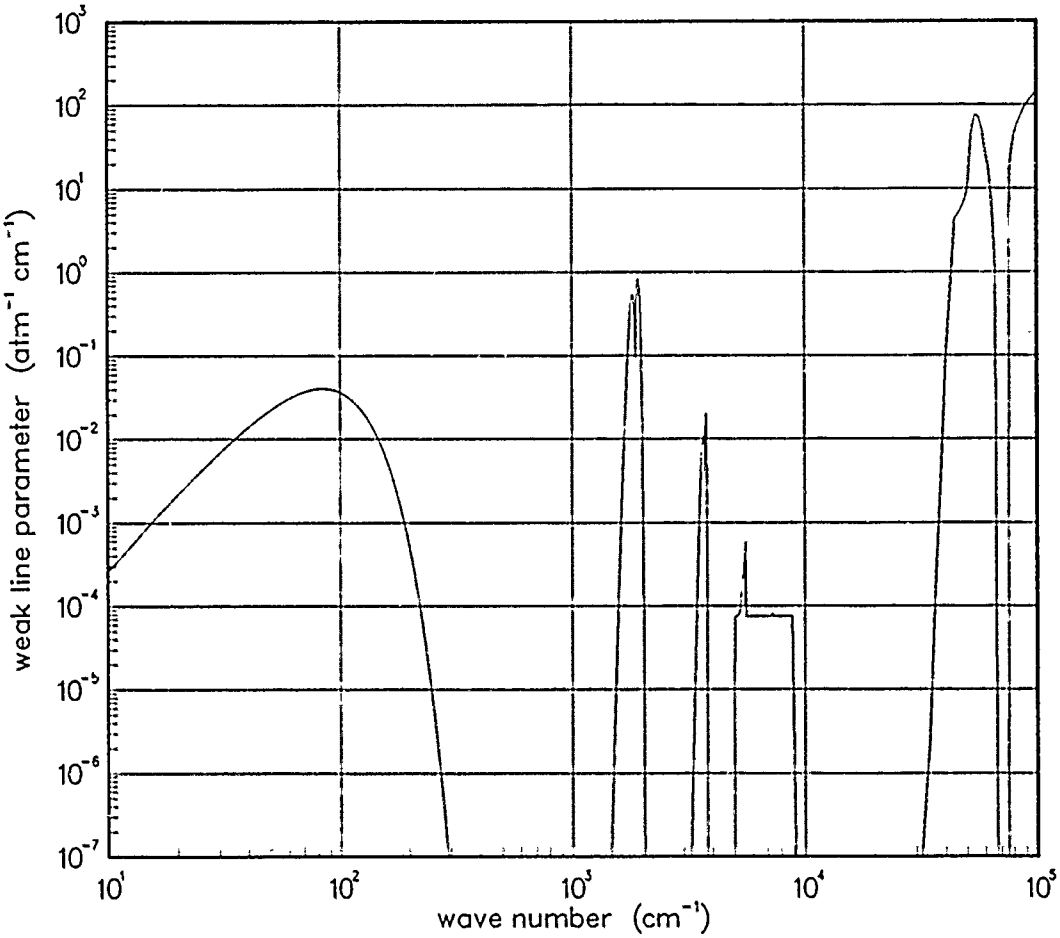

Figure 78. Weak-line parameter for NO at 1000°K.

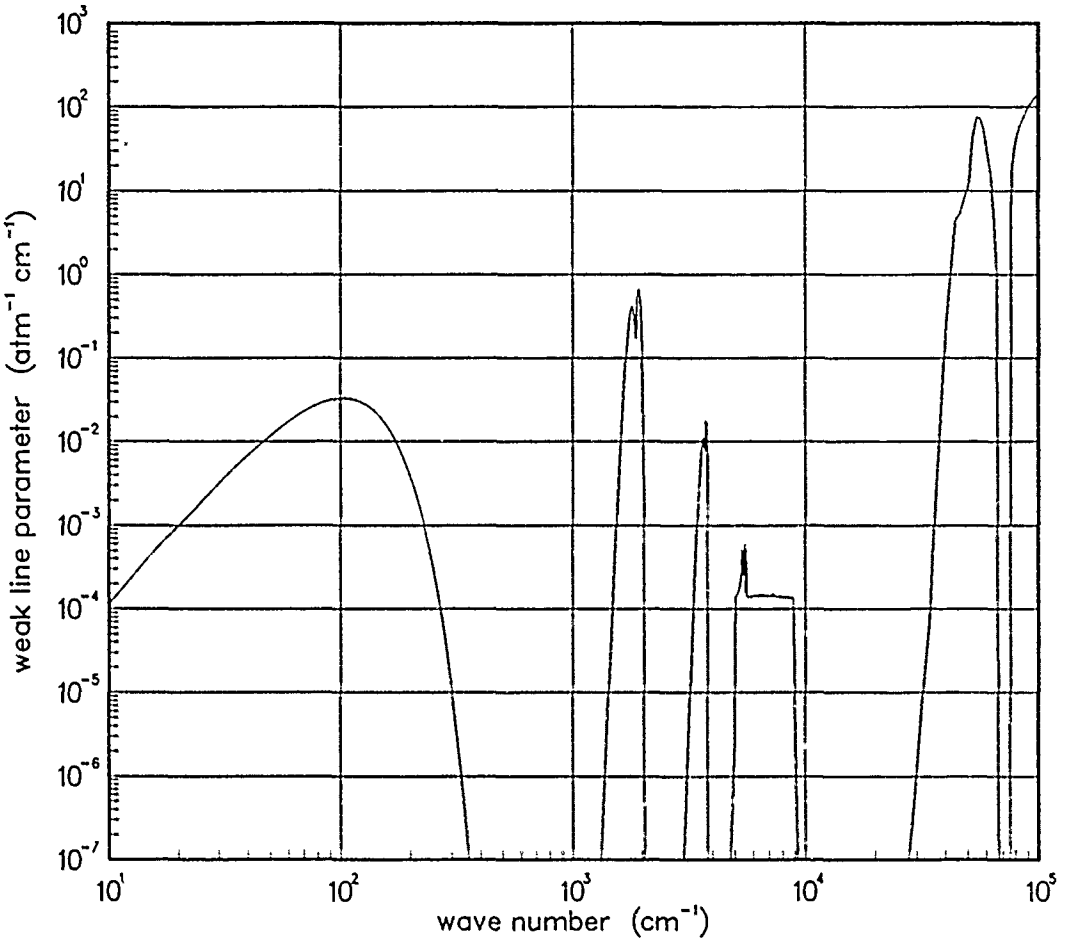

Figure 79. Weak-line parameter for NO at 1500°K.

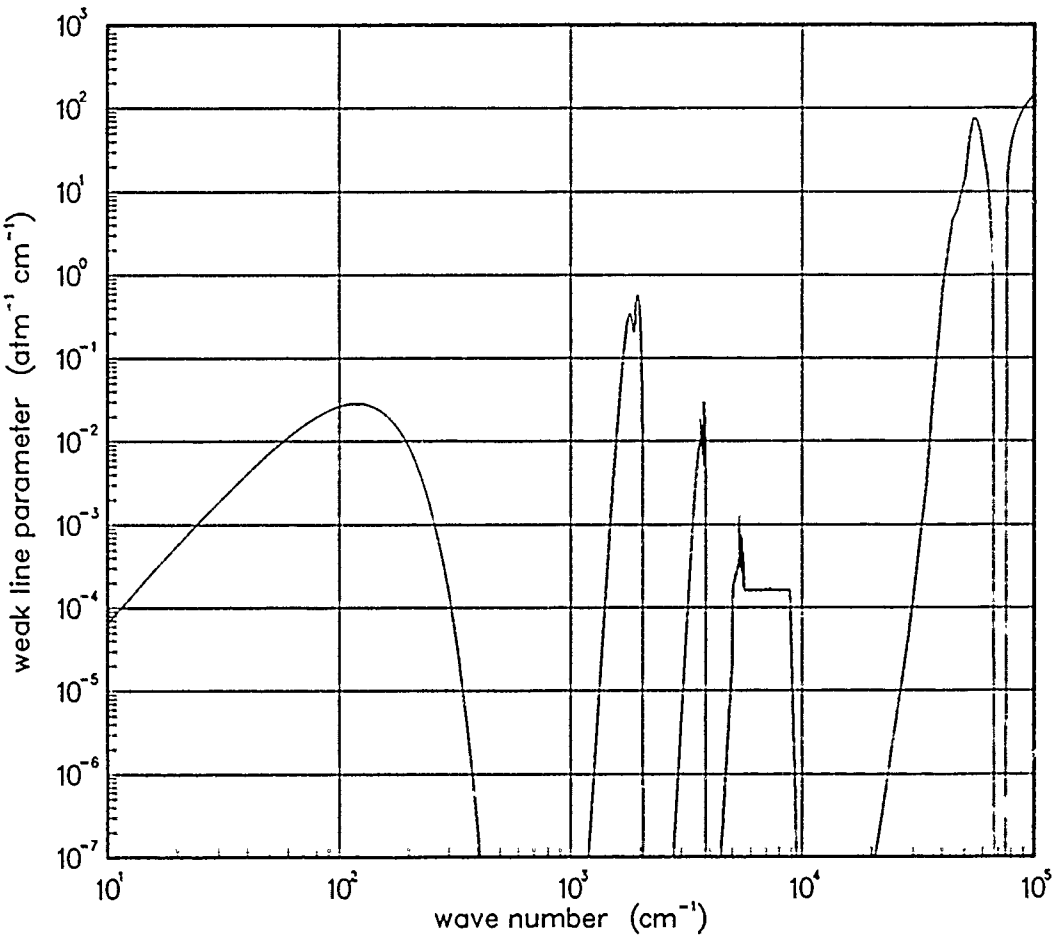

Figure 80. Weak-line parameter for NO at 2000°K.

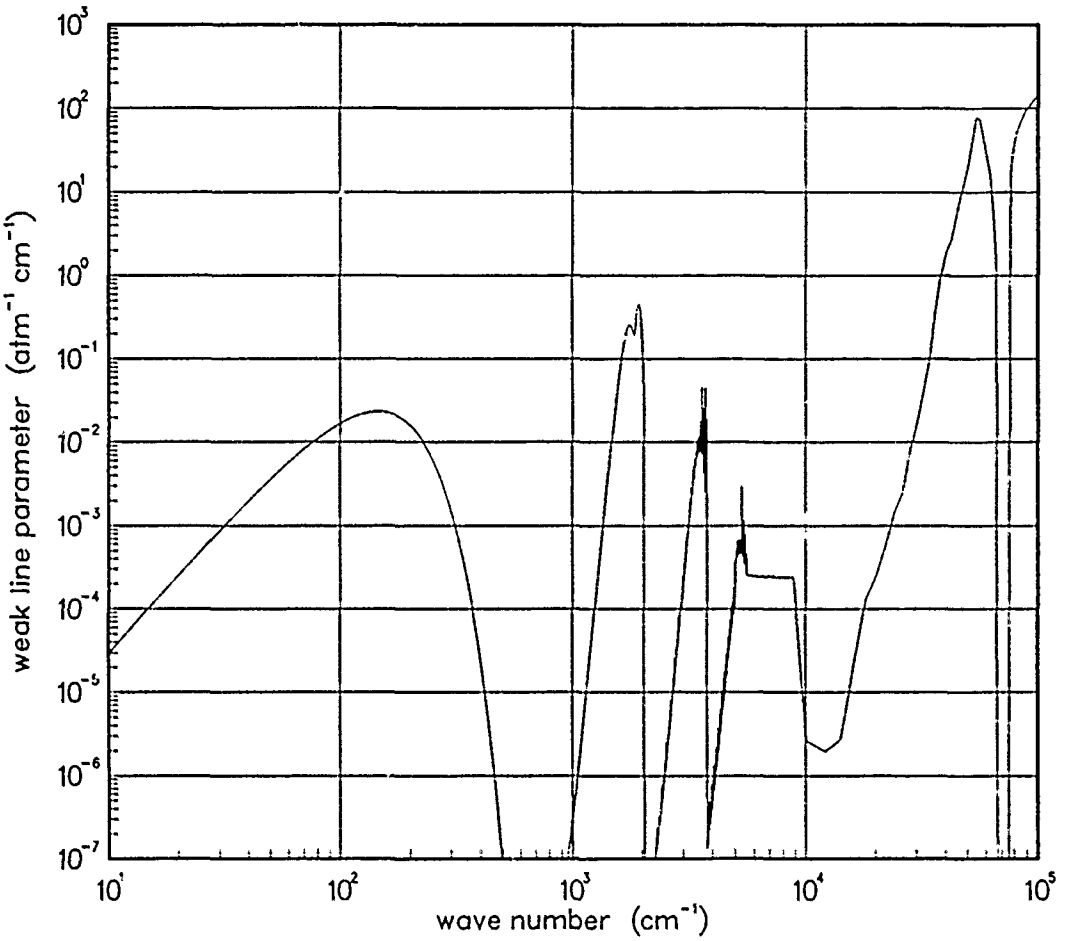

Figure 81. Weak-line parameter for NO at 3000°K.

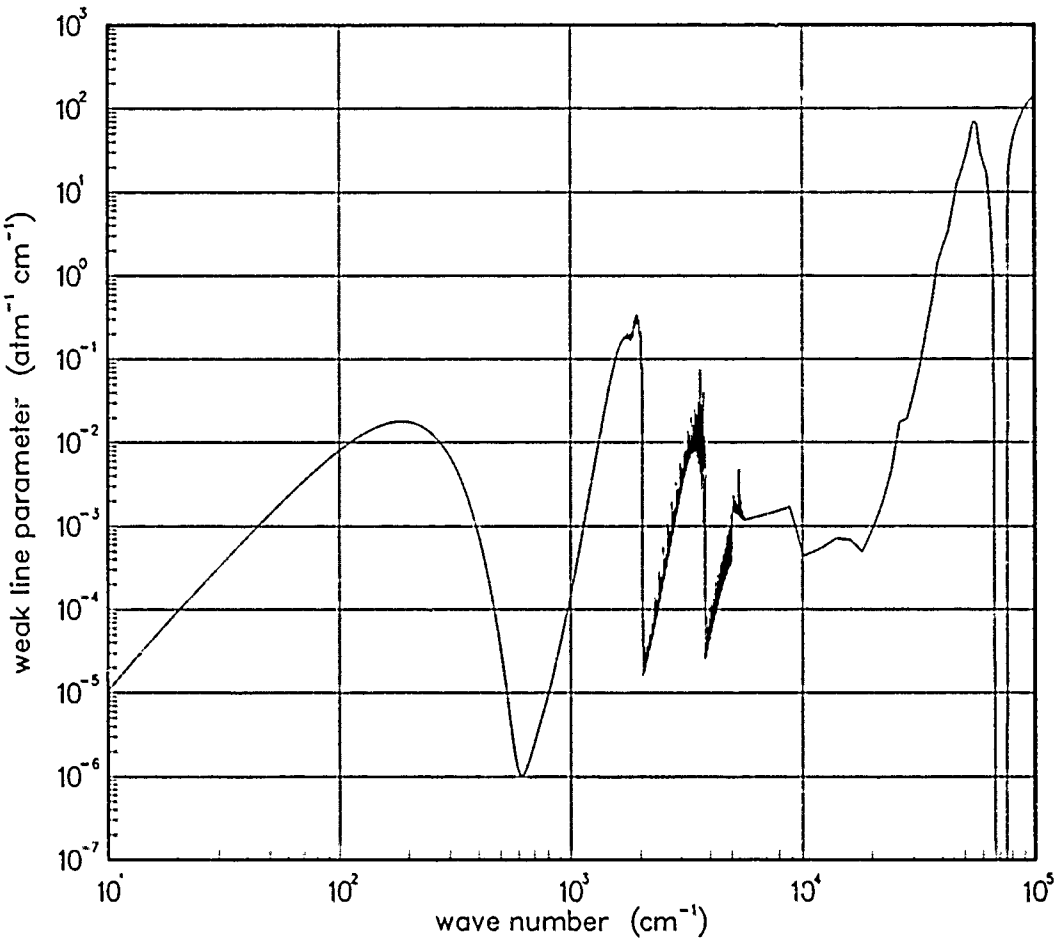

Figure 82. Weak-line parameter for NO at 5000°K.

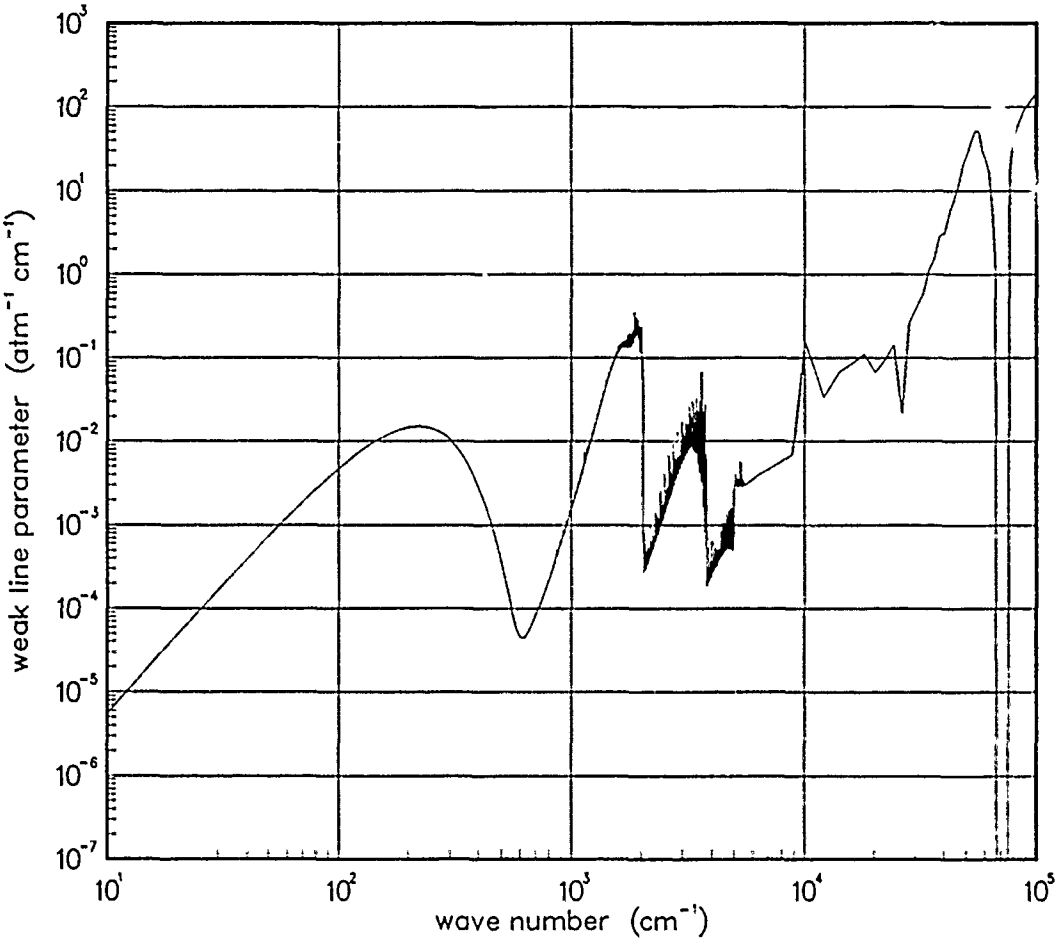

Figure 83. Weak-line parameter for NO at 7000°K.

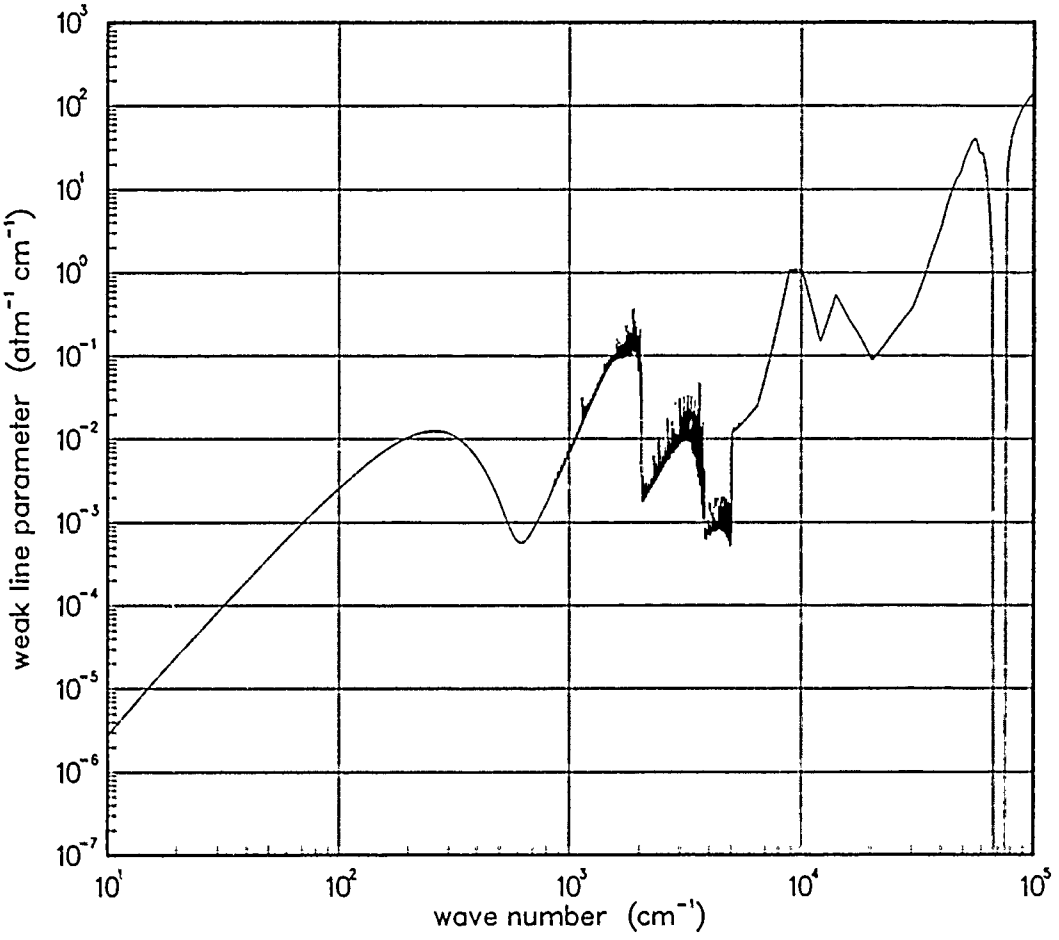

Figure 84. Weak-line parameter for NO at 10000°K.

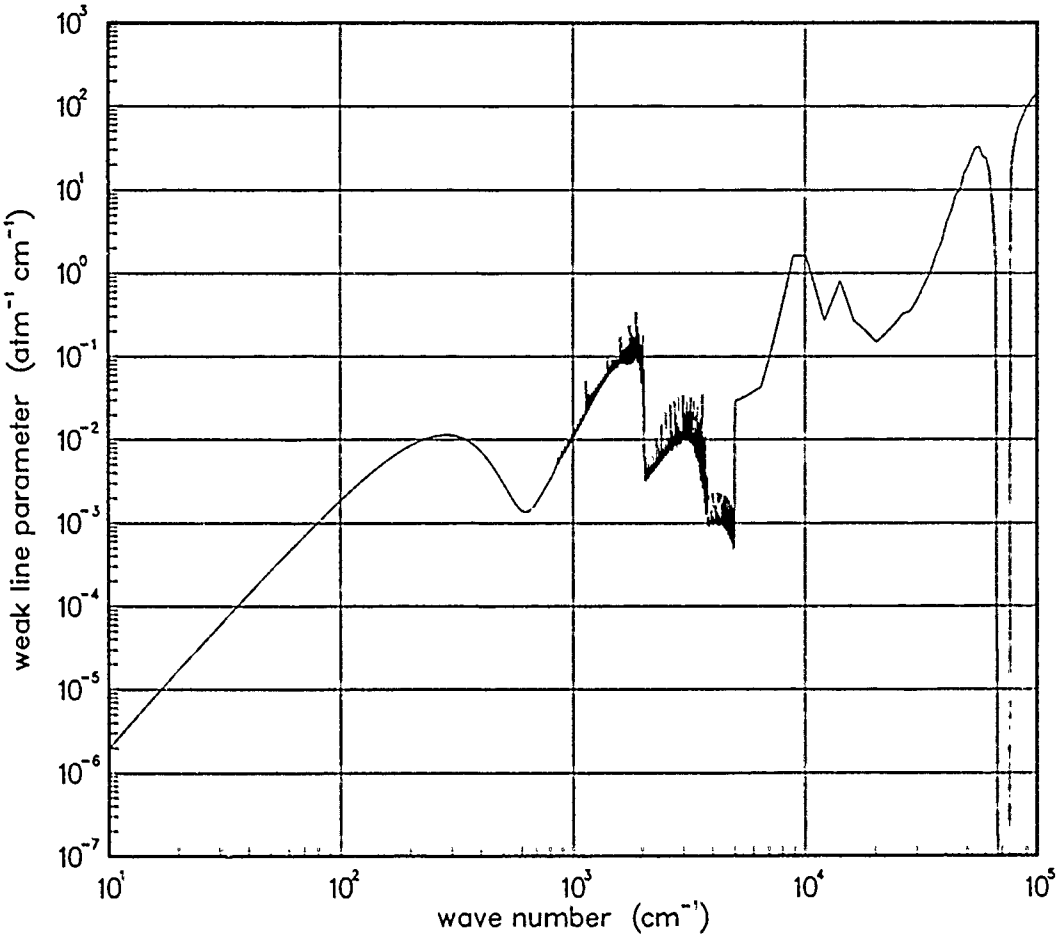

Figure 85. Weak-line parameter for NO at 12000°K.

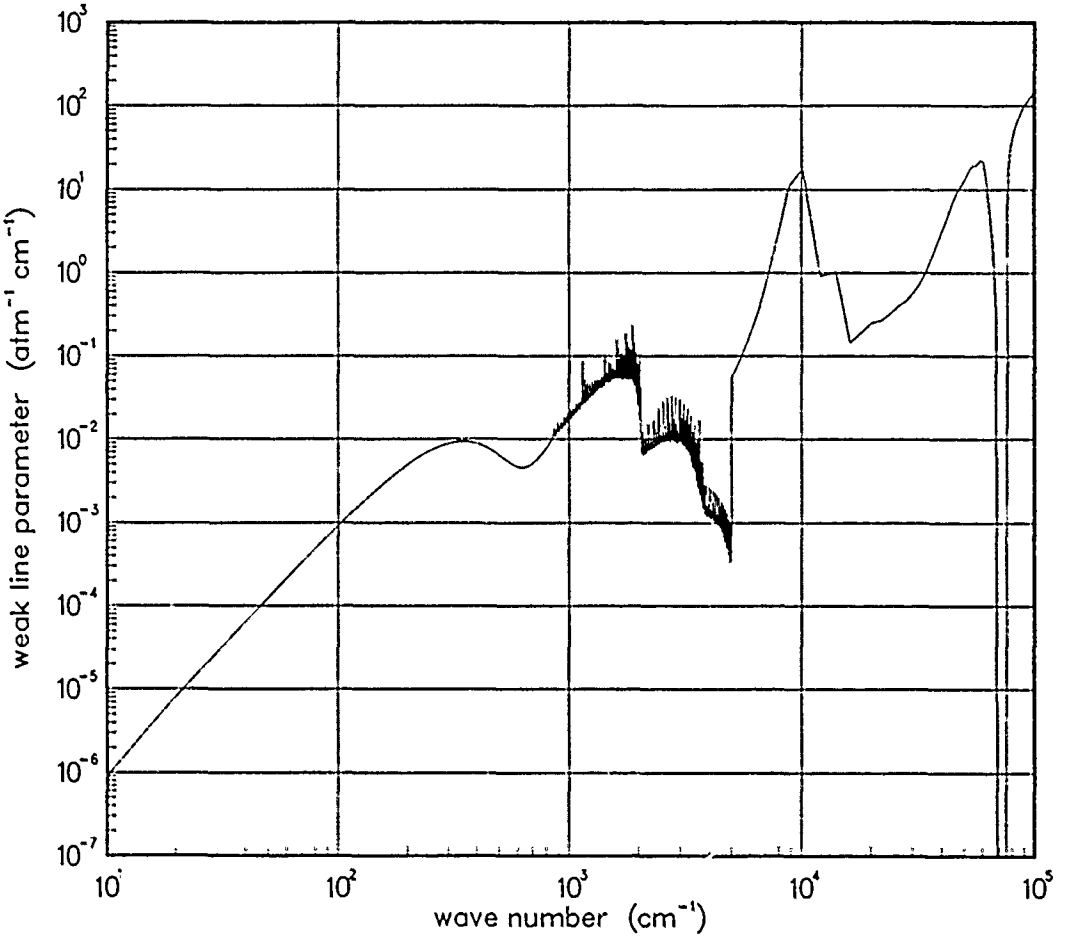

Figure 86. Weak-line parameter for NO at 18000°K.

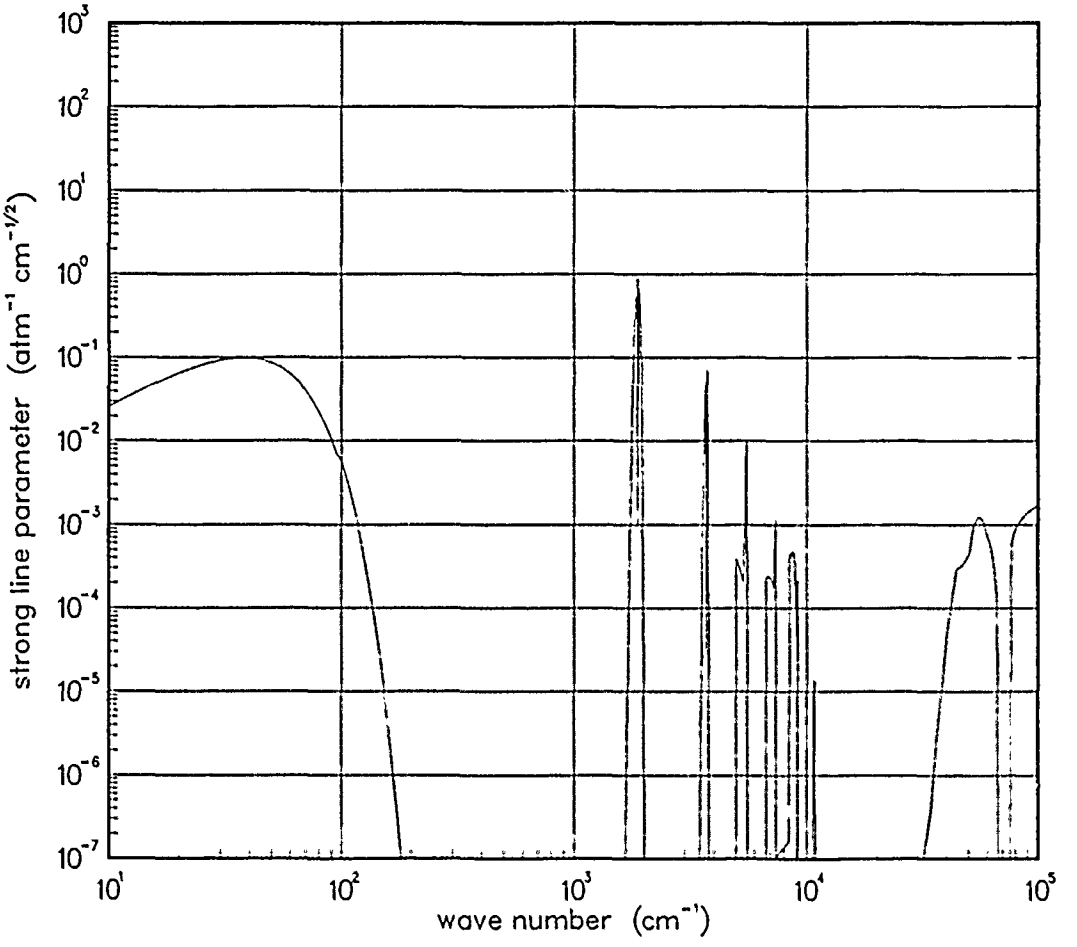

Figure 87. Strong-line parameter for NO at 200°K.

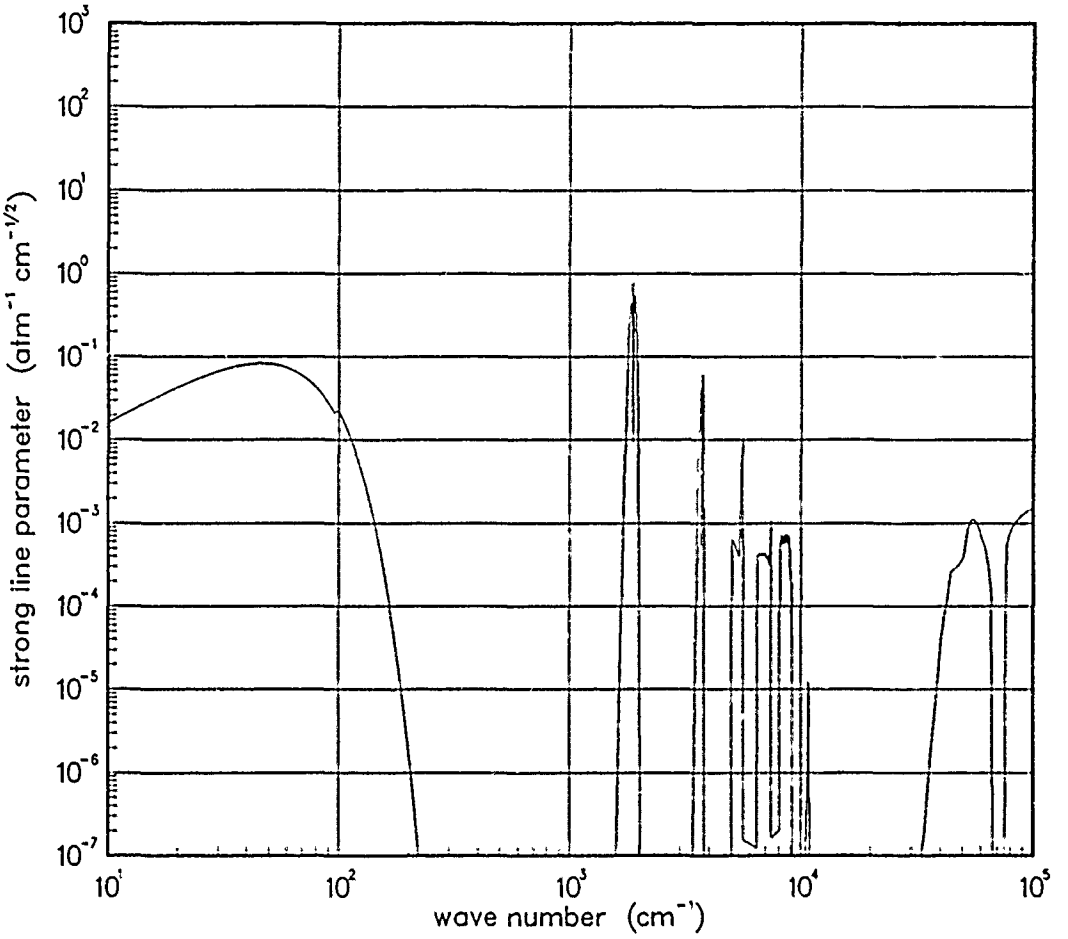

Figure 88. Strong-line parameter for NO at 300°K.

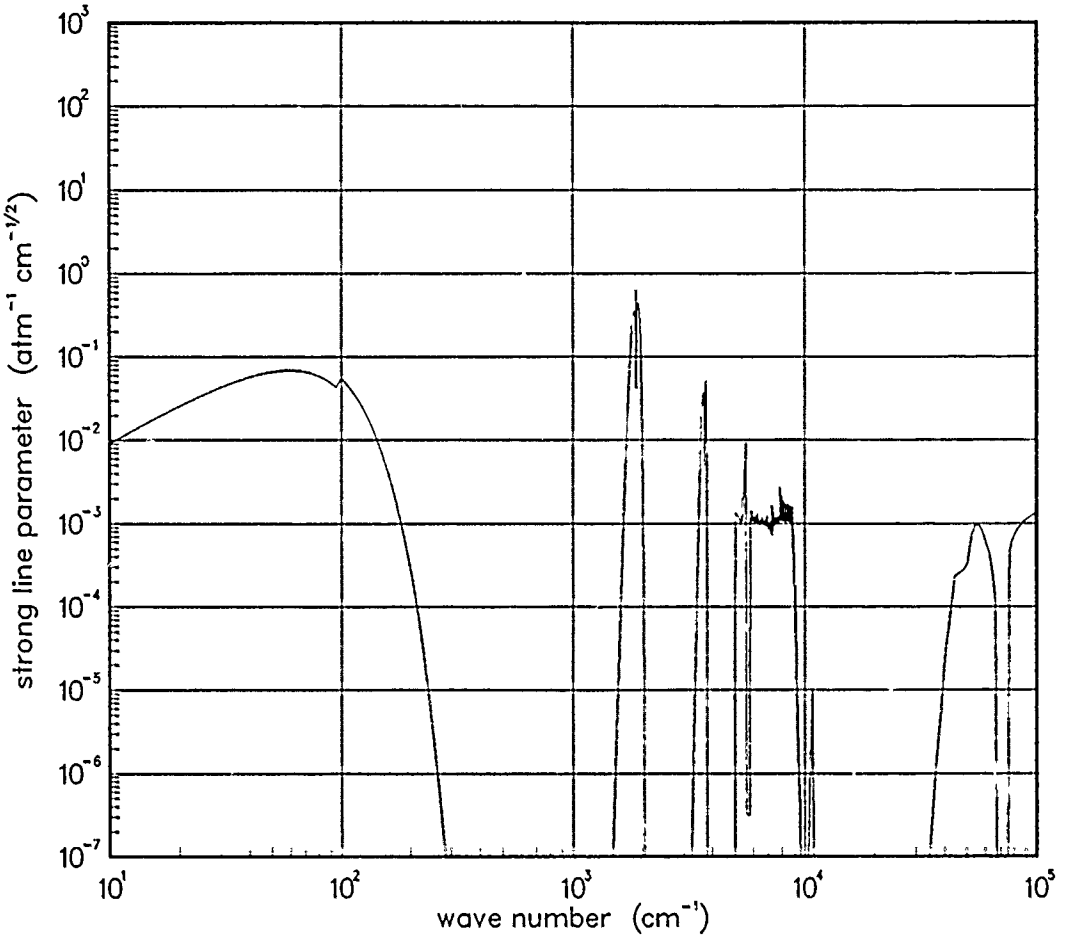

Figure 89. Strong-line parameter for NO at 500°K.

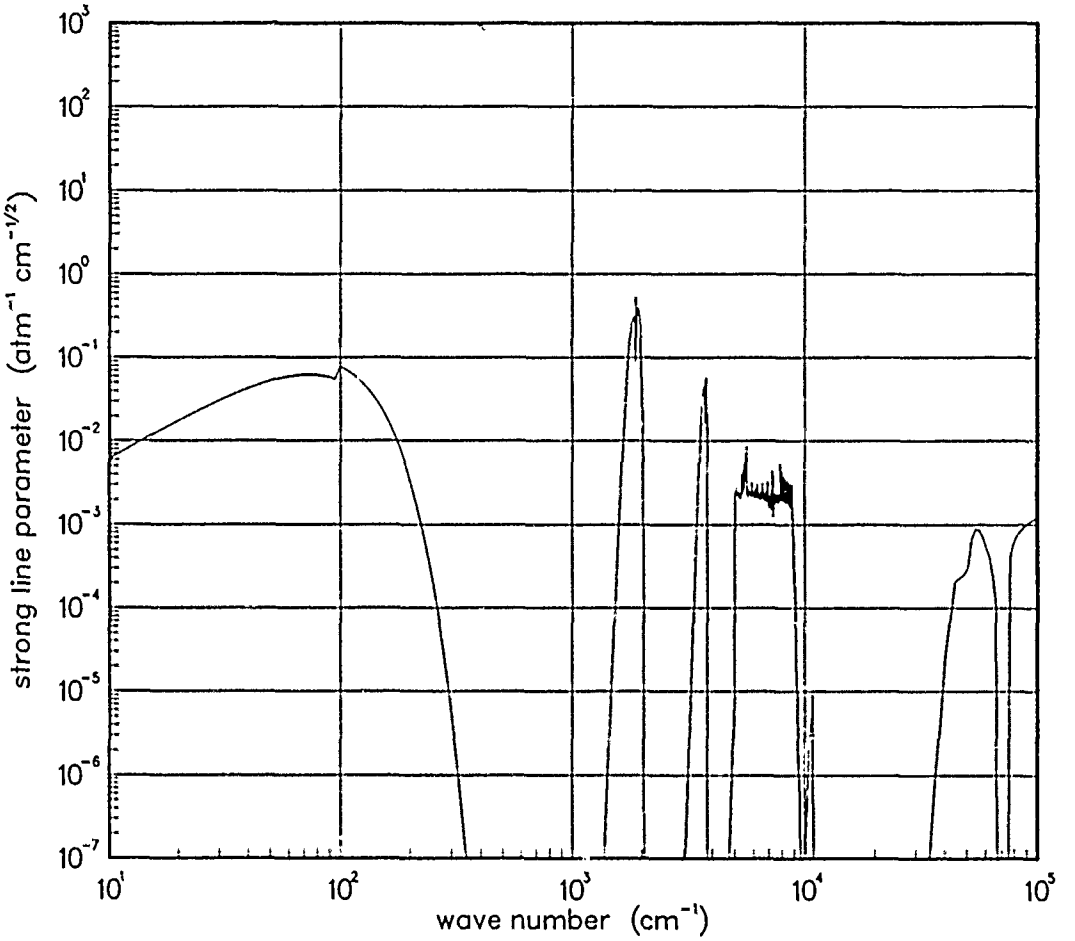

Figure 90. Strong-line parameter for NO at 750°K.

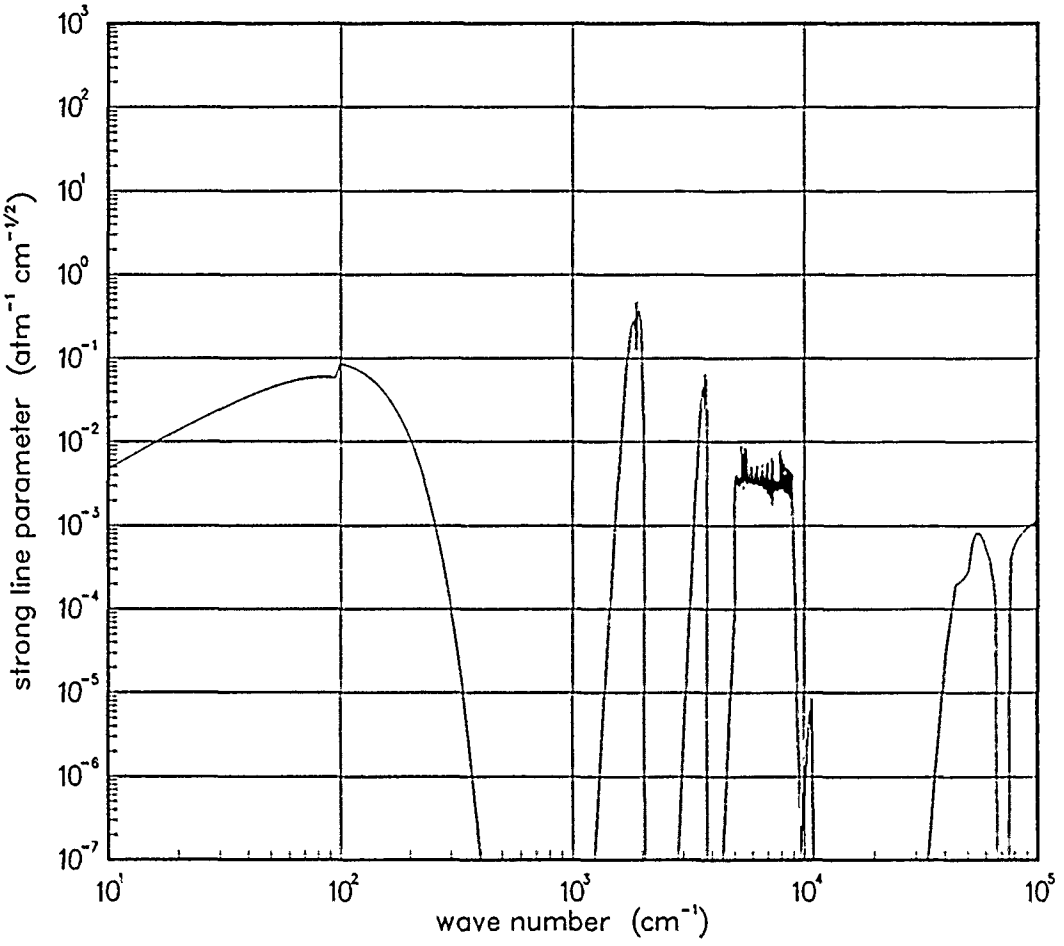

Figure 91. Strong-line parameter for NO at 1000°K.

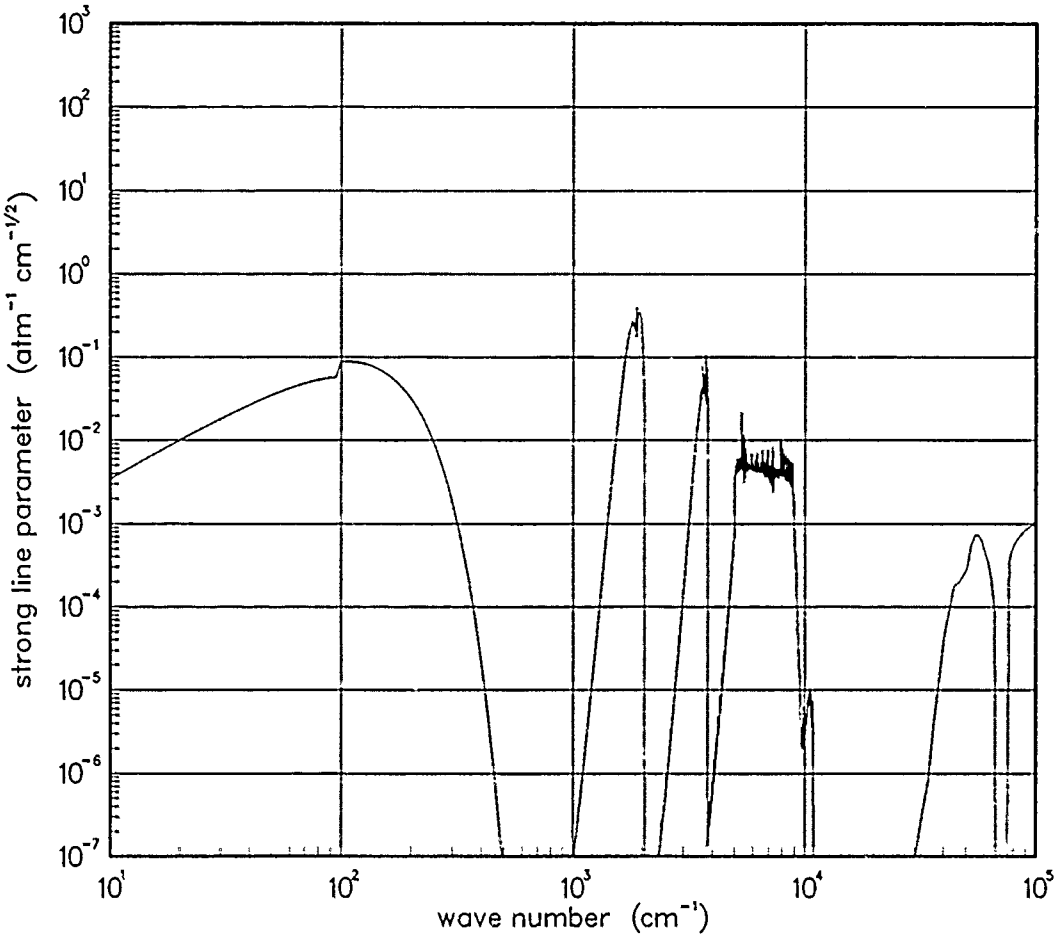

Figure 92. Strong-line parameter for NO at 1500°K.

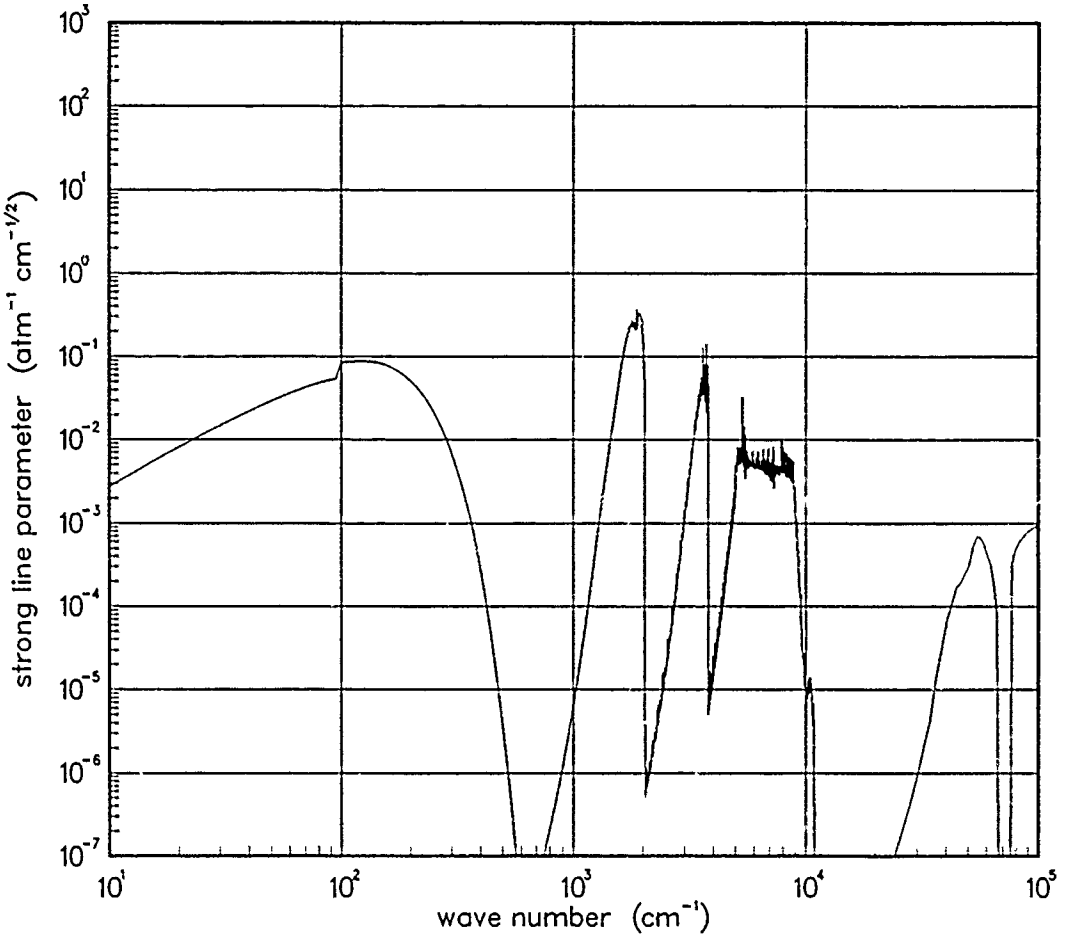

Figure 93. Strong-line parameter for NO at 2000°K.

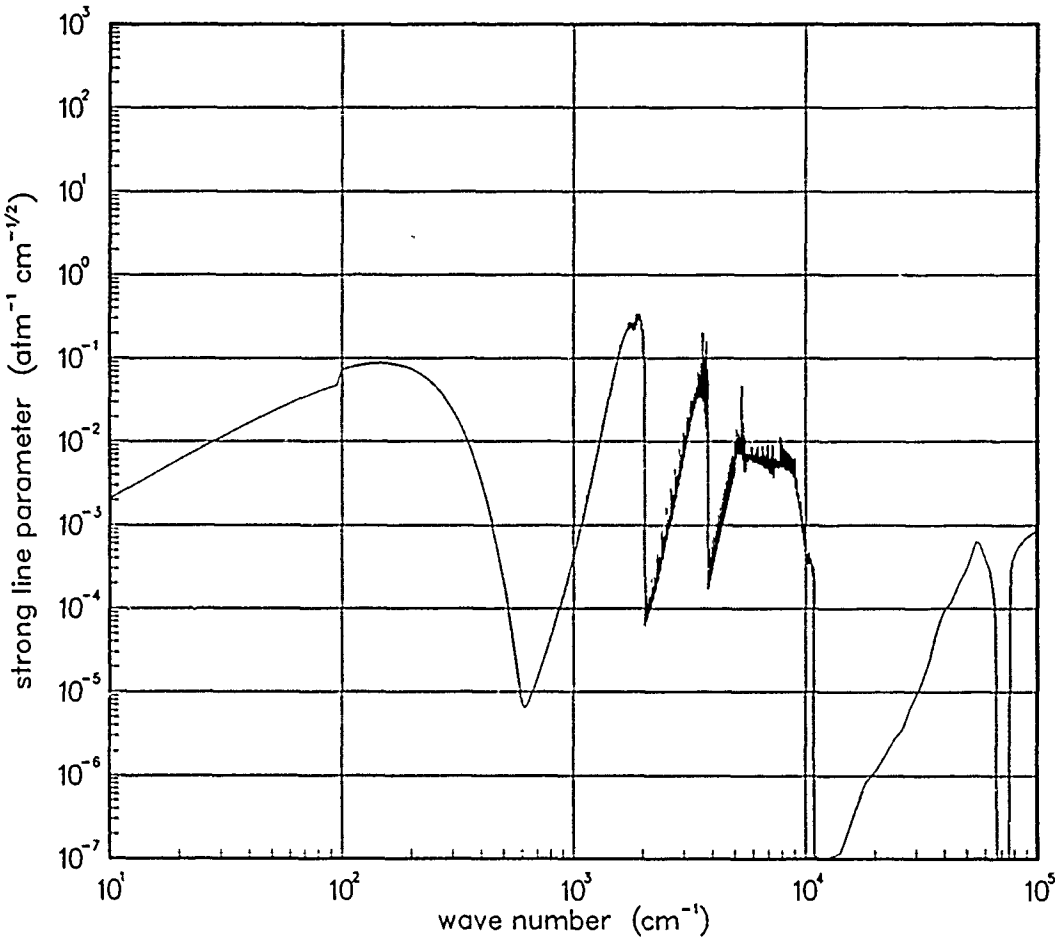

Figure 94. Strong-line parameter for NO at 3000°K.

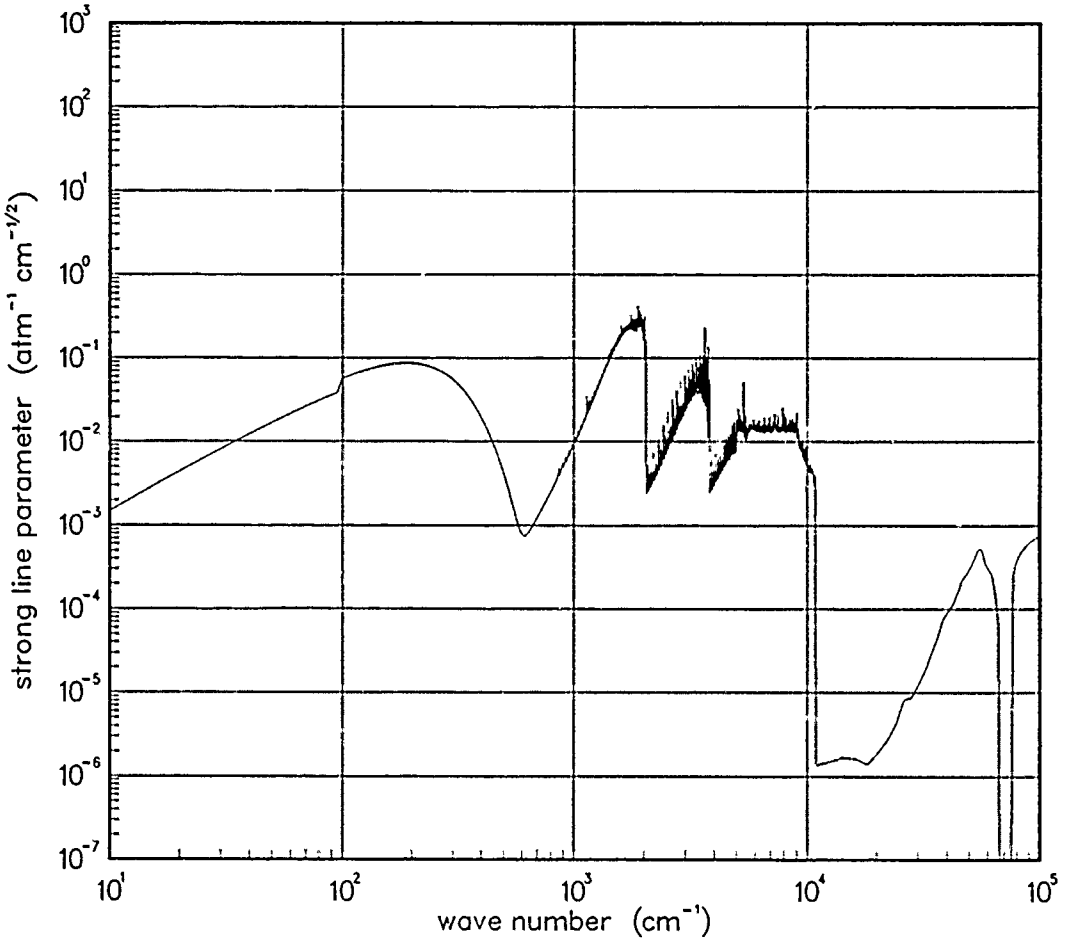

Figure 95. Strong-line parameter for NO at 5000°K.

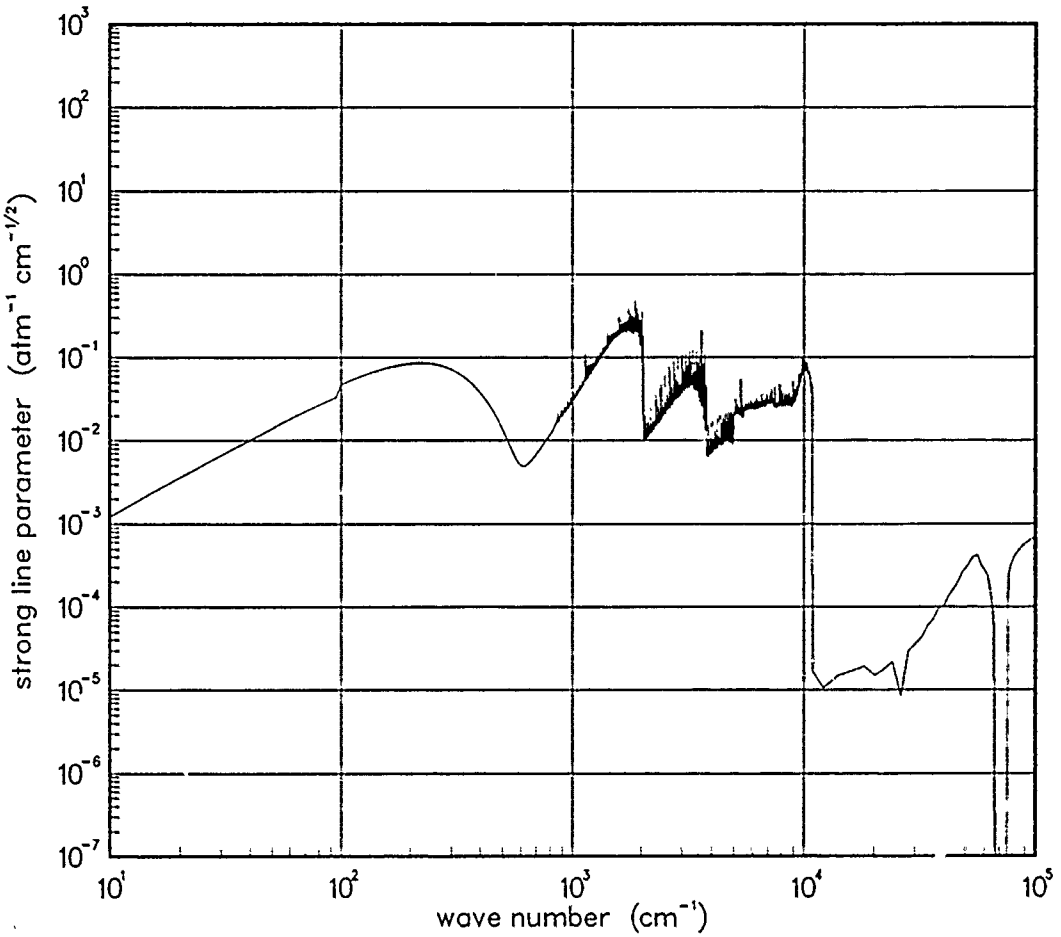

Figure 96. Strong-line parameter for NO at 7000°K.

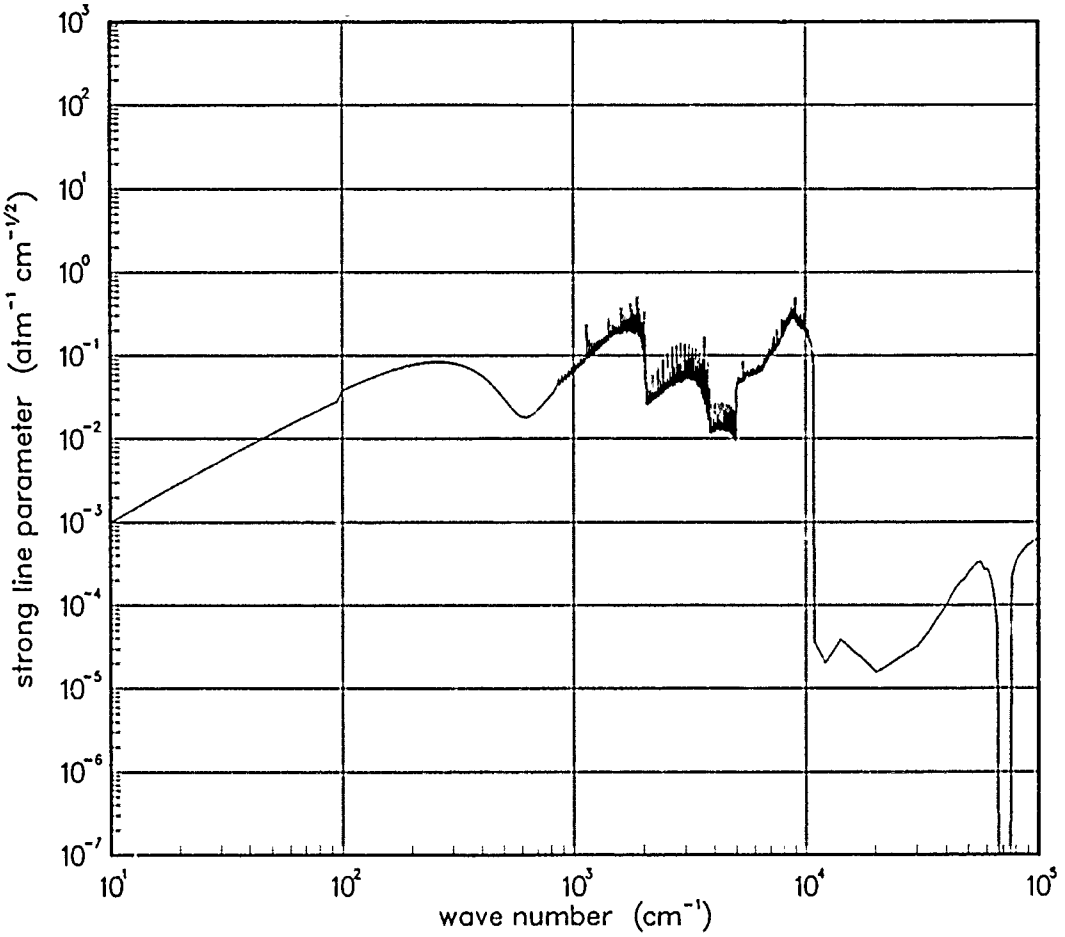

Figure 97. Strong-line parameter for NO at 10000°K.

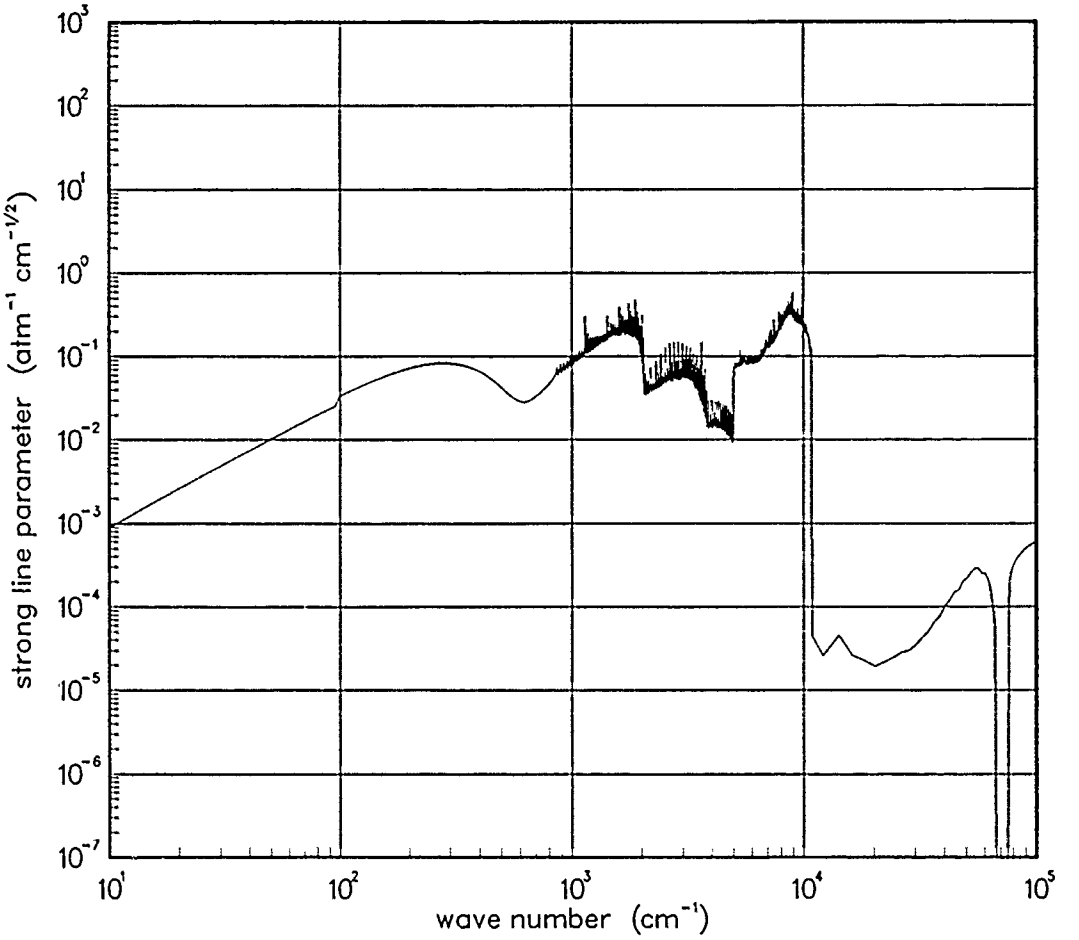

Figure 98. Strong-line parameter for NO at 12000°K.

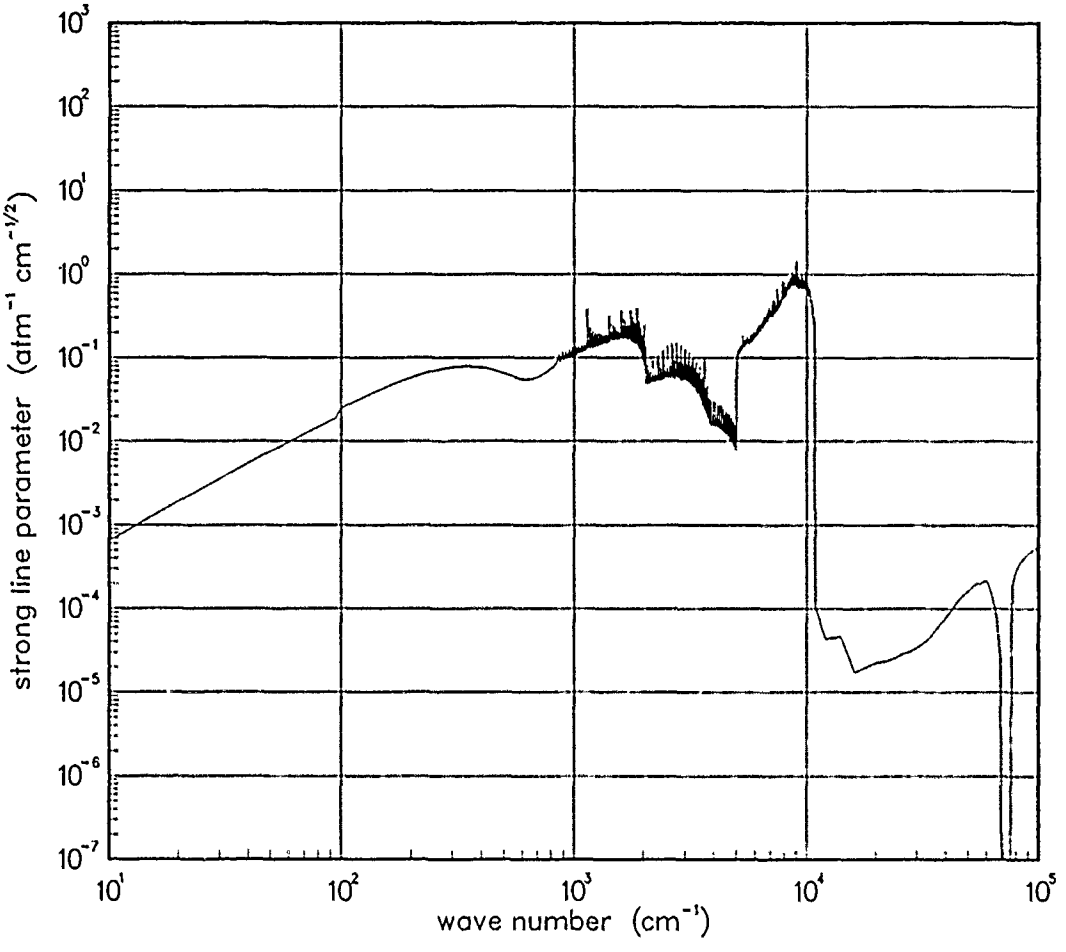

Figure 99. Strong-line parameter for NO at 18000°K.

Table 4. Spectroscopic data for NO^+.

$X\ ^1\Sigma^+$

$\omega_e = 2377.1^*$ $\quad \omega_e x_e = 16.35^*$
$\alpha_e = 0.0202^*$ $\quad B_e = 2.002^*$

$S_{10} = 70.83^\dagger$

$\gamma_\ell(300°K) = 0.04^\ddagger$

Data Source:

*E. Miescher, Helv. Phys. Acta., 29, 135, (1956).

†H.J. Werner, P. Rosmus, J. Mol. Spectrosc., 96, 362, (1982).

‡Estimate.

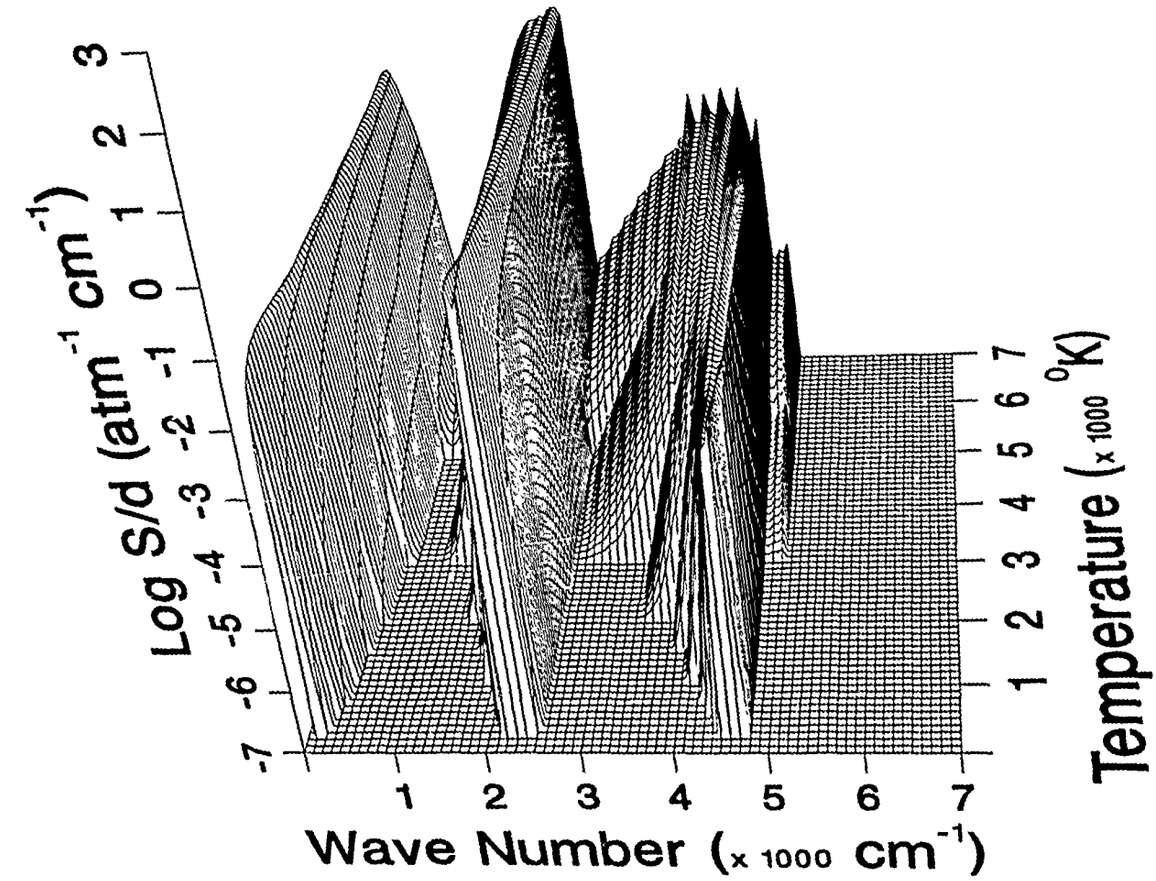

Figure 100. Weak-line parameter for NO^{+}.

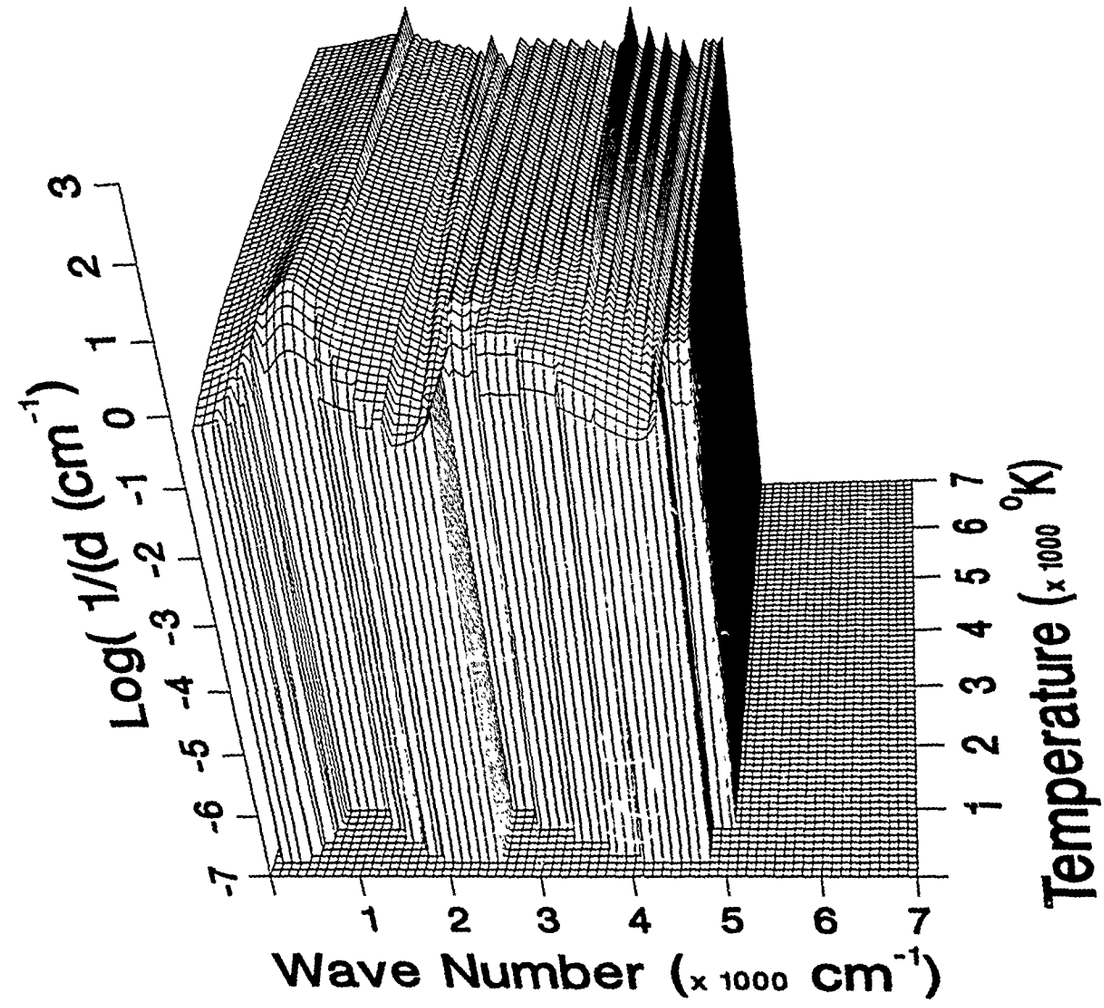

Figure 101. Inverse line spacing for NO^{+}.

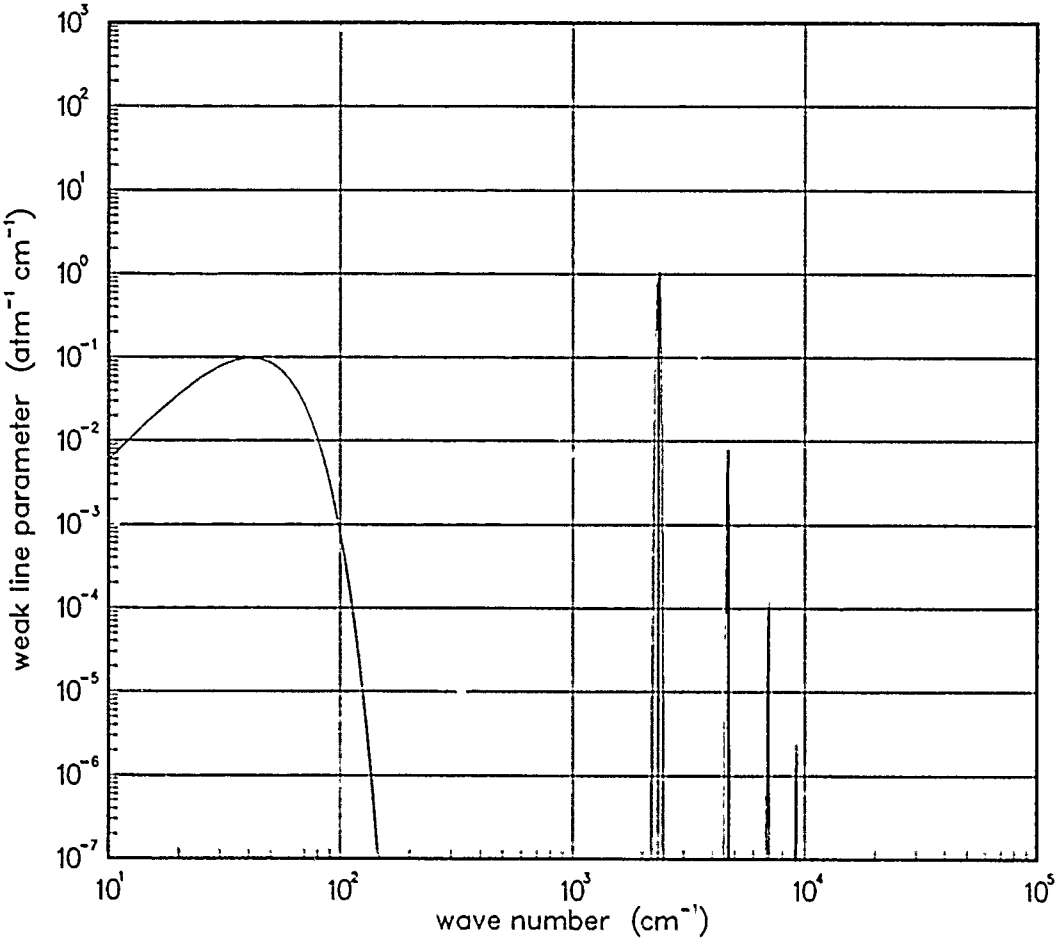

Figure 102. Weak-line parameter for NO^{+} at 200°K.

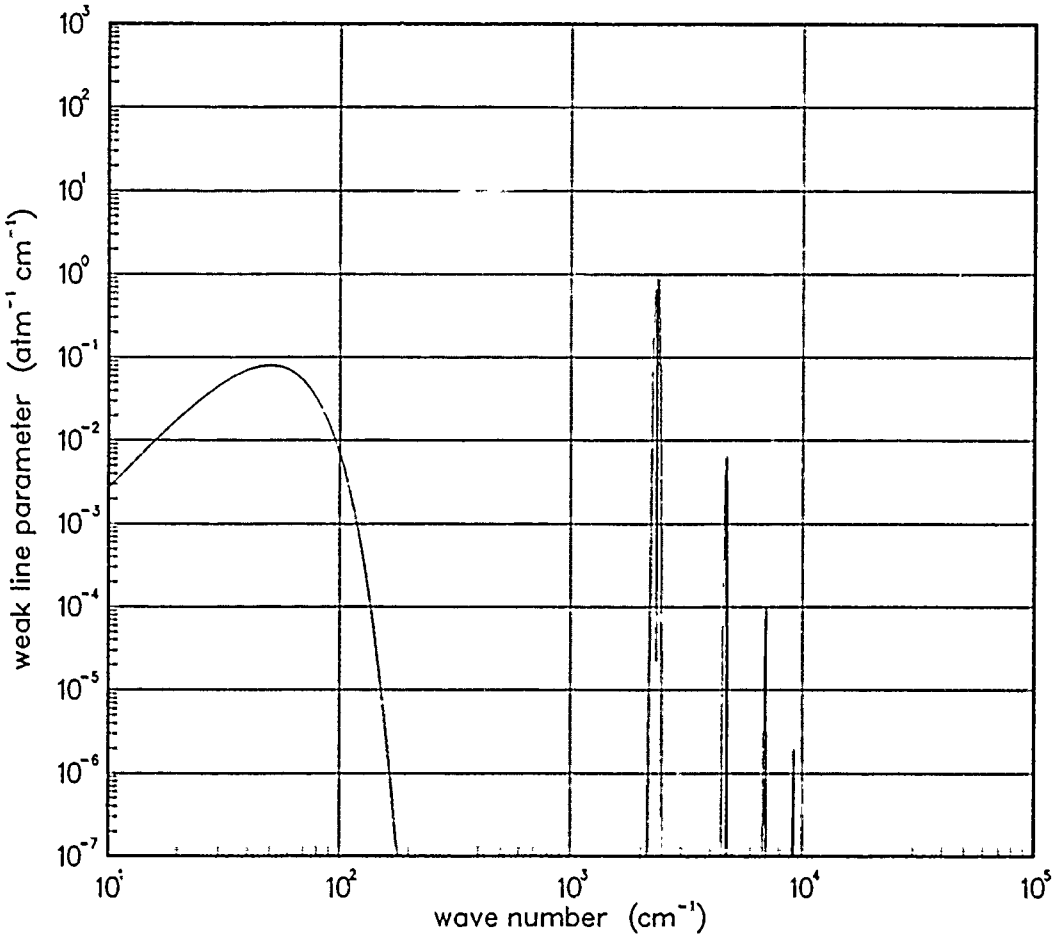

Figure 103. Weak-line parameter for NO^{+} at 300°K.

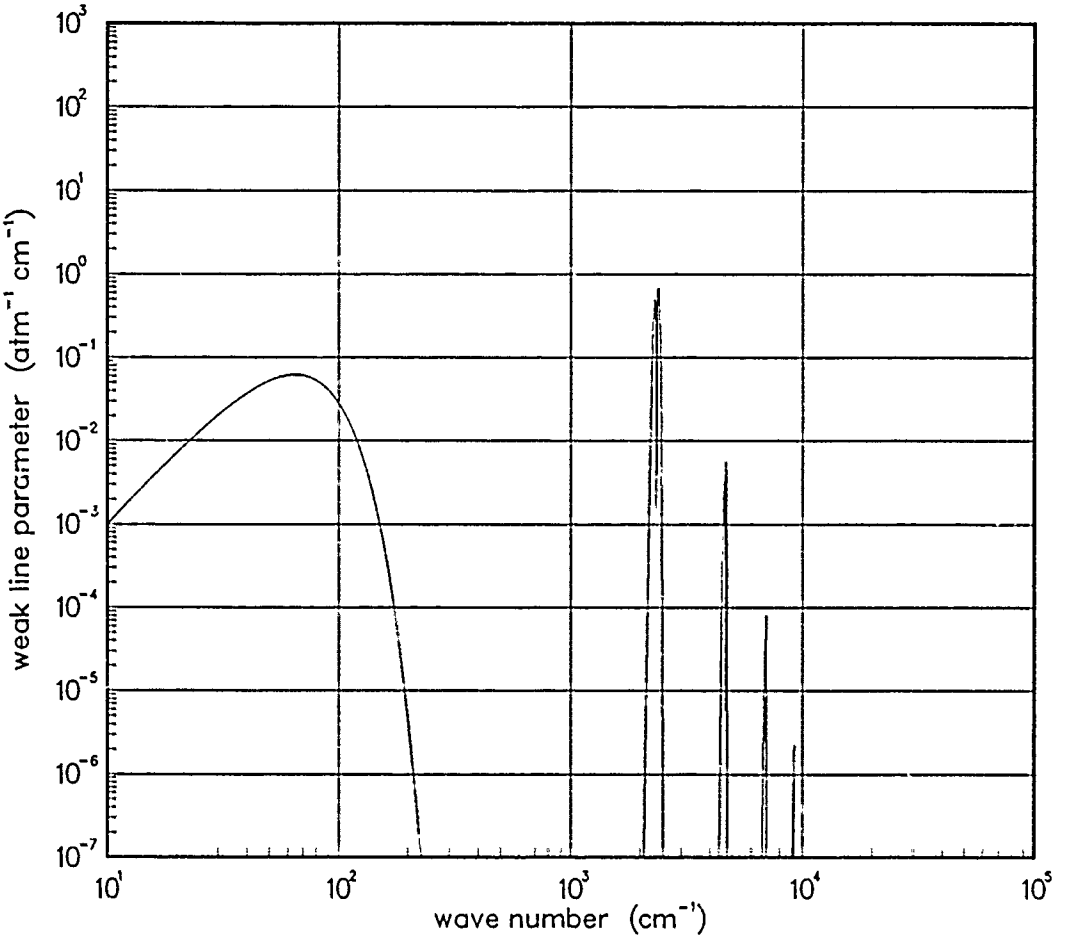

Figure 104. Weak-line parameter for NO^{+} at 500°K.

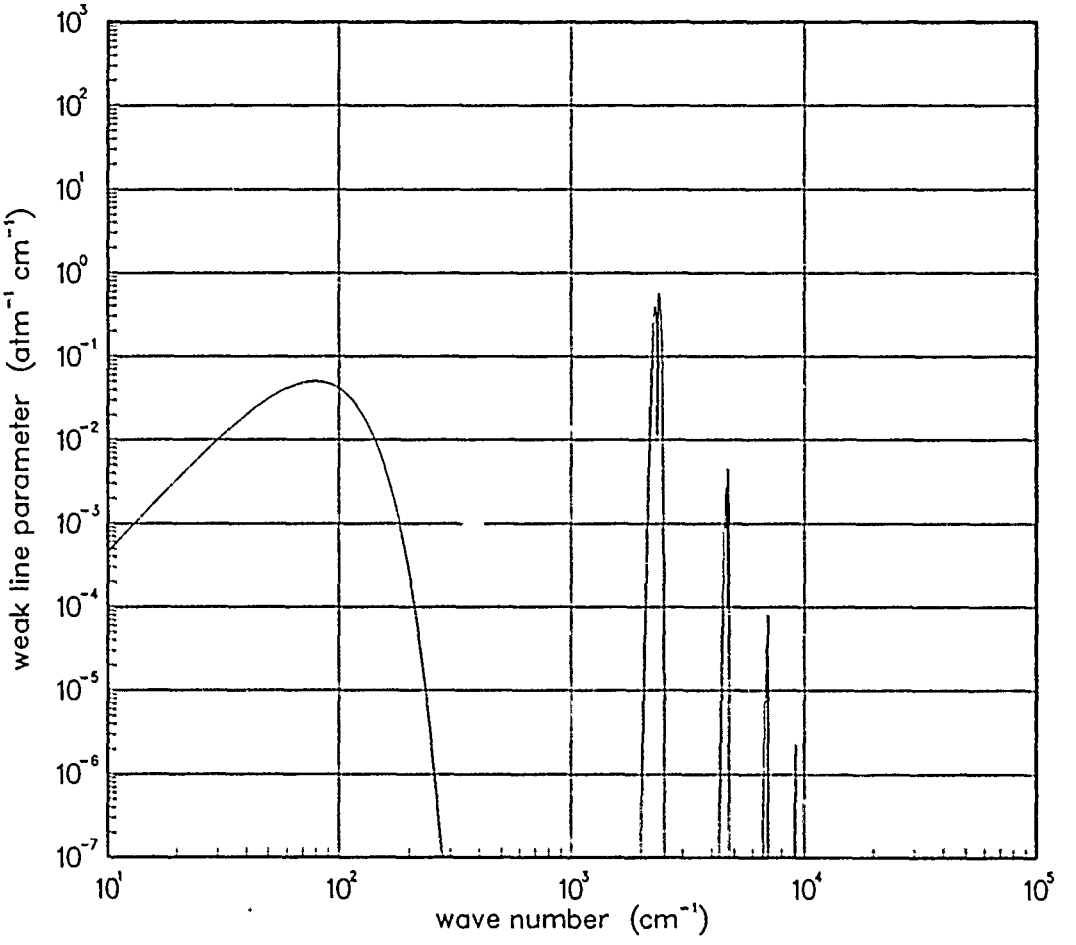

Figure 105. Weak-line parameter for NO^{+} at 750°K.

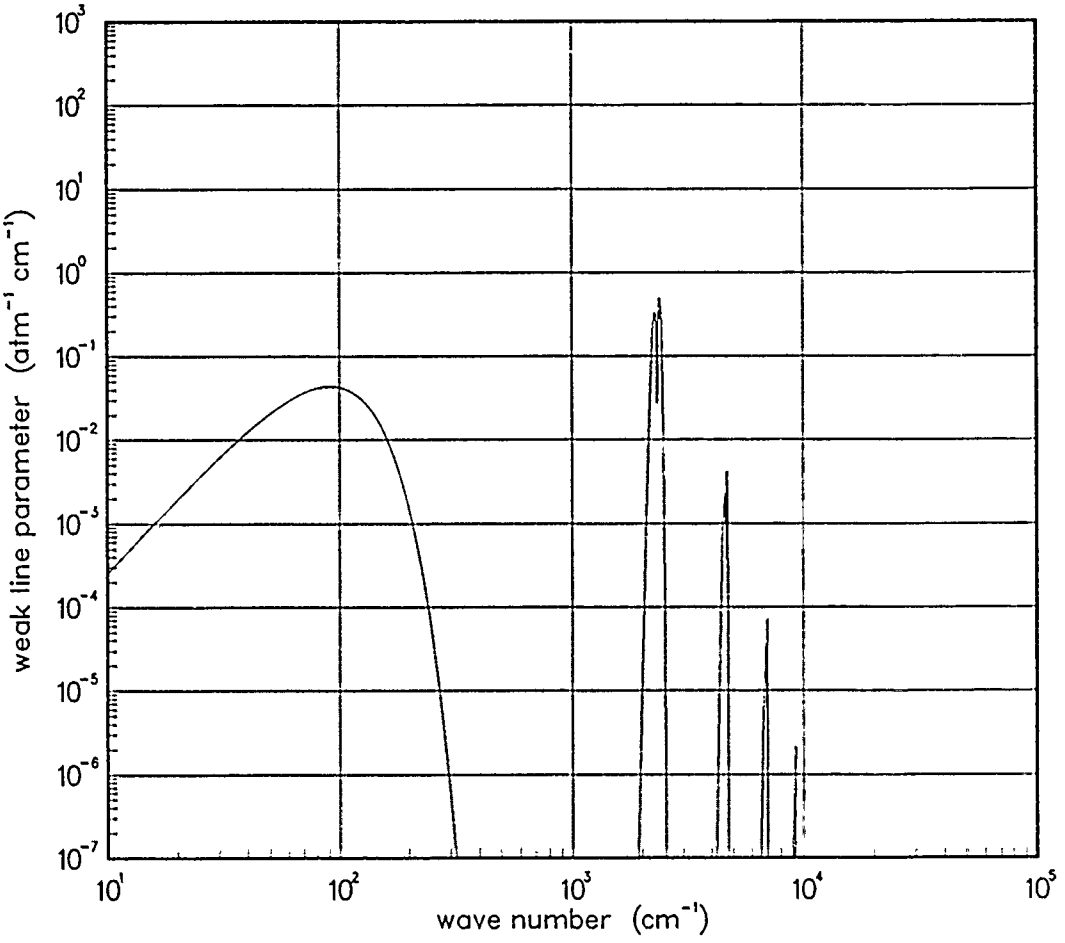

Figure 106. Weak-line parameter for NO^{+} at 1000°K.

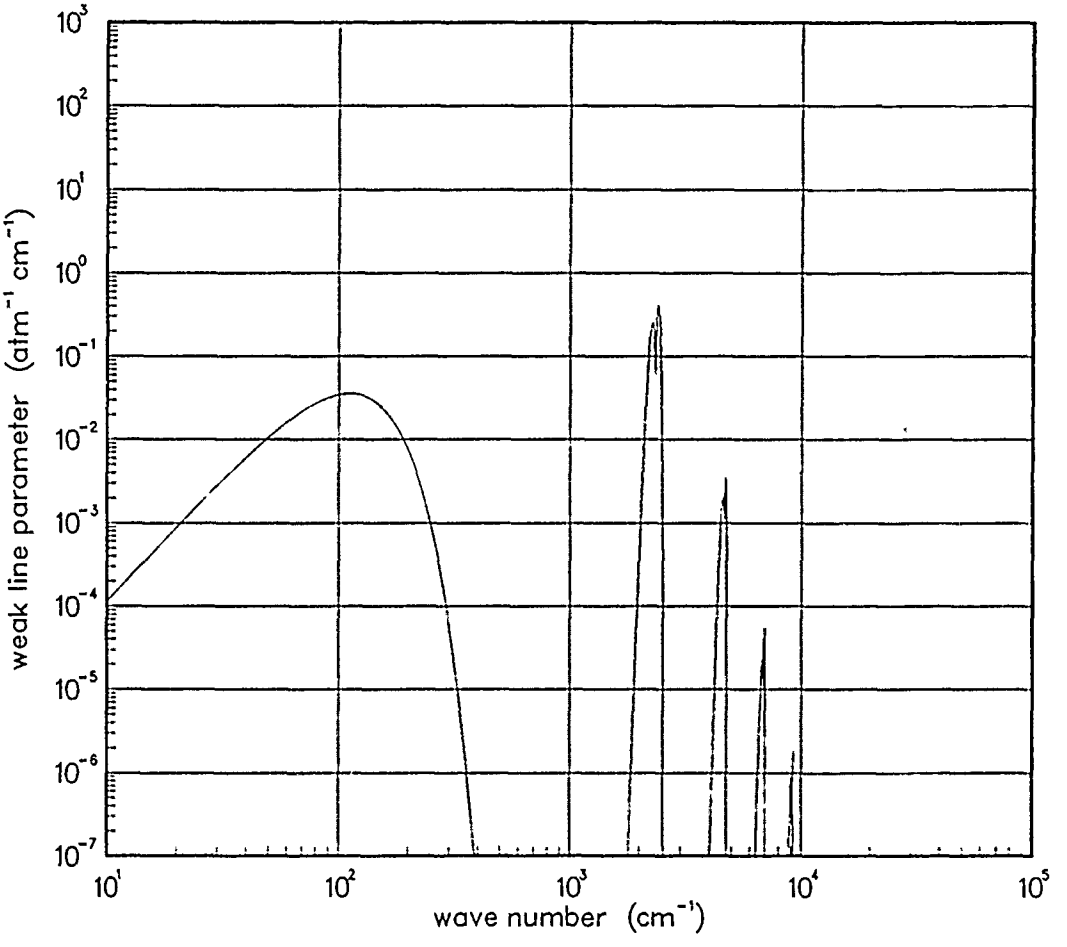

Figure 107. Weak-line parameter for NO^{+} at 1500°K.

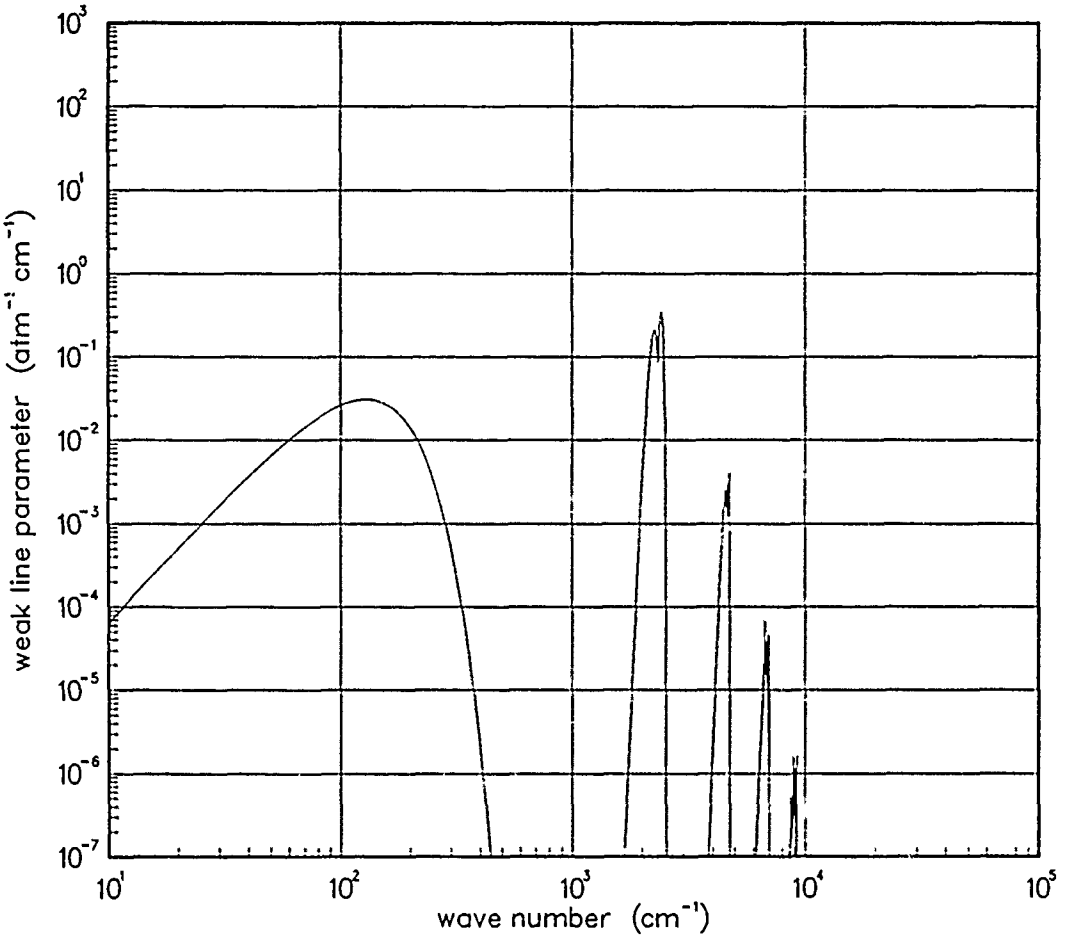

Figure 108. Weak-line parameter for NO^{+} at 2000°K.

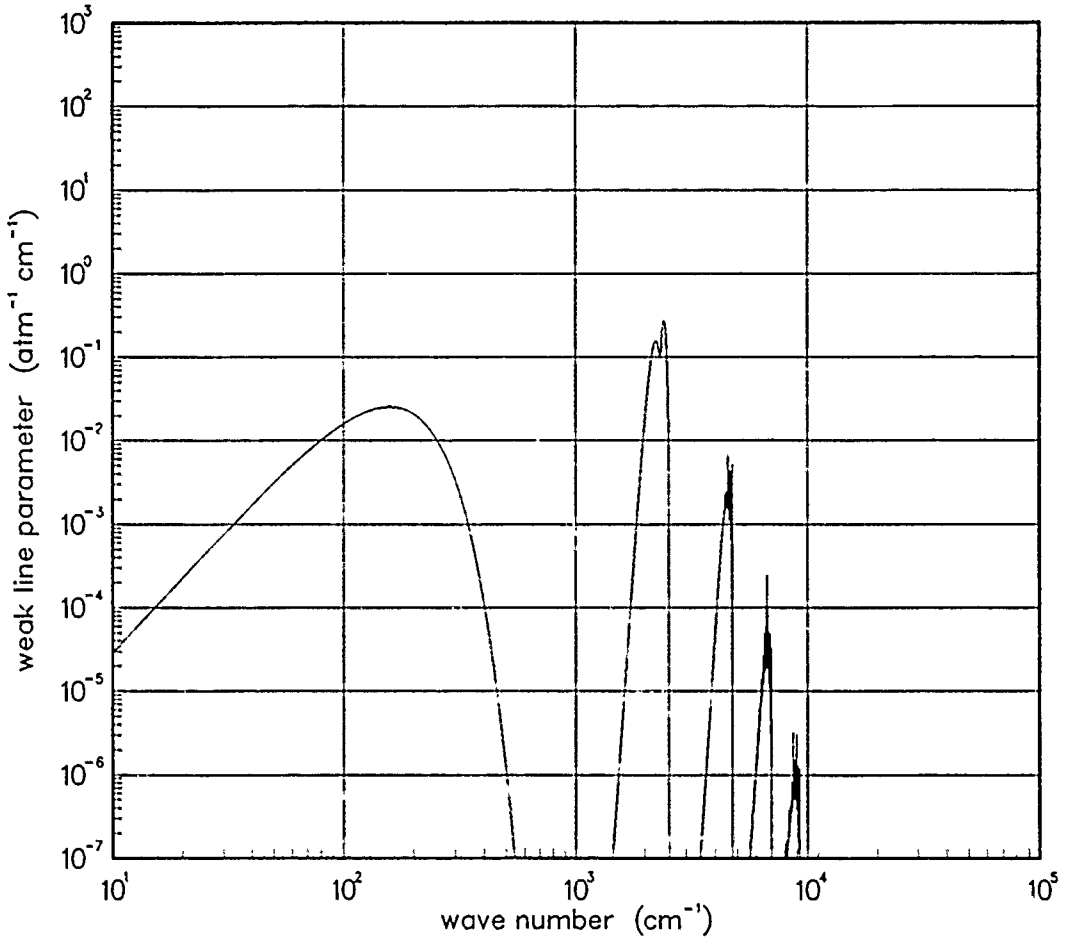

Figure 109. Weak-line parameter for NO^{+} at 3000°K.

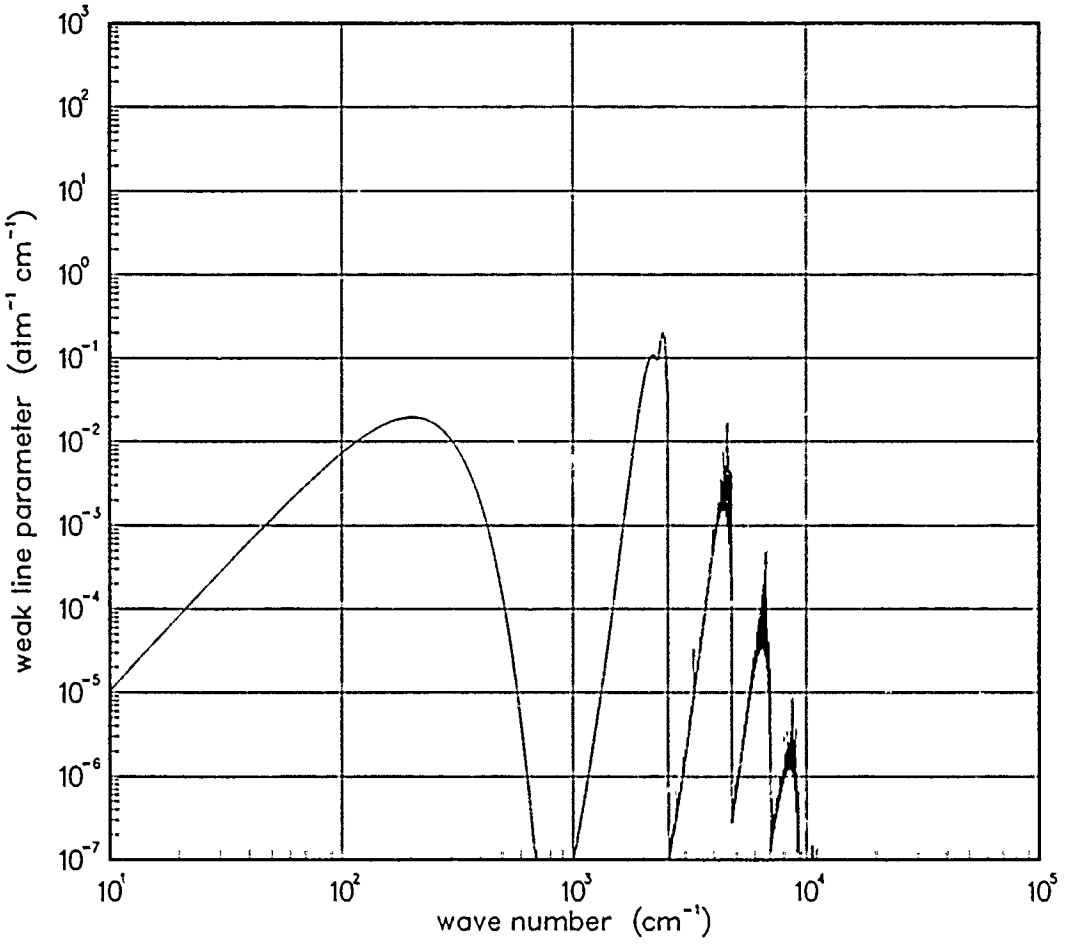

Figure 110. Weak-line parameter for NO^{+} at 5000°K.

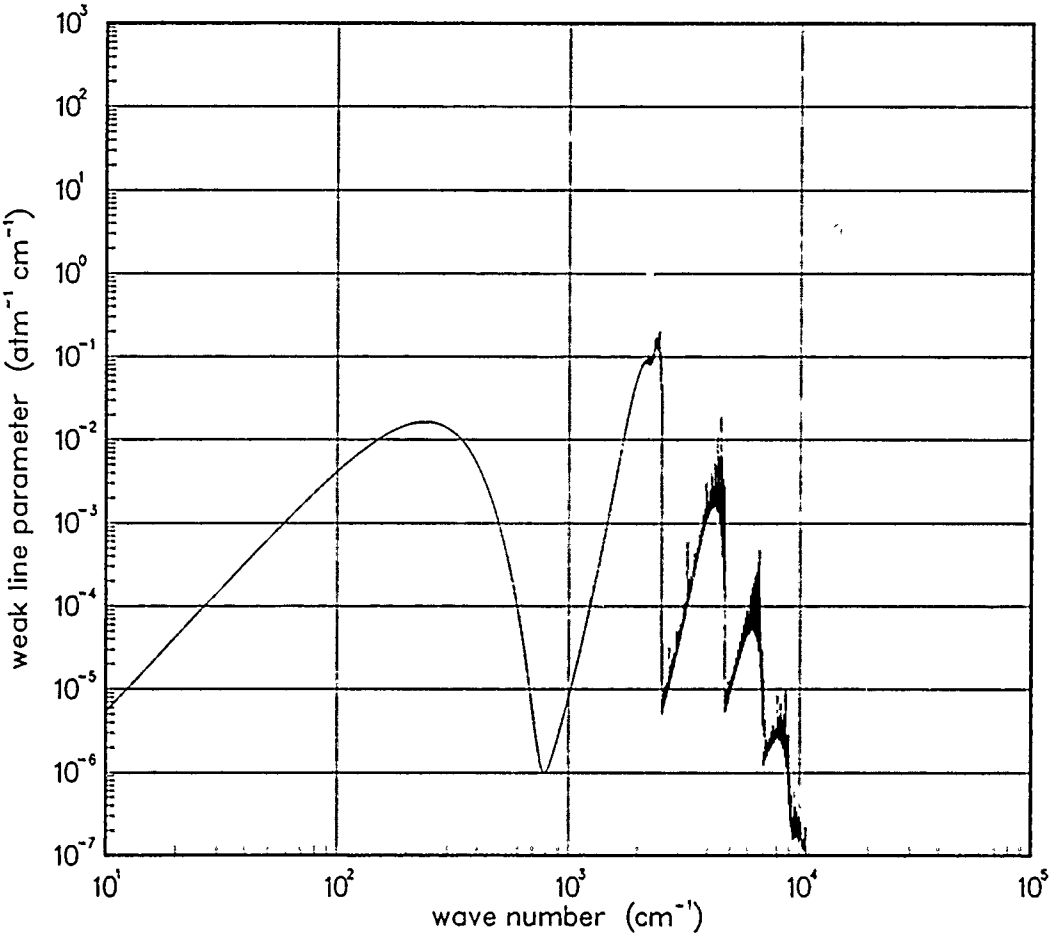

Figure 111. Weak-line parameter for NO^{+} at 7000°K.

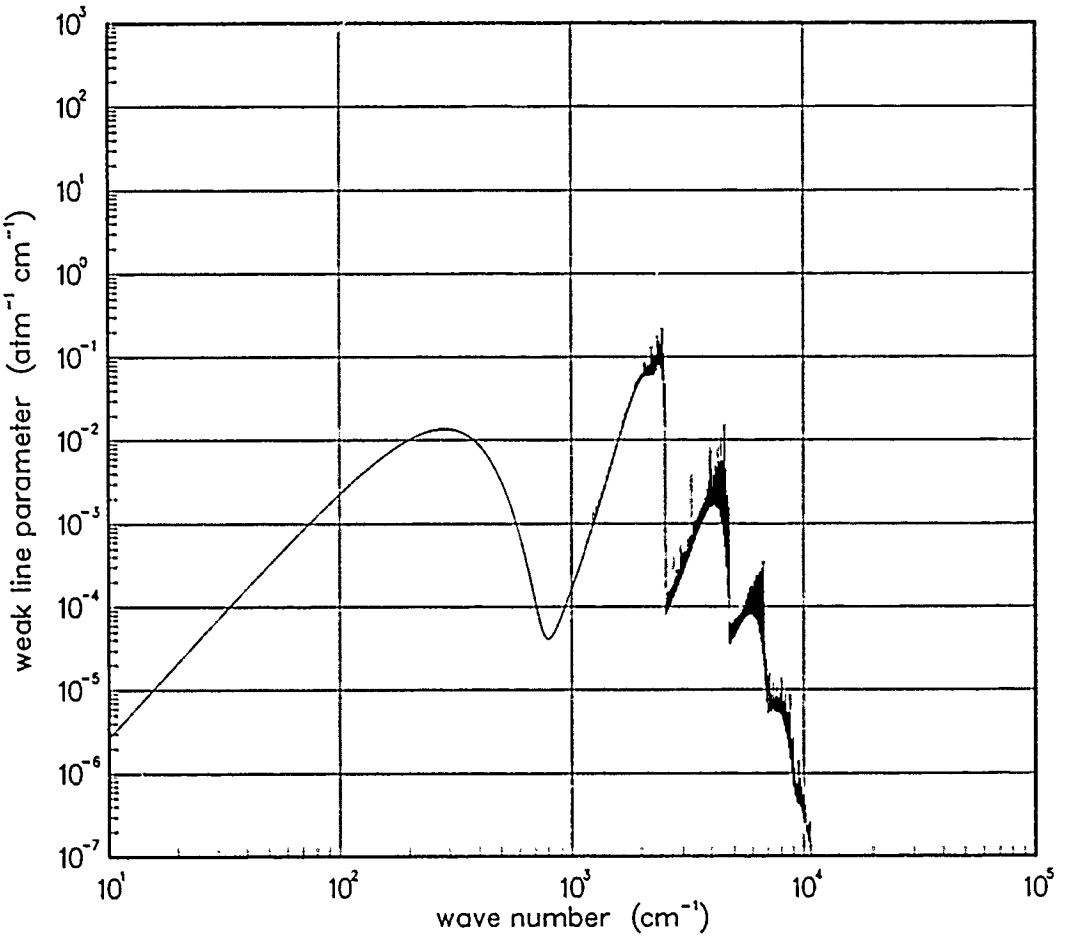

Figure 112. Weak-line parameter for NO^{+} at 10000°K.

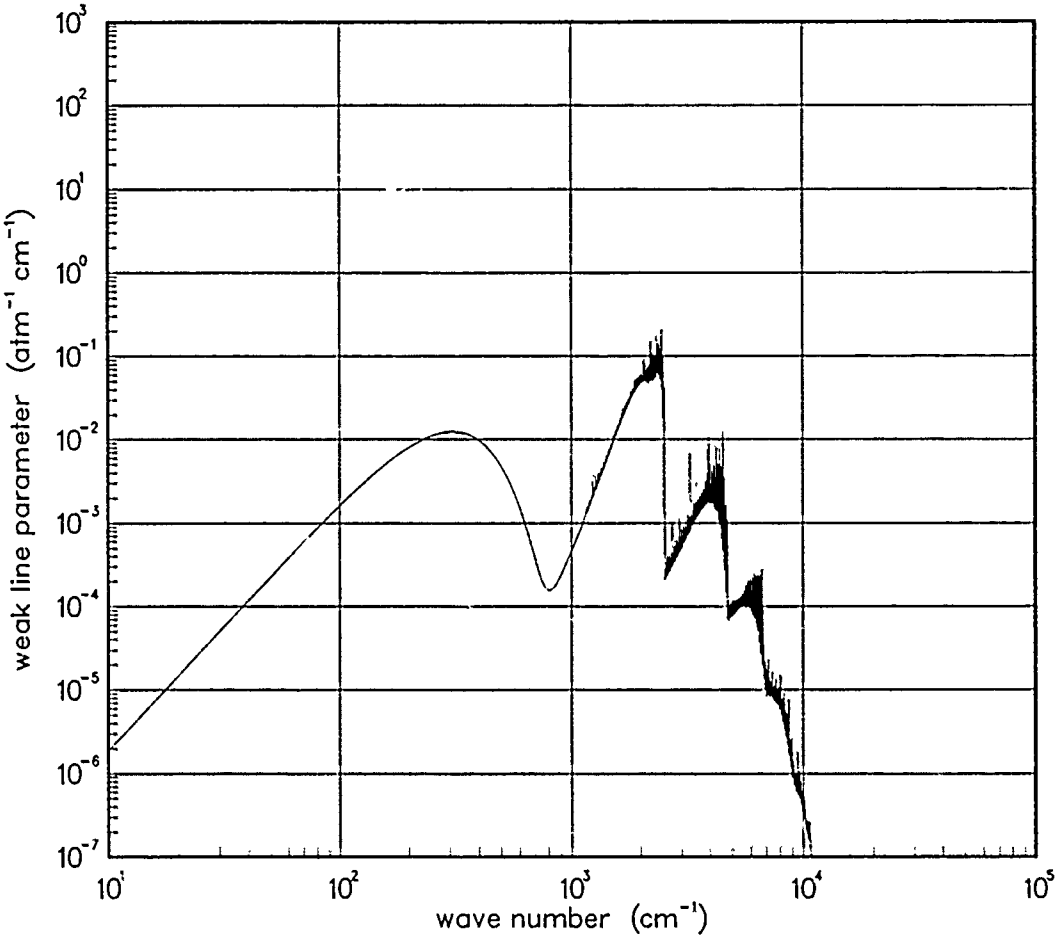

Figure 113. Weak-line parameter for NO^{+} at 12000°K.

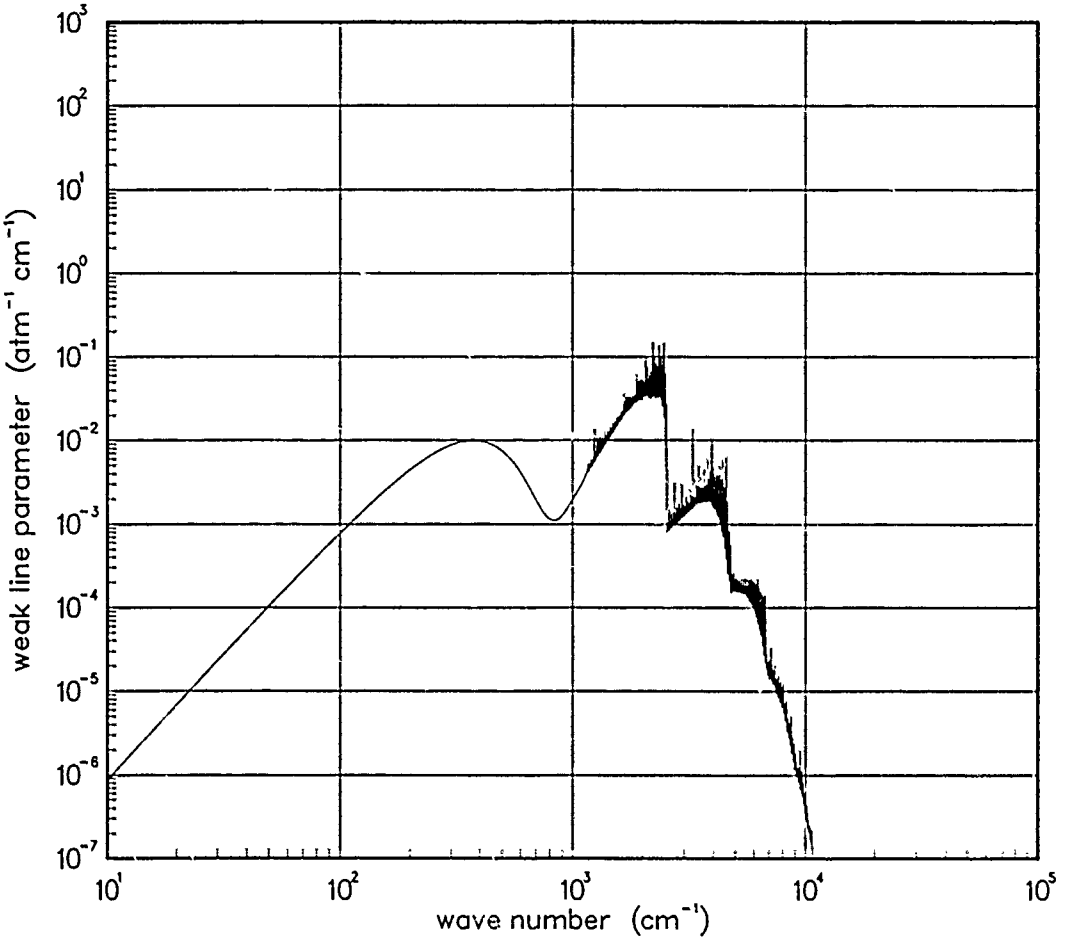

Figure 114. Weak-line parameter for NO^{+} at 18000°K.

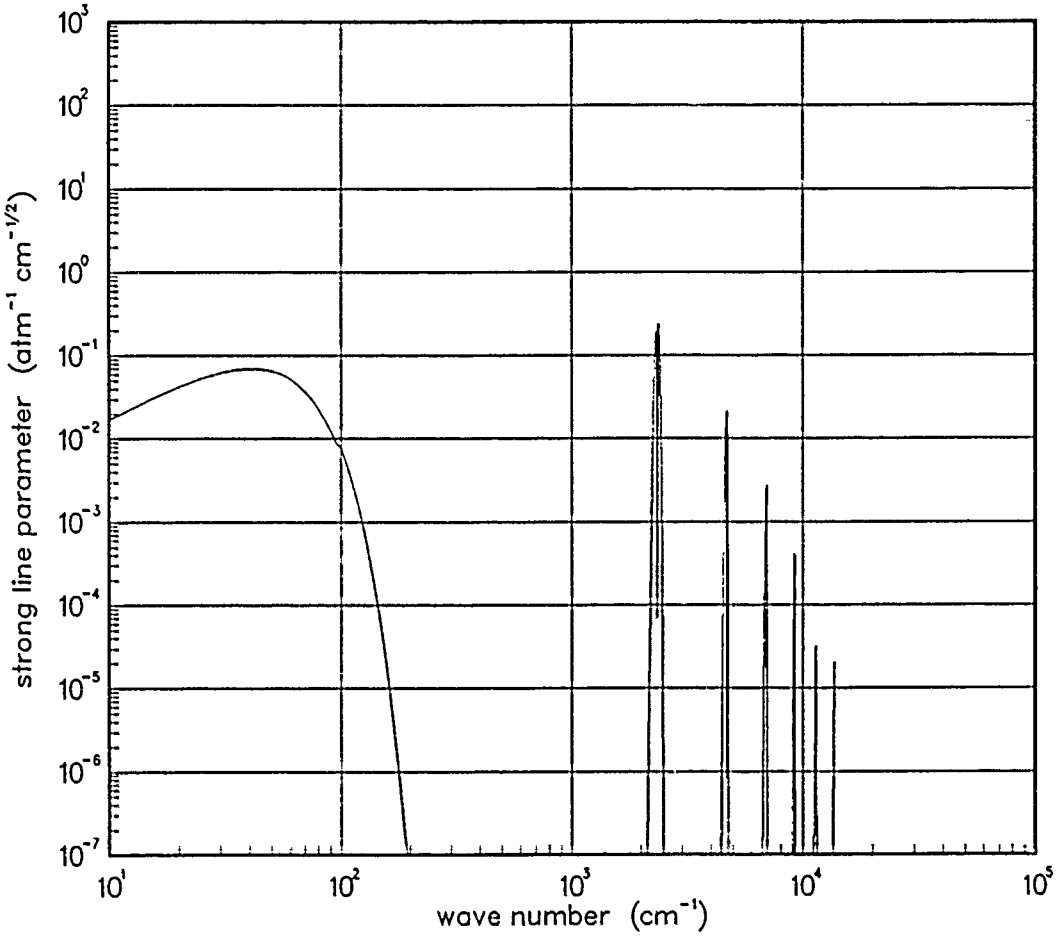

Figure 115. Strong-line parameter for NO^{+} at 200°K.

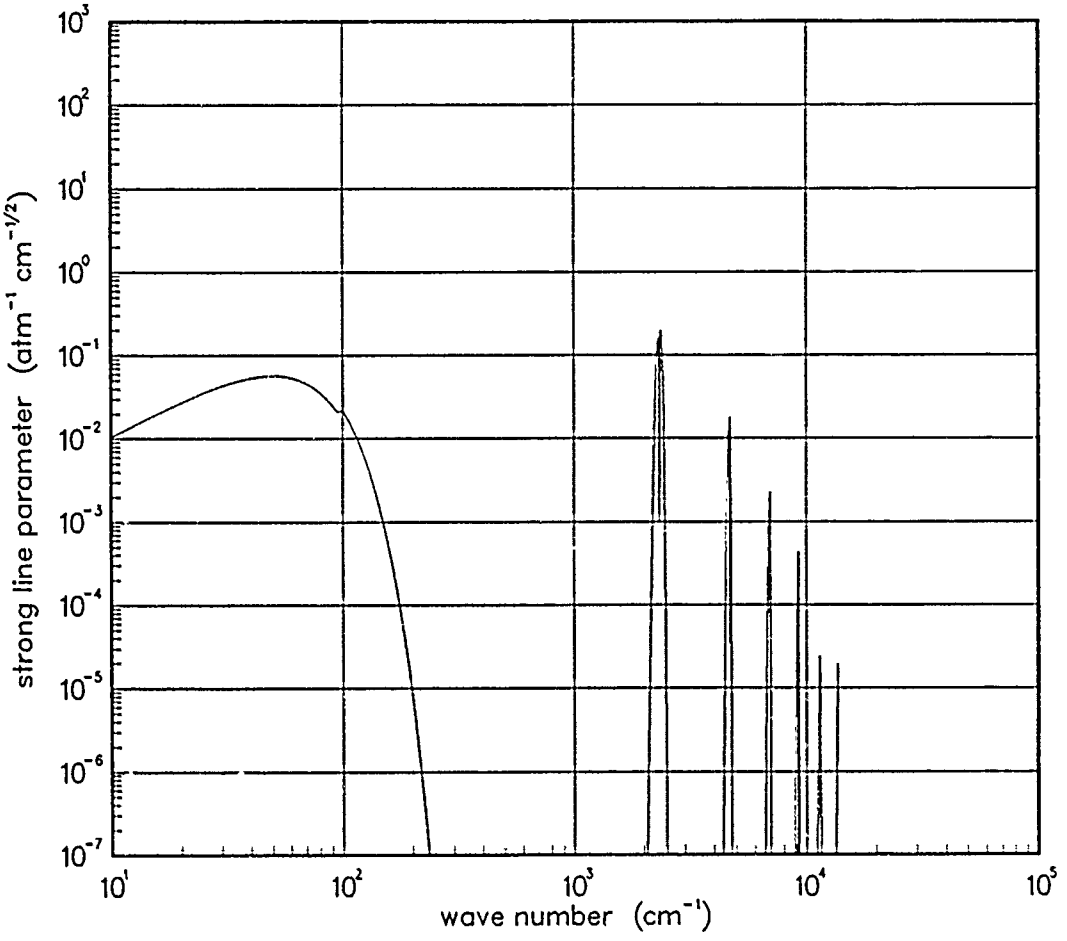

Figure 116. Strong-line parameter for NO^{+} at 300°K.

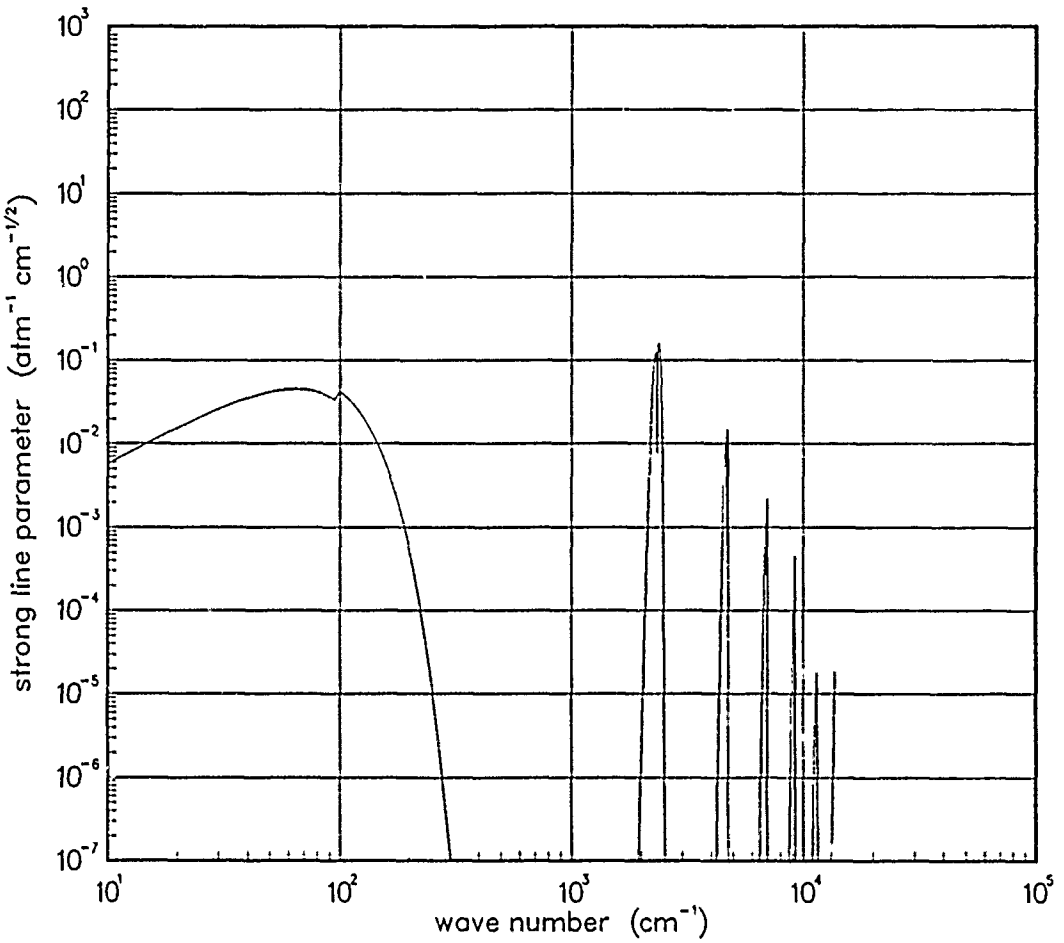

Figure 117. Strong-line parameter for NO^{+} at 500°K.

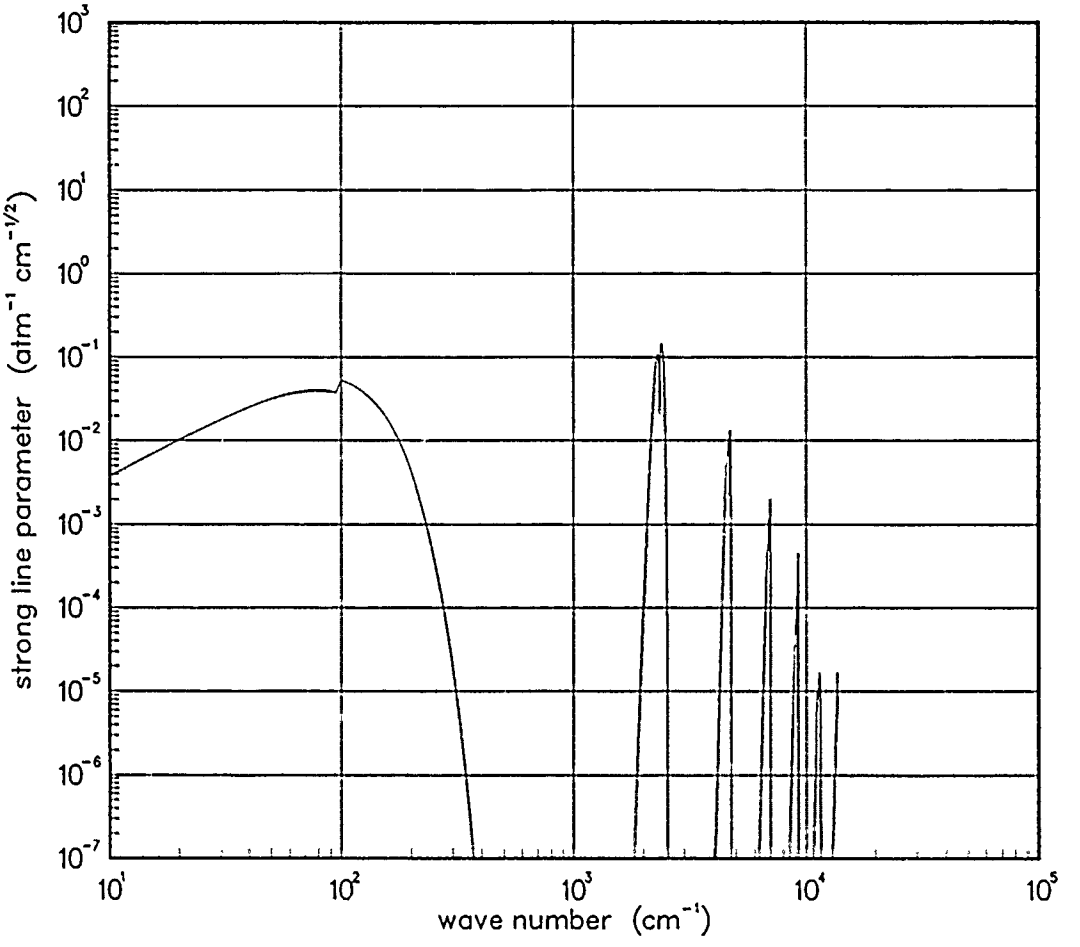

Figure 118. Strong-line parameter for NO^{+} at 750°K.

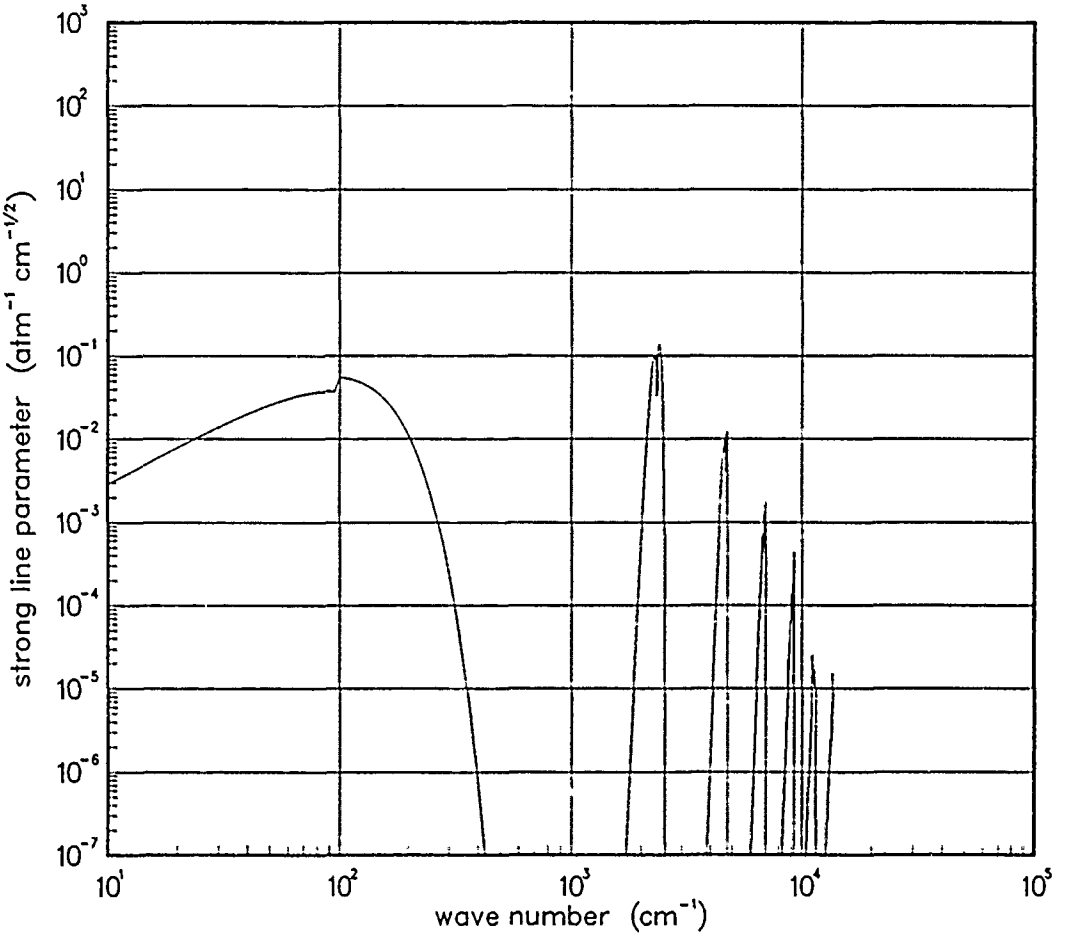

Figure 119. Strong-line parameter for NO^+ at 1000°K.

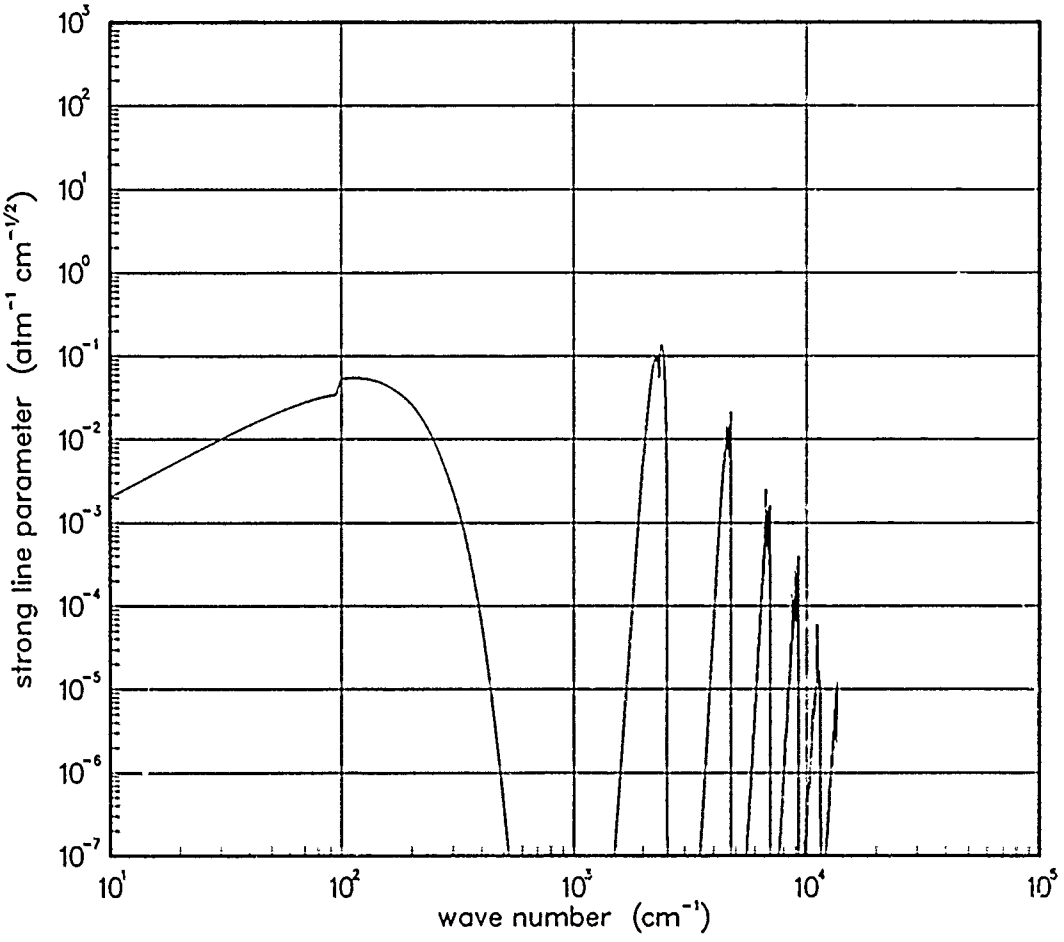

Figure 120. Strong-line parameter for NO^+ at 1500°K.

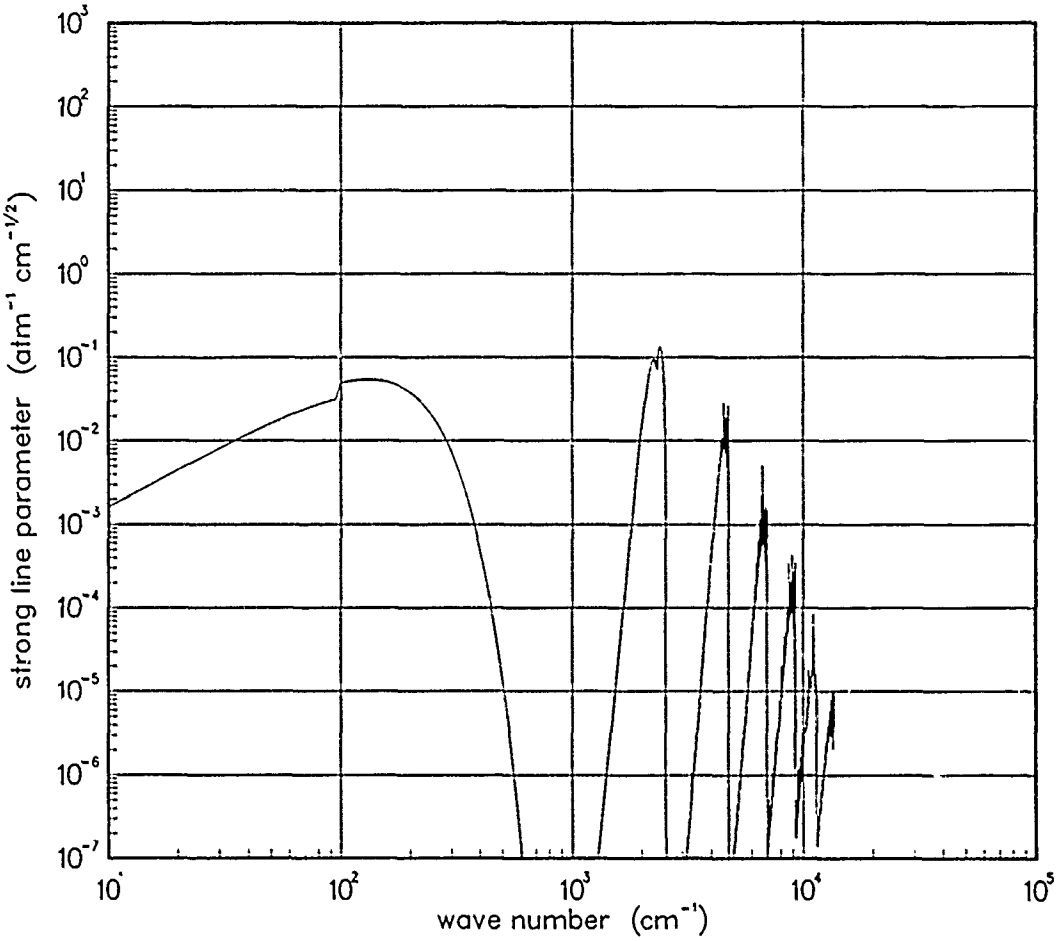

Figure 121. Strong-line parameter for NO^{+} at 2000°K.

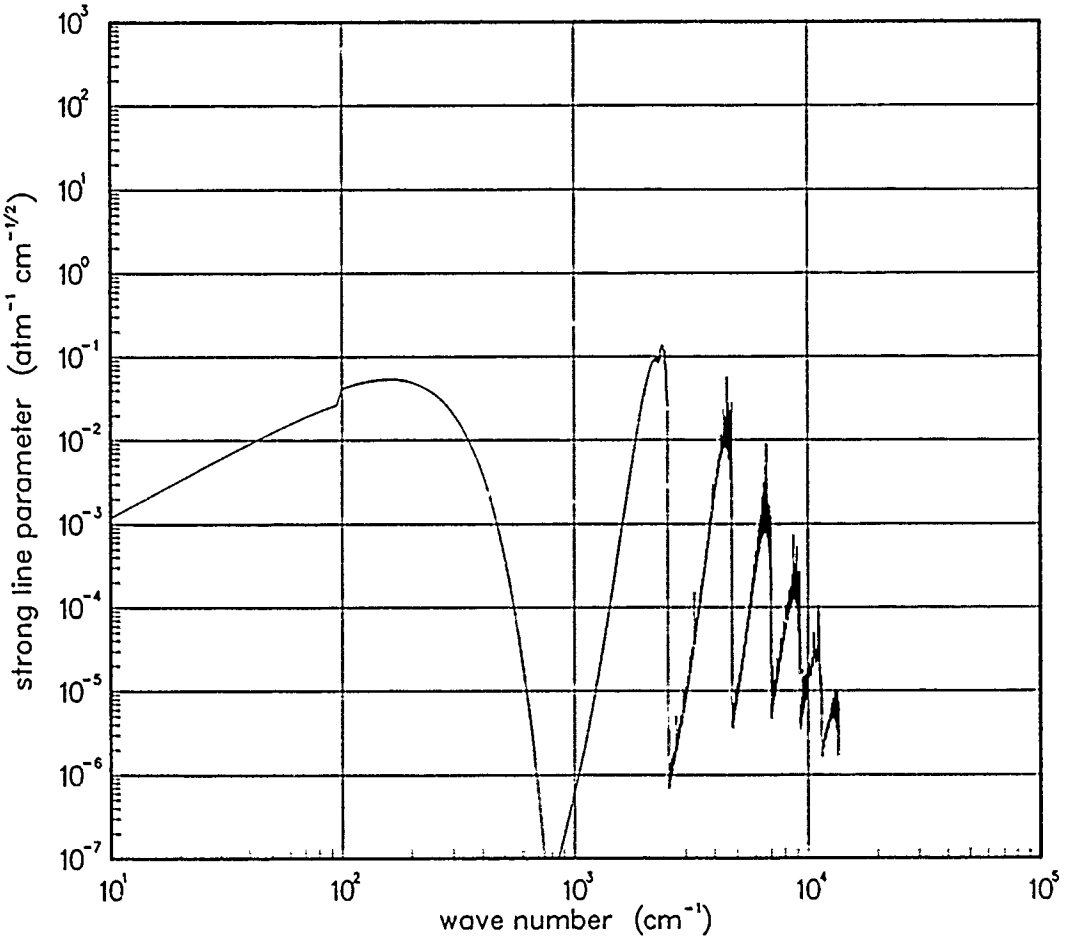

Figure 122. Strong-line parameter for NO^{+} at 3000°K.

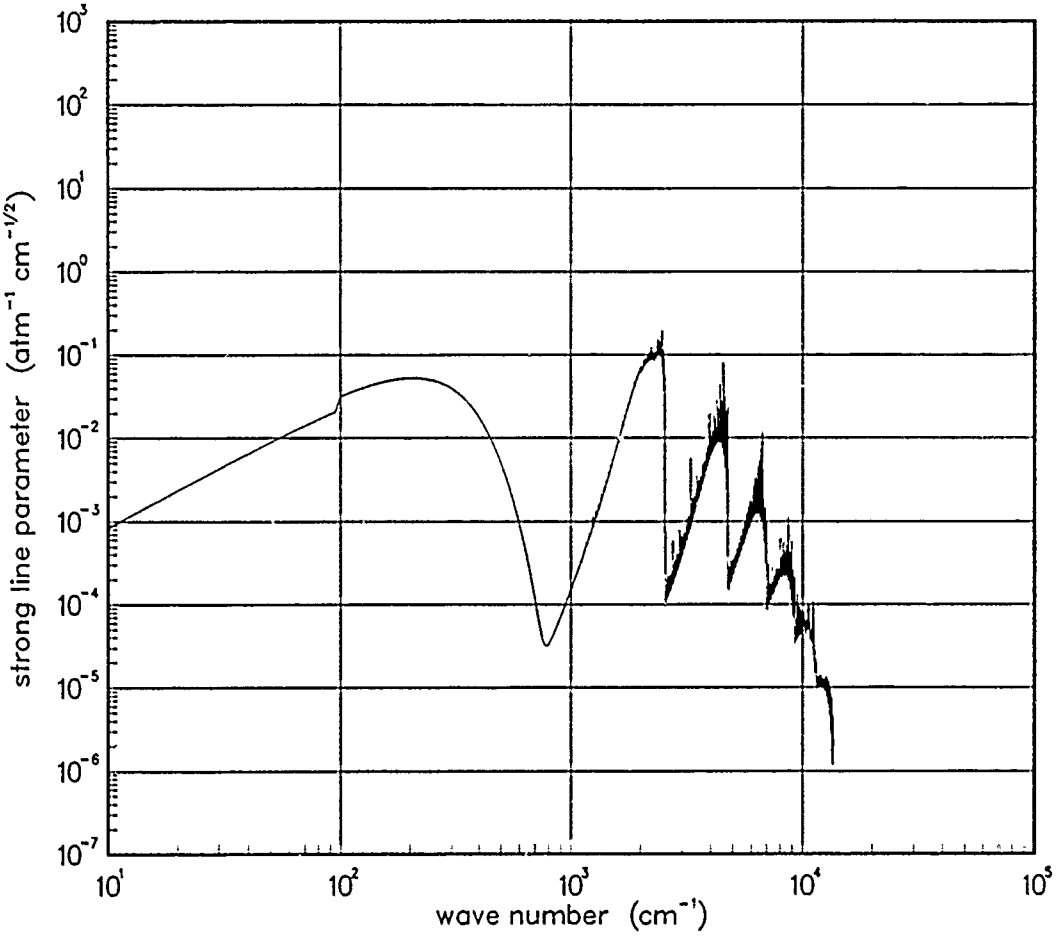

Figure 123. Strong-line parameter for NO^{+} at 5000°K.

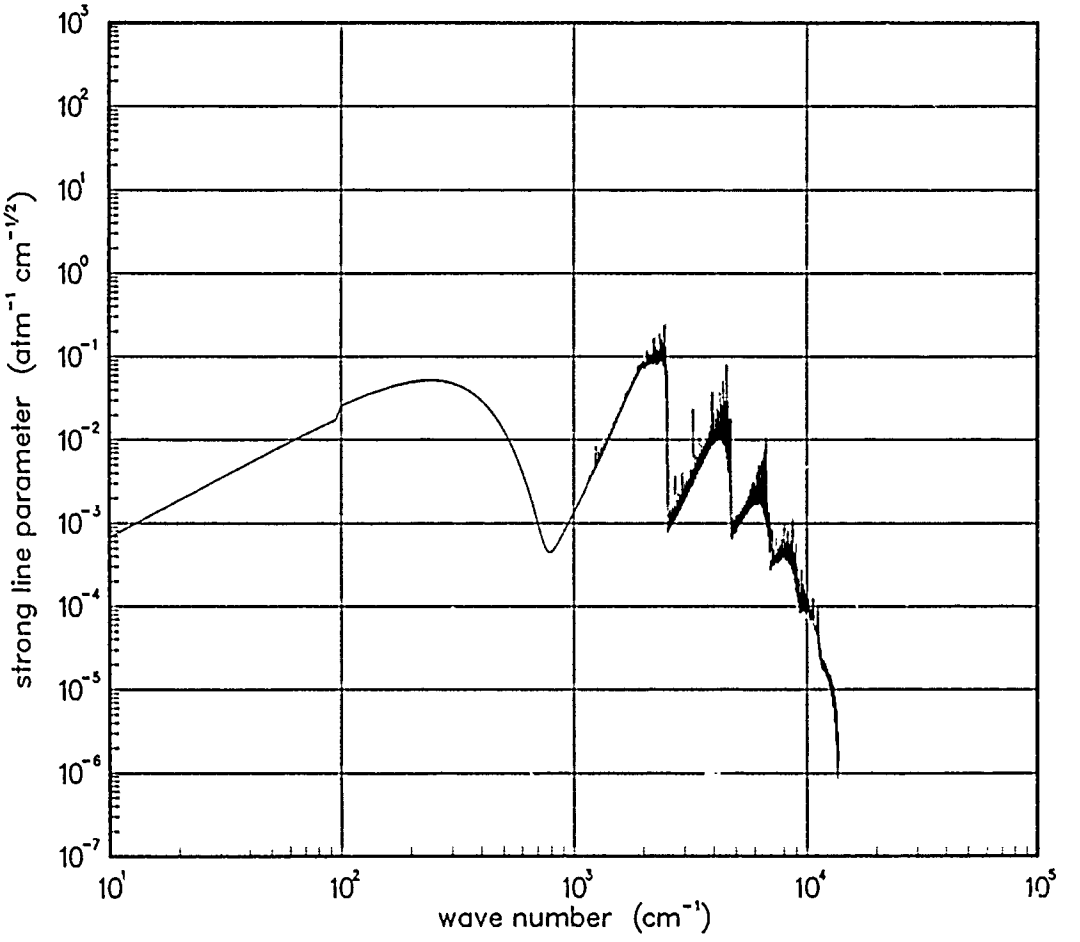

Figure 124. Strong-line parameter for NO^{+} at 7000°K.

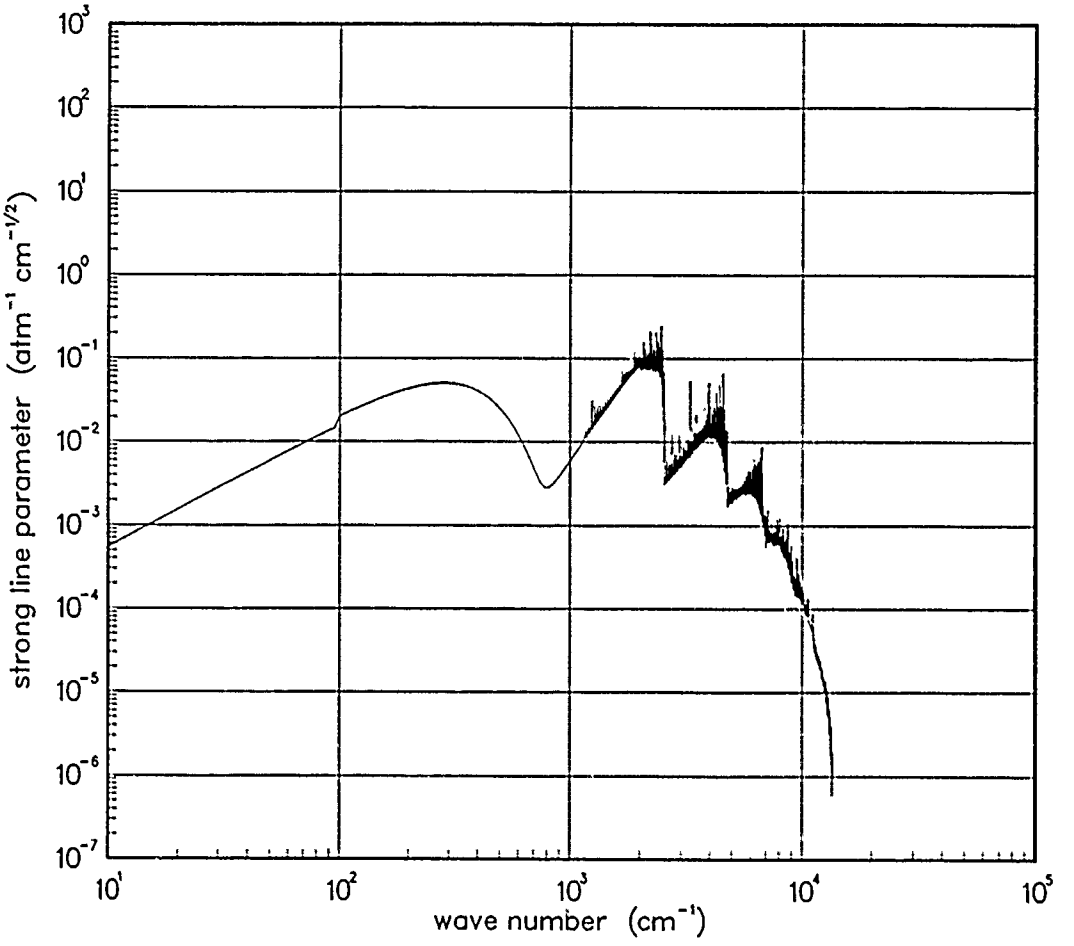

Figure 125. Strong-line parameter for NO^{+} at 10000°K.

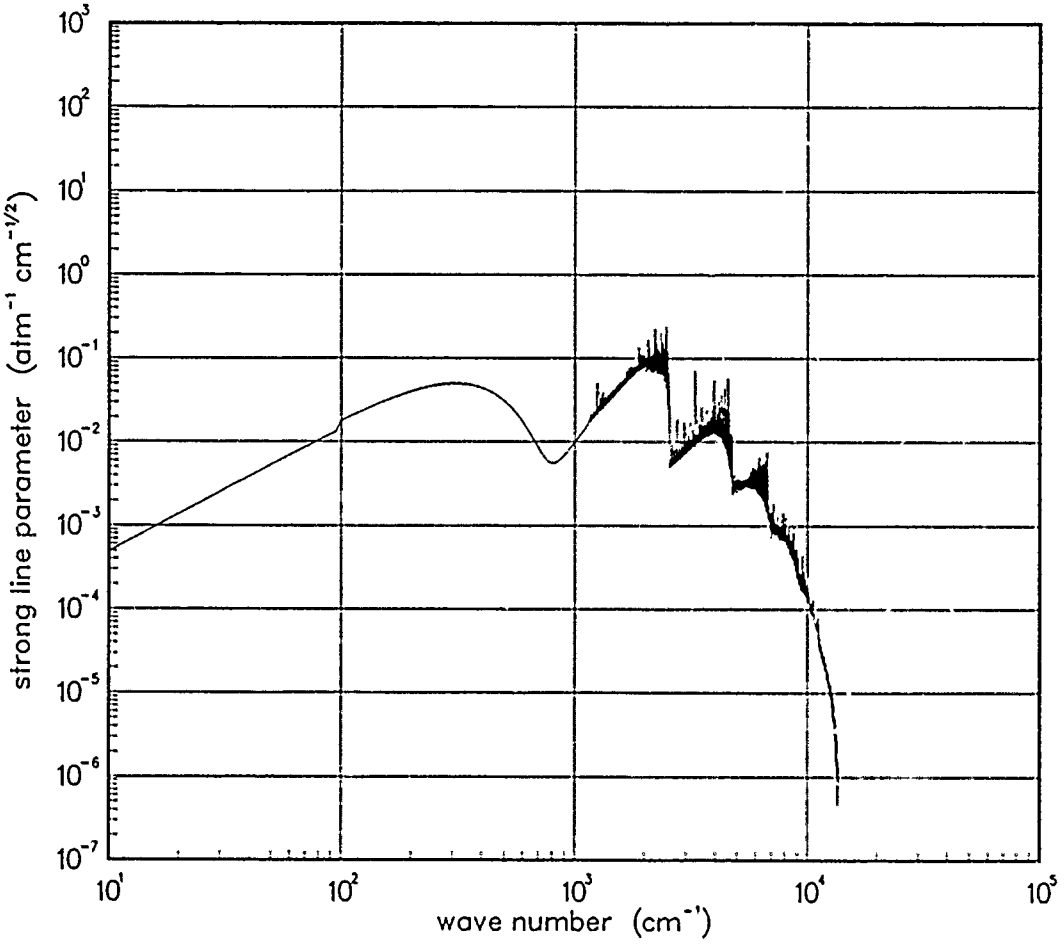

Figure 126. Strong-line parameter for NO^{+} at 12000°K.

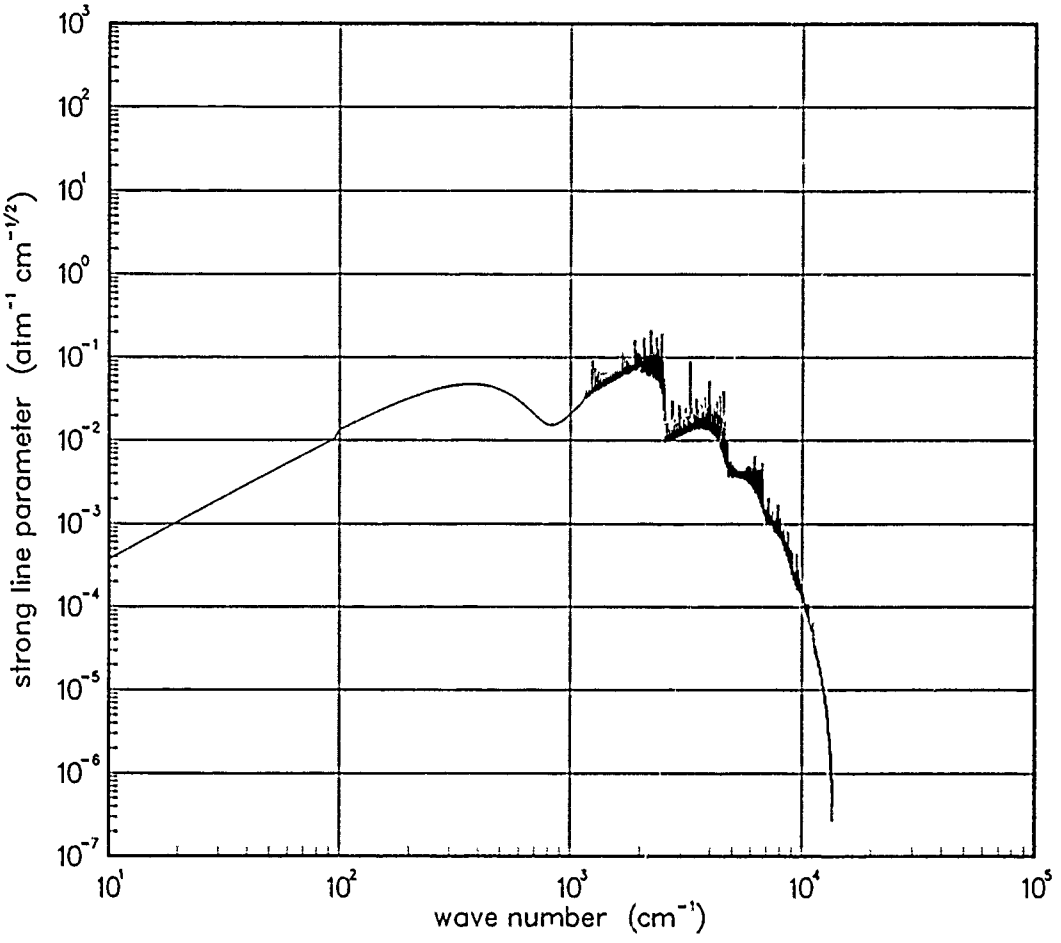

Figure 127. Strong-line parameter for NO^{+} at 18000°K.

4.5 OXYGEN (O_2).

The local thermal equilibrium emission spectra for the Oxygen molecule was calculated by VisiDyne Corporation* using an Air Force Weapons Laboratory opacity data base developed in the late sixties. Data for the weak-line parameter for O_2 in the visible region (5,000 cm^{-1} - 100,000 cm^{-1}) is available. There is no inverse line spacing information available for this molecule.

Data Source:

*H. Smith, T. Keneshea, VisiDyne Corporation, private communication (1986).

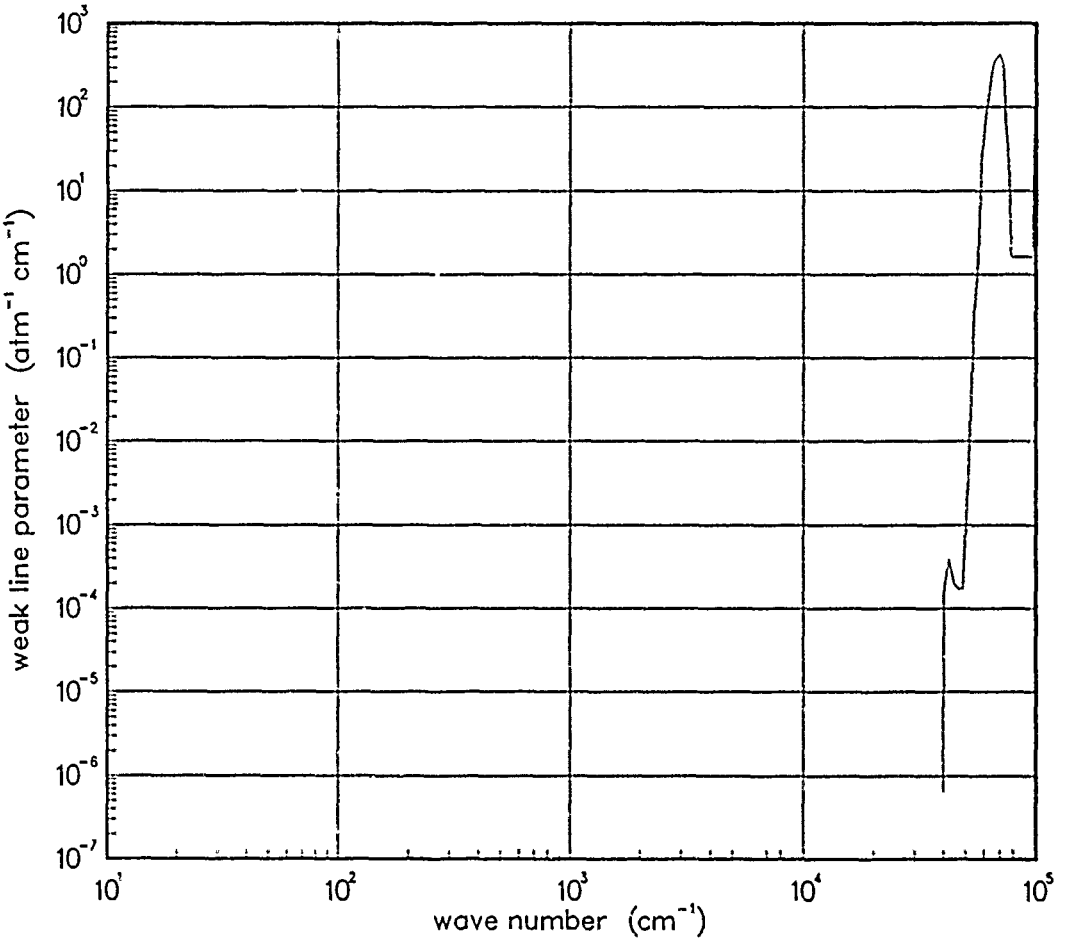

Figure 128. Weak-line parameter for O_2 at 200°K.

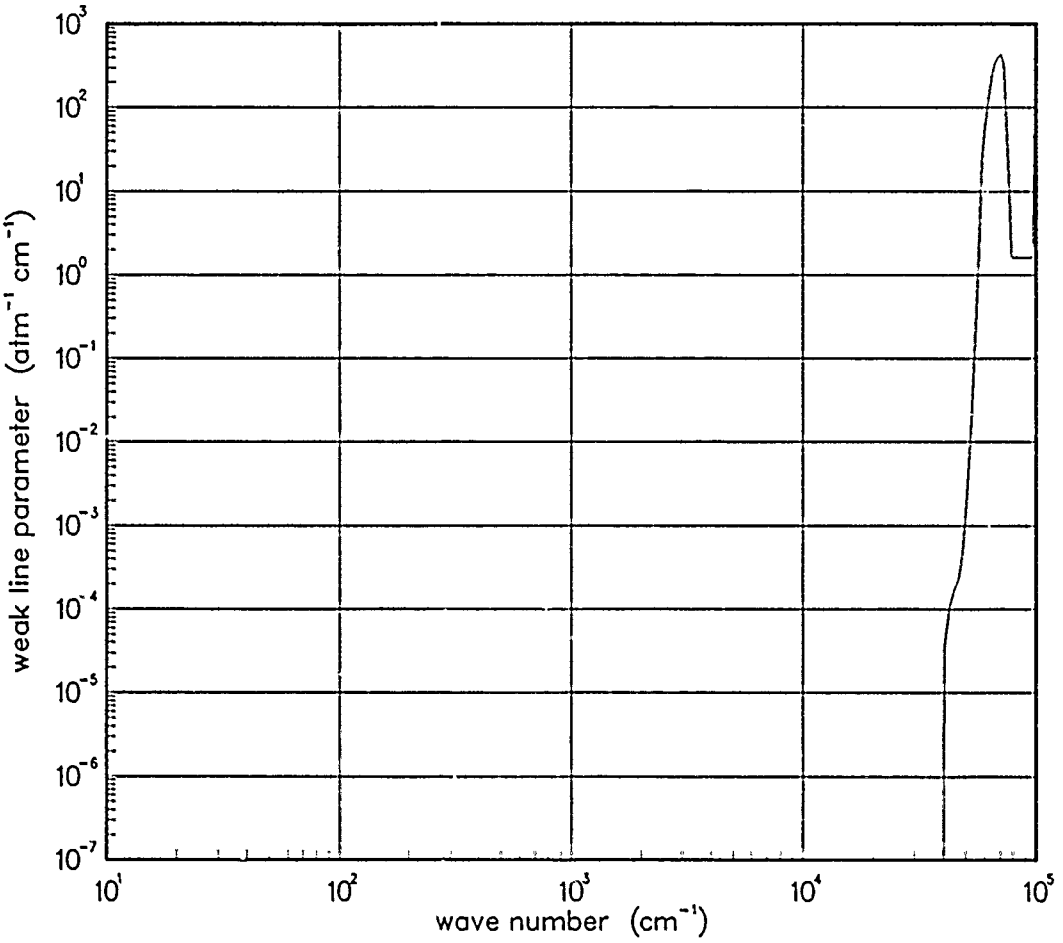

Figure 129. Weak-line parameter for O_2 at 300°K.

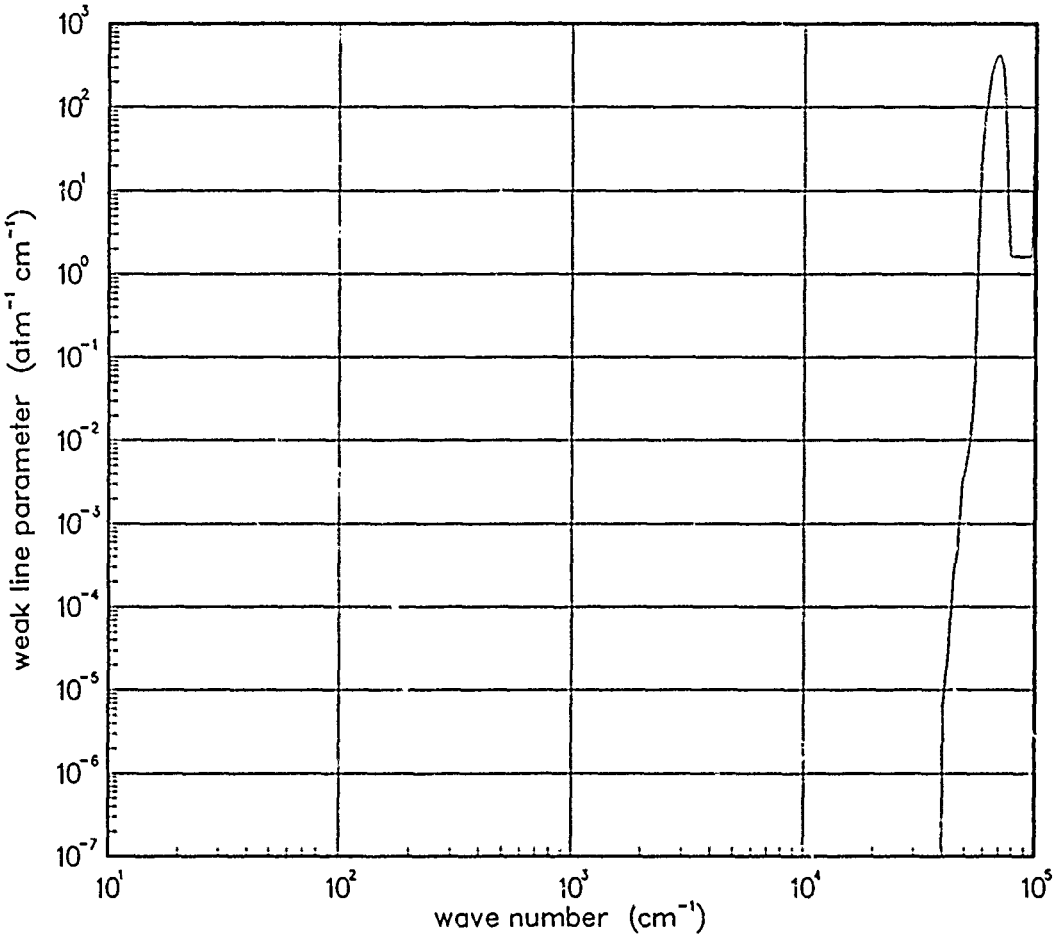

Figure 130. Weak-line parameter for O_2 at 500°K.

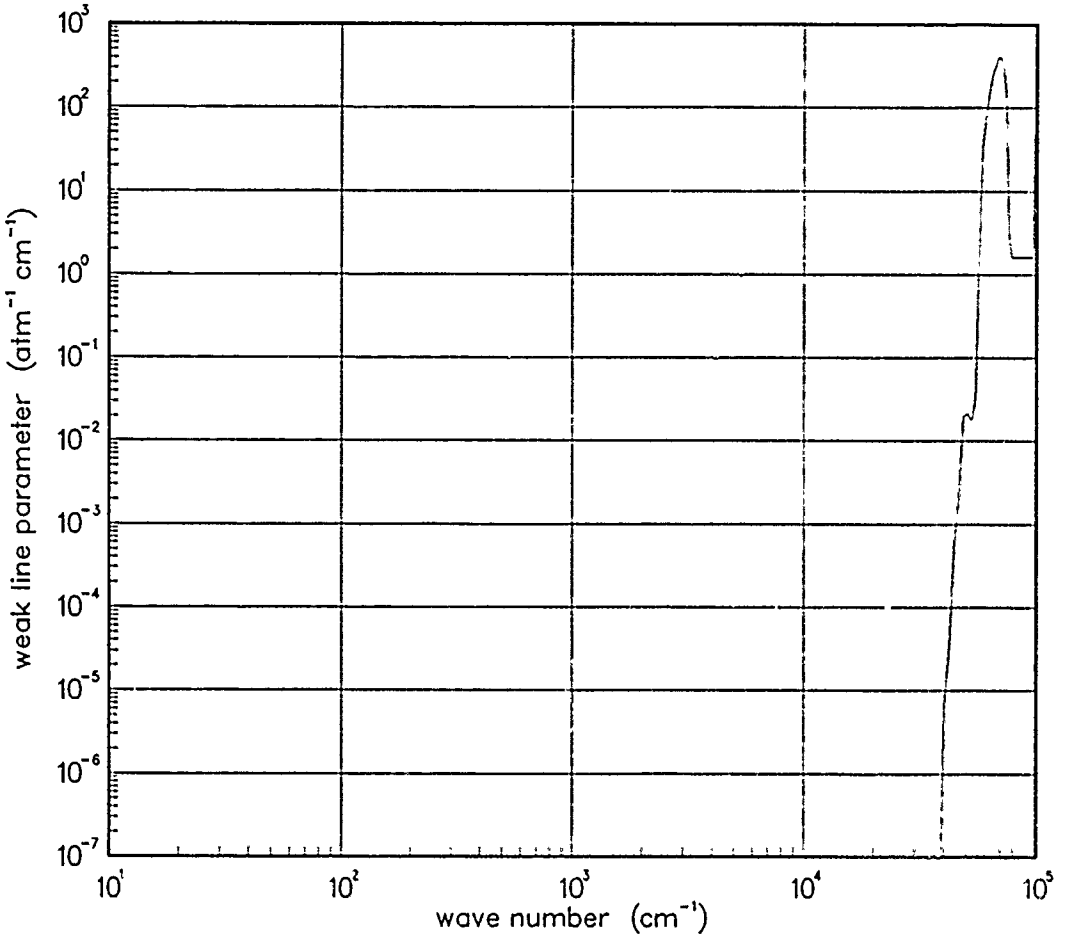

Figure 131. Weak-line parameter for O_2 at 750°K.

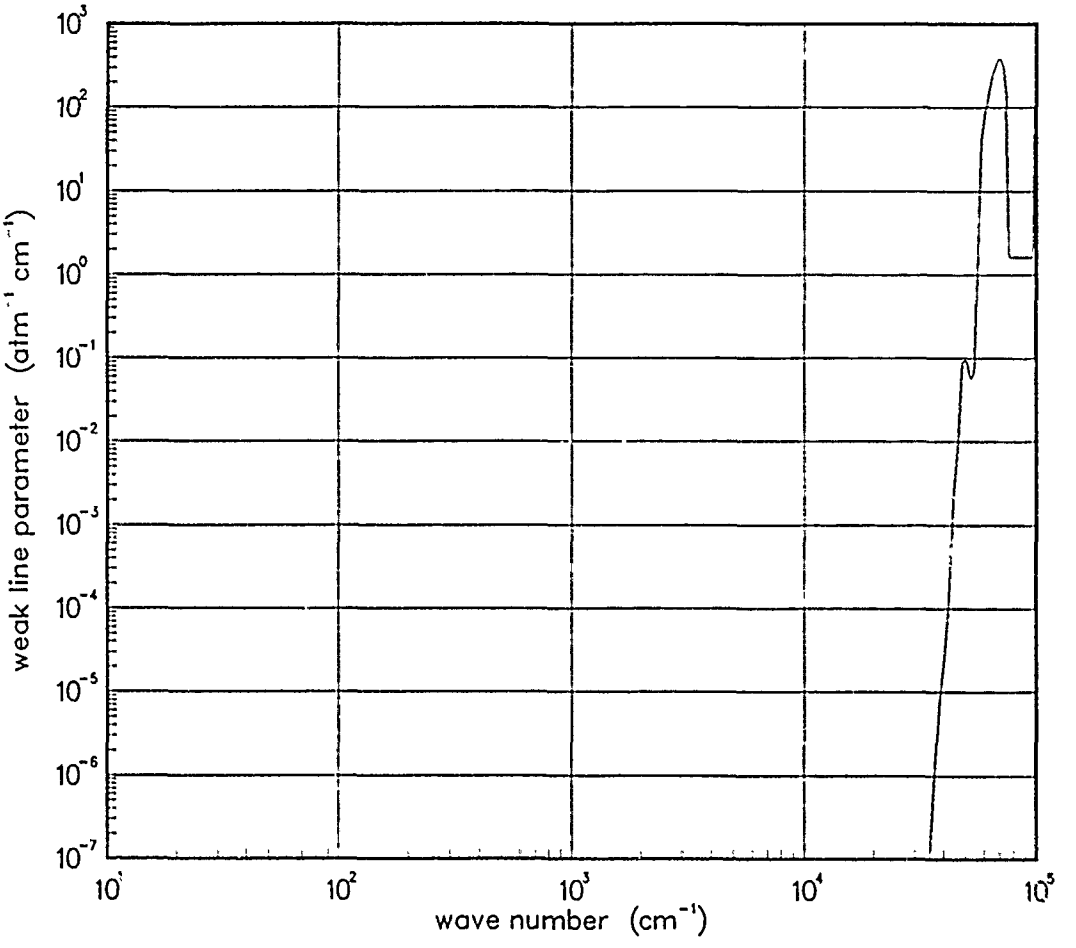

Figure 132. Weak-line parameter for O_2 at 1000°K.

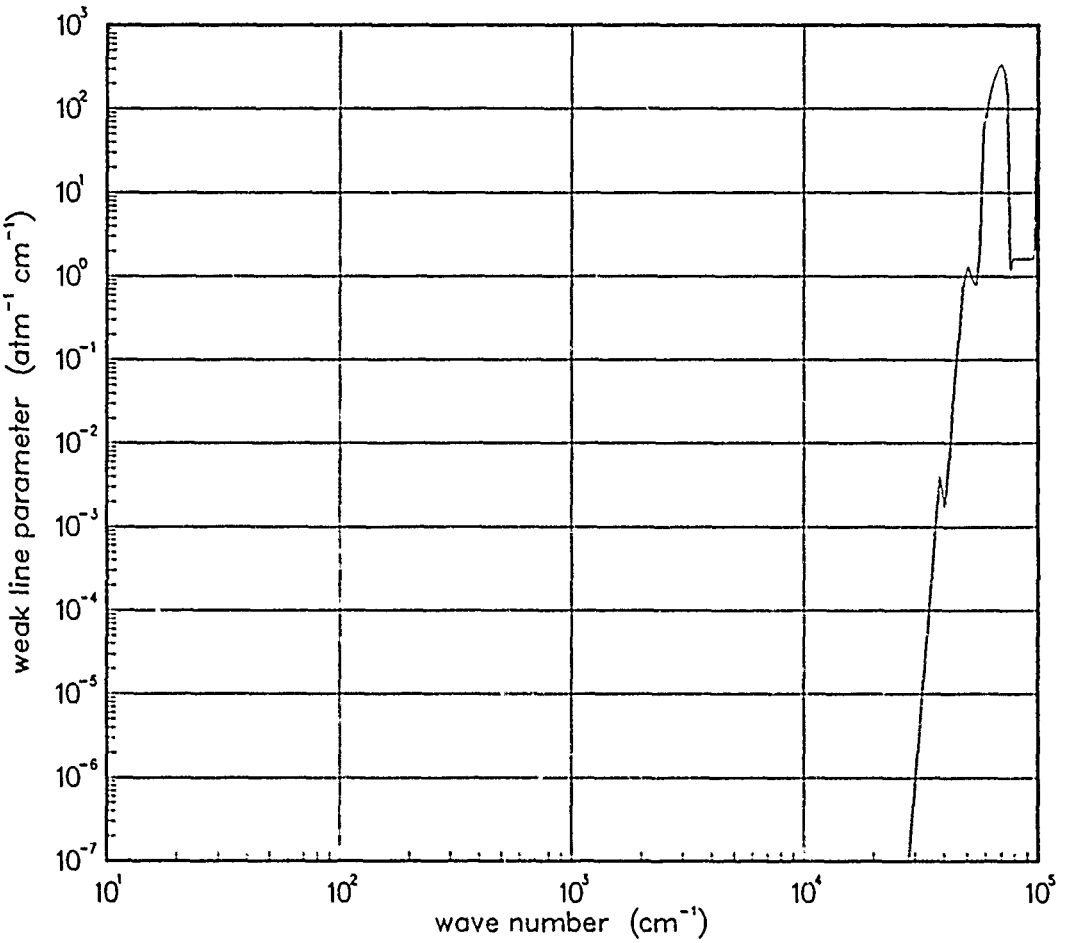

Figure 133. Weak-line parameter for O_2 at 1500°K.

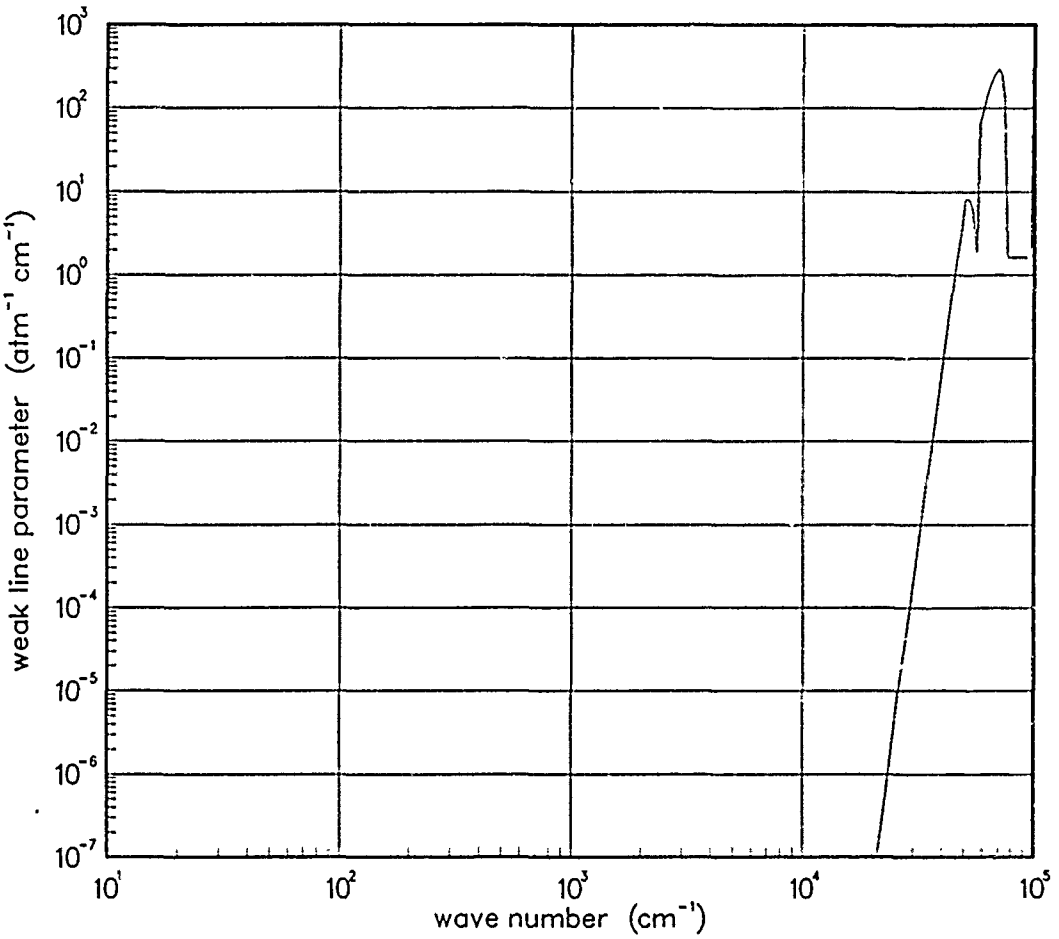

Figure 134. Weak-line parameter for O_2 at 2000°K.

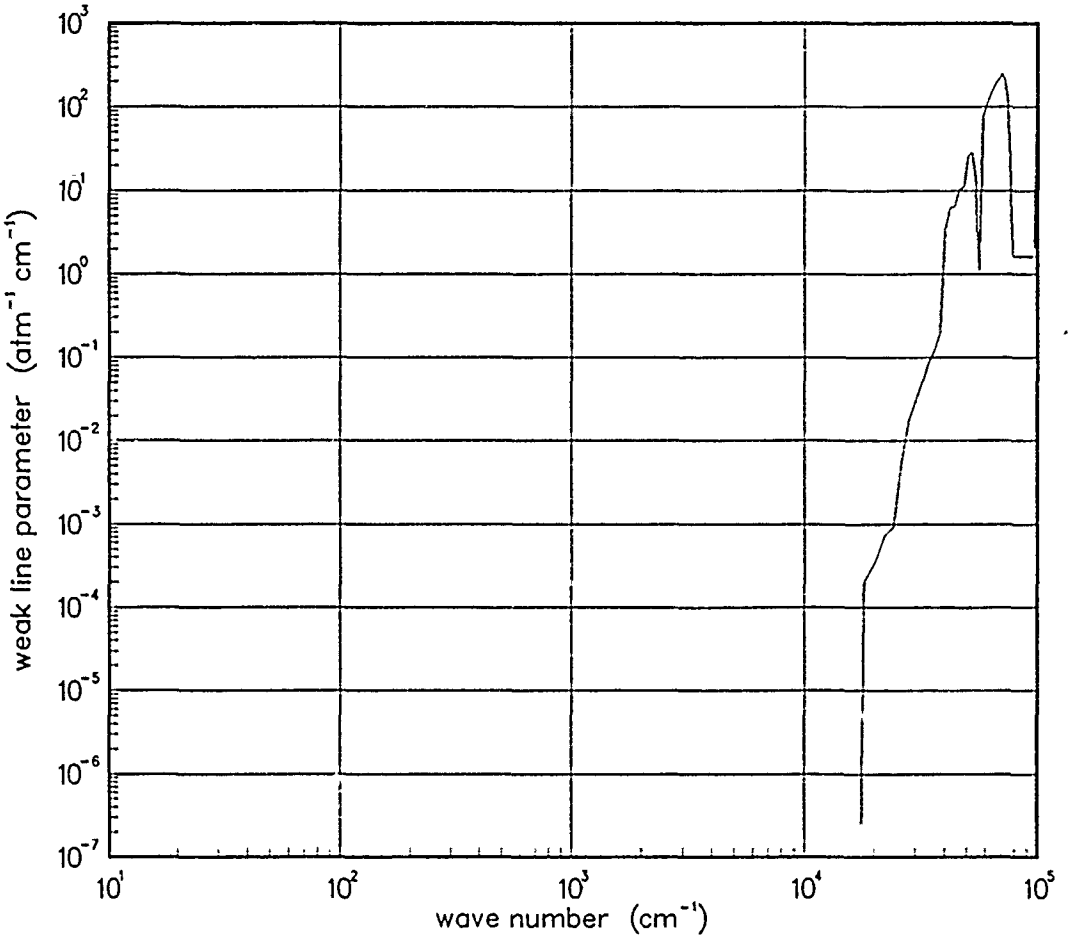

Figure 135. Weak-line parameter for O_2 at 3000°K.

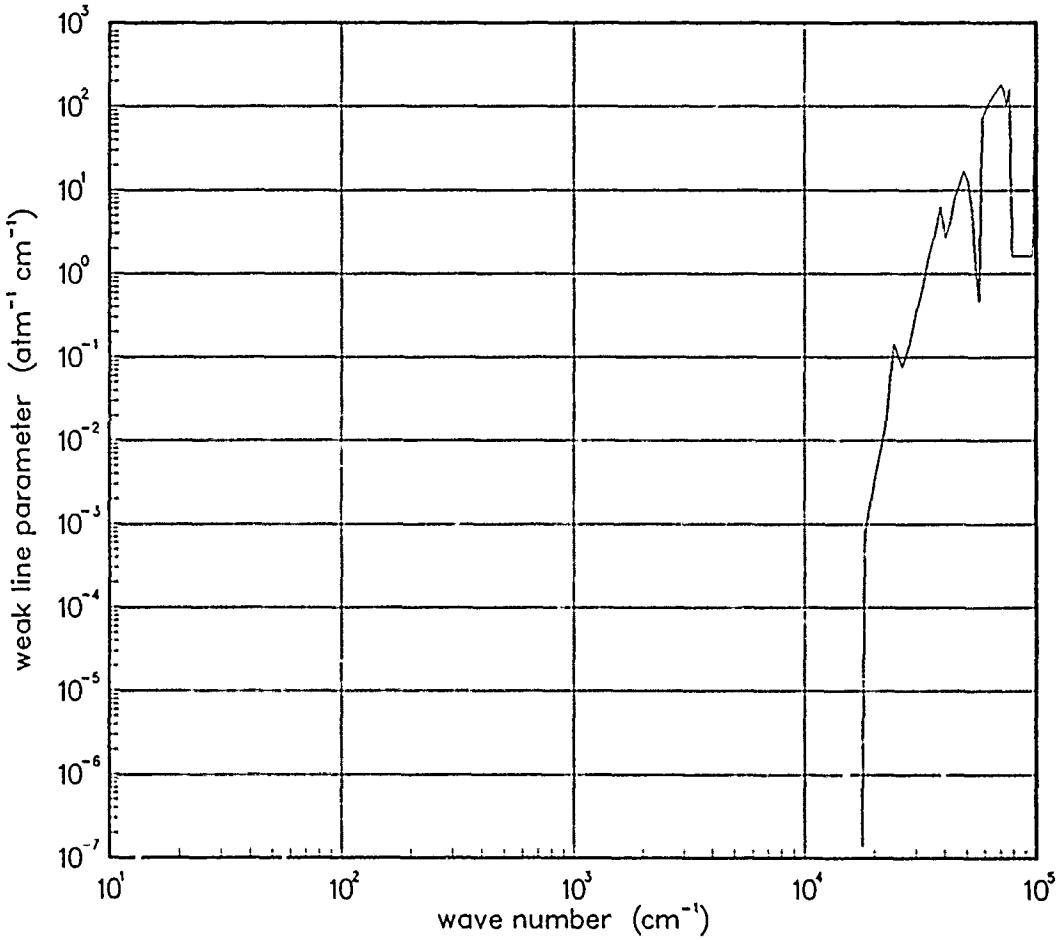

Figure 136. Weak-line parameter for O_2 at 5000°K.

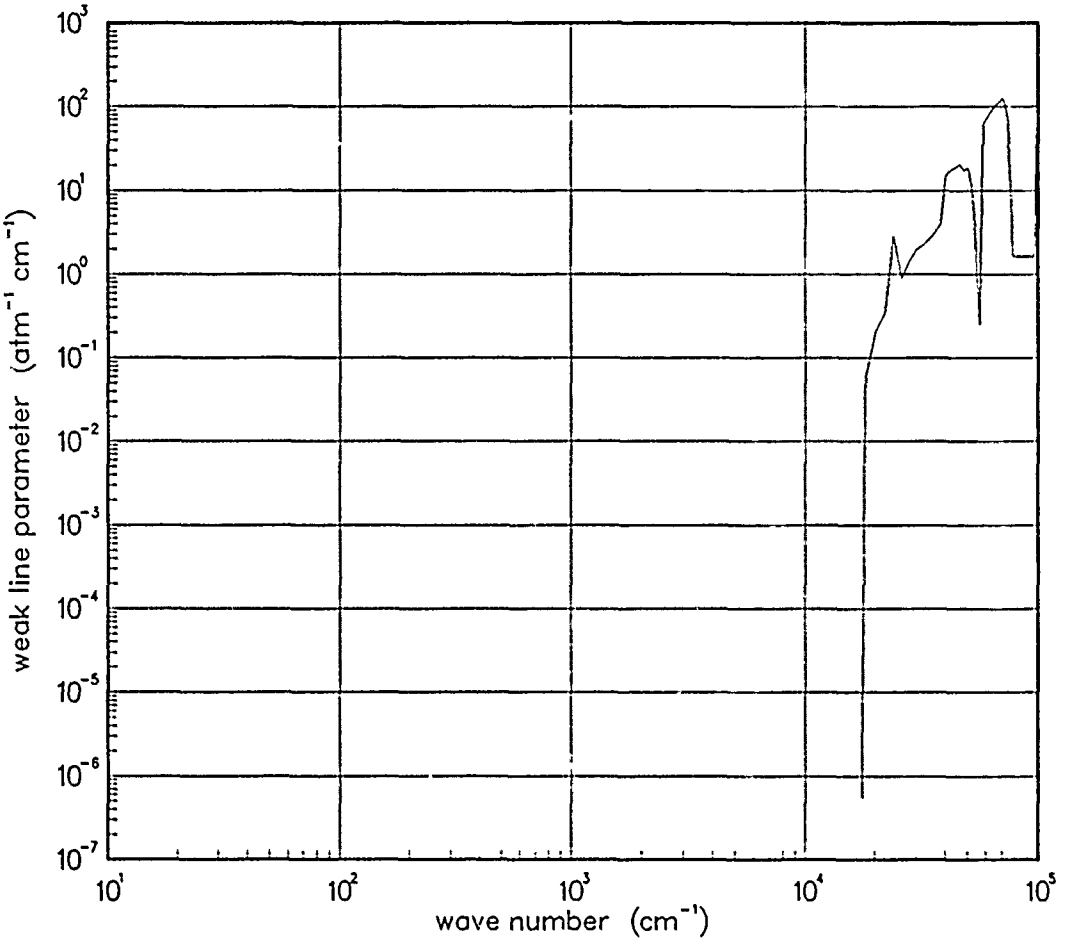

Figure 137. Weak-line parameter for O_2 at 7000°K.

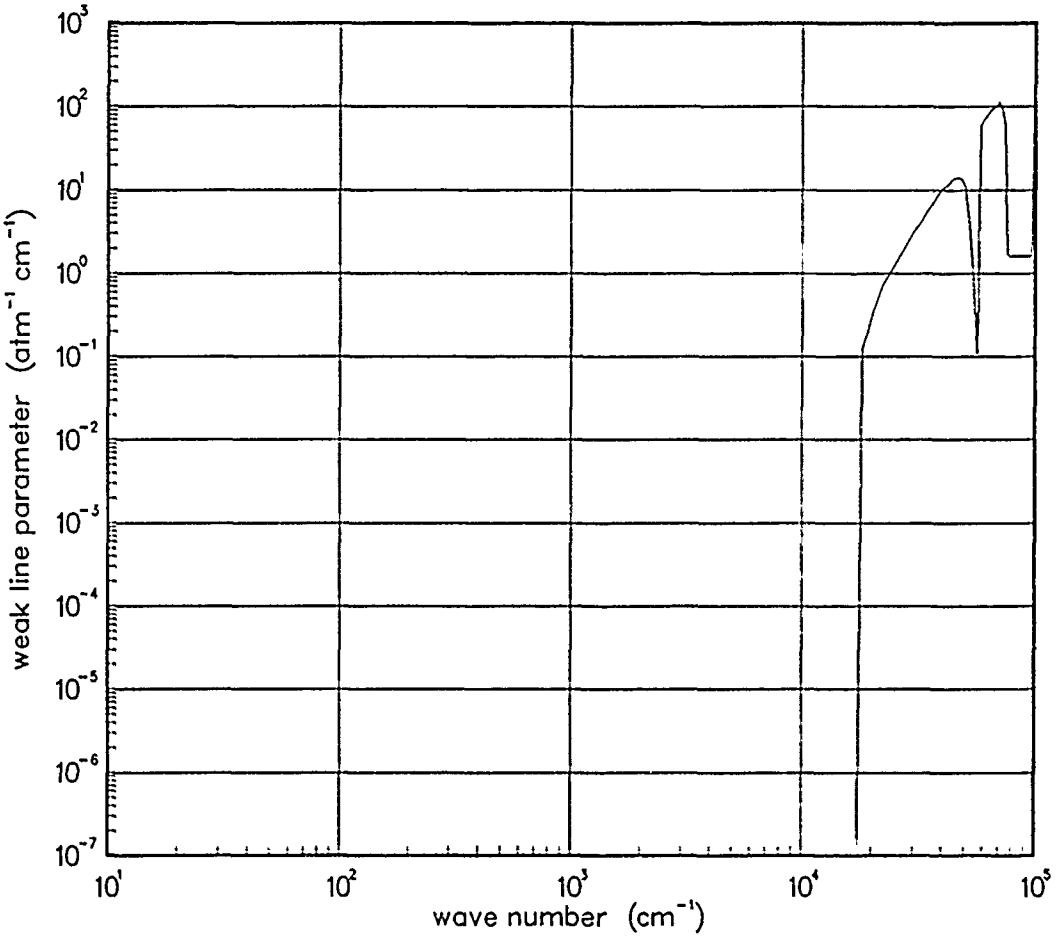

Figure 138. Weak-line parameter for O_2 at 10000°K.

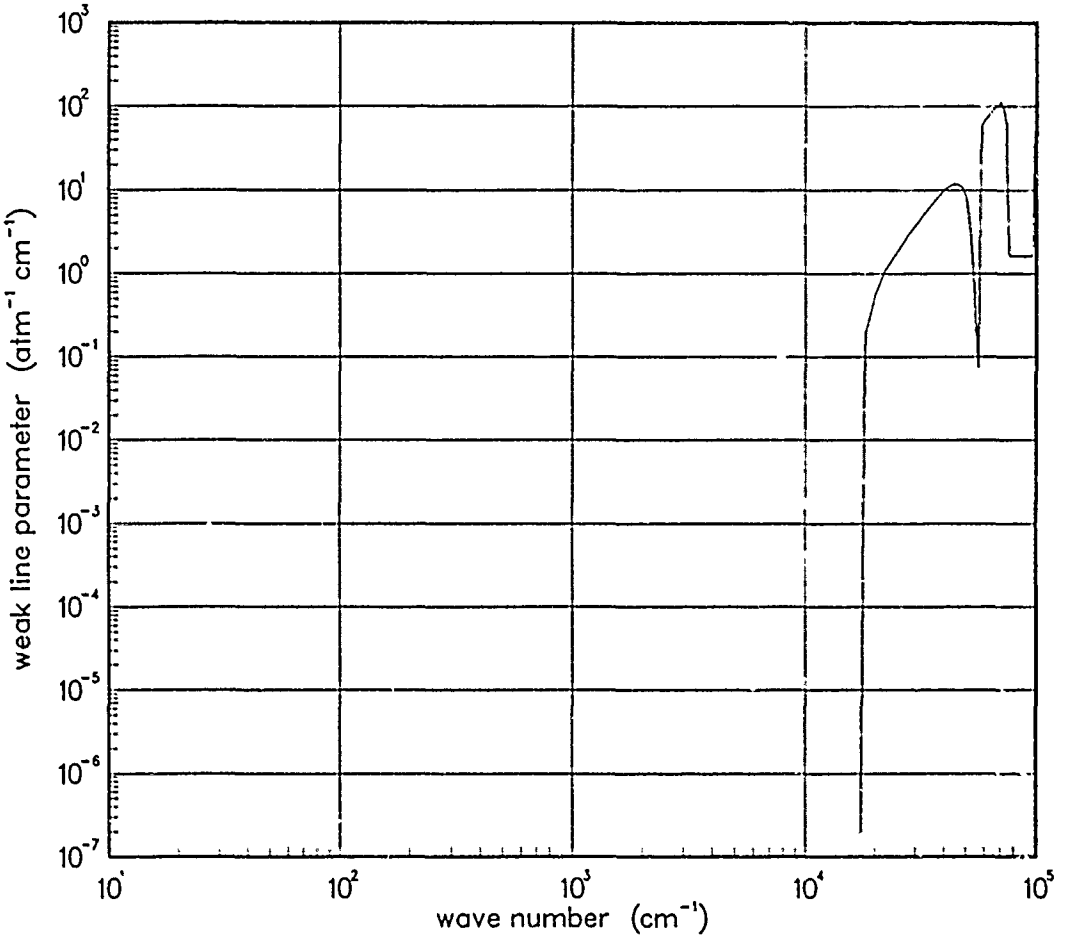

Figure 139. Weak-line parameter for O_2 at 12000°K.

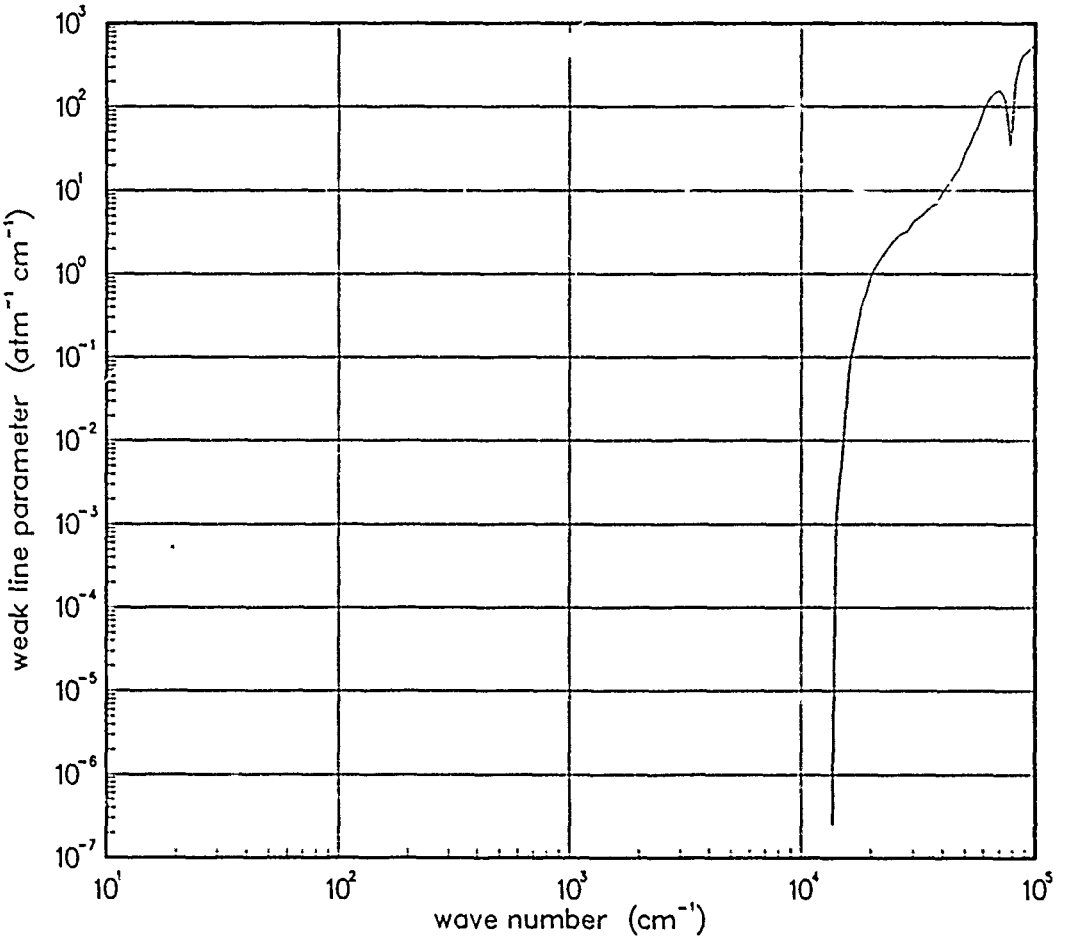

Figure 140. Weak-line parameter for O_2 at 18000°K.

SECTION 5
POLYATOMIC MOLECULES

The local thermal equilibrium emission spectra for polyatomics have been computed from a variety of sources including Triatomic Thermal Emission code (TATE), Air Force Geophysical Laboratory Line Atlas and the Air Force Weapons Laboratory Opacity Database.

5.1 AMMONIA (NH_3).

The local thermal equilibrium emission spectra for Ammonia has been developed from the Air Force Geophysical Laboratory line atlas for 200, 300, 500, 750, 1000 °K.

The NH_3 molecule has been included within the NORSE LTE data base because of its contribution to ambient atmospheric absorption. The inclusion of accurate parameters for this species above 1000 °K is felt to be of low priority.

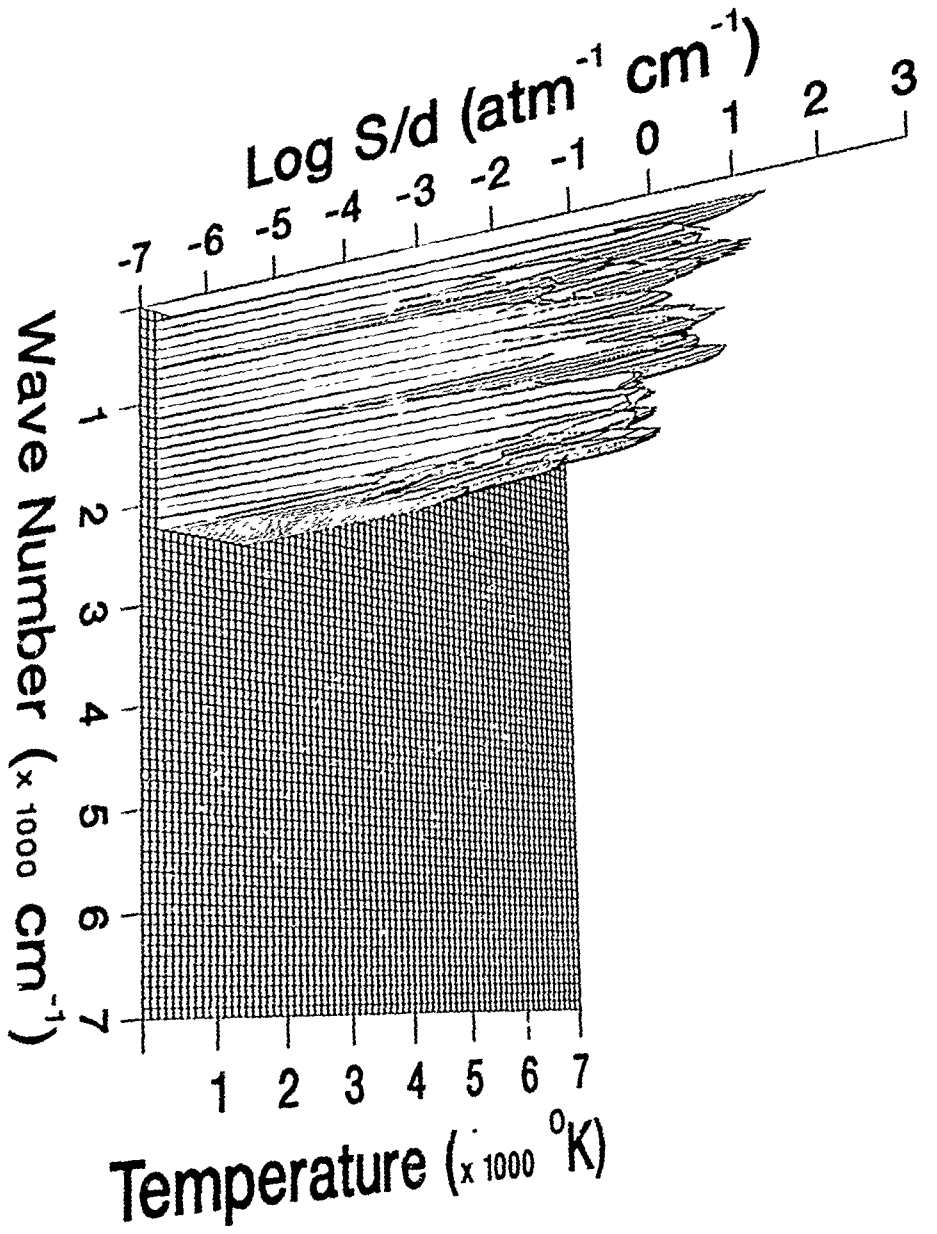

Figure 141. Weak-line parameter for NH_3.

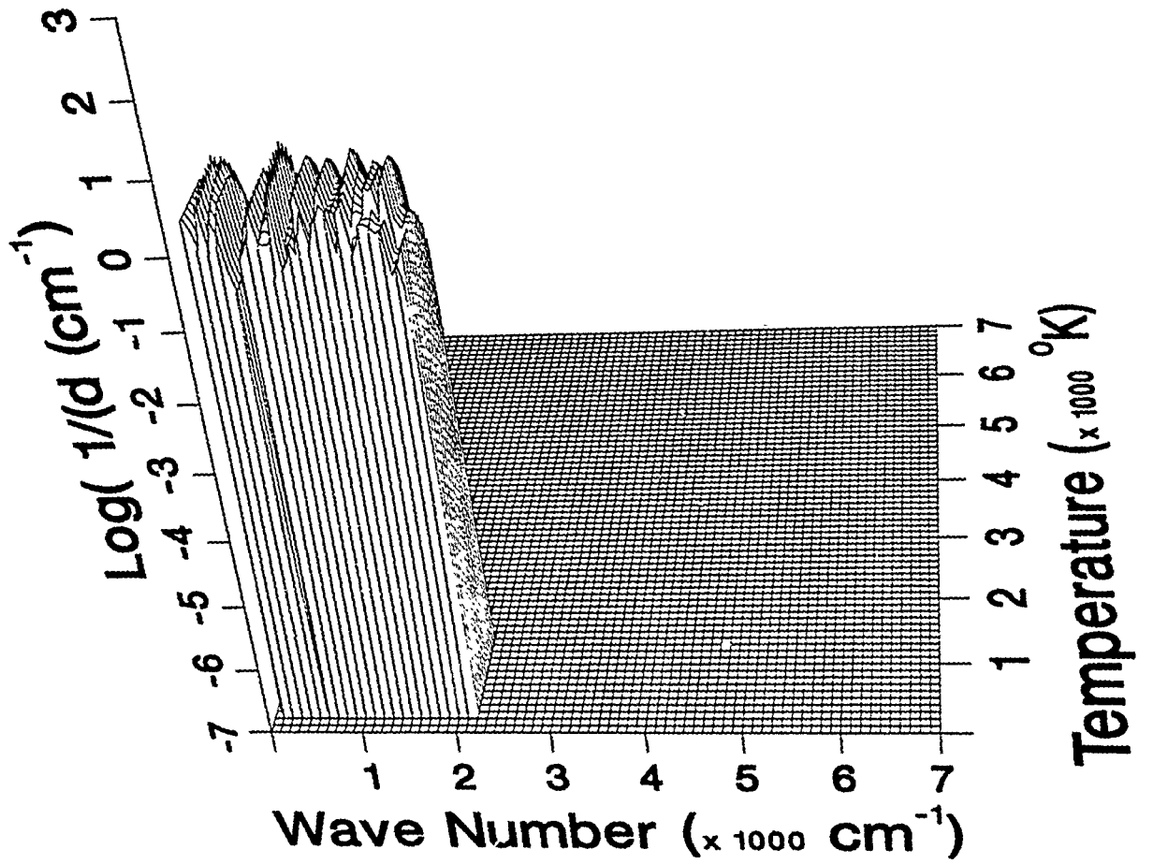

Figure 142. Inverse line spacing for NH_3.

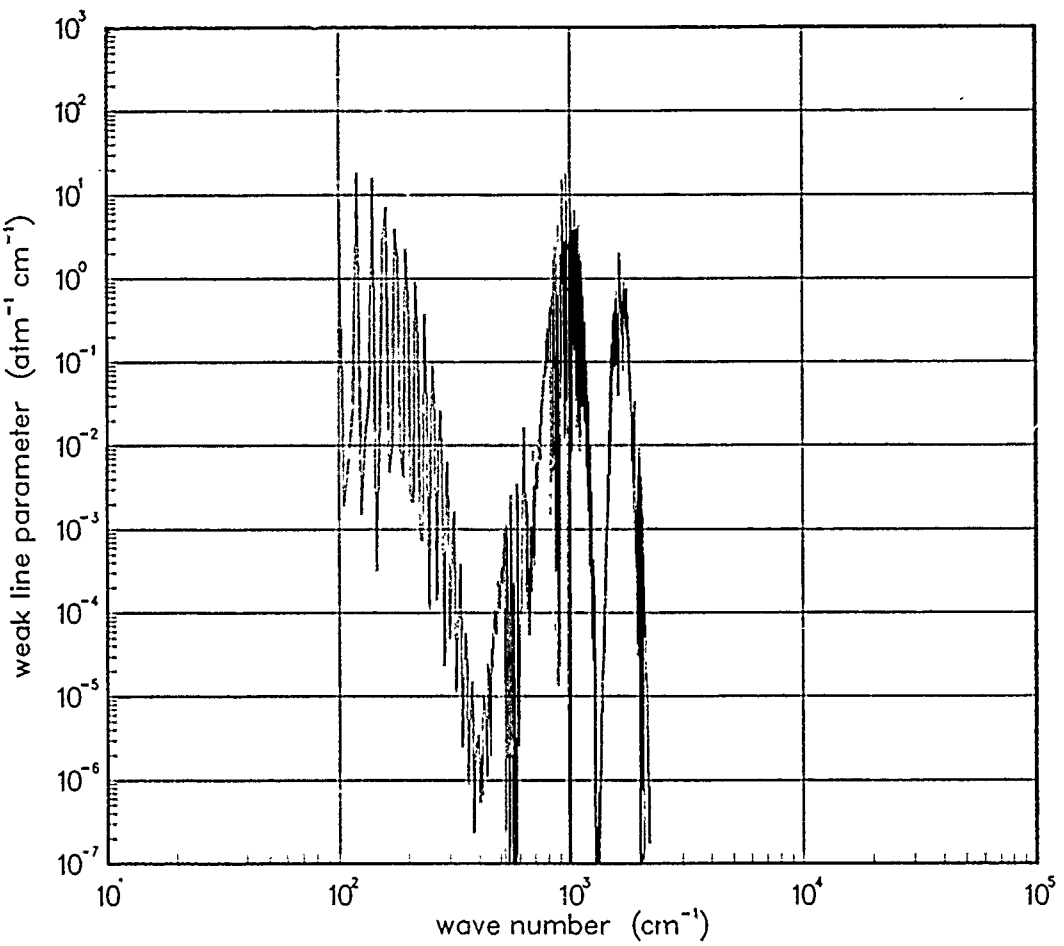

Figure 143. Weak-line parameter for NH_3 at 200°K.

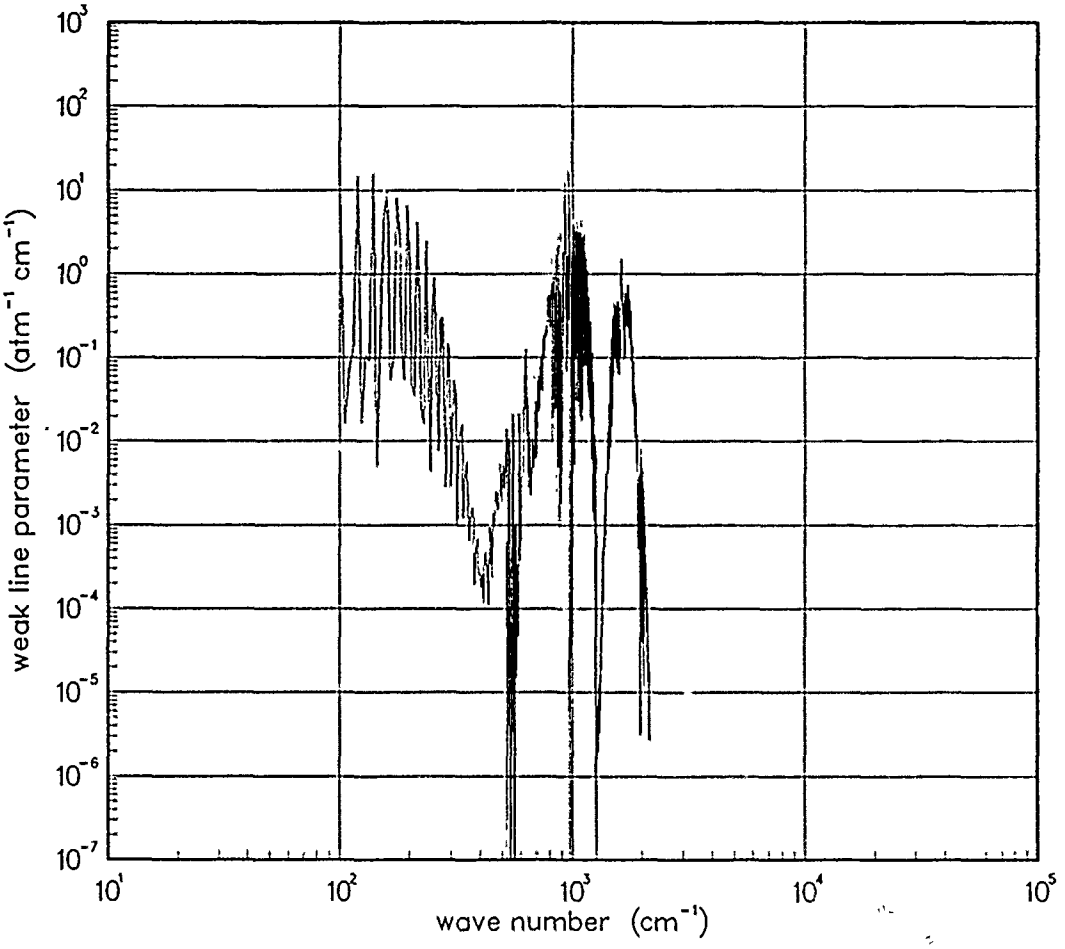

Figure 144. Weak-line parameter for NH_3 at 300°K.

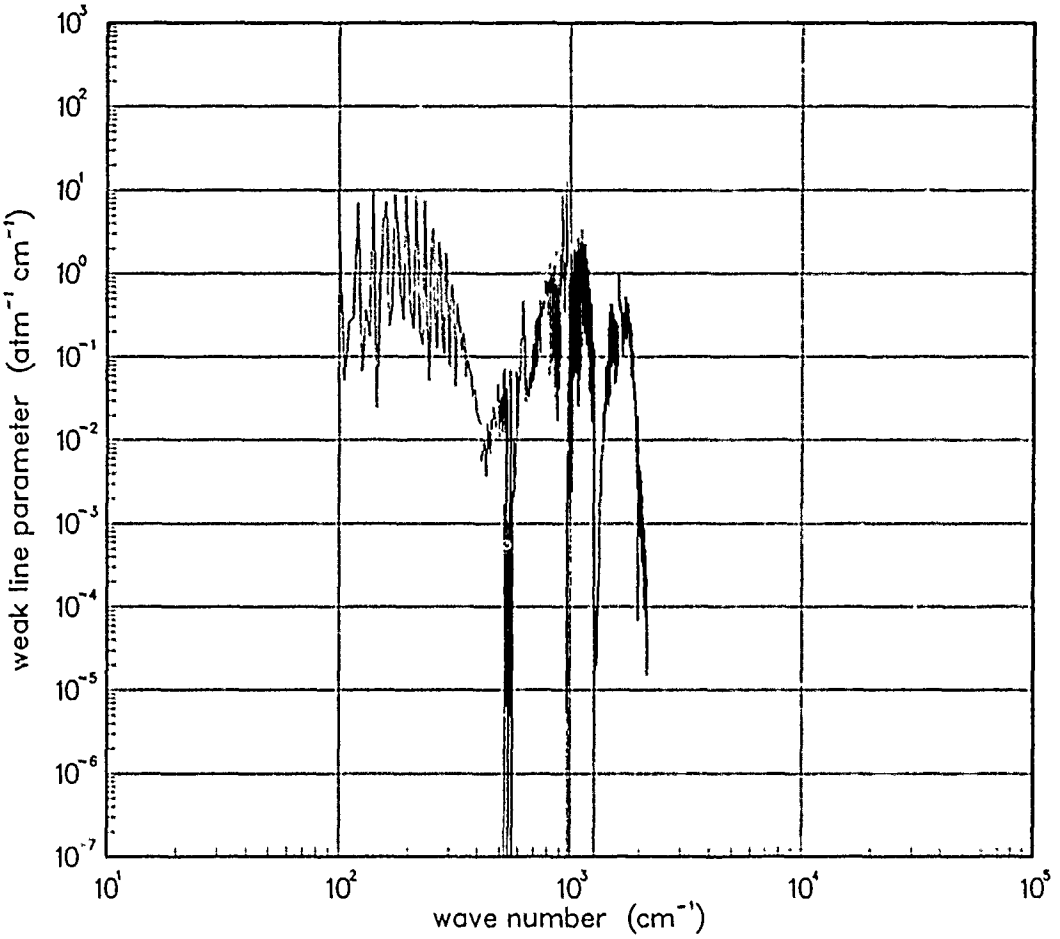

Figure 145. Weak-line parameter for NH_3 at 500°K.

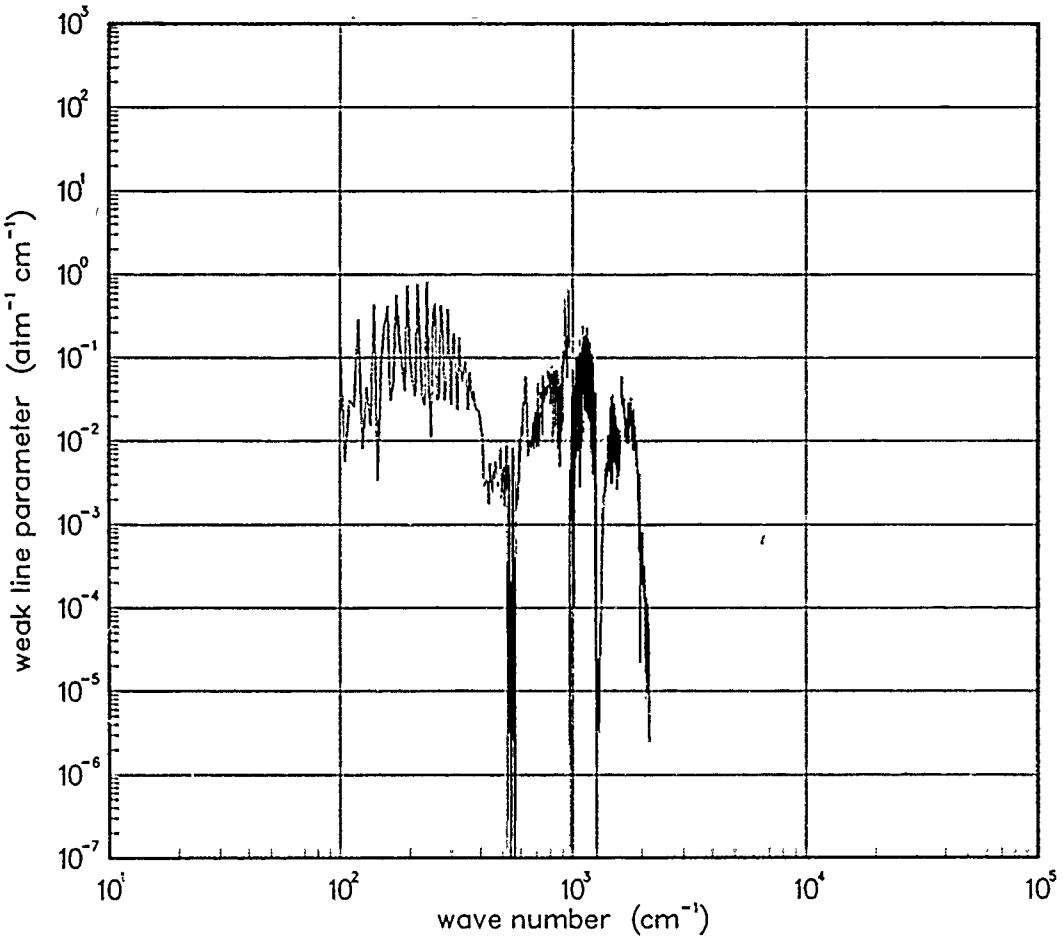

Figure 146. Weak-line parameter for NH_3 at 750°K.

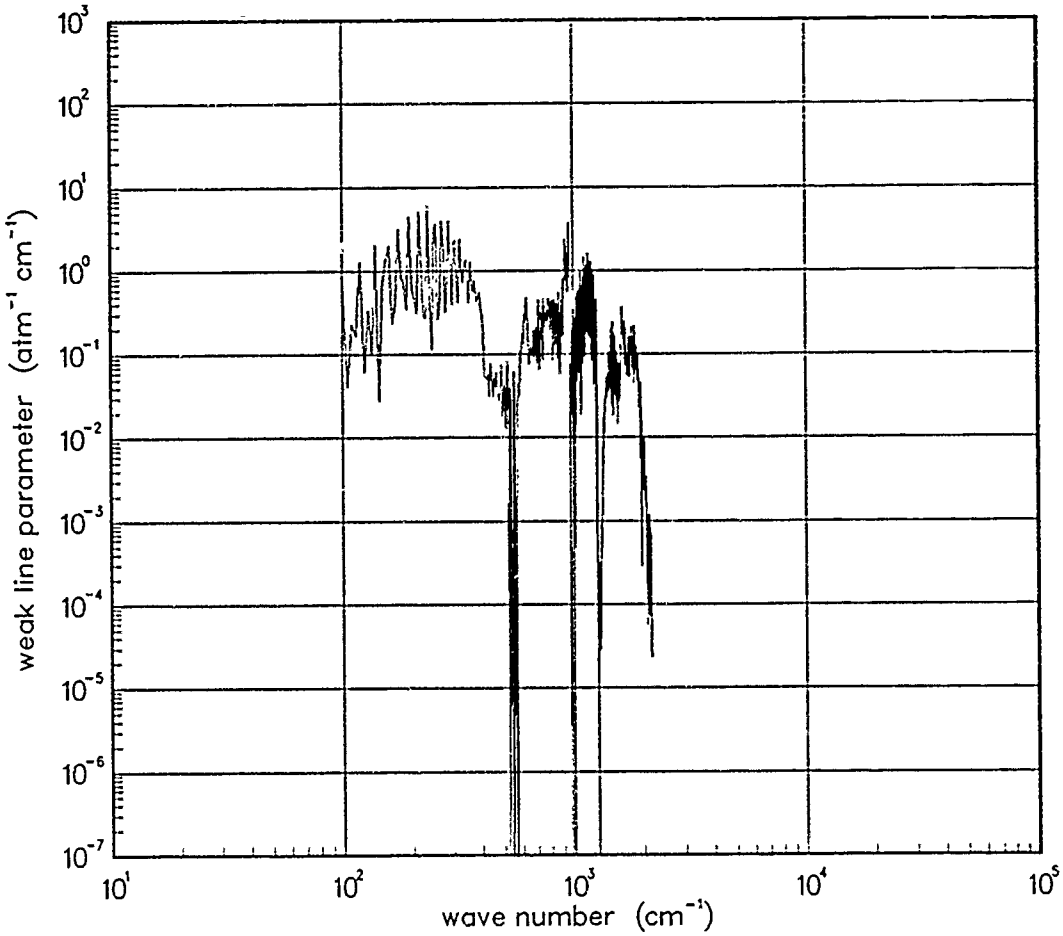

Figure 147. Weak-line parameter for NH_3 at 1000°K.

5.2 CARBON DIOXIDE (CO_2).

The weak-line and inverse line-spacing parameters for the eight most abundant isotopic species of CO_2 were calculated using the LTE smeared-band model code LINTRA*. The model requires band strengths and molecular constants for the contributing transitions; these constants were obtained from the Air Force Geophysical Laboratory†. Theoretical calculations for excited bands of the 626 isotopic species of CO_2 were obtained from VisiDyne‡. The smeared band model correctly accounts for the increased population of the rotational states with increasing temperature.

These band model parameters were calculated for each wavenumber between 100 cm^{-1} and 10,000 cm^{-1} and then averaged to obtain the required resolution for the NORSE optics database. The temperatures at which these calculations were performed were 200, 300, 500, 750, 1000, 1500, 2000, 3000, 5000, 7000, 10000, 12000, 18000 °K. The band model parameters calculated for temperatures much above 1500 °K are deficient due to the lack of essential experimental and theoretical data.

Data Source:

*LINTRA, (LINear TRiAtomic) smeared-line band model Fortran code developed by R. Parker, Physical Research Inc., 1987.

†L.S. Rothman, Appl. Opt., 25, 1975 (1986).

‡R.B. Wattson, L.S.Rothman, J. Mol. Spectrosc., 119, 83 (1986).

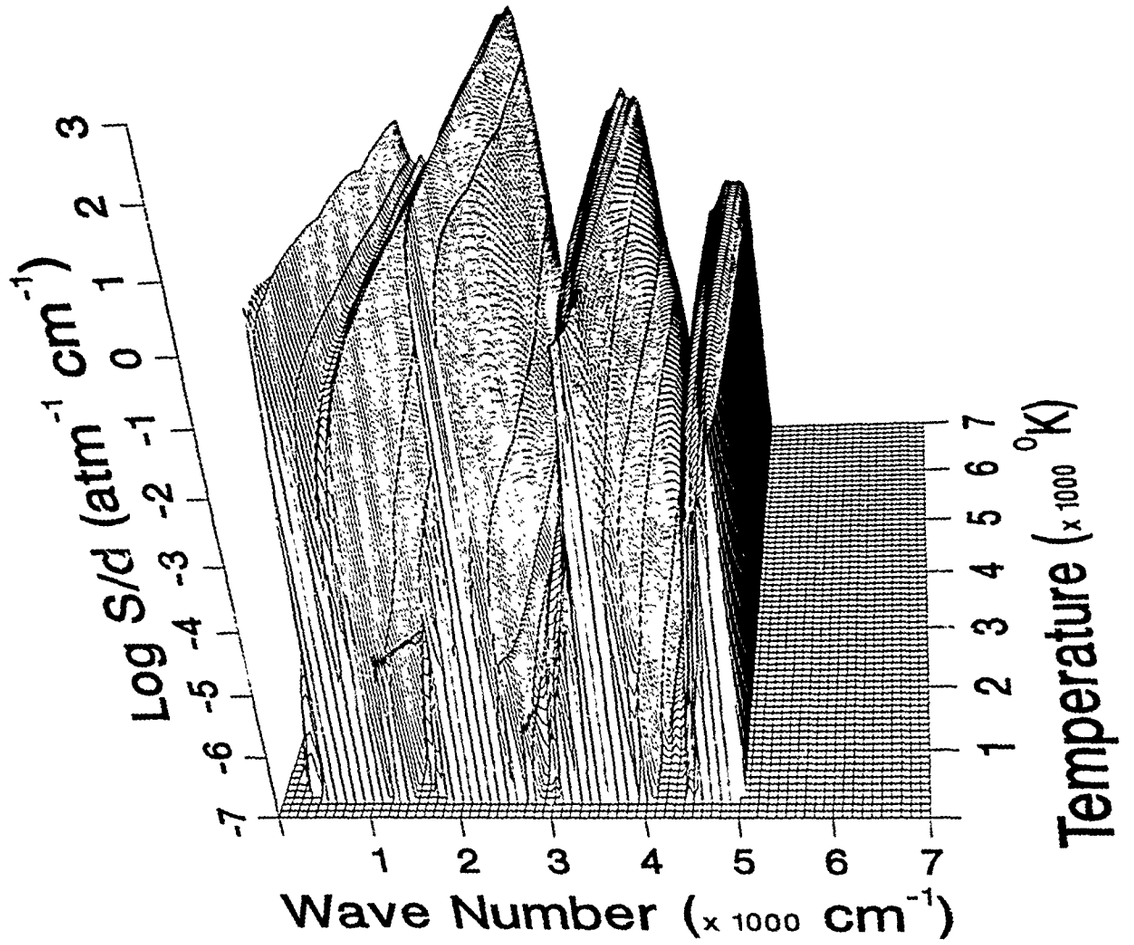

Figure 148. Weak-line parameter for CO_2.

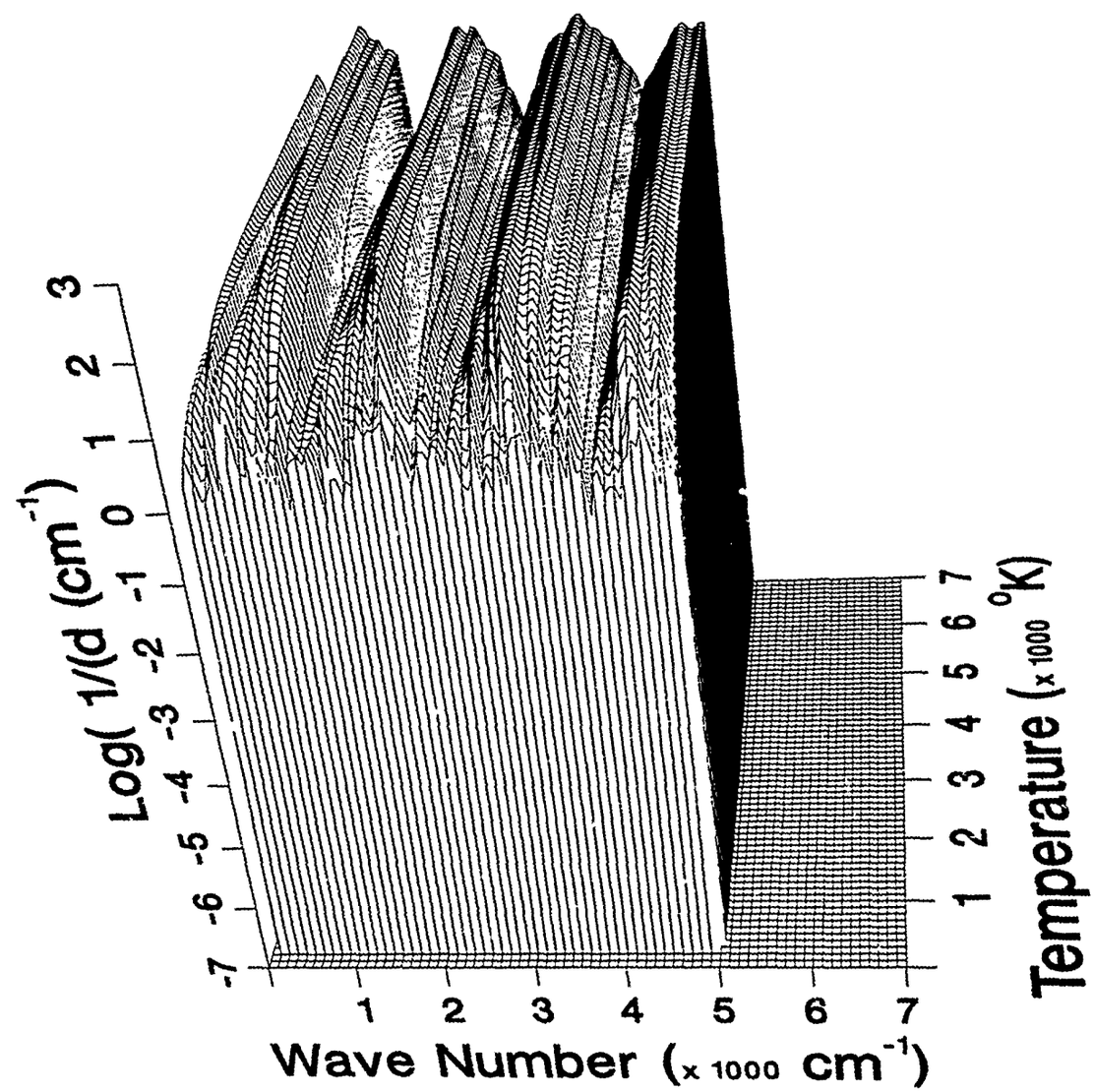

Figure 149. Inverse line spacing for CO_2.

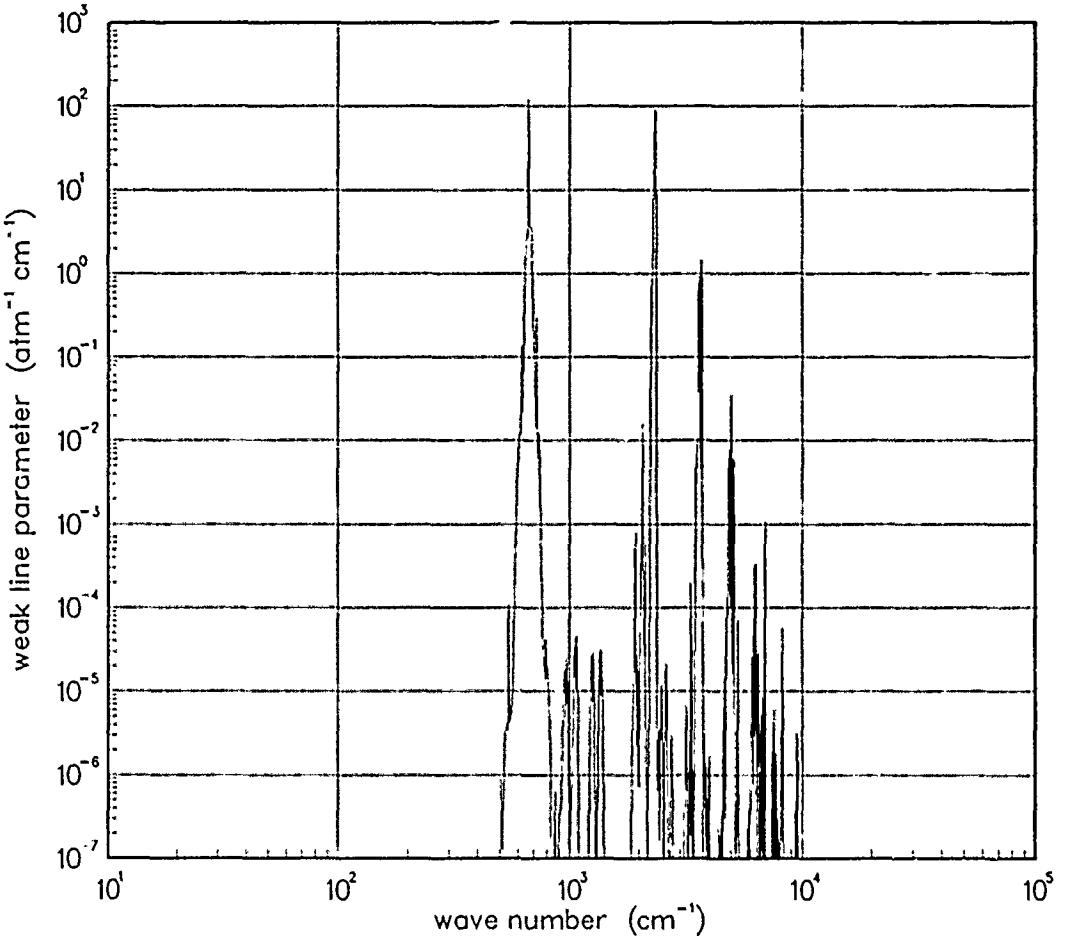

Figure 150. Weak-line parameter for CO_2 at 200°K.

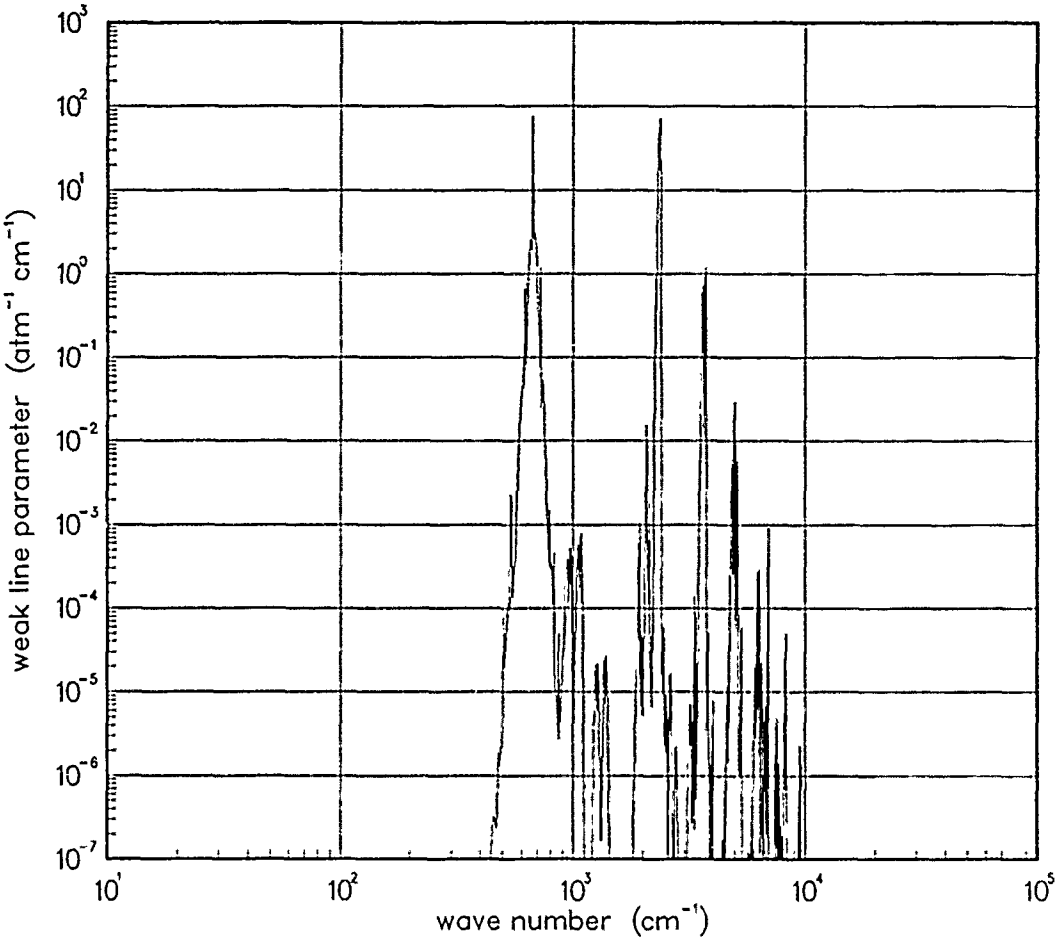

Figure 151. Weak-line parameter for CO_2 at 300°K.

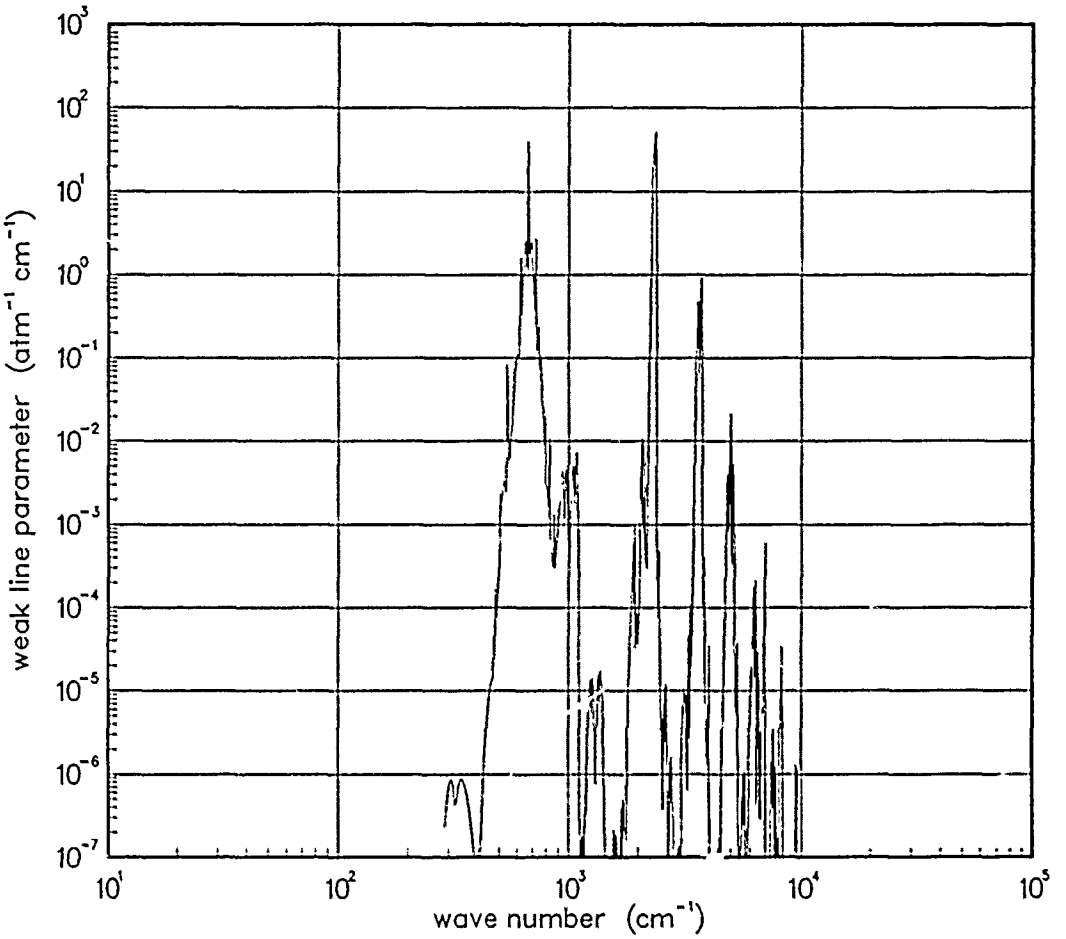

Figure 152. Weak-line parameter for CO_2 at 500°K.

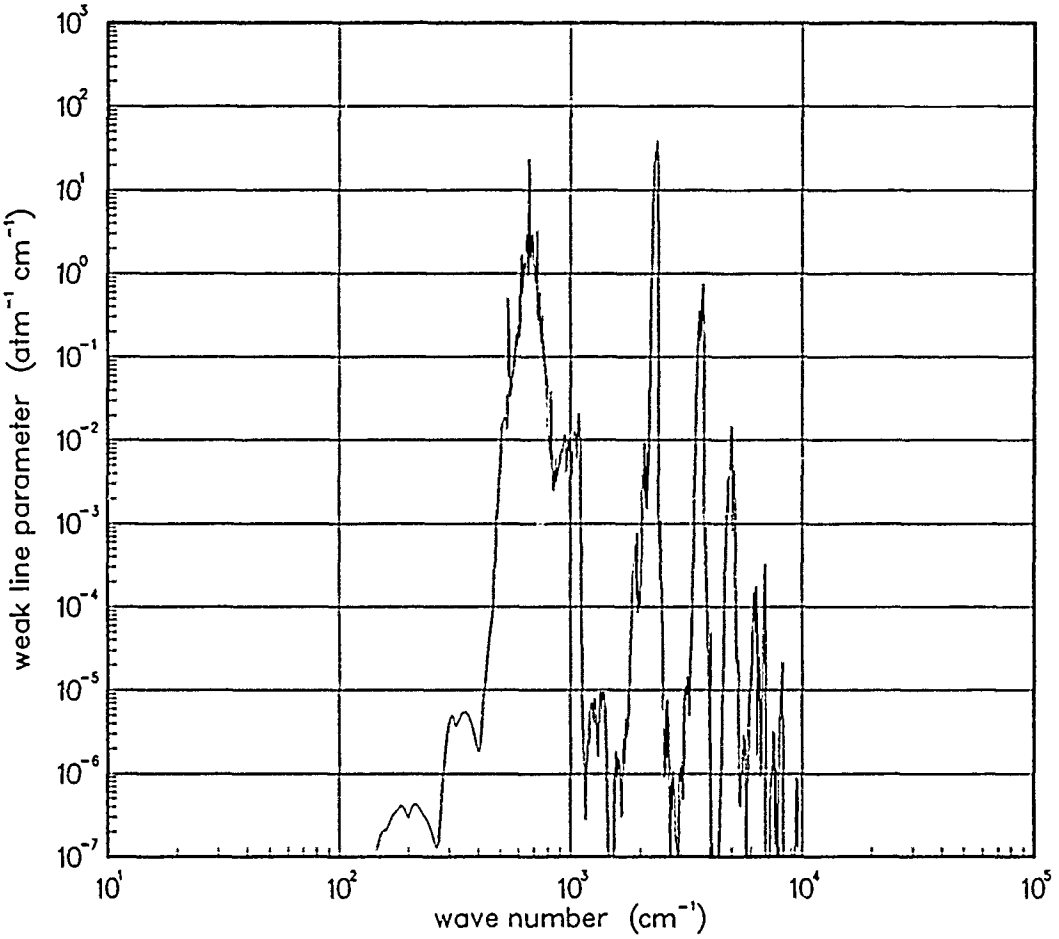

Figure 153. Weak-line parameter for CO_2 at 750°K.

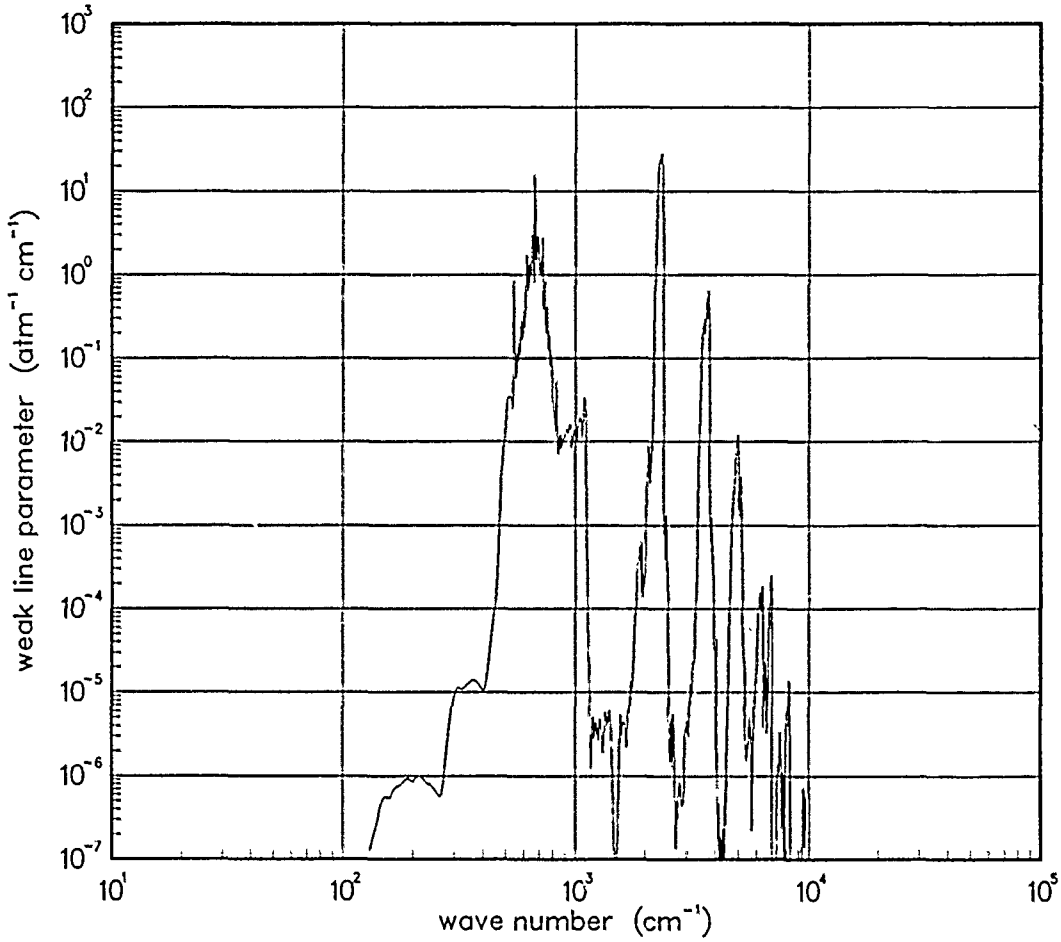

Figure 154. Weak-line parameter for CO_2 at 1000°K.

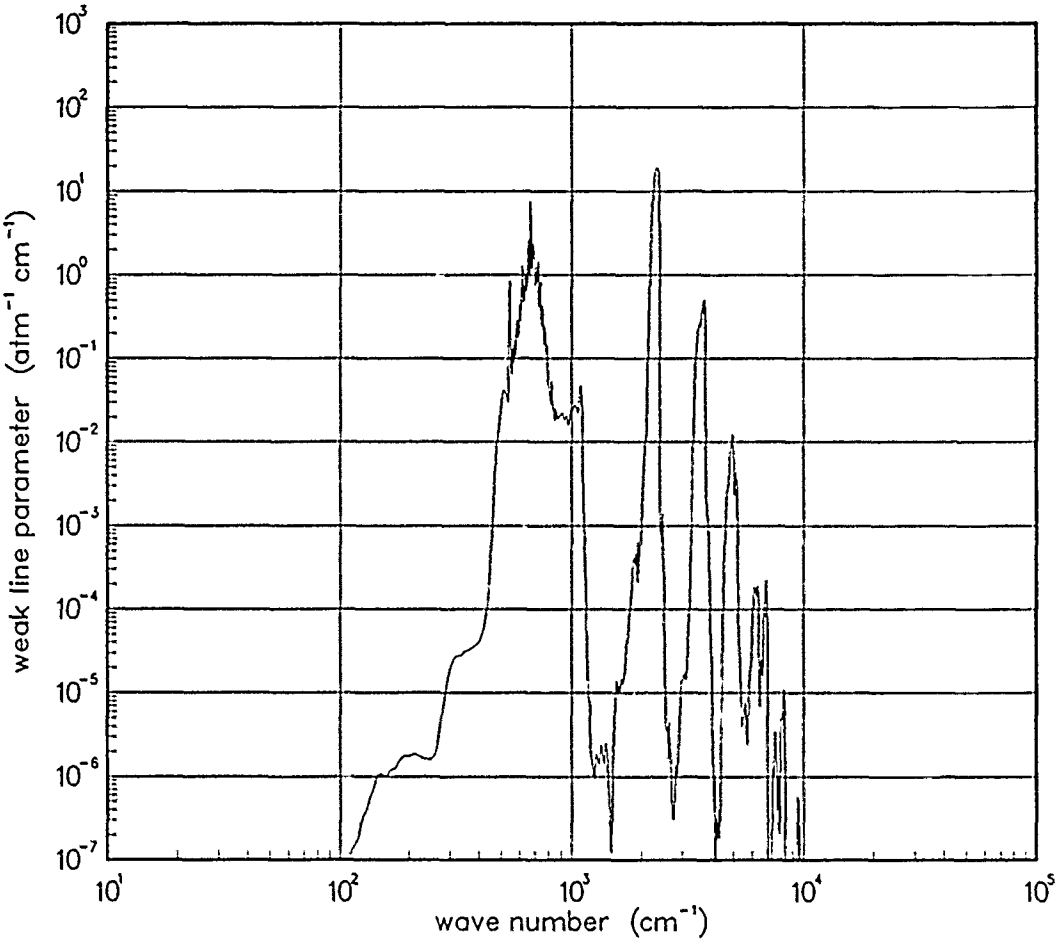

Figure 155. Weak-line parameter for CO_2 at 1500°K.

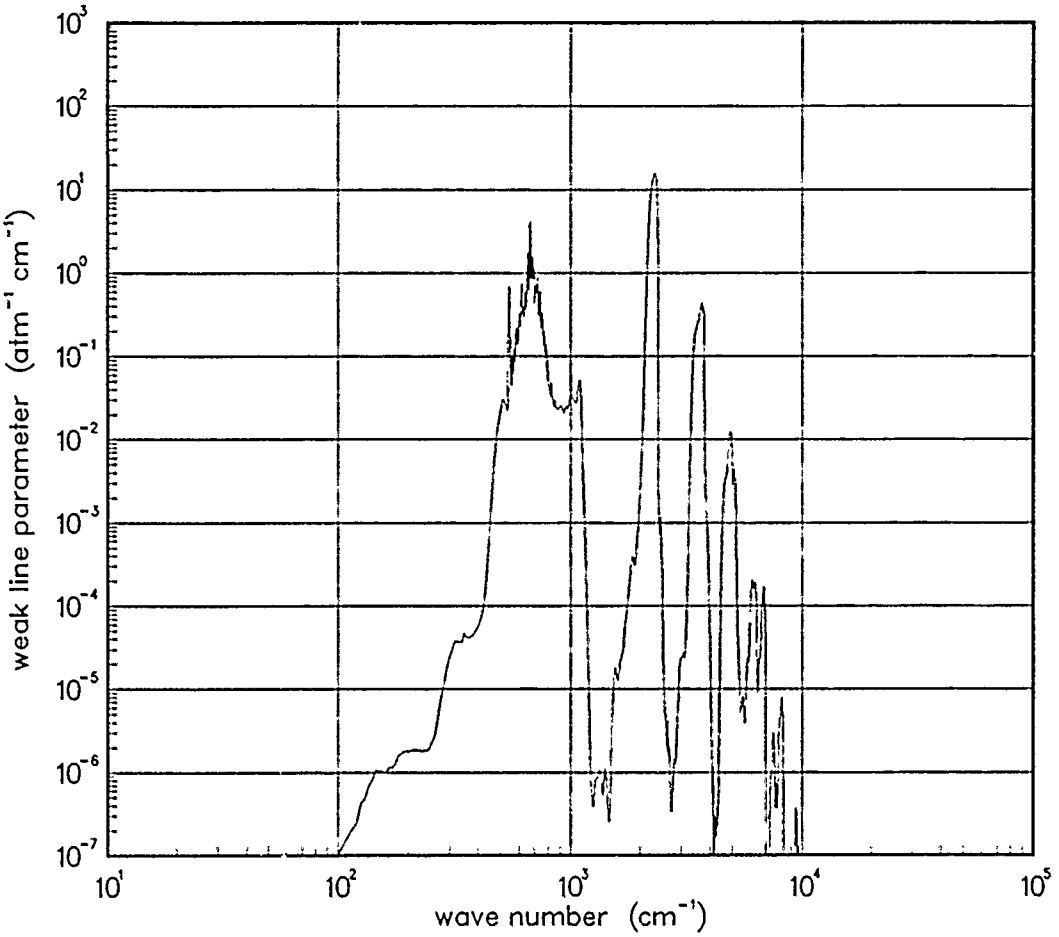

Figure 156. Weak-line parameter for CO_2 at 2000°K.

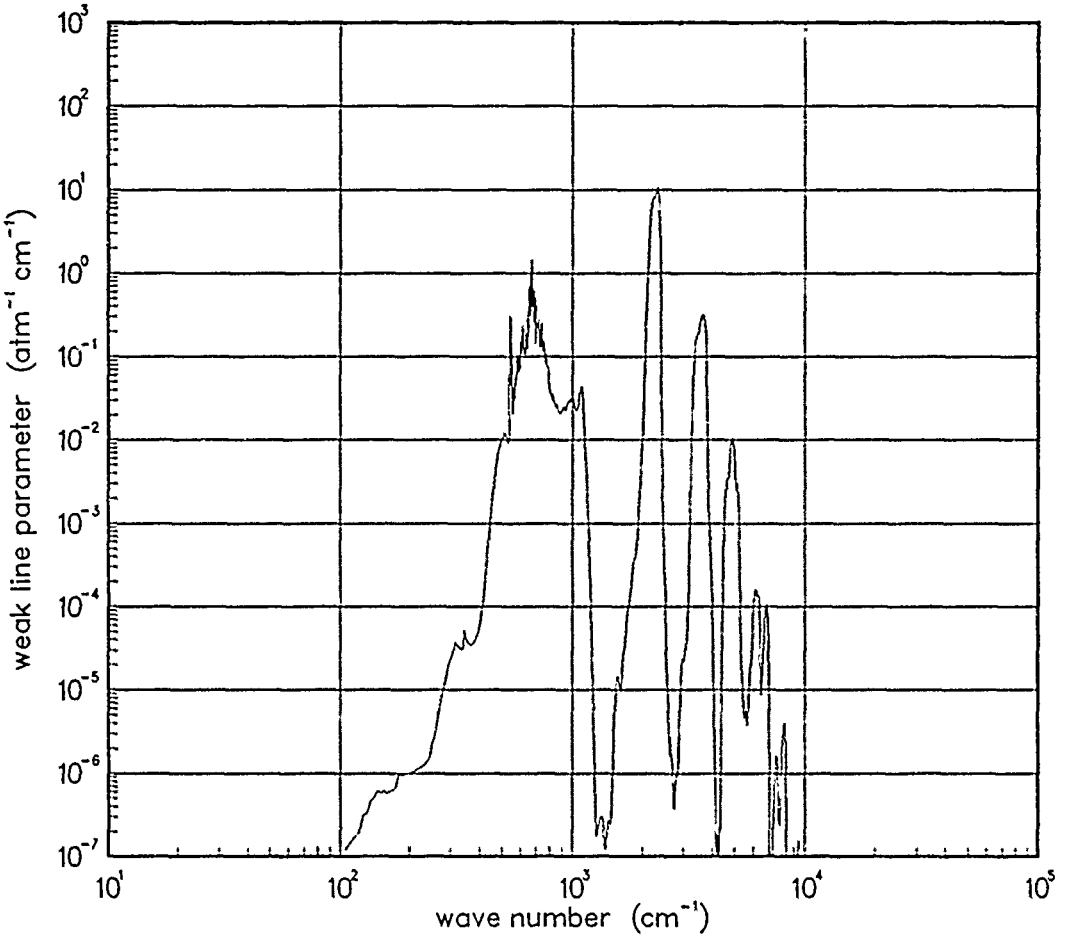

Figure 157. Weak-line parameter for CO_2 at 3000°K.

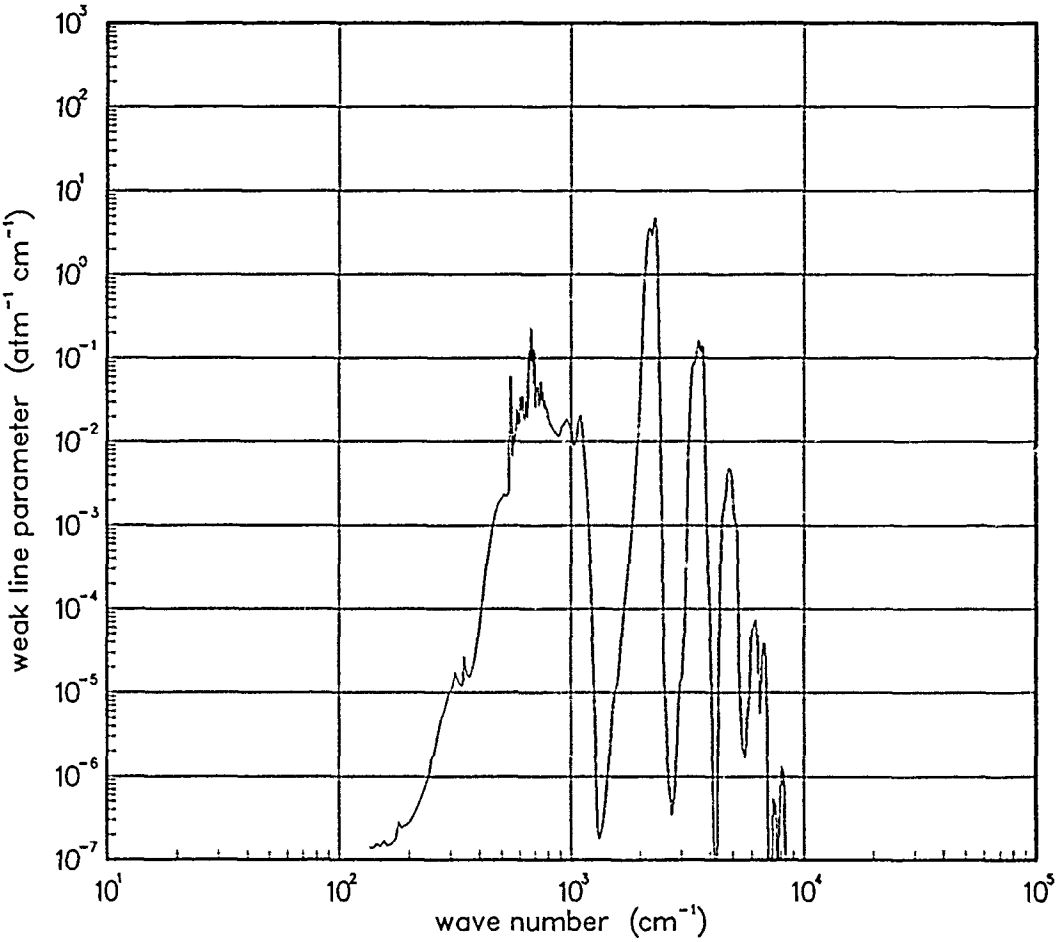

Figure 158. Weak-line parameter for CO_2 at 5000°K.

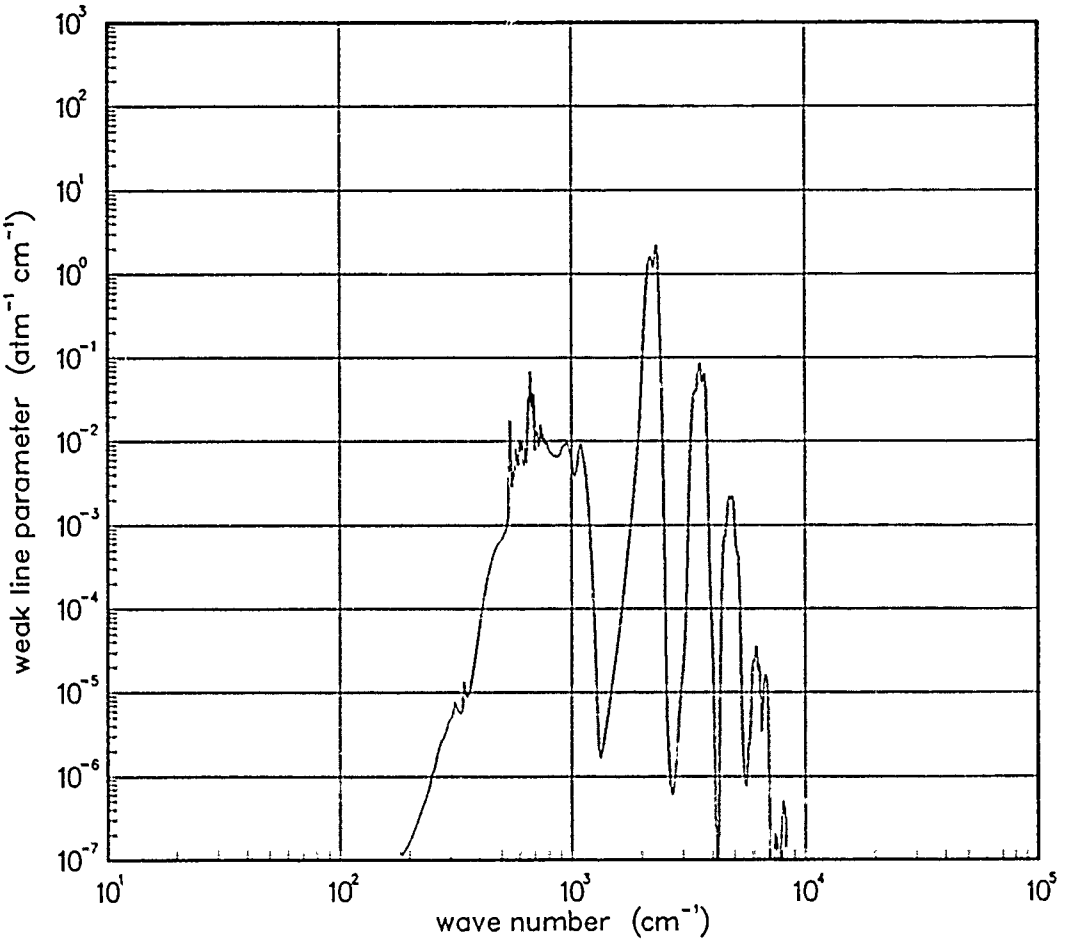

Figure 159. Weak-line parameter for CO_2 at 7000°K.

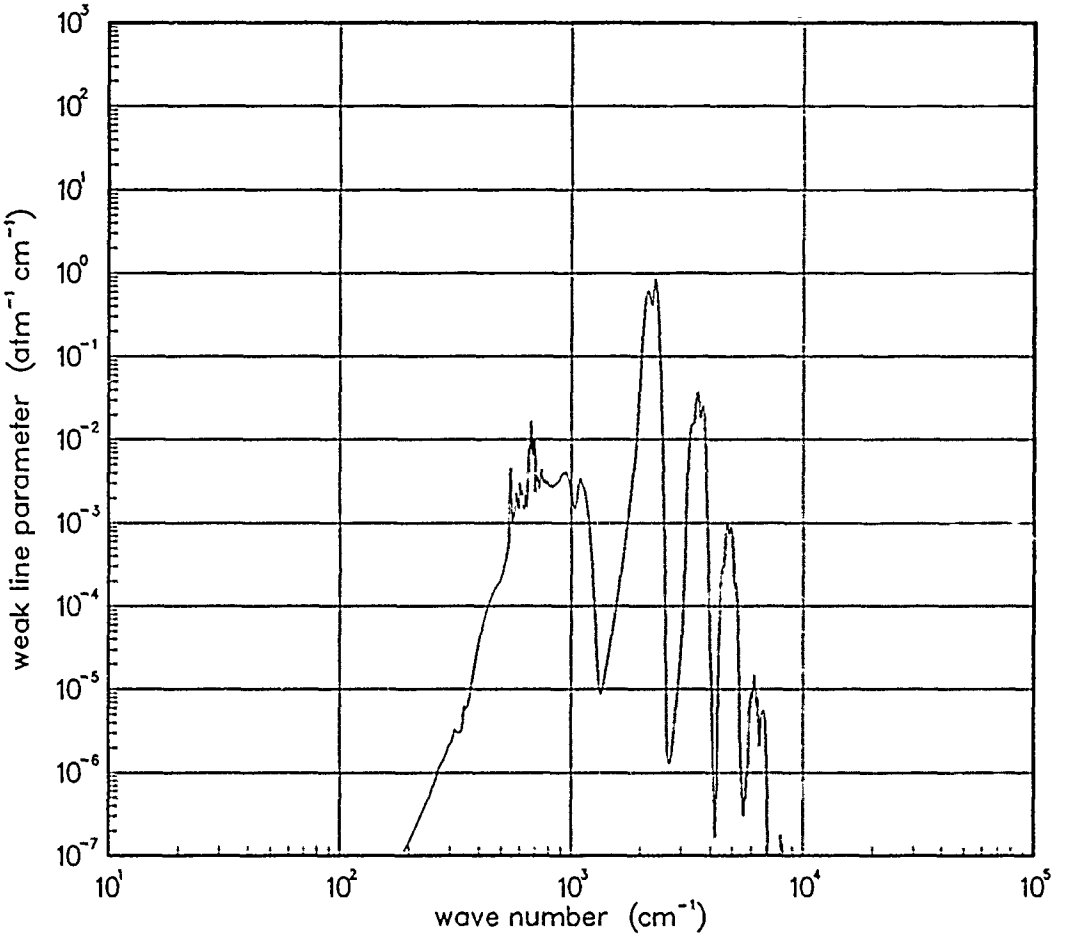

Figure 160. Weak-line parameter for CO_2 at 10000°K.

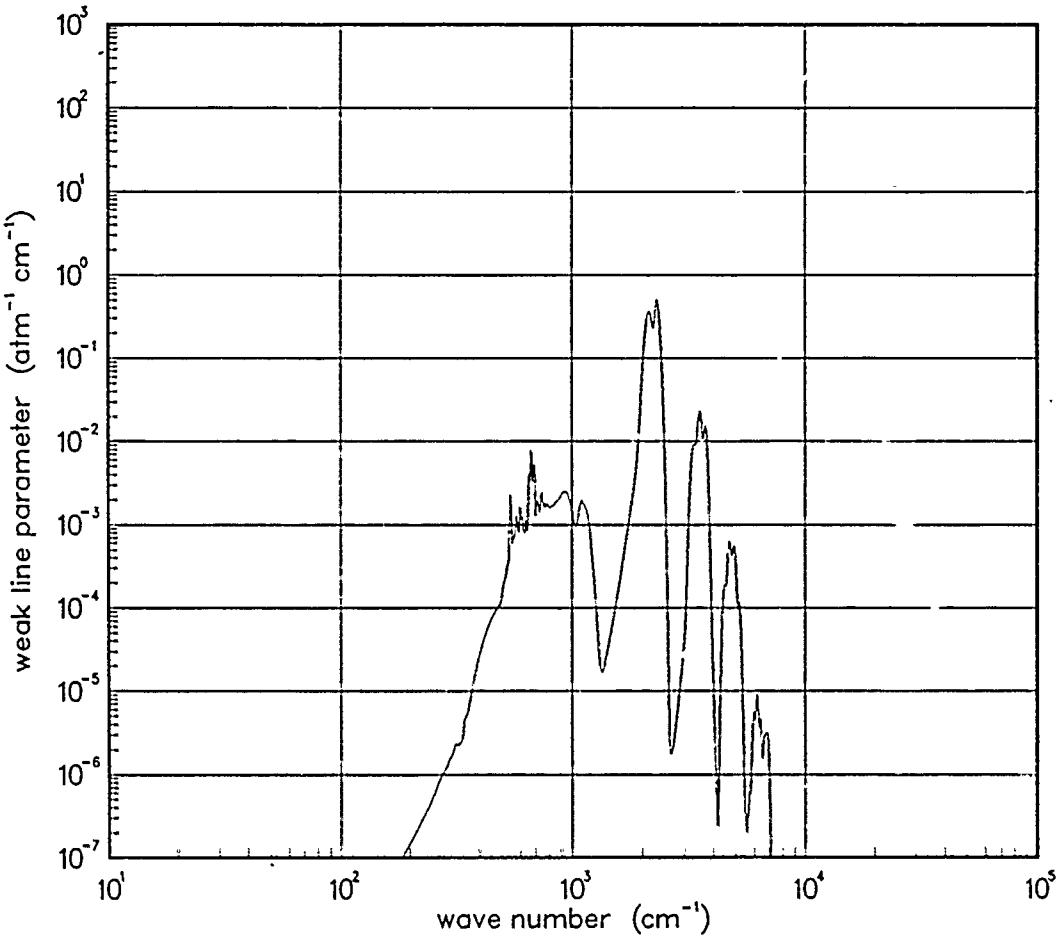

Figure 161. Weak-line parameter for CO_2 at 12000°K.

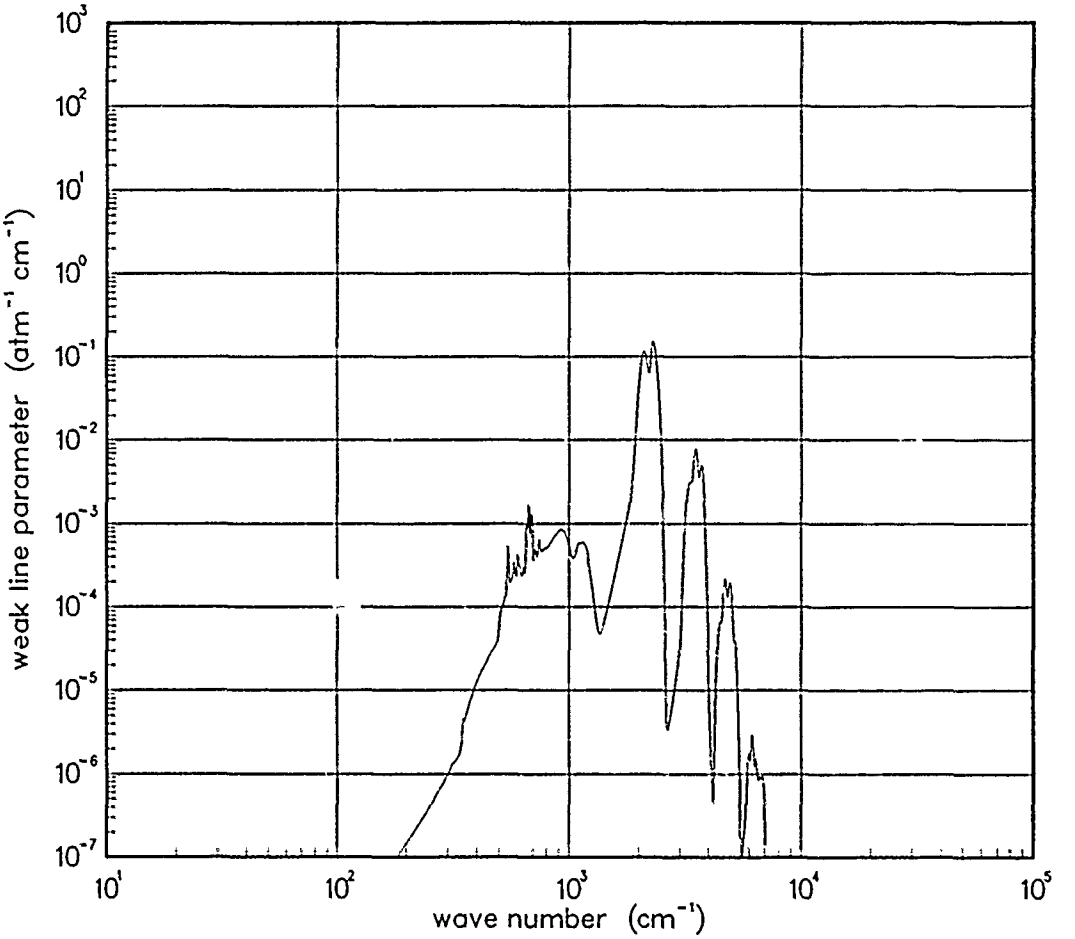

Figure 162. Weak-line parameter for CO_2 at 18000°K.

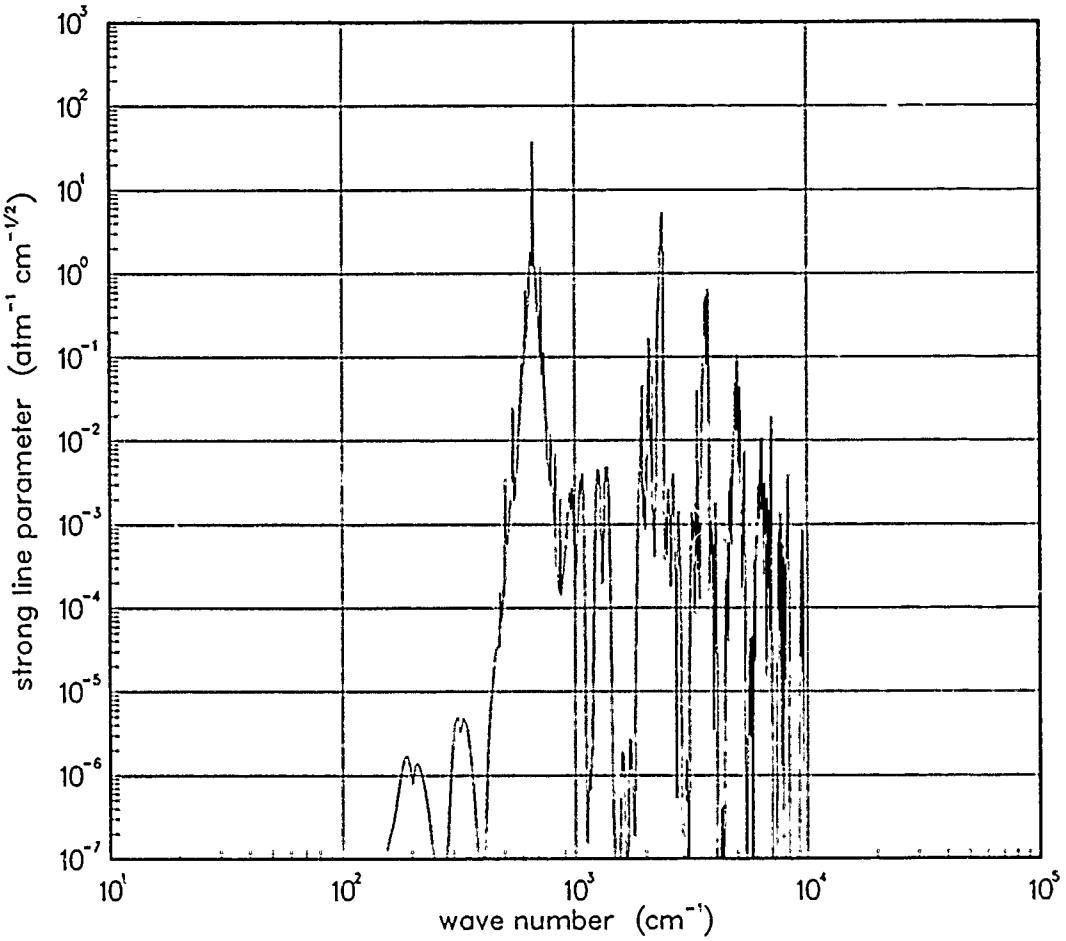

Figure 163. Strong-line parameter for CO_2 at 200°K.

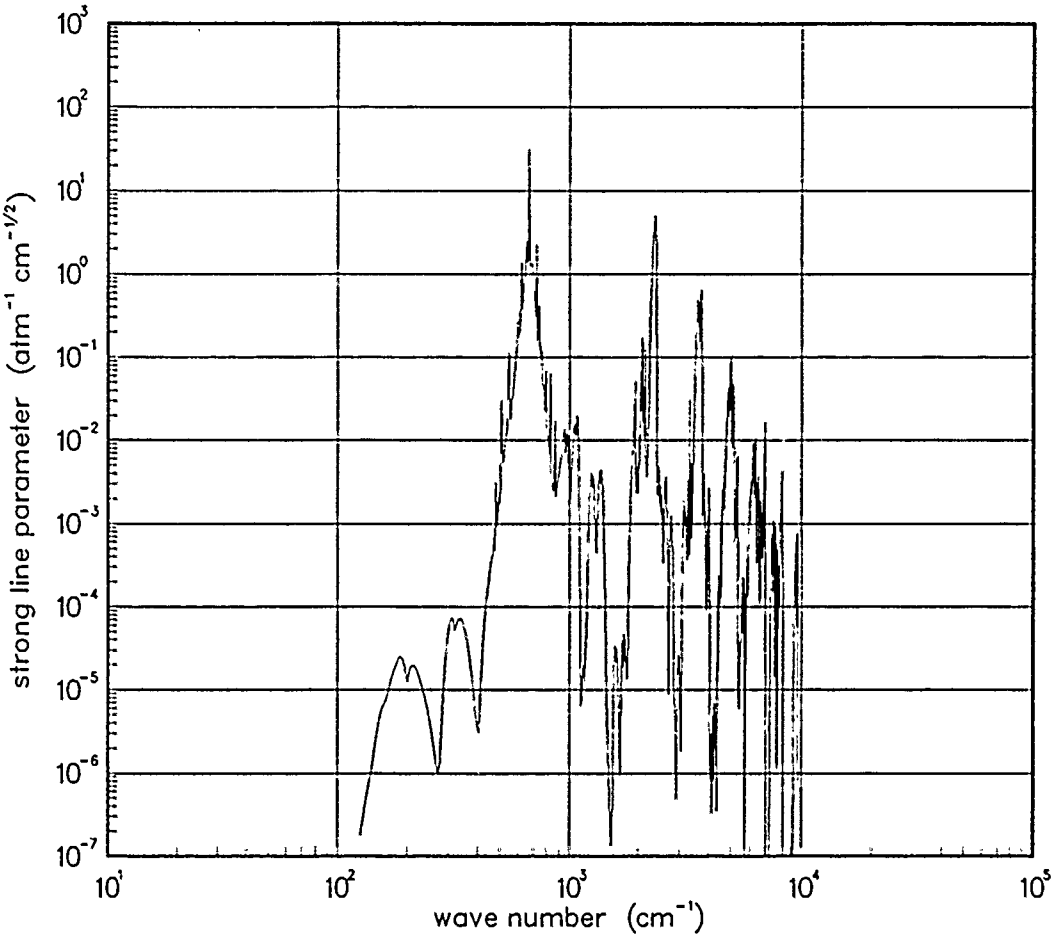

Figure 164. Strong-line parameter for CO_2 at 300°K.

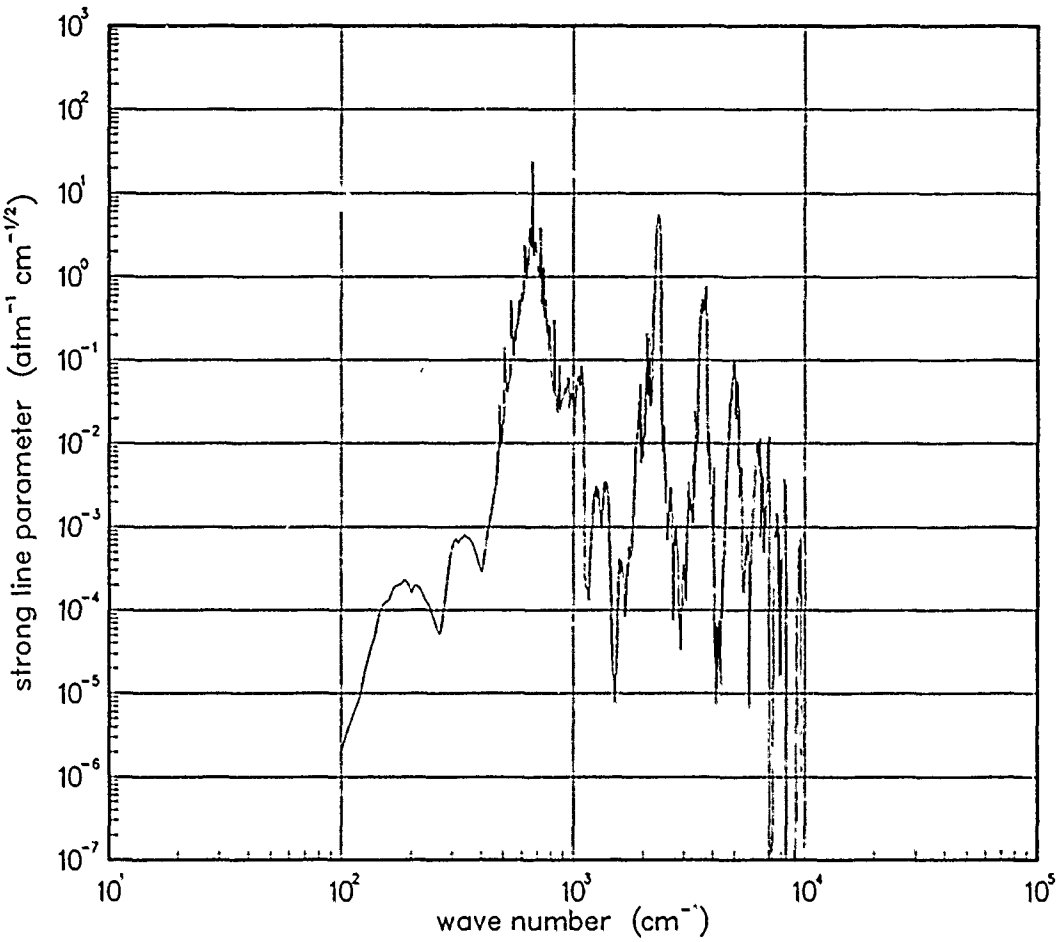

Figure 165. Strong-line parameter for CO_2 at 500°K.

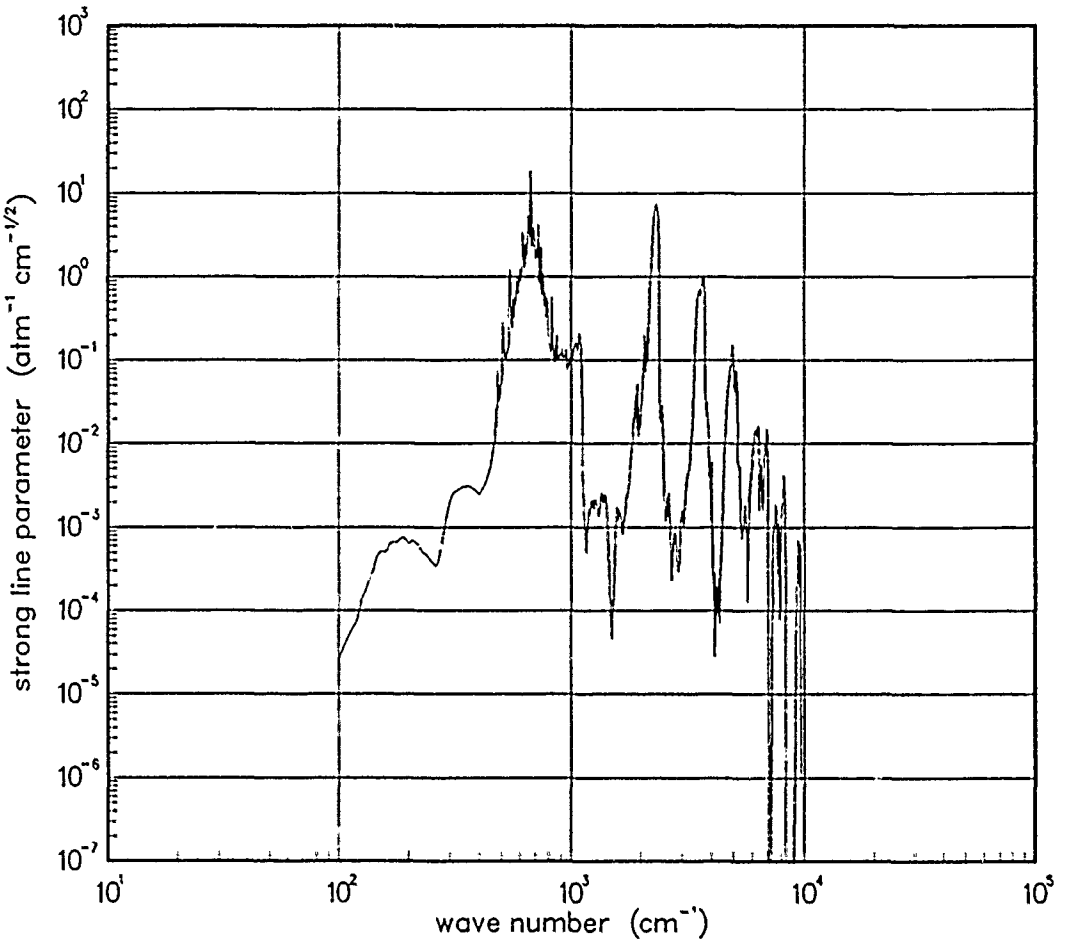

Figure 166. Strong-line parameter for CO_2 at 750°K.

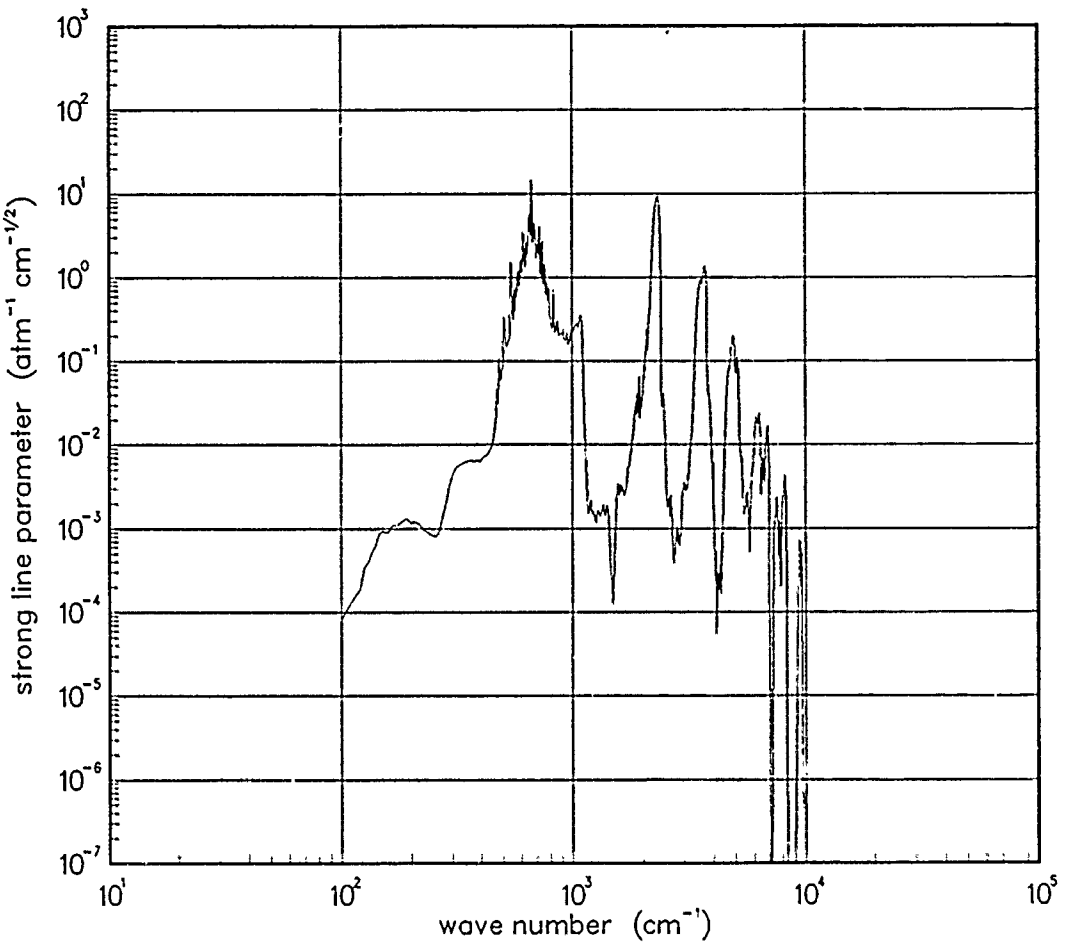

Figure 167. Strong-line parameter for CO_2 at 1000°K.

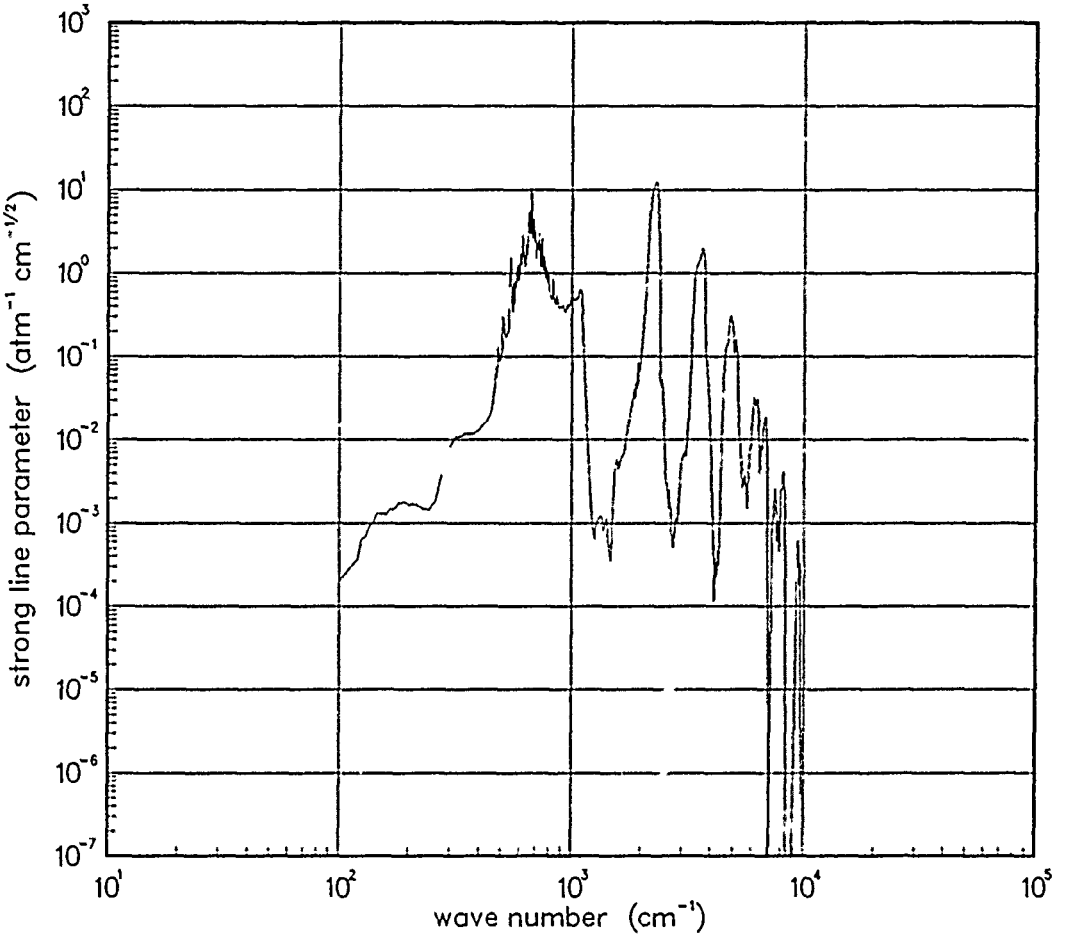

Figure 168. Strong-line parameter for CO_2 at 1500°K.

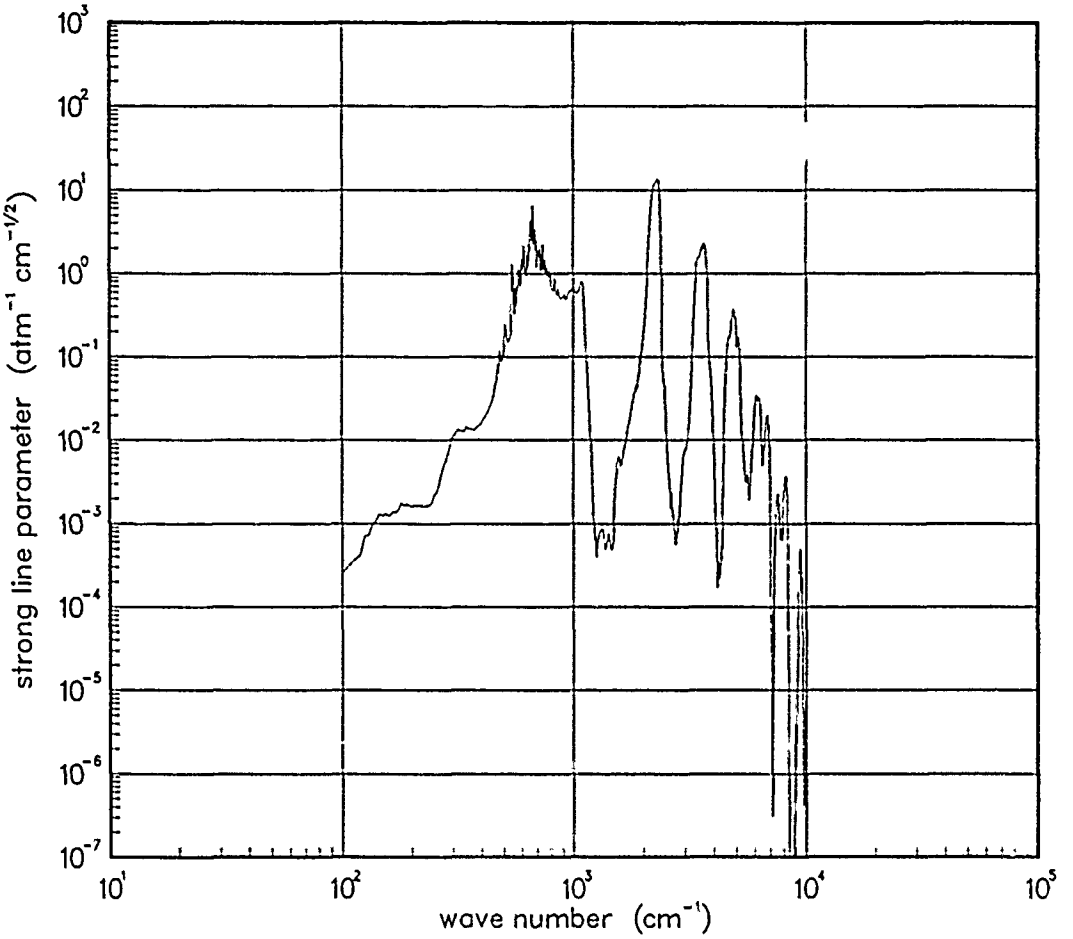

Figure 169. Strong-line parameter for CO_2 at 2000°K.

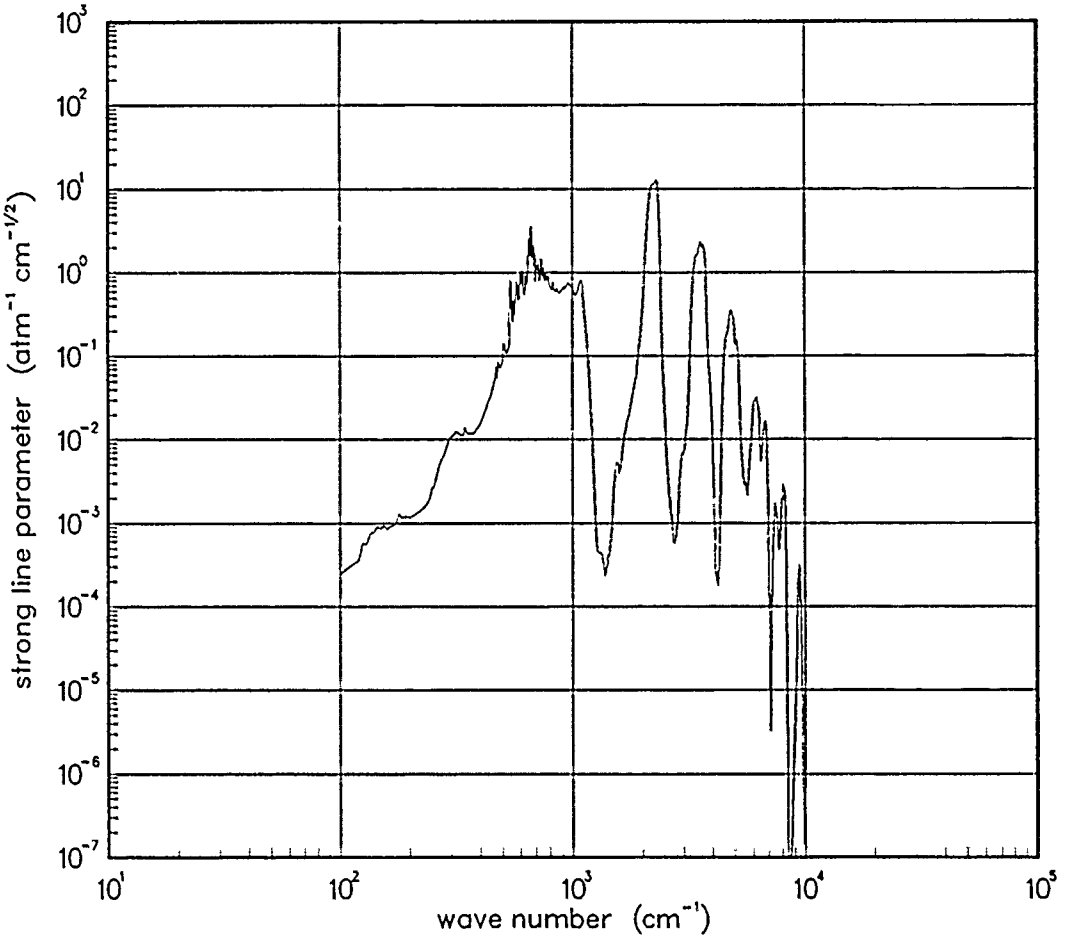

Figure 170. Strong-line parameter for CO_2 at 3000°K.

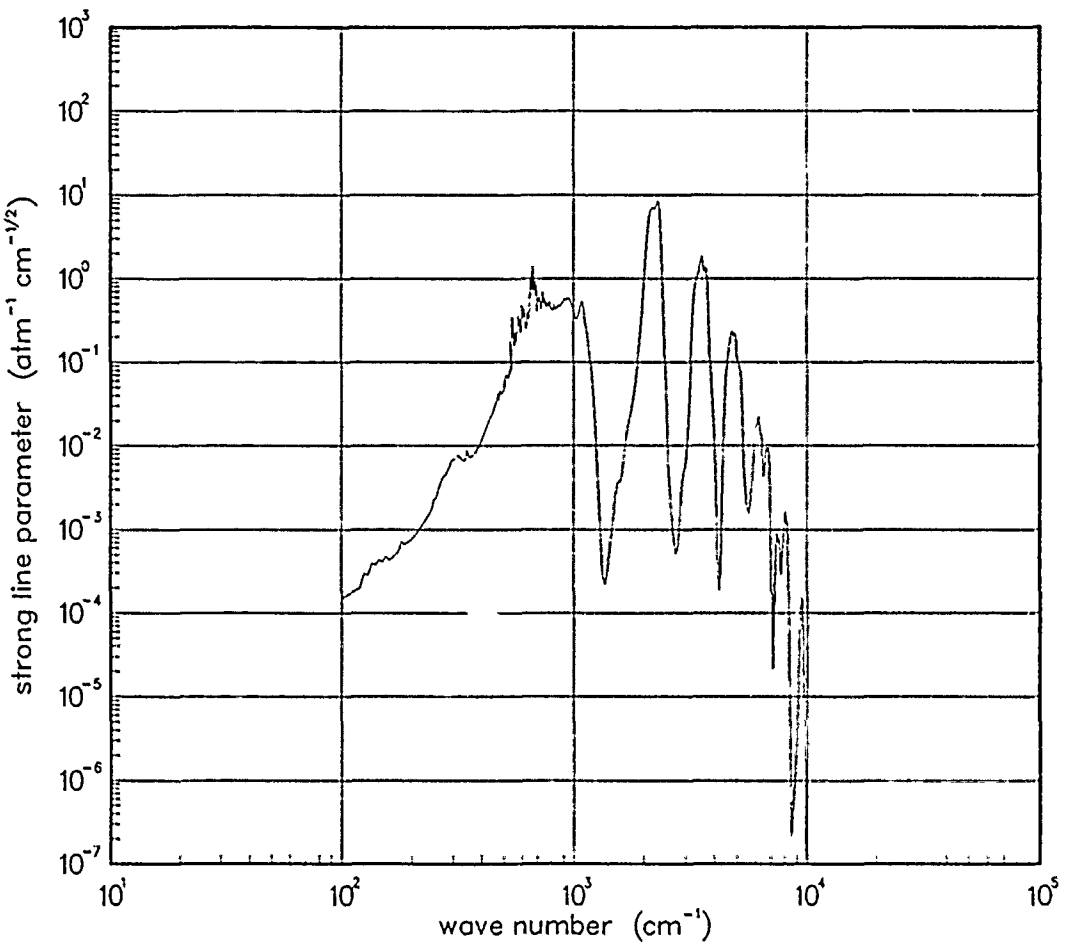

Figure 171. Strong-line parameter for CO_2 at 5000°K.

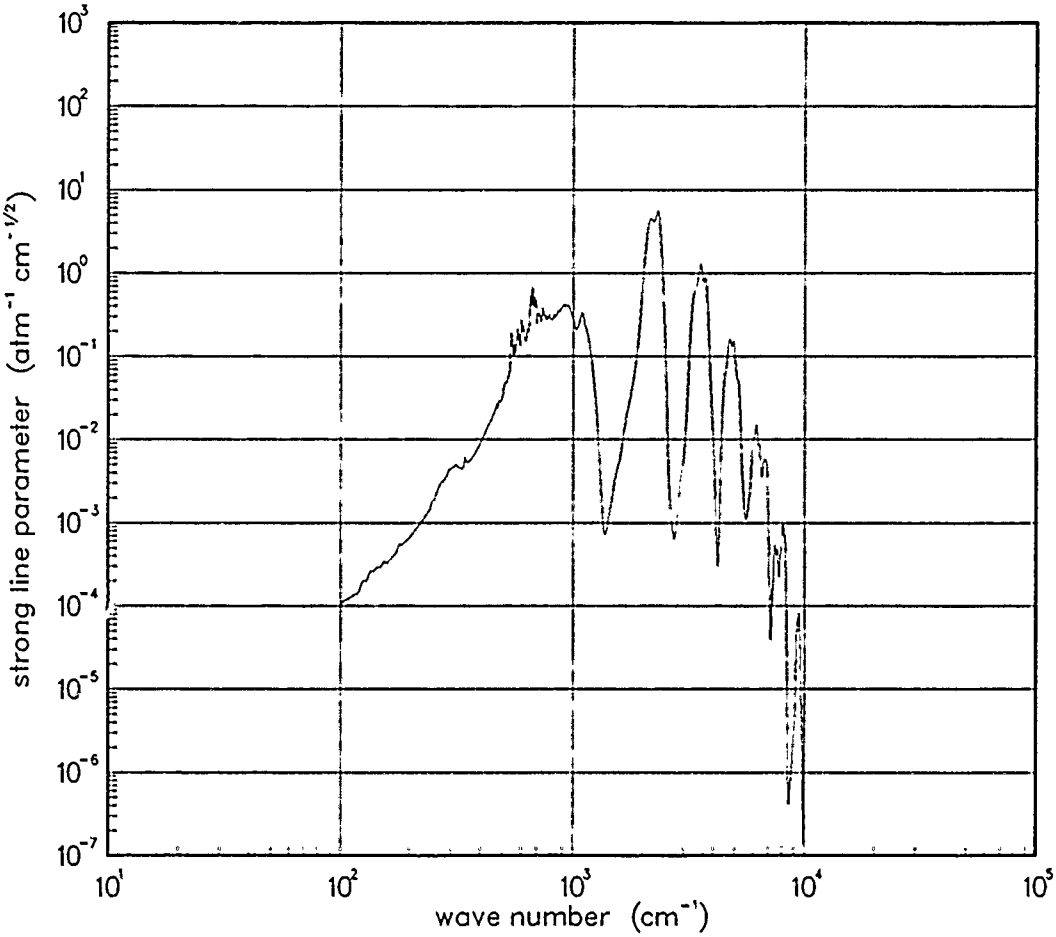

Figure 172. Strong-line parameter for CO_2 at 7000°K.

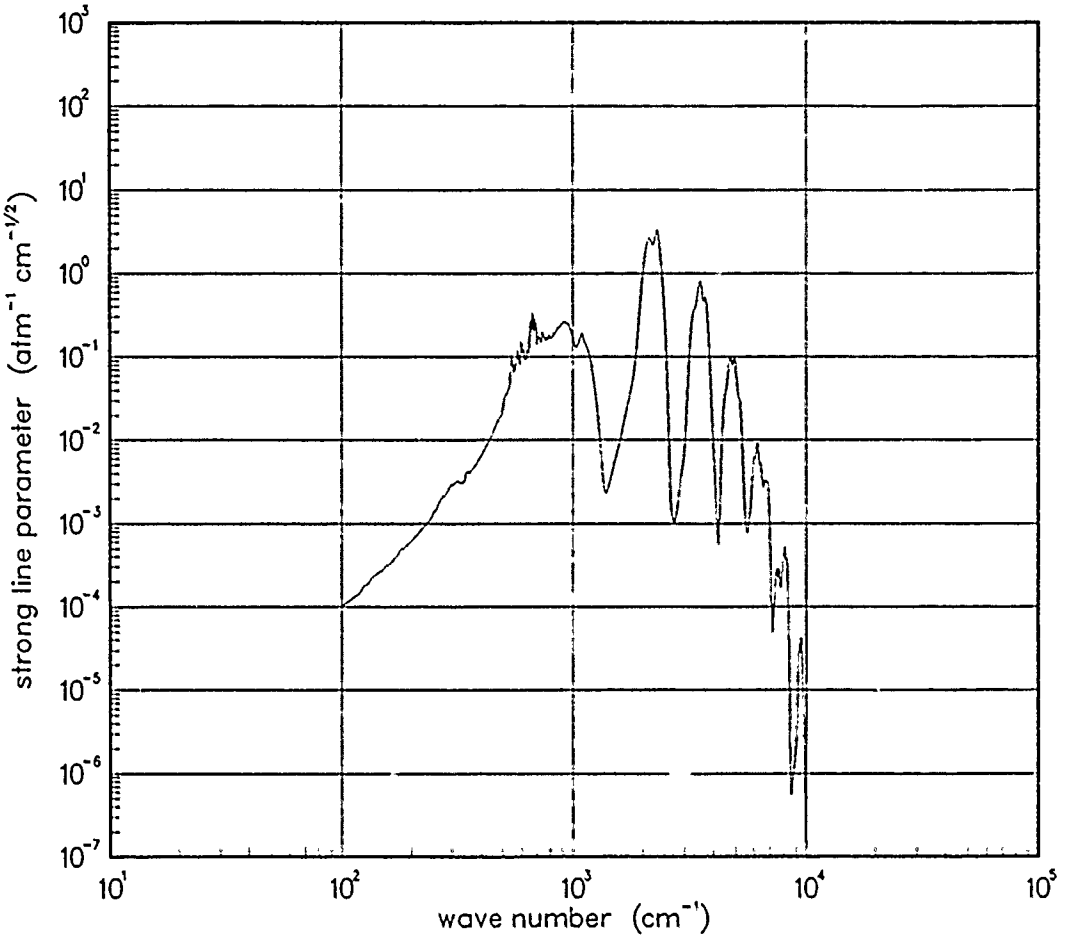

Figure 173. Strong-line parameter for CO_2 at 10000°K.

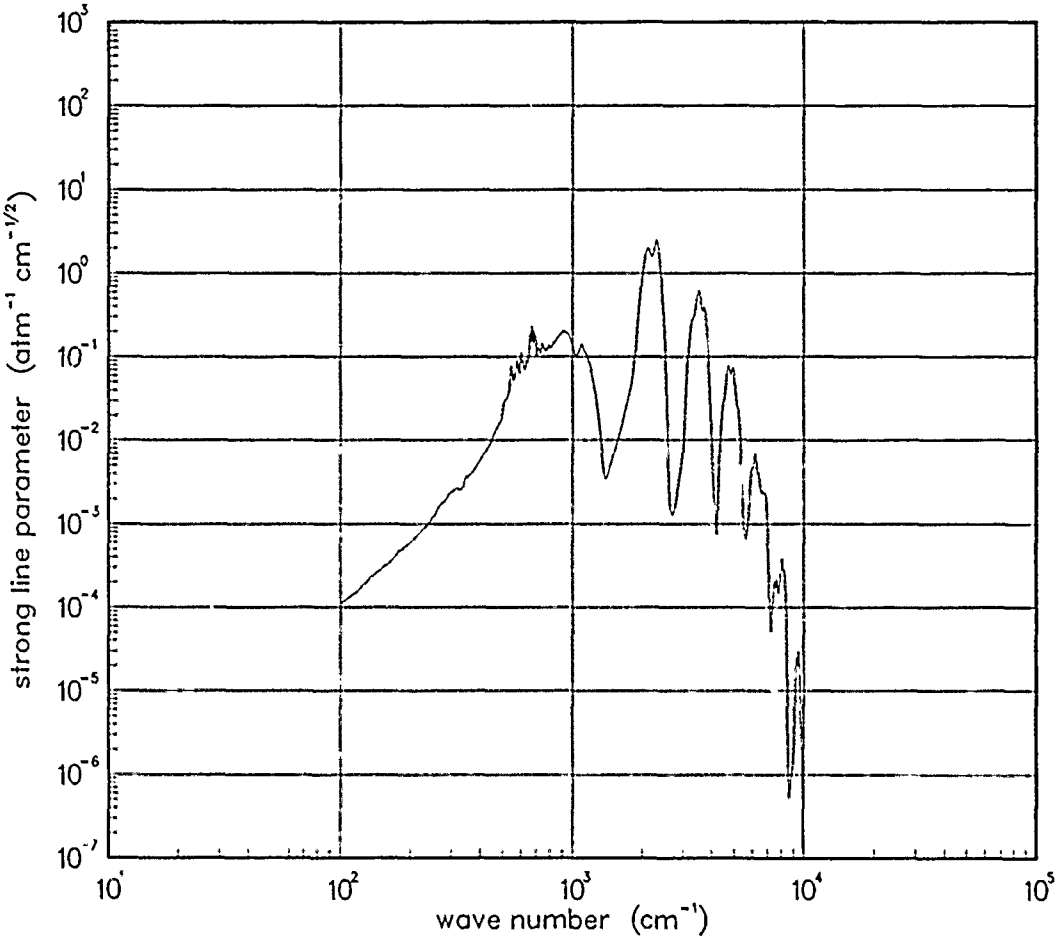

Figure 174. Strong-line parameter for CO_2 at 12000°K.

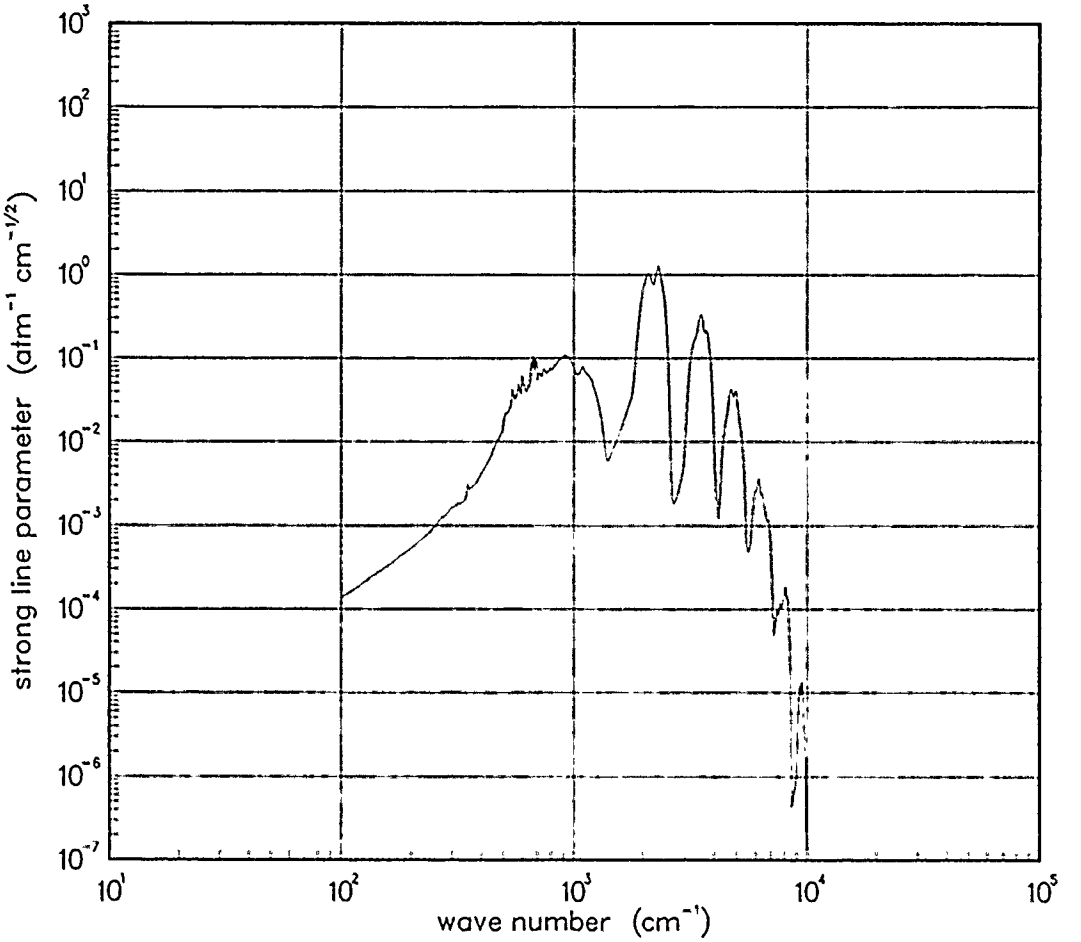

Figure 175. Strong-line parameter for CO_2 at 18000°K.

5.3 DINITROGEN OXIDE (N_2O).

The Data Curves for N_2O at temperatures < 1000 °K have been generated from the Air Force Geophysical Laboratory Line Atlas*. At temperatures above 1000 °K the curves were generated by combining the Air Force Geophysical Laboratory spectra at high temperatures with the "Boxcar" shapes†.

Data Source:

*R.A. McClatchey, et al, AFCRL Atmospheric Line Parameters Compilation , AFCRL-TR-73-0096, Air Force Cambridge Research Laboratories, (January 1973) 1982 version of the data tape.

†L.E. Ewing, Modeling Detail in the Weapon Optical Effects Code (U) , 69TMP-77, General Electric -- TEMPO, (October 1969) (Secret-Restricted Data).

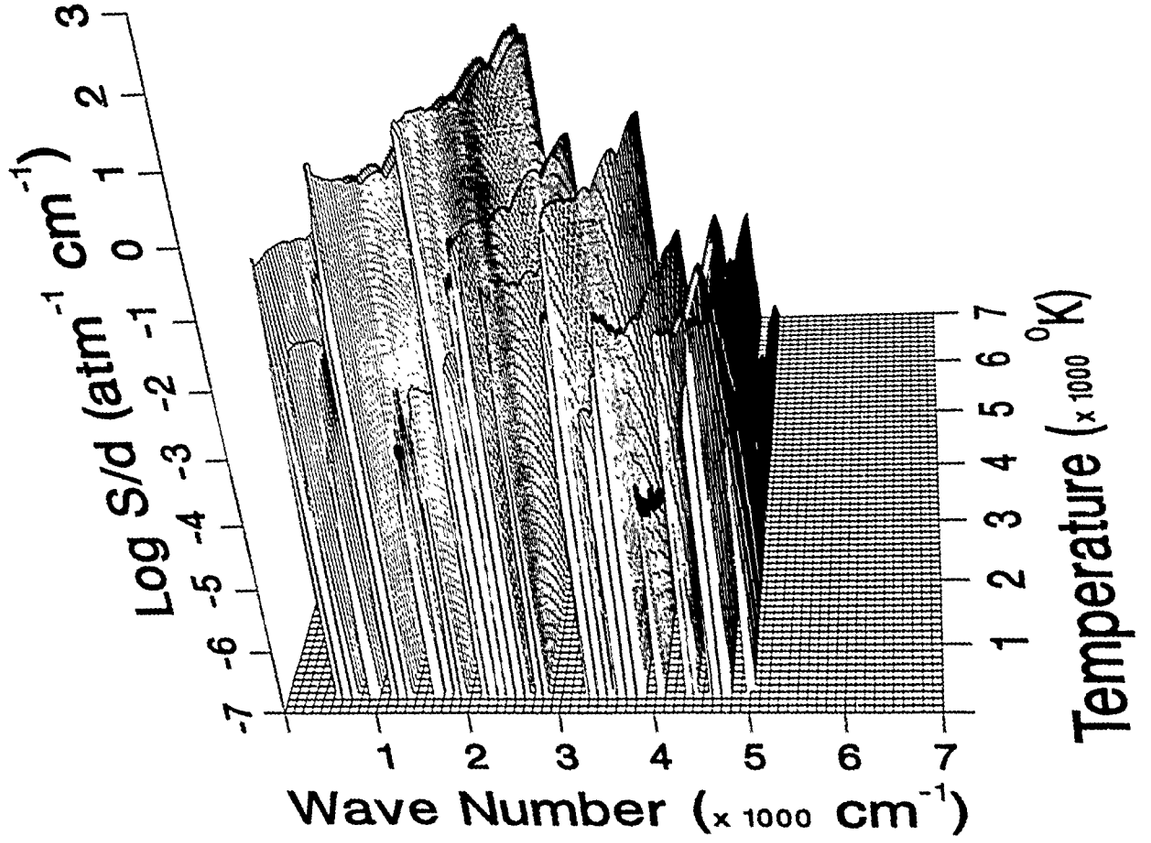

Figure 176. Weak-line parameter for N_2O.

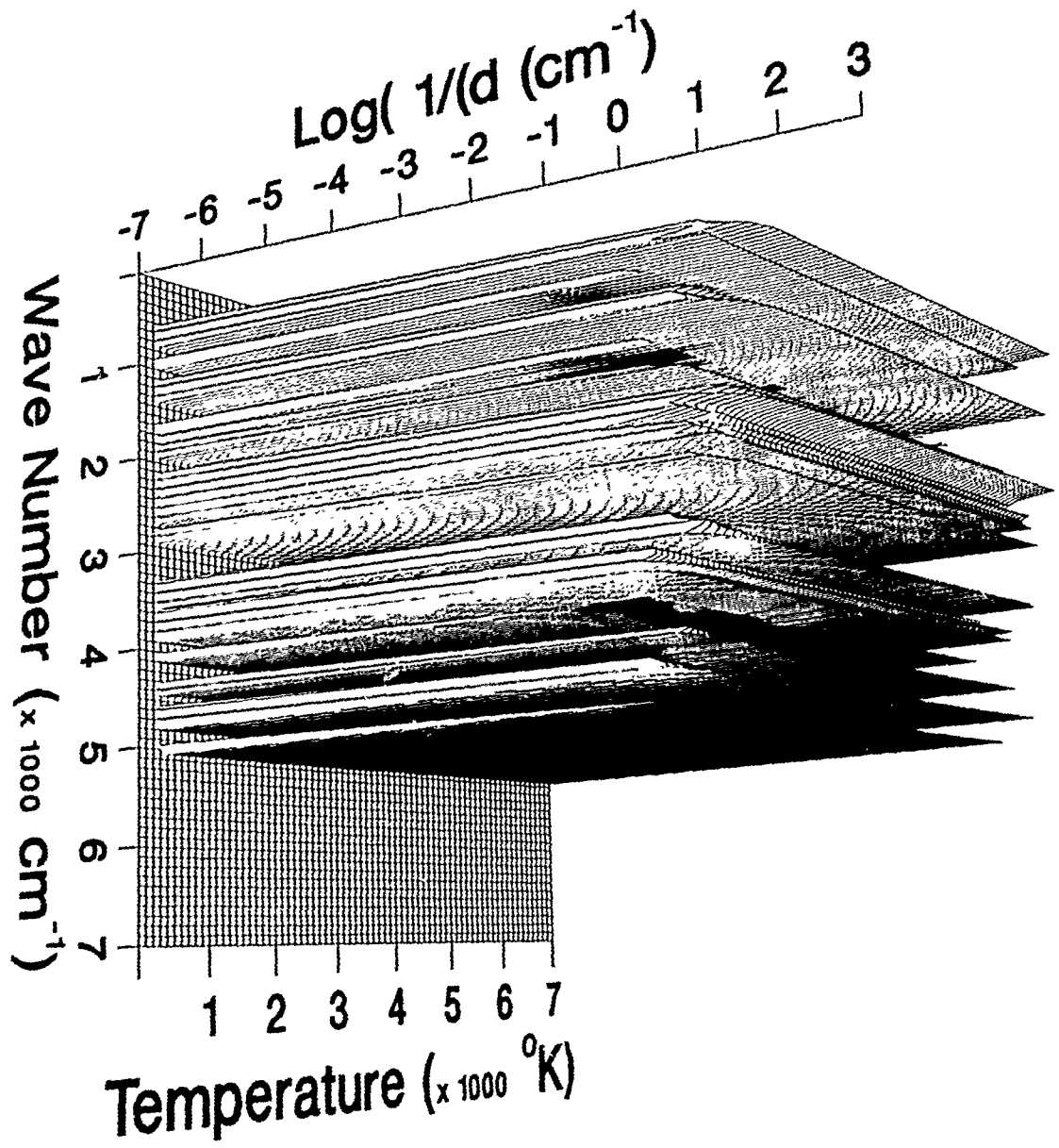

Figure 177. Inverse line spacing for N_2O.

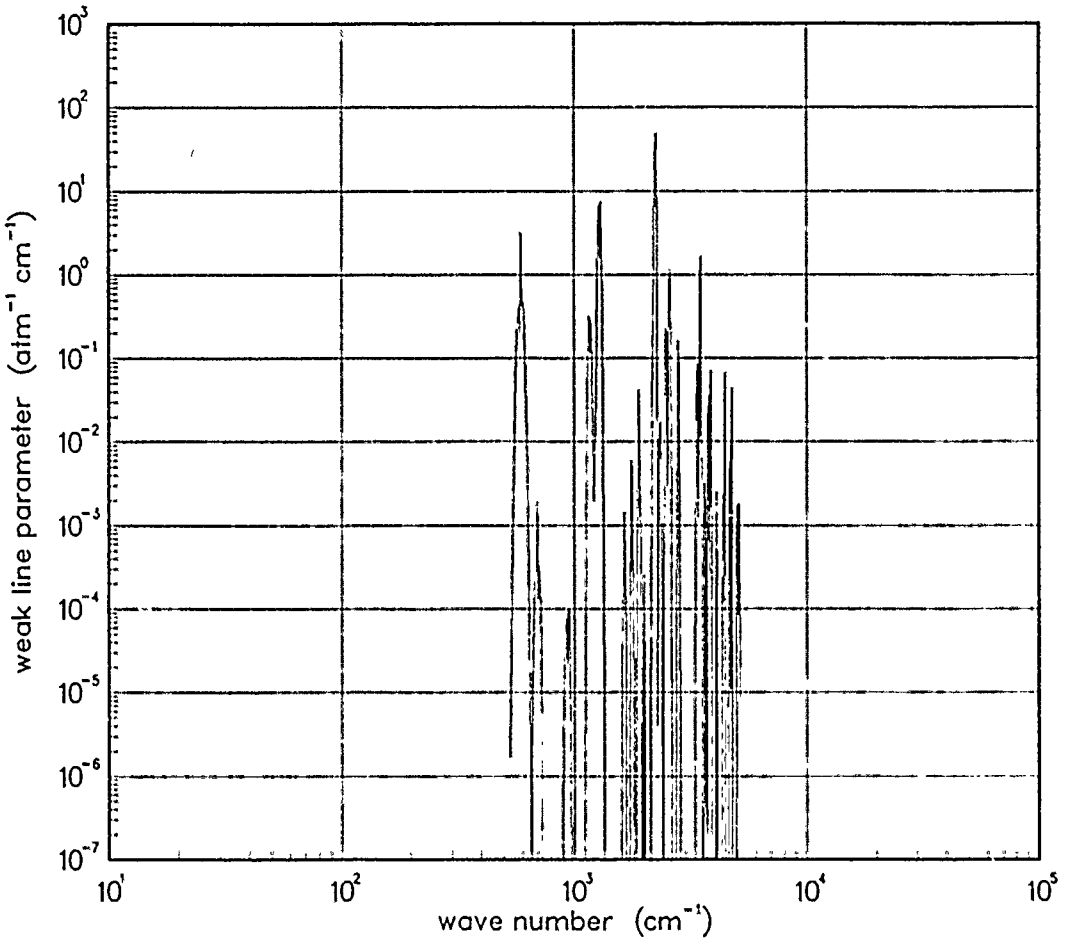

Figure 178. Weak-line parameter for N_2O at 200°K.

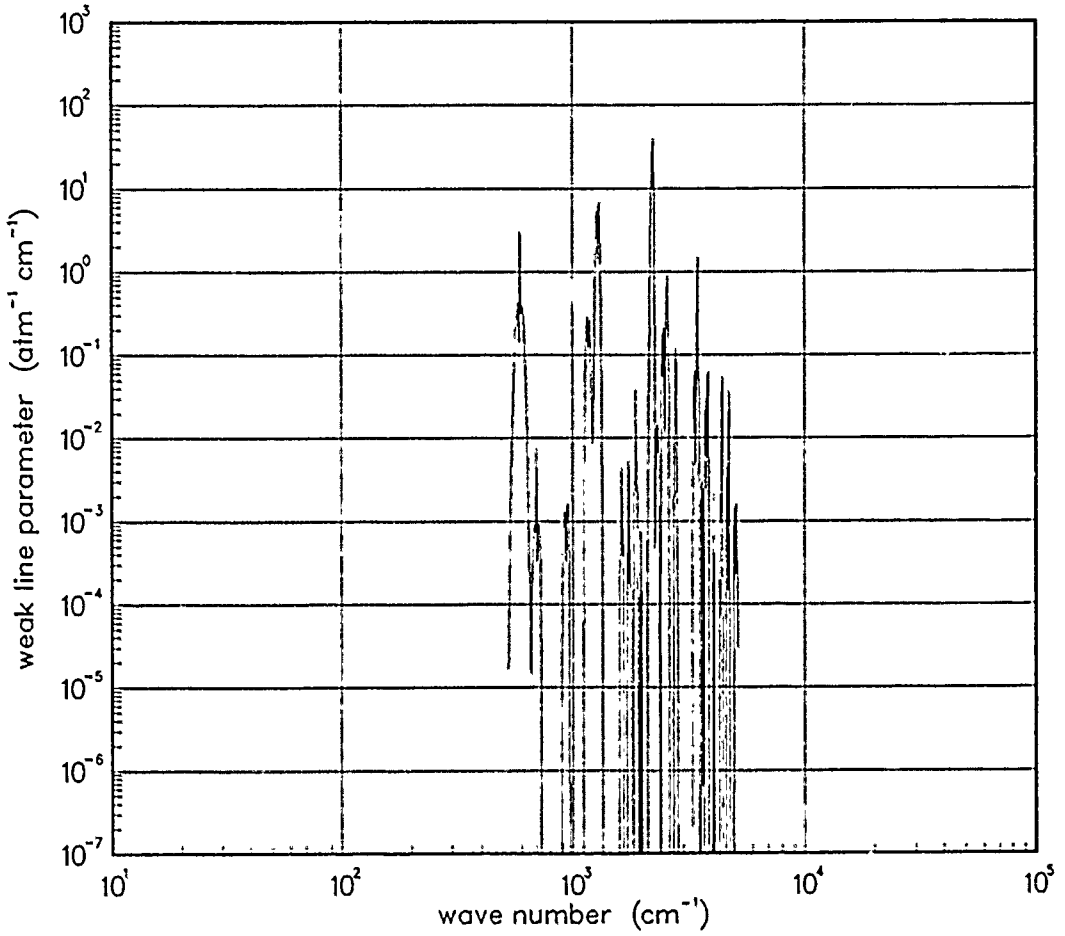

Figure 179. Weak-line parameter for N_2O at 300°K.

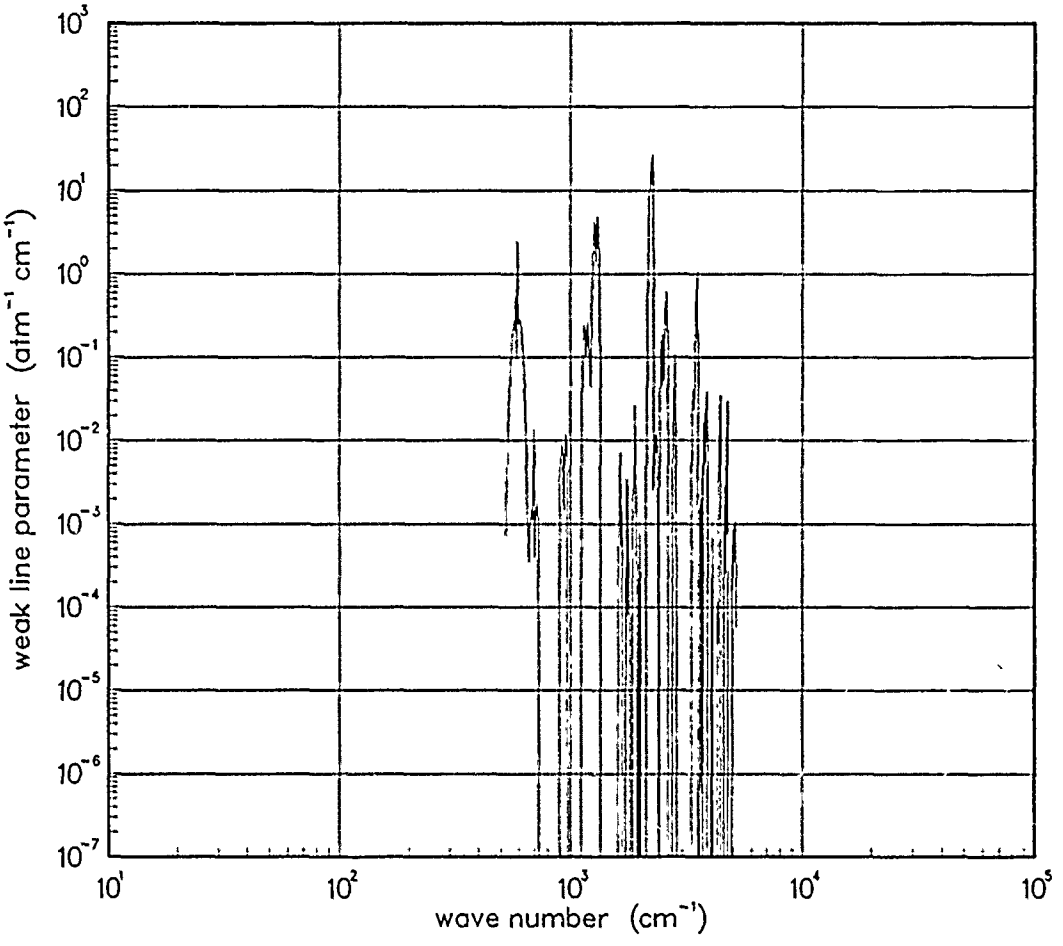

Figure 180. Weak-line parameter for N_2O at 500°K.

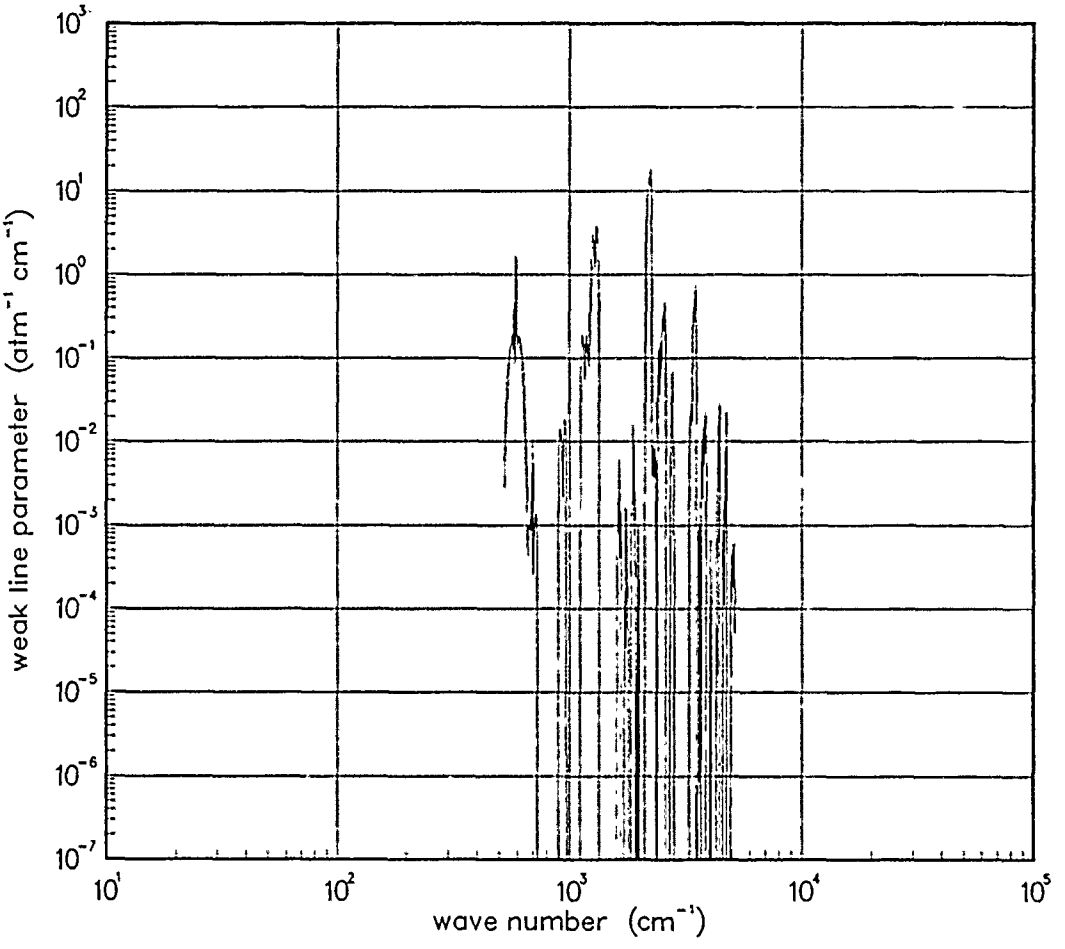

Figure 181. Weak-line parameter for N_2O at 750°K.

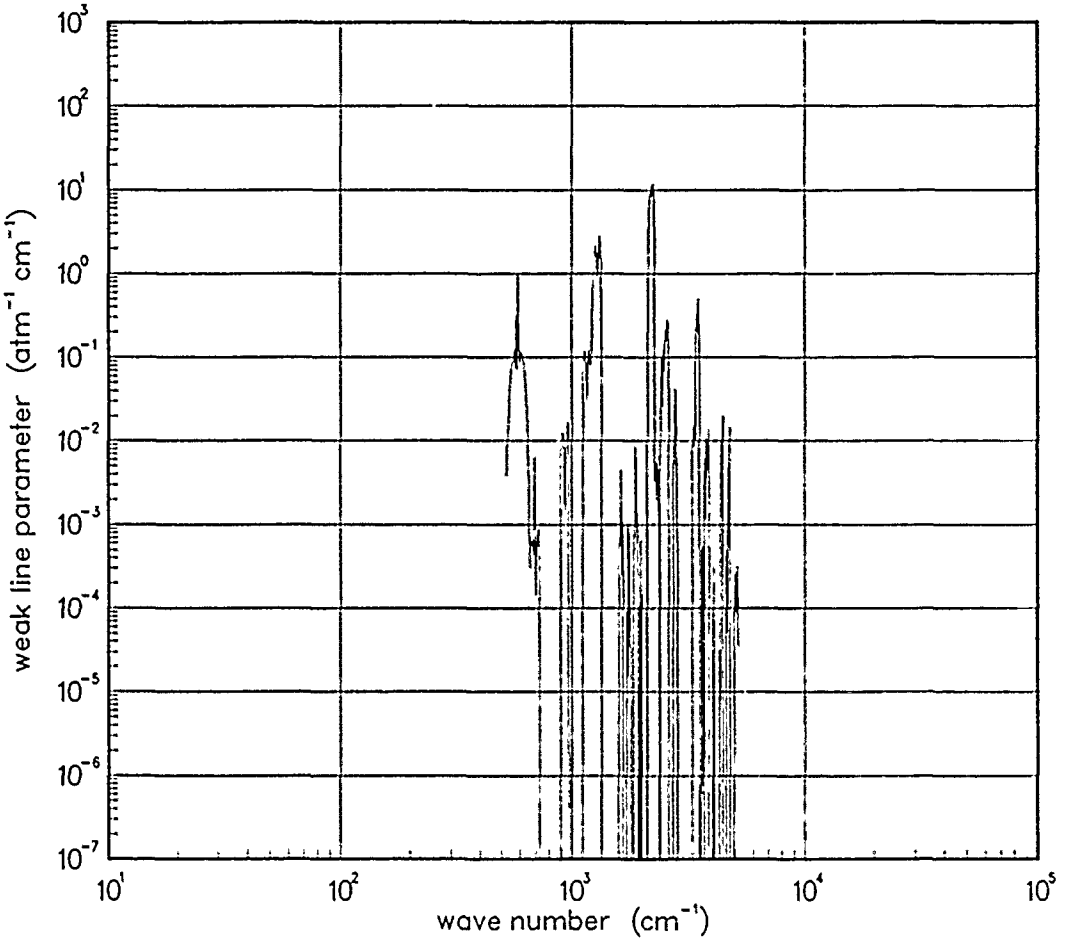

Figure 182. Weak-line parameter for N_2O at 1000°K.

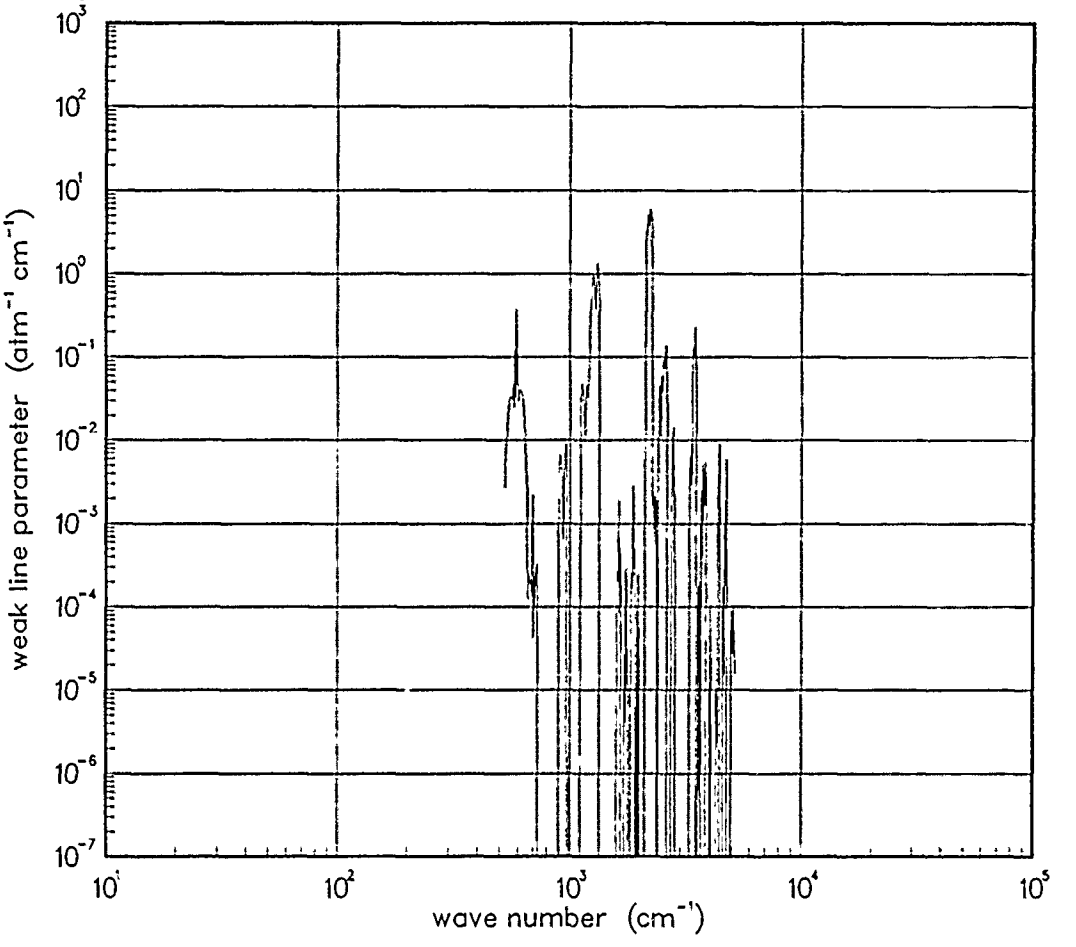

Figure 183. Weak-line parameter for N_2O at 1500°K.

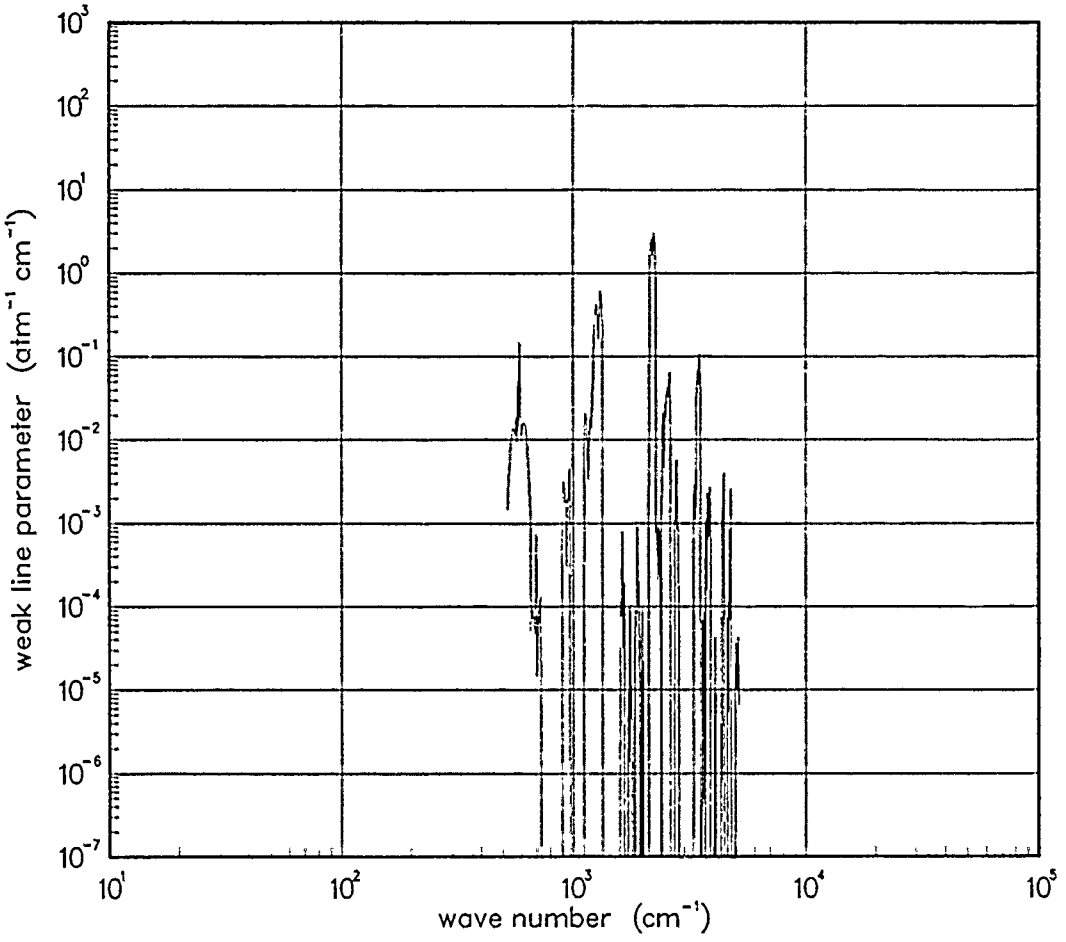

Figure 184. Weak-line parameter for N_2O at 2000°K.

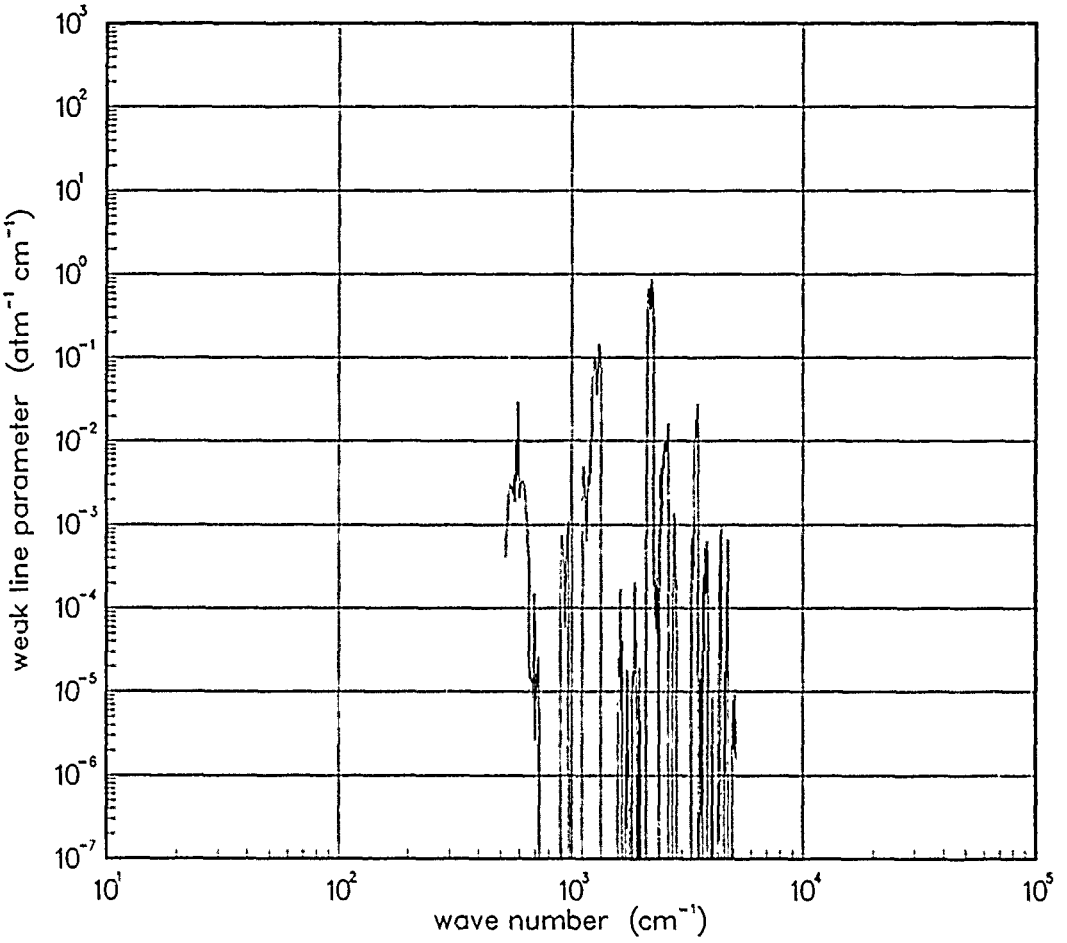

Figure 185. Weak-line parameter for N_2O at 3000°K.

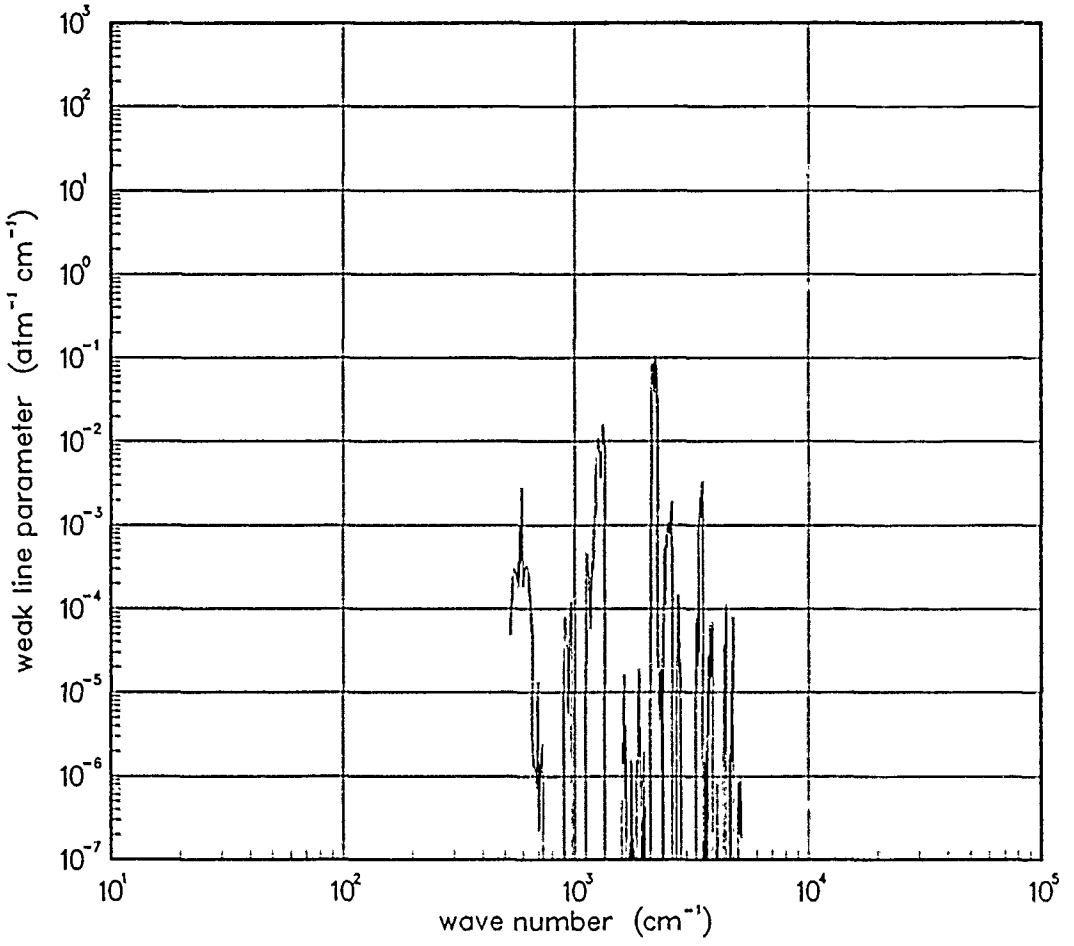

Figure 186. Weak-line parameter for N_2O at 5000°K.

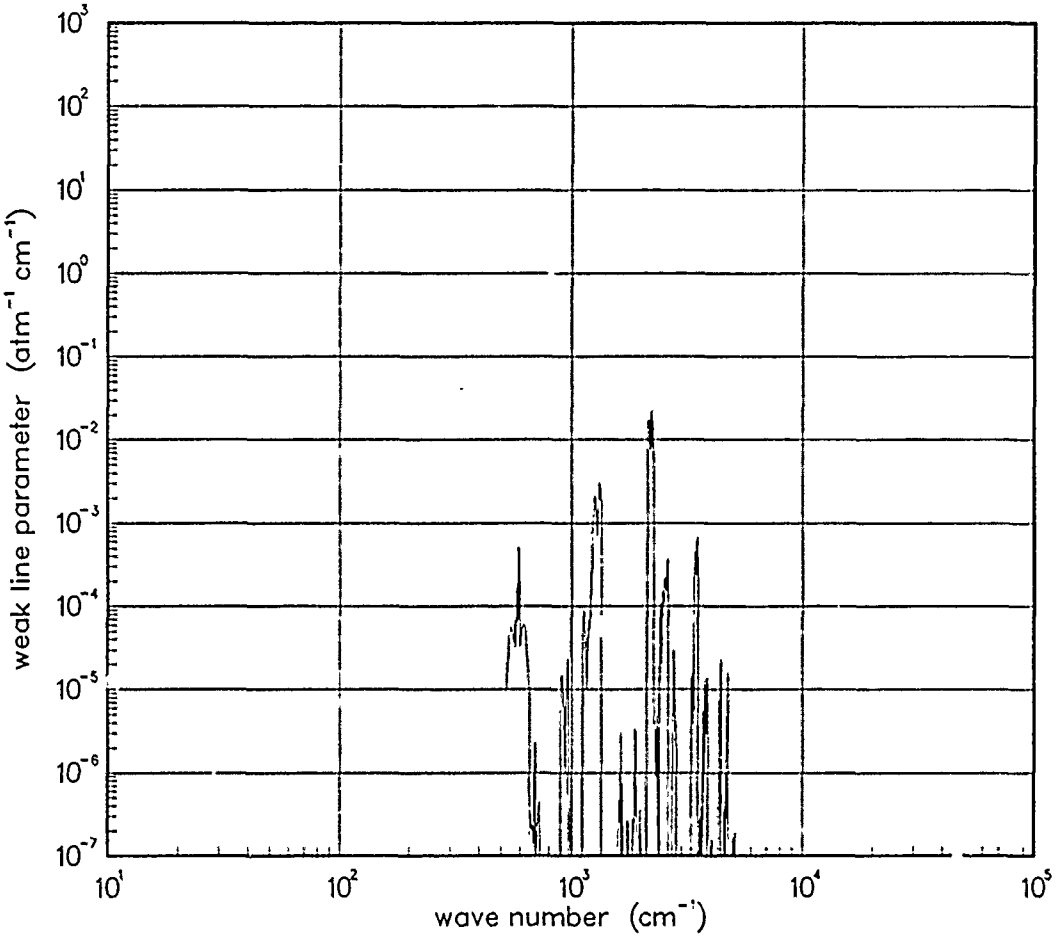

Figure 187. Weak-line parameter for N_2O at 7000°K.

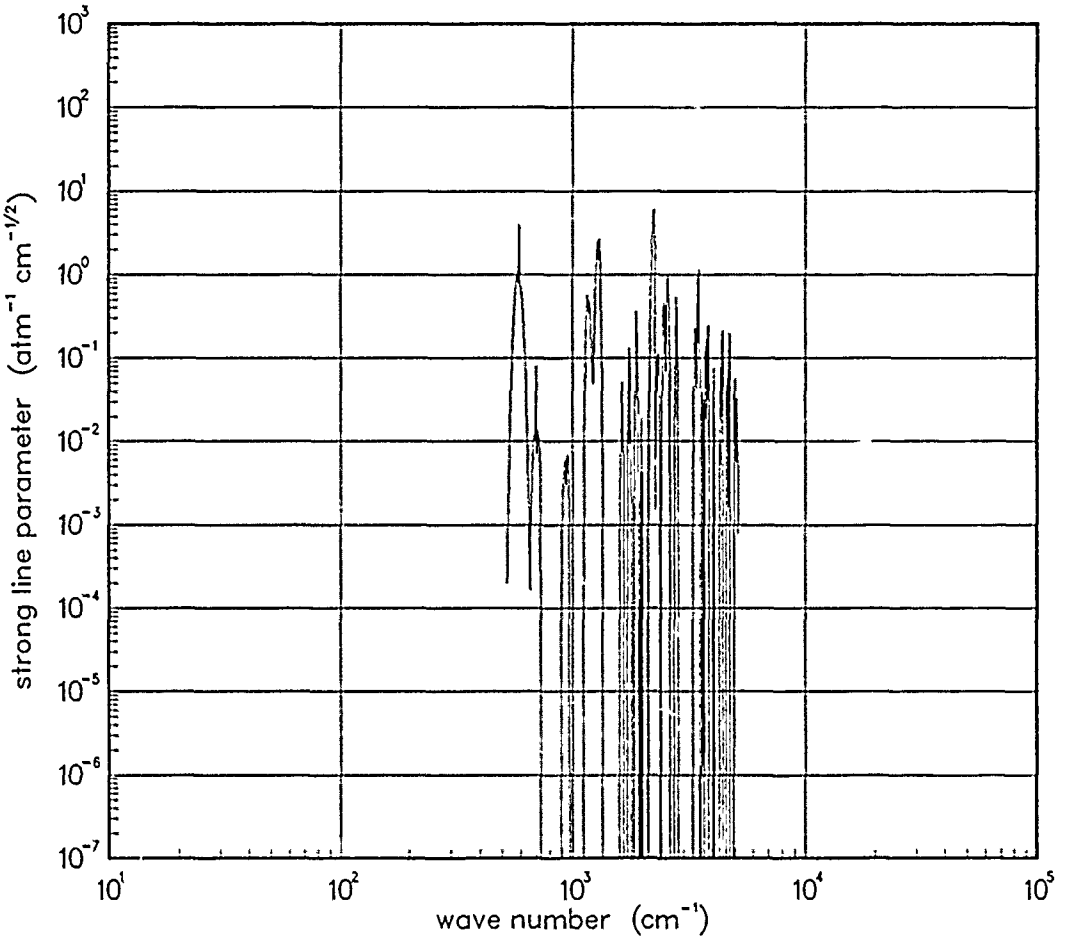

Figure 188. Strong-line parameter for N_2O at 200°K.

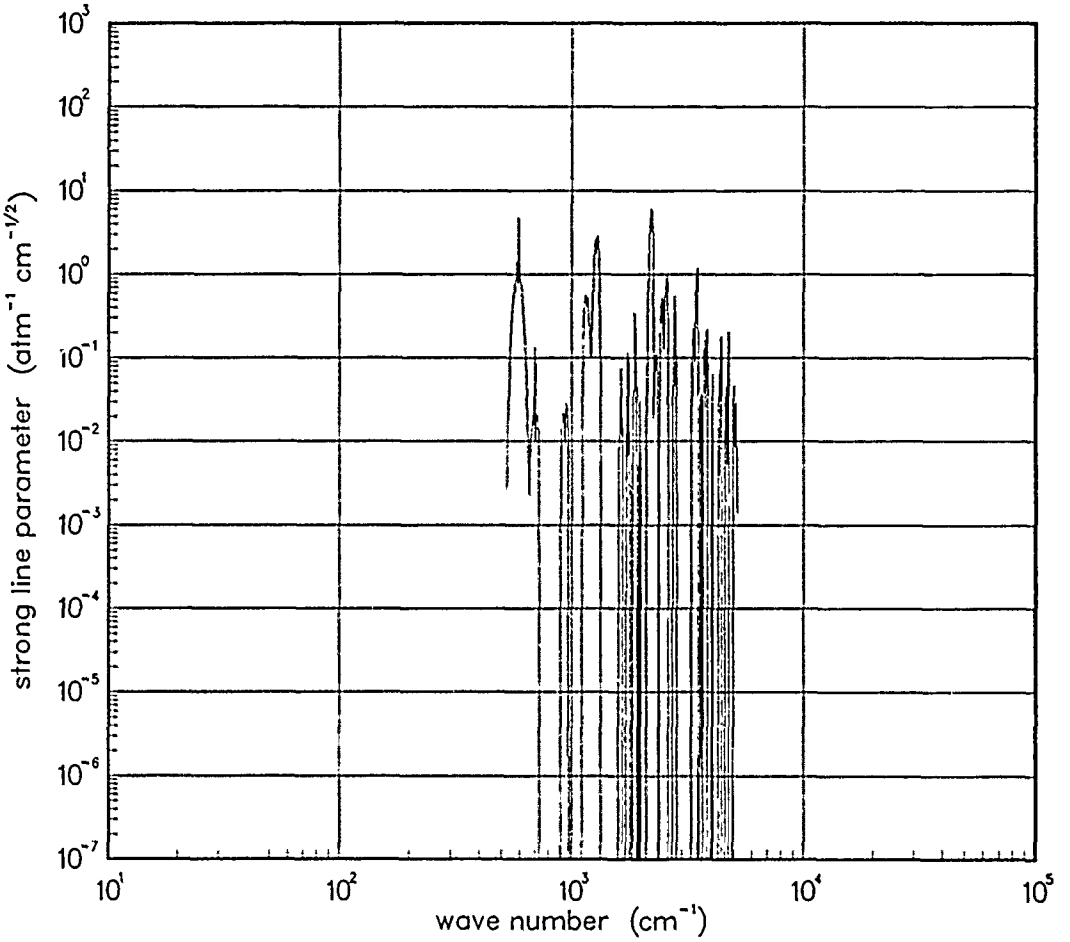

Figure 189. Strong-line parameter for N_2O at 300°K.

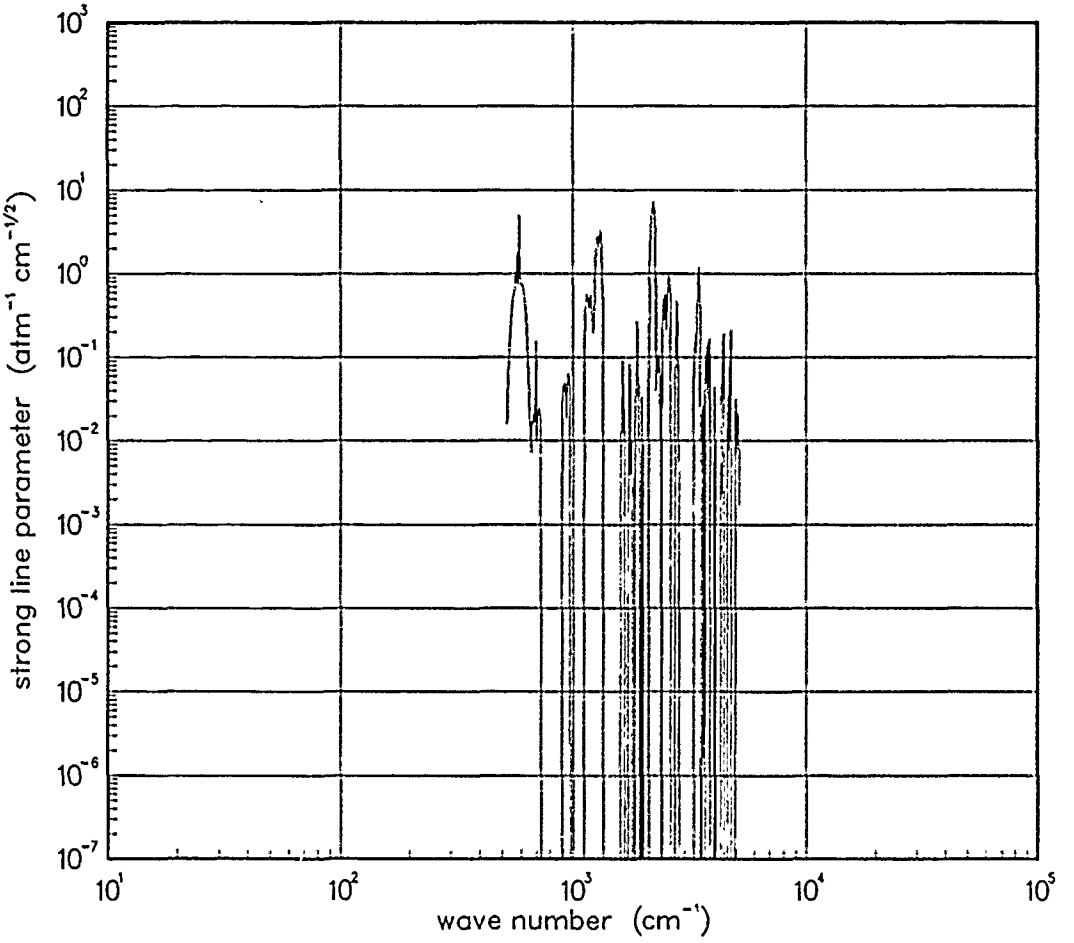

Figure 190. Strong-line parameter for N_2O at 500°K.

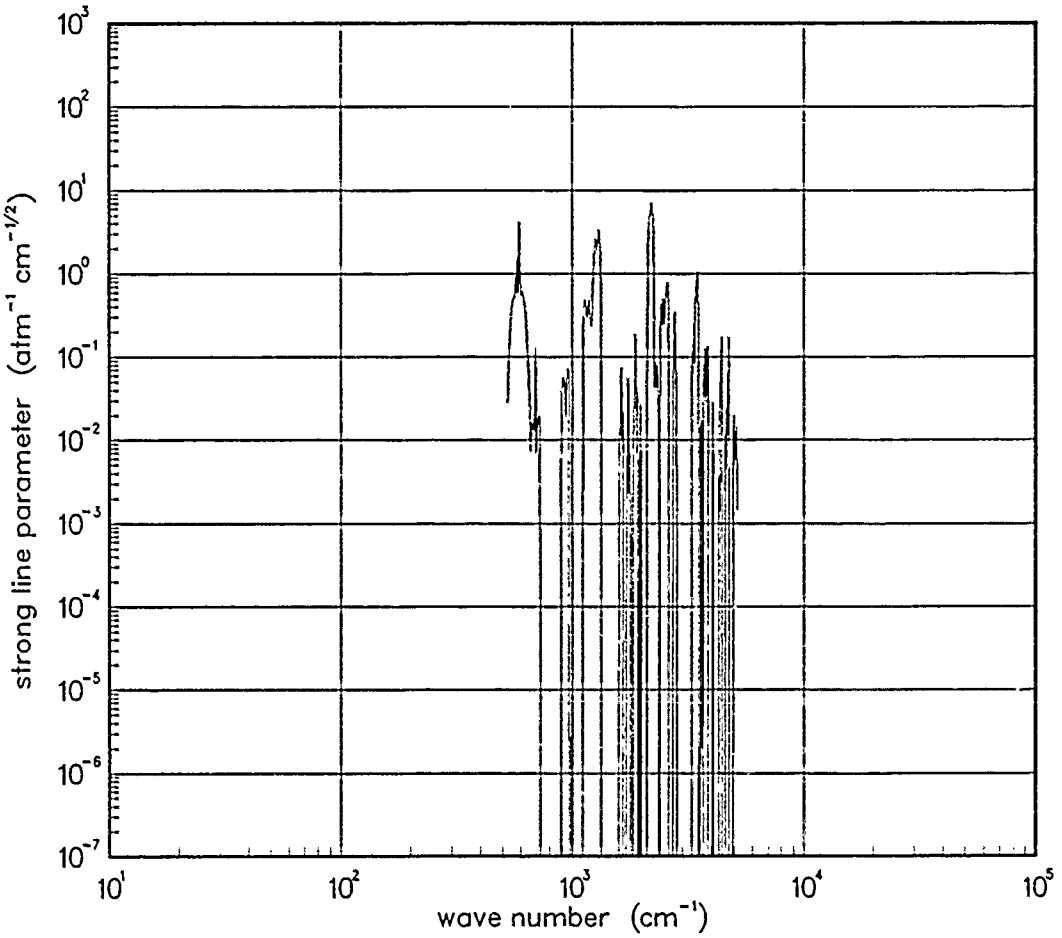

Figure 191. Strong-line parameter for N_2O at 750°K.

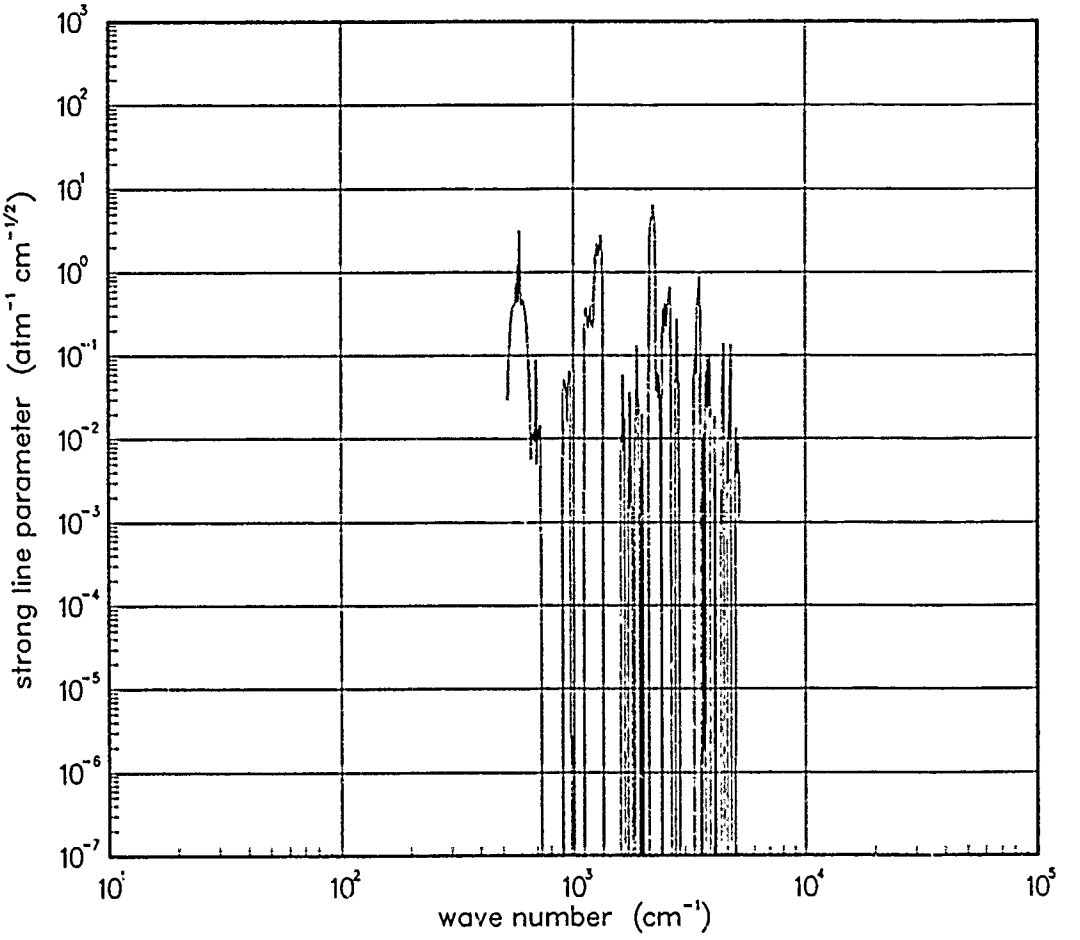

Figure 192. Strong-line parameter for N_2O at 1000°K.

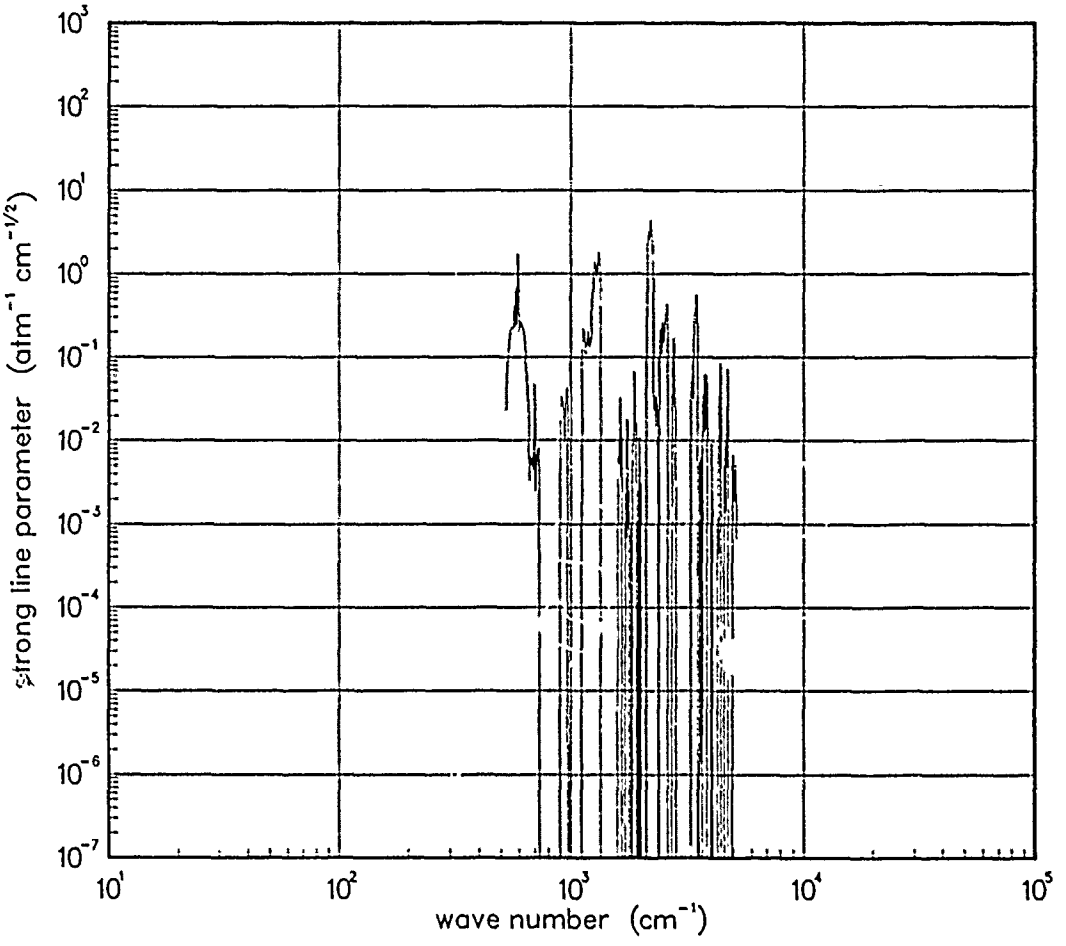

Figure 193. Strong-line parameter for N_2O at 1500°K.

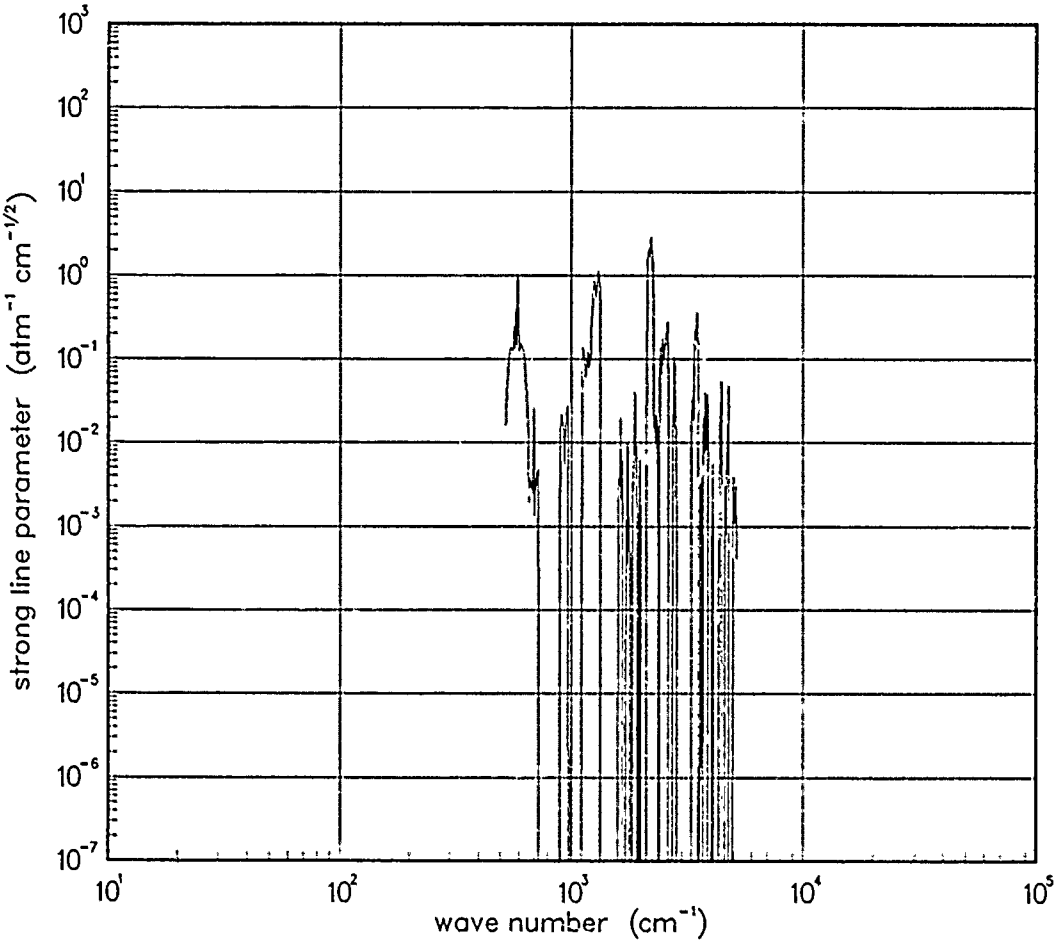

Figure 194. Strong-line parameter for N_2O at 2000°K.

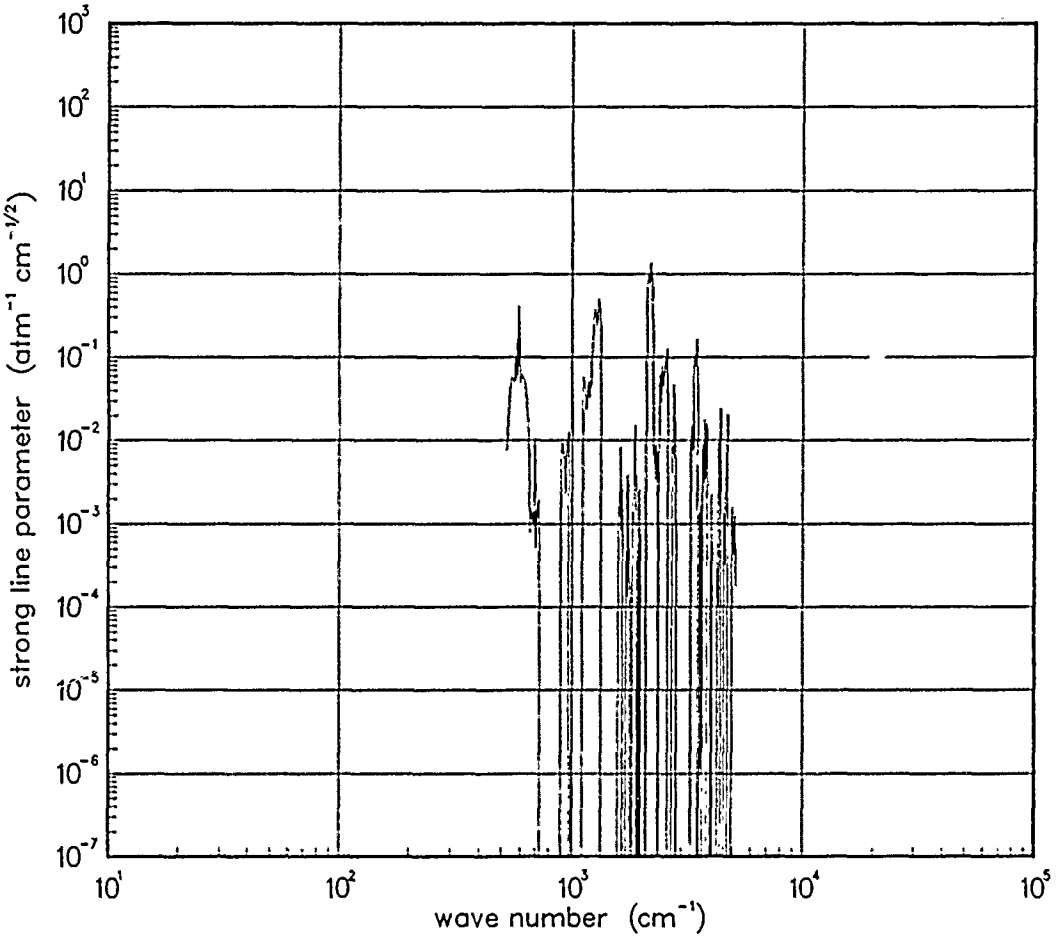

Figure 195. Strong-line parameter for N_2O at 3000°K.

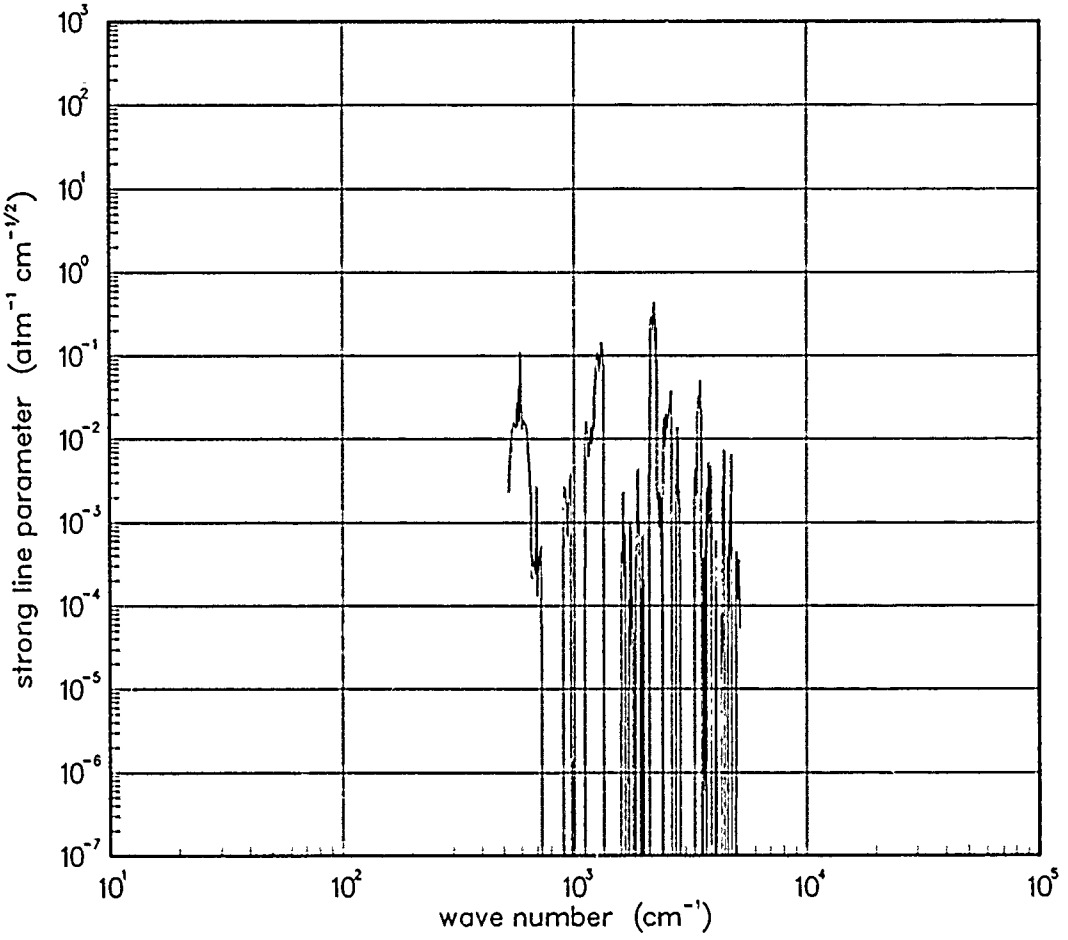

Figure 196. Strong-line parameter for N_2O at 5000°K.

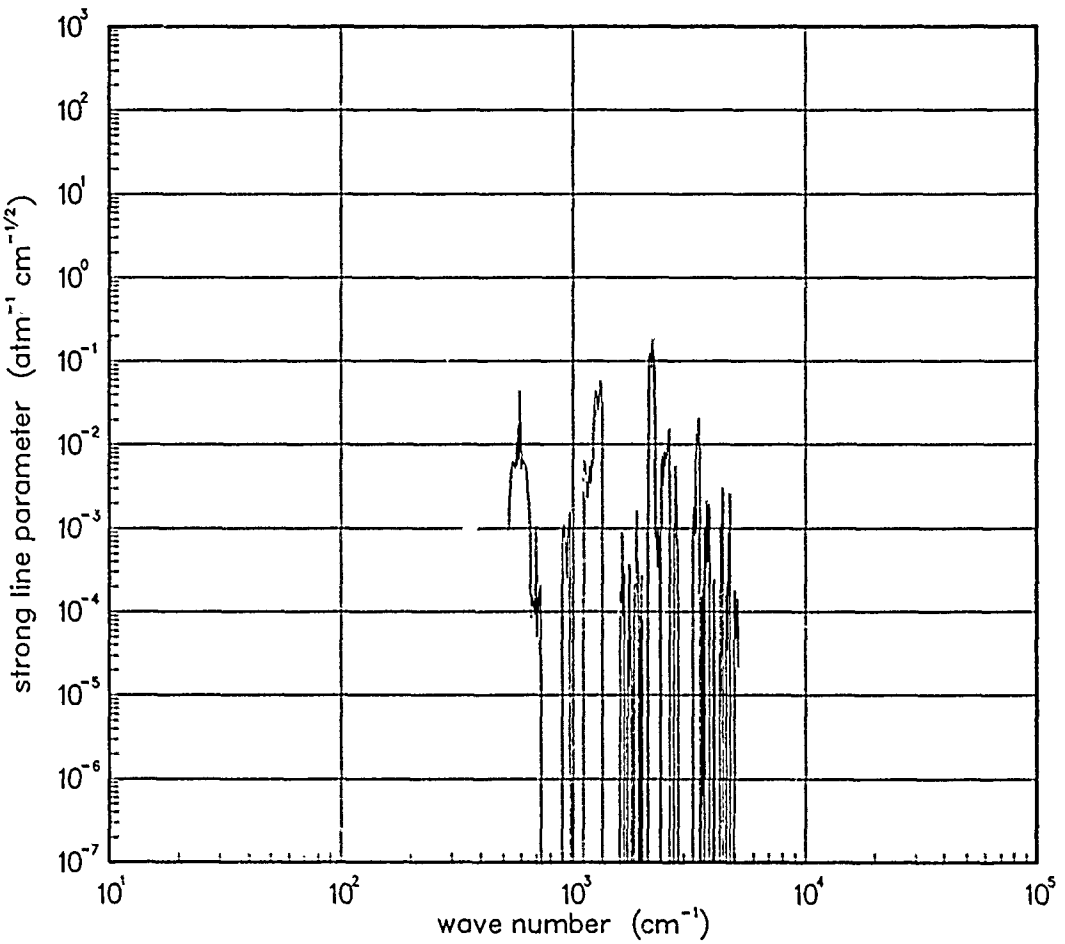

Figure 197. Strong-line parameter for N_2O at 7000°K.

5.4 METHANE (CH_4).

Local thermal equilibrium emission spectra for Methane has been developed from the Air Force Geophysical Laboratory line atlas for 200, 300, 500, 750, 1000 °K.

The CH_4 molecule has been included within the NORSE LTE data base because of its contribution to ambient atmospheric absorption. The inclusion of accurate parameters for this species above 1000 °K is felt to be of low priority.

Figure 198. Weak-line parameter for CH_4.

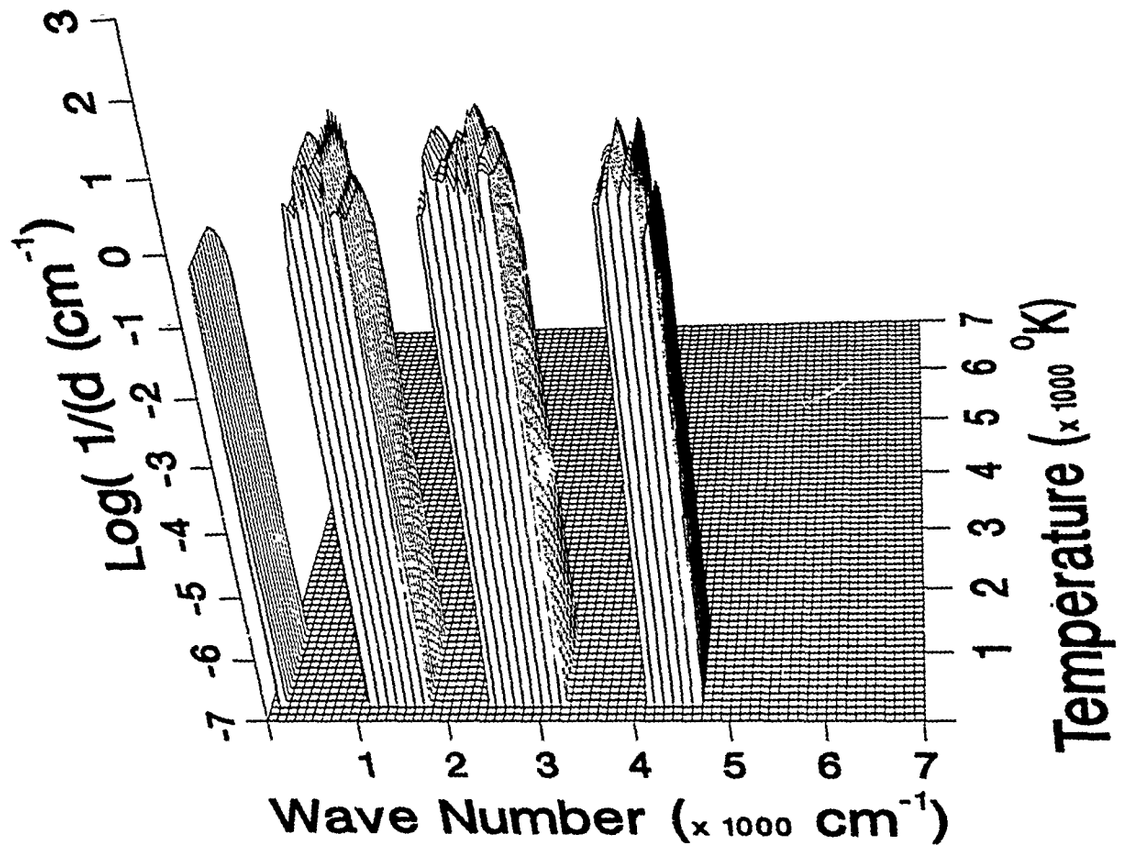

Figure 199. Inverse line spacing for CH_4.

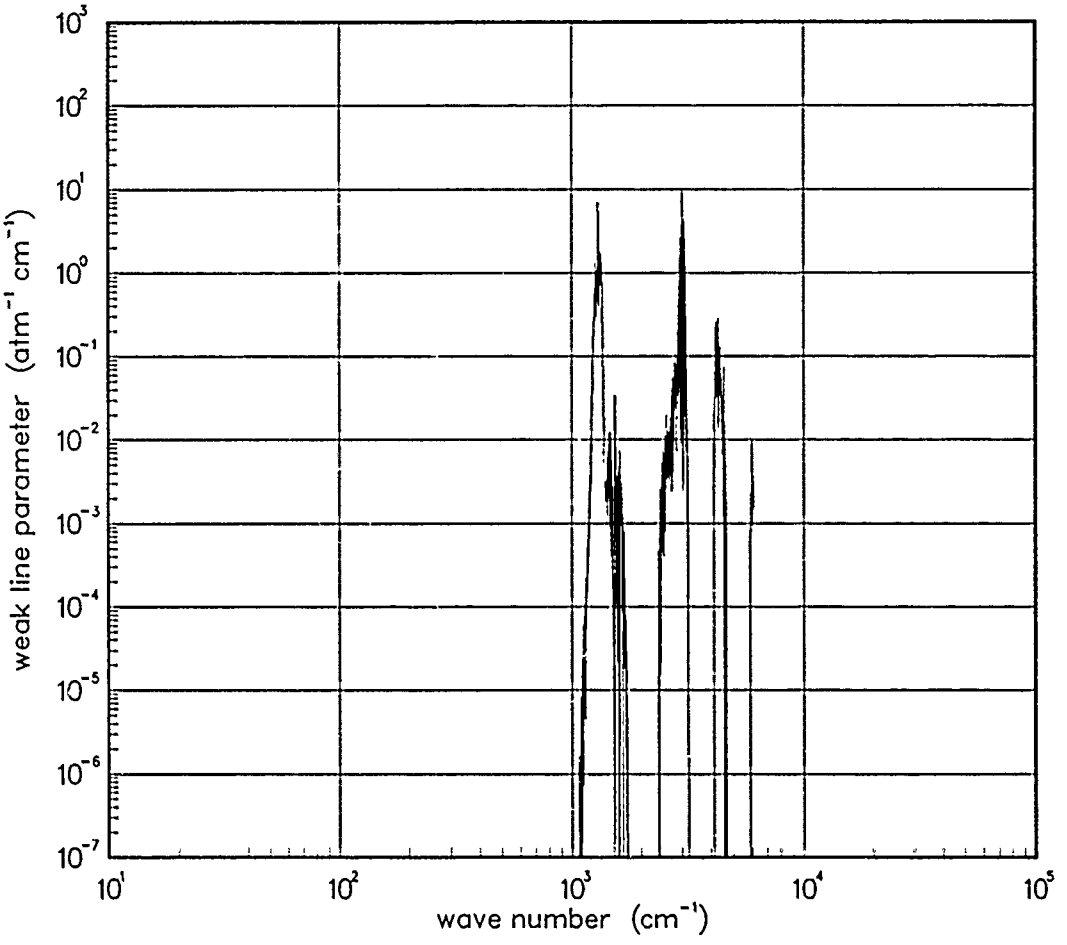

Figure 200. Weak-line parameter for CH_4 at 200°K.

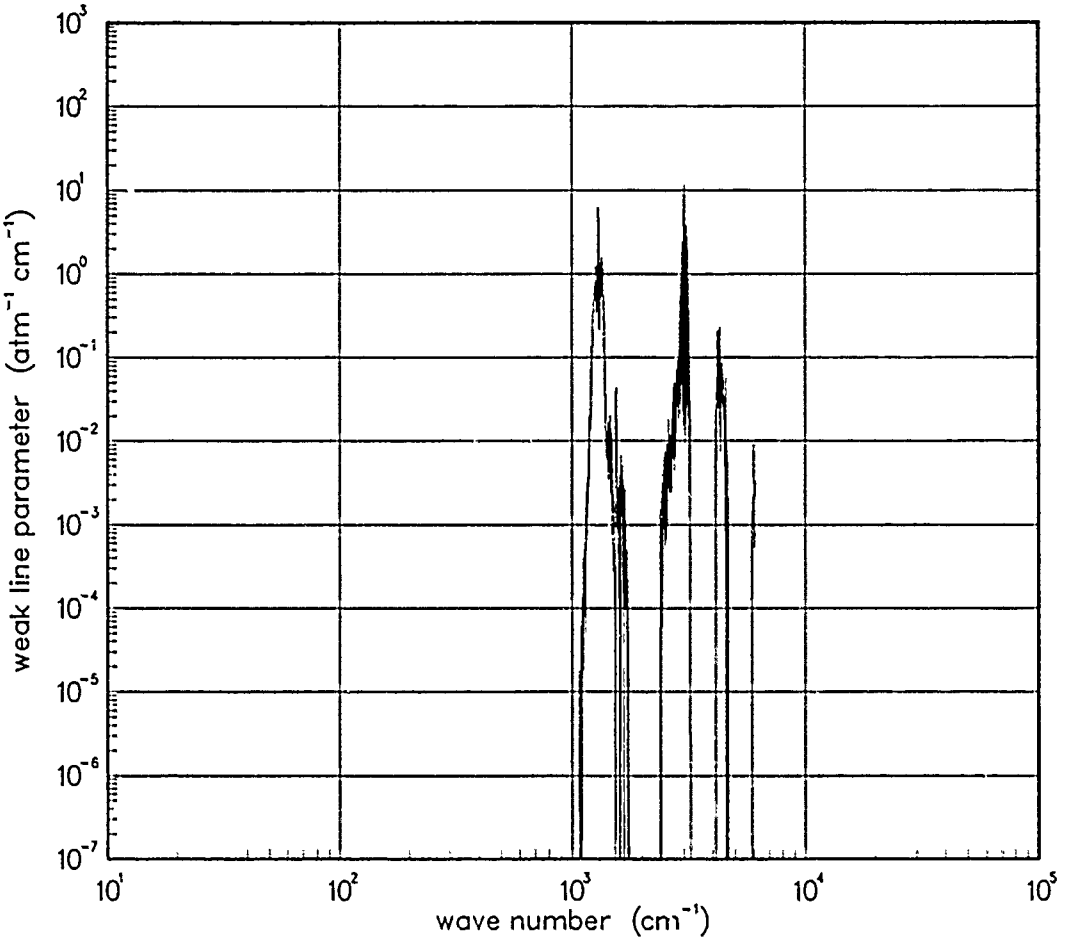

Figure 201. Weak-line parameter for CH_4 at 300°K.

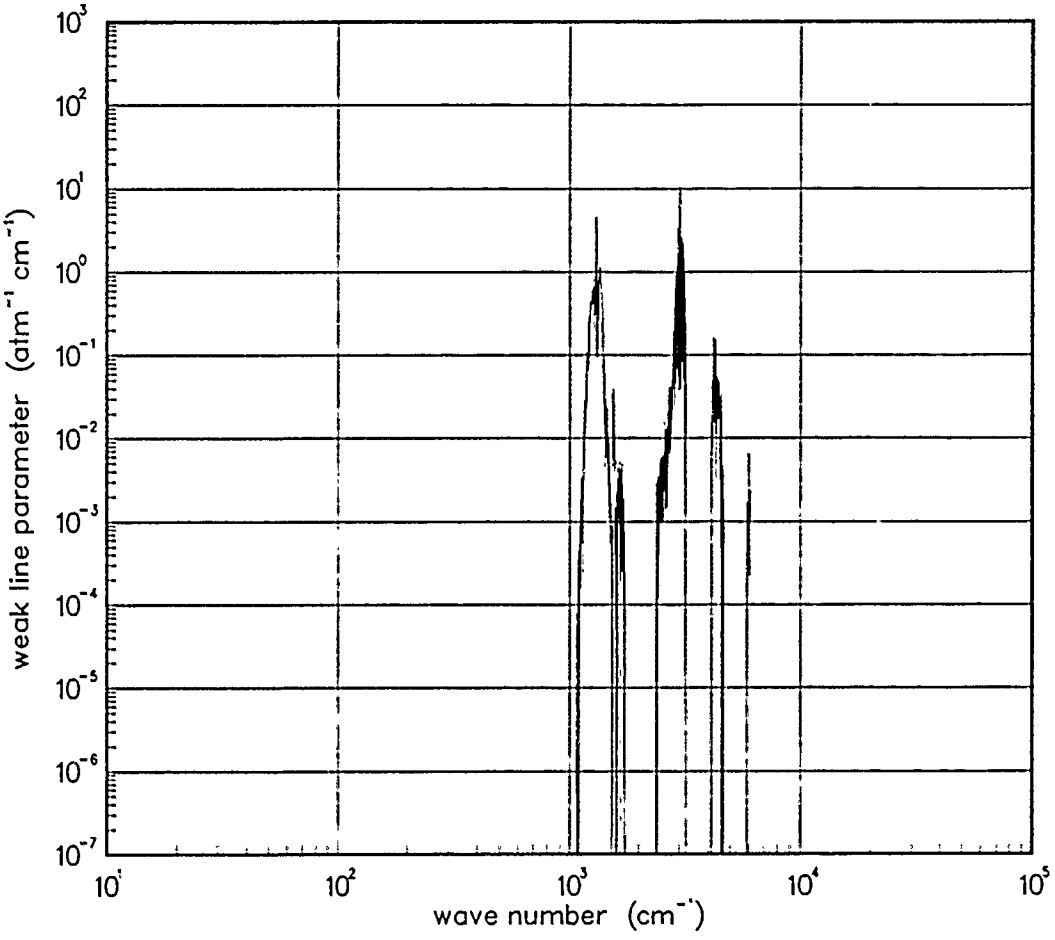

Figure 202. Weak-line parameter for CH_4 at 500°K.

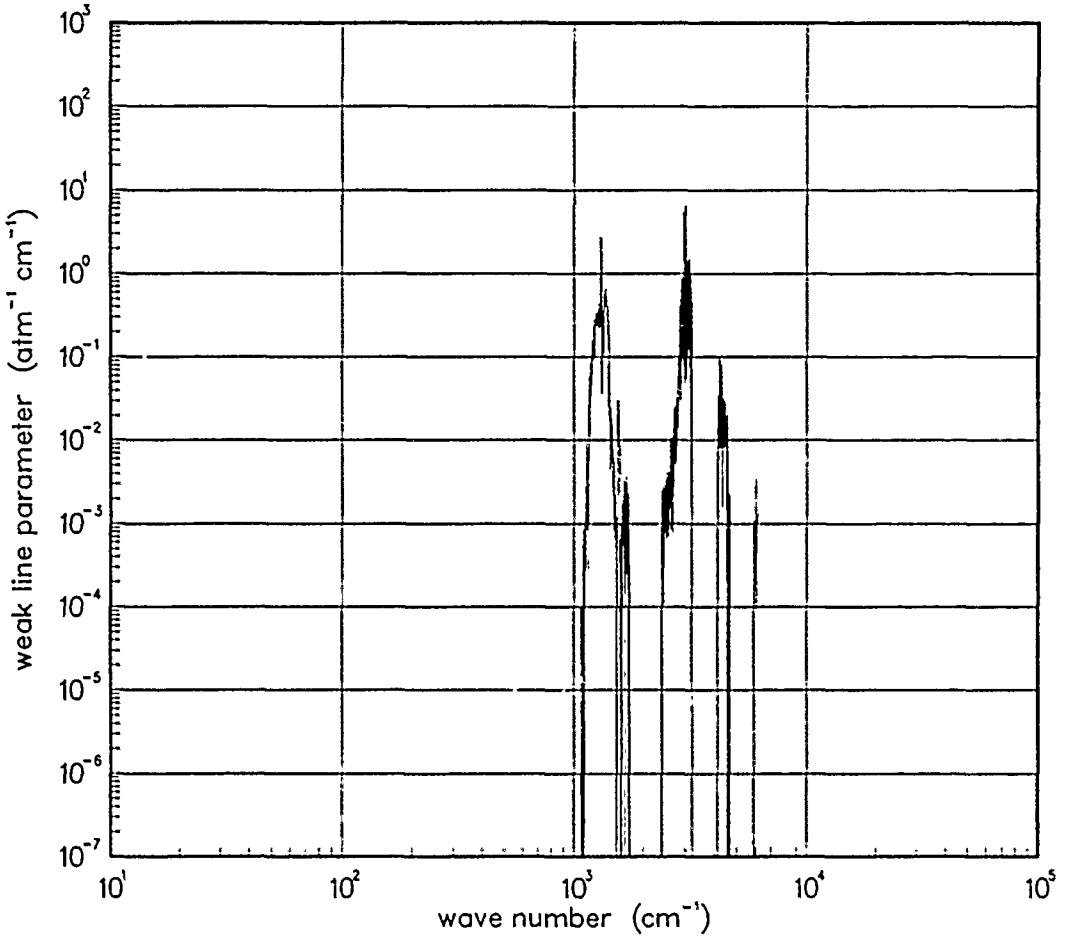

Figure 203. Weak-line parameter for CH_4 at 750°K.

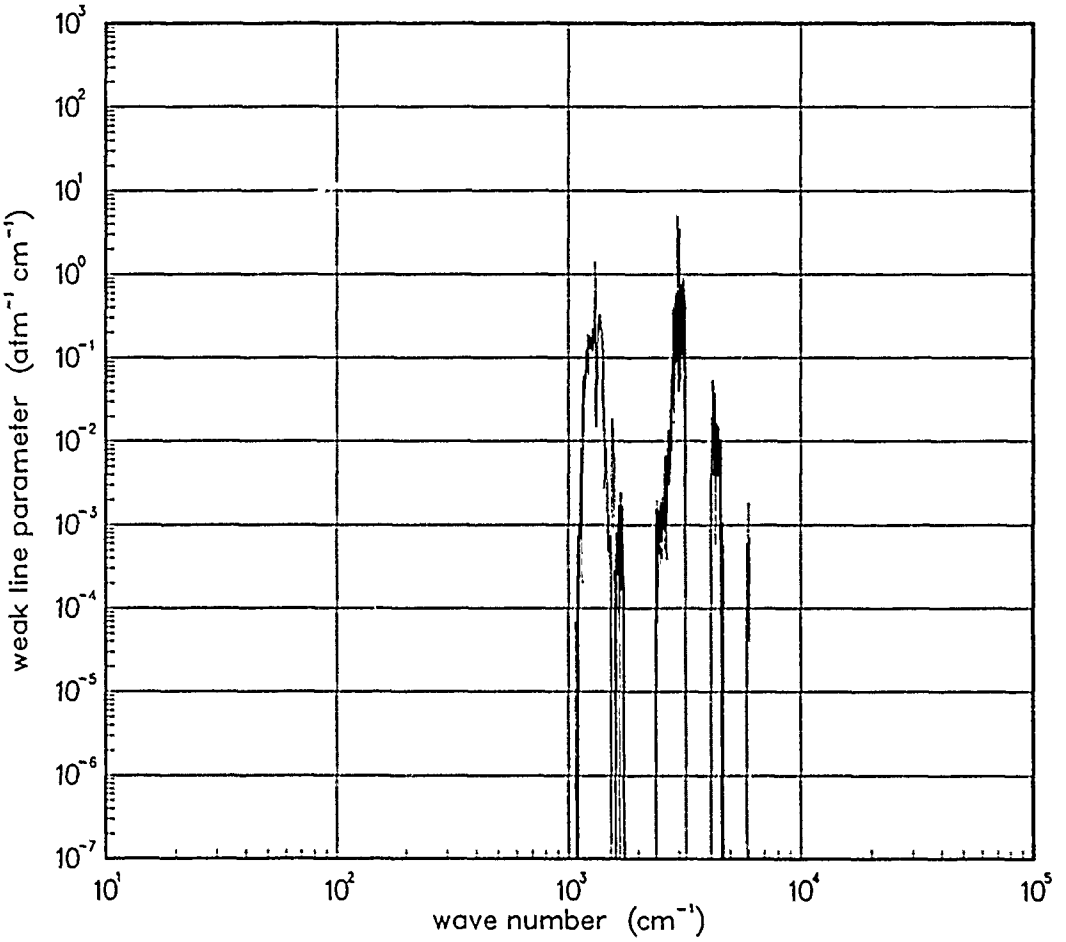

Figure 204. Weak-line parameter for CH_4 at 1000°K.

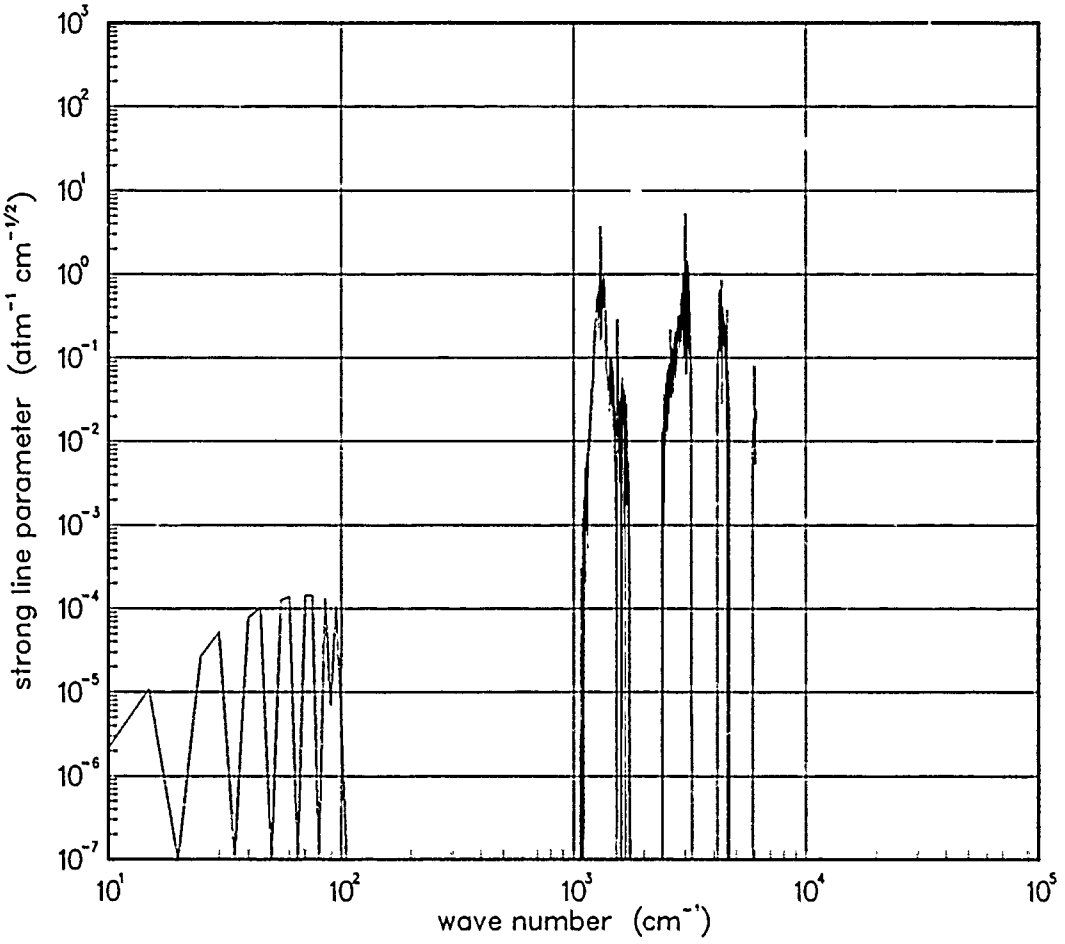

Figure 205. Strong-line parameter for CH_4 at 200°K.

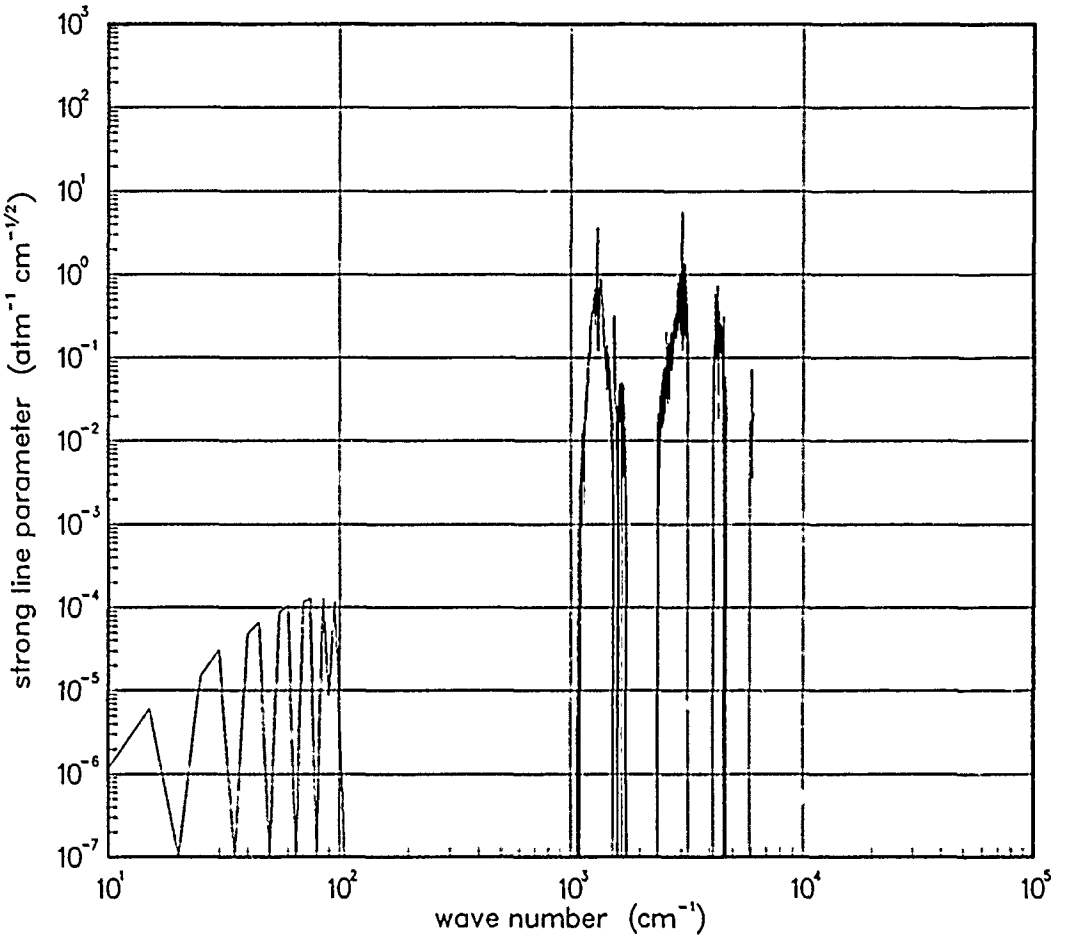

Figure 206. Strong-line parameter for CH_4 at 300°K.

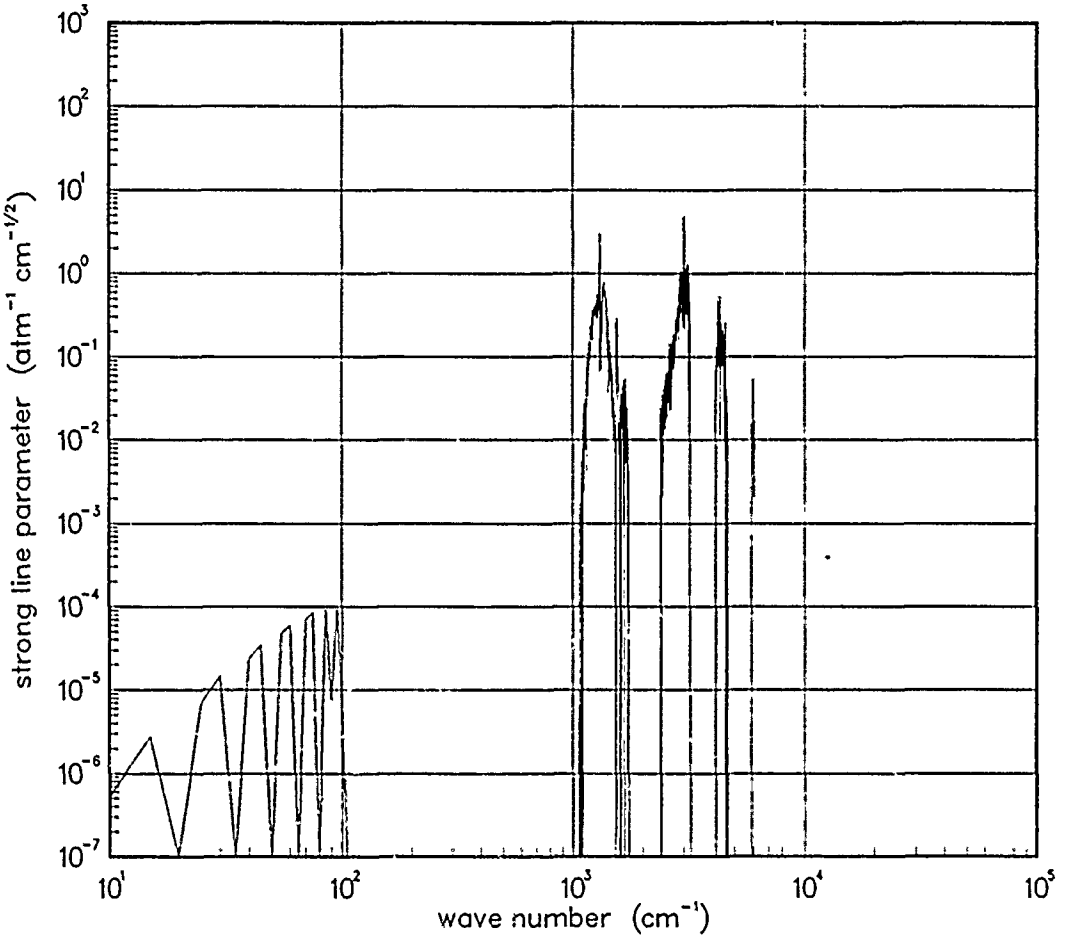

Figure 207. Strong-line parameter for CH_4 at 500°K.

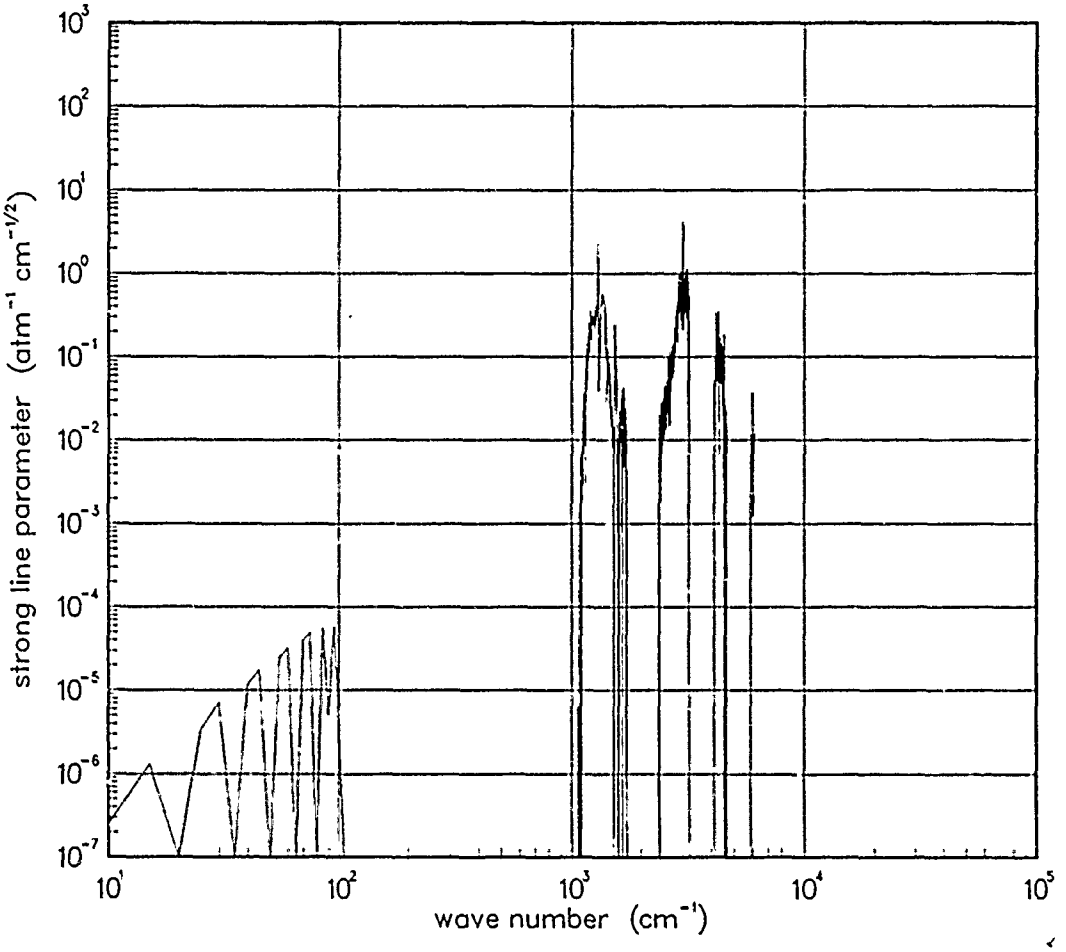

Figure 208. Strong-line parameter for CH_4 at 750°K.

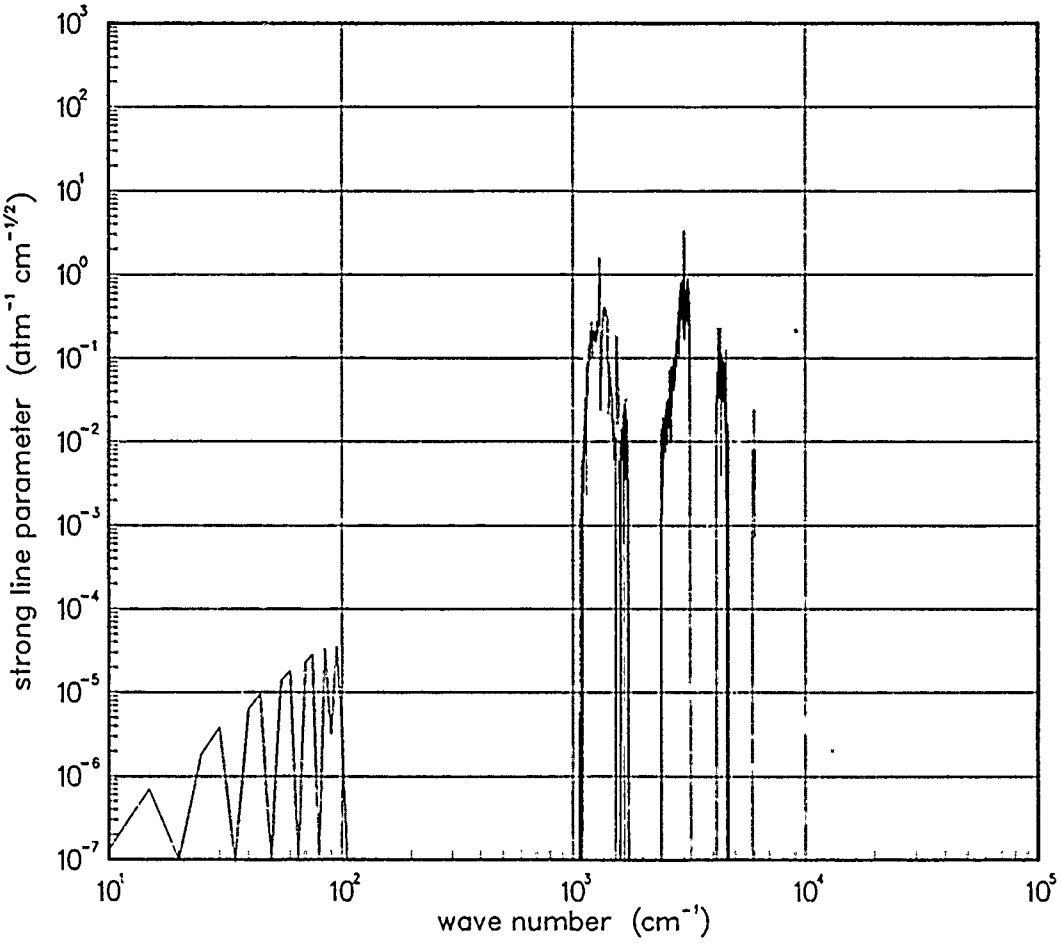

Figure 209. Strong-line parameter for CH_4 at 1000°K.

5.5 NITRIC ACID (HNO_3).

The local thermal equilibrium emission spectra for Nitric Acid has been developed from the 1982 Air Force Geophysical Laboratory Line Atlas for 300 °K.

The HNO_3 molecule has been included within the NORSE LTE data base because of its contribution to ambient atmospheric absorption. The inclusion of accurate parameters for this species at other temperatures is felt to be of low priority.

Figure 210. Weak-line parameter for HNO_3.

Figure 211. Inverse line spacing for HNO_3.

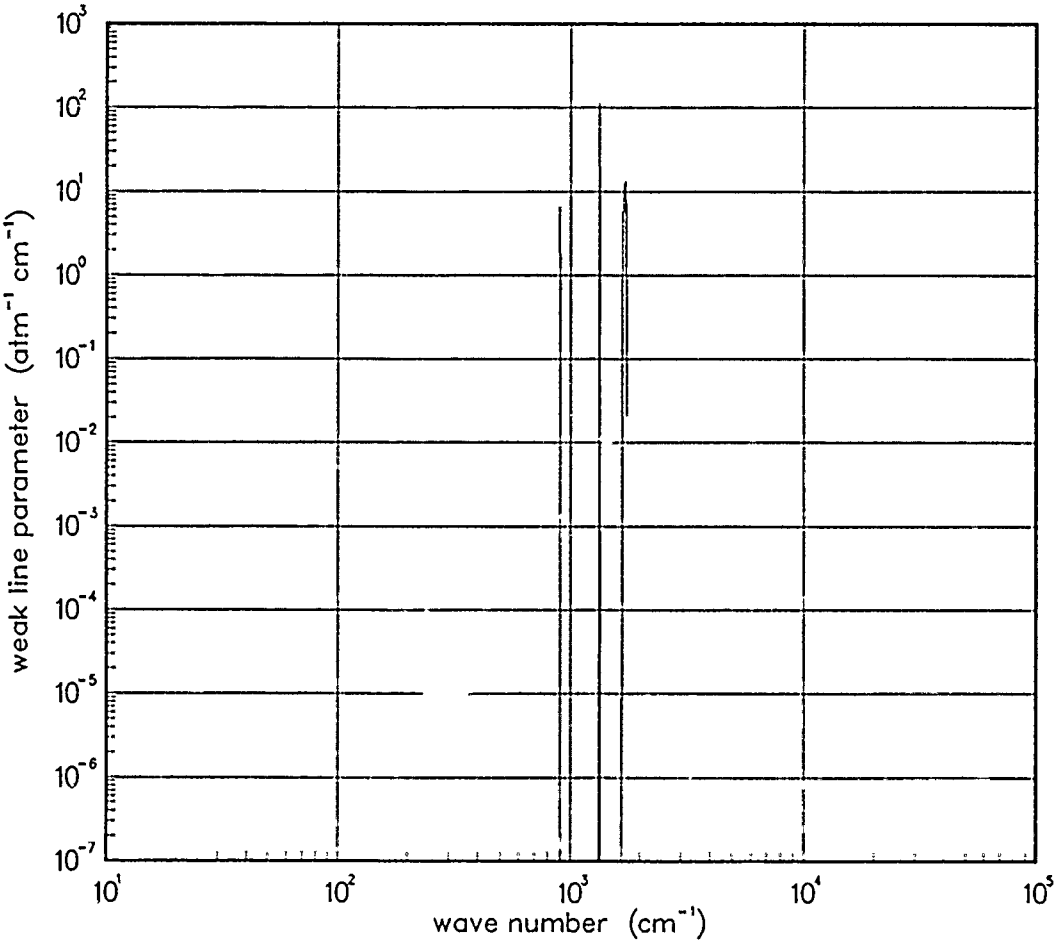

Figure 212. Weak-line parameter for HNO_3 at 300°K.

5.6 NITROGEN PEROXIDE (NO_2).

The local thermal equilibrium emission spectra for Nitrogen Peroxide was taken from the Roscoe IR database for the spectral region < 5,000 cm^{-1}. In the spectral region of 5,000 to 100,000 cm^{-1} the data was developed by the VisiDyne Corporation[‖] using a Air Force Weapons Laboratory database developed in the late sixties.

The calculation of the LTE NO_2 curves is discussed in ROSCOE Manual Volume 28[*]. The calculations (< 5,000 cm^{-1}) were performed with the TATE Code[†].

Table 5. Spectroscopic data for NO_2.

Ground Electronic State

ω_1 = 1326.8	ω_2 = 751.3[§]	ω_3 = 1632.8
χ_{11} = -7.9	χ_{22} = -1.6[§]	χ_{33} = -16.0
χ_{12} = -8.6[§]	χ_{13} = -29.5	χ_{23} = -11.3[§]

A_e = 8.0012 B_e = 0.43364 C_e = 0.41040

γ_ℓ(300 °K) = 0.10[‡]

Data Source:

[*]J.G. DeVore, and T.L. Stephens, Band Model Parameters for Thermal Emission (U) ,.72TMP-20, General Electric - TEMPO, (June 1972) (Secret).

[†]T.L. Stephens, V.R. Stull, A.L. Klein, and J.D. Losse, The ROSCOE Manual, Volume 28-Molecular Band Models for Thermal and Optically Pumped emissions (U) , GE78TMP-52, General Electric -- TEMPO (June 1978) (Confidential).

[‡]Estimate.

[§]Inferred (See The ROSCOE Manual Volume 28, GE78TMP-52).

[‖]H. Smith, T. Keneshea, VisiDyne Corporation, private communication (1986).

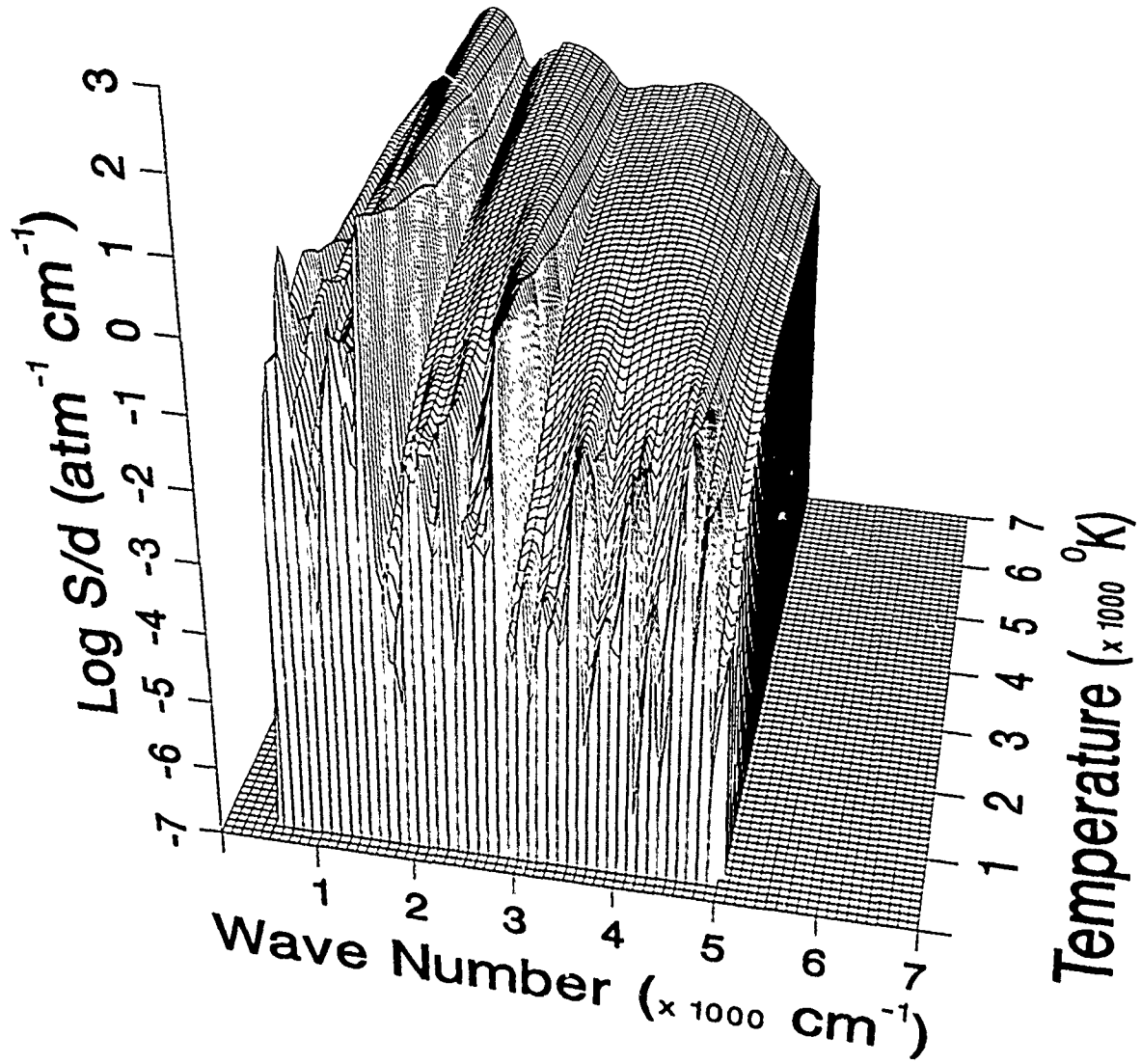

Figure 213. Weak-line parameter for NO_2.

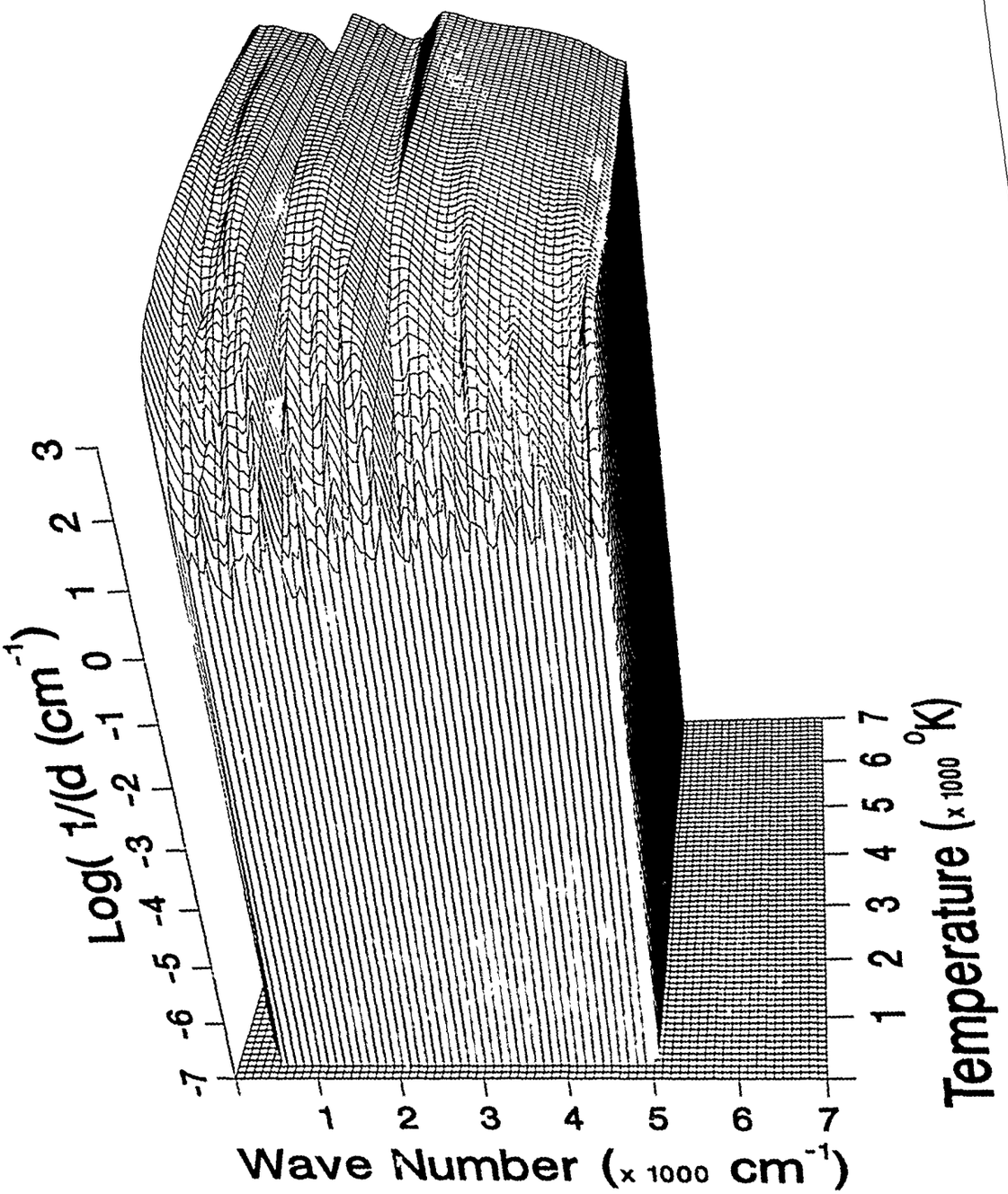

Figure 214. Inverse line spacing for NO_2.

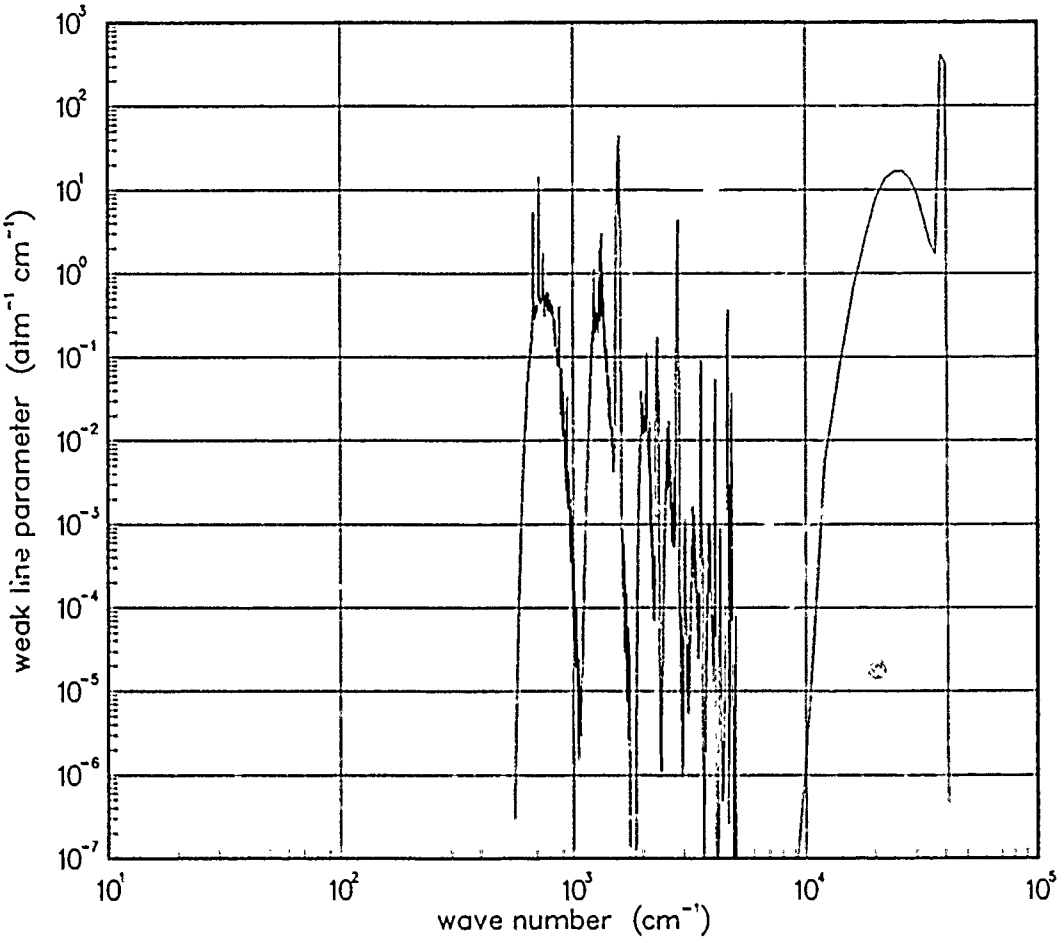

Figure 215. Weak-line parameter for NO_2 at 200°K.

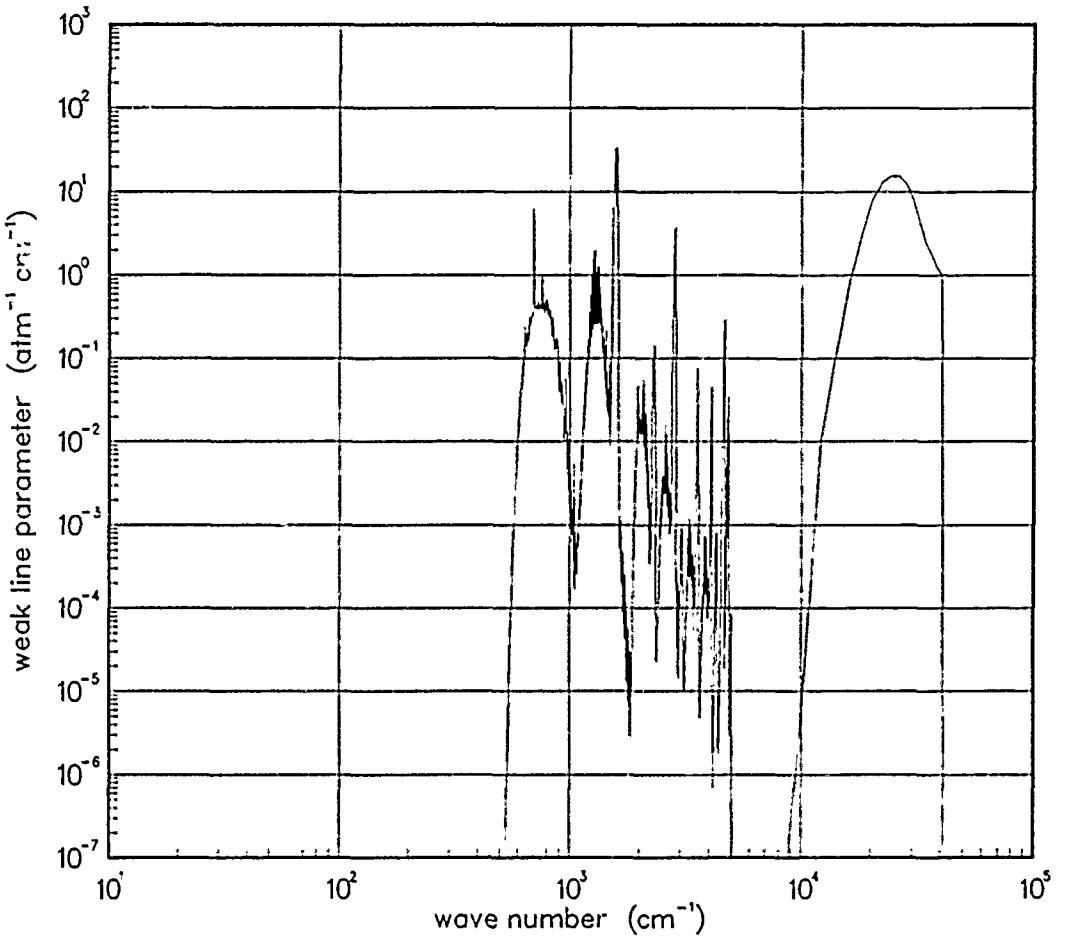

Figure 216. Weak-line parameter for NO_2 at 300°K.

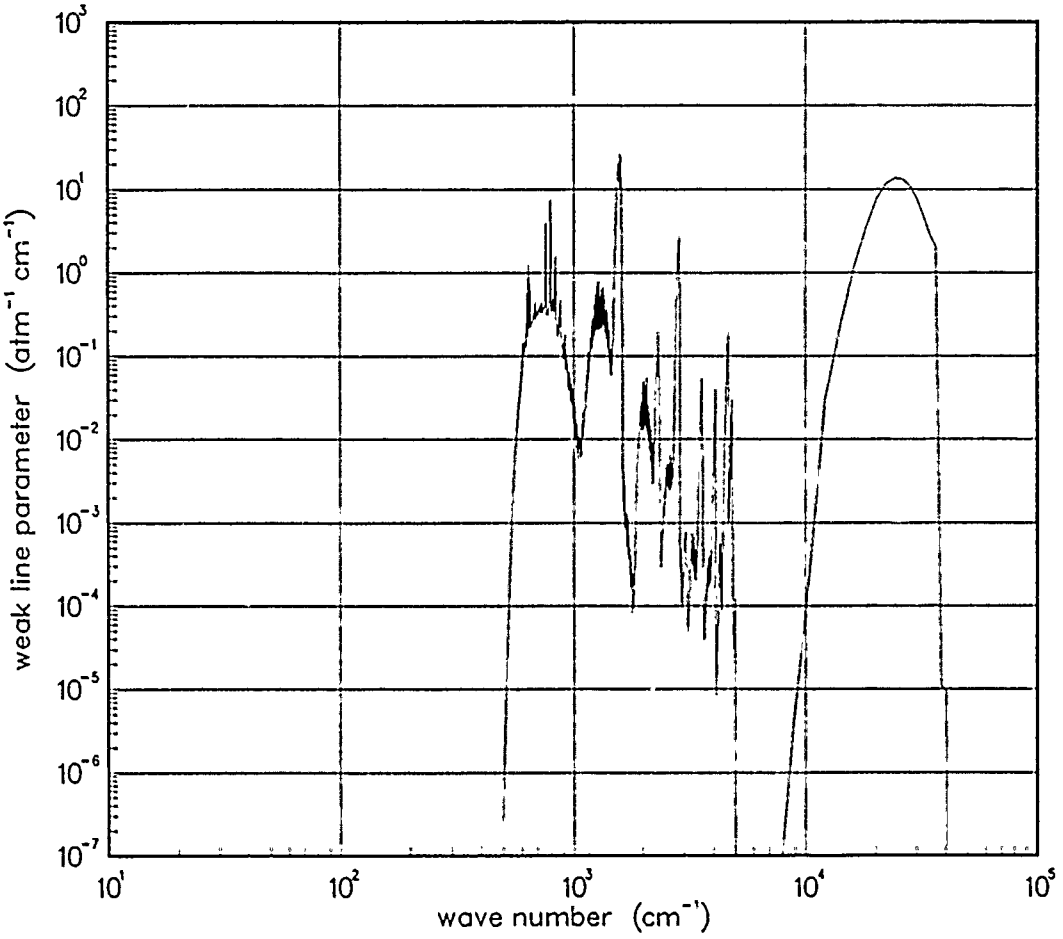

Figure 217. Weak-line parameter for NO_2 at 500°K.

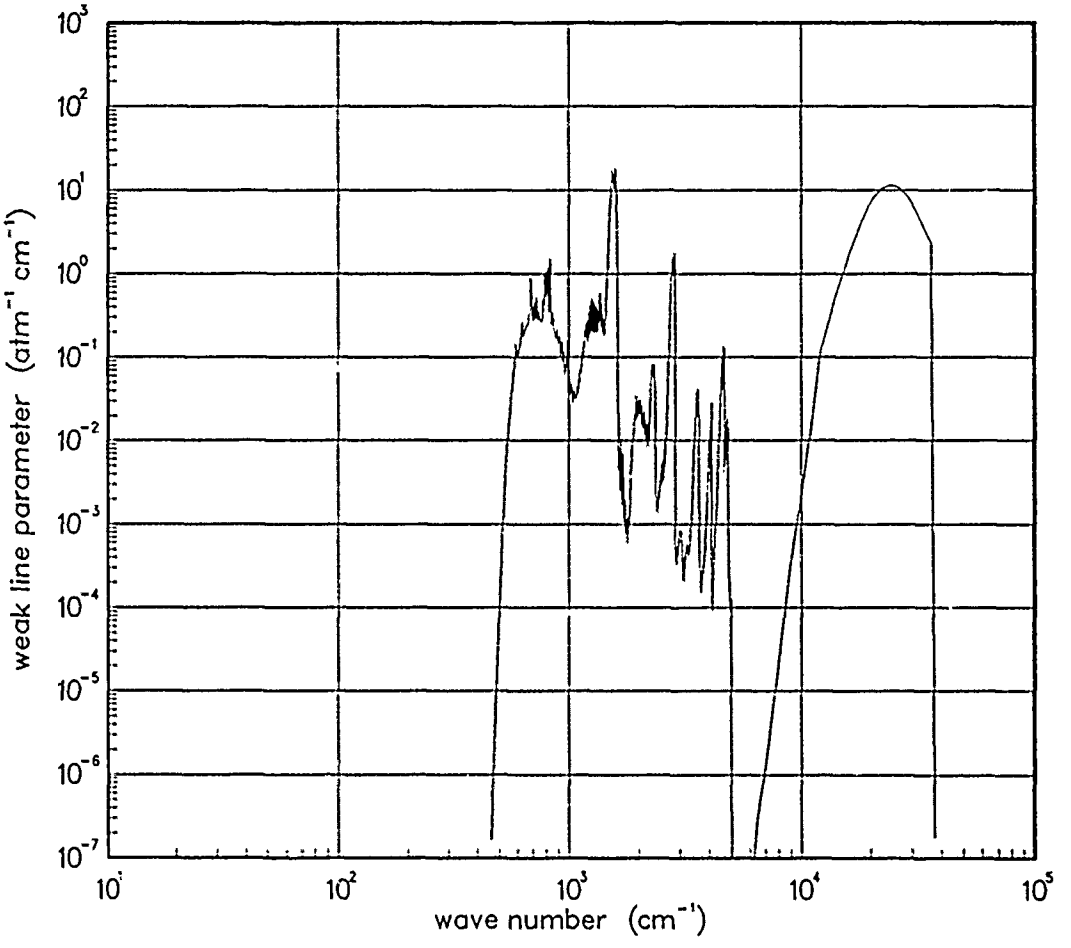

Figure 218. Weak-line parameter for NO_2 at 750°K.

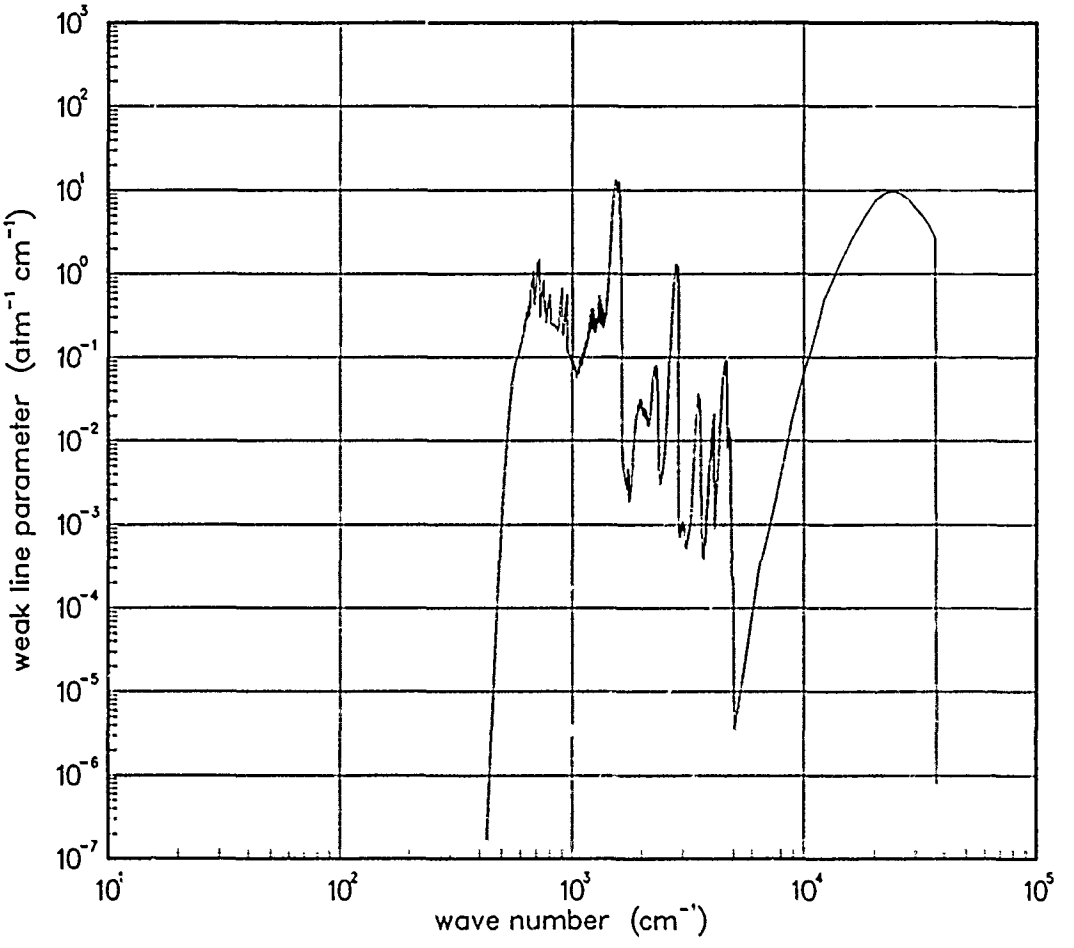

Figure 219. Weak-line parameter for NO_2 at 10° 0°K.

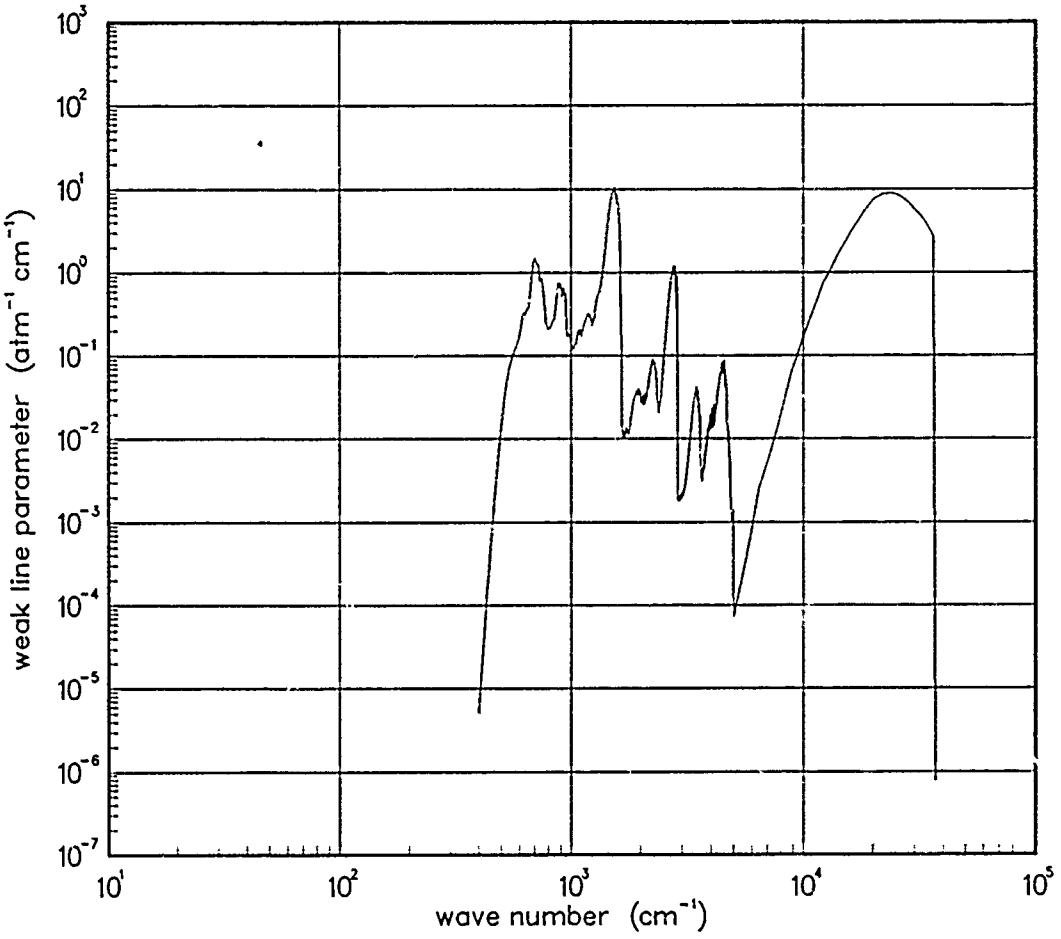

Figure 220. Weak-line parameter for NO_2 at 1500°K.

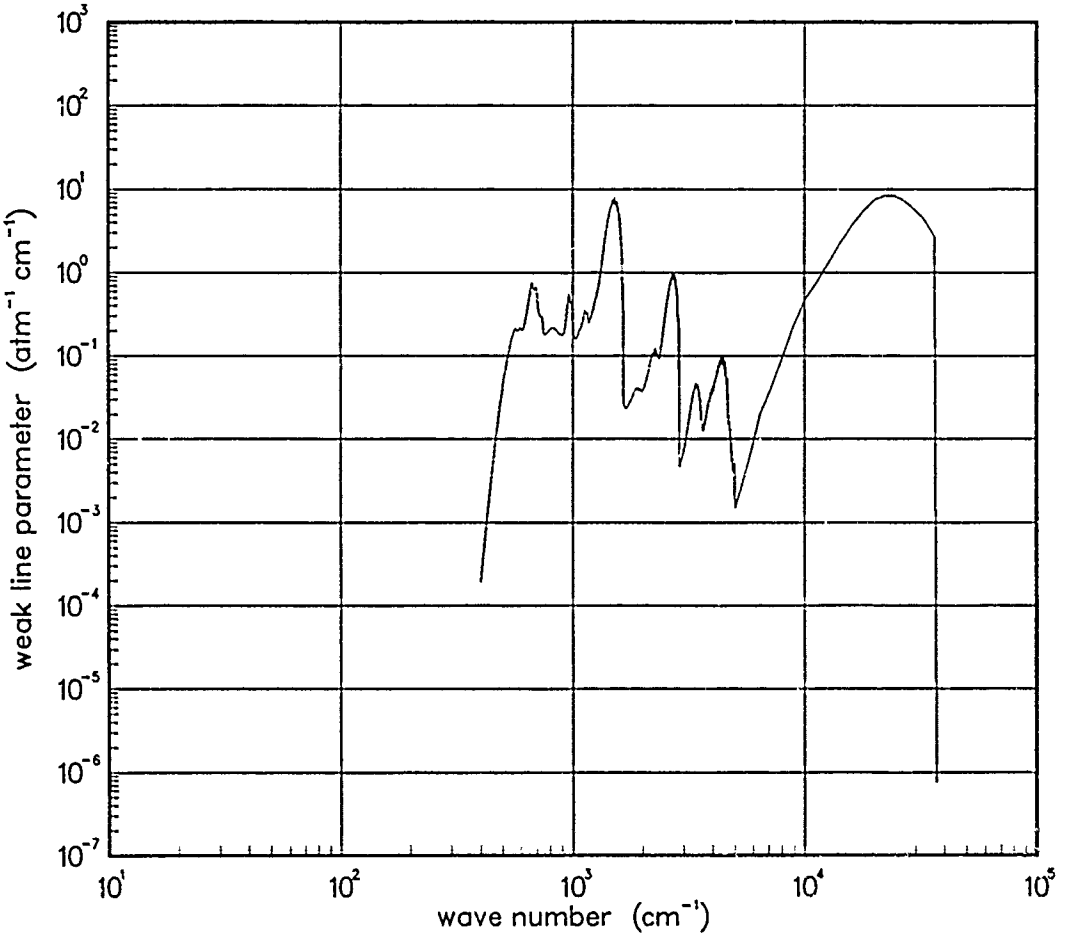

Figure 221. Weak-line parameter for NO_2 at 2000°K.

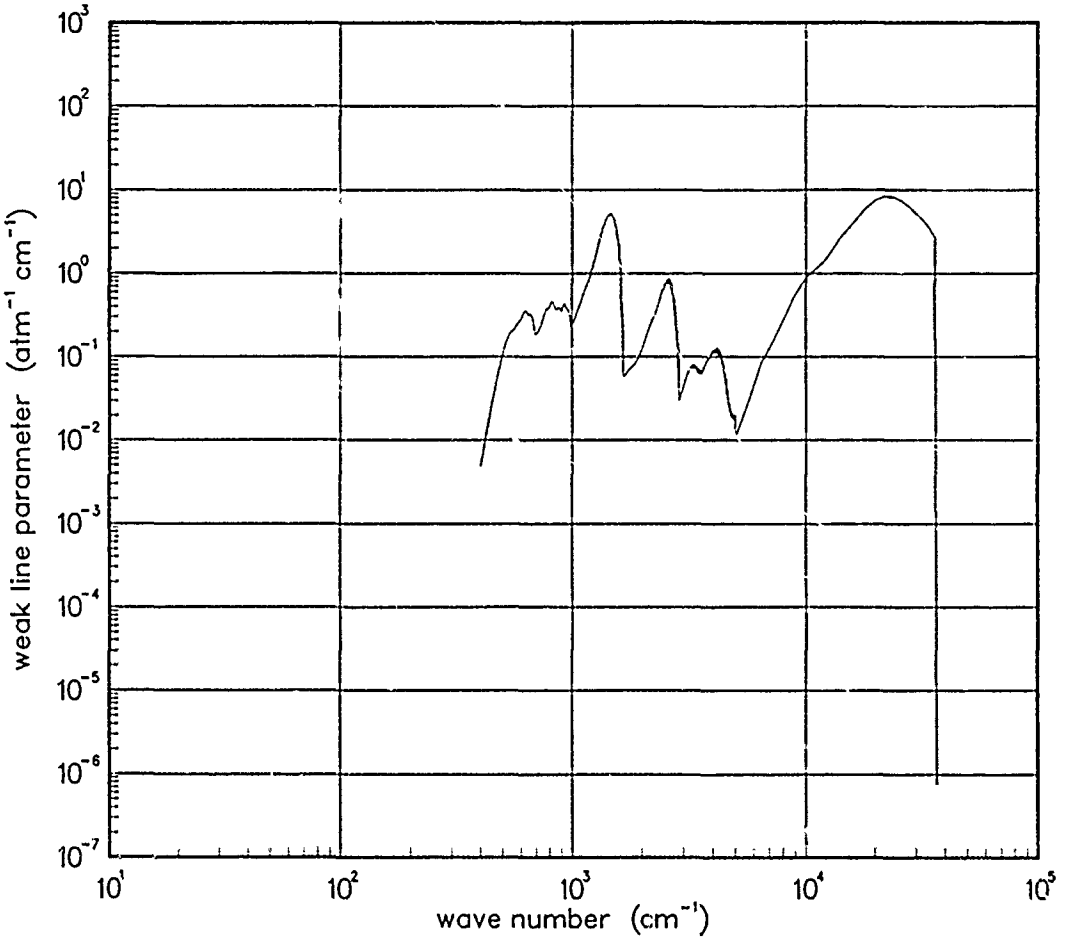

Figure 222. Weak-line parameter for NO_2 at 3000°K.

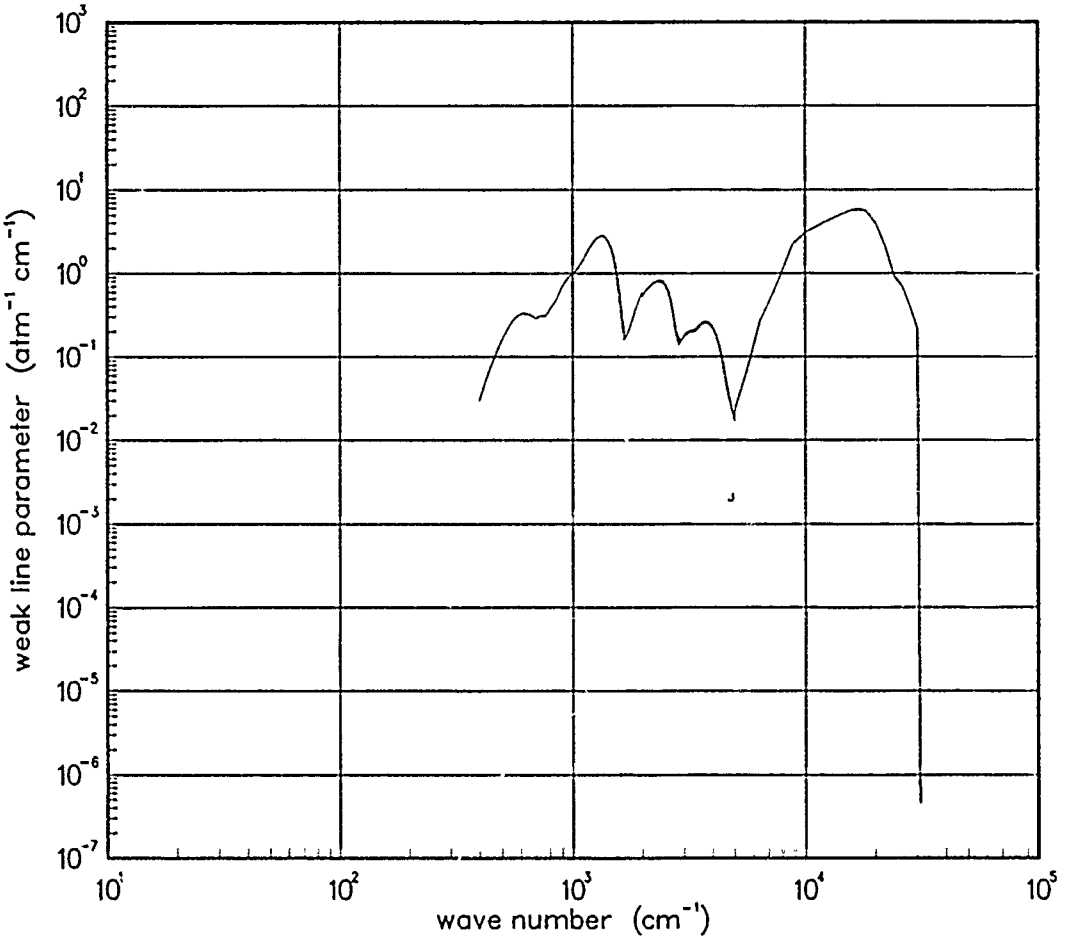

Figure 223. Weak-line parameter for NO_2 at 5000°K.

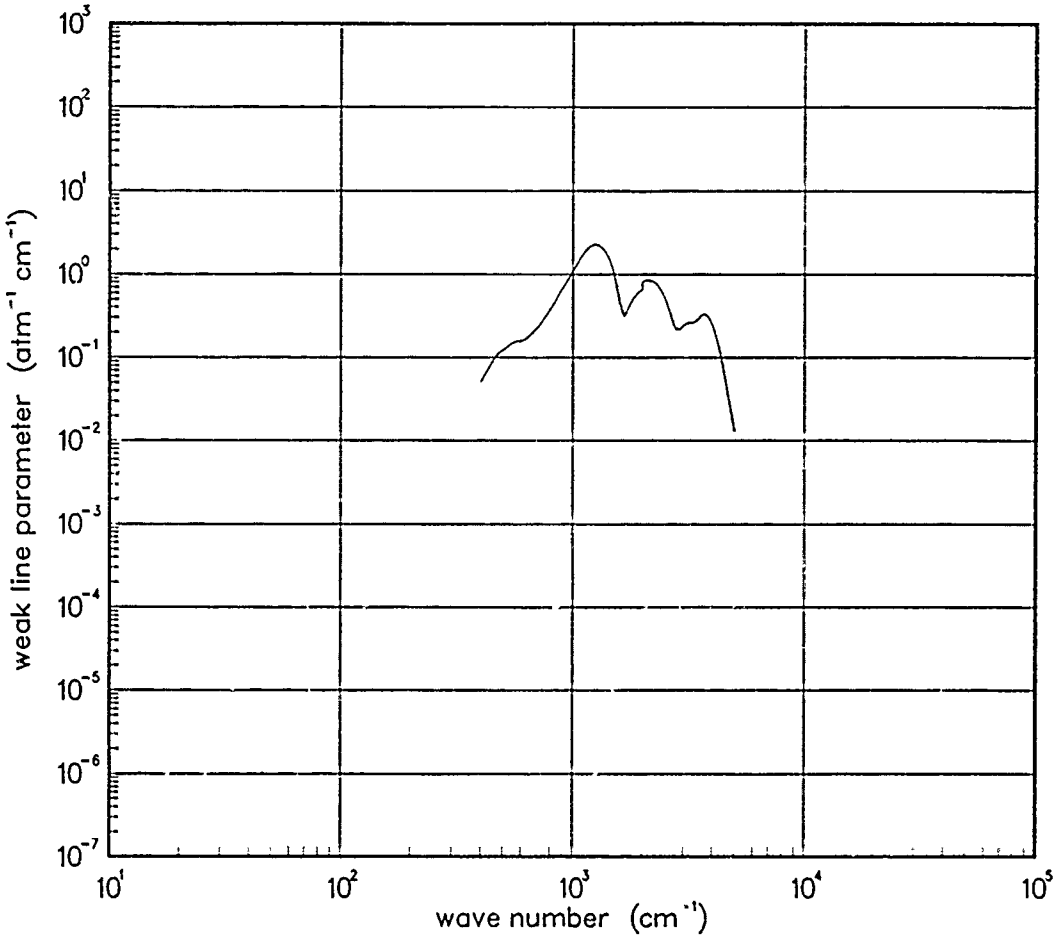

Figure 224. Weak-line parameter for NO_2 at 7000°K.

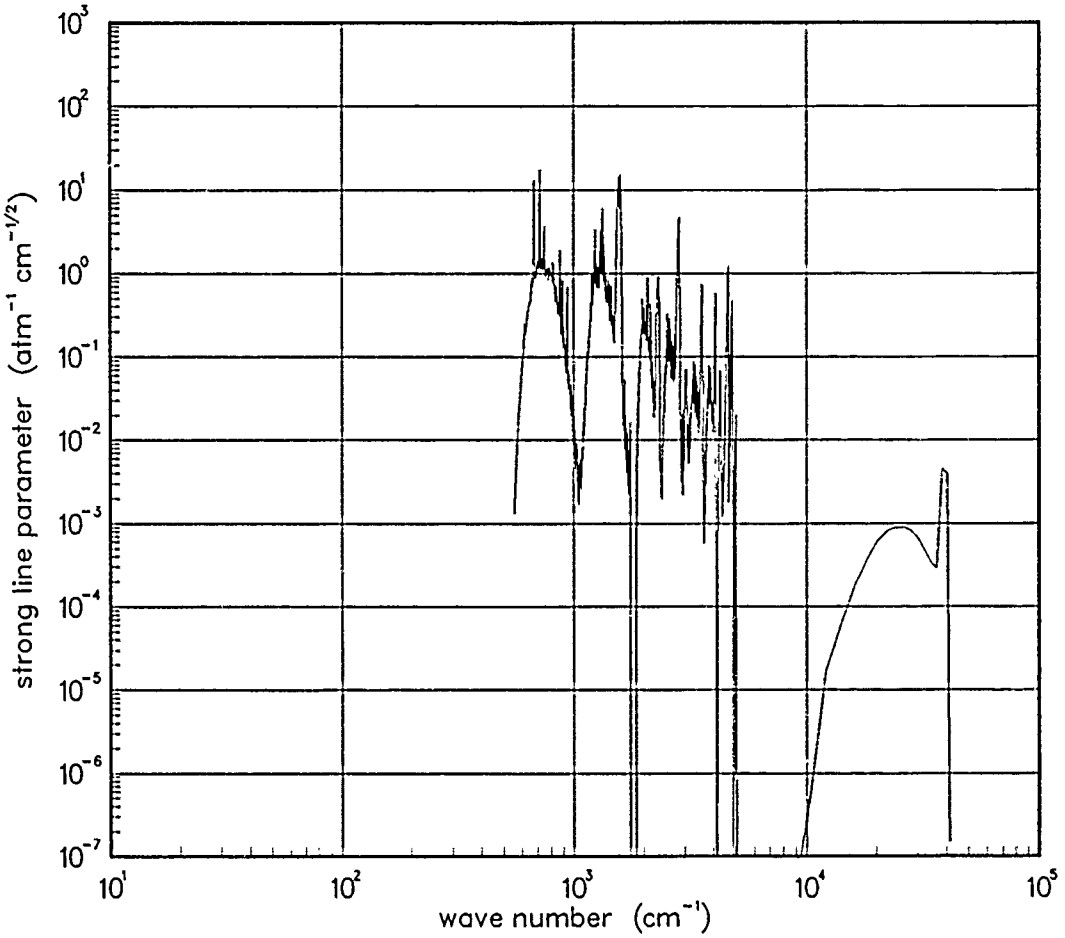

Figure 225. Strong-line parameter for NO_2 at 200°K.

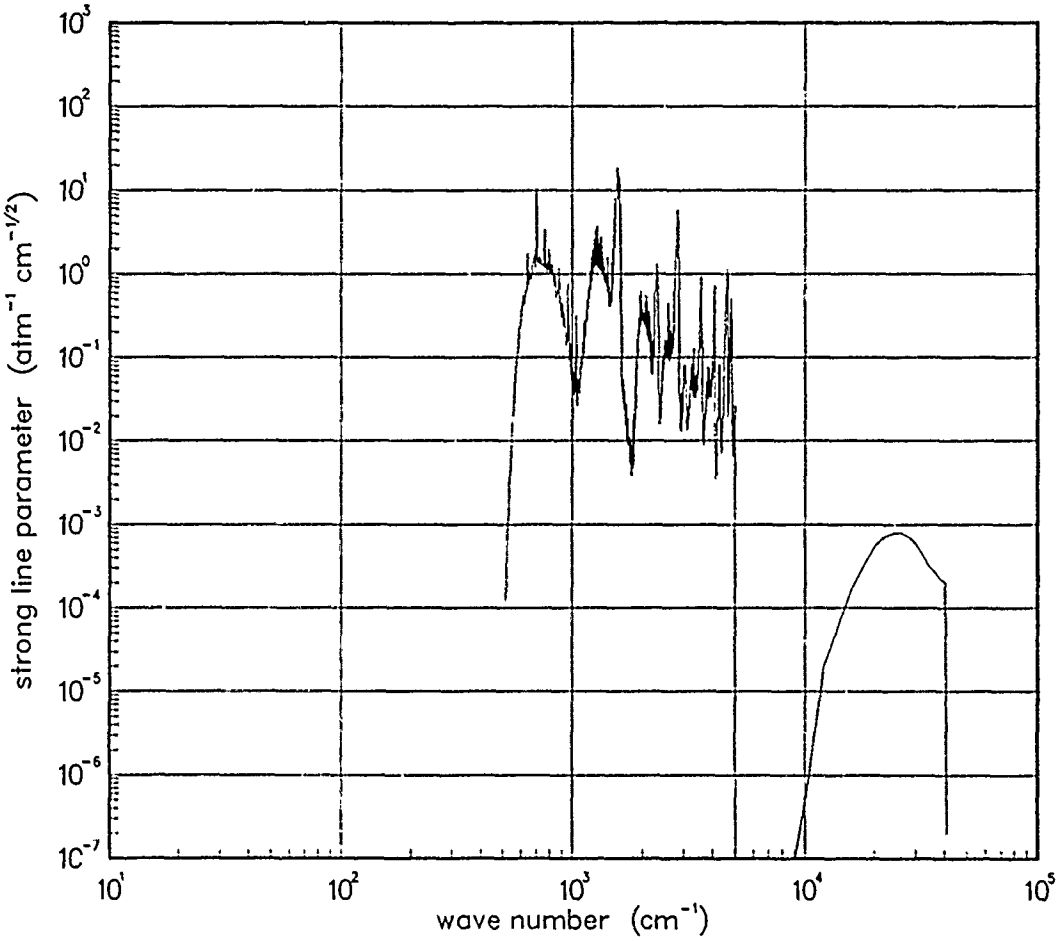

Figure 226. Strong-line parameter for NO_2 at 300°K.

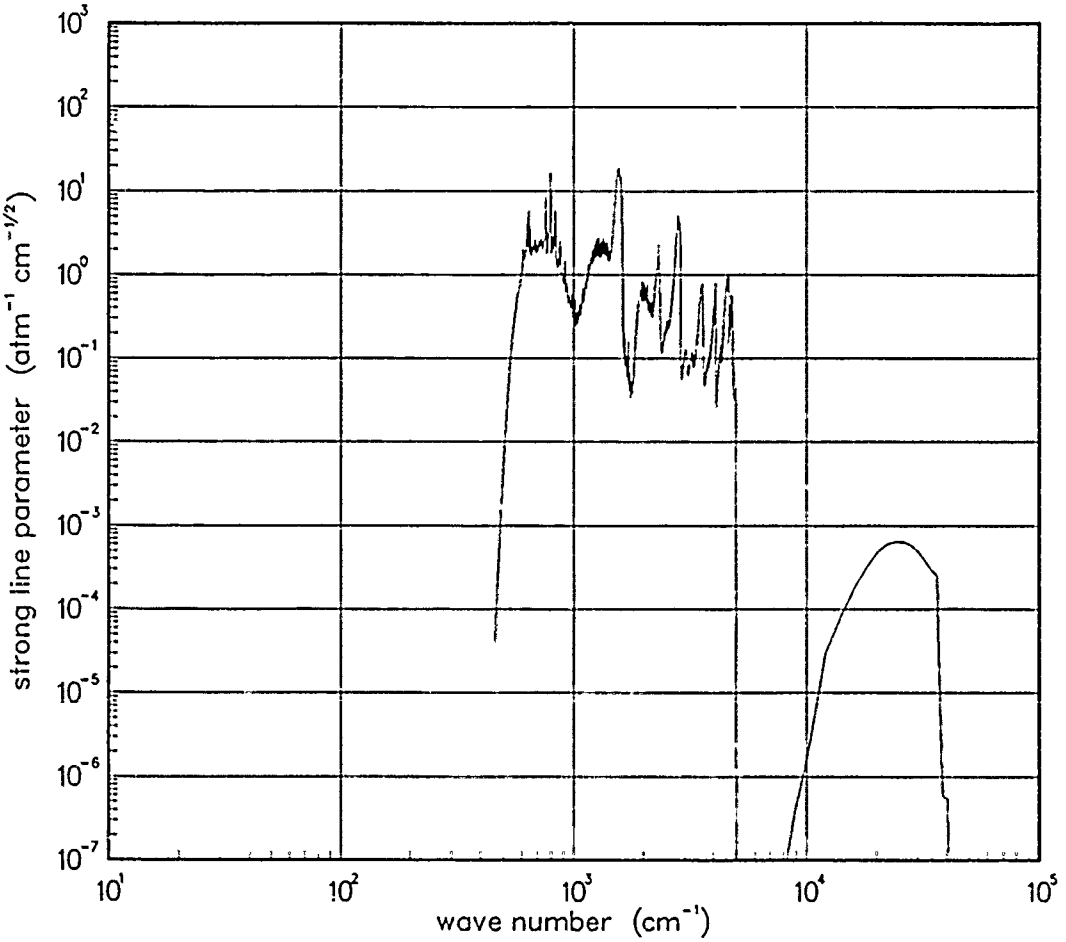

Figure 227. Strong-line parameter for NO_2 at 500°K.

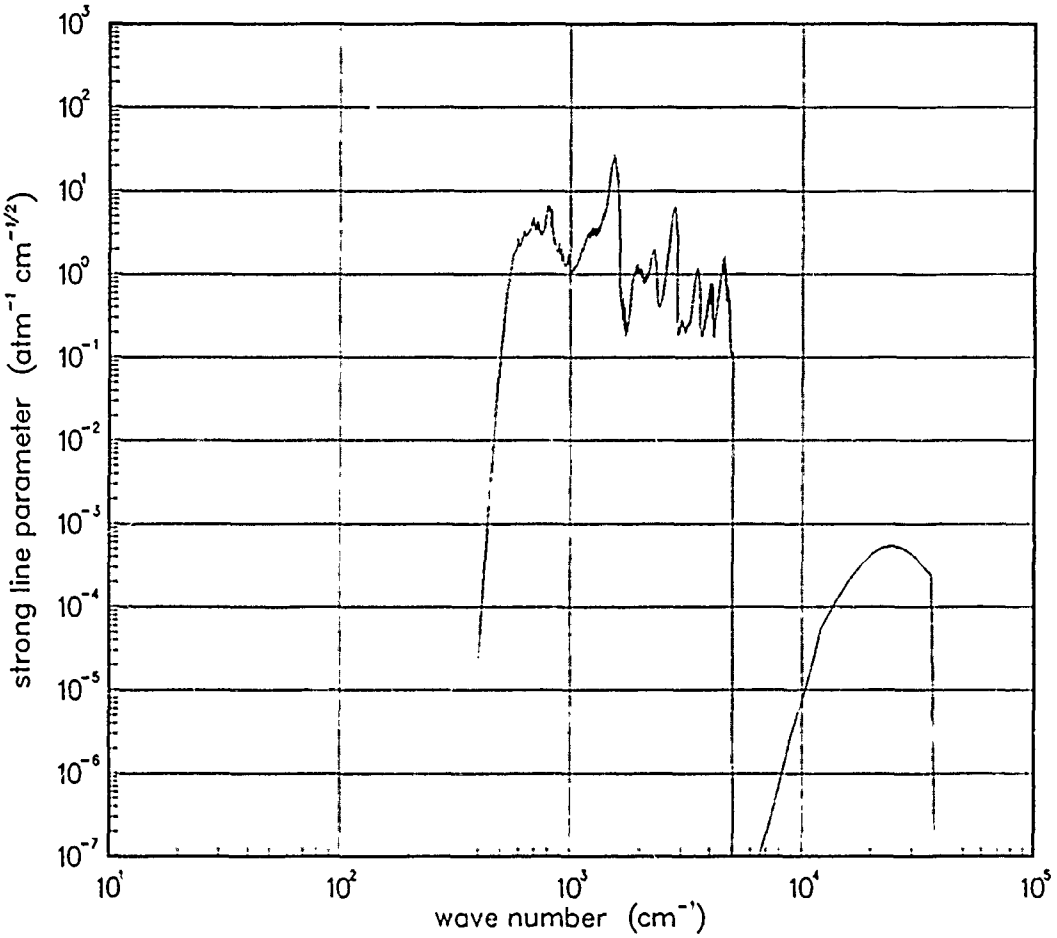

Figure 228. Strong-line parameter for NO_2 at 750°K.

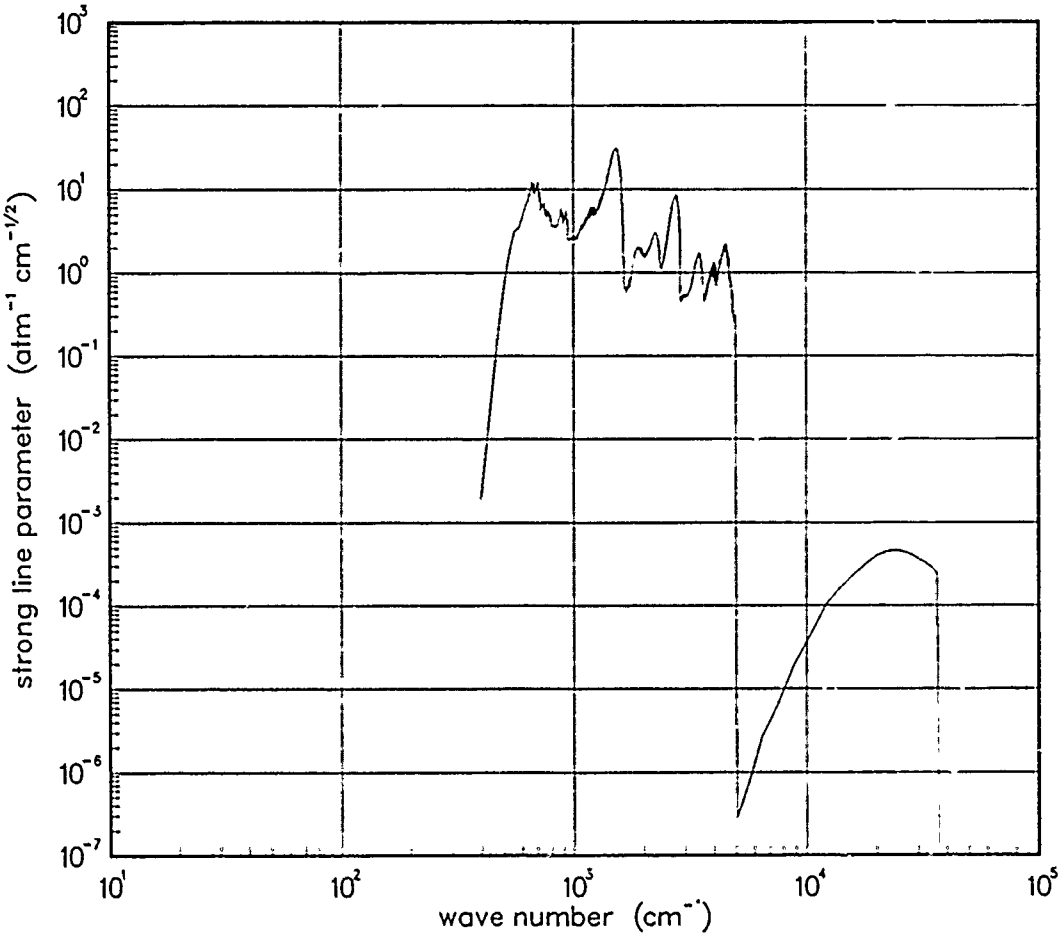

Figure 229. Strong-line parameter for NO_2 at 1000°K.

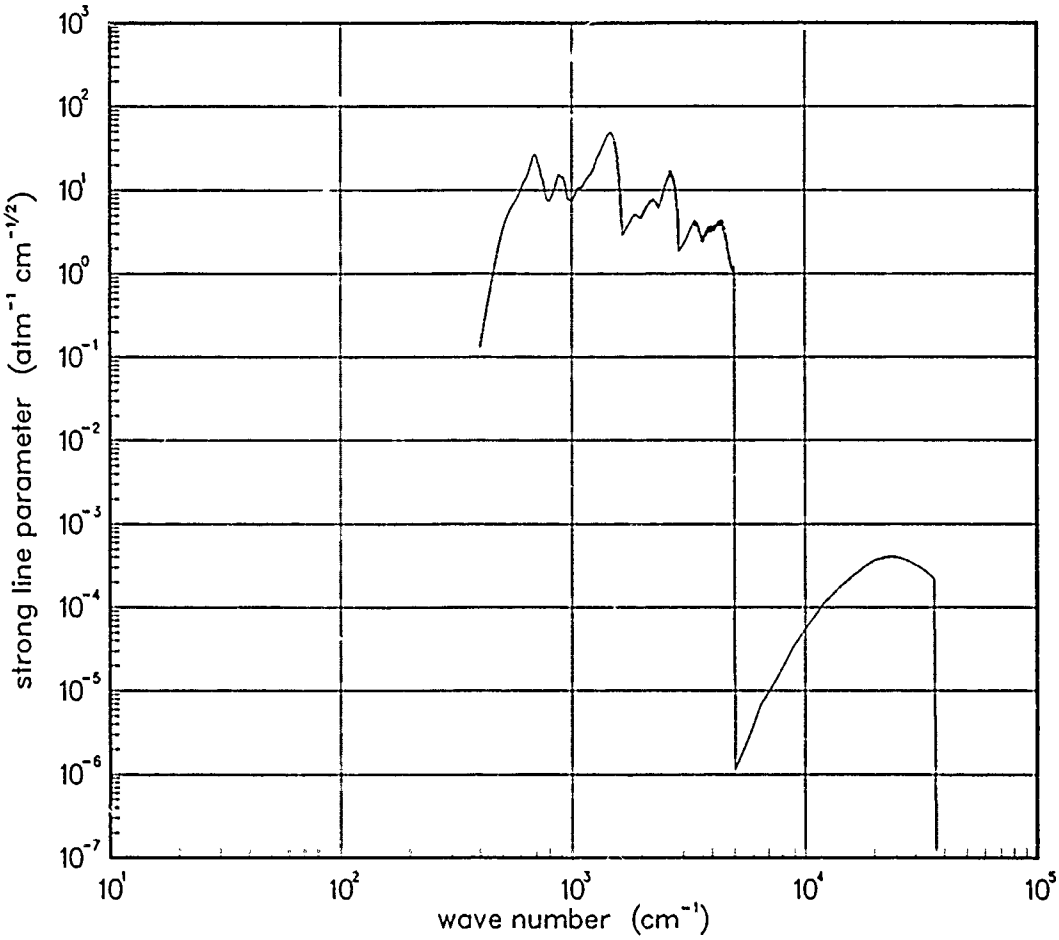

Figure 230. Strong-line parameter for NO_2 at 1500°K.

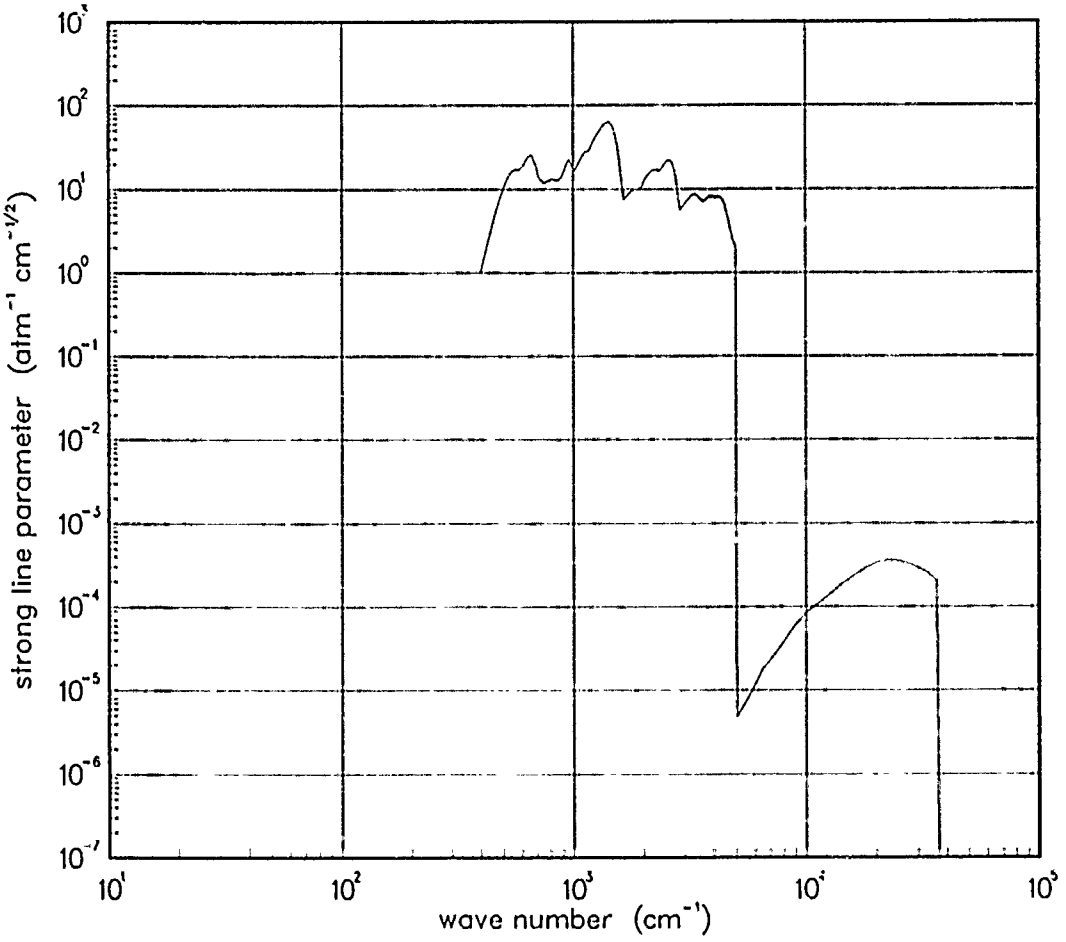

Figure 231. Strong-line parameter for NO_2 at 2000°K.

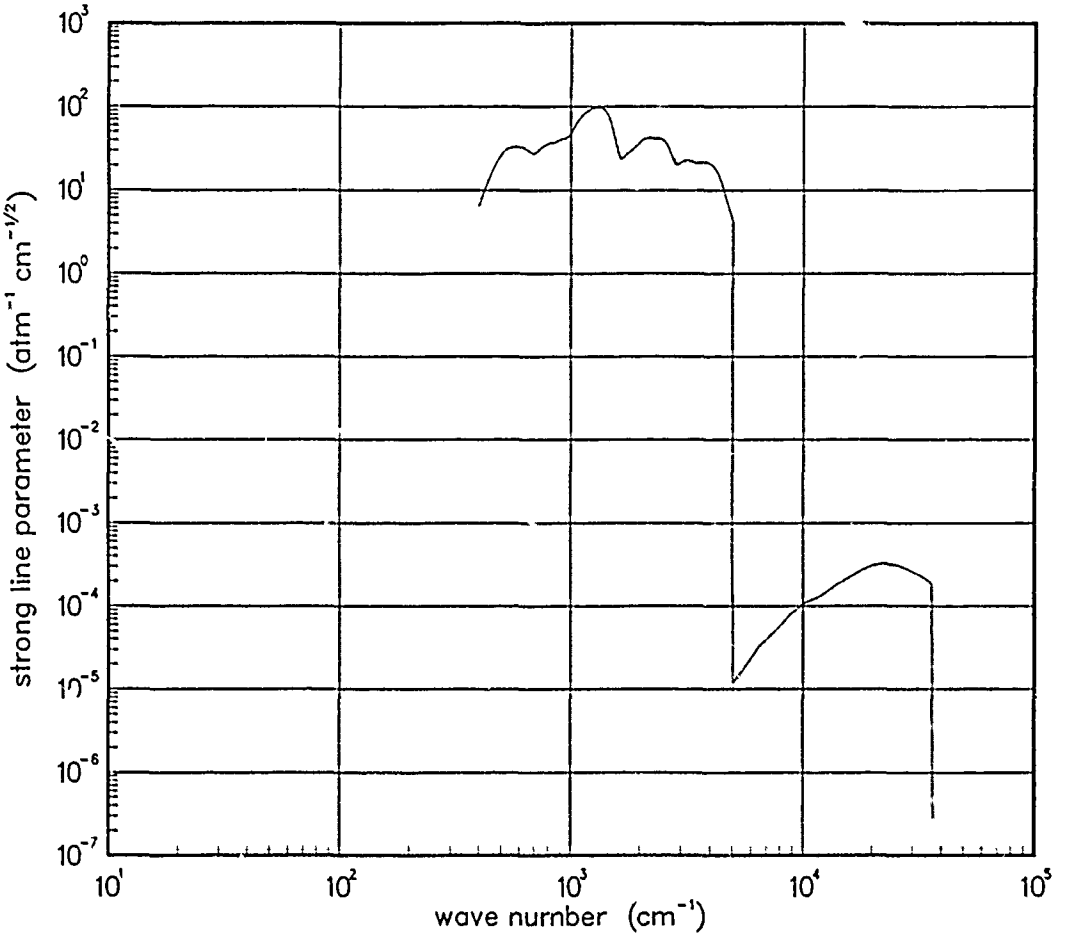

Figure 232. Strong-line parameter for NO_2 at 3000°K.

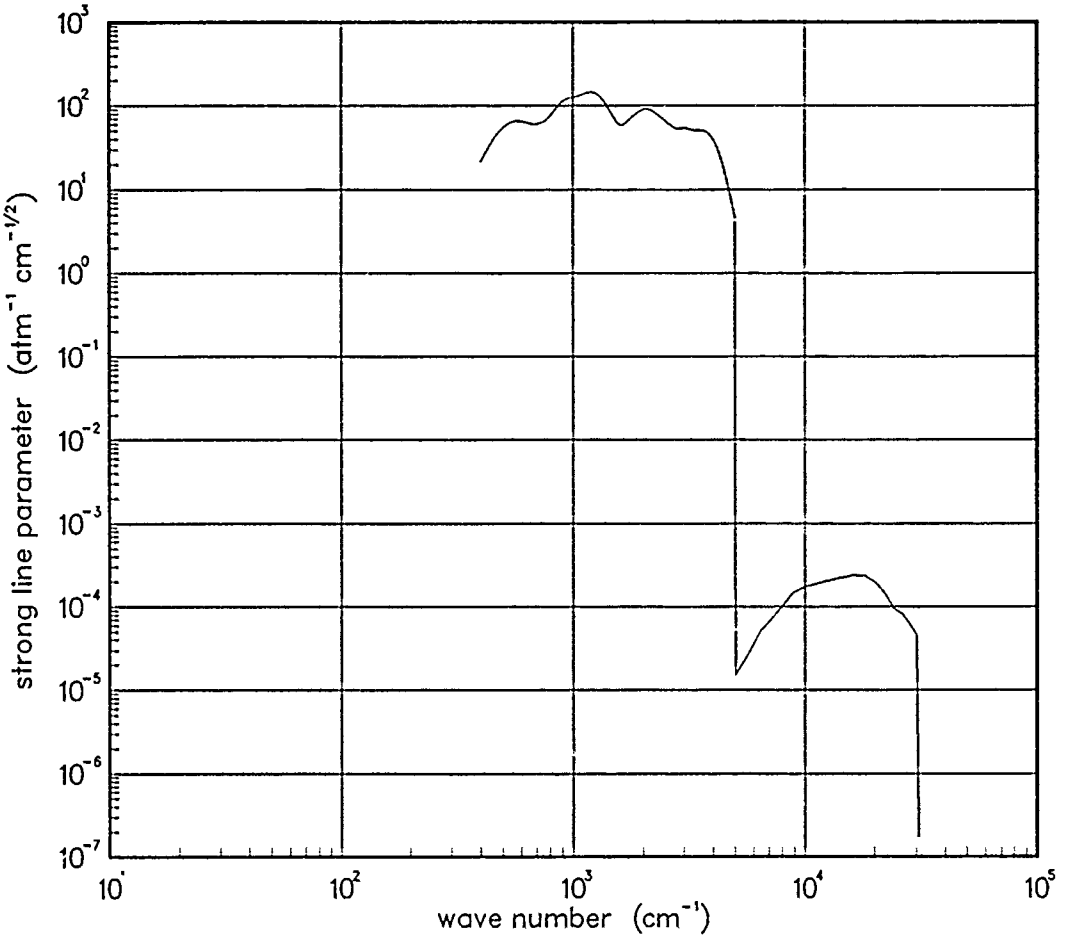

Figure 233. Strong-line parameter for NO_2 at 5000°K.

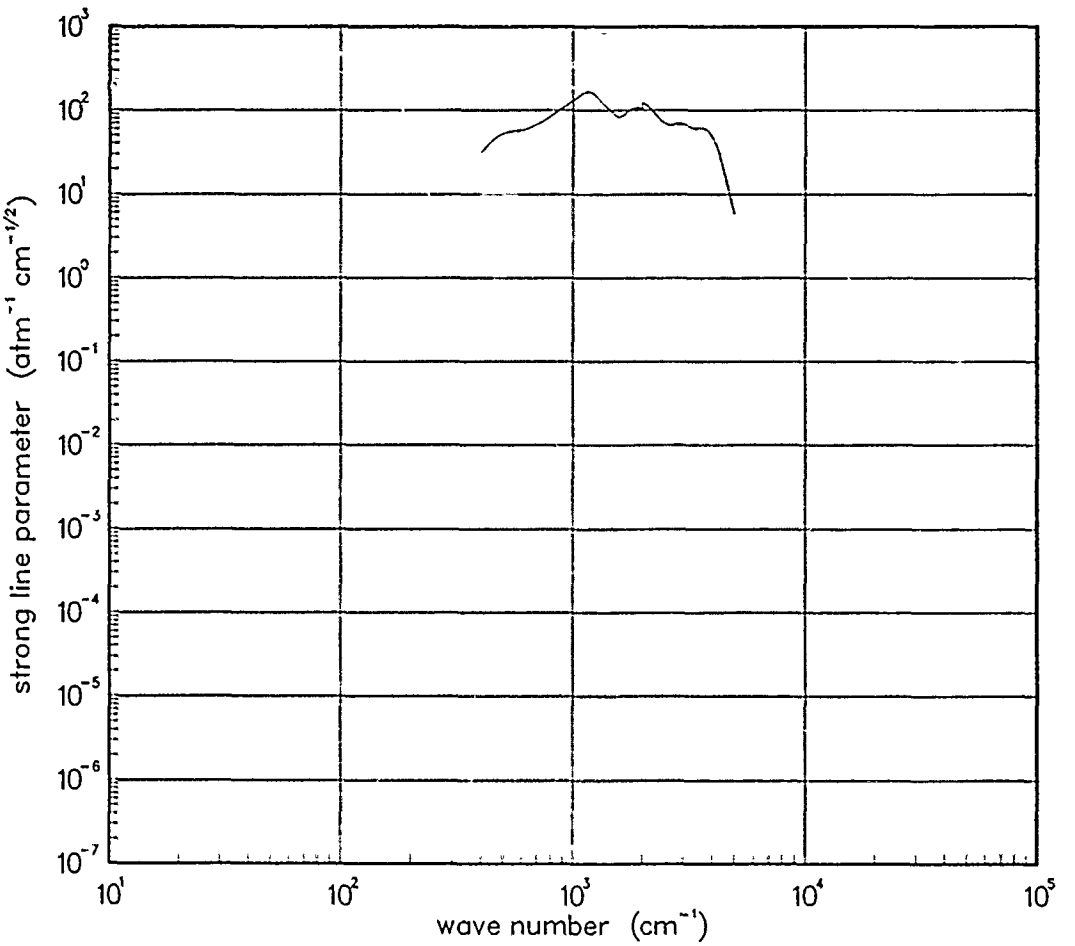

Figure 234. Strong-line parameter for NO_2 at 7000°K.

5.7 OZONE (O_3).

The local thermal equilibrium emission spectra for O_3 was taken from the ROSCOE LTE data base.

The computation of this data was performed with the TATE code*. The calculations are described in The ROSCOE Manual, Volume 28†.

Table 6. Spectroscopic data for O_3.

Ground Electronic State

ω_1 = 1123.1	ω_2 = 719.4	ω_3 = 1101.1
χ_{11} = 2.0	χ_{22} = -1.0	χ_{33} = -15.
χ_{12} = -11.	χ_{13} = -39.	χ_{23} = -21.

A_e = 3.55196 B_e = 0.444917 C_e = 0.39476

γ_ℓ(300 °K) = 0.11

Data Source:

*J.G. DeVore, and T.L. Stephens, Band Model Parameters for Thermal Emission (U) , 72TMP-20, General Electric - TEMPO (June 1972) (Secret).

†T.L. Stephens, V.R. Stull, A.L. Klein, and J.D. Losse, The ROSCOE Manual, Volume 28-Molecular Band Models for Thermal and Optically Pumped Emissions (U) , GE78TMP-52, General Electric -- TEMPO (June 1978) (Confidential).

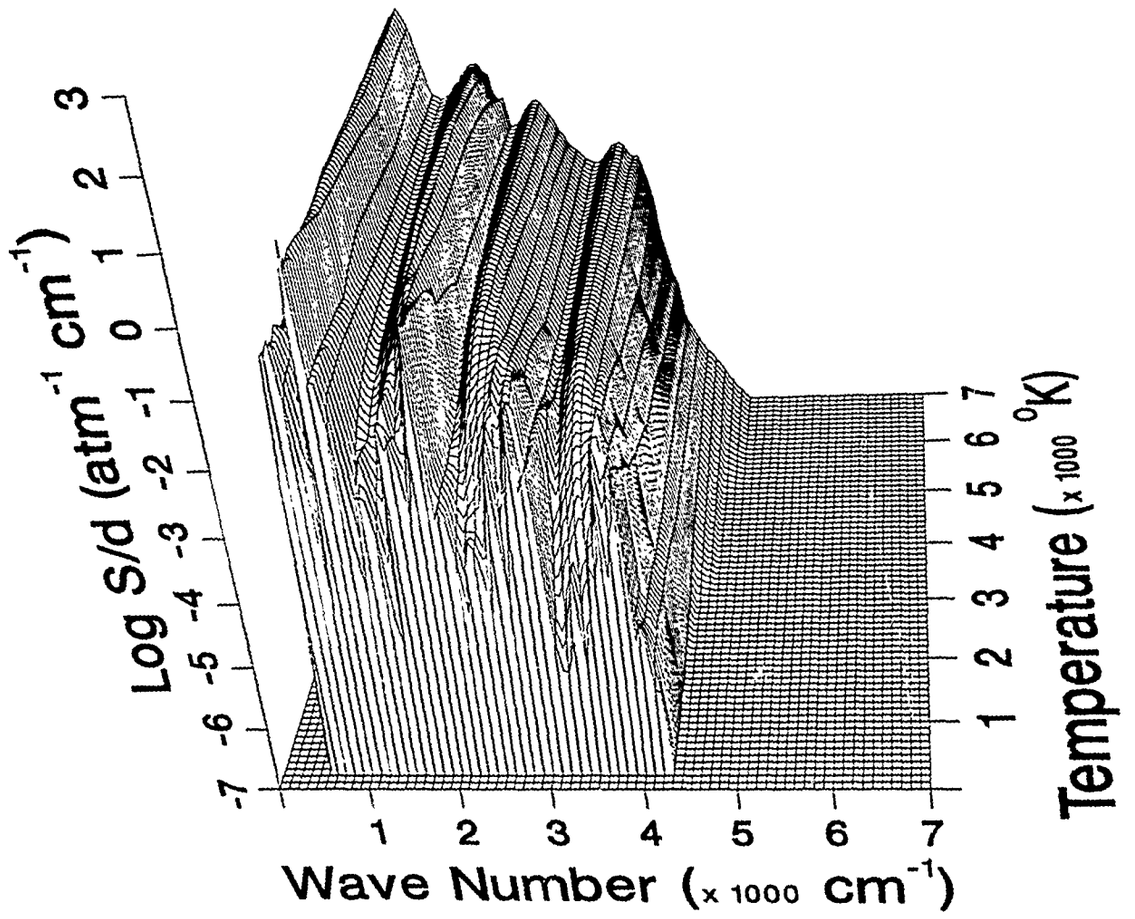

Figure 235. Weak-line parameter for O_3.

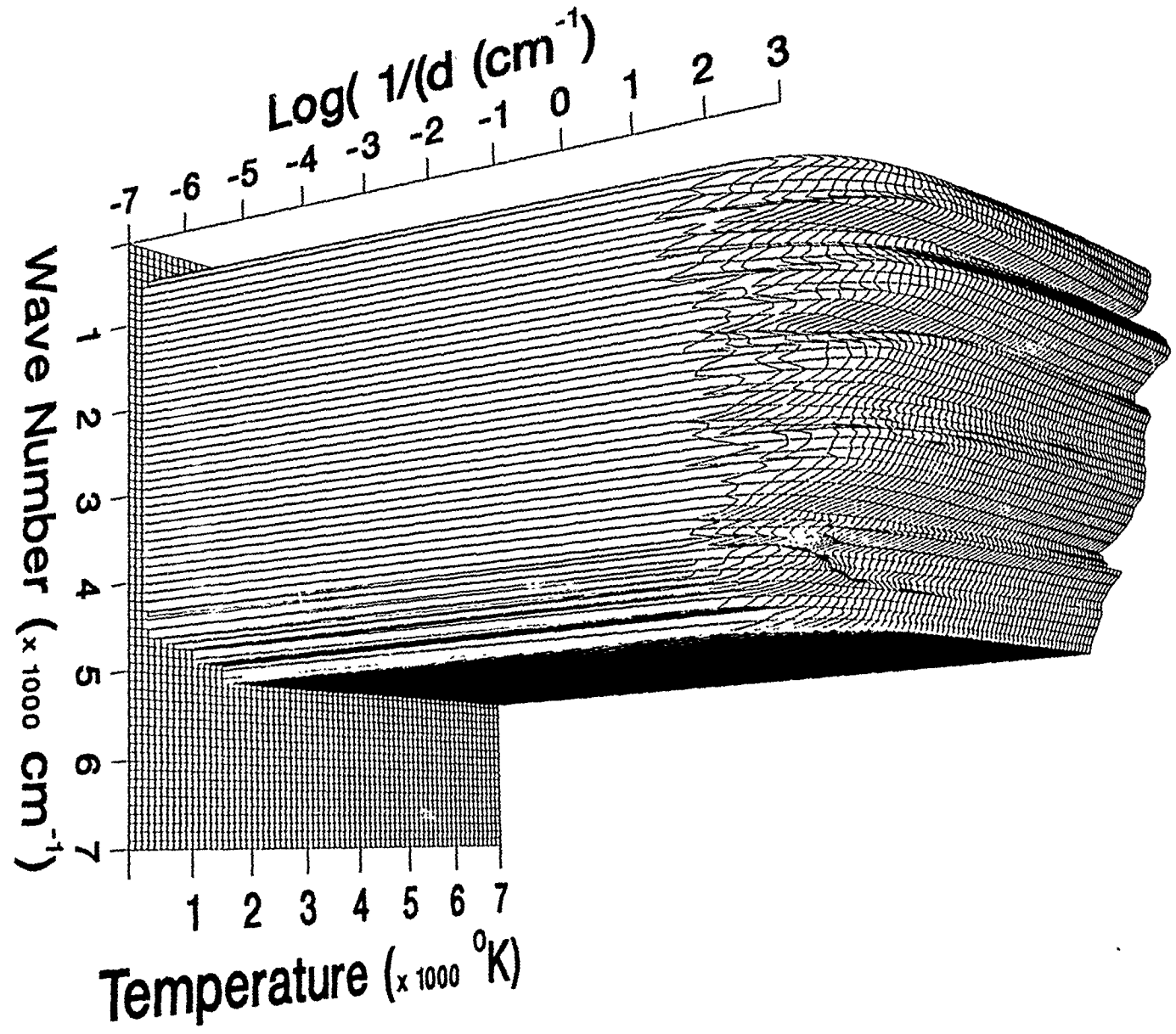

Figure 236. Inverse line spacing for O_3.

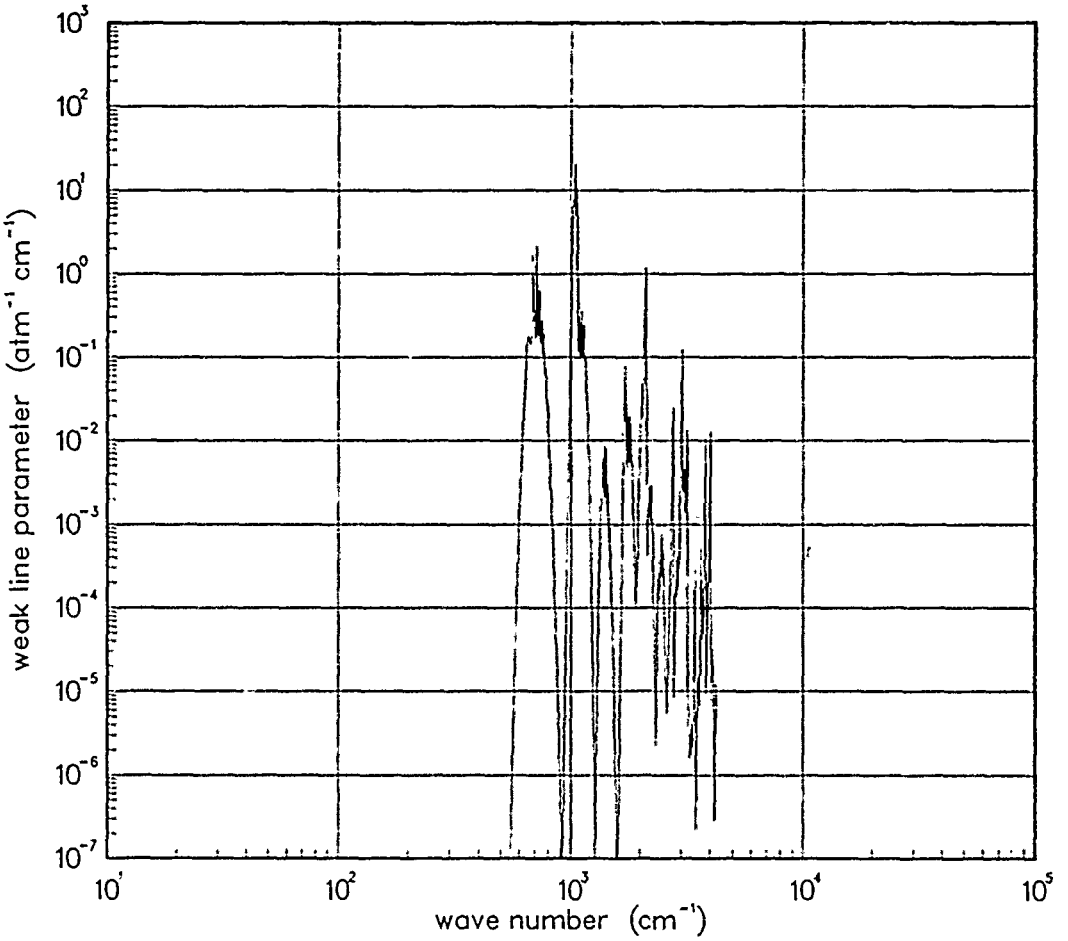

Figure 237. Weak-line parameter for O_3 at 200°K.

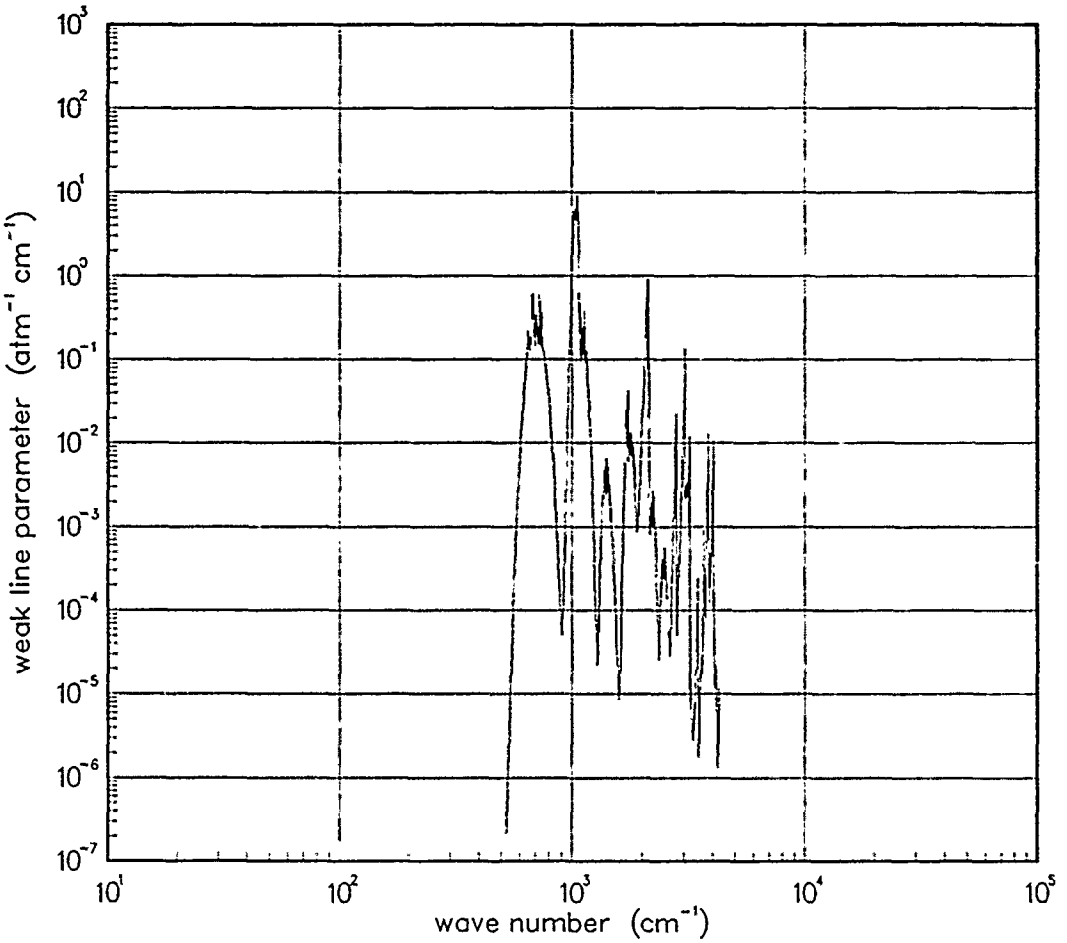

Figure 238. Weak-line parameter for O_3 at 300°K.

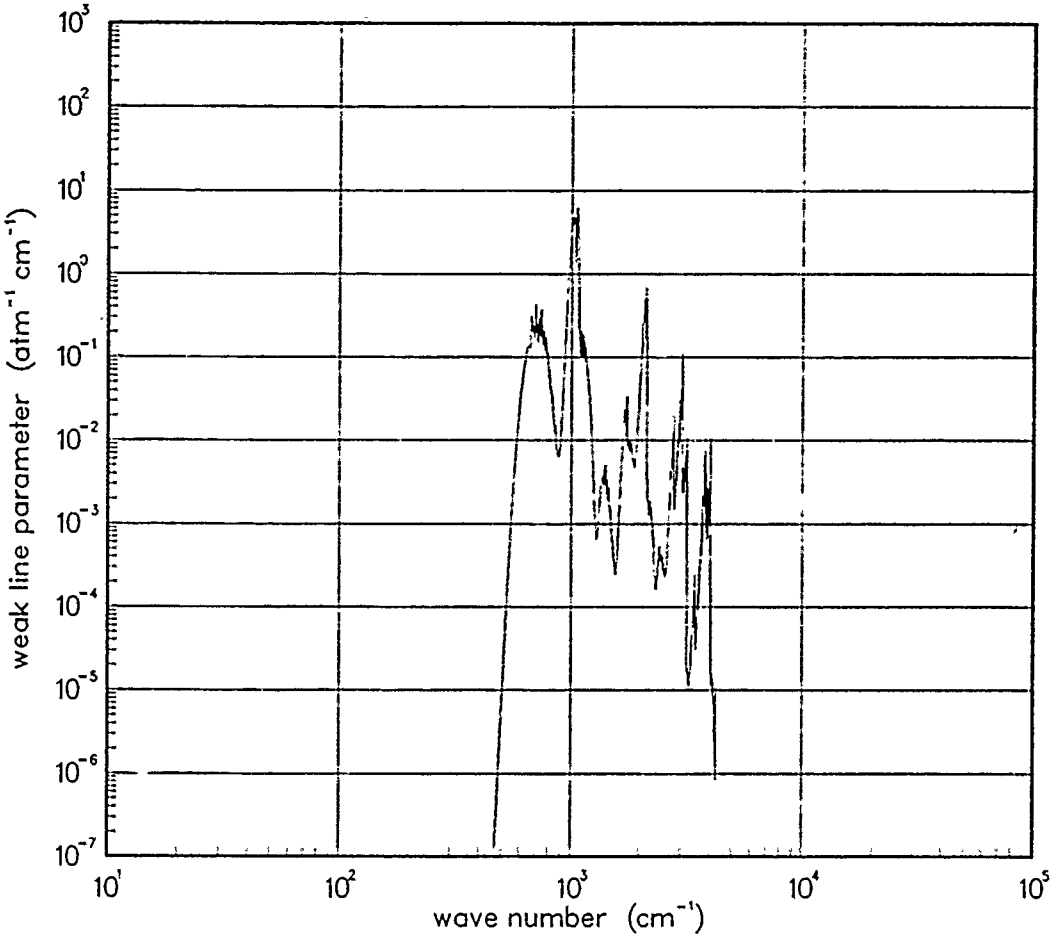

Figure 239. Weak-line parameter for O_3 at 500°K.

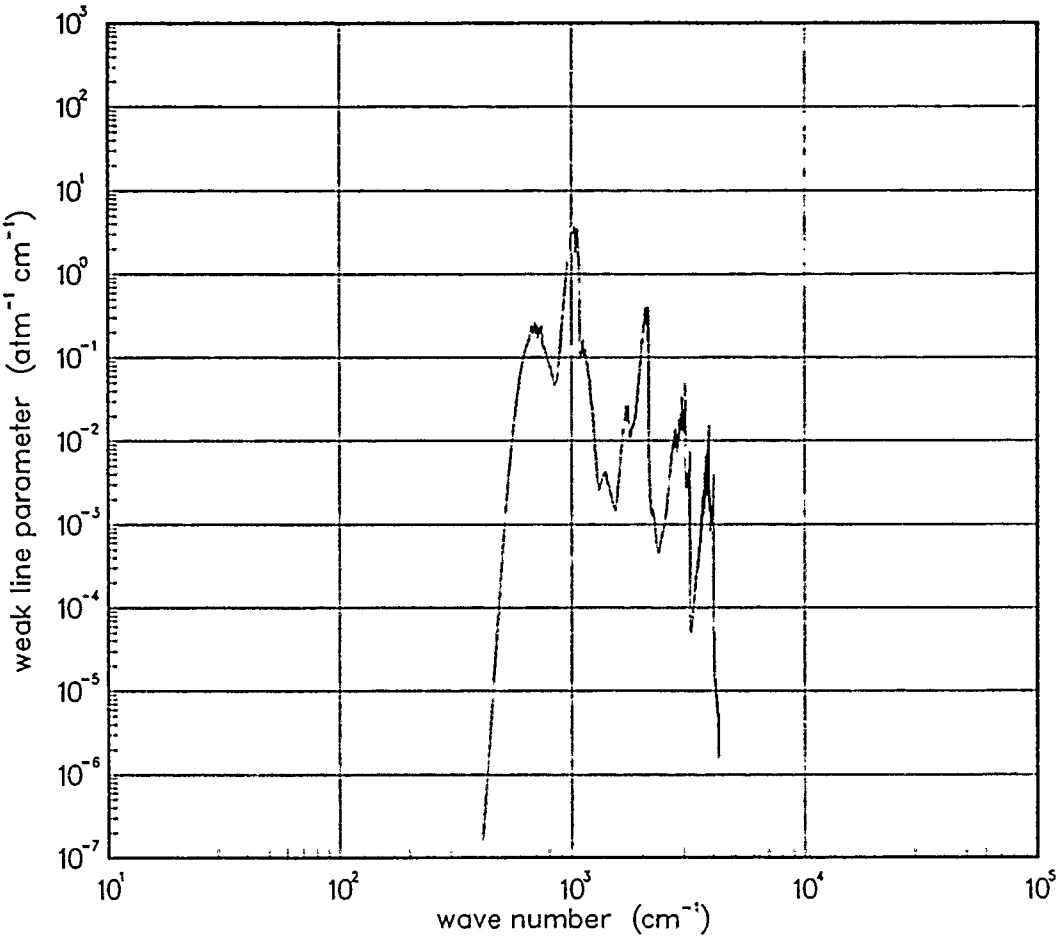

Figure 240. Weak-line parameter for O_3 at 750°K.

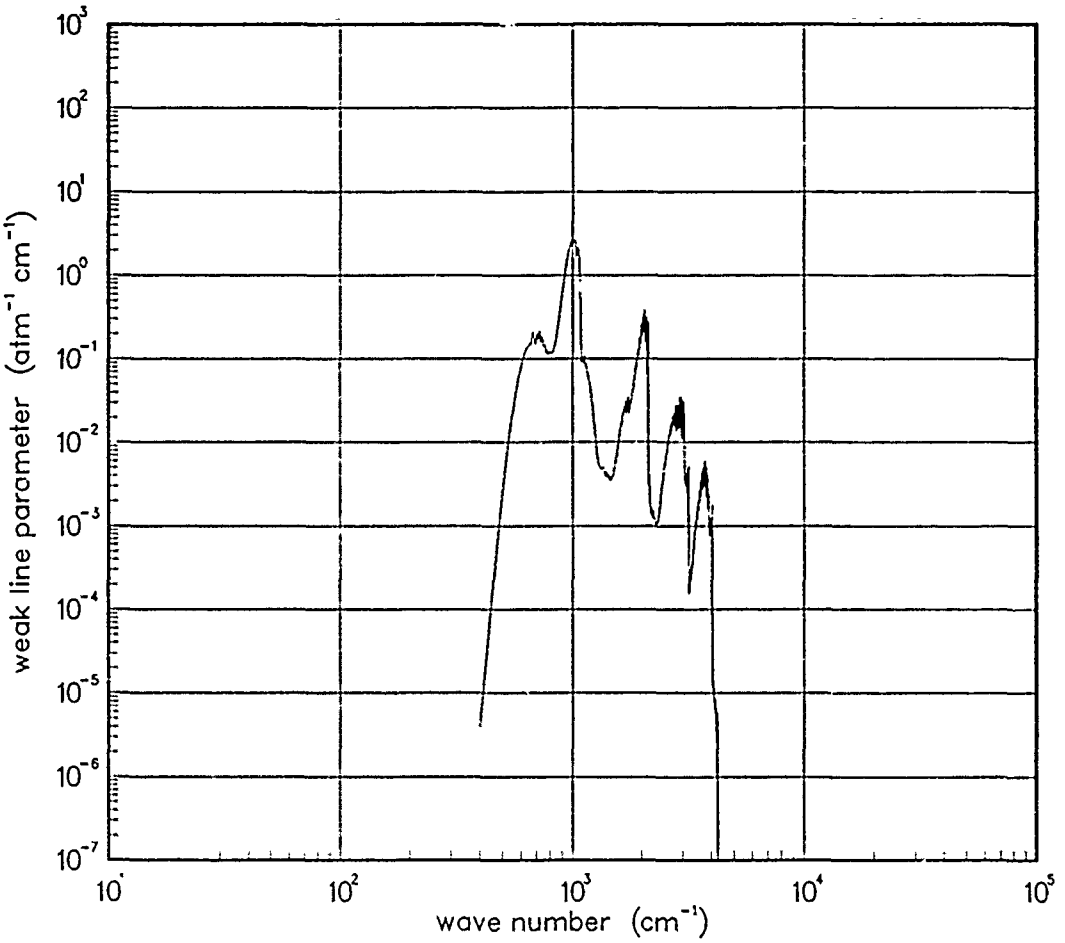

Figure 241. Weak-line parameter for O_3 at 1000°K.

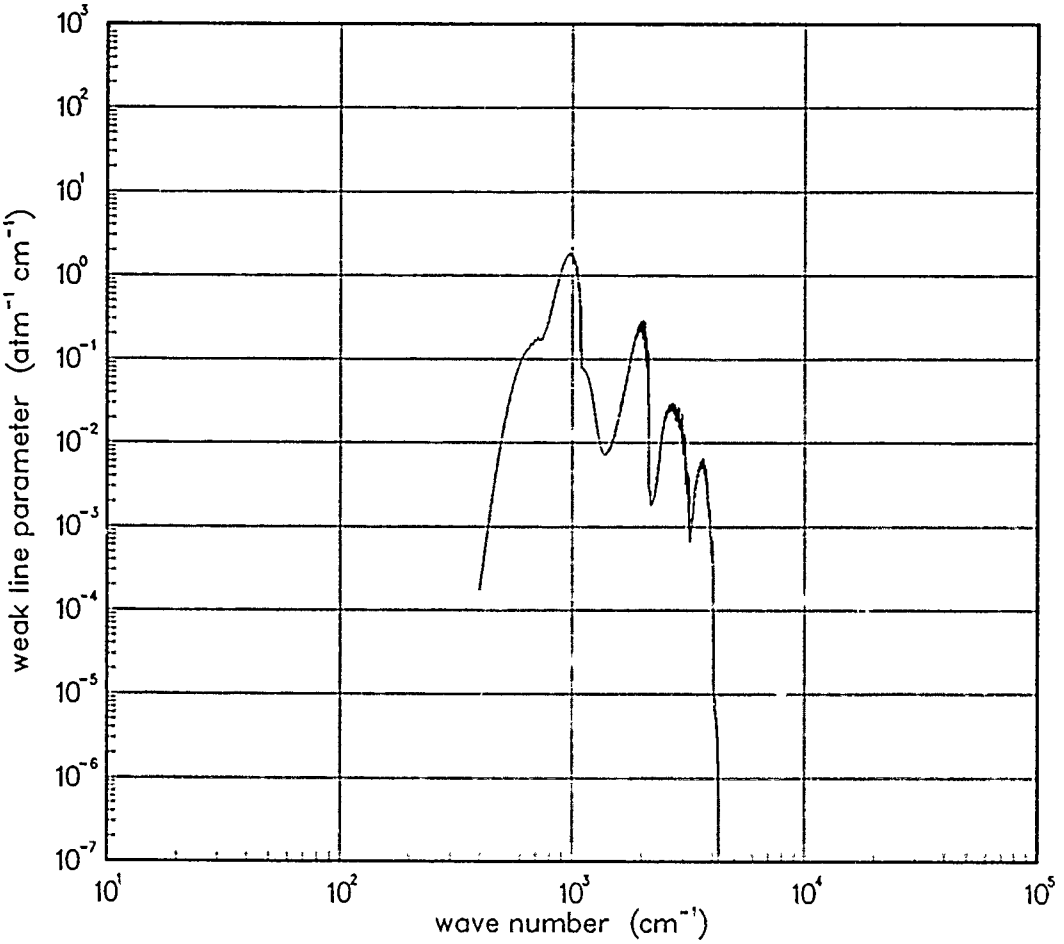

Figure 242. Weak-line parameter for O_3 at 1500°K.

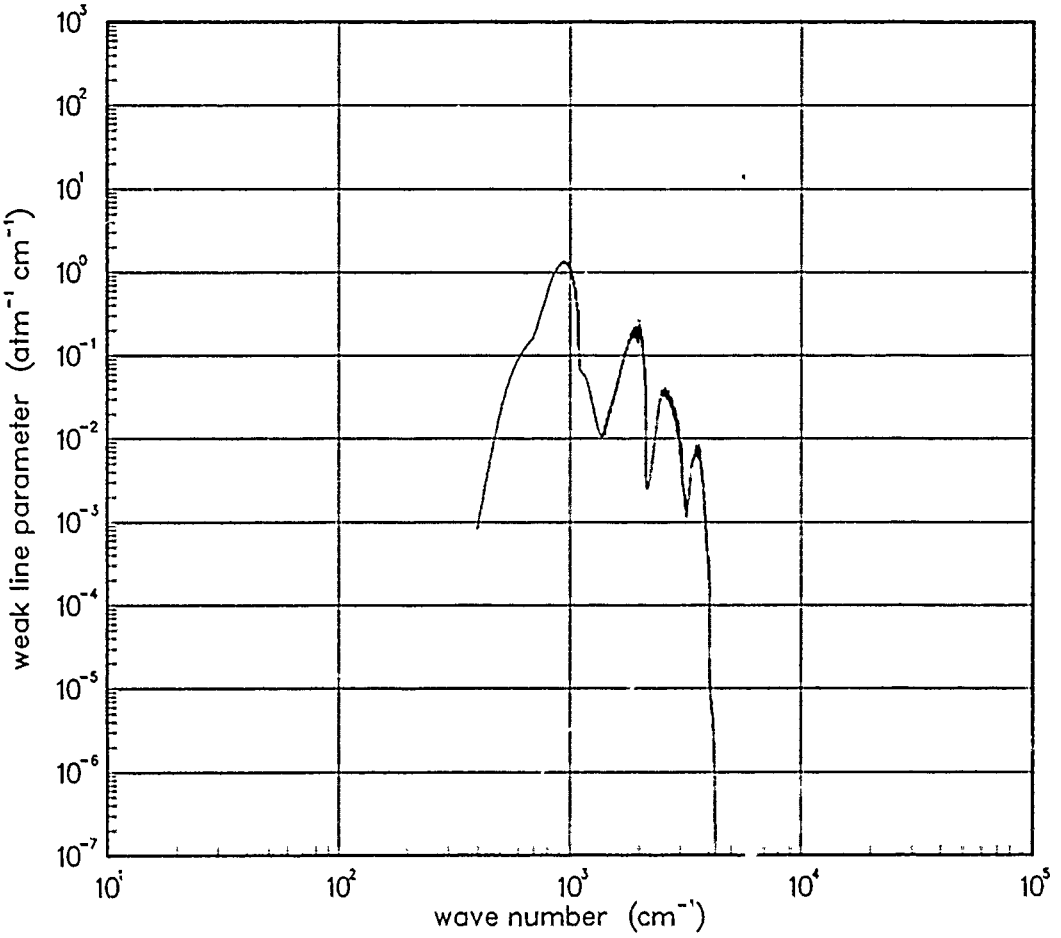

Figure 243. Weak-line parameter for O_3 at 2000°K.

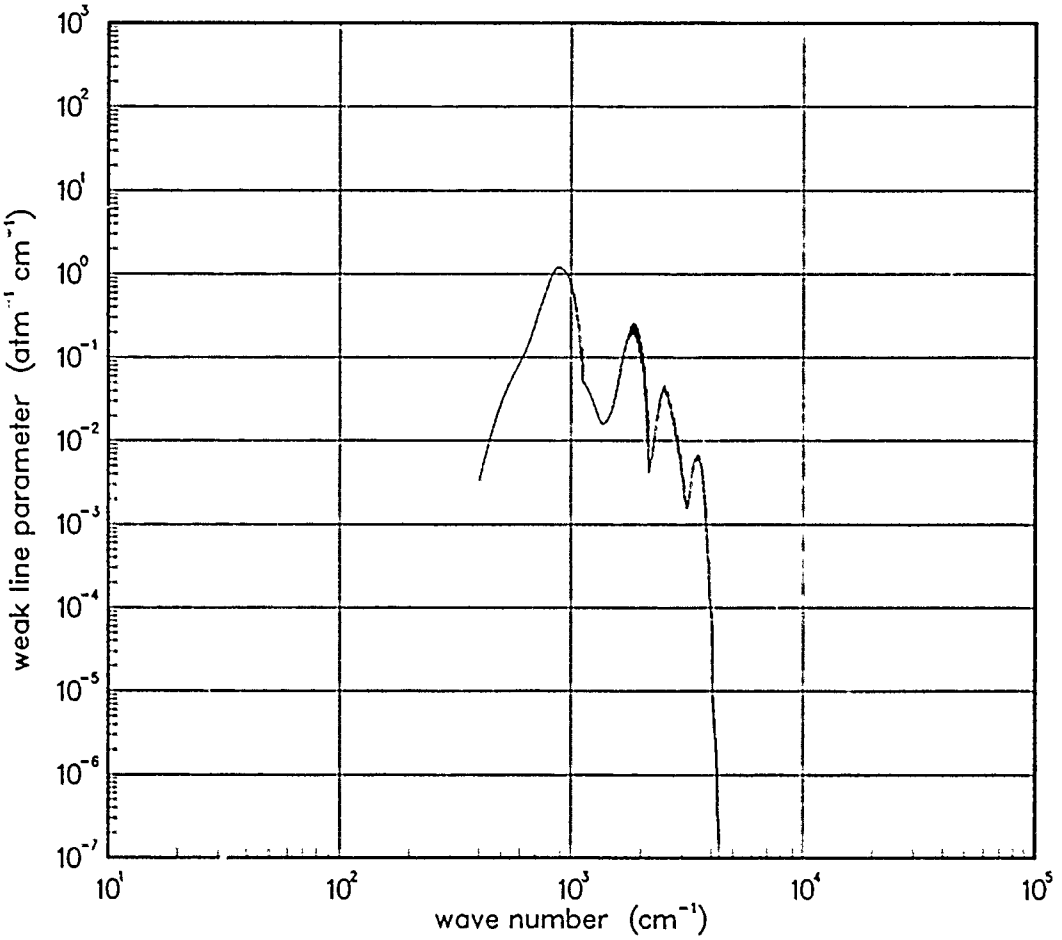

Figure 244. Weak-line parameter for O_3 at 3000°K.

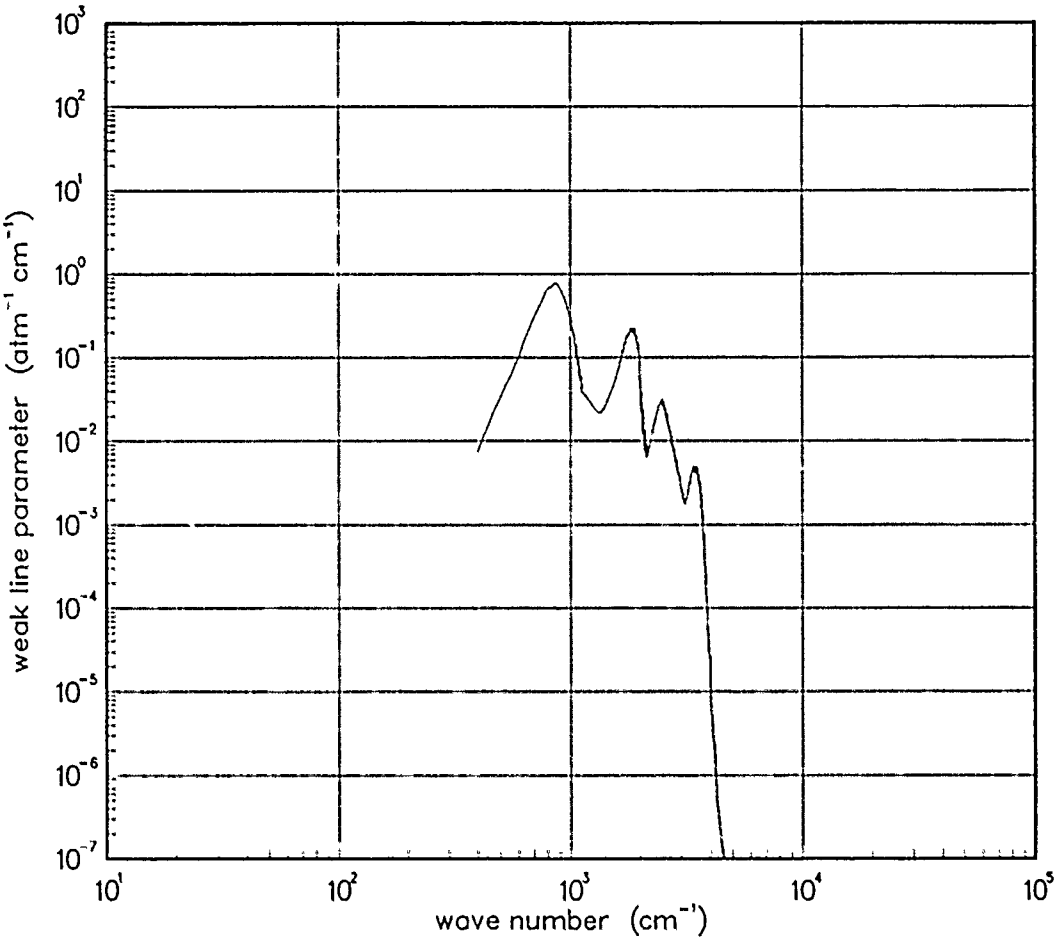

Figure 245. Weak-line parameter for O_3 at 5000°K.

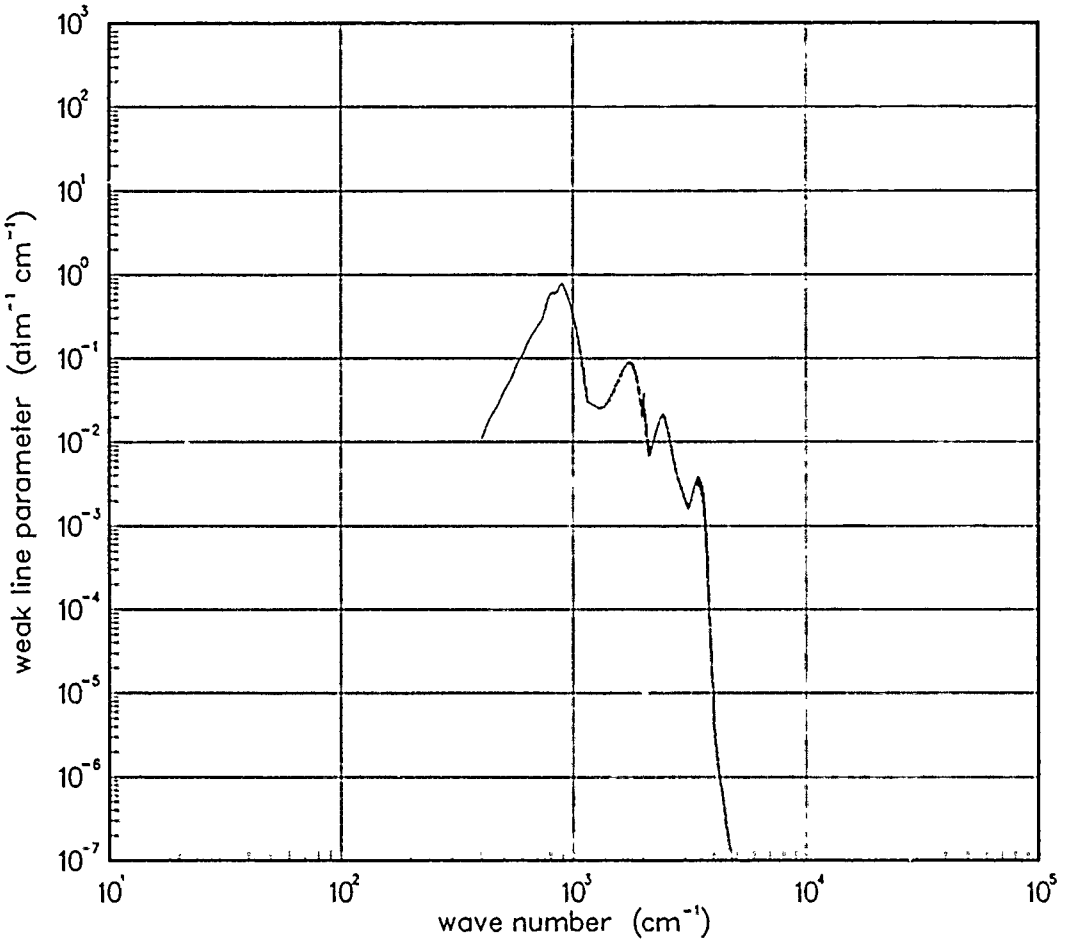

Figure 246. Weak-line parameter for O_3 at 7000°K.

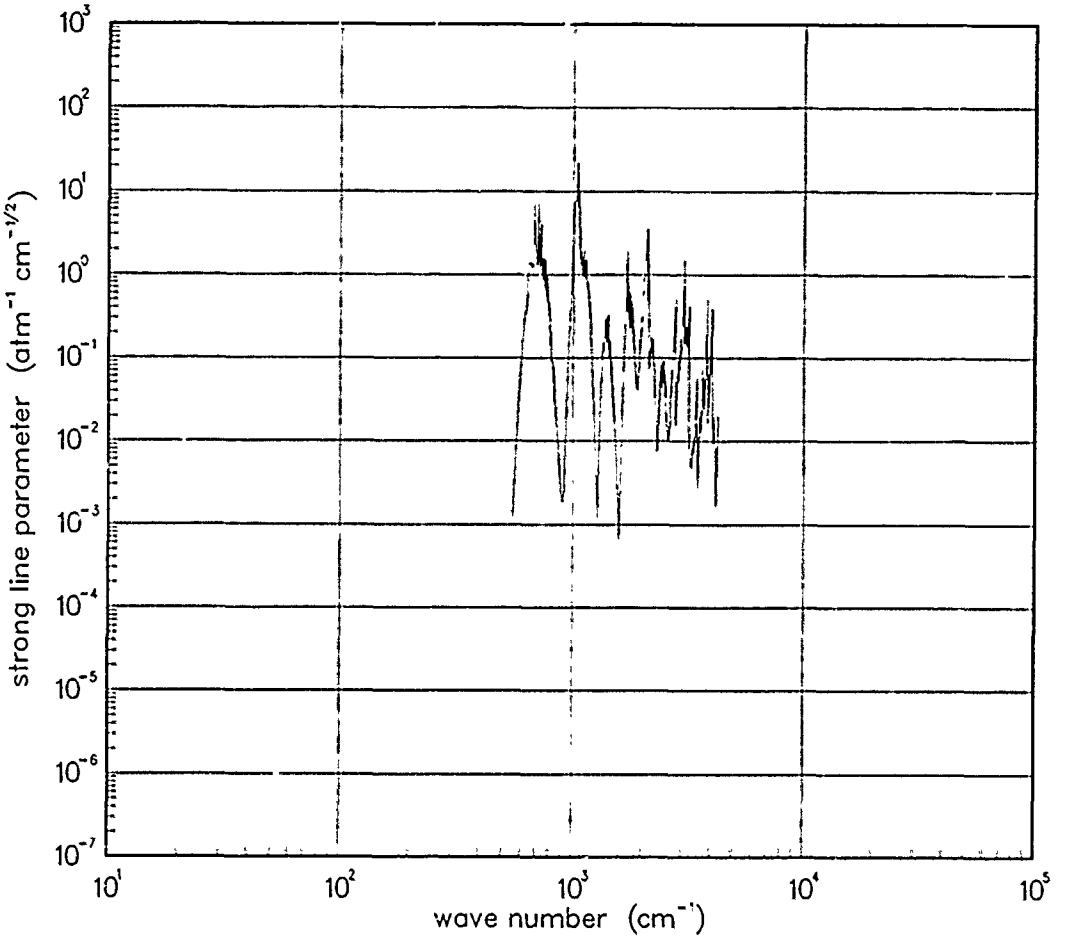

Figure 247. Strong-line parameter for O_3 at 200°K.

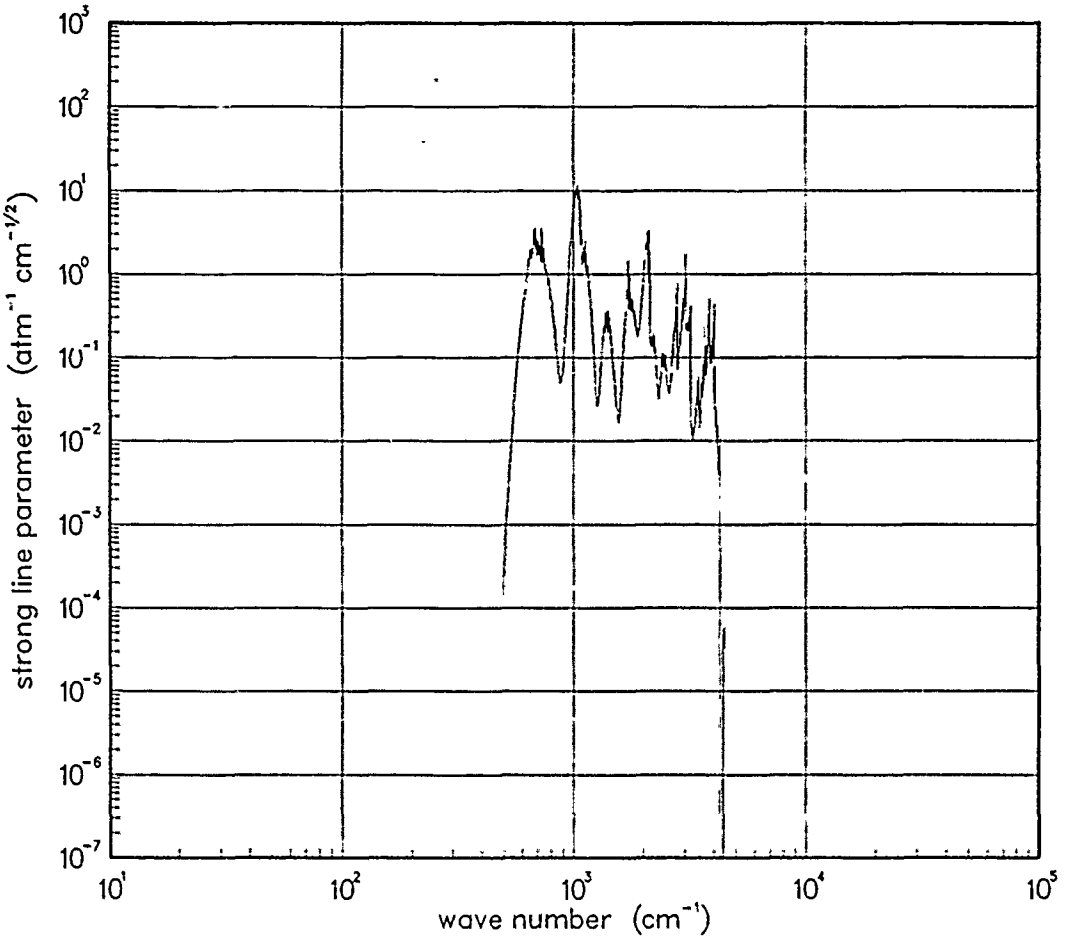

Figure 248. Strong-line parameter for O_3 at 300°K.

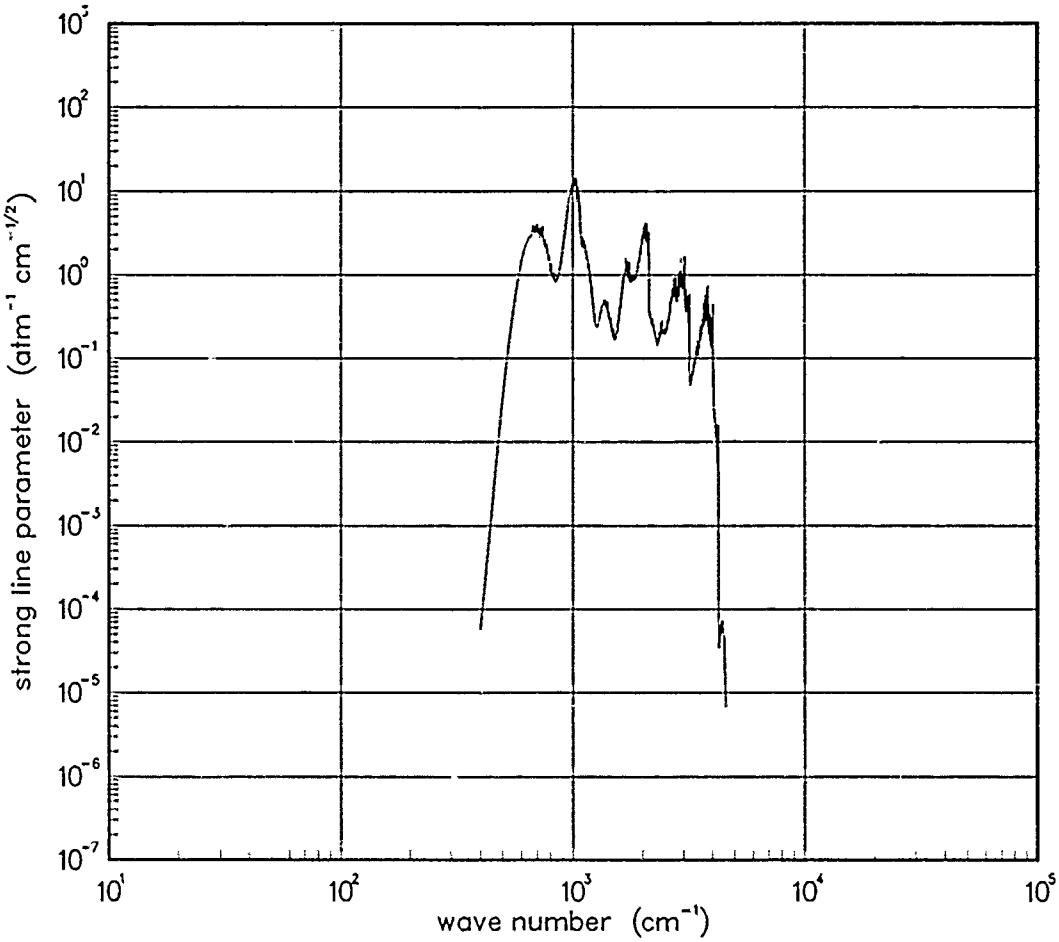

Figure 249. Strong-line parameter for O_3 at 500°K.

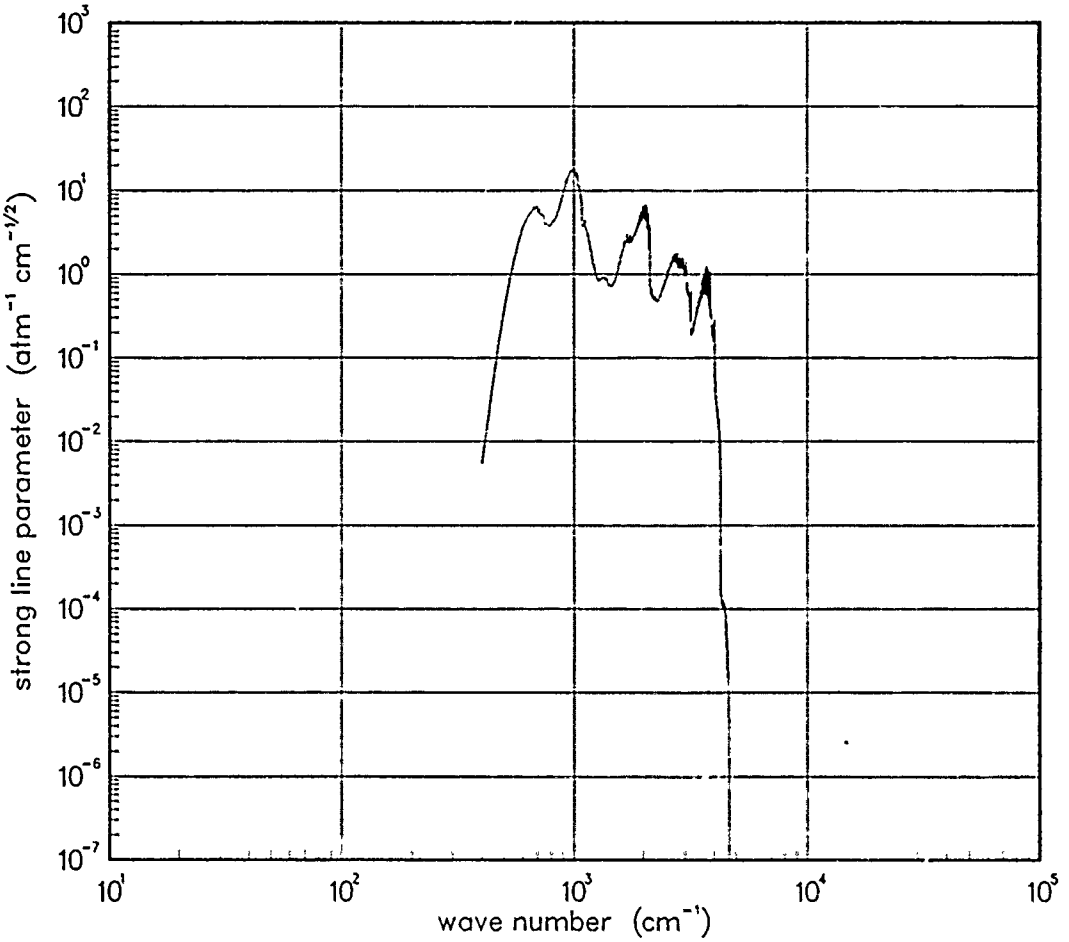

Figure 250. Strong-line parameter for O_3 at 750°K.

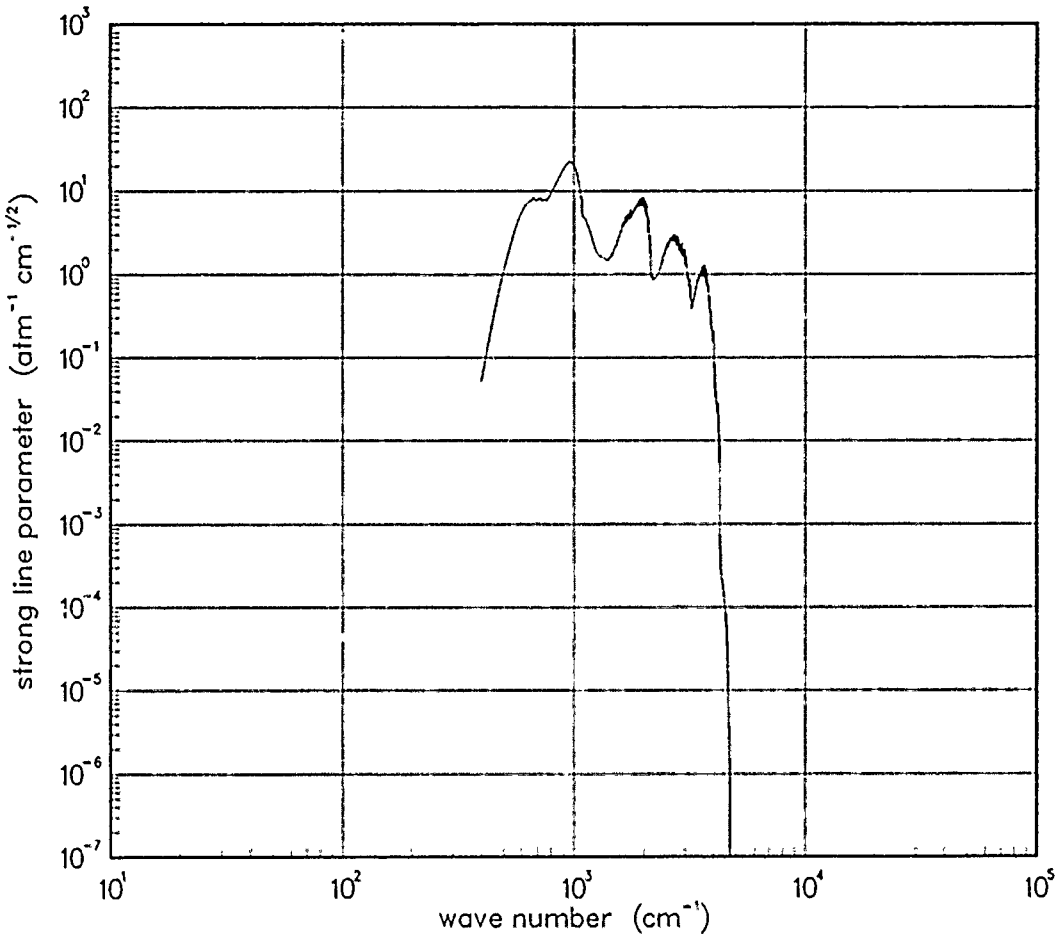

Figure 251. Strong-line parameter for O_3 at 1000°K.

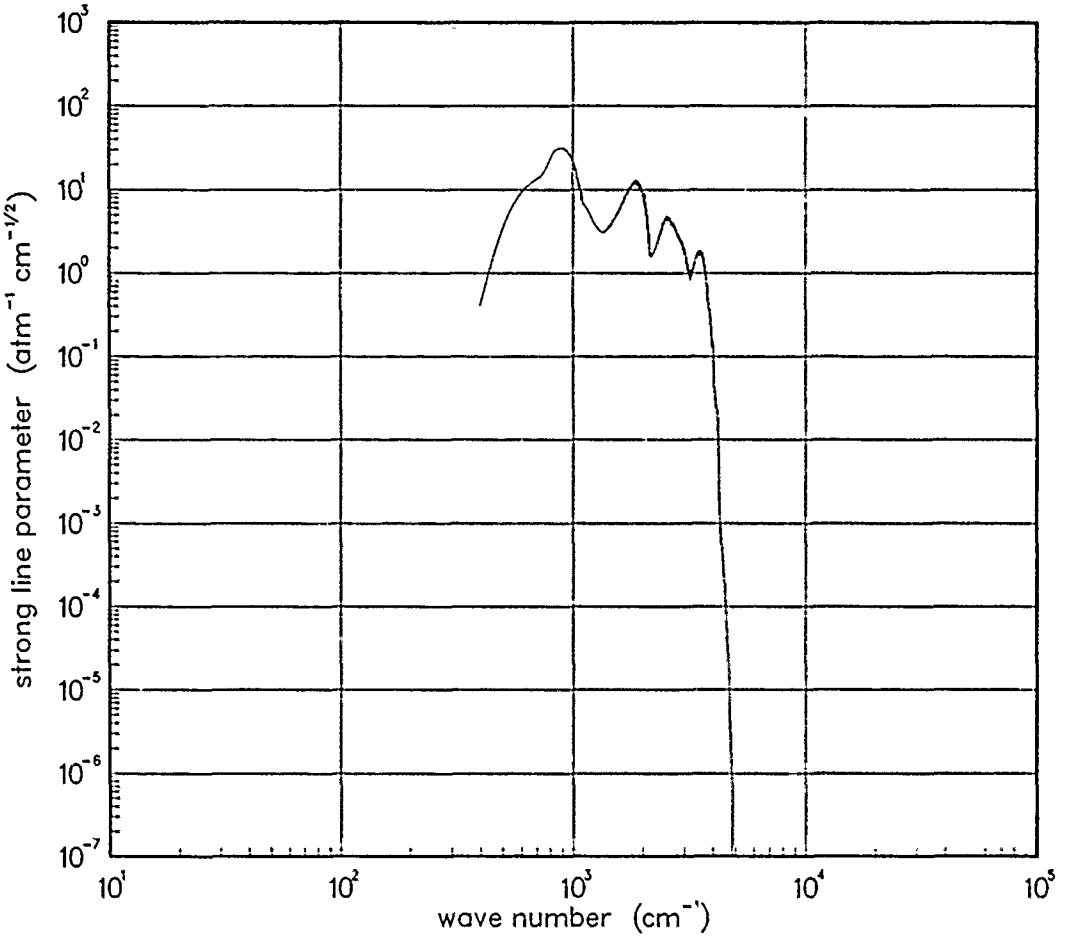

Figure 252. Strong-line parameter for O_3 at 1500°K.

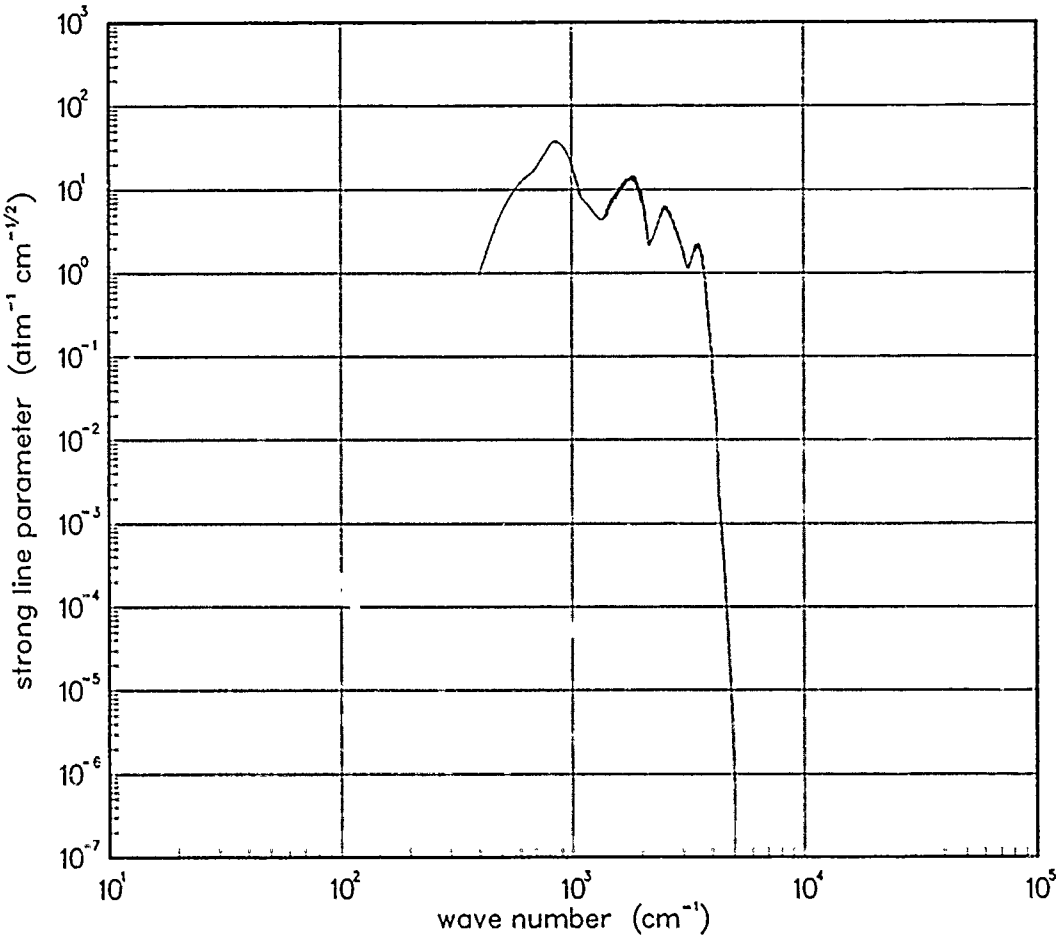

Figure 253. Strong-line parameter for O_3 at 2000°K.

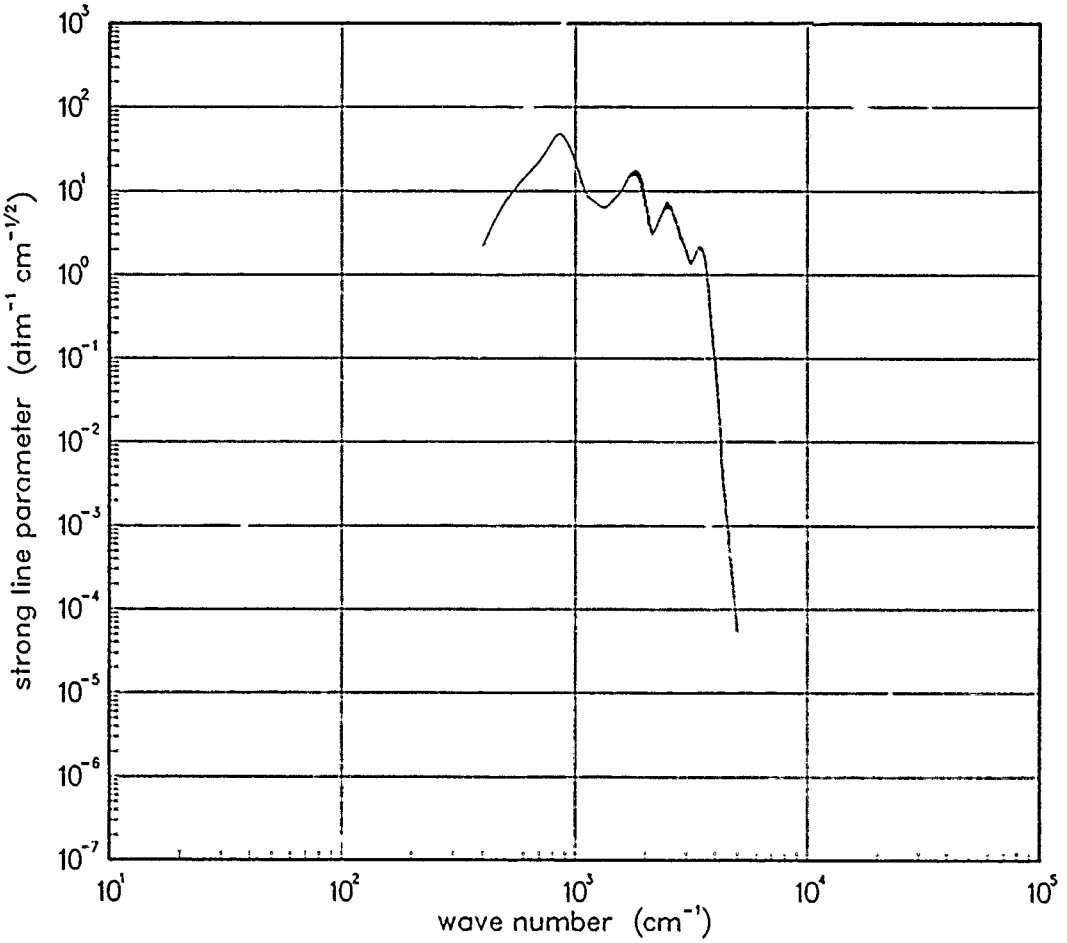

Figure 254. Strong-line parameter for O_3 at 3000°K.

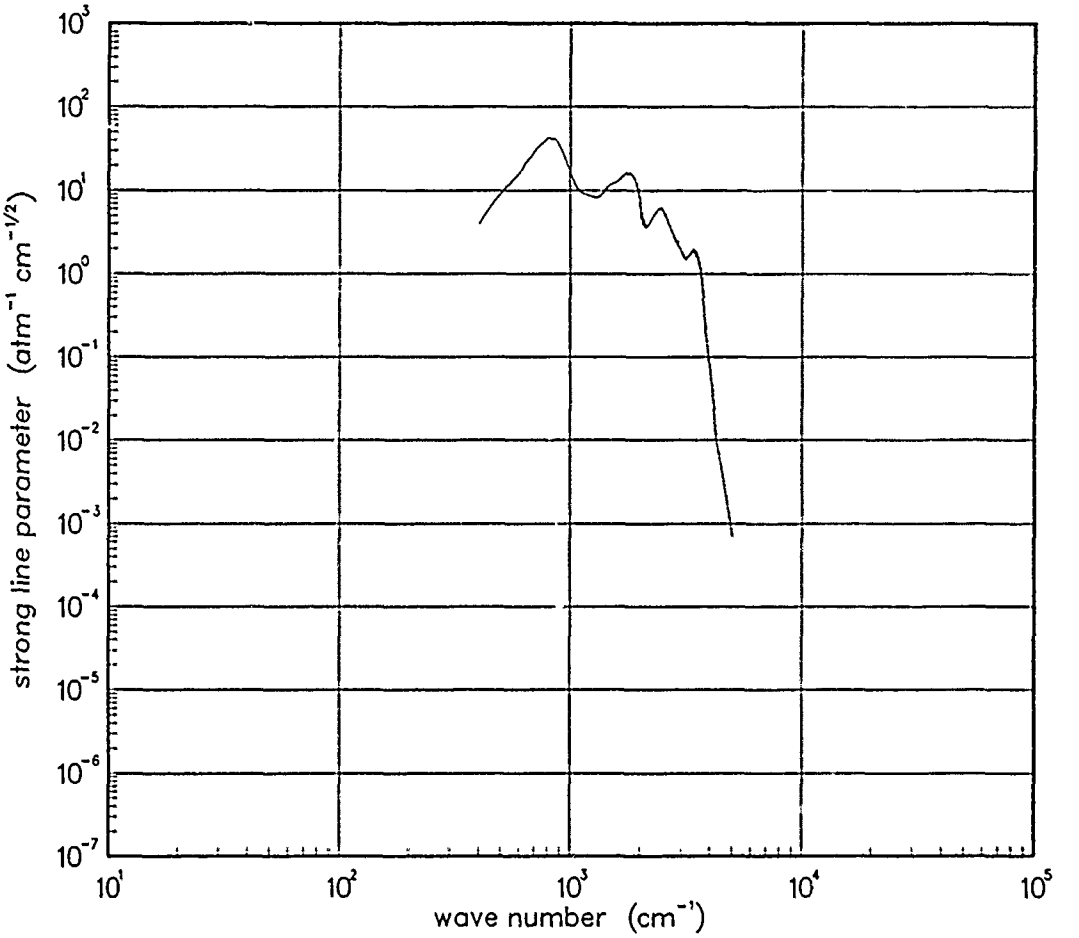

Figure 255. Strong-line parameter for O_3 at 5000°K.

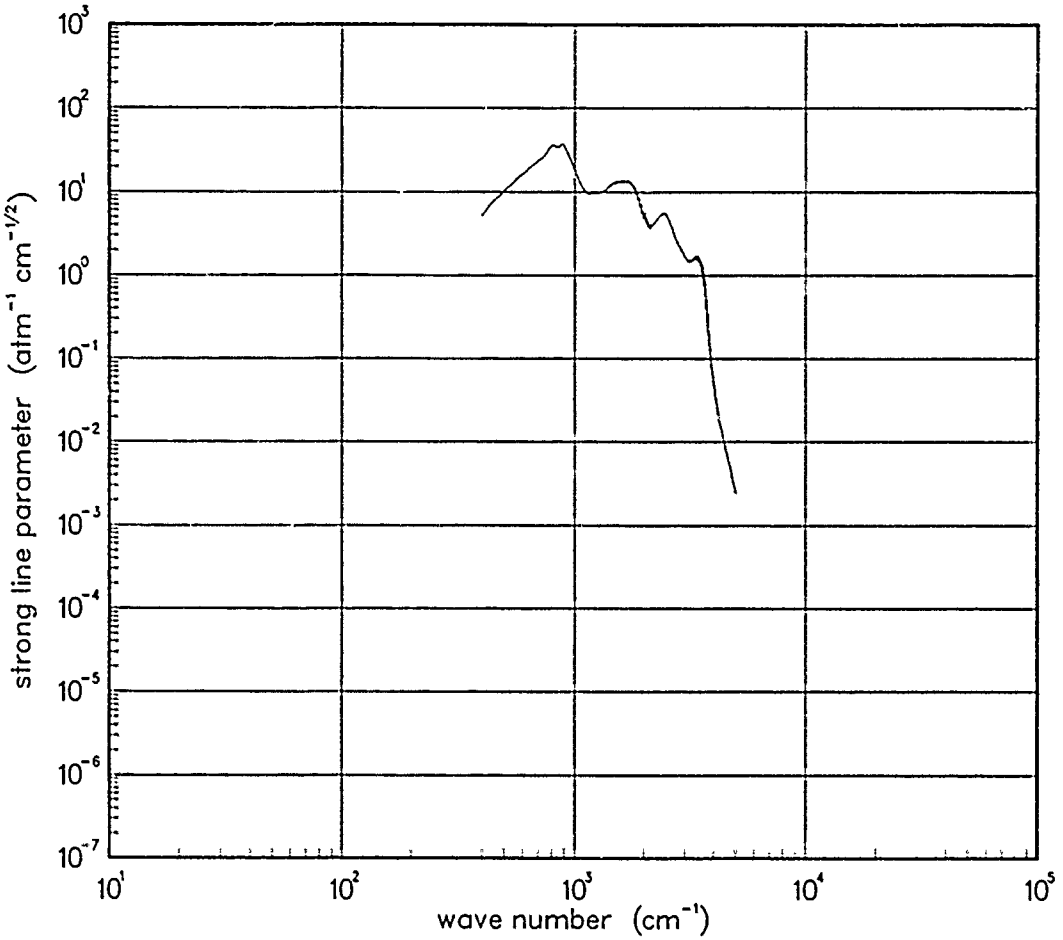

Figure 256. Strong-line parameter for O_3 at 7000°K.

5.8 SULFUR DIOXIDE (SO_2).

The local thermal equilibrium emission spectra for Sulfur Dioxide has been developed from the Air Force Geophysical Laboratory line atlas for 200, 300, 500, 750, 1000 °K.

The SO_2 molecule has been included within the NORSE LTE data base because of its contribution to ambient atmospheric absorption. The inclusion of accurate parameters for this species above 1000 °K is felt to be of low priority.

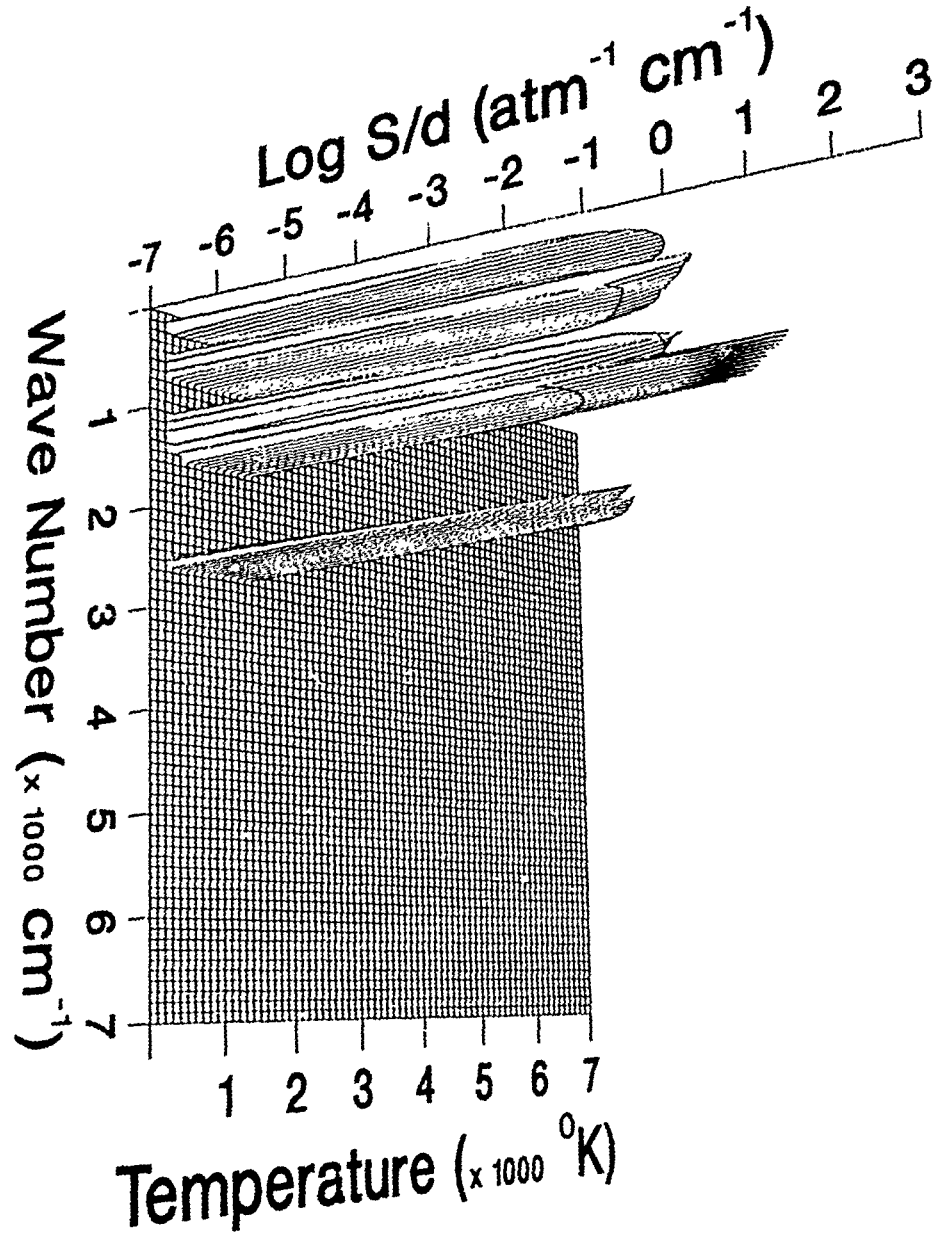

Figure 257. Weak-line parameter for SO_2.

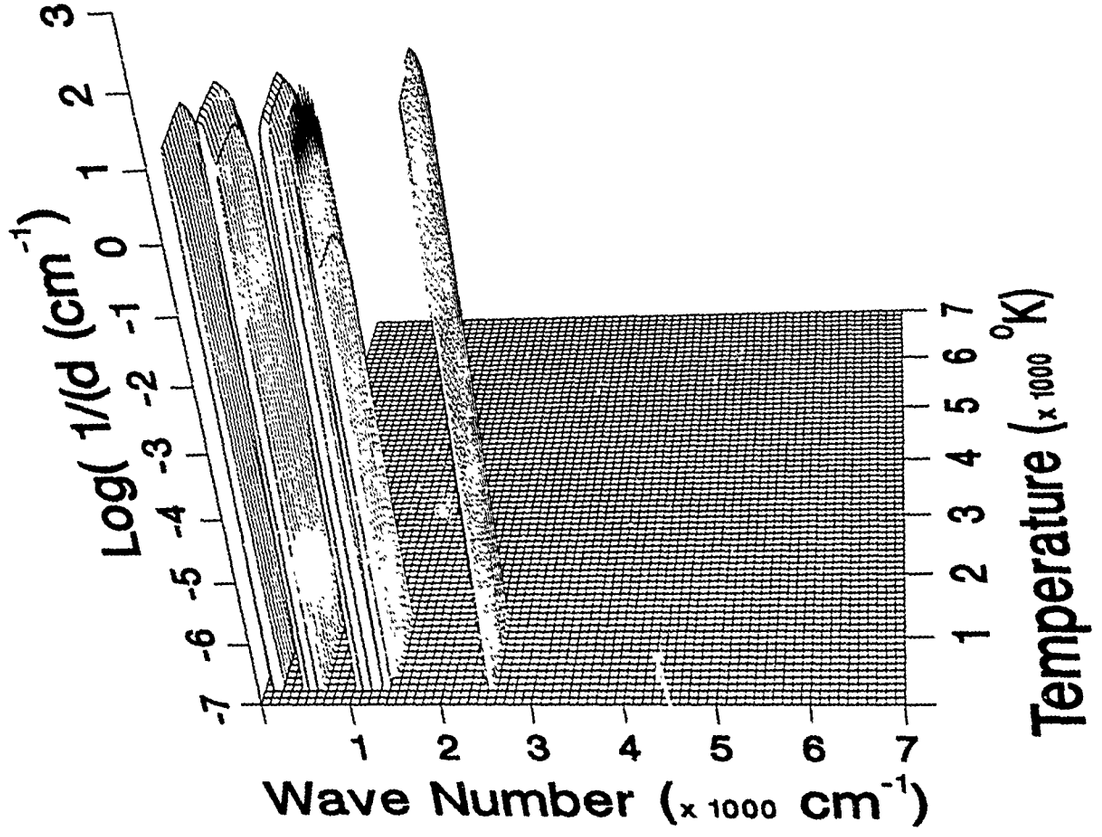

Figure 258. Inverse line spacing for SO_2.

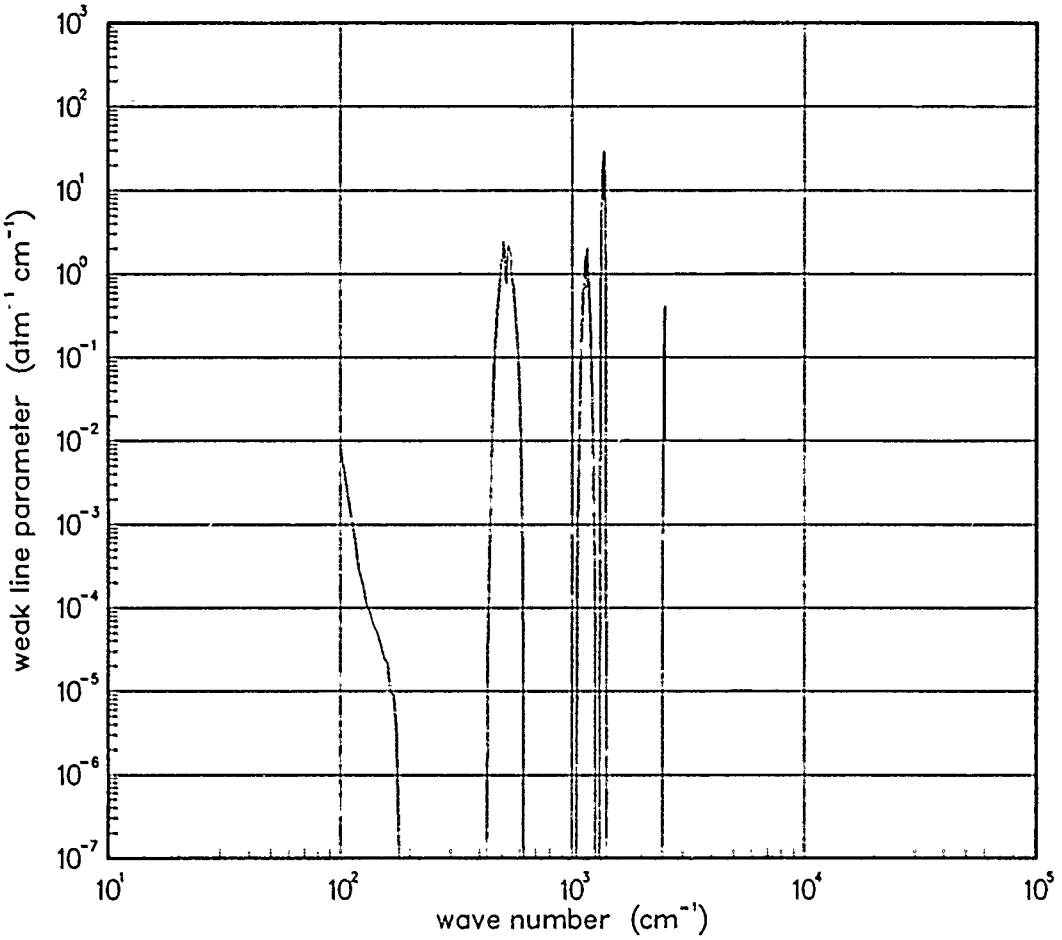

Figure 259. Weak-line parameter for SO_2 at 200°K.

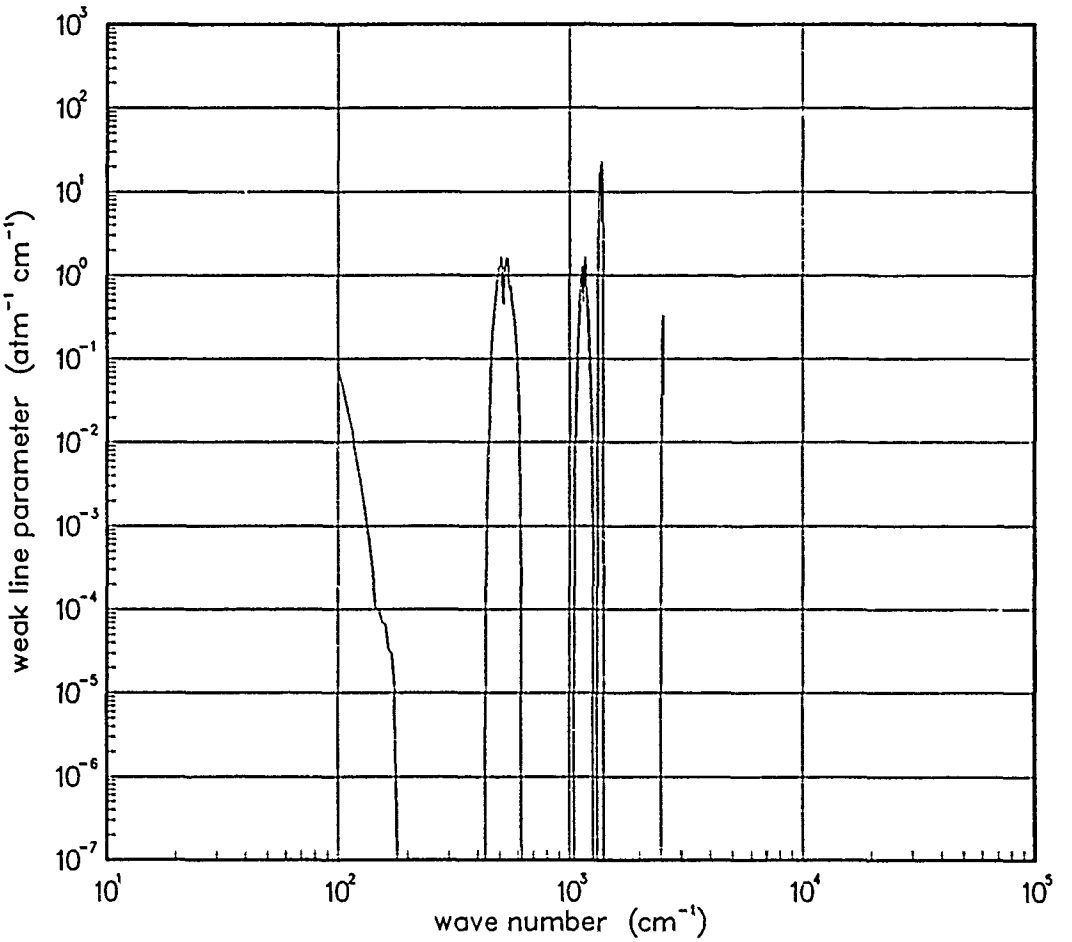

Figure 260. Weak-line parameter for SO_2 at 300°K.

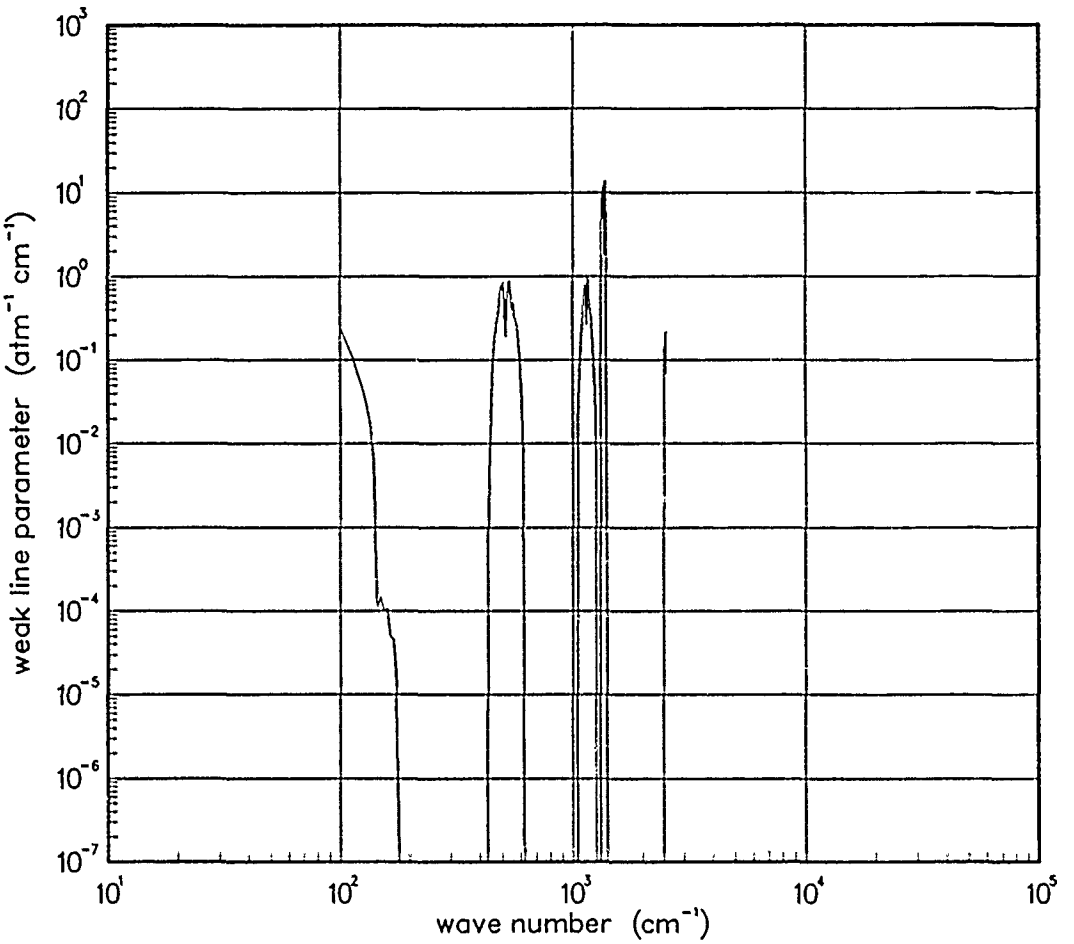

Figure 261. Weak-line parameter for SO_2 at 500°K.

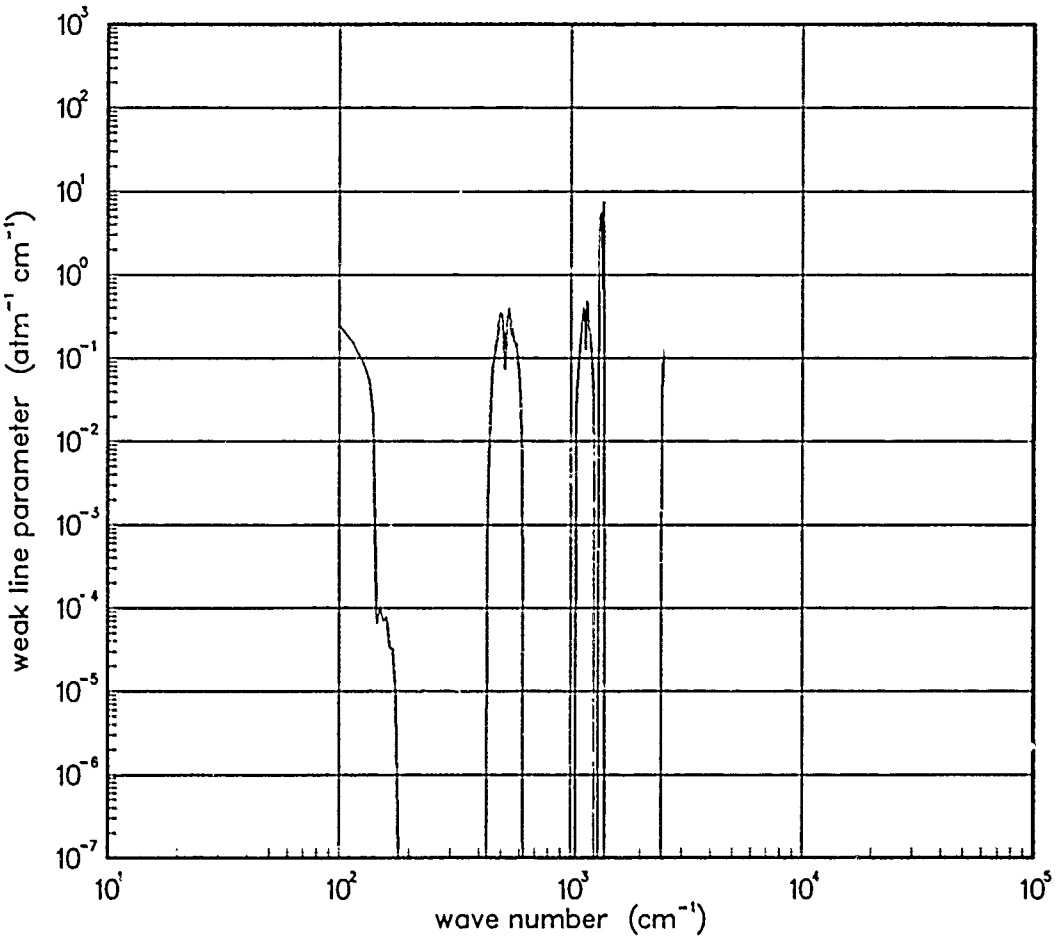

Figure 262. Weak-line parameter for SO_2 at 750°K.

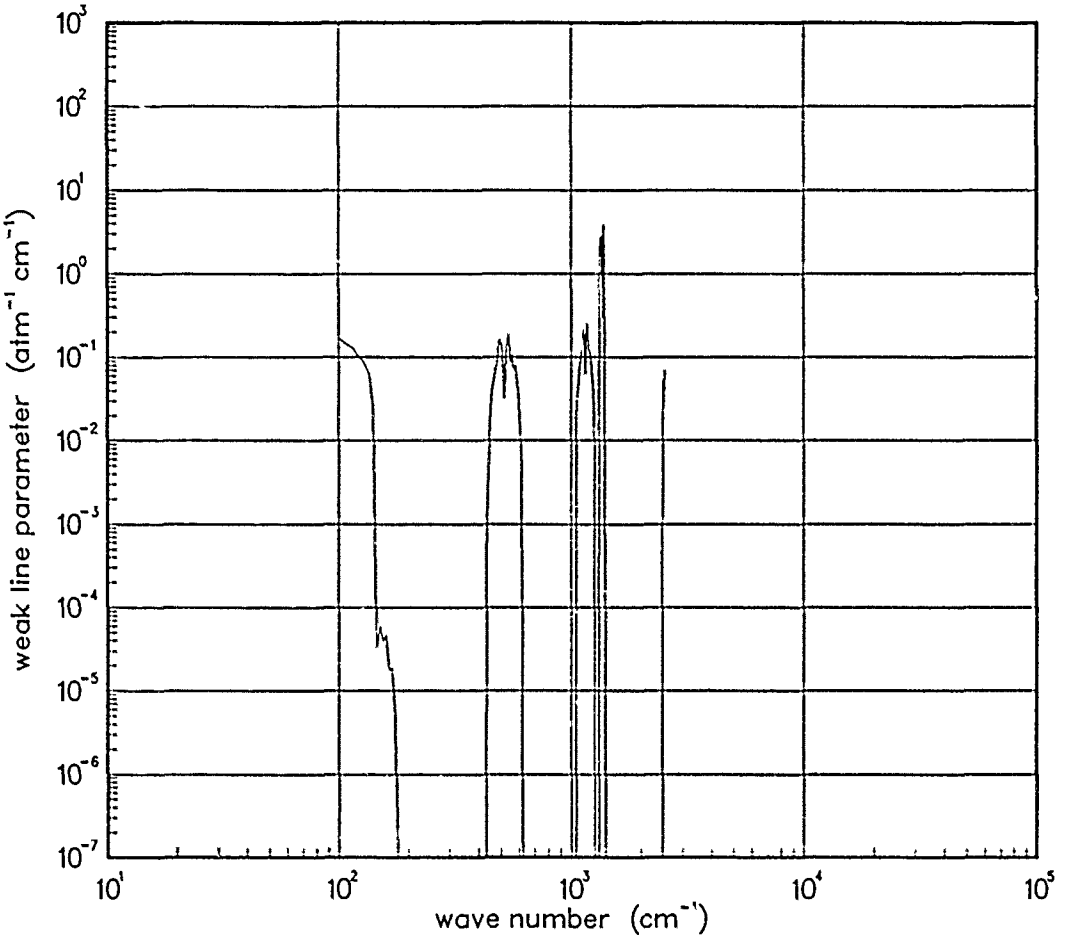

Figure 263. Weak-line parameter for SO_2 at 1000°K.

5.9 WATER (H_2O).

The local thermal equilibrium emission spectra for H_2O was taken from the ROSCOE LTE data base.

Low temperature (200, 300, 500 °K) H_2O data was derived from the Air Force Geophysical Laboratory Line Atlas*. For temperatures above 500 °K the curves were extracted from the WOE fireball LTE parameters† except in the spectral region 2000 - 5000 cm^{-1} were ROSCOE-IR results were used. Both the WOE high temperature data and the ROSCOE-IR data are based on measurements preformed at Convair‡.

Data Source:

*R.A. McClatchey, et al, AFCRL Atmospheric Line Parameters Compilation , AFCRL-TR-73-0096, Air Force Cambridge Research Laboratories, (January 1973) 1982 version of the data tape.

†J.G. DeVore, and T.L. Stephens, Band Model Parameters for Thermal Emission (U) , 72TMP-20, General Electric - TEMPO, June 1972 (Secret).

‡C.C. Ferriso, C.B. Ludwig, and A.L. Thomson,J. Quant. Spectrosc. Radiat. Transfer 6, 241 (1966). C.B. Ludwig, Appl. Opt. 10 (1971).

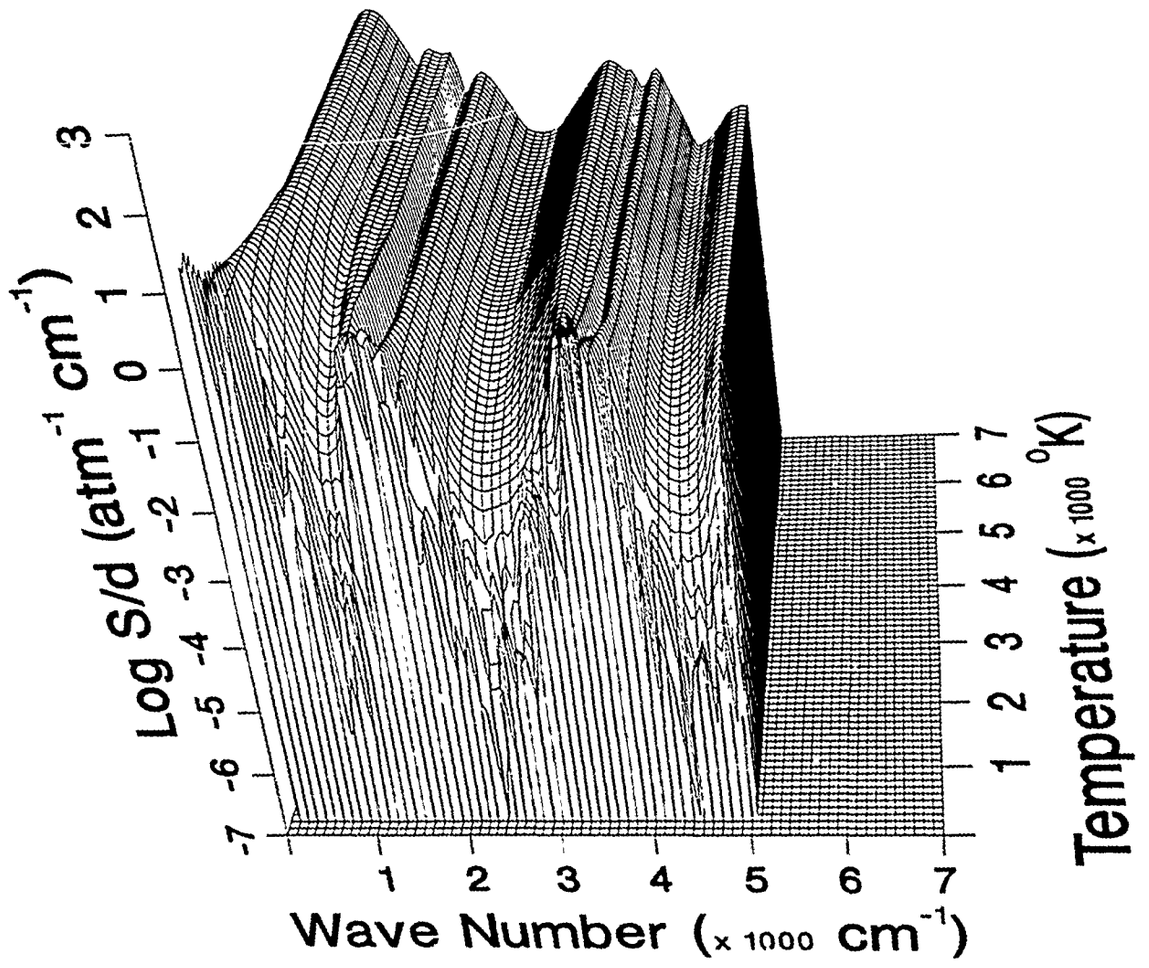

Figure 264. Weak-line parameter for H_2O.

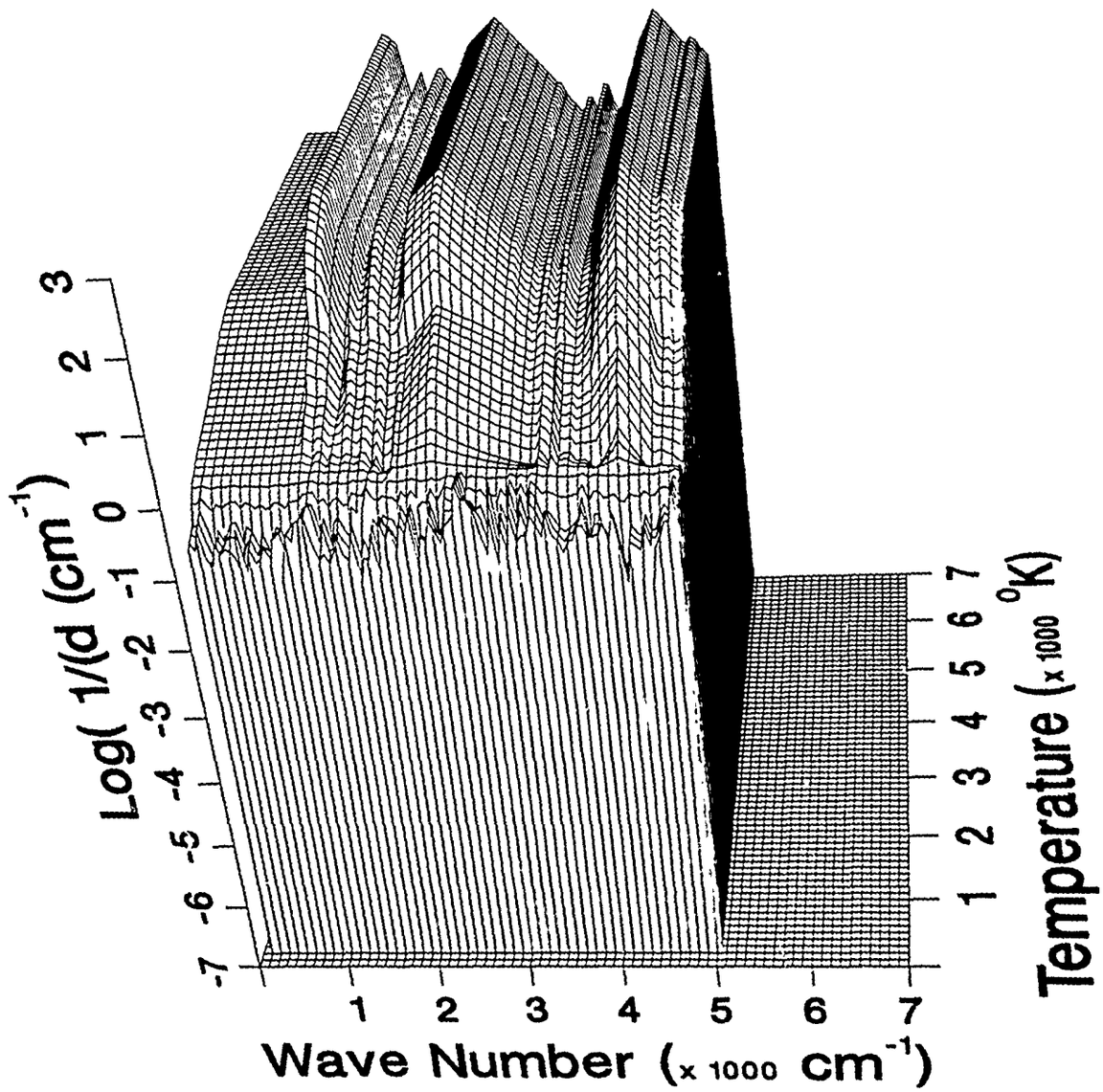

Figure 265. Inverse line spacing for H_2O.

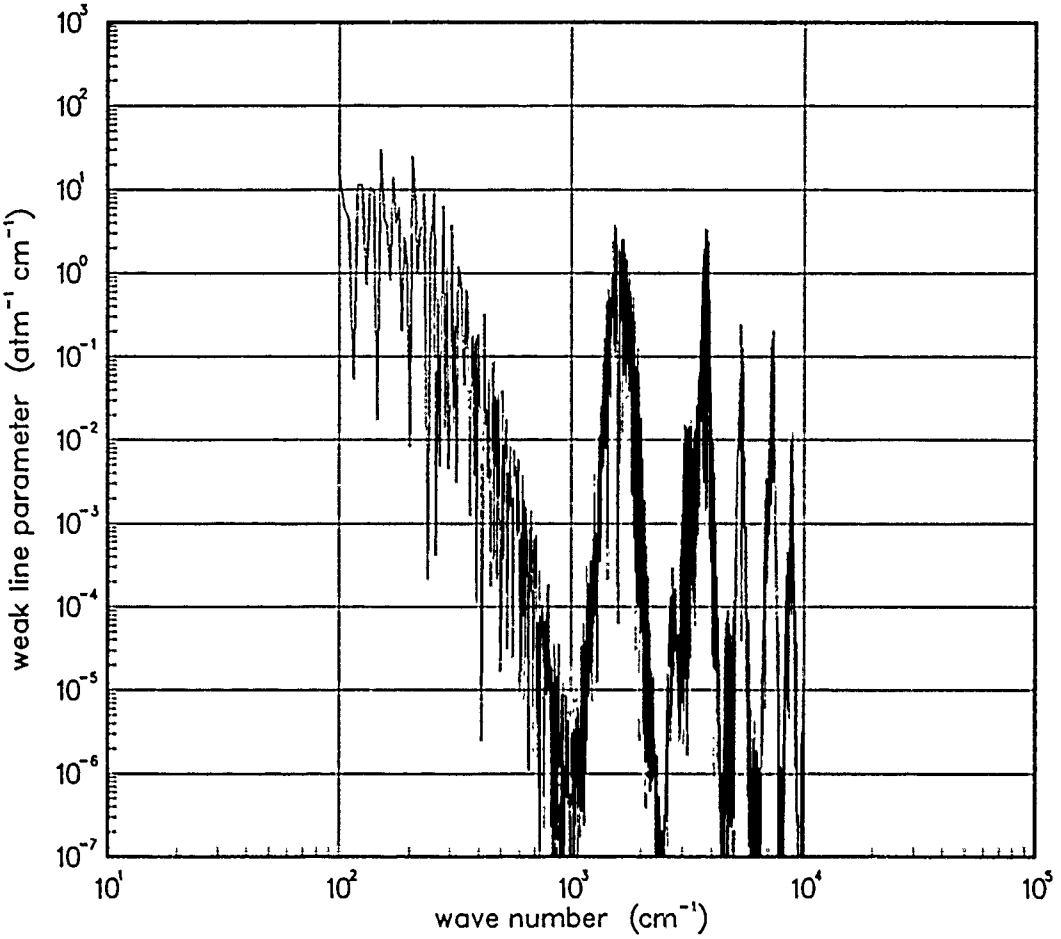

Figure 266. Weak-line parameter for H_2O at 200°K.

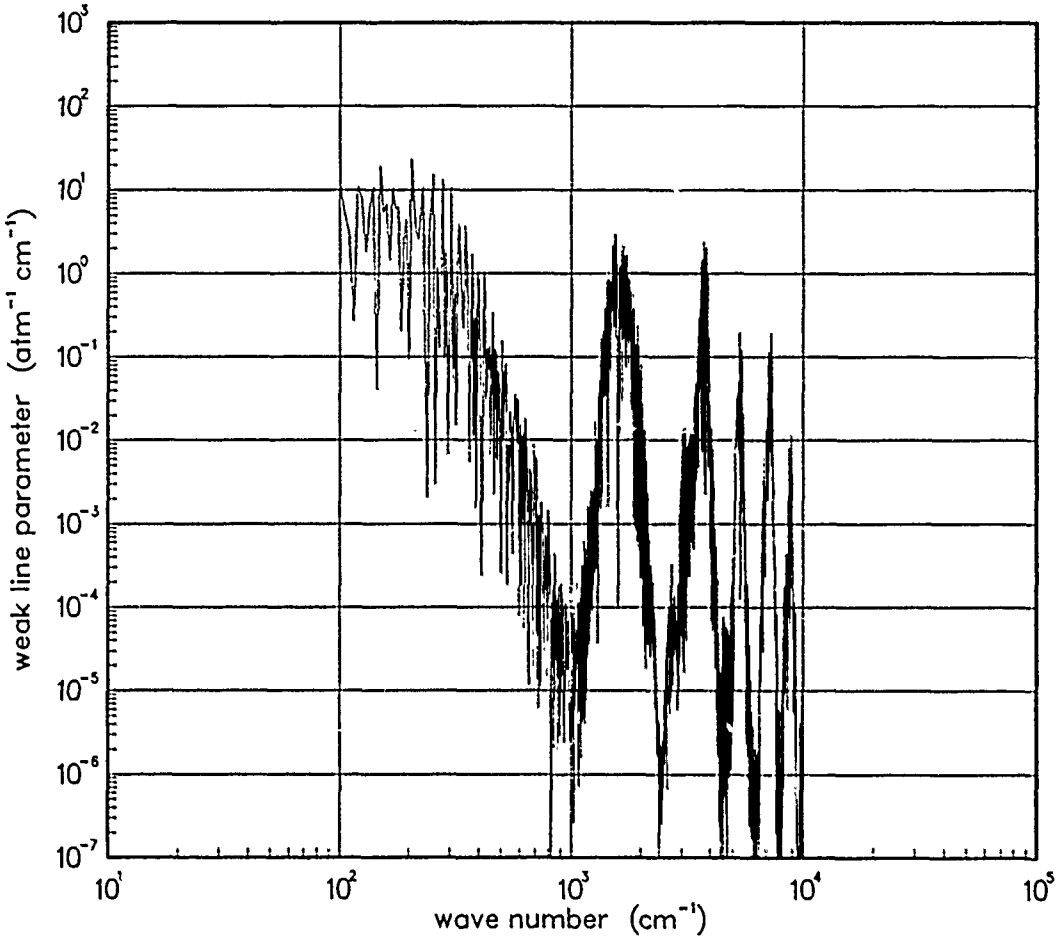

Figure 267. Weak-line parameter for H_2O at 300°K.

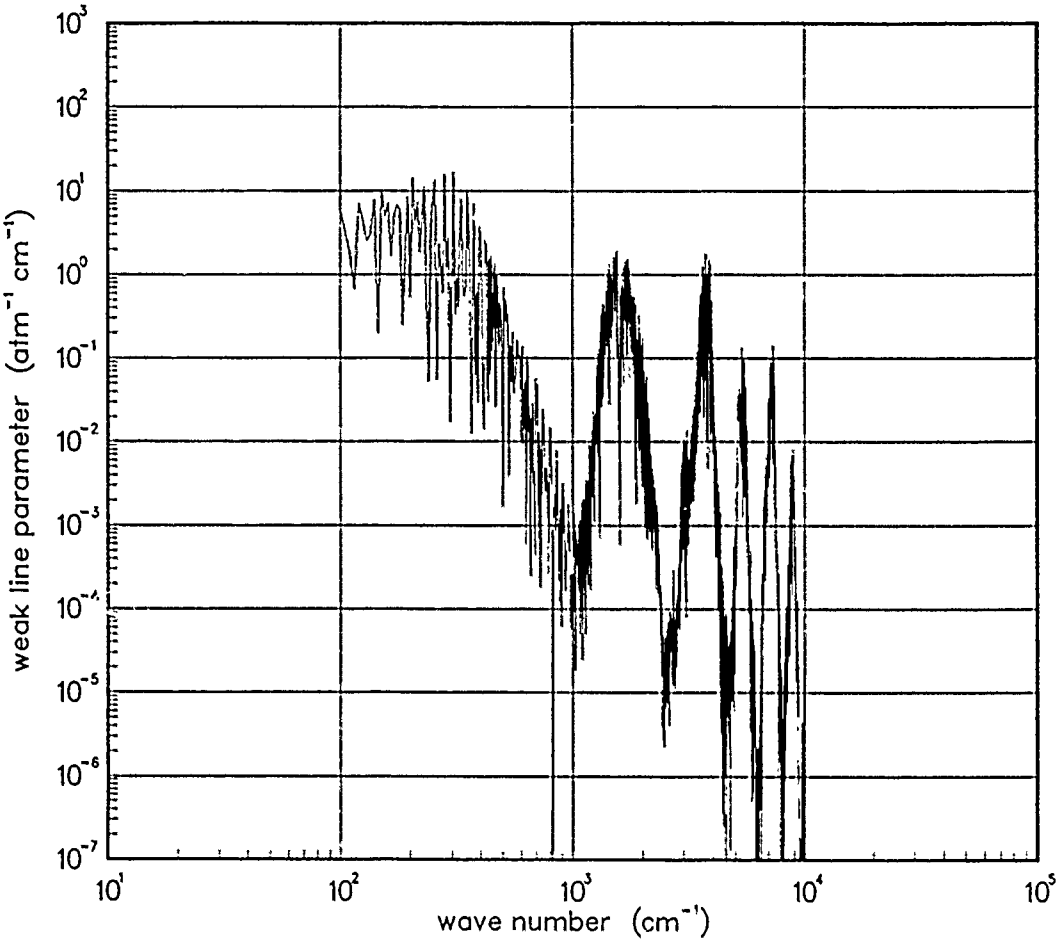

Figure 268. Weak-line parameter for H_2O at 500°K.

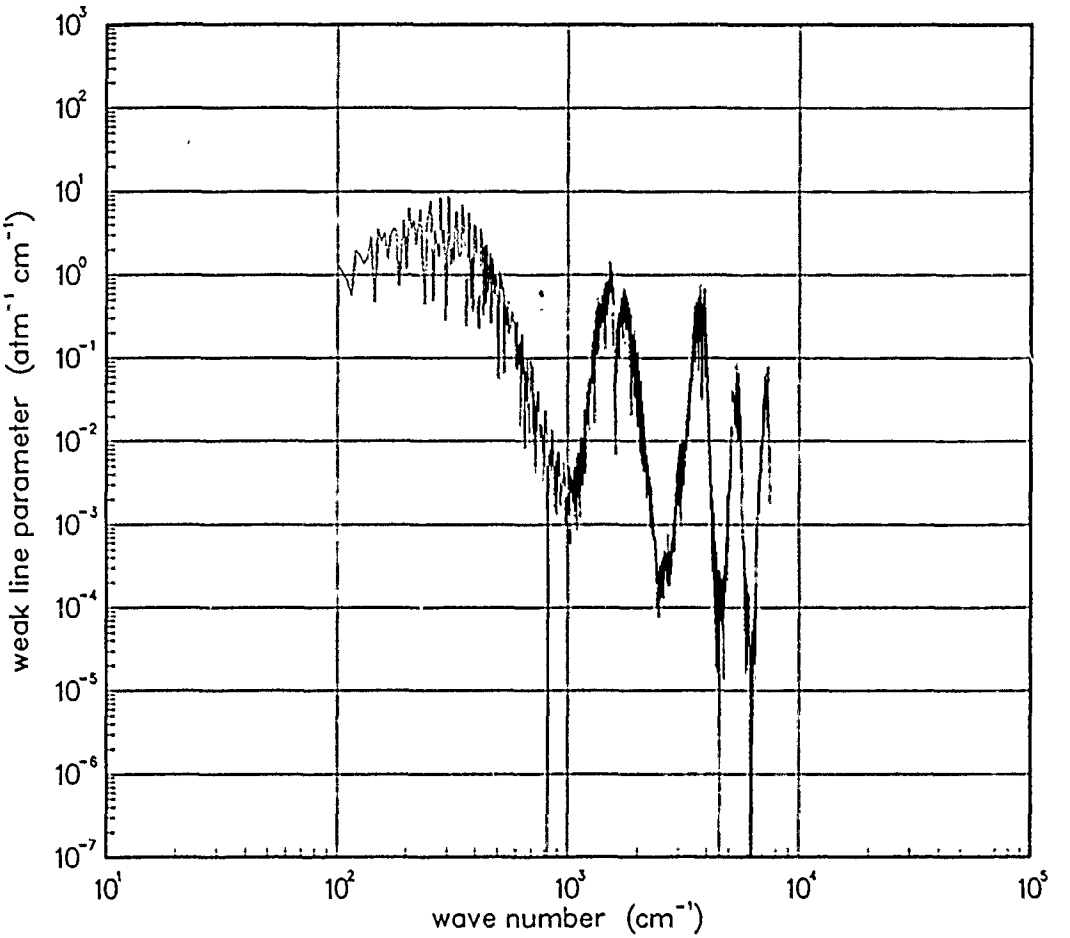

Figure 269. Weak-line parameter for H_2O at 750°K.

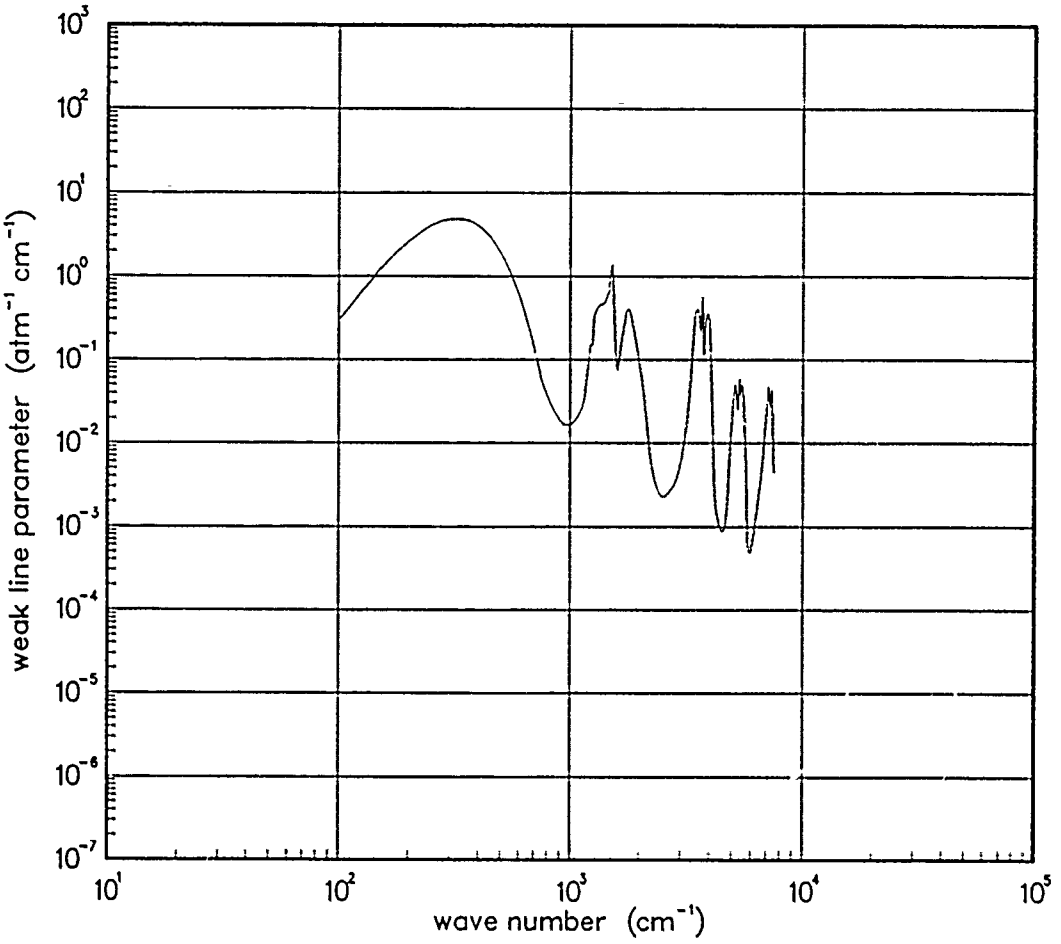

Figure 270. Weak-line parameter for H_2O at 1000°K.

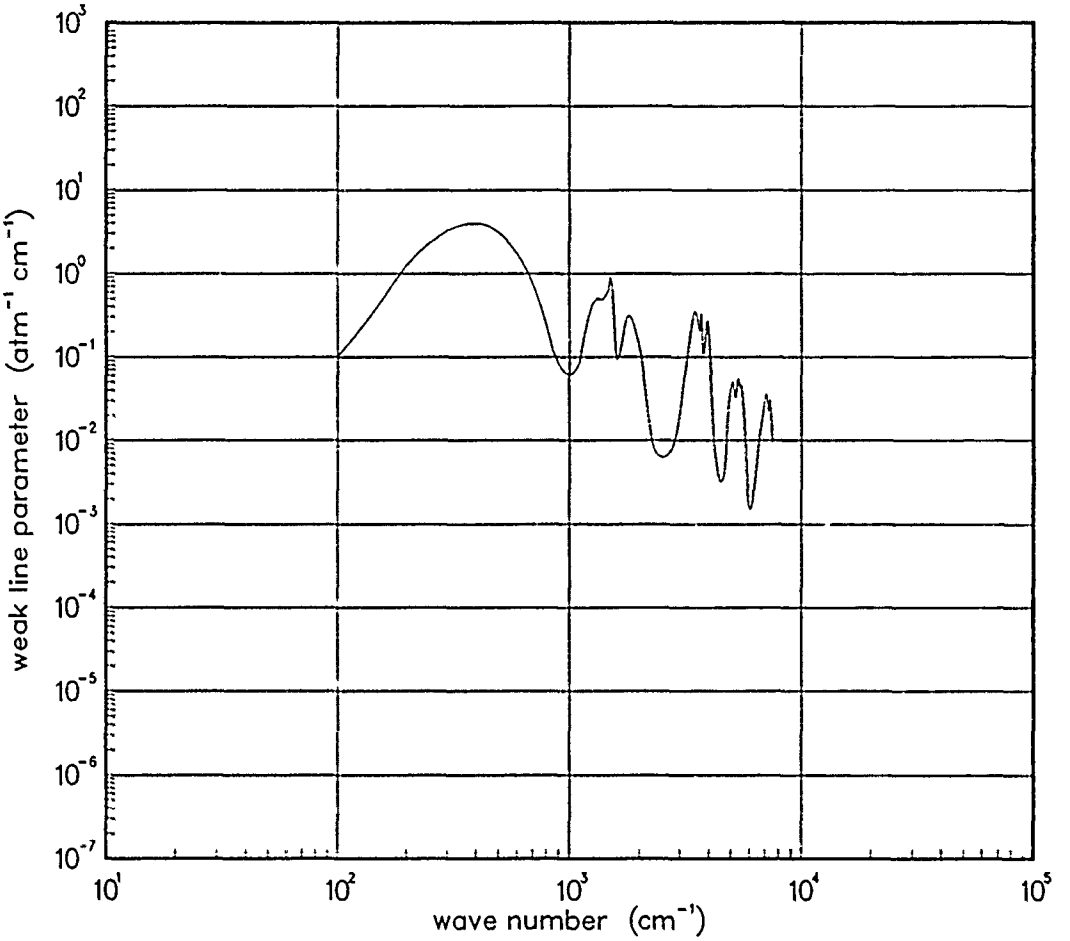

Figure 271. Weak-line parameter for H_2O at 1500°K.

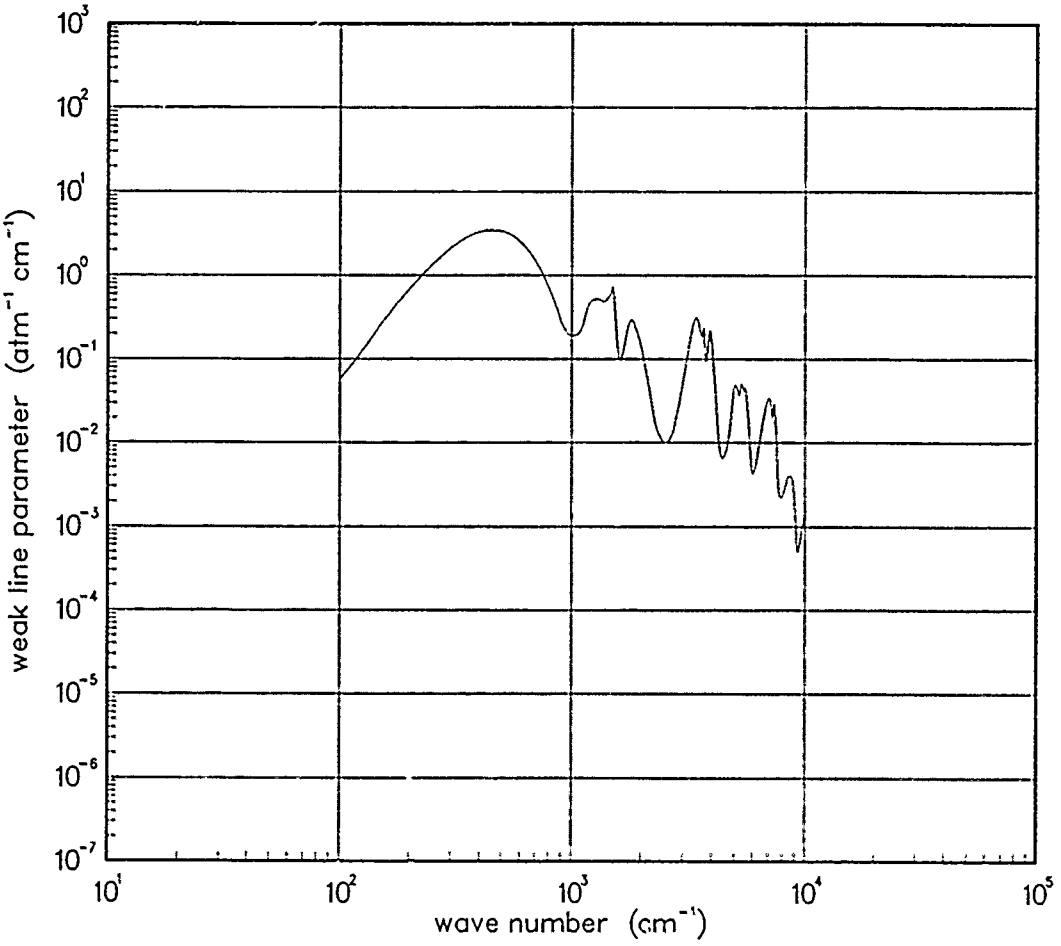

Figure 272. Weak-line parameter for H_2O at 2000°K.

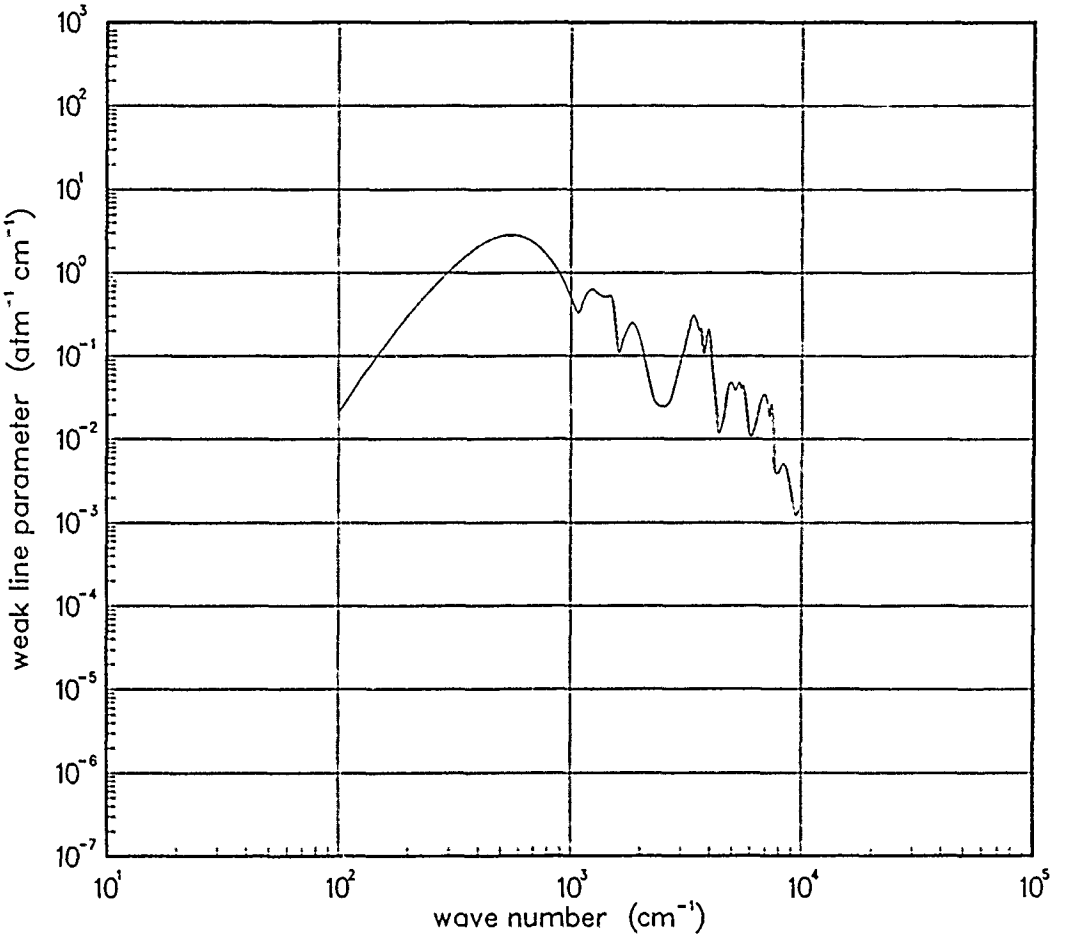

Figure 273. Weak-line parameter for H_2O at 3000°K.

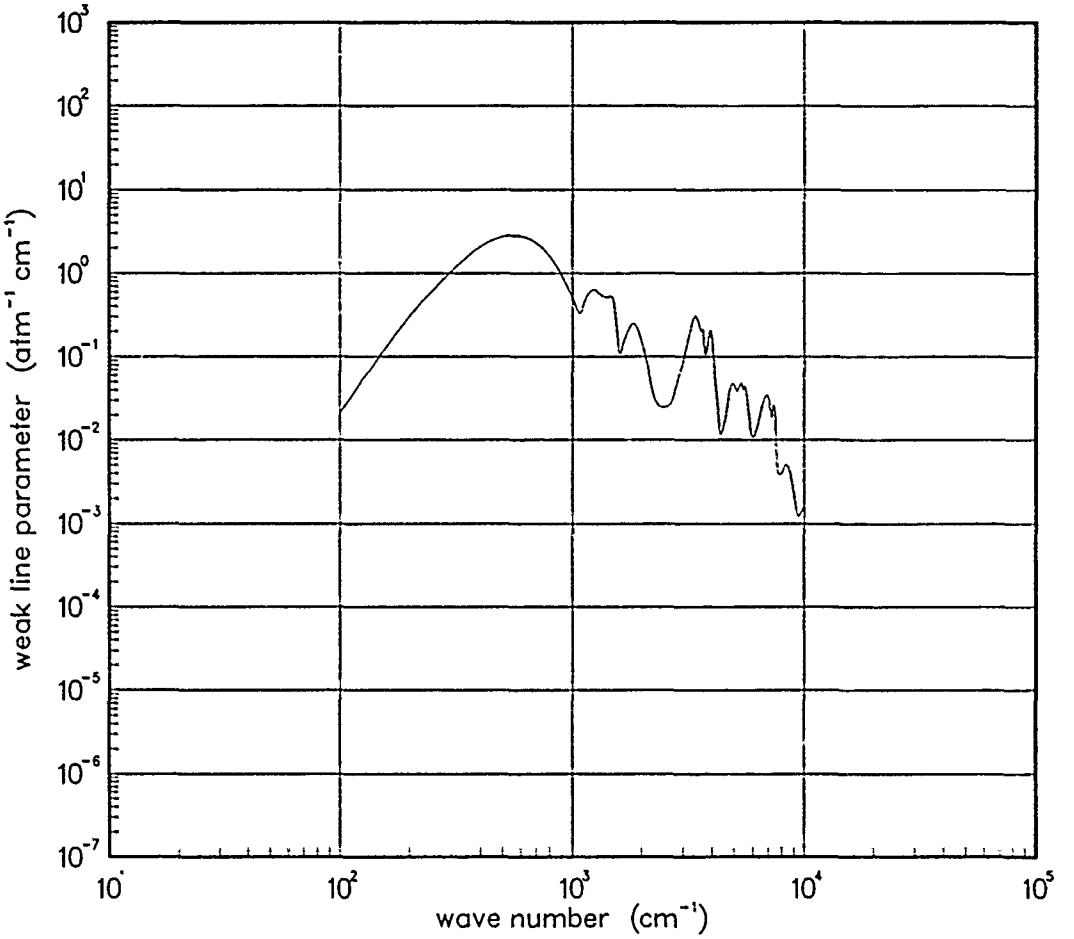

Figure 274. Weak-line parameter for H_2O at 5000°K.

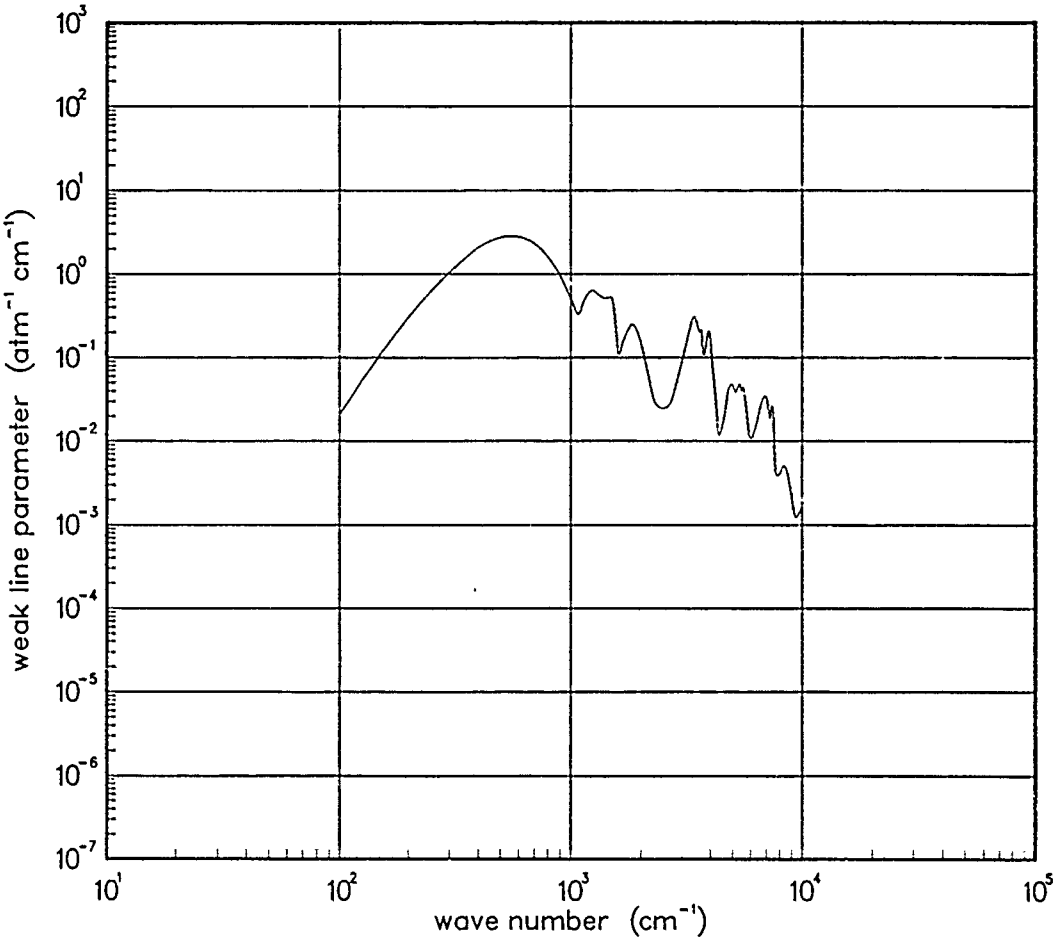

Figure 275. Weak-line parameter for H_2O at 7000°K.

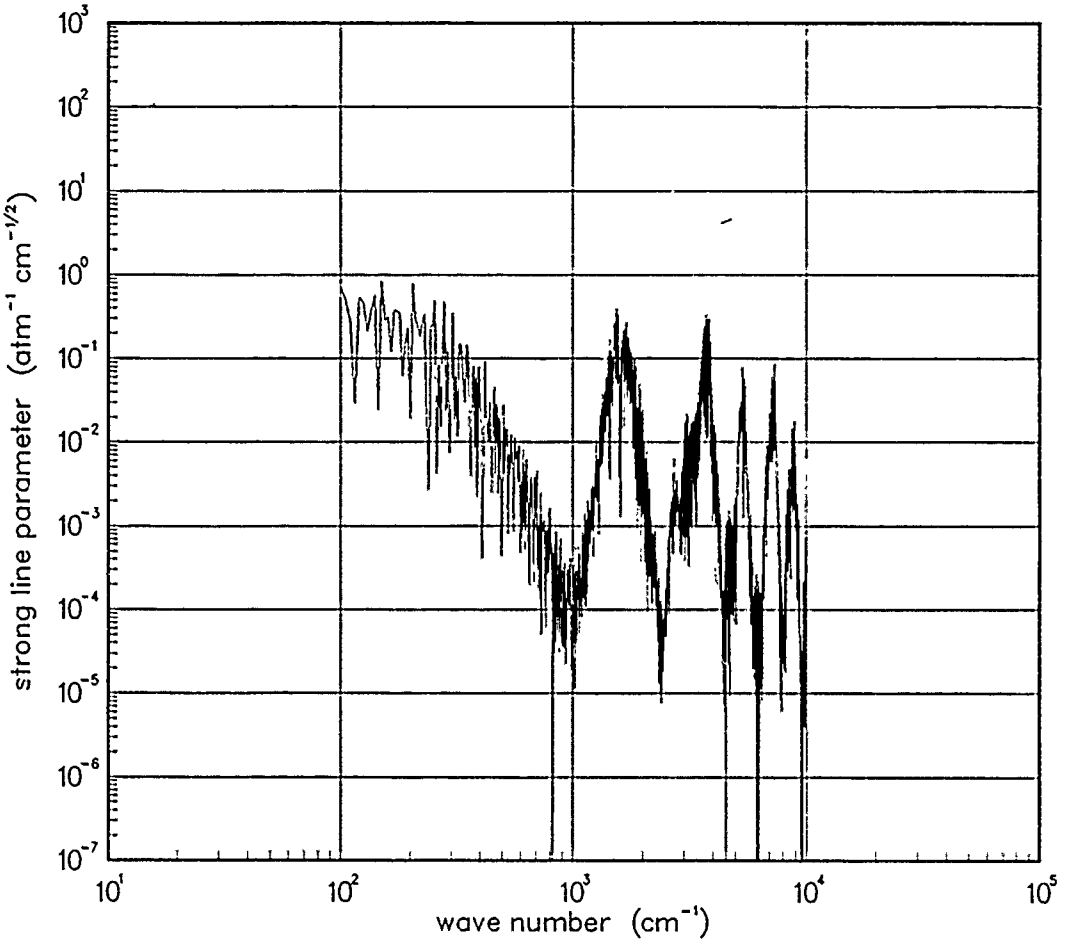

Figure 276. Strong-line parameter for H_2O at 200°K.

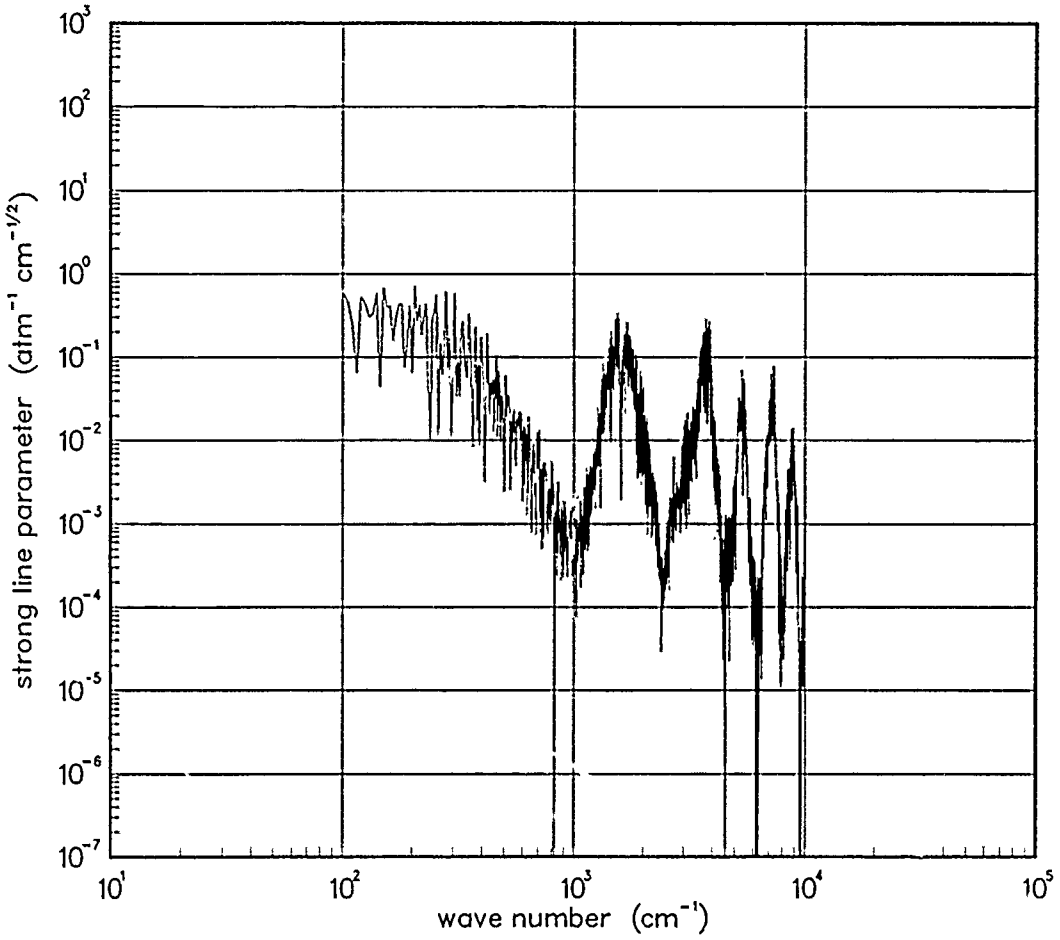

Figure 277. Strong-line parameter for H_2O at 300°K.

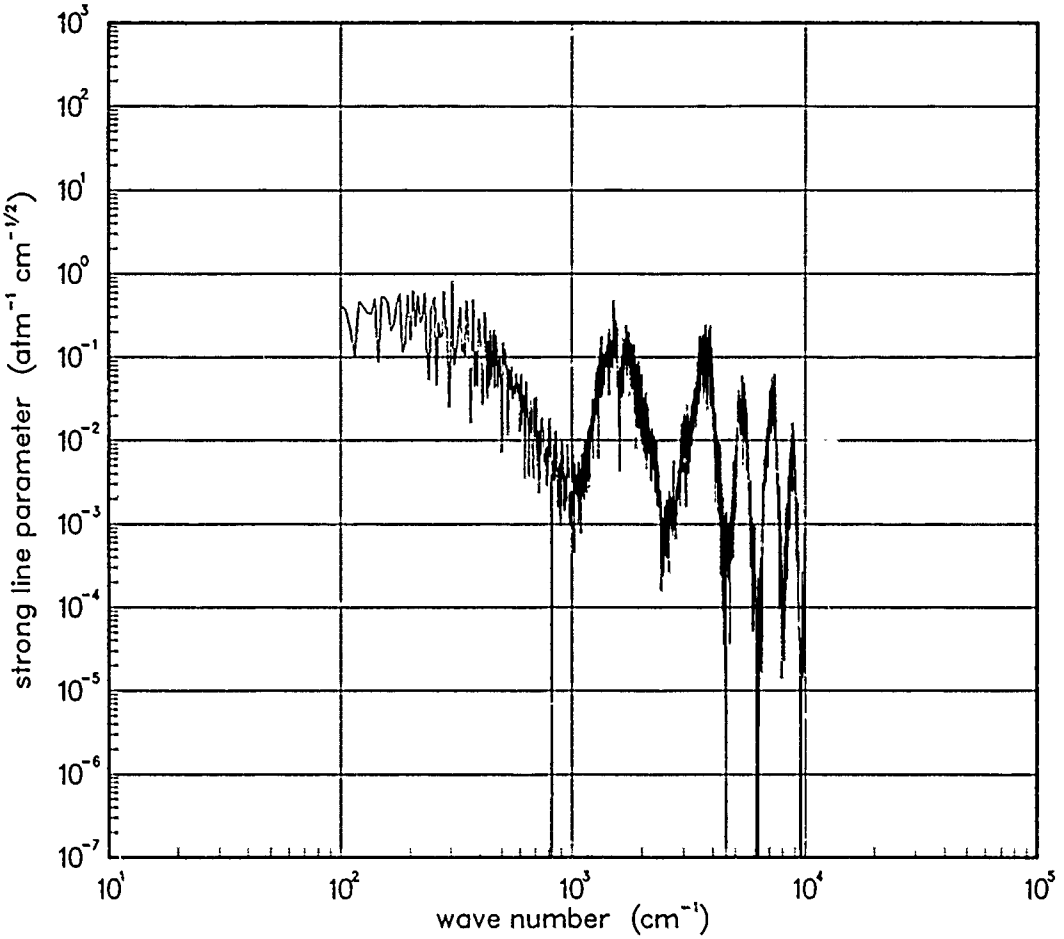

Figure 278. Strong-line parameter for H_2O at 500°K.

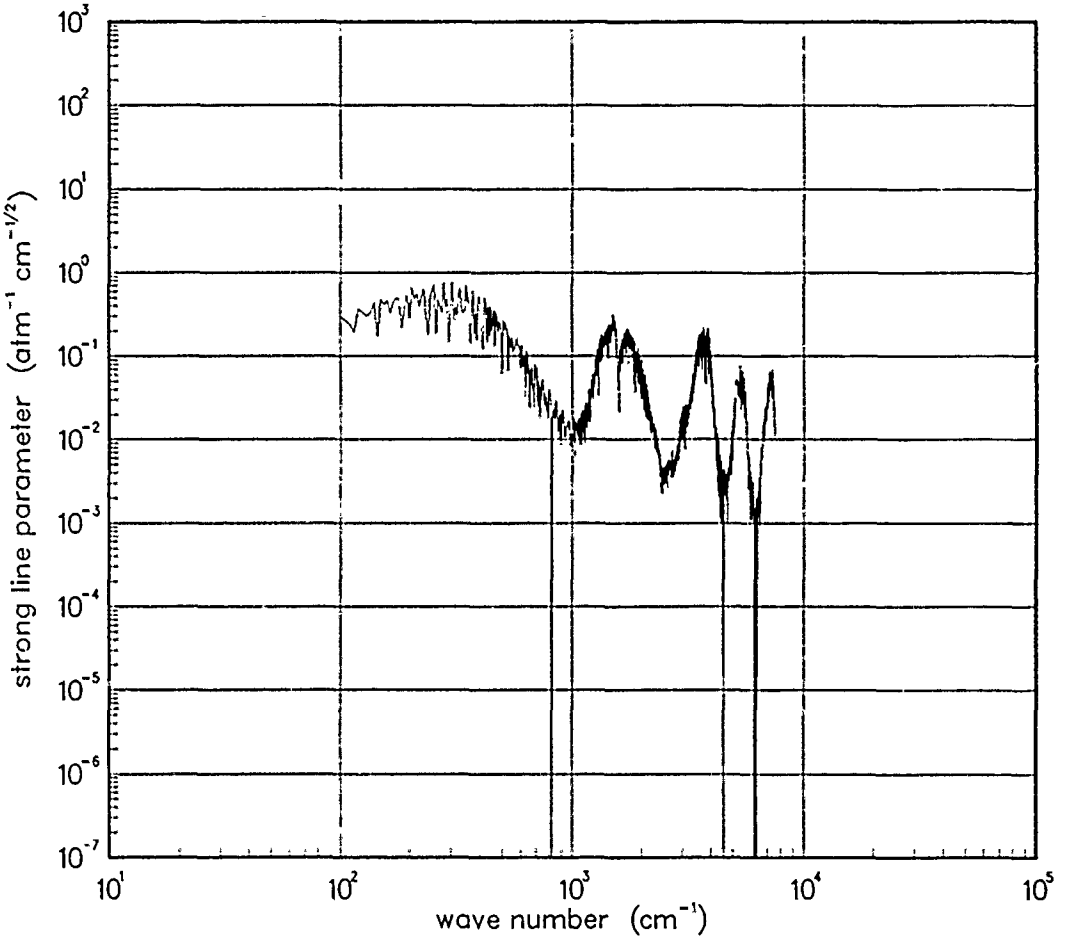

Figure 279. Strong-line parameter for H_2O at 750°K.

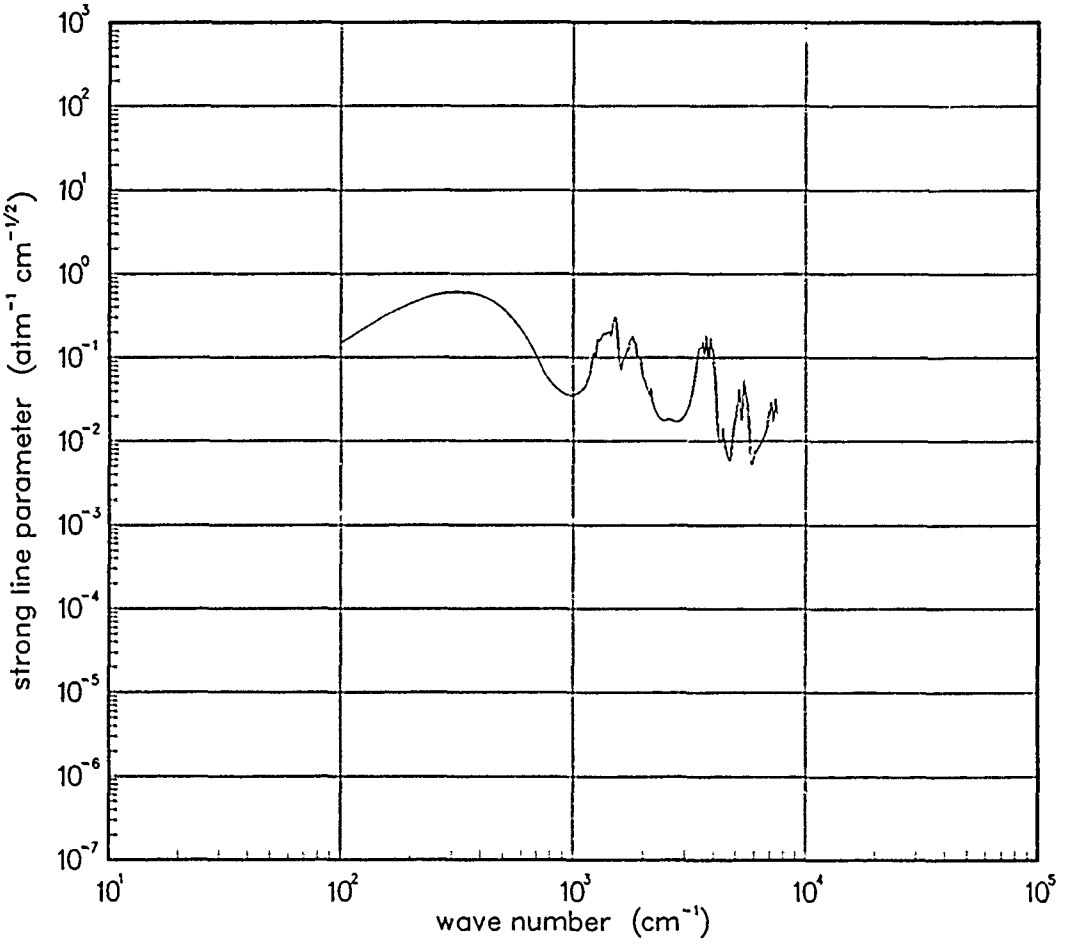

Figure 280. Strong-line parameter for H_2O at 1000°K.

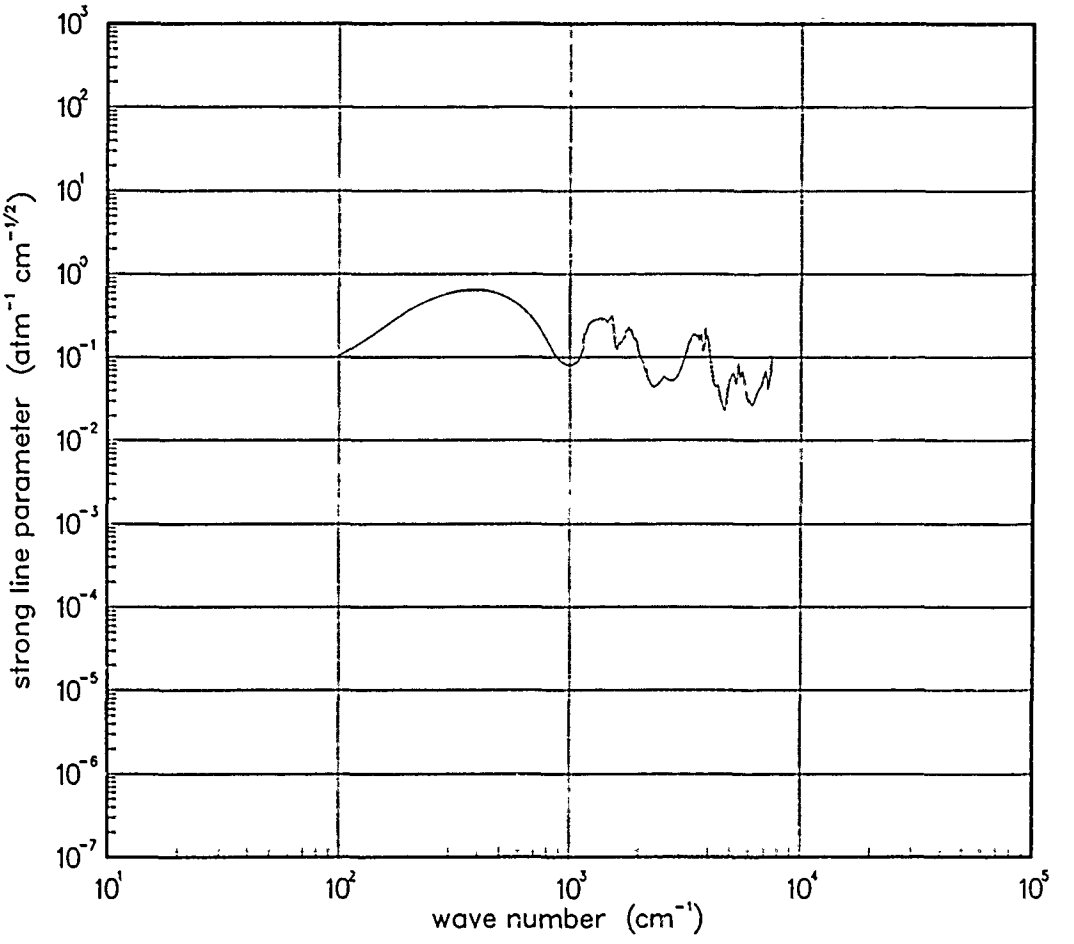

Figure 281. Strong-line parameter for H_2O at 1500°K.

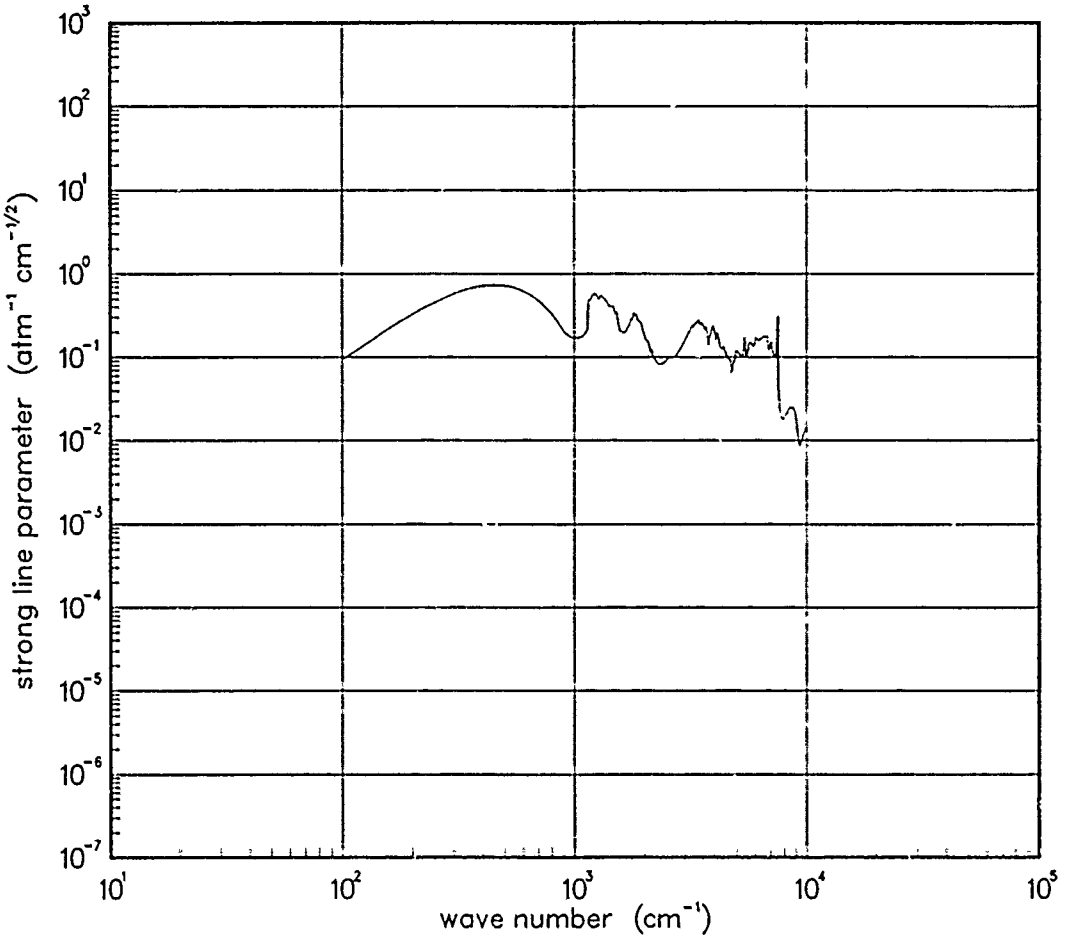

Figure 282. Strong-line parameter for H_2O at 2000°K.

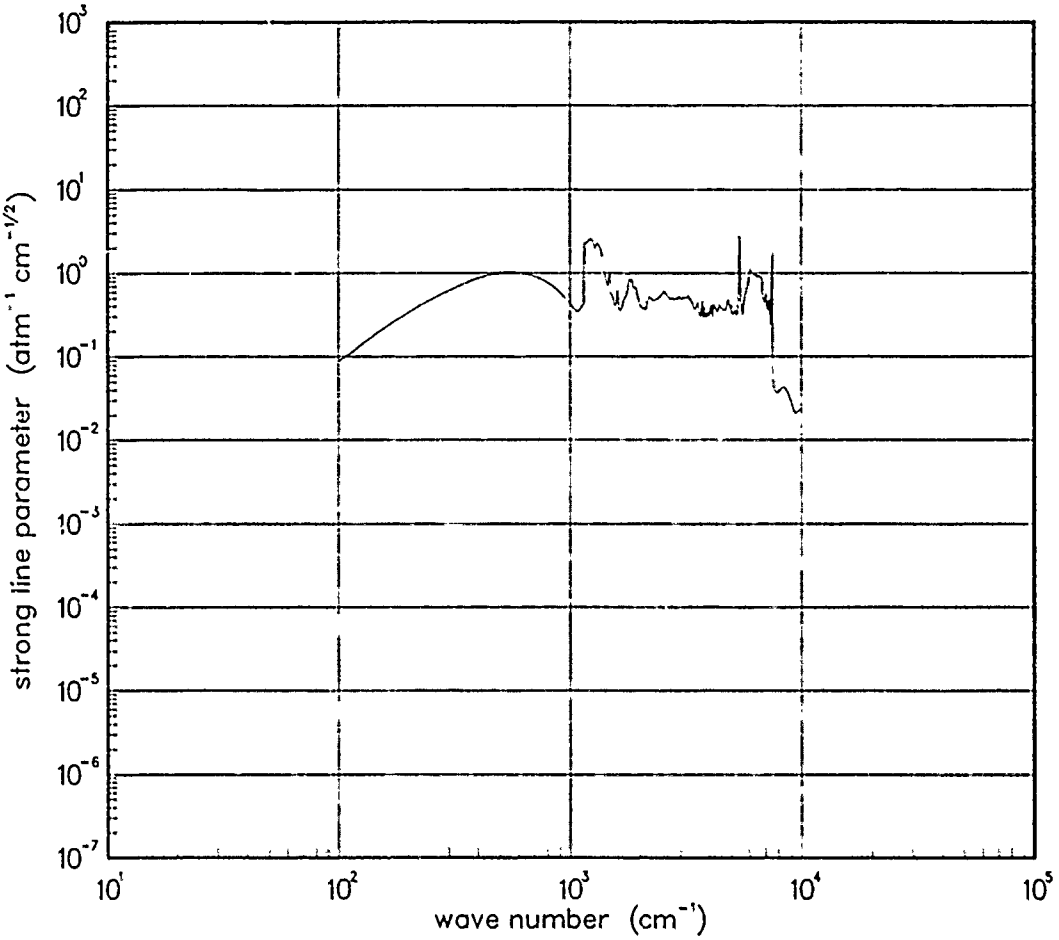

Figure 283. Strong-line parameter for H_2O at 3000°K.

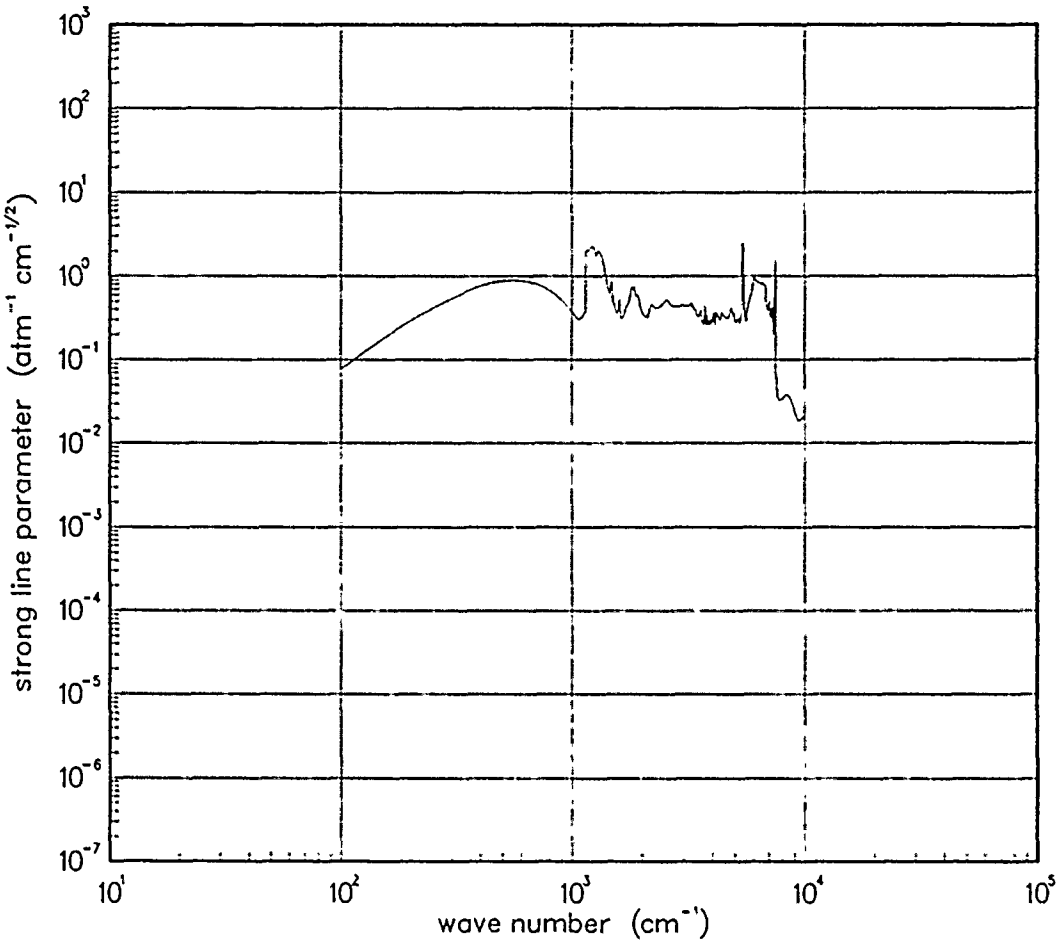

Figure 284. Strong-line parameter for H_2O at 5000°K.

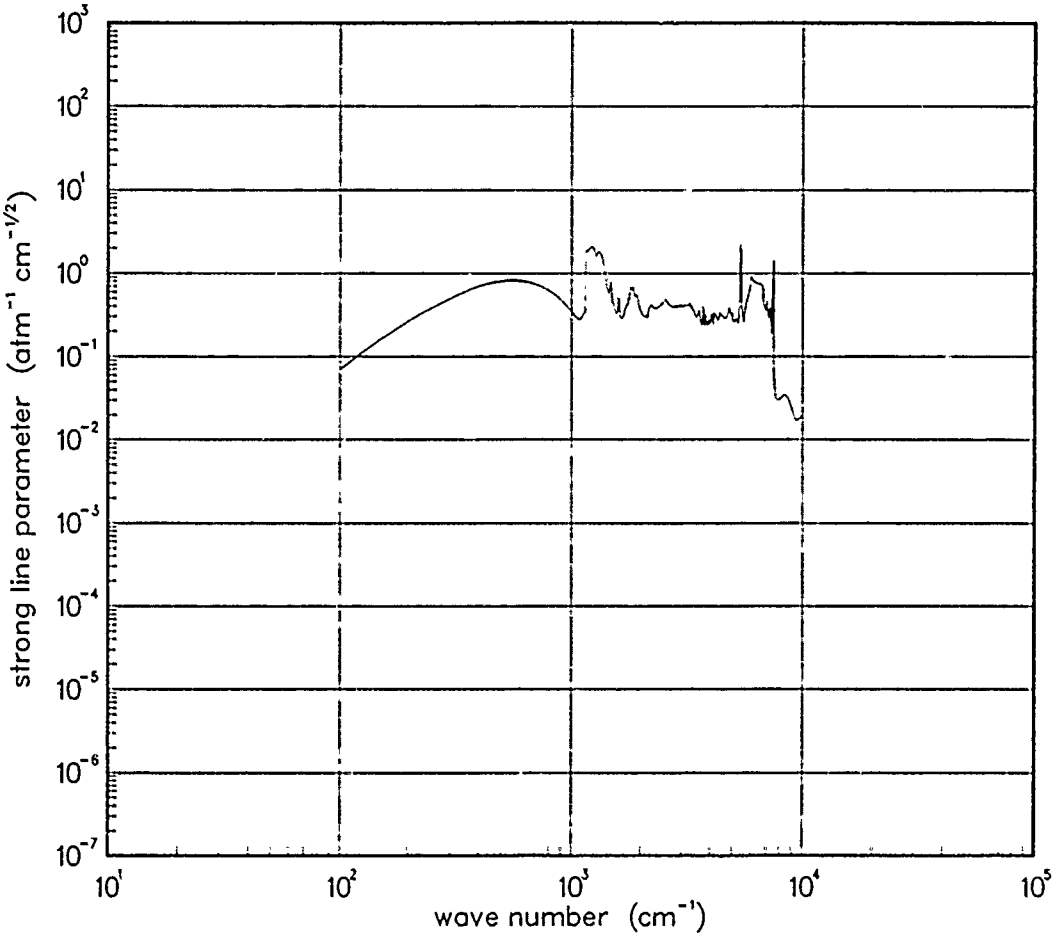

Figure 285. Strong-line parameter for H_2O at 7000°K.

SECTION 6
METAL OXIDES

LTE information for all of the metal oxides within the spectral range: 10 - 10,000 cm^{-1} have been computed using the DATE code. The DATE code has been discussed in detail in Reference 3.

6.1 ALUMINUM OXIDE (AℓO).

Aluminum Oxide at temperatures from 200 - 18,000 °K was calculated using the DATE code.

Table 7. Spectroscopic data for AℓO.

$X\ ^2\Sigma^+$

$\omega_e = 979.23^*$ $\omega_e x_e = 6.97^*$ $A_e = 123.61$
$\alpha_e = 0.0058^*$ $B_e = .64136^*$ $E_e = 0.0$

$S_{10} = 204.0^\dagger$ $S_{20} = 1.05^\dagger$ $S_{30} = 0.00381^\dagger$

$\gamma_\ell(300°K) = 0.04^\S$

Data Source:

*B. Rosen, ed.,Spectroscopic Data Relative to Diatomic Molecules, Pergamon Press, New York (1970).

†H.H. Michels, Diatomic Oxide Vibrational Band Intensities , United Aircraft Research Laboratories, K921094-4 (May 1971).

‡J.K. McDonald, and K.K. Innes, A Low-Lying Excited Electronic State of the AℓO Molecule and the Ground-State Dissociation Energy, Journal of Molecular Spectroscopy, 32, pp 501-510 (1969).

§Estimate

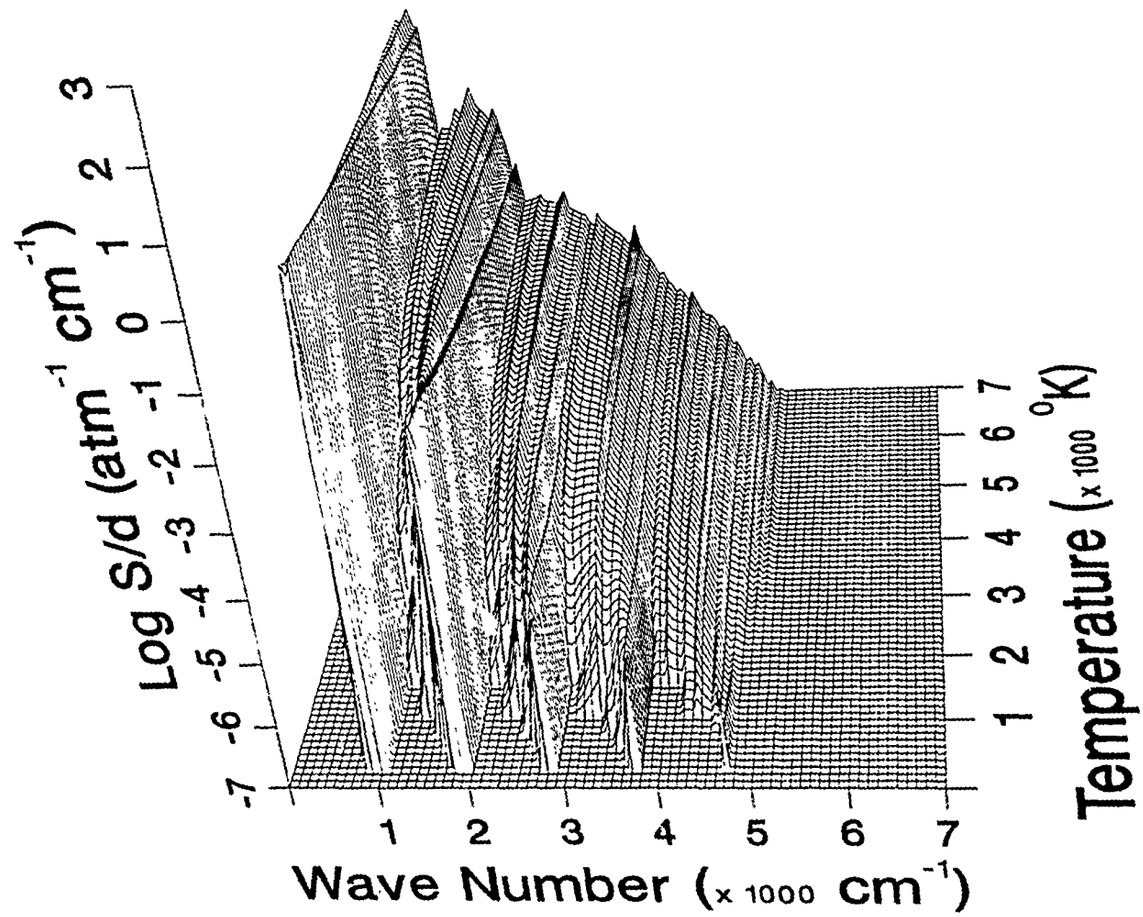

Figure 286. Weak-line parameter for A&O.

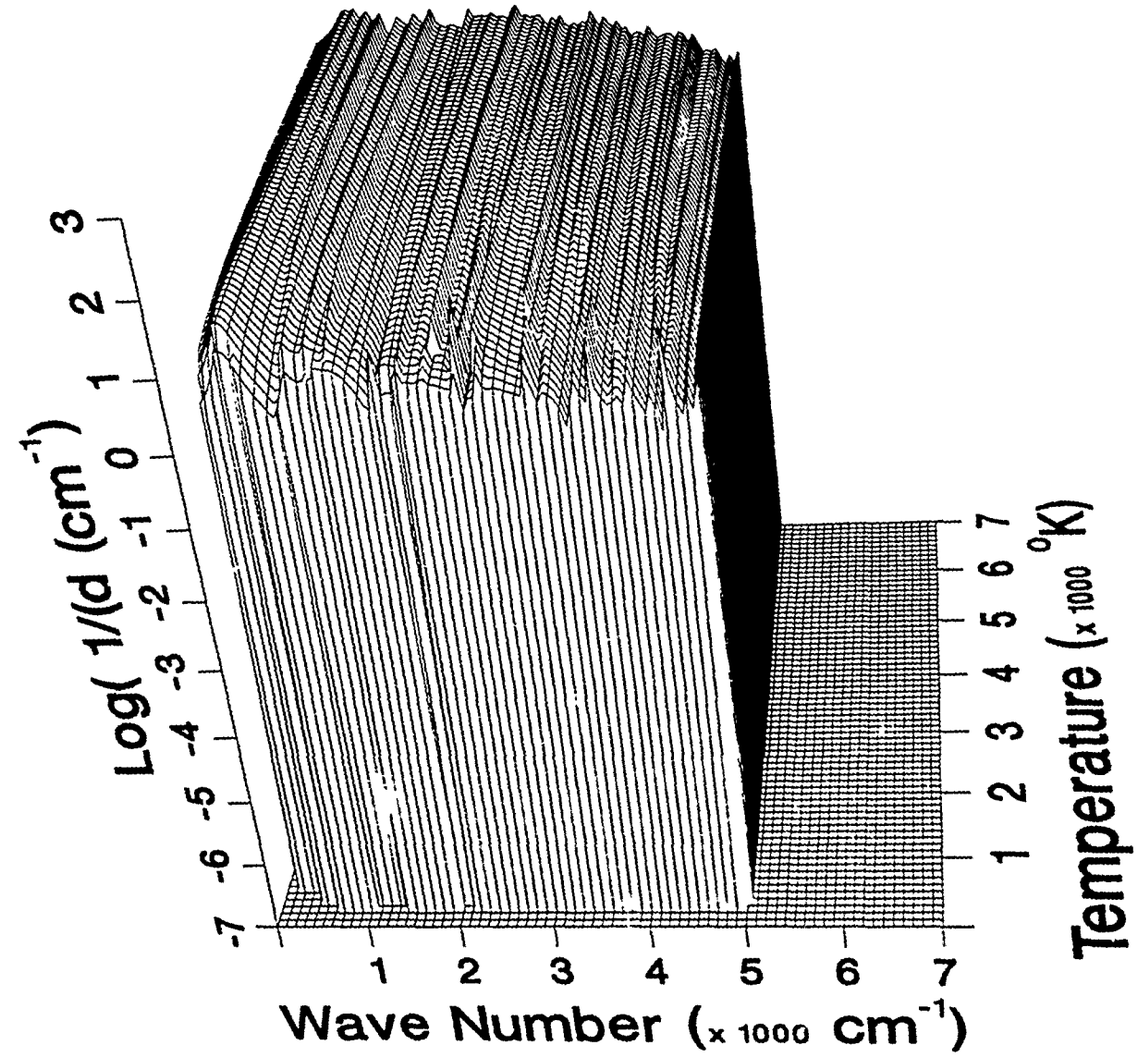

Figure 287. Inverse line spacing for AℓO.

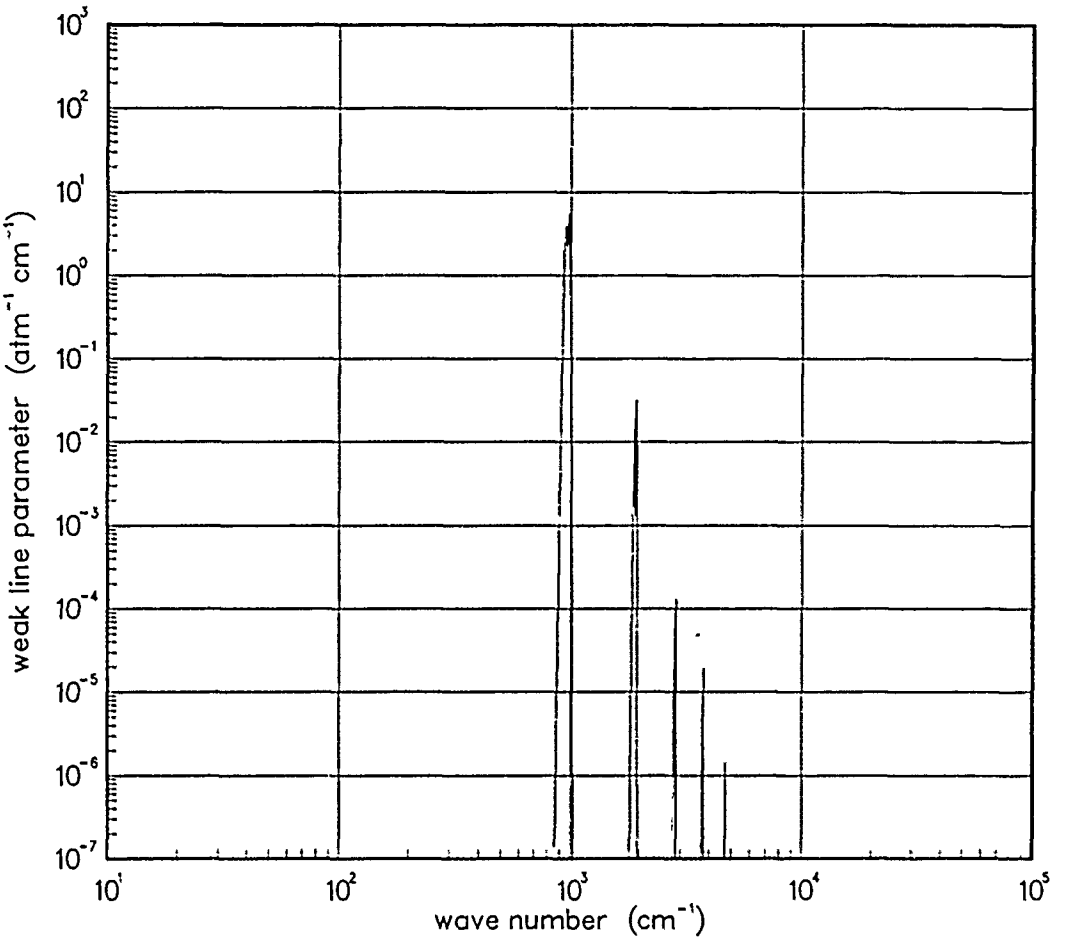

Figure 288. Weak-line parameter for AℓO at 200°K.

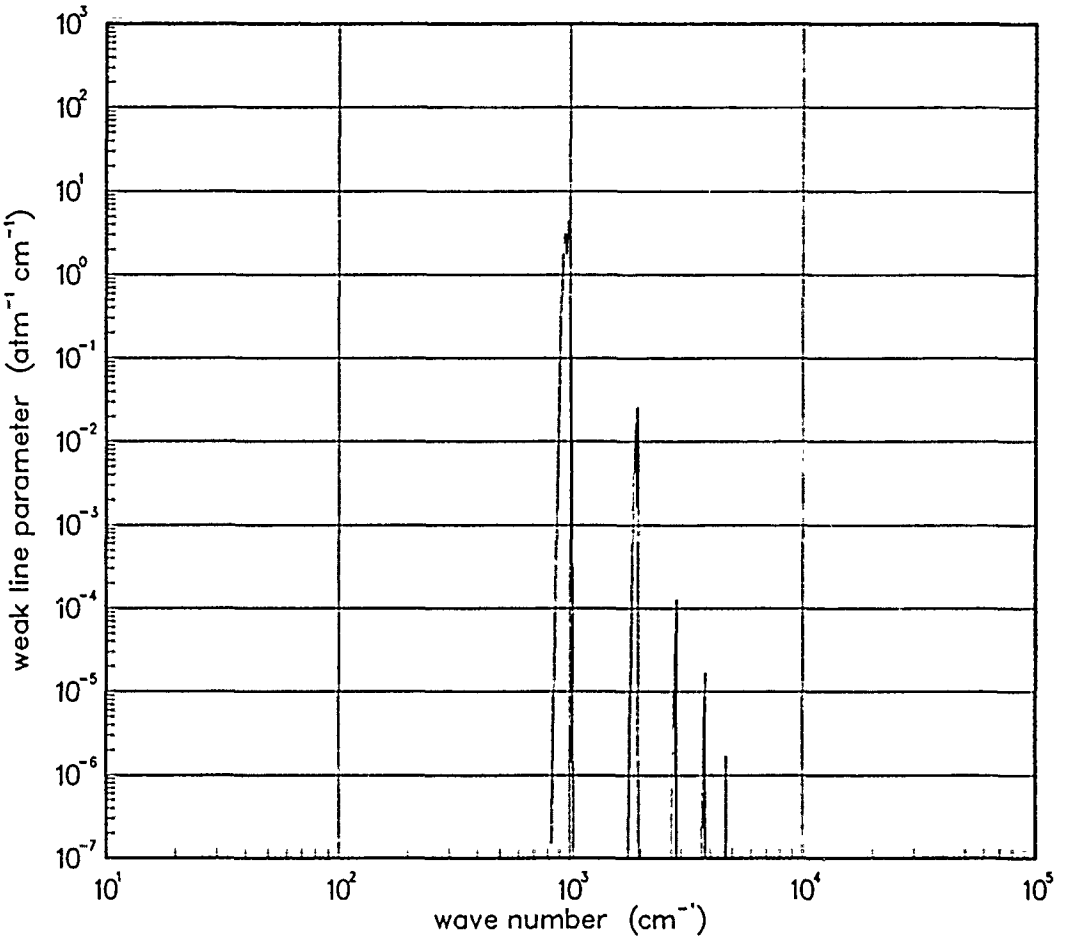

Figure 289. Weak-line parameter for AℓO at 300°K.

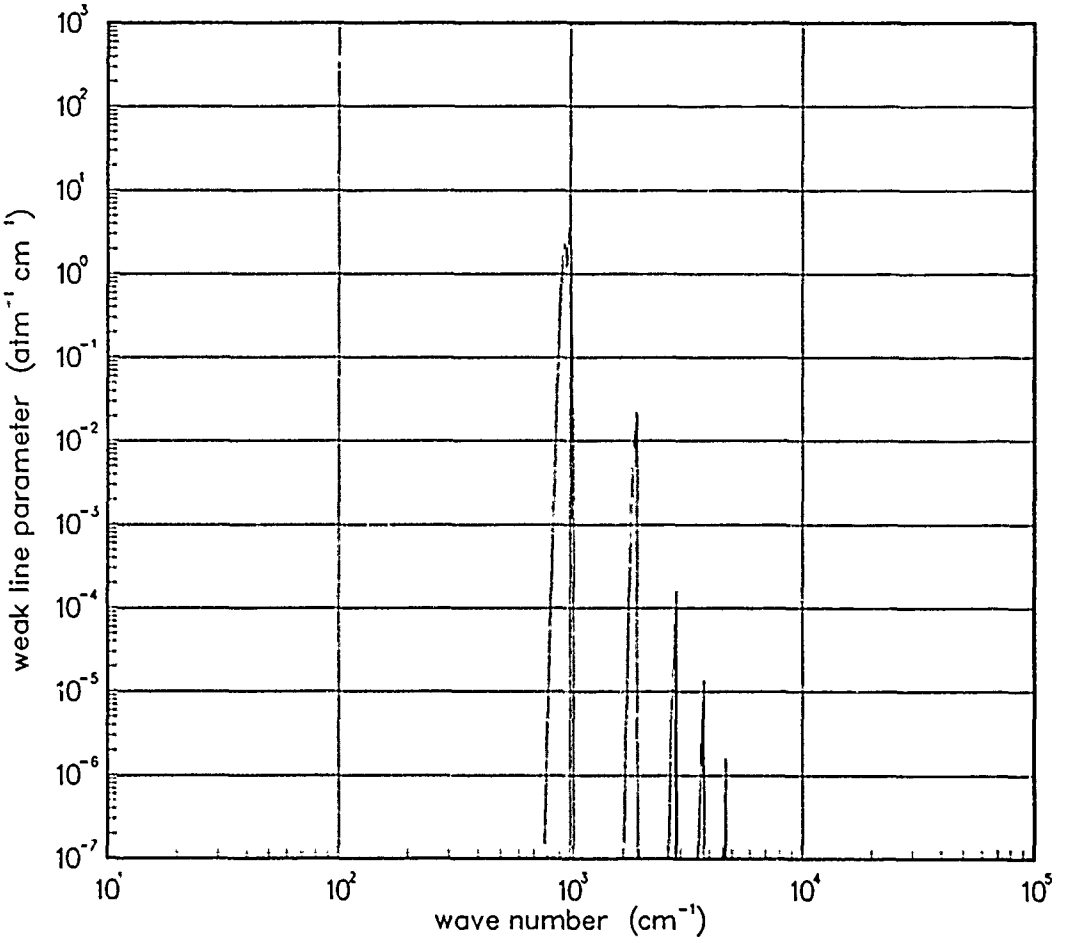

Figure 290. Weak-line parameter for AℓO at 500°K.

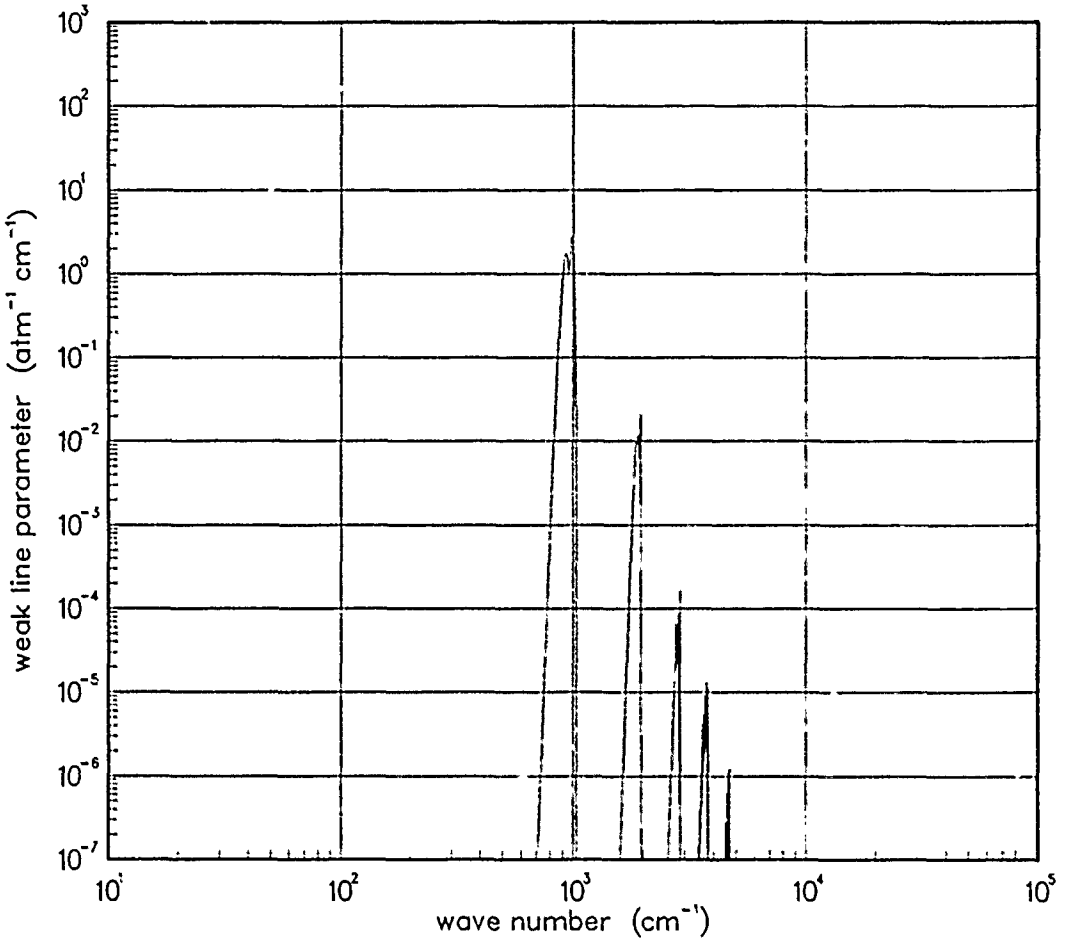

Figure 291. Weak-line parameter for AℓO at 750°K.

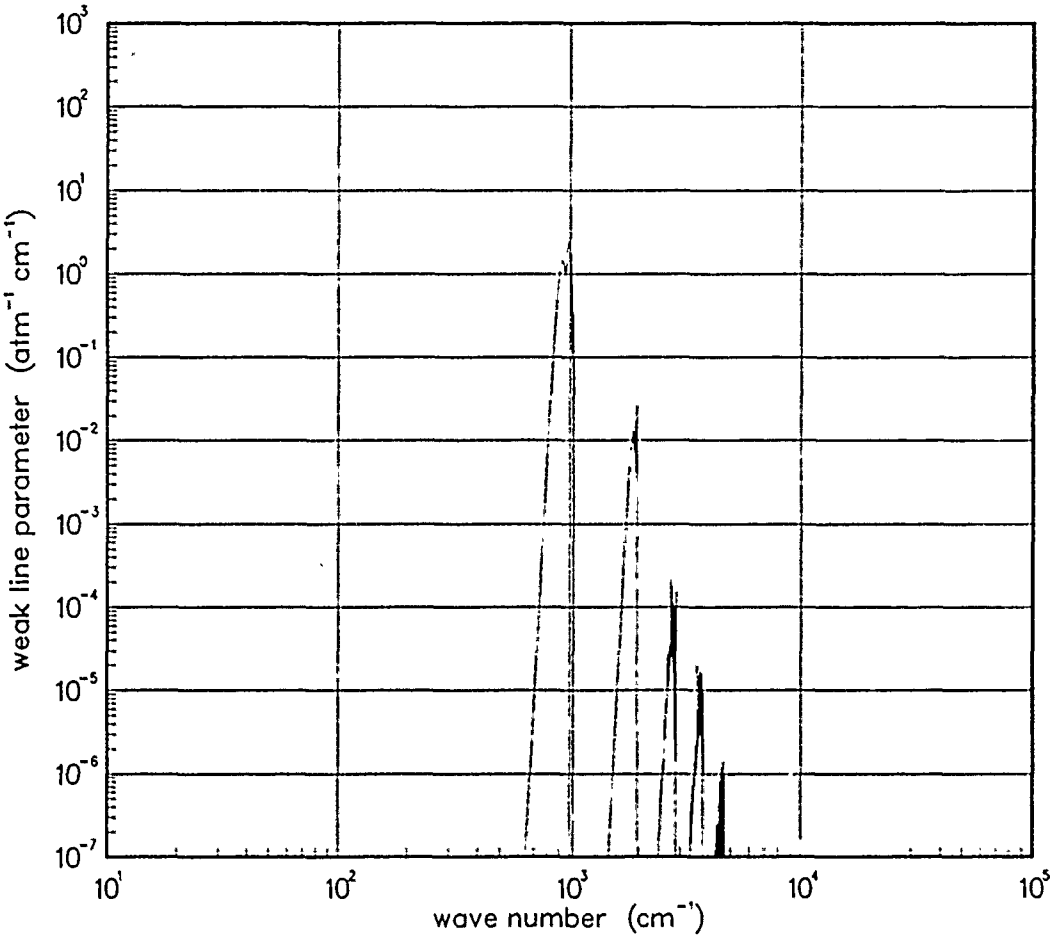

Figure 292. Weak-line parameter for AℓO at 1000°K.

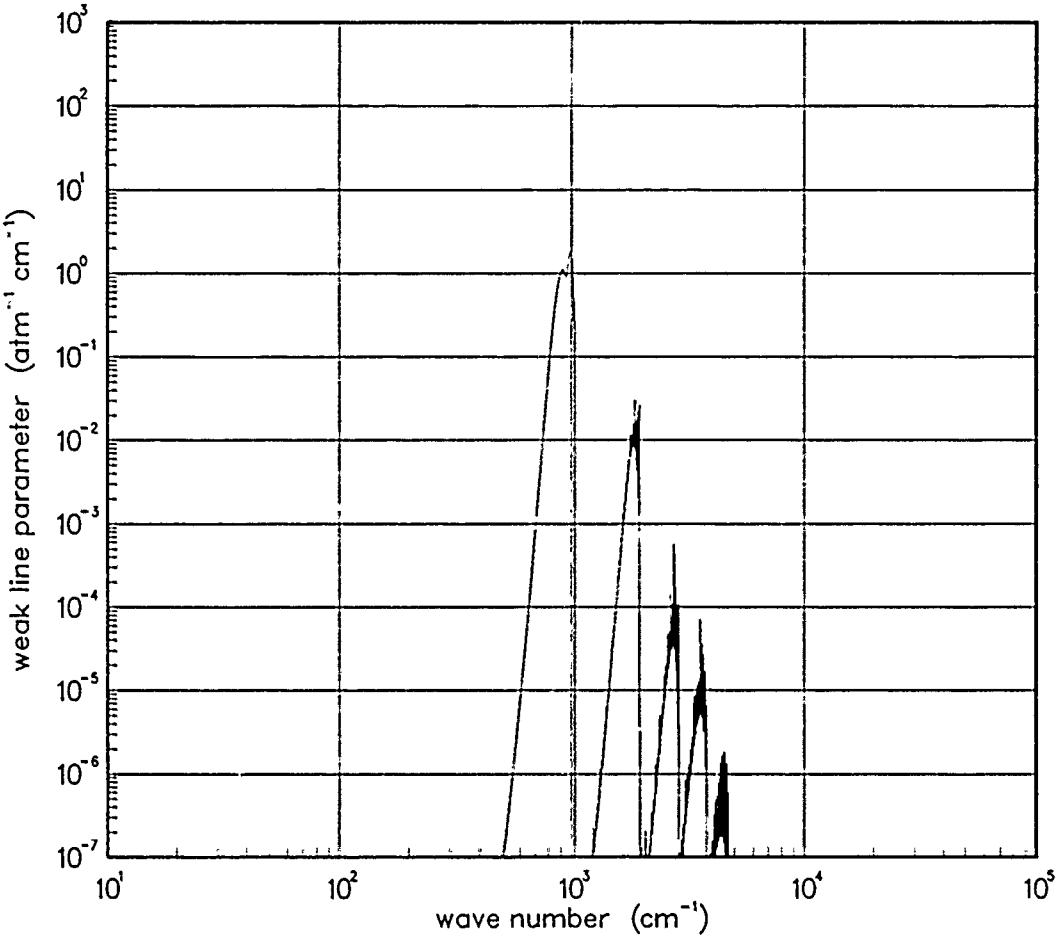

Figure 293. Weak-line parameter for AℓO at 1500°K.

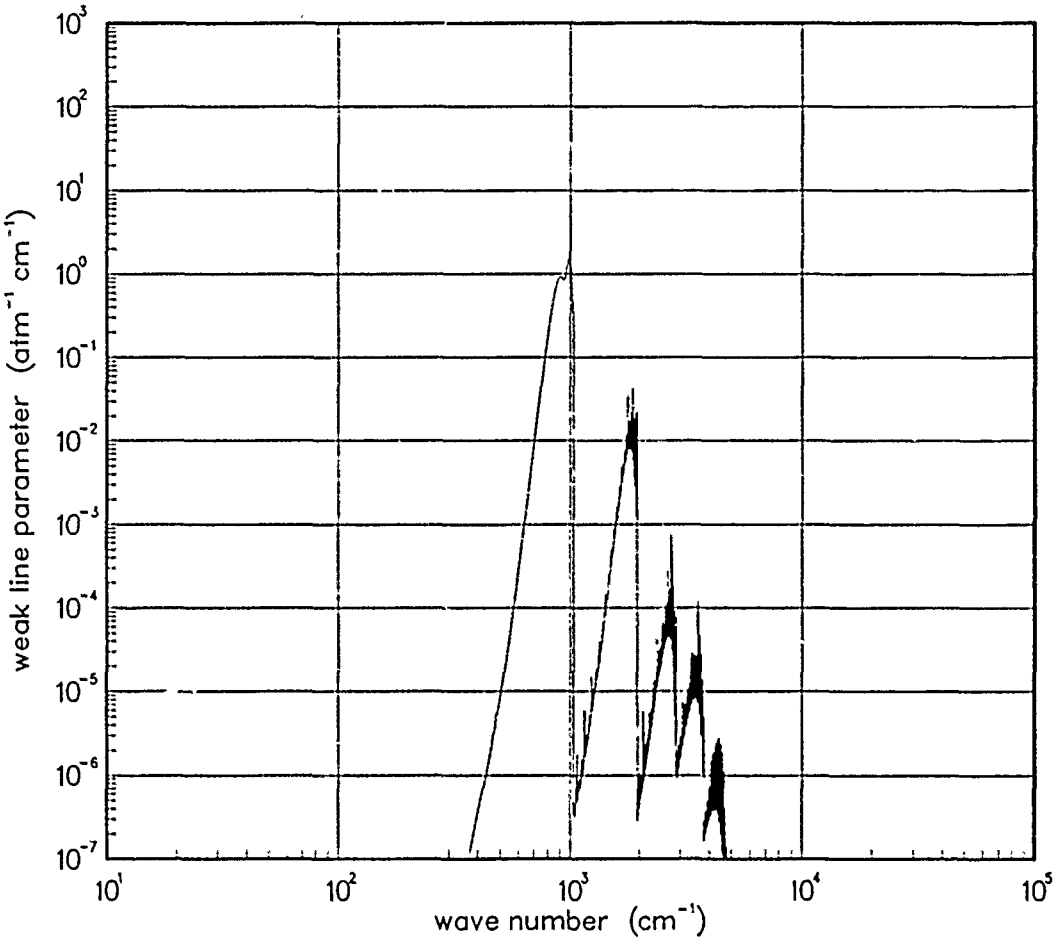

Figure 294. Weak-line parameter for AℓO at 2000°K.

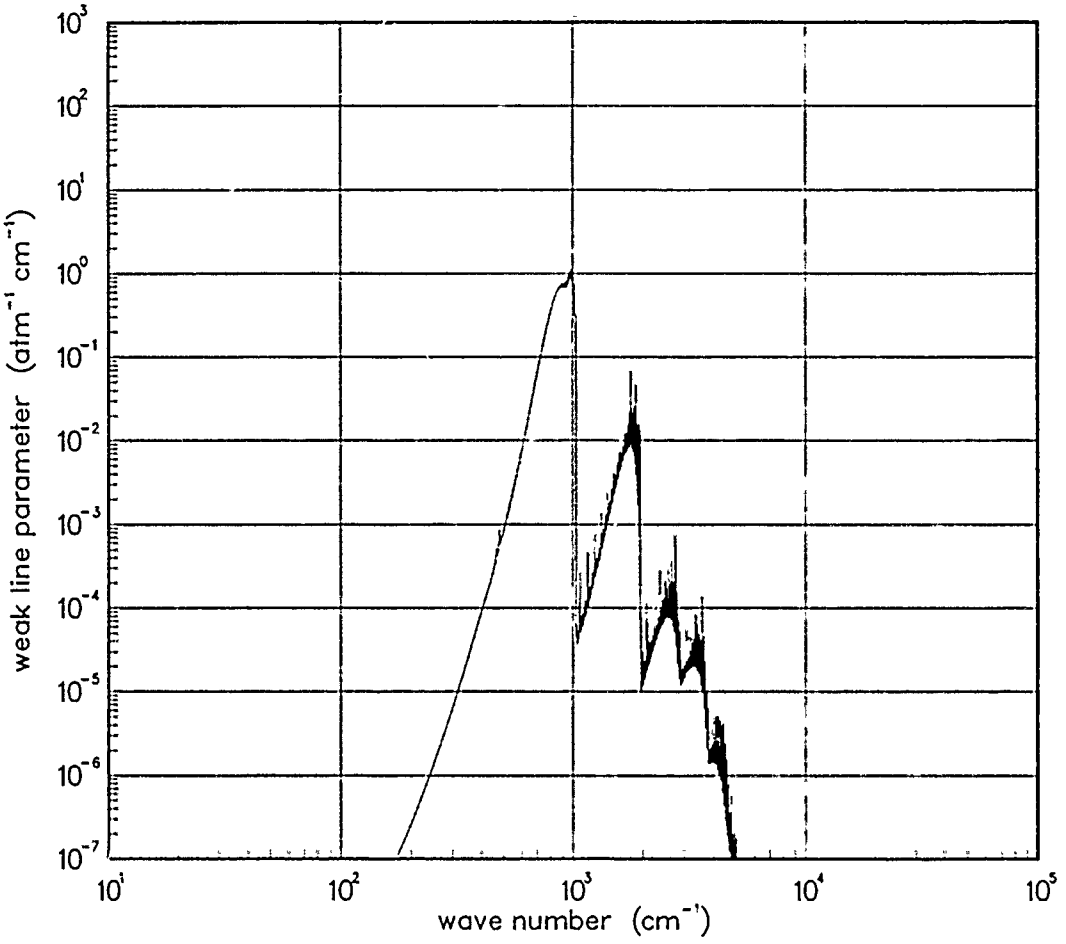

Figure 295. Weak-line parameter for AℓO at 3000°K.

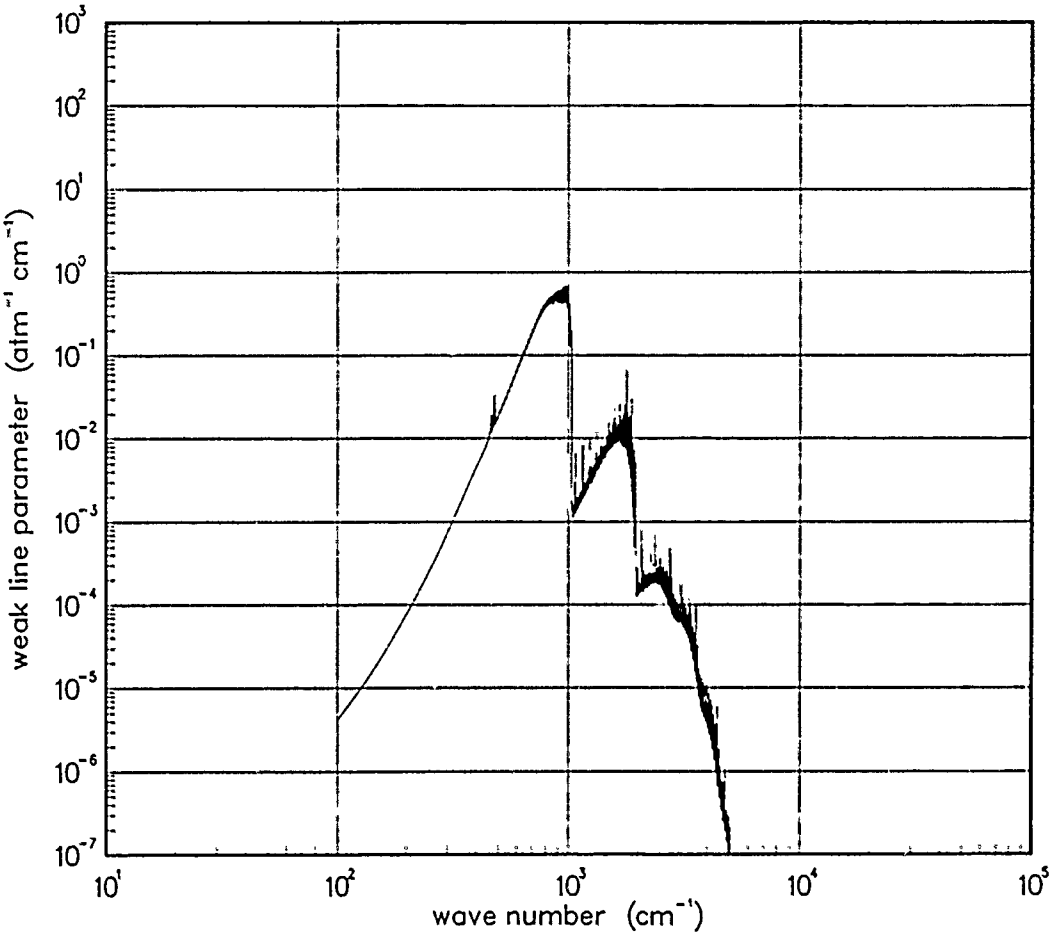

Figure 296. Weak-line parameter for AℓO at 5000°K.

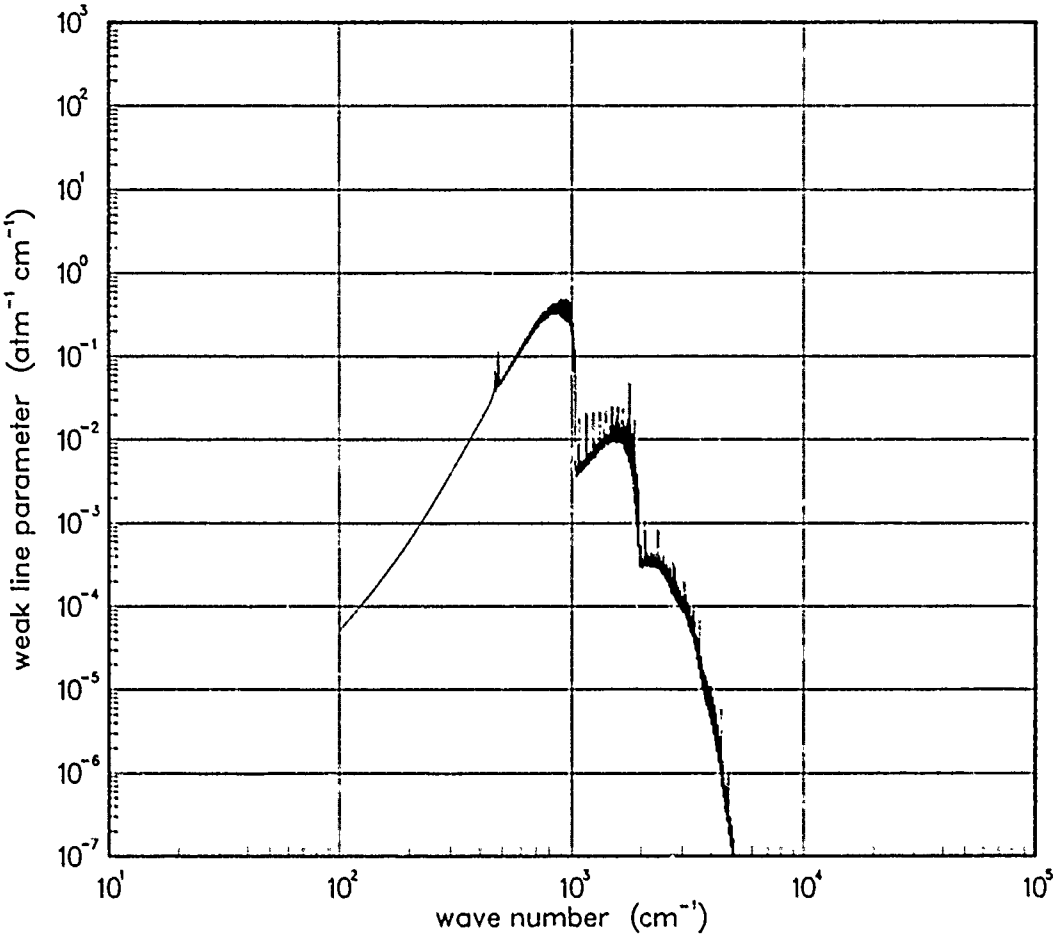

Figure 297. Weak-line parameter for AℓO at 7000°K.

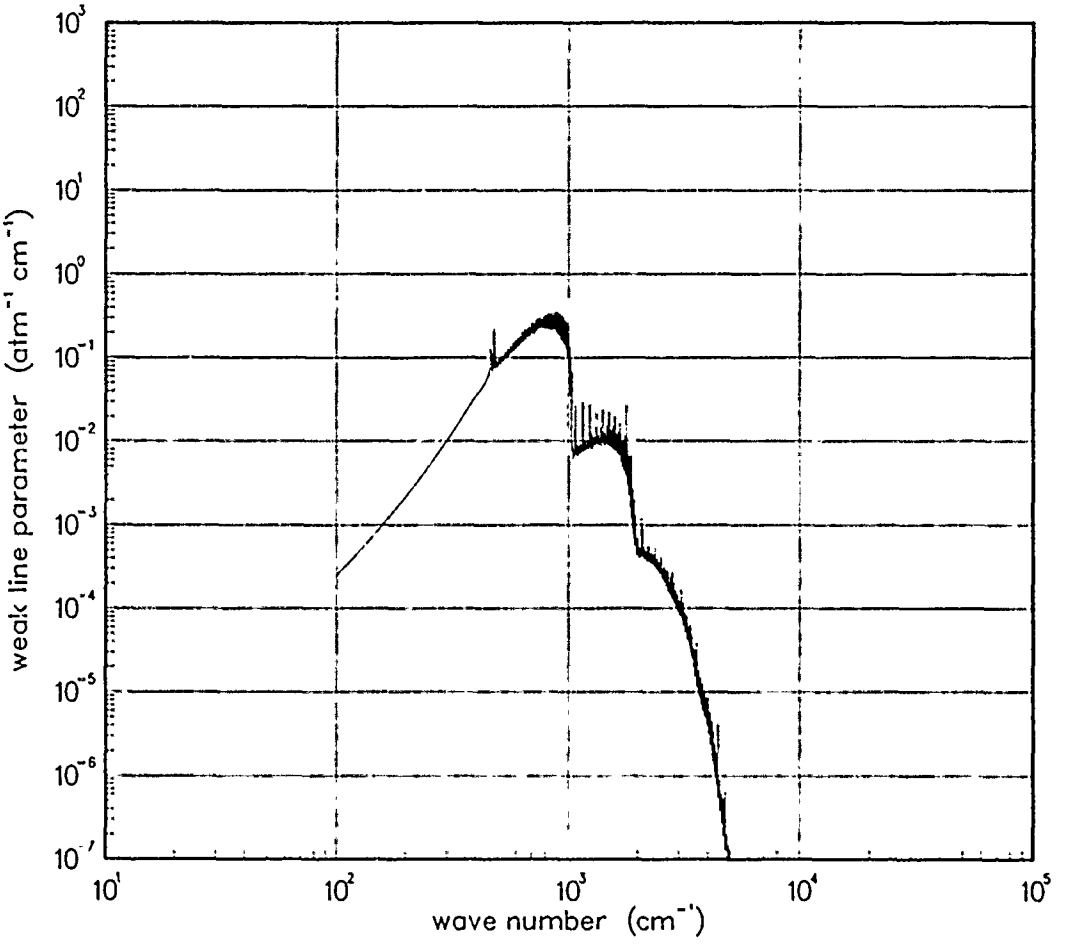

Figure 298. Weak-line parameter for AℓO at 10000°K.

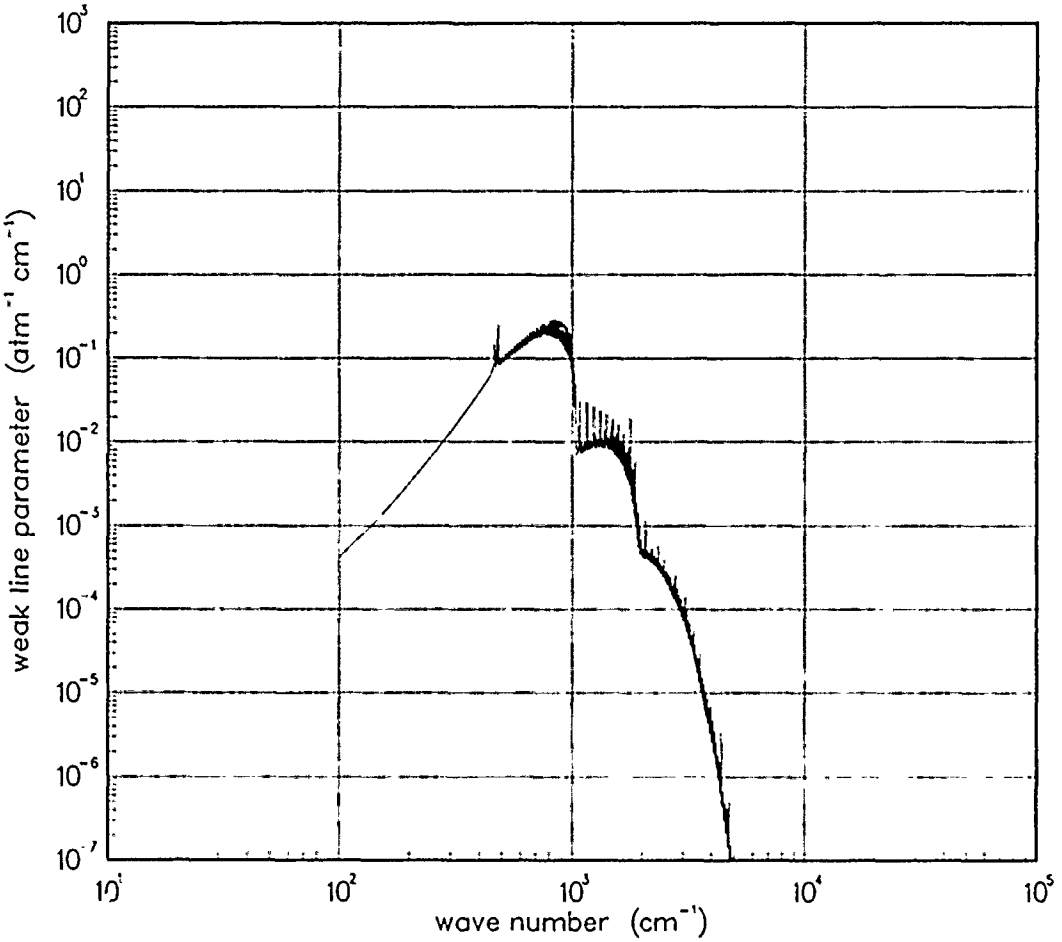

Figure 299. Weak-line parameter for AℓO at 12000°K.

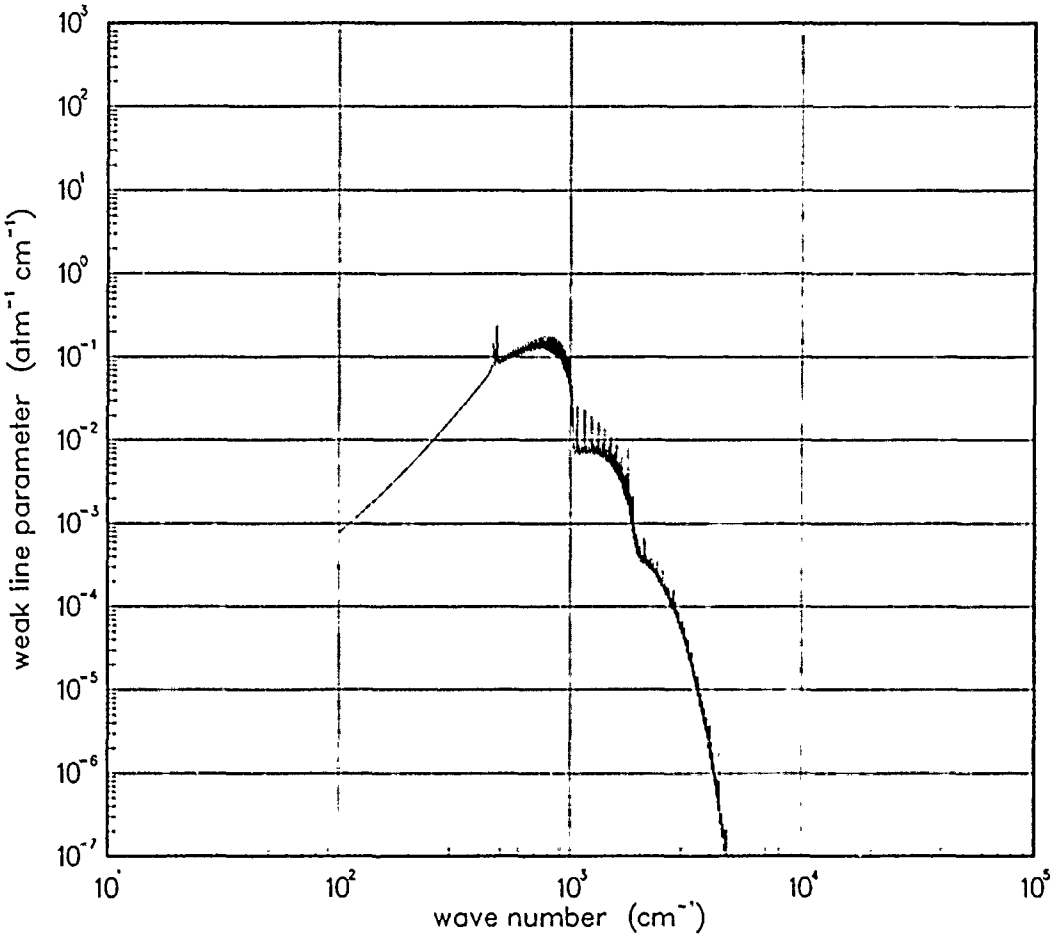

Figure 300. Weak-line parameter for AℓO at 18000°K.

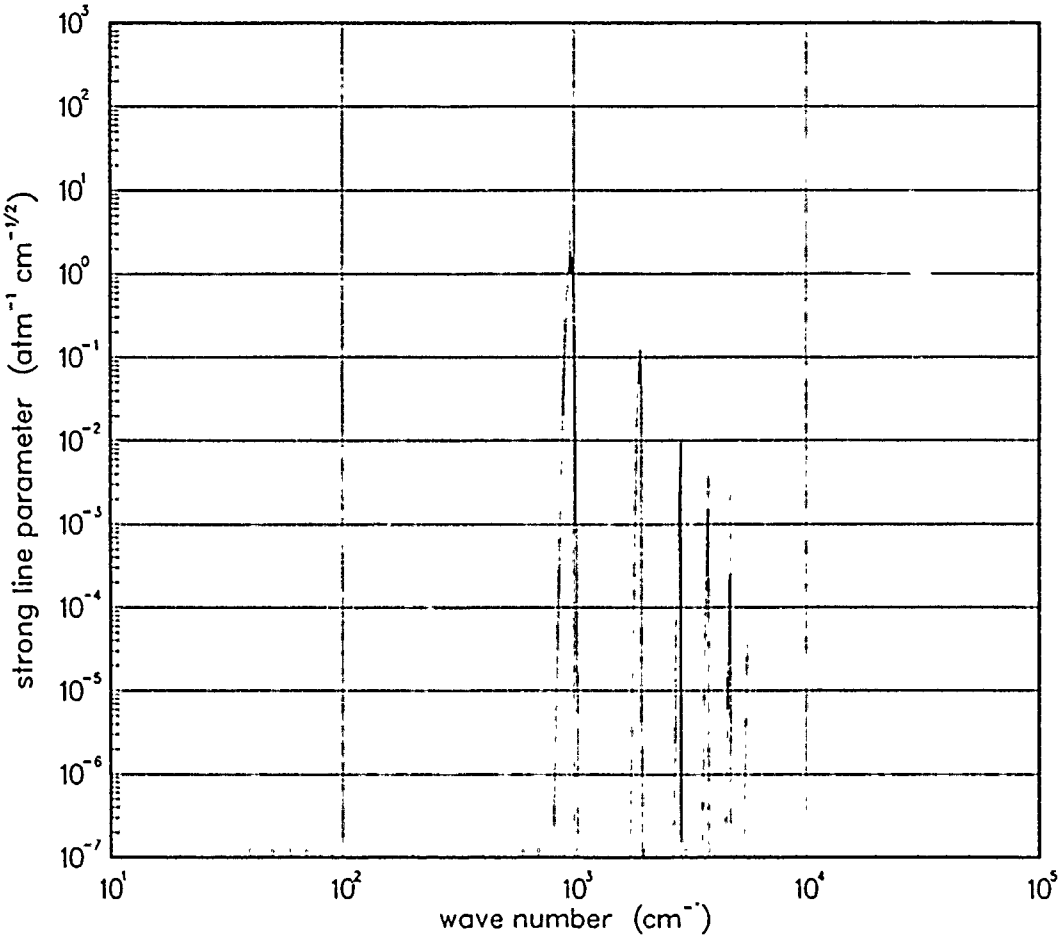

Figure 301. Strong-line parameter for AℓO at 200°K.

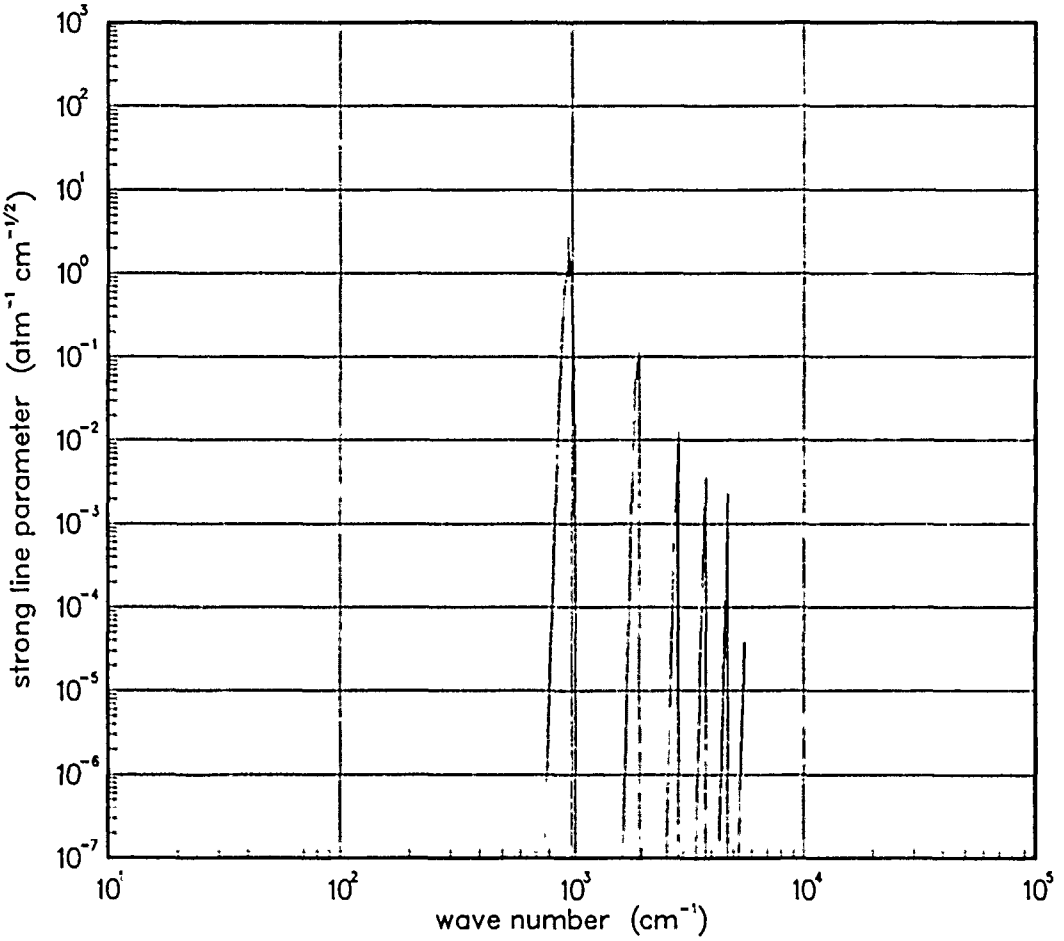

Figure 302. Strong-line parameter for AℓO at 300°K.

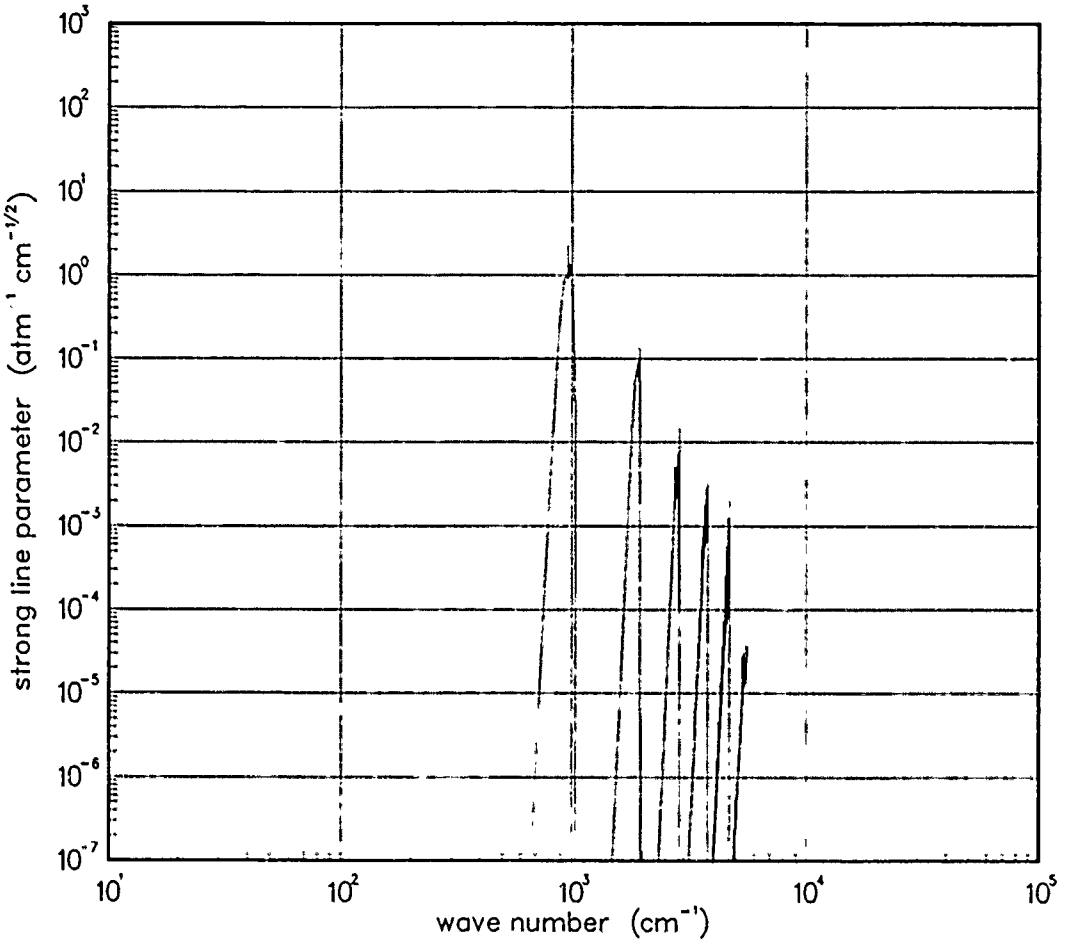

Figure 303. Strong-line parameter for AℓO at 500°K.

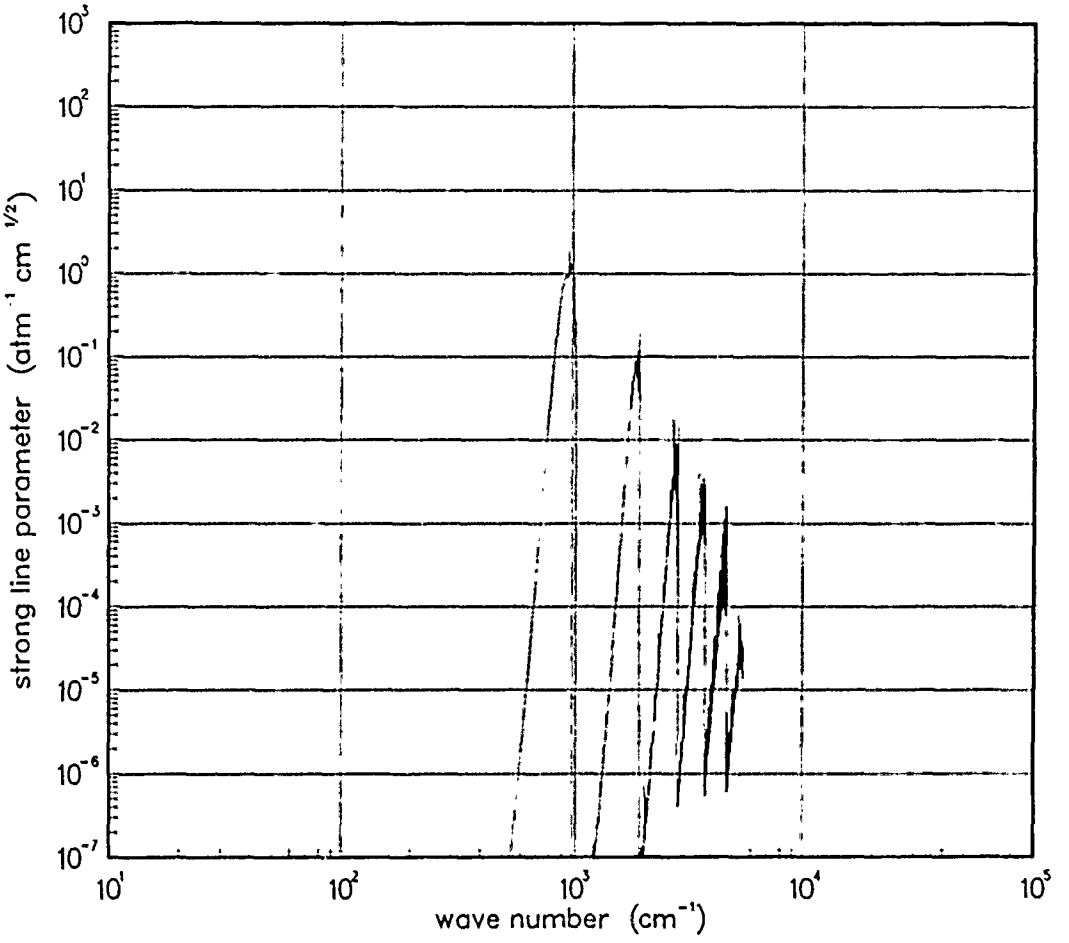

Figure 304. Strong-line parameter for AℓO at 750°K.

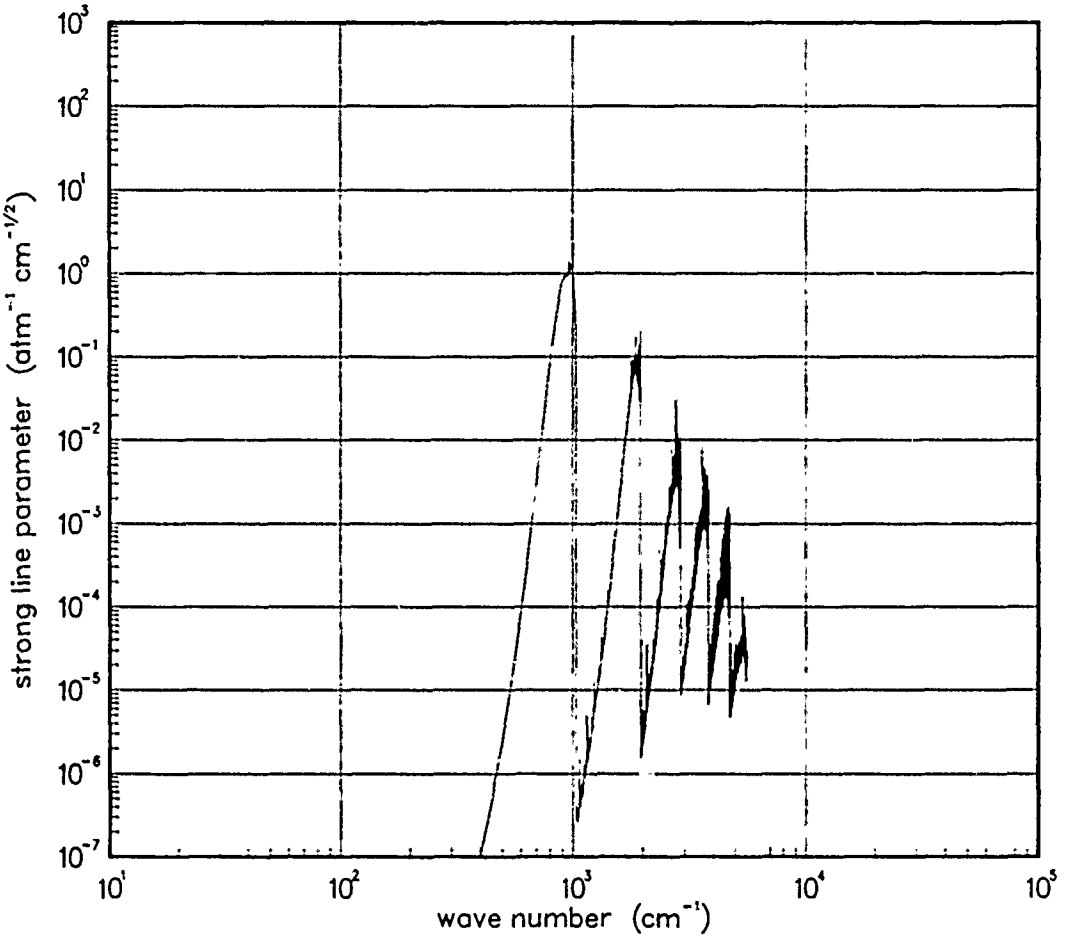

Figure 305. Strong-line parameter for AℓO at 1000°K.

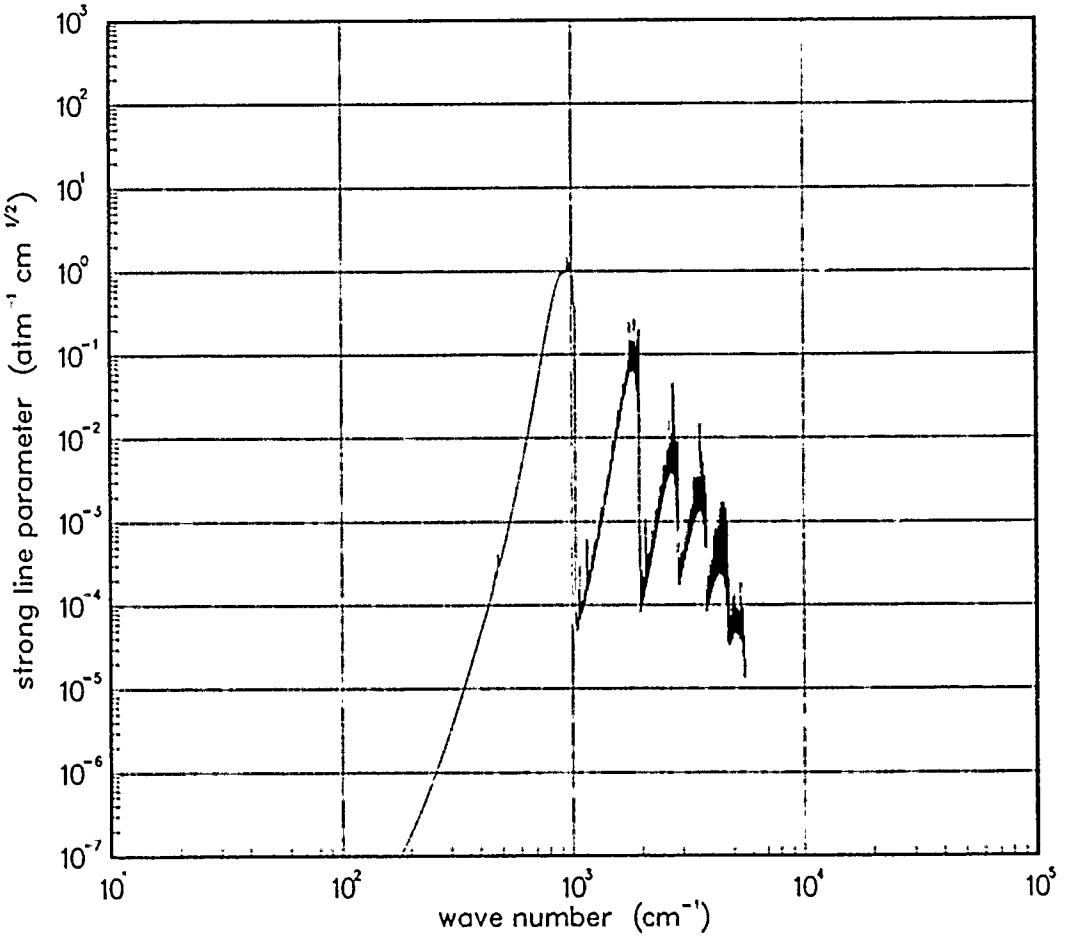

Figure 306. Strong-line parameter for AℓO at 1500°K.

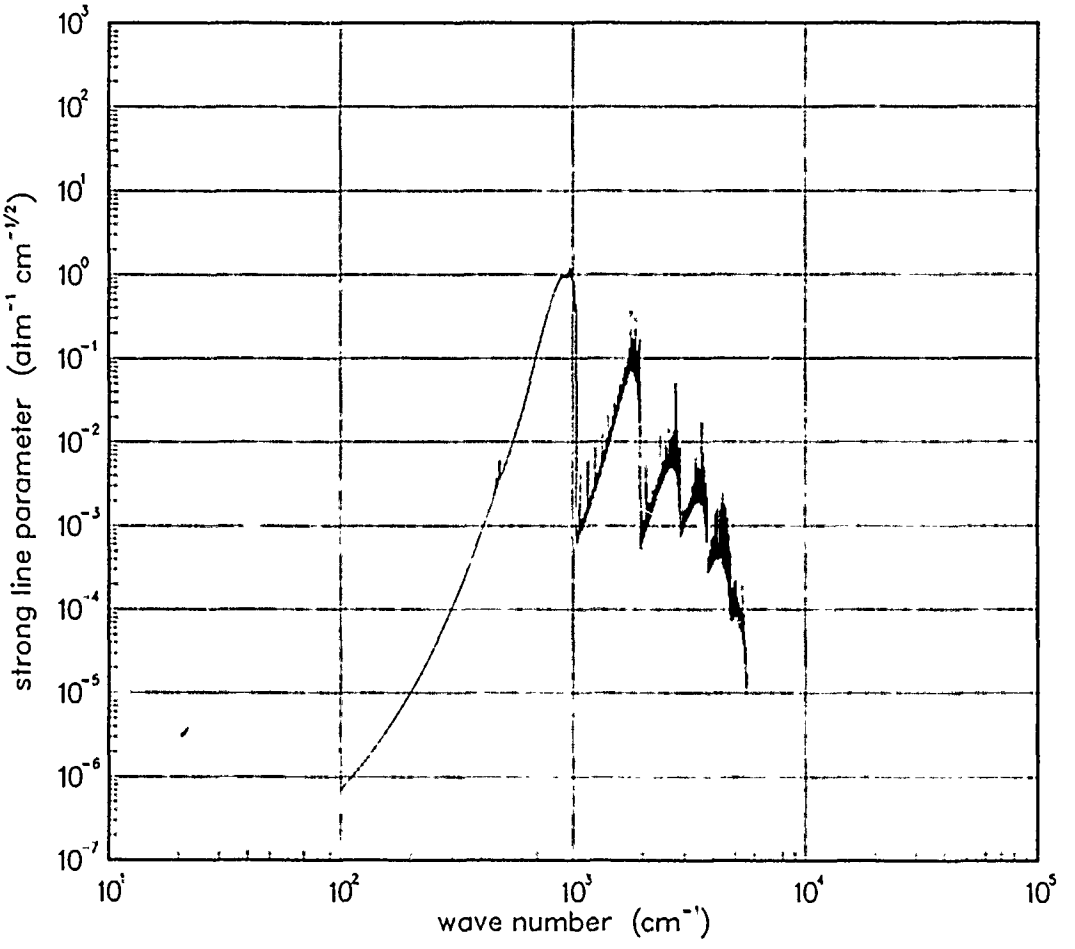

Figure 307. Strong-line parameter for AℓO at 2000°K.

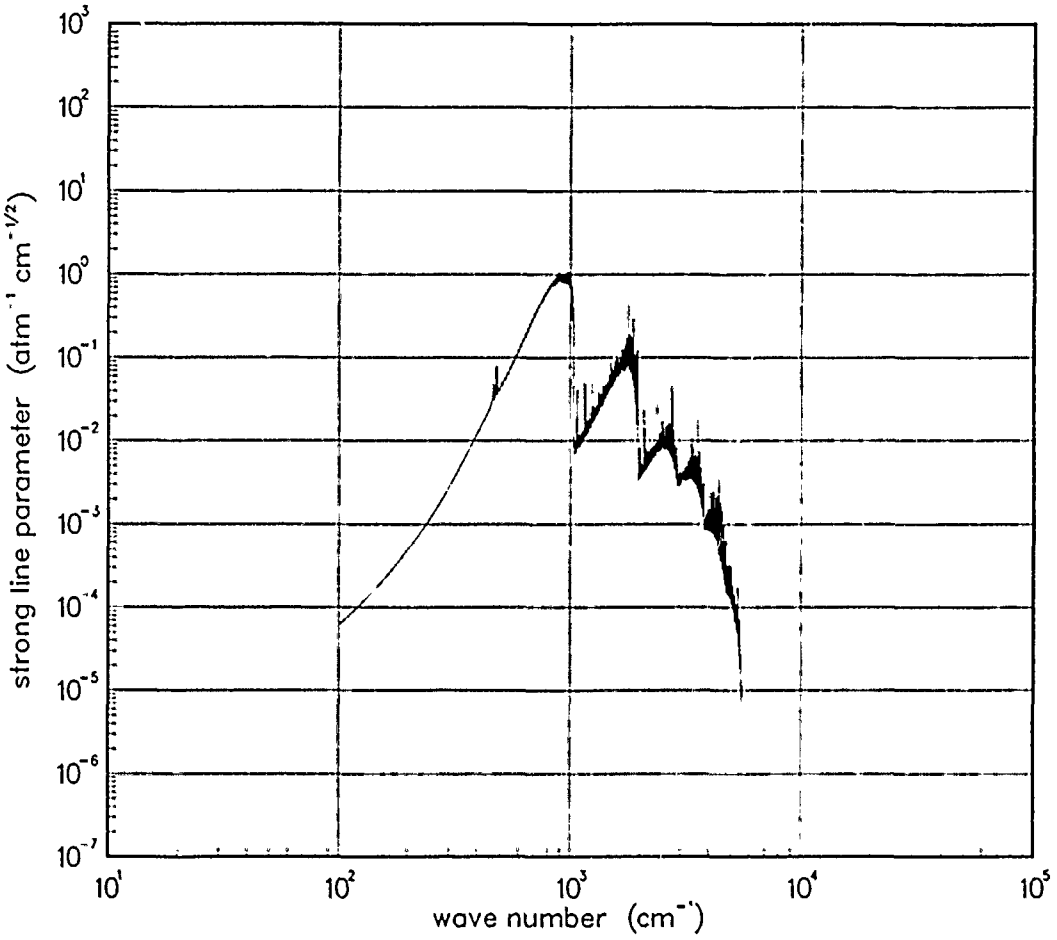

Figure 308. Strong-line parameter for AℓO at 3000°K.

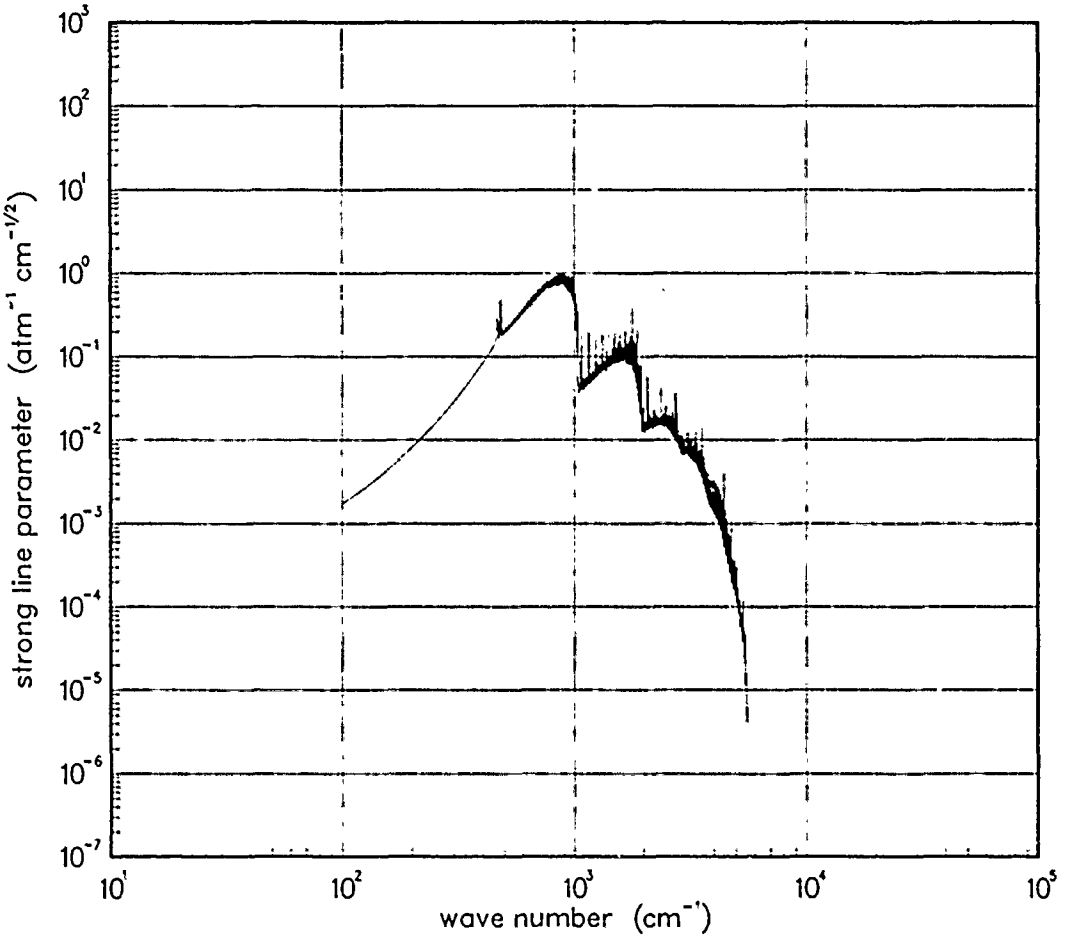

Figure 309. Strong-line parameter for AℓO at 5000°K.

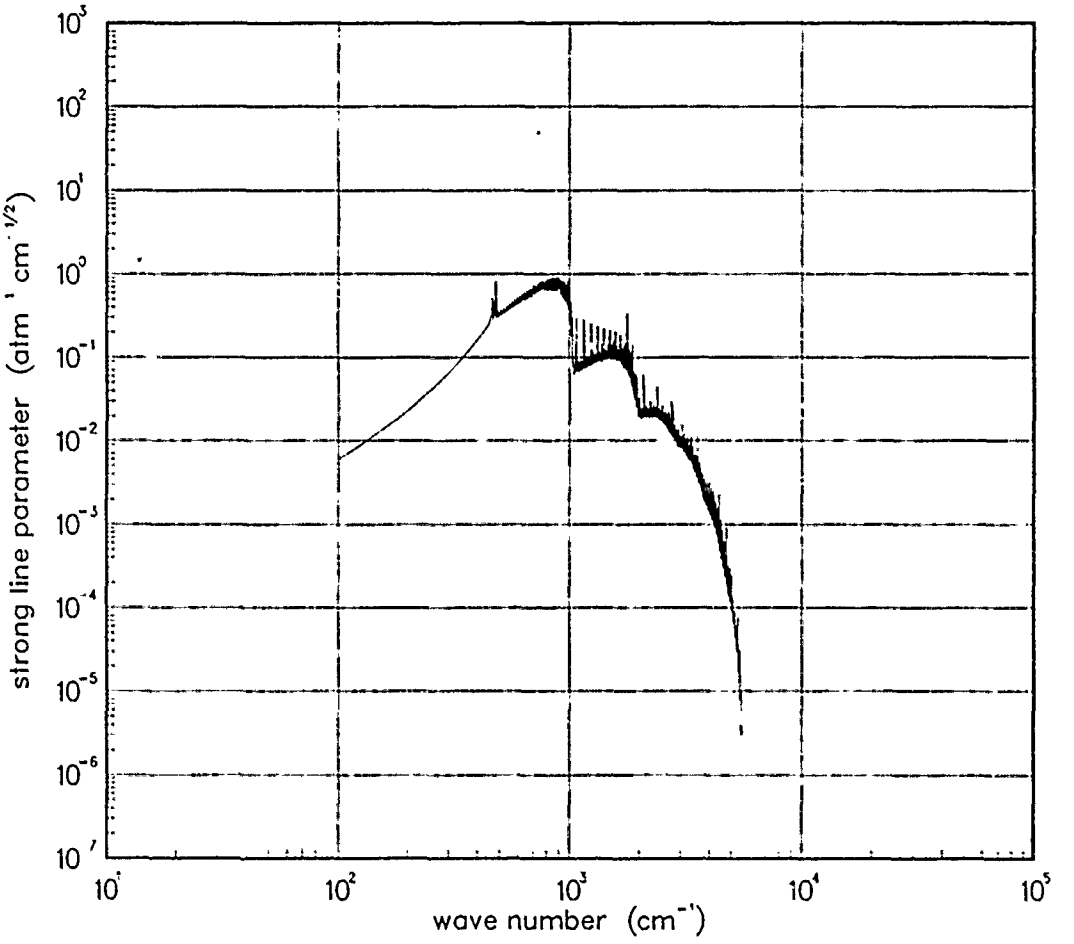

Figure 310. Strong-line parameter for AℓO at 7000°K.

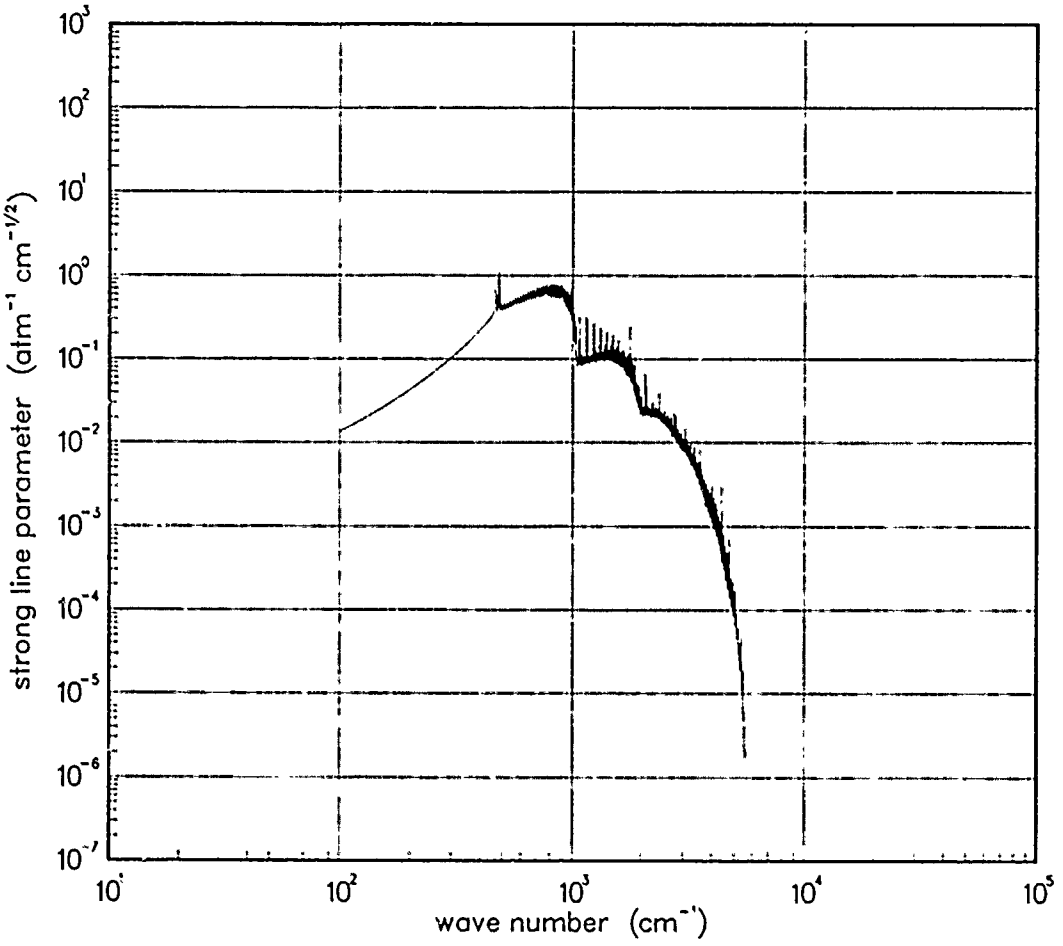

Figure 311. Strong-line parameter for AℓO at 1[illegible]00°K.

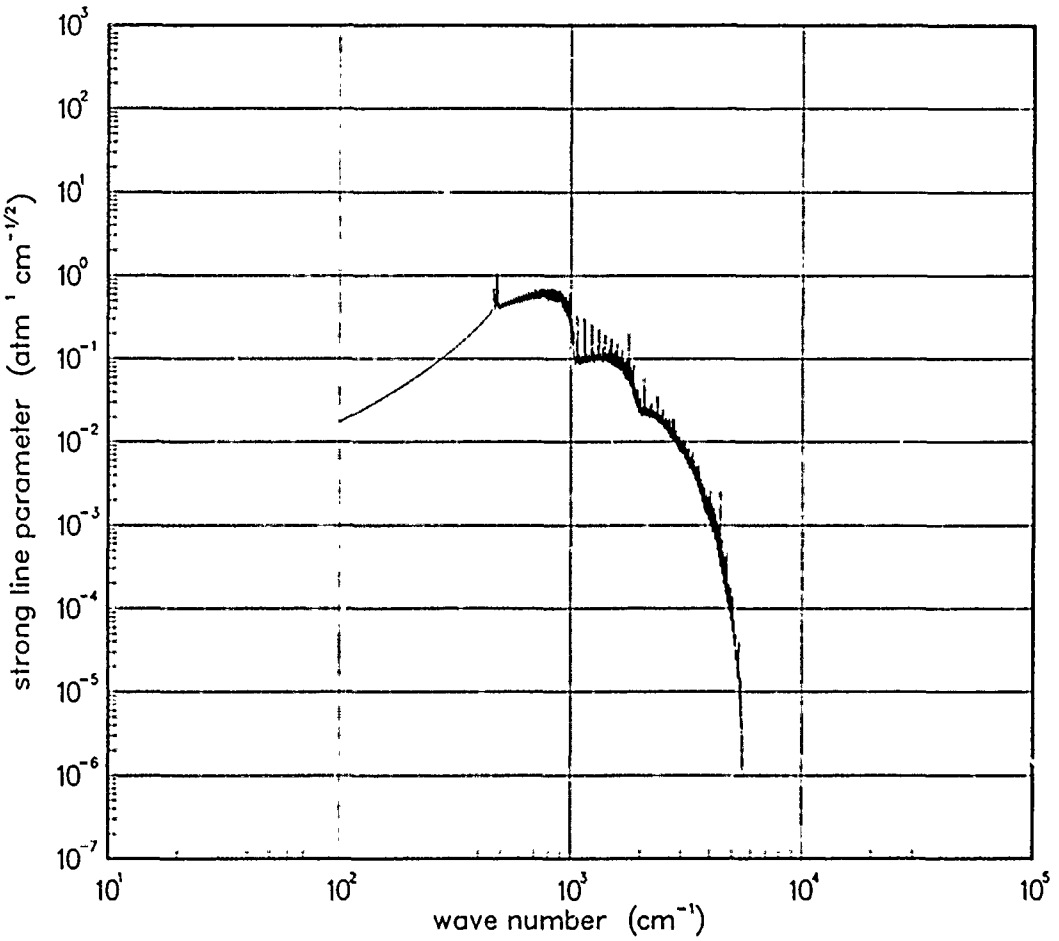

Figure 312. Strong-line parameter for AℓO at 12000°K.

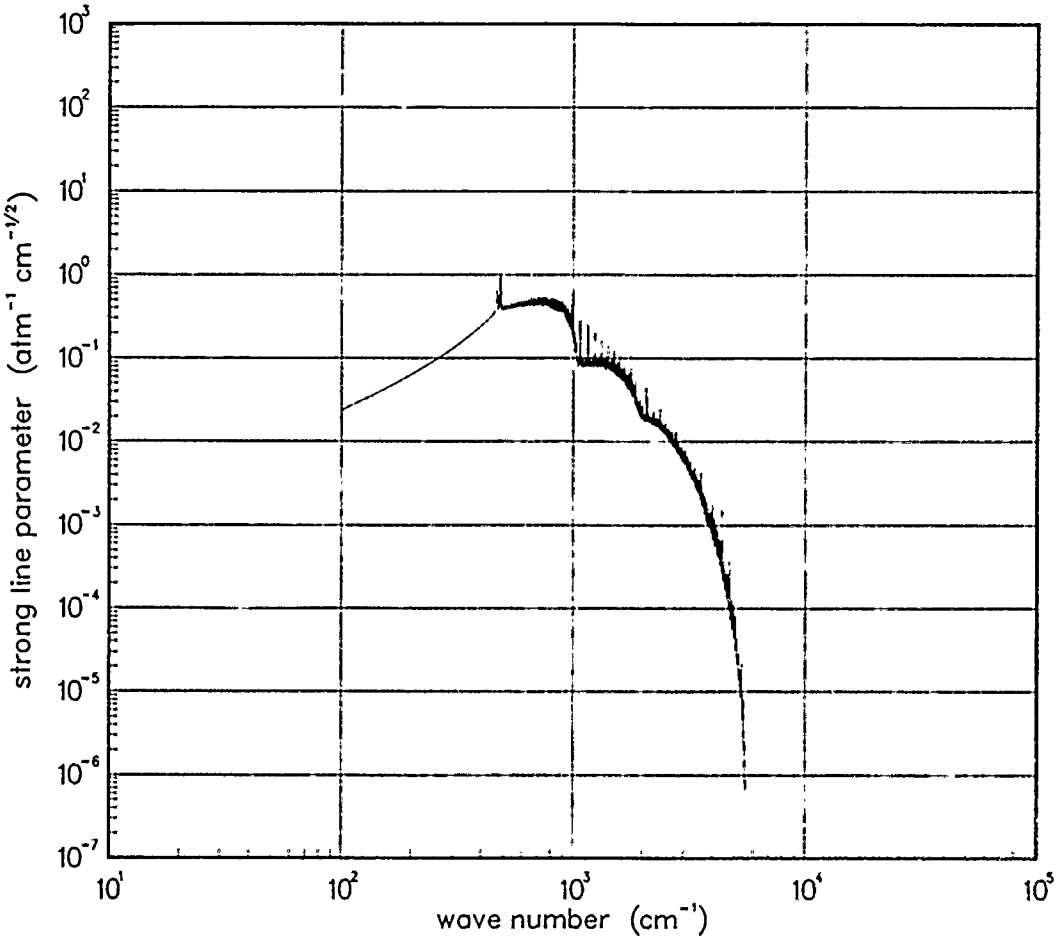

Figure 313. Strong-line parameter for AℓO at 18000°K.

6.2 COPPER OXIDE (CuO).

Table 8. Spectroscopic data for CuO.

$X\ ^2\Pi^*$

$\omega_e = 633.^\dagger$ $\omega_e x_e = 4.5^\dagger$ $A_e = 275.00^\dagger$
$\alpha_e = .0058^\ddagger$ $A_e = 275.0^\dagger$ $B_e = 0.53530^\ddagger$ $E_e = 0.0$

$S_{10} = 450.^\ddagger$

$\gamma_\ell(300°K) = 0.04^\S$

Data Source:

*A. Antic-Jovanovic, D.S. Pesic, and A.G. Gaydon, Proc. Roy. 307 399 (1968).

†J.S. Shirk, and A.M. Bass, J. Chem. Phys. 52 (1970).

‡T.L. Stephens, and J.G. DeVore, Band Models for Calculating Fireball Thermal Emission (U) , 71TMP-35, General Electric-TEMPO, Santa Barbara, California (May 1971).

§Estimate.

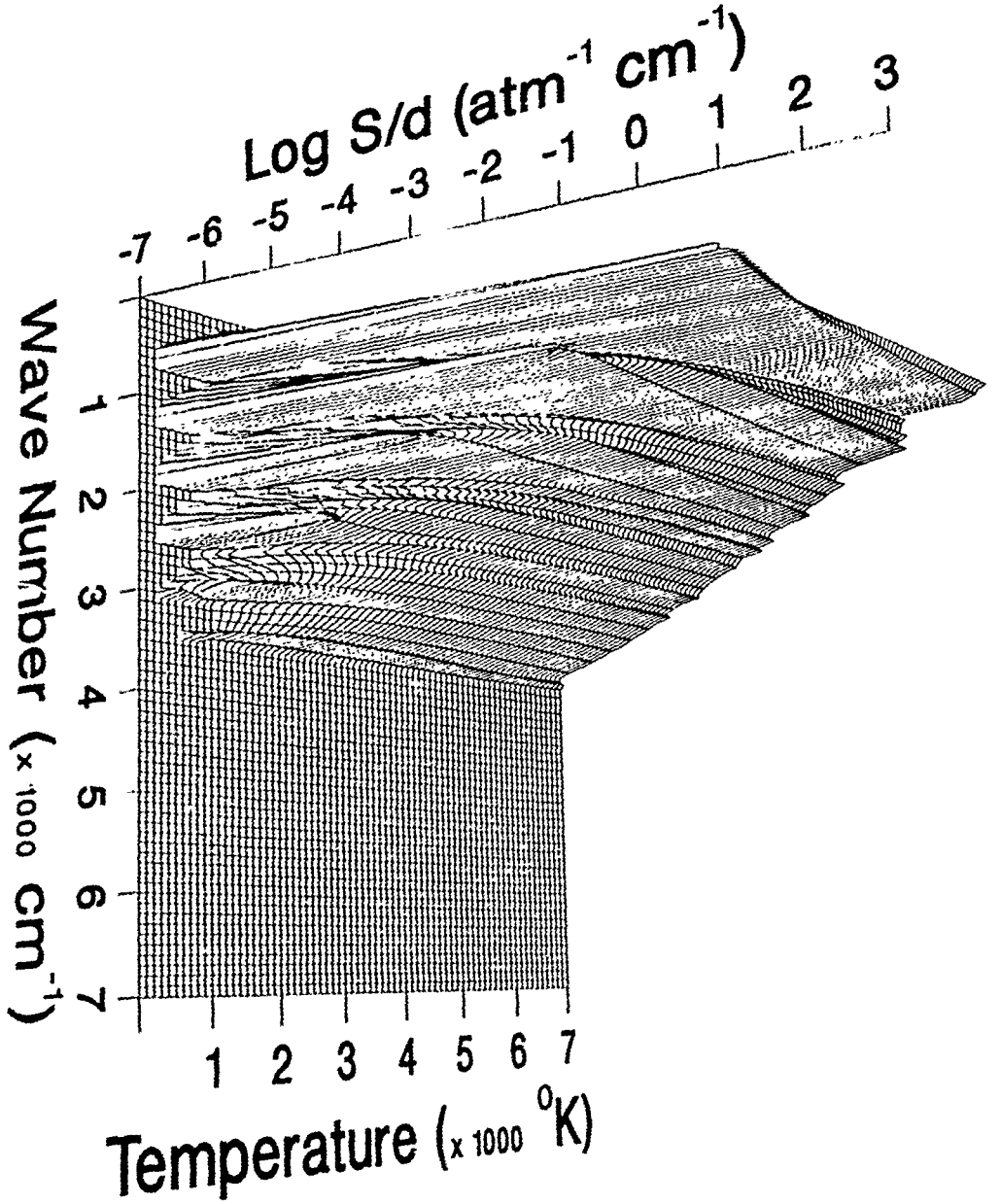

Figure 314. Weak-line parameter for CuO.

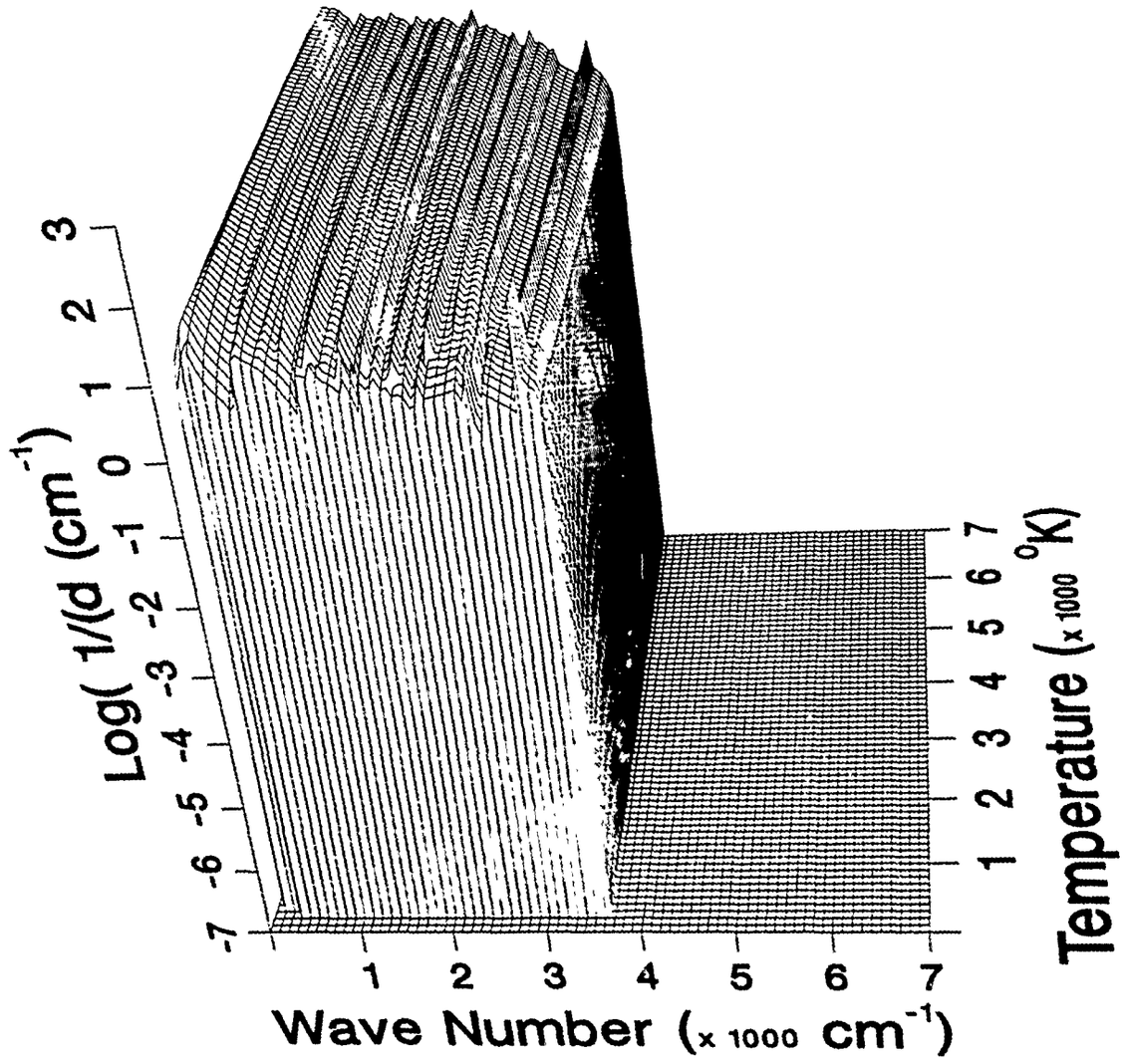

Figure 315. Inverse line spacing for CuO.

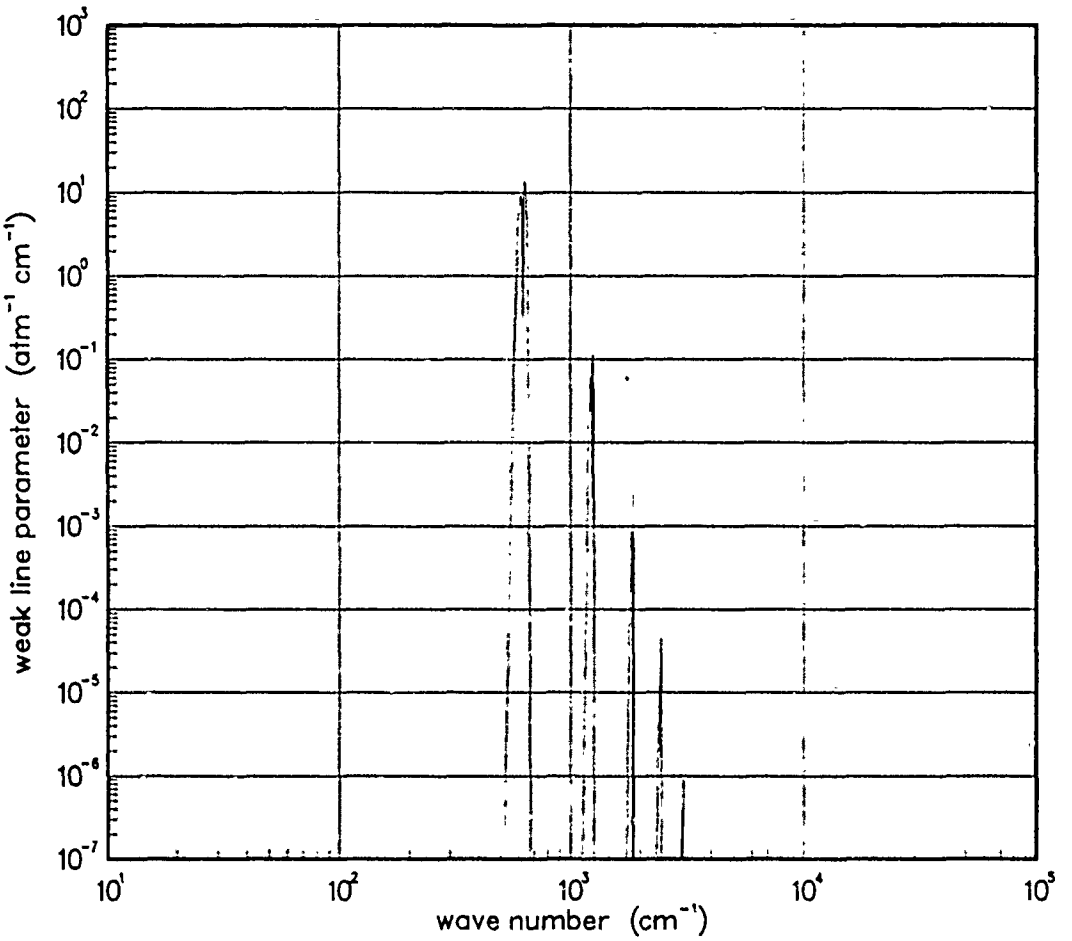

Figure 316. Weak-line parameter for CuO at 200°K.

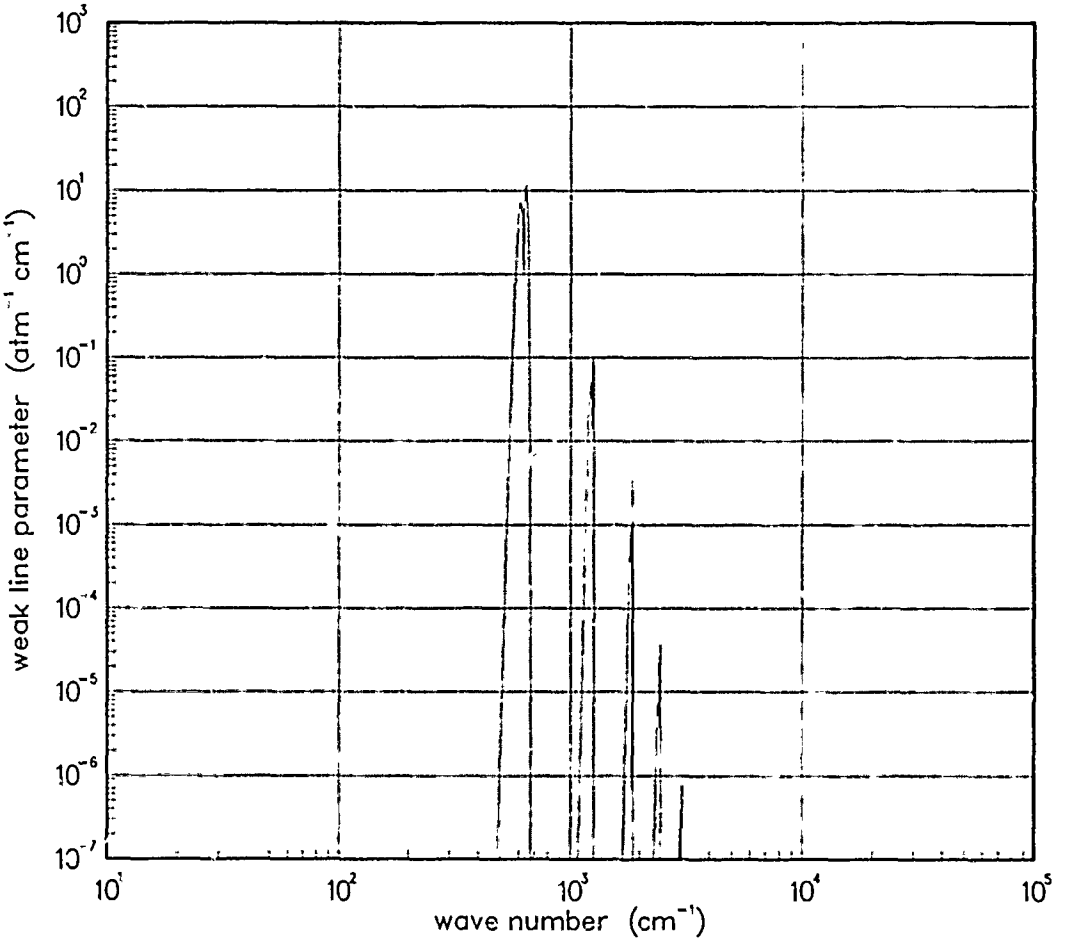

Figure 317. Weak-line parameter for CuO at 300°K.

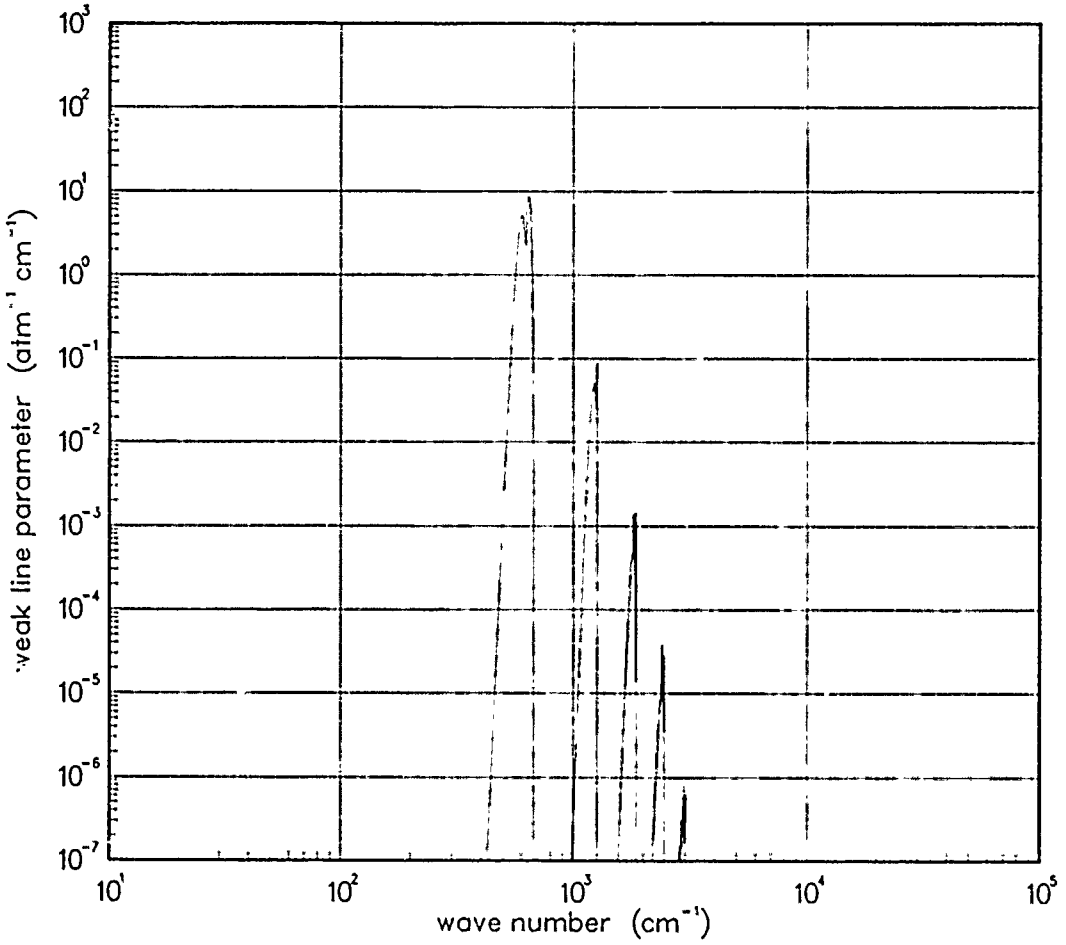

Figure 318. Weak-line parameter for CuO at 500°K.

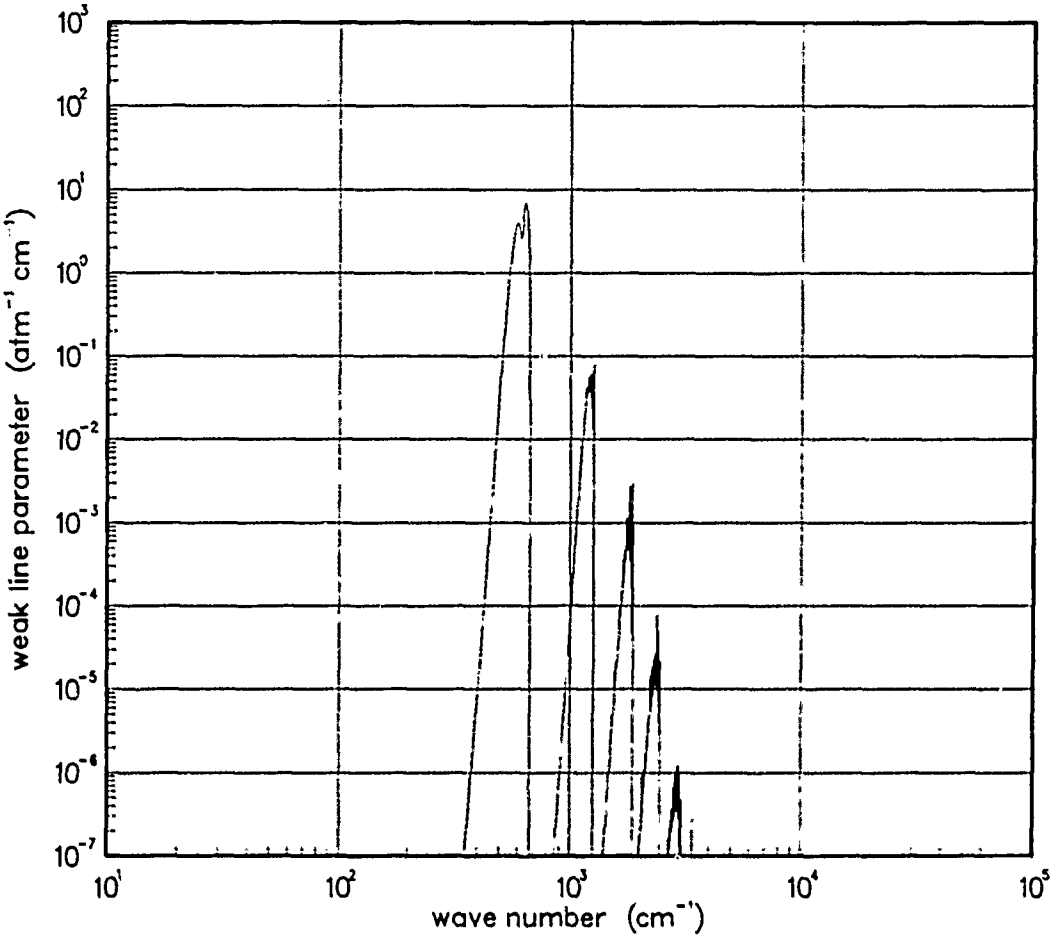

Figure 319. Weak-line parameter for CuO at 750°K.

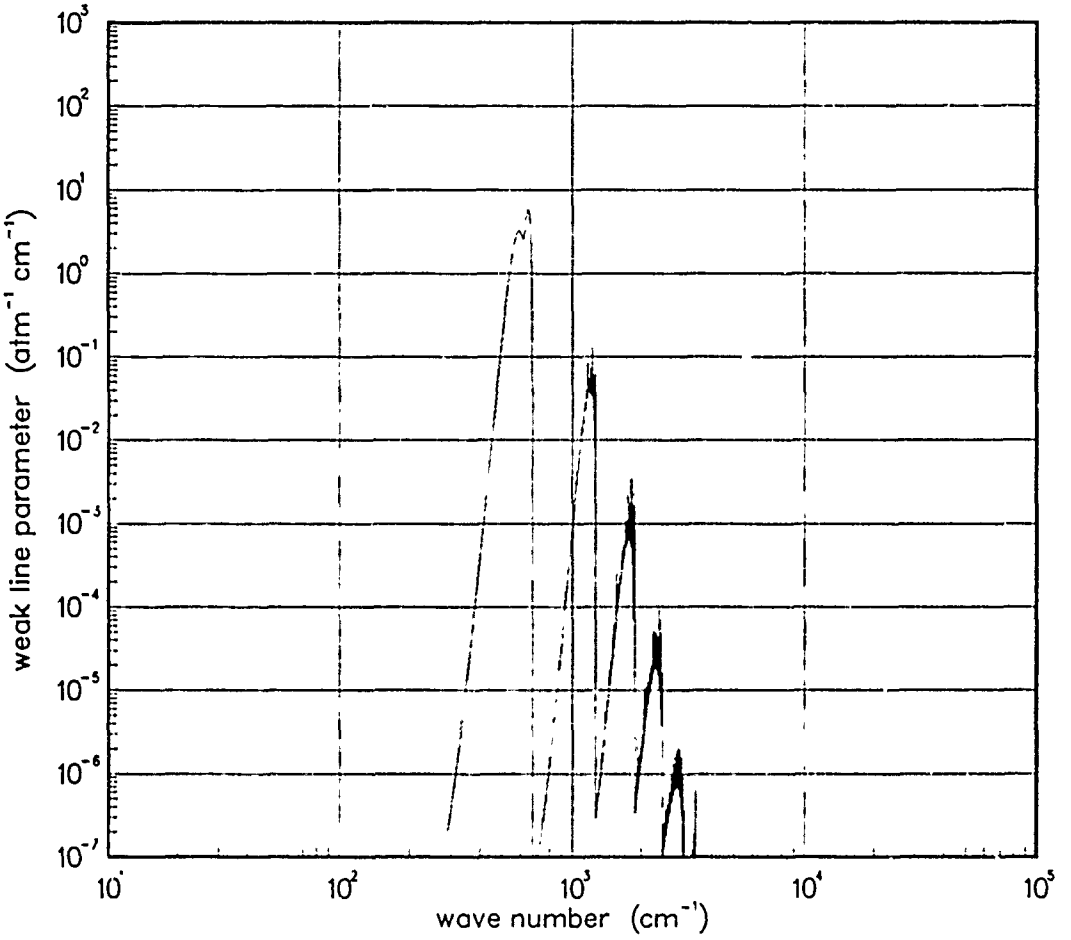

Figure 320. Weak-line parameter for CuO at 1000°K.

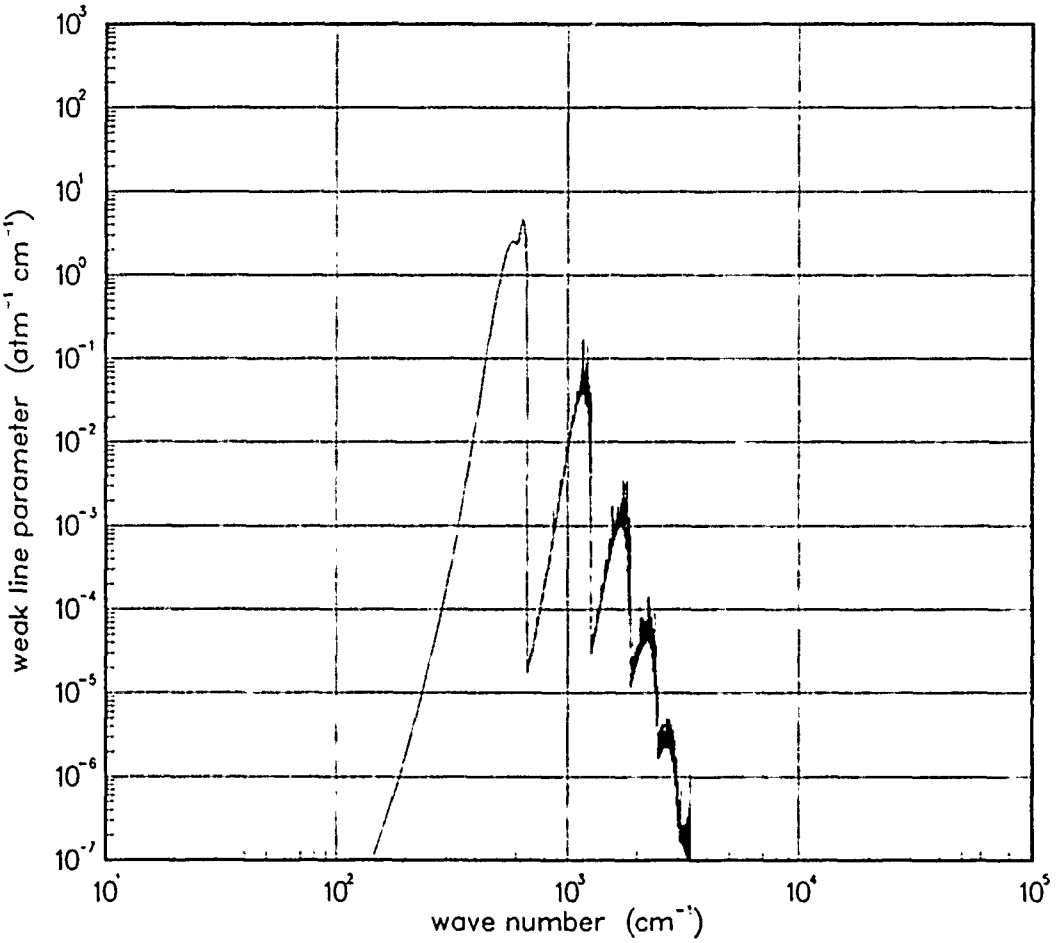

Figure 321. Weak-line parameter for CuO at 1500°K.

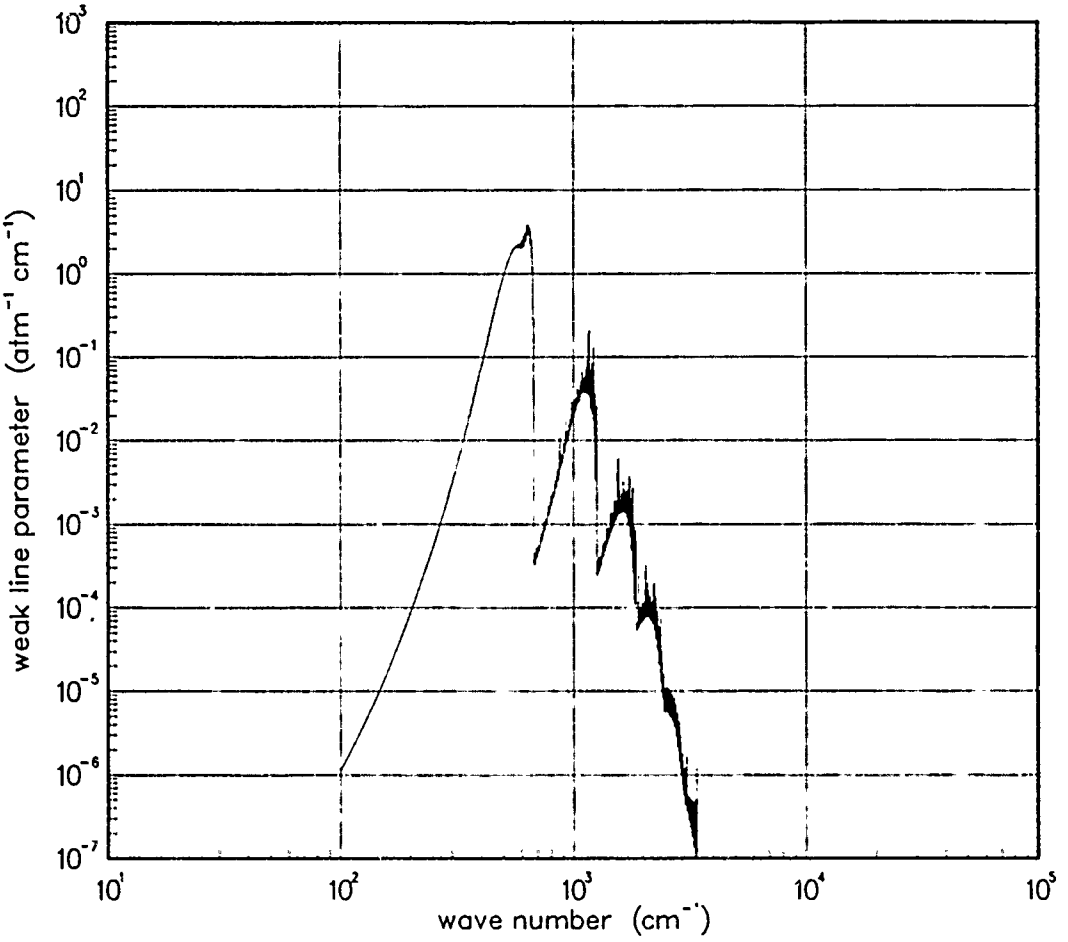

Figure 322. Weak-line parameter for CuO at 2000°K.

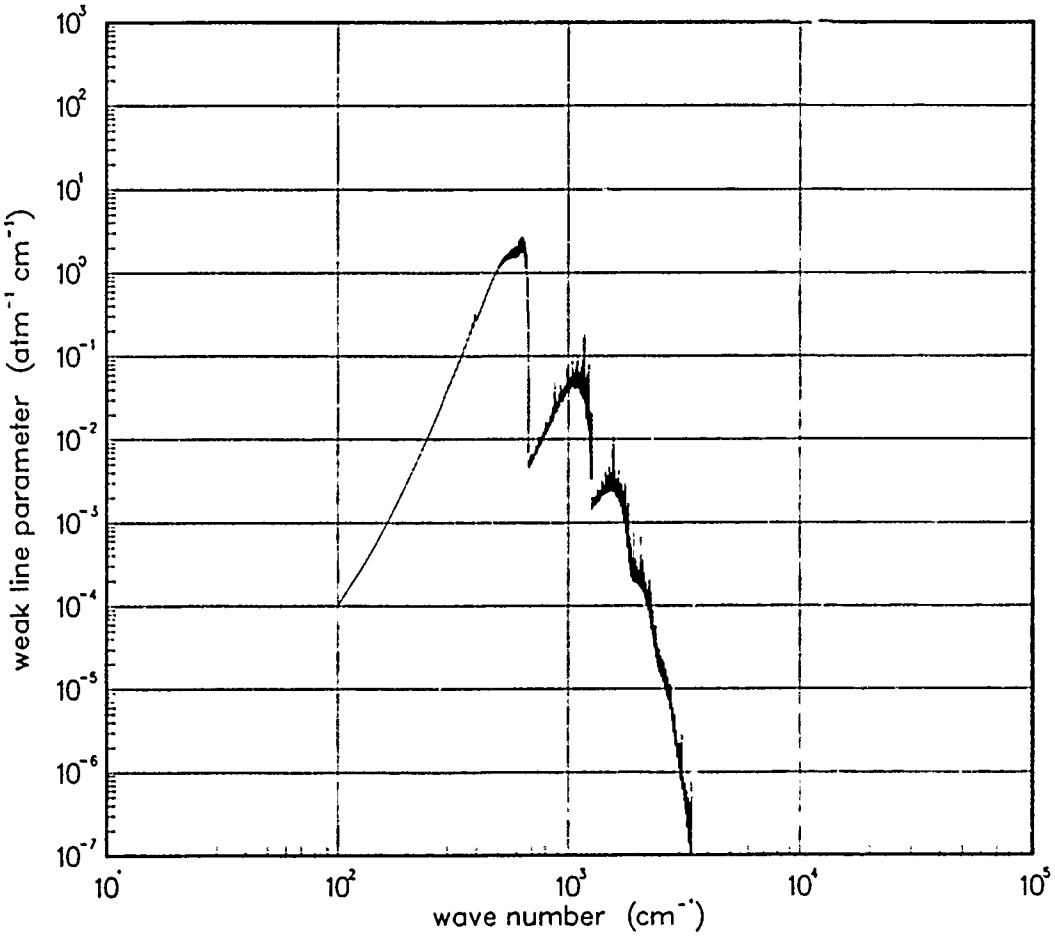

Figure 323. Weak-line parameter for CuO at 3000°K.

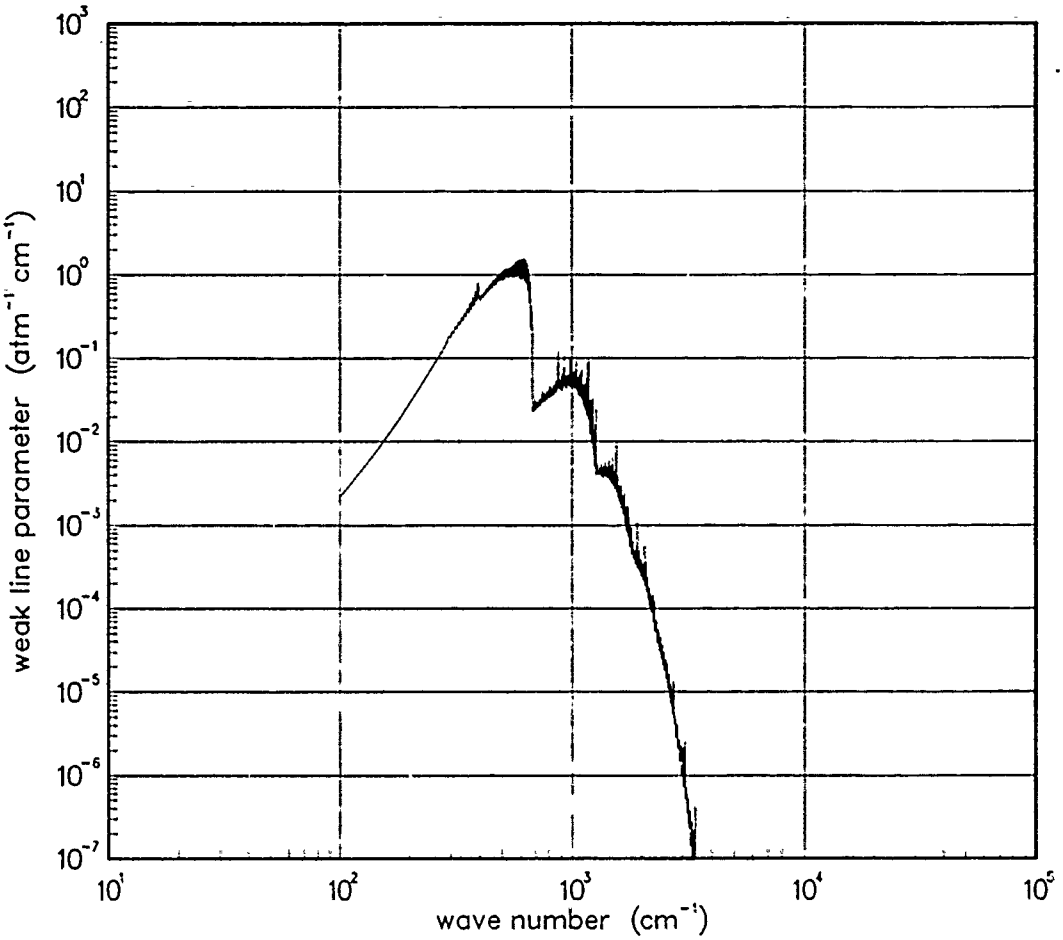

Figure 324. Weak-line parameter for CuO at 5000°K.

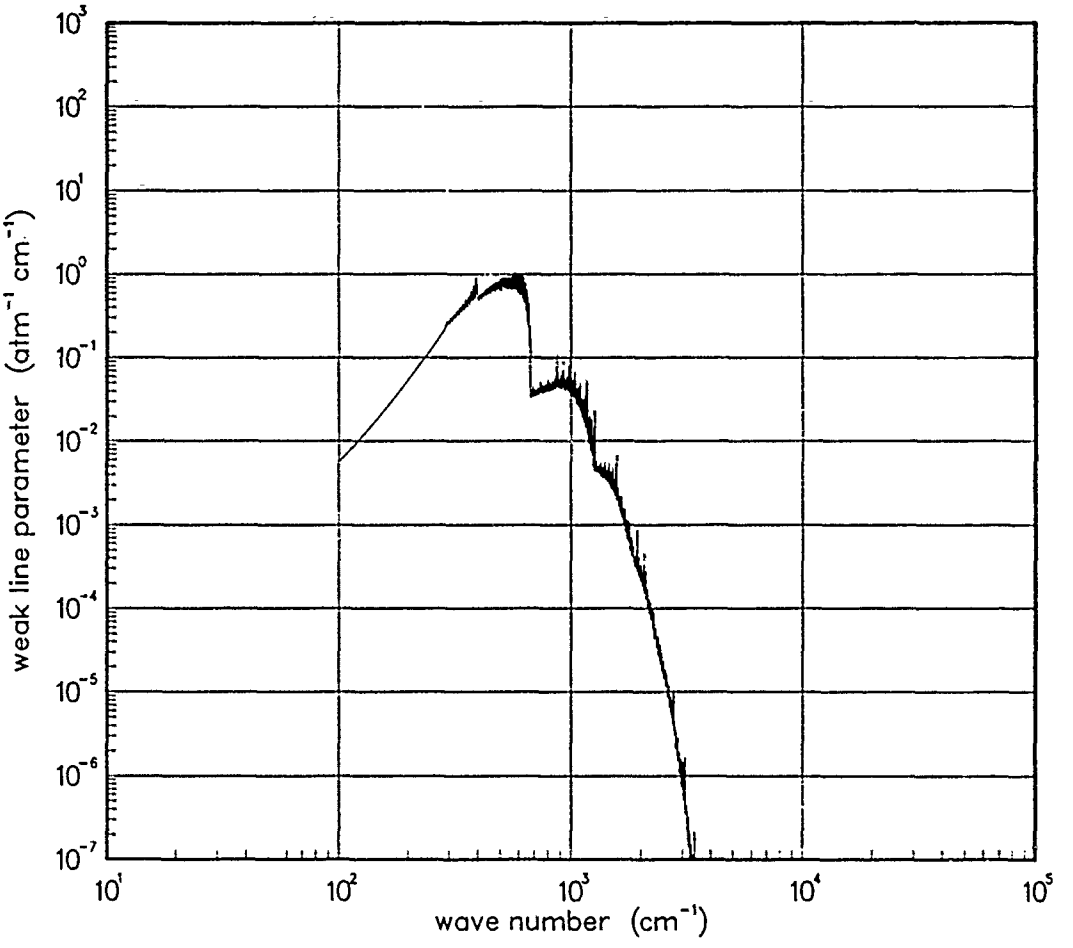

Figure 325. Weak-line parameter for CuO at 7000°K.

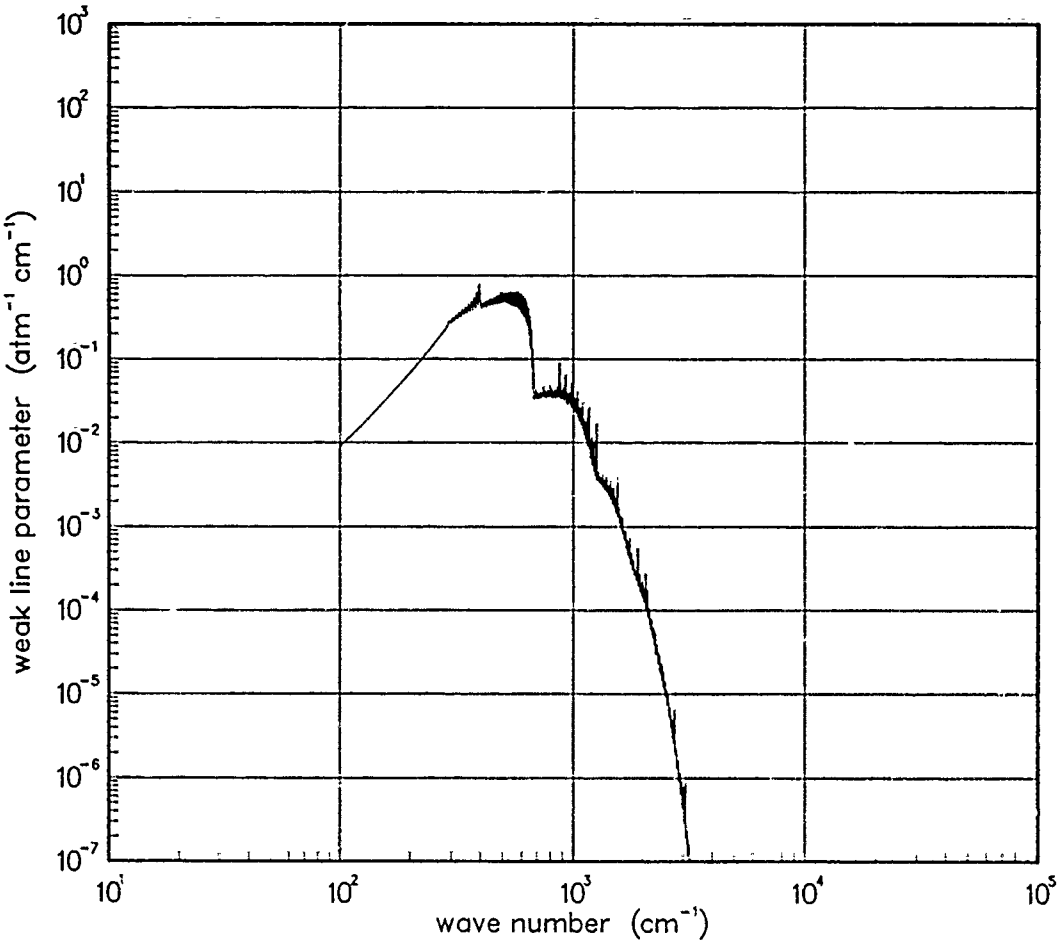

Figure 326. Weak-line parameter for CuO at 10000°K.

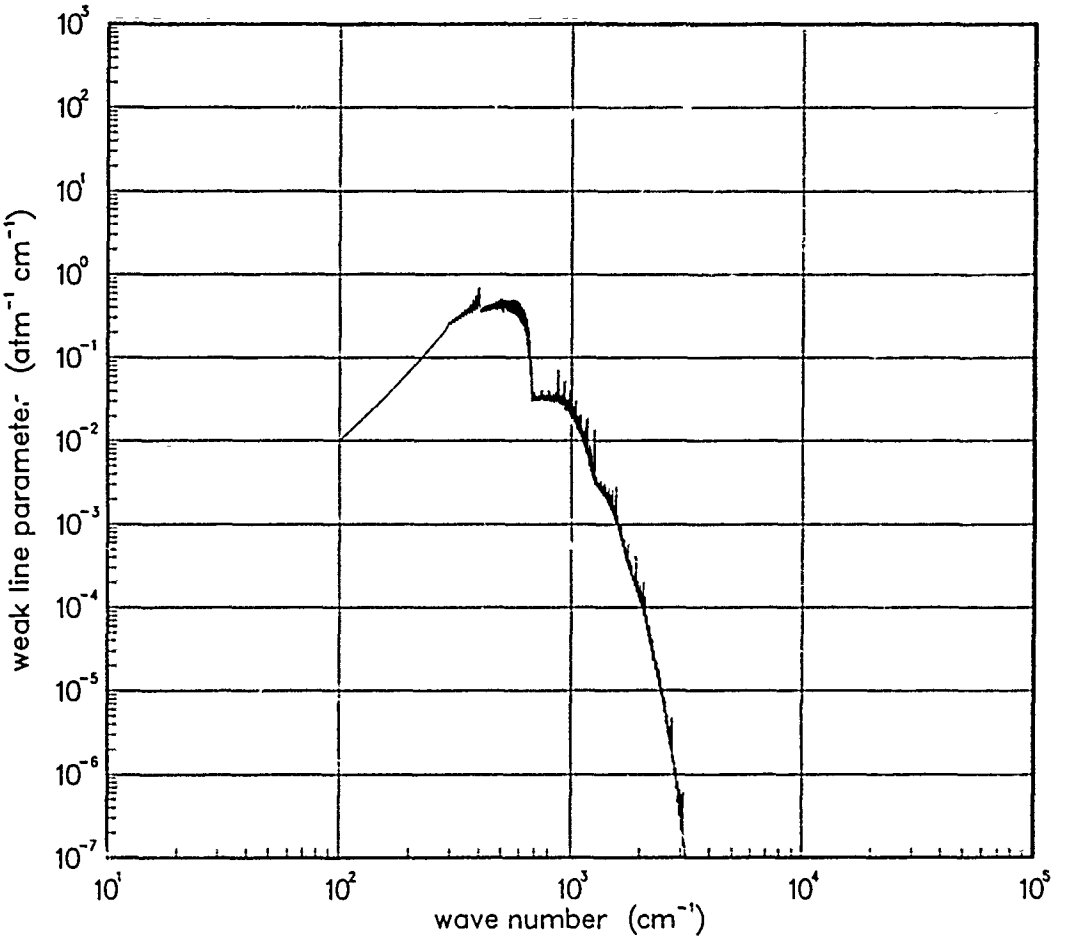

Figure 327. Weak-line parameter for CuO at 12000°K.

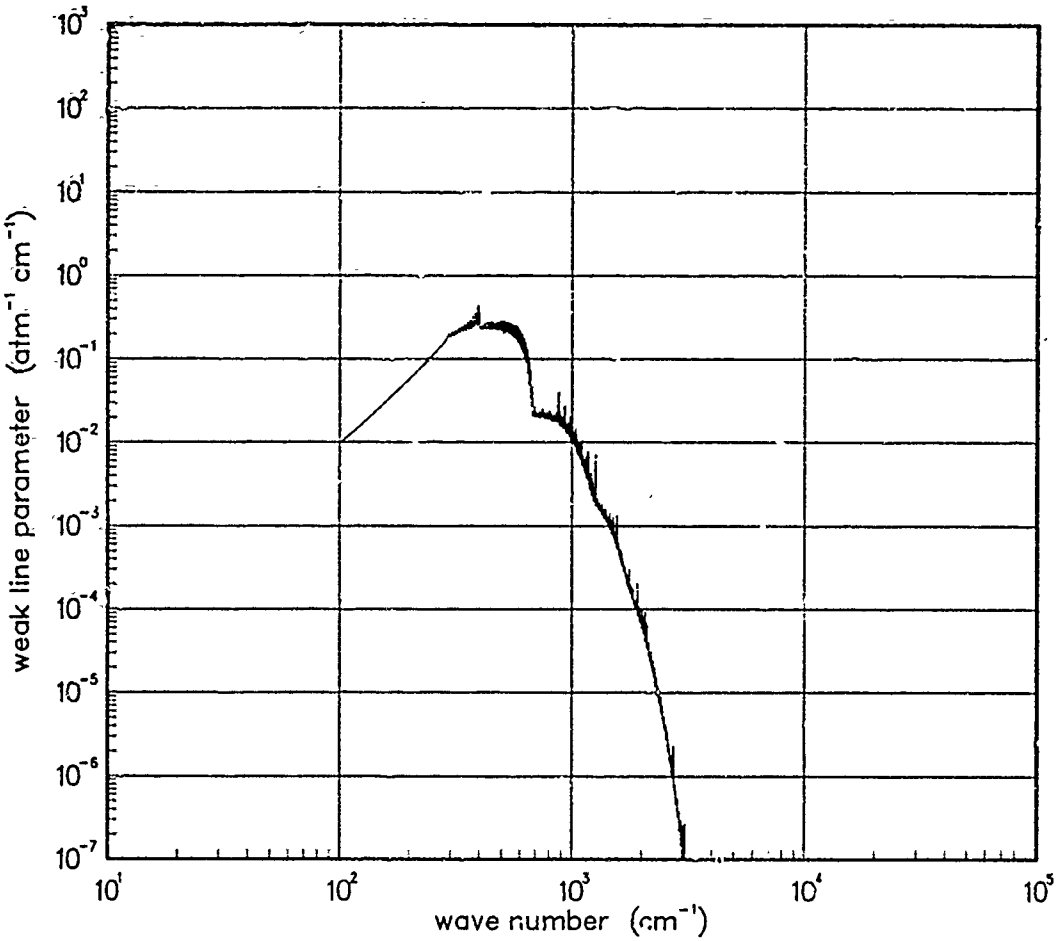

Figure 328. Weak-line parameter for CuO at 18000°K.

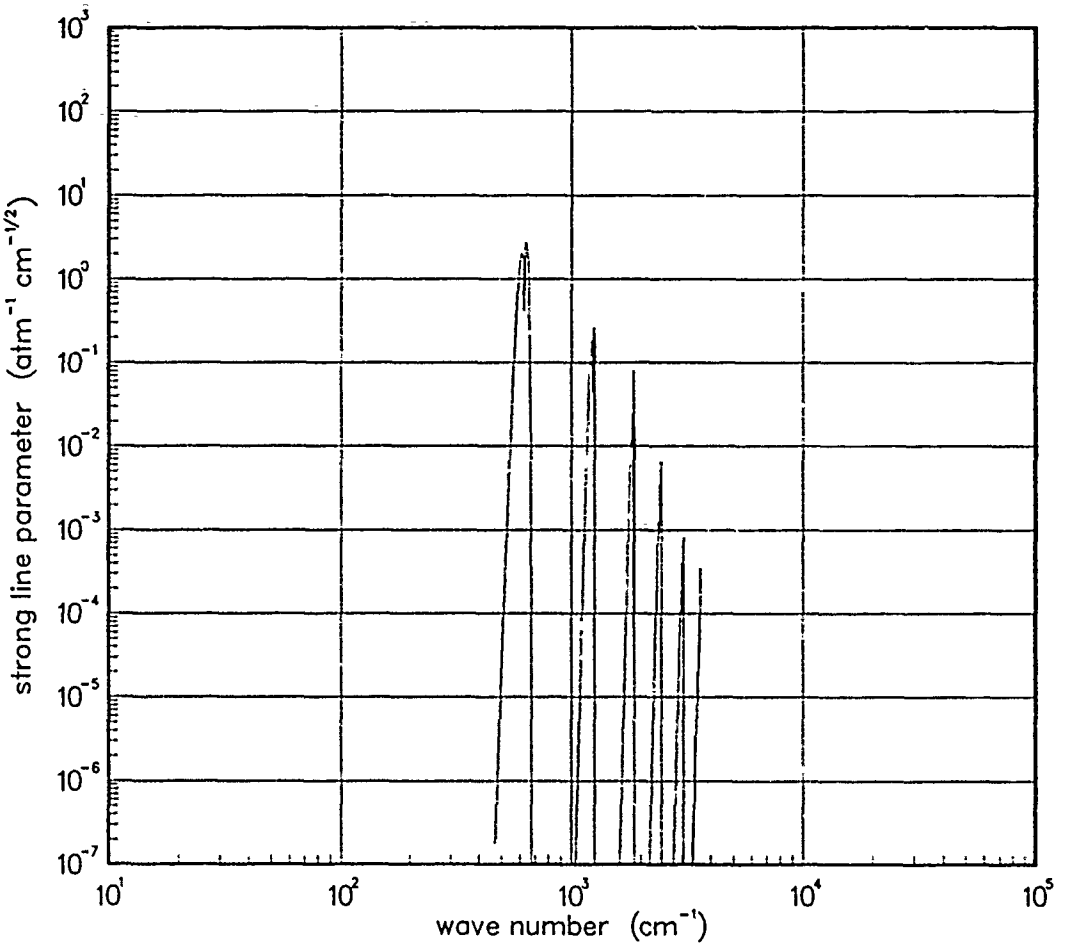

Figure 329. Strong-line parameter for CuO at 200°K.

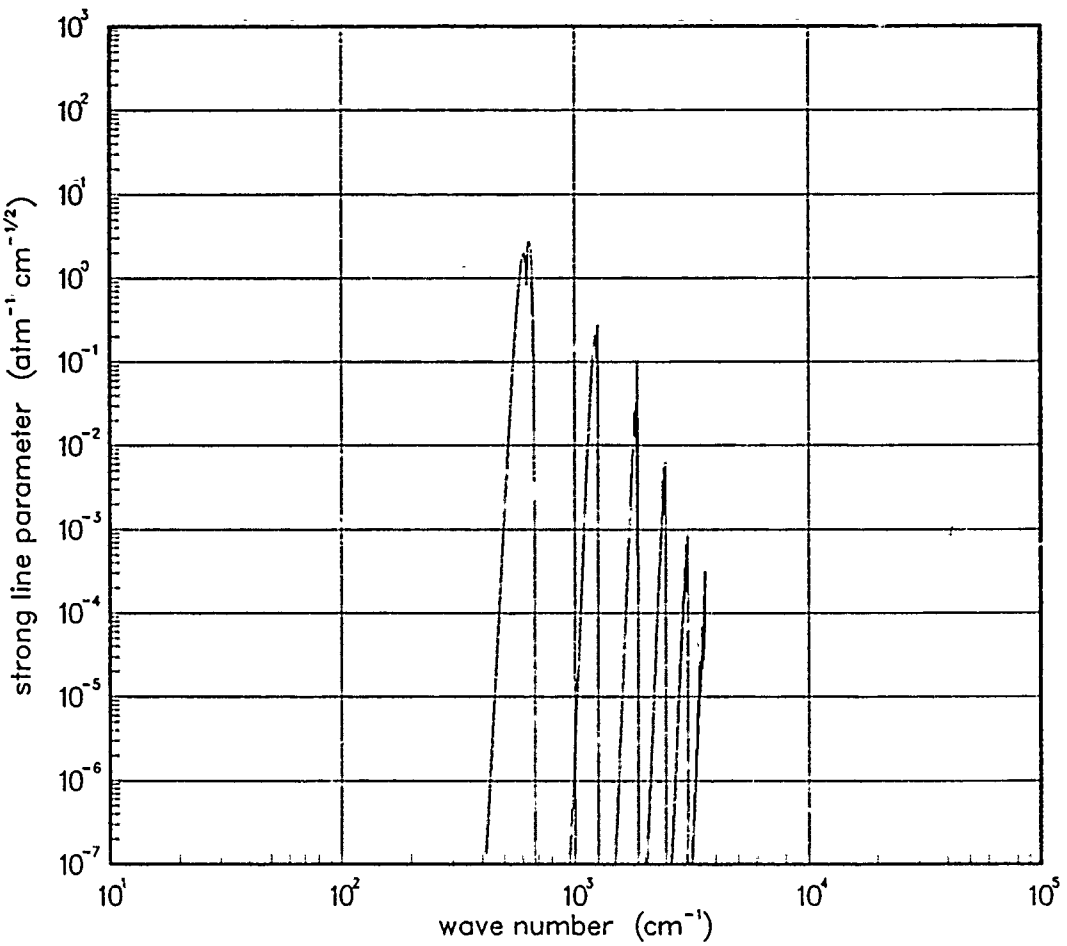

Figure 330. Strong-line parameter for CuO at 300°K.

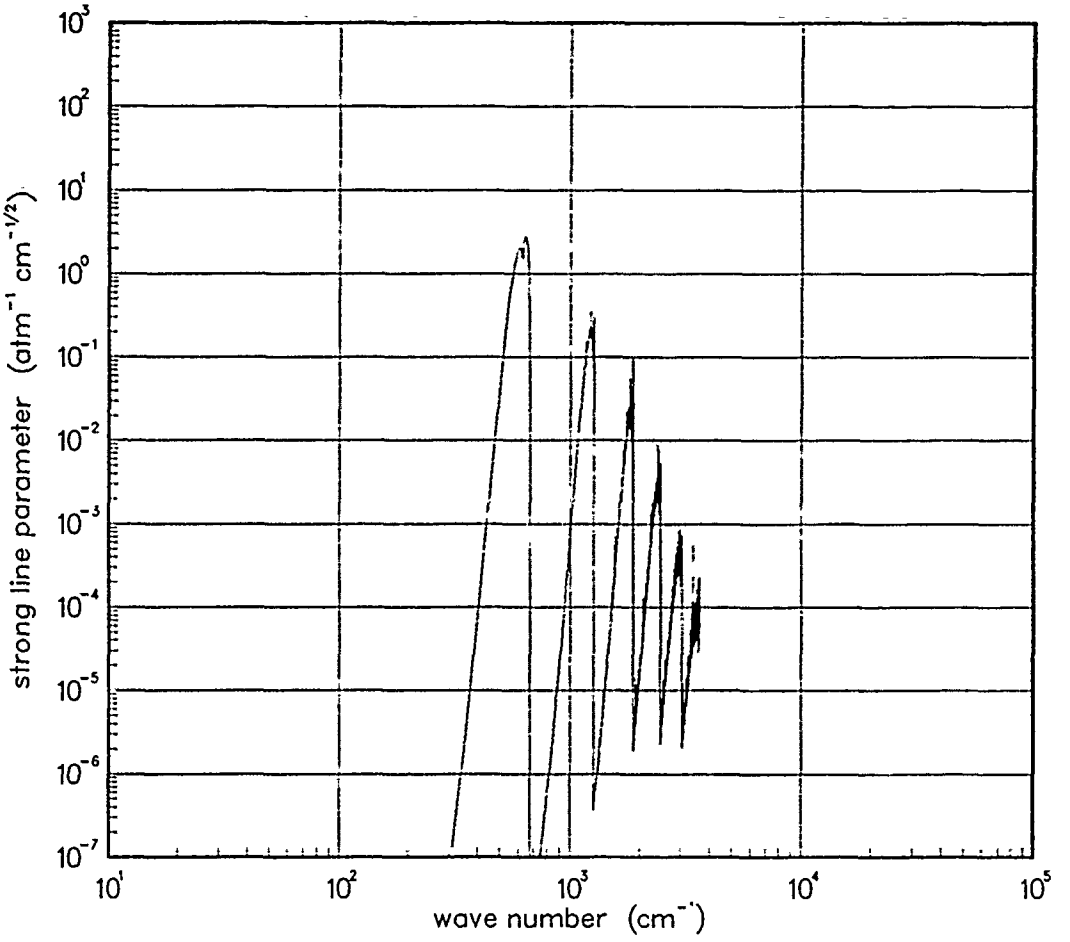

Figure 331. Strong-line parameter for CuO at 500°K.

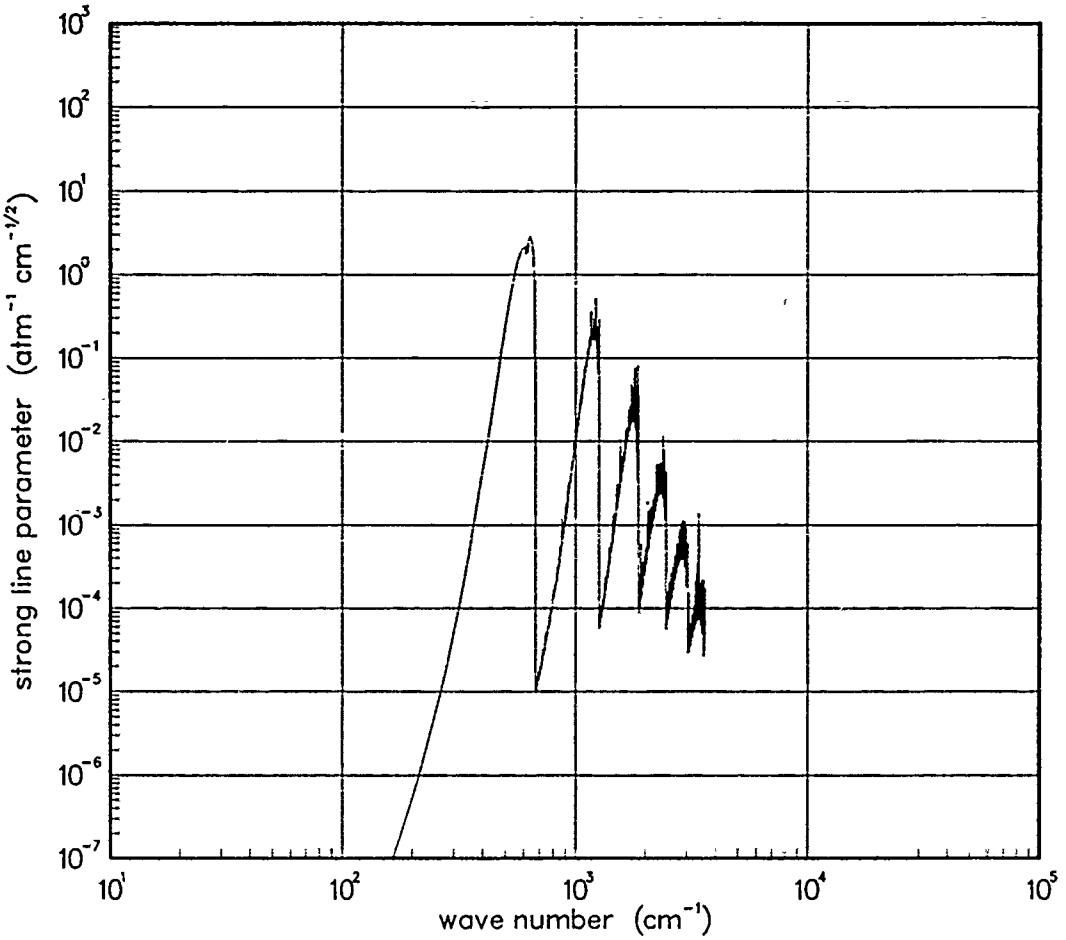

Figure 332. Strong-line parameter for CuO at 750°K.

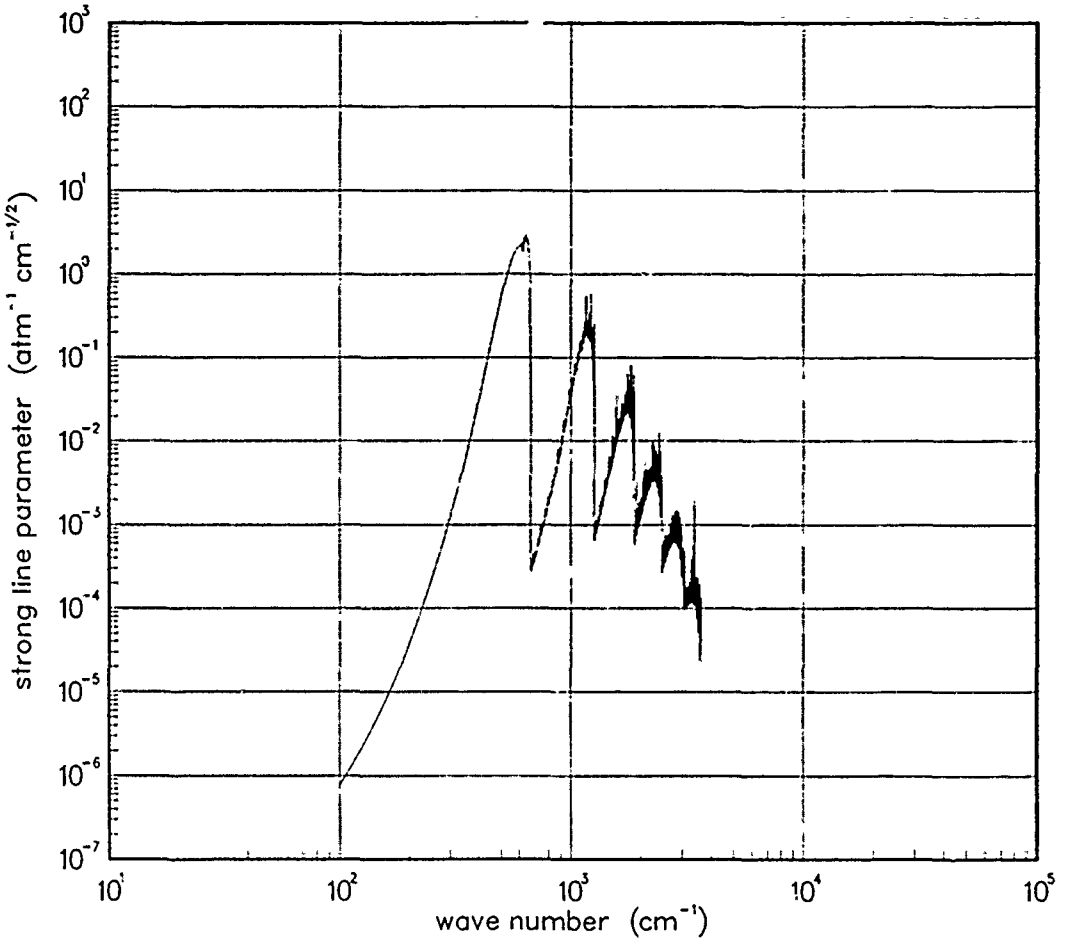

Figure 333. Strong-line parameter for CuO at 1000°K.

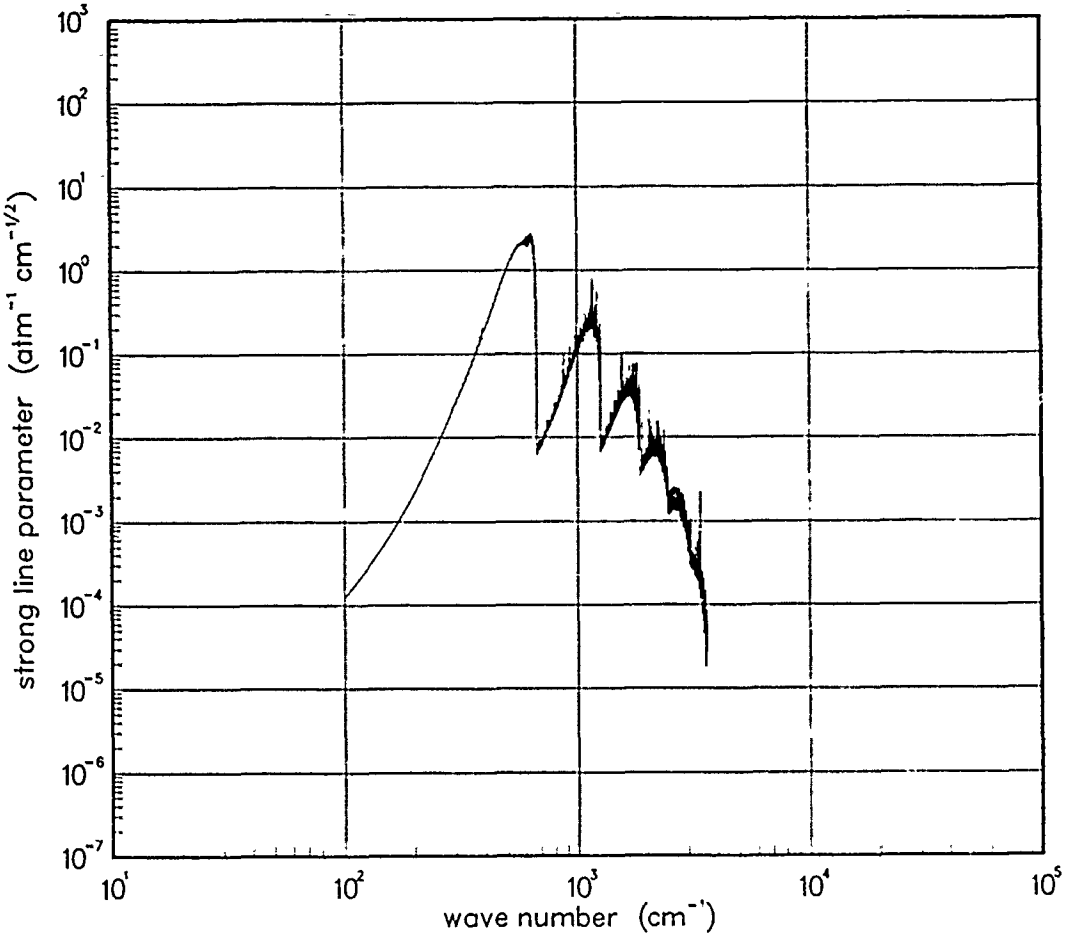

Figure 334. Strong-line parameter for CuO at 1500°K.

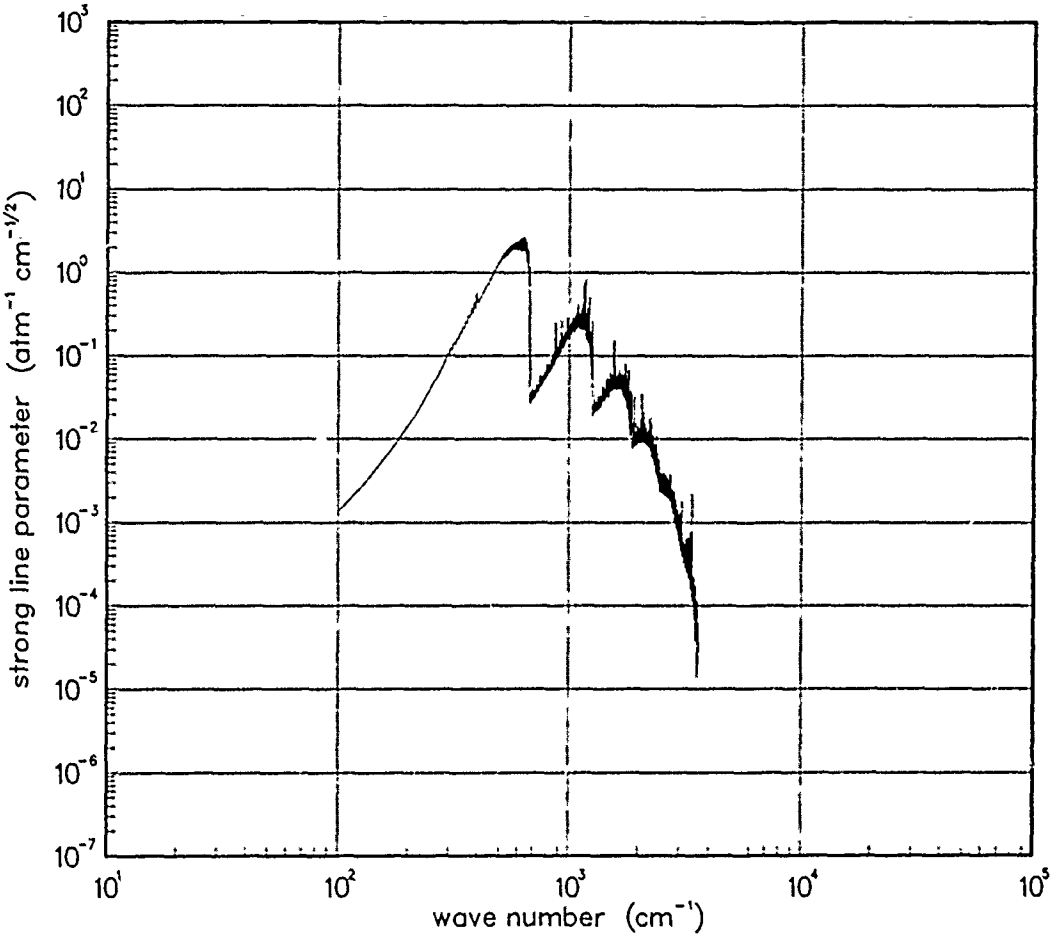

Figure 335. Strong-line parameter for CuO at 2000°K.

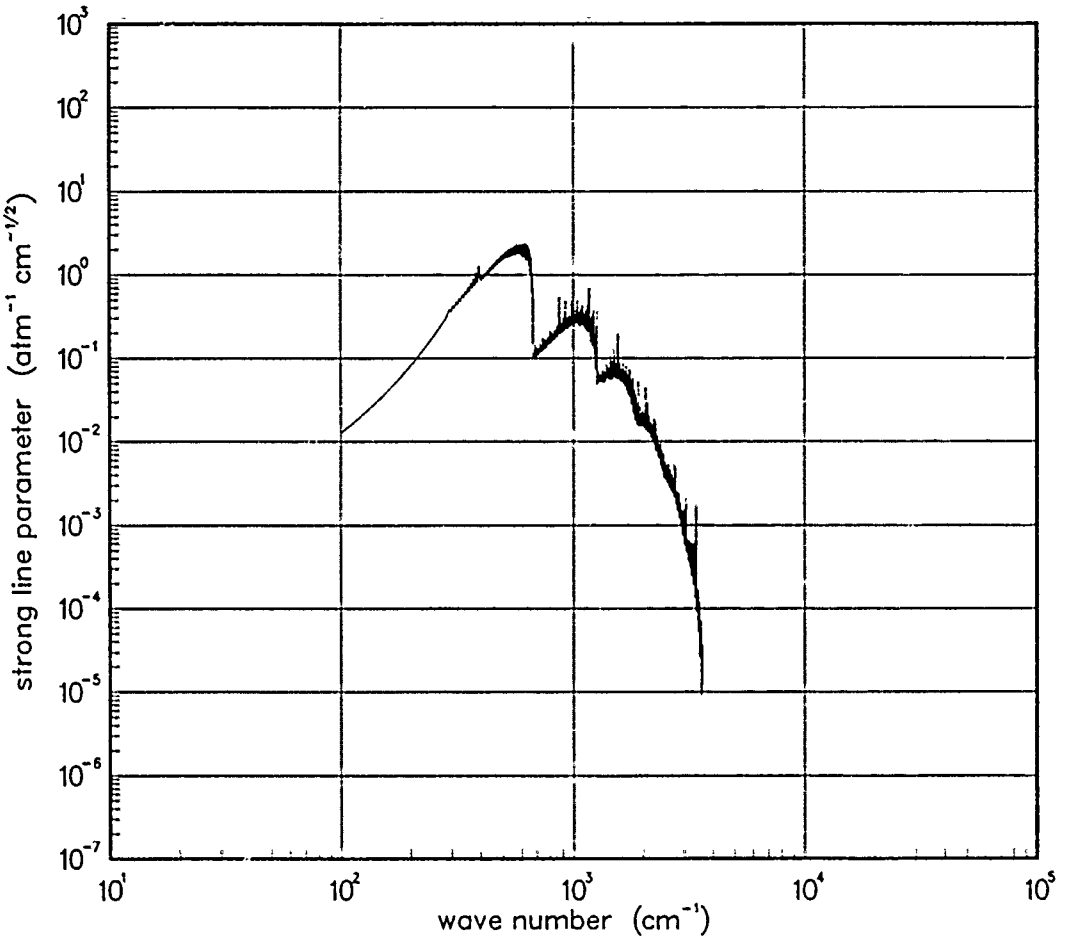

Figure 336. Strong-line parameter for CuO at 3000°K.

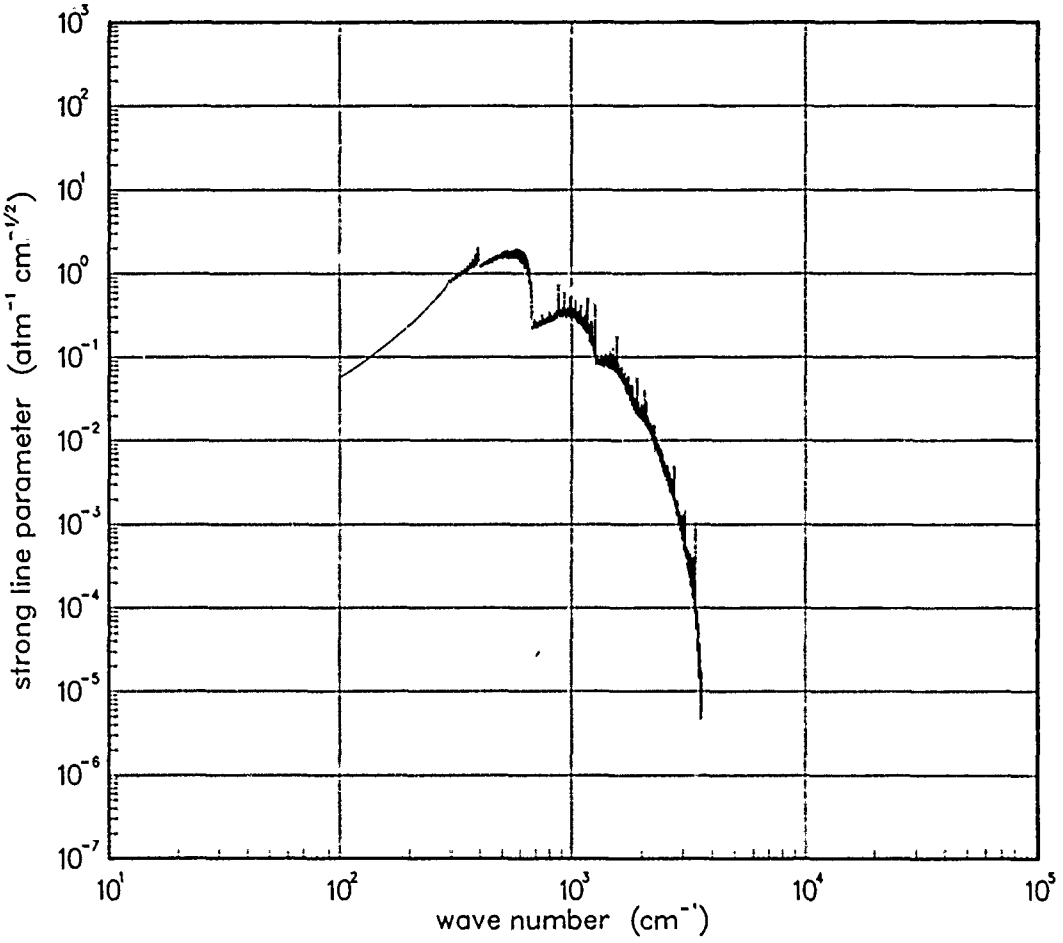

Figure 337. Strong-line parameter for CuO at 5000°K.

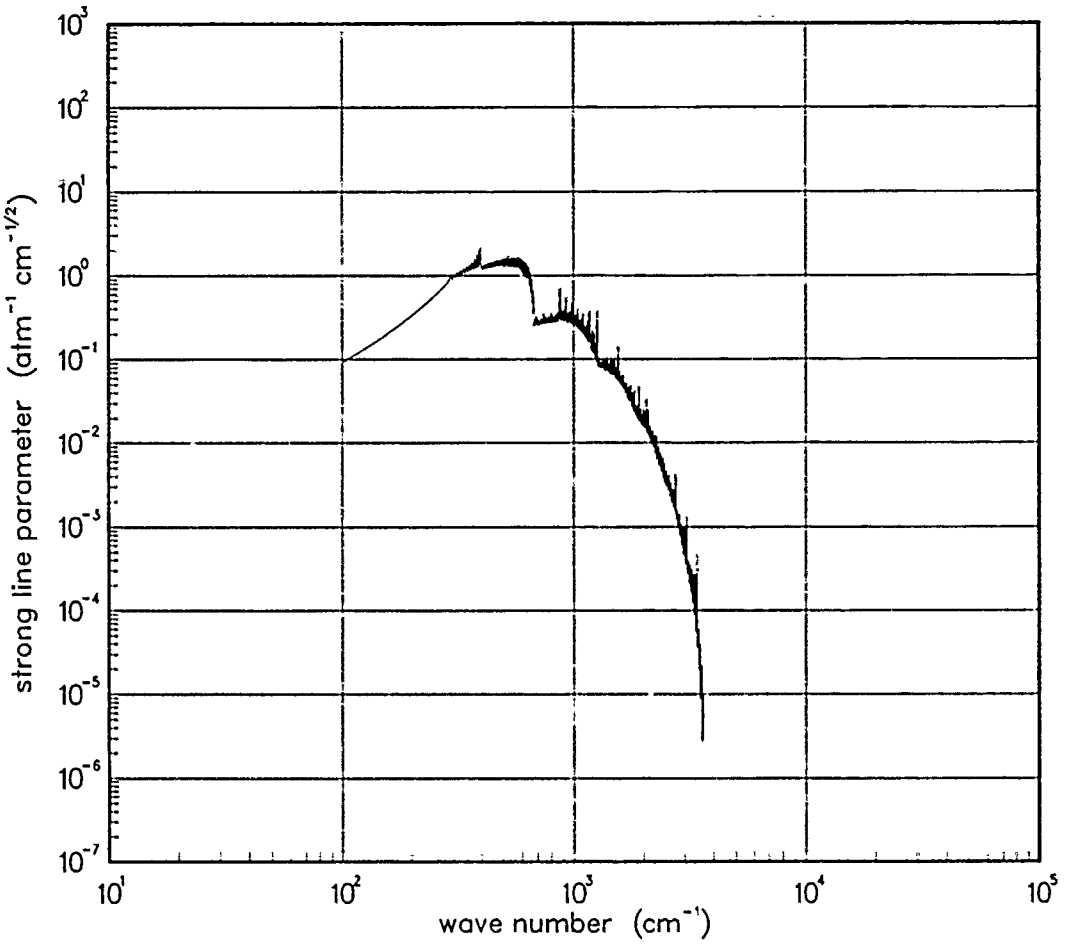

Figure 338. Strong-line parameter for CuO at 7000°K.

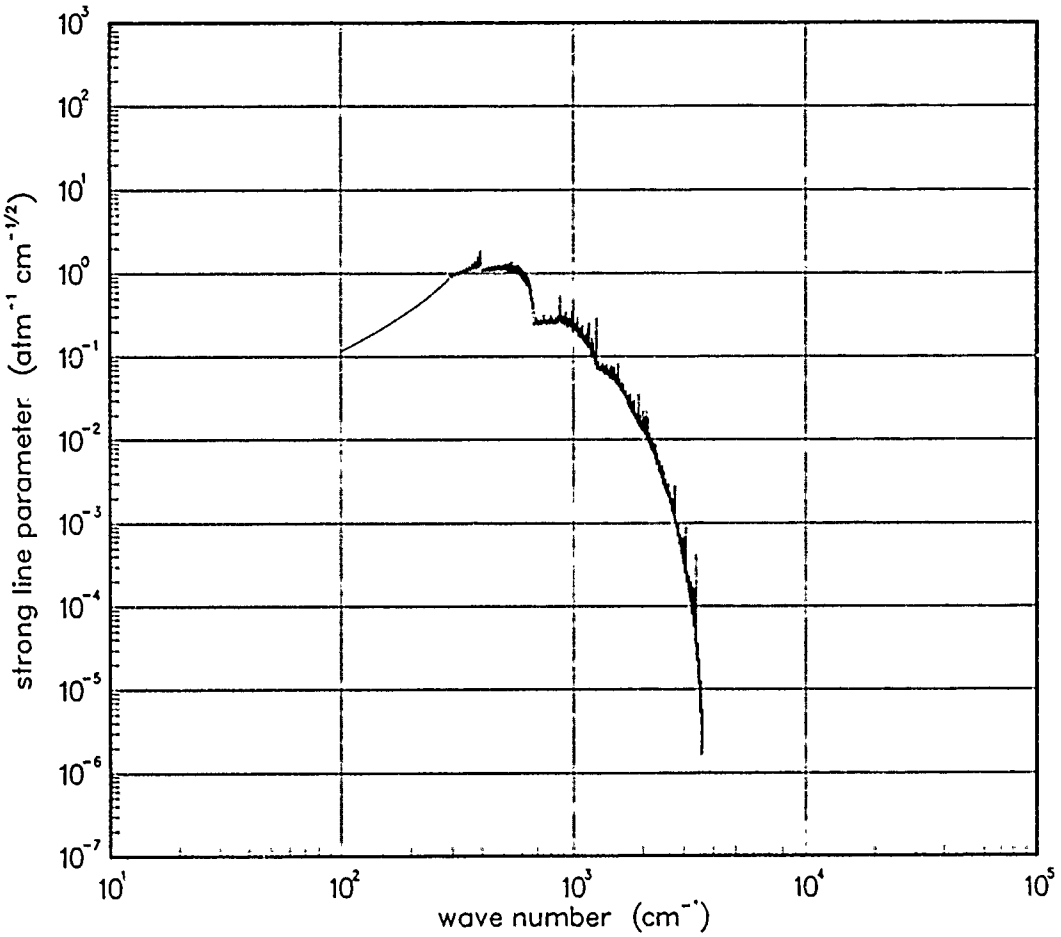

Figure 339. Strong-line parameter for CuO at 10000°K.

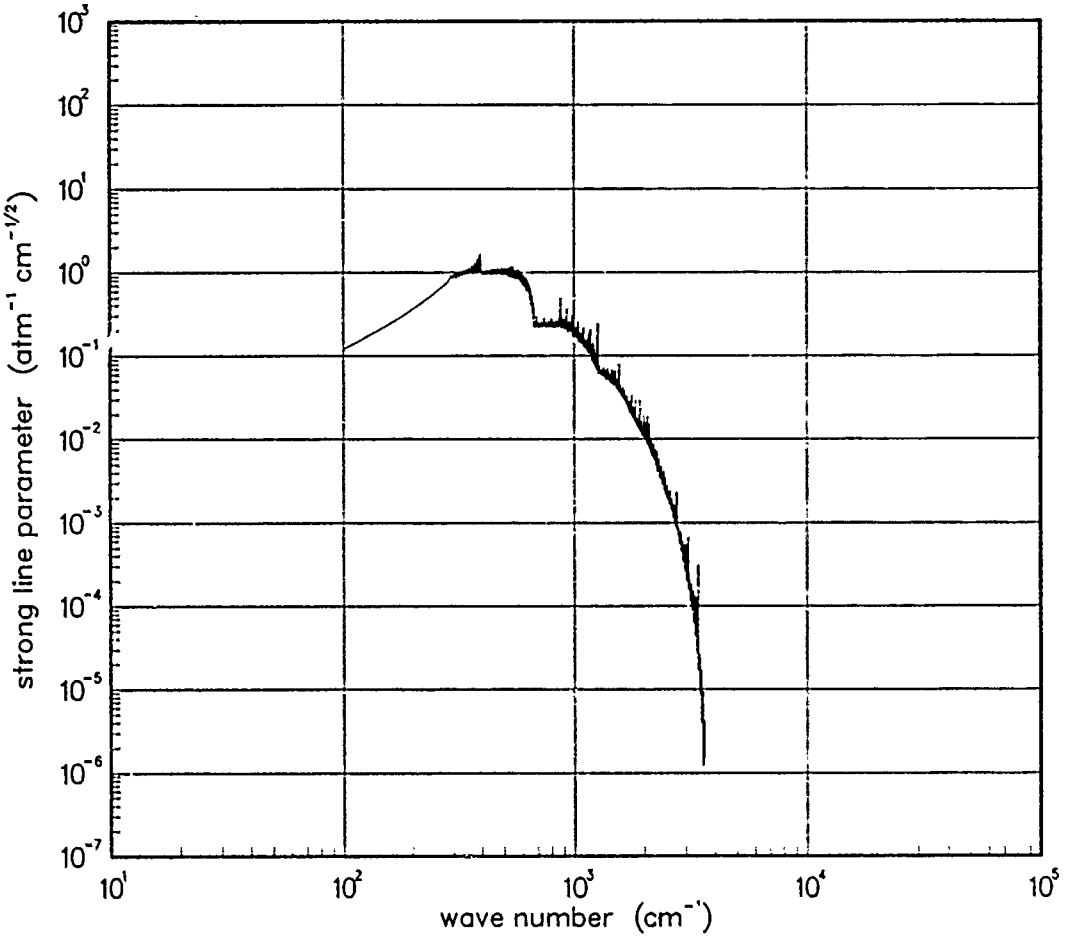

Figure 340. Strong-line parameter for CuO at 12000°K.

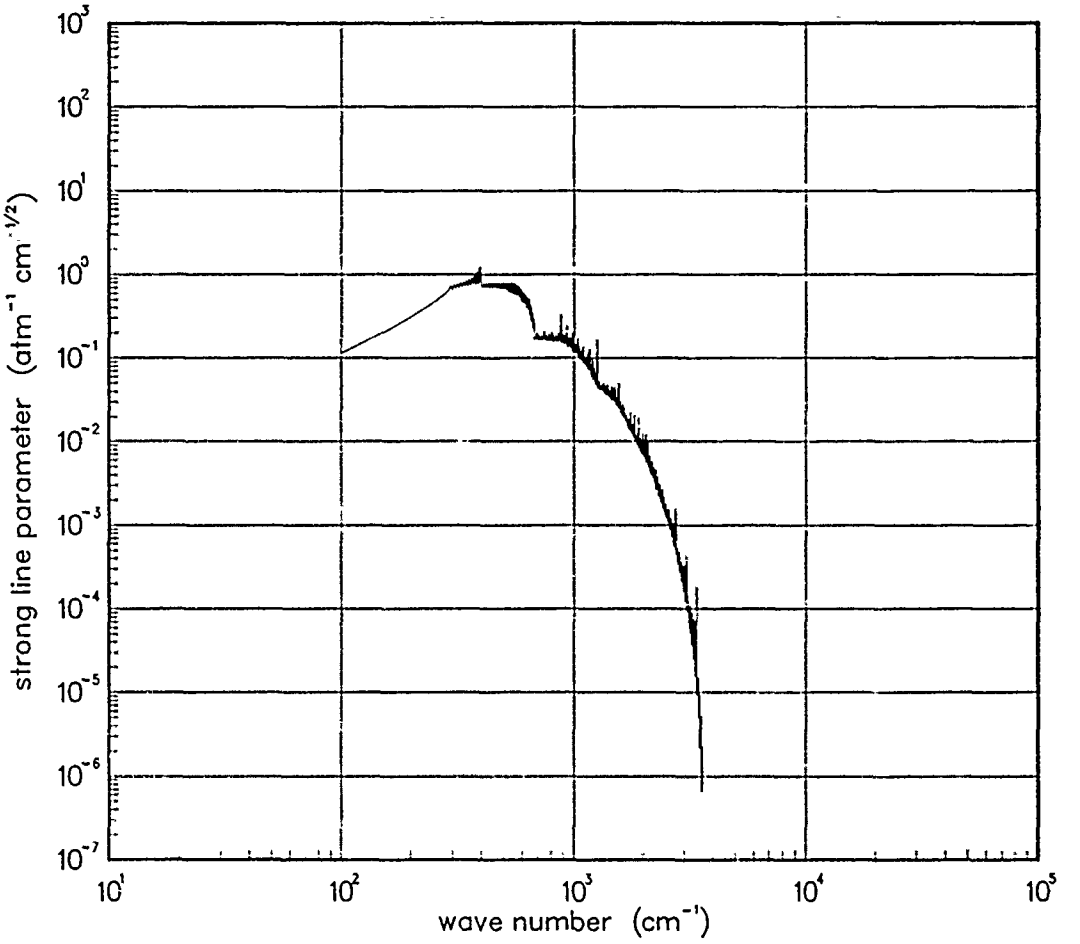

Figure 341. Strong-line parameter for CuO at 18000°K.

6.3 IRON OXIDE (FeO).

Table 9. Spectroscopic data for FeO.

$X\ ^7\Sigma$

$\omega_e = 880.53^*$ $\quad \omega_e x_e = 4.63^*$
$\alpha_e = 0.00376^*$ $\quad B_e = 0.51271^*$

$S_{10} = 450^\dagger$

$\gamma_e(300\ ^\circ K) = 0.04^\ddagger$

Data Source:

*R.F. Barrow, and M. Senior, Nature 223 1359 (1969).

†K. Wray, AVCO, Mass., Contribution to DASA/ARPA Working Group, p. 26 Palo Alto, Ca. (October 1970).

‡Estimate.

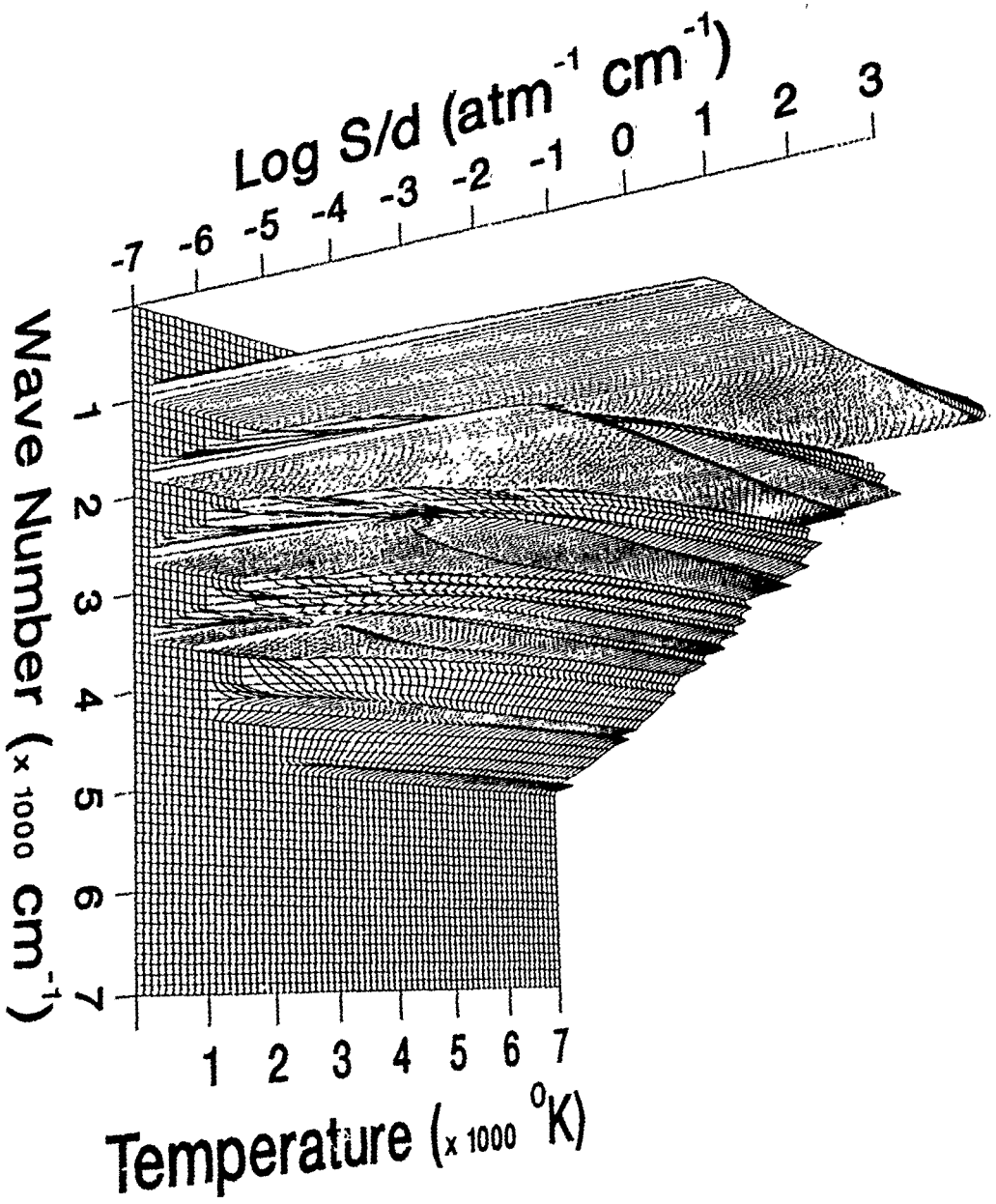

Figure 342. Weak-line parameter for FeO.

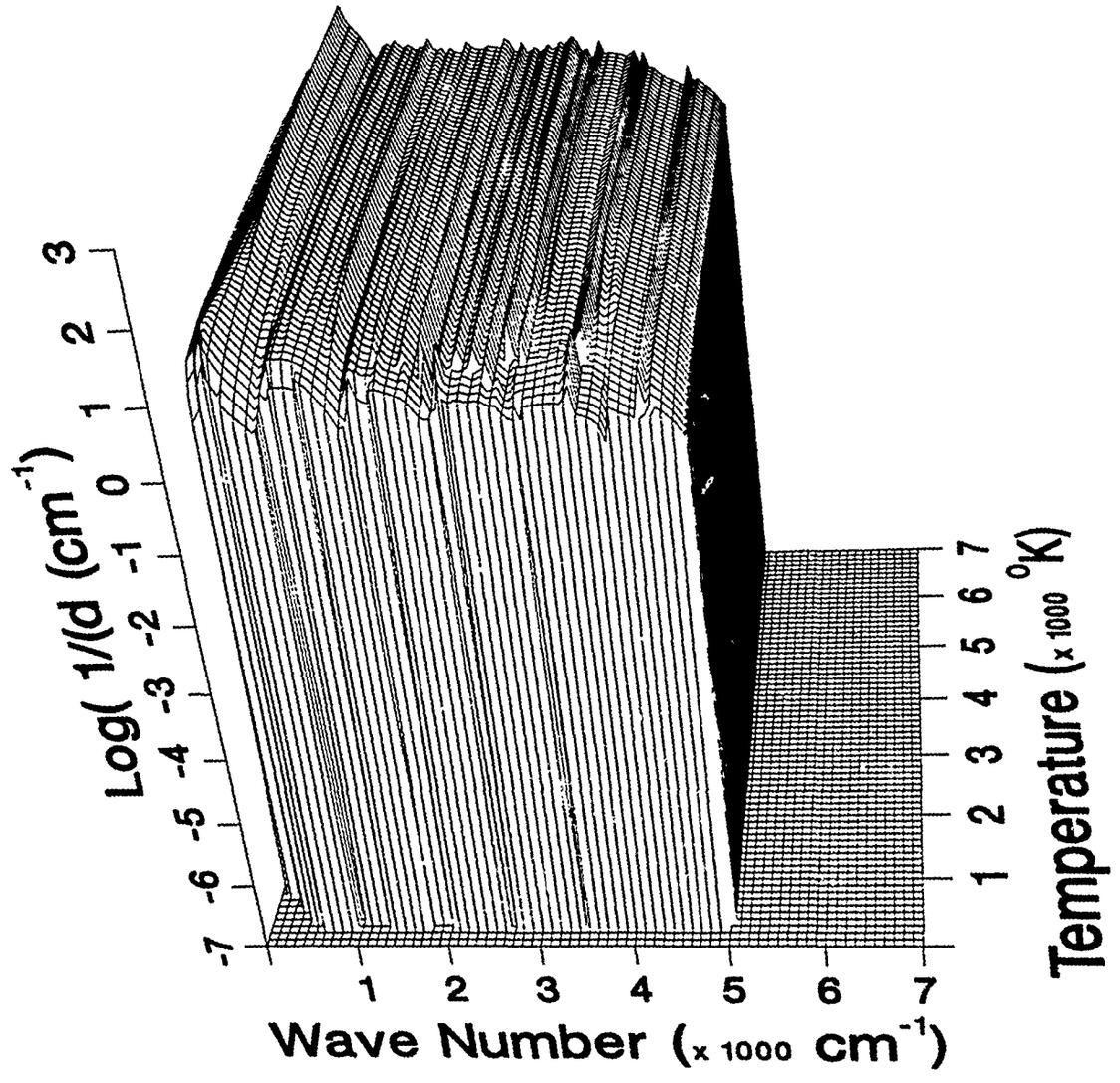

Figure 343. Inverse line spacing for FeO.

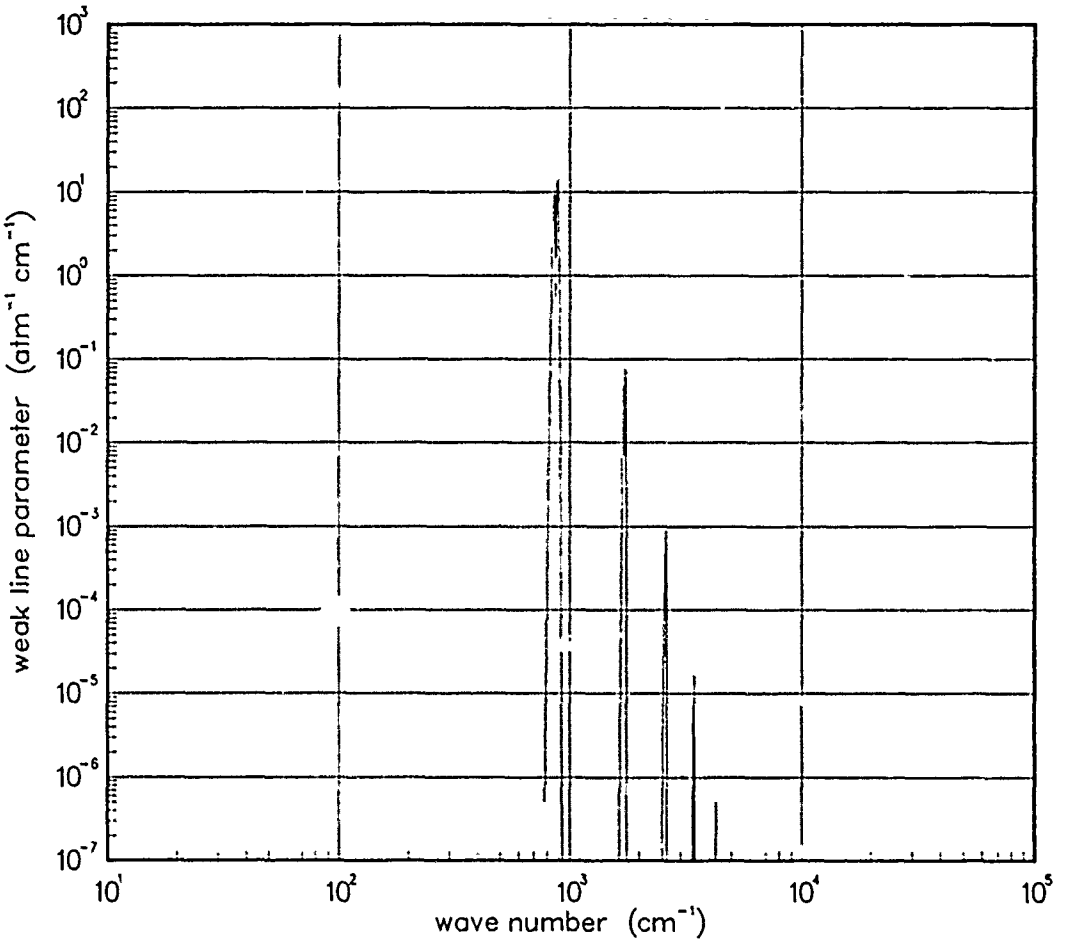

Figure 344. Weak-line parameter for FeO at 200°K.

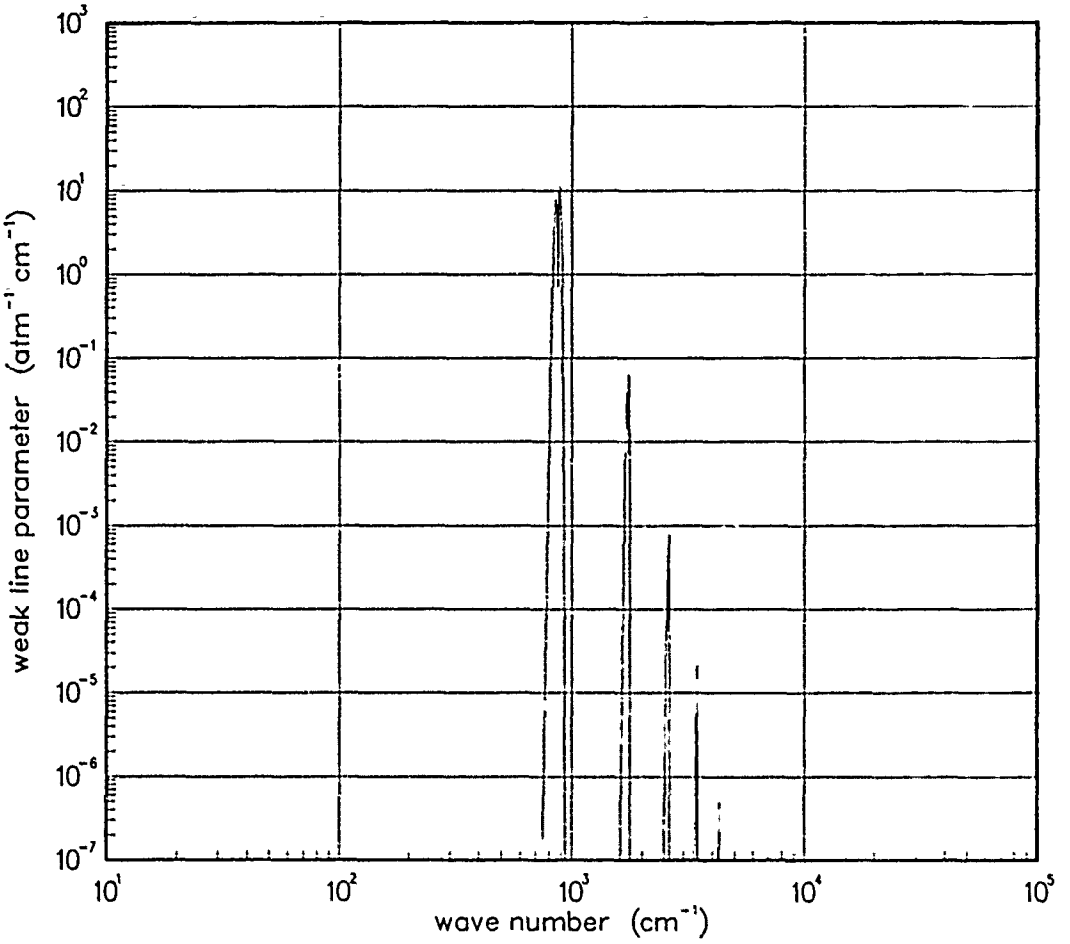

Figure 345. Weak-line parameter for FeO at 300°K.

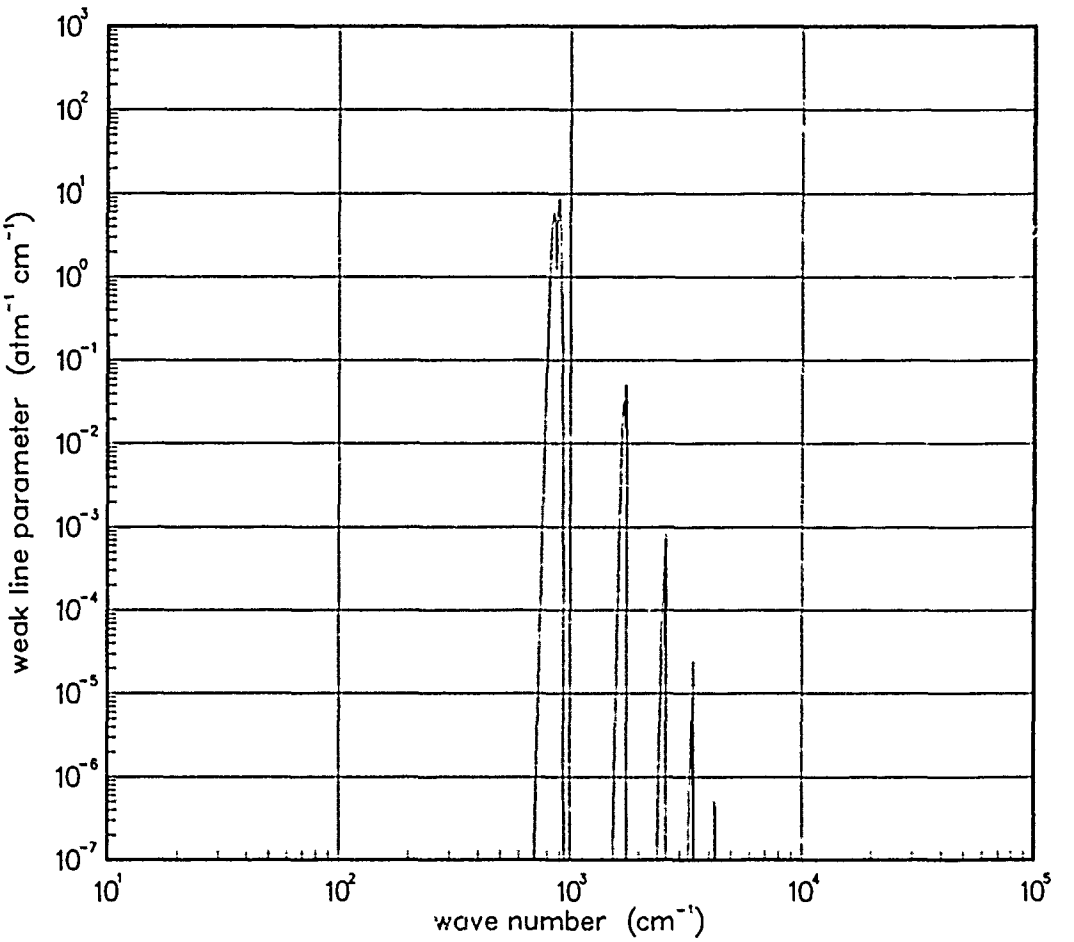

Figure 346. Weak-line parameter for FeO at 500°K.

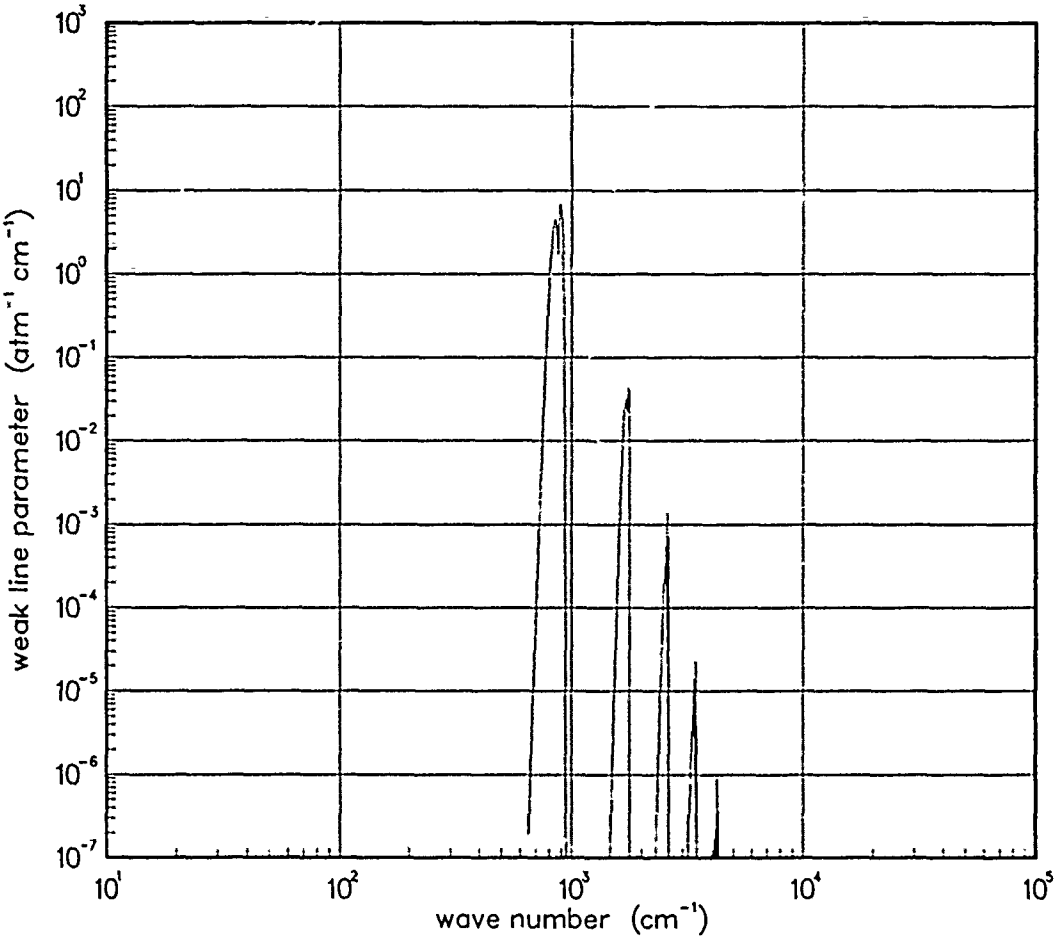

Figure 347. Weak-line parameter for FeO at 750°K.

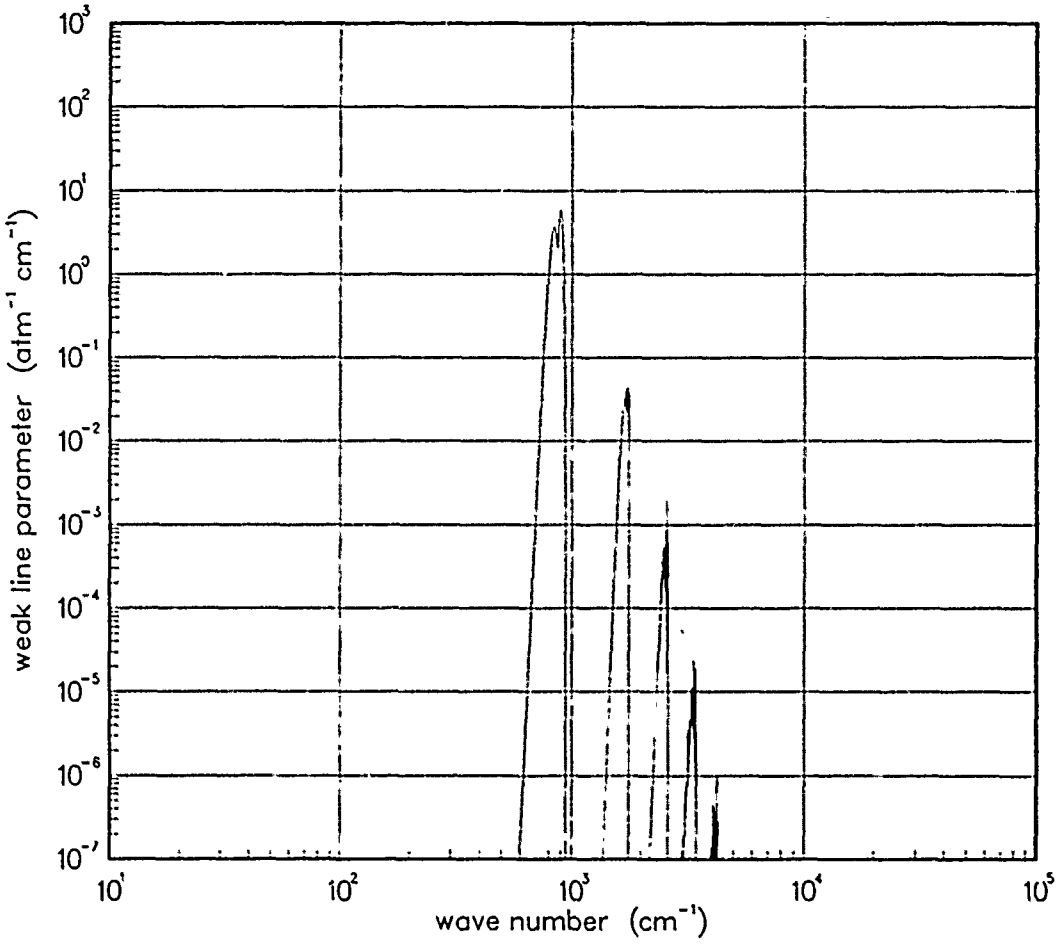

Figure 348. Weak-line parameter for FeO at 1000°K.

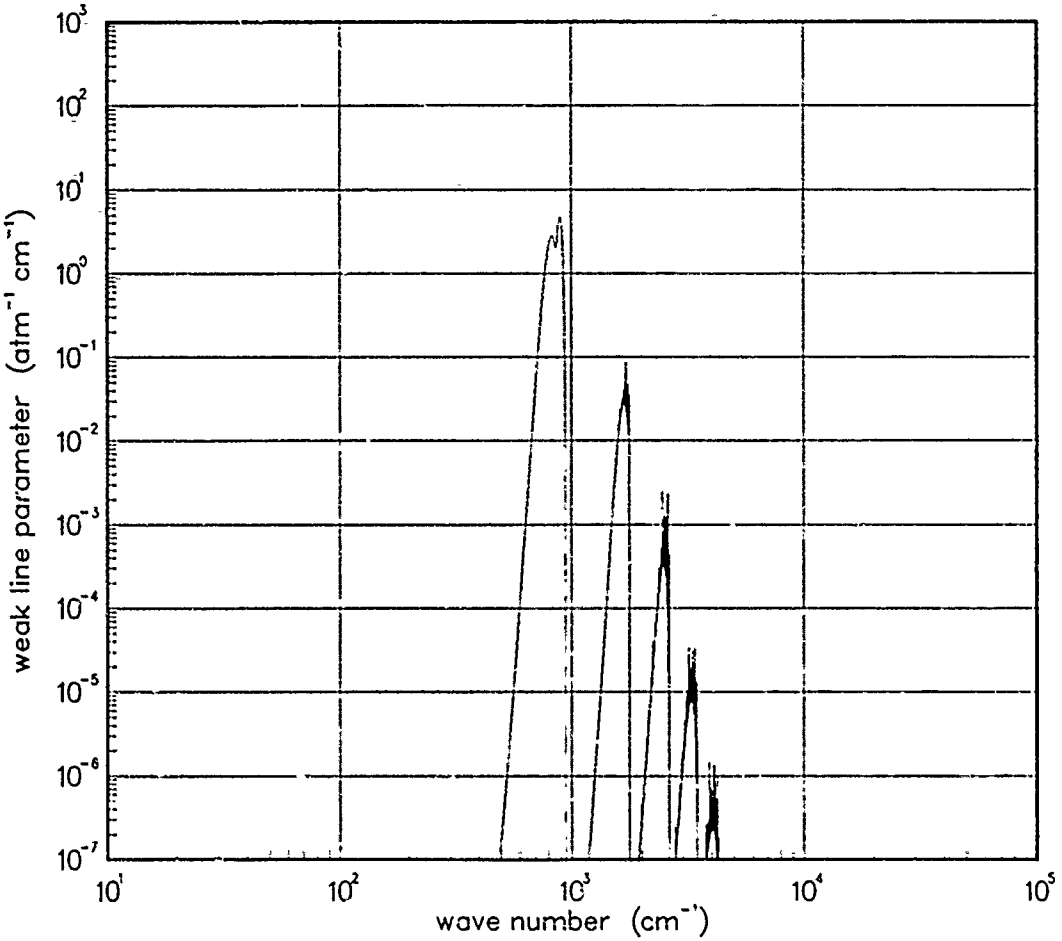

Figure 349. Weak-line parameter for FeO at 1500°K.

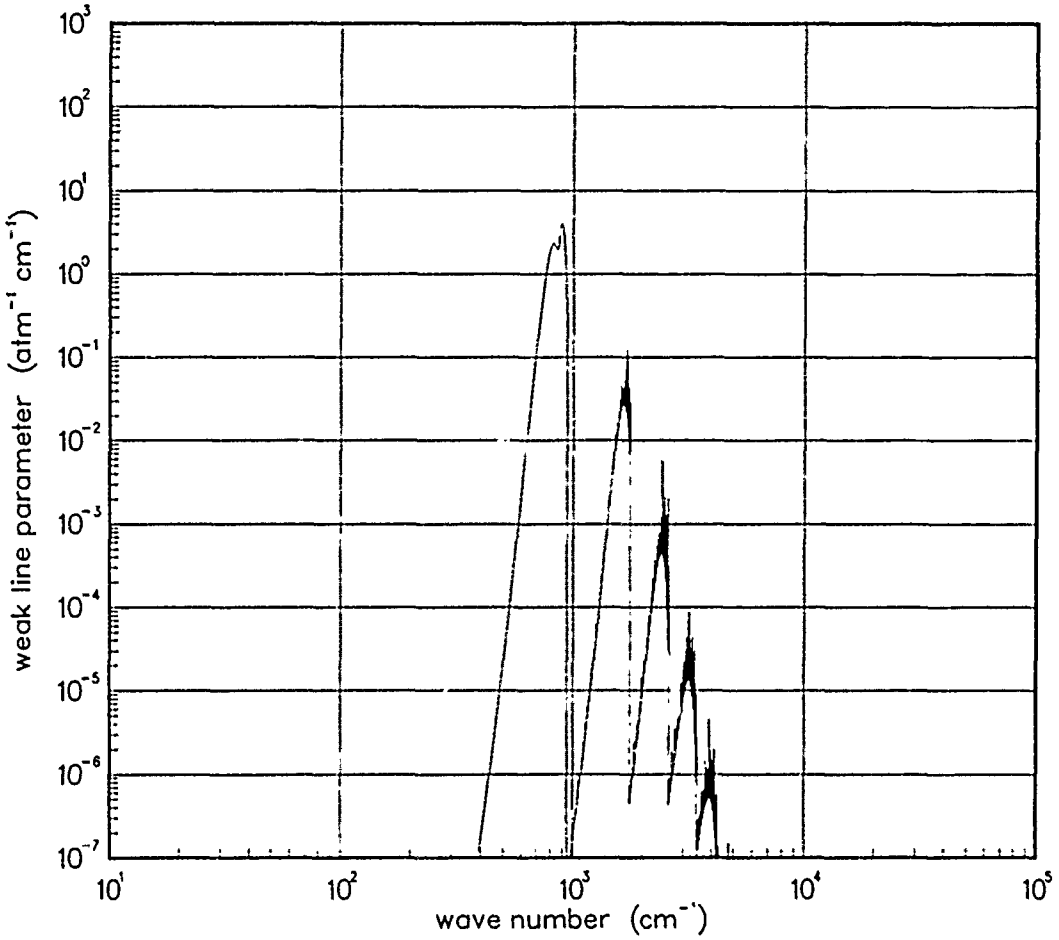

Figure 350. Weak-line parameter for FeO at 2000°K.

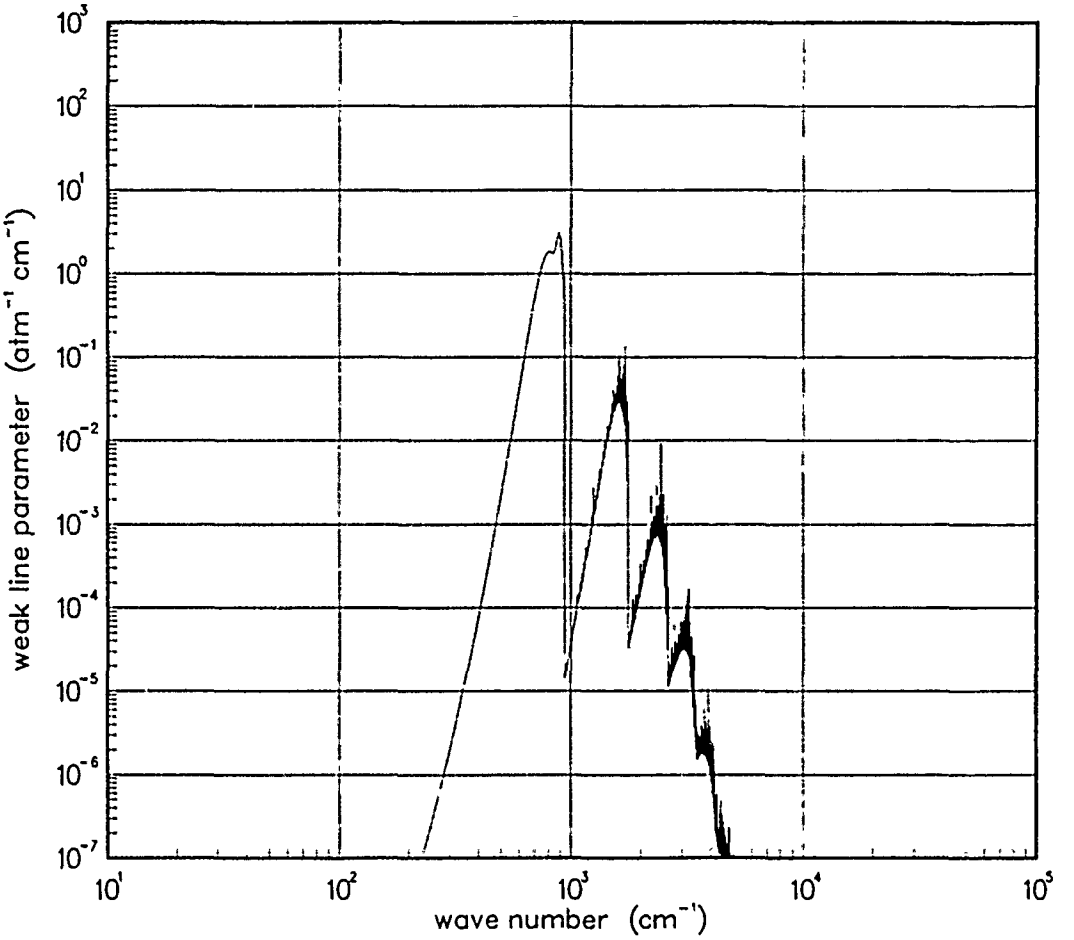

Figure 351. Weak-line parameter for FeO at 3000°K.

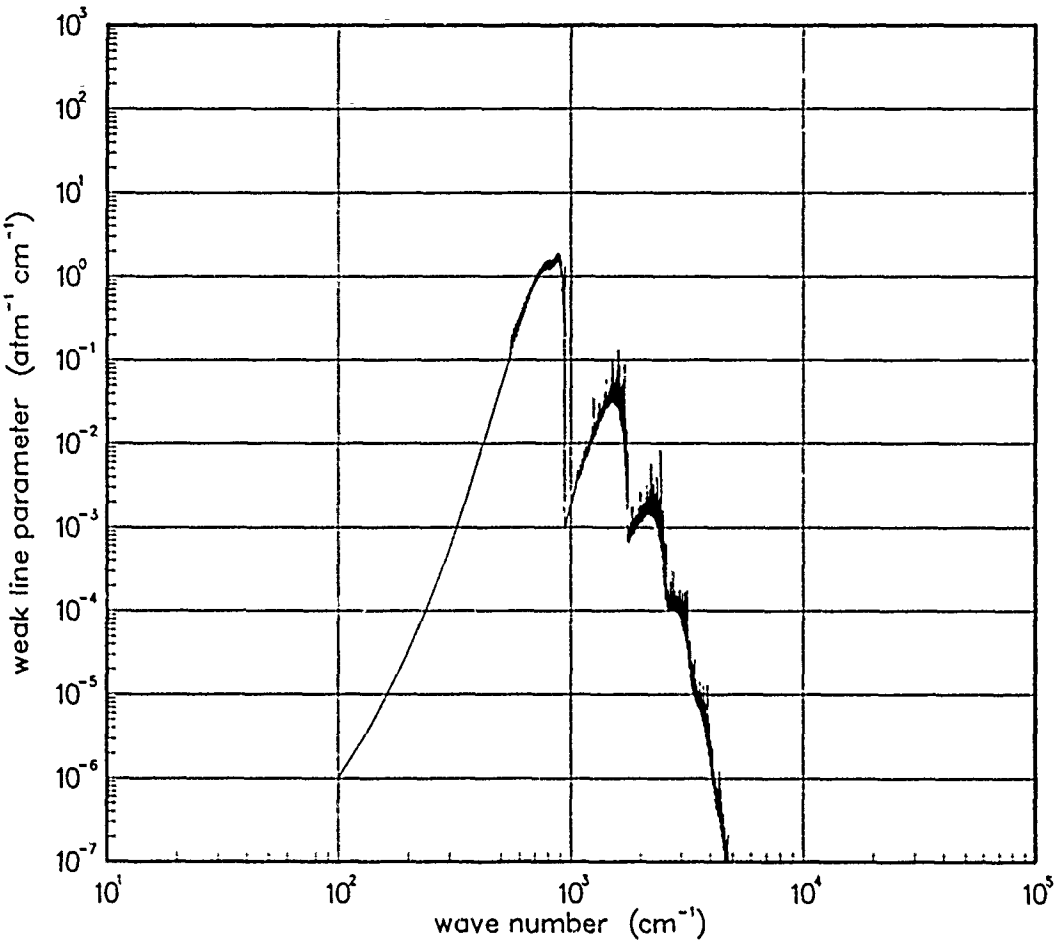

Figure 352. Weak-line parameter for FeO at 5000°K.

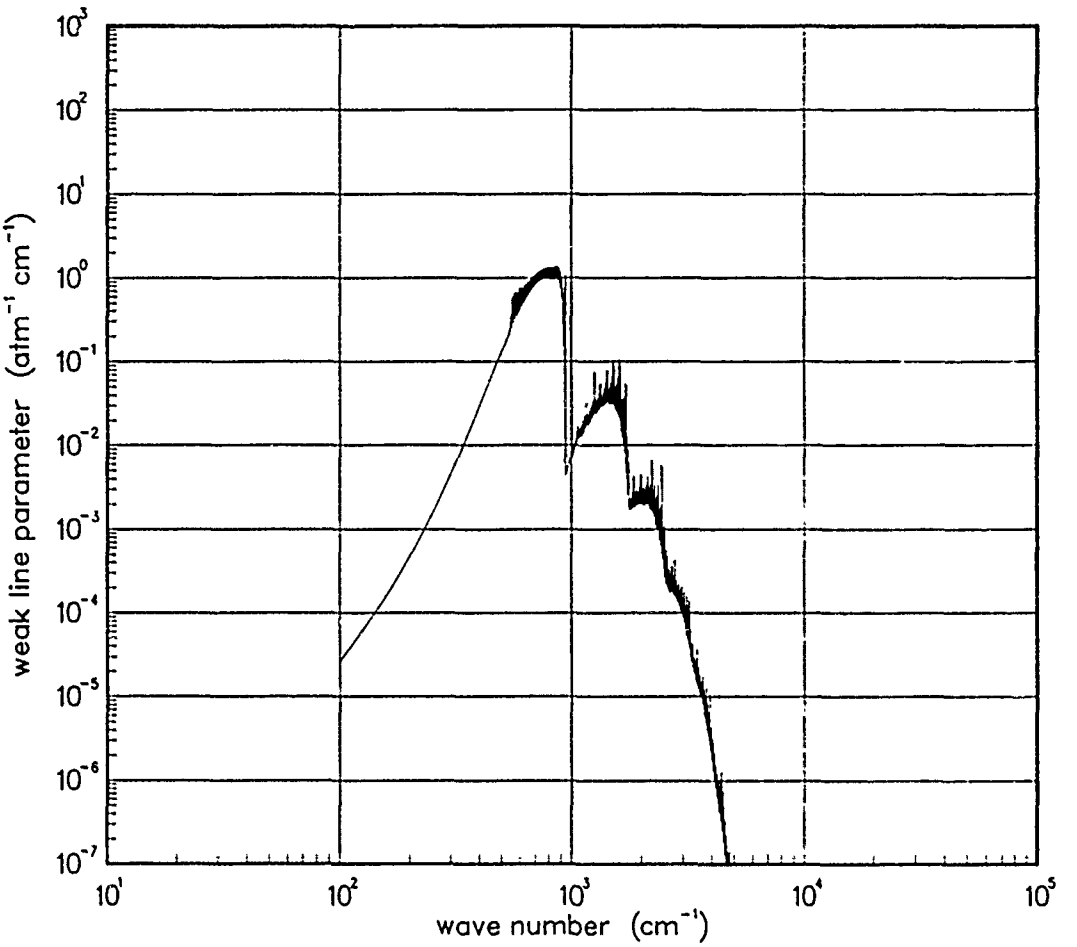

Figure 353. Weak-line parameter for FeO at 7000°K.

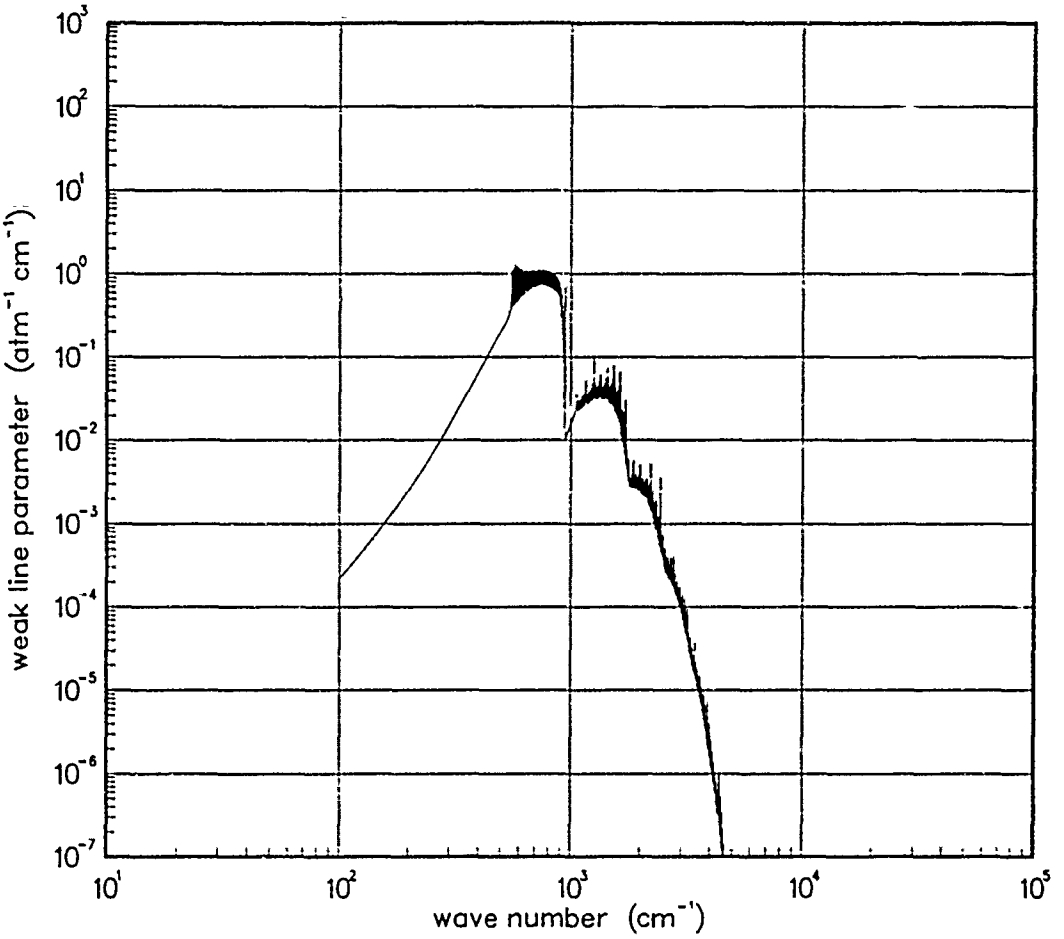

Figure 354. Weak-line parameter for FeO at 10000°K.

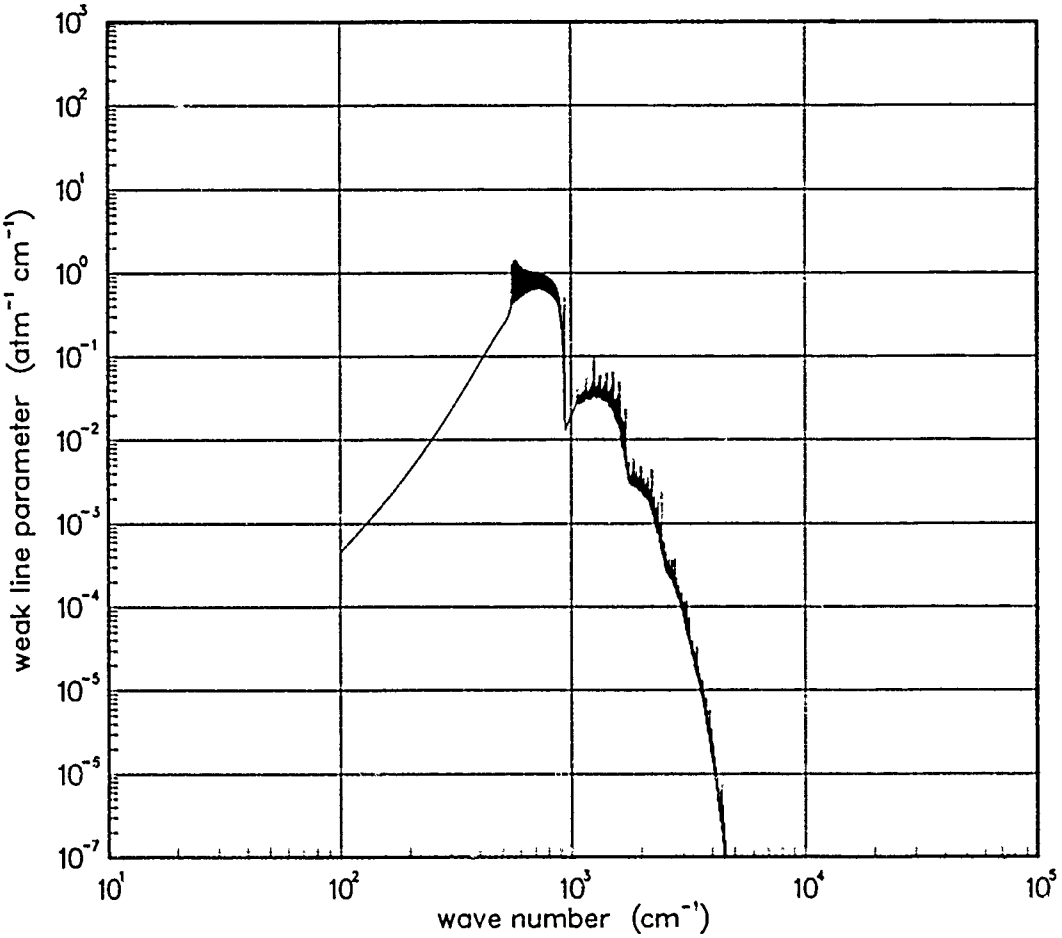

Figure 355. Weak-line parameter for FeO at 12000°K.

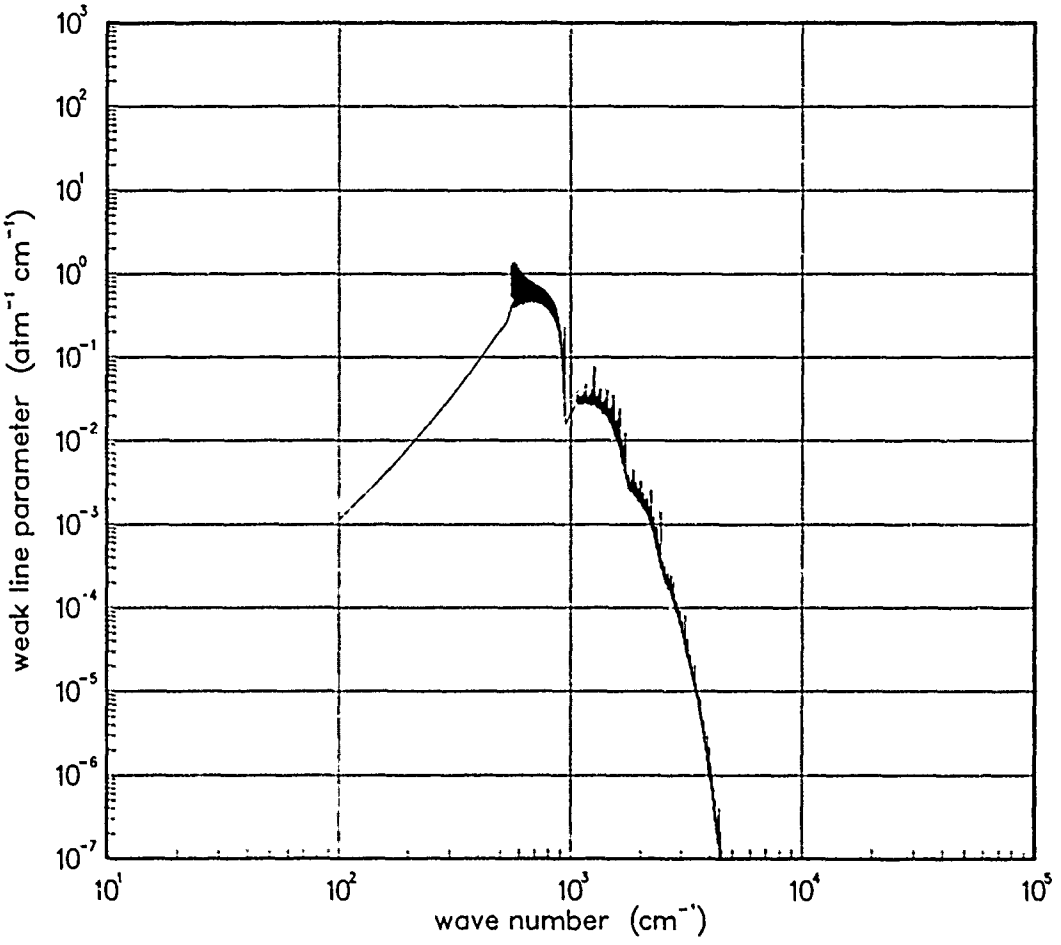

Figure 356. Weak-line parameter for FeO at 18000°K.

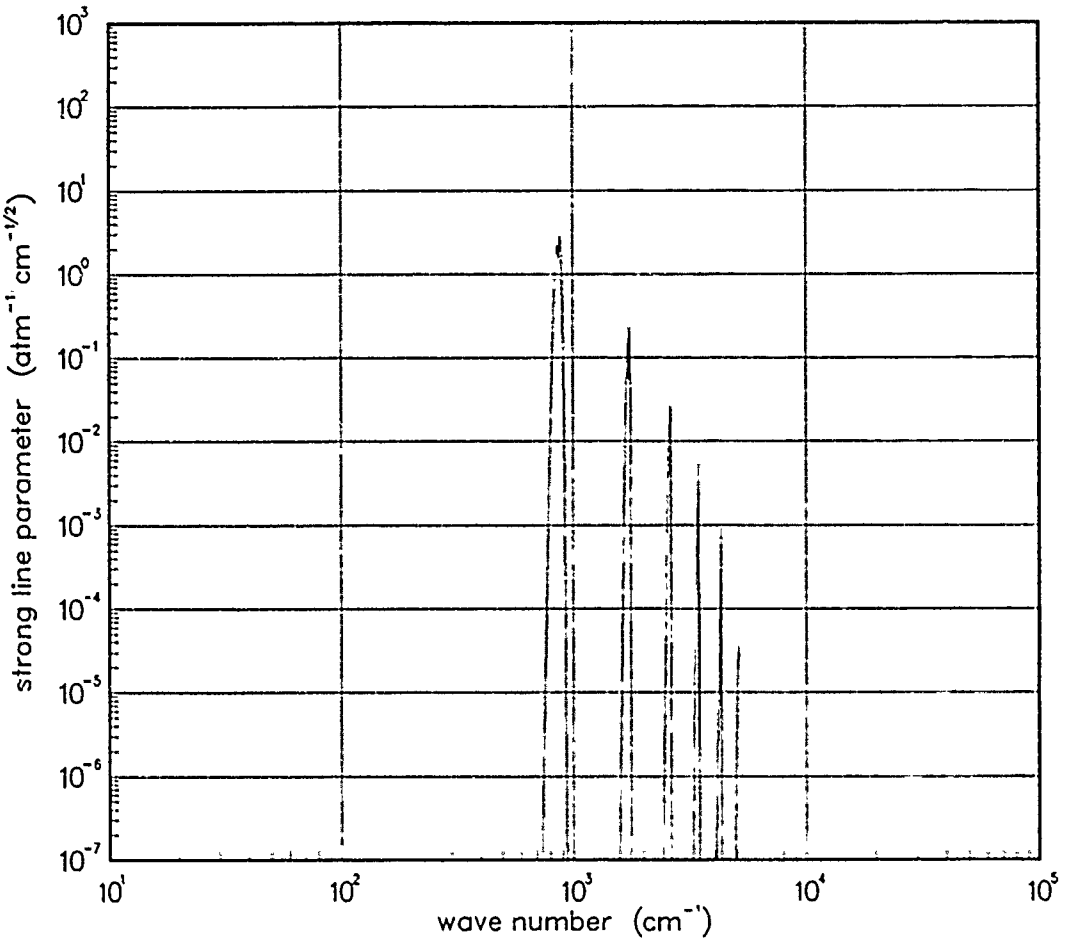

Figure 357. Strong-line parameter for FeO at 200°K.

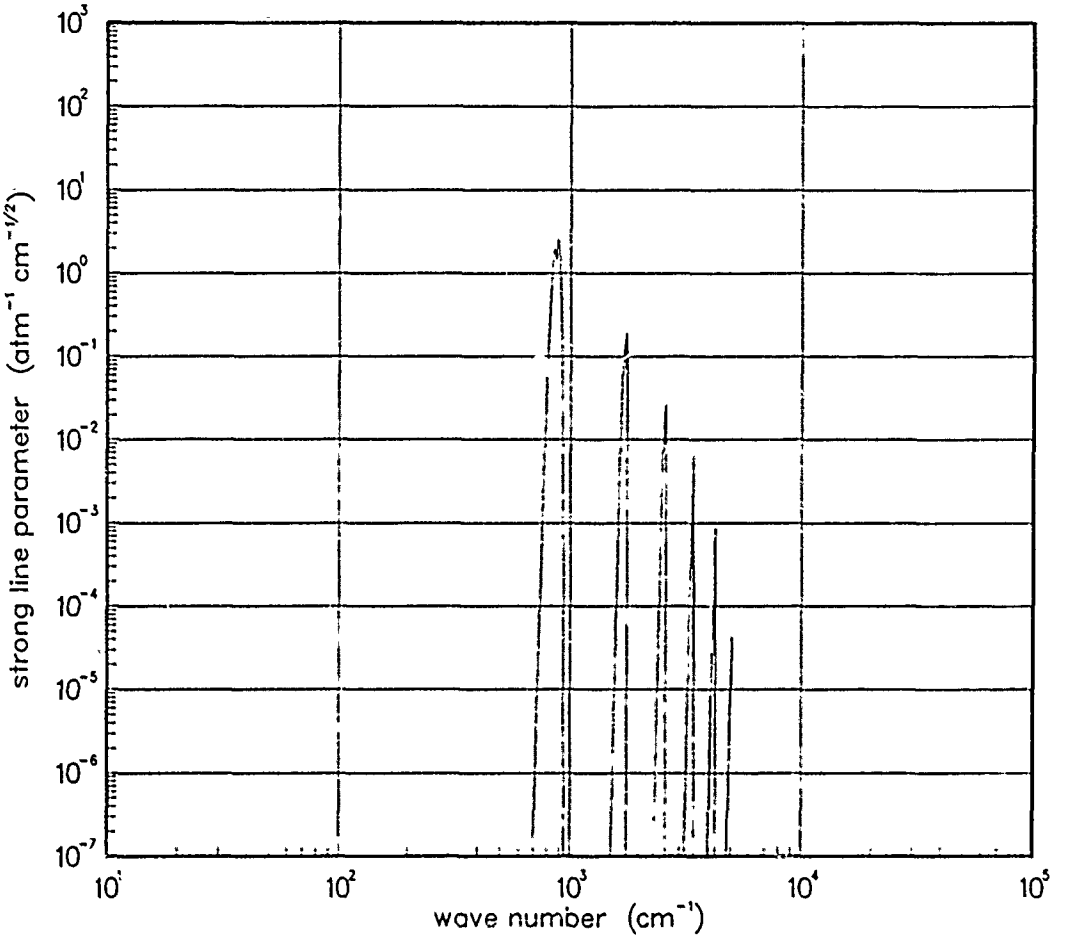

Figure 358. Strong-line parameter for FeO at 300°K.

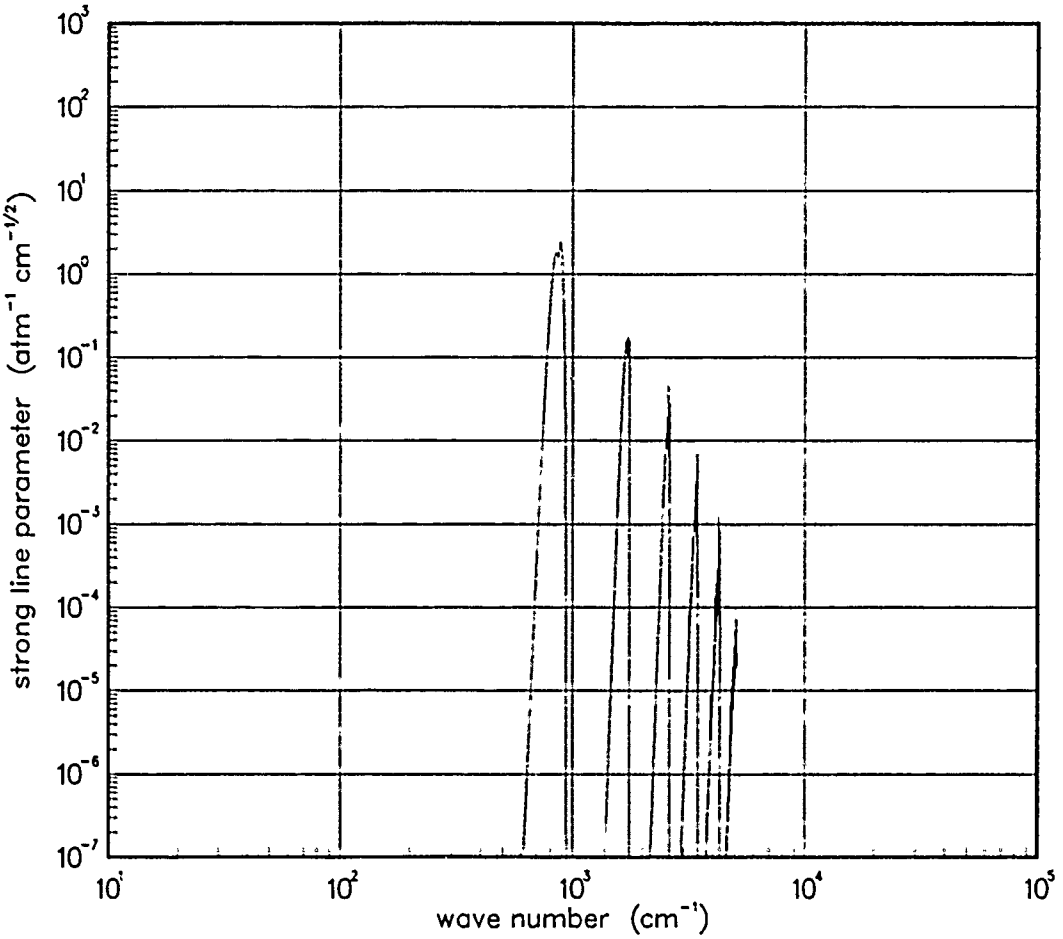

Figure 359. Strong-line parameter for FeO at 500°K.

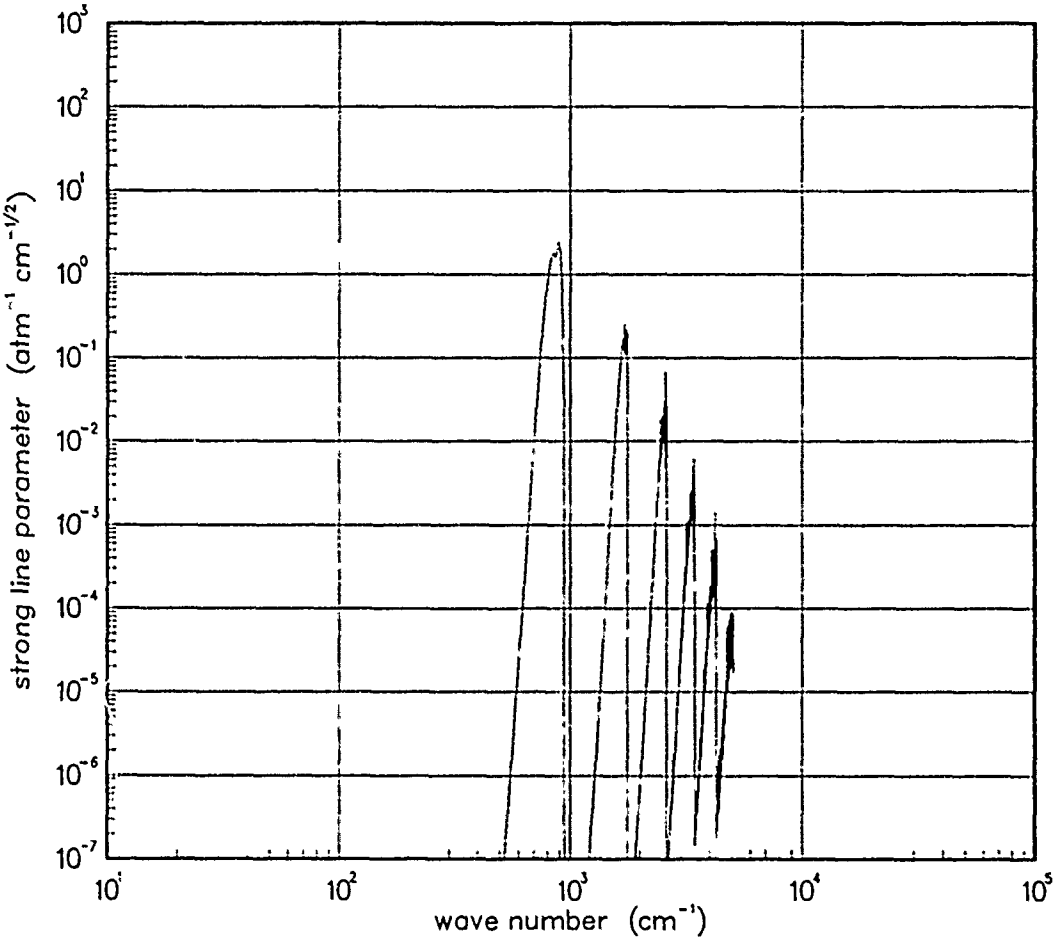

Figure 360. Strong-line parameter for FeO at 750°K.

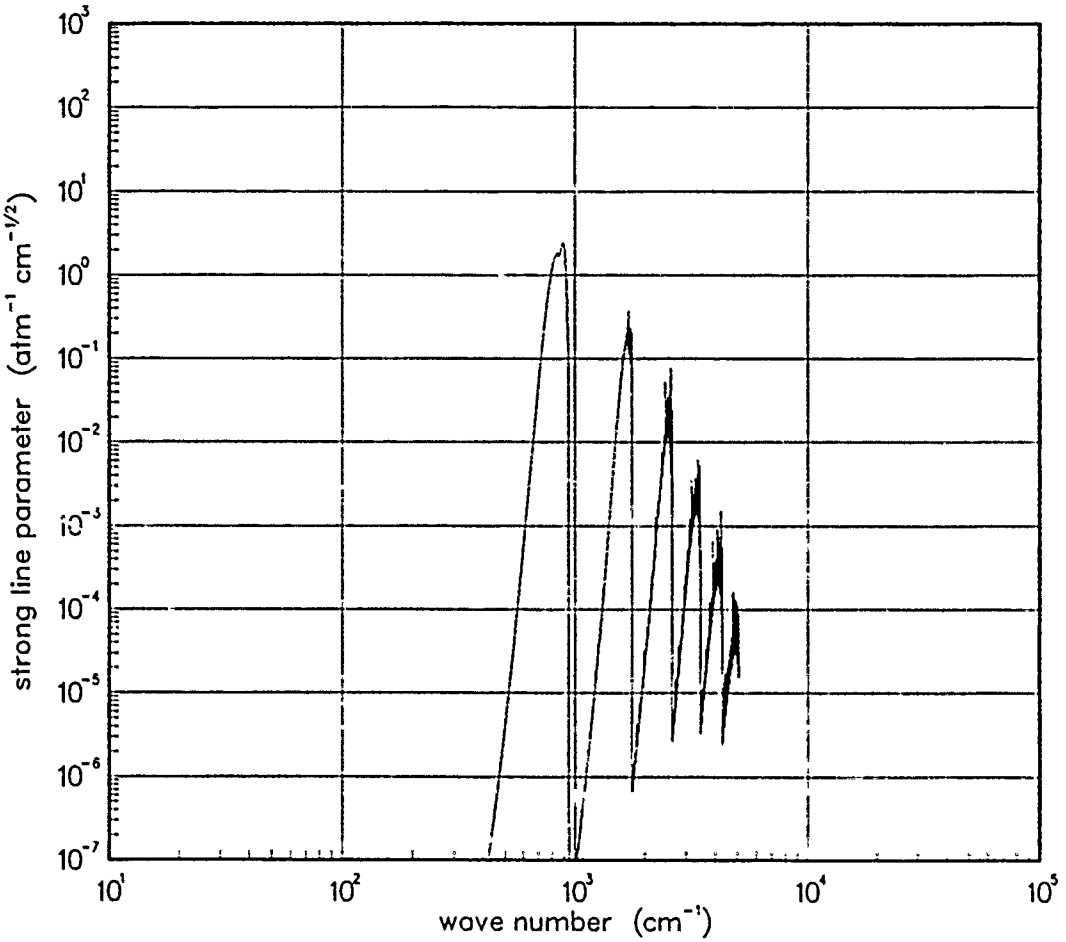

Figure 361. Strong-line parameter for FeO at 1000°K.

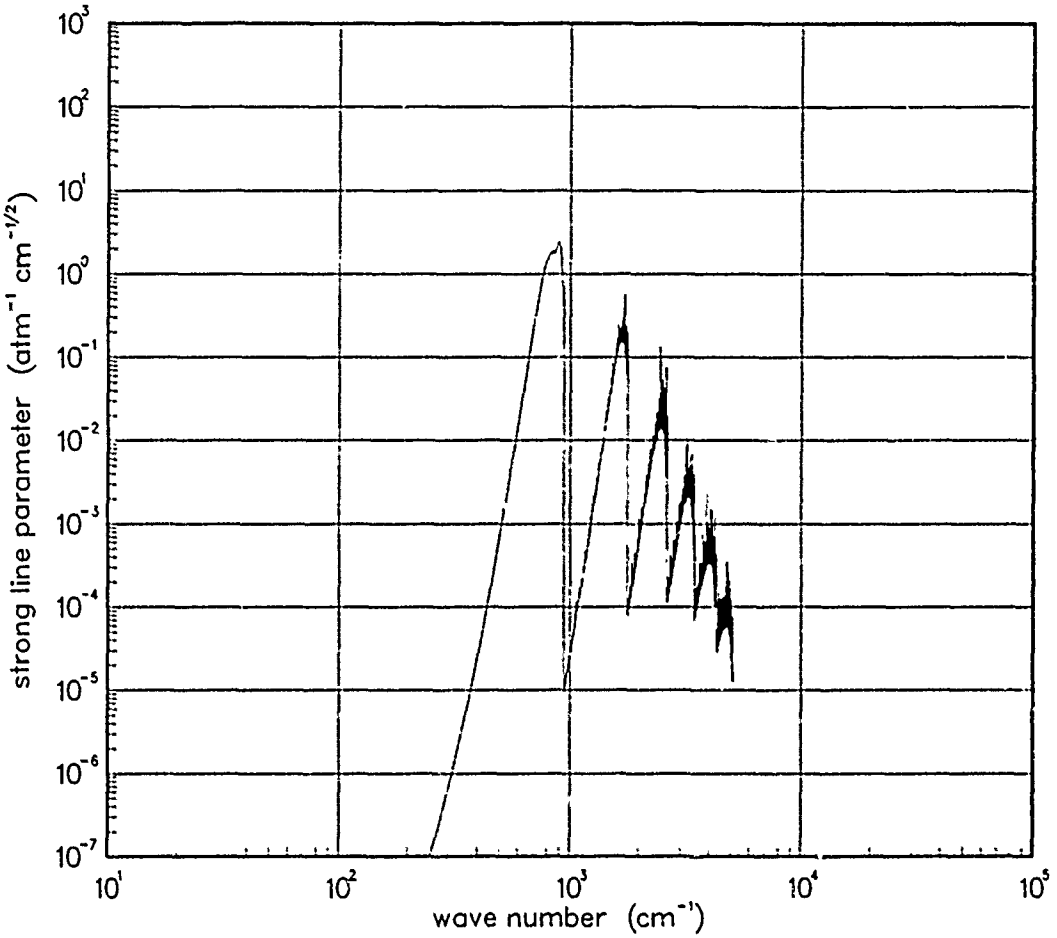

Figure 362. Strong-line parameter for FeO at 1500°K.

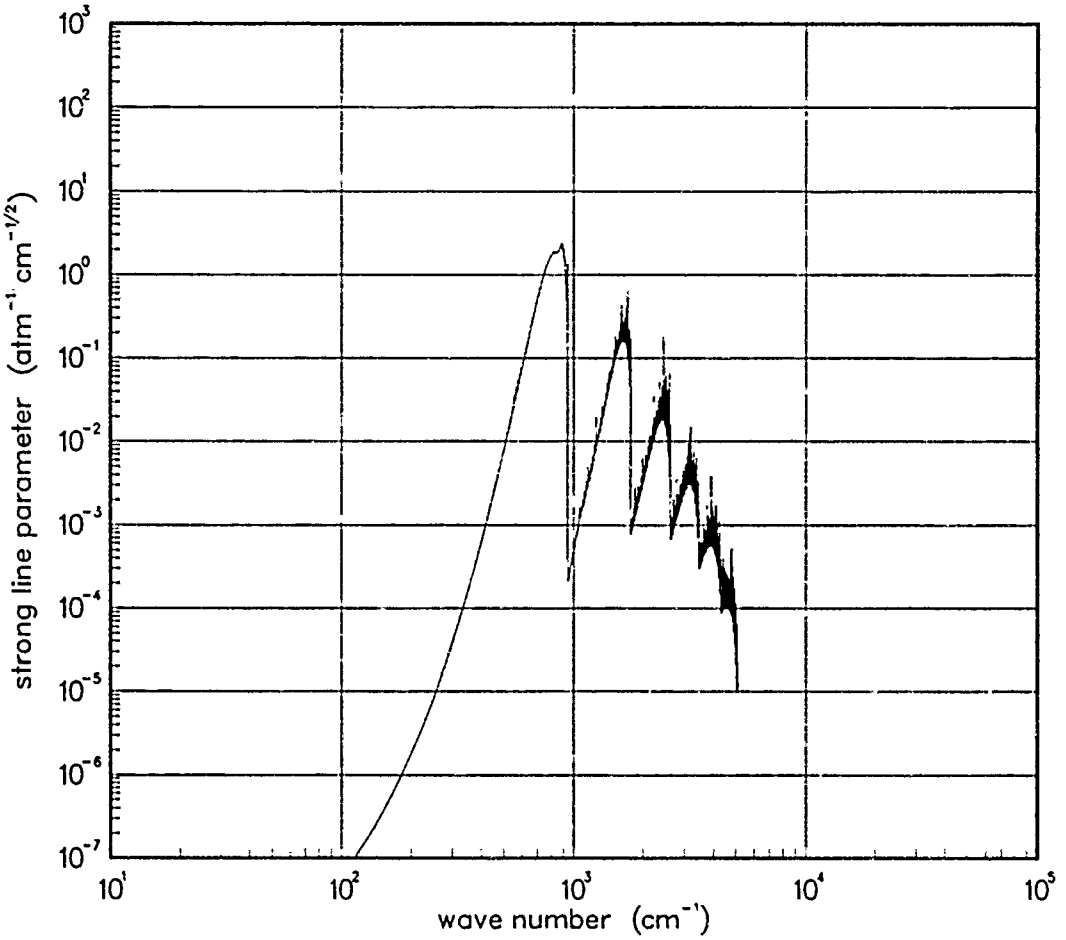

Figure 363. Strong-line parameter for FeO at 2000°K.

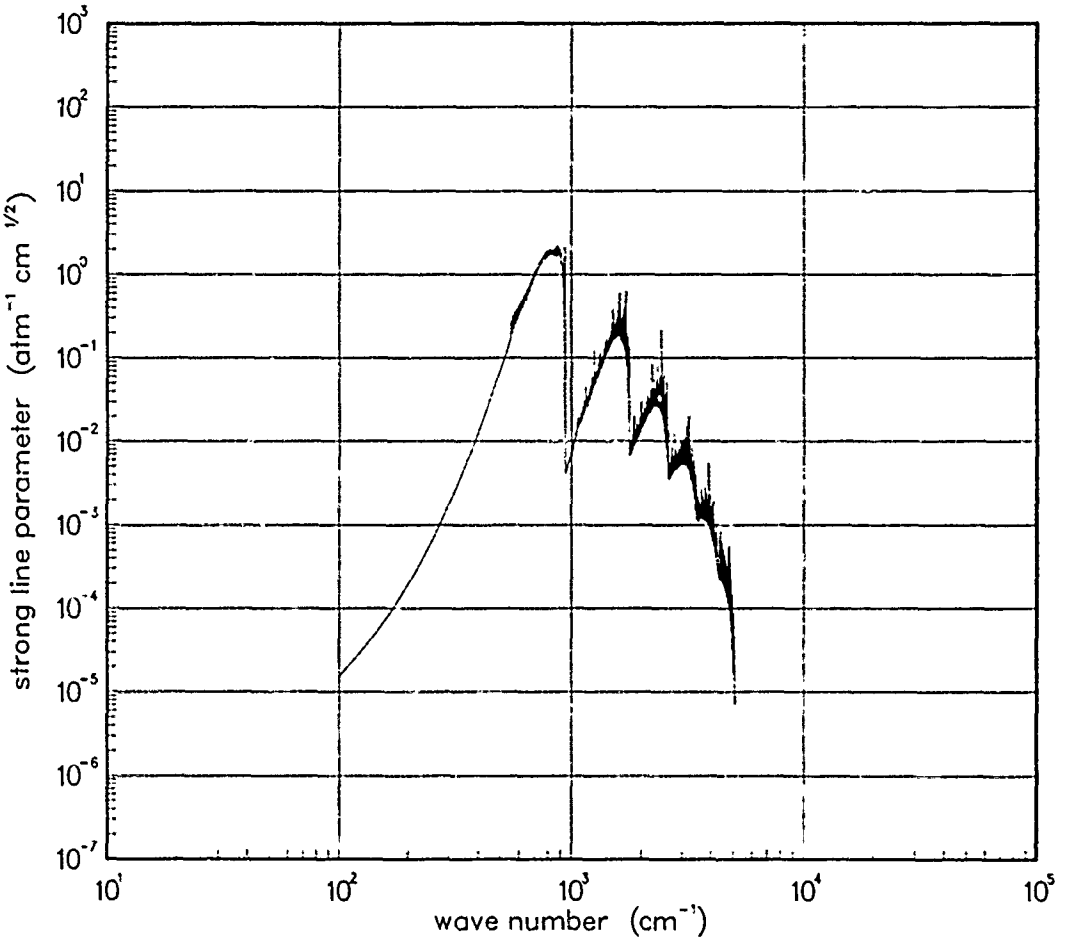

Figure 364. Strong-line parameter for FeO at 3000°K.

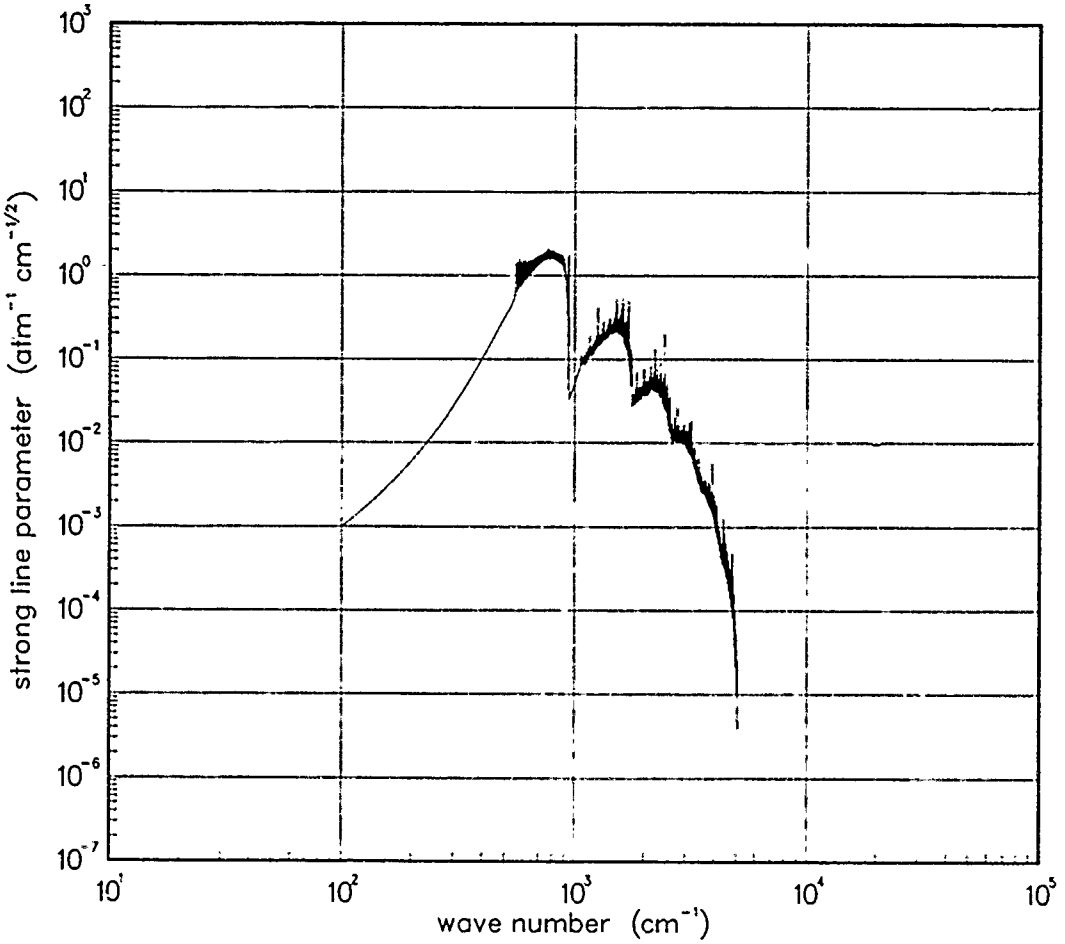

Figure 365. Strong-line parameter for FeO at 5000°K.

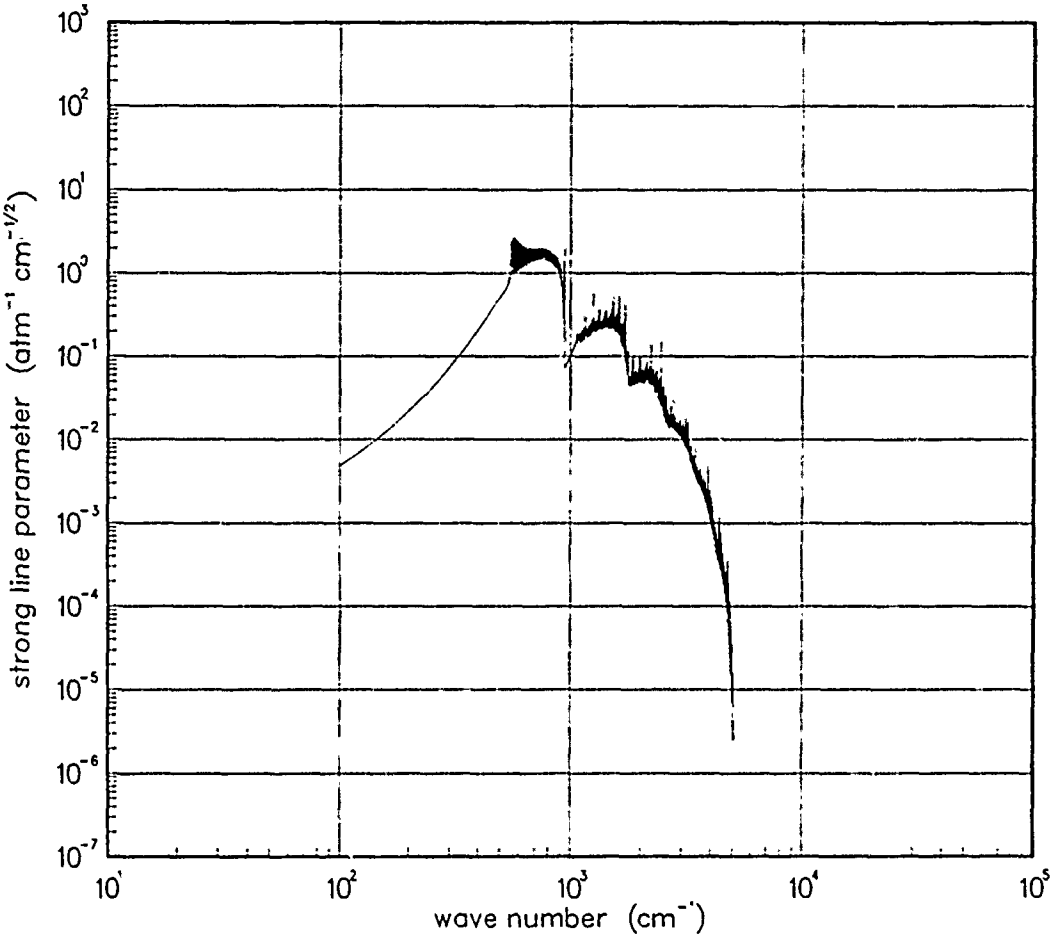

Figure 366. Strong-line parameter for FeO at 7000°K.

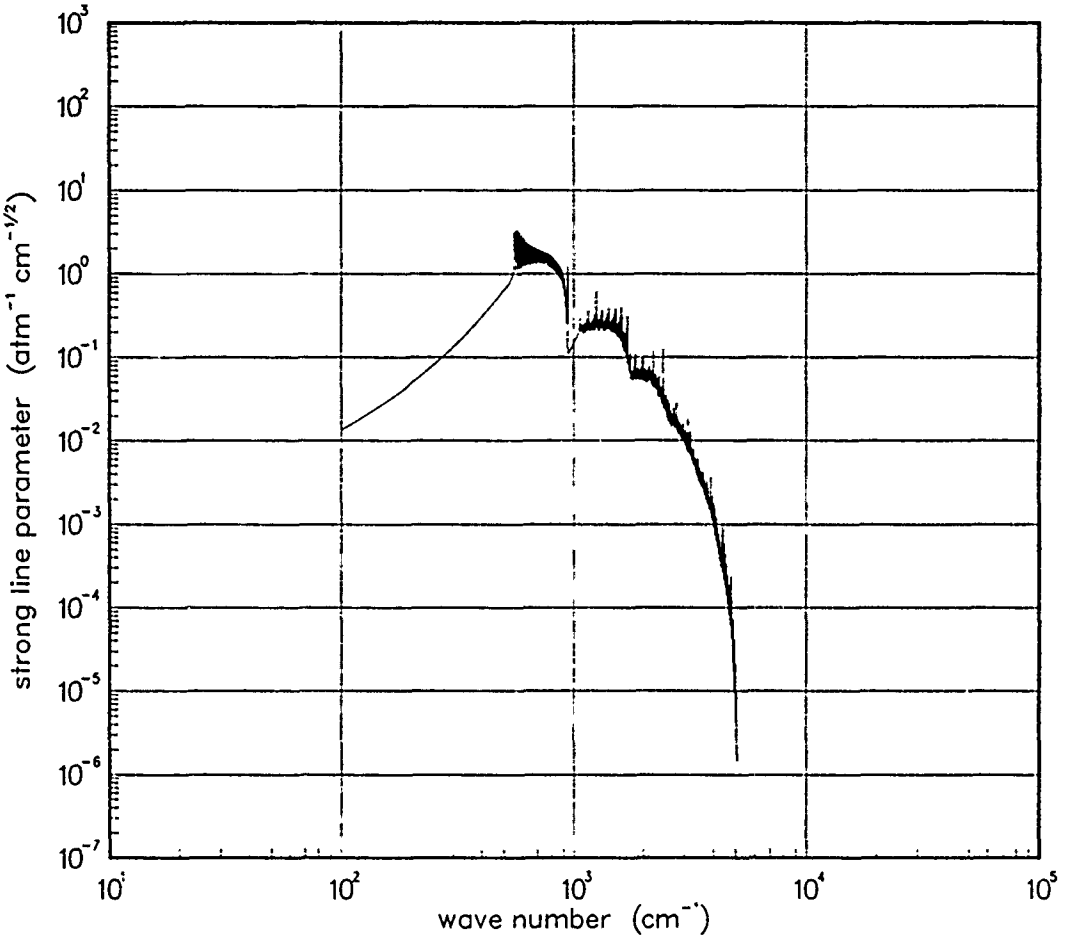

Figure 367. Strong-line parameter for FeO at 10000°K.

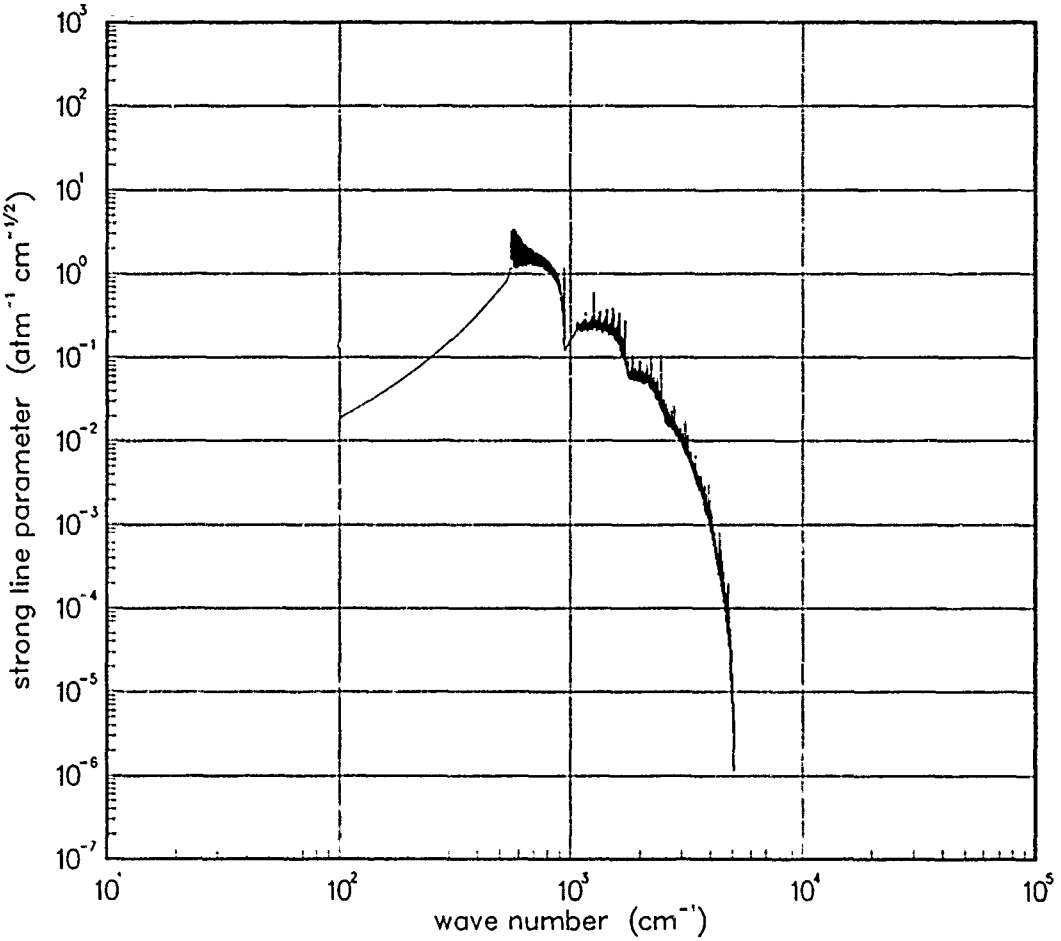

Figure 368. Strong-line parameter for FeO at 12000°K.

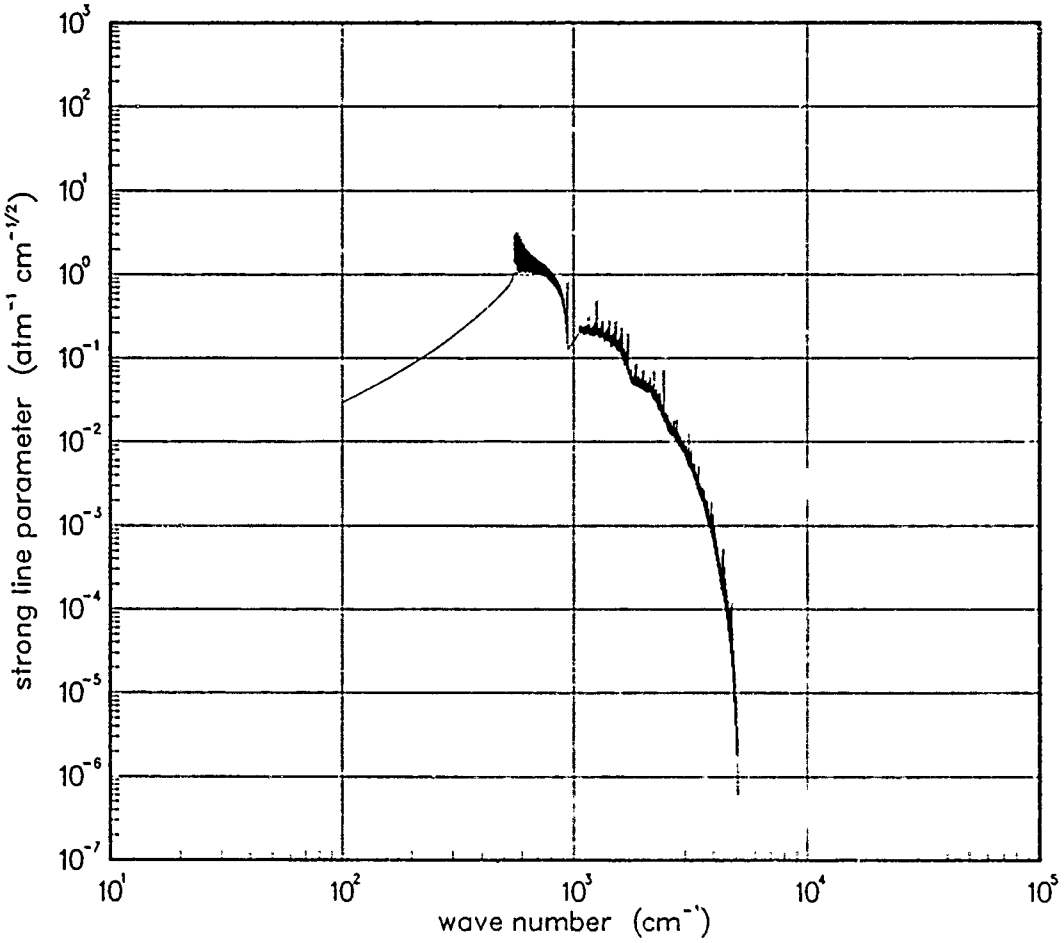

Figure 369. Strong-line parameter for FeO at 18000°K.

6.4 LITHIUM OXIDE (LiO).

Table 10. Spectroscopic data for LiO.

$X\ ^2\Pi$

$\omega_e = 848.6^*$ $\omega_e x_e = 5.4^\dagger$ $E_e = 0.0$
$\alpha_e = 0.012^\dagger$ $A_e = -112.0^*$ $B_e = 1.222^*$

$S_{10} = 450.^\dagger$

$\gamma_\ell(300°K) = 0.04^\dagger$

$A\ ^2\Sigma^+$

$\omega_e = 871.0^*$ $\omega_e x_e = 5.6^\dagger$ $E_e = 2800.^*$
$\alpha_e = 0.013^\dagger$ $B_e = 1.35^*$

$S_{10} = 450.^\dagger$

$\gamma_\ell(300°K) = 0.04^\dagger$

Data Source:

*S.M. Freund, E. Herbst, R.P. Mariella, Jr., and W. Klemperer, Radio Frequency Spectrum of the X $^2\Pi$ State of $^7Li^{16}O$, (preprint), Harvard University (1971).
†Estimate.

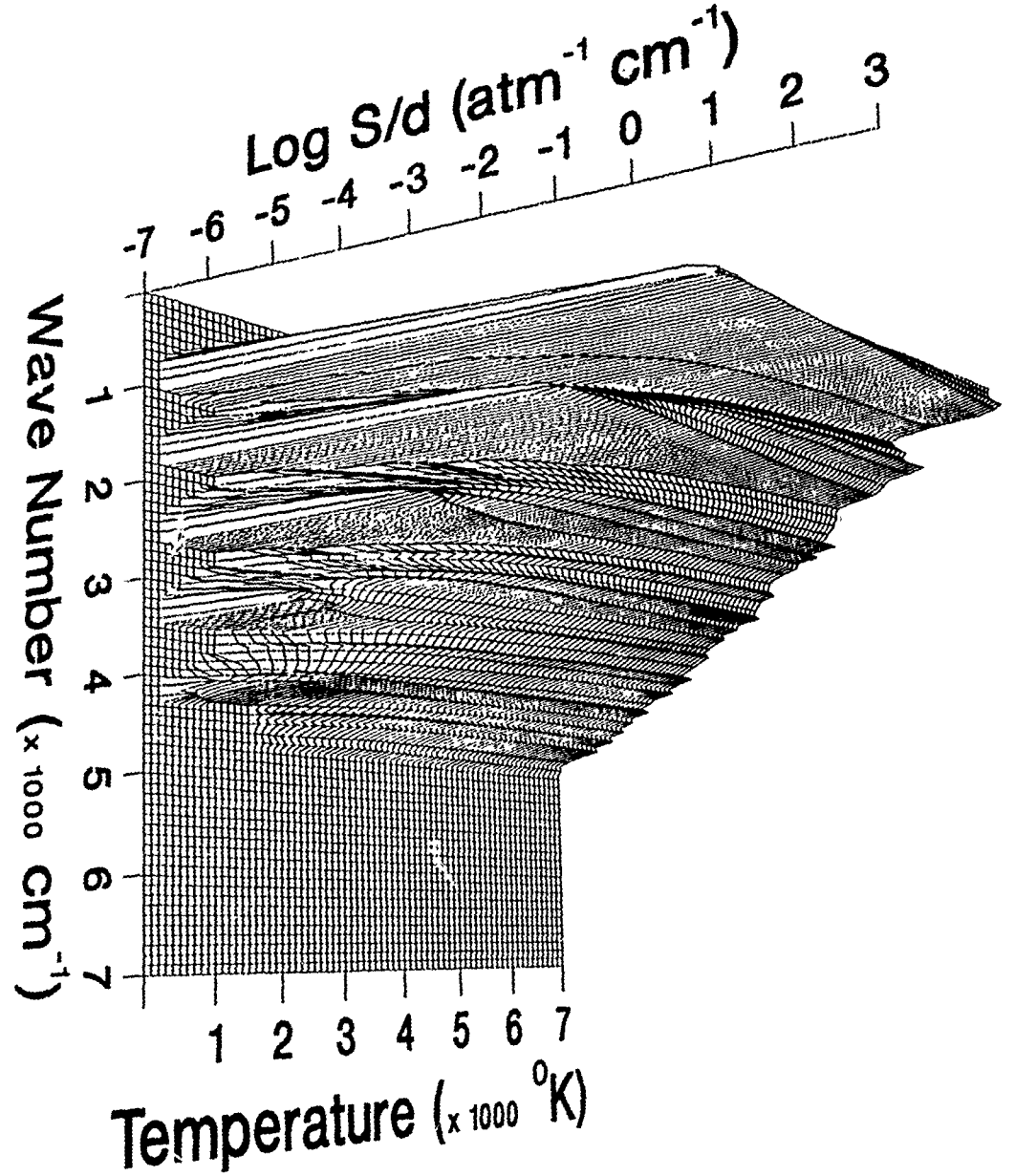

Figure 370. Weak-line parameter for LiO.

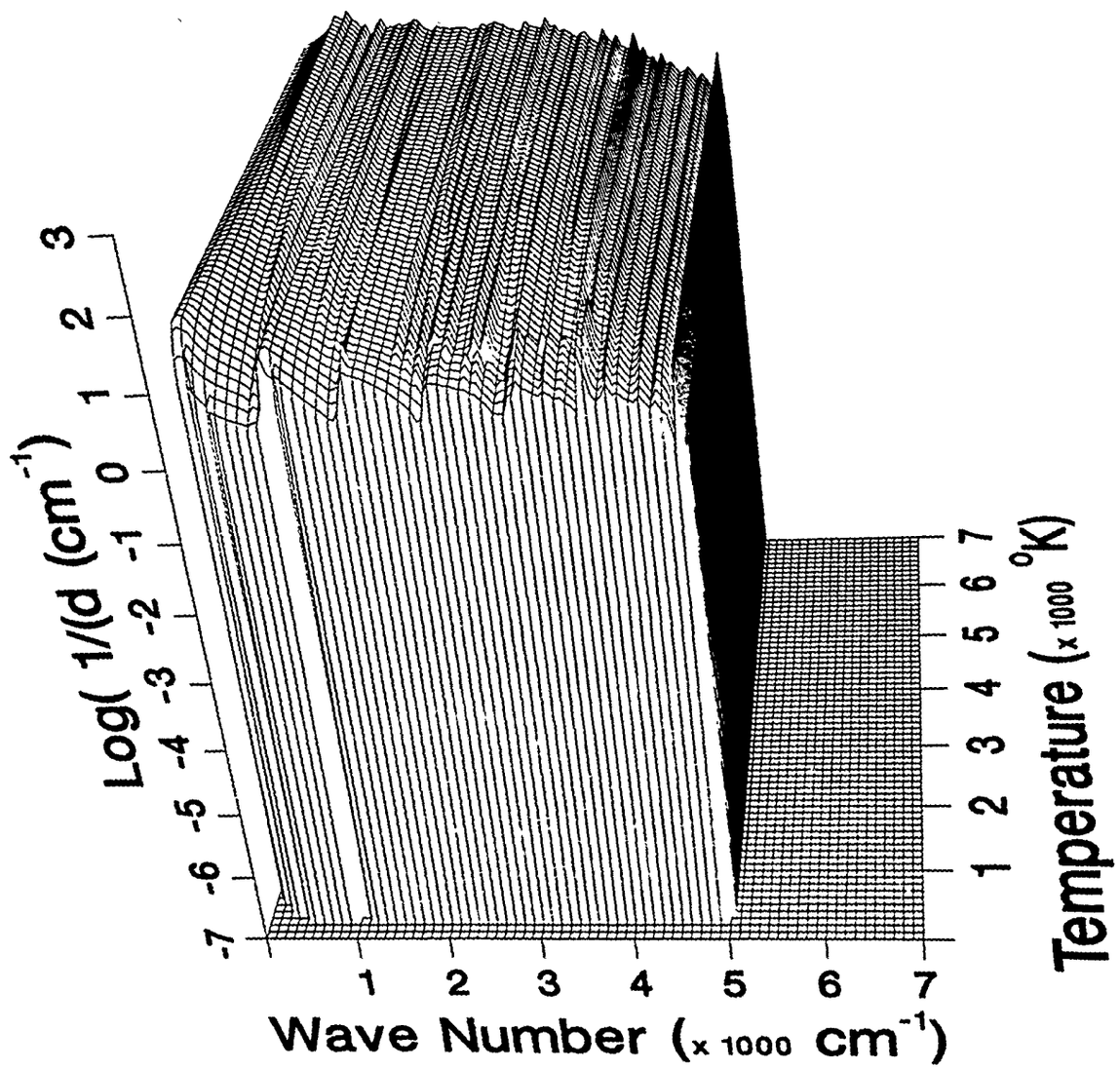

Figure 371. Inverse line spacing for LiO.

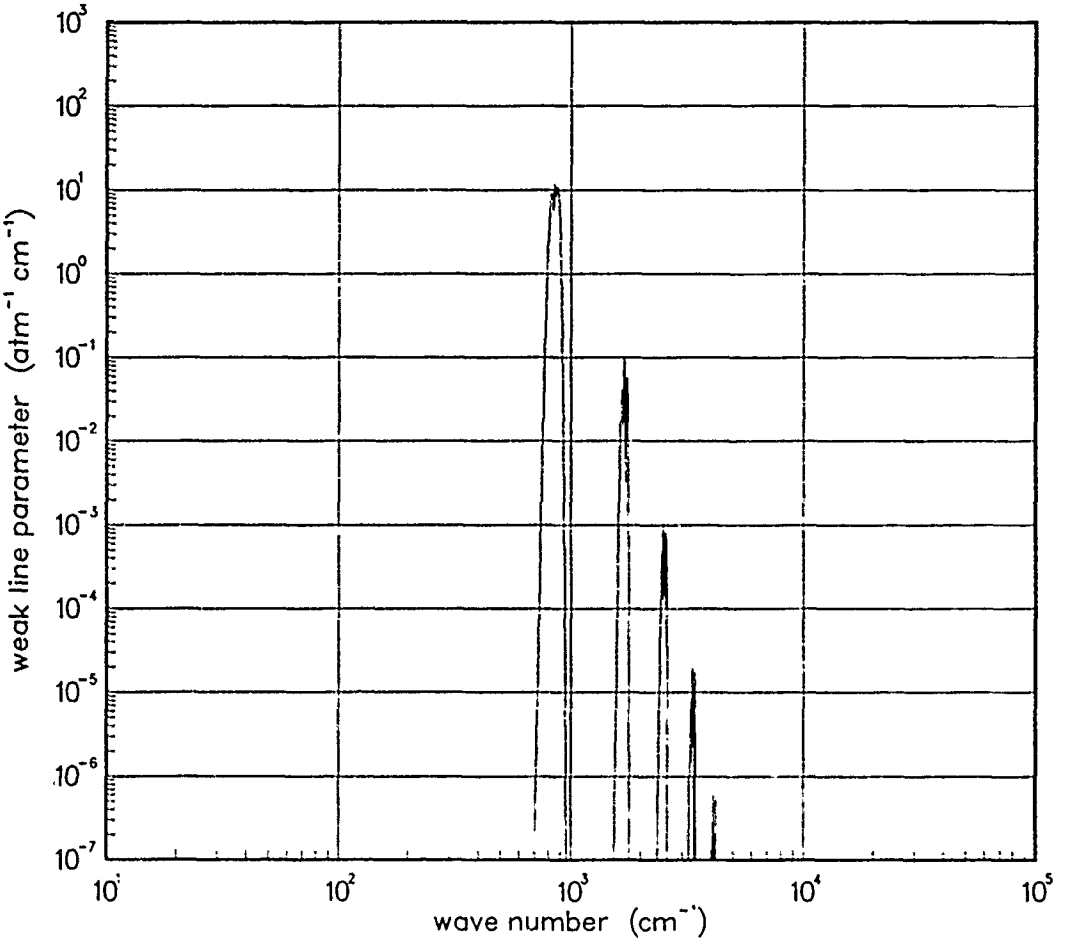

Figure 372. Weak-line parameter for LiO at 200°K.

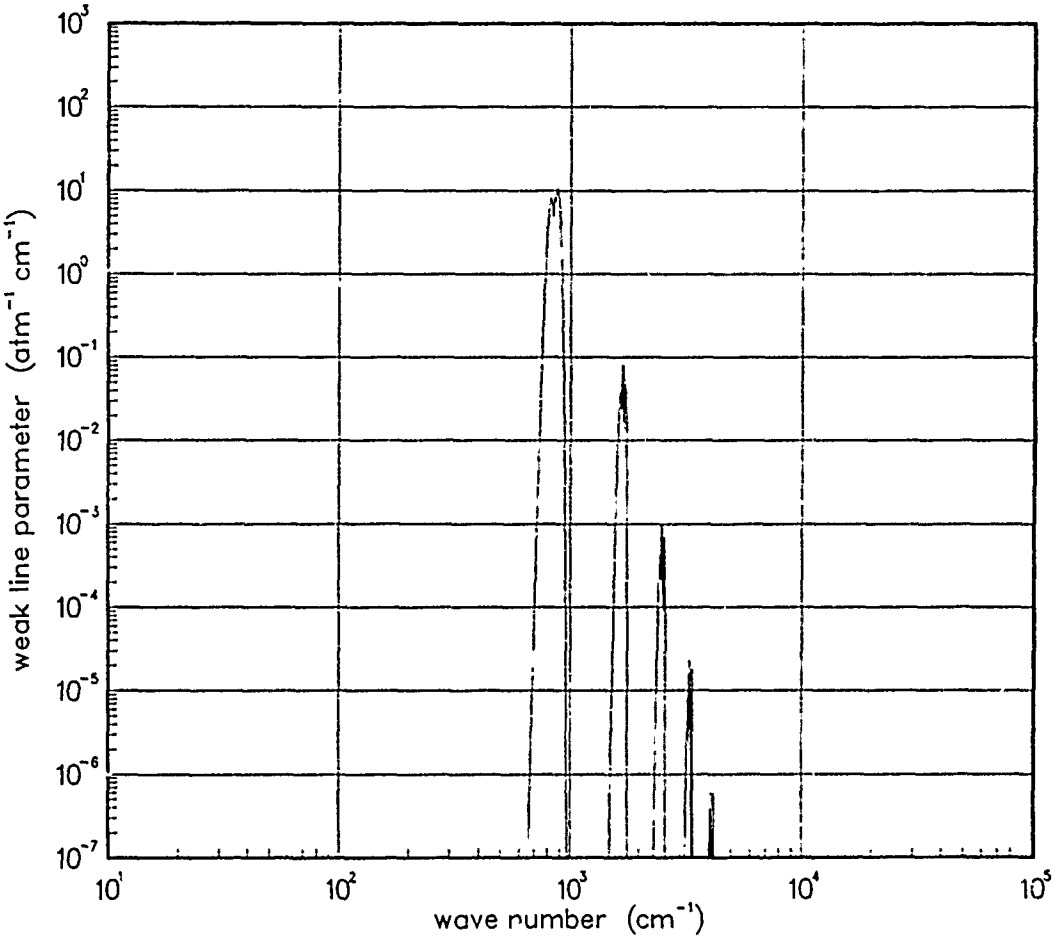

Figure 373. Weak-line parameter for LiO at 300°K.

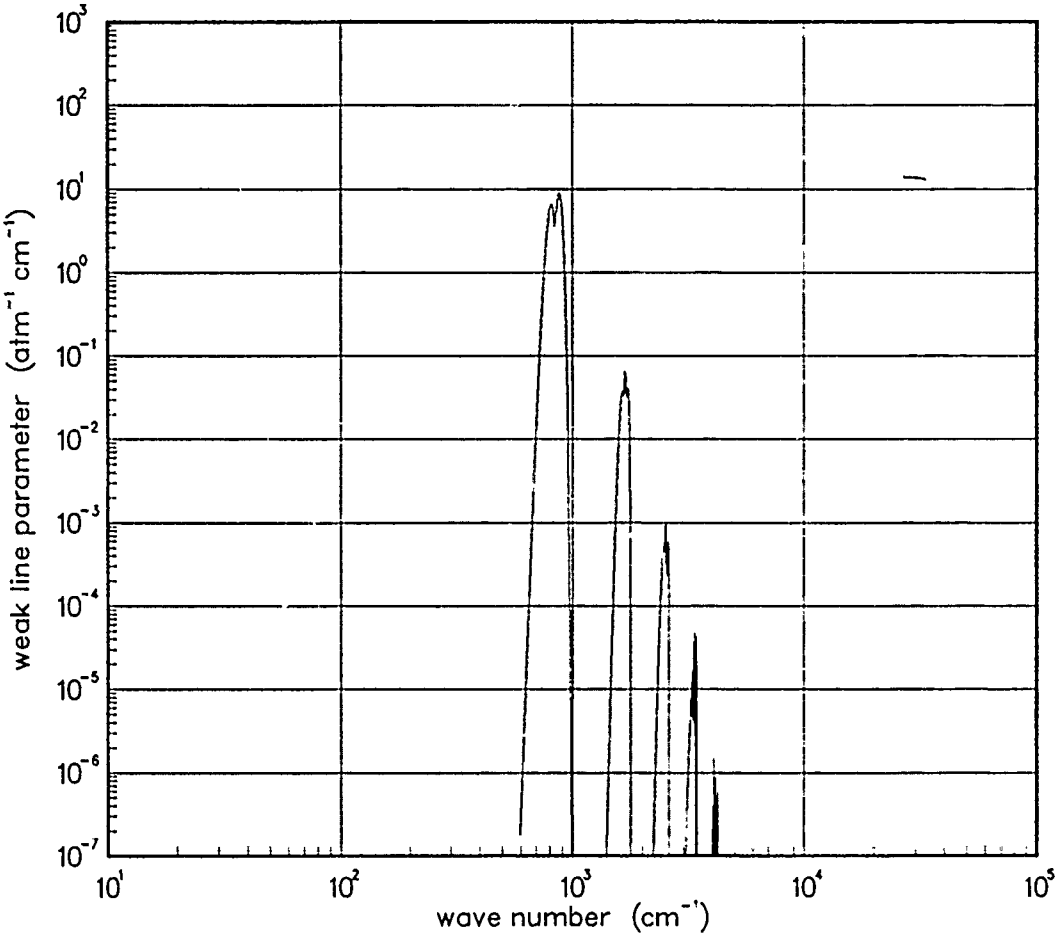

Figure 374. Weak-line parameter for LiO at 500°K.

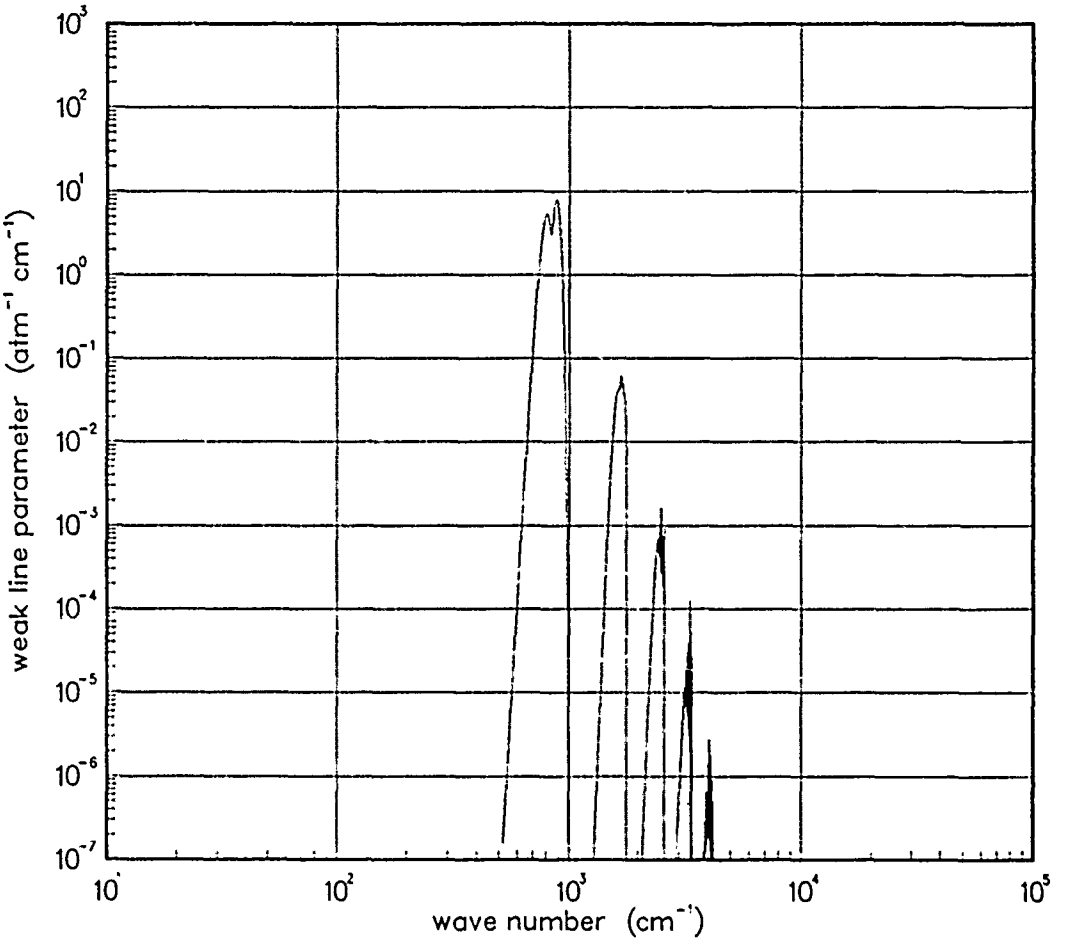

Figure 375. Weak-line parameter for LiO at 750°K.

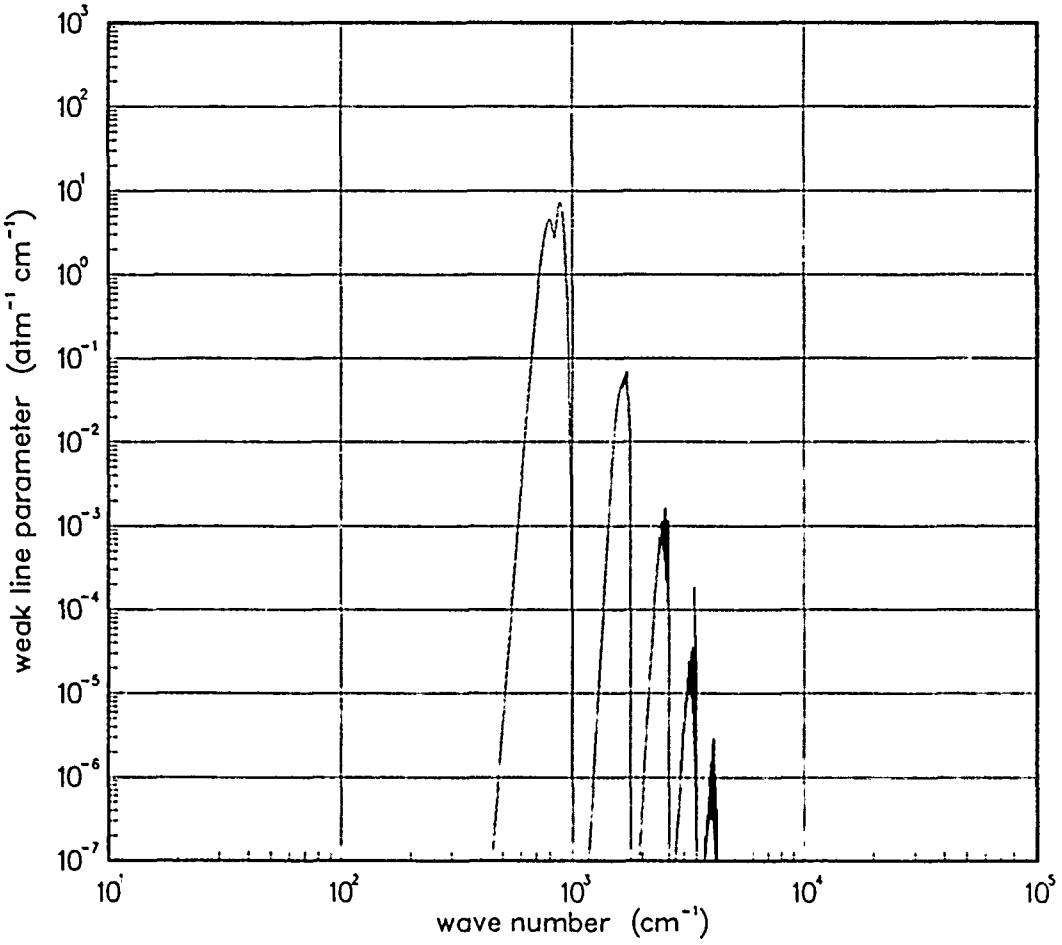

Figure 376. Weak-line parameter for LiO at 1000°K.

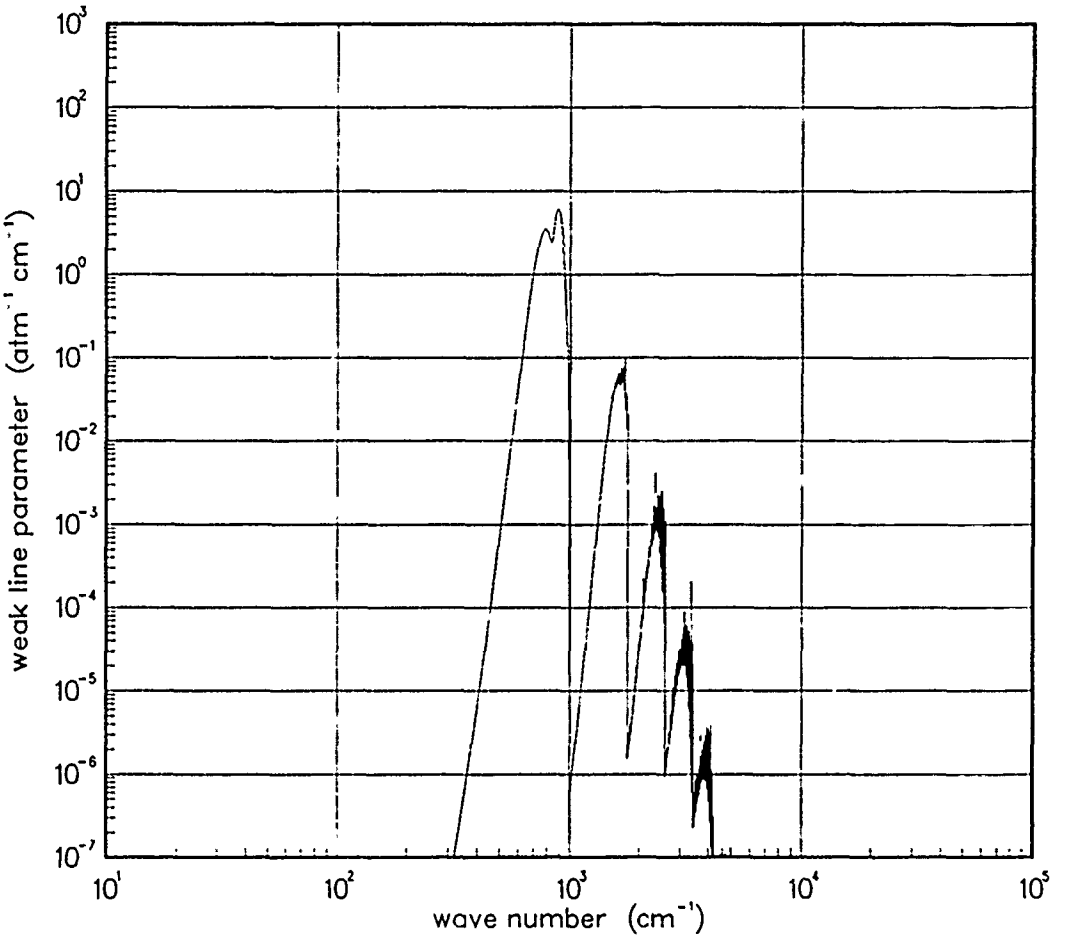

Figure 377. Weak-line parameter for LiO at 1500°K.

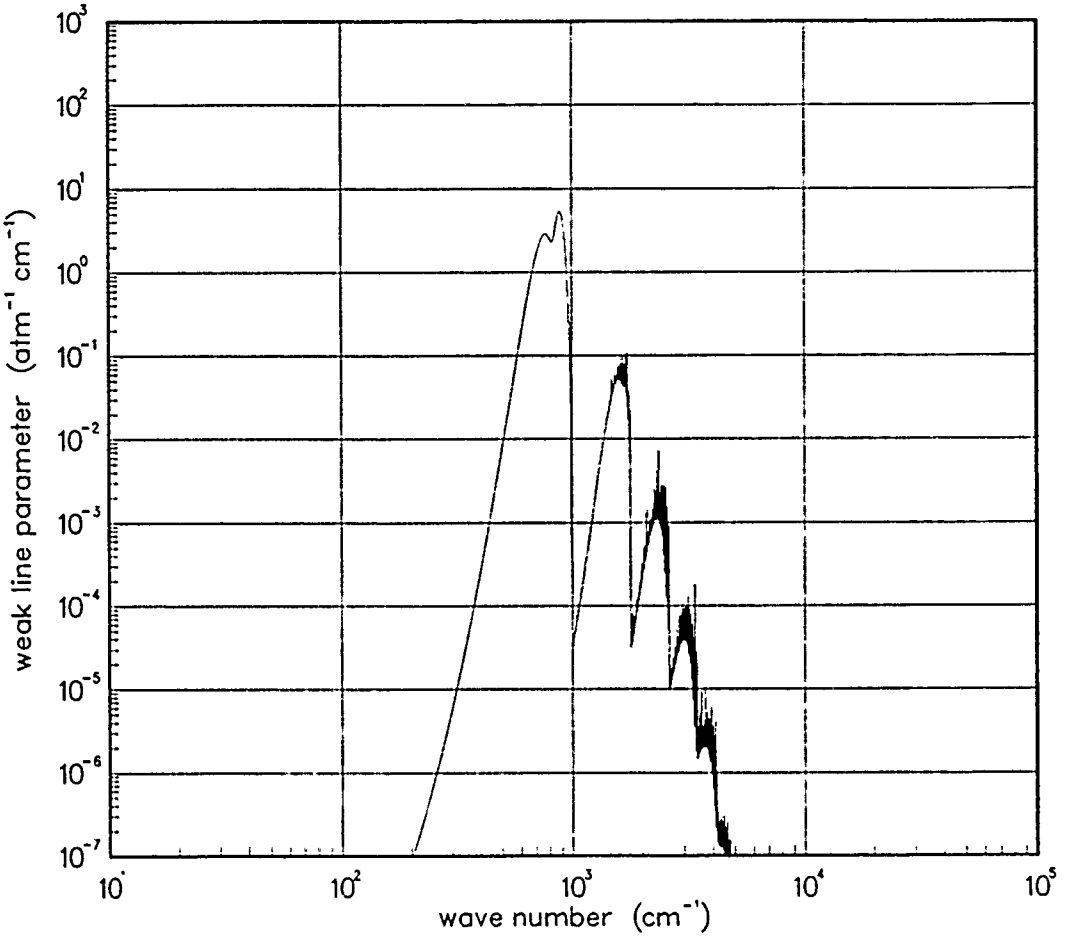

Figure 378. Weak-line parameter for LiO at 2000°K.

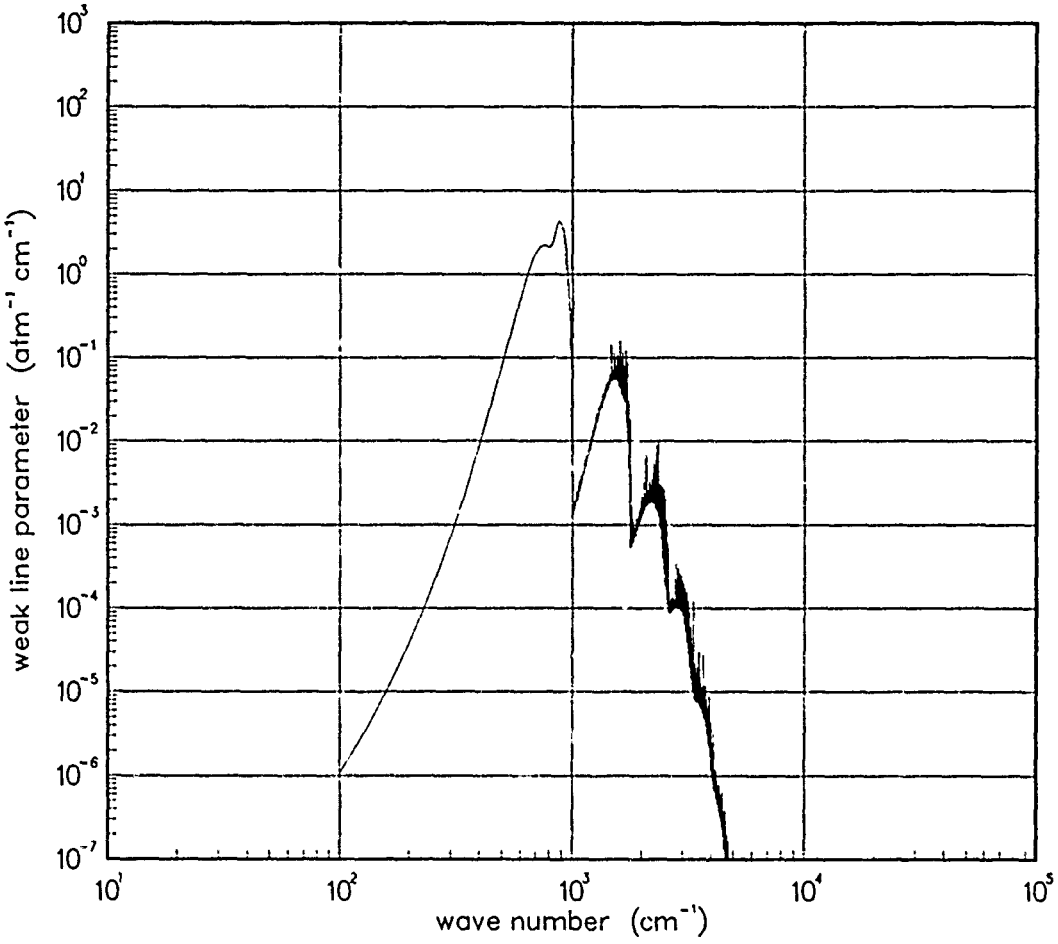

Figure 379. Weak-line parameter for LiO at 3000°K.

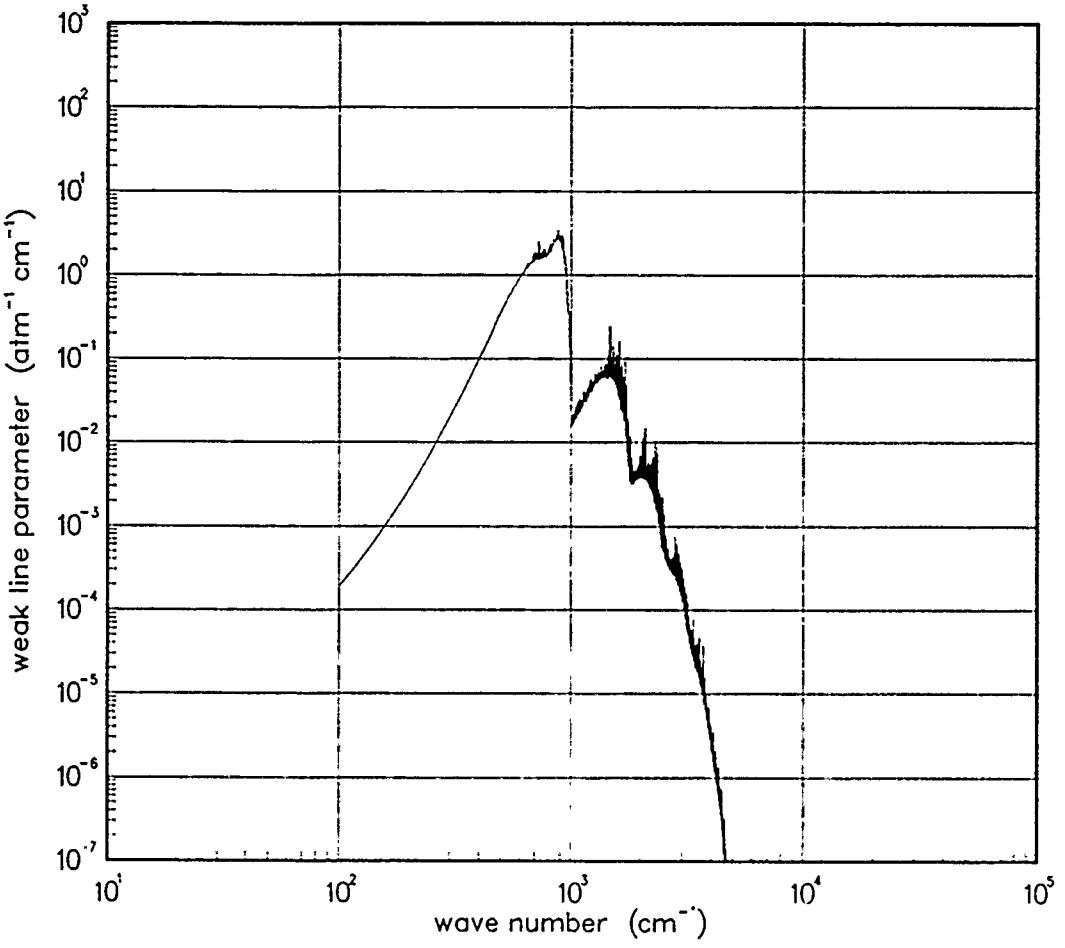

Figure 380. Weak-line parameter for LiO at 5000°K.

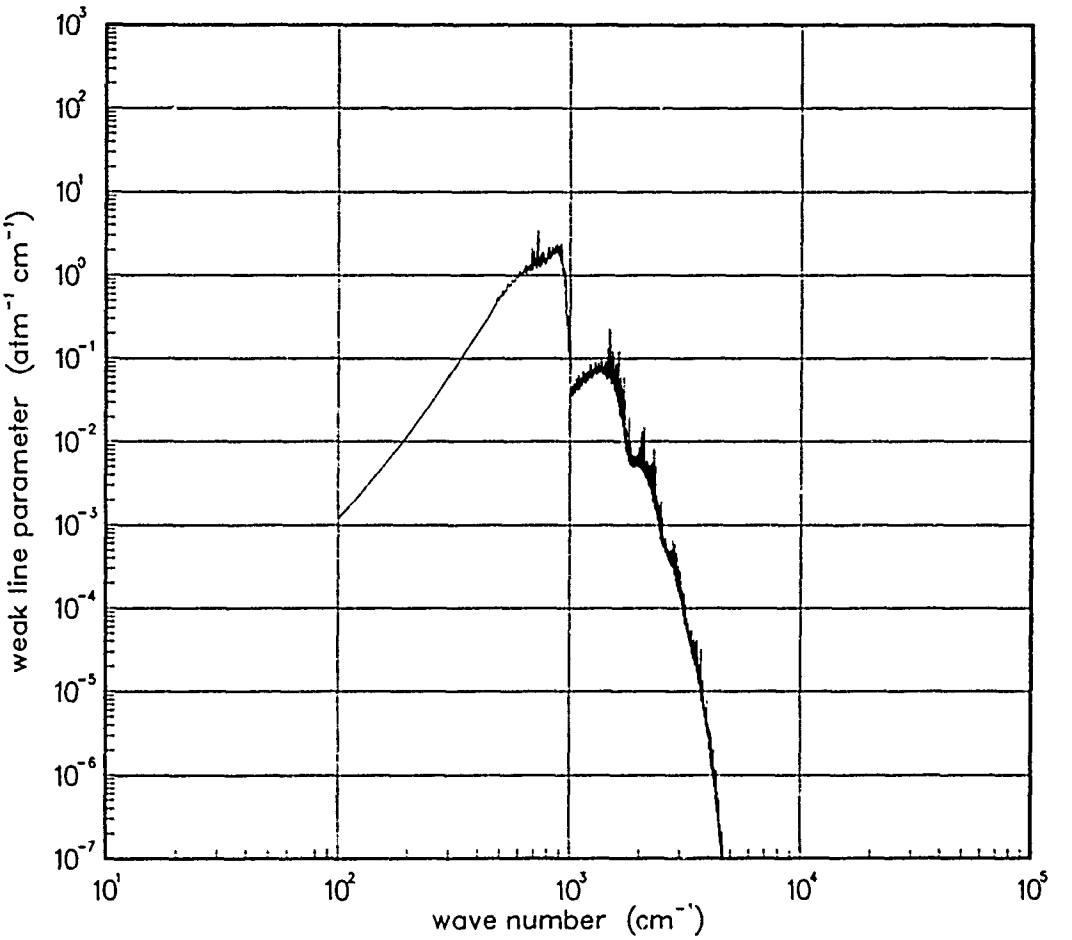

Figure 381. Weak-line parameter for LiO at 7000°K.

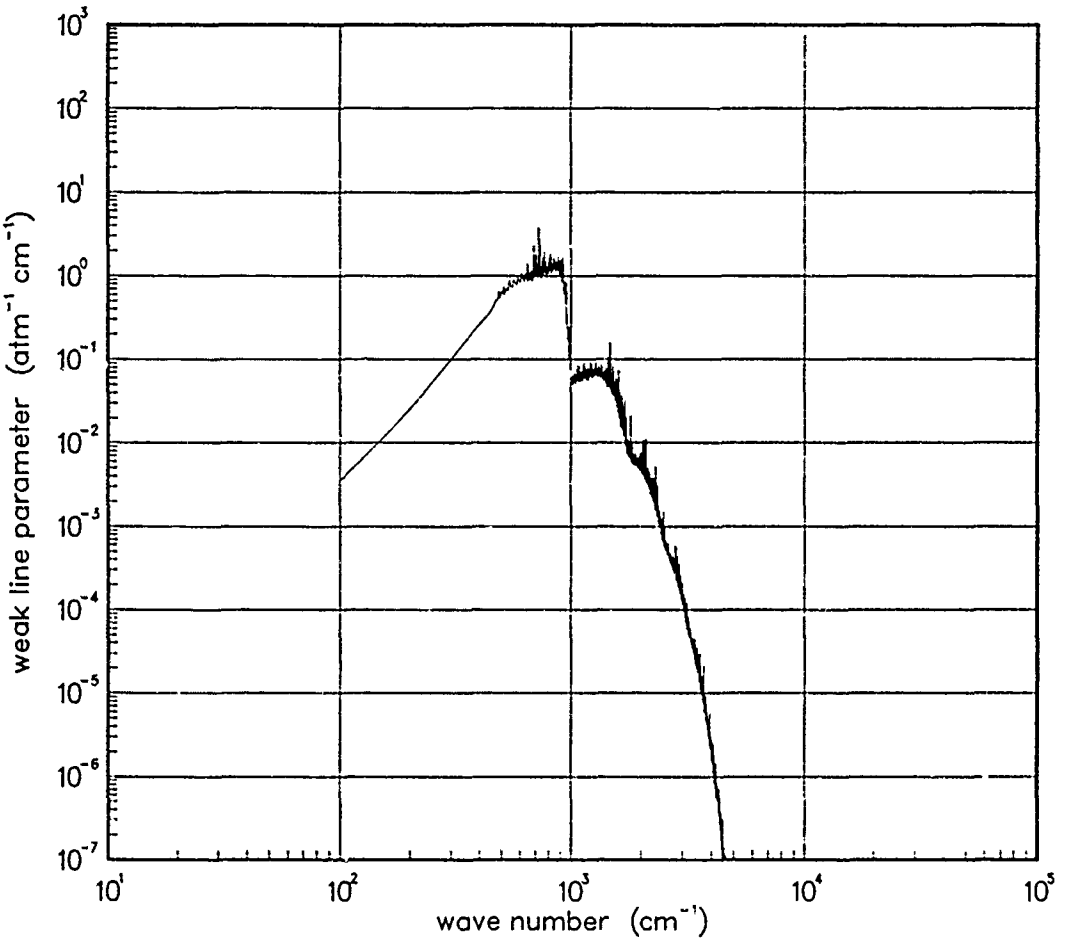

Figure 382. Weak-line parameter for LiO at 10000°K.

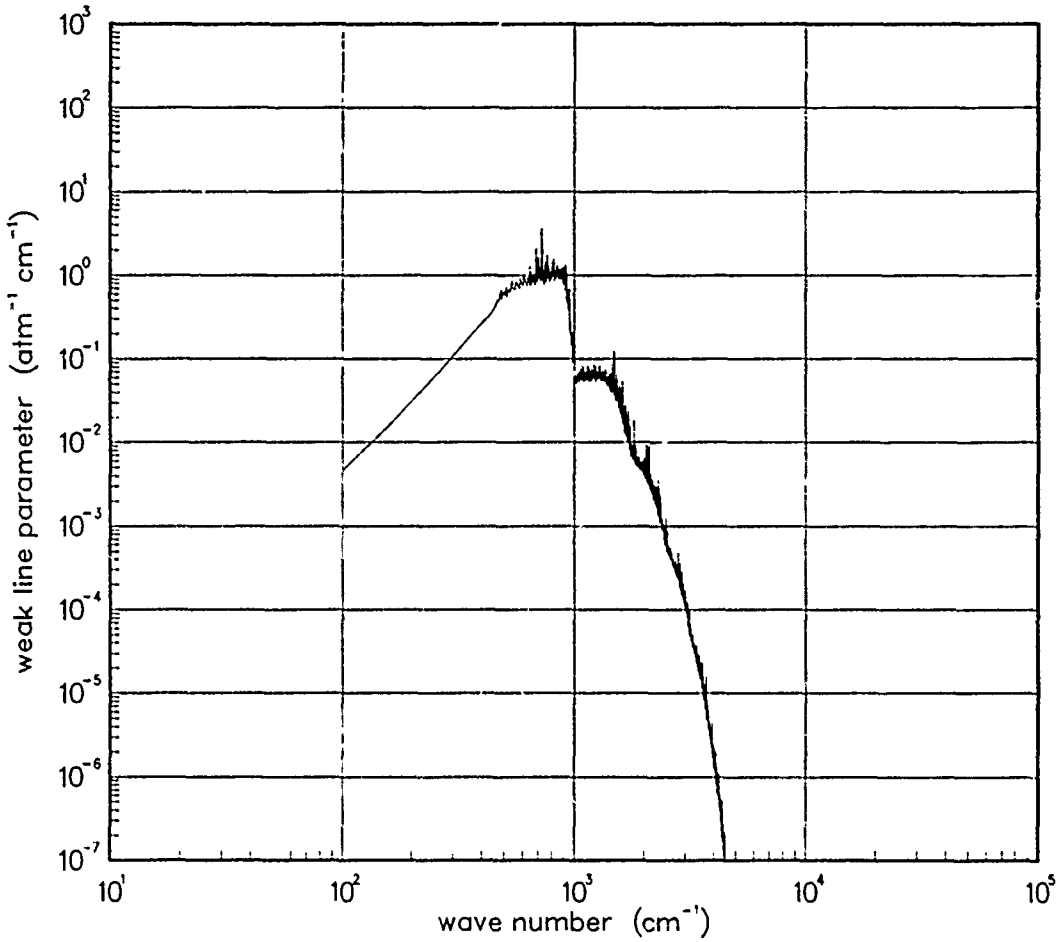

Figure 383. Weak-line parameter for LiO at 12000°K.

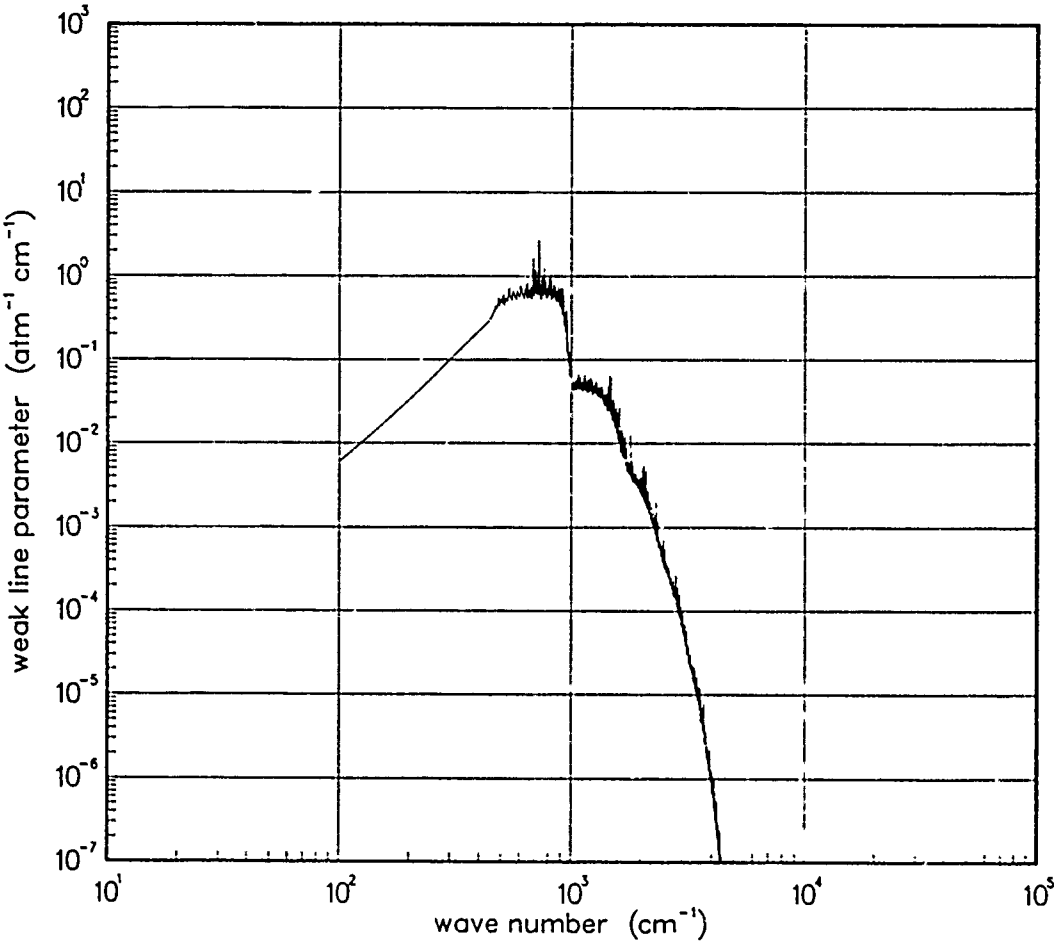

Figure 384. Weak-line parameter for LiO at 18000°K.

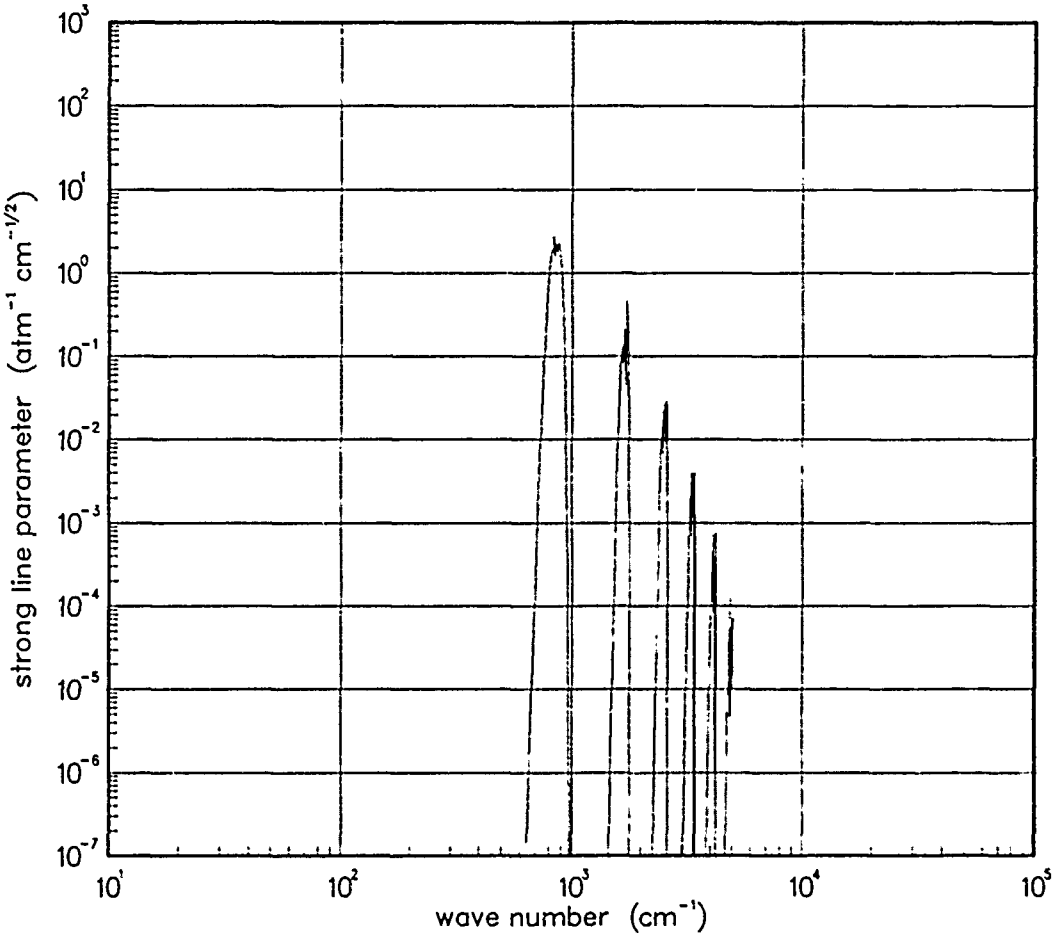

Figure 385. Strong-line parameter for LiO at 200°K.

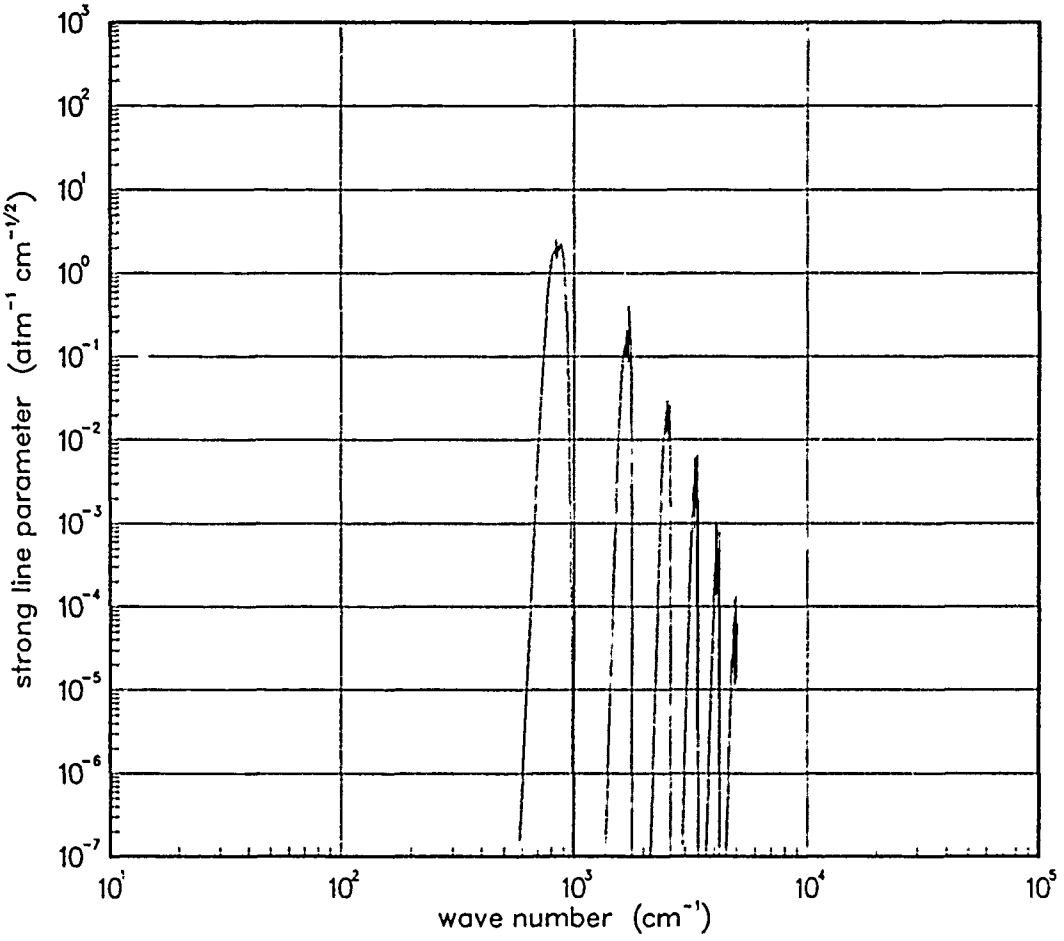

Figure 386. Strong-line parameter for LiO at 300°K.

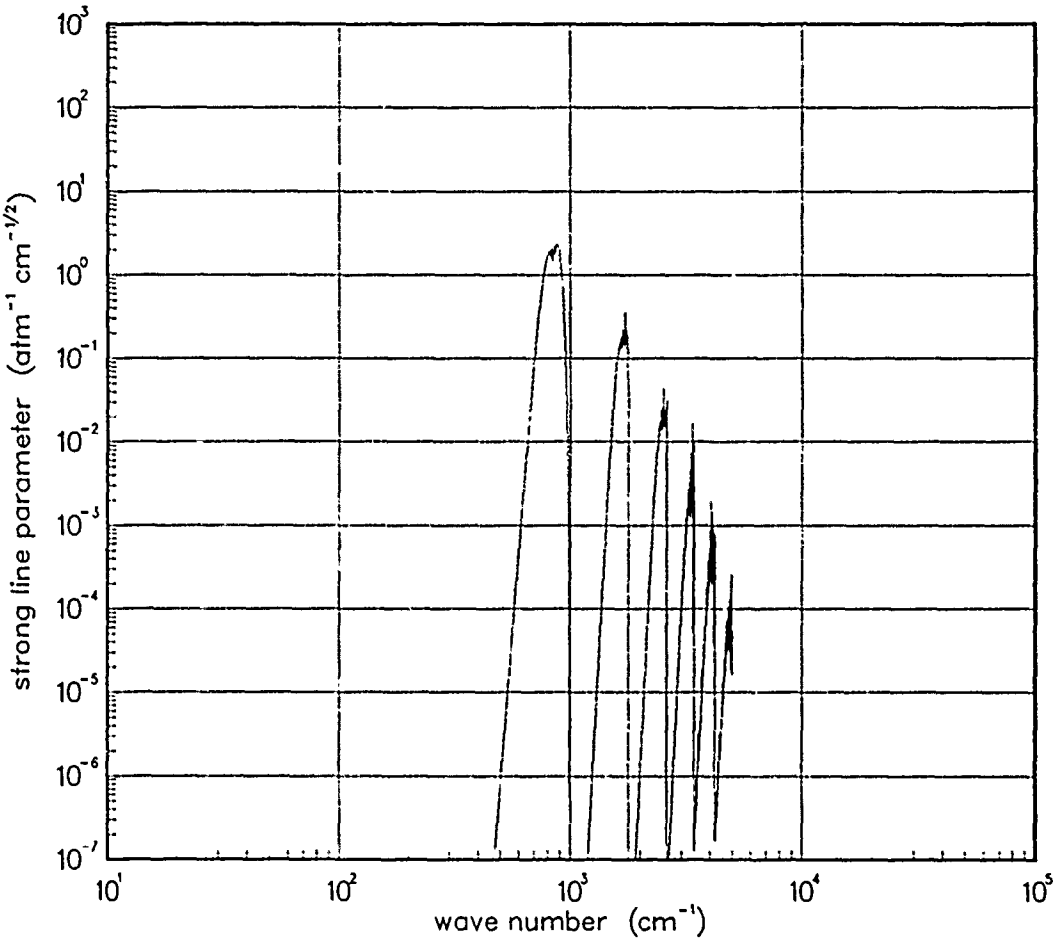

Figure 387. Strong-line parameter for LiO at 500°K.

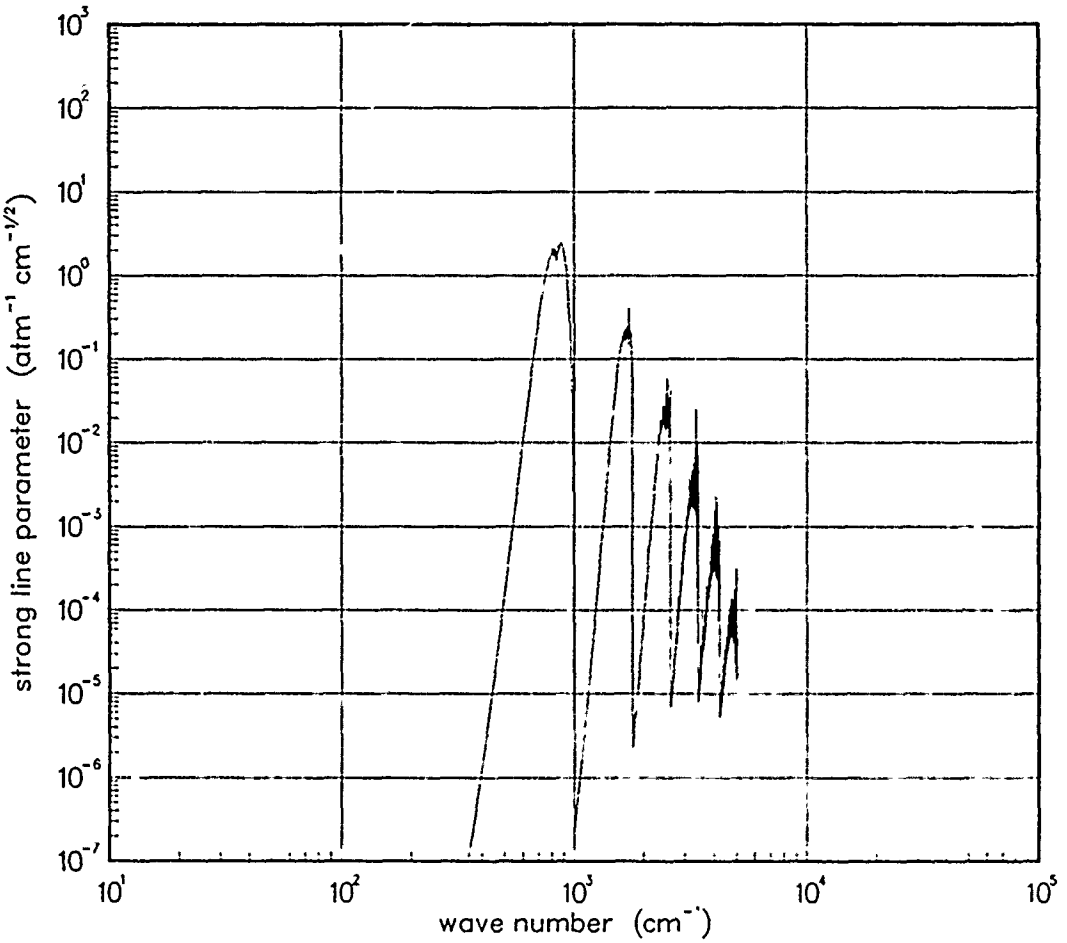

Figure 388. Strong-line parameter for LiO at 750°K.

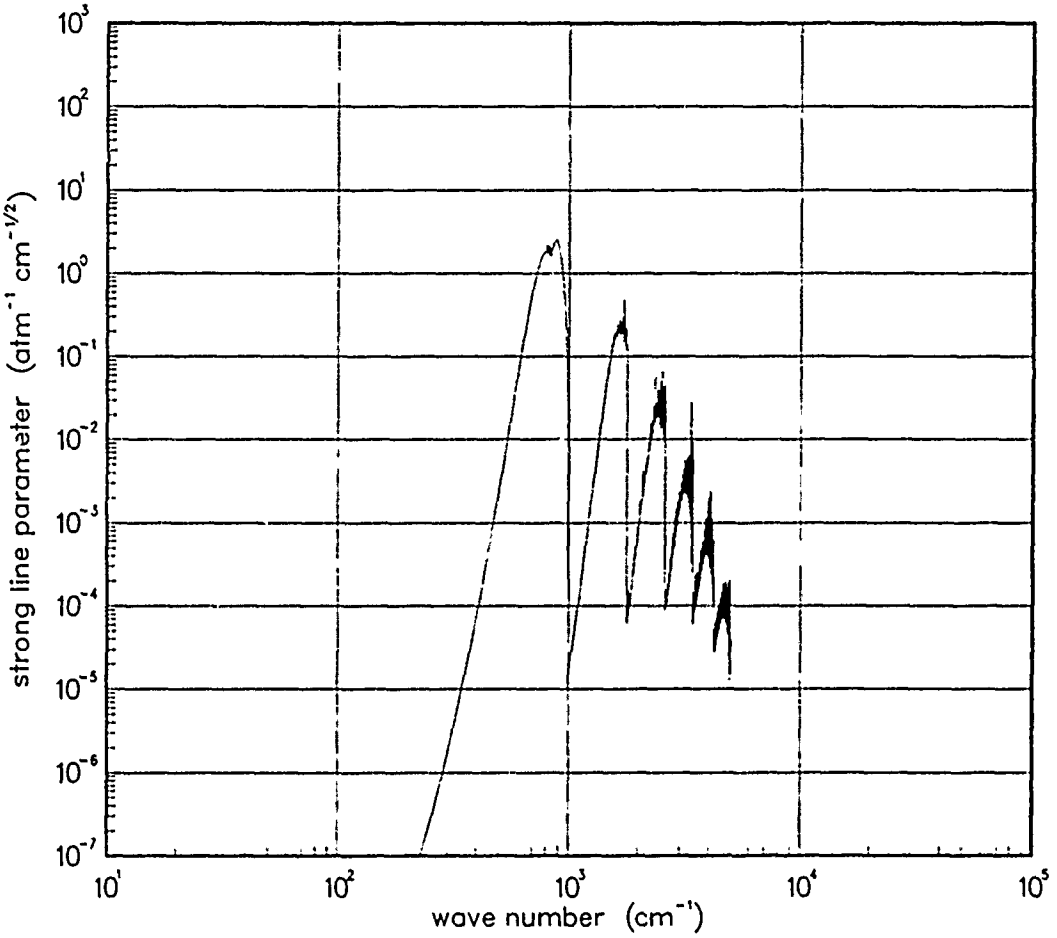

Figure 389. Strong-line parameter for LiO at 1000°K.

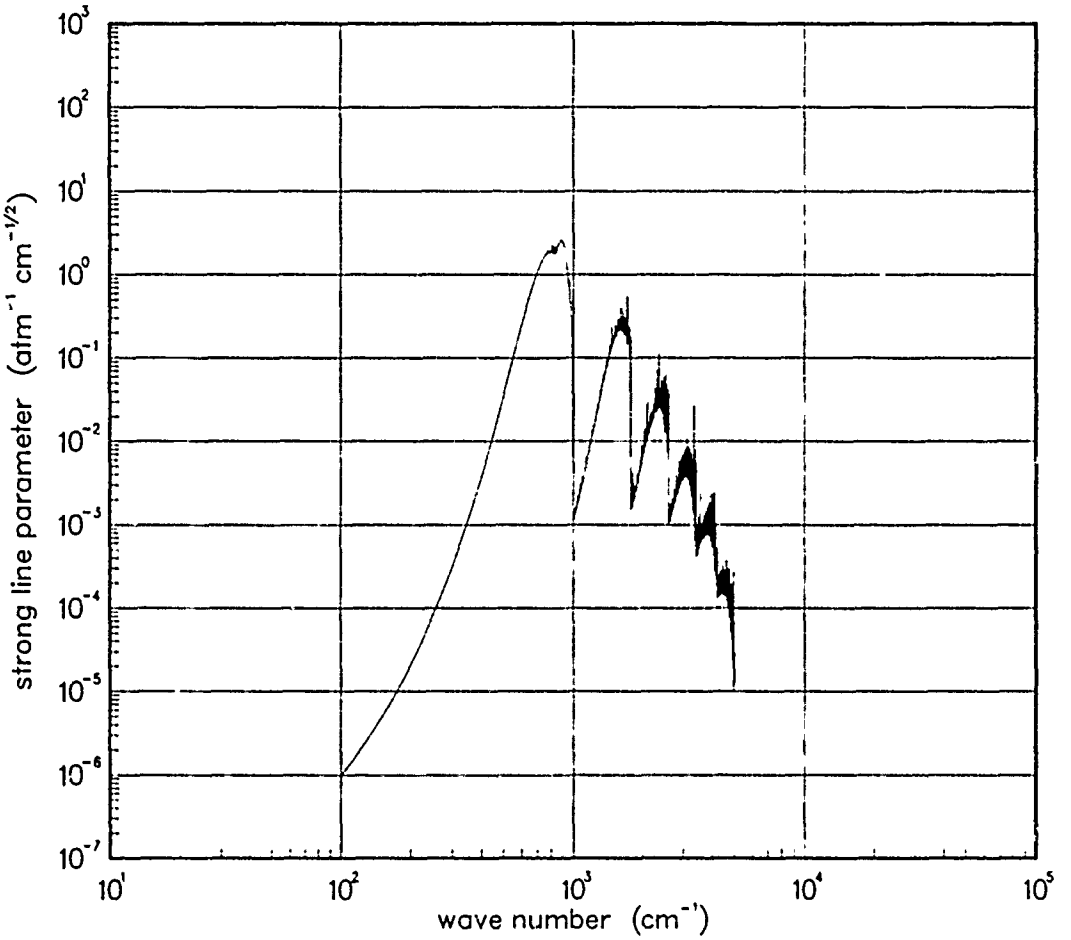

Figure 390. Strong-line parameter for LiO at 1500°K.

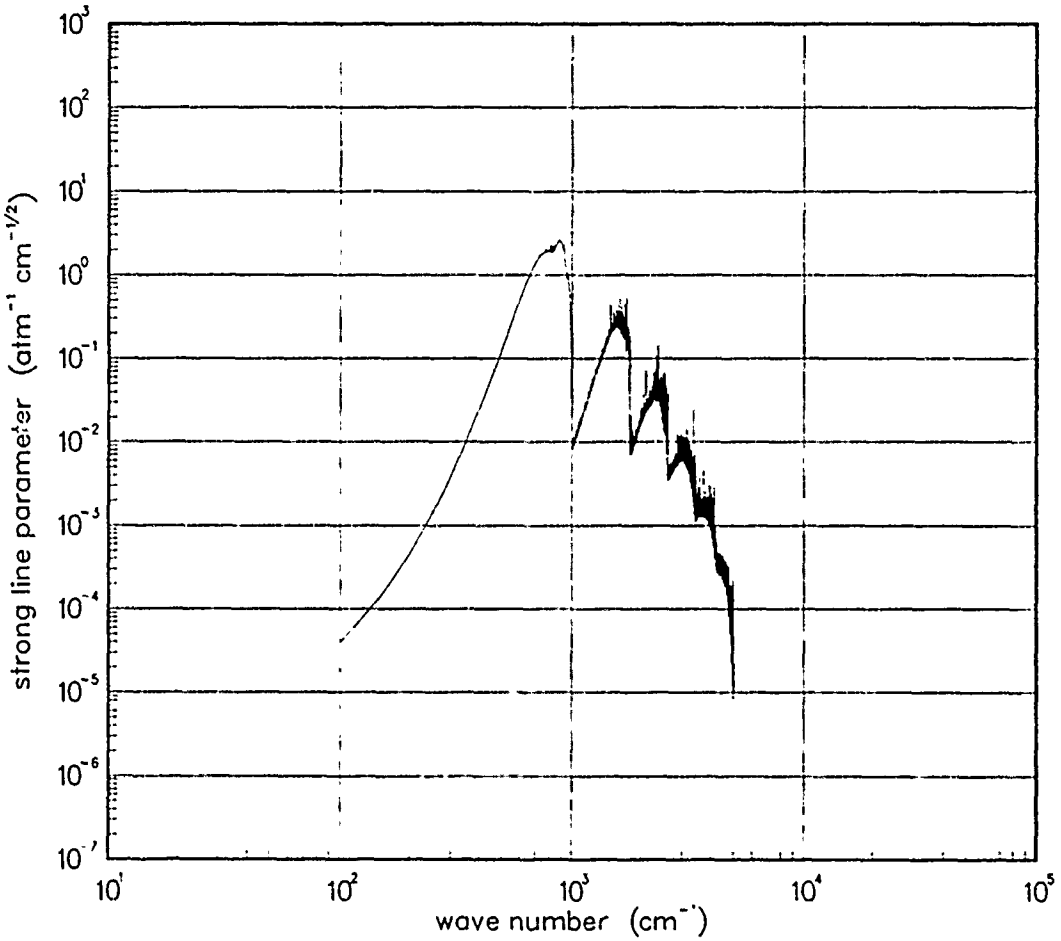

Figure 391. Strong-line parameter for LiO at 2000°K.

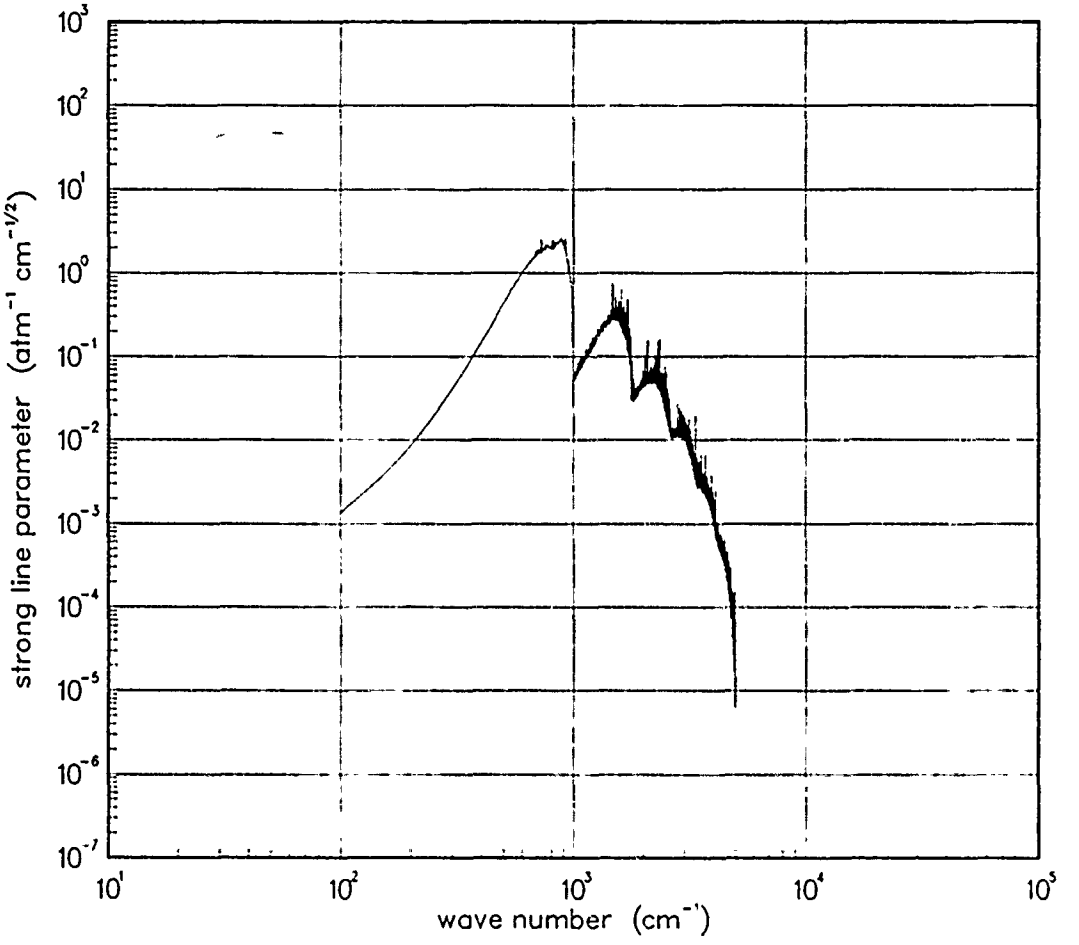

Figure 392. Strong-line parameter for LiO at 3000°K.

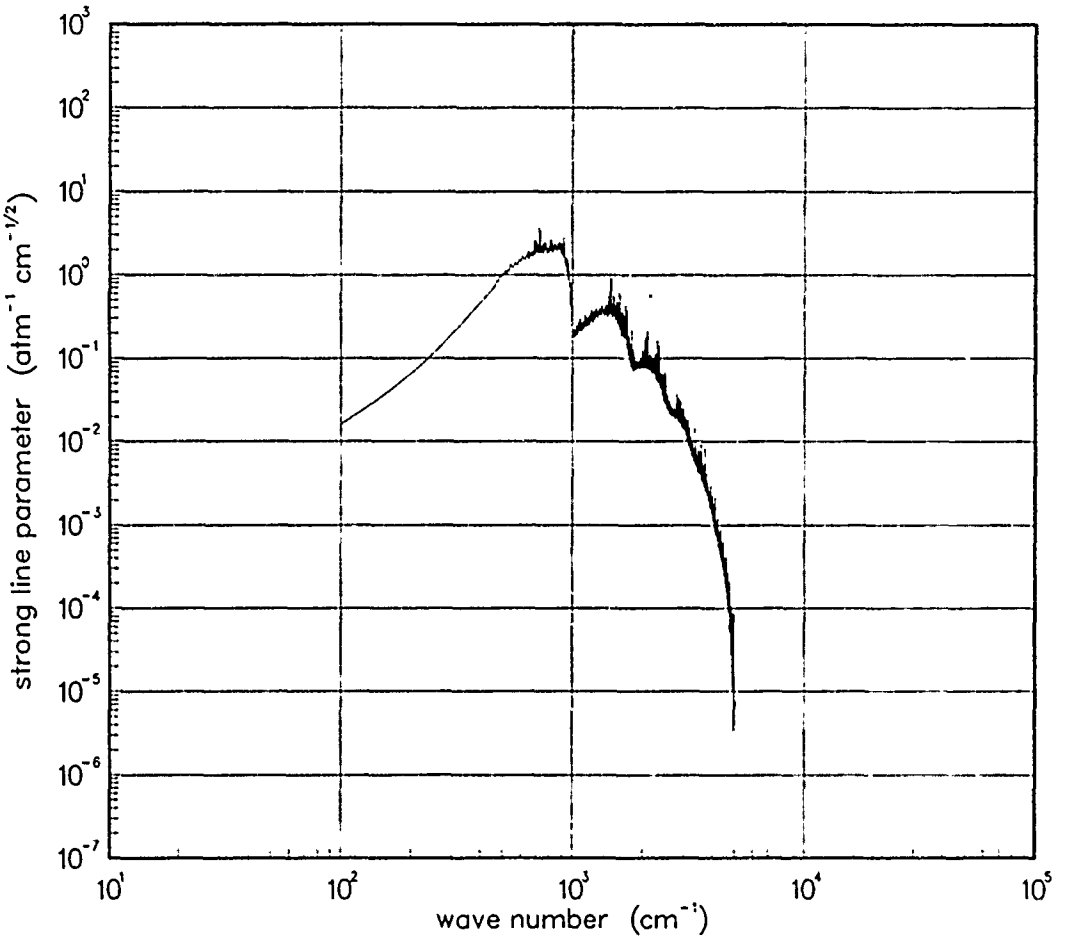

Figure 393. Strong-line parameter for LiO at 5000°K.

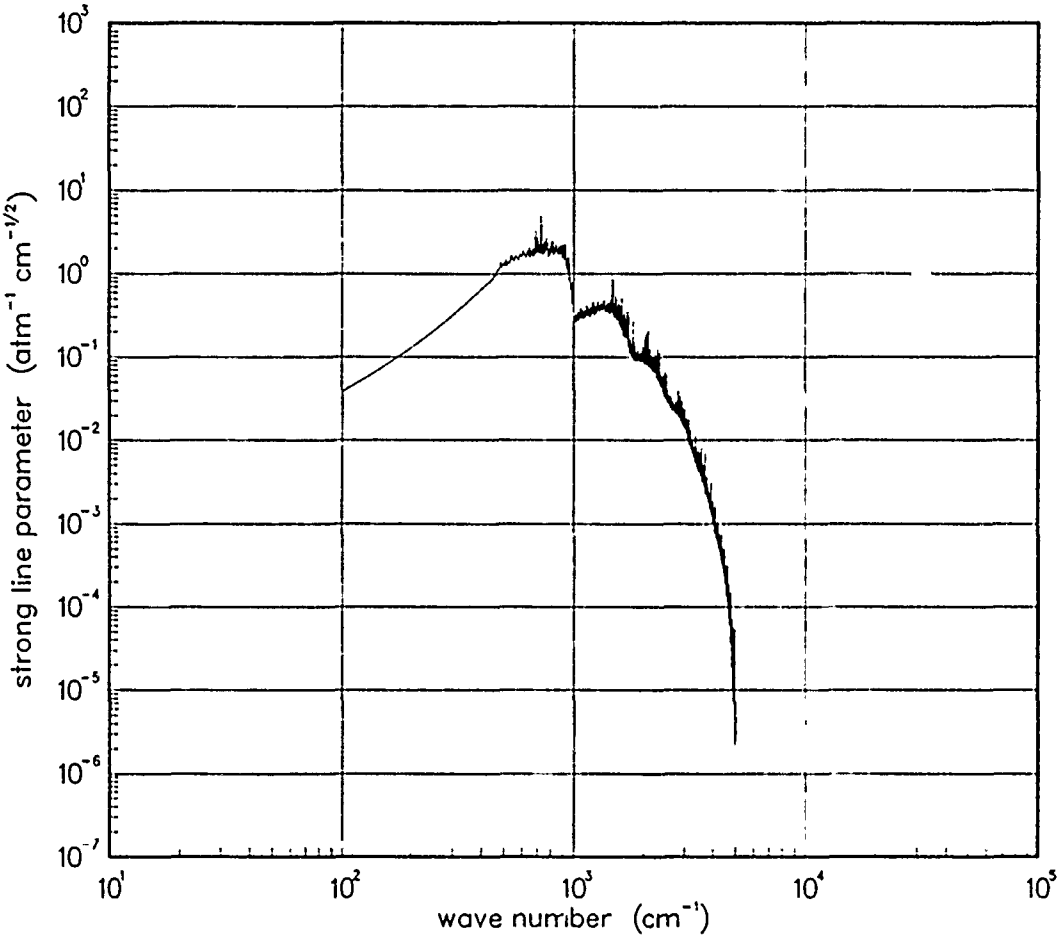

Figure 394. Strong-line parameter for LiO at 7000°K.

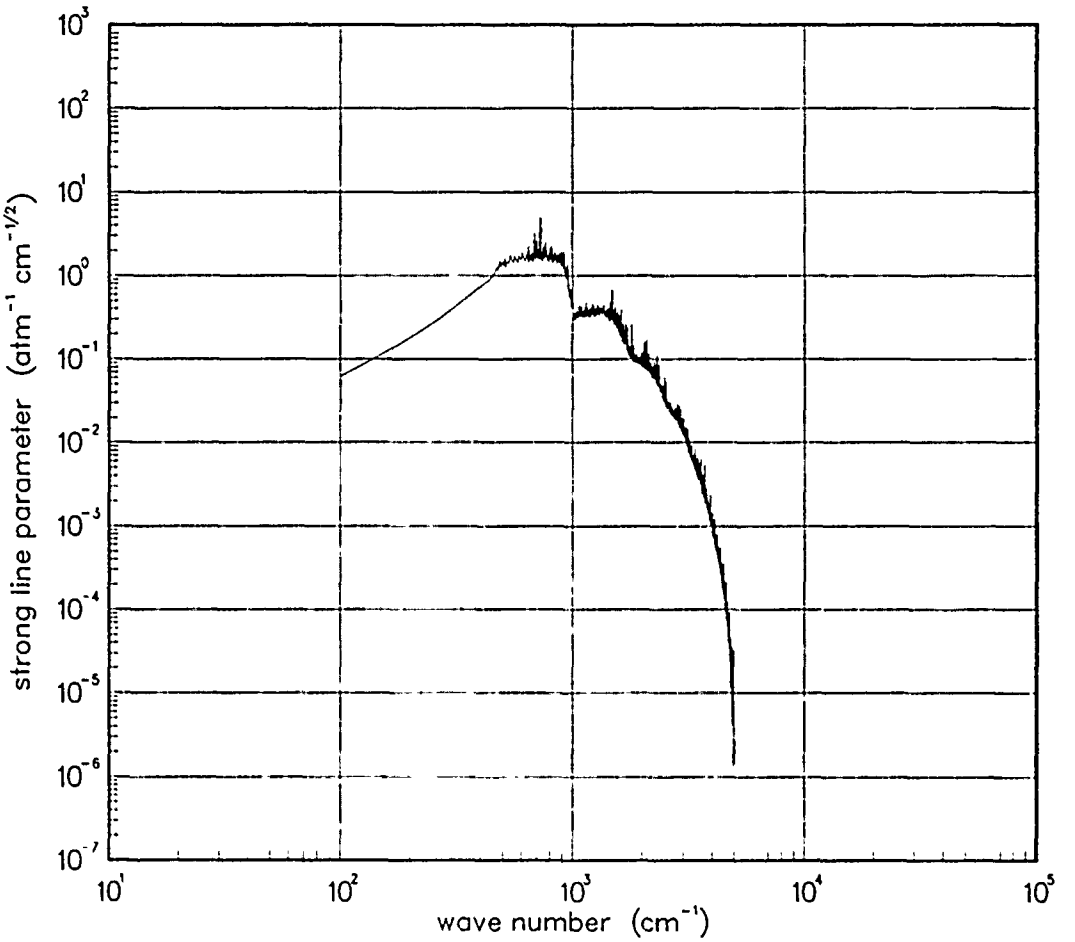

Figure 395. Strong-line parameter for LiO at 10000°K.

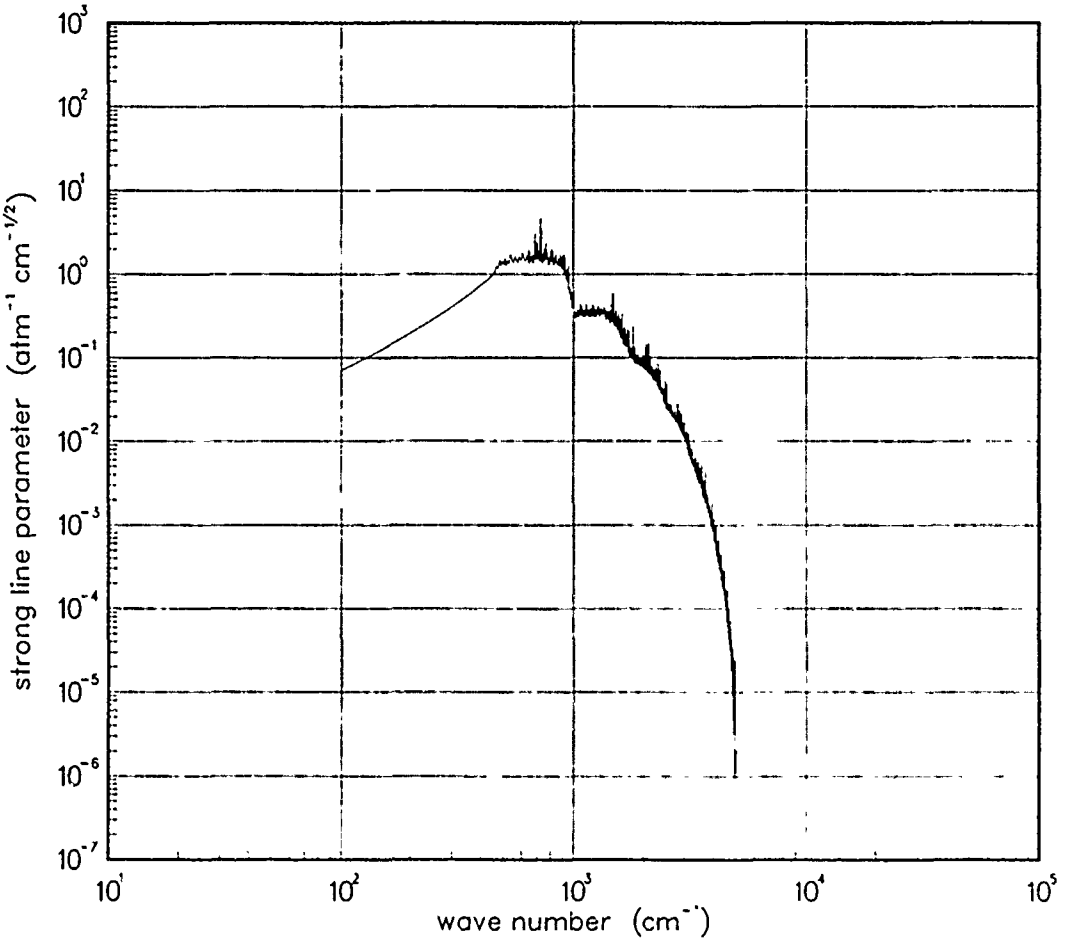

Figure 396. Strong-line parameter for LiO at 12000°K.

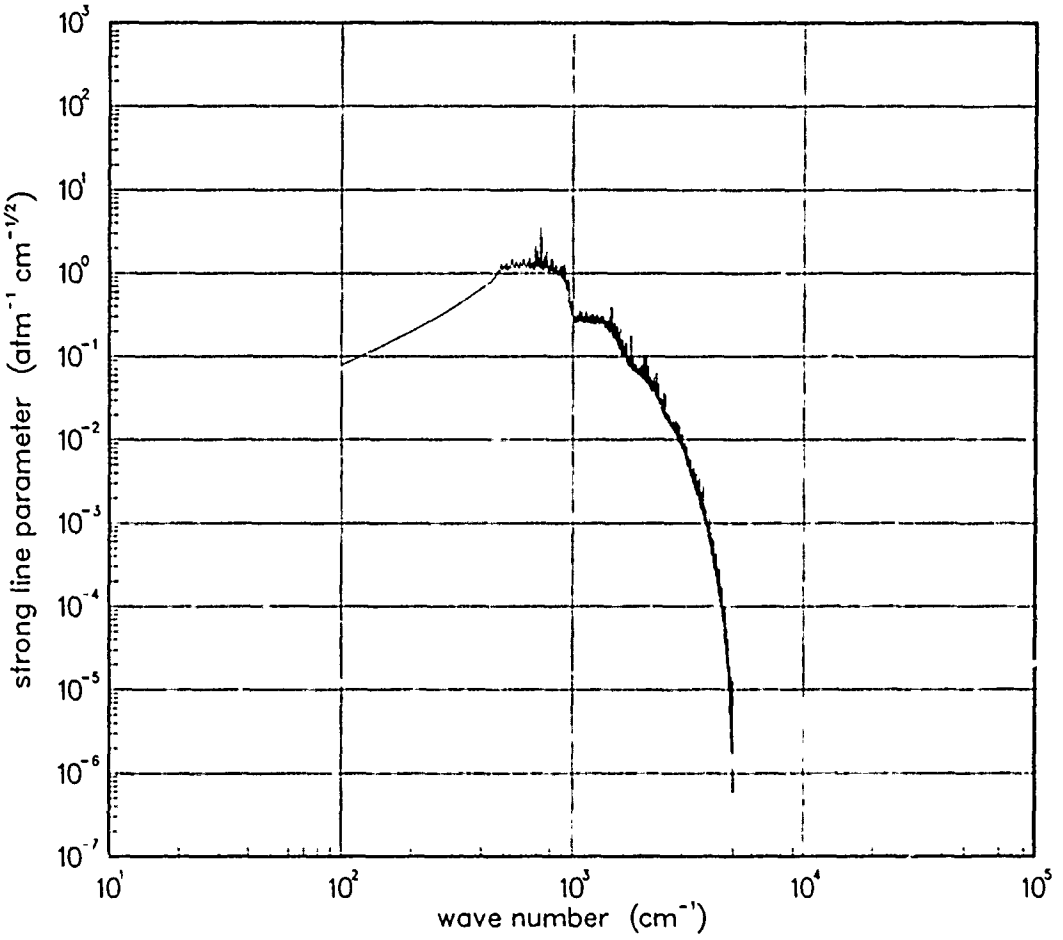

Figure 397. Strong-line parameter for LiO at 18000°K.

6.5. MAGNESIUM OXIDE (MgO).

Table 11. Spectroscopic data for MgO.

$X\ ^1\Sigma$

$\omega_e = 785.06^*$ $\omega_e x_e = 5.18^*$
$\alpha_e = 0.0050^*$ $B_e = 0.57430^*$

$S_{10} = 440.^\dagger$

$\gamma_\ell(300°K) = 0.04^\ddagger$

$X\ ^1\Pi$

$\omega_e = 664.4^*$ $\omega_e x_e = 3.9^*$ $E_e = 3563.30^*$
$\alpha_e = 0.0040^*$ $B_e = 0.505^*$

$S_{10} = 440.^\ddagger$

$\gamma_\ell(300°K) = 0.04^\ddagger$

Data Source:

*B. Rosen, ed., Spectroscopic Data Relative to Diatomic Molecules, Pergamon Press, New York (1970).

†M. Yoshimine, J. Phys. Soc. Japan 25, 1100 (1968).

‡Estimate.

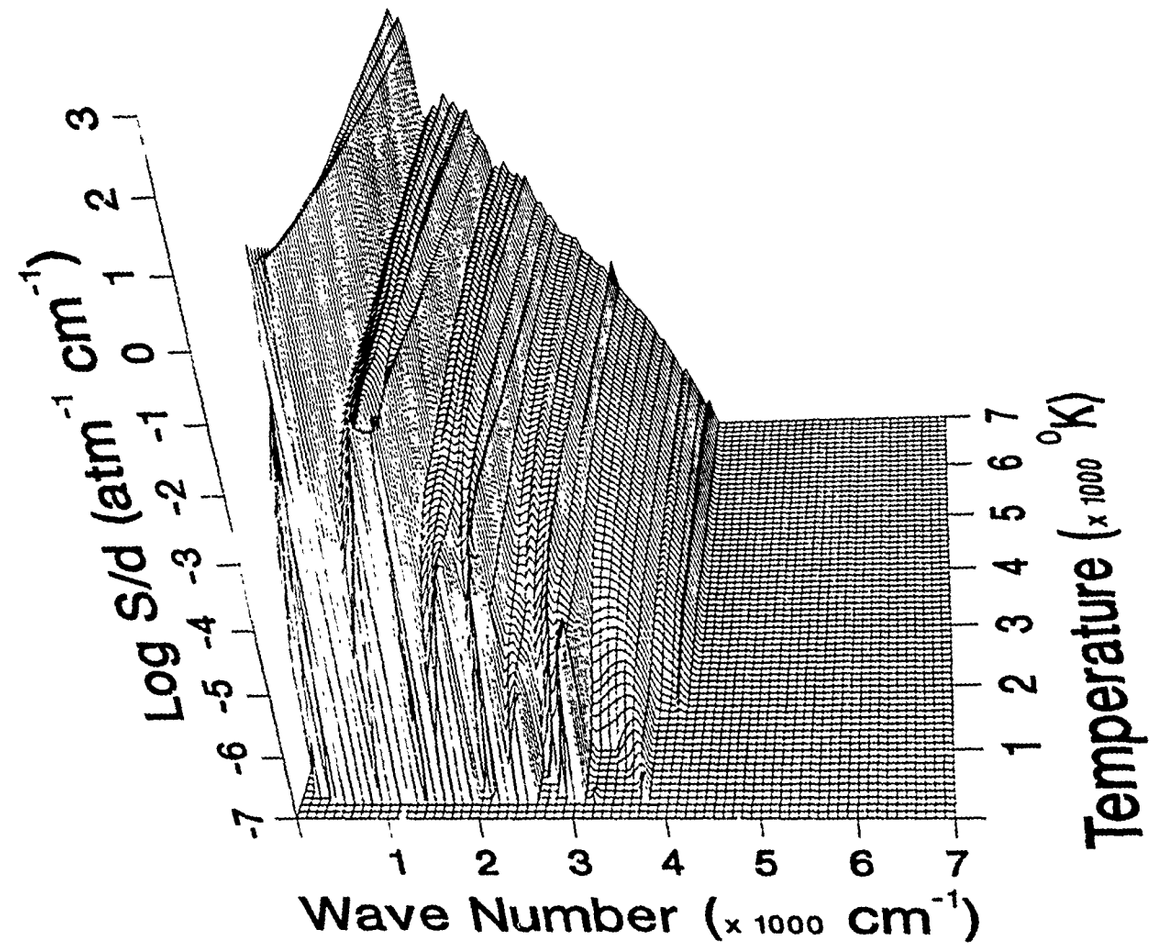

Figure 398. Weak-line parameter for MgO.

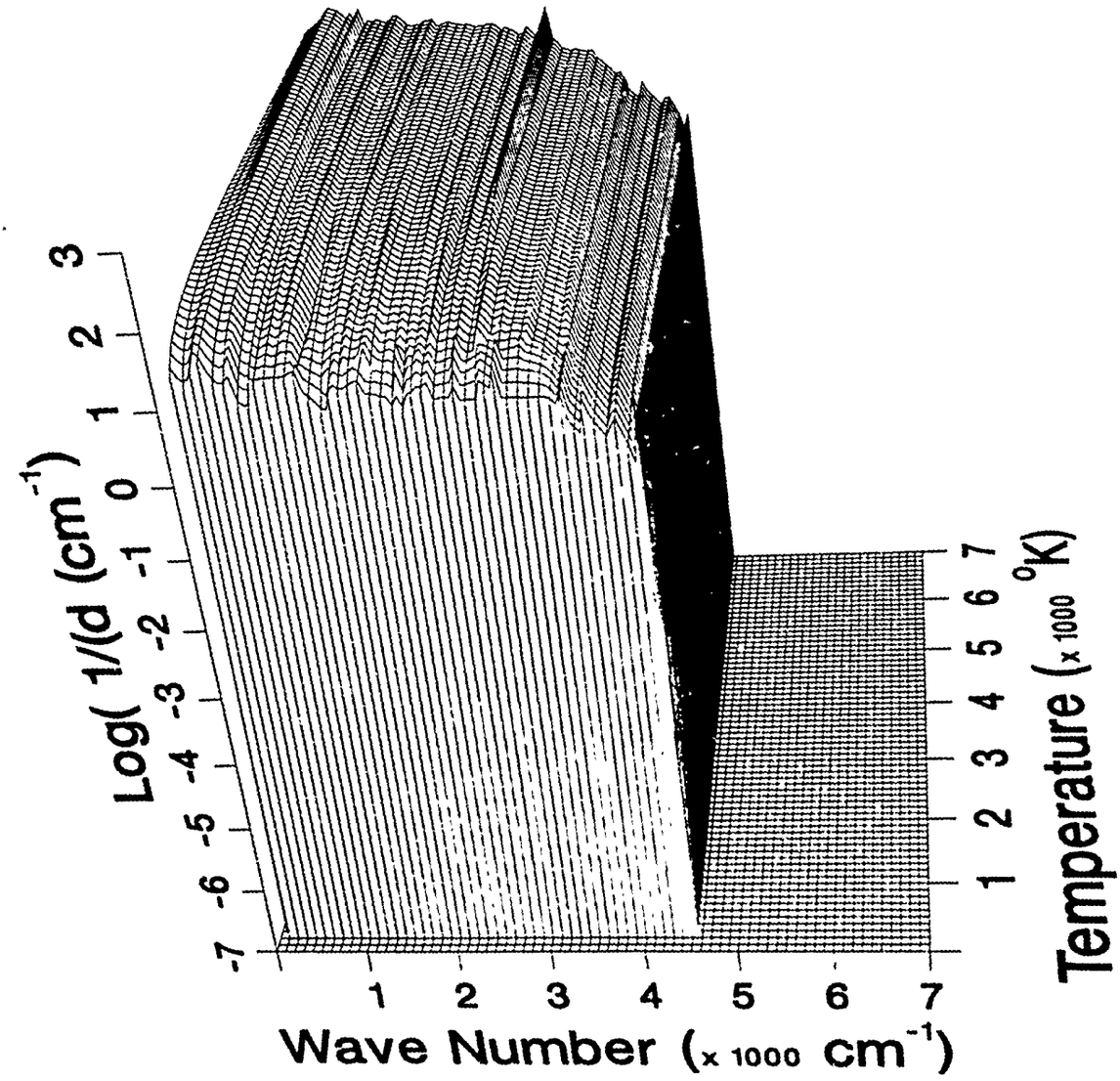

Figure 399. Inverse line spacing for MgO.

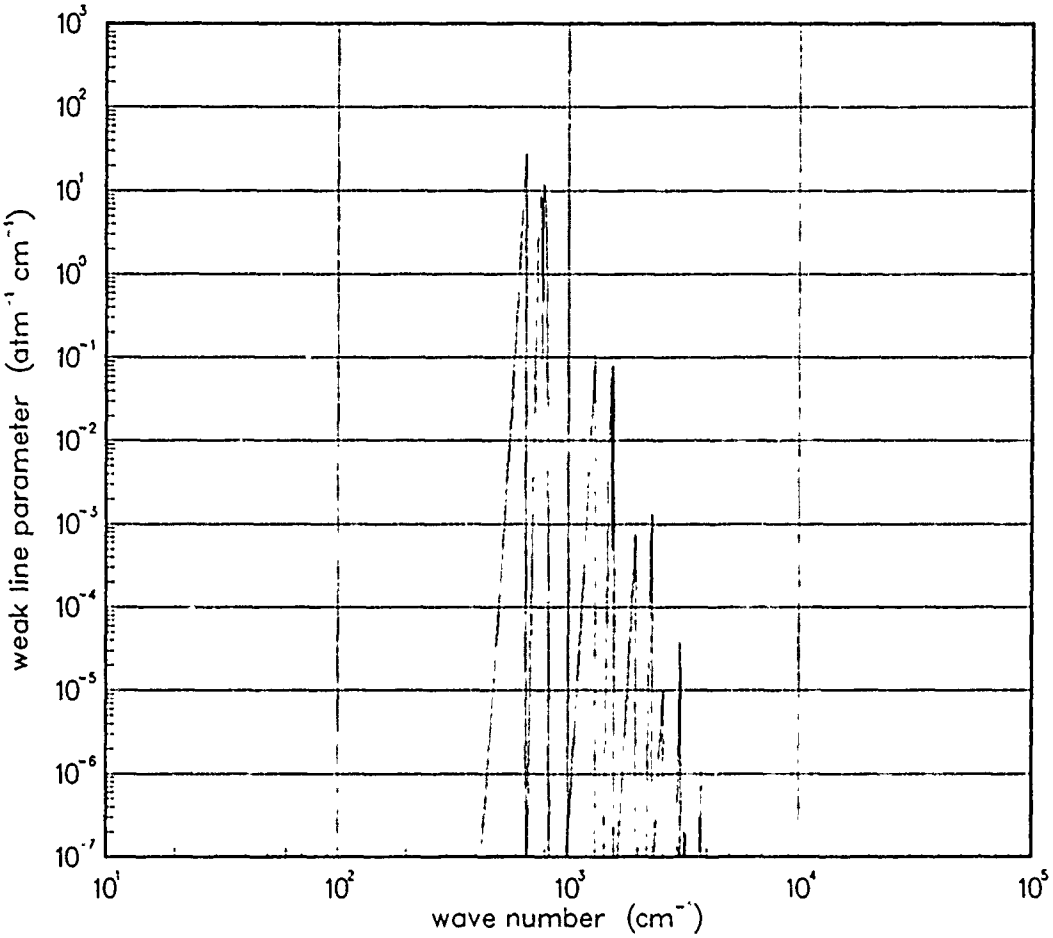

Figure 400. Weak-line parameter for MgO at 200°K.

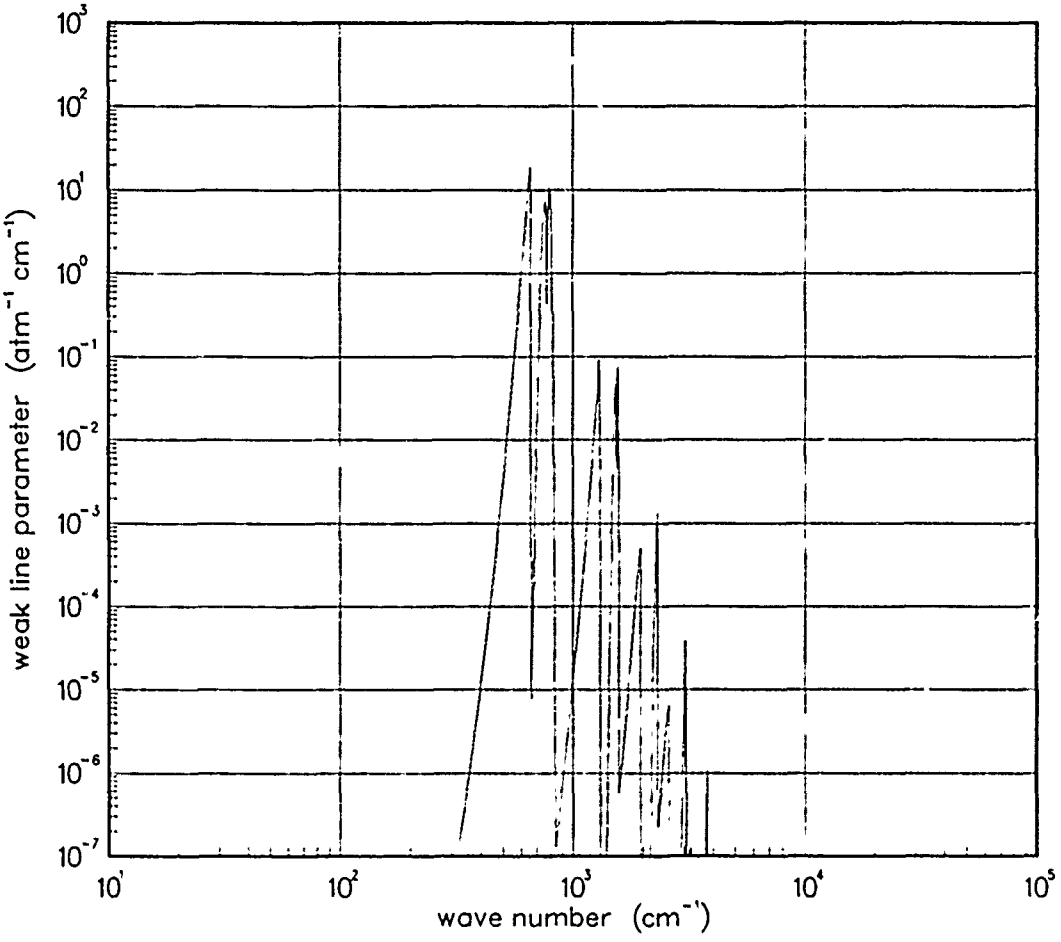

Figure 401. Weak-line parameter for MgO at 300°K.

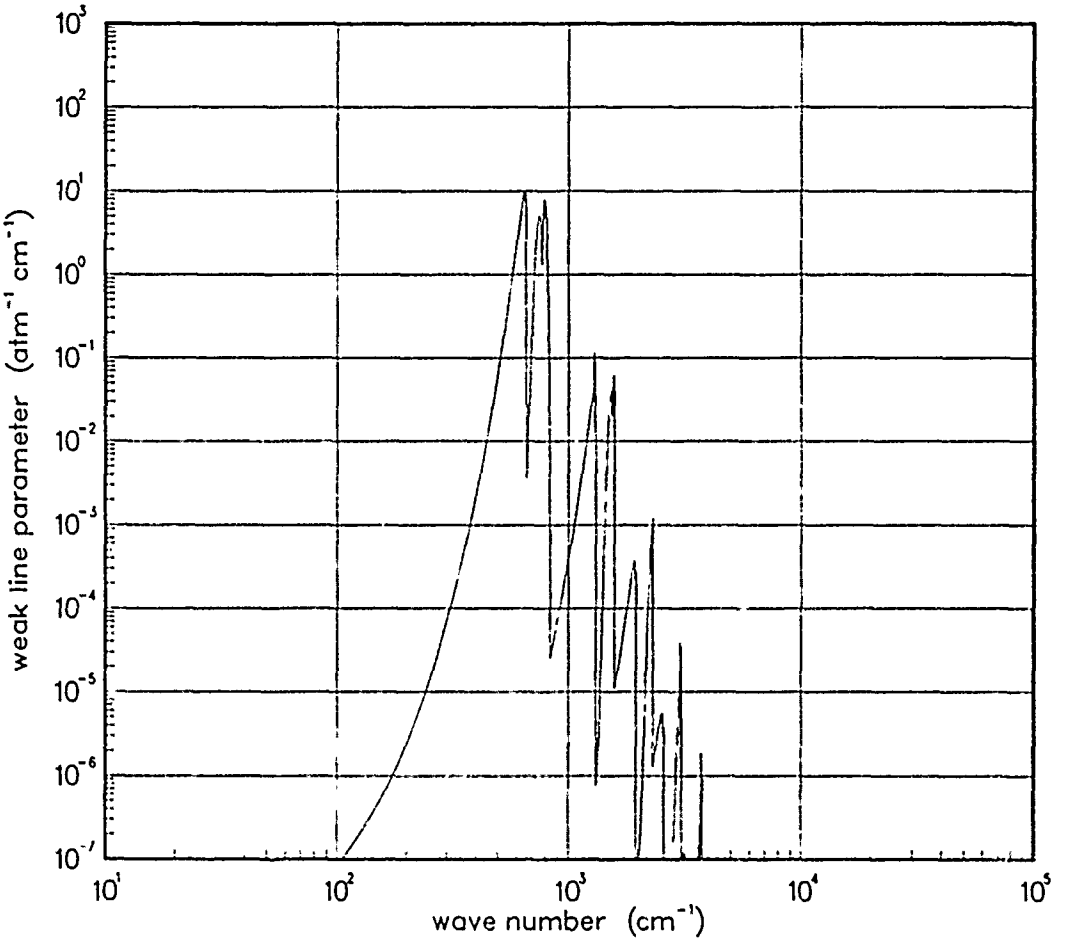

Figure 402. Weak-line parameter for MgO at 500°K.

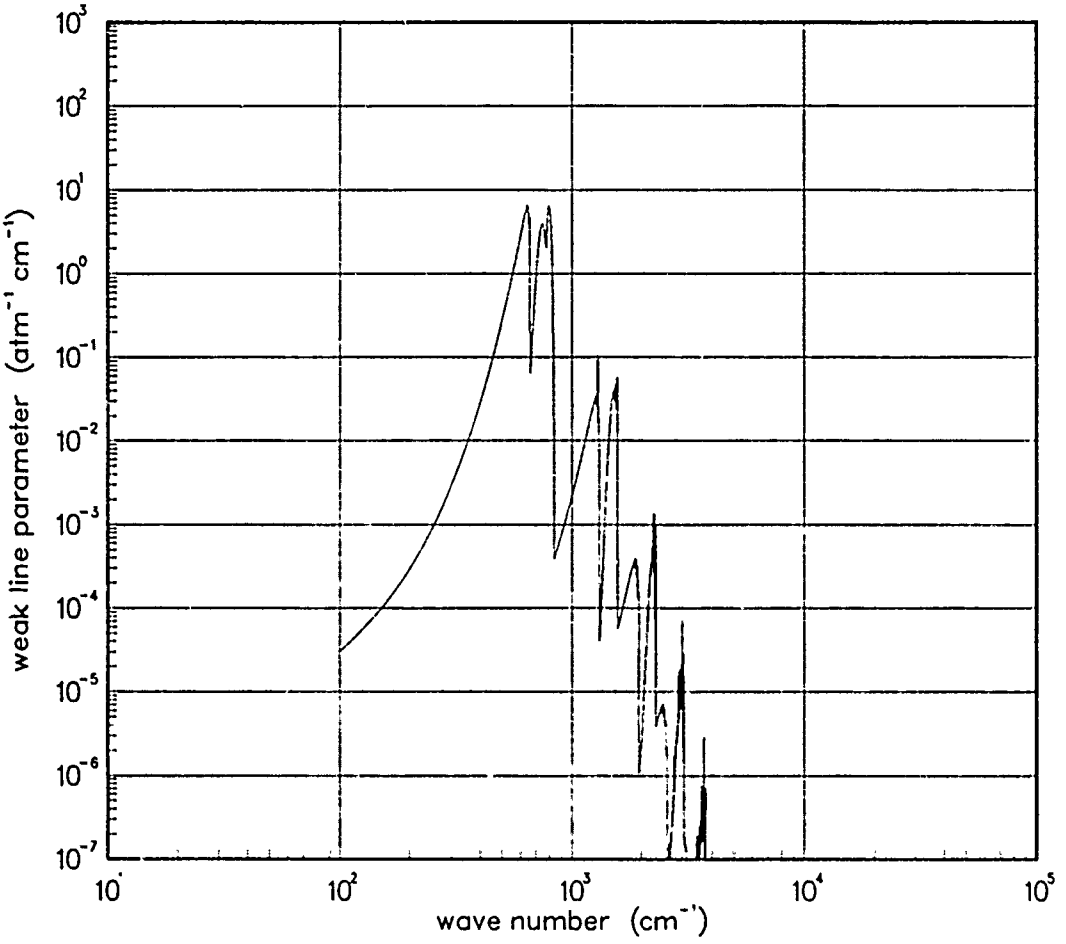

Figure 403. Weak-line parameter for MgO at 750°K.

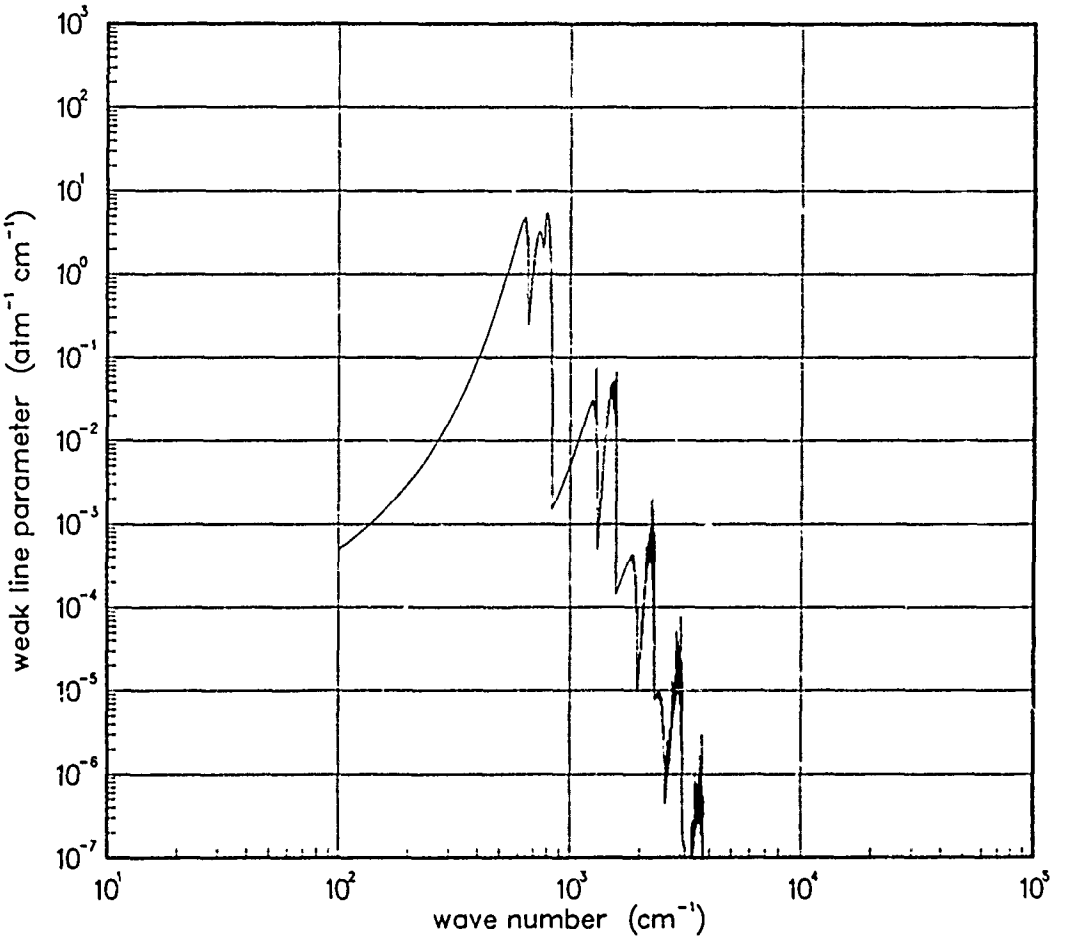

Figure 404. Weak-line parameter for MgO at 1000°K.

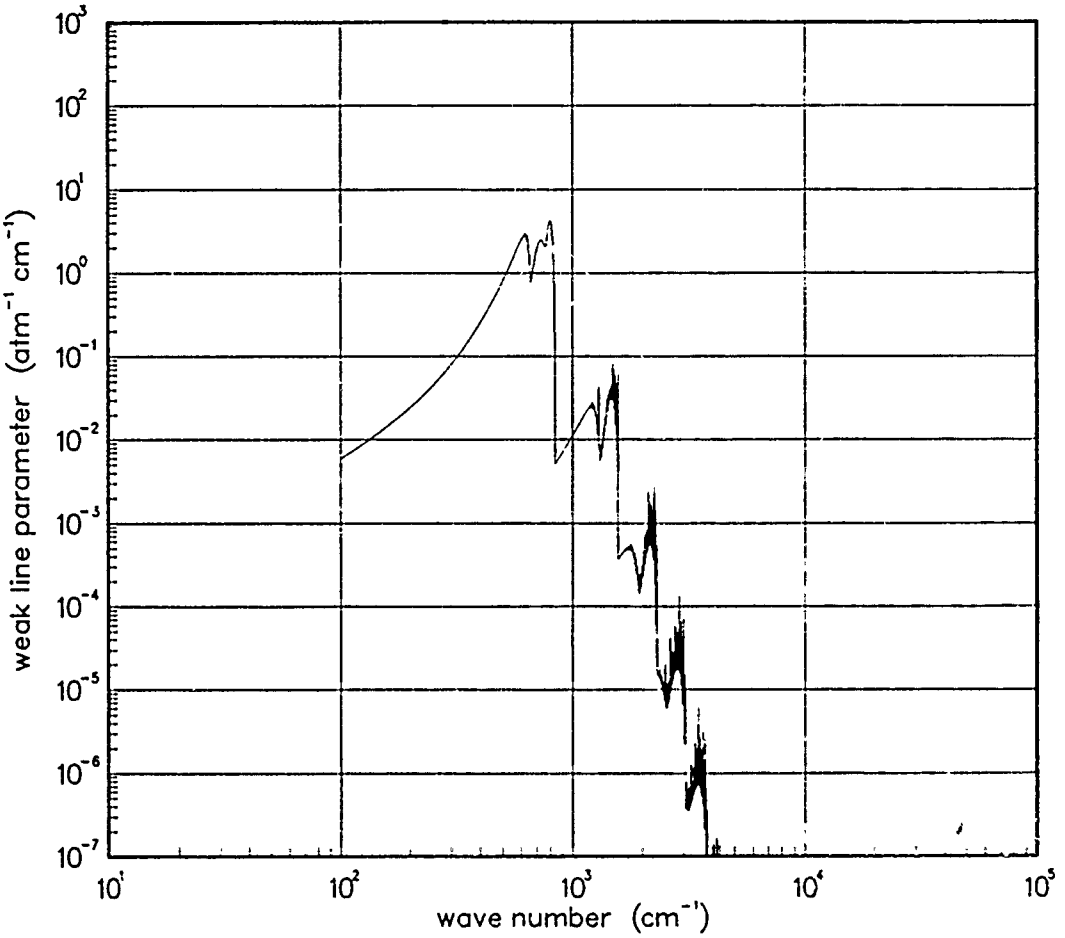

Figure 405. Weak-line parameter for MgO at 1500°K.

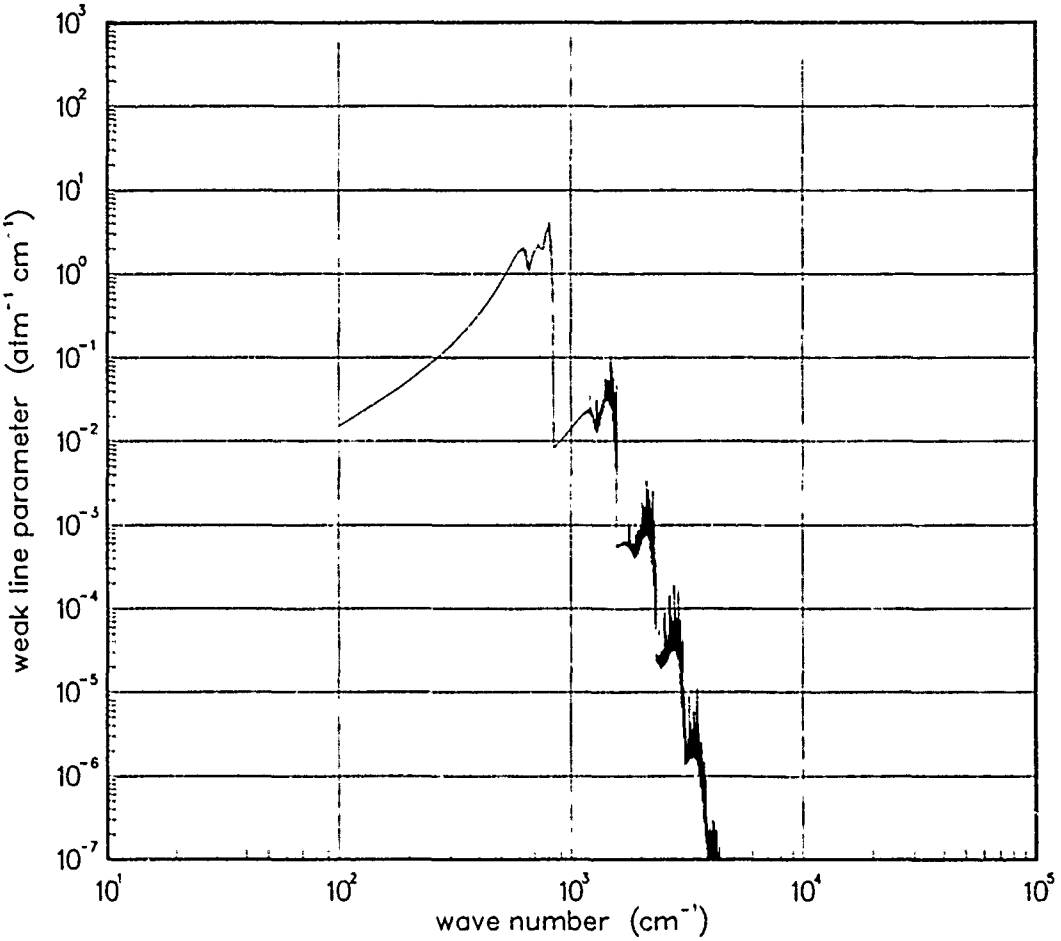

Figure 406. Weak-line parameter for MgO at 2000°K.

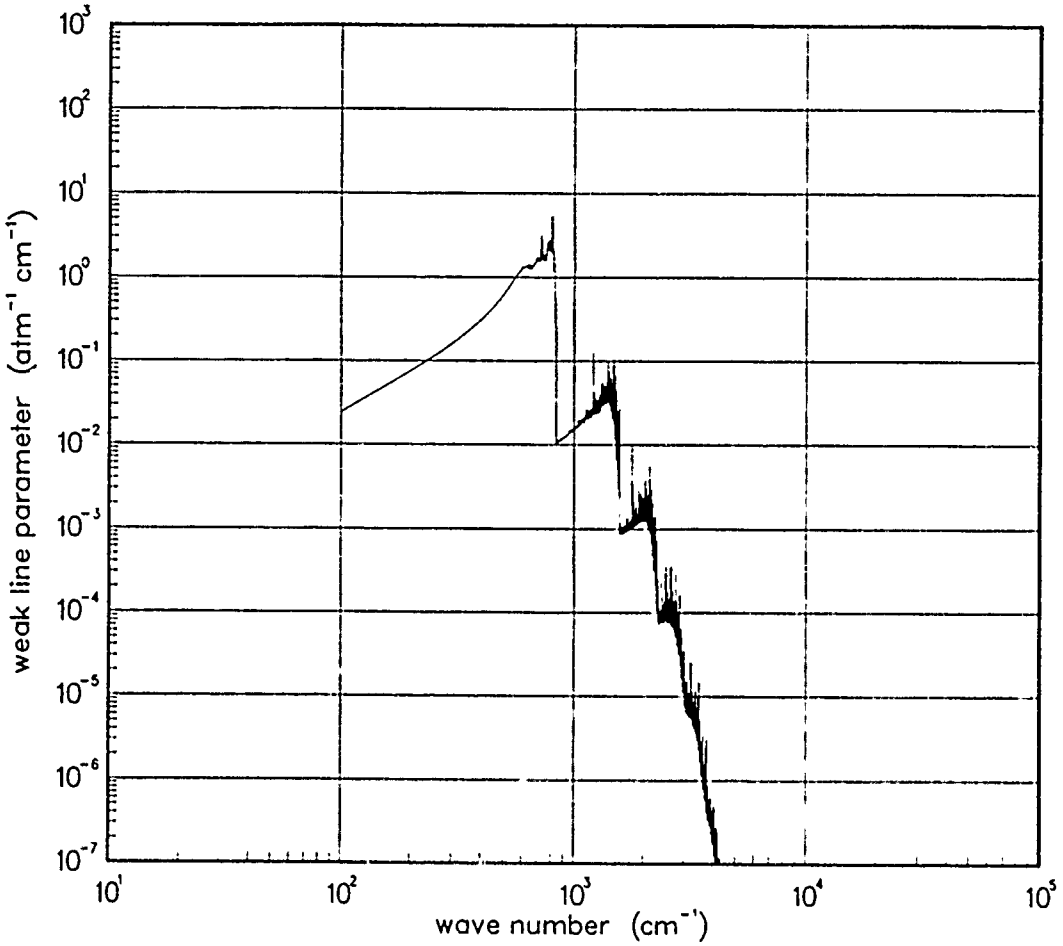

Figure 407. Weak-line parameter for MgO at 3000°K.

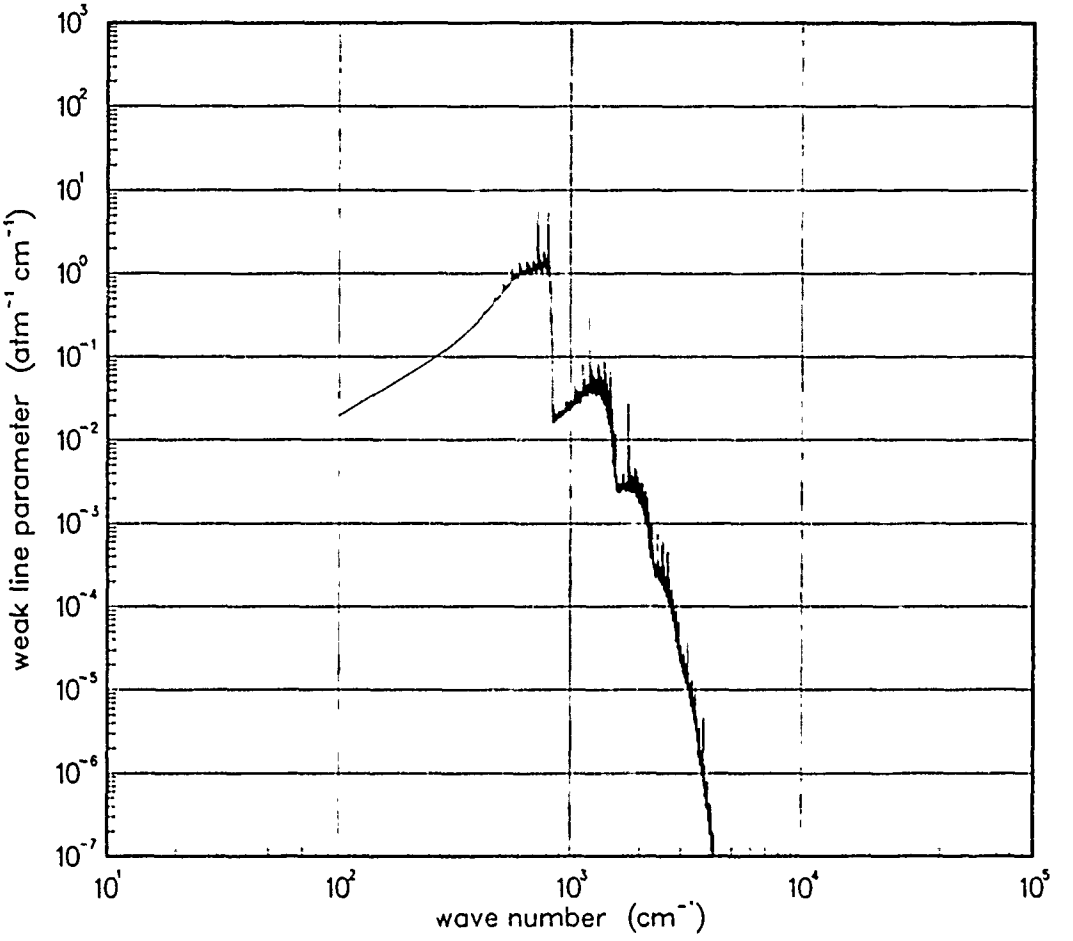

Figure 408. Weak-line parameter for MgO at 5000°K.

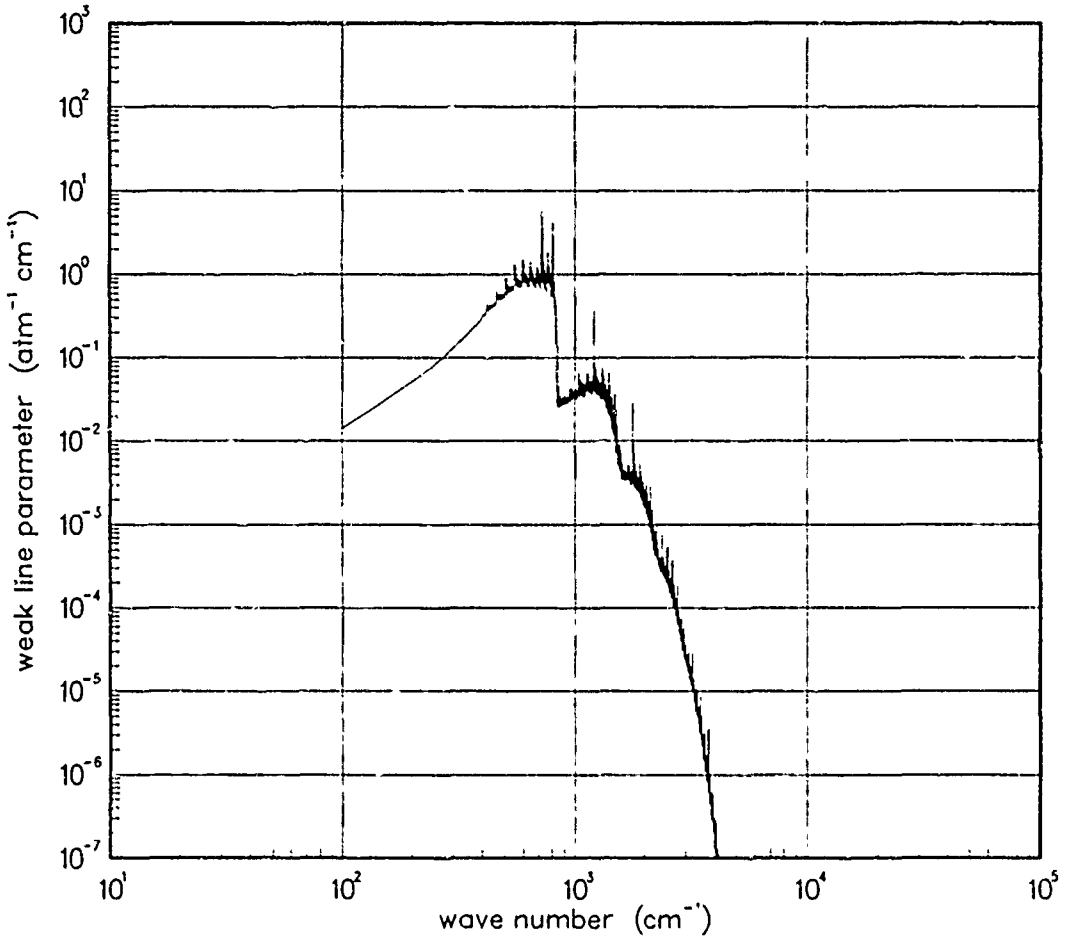

Figure 409. Weak-line parameter for MgO at 7000°K.

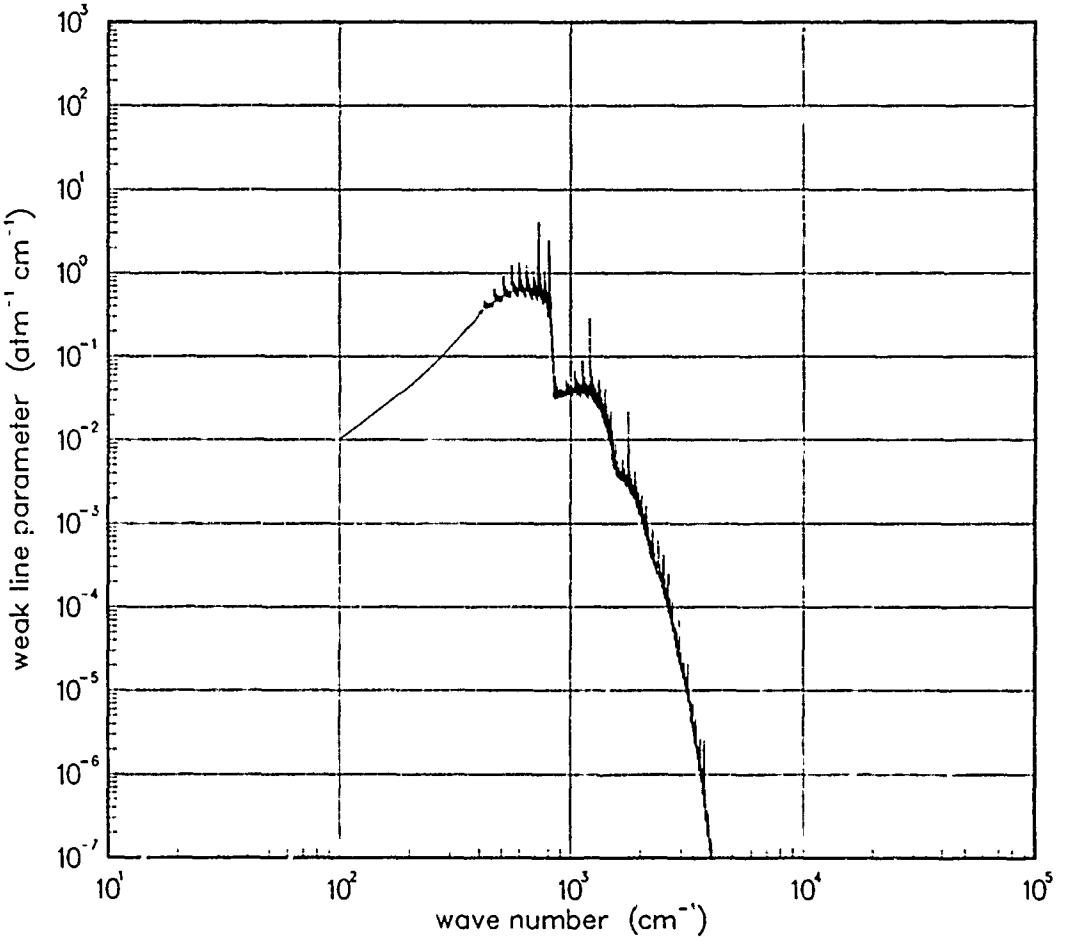

Figure 410. Weak-line parameter for MgO at 10000°K.

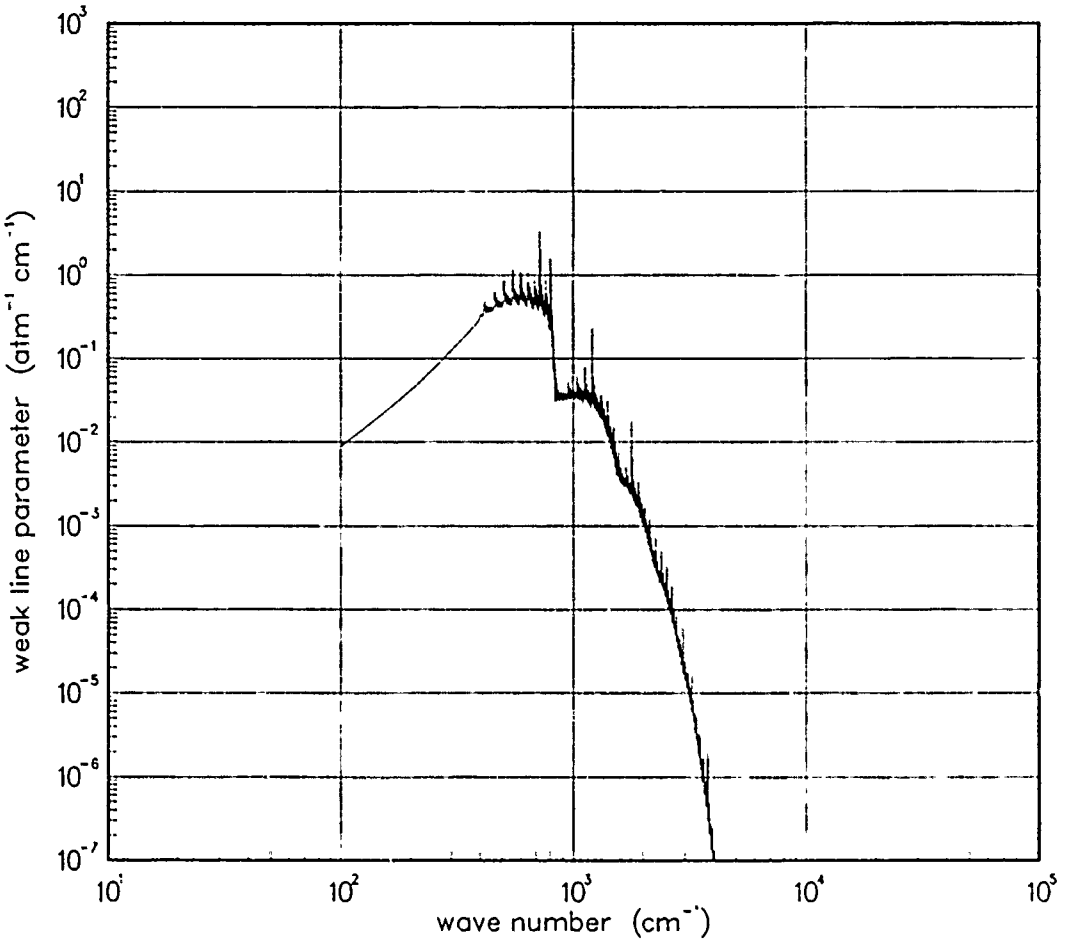

Figure 411. Weak-line parameter for MgO at 12000°K.

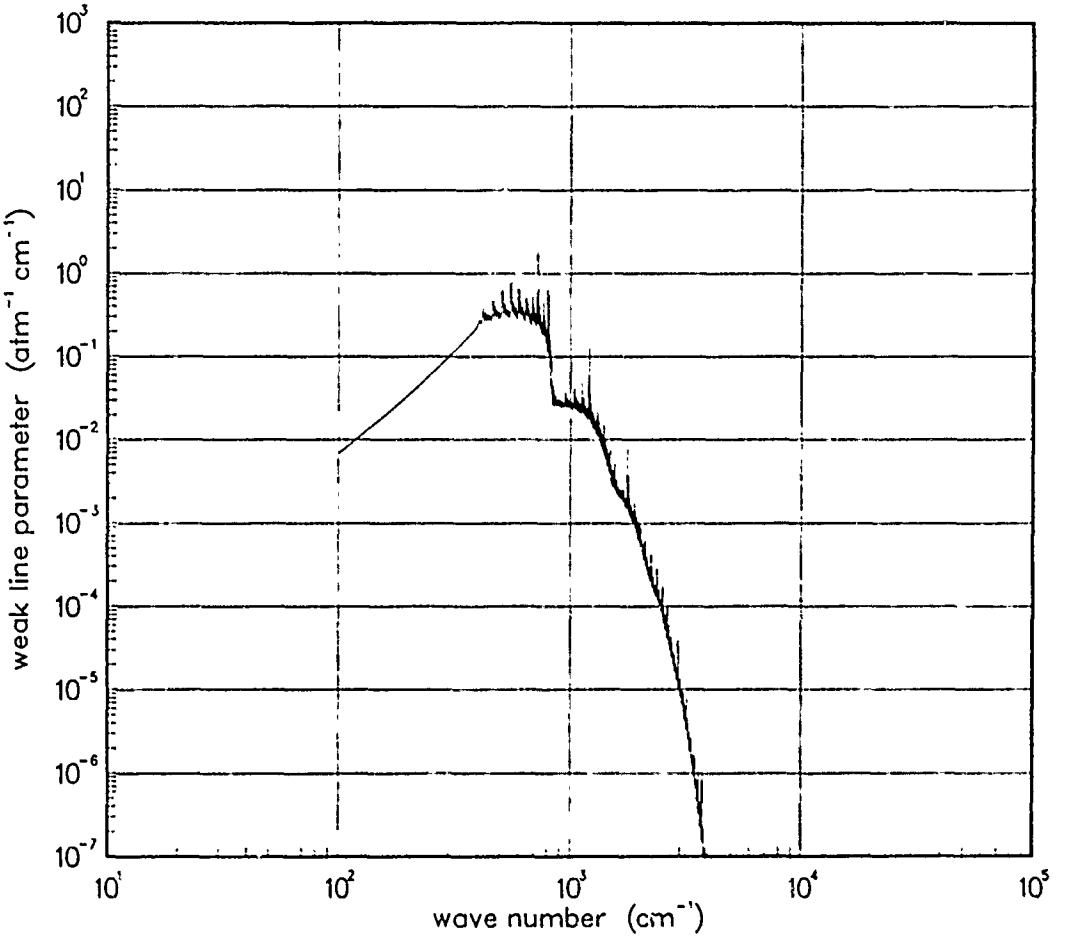

Figure 412. Weak-line parameter for MgO at 18000°K.

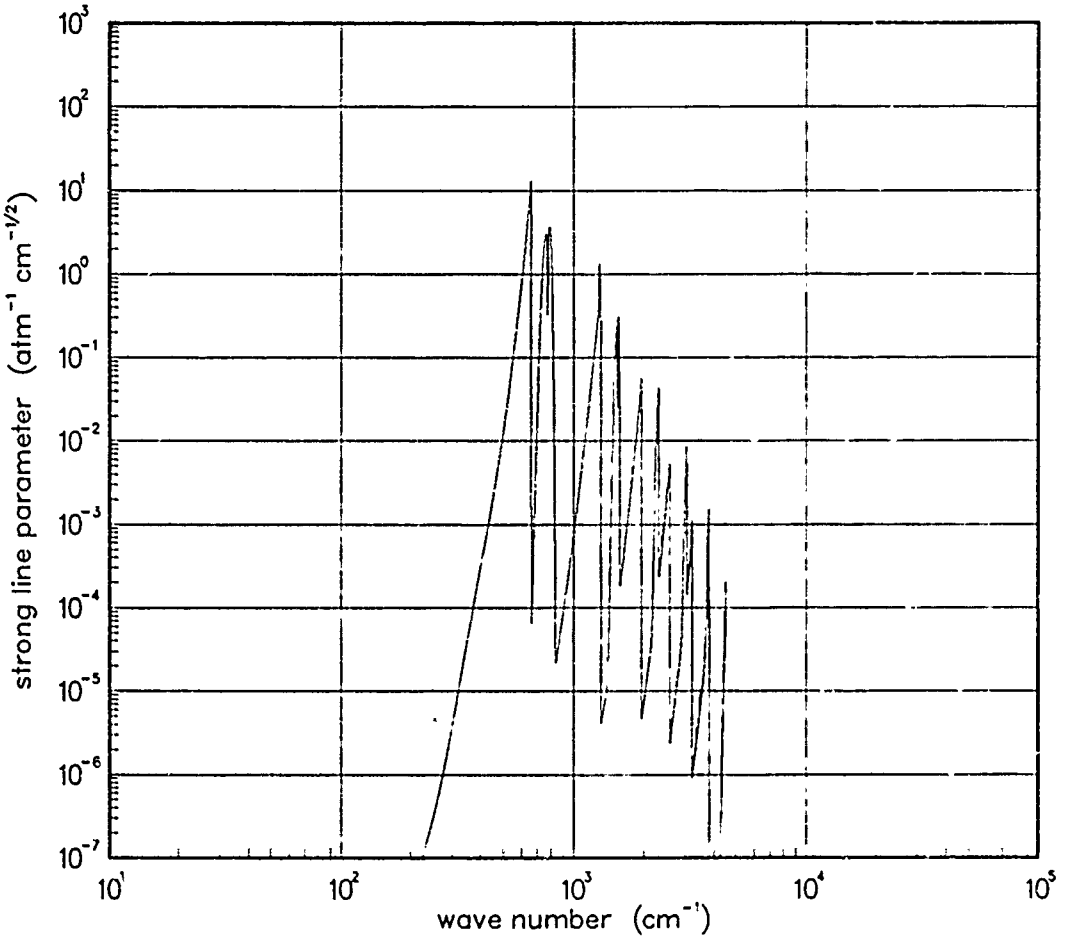

Figure 413. Strong-line parameter for MgO at 200°K.

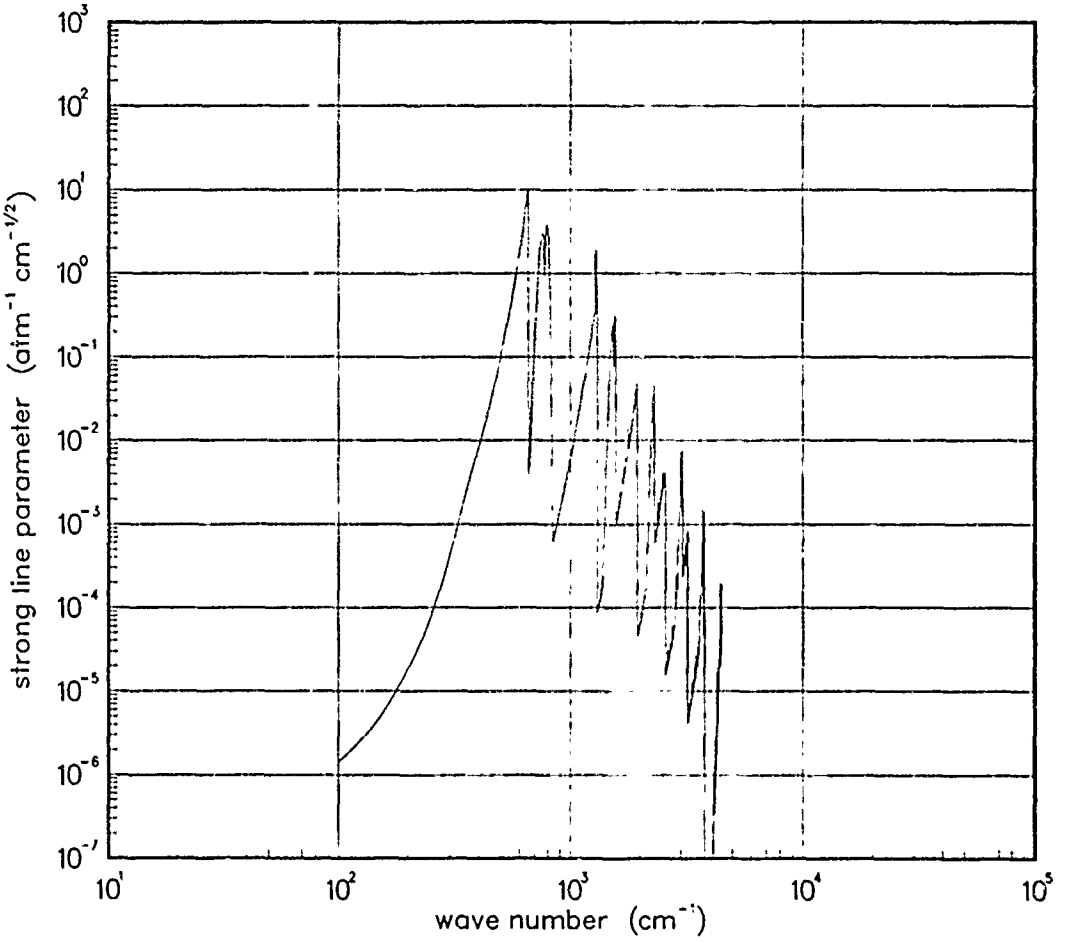

Figure 414. Strong-line parameter for MgO at 300°K.

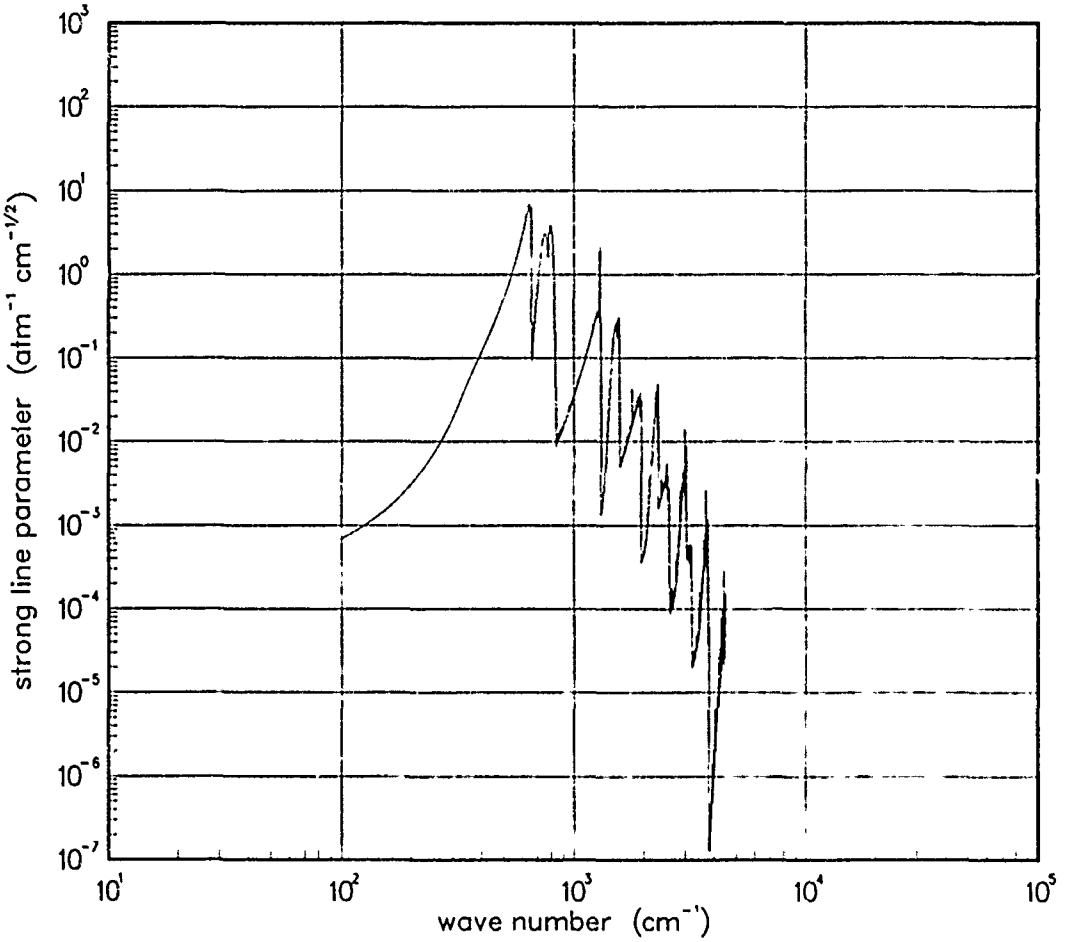

Figure 415. Strong-line parameter for MgO at 500°K.

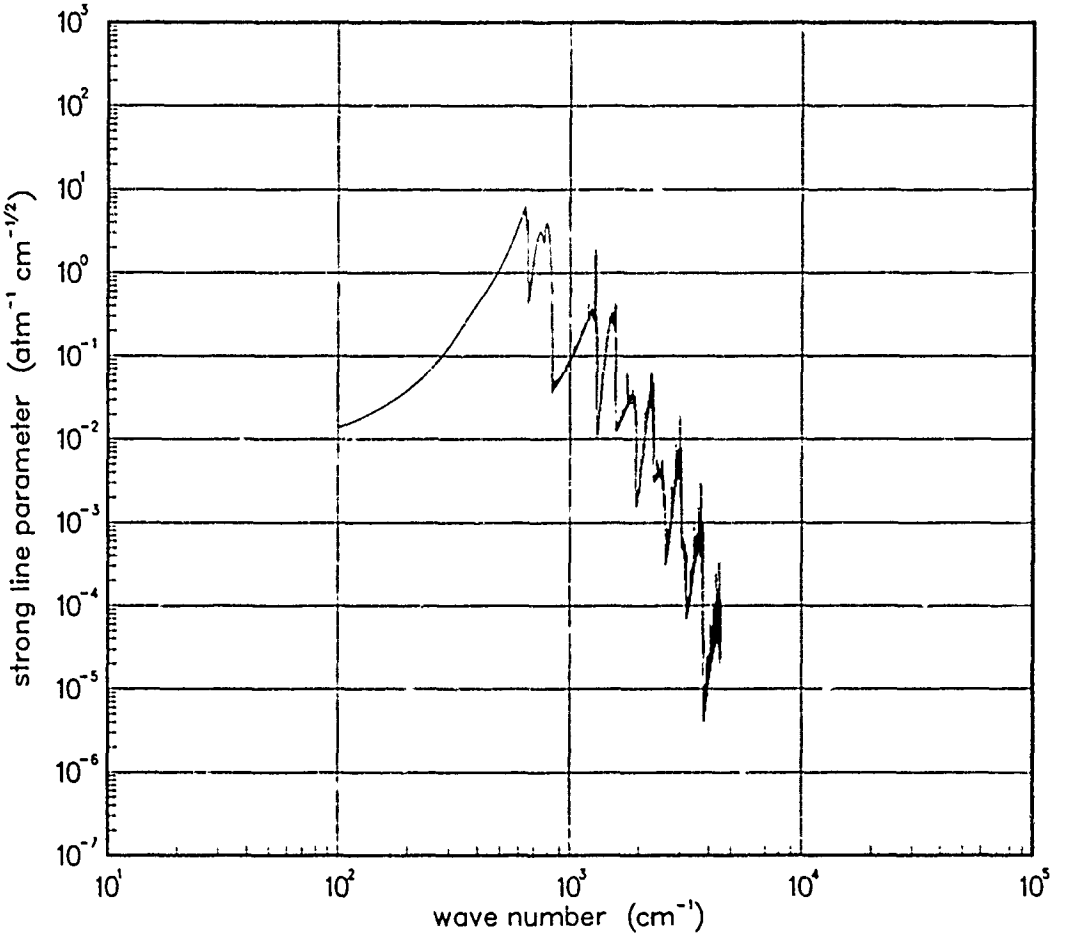

Figure 416. Strong-line parameter for MgO at 750°K.

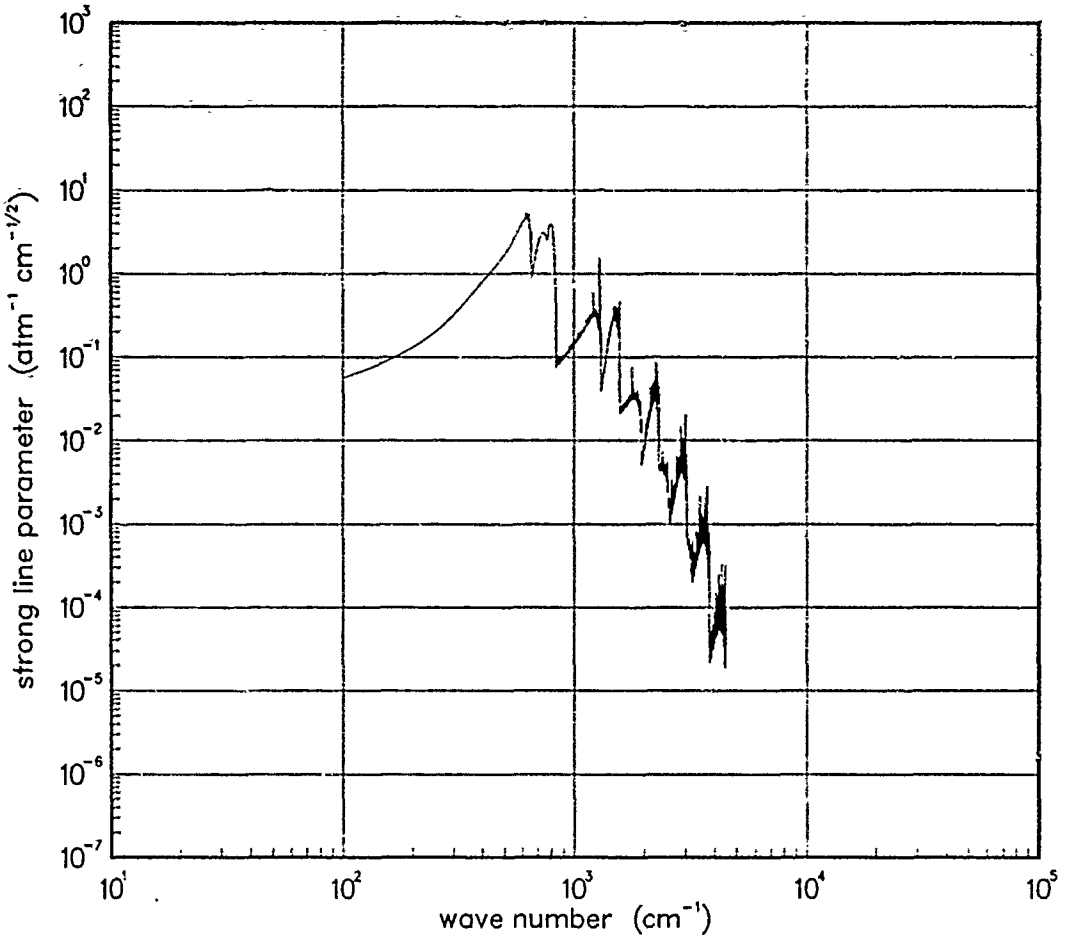

Figure 417. Strong-line parameter for MgO at 1000°K.

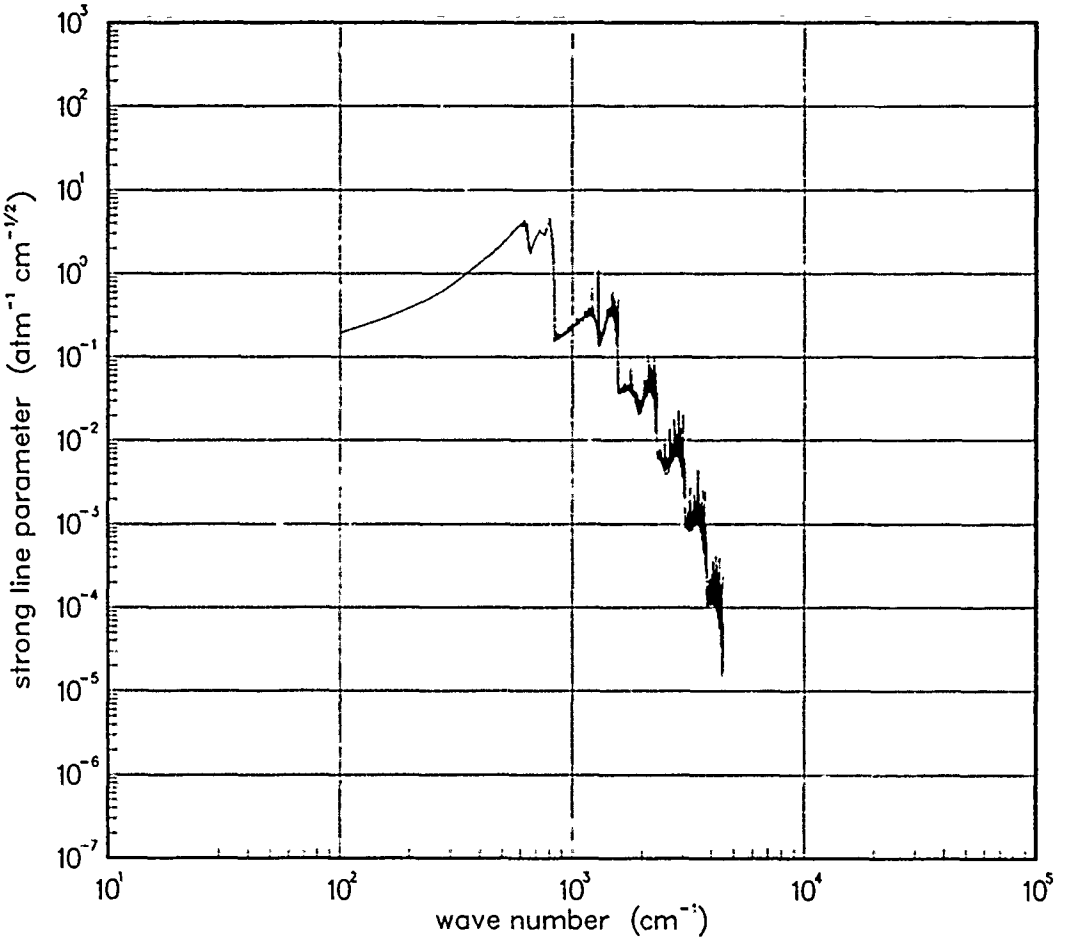

Figure 418. Strong-line parameter for MgO at 1500°K.

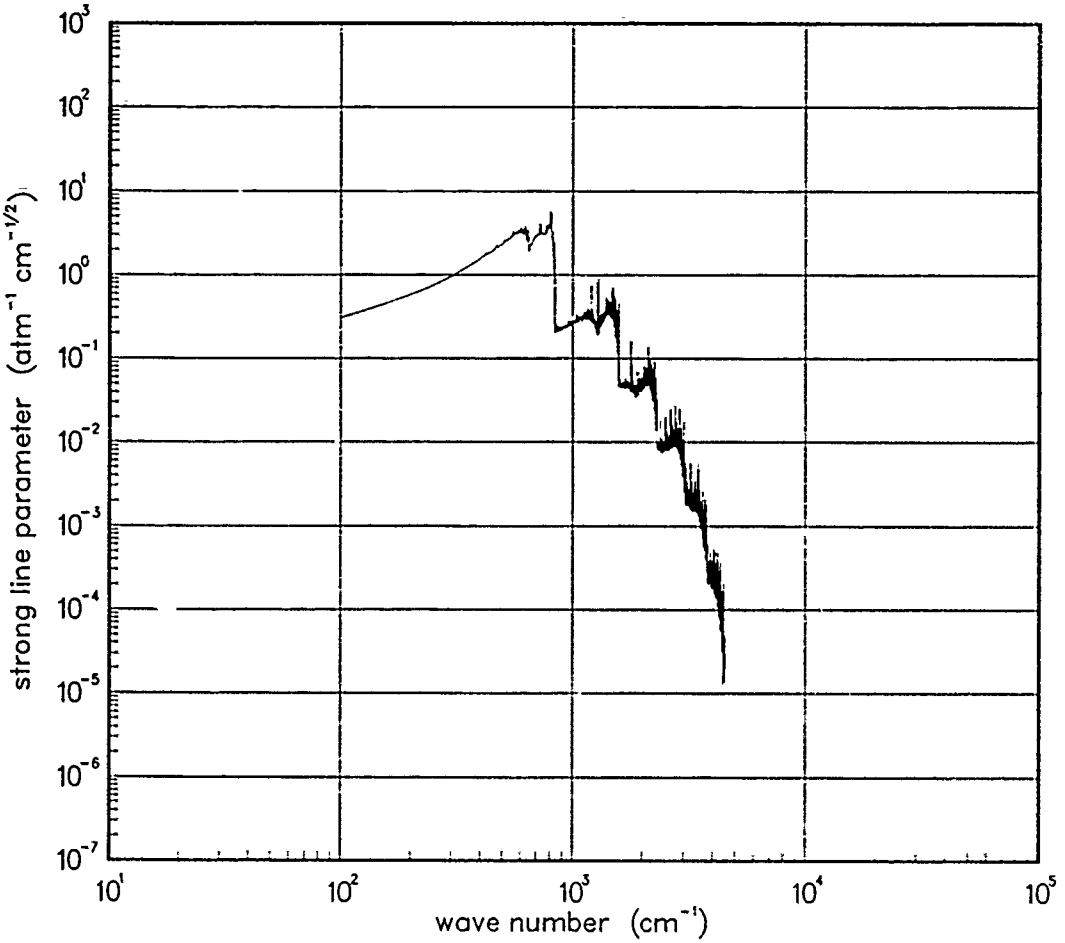

Figure 419. Strong-line parameter for MgO at 2000°K.

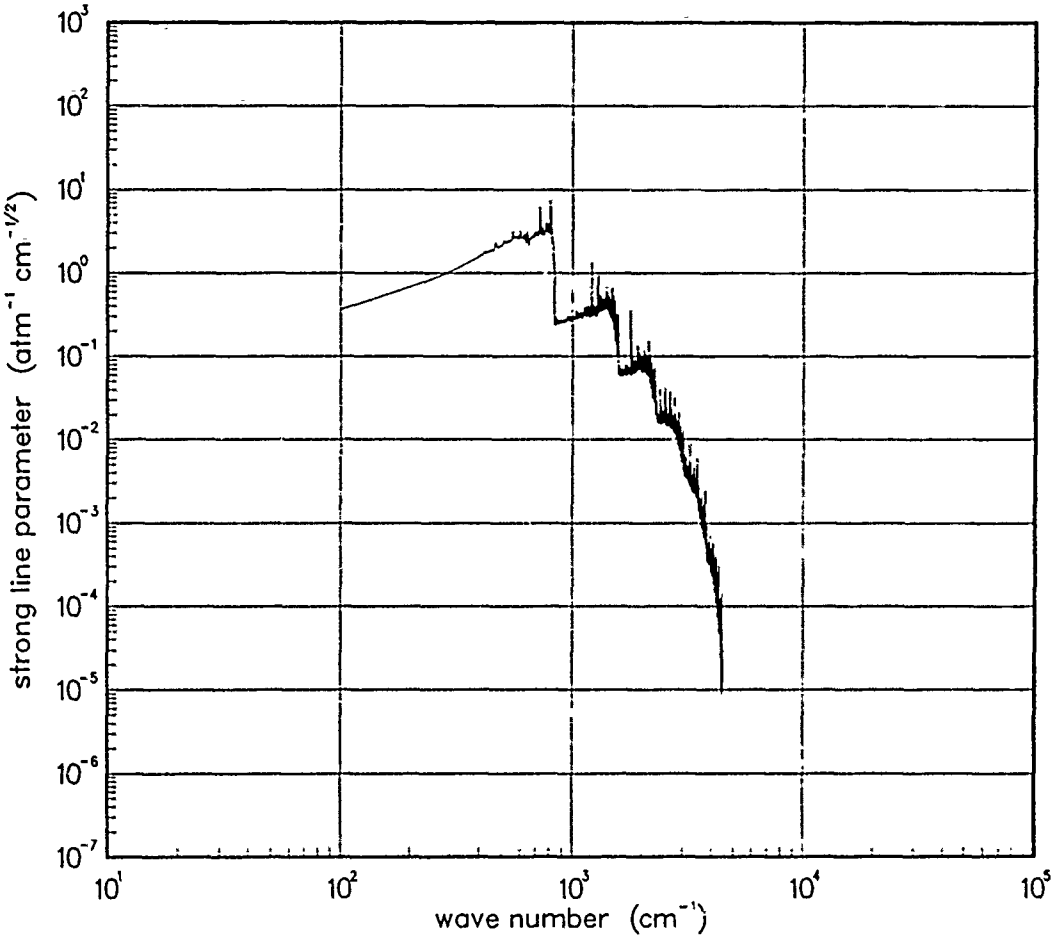

Figure 420. Strong-line parameter for MgO at 3000°K.

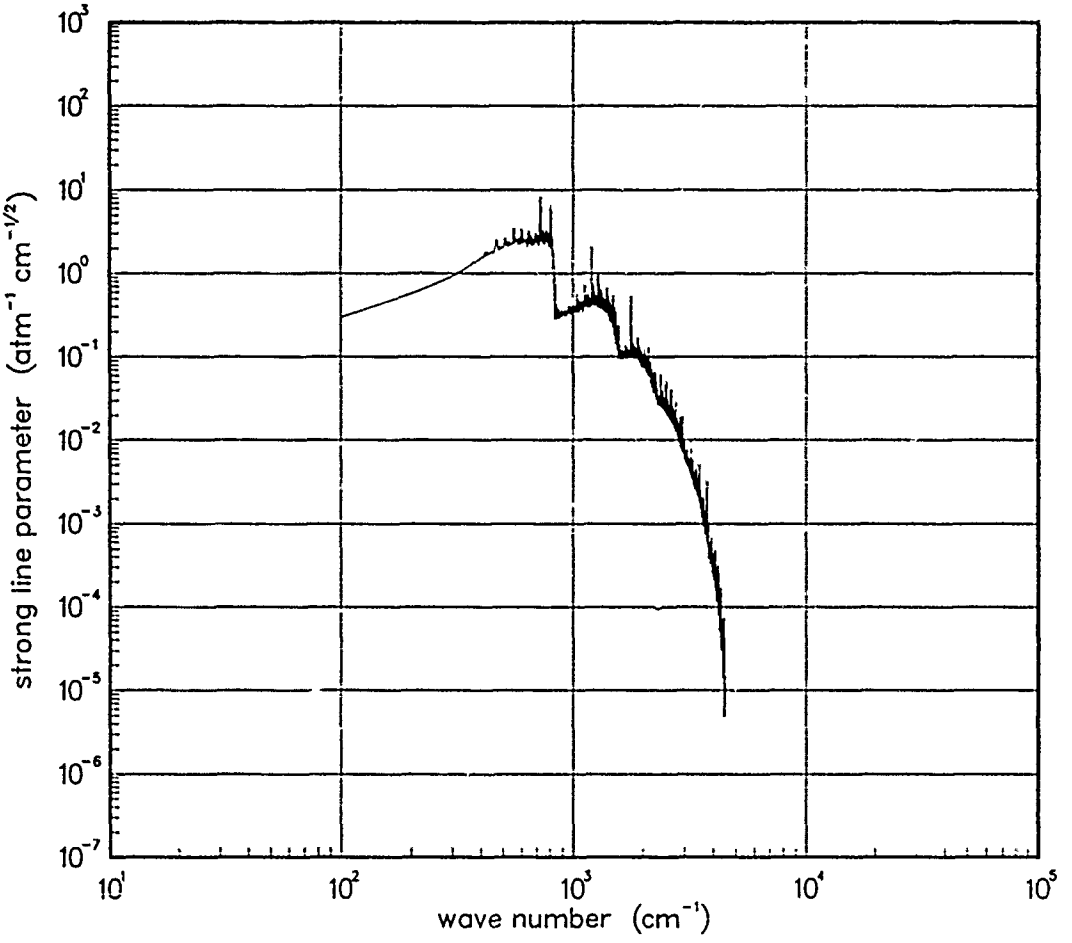

Figure 421. Strong-line parameter for MgO at 5000°K.

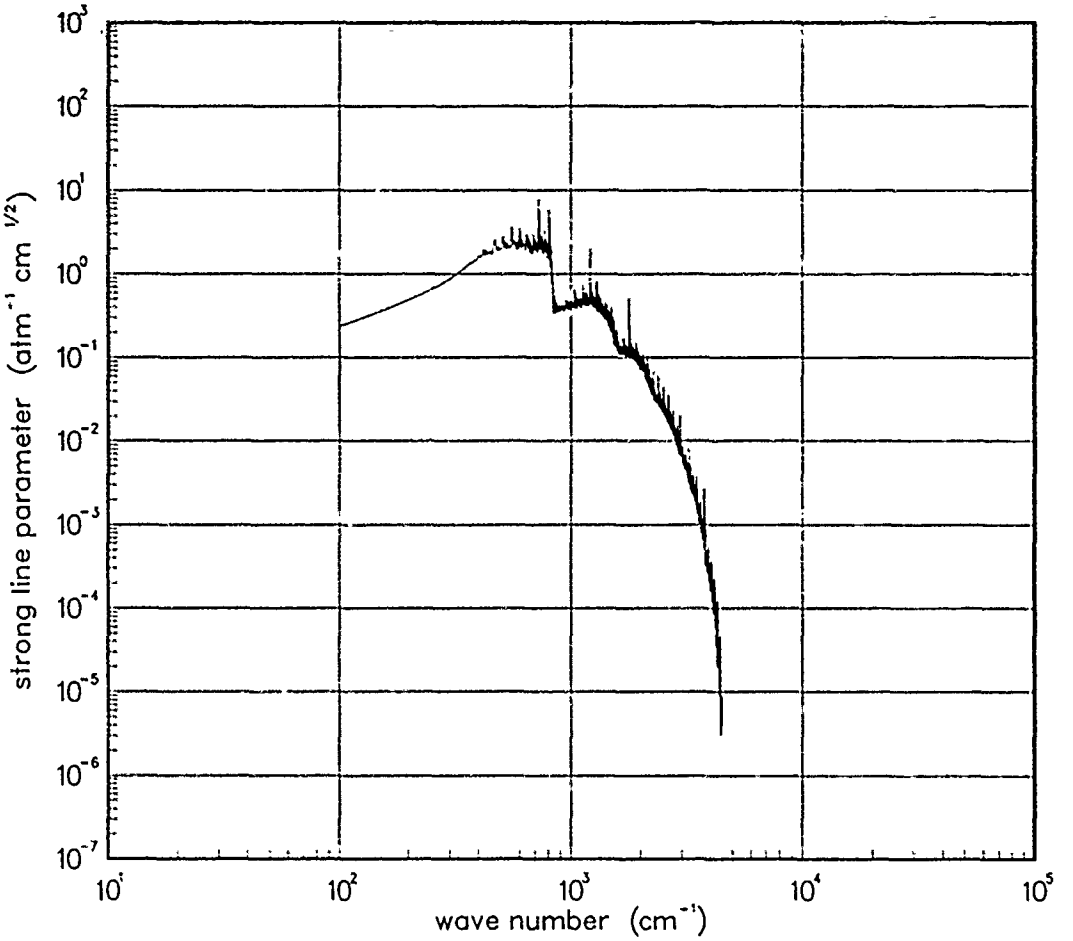

Figure 422. Strong-line parameter for MgO at 7000°K.

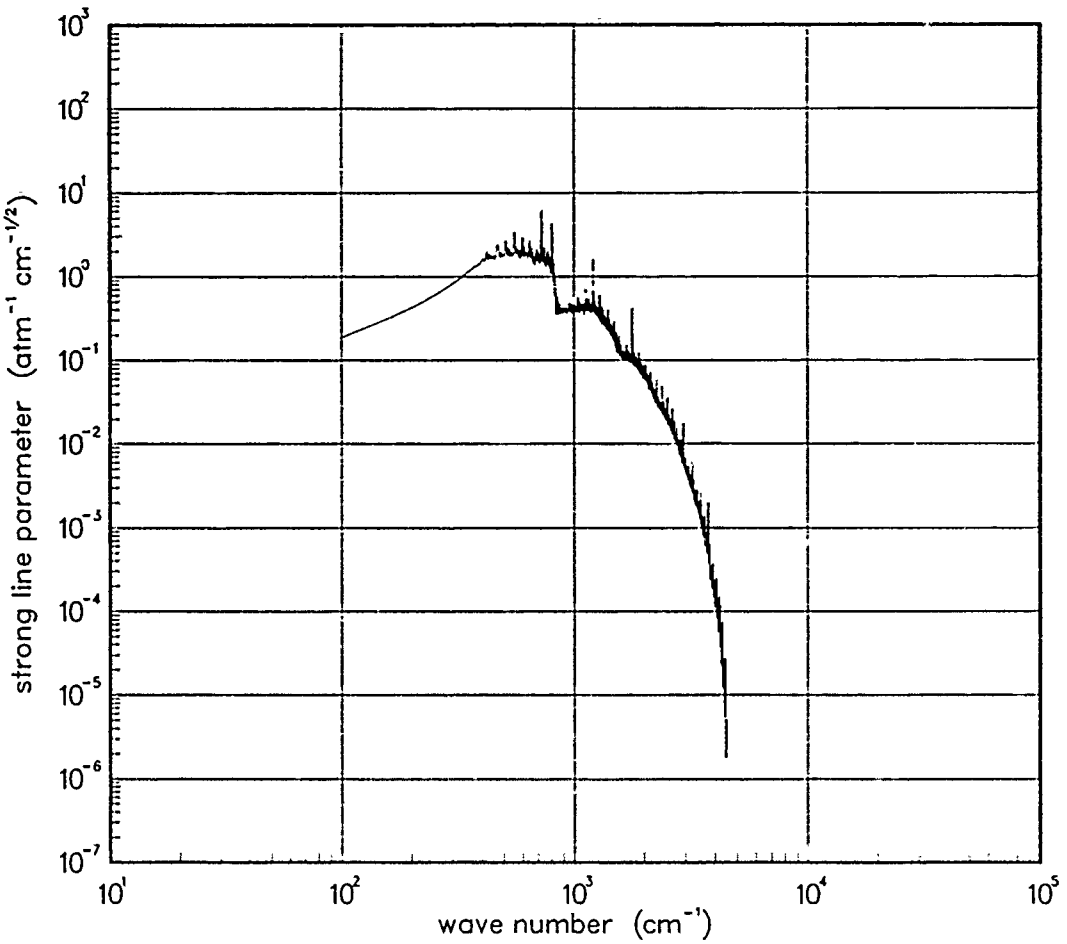

Figure 423. Strong-line parameter for MgO at 10000°K.

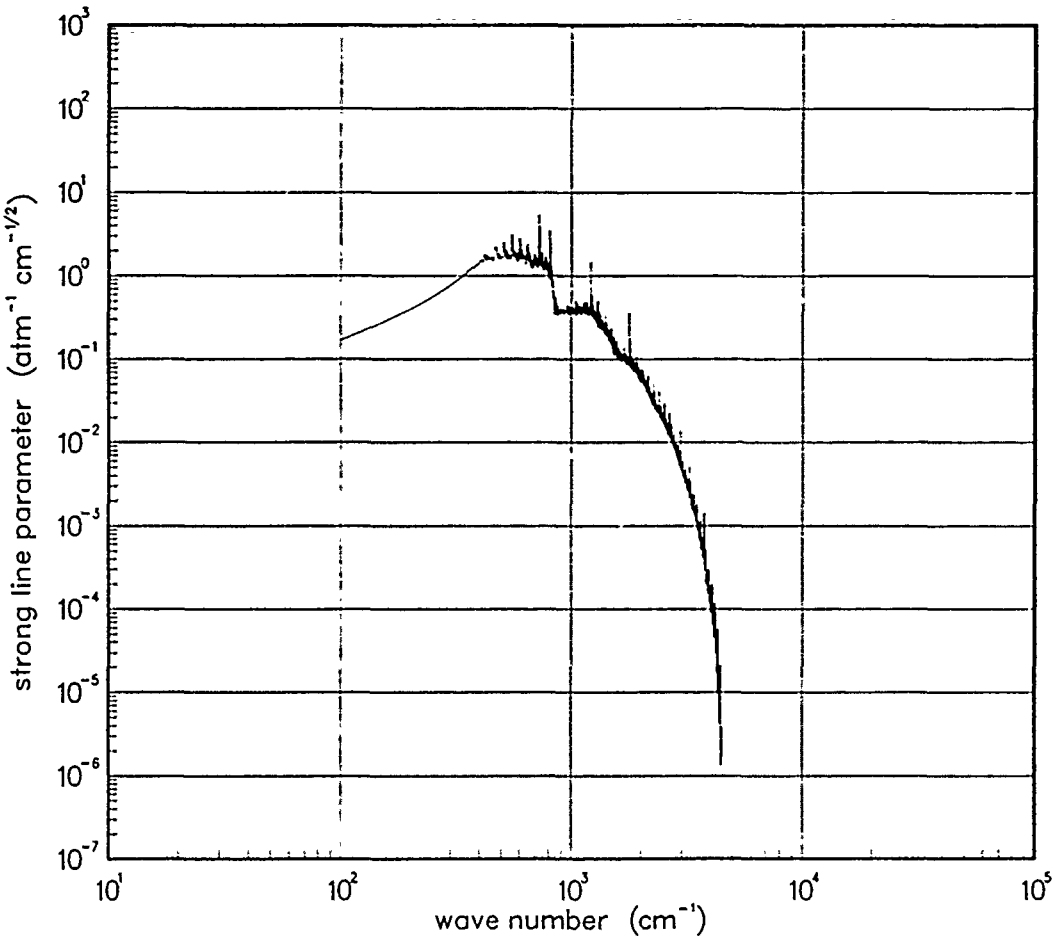

Figure 424. Strong-line parameter for MgO at 12000°K.

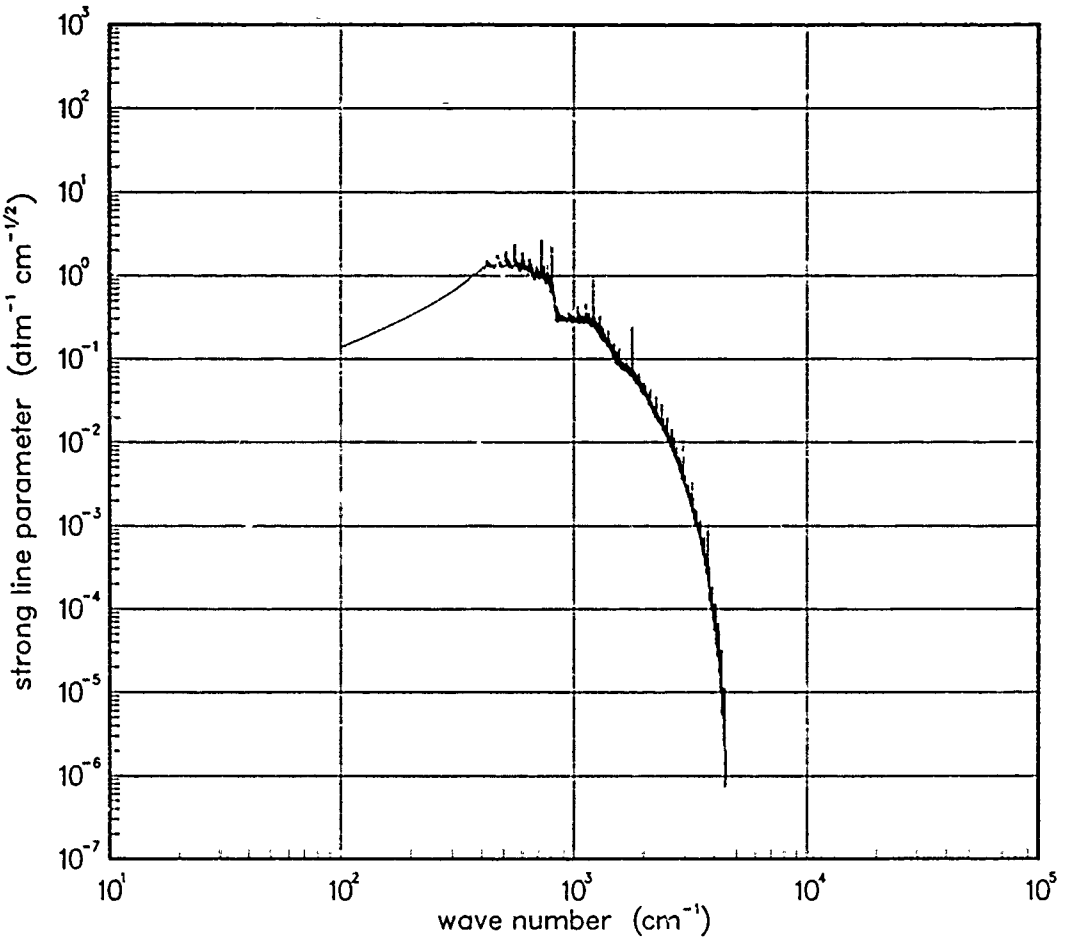

Figure 425. Strong-line parameter for MgO at 18000°K.

6.6 SILICON OXIDE (SiO).

Table 12. Spectroscopic data for SiO.

$X\ ^1\Sigma^+$

$\omega_e = 1241.44^*$ $\omega_e x_e = 5.92^*$
$\alpha_e = .00504^*$ $B_e = 0.72675^*$

$S_{10} = 90.6^\dagger$ $S_{20} = .428^\dagger$ $S_{30} = 0.020^\dagger$

$\gamma_\ell(300°K) = 0.04$

Data Source:

*B. Rosen, ed.,Spectroscopic Data Relative to Diatomic Molecules, Pergamon Press, New York (1970).

†H.H. Michels, Diatomic Oxide Vibrational Band Intensities , United Aircraft Research Laboratories, K921094-4 (May 1971).

‡Fit to the Oscillator Strength data in Note †.

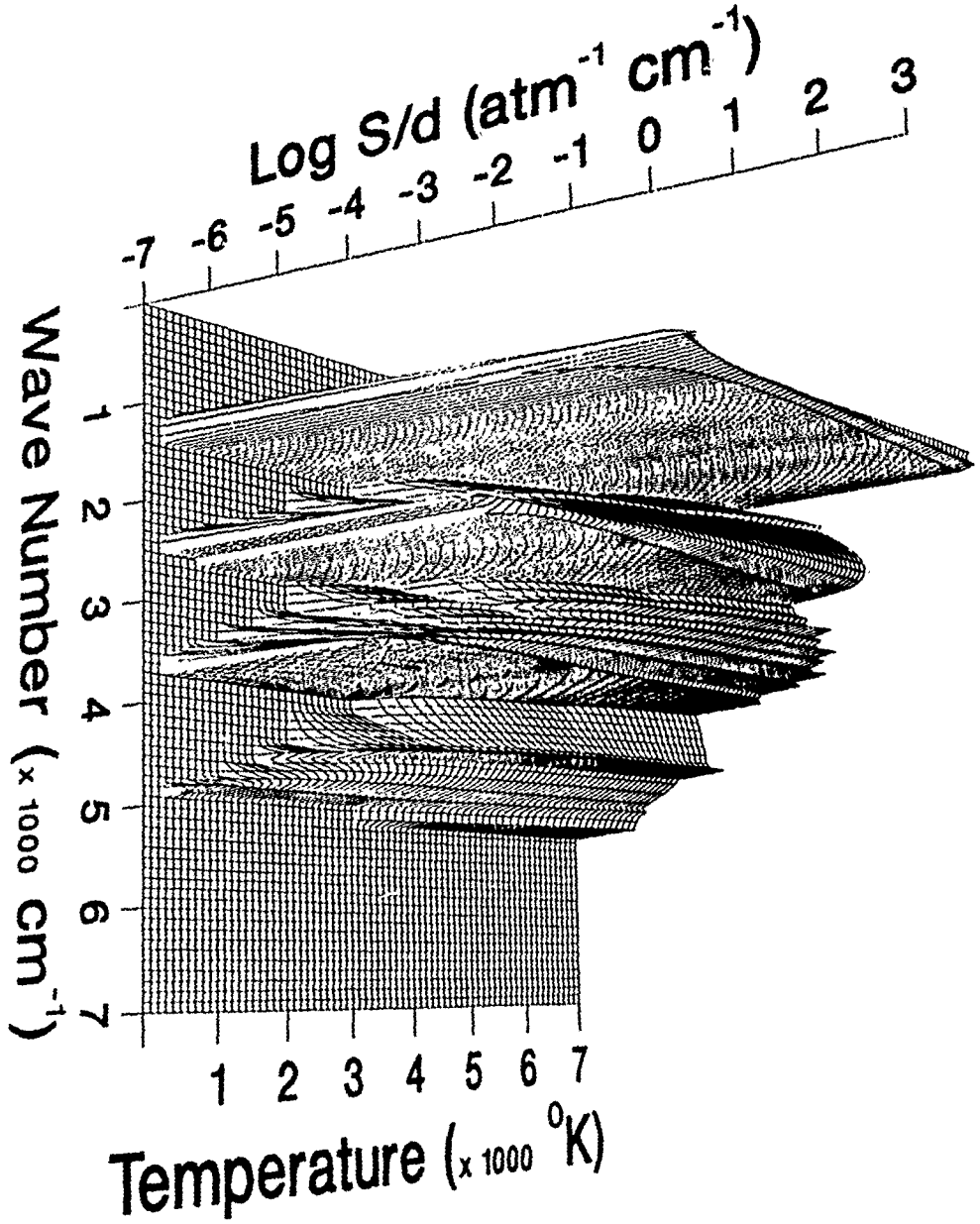

Figure 426. Weak-line parameter for SiO.

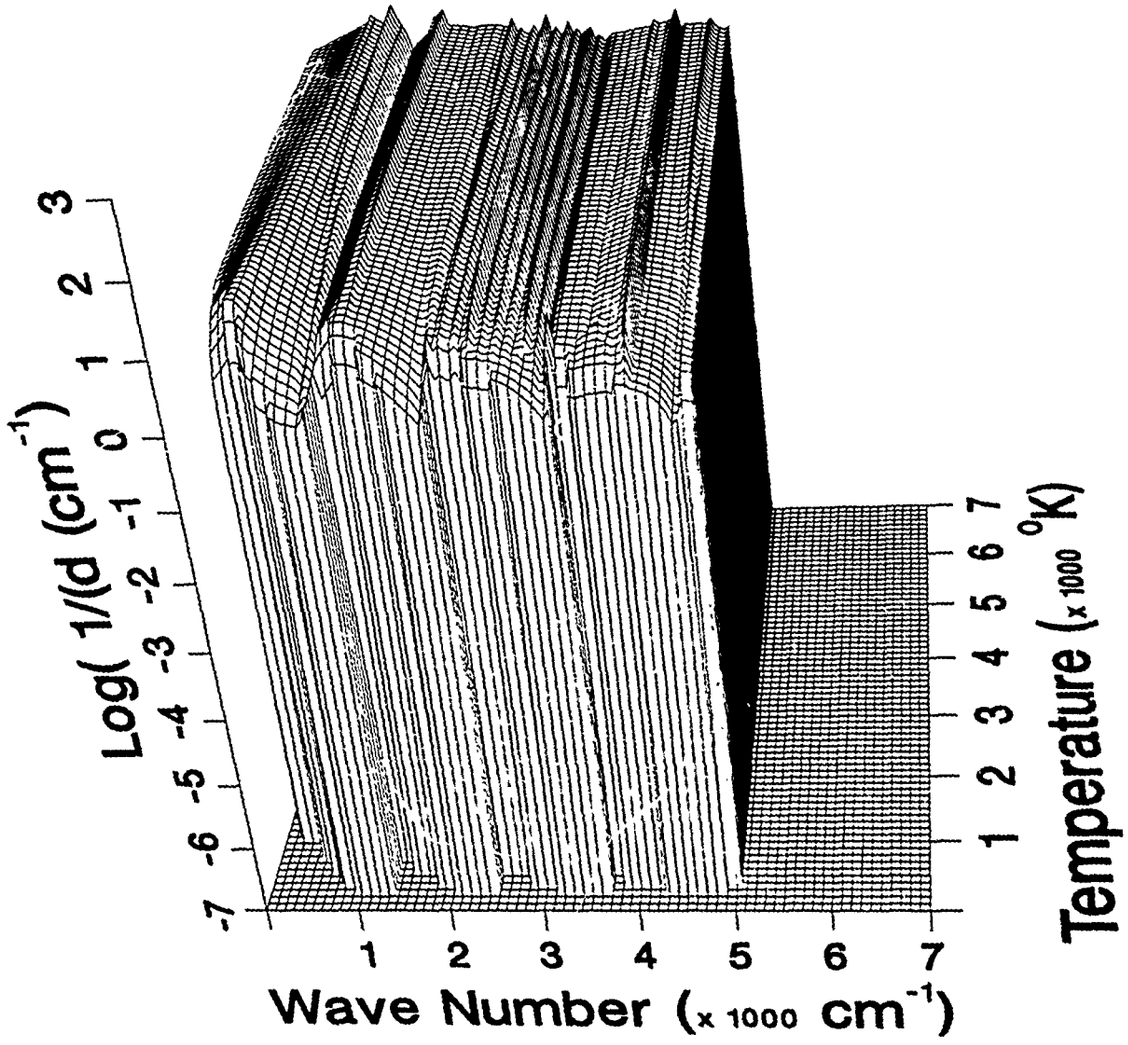

Figure 427. Inverse line spacing for SiO.

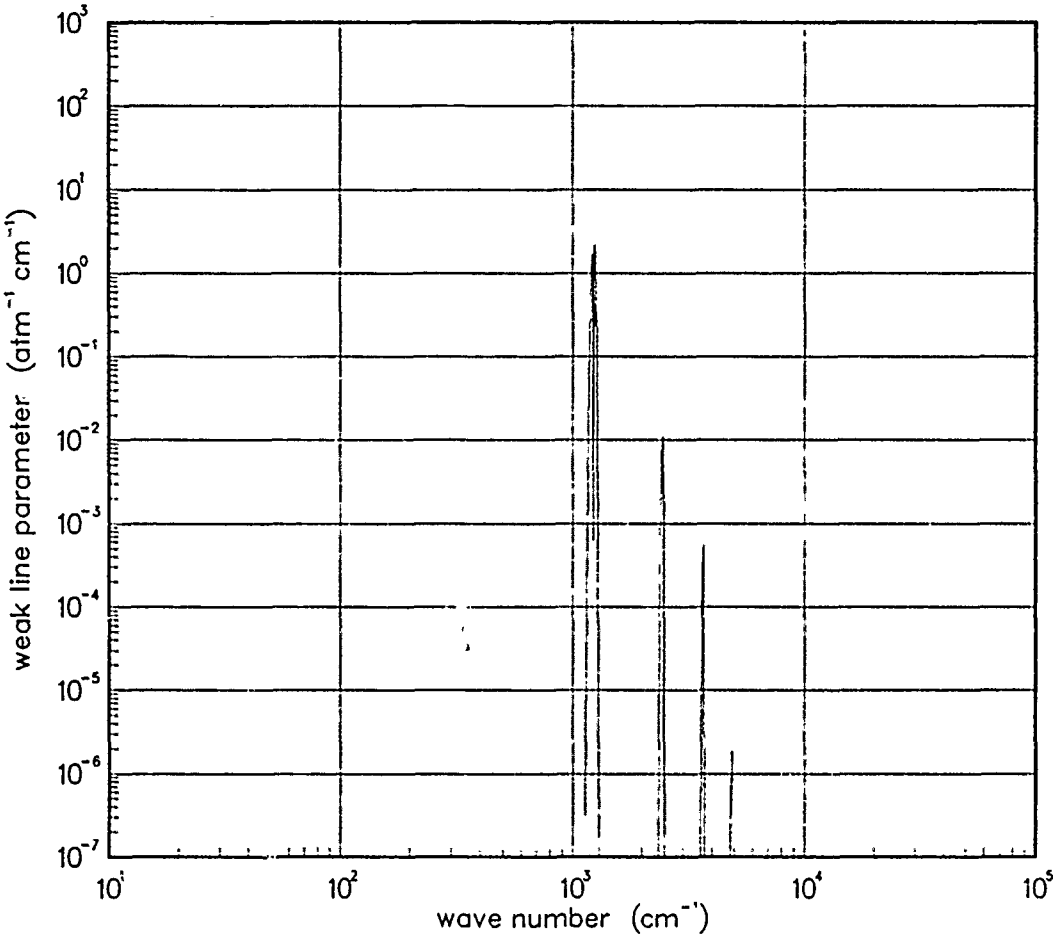

Figure 428. Weak-line parameter for SiO at 200°K.

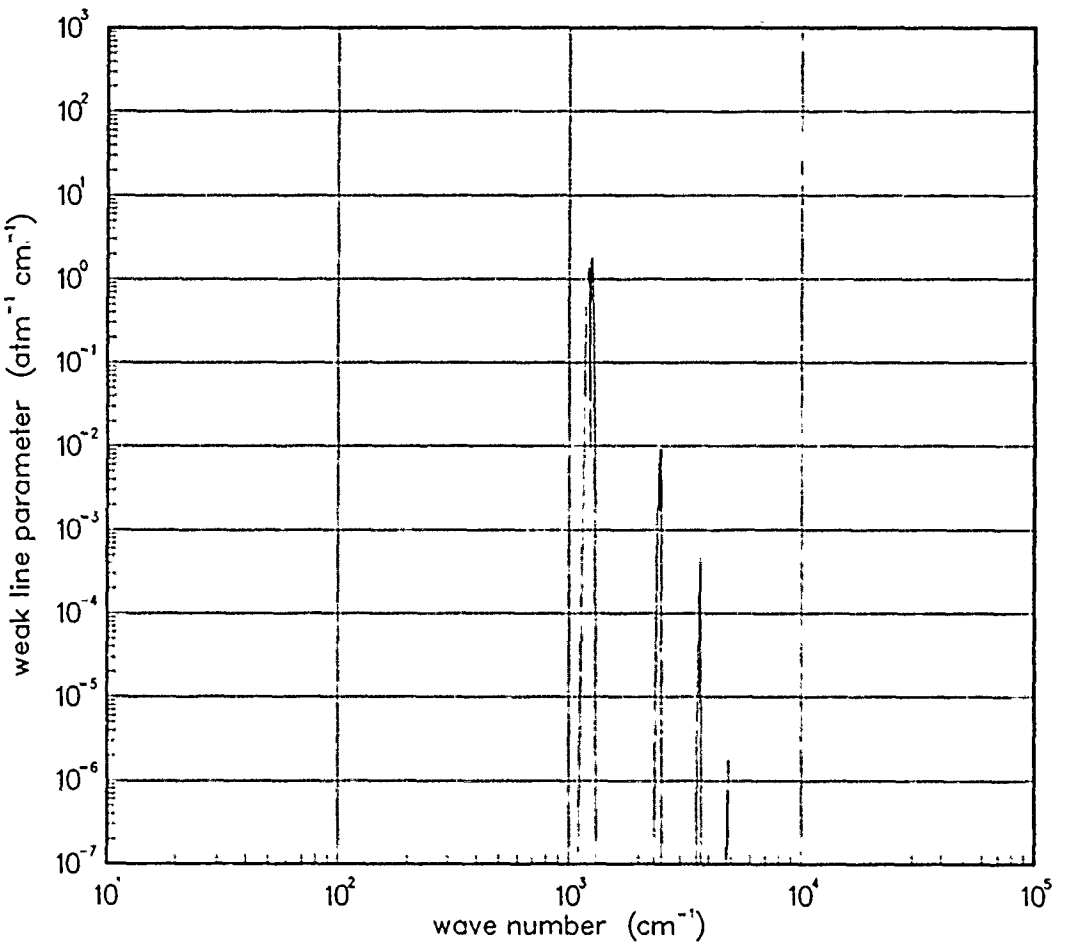

Figure 429. Weak-line parameter for SiO at 300°K.

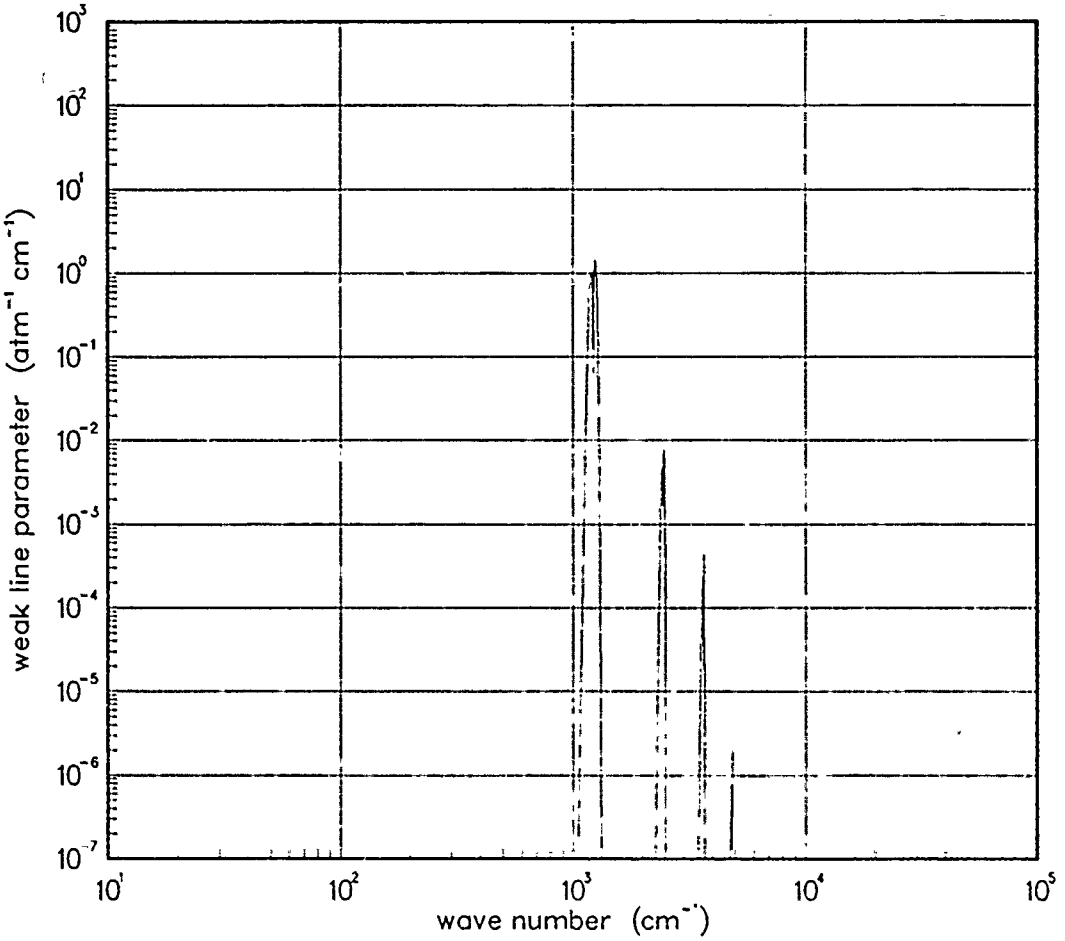

Figure 430. Weak-line parameter for SiO at 500°K.

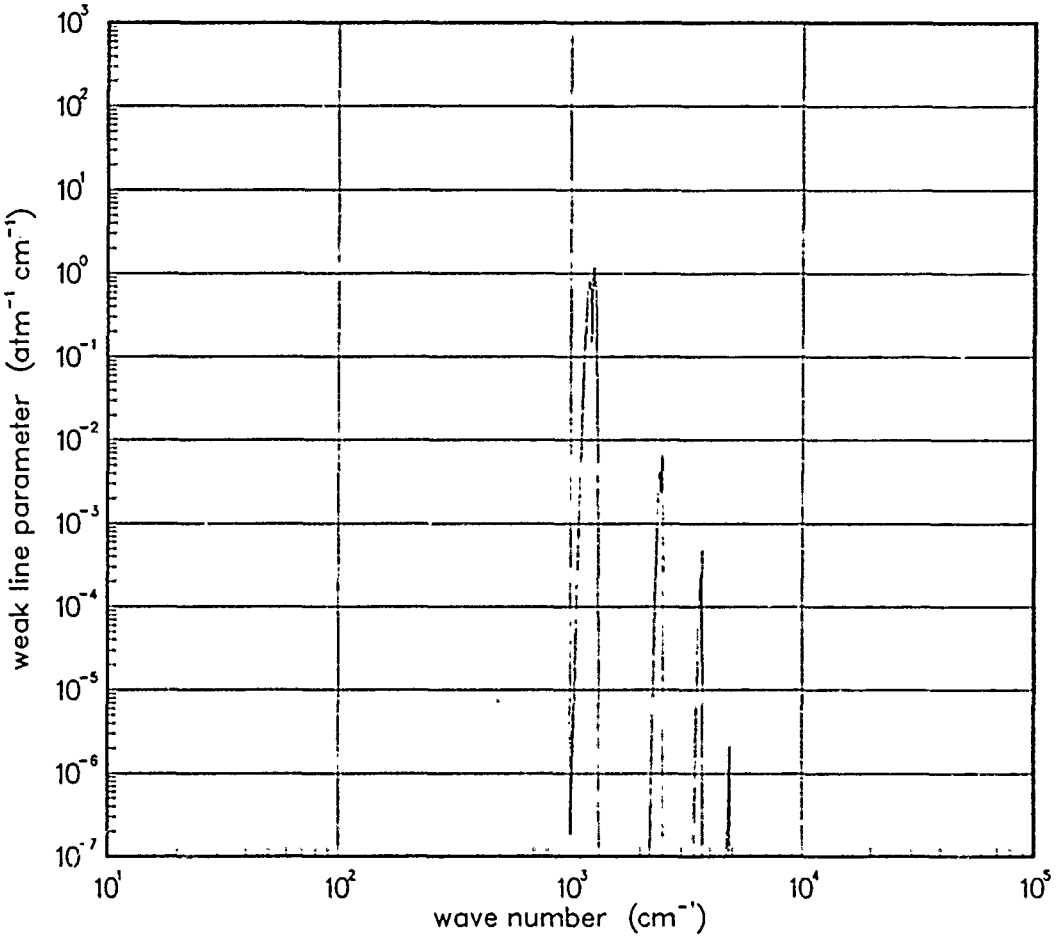

Figure 431. Weak-line parameter for SiO at 750°K.

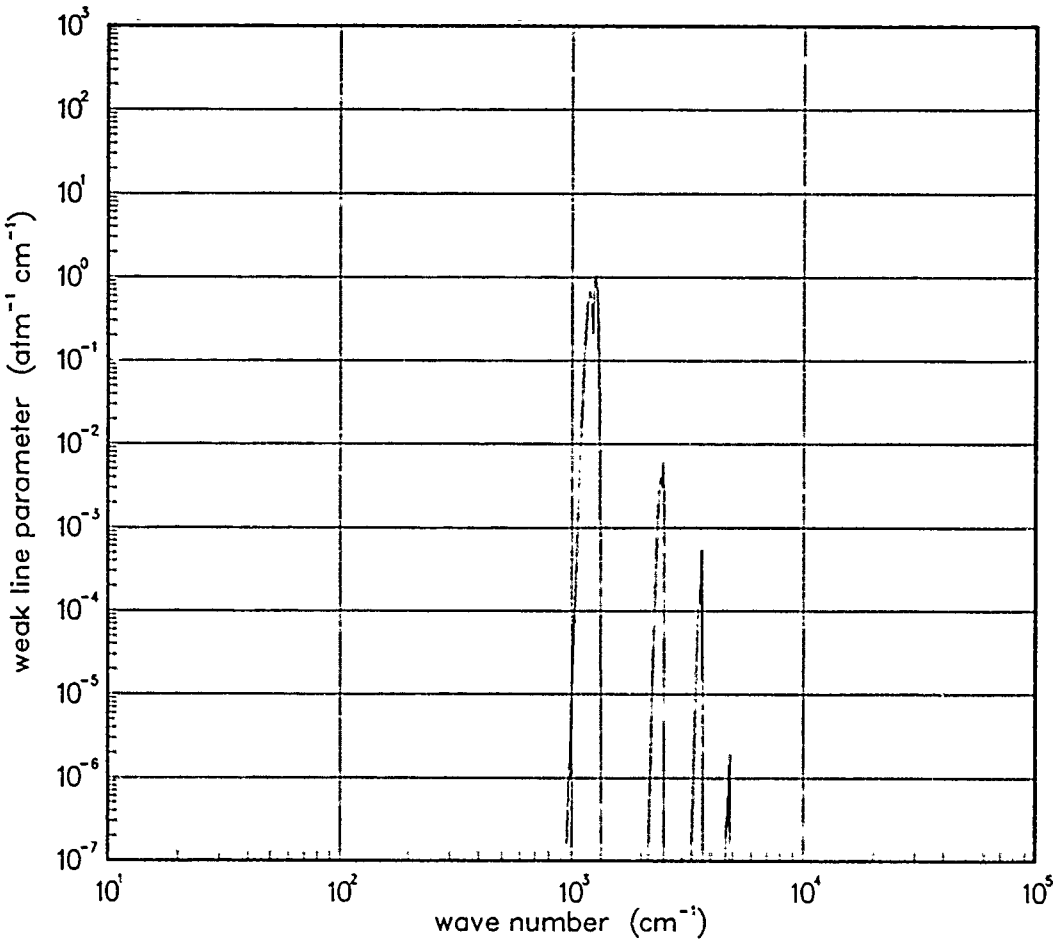

Figure 432. Weak-line parameter for SiO at 1000°K.

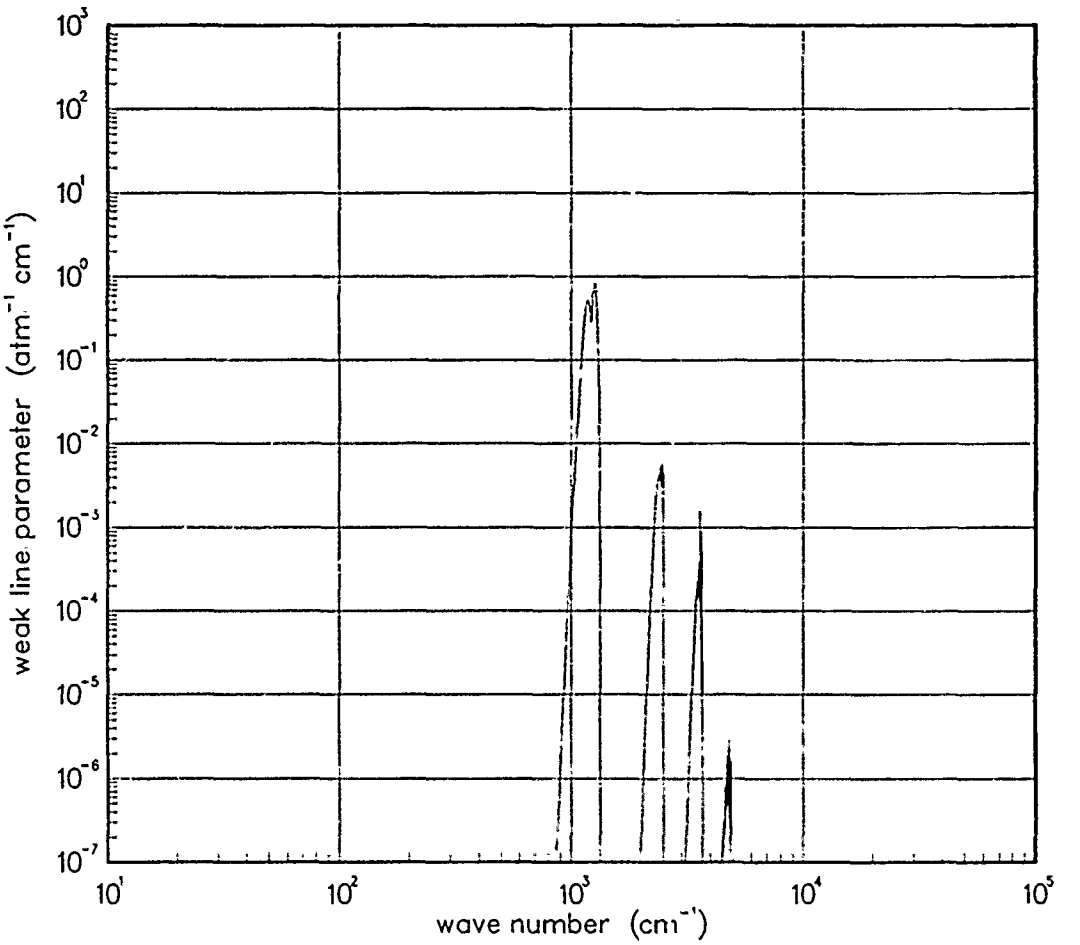

Figure 433. Weak-line parameter for SiO at 1500°K.

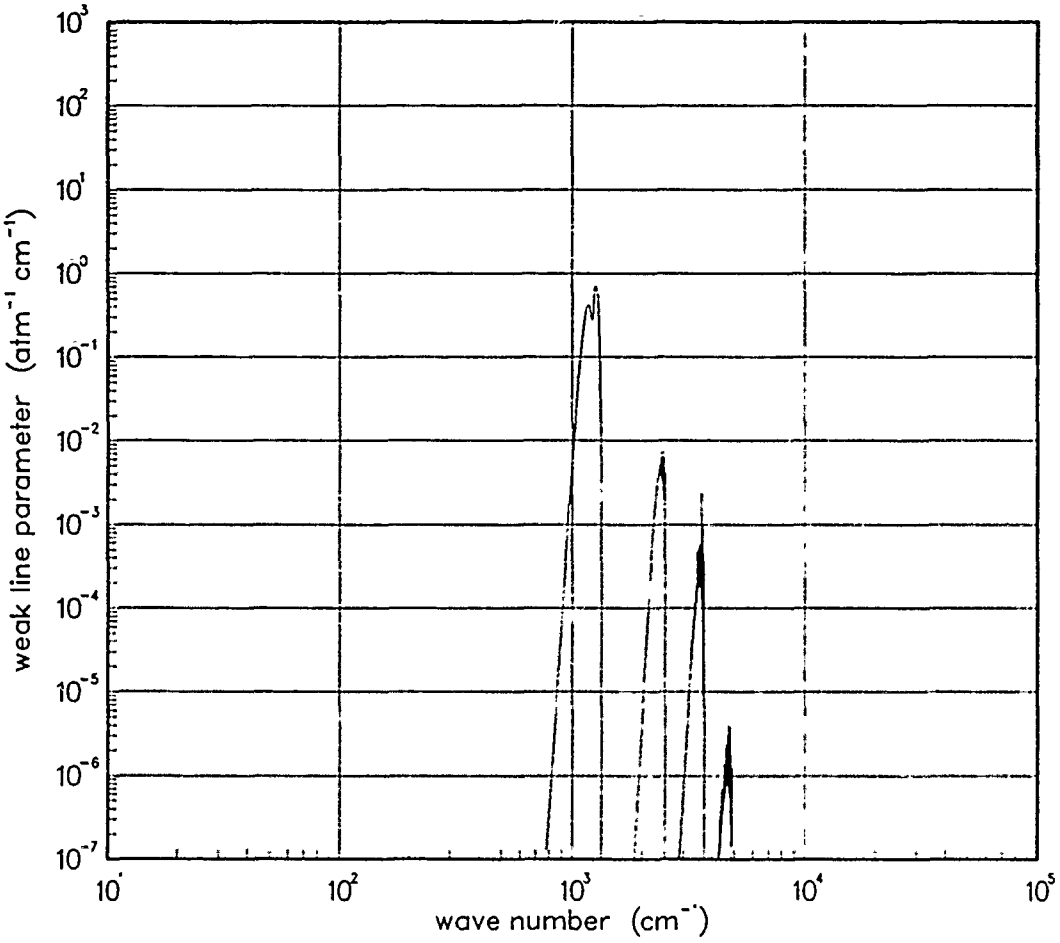

Figure 434. Weak-line parameter for SiO at 2000°K.

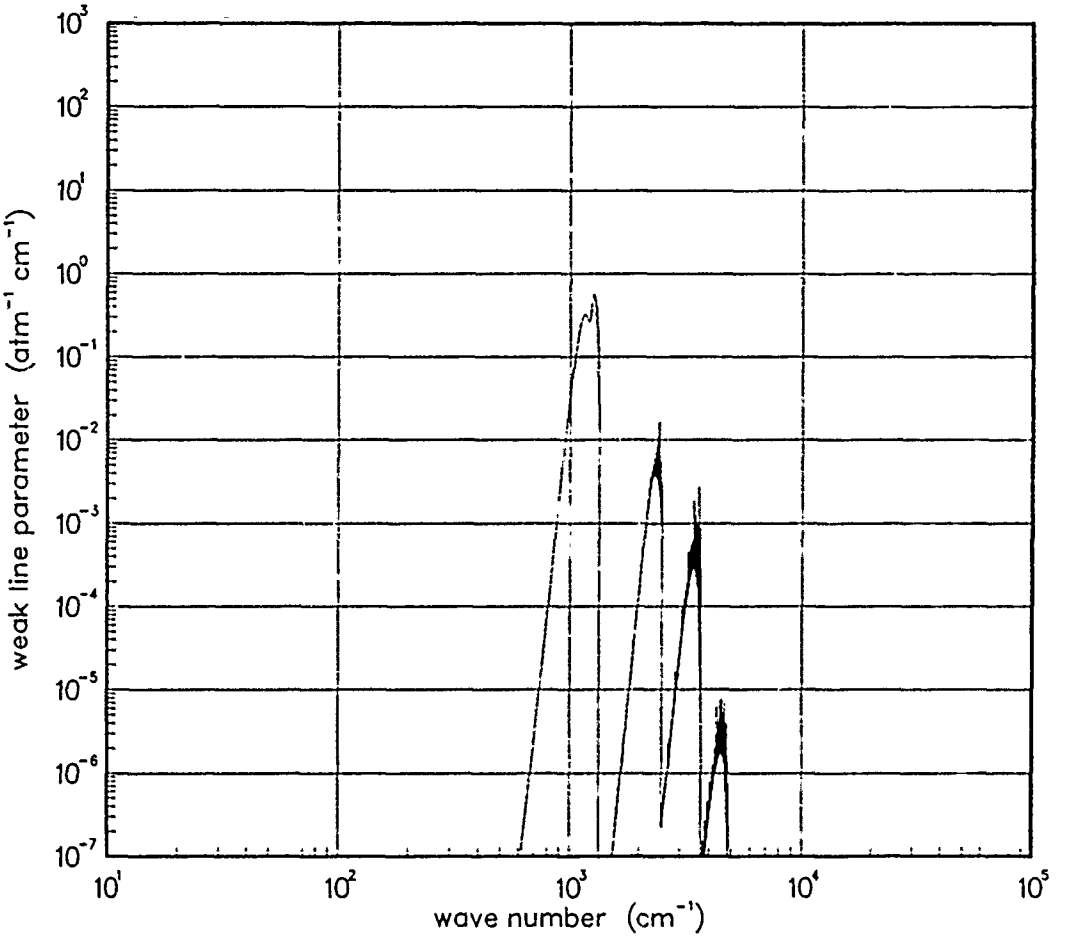

Figure 435. Weak-line parameter for SiO at 3000°K.

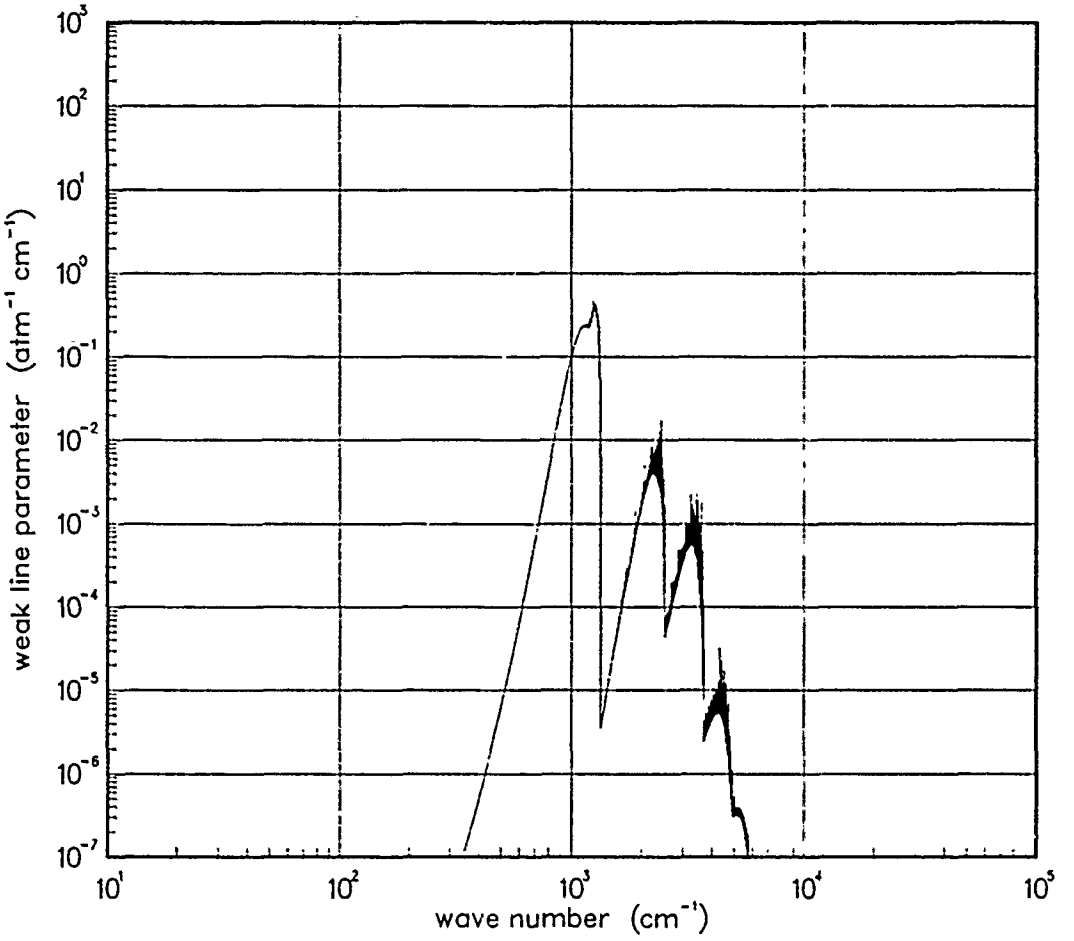

Figure 436. Weak-line parameter for SiO at 5000°K.

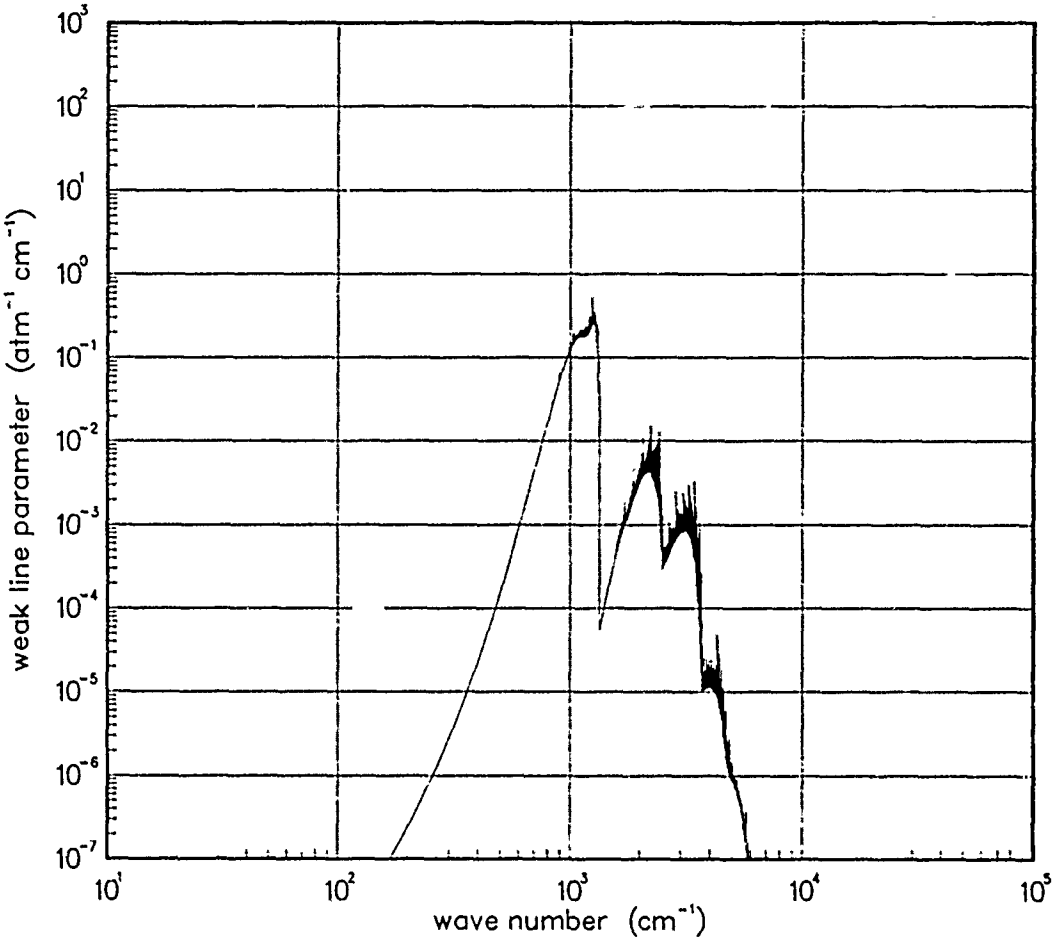

Figure 437. Weak-line parameter for SiO at 7000°K.

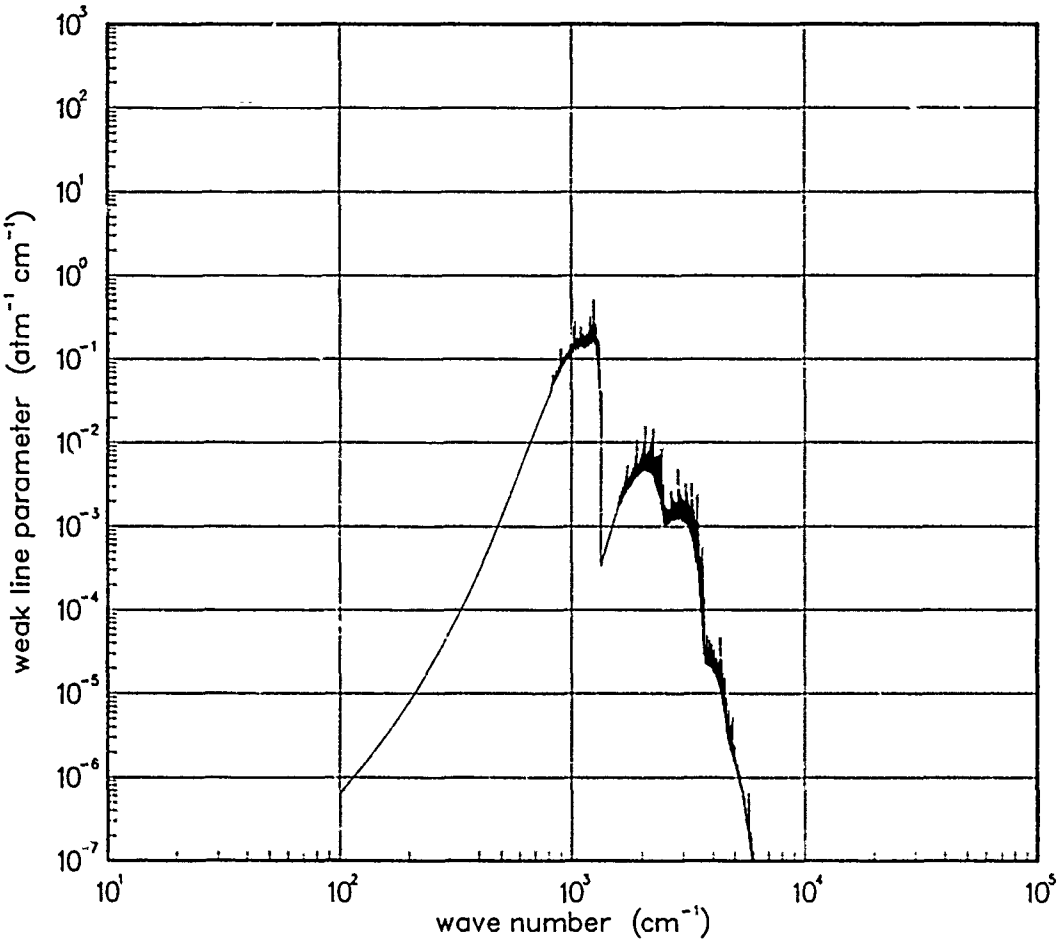

Figure 438. Weak-line parameter for SiO at 10000°K.

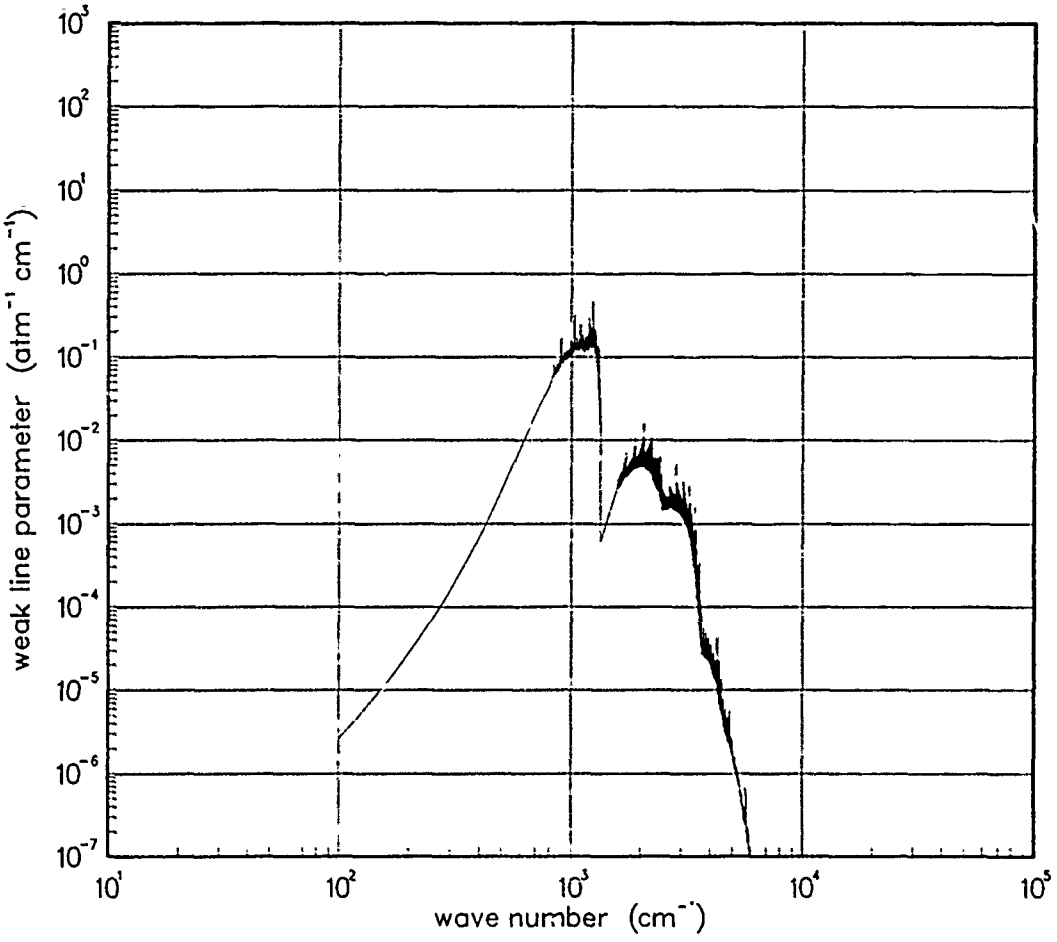

Figure 439. Weak-line parameter for SiO at 12000°K.

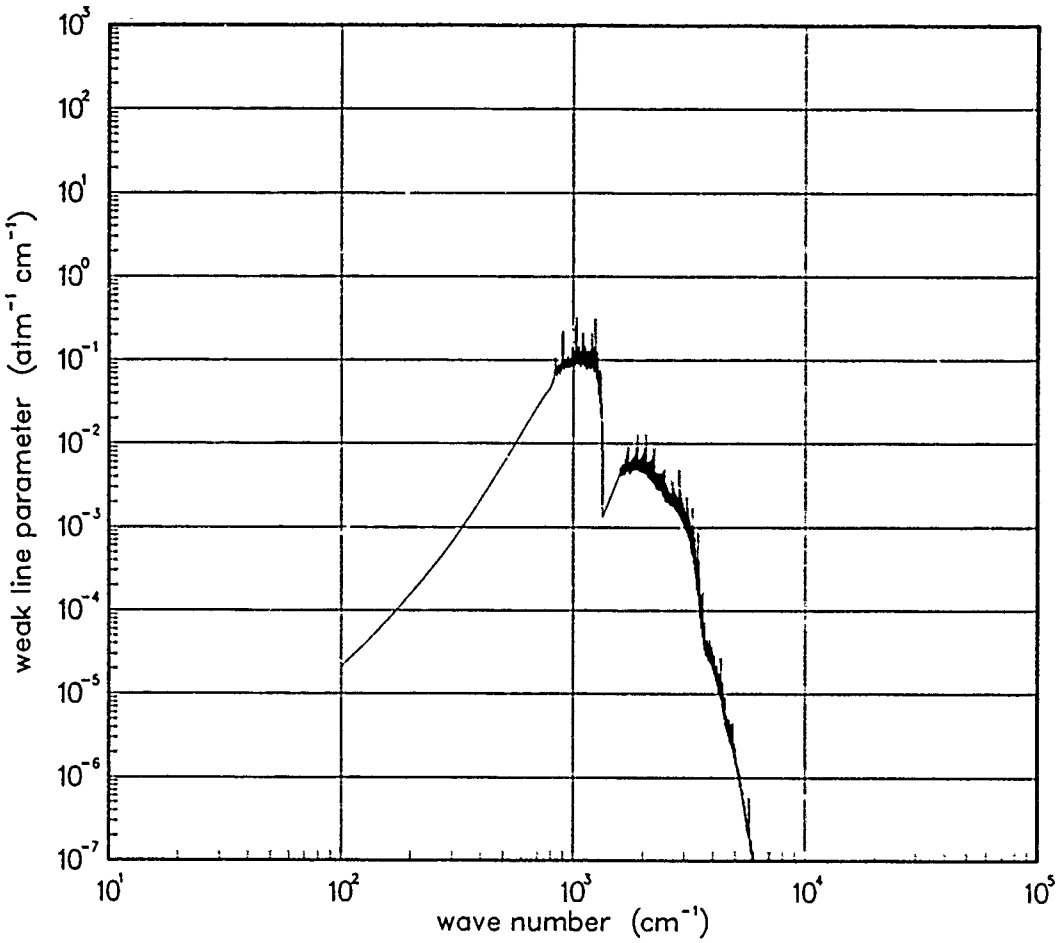

Figure 440. Weak-line parameter for SiO at 18000°K.

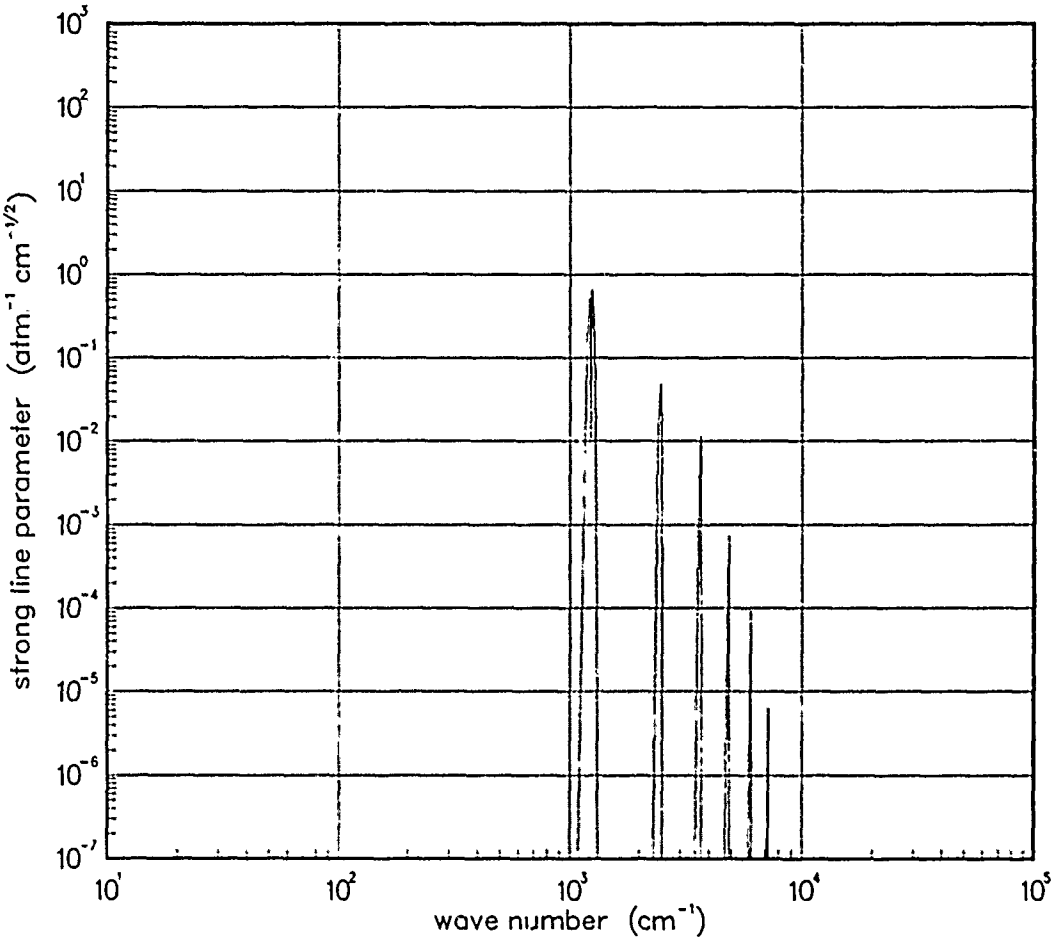

Figure 441. Strong-line parameter for SiO at 200°K.

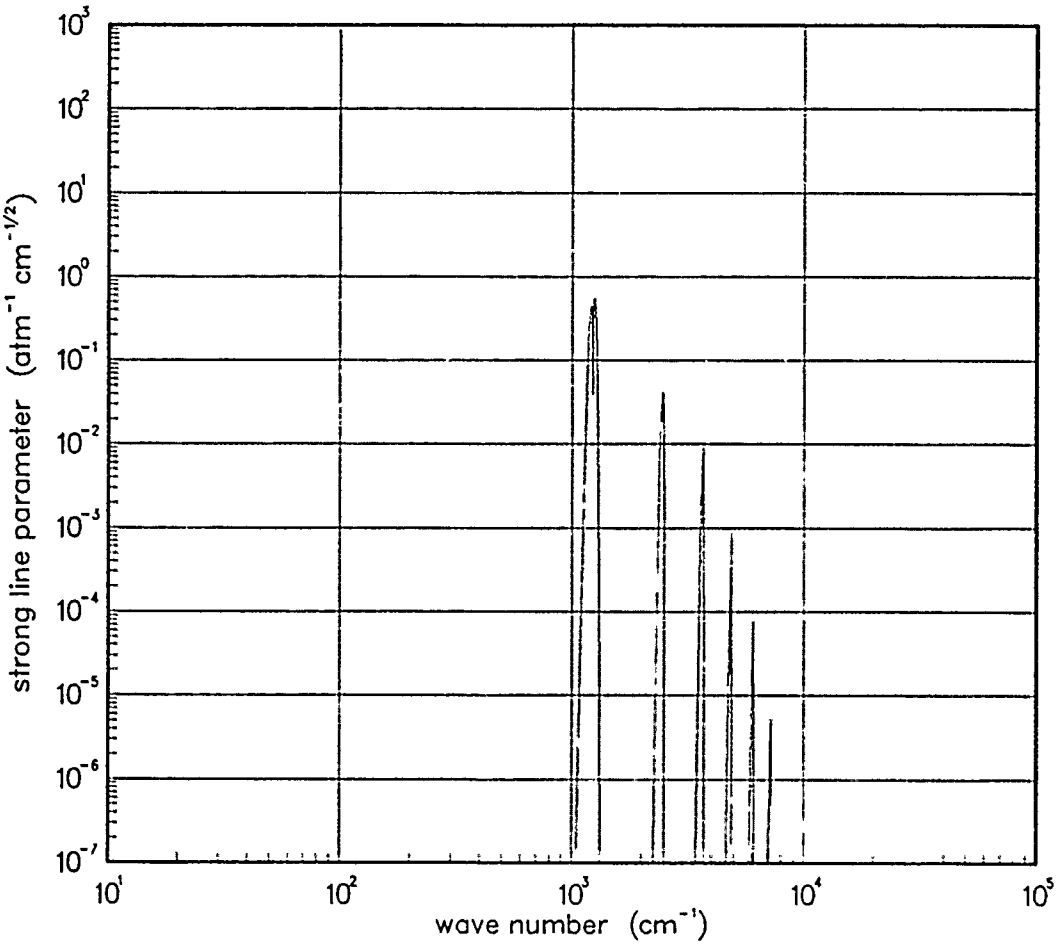

Figure 442. Strong-line parameter for SiO at 300°K.

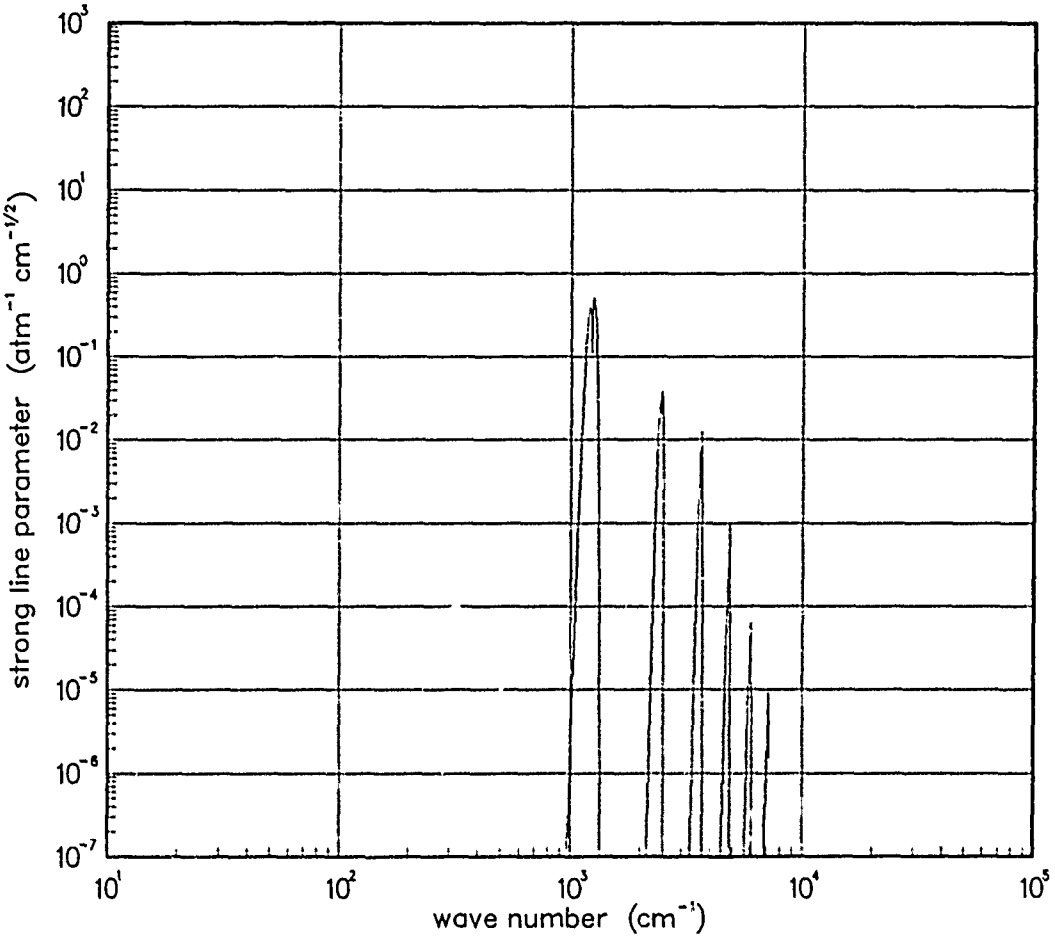

Figure 443. Strong-line parameter for SiO at 500°K.

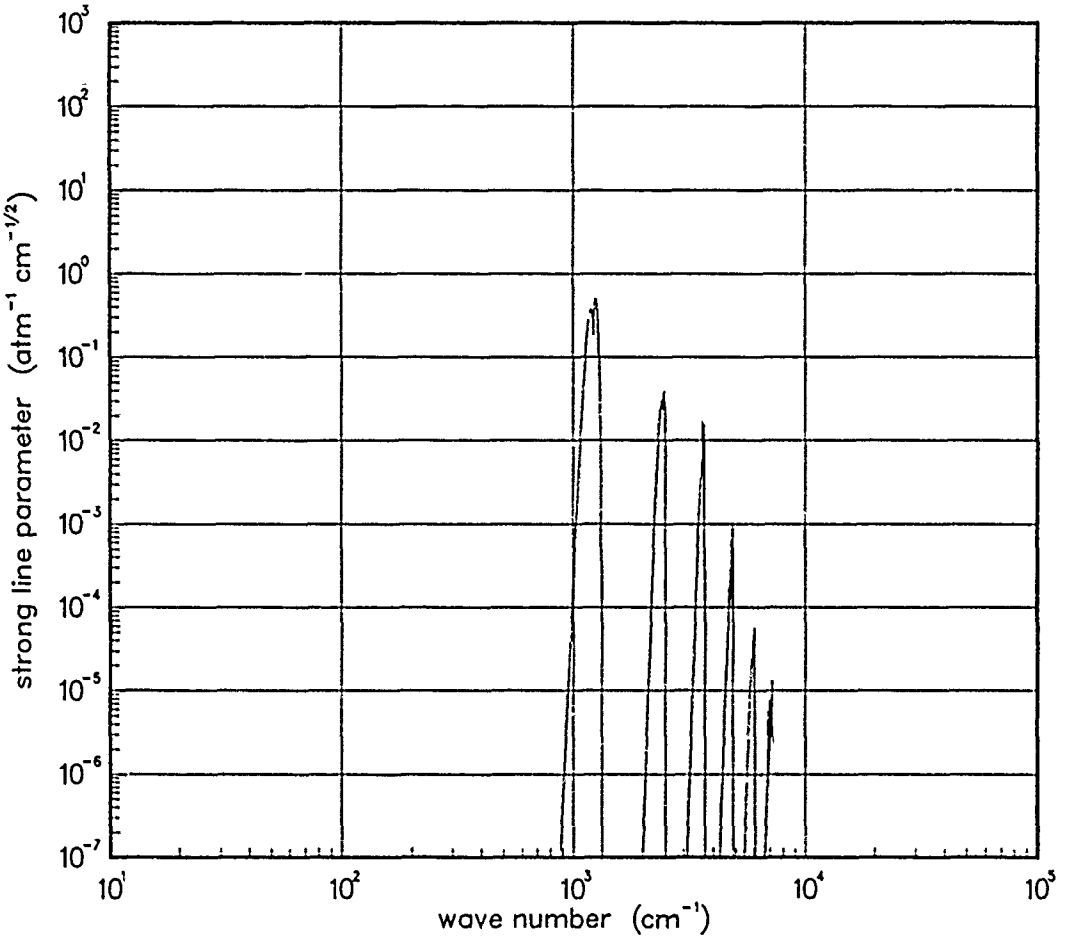

Figure 444. Strong-line parameter for SiO at 750°K.

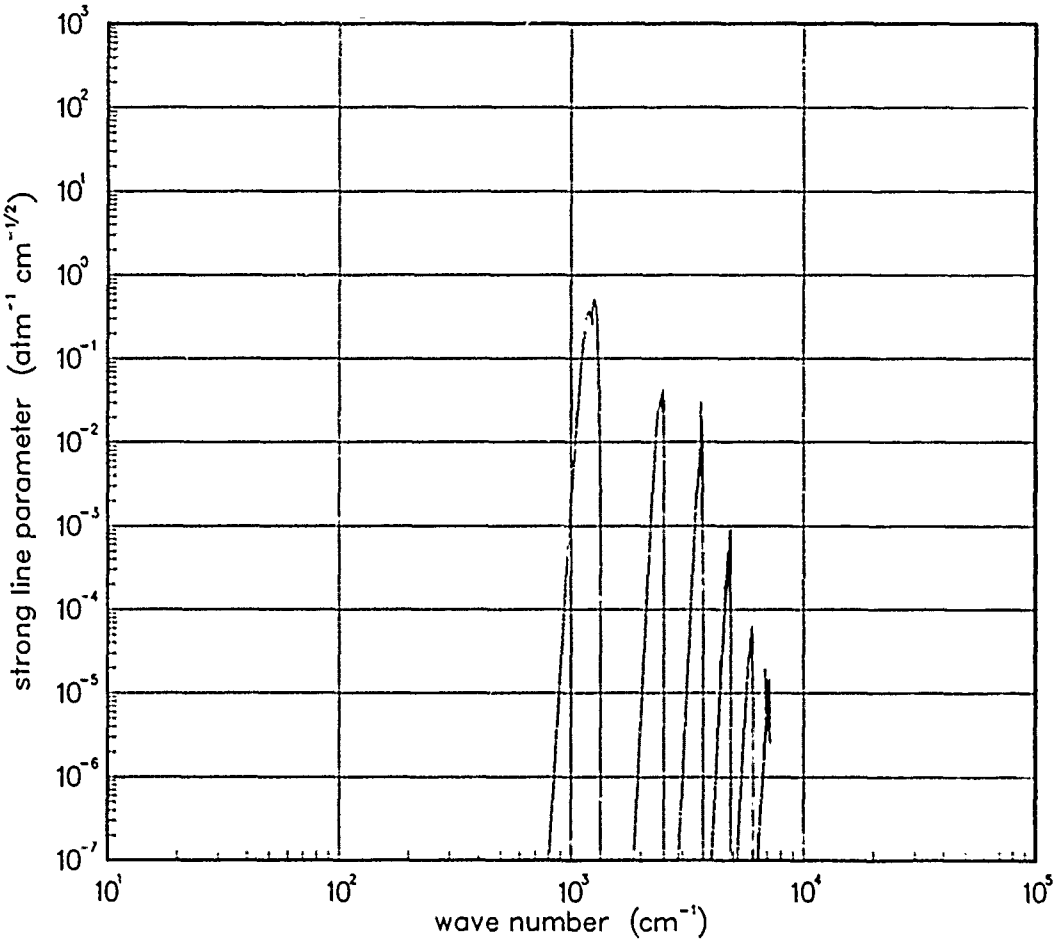

Figure 445. Strong-line parameter for SiO at 1000°K.

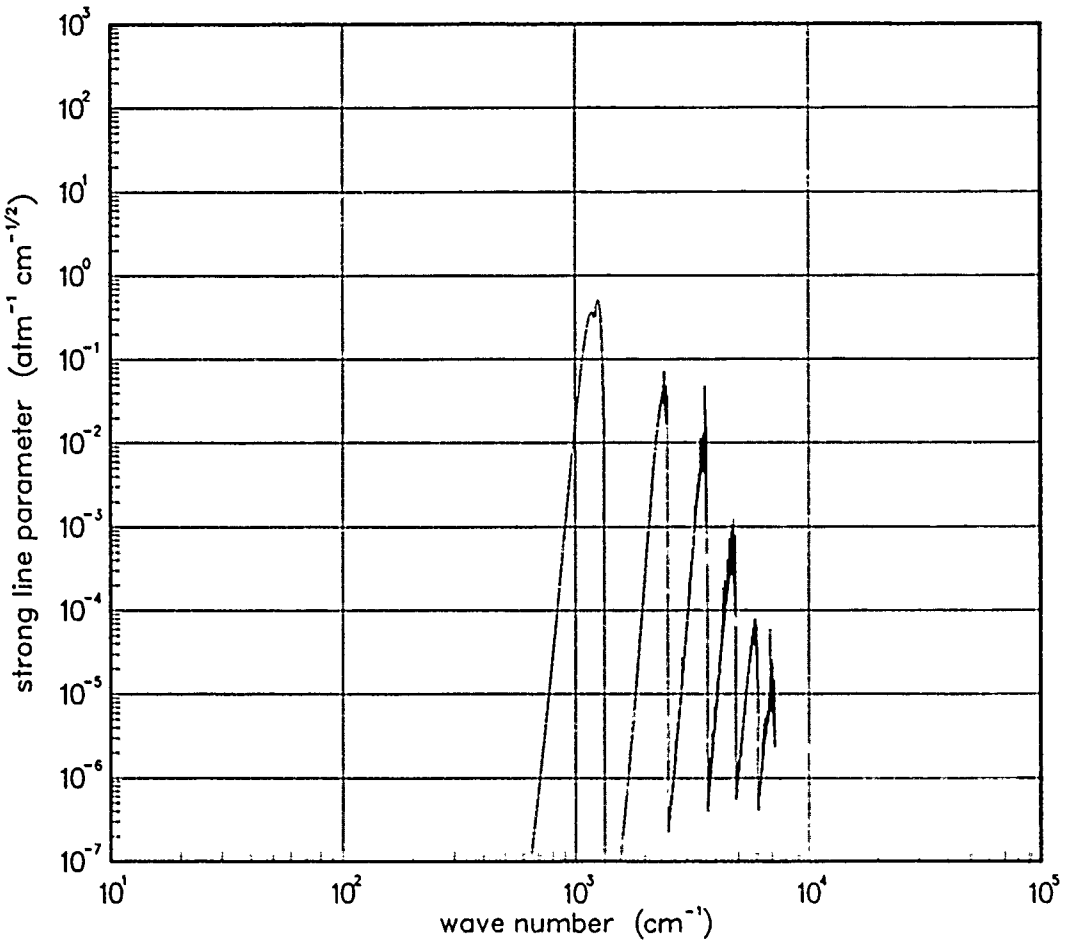

Figure 446. Strong-line parameter for SiO at 1500°K.

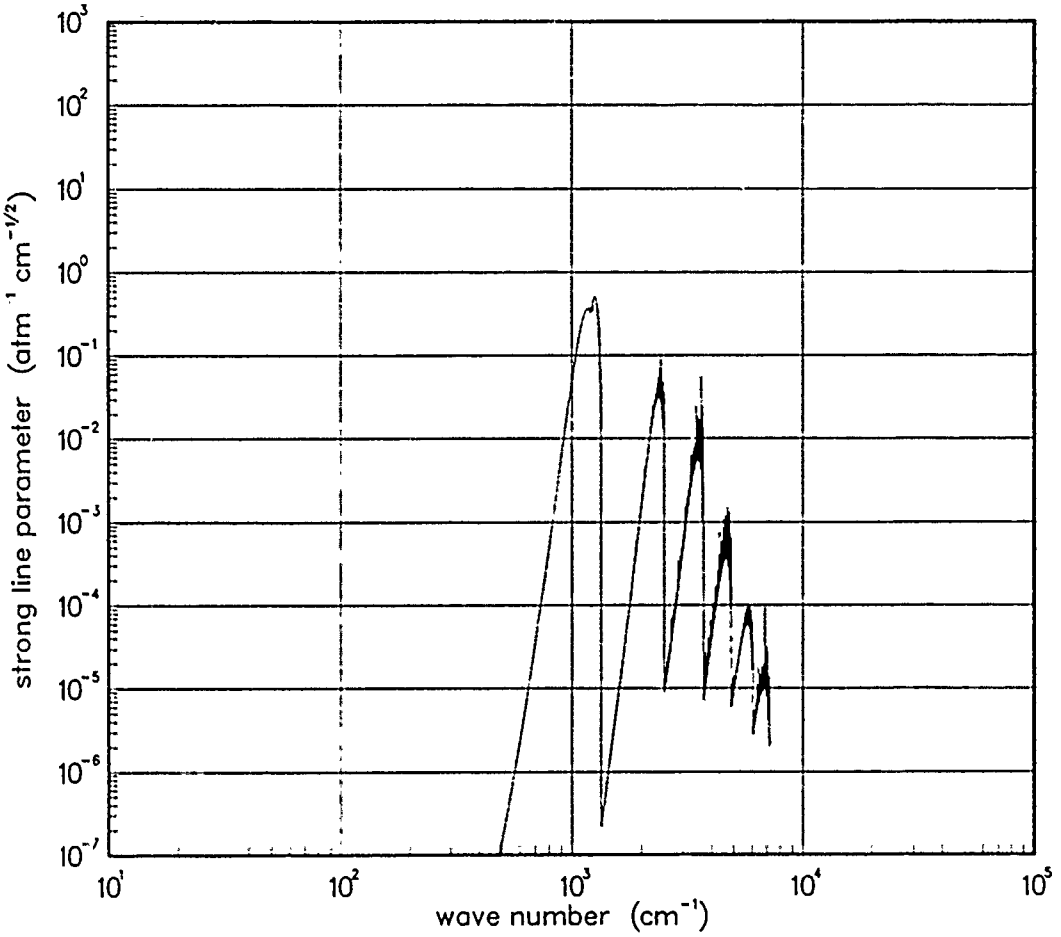

Figure 447. Strong-line parameter for SiO at 2000°K.

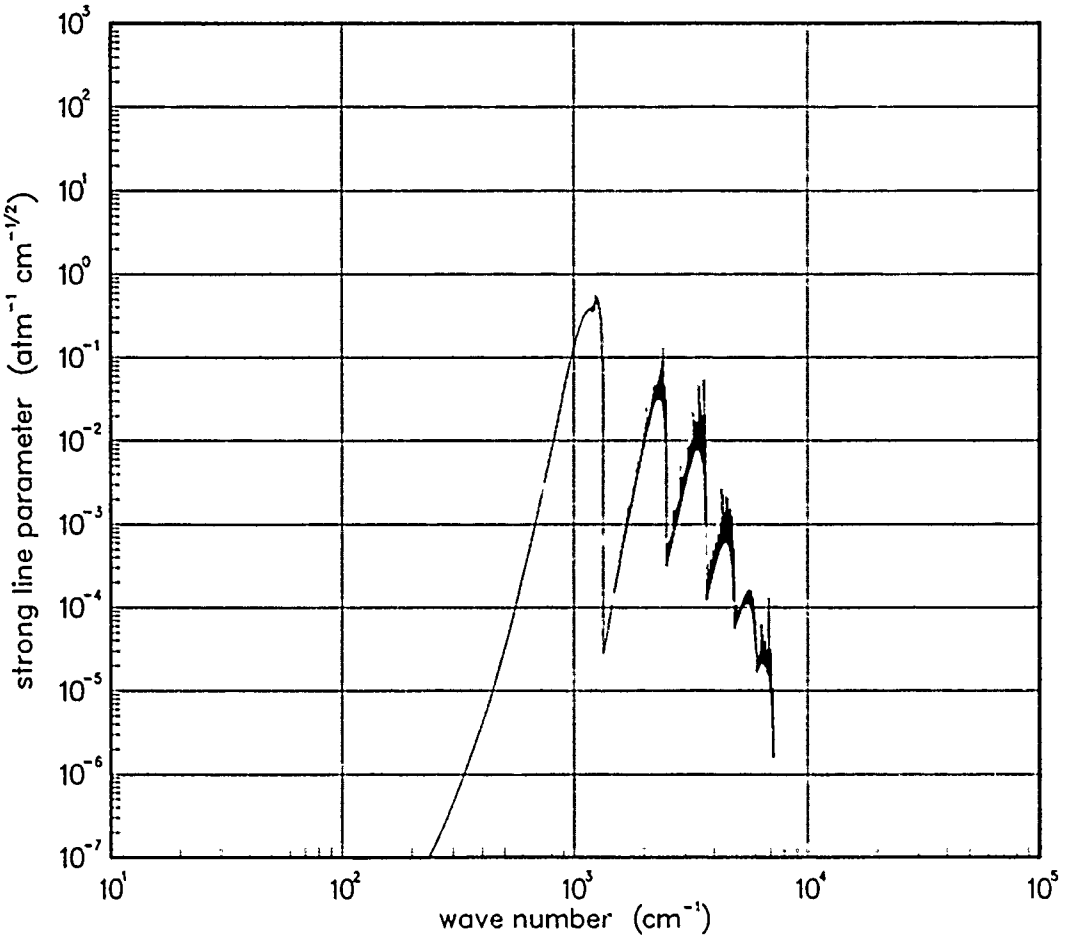

Figure 448. Strong-line parameter for SiO at 3000°K.

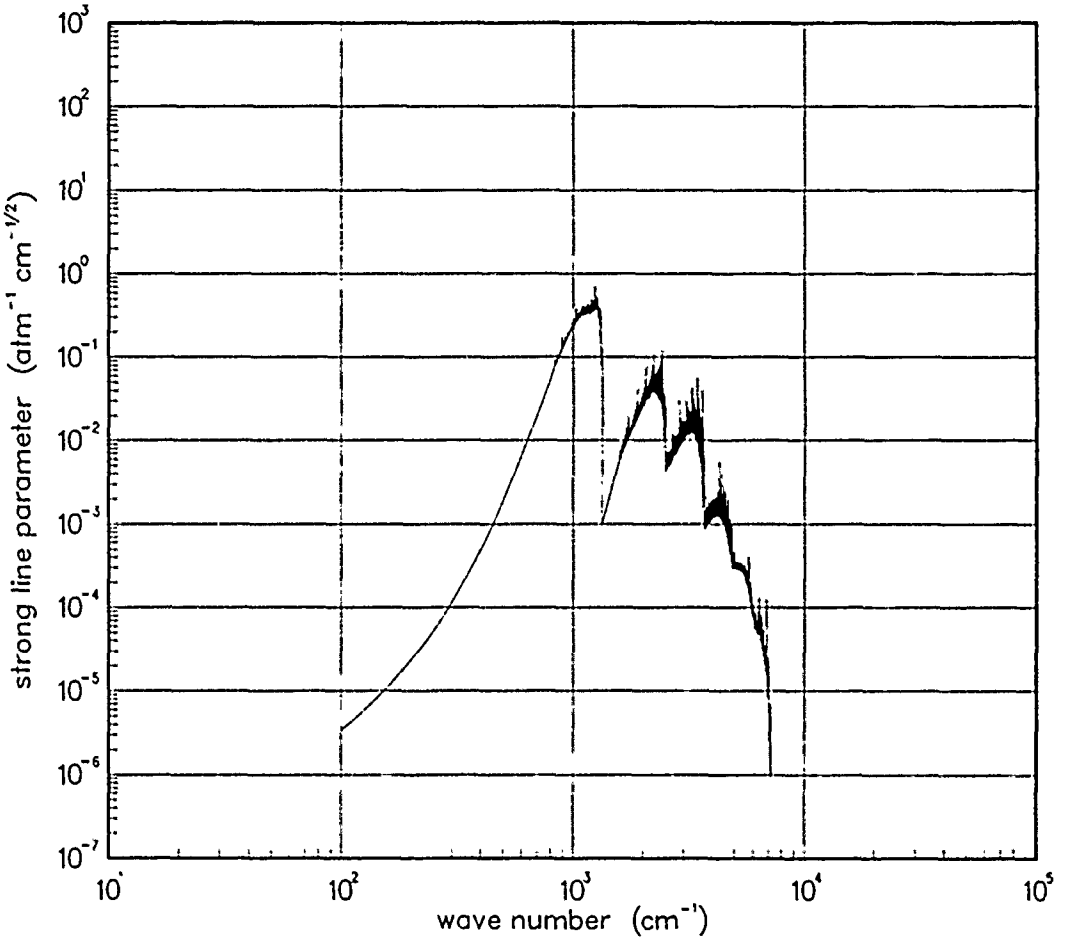

Figure 449. Strong-line parameter for SiO at 5000°K.

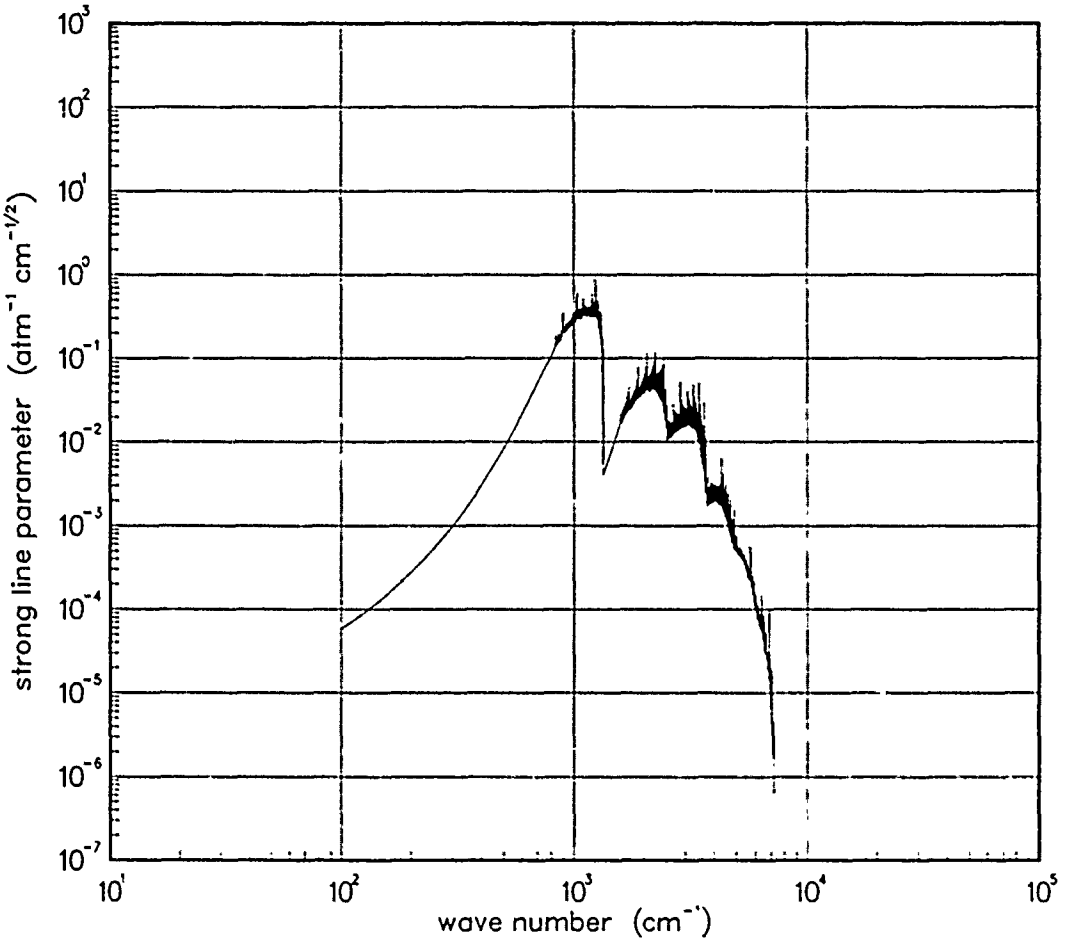

Figure 450. Strong-line parameter for SiO at 7000°K.

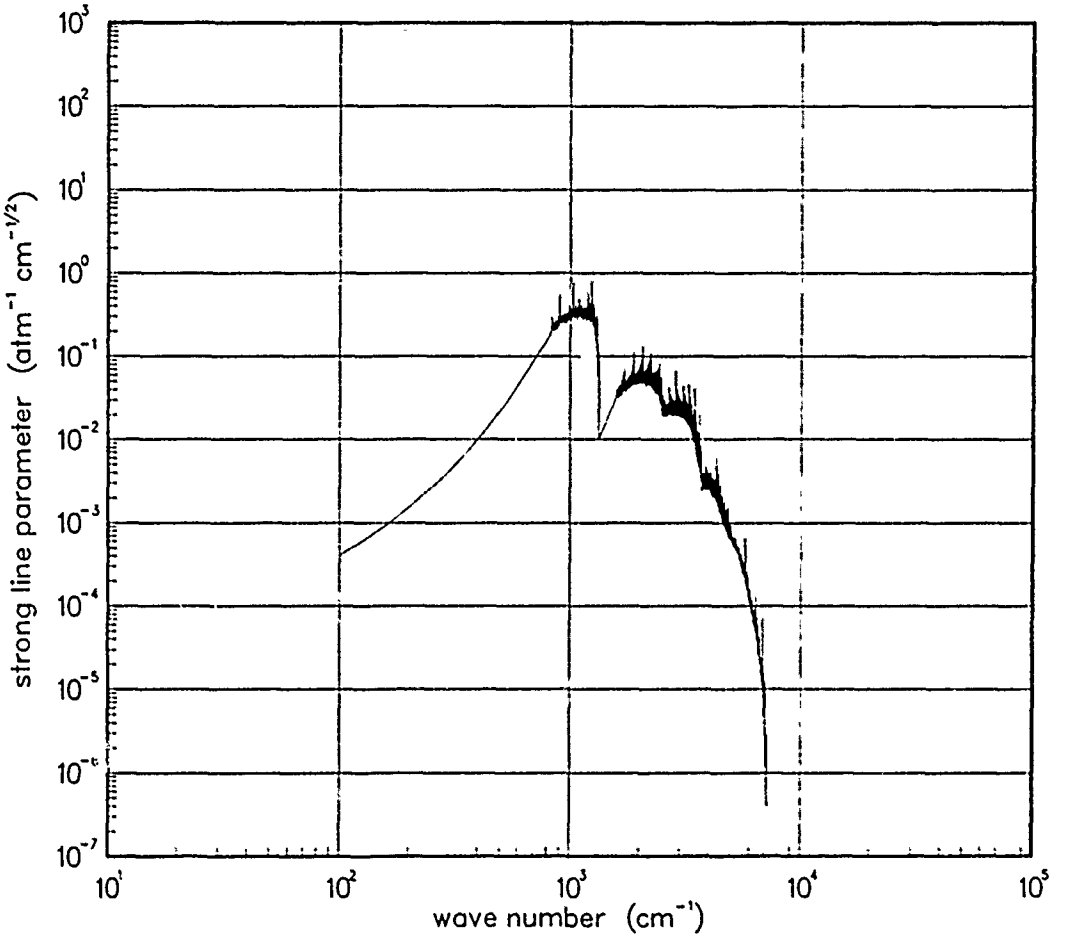

Figure 451. Strong-line parameter for SiO at 10000°K.

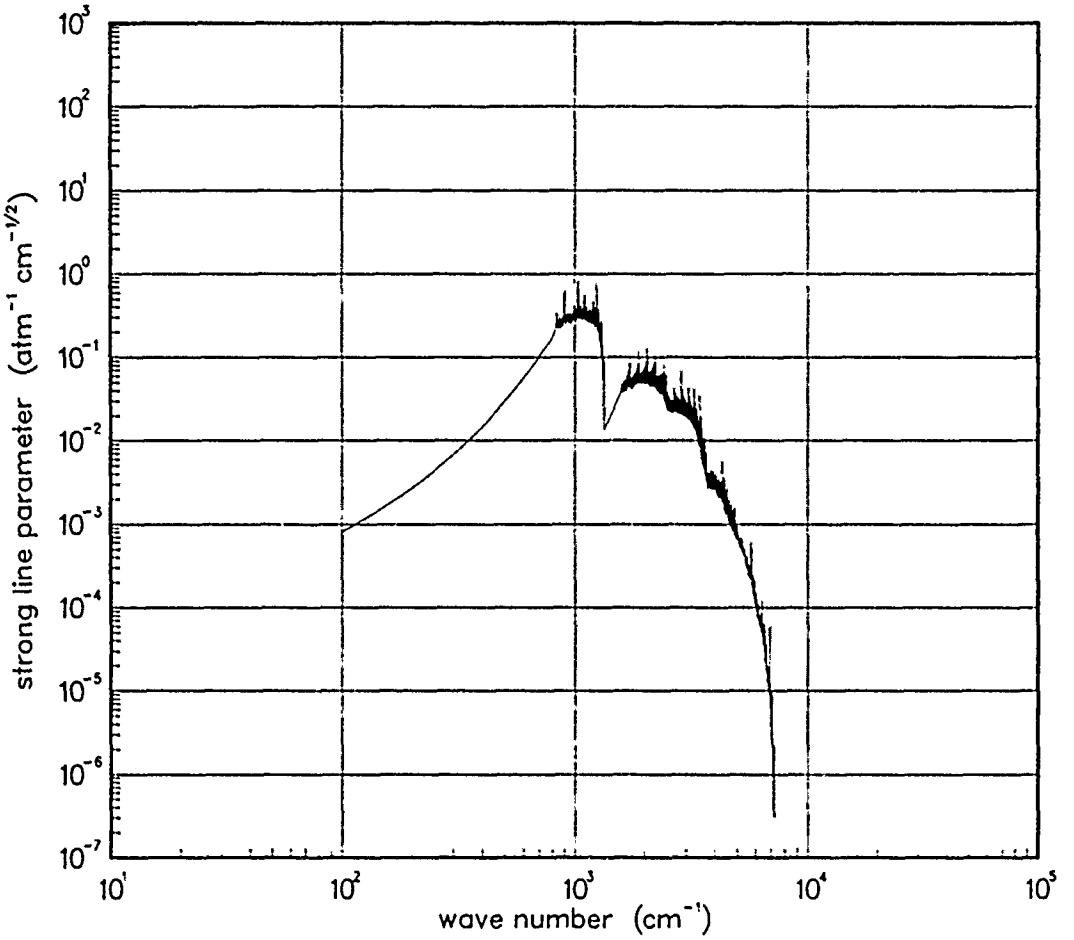

Figure 452. Strong-line parameter for SiO at 12000°K.

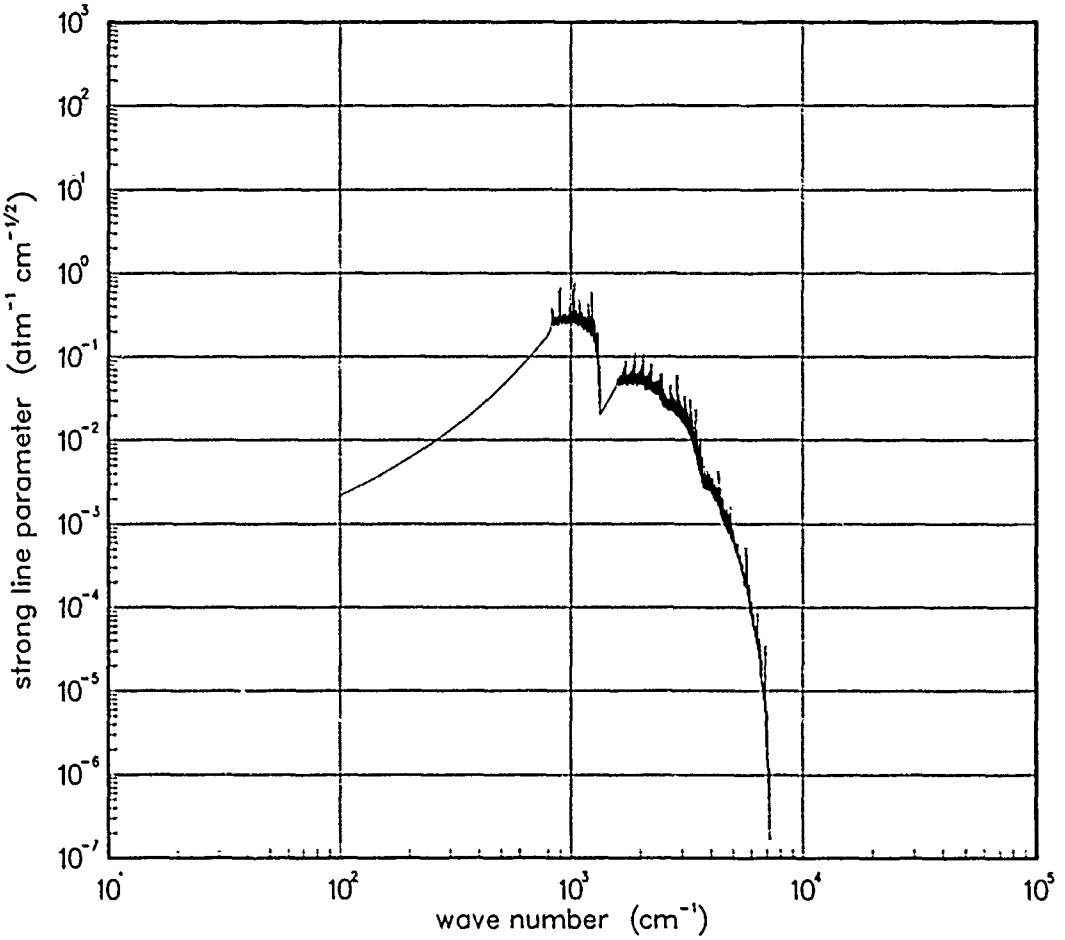

Figure 453. Strong-line parameter for SiO at 18000°K.

6.7 TITANIUM OXIDE (TiO).

Table 13. Spectroscopic data for TiO.

$X\ ^3\Delta$

$\omega_e = 1008.26^{\dagger}$ $\omega_e x_e = 4.13^{\dagger}$
$\alpha_e = .0031^{\dagger}$ $A_e = 48.3^{*}$ $B_e = .5354^{\dagger}$ $E_e = 0.0$

$S_{10} = 149.0^{\ddagger}$ $S_{20} = .549^{\ddagger}$ $S_{30} = 0.076^{\ddagger}$

Data Source:

*J.D. Phillips, Astrophys. J. 169, 185 (1971).

†B. Rosen, ed.,Spectroscopic Data Relative to Diatomic Molecules, Pergamon Press, New York (1970).

‡H.H. Michels, Diatomic Oxide Vibrational Band Intensities , United Aircraft Research Laboratories, K921094-4 (May 1971).

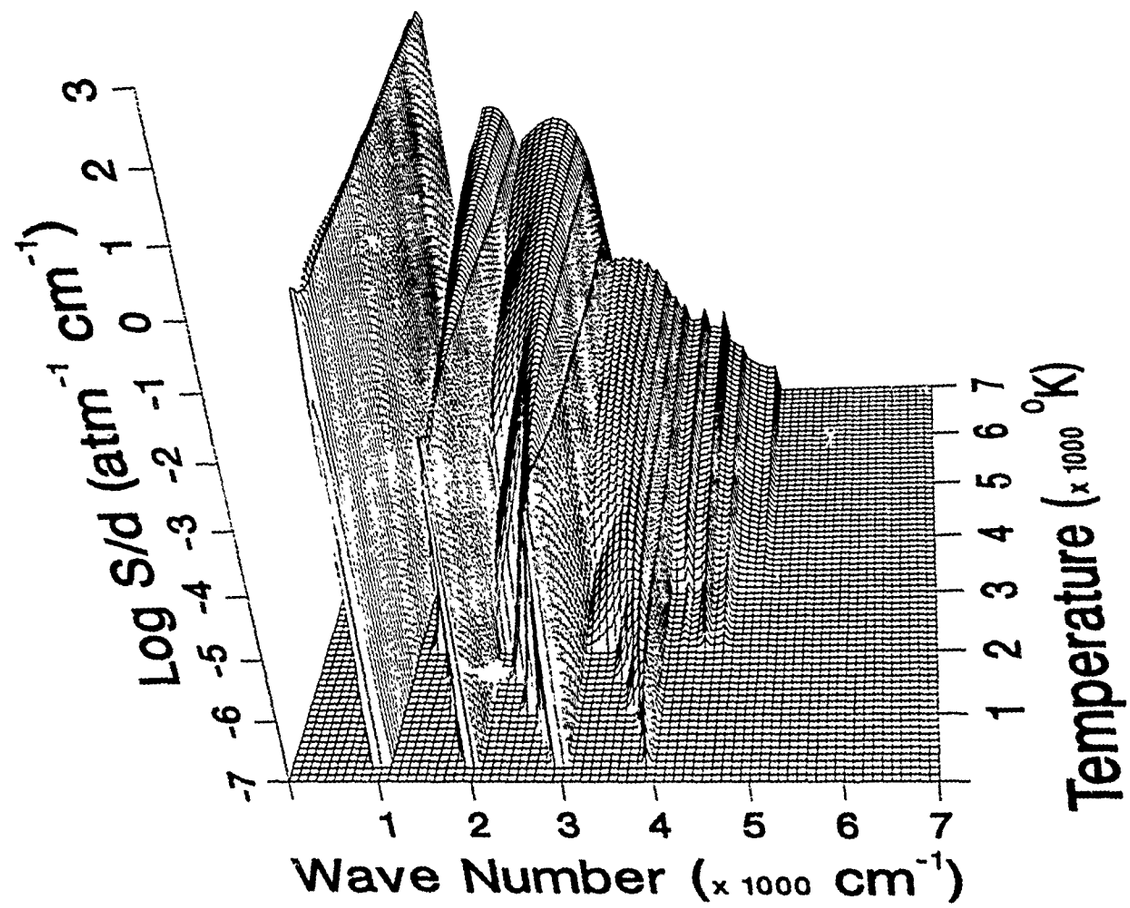

Figure 454. Weak-line parameter for TiO.

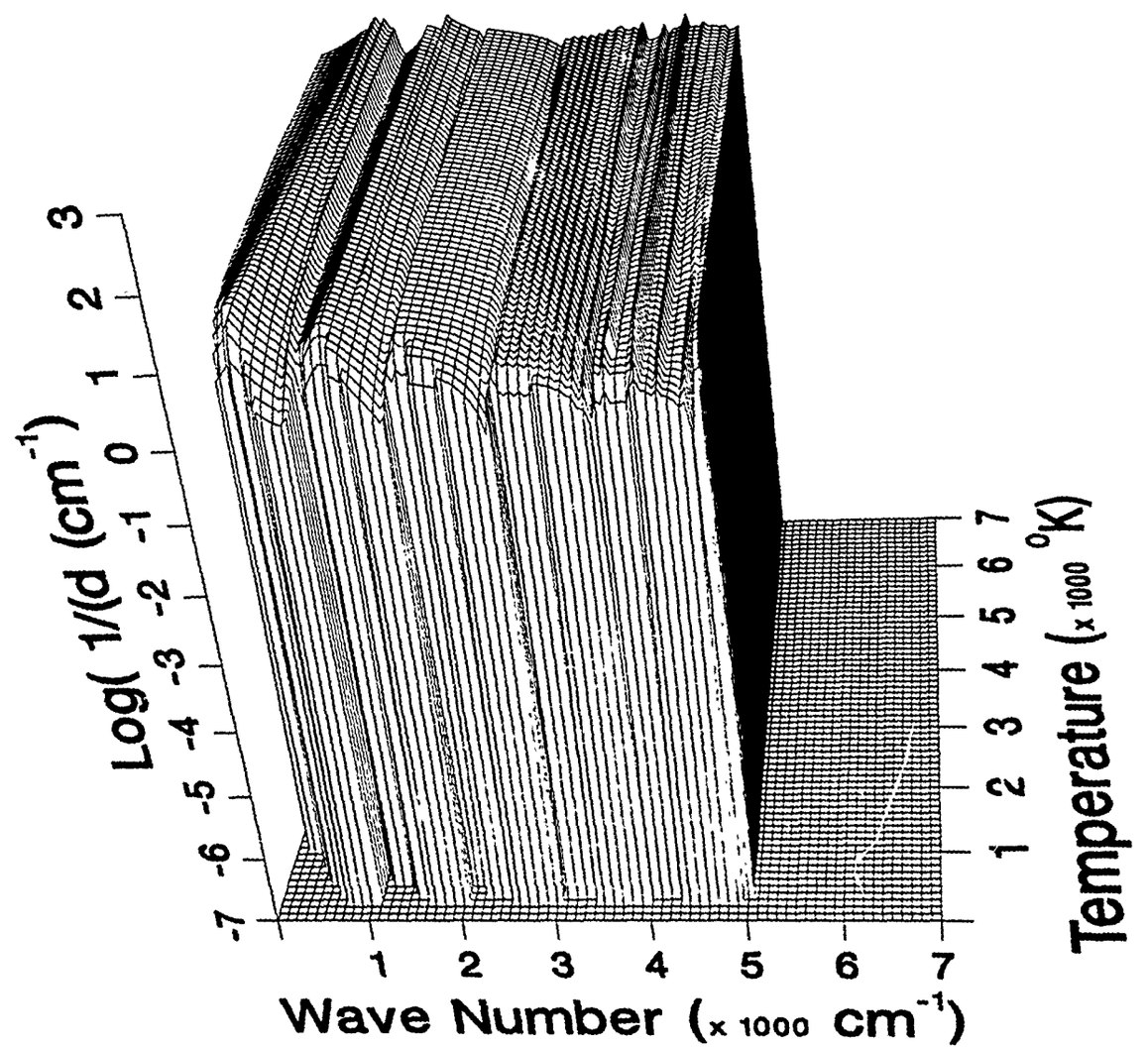

Figure 455. Inverse line spacing for TiO.

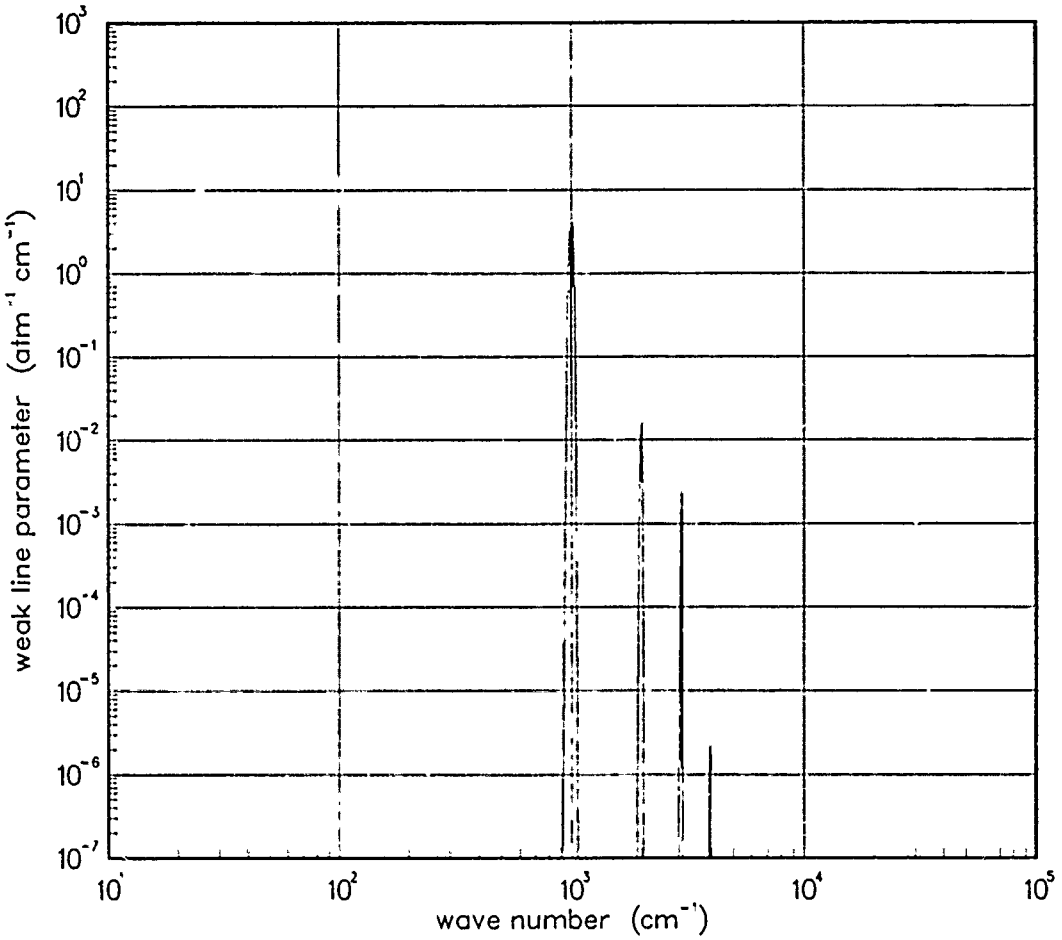

Figure 456. Weak-line parameter for TiO at 200°K.

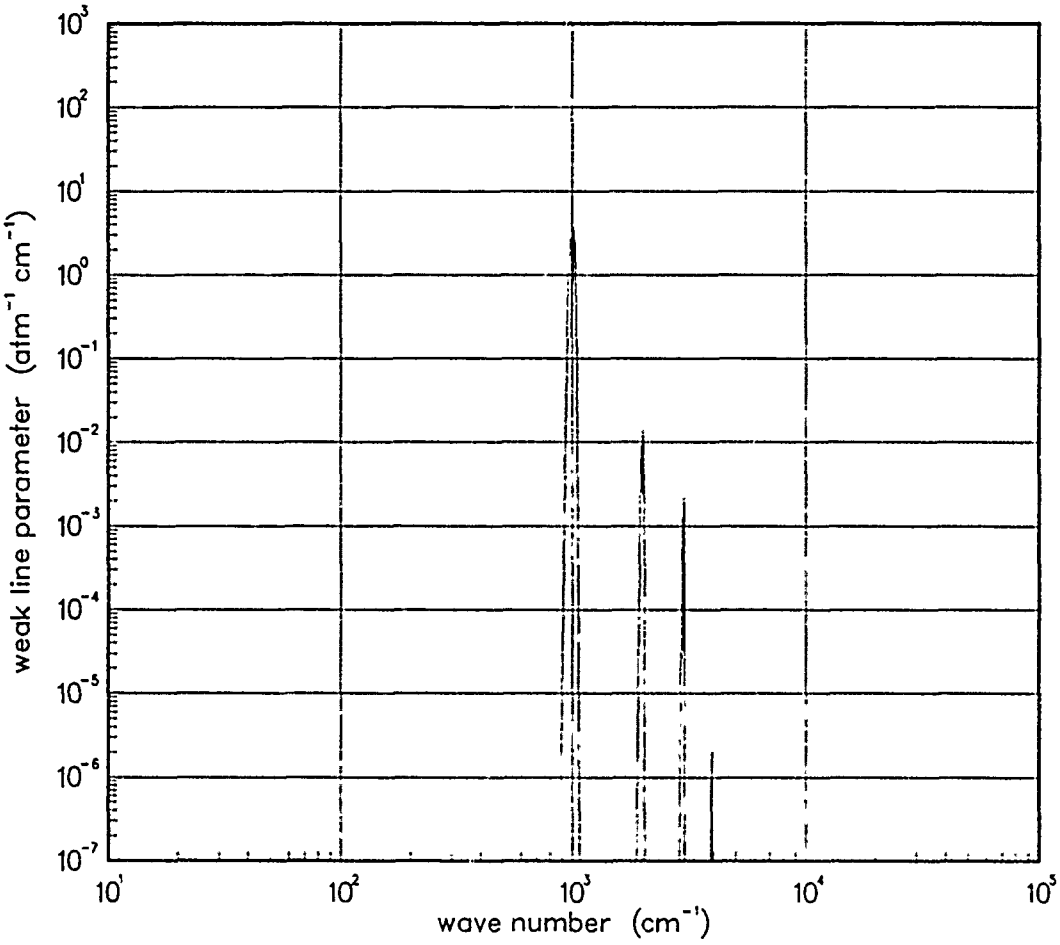

Figure 457. Weak-line parameter for TiO at 300°K.

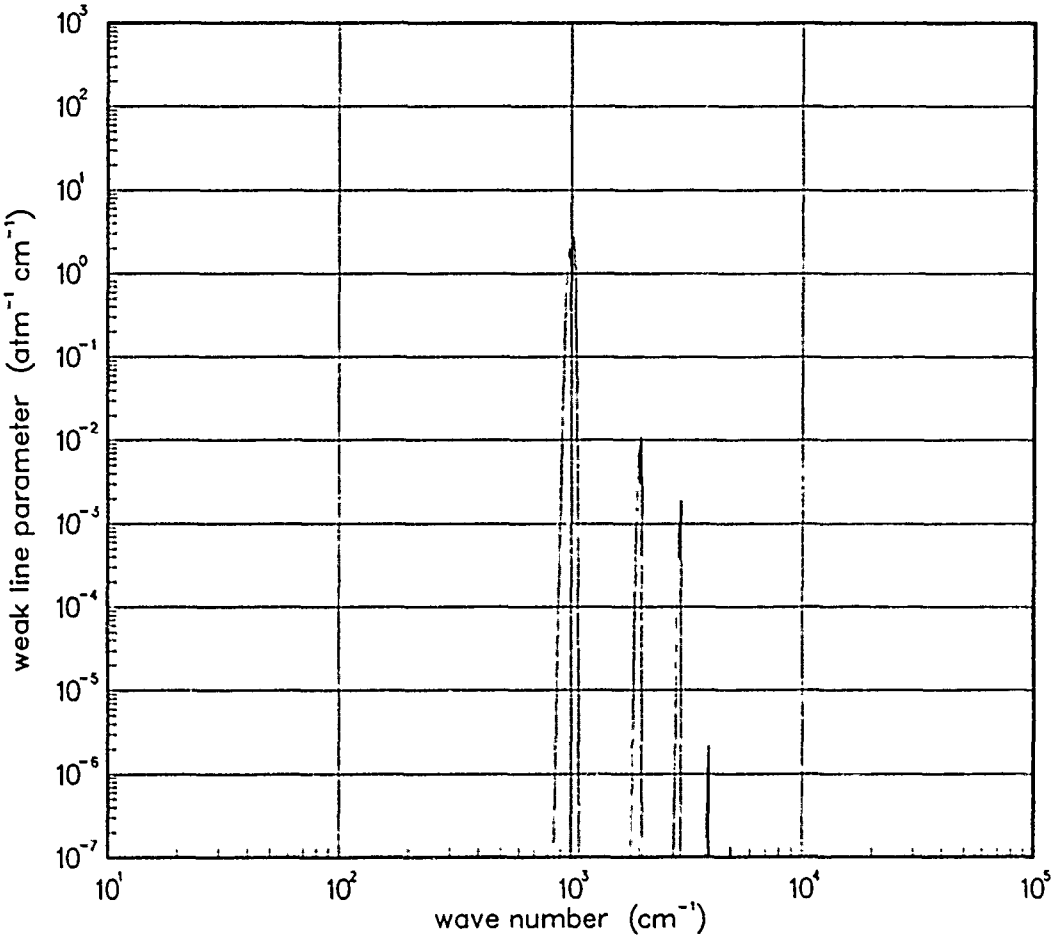

Figure 458. Weak-line parameter for TiO at 500°K.

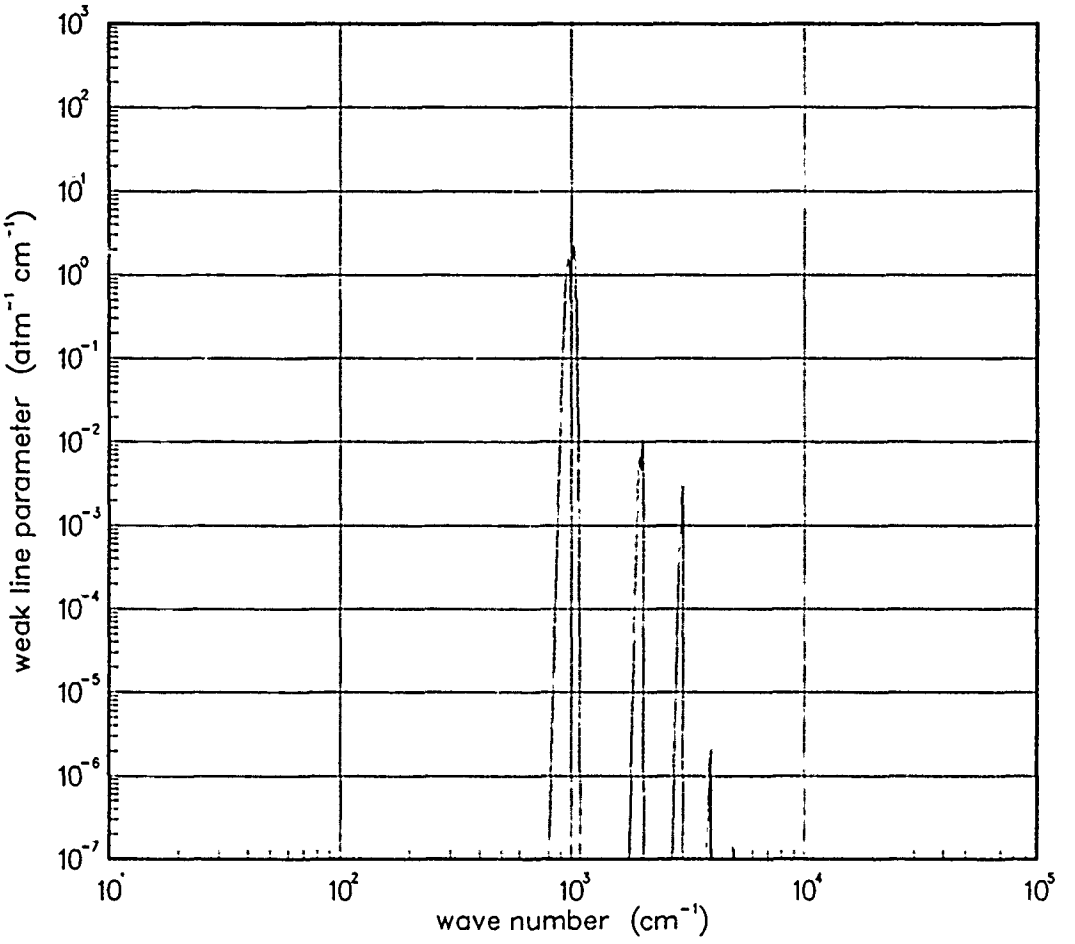

Figure 459. Weak-line parameter for TiO at 750°K.

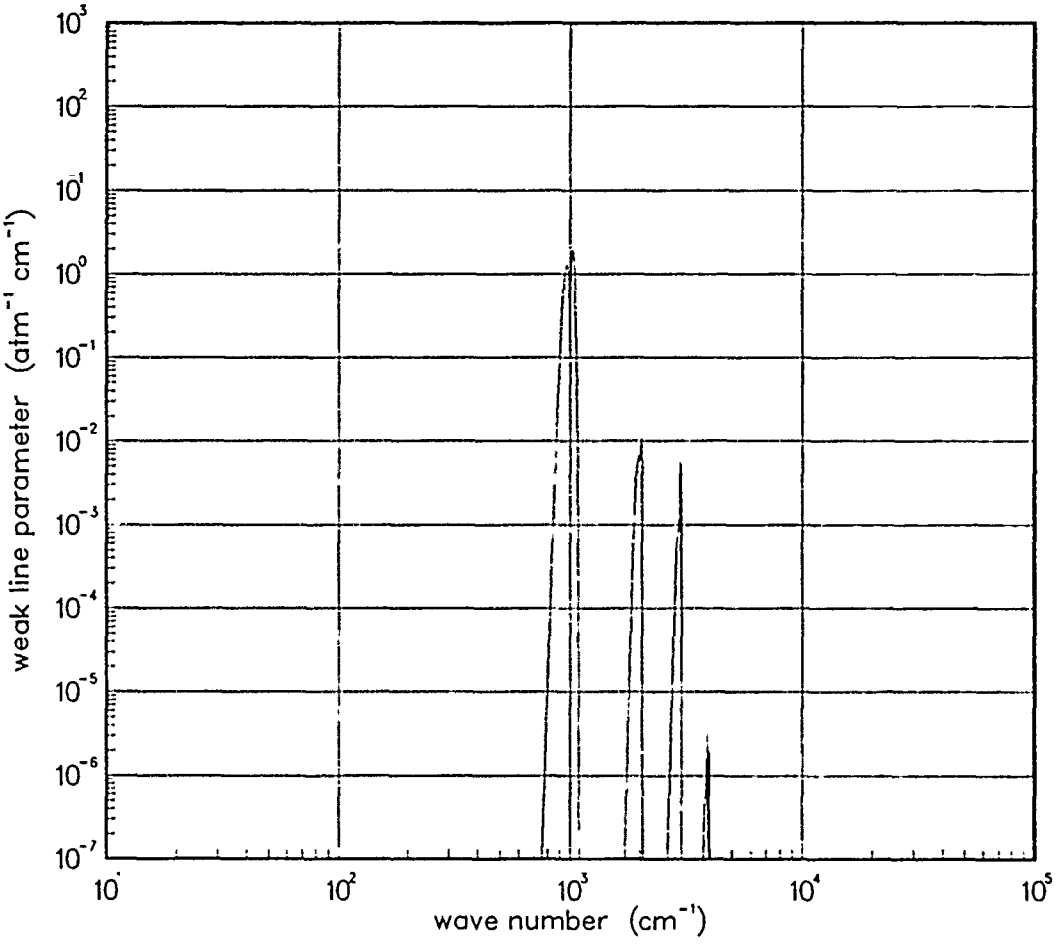

Figure 460. Weak-line parameter for TiO at 1000°K.

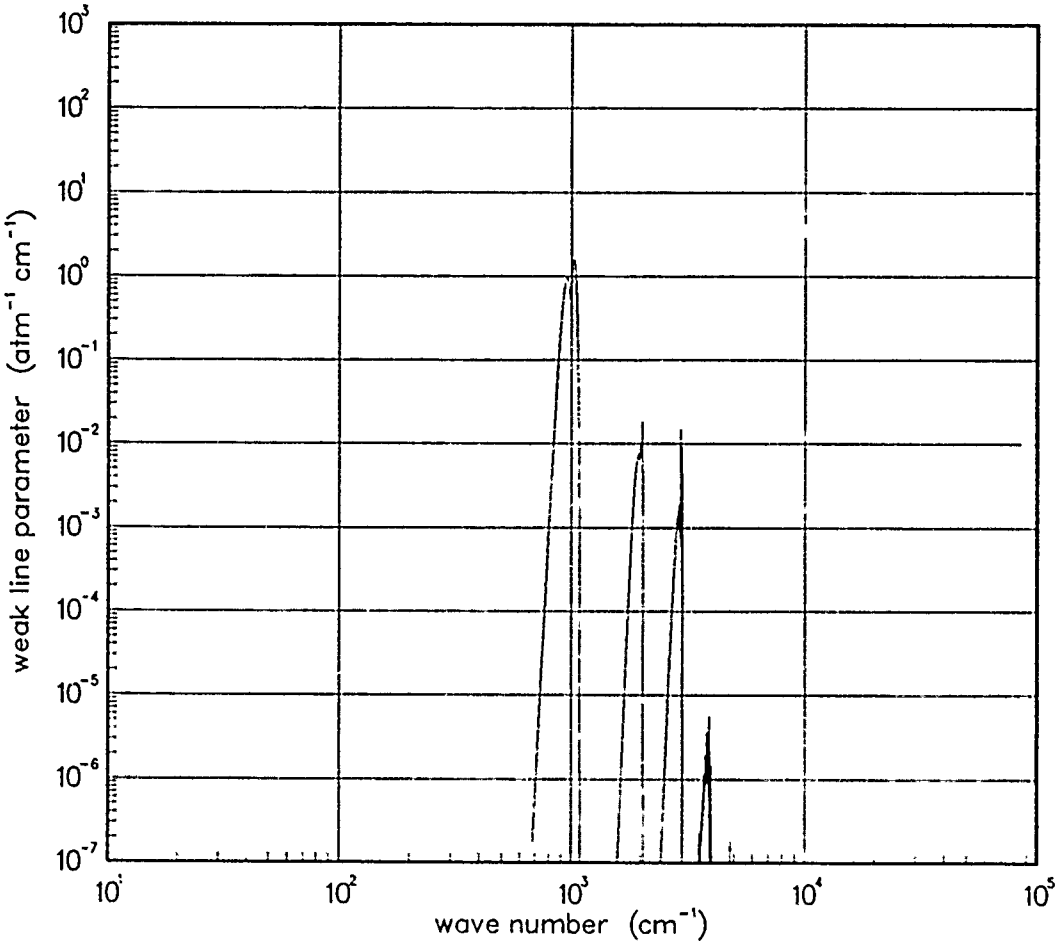

Figure 461. Weak-line parameter for TiO at 1500°K.

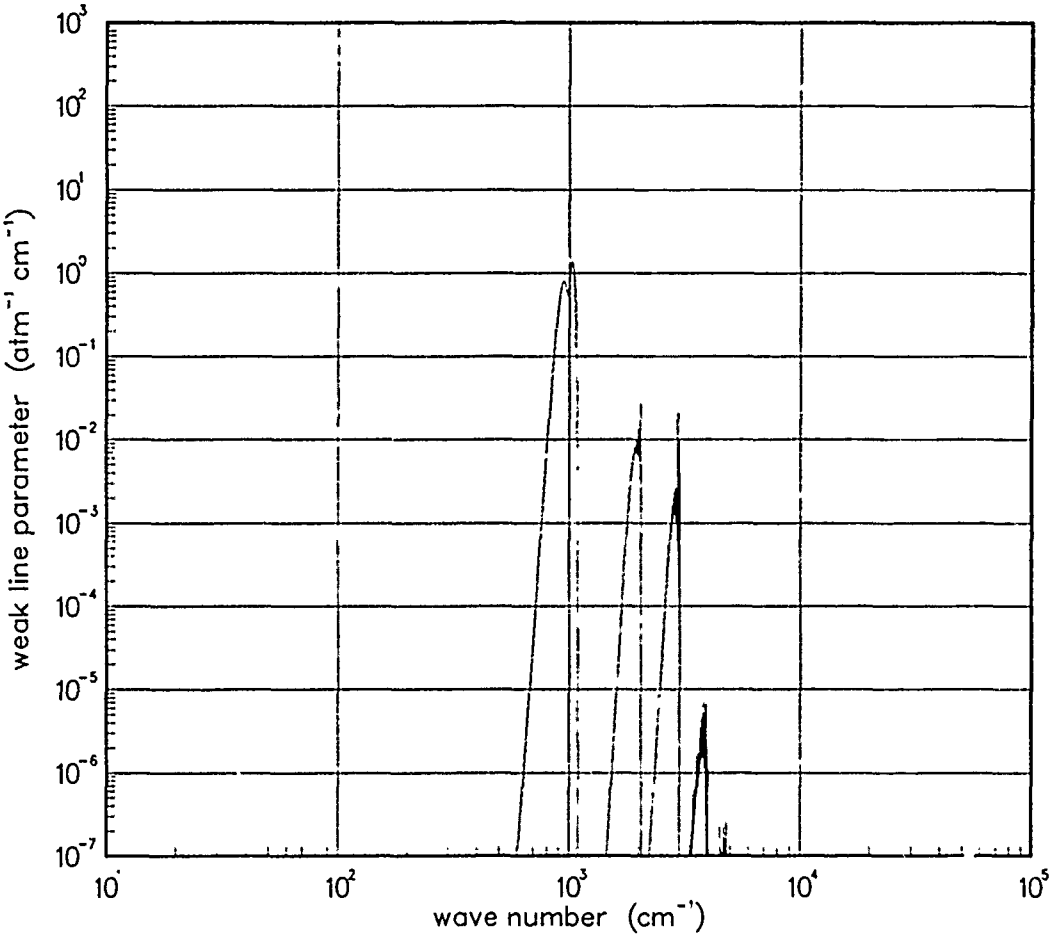

Figure 462. Weak-line parameter for TiO at 2000°K.

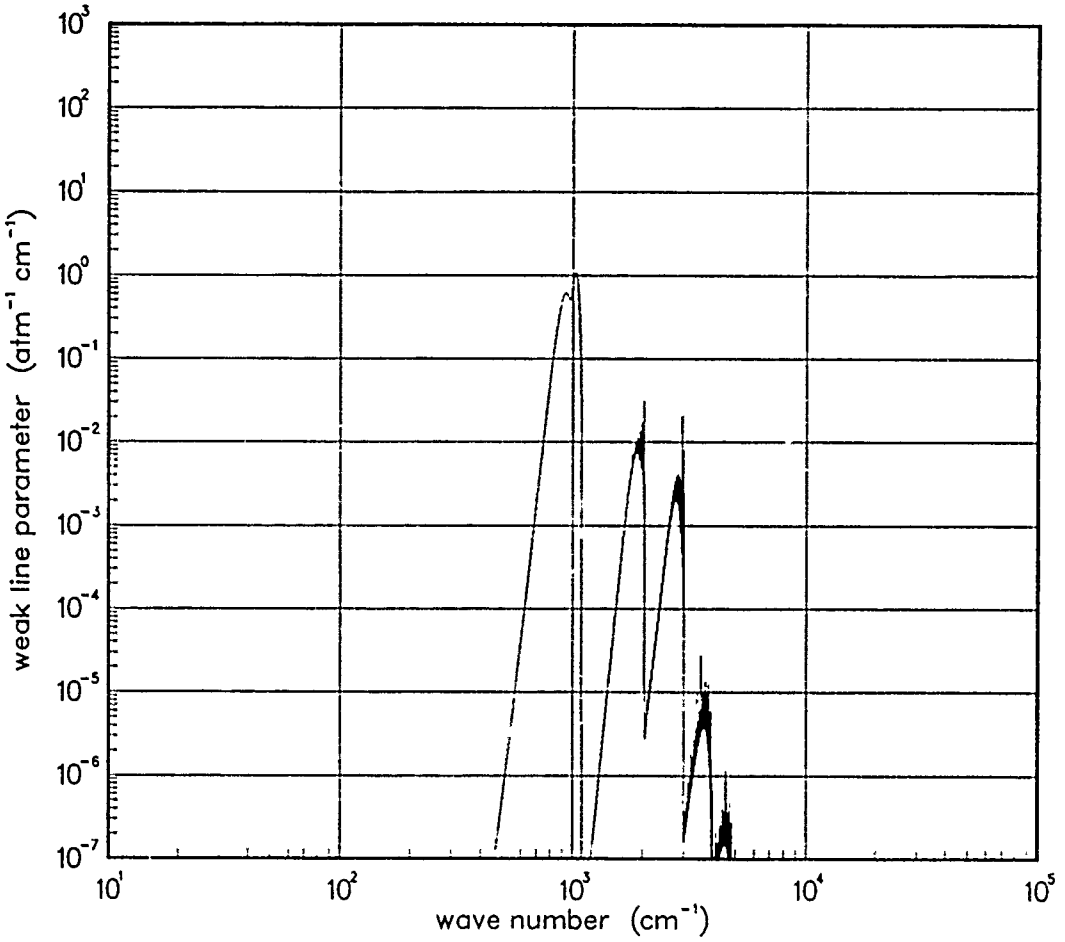

Figure 463. Weak-line parameter for TiO at 3000°K.

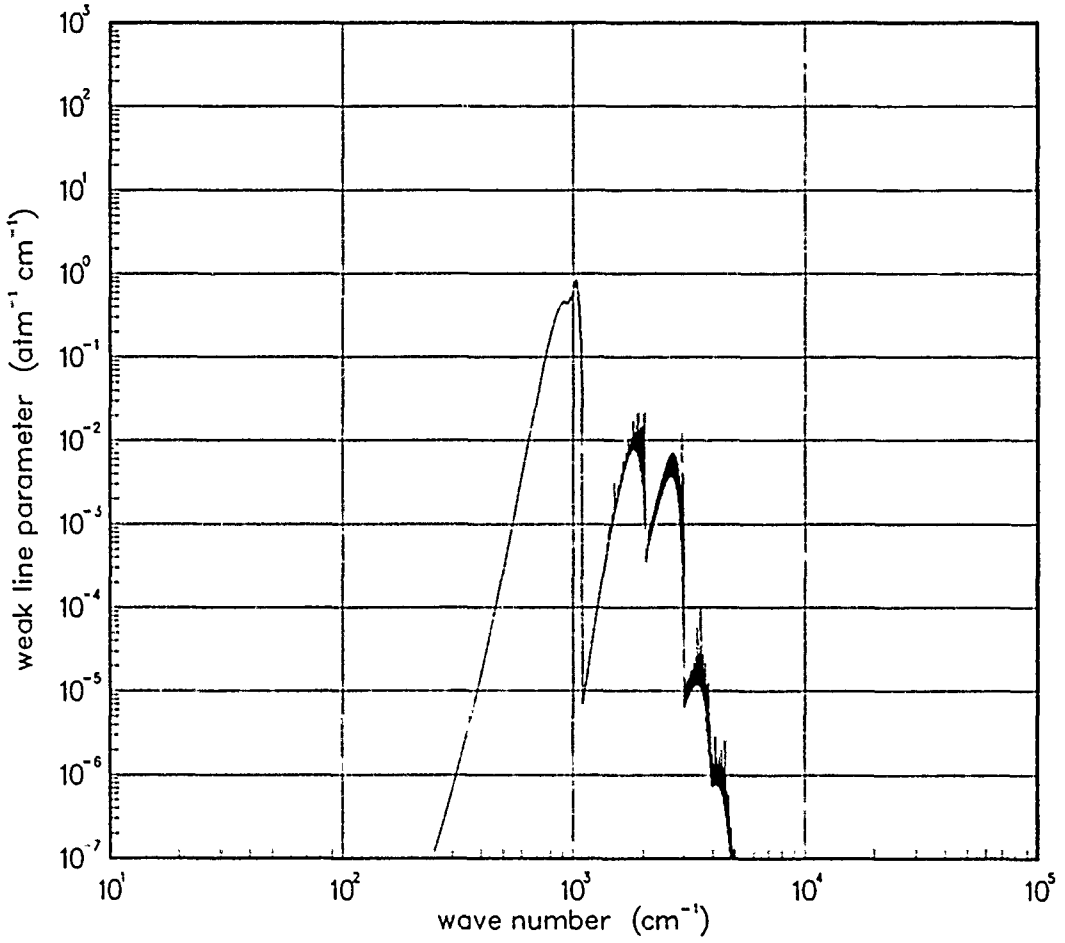

Figure 464. Weak-line parameter for TiO at 5000°K.

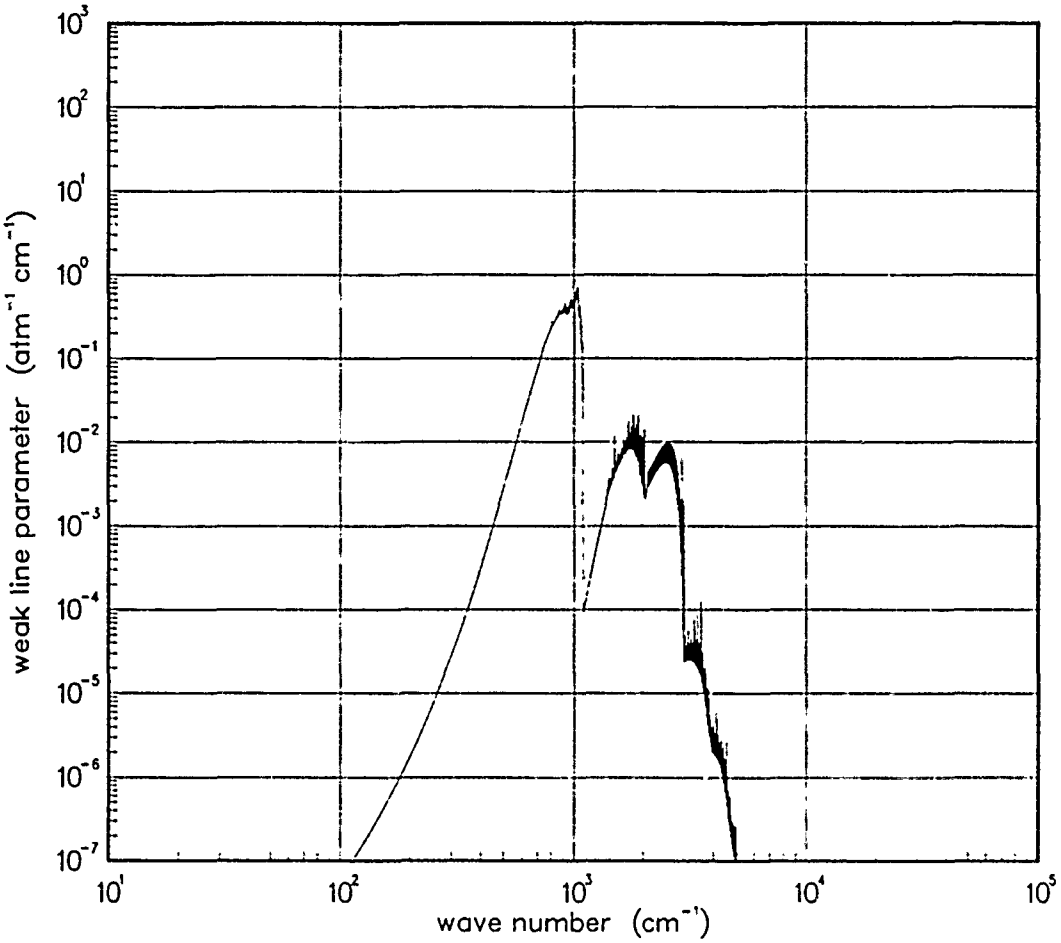

Figure 465. Weak-line parameter for TiO at 7000°K.

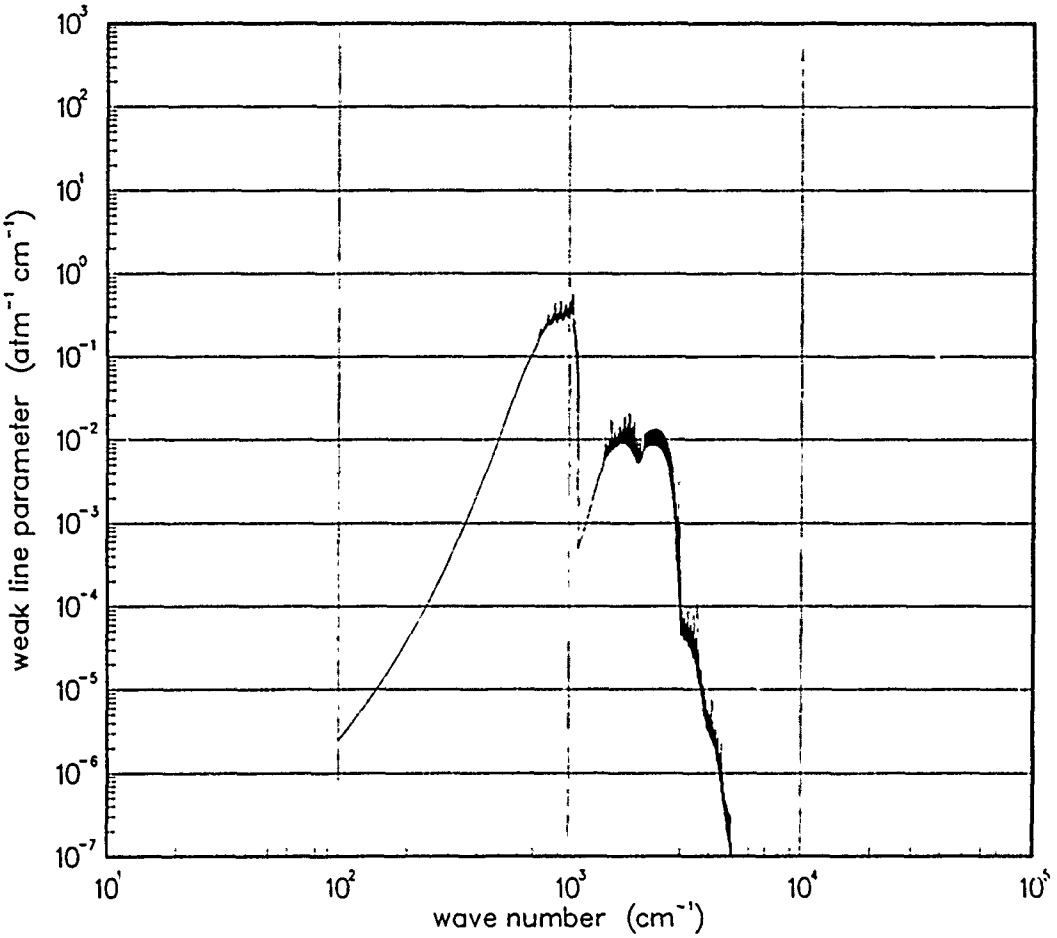

Figure 466. Weak-line parameter for TiO at 10000°K.

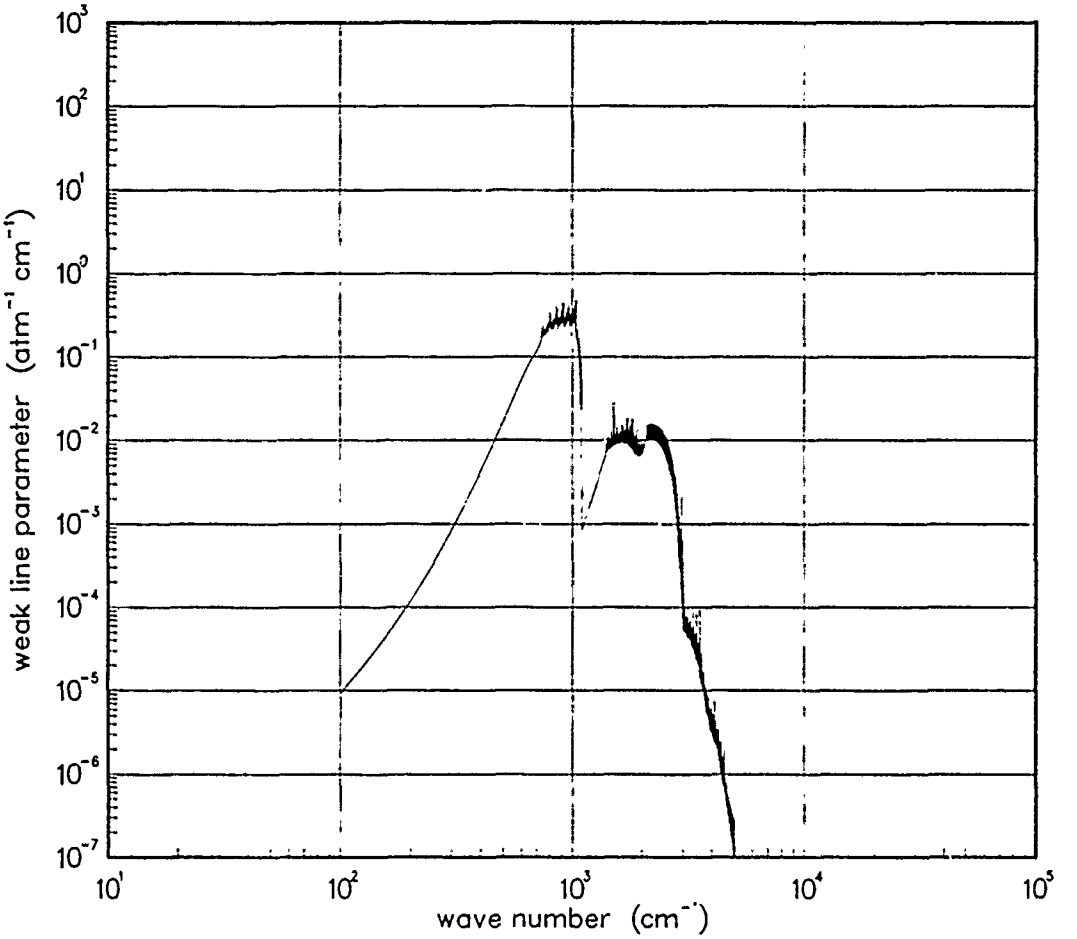

Figure 467. Weak-line parameter for TiO at 12000°K.

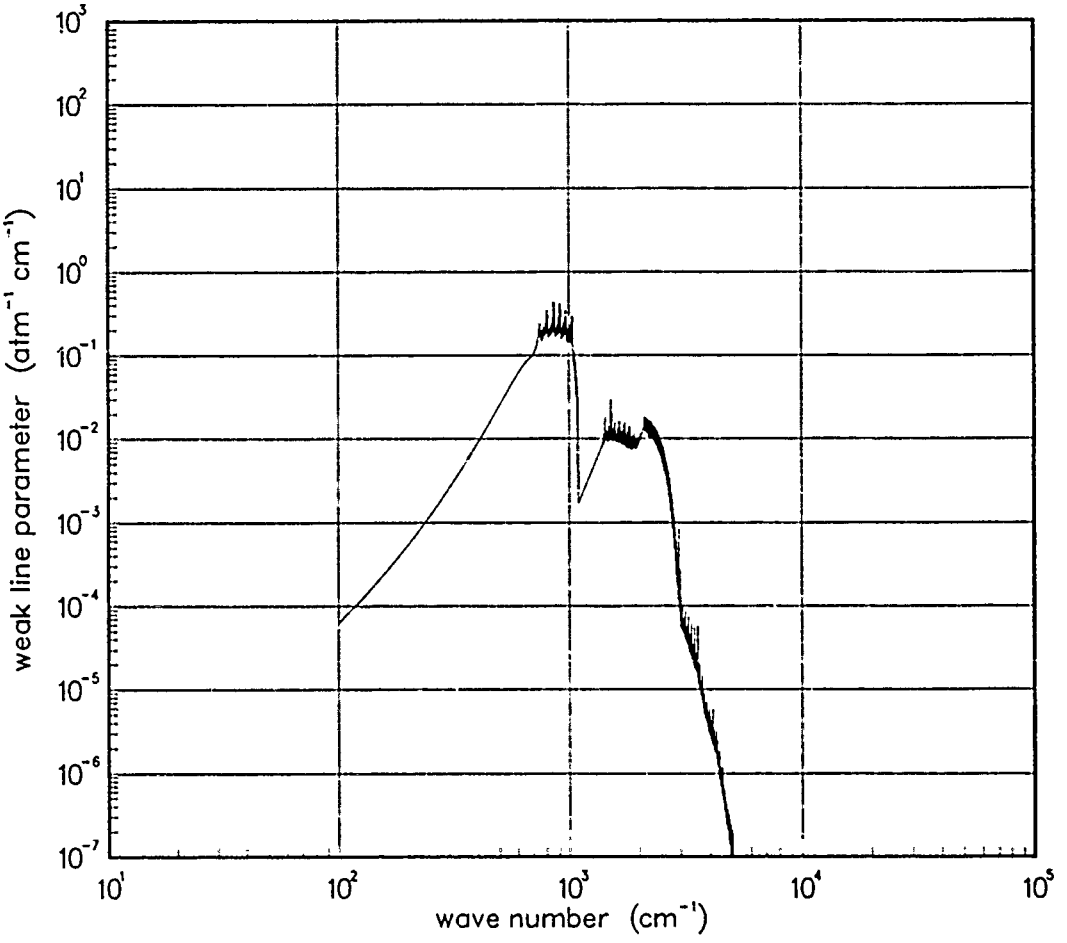

Figure 468. Weak-line parameter for TiO at 18000°K.

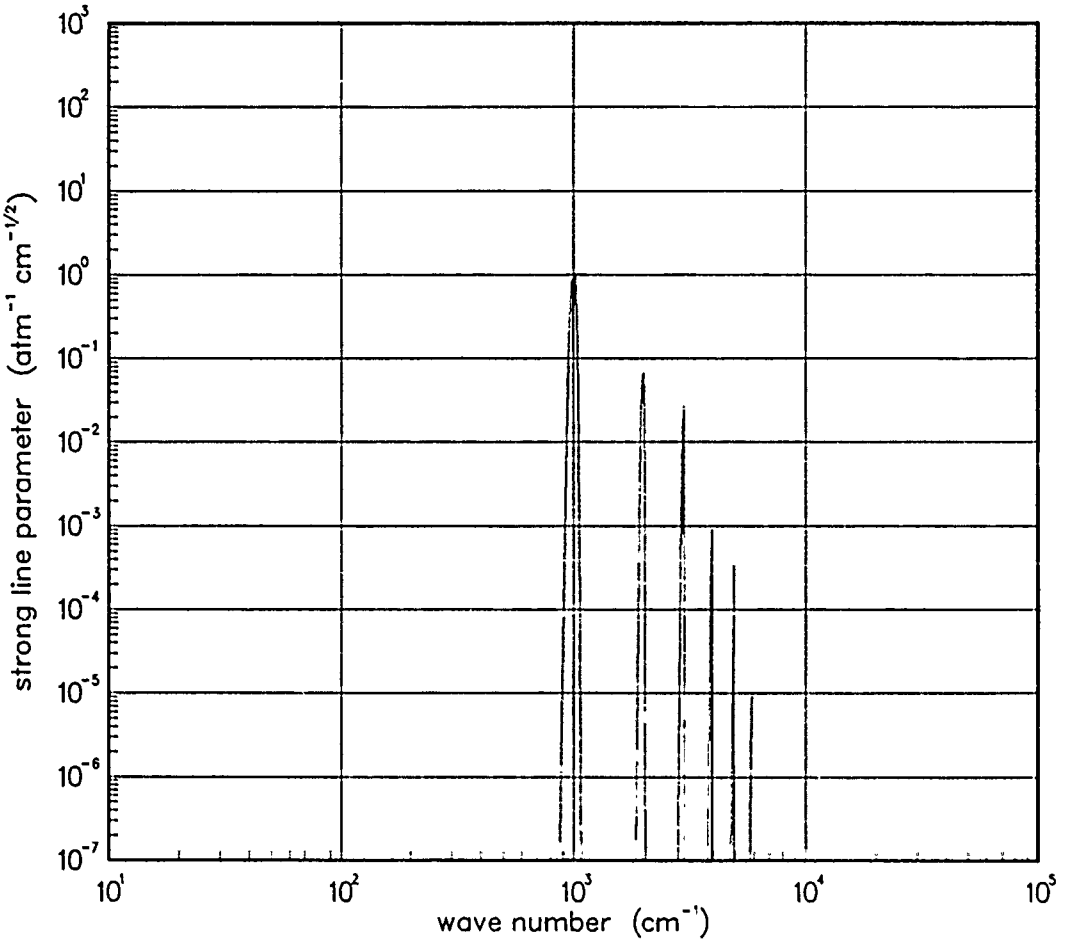

Figure 469. Strong-line parameter for TiO at 200°K.

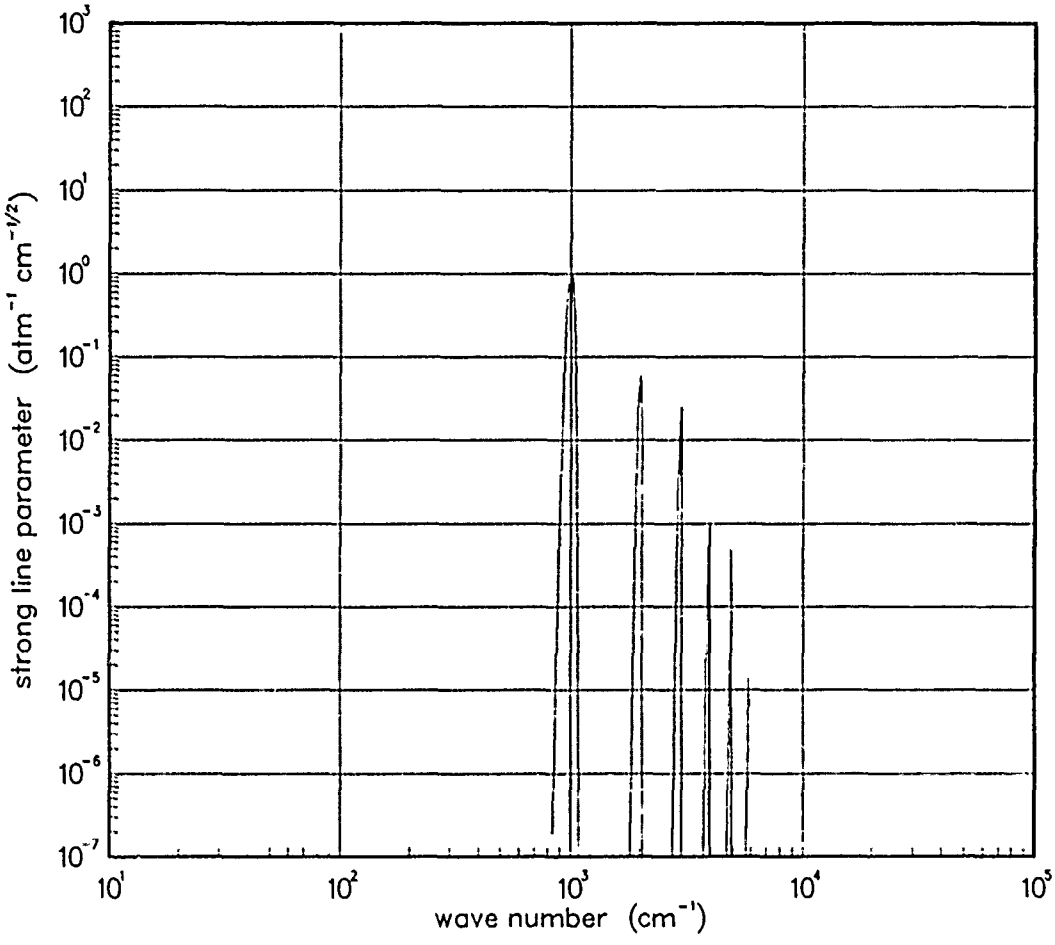

Figure 470. Strong-line parameter for TiO at 300°K.

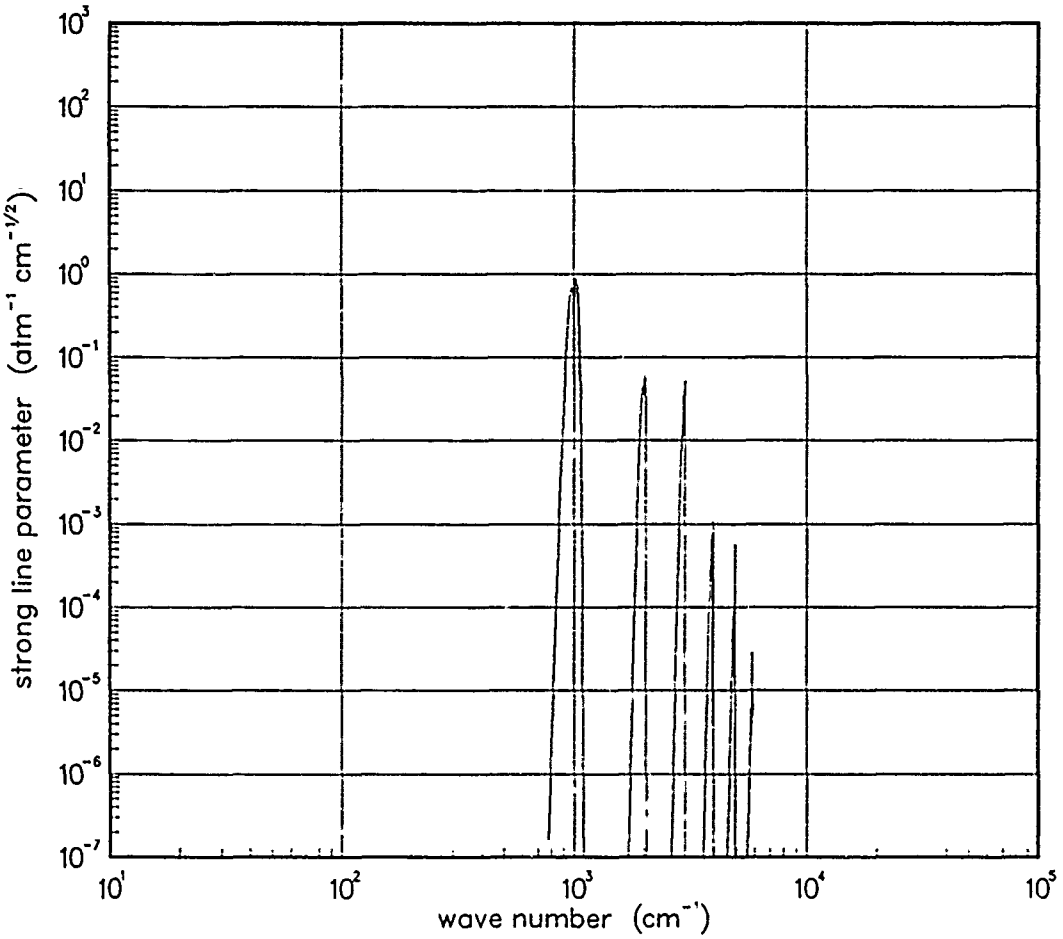

Figure 471. Strong-line parameter for TiO at 500°K.

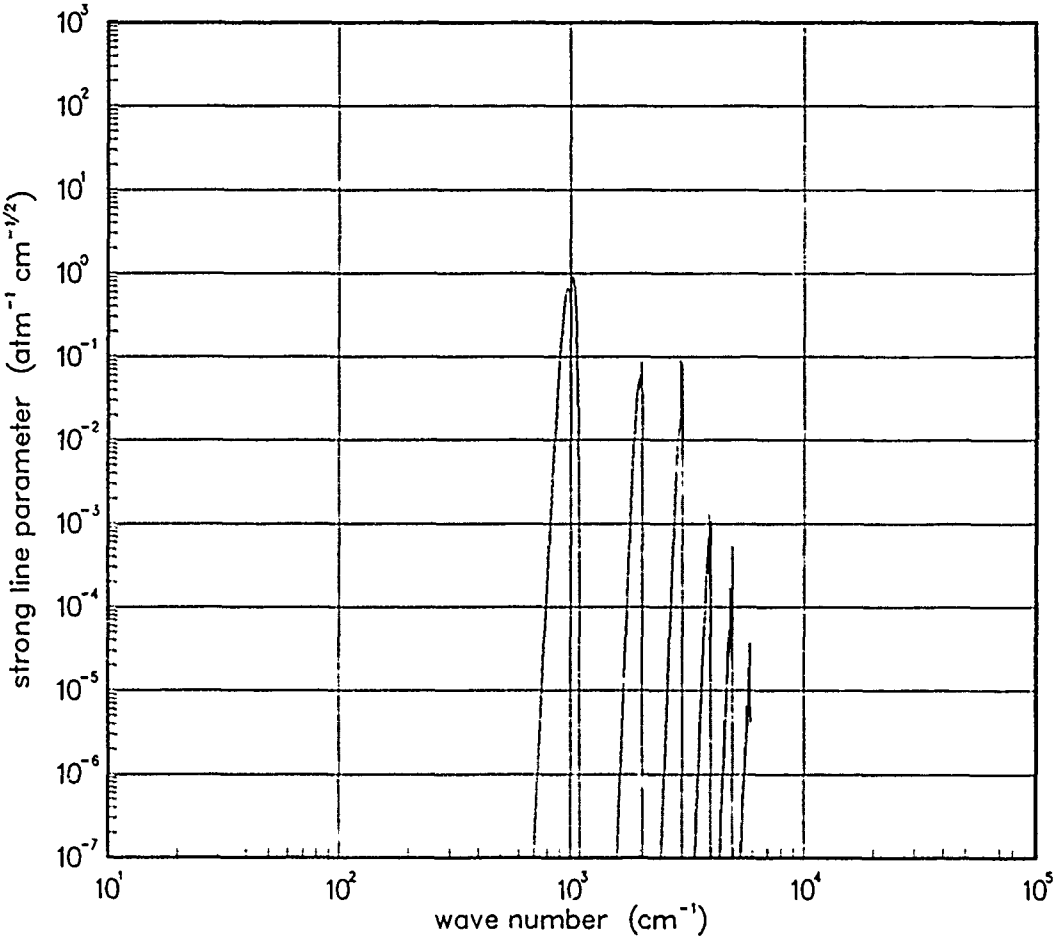

Figure 472. Strong-line parameter for TiO at 750°K.

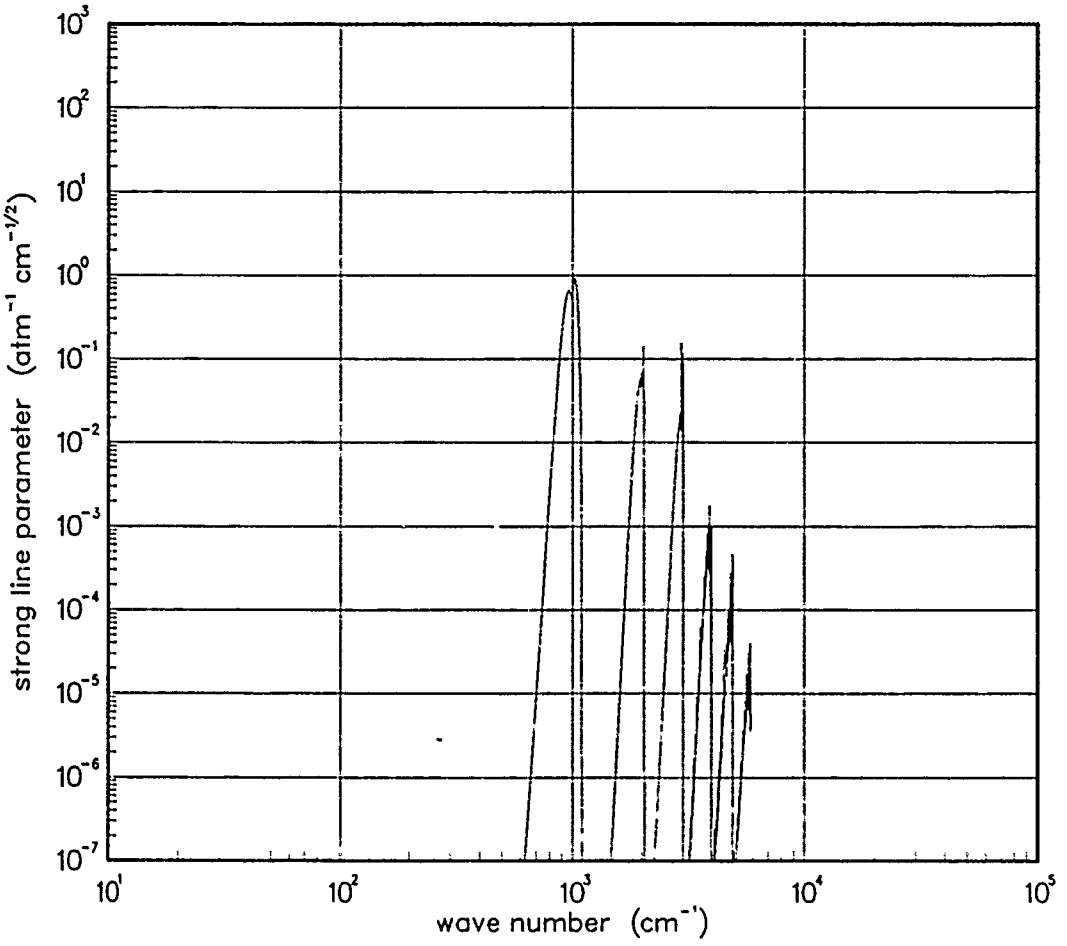

Figure 473. Strong-line parameter for TiO at 1000°K.

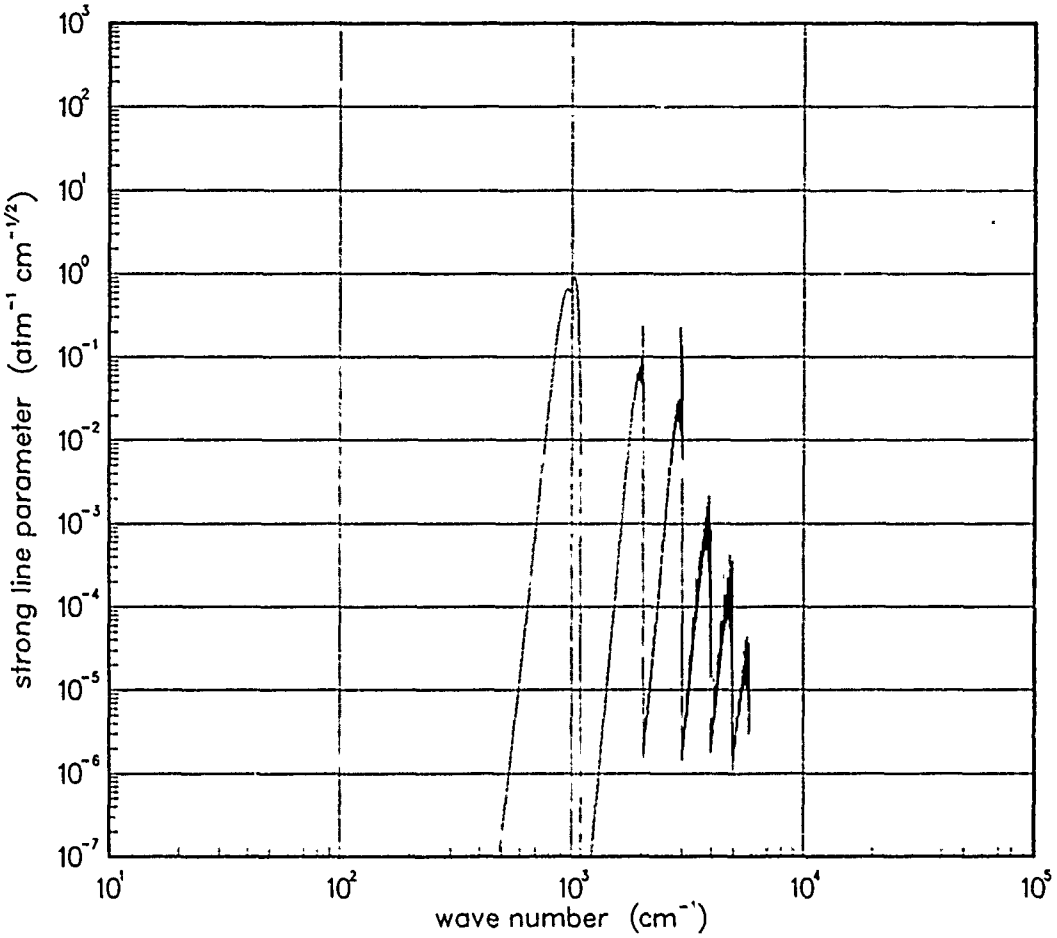

Figure 474. Strong-line parameter for TiO at 1500°K.

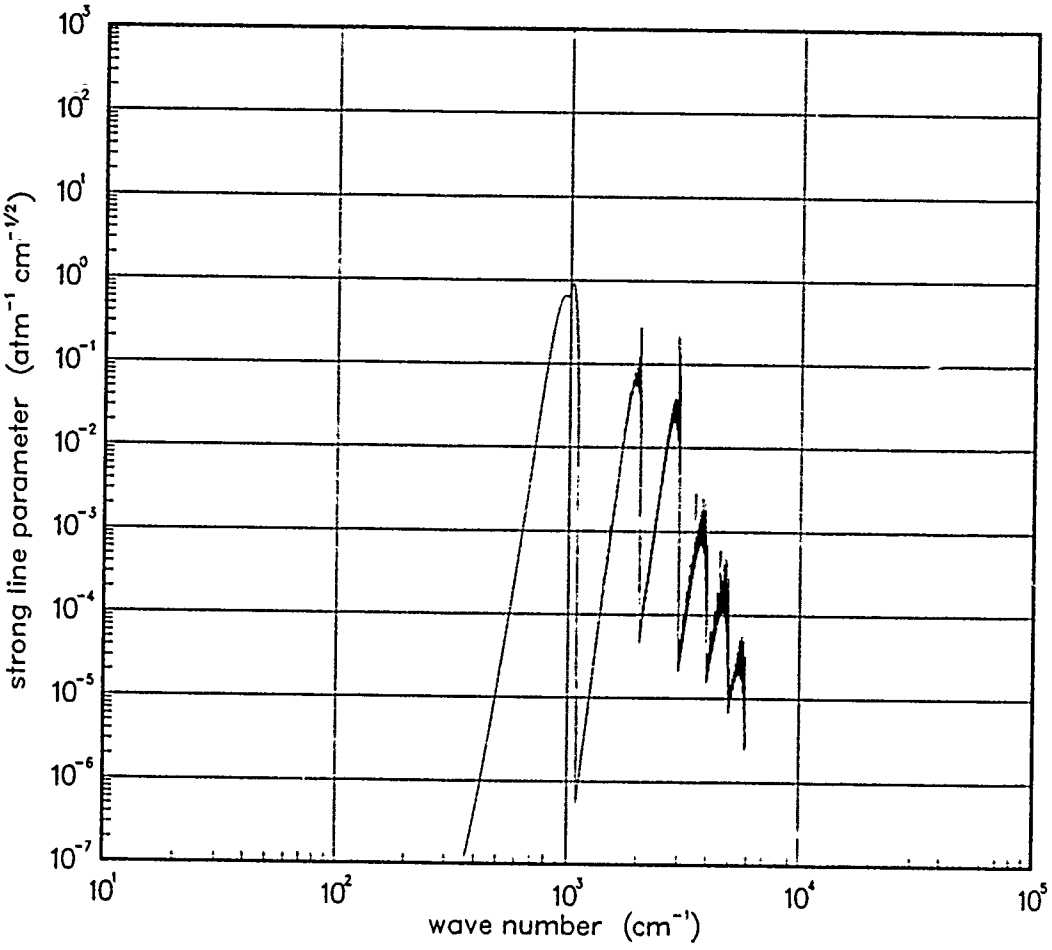

Figure 475. Strong-line parameter for TiO at 2000°K.

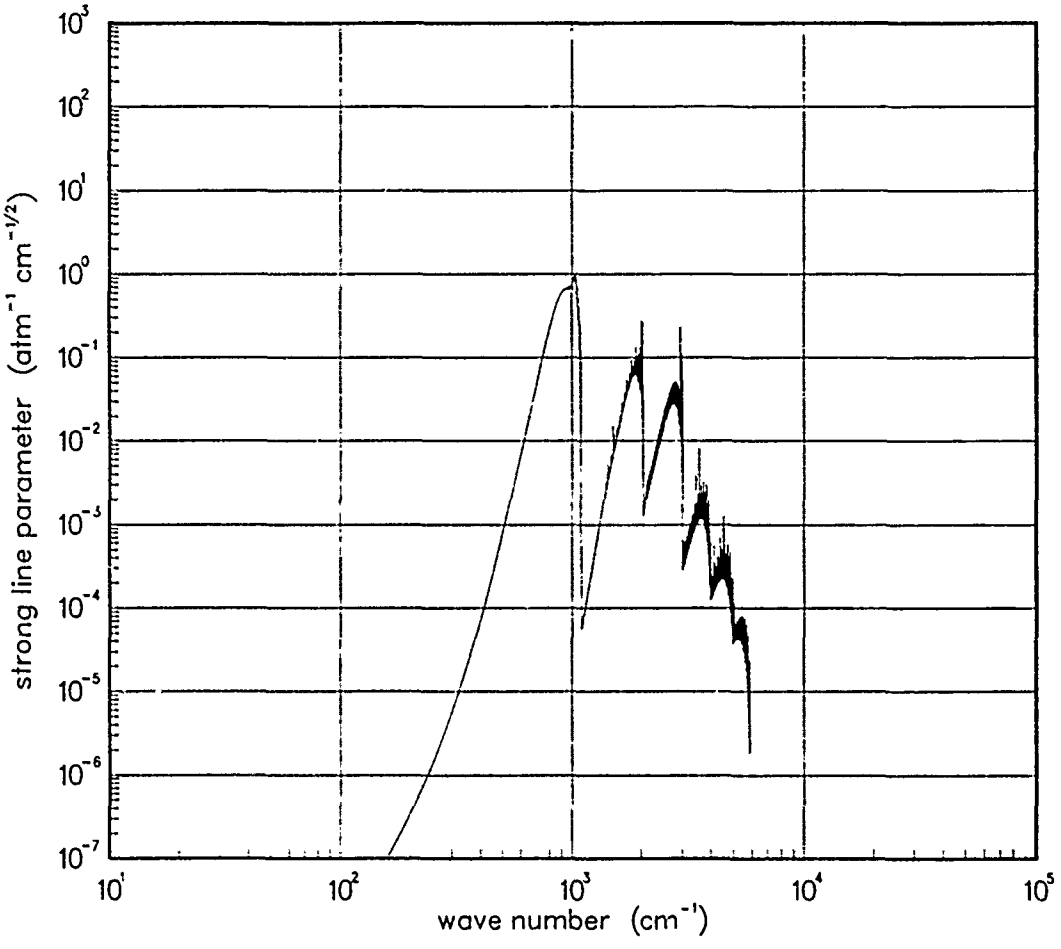

Figure 476. Strong-line parameter for TiO at 3000°K.

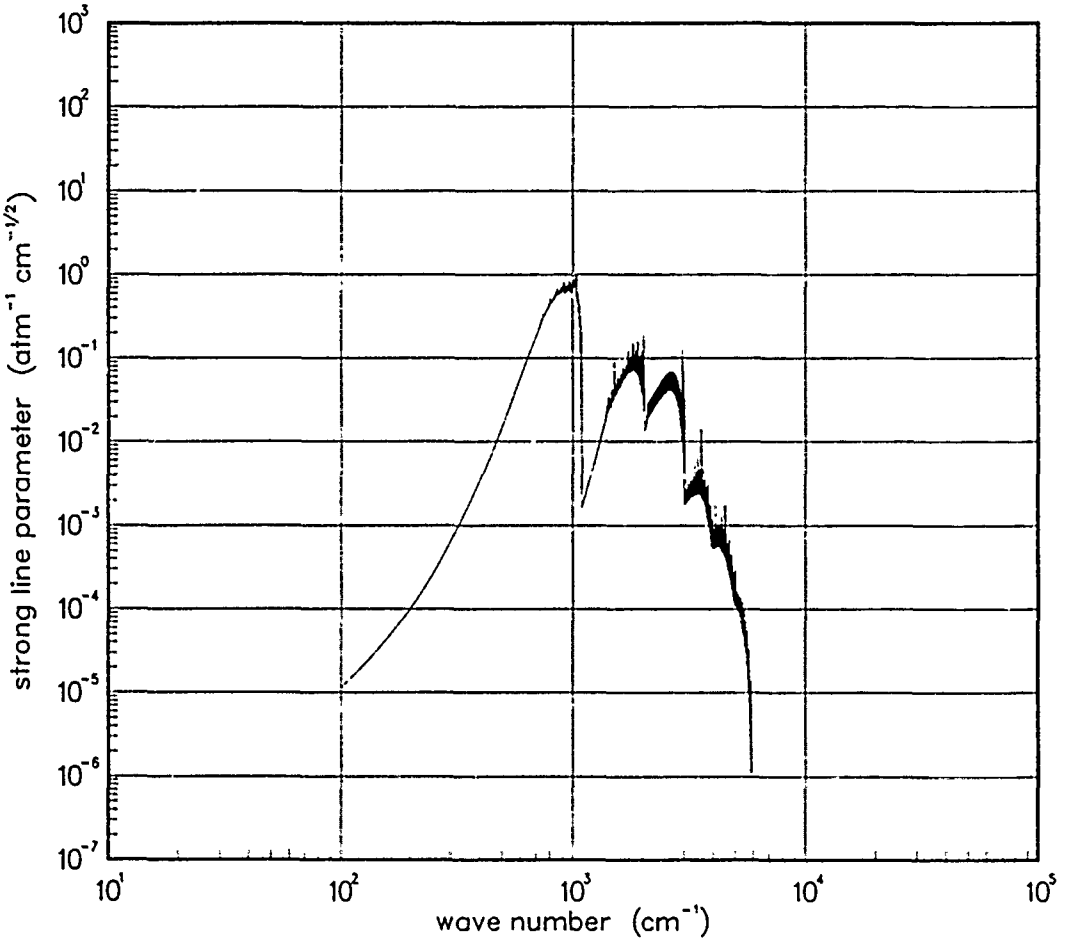

Figure 477. Strong-line parameter for TiO at 5000°K.

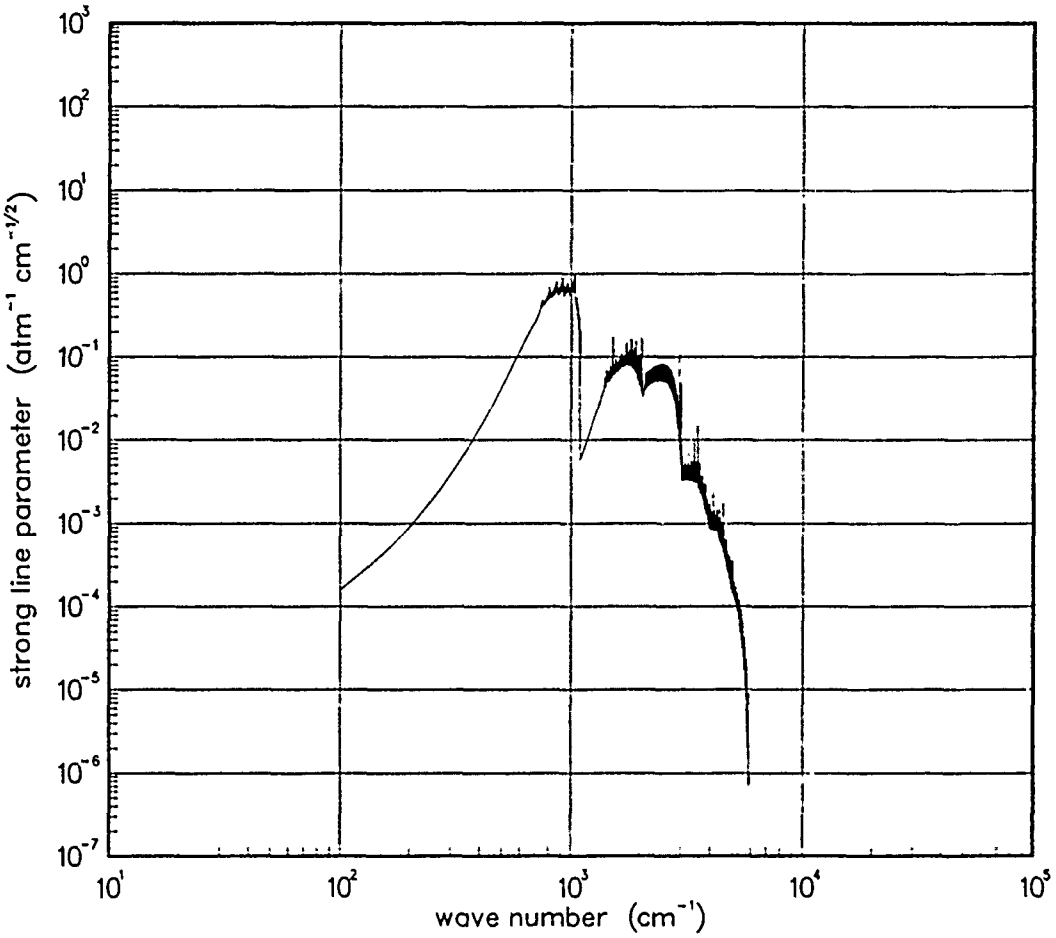

Figure 478. Strong-line parameter for TiO at 7000°K.

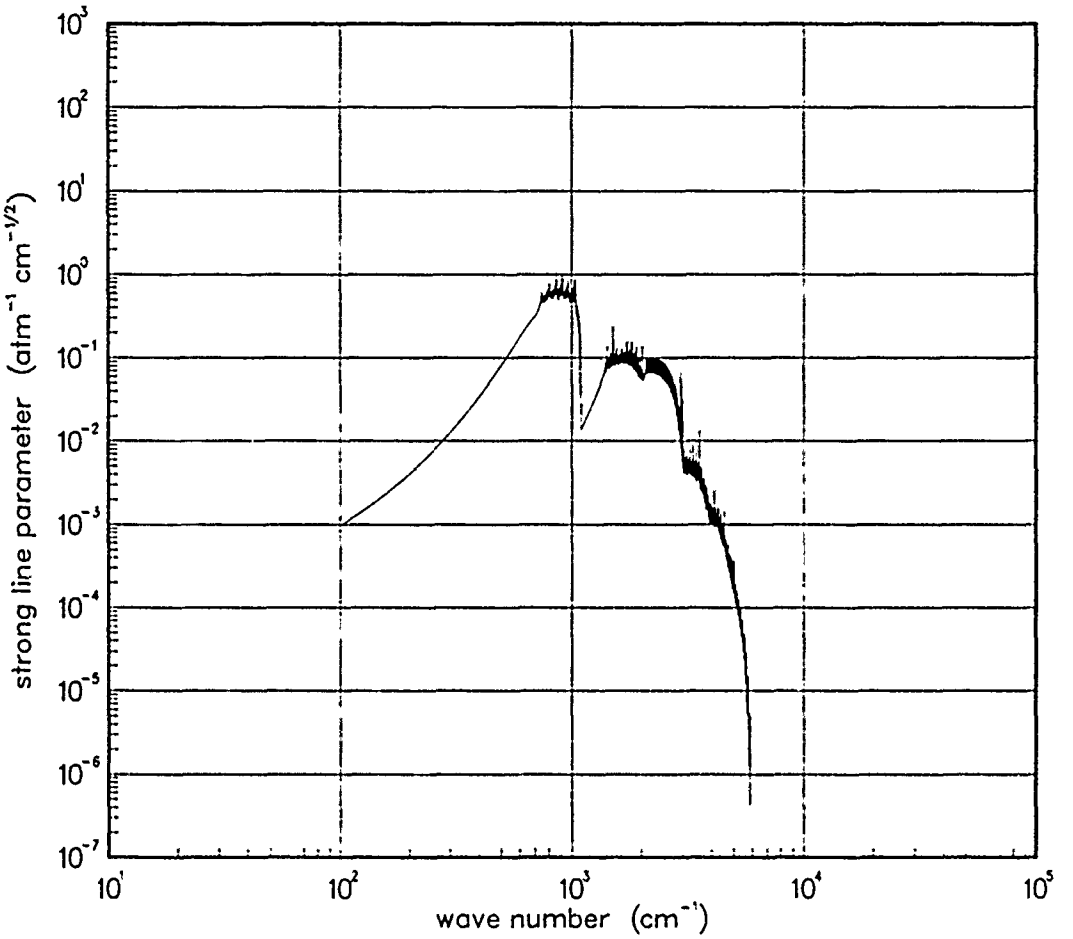

Figure 479. Strong-line parameter for TiO at 10000°K.

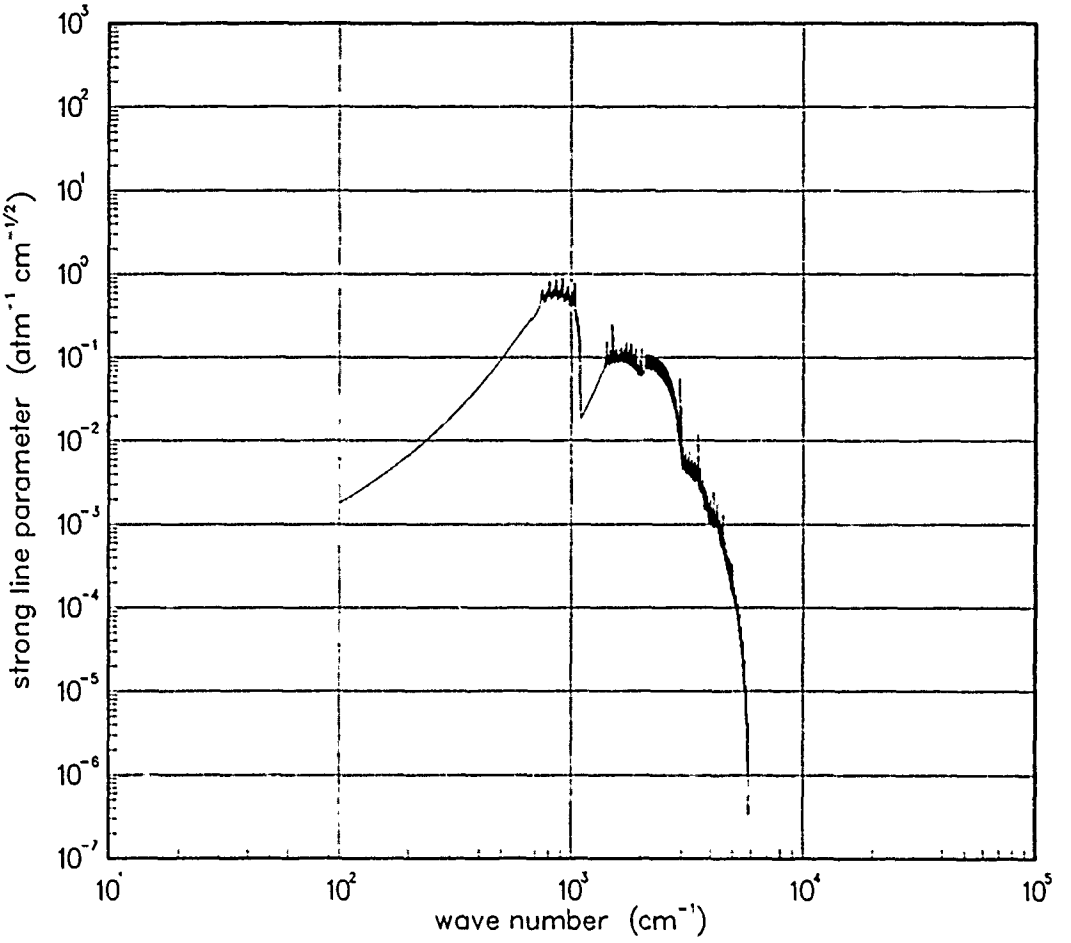

Figure 480. Strong-line parameter for TiO at 12000°K.

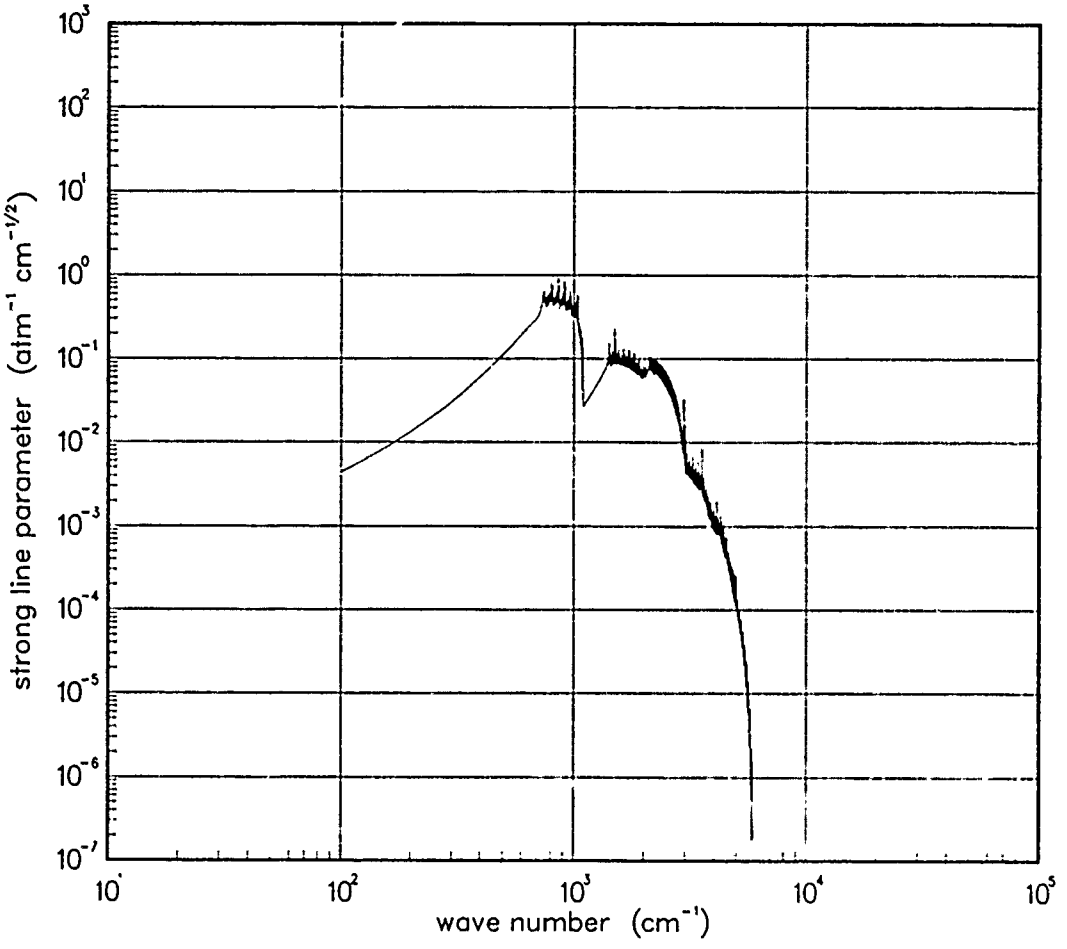

Figure 481. Strong-line parameter for TiO at 18000°K.

6.8 URANIUM OXIDE (UO).

The emissions from the Uranium Oxide molecule and Uranium Oxide Ion were calculated with the DATE program.

Table 14. Spectroscopic data for UO.

$X\ ^{1}\Sigma^{*}$

$\omega_e = 783.2^{\dagger}$ $\omega_e x_e = 5.09^{\dagger}$
$\alpha_e = .0028^{\ddagger}$ $B_e = 0.368^{\ddagger}$

$S_{10} = 450.^{\ddagger}$

$\gamma_\ell(300°K) = 0.04^{\S}$

Data Source:

*The symmetry of the ground state is not known. However, the nature of the state will affect only the strong-line parameter to any significant degree.

†ω_e is calculated using the band center (773 cm^{-1}) given in Note ‖ along with an estimate of 0.0065 for x_e. See Note ‡.

‡T.L. Stephens, and J.G. DeVore, Band Models for Calculating Fireball Thermal Emission (U) , 71TMP-35, General Electric-TEMPO, Santa Barbara, California, (May 1971).

§Estimate.

‖H.J. Leary, et al., High Temp. Sci. 3, 433 (1971).

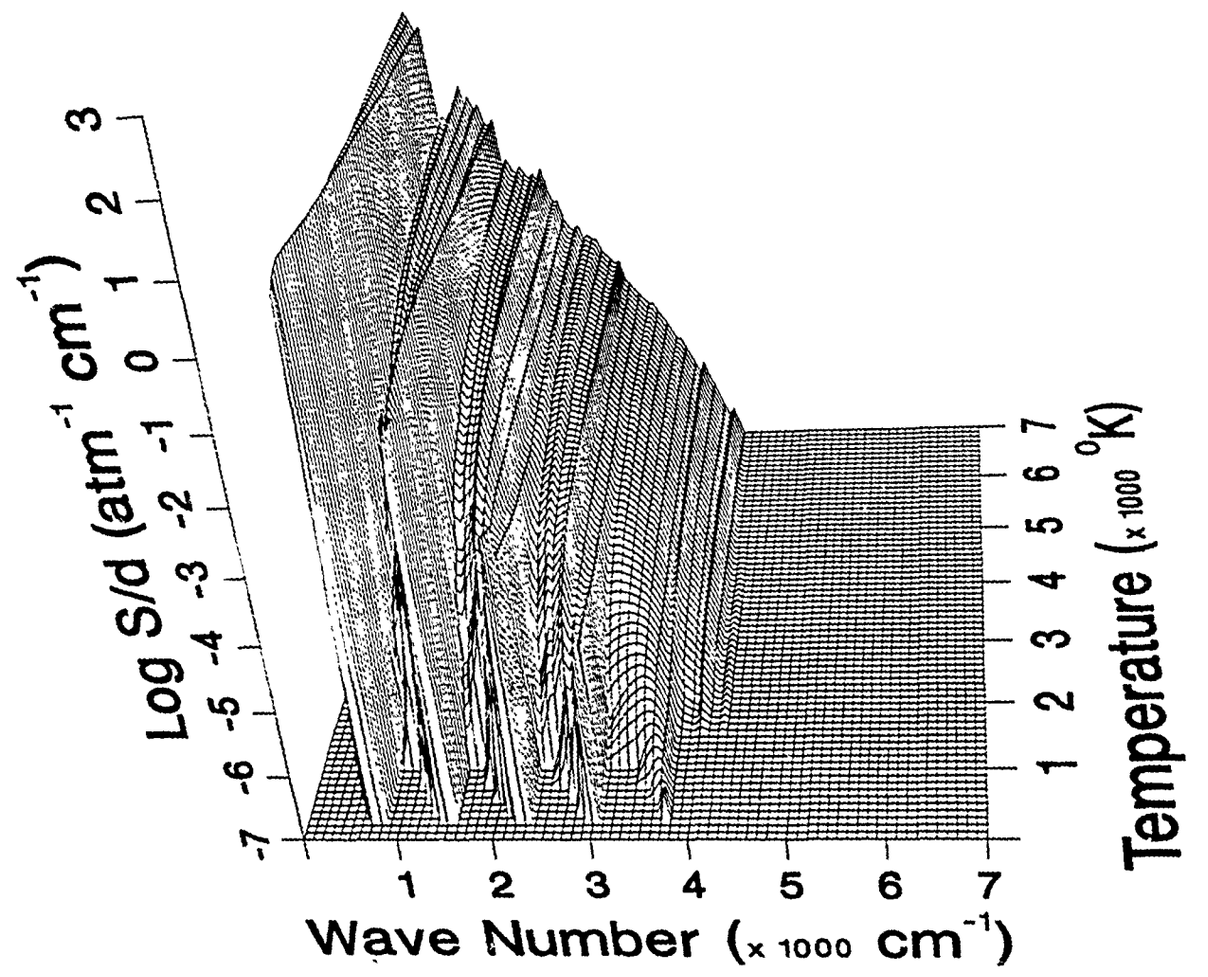

Figure 482. Weak-line parameter for UO.

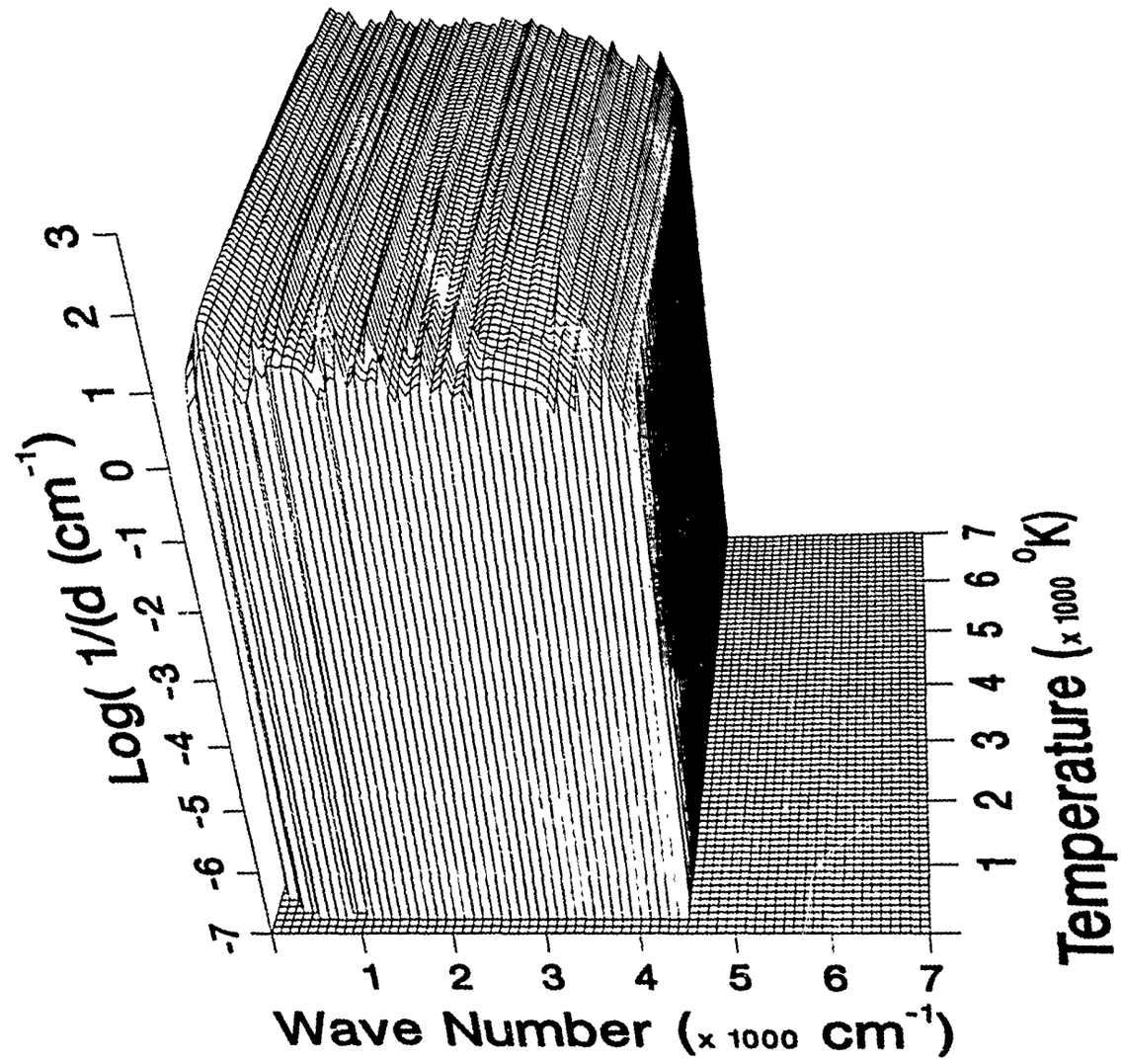

Figure 483. Inverse line spacing for UO.

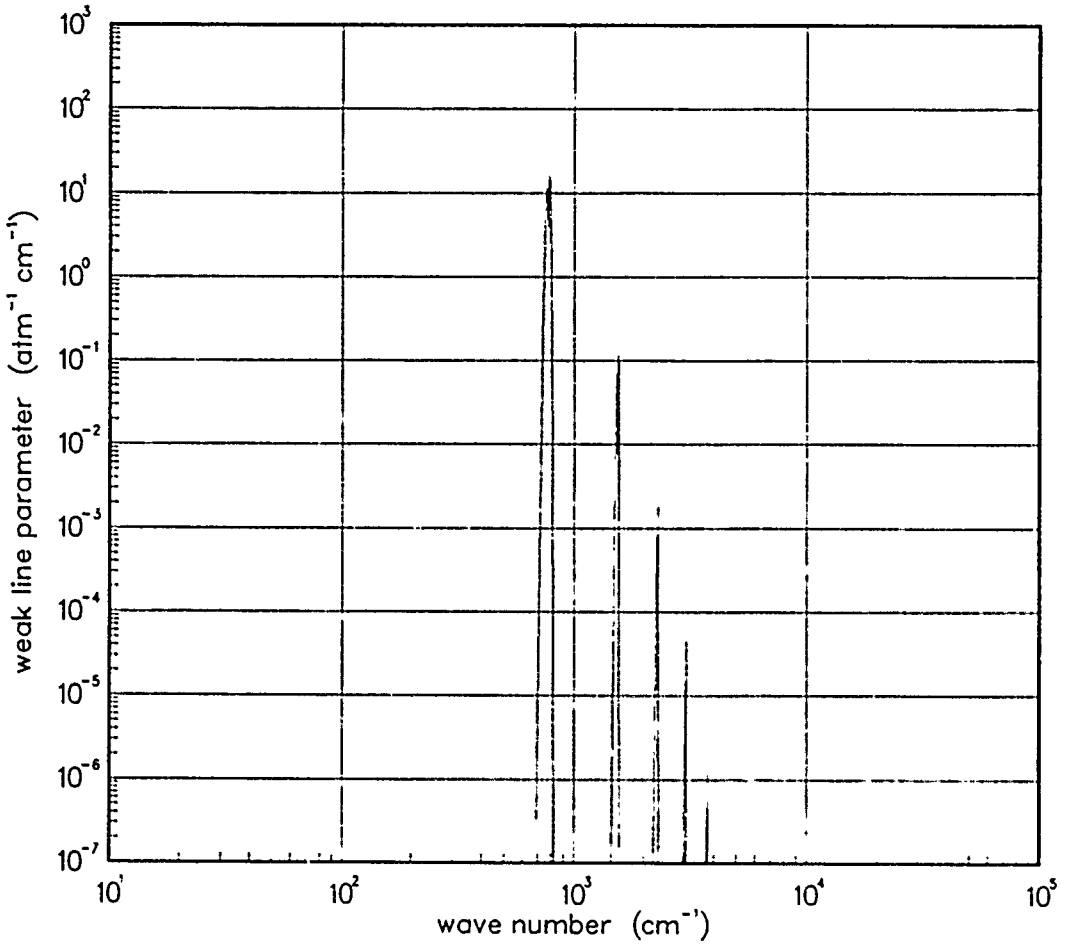

Figure 484. Weak-line parameter for UO at 200°K.

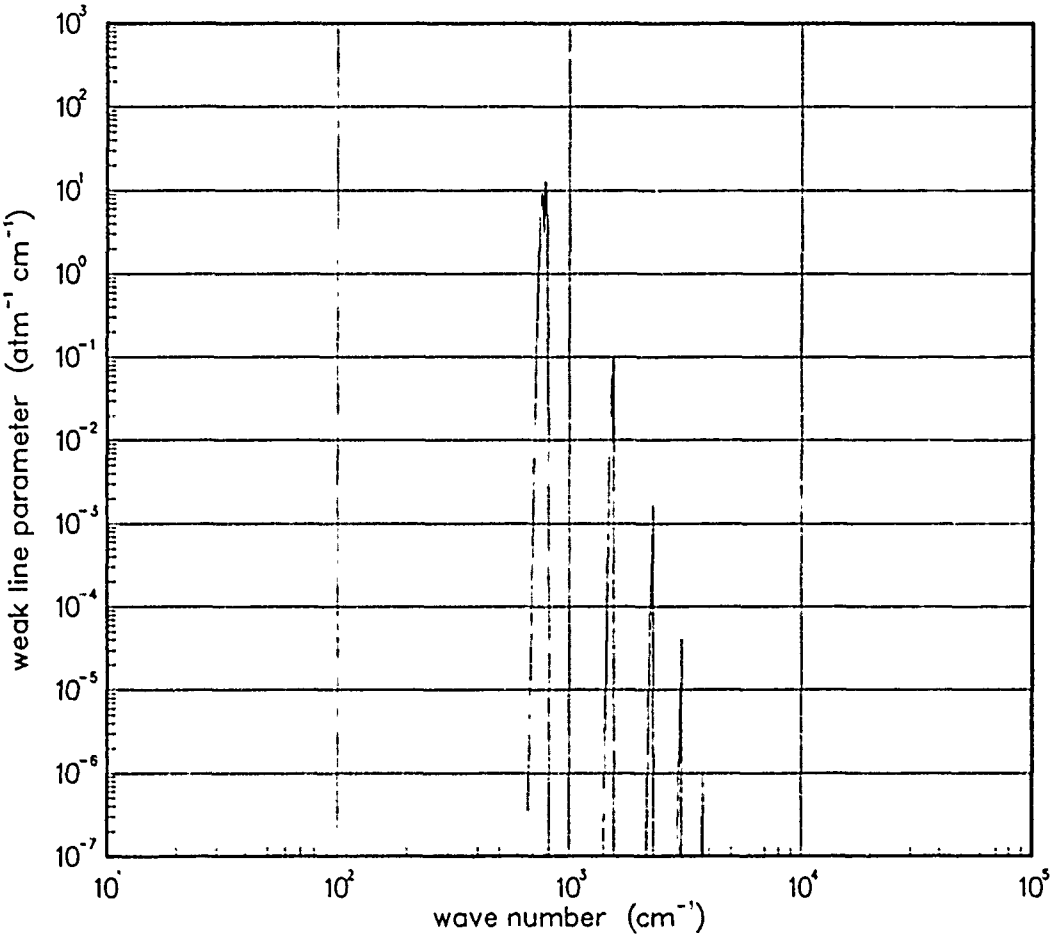

Figure 485. Weak-line parameter for UO at 300°K.

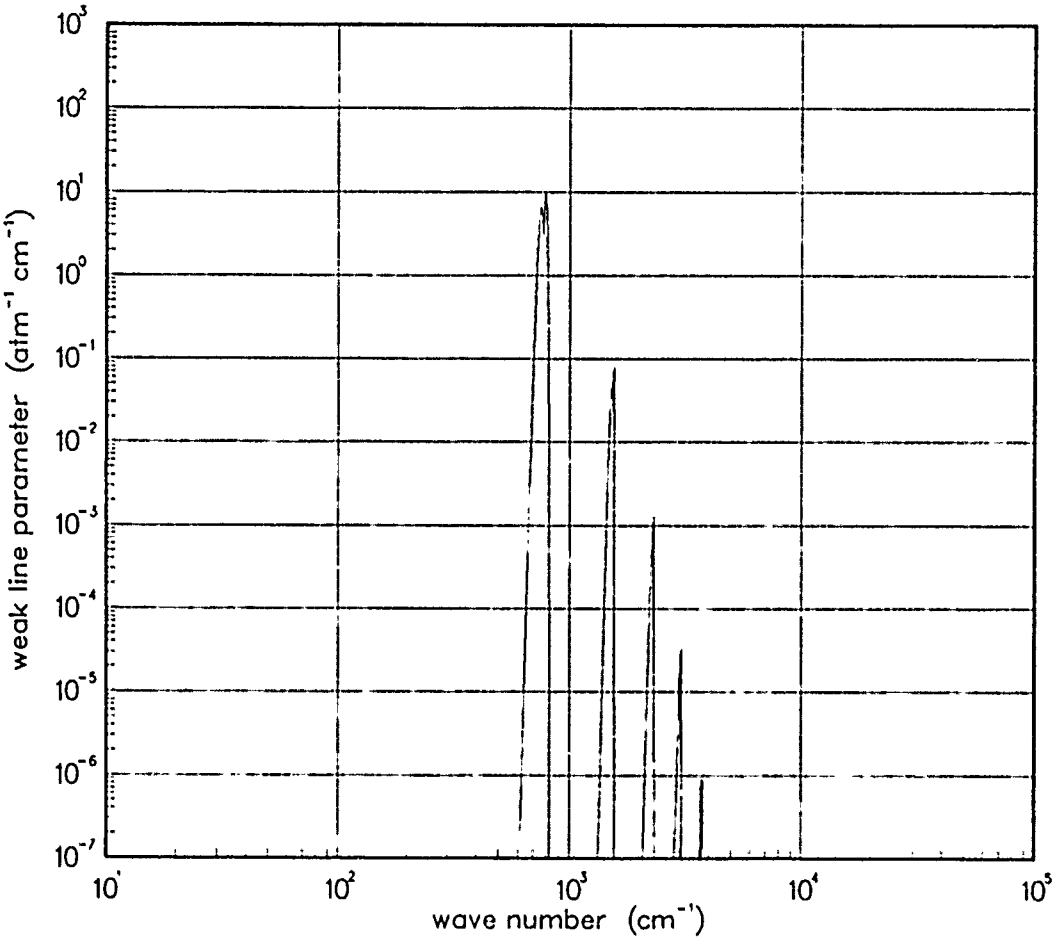

Figure 486. Weak-line parameter for UO at 500°K.

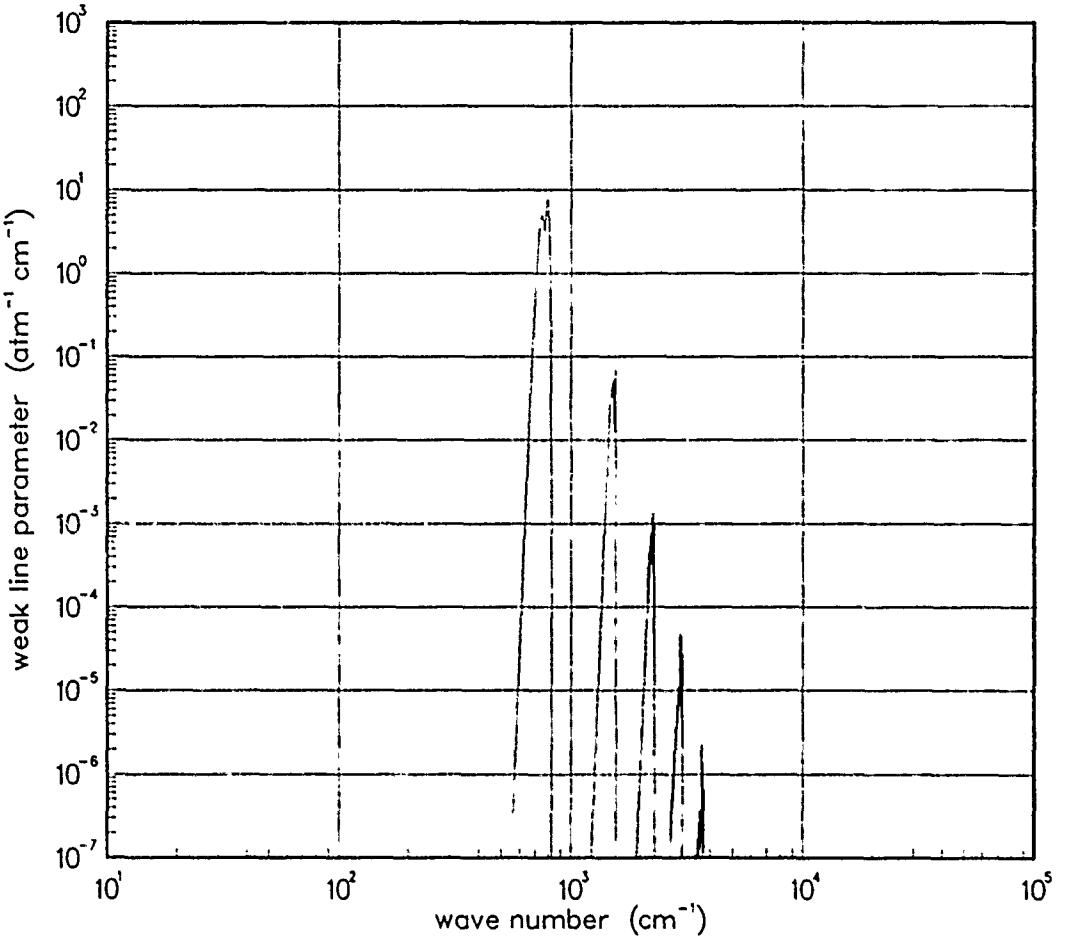

Figure 487. Weak-line parameter for UO at 750°K.

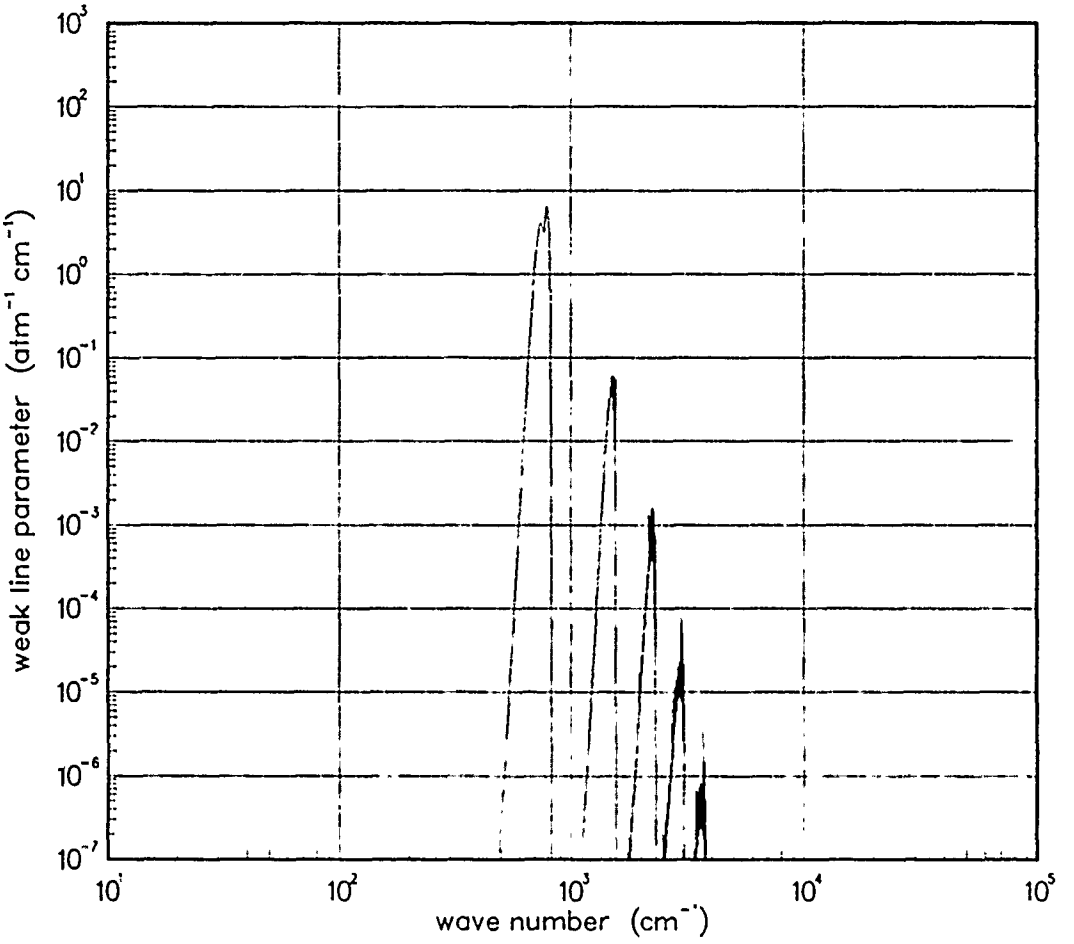

Figure 488. Weak-line parameter for UO at 1000°K.

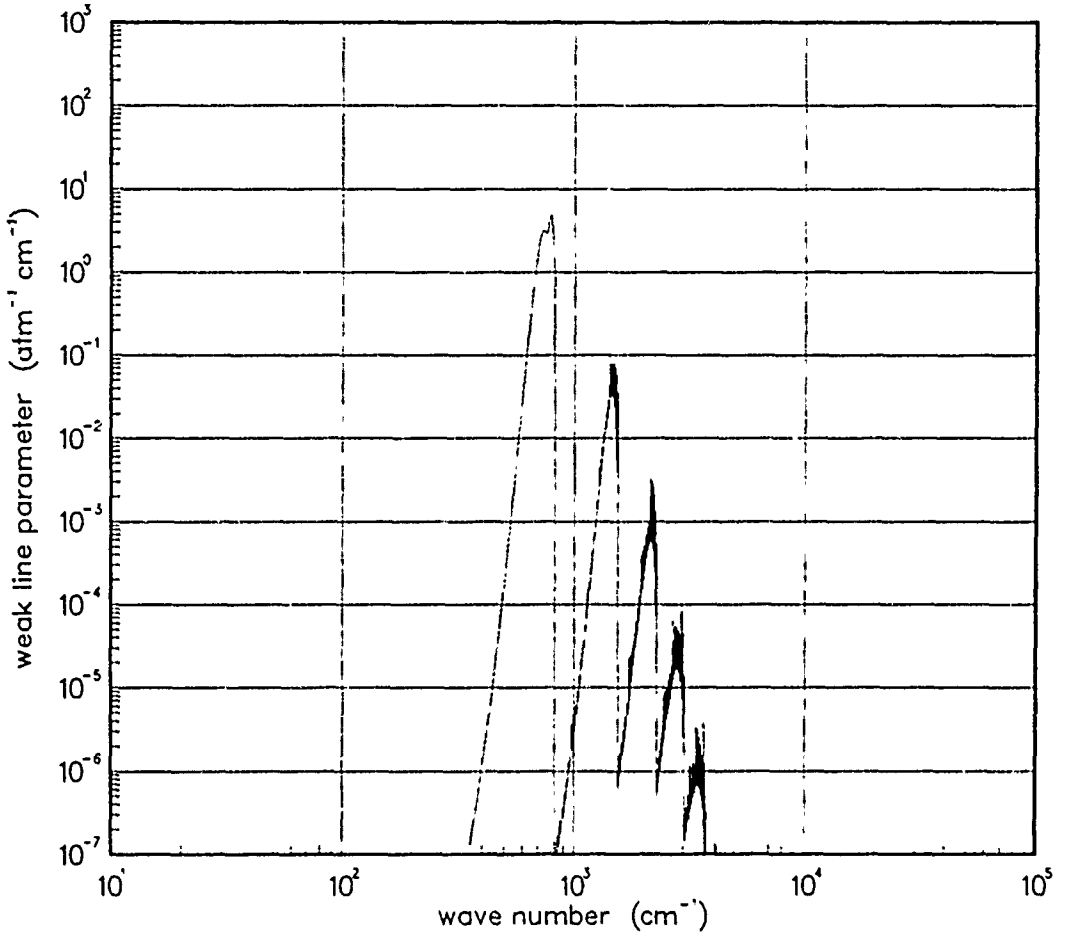

Figure 489. Weak-line parameter for UO at 1500°K.

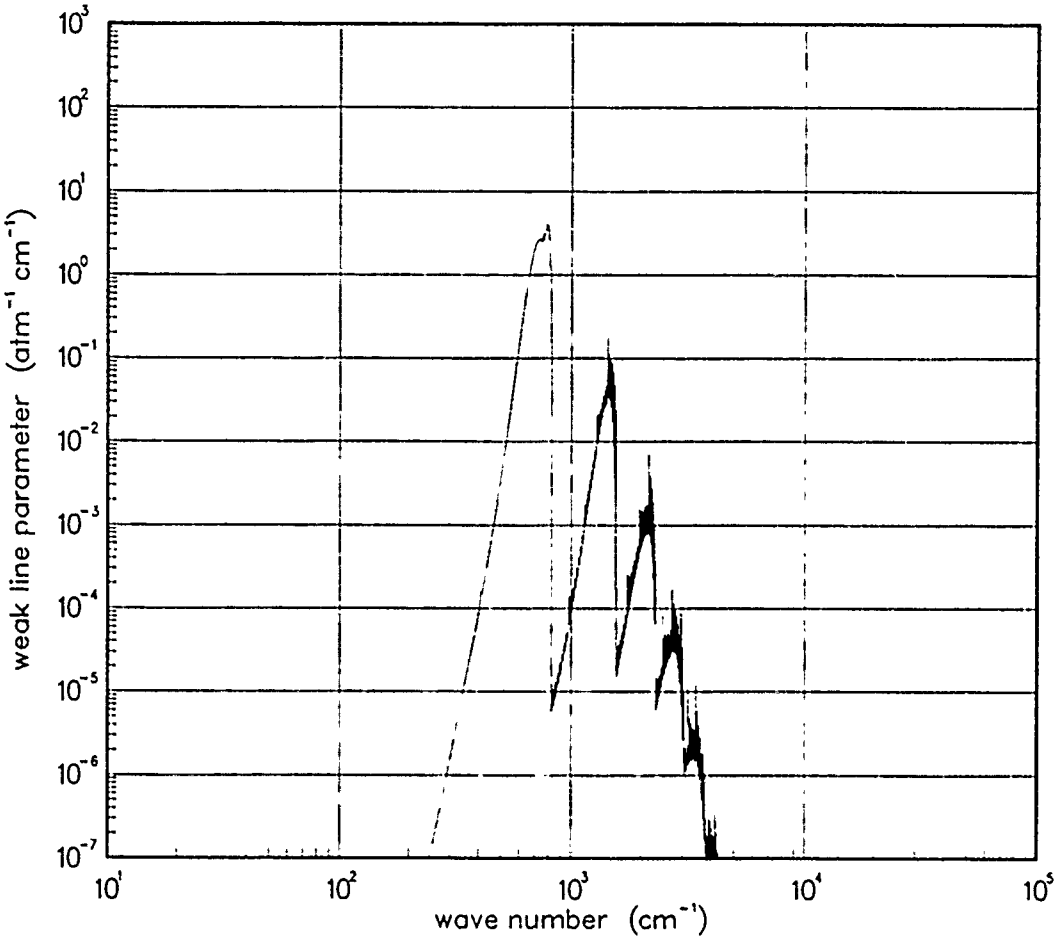

Figure 490. Weak-line parameter for UO at 2000°K.

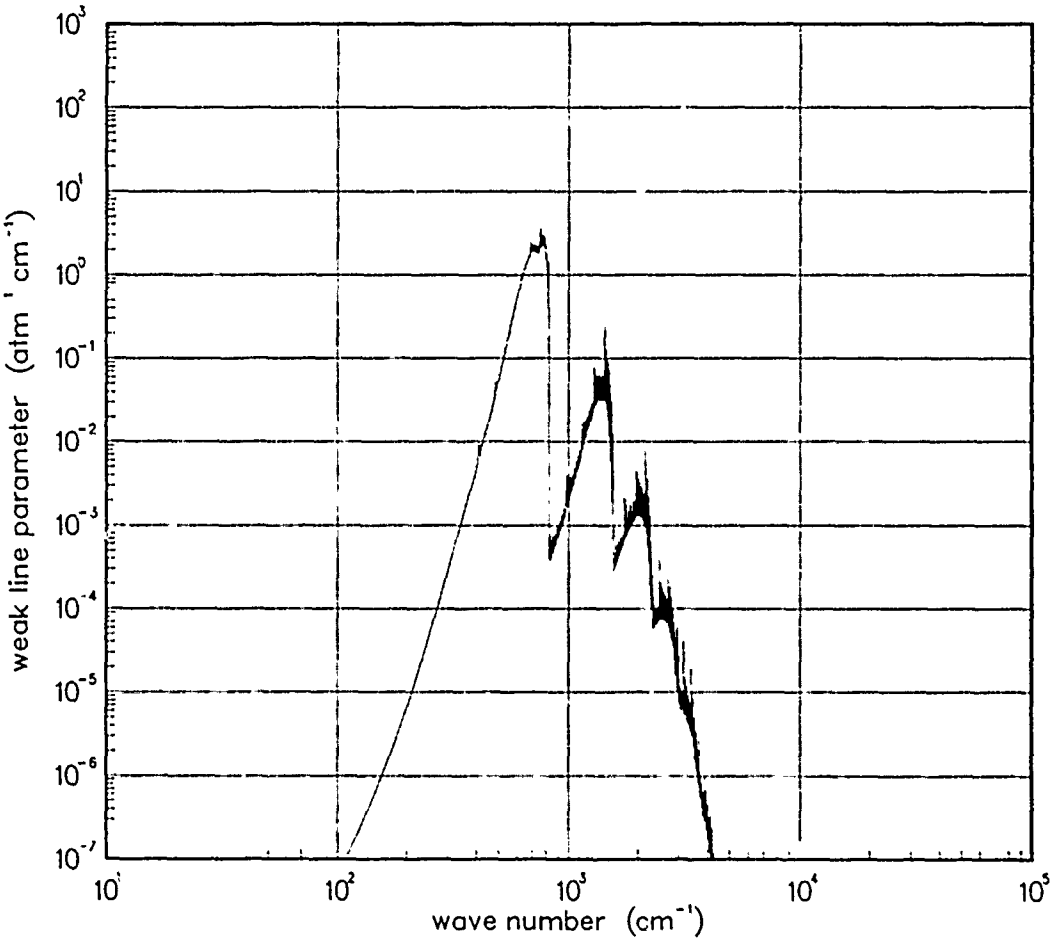

Figure 491. Weak-line parameter for UO at 3000°K.

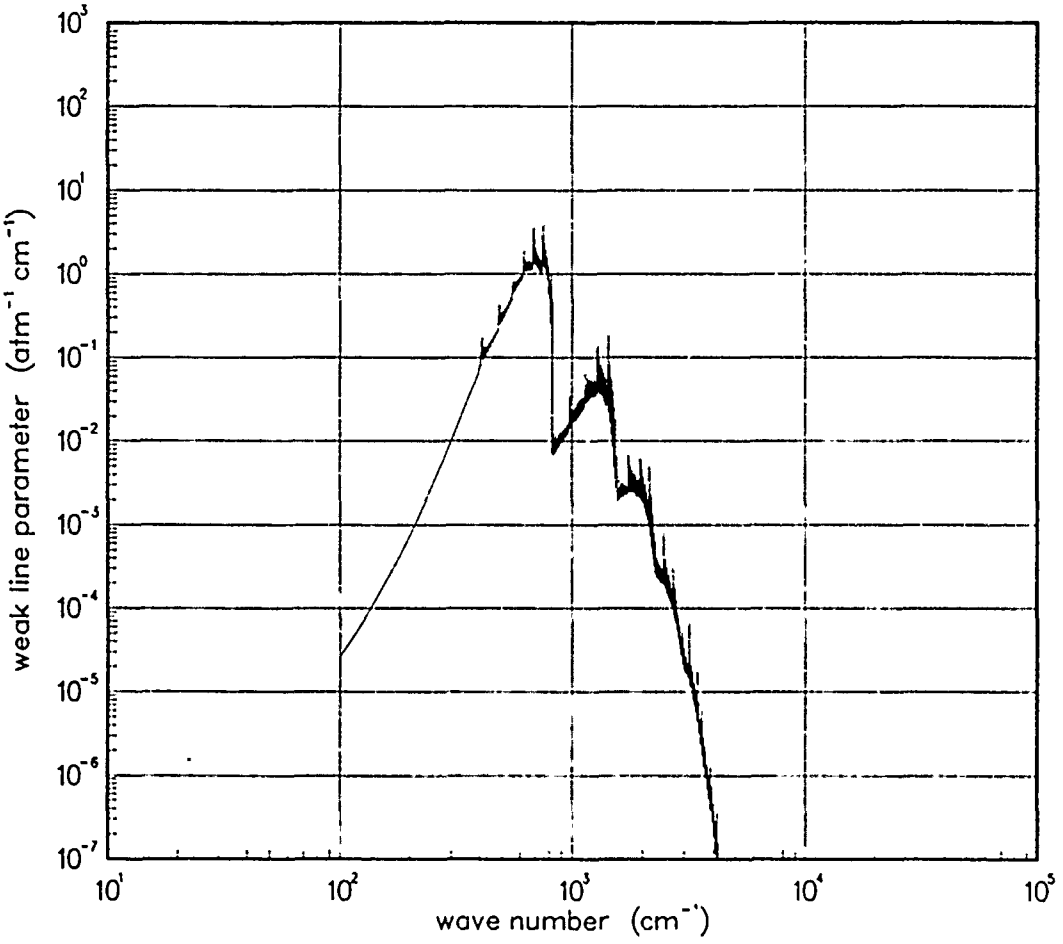

Figure 492. Weak-line parameter for UO at 5000°K.

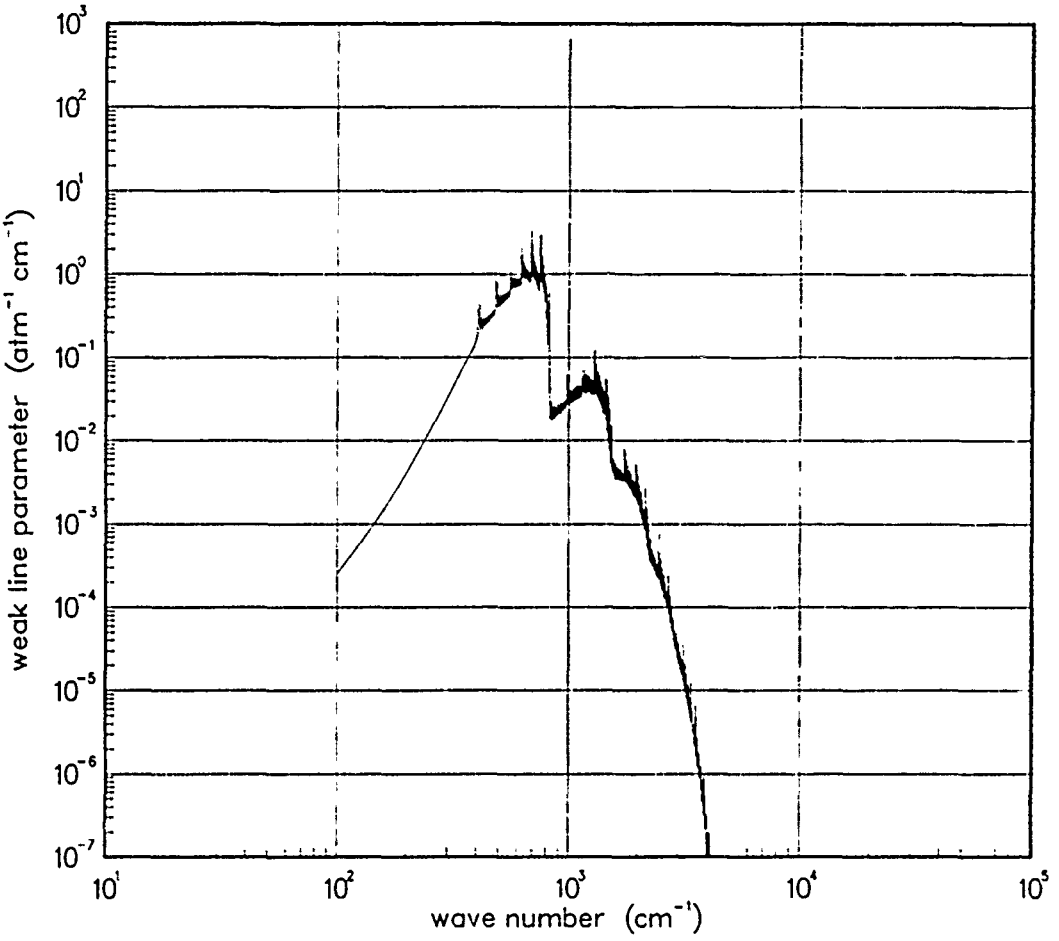

Figure 493. Weak-line parameter for UO at 7000°K.

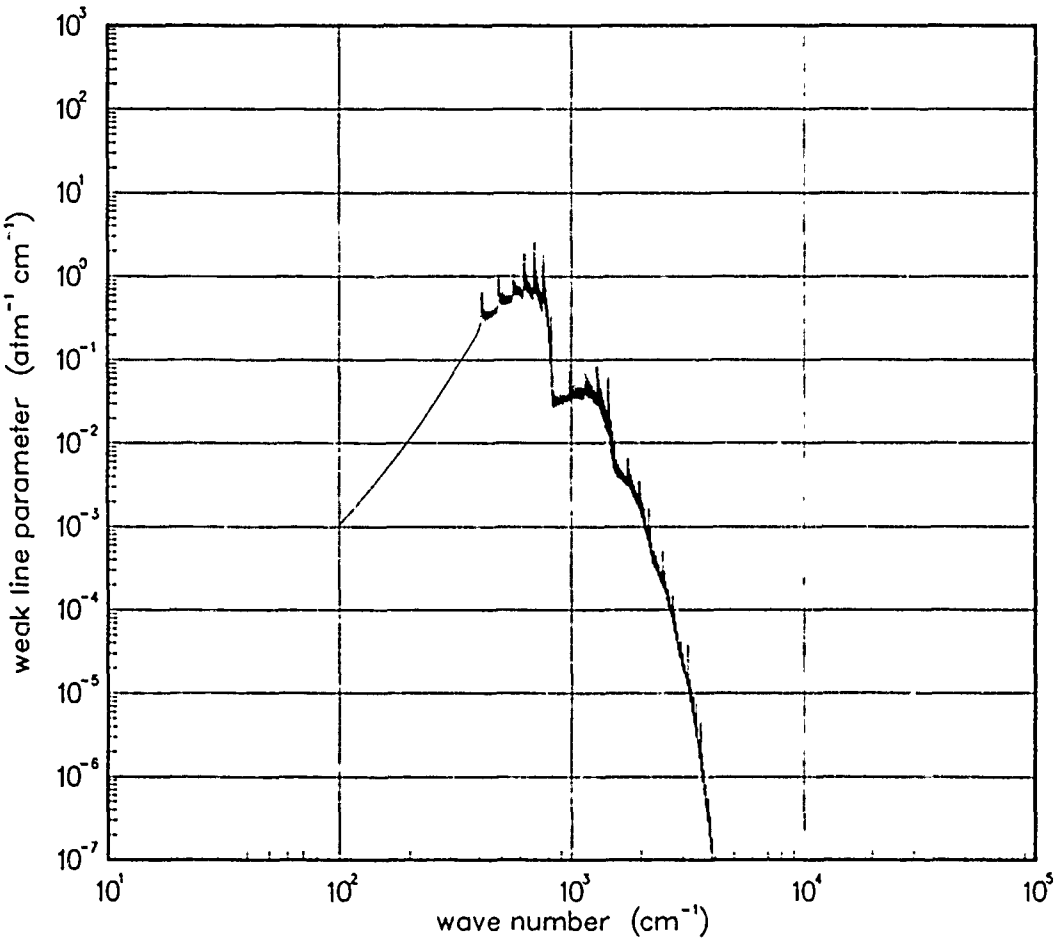

Figure 494. Weak-line parameter for UO at 10000°K.

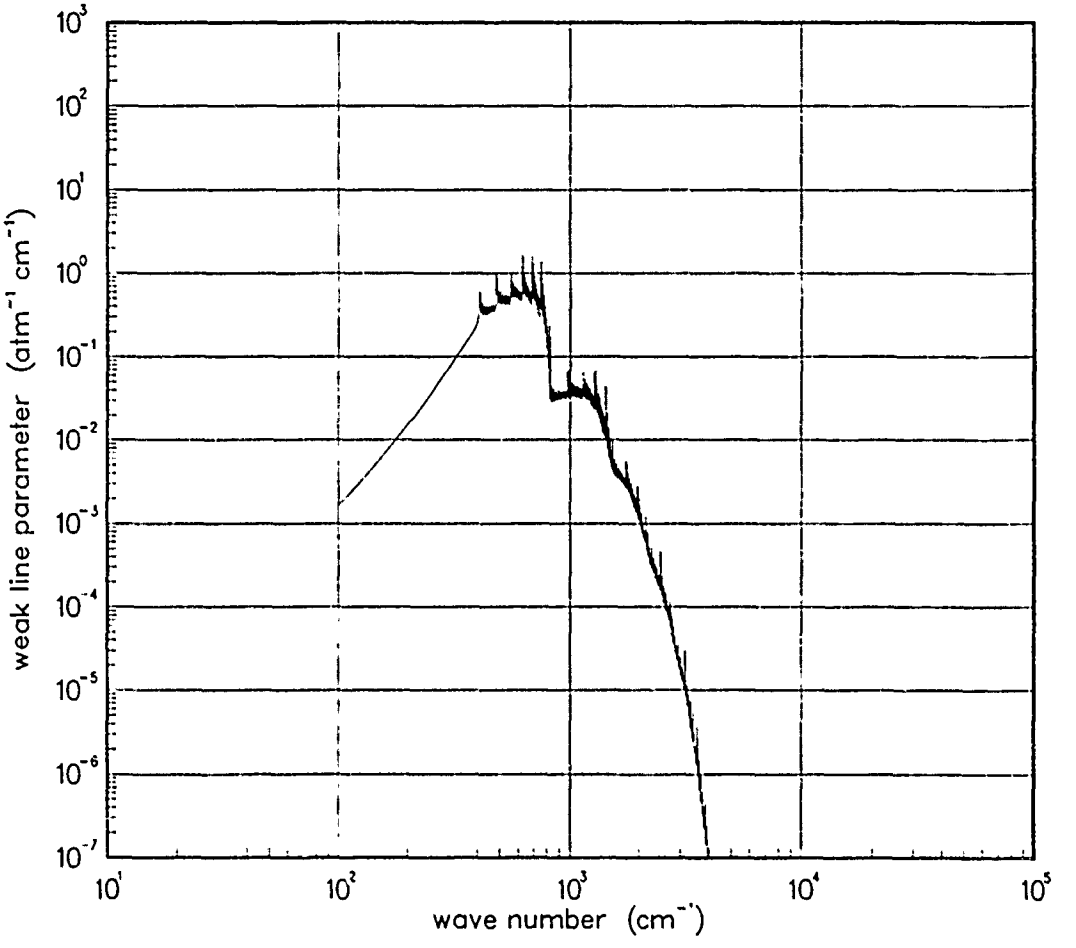

Figure 495. Weak-line parameter for UO at 12000°K.

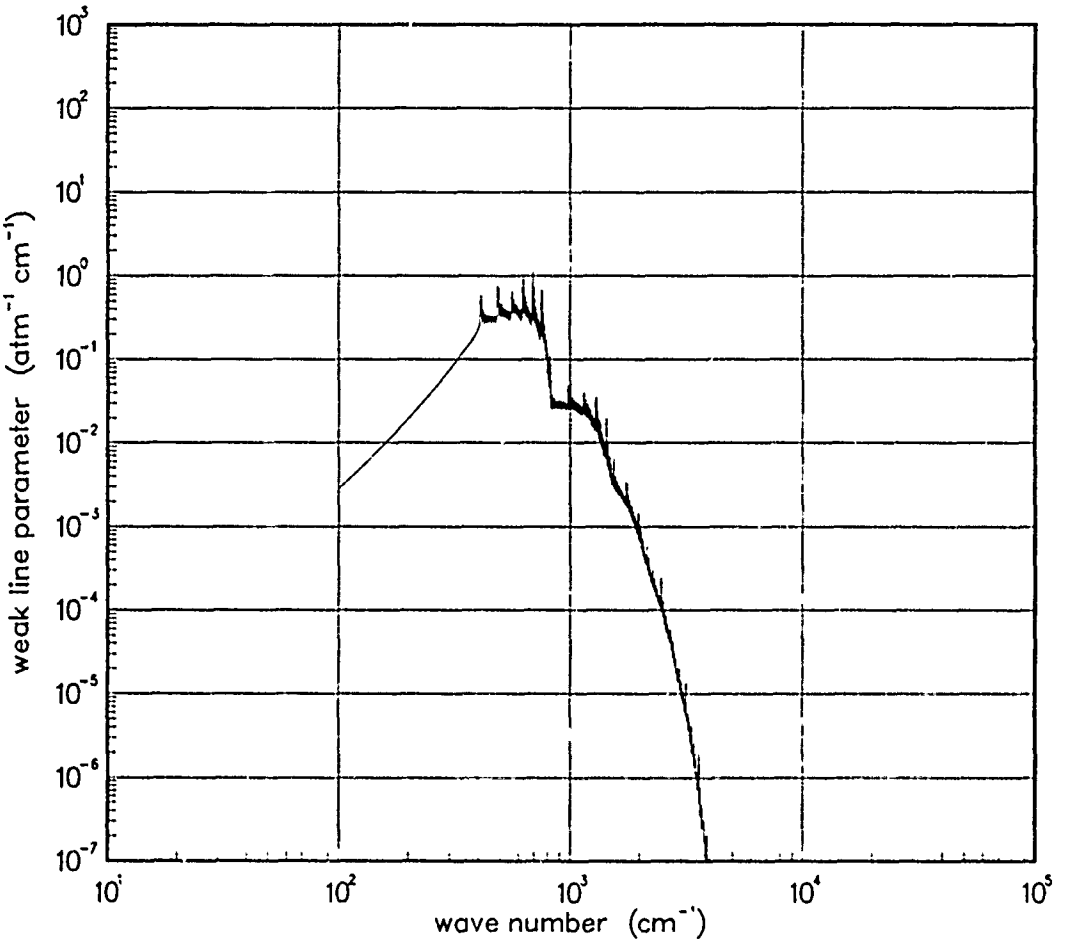

Figure 496. Weak-line parameter for UO at 180.0°K.

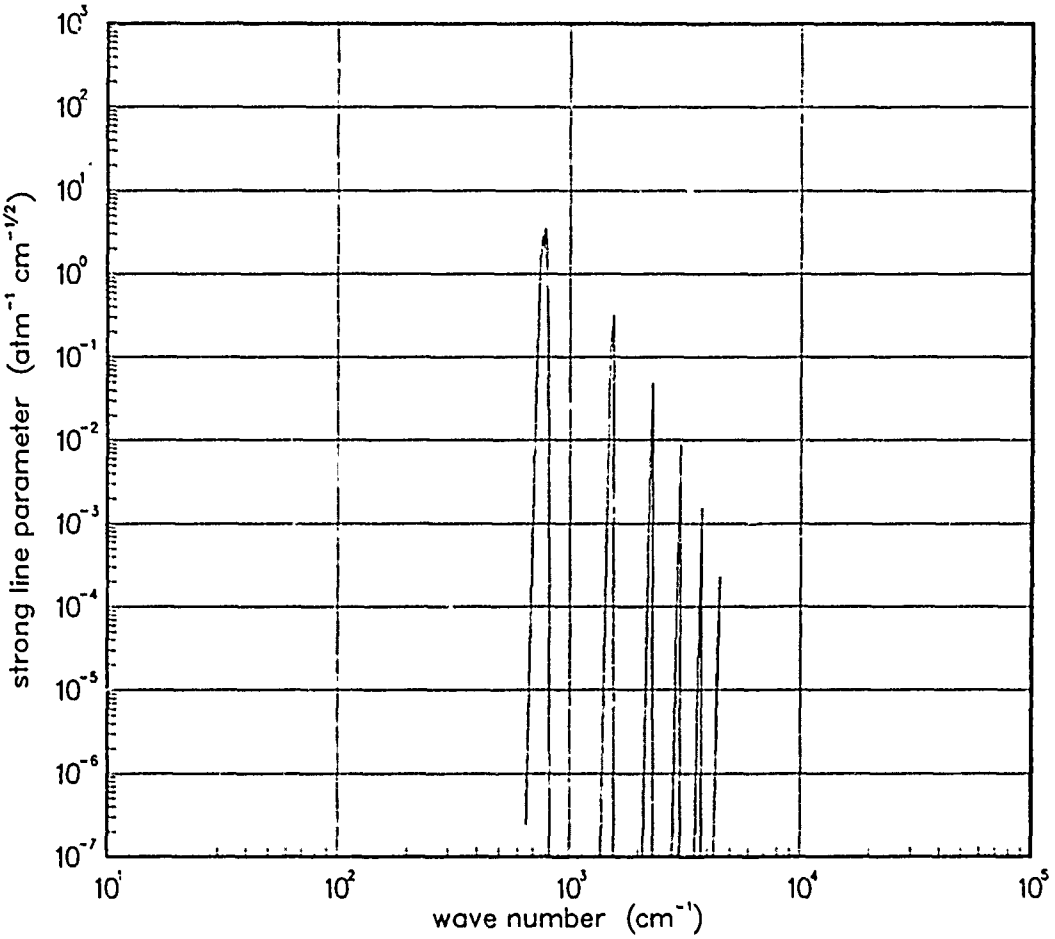

Figure 497. Strong-line parameter for UO at 200°K.

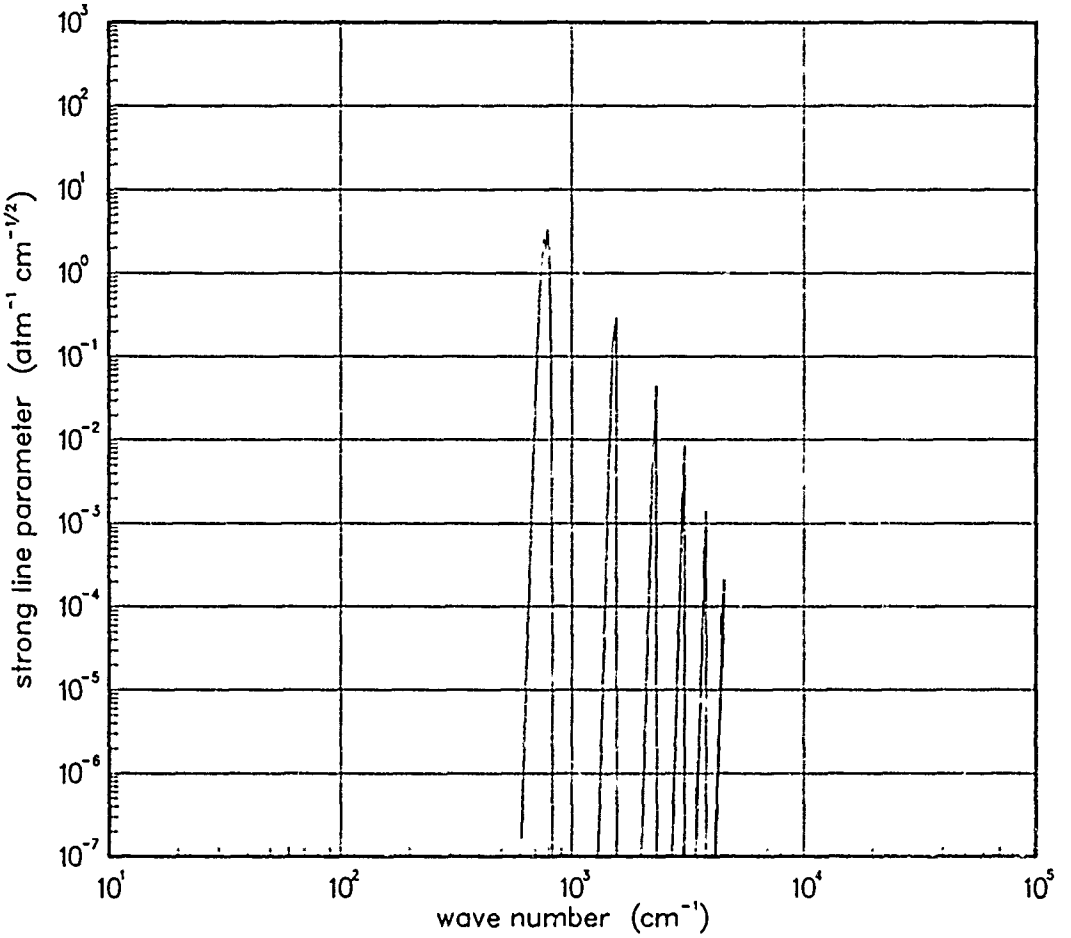

Figure 498. Strong-line parameter for UO at 300°K.

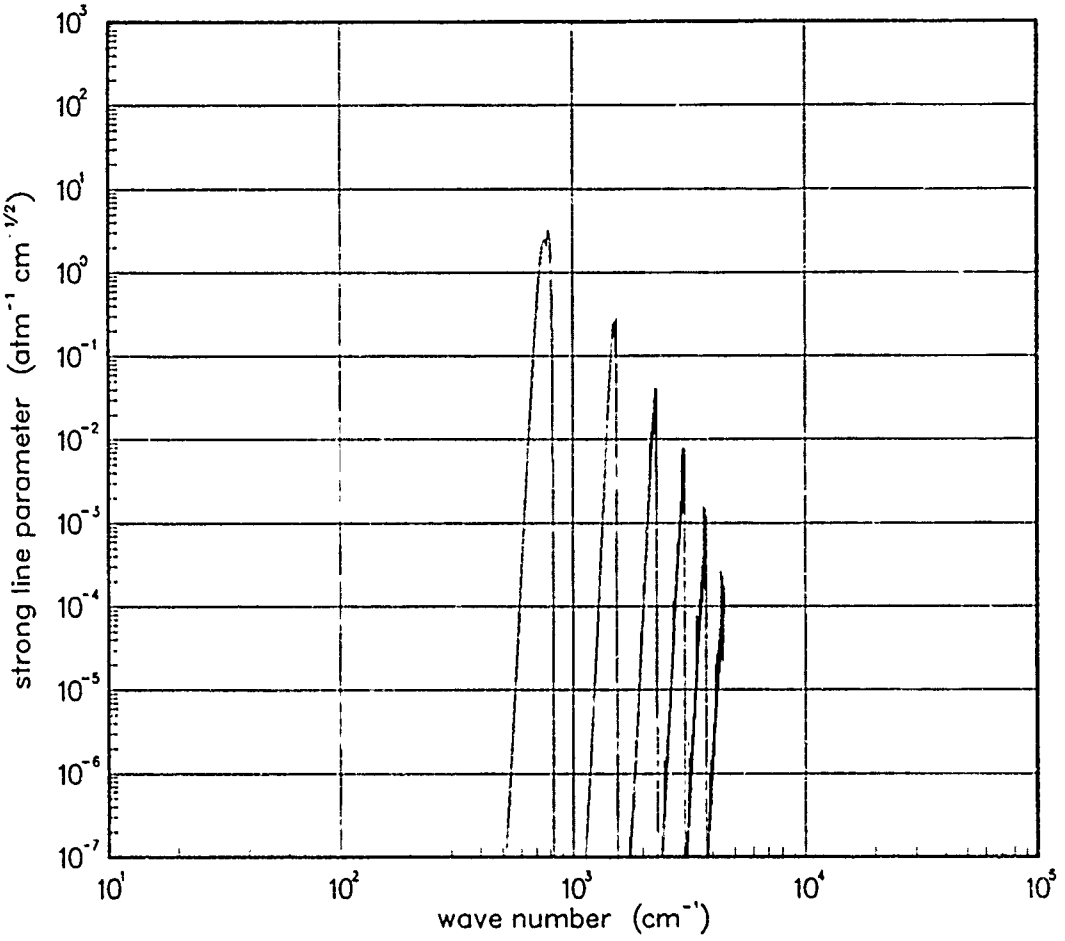

Figure 499. Strong-line parameter for UO at 500°K.

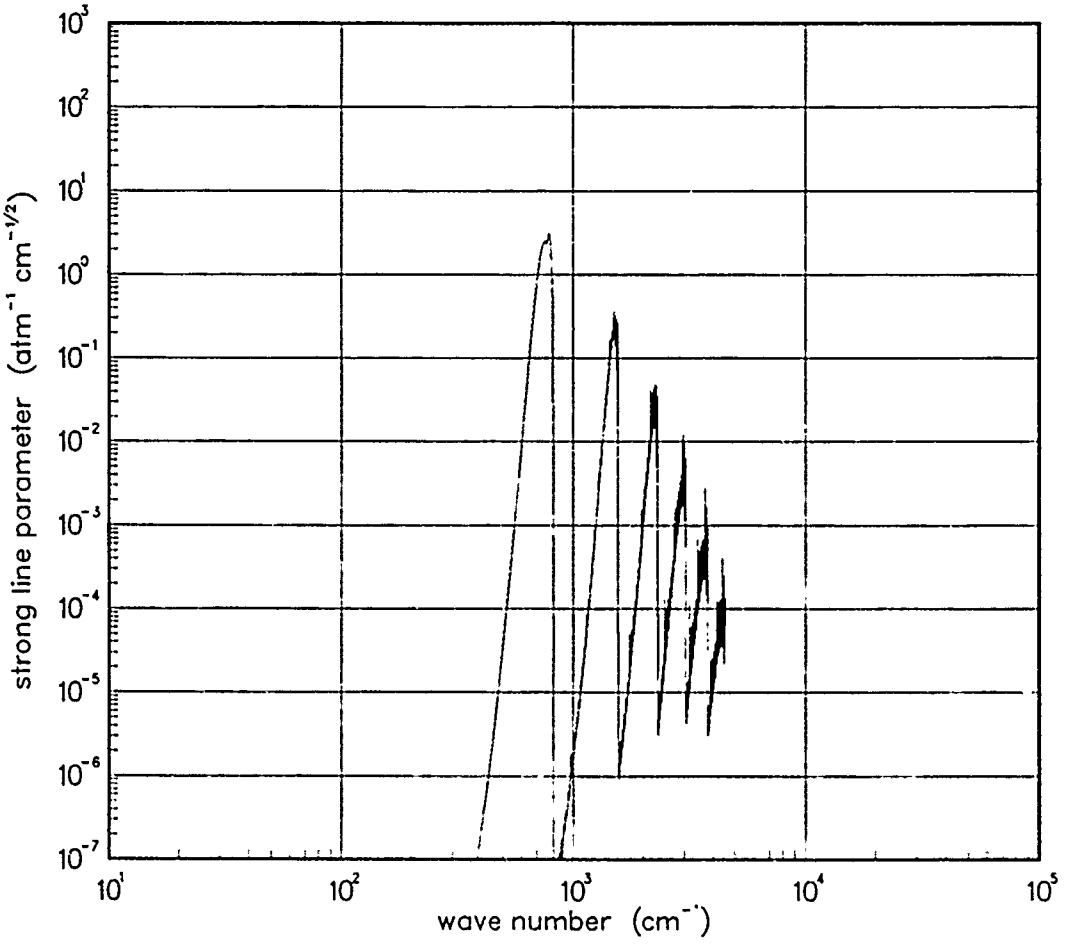

Figure 500. Strong-line parameter for UO at 750°K.

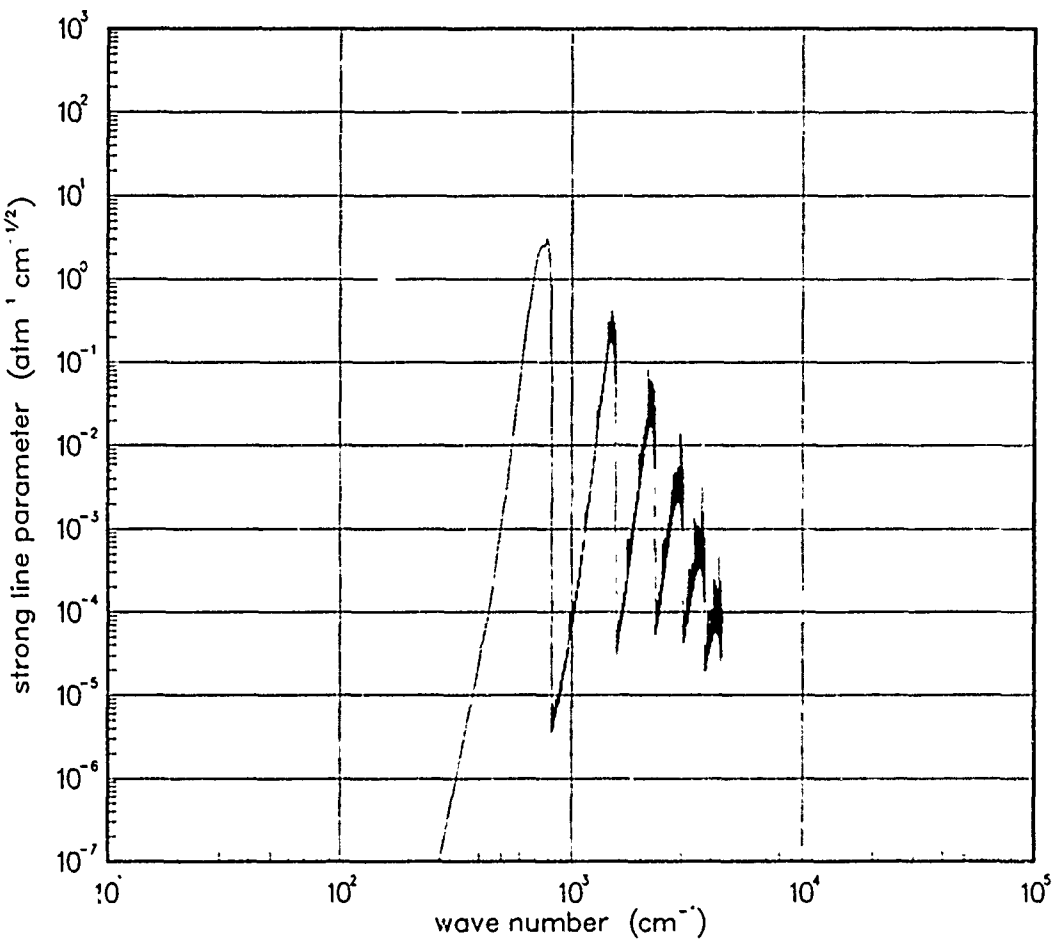

Figure 501. Strong-line parameter for UO at 1000°K.

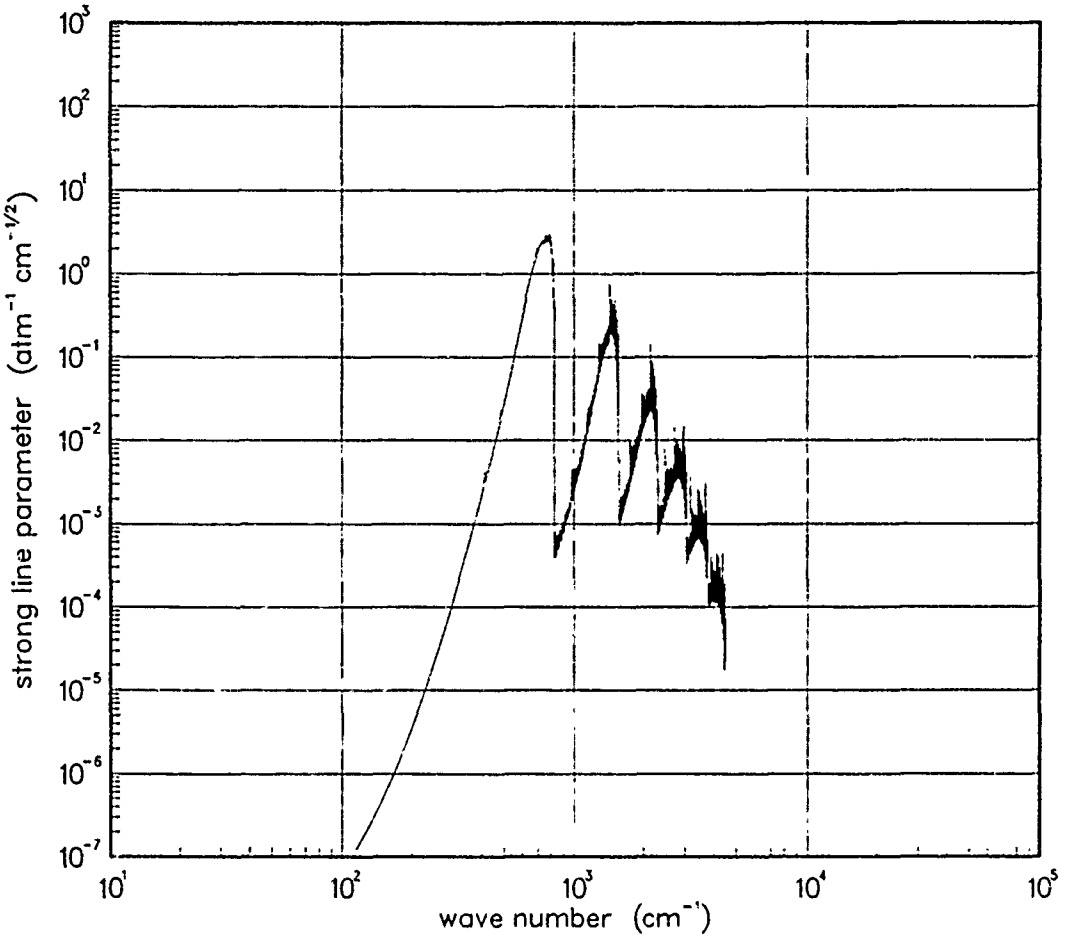

Figure 502. Strong-line parameter for UO at 1500°K.

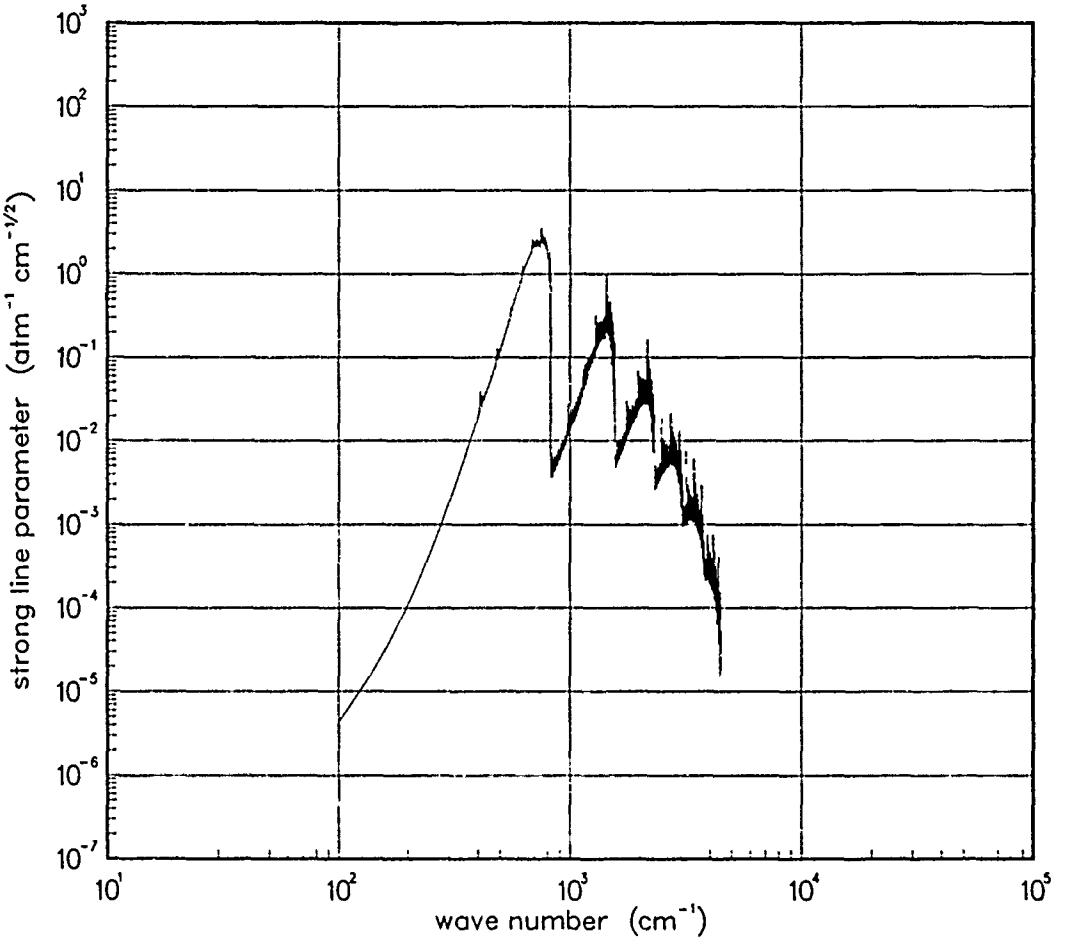

Figure 503. Strong-line parameter for UO at 2000°K.

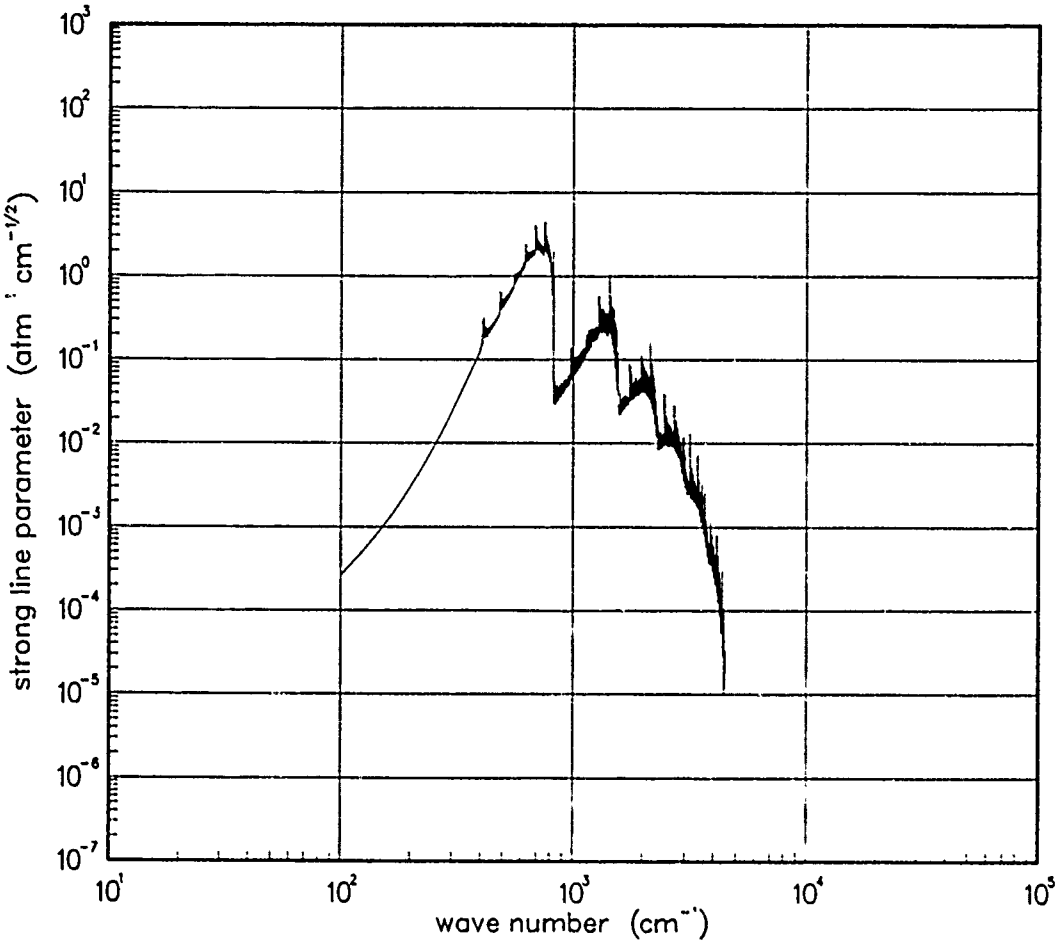

Figure 504. Strong-line parameter for UO at 3000°K.

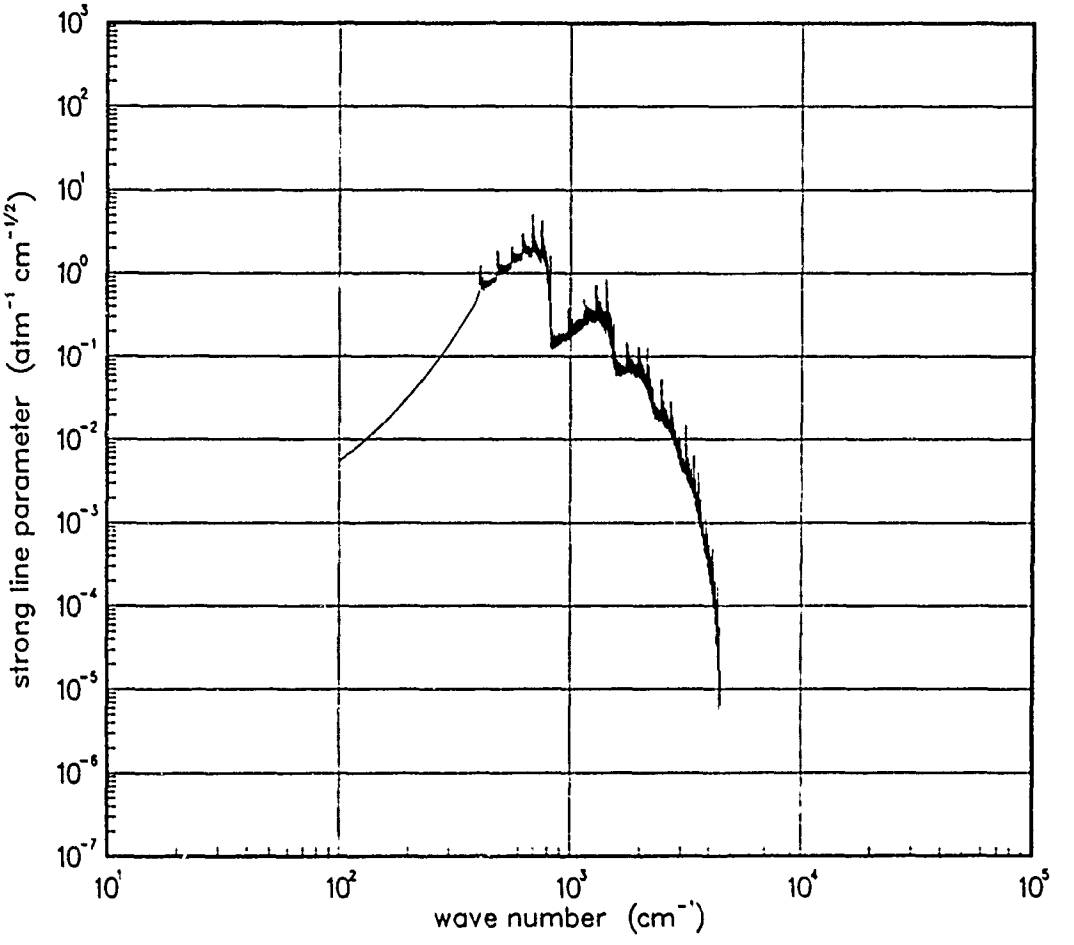

Figure 505. Strong-line parameter for UO at 5000°K.

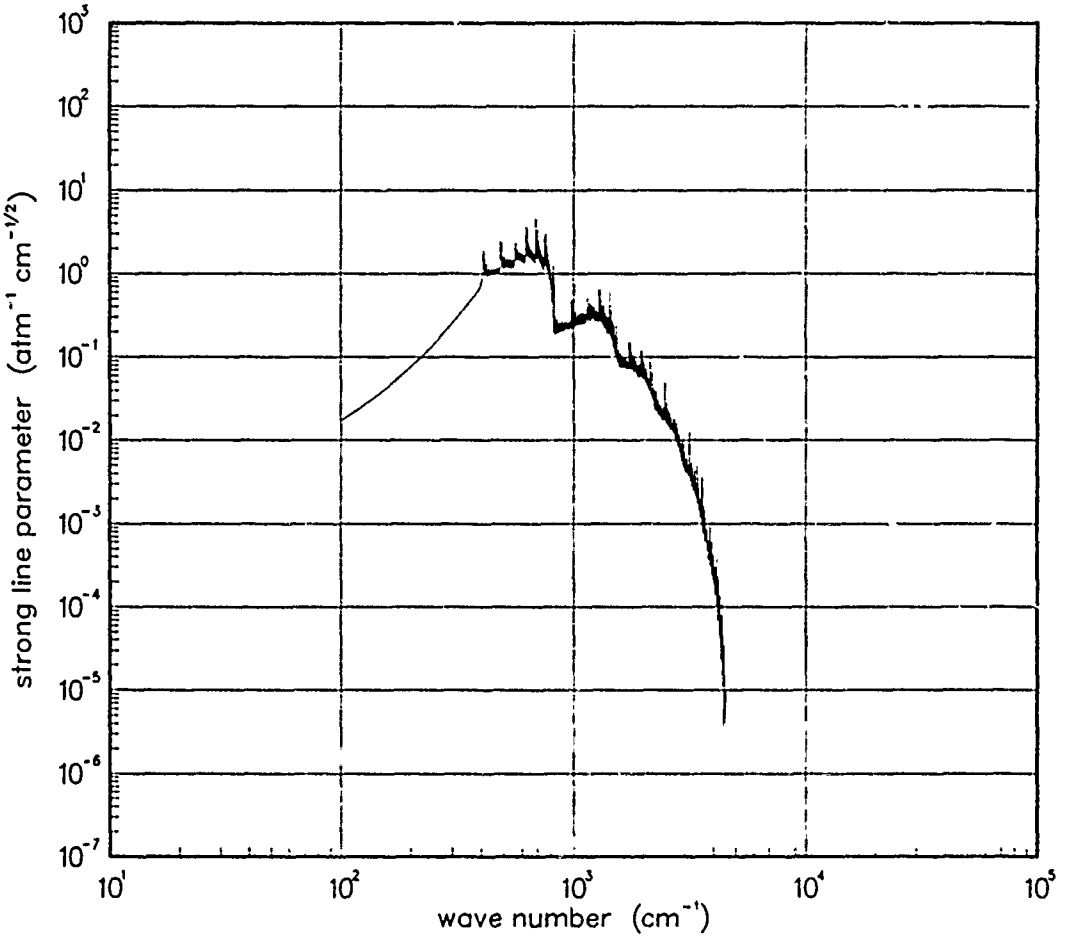

Figure 506. Strong-line parameter for UO at 7000°K.

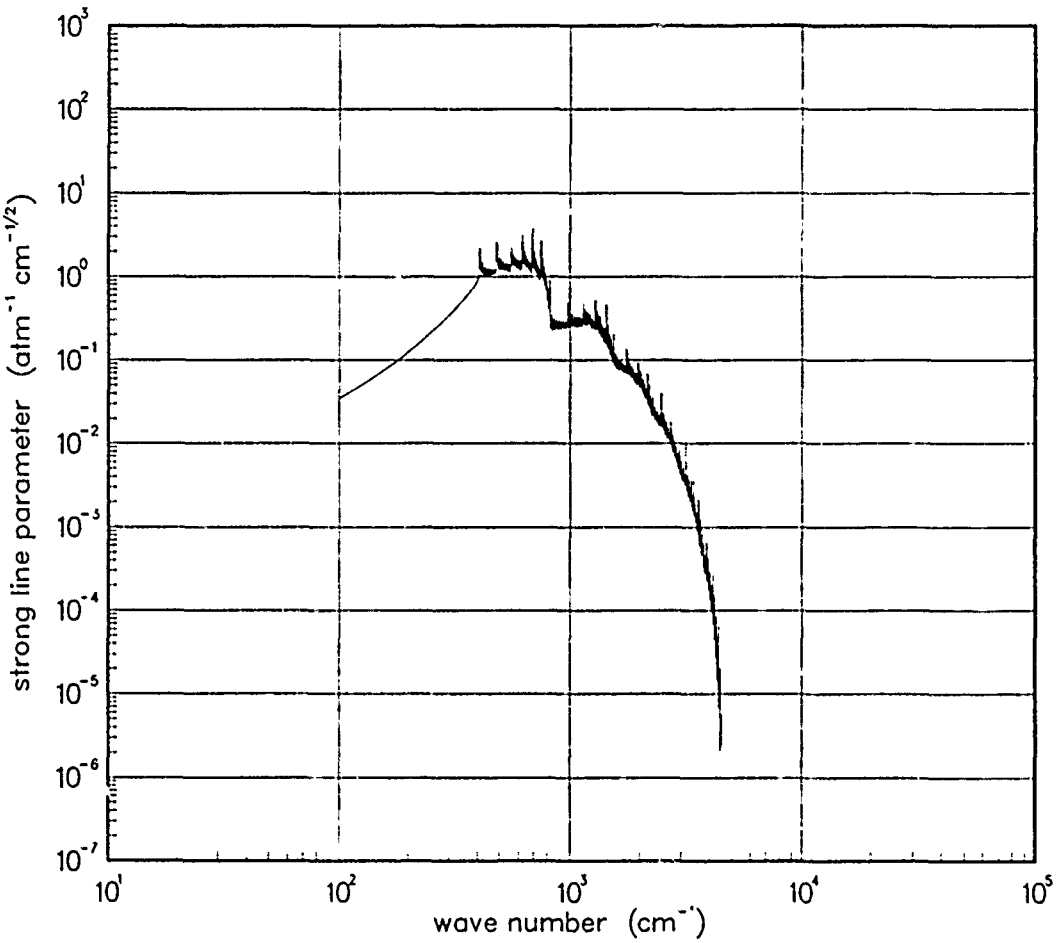

Figure 507. Strong-line parameter for UO at 10000°K.

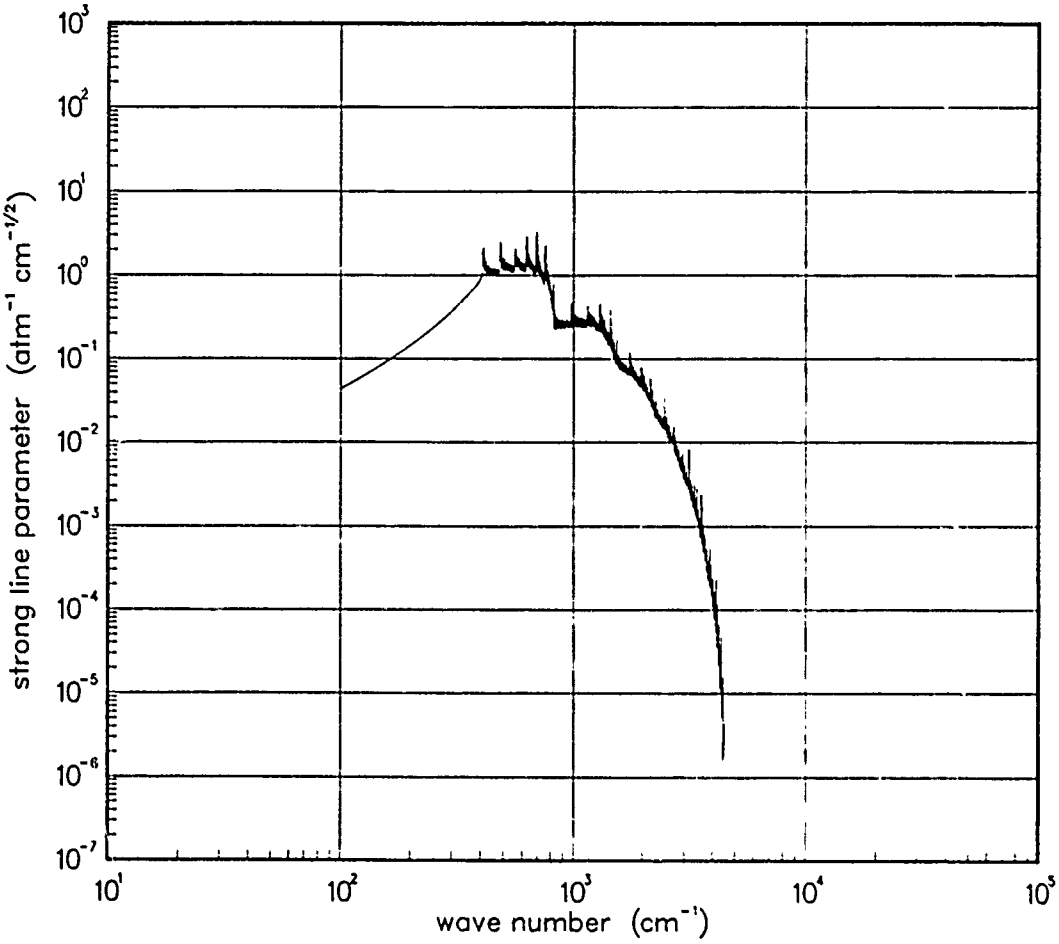

Figure 508. Strong-line parameter for UO at 12000°K.

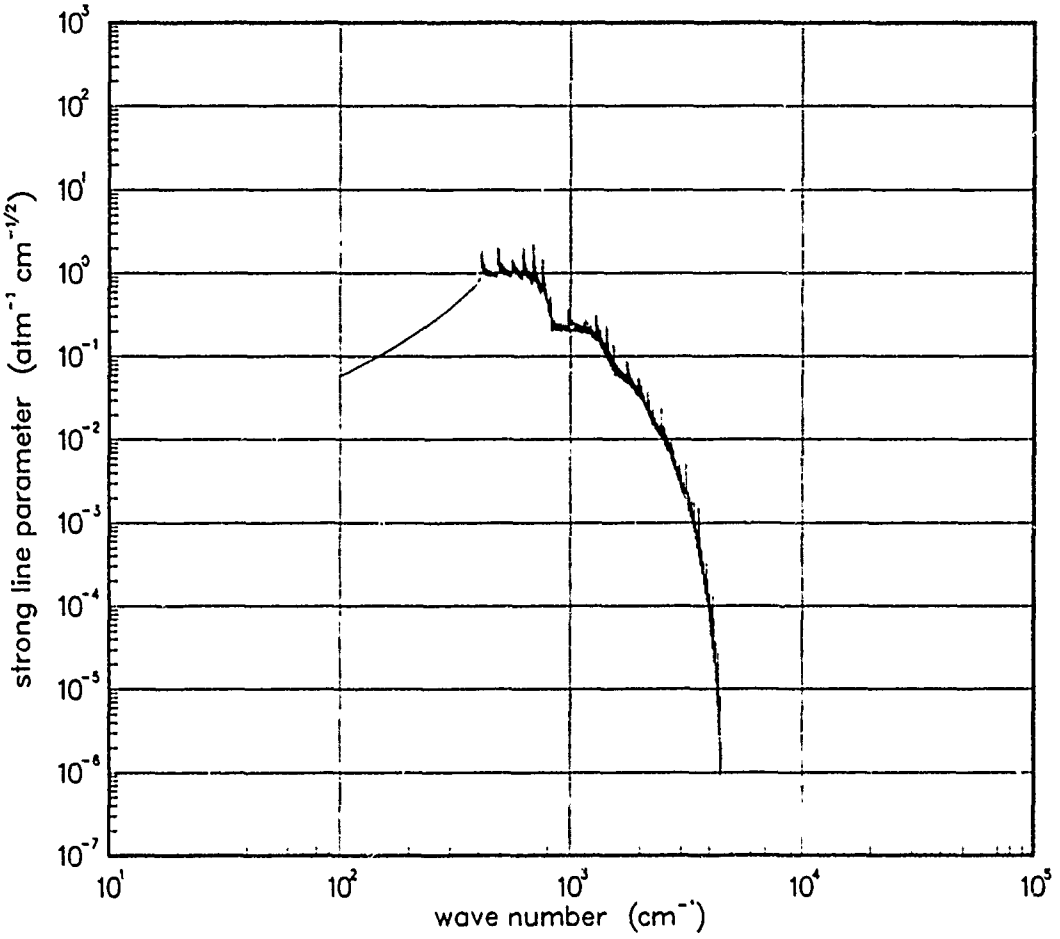

Figure 509. Strong-line parameter for UO at 18000°K.

The SOD and DEI's for UO^+ were calculated in 1985. The source of the molecular constants that were used in these calculations is unknown.

Table 15. Spectroscopic data for UO^+.

Ground Electronic State

ω_e = 925.00 $\omega_e x_e$ = 2.70
α_e = .0020 B_e = 0.330

S_{10} = 1190.0

γ_e(300°K) = 0.04*

Data Source:

*Estimate.

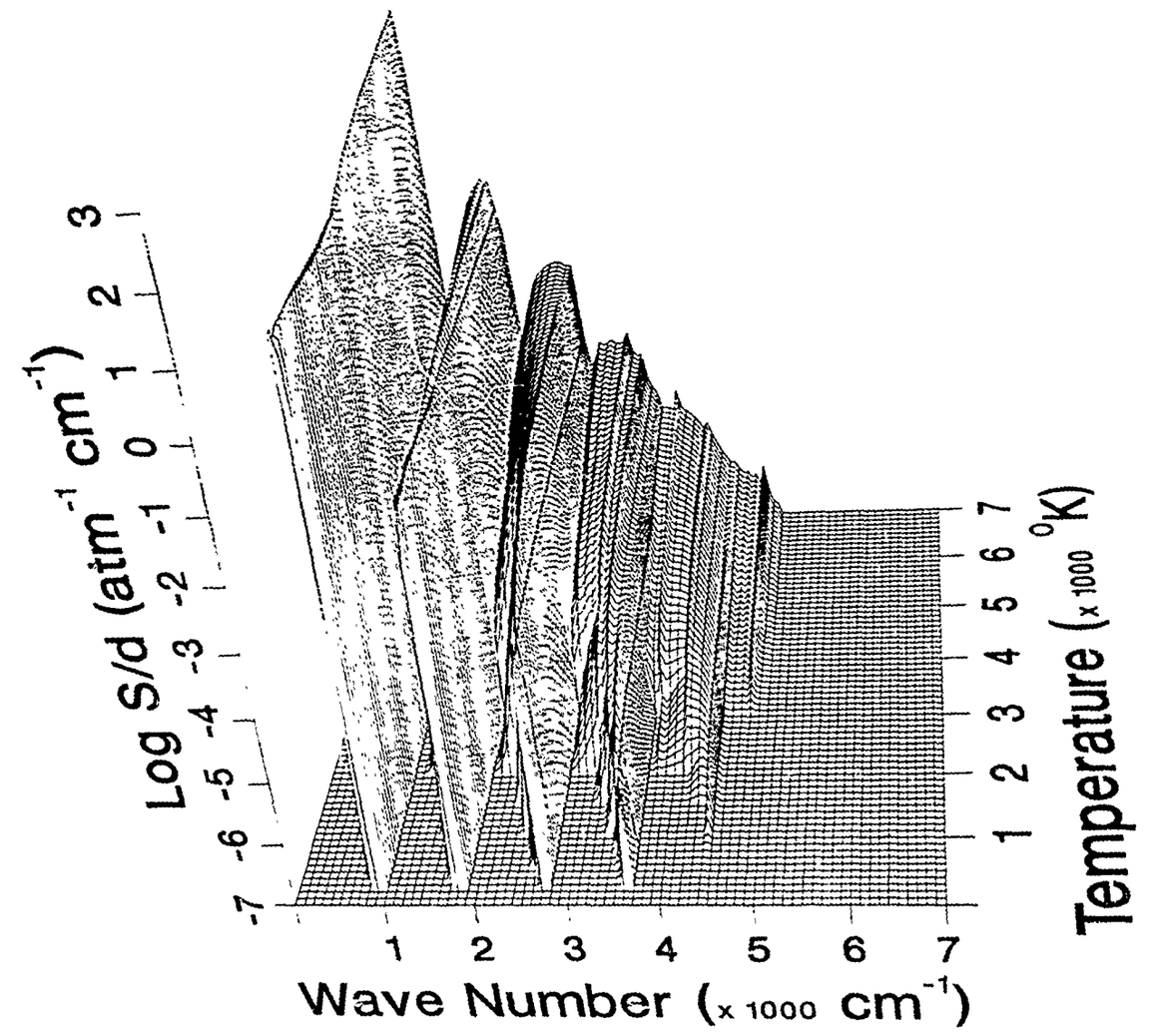

Figure 510. Weak-line parameter for UO^{+}.

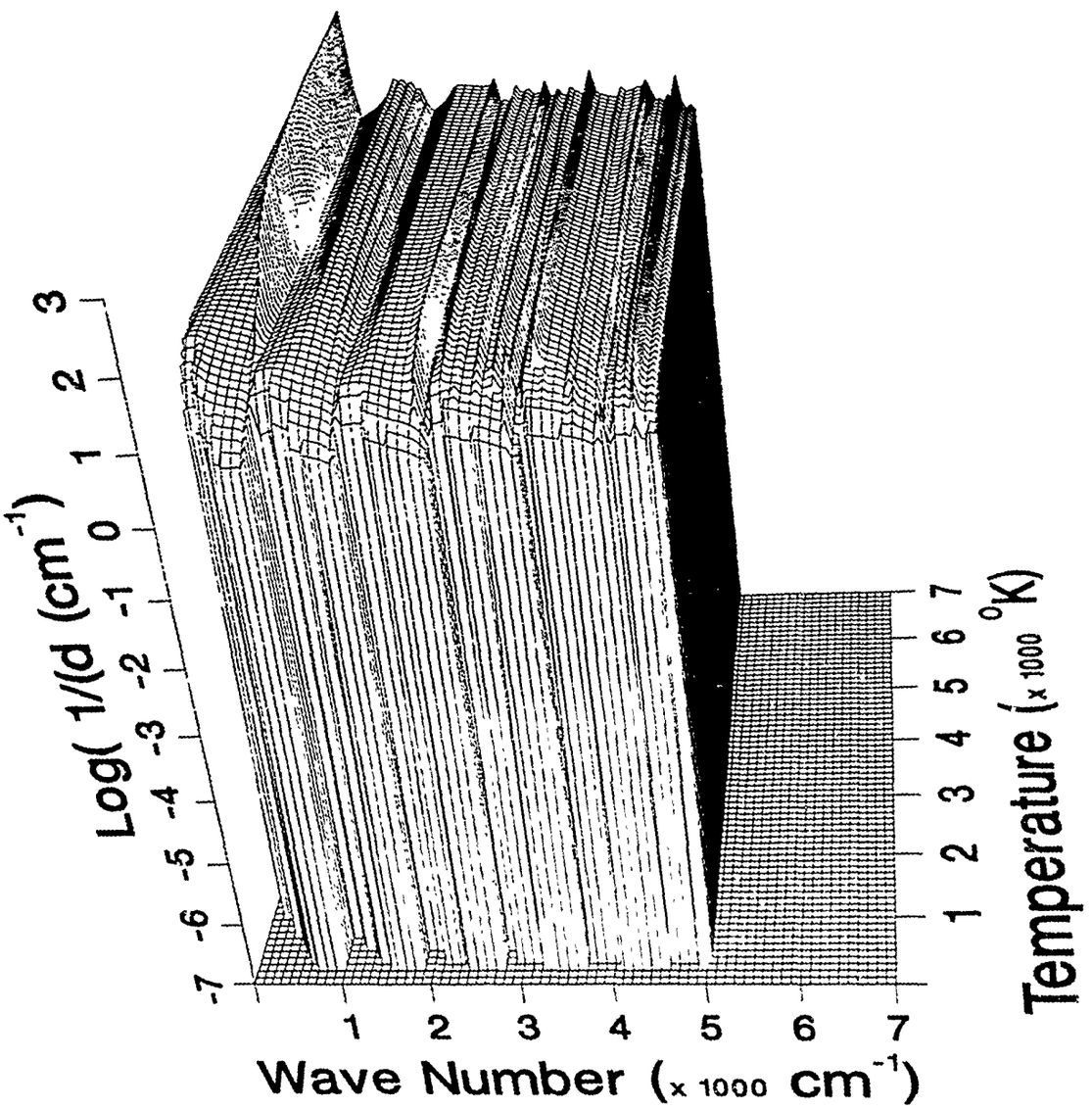

Figure 511. Inverse line spacing for UO^{+}.

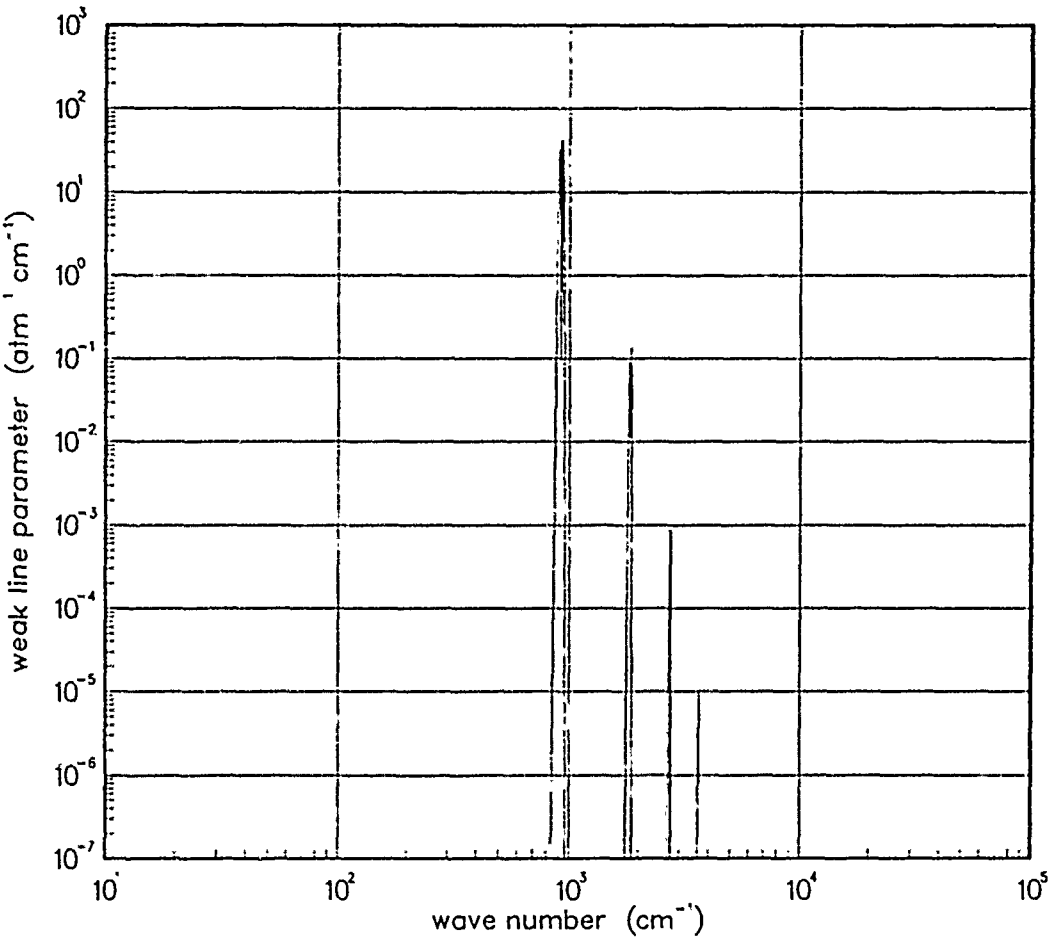

Figure 512. Weak-line parameter for UO^+ at 200°K.

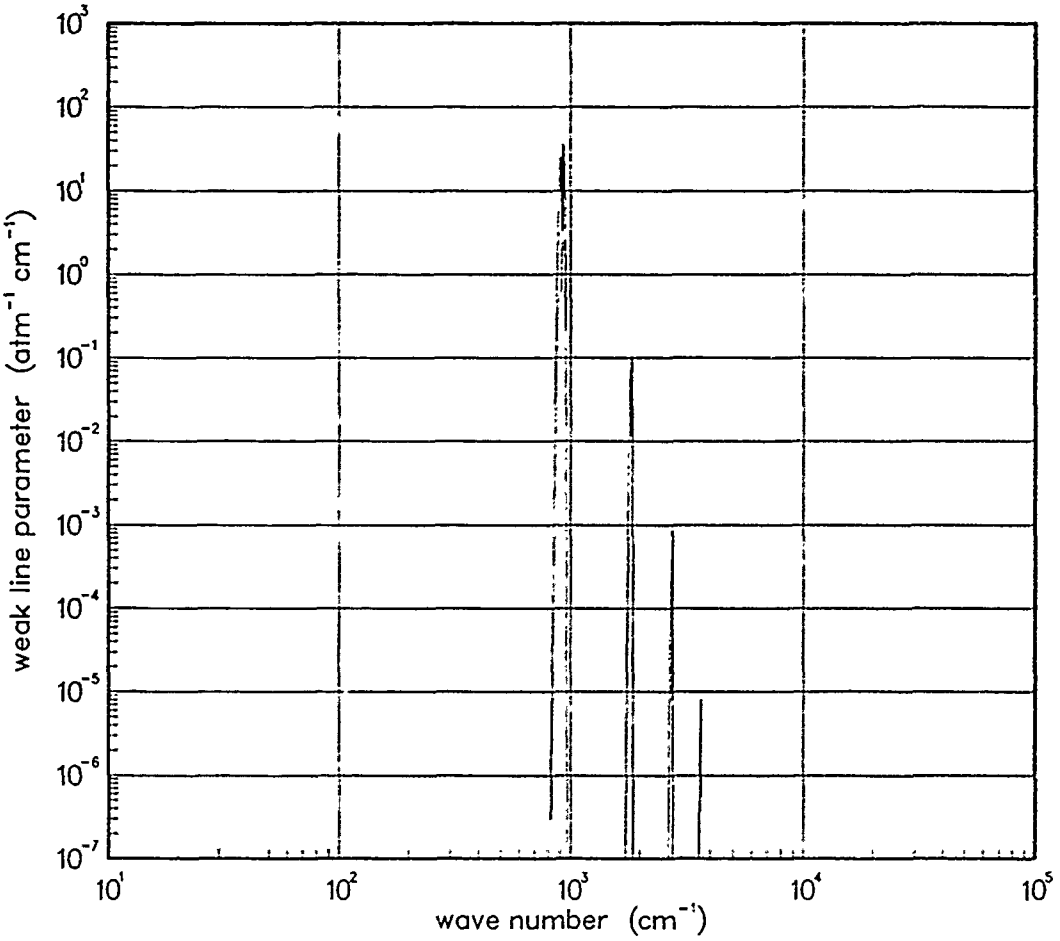

Figure 513. Weak-line parameter for UO^{+} at 300°K.

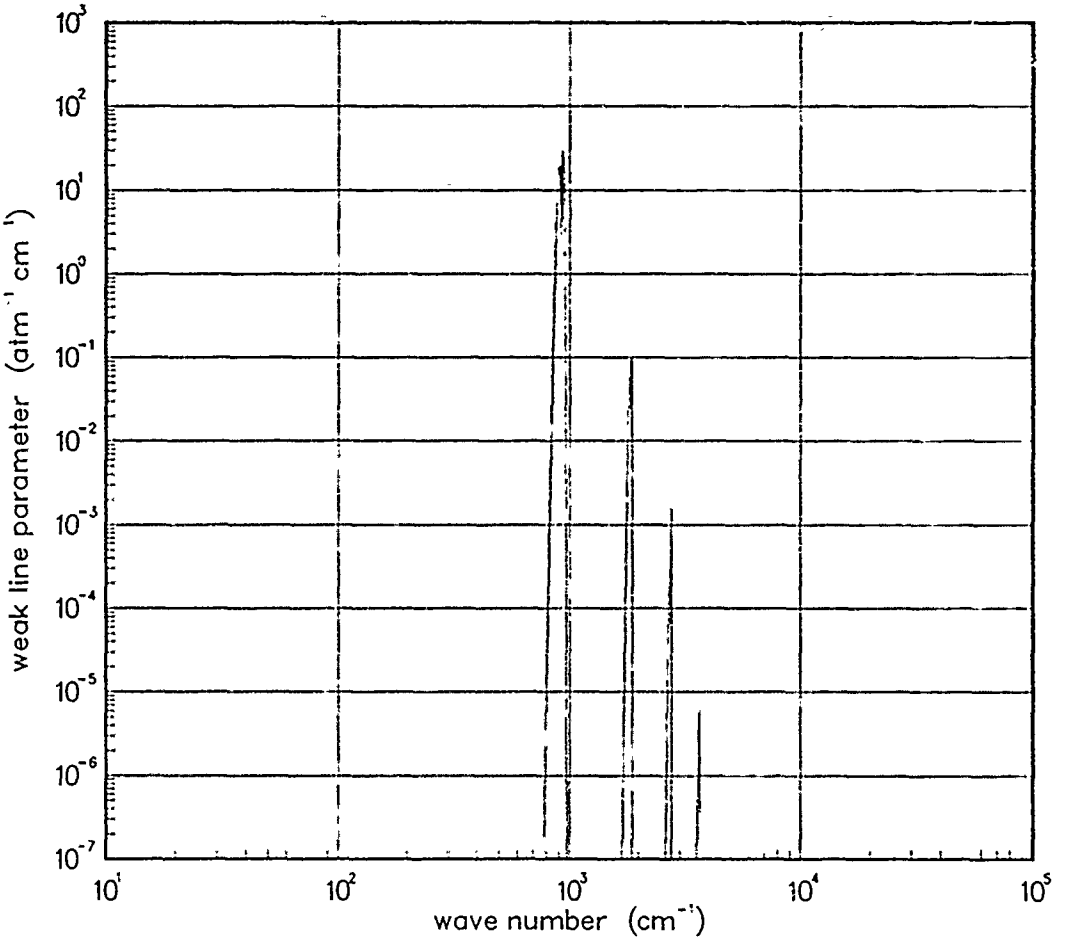

Figure 514. Weak-line parameter for UO^+ at 500°K.

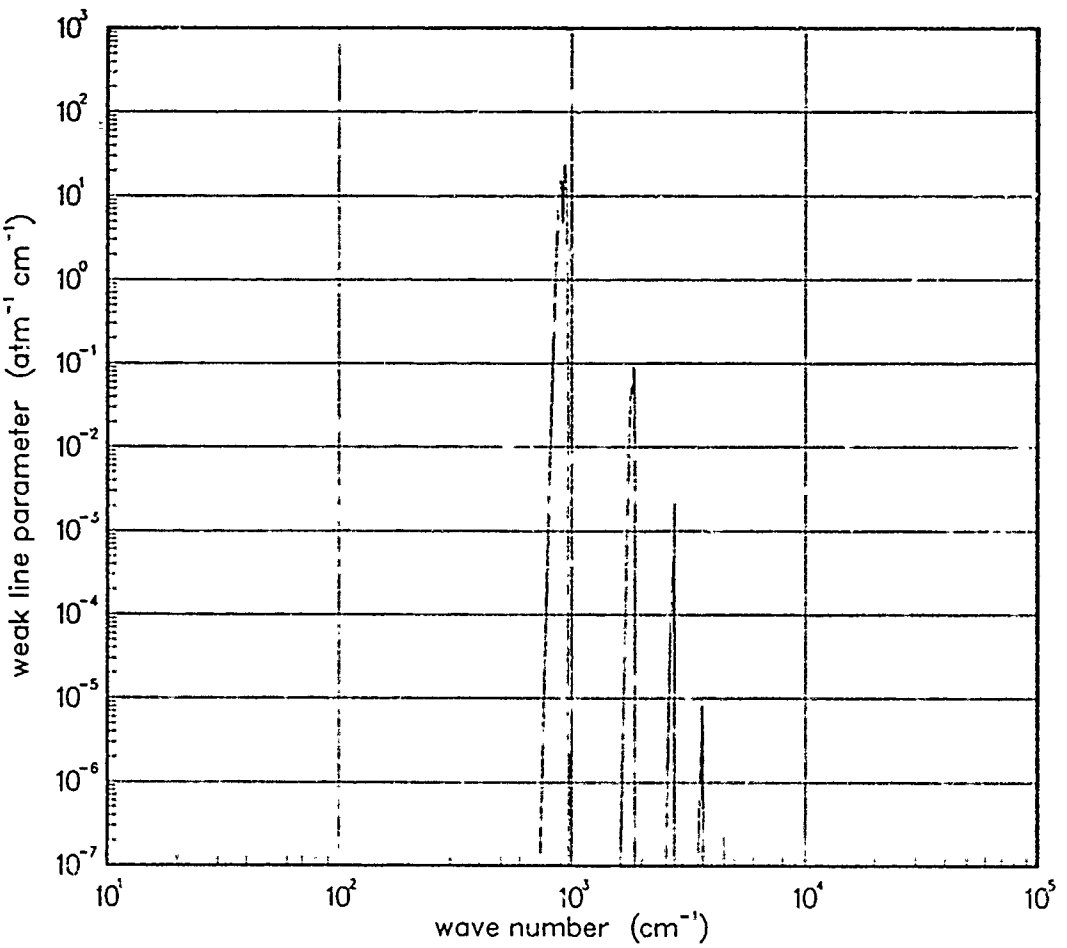

Figure 515. Weak-line parameter for UO^{+} at 750°K.

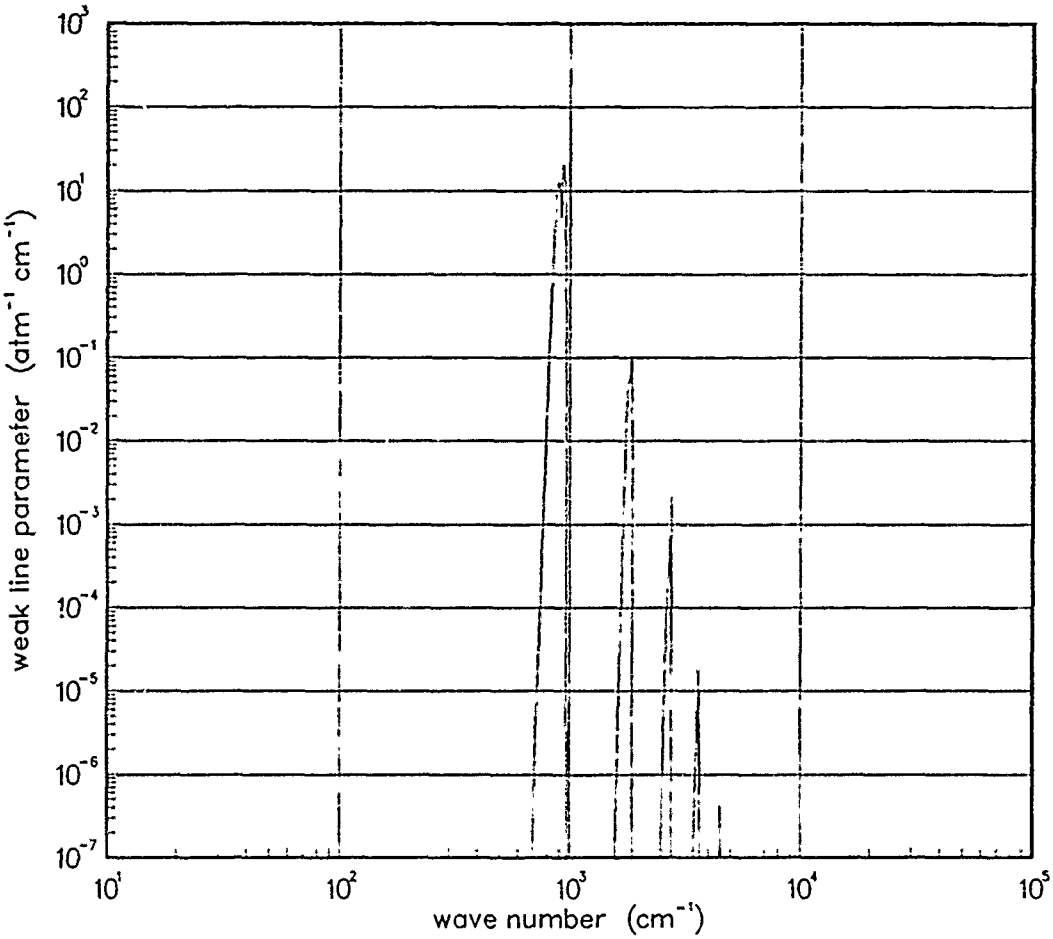

Figure 516. Weak-line parameter for UO^{+} at 1000°K.

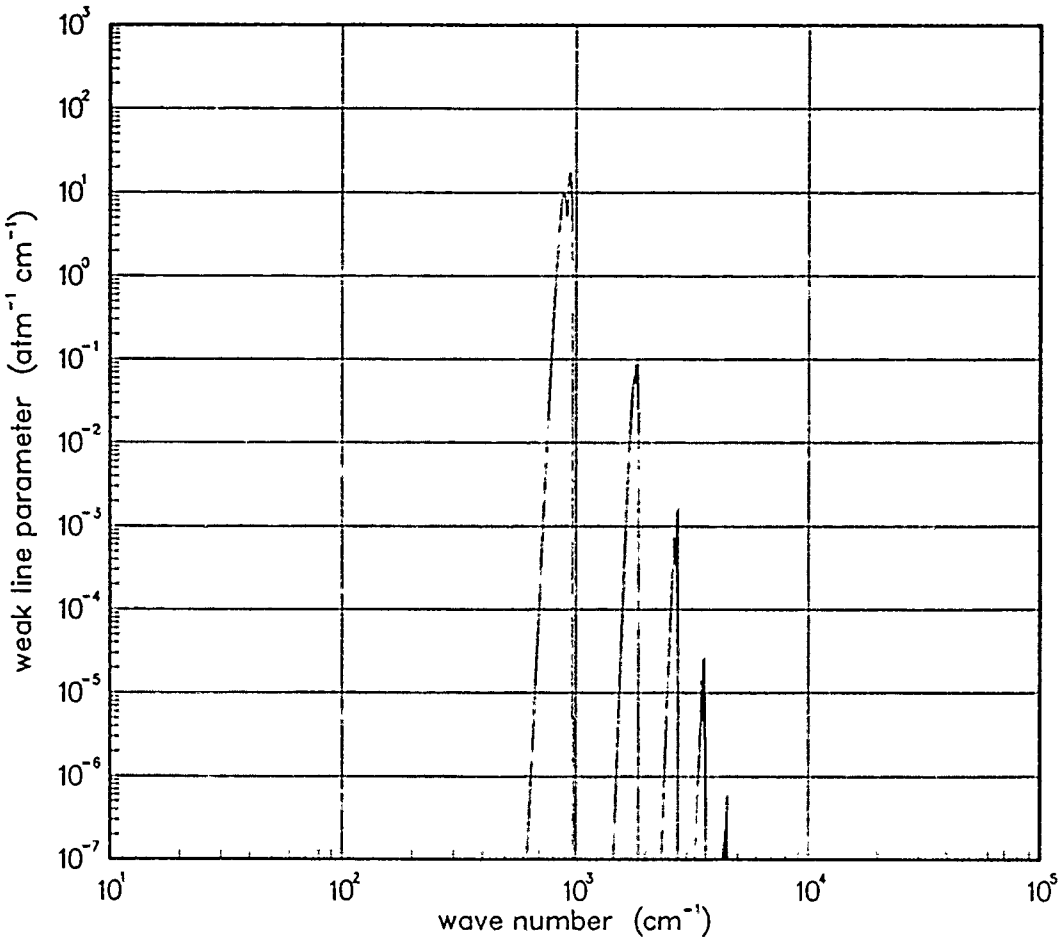

Figure 517. Weak-line parameter for UO^{+} at 1500°K.

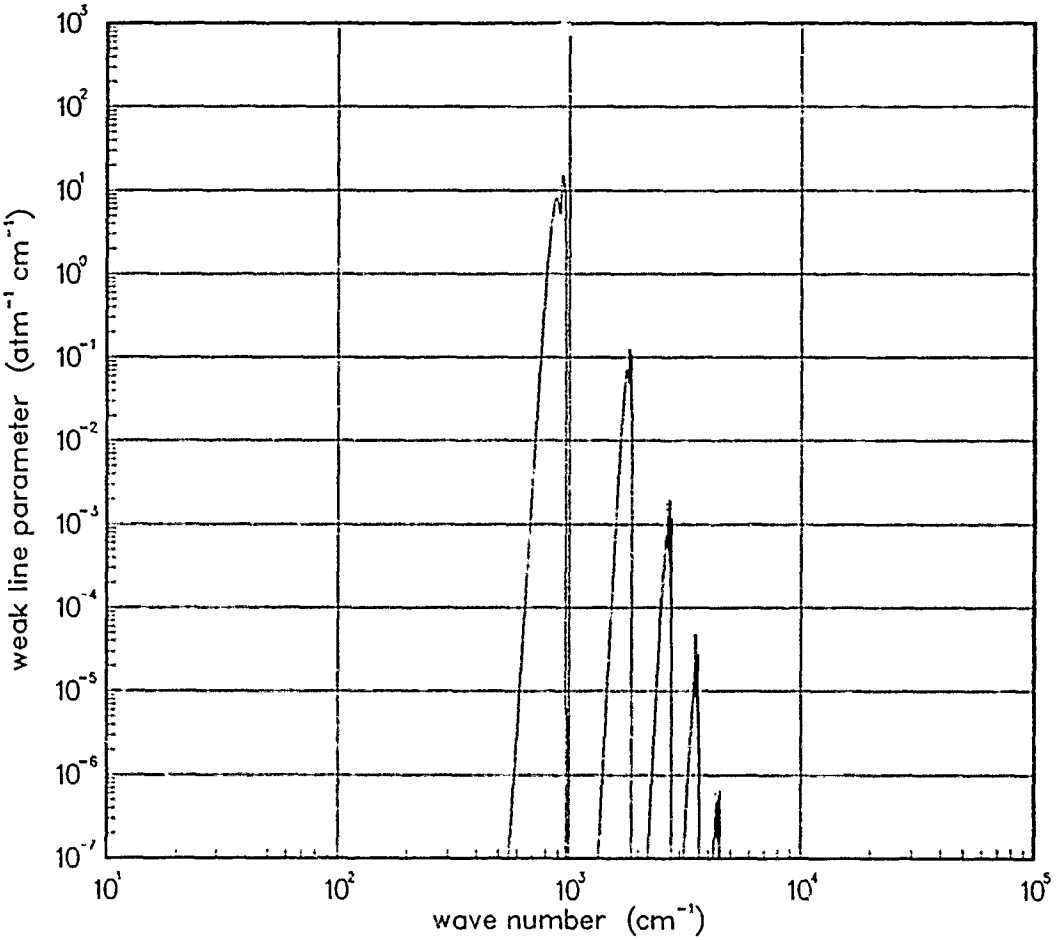

Figure 518. Weak-line parameter for UO^{+} at 2000°K.

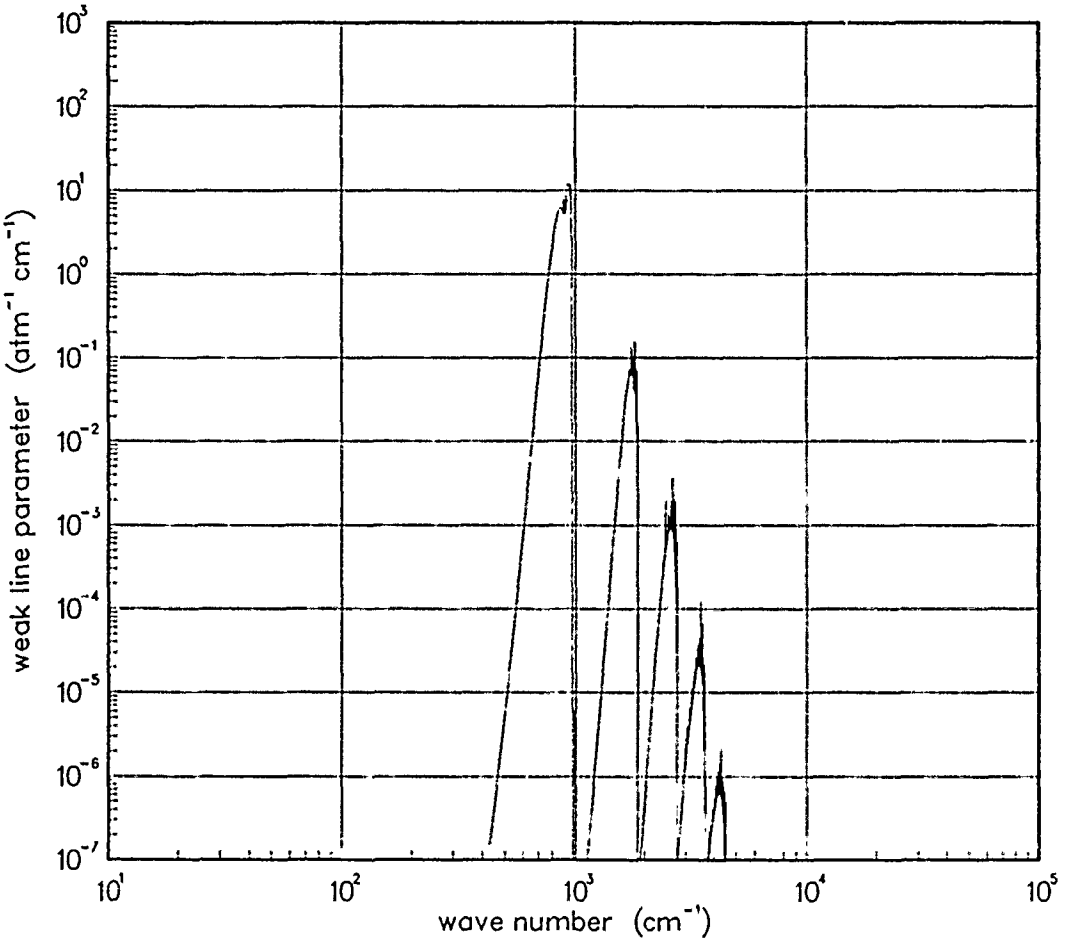

Figure 519. Weak-line parameter for UO^{+} at 3000°K.

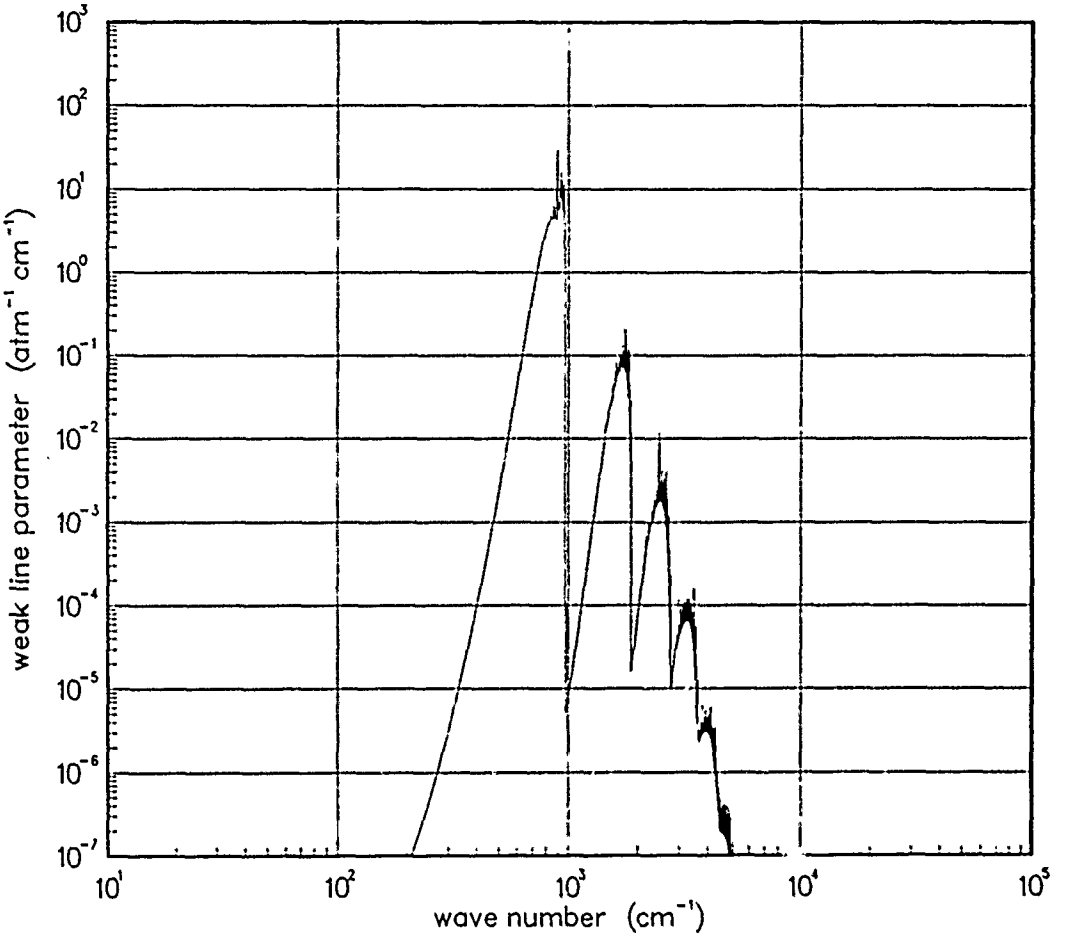

Figure 520. Weak-line parameter for UO^{+} at 5000°K.

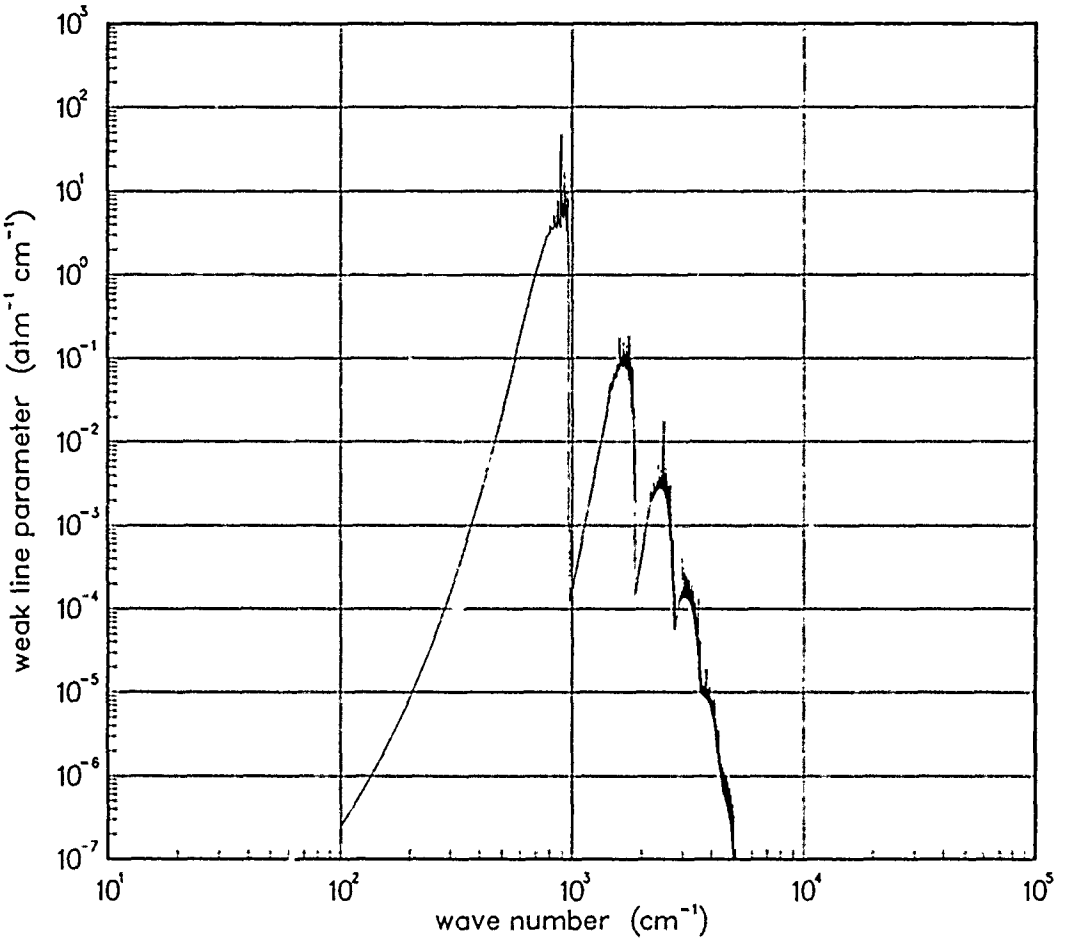

Figure 521. Weak-line parameter for UO^{+} at 7000°K.

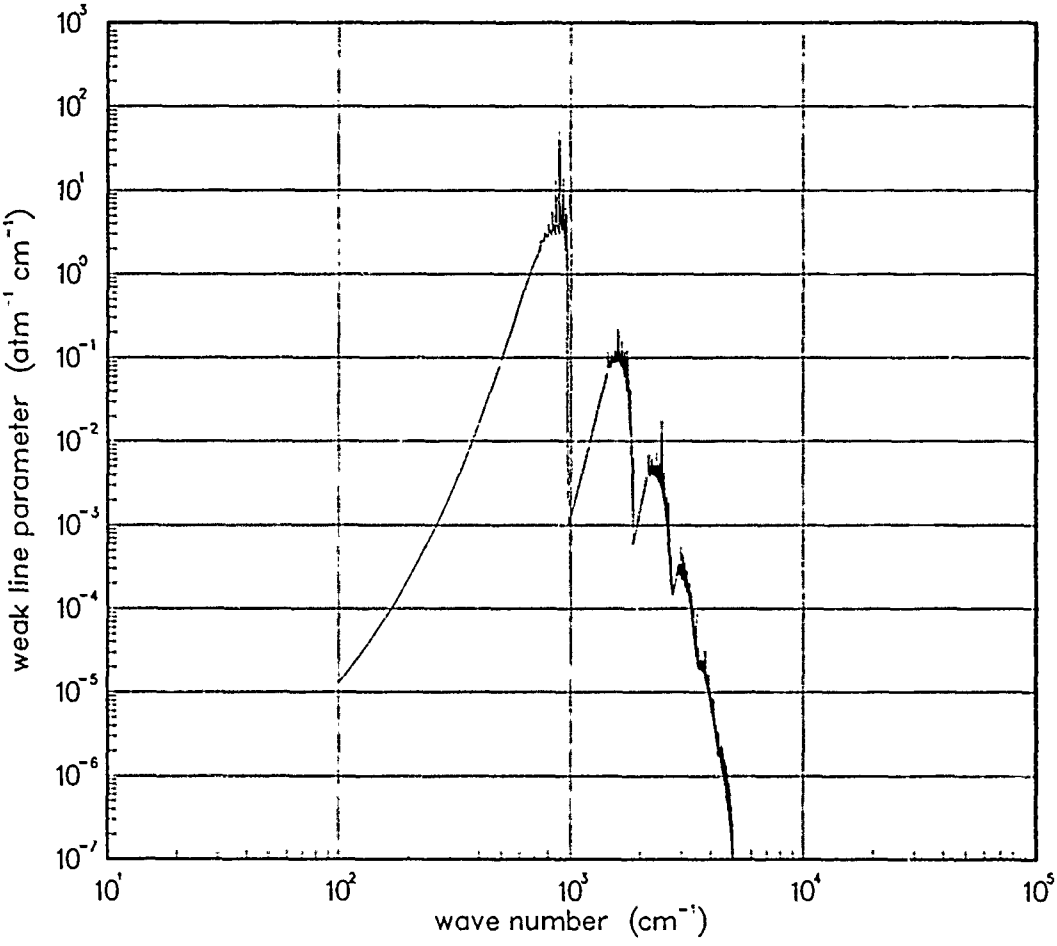

Figure 522. Weak-line parameter for UO^{+} at 10000°K.

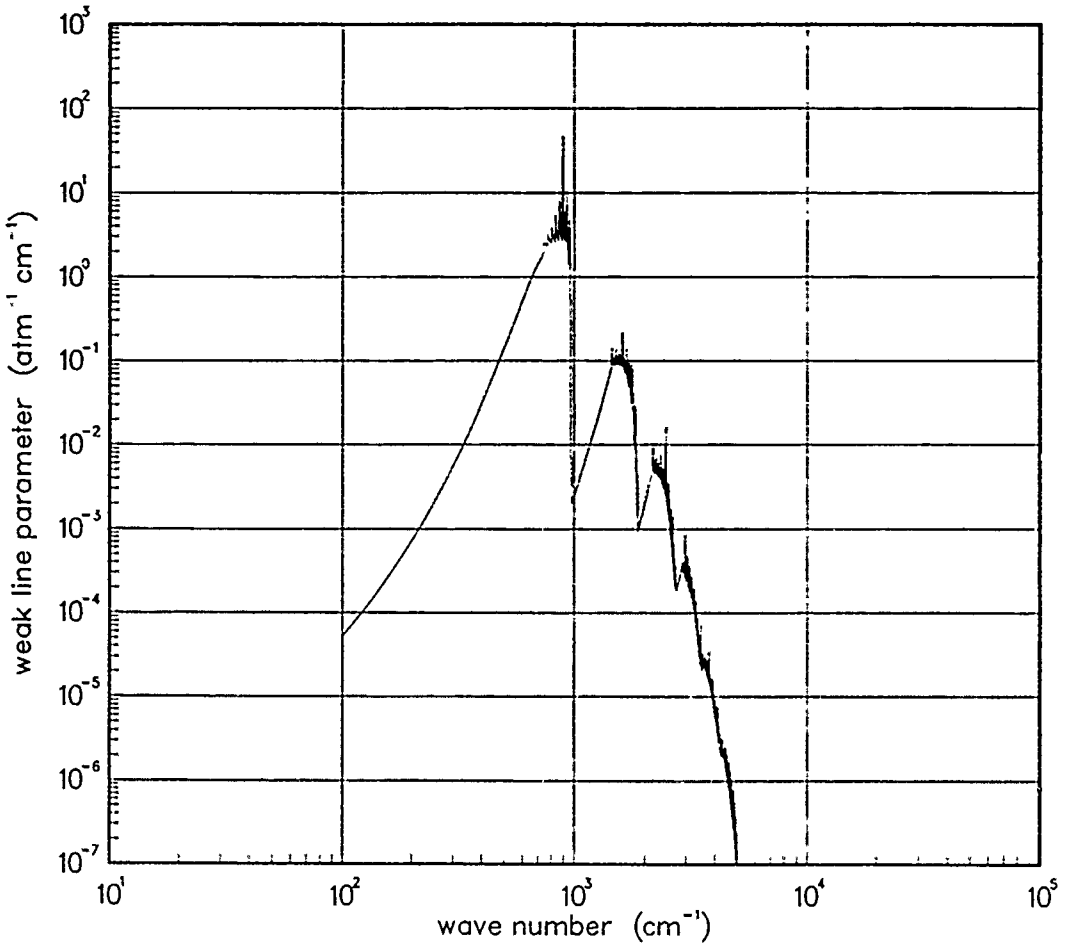

Figure 523. Weak-line parameter for UO^{+} at 12000°K.

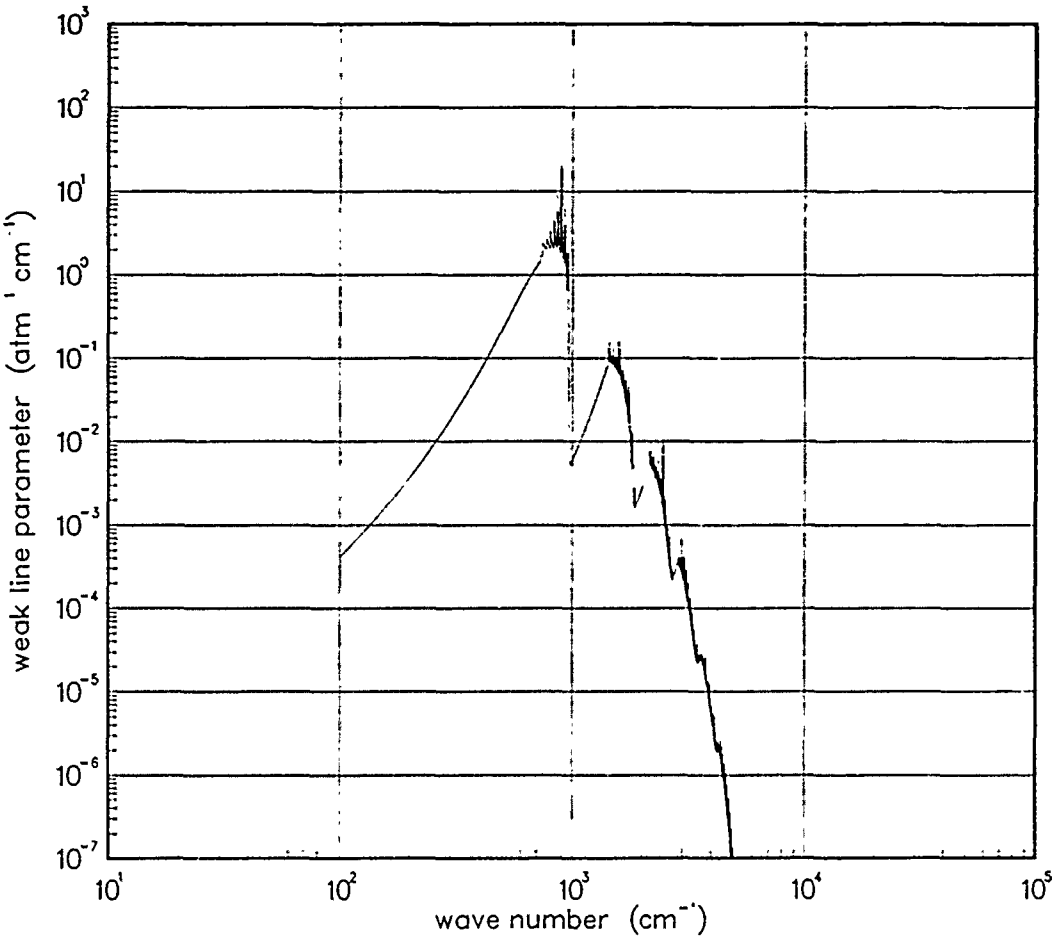

Figure 524. Weak-line parameter for UO^+ at 18000°K.

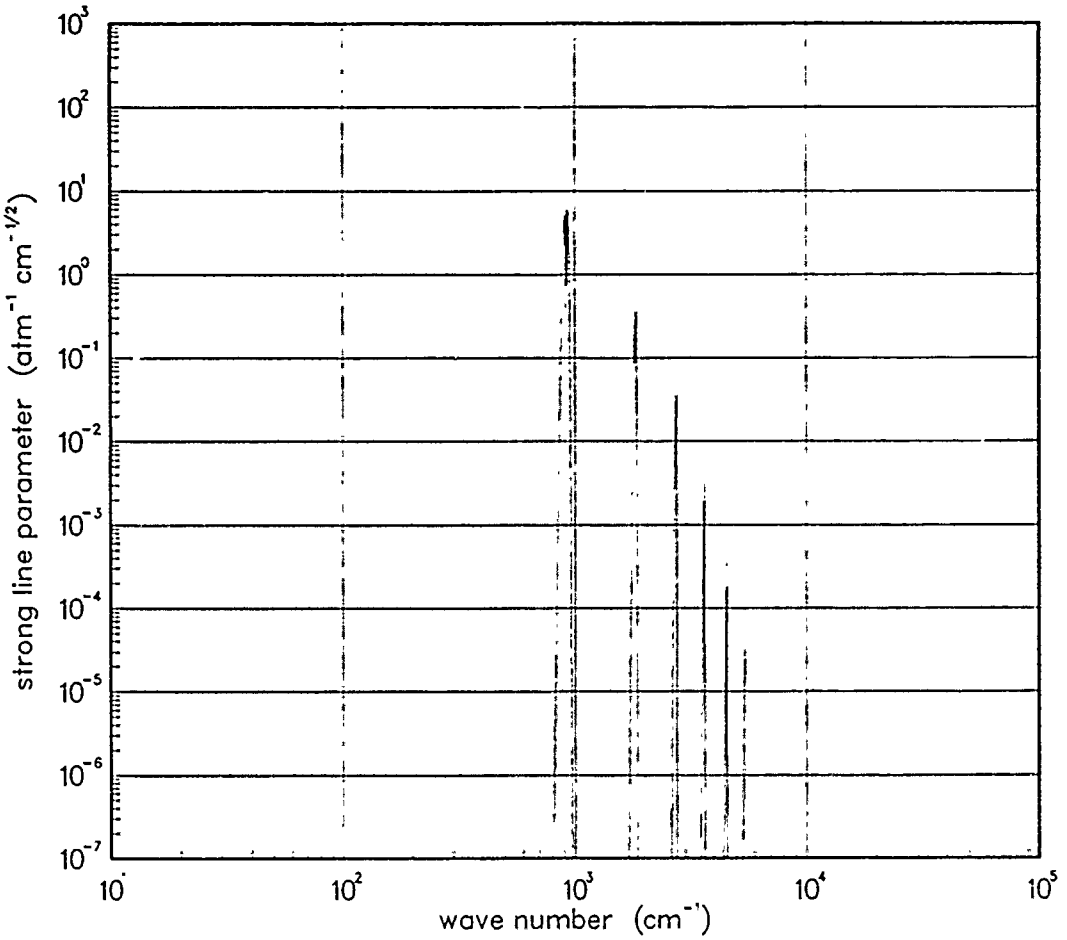

Figure 525. Strong-line parameter for UO^{+} at 200°K.

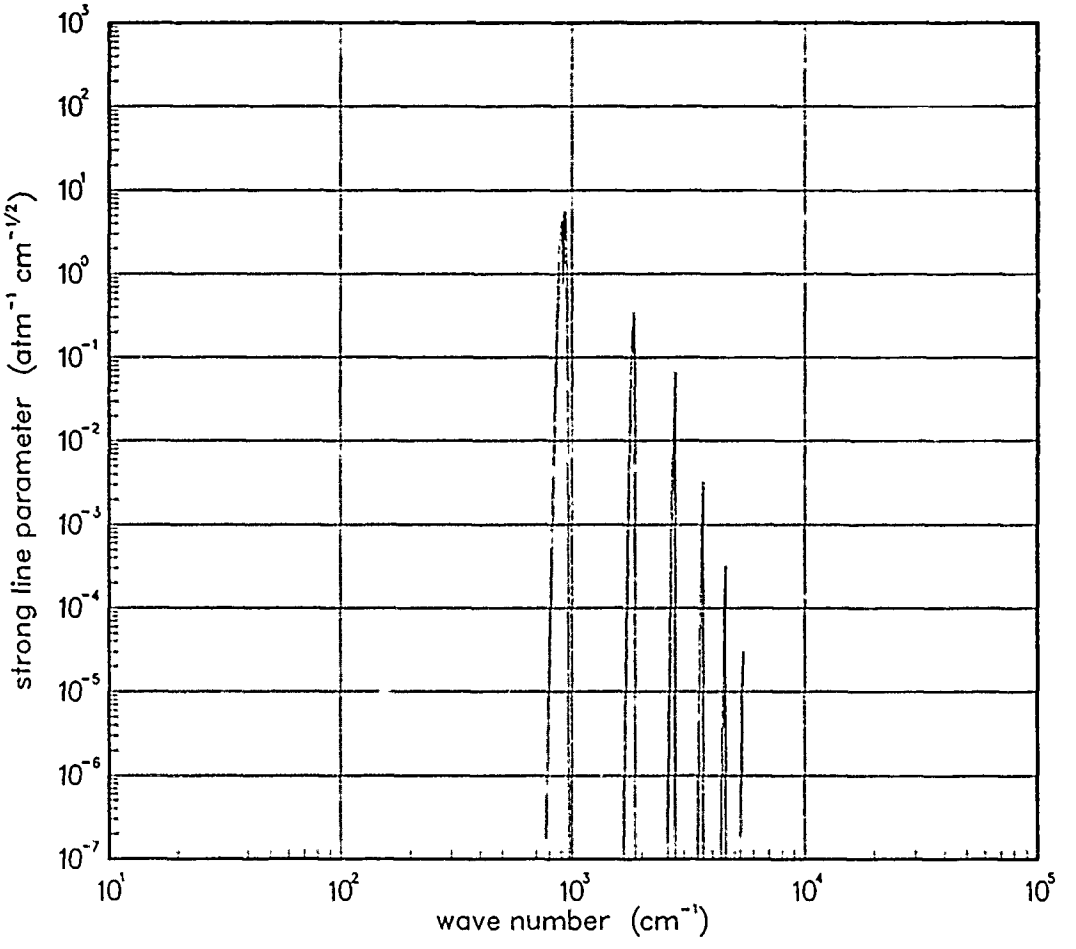

Figure 526. Strong-line parameter for UO^{+} at 300°K.

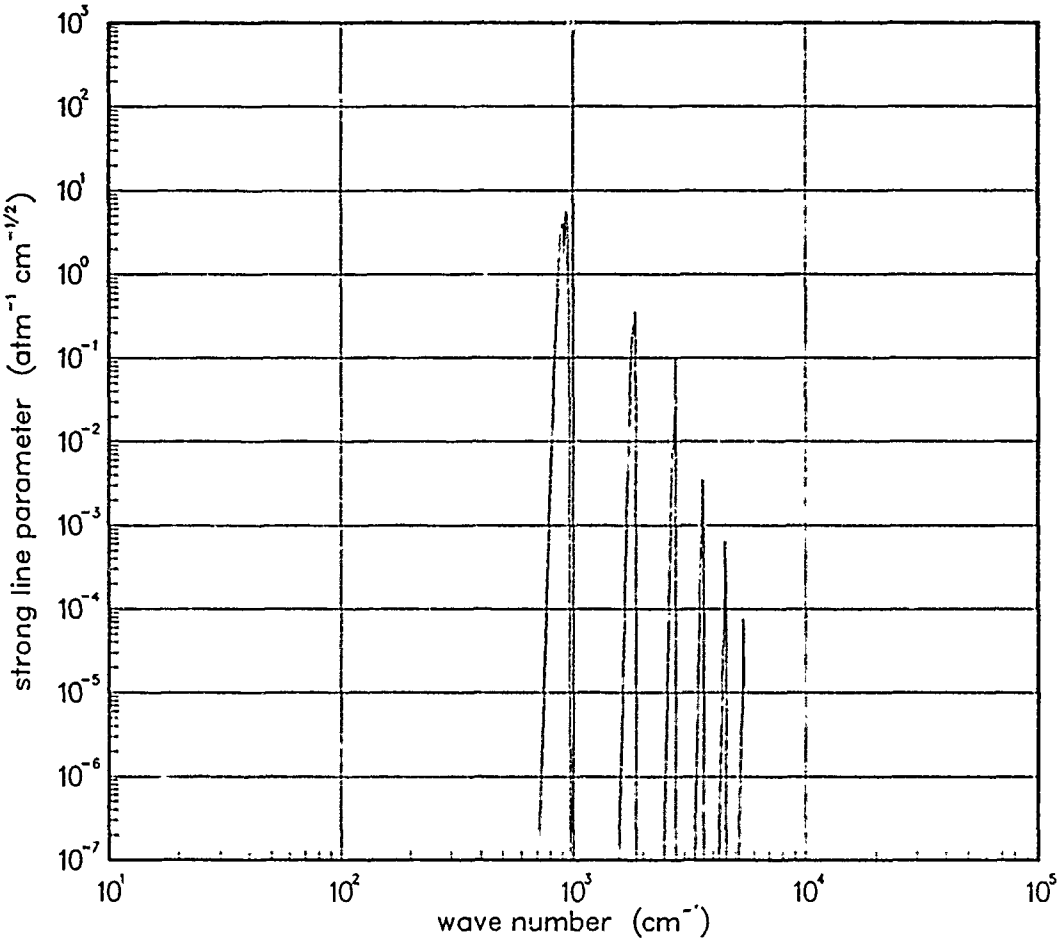

Figure 527. Strong-line parameter for UO^{+} at 500°K.

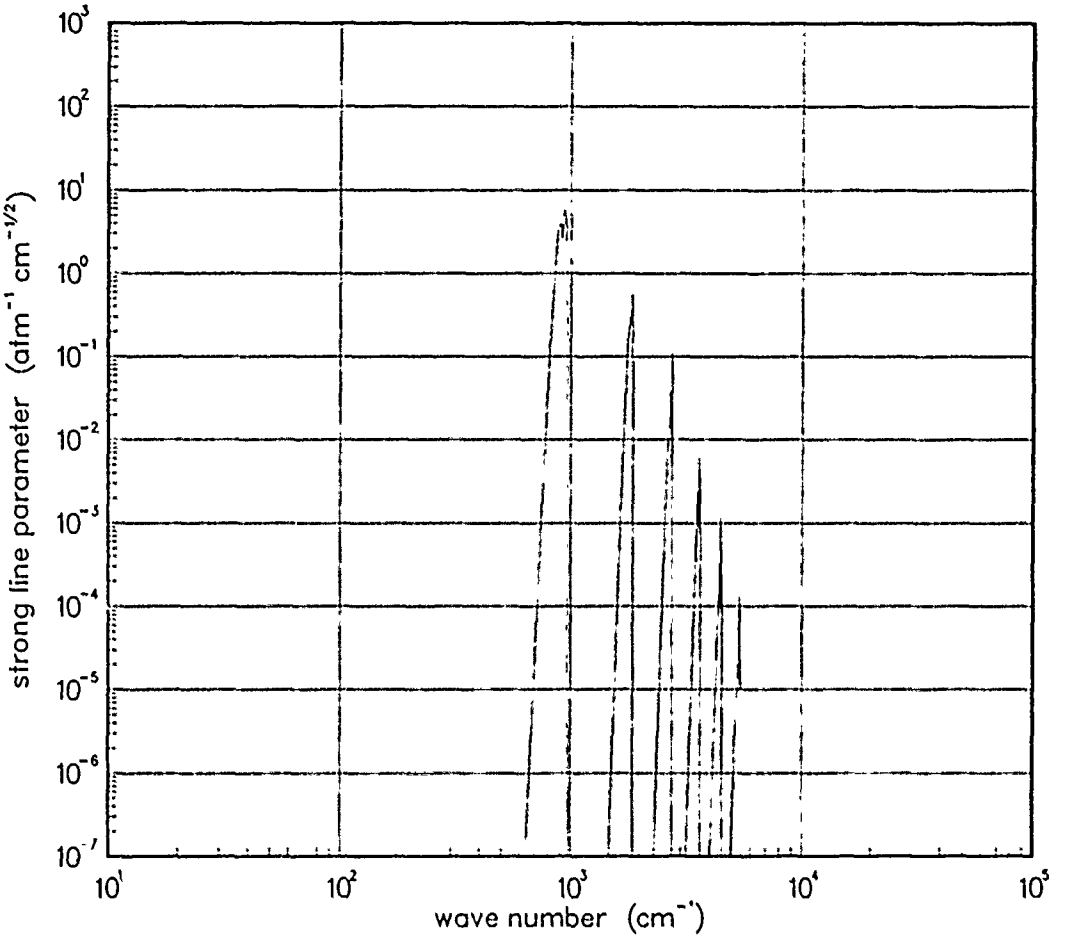

Figure 528. Strong-line parameter for UO^{+} at 750°K.

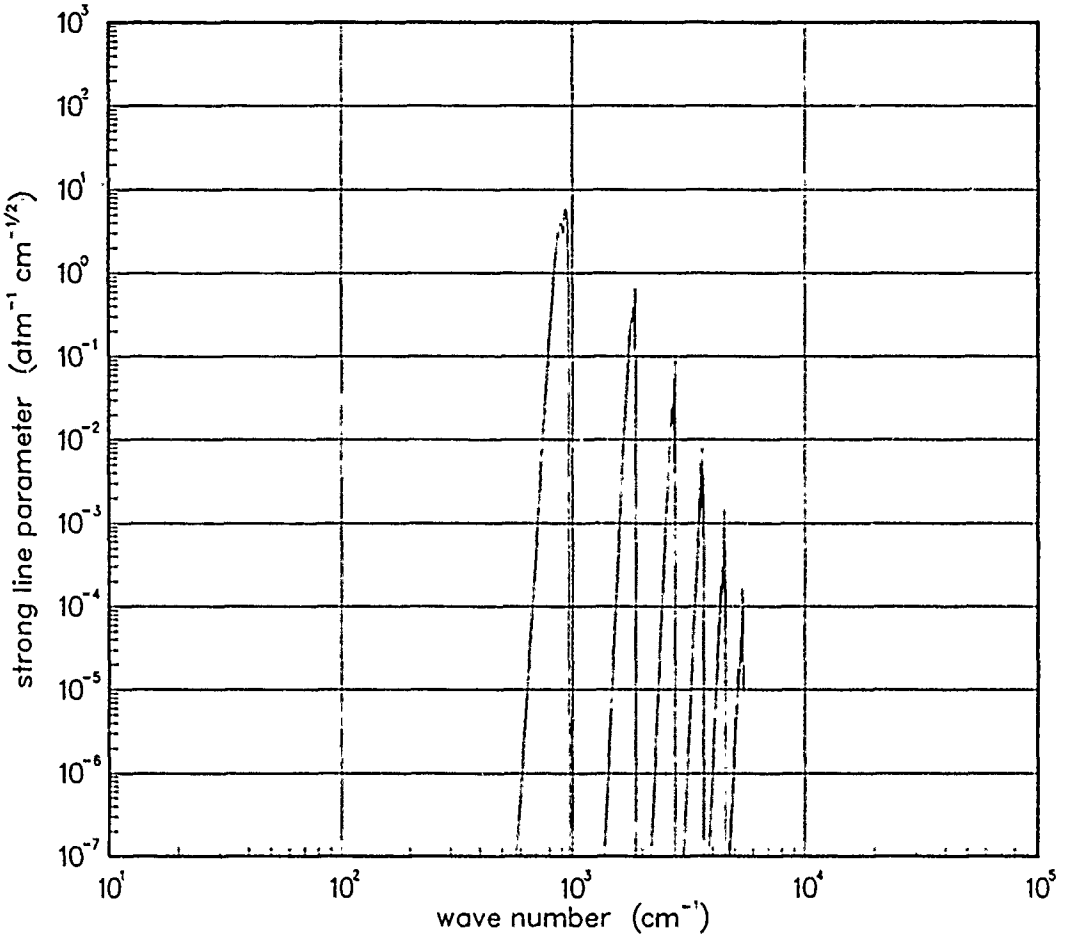

Figure 529. Strong-line parameter for UO^{+} at 1000°K.

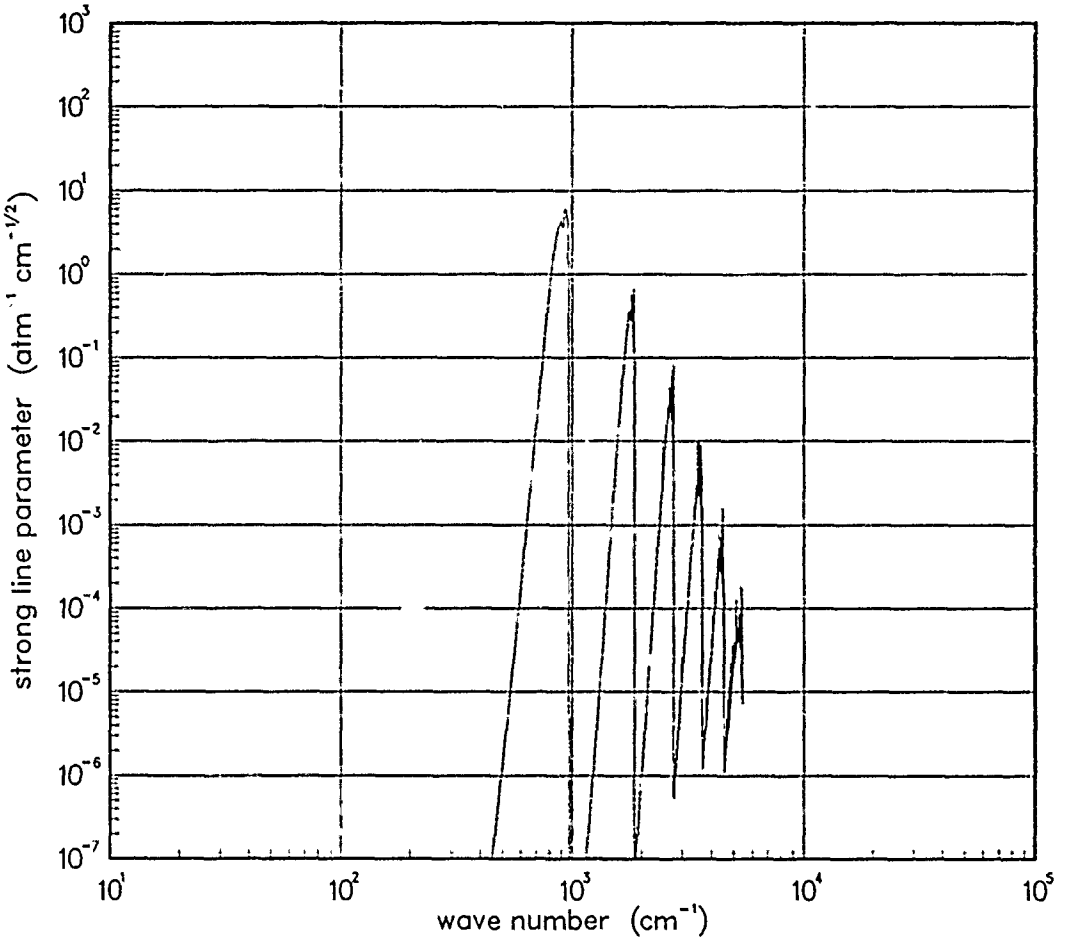

Figure 530. Strong-line parameter for UO^{+} at 1500°K.

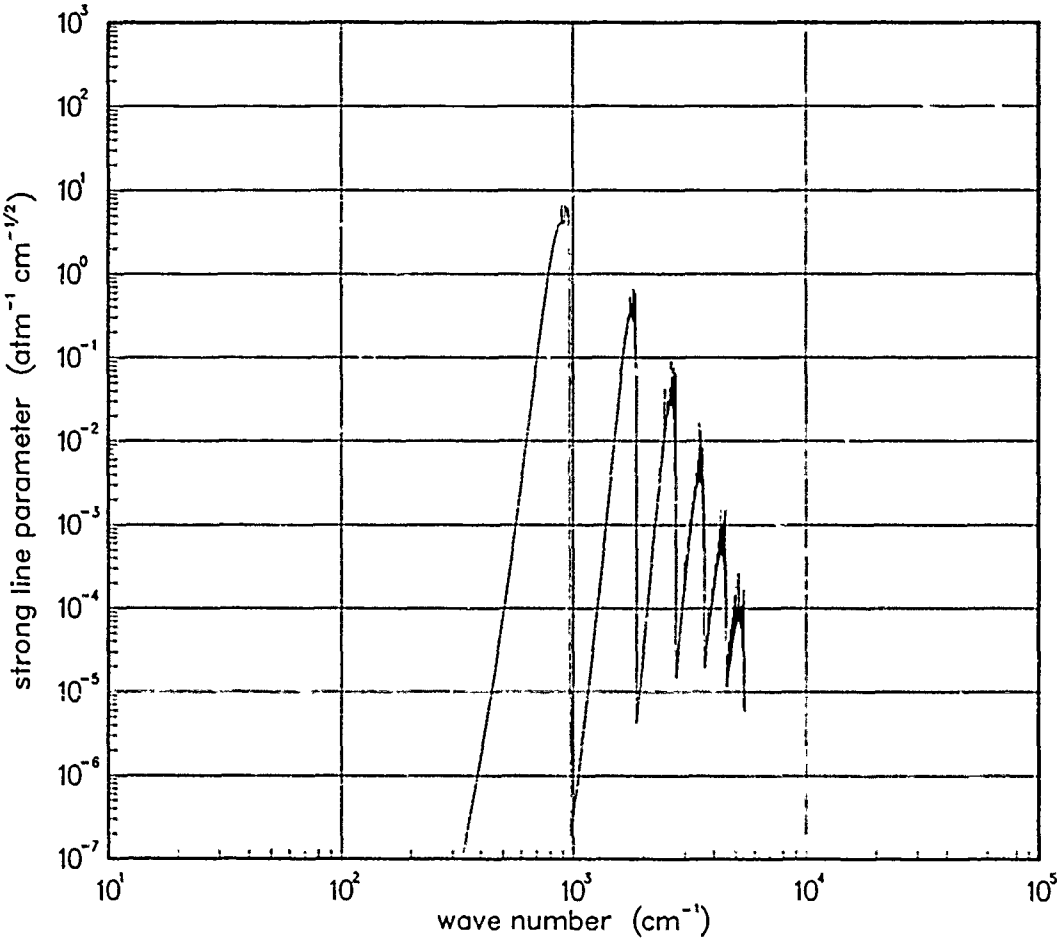

Figure 531. Strong-line parameter for UO^{+} at 2000°K.

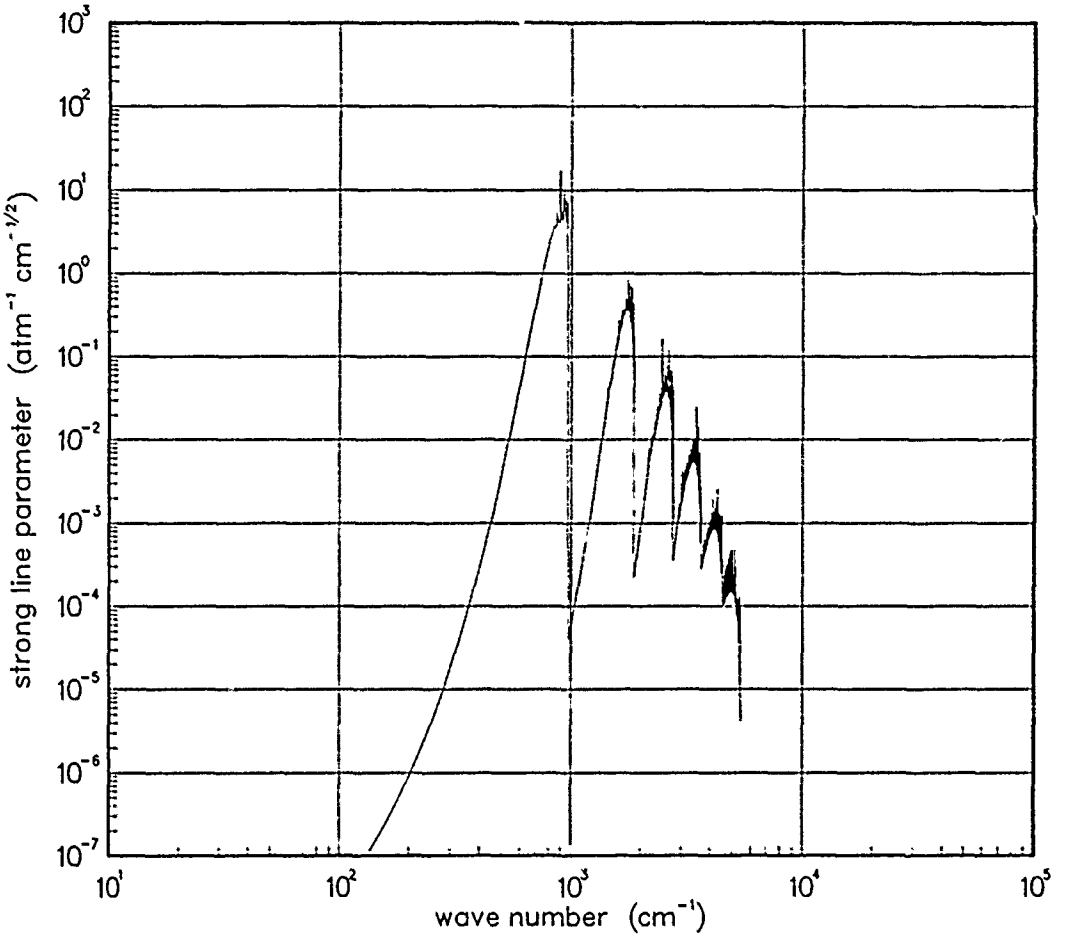

Figure 532. Strong-line parameter for UO^{+} at 3000°K.

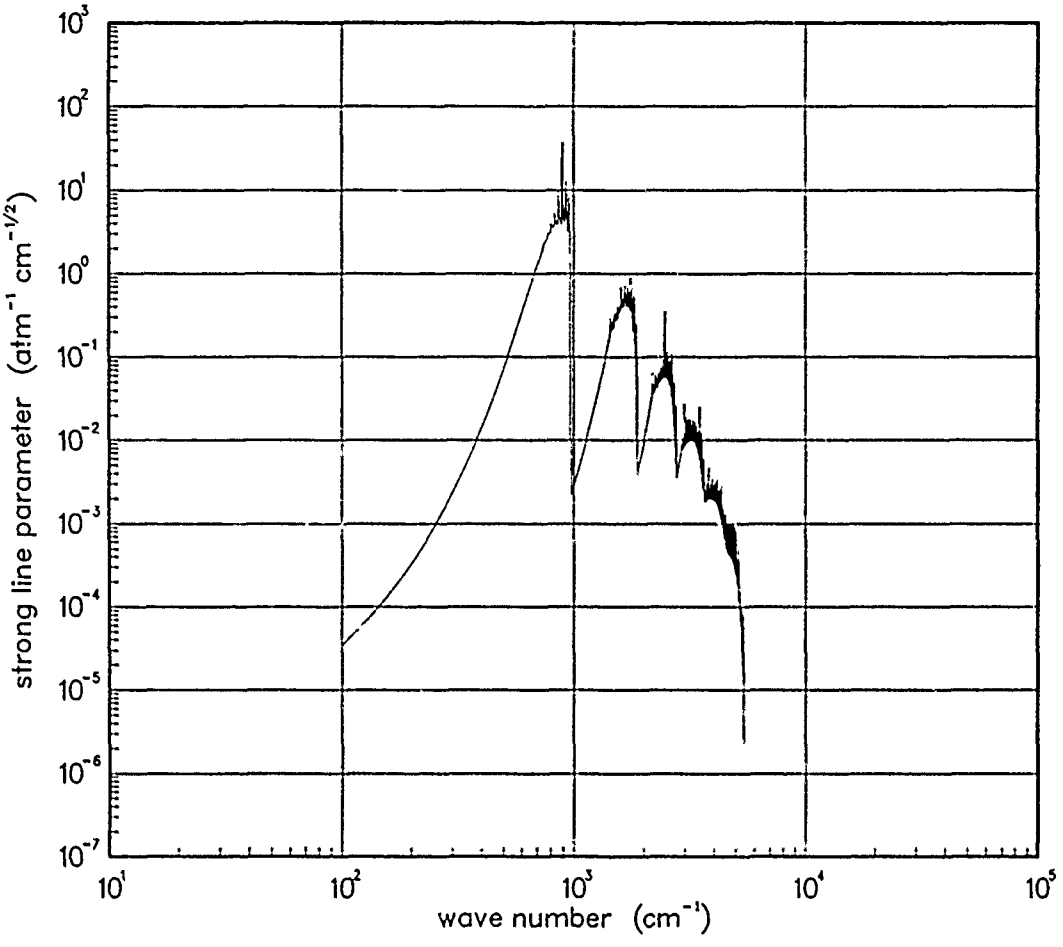

Figure 533. Strong-line parameter for UO^{+} at 5000°K.

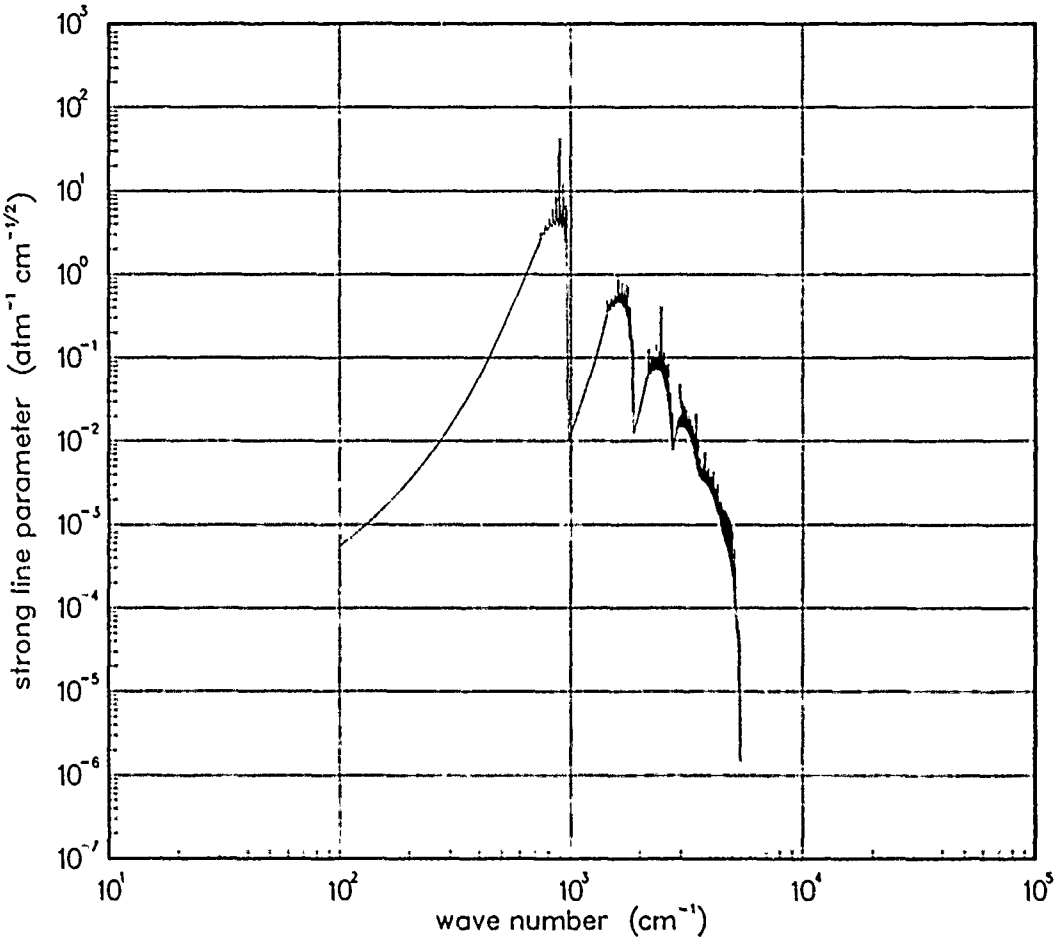

Figure 534. Strong-line parameter for UO^{+} at 7000°K.

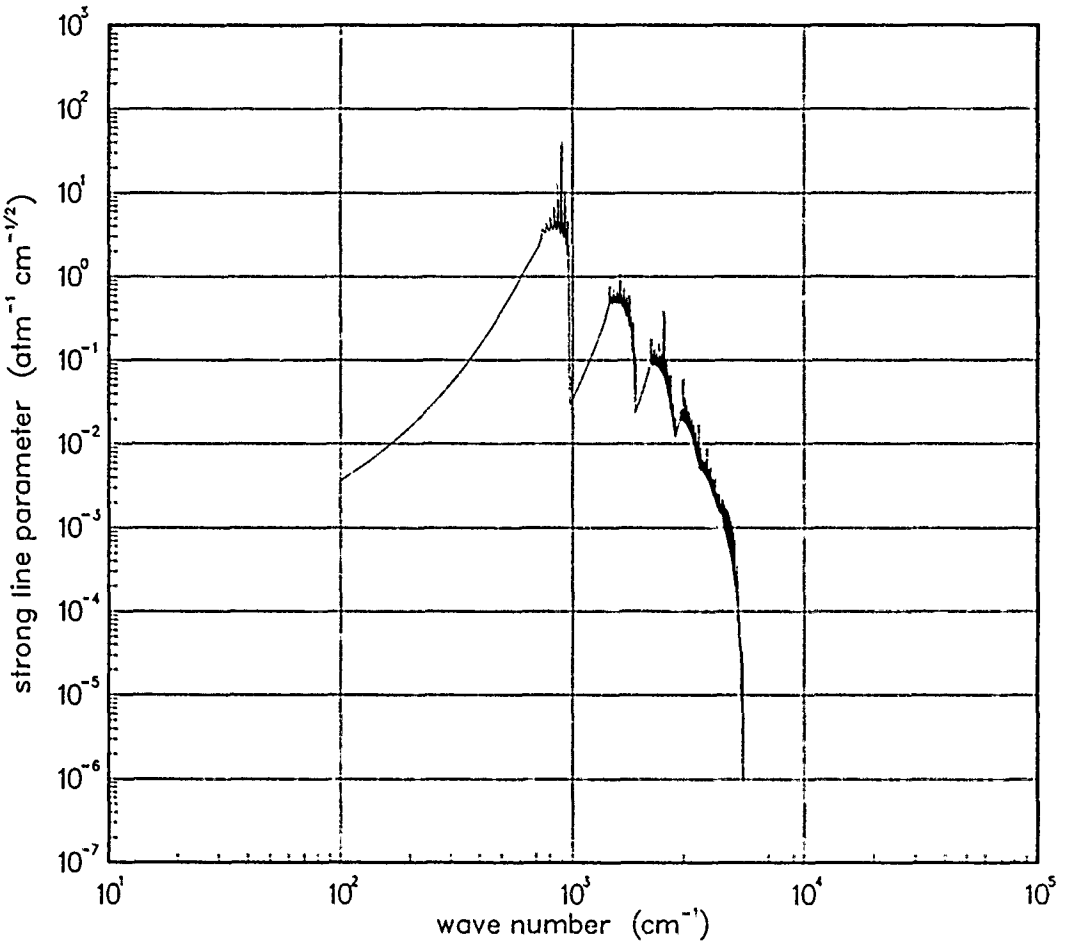

Figure 535. Strong-line parameter for UO^{+} at 10000°K.

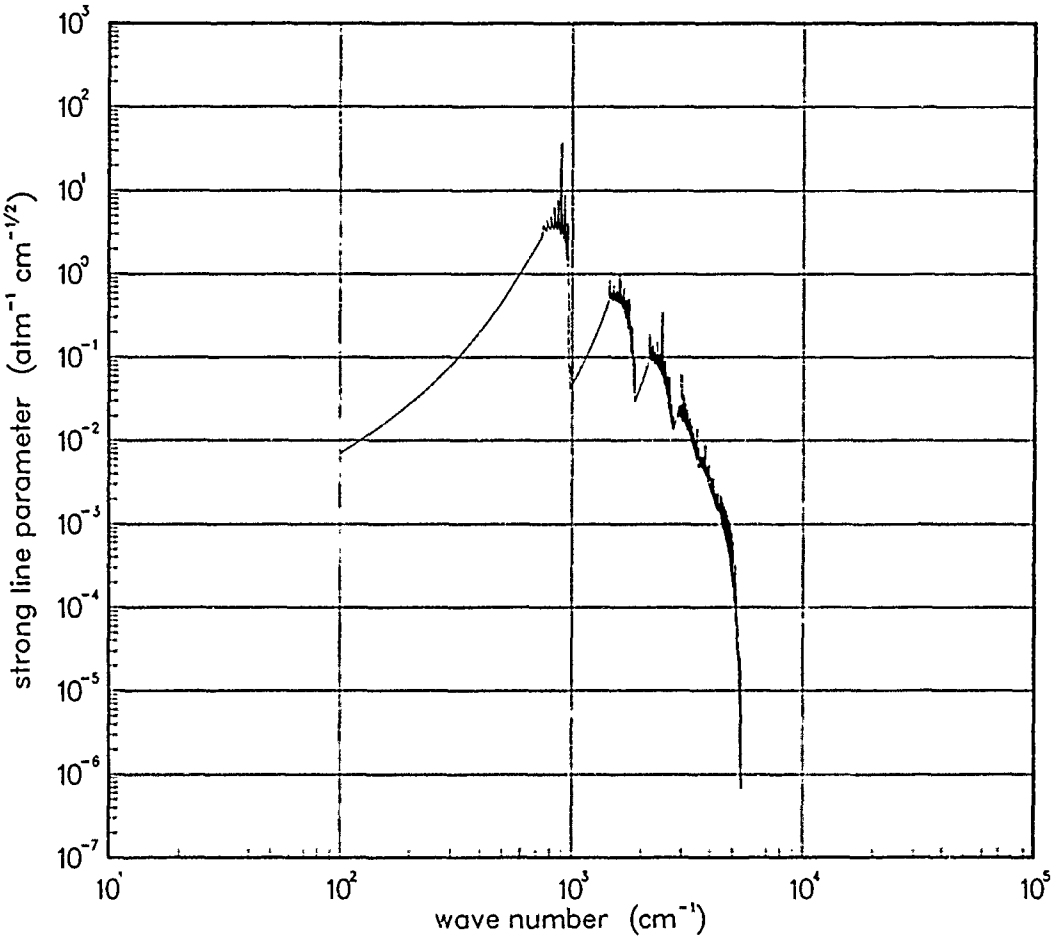

Figure 536. Strong-line parameter for UO^{+} at 12000°K.

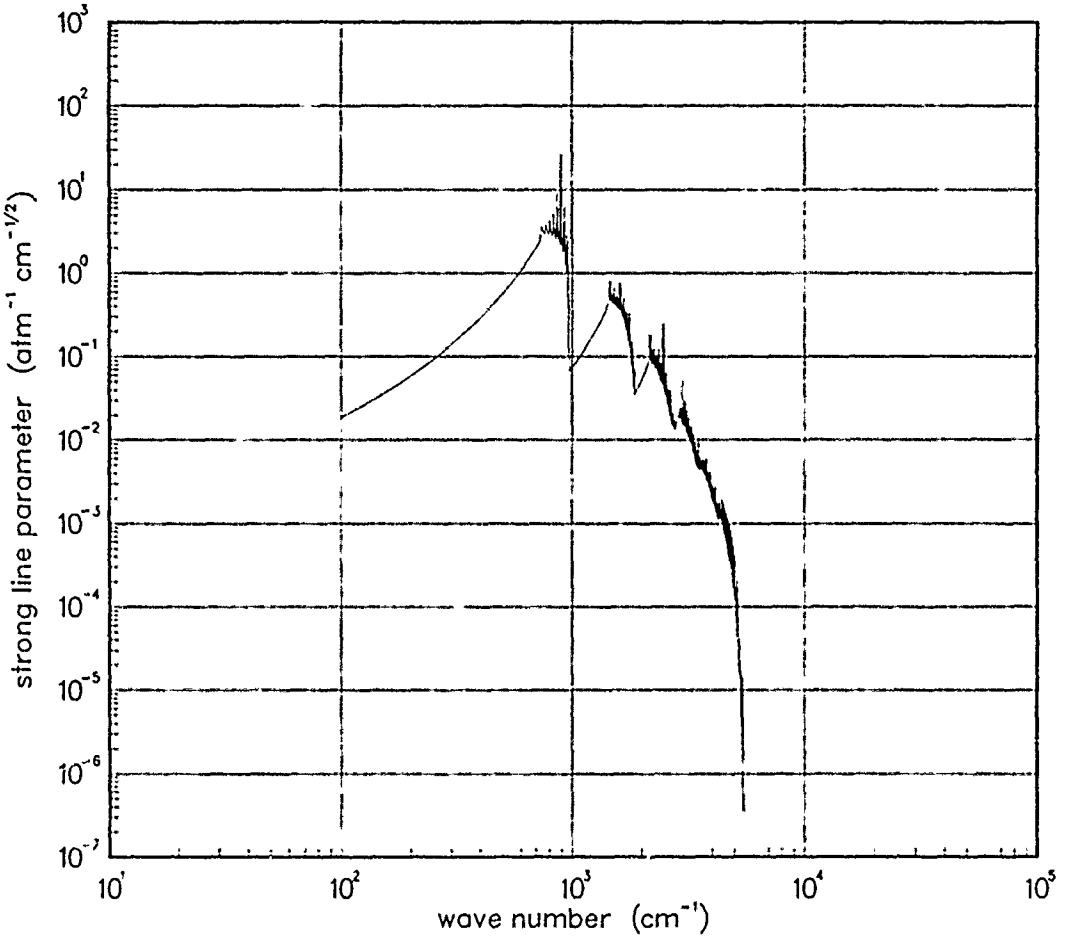

Figure 537. Strong-line parameter for UO^{+} at 18000°K.

SECTION 7
LIST OF REFERENCES

1. J. G. DeVore, "The NORSE Manual Volume 4-10: Model Data Files", (1985).

2. Physical Research, Inc., "Capabilities of Nuclear Weapons (EM-1), Chapter 13 - Optical System Degradation", Unpublished.

3. General Electric - TEMPO, "Band Models for Calculating Fireball Thermal Emission", Unpublished.

4. General Electric - TEMPO, "The ROSCOE Manual, Volume 28- Molecular Band Models for Thermal and Optically Pumped Emissions", Unpublished.

5. R. Levi Di Leon and J. Taine, J. Quant. Spectrosc. Radiat. Transfer, 35, 337 (1986).

6. W. Malkmus, J. Opt. Soc. Am. 57, 323 (1967).

7. W. Malkmus, J. Opt. Soc. Am. 53, 951 (1963).

8. General Electric - TEMPO, "Band Model Parameters for Thermal Emission", Unpublished.

APPENDIX A

BIBLIOGRAPHY

1. G. Herzberg, Molecular Spectra and Molecular Structure, D. Van Nostrand, Princeton, New Jersey (in 3 volumes) (1945).

2. T.L. Stephens, Atmospheric Transmission in the Optical Range , 68TMP-79, General Electric -- TEMPO, (July 1968), and Supplement.

3. The ROSCOE Manual, Vol 28-1 -- Molecular Band Model Parameters for Thermal Emissions: Expanded Wavelength Coverage, DNA 3964F-28-1, Kaman Tempo, (January 1981).

4. R.A. McClatchey, et al, AFCRL Atmospheric Line Parameters Compilation , AFCRL-TR-73-0096, Air Force Cambridge Research Laboratories, (January 1973).

APPENDIX B

GLOSSARY

NORSE	Nuclear and Optical Radar and Systems Effects code.
LTE	Local Thermal Equibrium.
DEI	Inverse line spacing.
SOD	Strength Over line spacing (Distance).
RADFLO	RADiation FLOw Code.
LINTRA	LINear TRiAtomic smeared band model.
WOE	Weapons Optical Effects code.
TATE	TriAtomic Thermal Emissions code.
STP	Standard Temperature and Pressure.

APPENDIX C

LIST OF SYMBOLS

A	Area
$\mathfrak{A}$	Malkmus strong-line parameter
A_L	Effective band width
$\bar{A}_{ij}$	Effective line width
a_ν	Line absorption coefficient
$a_{\nu_{ij}}$	Line absorption coefficient where ij indicates the upper and lower levels involved in the line transition
b_{ij}	Line profile
E_a	Energy absorbed
E_e	Energy emitted
I_ν	Intensity at energy ν
I_ν^b	Blackbody emission intensity, at energy ν
P	Pressure
$P(S)$	Probability distribution function
T	Temperature, Absolute
s	Path length
u	Adjusted path length
χ	Mole fraction
γ_d	Doppler width
γ_L	Lorentzian width
ν	Energy
Ω	Solid angle

LIST OF SYMBOLS (Continued)

ω_e	Spectroscopic constant
$\omega_e x_e$	Spectroscopic constant
α_e	Spectroscopic constant
B_e	Spectroscopic constant
A_e	Spectroscopic constant
S_{10}	Band Strength 1-0 transition
S_{20}	Band Strength 1-0 transition
S_{30}	Band Strength 1-0 transition
γ_L	Lorentz Line Width

DISTRIBUTION LIST

DNA-TR-87-239-V2A-10A

DEPARTMENT OF DEFENSE

US NUCLEAR COM & CENTRAL SYST SUPPORT STAFF
ATTN: SAB H SEQUINE

ASSISTANT TO THE SECRETARY OF DEFENSE
ATOMIC ENERGY
ATTN: EXECUTIVE ASSISTANT

DEFENSE ADVANCED RSCH PROJ AGENCY
ATTN: DR MANSFIELD
ATTN: GSD R ALEWINE

DEFENSE COMMUNICATIONS AGENCY
ATTN: J DIETZ

DEFENSE COMMUNICATIONS AGENCY
ATTN: A320

DEFENSE COMMUNICATIONS ENGINEER CENTER
ATTN: CODE R410

DEFENSE INTELLIGENCE AGENCY
ATTN: DC-6
ATTN: DIR
ATTN: DT-1B
ATTN: RTS-2B
ATTN: VP-TPO

DEFENSE NUCLEAR AGENCY
ATTN: DFSP G ULLRICH
ATTN: NANF
ATTN: NASF
ATTN: OPNA
ATTN: PRPD R YOHO
3 CYS ATTN: RAAE
ATTN: RAAE A MARDIGUIAN
ATTN: RAAE K SCHWARTZ
ATTN: RAAE L SCHROCK
ATTN: RAAE L WITTWER
ATTN: RAAE M CRAWFORD
ATTN: RAAE P FLEMING
ATTN: RAAE S BERGGREN
ATTN: RAEE
4 CYS ATTN: TITL

DEFENSE NUCLEAR AGENCY
ATTN: TDNM
ATTN: TDTT
2 CYS ATTN: TDTT W SUMMA

DEFENSE TECHNICAL INFORMATION CENTER
2 CYS ATTN: DTIC/FDAB

JOINT DATA SYSTEM SUPPORT CTR
ATTN: R MASON

JOINT STRAT TGT PLANNING STAFF
ATTN: JK (ATTN: DNA REP)
ATTN: JKCS, STUKMILLER
ATTN: JLWT (THREAT ANALYSIS)
ATTN: JPEM
ATTN: JPSS

NATIONAL SECURITY AGENCY
ATTN: C GOEDEKE

OFFICE OF THE JOINT CHIEFS OF STAFF
ATTN: J6

STRATEGIC DEFENSE INITIATIVE ORGANIZATION
ATTN: C GIESE
ATTN: CS O JUDD
ATTN: K OBRIEN
ATTN: KE
ATTN: PGM OPNS MR SNYDER
ATTN: S/AA COL GUIBERSON
ATTN: S/AA COL RIVA
ATTN: S/AA W SEIBERLING
ATTN: SLKT
ATTN: SN
ATTN: T/SK COL MILL
ATTN: T/SK COL R ROSS
ATTN: T/SK E IMKER

UNDER SECRETARY OF DEFENSE
ATTN: STRAT & THTR NUC FOR G SEVIN

DEPARTMENT OF THE ARMY

U S ARMY FOREIGN SCIENCE & TECH CTR
ATTN: DRXST-SD

U S ARMY MISSILE COMMAND/AMSMI-RD-CS-R
ATTN: AMSMI-RD-CS-R (DOCS)

U S ARMY NUCLEAR & CHEMICAL AGENCY
ATTN: MONA-NU

U S ARMY RESEARCH OFFICE
ATTN: R MACE

U S ARMY STRATEGIC DEFENSE CMD
ATTN: CSSD-H-TT H POPE
ATTN: DASD-H-SA R BRADSHAW
ATTN: DASD-H-SA/R SMITH
ATTN: DASD-H-SAV

U S ARMY STRATEGIC DEFENSE COMMAND
ATTN: ATC-O W DAVIES
ATTN: BMDATC-R W DICKERSON

DEPARTMENT OF THE NAVY

COMMAND & CONTROL PROGRAMS
ATTN: OP 941

NAVAL RESEARCH LABORATORY
ATTN: CODE 2627 (TECH LIB)
ATTN: CODE 4121.8 H HECKATHORN
ATTN: CODE 4700 S OSSAKOW
ATTN: CODE 4780 J HUBA

NAVAL SURFACE WARFARE CENTER
ATTN: CODE X211 (TECH LIB)

NAVAL TECHNICAL INTELLIGENCE CTR
ATTN: NISC-50

OFFICE OF NAVAL RESEARCH
ATTN: A TUCKER

DEPARTMENT OF THE AIR FORCE

AIR FORCE CTR FOR STUDIES & ANALYSIS
ATTN: AFCSA/SAMI (R GRIFFIN)
ATTN: AFCSA/SASC

AIR FORCE GEOPHYSICS LABORATORY
ATTN: OPE/H GARDINER
ATTN: PHP/W SWIDER

AIR FORCE OFFICE OF SCIENTIFIC RSCH
ATTN: AFOSR/NC

AIR FORCE SPACE SYSTEMS DIVISION
ATTN: CNSC/CAPT T ABBOUSHI
ATTN: YA
2 CYS ATTN: YN

AIR FORCE TECHNICAL APPLICATIONS CTR
ATTN: TN
ATTN: TX

BALLISTIC MISSILE OFFICE
ATTN: ENSE
ATTN: PK

SPACE DIVISION/AQ
ATTN: WE

SPACE DIVISION/YA
ATTN: YAR

SPACE DIVISION/YG
ATTN: CNDA
ATTN: YGJB P KELLY

WEAPONS LABORATORY
ATTN: NTCA
ATTN: NTN
ATTN: SUL

DEPARTMENT OF ENERGY

LAWRENCE LIVERMORE NATIONAL LAB
ATTN: G SIMONSON
ATTN: L-10 A GROSSMAN
ATTN: L-84 H KRUGER

LOS ALAMOS NATIONAL LABORATORY
ATTN: D SAPPENFIELD
ATTN: D SIMONS
ATTN: D SUTHERLAND
ATTN: E SYMBALISTY
ATTN: MS J ZINN
ATTN: P364 REPORT LIBRARY
ATTN: REPORT LIBRARY

SANDIA NATIONAL LABORATORIES
ATTN: D HARTLEY

SANDIA NATIONAL LABORATORIES
ATTN: CODE 9014 R BACKSTROM
ATTN: TECH LIB (RPTS REC CLRK)

OTHER GOVERNMENT

CENTRAL INTELLIGENCE AGENCY
ATTN: OSWR/NED
ATTN: OSWR/SSD FOR L BERG

DEPARTMENT OF DEFENSE CONTRACTORS

AERODYNE RESEARCH, INC
ATTN: C KOLB

AEROJET ELECTRO-SYSTEMS CO
ATTN: J GRAHAM

AEROSPACE CORP
ATTN: A LIGHTY
ATTN: C CREWS
ATTN: C RICE
ATTN: D RUDOLPH
ATTN: G LIGHT

ANALYTICAL SYSTEMS ENGINEERING CORP
ATTN: SECURITY

BDM INTERNATIONAL INC
ATTN: L JACOBS

BERKELEY RSCH ASSOCIATES, INC
ATTN: J WORKMAN
ATTN: S BRECHT

BOEING CO
ATTN: M/S 48-88 G HALL

CALIFORNIA RESEARCH & TECHNOLOGY, INC
ATTN: M ROSENBLATT

CALSPAN CORP
ATTN: C TREANOR
ATTN: J GRACE
ATTN: M DUNN

EOS TECHNOLOGIES, INC
ATTN: B GABBARD
ATTN: W LELEVIER

GENERAL ELECTRIC CO
ATTN: C ZIERDT
ATTN: R EDSALL

GRUMMAN AEROSPACE CORP
ATTN: J DIGLIO

HSS, INC
ATTN: D HANSEN
ATTN: M SHULER

INFORMATION SCIENCE, INC
ATTN: W DUDZIAK

INSTITUTE FOR DEFENSE ANALYSES
ATTN: E BAUER
ATTN: H WOLFHARD

JAMIESON SCIENCE & ENGINEERING
ATTN: J JAMIESON

KAMAN SCIENCES CORP
ATTN: D PERIO
ATTN: P TRACY

KAMAN SCIENCES CORP
ATTN: E CONRAD
ATTN: G DITTBERNER

KAMAN SCIENCES CORPORATION
ATTN: B GAMBILL
5 CYS ATTN: DASIAC
ATTN: R RUTHERFORD

KAMAN SCIENCES CORPORATION
ATTN: DASIAC

LOCKHEED MISSILES & SPACE CO, INC
ATTN: J HENLEY
ATTN: R SEARS

MARTIN MARIETTA DENVER AEROSPACE
ATTN: H VON STRUVE III
ATTN: J BENNETT

MCDONNELL DOUGLAS CORP
ATTN: T CRANOR

MCDONNELL DOUGLAS CORPORATION
ATTN: J GROSSMAN
ATTN: R HALPRIN

MISSION RESEARCH CORP
ATTN: J KENNEALY
ATTN: R ARMSTRONG
ATTN: S BELANGER
ATTN: W WHITE

MISSION RESEARCH CORP
ATTN: D LANDMAN
ATTN: F FAJEN
ATTN: F GUIGLIANO
ATTN: G MCCARTOR
ATTN: K COSNER
ATTN: M FIRESTONE
ATTN: R BIGONI
ATTN: R BOGUSCH
ATTN: TECH INFO CENTER
2 CYS ATTN: TECH LIBRARY

MISSION RESEARCH CORP
ATTN: R STELLINGWERF

NICHOLS RESEARCH CORP INC
ATTN: J EOLL

NICHOLS RESEARCH CORP, INC
ATTN: R BYRN

PACIFIC-SIERRA RESEARCH CORP
ATTN: E FIELD JR
ATTN: F THOMAS
ATTN: H BRODE, CHAIRMAN SAGE

PHOTOMETRICS, INC
ATTN: I L KOFSKY

PHOTON RESEARCH ASSOCIATES
ATTN: D BURWELL
ATTN: O LEWIS

PHYSICAL RESEARCH INC
ATTN: W. SHIH

PHYSICAL RESEARCH INC
ATTN: H FITZ
ATTN: P LUNN

PHYSICAL RESEARCH INC
2 CYS ATTN: J GENEROSA
2 CYS ATTN: R PARKER
2 CYS ATTN: T GORMAN

PHYSICAL RESEARCH, INC
ATTN: T STEPHENS

PHYSICAL RESEARCH, INC
ATTN: J DEVORE
ATTN: J THOMPSON
ATTN: W SCHLUETER

R & D ASSOCIATES
ATTN: F GILMORE

RJO ENTERPRISES/POET FAC
ATTN: A ALEXANDER
ATTN: W BURNS

S-CUBED
ATTN: C NEEDHAM
ATTN: T CARNEY

SCIENCE APPLICATIONS INTL CORP
ATTN: D HAMLIN
ATTN: D SACHS

SCIENCE APPLICATIONS INTL CORP
ATTN: E HYMAN

SCIENCE APPLICATIONS INTL CORP
ATTN: M CROSS

SRI INTERNATIONAL
ATTN: W CHESNUT

TELEDYNE BROWN ENGINEERING
ATTN: J CATO
ATTN: J WOLFSBERGER, JR
ATTN: TECH LIBRARY (P SHELTON)
ATTN: N PASSINO

TOYON RESEARCH CORP
ATTN: J ISE

TRW INC
ATTN: DR D GRYBOS
ATTN: R PLEBUCH, HARDNESS & SURV LAB
ATTN: H CULVER

TRW SPACE & DEFENSE SYSTEMS
ATTN: D M LAYTON

USER SYSTEMS, INC
ATTN: S W MCCANDLESS, JR

VISIDYNE, INC
ATTN: J CARPENTER